SUMMARY OF SIGNIFICANT RESULTS IN—

Mineral resources
Water resources
Engineering geology and hydrology
Regional geology
Principles and processes
Laboratory and field methods
Topographic surveys and mapping
Management of resources on public lands
Land information and analysis
Investigations in other countries

LIST OF—

Investigations in progress

GEOLOGICAL SURVEY RESEARCH 1979

GEOLOGICAL SURVEY PROFESSIONAL PAPER 1150

GEOLOGICAL SURVEY RESEARCH 1979

GEOLOGICAL SURVEY PROFESSIONAL PAPER 1150

A summary of recent significant scientific and economic results accompanied by a list of geologic and hydrologic investigations in progress and a report on the status of topographic mapping

UNITED STATES GOVERNMENT PRINTING OFFICE, WASHINGTON, D.C.: 1979

UNITED STATES DEPARTMENT OF THE INTERIOR

CECIL D. ANDRUS, *Secretary*

GEOLOGICAL SURVEY

H. William Menard, *Director*

Library of Congress catalog-card No. 68-46150

For sale by the Superintendent of Documents, U.S. Government Printing Office
Washington, D.C. 20402

CONTENTS

	Page
Abbreviations	vii
SI units and inch-pound system equivalents	ix
Mineral-resource investigations	1
United States and world mineral-resource assessments	1
Geologic studies of mining districts and mineral-bearing regions	3
Mineral-resource investigations of wilderness areas	9
Geochemical and geophysical techniques in resource assessments	10
Geochemical-reconnaissance results	10
Geophysical exploration	11
Lead isotopes applied to mineral exploration	12
Volatile gases useful in geochemical exploration	12
Biogeochemical investigations	12
Botanical investigations	12
Analytical methodology useful in geochemical exploration	12
Resource information systems and analysis	13
Resource information systems	13
Resource analysis	13
Chemical resources	15
Lithium investigations in sedimentary and volcanic rocks	15
Phosphate investigation	17
Novaculite in Nevada	18
Mineral-fuel investigations	19
Coal analysis	19
Field studies	19
Dating, geochemistry, and petrology of peat, lignite, and coal	21
Oil and gas resources	23
Alaska	23
Rocky Mountains and Great Plains	25
Great Basin and Southwestern United States	28
California	30
Gulf of Mexico and Florida	30
Appalachian Basin	31
New exploration and production techniques	33
Oil-shale resources	35
Nuclear-fuel resources	36
Geothermal resources	53
Regional geologic investigations	56
New England and the Adirondacks	56
Appalachian Highlands and the Coastal Plains	60
Central region	65
Lake Michigan	65
Michigan	65
Regional geologic investigations—Continued	
Central region—Continued	
Minnesota	66
Mississippi embayment	66
Rocky Mountains and Great Plains	67
Stratigraphic studies	67
Igneous studies	71
Tectonic and geophysical studies	73
Basin and Range region	78
Mineral-resource studies	78
Stratigraphic and structural studies	80
Pacific coast region	83
California	83
Oregon	87
Washington	88
Alaska	91
Statewide	91
Northern Alaska	94
East-central Alaska	95
Southern Alaska	96
Southwestern Alaska	97
Southeastern Alaska	97
Regional studies and compilations of large areas	99
Water-resource investigations	101
Northeastern region	102
Regional studies	103
Illinois	103
Indiana	103
Maryland	105
Massachusetts	105
Michigan	105
Minnesota	106
Minnesota and Wisconsin	108
New Hampshire	108
New Jersey	109
New York	109
Ohio	110
Pennsylvania	110
Vermont	110
Virginia	110
Wisconsin	111
Southeastern region	112
Alabama	112
Florida	112
Georgia	116
North Carolina	116
Tennessee	118
Central region	118
Multistate studies	120
Colorado	120
Iowa	121

Page

Water-resource investigations—Continued
Central region—Continued
Multistate studies—Continued
Kansas 122
Louisiana 122
Missouri 123
Montana 123
New Mexico 124
North Dakota 126
South Dakota 127
Texas 127
Utah 127
Western region 128
Alaska 129
Arizona 130
California 130
Idaho 131
Nevada 132
Oregon 132
Washington 133
Special water-resource programs 134
Data coordination, acquisition, and storage 134
Office of Water-Data Coordination 134
Water-data storage system 135
National Water Data Exchange 135
Urban water program 136
Water use 137
National water quality programs 138
The Regional Aquifer-System Analysis program 139
Marine geology and coastal hydrology 141
Coastal and marine geology 141
Atlantic continental margin 141
Gulf of Mexico 145
Pacific continental margin 146
California to Washington 146
Alaskan continental margin 150
Island possessions and territories 155
Deep-sea relief, sediments, and mineral deposits 156
Marine geologic processes 157
Estuarine and coastal hydrology 158
Gulf coast 158
Atlantic coast 159
Pacific coast 159
Management of natural resources on Federal and Indian lands 163
Classification and evaluation of mineral lands 163
Classified land 163
Known Geologic Structures of producing oil and gas fields 163
Known Geothermal Resource Areas 164
Known Recoverable Coal Resource Areas 164
Coal Resource Occurrence/Coal Development Potential (CRO/CDP) reports 164
Known leasing areas for potassium, phosphate, and sodium 164
Waterpower classification—preservation of reservoir sites 164
Supervision of mineral leasing 165
Management of oil and gas resources on the Outer Continental Shelf 165

Page

Geologic and hydrologic principles, processes, and techniques 167
Geophysics 167
Rock magnetism 167
Geomagnetism 168
Petrophysics 169
Applied geophysical techniques 172
Geochemistry, mineralogy, petrology 176
Experimental and theoretical geochemistry 176
Mineralogic studies and crystal chemistry 176
Minerals and environmental health 177
Volcanic rocks and processes 178
Hawaiian volcano studies 178
Hawaiian Island—Emperor Seamount studies 180
Cenozoic volcanism in Western United States 181
Studies of volcanic ejecta and gases 183
Plutonic rocks and magmatic processes 184
Metamorphic rocks and processes 184
Geochemistry of water 185
Water-rock interactions 185
Hydrochemistry of volcanic aquifers 185
Evaluation of brines 185
Statistical geochemistry and petrology 187
Extended *Q*-mode factor analysis 187
Isotope and nuclear geochemistry 188
Isotope tracer studies 188
Stable isotopes 190
Advances in geochronometry 191
Geothermal systems 192
Sedimentology 200
Glaciology 203
Climate 205
Ground-water hydrology 207
Aquifer-model studies 208
Recharge studies 209
Disposal and storage studies 210
Summary appraisals of the Nation's ground-water resources 210
Miscellaneous studies 211
Surface-water hydrology 211
Paleontology 214
Mesozoic and Cenozoic studies 214
Paleozoic studies 218
Precambrian studies 219
Plant ecology 220
Chemical, physical, and biological characteristics of water 220
Relation between surface water and ground water 224
Evaporation and transpiration 226
Limnology and potamology 227
New hydrologic instruments and techniques 229
Sea-ice studies 230
Analytical methods 231
Analytical chemistry 231
Emission spectroscopy 231
Neutron activation 232
X-ray fluorescence 232
Analysis of water 232

Page

Geology and hydrology applied to hazard assessment and environment 235
Earthquake studies 235
Seismicity 235
Earthquake mechanics and prediction studies 238
Seismicity 238
Foreshock studies 239
Seismic gaps 239
Gravity surveys 240
Crustal deformation 240
Fault stability 241
Earthquake precursors 242
Earthquake swarms 242
The Thessaloniki earthquake 243
Earthquake hazards studies 243
Engineering geology 251
Landslide hazards 253
Reactor hazards 257
Hydrologic aspects of energy 260
Geology and hydrology related to national security 261
Radioactive wastes and the geologic and hydrologic environments 263
Studies of low-level radioactive waste disposal sites 264
Regional studies 264
Waste isolation pilot plant site, southeastern New Mexico 267
Geophysics 267
Geochemistry 268
Floods 269
Outstanding floods 269
Flood-frequency studies 270
Flood mapping 271
Effects of pollutants on water quality 272
Environmental geochemistry 275
Land subsidence 275
Hazards information and warnings 277
Astrogeology 279
Planetary investigations 279
Lunar investigations 285
Remote sensing and advanced techniques 290
Earth Resources Observation Systems program 290
Data analysis laboratory 290
Integration of remotely sensed data with other data 290
Correction of Landsat images 290
Water depth from Landsat images 290
Monitoring the environment 290
Cooperative projects with the Bureau of Land Management 290
Cooperative projects with the National Park Service 291
Cooperative projects with the U.S. Fish and Wildlife Service 291
Cooperative projects with the Mine Safety and Health Administration 292
Cooperative projects with the Bureau of Reclamation 292
Impact of surface mining 292
Cooperative projects with States 293
Forest defoliation 294
Cape Cod, Massachusetts 294

Page

Remote sensing and advanced techniques—Continued
Earth Resources Observation Systems program—Continued
Monitoring the environment—Continued
Targeting, inventorying, and monitoring ground-water resources 294
Studying the global environment 294
Monitoring desertification 294
Satellite image atlas of glaciers 295
Integrated terrain mapping 295
Targeting mineral exploration 295
Mineral exploration at Claunch, New Mexico 295
Petroleum in northwestern Colorado 295
Porphyry copper in Arizona 295
Copper and molybdenum in Nabesna, Alaska 296
Data from airborne instruments 296
Fraunhofer line discriminator experiments 296
Applications to geologic studies 297
Applications to hydrologic studies 300
Land use and environmental impact 302
Multidisciplinary studies in support of land-use planning and decisionmaking 302
Land use and land cover maps and data and other geographic studies 304
Environmental impact studies 310
International cooperation in the earth sciences 311
Scientific and technical assistance 311
Scientific cooperation and research 313
International commissions and representation 319
International hydrological program 320
Summary by country 321
Afghanistan-Iran-Turkey 321
Bolivia 321
Brazil 321
Djibouti 322
Egypt 322
Guatemala 323
Hungary 323
India 323
Indonesia 324
Iran 325
Israel 325
Japan 325
Jordan 326
Kenya 326
Liberia 326
Mexico 326
Oman 327
New Zealand 328
Pakistan 328
People's Republic of China 329
Peru 330
Poland 331
Saudi Arabia 332
Turkey 334
Venezuela 336
Antarctic programs 336

	Page
Topographic surveys and mapping	339
Field surveying	339
Surveying from the air using inertial technology	339
Inertial surveying with SPAN MARK	339
Photogrammetry	340
Arbitrary-photocoordinate pass points	340
Mapping from high-resolution high-altitude panchromatic photographs	340
Building DLG–2 digital files directly from stereomodels	340
Numerical orientation of Kelsh K–100 plotter	341
Point-transfer eye test	341
Planimetric compilation from orthophotographs	341
Photogrammetric archival storage system	342
Image control targets	342
"Natural" color image maps from color infrared film	342
Digital cartography	342
Digital data editing system	343
Digital Profile Recording and Output System	343
Digital readout and reference system for cartographic camera	343
Topographic surveys and mapping—Continued	
Digital cartography—Continued	
Coordinate Transformation System	343
Satellite technology	344
Landsat 3 return beam vidicon images	344
Satellite image maps	344
Space Oblique Mercator projection	345
Cartographic equipment	345
Microdotter	345
Computer technology	346
Time sharing	346
Batch computing	346
Computer managed meetings	346
U.S. Geological Survey publications	347
Publications program	347
Publications issued	348
How to obtain publications	349
Over the counter	349
By mail	350
References cited	351
Investigations in progress	365
Indexes	404
Subject index	404
Investigator index	440

ILLUSTRATIONS

	Page
FIGURE 1.—Lithium distribution illustrated by a neutron-induced radioluxograph	17
2.—Index map of the conterminous United States showing areal subdivisions used in the discussion of water resources	101
3.—Landslide concentration map for Guatemala City area	256
4.—Status of land use and land cover mapping as of October 1978	305

TABLES

	Page
TABLE 1.—Revised estimates of major United States and world identified, economic, and selected paramarginal resources	2
2.—Mineral production, value, and royalty for calendar year 1978	165
3.—Summary of CY 1978	166
4.—Technical assistance to other countries provided by the USGS during FY 1978	314
5.—Technical and administrative documents issued during the period October 1977 through October 1978 as a result of USGS technical and scientific cooperation programs	317

ABBREVIATIONS

A — angstrom
ABAG — Association of Bay Area Governments
a.c. — alternating current
A.D. — anno Domini
AESOP — Automatic Surface Observation Platforms
AGID — Association of Geoscientists for International Development
AGWAT — Ministry of Agriculture and Water
AIDJEX — Arctic Ice Dynamics Joint Experiment
AMRAP — Alaska Mineral Resource Assessment Program
ANCSA — Alaska Native Claims Settlement Act
AOCS — Atlantic Outer Continental Shelf
APD — antiphase domain
ARPA — Advanced Research Projects Agency
ASL — Albuquerque Seismological Laboratory
ASRO — Advanced Seismological Research Observatories
atm — atmosphere

bbl — barrel
BLM — Bureau of Land Management
BOD — biochemical oxygen demand
B.P. — before present
Btu — British thermal unit

°C — degrees Celsius
CAI — Color alteration index
cal — calorie
CARETS — Central Atlantic Regional Ecological Test Site project
CCD — Computer Center Division
CCOP — U.N. Committee for Coordination of Joint Prospecting for Mineral Resources in Asian Offshore Areas
CCT — computer-compatible tape
C/DCP — convertible data-collection platforms
CDP — common depth point
CENTO — Central Treaty Organization
CEQ — Council on Environmental Quality
CFRUC — Colorado Front Range Urban Corridor Project
CGIS — Canada Geographic Information System
cgs — centimeter-gram-second
Ci — curie
cm — centimeter
COD — chemical oxygen demand
COM — computer-oriented microform
COST — Continent Offshore Stratigraphic Test Group
CPU — central processing unit
CRIB — Computerized Resource Information Bank
CV — characteristic value

d — day
d.c. — direct current
DCAP — Digital Cartographic Applications Program
DCS — Data-collection system
DEROCS — Development of Energy Resources of the Outer Continental Shelf
DMA — Defense Mapping Agency
DNPM — Departmento Nacional da Producão Mineral
DO — dissolved oxygen
DOMES — Deep Ocean Mining Environmental Study
DSDP — Deep Sea Drilling Project

EIA — Environmental Impact Analysis
EIS — environmental impact statement
EM — electromagnetic (soundings)
EMRIA — Energy Mineral Rehabilitation Inventory and Analysis
emu — electromagnetic unit
EPA — Environmental Protection Agency
ERDA — Energy Research and Development Administration
EROS — Earth Resources Observation System
ERTS — Earth Resources Technology Satellite
ESCAP — Economic and Social Commission for Asia and the Pacific Committee on Natural Resources

eV — electronvolt

FAO — Food and Agriculture Organization
f.l. — focal length
FLD — Fraunhofer line discriminator
FY — fiscal year

g — gram
GHz — gigahertz
GIPSY — General Information Processing System
GIRAS — Geographic Information Research and Analysis System
GOES — Geostationary Operational Environmental Satellite
GPa — gigapascal
GRASP — Geologic Retrieval and Synopsis Program

h — hour
ha — hectare
HFU — heat-flow unit
HIPLEX — High Plains Cooperative Program
hm — hectometer
HUD — Department of Housing and Urban Development
Hz — hertz

IAH — International Association of Hydrogeologists
IAHS — International Association of Hydrological Scientists
ICAT — Inorganic Chemical Analysis Team
IDB — Inter-American Development Bank
IDIMS — Interactive Display Image Manipulation System
IDOE — International Decade of Ocean Exploration
IGCP — International Geological Correlation Program
IGU — International Geographical Union
IHD — International Hydrological Decade
IHP — International Hydrological Program
IMW — International Map of the World
in. — inch
IR — infrared
ISAM — Index Sequential Access Method
ISO — International Standardization Organization
IUGS — International Union of Geologic Sciences

J — joule
JECAR — Joint Commission of Economic Cooperation
JPL — Jet Propulsion Laboratory
JTU — Jackson turbidity unit

K — kelvin
kbar — kilobar
KCLA — Known Coal Leasing Area
KeV — kiloelectronvolt
kg — kilogram
KGRA — Known Geothermal Resources Area
KGS — Known Geologic Structure
kHz — kilohertz
km — kilometer
KREEP — potassium-rare-earth element-phosphorus
kWh — kilowatt-hour

L — liter
LARS — Laboratory for Applications of Remote Sensing
lat — latitude
LMF — lithic matrix fragments
long — longitude

m — meter
M — magnitude (earthquake)
m_b — magnitude from body waves
m_L — Richter magnitude
m_s — magnitude from surface waves
mcal — millicalorie
MEF — maximum evident flood
mGal — milligal
mi — mile
min — minute

mg — milligram
ml — milliliter
mm — millimeter
MN — meganewton
mo — month
MPa — megapascal
MSS — multispectral scanner
mV — millivolt
MW — megawatt
MWe — megawatts electrical
m.y. — million years
μ — micron
μcal — microcalorie
μg — microgram
μGal — microgal
μm — micrometer
μmho — micrombo
μstrain/yr — engineering shear

NASA — National Aeronautics and Space Administration
NASQAN — National Stream Quality Accounting Network
NAWDEX — National Water Data Exchange
NCRDS — National Coal Resources Data System
NEIS — National Earthquake Information Service
NEPA — National Environmental Policy Act
ng — nanogram
NLCR — nonlinear complex resistivity
nm — nanometer
NOAA — National Oceanic and Atmospheric Administration
NOS — National Ocean Survey
NPR — Naval Petroleum Reserve
NRA — National Resources Agency
NRA — Nuclear Regulatory Agency
nT — nanotesla
NTIS — National Technical Information Service
NTS — Nevada Test Site

OAS — Organization of American States
OCS — Outer Continental Shelf
oe — Oersted
ohm-m — ohm-meter
OIA — Office of International Activities
OME — Office of Minerals Exploration
ORNL — Oak Ridge National Laboratory
OWDC — Office of Water-Data Coordination
Ω — ohm

PAIGH — Pan American Institute of Geography and History
PCB — polychlorinated biphenyls
pCi — picocurie
ppb — part per billion
ppm — part per million
PSRV — pseudo-relative velocity

R — range
RASS — Rock Analysis Storage System
REE — rare-earth element
RF — radio frequency
RMSE — root mean square error
R/V — research vessel

s — second
SFBRS — San Francisco Bay Region Environment and Resources Planning Study
SIP — strongly implicit procedure
SLAR — side-looking airborne radar
SMS — Synchronous Meteorological Satellite
SOM — Space Oblique Mercator
SP — self potential
SRO — Seismic Research Observatory

t — tonne
T — township
TEM — transmission electron microscopy
TIU — Thermal-inertia unit

TL ---------- thermoluminescence
TVA ---------- Tennessee Valley Authority

UNDP ---------- U.N. Development Program
UNESCO --- United Nations Educational, Scientific and Cultural Organization
USAID ---- U.S. Agency for International Development
USBM ---------- U.S. Bureau of Mines
USDA ---------- U.S. Department of Agriculture
USGS ---------- U.S. Geological Survey
USNC/SH --- United Nations Educational, Scientific and Cultural Organization
USPHS ---------- U.S. Public Health Service
U.S.S.R. ---------- Union of Soviet Socialist Republics
UTM ---------- Universal Transverse Mercator

V ---------- volt
VDETS ---------- Voice Data Entry Terminal System
VES ---------- Vertical electric soundings
VHRR ---------- very high resolution radiometer
VLF ---------- very low frequency

W ---------- watt
WMO ---------- World Meteorological Organization
WRC ---------- Water Resources Council
WRDD ----- Water Resources Development Department
WWSSN Worldwide Standardized Seismograph Network

yr ---------- year

SI UNITS AND INCH-POUND SYSTEM EQUIVALENTS

[SI, International System of Units, a modernized metric system of measurement. All values have been rounded to four significant digits except 0.01 bar, which is the exact equivalent of 1 kPa. Use of hectare (ha) as an alternative name for square hectometer (hm^2) is restricted to measurement of land or water areas. Use of liter (L) as a special name for cubic decimeter (dm^3) is restricted to the measurement of liquids and gases; no prefix other than milli should be used with liter. Metric ton (t) as a name for megagram (Mg) should be restricted to commercial usage, and no prefixes should be used with it. Note that the style of meter² rather than square meter has been used for convenience in finding units in this table. Where the units are spelled out in text, Survey style is to use square meter]

SI unit		Inch-Pound equivalent	
Length			
millimeter (mm)	=	0.039 37	inch (in)
meter (m)	=	3.281	feet (ft)
	=	1.094	yards (yd)
kilometer (km)	=	0.621 4	mile (mi)
	=	0.540 0	mile, nautical (nmi)
Area			
centimeter² (cm^2)	=	0.155 0	inch² (in^2)
meter² (m^2)	=	10.76	feet² (ft^2)
	=	1.196	yards² (yd^2)
	=	0.000 247 1	acre
hectometer² (hm^2)	=	2.471	acres
	=	0.003 861	section (640 acres or 1 mi²)
kilometer² (km^2)	=	0.386 1	mile² (mi^2)
Volume			
centimeter³ (cm^3)	=	0.061 02	inch³ (in^3)
decimeter³ (dm^3)	=	61.02	inches³ (in^3)
	=	2.113	pints (pt)
	=	1.057	quarts (qt)
	=	0.264 2	gallon (gal)
	=	0.035 31	foot³ (ft^3)
meter³ (m^3)	=	35.31	feet³ (ft^3)
	=	1.308	yards³ (yd^3)
	=	264.2	gallons (gal)
	=	6.290	barrels (bbl) (petroleum, 1 bbl=42 gal)
	=	0.000 810 7	acre-foot (acre-ft)
hectometer³ (hm^3)	=	810.7	acre-feet (acre-ft)
kilometer³ (km^3)	=	0.239 9	mile³ (mi^3)
Volume per unit time (includes flow)			
decimeter³ per second (dm^3/s)	=	0.035 31	foot³ per second (ft^3/s)
	=	2.119	feet³ per minute (ft^3/min)
Volume per unit time (includes flow)—Continued			
decimeter³ per second (dm^3/s)	=	15.85	gallons per minute (gal/min)
	=	543.4	barrels per day (bbl/d) (petroleum, 1 bbl=42 gal)
meter³ per second (m^3/s)	=	35.31	feet³ per second (ft^3/s)
	=	15 850	gallons per minute (gal/min)
Mass			
gram (g)	=	0.035 27	ounce avoirdupois (os avdp)
kilogram (kg)	=	2.205	pounds avoirdupois (lb avdp)
megagram (Mg)	=	1.102	tons, short (2 000 lb)
	=	0.984 2	ton, long (2 240 lb)
Mass per unit volume (includes density)			
kilogram per meter³ (kg/m^3)	=	0.062 43	pound per foot³ (lb/ft^3)
Pressure			
kilopascal (kPa)	=	0.145 0	pound-force per inch² (lbf/in^2)
	=	0.009 869	atmosphere, standard (atm)
	=	0.01	bar
	=	0.296 1	inch of mercury at 60°F (in Hg)
Temperature			
temp kelvin (K)	=	[temp deg Fahrenheit (°F) +459.67]/1.8	
temp deg Celsius (°C)	=	[temp deg Fahrenheit (°F) −32]/1.8	

Any use of trade names and trademarks in this publication is for descriptive purposes only and does not constitute endorsement by the U.S. Geological Survey.

GEOLOGICAL SURVEY RESEARCH 1979

MINERAL-RESOURCE INVESTIGATIONS

UNITED STATES AND WORLD MINERAL-RESOURCE ASSESSMENTS

The development of new concepts on the origin and occurrence of mineral deposits can significantly change the United States and world resource picture. Thus, as new data becomes available, it must be analyzed in terms of its impact on the outlook for future supplies of mineral raw materials. In 1978, such analyses led to statements on the resources of a number of commodities.

World aluminum (bauxite) resources

In updating information on aluminum resources, S. H. Patterson (USGS) and H. F. Kurtz (USBM) estimated total bauxite reserves to be 27 billion tons, and total resources (reserves plus subeconomic and undiscovered deposits) are estimated at 40 to 50 billion tons. These resources (in millions of tons) are located as follows: United States—300 to 325 (includes bauxite materials for refractory and chemical use); Caribbean and Central America region—3,000 to 4,000; South America—8,000 to 10,000; Europe—2,000 to 3,000; Africa—12,000 to 15,000; Asia—7,000 to 9,000; Oceania—8,000 to 9,000.

Chromite resources

Chromite is mined almost exclusively from either podiform or stratiform deposits, according to B. R. Lipin and T. P. Thayer. Podiform deposits, which seldom contain more than a million tons each of chromite, are an uncertain future source of chromite. Although there are probably 200 million tons of minable chromite in podiform deposits yet to be discovered in known districts, these are extremely difficult to find, and no single geophysical technique is adequate in their discovery. Research into using a combination of techniques is underway but such exploration is very costly.

Stratiform chromite deposits are almost always large (more than 5 million metric tons each) and contain more than 99 percent of the world's total resources of chromite, which are estimated to be more than 33 billion tons. The stratiform deposits in South Africa and Rhodesia contain 66 and 33 percent, respectively, of the world's chromite resources, but these countries contributed only 34 percent of the 8 million tons produced in 1977. Demand for chromium will probably remain high because of the lack of substitutes in making corrosion-resistant steel. At the 1977 production rate, resources of chromite in most other countries, with the possible exception of the U.S.S.R., will be depleted within 20 years.

Fluorspar resources of Africa

An investigation of fluorspar resources by R. E. Van Alstine and P. G. Schruben showed that imports of African fluorspar increased from 4 percent to 22 percent of our total fluorspar imports from 1975 through 1977. Manto deposits in carbonate rocks in South Africa, Kenya, Tunisia, and Morocco; pipe-like deposits in South Africa; and stockwork deposits in South Africa and Namibia have been most productive. The major fluorspar deposits of Africa, as elsewhere around the world (Van Alstine, 1976), are associated with large rift zones. Fluorite has been reported from 24 of 115 carbonatites found near the rift zones.

Estimates of African fluorspar reserves of proved and probable ore total about 192 million metric tons and average 22 percent C_aF_2. South Africa accounts for about 86 percent of this total and ranks first in world reserves of fluorspar. Africa is thus able to provide an increasing and major share of the world's fluorspar supply.

Phosphate resources of the circumpacific region

The circumpacific region contains four major phosphogenic provinces. These include (1) North American province, (2) South American marine phosphogenic provinces, (3) the Oceania insular province, and (4) the Australian-Asian Proterozoic and lower Paleozoic province. The first three of these have been actively forming until the recent geologic past, but the last one is extinct.

The phosphate resources in these provinces throughout the circumpacific region exceed 26 billion tons of phosphate rock according to R. P. Sheldon. In spite of this amount, little phosphate rock at present is mined, and many countries of the region, including some with the greatest need for fertilizer,

lack phosphate resources. However, exploration is not complete in much of the region, particularly southern Asia, and there are many opportunities for development of phosphate resources to meet the agricultural needs of the region.

Lead and zinc resources of the United States and of the world

The table below is the result of revision by J. A. Briskey, Jr., and H. T. Morris of some of the reserve-resource data presented in USGS Professional Paper 820 to allow for past production and major new

TABLE 1.—*Revised estimates of major United States and world identified, economic, and selected paramarginal resources* [1]

[Thousands of short tons]

	USGS PP 820		Known additions 1973–77		Production [2] 1973–77		Current revised estimates	
	lead	zinc	lead	zinc	lead	zinc	lead	zinc
UNITED STATES								
Lead:								
Missouri	30,250		10,000		2,566		37,684	
NE Washington; Coeur d'Alene District, Idaho; and Butte District, Montana	2,150		1,000		273		2,877	
Great Basin and Rocky Mountains (chiefly Colorado, Utah, New Mexico, Arizona, Nevada, and California)	3,500		84		210		3,374	
Others	2,285		40		38		2,287	
Zinc:								
Appalachian (chiefly New Jersey, Pennsylvania, New York, Virginia, East Tennessee, and Maine)		16,400		3,000		1,123		18,277
Mississippi Valley (chiefly Missouri, Illinois, Wisconsin, and middle Tennessee)		19,200		7,140		561		25,779
Rocky Mountains, Great Basin, and Pacific Coast (chiefly Colorado, Utah, New Mexico, Arizona, Nevada, Idaho, Montana, Washington, California, and Alaska)		9,400		597		707		9,290
U.S. TOTALS	38,185	45,000	11,124	10,737	3,087	2,391	46,222	53,346
NORTH AMERICA (including Greenland)	54,105	84,000	28,705	45,377	4,884	8,882	77,926	120,495
SOUTH AND CENTRAL AMERICA, AND MEXICO	11,025	16,000	429	800	2,583	4,221	8,871	12,579
EUROPE	24,625	58,000	+[3]	+[3]	3,555	5,901	21,070+	52,099+
AFRICA	5,200	14,000	3,228	11,188	892	1,702	7,536	23,486
ASIA [4] (including U.S.S.R.)	27,495	42,000	721+[3]	1,573+[3]	5,402	9,354	22,814+	34,219+
OCEANIA (including Australia, New Zealand, and Tasmania)	18,500	21,000	7,855	8,064	2,126	2,496	24,229	26,568
WORLD TOTAL	140,950	235,000	40,938	67,002+	19,442	32,556	162,446	269,446+

[1] Includes measured, indicated, and some inferred reserves, as well as those paramarginal resources that have highly promising potential for near-term development (i.e., Crandon, Wisconsin; Howard's Pass, Yukon; Gamsberg, South Africa; and Elura, Australia).

[2] Data from American Bureau of Metal Statistics, U.S. Bureau of Mines, and World Mining publications. Production by geographic region within the United States for 1976–77 and production outside of North America for 1977 have been estimated.

[3] Current, reliable data on new discoveries in Communist countries are lacking, although there apparently have been several major new finds in the 1973–77 period.

[4] Known additions, 1973–77, are in India and Thailand.

additions of minable reserves and near-minable resources that have been discovered or have changed status since 1972. At current levels of production in an economically and politically favorable environment, ignoring the certainty of future additional discoveries of ore, lead and zinc supplies are potentially adequate for at least 75 and 112 years, respectively, for the United States and at least 42 and 41 years, respectively, for the world.

Peat resources in Minnesota and Maine

Field reconnaissance by C. C. Cameron of peat deposits in Lake of the Woods County, Minnesota, and in Hancock and Penobscot Counties, Maine, shows distinct contrasts which reflect different problems to be encountered in exploitation and (or) environmental evaluations. In Minnesota, a few comparatively shallow deposits meeting minimum standards for thickness (at least 1.5 m) and quality (peat containing less than 25 percent ash dry weight) occur within vast areas of organic deposits in marshes and swamps; areas totaling 62.5 km^2 of peat meeting minimum conditions for commercial exploitation contain an estimated 20,403,900 metric tons of air-dried peat chiefly of the reed-sedge type. In contrast, the 26 Maine deposits meeting minimum standards of thickness and quality for commercial exploitation are thicker and lie in discrete bogs; areas totaling about 19.5 km^2 contain an estimated 27,385,300 metric tons of air-dried peat of the moss and reed-sedge type. Minnesota deposits are on the raised floor of glacial Lake Agassiz. The Maine deposits occur chiefly in glacial ice margin-marine settings.

Extension of phosphorite-bearing strata underneath Atlantic Continental Shelf of United States

Analysis by F. T. Manheim and C. C. Woo of drill cores from the USGS Atlantic Continental Margin Coring Project (AMCOR) reveals that phosphate-enriched sediments of Miocene age are continuous between the Florida and South Carolina-Georgia phosphorite deposits and those of the Blake Plateau. The latter aggregate 2.27 billion tons. Whereas such marine phosphorites have been considered uneconomic in the past in comparison with land deposits, new factors and methods of use may render them useful resources in the future, especially as a soil additive in moist, tropical environments.

Small-scale distribution patterns of manganese nodules

Sea floor manganese nodules can be seen in most of about 15,000 photographs recently taken during the NOAA-sponsored Deep Ocean Mining Environmental Study, according to W. F. Cannon. Several types of small-scale patterns are evident in individual photographs. These patterns were studied by nearest neighbor analysis to determine if statistically significant nonrandom patterns were present. Most photographs show distribution patterns that are either random with a high degree of confidence in cases where nodule abundance is low or varied from random toward a uniform distribution in cases of higher abundance. In other words, as complete coverage of the bottom by nodules is approached, the distribution necessarily approaches uniform. However, two significant features were recognized. First, a distinct nodule facies, recognized previously, has a strong trend toward uniform distribution of nodules even where abundance is low. Second, none of the 15,000 photographs displayed a statistically significant clustering of nodules; that is, observed groupings of nodules are no more pronounced than expected through a random distribution.

GEOLOGIC STUDIES OF MINING DISTRICTS AND MINERAL-BEARING REGIONS

The assessment of the mineral potential of public and other lands requires an ever-increasing knowledge of mineral deposits and the conditions of their formation. This knowledge, obtained through studies of known deposits and districts, can be applied to new areas having similar characteristics. During 1978, field and laboratory studies added to our understanding of mineral deposits in a large number of areas.

Quartz Hill molybdenum deposit, Ketchikan quadrangle, Alaska

A large porphyry-type molybdenum deposit (Quartz Hill) has been discovered recently in the heart of the Coast Range batholithic complex about 70 km east of Ketchikan, southeastern Alaska. T. L. Hudson, J. G. Smith, and R. L. Elliott report that intrusive rocks associated with the mineral deposit form two composite epizonal to hypabyssal stocks separated by a narrow septum of gneiss. The stocks have a fairly uniform granite composition, but they contain a variety of textural rock types ranging from approximately equigranular biotite granite to porphyries characterized by aphanitic to very fine grained and aplitic groundmasses. The porphyries are somewhat more albitic than the granites; miarolitic cavities and pegmatite pods and dikes are associated with some porphyritic rocks. Trace-element concentration in the intrusive rocks are distinctly

low for many elements. Field relations indicate that the stocks were emplaced after regional uplift and erosion of the Coast Range batholithic complex. Potassium-argon data show that some granite crystallized about 30 million years ago and that extensive alteration and mineralization took place at least 27 million years ago; at least two stages of intrusion are indicated.

All observed mineralization is within the northern stock (Quartz Hill stock) where molybdenite occurs in a complex fracture and vein stockwork. Molybdenite forms fracture coatings and occurs within veins accompanied primarily by quartz. Sericite, chlorite, and pyrite also occur locally in veins. Silicification, potassium-silicate alterations, phyllitic alteration, and zeolitization have been recognized in the Quartz Hill stock. Data from the Ketchikan quadrangle indicate that Quartz Hill and probably other porphyry-type molybdenum deposits in the Coast Range batholithic complex of southeastern Alaska and nearby parts of Canada (called Coast Plutonic Complex) are associated with a regionally extensive middle Tertiary episode of felsic magmatism. Emplacement of these magmas in the Coast Range batholithic complex may be primarily controlled by structural features.

Geochemical anomalies in the Mystery Mountains, Medfra quadrangle, Alaska

M. L. Silberman and C. L. Connor located an area of approximately 4 km^2 in the southeastern corner of the Medfra C–4 quadrangle where anomalous concentrations of copper, tin, boron, and silver are associated with small porphyritic dacite(?) intrusions which cut clastic sedimentary rocks of the Nixon Fork terrain. Sericitic alteration has affected hypabyssal intrusive rocks over about an 8- to 10-km^2 area. The tin, copper, and other trace metal anomalies are found in both the intrusive rocks and the sedimentary wall rocks. Many of the small intrusive bodies are brecciated and cemented by tourmaline. Tourmaline veinlets and irregular segregations are common throughout all of the rocks in the area. Copper appears to occur principally as chalcopyrite disseminated throughout the intrusive and intruded rocks and as supergene malachite and azurite in brecciated hornfels surrounding some of the intrusions. Copper in grab samples of hornfels, sandstones, and porphyritic dacite varies from several hundred ppm to a high value of 2 percent. Tin content in the same samples varies from less than 10 ppm to 200 ppm. The tin and copper appear to be associated. In some samples of porphyry, tourmaline clots are surrounded by and contain disseminated chalcopyrite. The source of tin in the rocks has not yet been determined.

Metallogeny in California

Metallogeny studies by J. P. Albers in California reveal that specific metallic mineral deposit types correlate with discrete geotectonic units that make up the major geologic terranes. These major terranes are continental crust, including craton and miogeoclinal, batholithic, oceanic crust, and island arc. Lead-silver-zinc replacement and most contact metasomatic iron deposits are confined to Paleozoic carbonate miogeoclinal and craton facies rocks; tungsten and molybdenum are in carbonate roof pendants and in quartz veins in batholithic rocks; massive sulfide deposits are in the silicic volcanic rocks of island-arc terranes; and mercury, manganese, and chromite are in various rocks composing oceanic crust. Gold quartz veins occur in rocks of all four major terranes, but the major deposits seem to show a marked preference for oceanic crust. Recognition of a correlation between mineral deposit types and lithologic-tectonic units can be an aid to exploration and in estimating the mineral potential of individual geotectonic units.

Volcanogenic massive sulfide deposits in the northern Klamath Mountains, California and Oregon

Preliminary field and petrographic investigations by R. A. Koski and R. P. George, Jr., indicate that numerous stratiform massive Fe-Cu-Zn sulfide deposits in the northern Klamath Mountains of California and Oregon represent submarine volcanogenic mineralization in diverse volcanic-sedimentary and tectonic environments. The deposits are typically simple assemblages of pyrite and (or) pyrrhotite with subordinate but variable chalcopyrite and sphalerite and occur as discontinuous tabular or lensoid bodies and disseminations conformable with local stratigraphy. There are no obvious indications of root-zone stockwork mineralization and alteration. Sulfide accumulations associated with dacitic to andesitic lava flows and breccias at the Silver Peak and Almeda deposits, alternating phyllites, graphite schists, and schistose metatuffs(?) at the Gray Eagle deposit, and pillow basalt and serpentinite at the Queen of Bronze, Cowboy, and Turner-Albright deposits may represent proximal island arc, near-arc basin, and ocean-crust mineralization events, respectively.

Selenium in Paleozoic eugeosynclinal rocks in central Nevada

F. G. Poole, G. A. Desborough, and J. S. Wahlberg have found that many kerogen-rich mudstone, siltstone, chert, and dolomitic rocks of Ordovician and Devonian age in Nevada contain anomalously high concentrations of selenium. Of 37 samples analyzed, selenium values range widely from 0.2 to 360 ppm with an average of 32 ppm. These marine strata are considered by them to be a large low-grade selenium resource.

Gold-mineralized areas in Manhattan quadrangle have potential for molybdenum-porphyry deposits

According to D. R. Shawe, rock geochemical samples collected in two areas in the Manhattan, Nev., 7½-minute quadrangle show anomalous 20 to 300 ppm amounts of molybdenum. About 6 km north of the town of Manhattan and to the west of the site of North Manhattan, molybdenum-mineralized Tertiary volcanic rocks covering about 2 km^2 are associated with thin gold-bearing quartz veins. In the Manhattan district, proper molybdenum-mineralized Tertiary volcanic rocks and Paleozoic sedimentary rocks covering more than 10 km^2 are associated with a west-northwest-trending belt of gold deposits. Coarse-grained potassium feldspar that contains molybdenite and chalcopyrite, collected from a mine dump on April Fool Hill at Manhattan, suggests temperatures of mineralization well above those of the low-temperature (200° to 235° C) gold mineralization (Nash, 1972). The gold and molybdenum mineralization west of North Manhattan and in the Manhattan district may represent hydrothermal activity peripheral to deeper and hotter molybdenum-porphyry mineralized systems.

Zoned mineralization around a hidden stock in west-central Utah

Available structural and mineralogical data led T. A. Stevens and C. G. Cunningham to suggest that the Deer Trail Mountain-Alunite Ridge mining area near Marysville, west-central Utah, is centered above a 14-million-year-old epizonal stock that caused local doming (Cunningham and Steven, 1978). A highly acidic wet-stream environment developed above the stock, and the fractures were filled with vein-type alunite; hydrothermal alteration of adjacent rocks developed a zonal assemblage that changes progressively outward from alunite, to kaolinite, to chlorite-calcite. Economic mineral deposits are zoned around a barren sulfate-dominated core surrounded by a belt containing epithermal base- and precious-metal veins and mantos. The hidden stock is interpreted to have excellent potential for hosting a porphyry-type deposit, possibly of molybdenum.

Geochronology of intrusion and porphyry copper ores, Globe-Miami, Arizona

S. C. Creasey reports that the geochronology of the stocks and deposition of porphyry copper ores in the Globe-Miami district in Arizona indicates that only one stock (Schultze Granite) is of Laramide age, the others are Precambrian, and the ores of two statistically distinct ages are spatially and temporally related to the porphyry phase of the Schultze Granite. The district contains several stocks presumed to be Laramide, although there were no unequivocal geologic relations indicating a Laramide age. The K-Ar isotopic ages clearly reveal that all the stocks but the Schultze Granite are Precambrian. The precise ages of most of the Precambrian stocks, however, are not known because the ages were partly to completely reset by heat and emanations from the Schultze Granite.

The Schultze Granite is a composite comprising an early granodiorite phase, an intermediate porphyritic quartz monzonite phase (main phase), and late porphyry phases; the porphyry phases were not all intruded at the same time.

Geologic relations show that the porphyry copper mineralization is spatially related to the porphyry phase of the Schultze Granite and that the entire district is cut by regional quartz-sericite-sulfide veins localized along northwest-, northeast-, and north-striking high-angle fractures. Potassium-argon isotopic ages indicate that the regional quartz-sericite-sulfide veins are the same age as the main phase of the Schultze Granite and statistically older than the porphyry copper mineralization in the Miami-Inspiration and Pinto Valley porphyry copper deposits. However, the veins are statistically younger than the Copper Cities porphyry copper deposit. The ages clearly indicate that the Copper Cities porphyry copper ore deposit is statistically older than either the Miami-Inspiration or the Pinto Valley porphyry coppers which are the same age within the precision limits of the K-Ar age dating method. The suggestion is strong, therefore, from both geologic relations and K-Ar isotopic ages that the magma for the Schultz Granite regenerated following earlier intrusions and that ore bodies formed from successive magma generations.

Proterozoic Z stratabound copper occurrences

Mineral potential of stratabound copper-silver occurrences in the Belt Supergroup (Proterozoic Z)

of western Montana and northern Idaho has been difficult to evaluate, according to J. E. Harrison. One type of occurrence, in green argillitic beds, is common throughout most of the 130,000 km of known Belt rock exposure. The geologic history of the old sedimentary basin is highly complicated, and the factor or factors that may have formed ore deposits are not understood. No current hypothesis seems adequate to explain the occurrence.

The new Conterminous United States Mineral Appraisal Program (CUSMAP) has made possible a research project aimed at developing a model for the green-bed copper occurrences as an aid to mineral resource appraisal of the Belt basin, most of which is covered by Federal lands. The model-building attempt was begun by core drilling a zone at the top of the Spokane Formation to acquire three-dimensional data on the distribution of copper-silver in five green argillite beds that alternate with purple argillite and siltite beds. Twenty-two core holes ranging in depth from 9 to 46 m were drilled on a grid system in an area about 150 m long and 50 m wide in relatively flat-lying beds on the top of Blacktail Mountain, which is about 10 km west of the north end of Flathead Lake, Mont.

Preliminary logging of the core at the drilling site by Harrison indicates that two of the five green beds consistently contain copper sulfides but that the copper-bearing zone is not precisely in the same position within the green beds from hole to hole. Small amounts of copper sulfides are also present as widely scattered grains or tiny clots in some purple beds. Detailed logging by M. W. Reynolds of slabbed core from selected holes was done during the drilling period as a guide to drill-plan modification. Preliminary sedimentological results from that logging suggest that the sedimentary environment of deposition was a remarkably stable tidal flat. Beds as thin as 2 cm can be correlated from hole to hole.

Faulting in banded upper zone of the Stillwater Complex

Closely spaced growth faults, approximately normal to layering in the ultramafic zone of the Stillwater Complex, die out in the lower 500 to 1,000 m of the banded upper zone. There, a system of faults subparallel to the layering dominates the structure, according to Kenneth Segerstrom and R. R. Carlson. Detailed mapping, supplemented by drill-hole data supplied by Johns-Manville Stillwater Corporation, now reveals the complexity of this system, especially on the west side of West Fork gorge, where branching faults have repeatedly offset a Paleozoic inlier and underlying banded Stillwater layers that enclose a zone of primary sulfides. These sulfides have anomalously high values in platinum-group elements, and their future exploitation will be severely hampered by the complicated structure.

Platinum-group minerals in the New Rambler copper-nickel deposit, southeastern Wyoming

Copper-nickel ores of the New Rambler mine in the Medicine Bow Mountains of southeastern Wyoming contain appreciable concentrations of palladium and platinum (average 75 ppm and 4 ppm, respectively) that occur principally as discrete platinoid minerals (McCallum and others, 1976). Rhodium, ruthenium, and iridium are present as minor constituents in the ores and appear to be related substitutionally to the platinum and palladium minerals.

Nine platinum-group minerals have been recognized by M. E. McCallum (USGS) and R. R. Loucks (Howard Univ.) during preliminary mineragraphic and electron microprobe studies of ore samples (Loucks and McCallum, 1978). There are sperrylite (commonly rhodian), moncheite, platinian merenskyite, antimonian michenerite, kotulskite, temagamite, and three unidentified compounds referred to as "Ph phase B" [$\sim$(Pd, Pt)$_5$(Te, Bi, Sb)$_2$], "Pd phase C" (Pd,Te$_2$), and "Pd phase D" [inferred stoichiometry $\sim$(Pd, Pt, Bi)$_2$ $BiTeO_4 \cdot 2H_2O$]. Another Pd compound that was provisionally termed "Pd phase A" (McCallum and others, 1976) ranges in composition from approximately Be$_5$ (Bi, Sb)$_2$Te$_4$ to (Pd, Pt) (Te, Bi) and is perhaps a variety of antimonian, platinian kotulskite. Palladian pyrite (as much as 60 ppm Pd) is present in the earliest stage Cu-Ni ore of the deposit.

Origin and value of Dickie Springs gold placer deposits, central Wyoming

The Dickie Springs gold placer deposits at the south end of the Wind River Range have been known for more than 100 years, but development was hampered by lack of water, the low price of gold, and inadequate information on the geology of the area. As of October 1978, the area remained inactive.

Surface and subsurface studies and analyses by J. D. Love, J. C. Antweiler, and E. L. Mosier (1978) suggest that, in an area of 21 km^2, Eocene granite boulder conglomerate in the upper part of the Wasatch Formation and alluvium derived from it contain more than a billion dollars' worth of gold

(at $175 per ounce). The gold is relatively coarse, and many particles exceed 5 mm in diameter. The 31 samples from the conglomerate average 35 cents per cubic meter at $175 per oz. The average gold content of 27 samples of alluvium derived from the conglomerate is $1.41 per cubic meter. In addition, an unpublished report (that was lost for 80 years) made for a private company gives 2,712 fire assays in a thoroughly sampled area of 5,843 acres of alluvium at and near the alluvial sites sampled by the USGS. The fire assays average (at $175 per ounce) $8.86 per cubic meter.

Samples from oil wells drilled in the area show at least 396 m of Eocene conglomerate. The present surface relief on the nearly flat-lying conglomerate where the samples were taken is about 185 m, and apparently there is no appreciable variation in gold content from one stratigraphic horizon to another.

The source of the gold has previously been assumed to be gold-bearing veins in Precambrian rocks of the Atlantic City-South Pass district 16 to 24 km northeast of Dickie Springs. The trace element content of gold in these two areas is so different, however, that it seems more likely that the Dickie Springs gold came from a different source, probably now-buried Precambrian rocks directly north of Dickie Springs. The Atlantic City-South Pass vein gold contains Zn, Cr, Ni, Co, and Te; whereas, the Dickie Springs placer gold contains Be, Cd, As, Sb, Bi, V, W, Sn, Mo, and B.

The geologic history of the Dickie Springs gold placer deposits was reconstructed as extensive hypothermal gold-bearing veins emplaced in a granitic and metamorphic terrane directly north of the Dickie Springs area in Precambrian time. During the Laramide Revolution, the Wind River Range was uparched and eroded to its Precambrian core in Paleocene and early Eocene time and thrust west and southwest over Cretaceous and Paleocene sedimentary rocks. In late early or early middle Eocene time the Precambrian thrust plate was cut by the ancestral Continental fault that raised the mountain block a thousand meters or more. Giant granite boulders and gold-bearing fines were shed off this rising scarp and deposited as fans in the Dickie Springs area. Conglomerate deposition ceased abruptly in middle Eocene time, and middle and upper Eocene, Oligocene, and Miocene lacustrine and fluviatile strata buried the conglomerates. In late Miocene or subsequent time the Continental fault was reactivated, only now the direction of movement was reversed. The mountain block went down a thousand meters or more, and the gold-bearing conglomerate in the Dickie Springs area was exhumed. Some of the gold-bearing conglomeratic debris from this rising block was transported northward onto the Miocene strata burying the mountain block (including the gold source area) north of Dickie Springs. This debris now comprises the gold-bearing alluvium.

Sapphirine in host rocks of Precambrian sulfide deposits, Wet Mountains, Colorado

During recent investigations in Colorado, W. H. Raymond, P. A. Leiggi, and D. M. Sheridan discovered the rather rare mineral sapphirine in the host rocks of two Precambrian sulfide deposits in the southern Wet Mountains. The sapphirine was noted first in a thin section of gahnite-bearing sample from one of the deposits and then was identified by X-ray diffraction analyses. Additional fieldwork has shown that sapphirine is abundant in gahnite-bearing anthophyllite-cordierite-biotite gneiss at one of the deposits and is locally abundant in amphibole-mica gneiss at the other deposits. These rocks, together with interlayered impure marble and calc-silicate gneiss, are the host rocks of Precambrian sphalerite-chalcopyrite-galena deposits at these localities. The metamorphic rocks occur as very large xenoliths or roof pendants in a region dominated by several phases of the Precambrian San Isabel Granite of Boyer (1962). Although sapphirine has been reported in eastern North America and as far west as Kansas, the Colorado occurrences are believed to be the first reported from the Rocky Mountains in western North America.

Copper, cobalt, and nickel in Viburnum Trend

Mapping and sampling by A. V. Heyl in the Magmont mine in the Viburnum Trend suggest that copper, cobalt, and nickel minerals are concentrated in areas of greatest solution thinning of carbonate rocks leached by heated brines of three or more successive generations. The resulting thinned zones in former limestone units, now replaced by dolomite, are characterized by breccias and inclined collapse fractures which are concentrated along and near northward and northeastward-trending strike-slip faults of relatively small displacement, especially at the intersections of these faults. The minerals (chalcopyrite, bornite, siegenite, and less common cobalt-nickel minerals) are commonly most abundant in the lower parts of the ore bodies and are concentrated in the largest solution collapse breccias along these faults.

Chemical data from the Hemlock Formation, Ned Lake quadrangle, Michigan

Chemical data obtained by M. P. Foose show the exposed portion of the Hemlock Formation in the Ned Lake 15-minute quadrangle, Michigan, to be of tholeiitic affinity. Flows exhibit a strong trend towards iron enrichment; however, volcaniclastic rocks exhibit little iron enrichment. Interlayers of sedimentary rocks within the volcanic rocks show some slightly anomalous copper values, but otherwise no significantly high metal values are observed. The intermediate composition of these volcanic rocks and their tholeiitic affinity reduce the chances that they may host stratabound sulfide deposits.

Rare-earth borosilicate in magnetite ore

In an investigation of potential byproduct or coproduct minerals in magnetite ore of the Old Bed orebody at Mineville, Essex County, New York, a light-gray to pink mineral found by Harry Klemic was identified as stillwellite (Ce, La, Ca) B SiO_5, by P. J. Loferski. This is the first known reported occurrence of stillwellite in the United States. The presence of stillwellite in association with rare-earth-bearing apatite in faulted and sheared magnetite ore indicates that boron- and silica-bearing solutions permeated the fault zones and reacted with the rare-earth-bearing apatite that is prevalent in the ore.

Geology of the Roseland district, Virginia Blue Ridge

The Roseland district of Virginia was formerly an important rutile- and ilmenite-producing area. Norman Herz and E. R. Force have found that the rutile occurs along the contact of the anorthosite pluton at Roses Mill with the granulite and charnockite, which it intrudes. The intruded granulite, a banded graphite-garnet-pyrrohotite-pyroxene gneiss, and the charnockite were deformed and metamorphosed before emplacement of the Roses Mill pluton in Grenville time. An ilmenite-apatite-rich facies of the Roses Mill pluton grades into nelsonite (ilmenite-apatite veins), and much of the Roses Mill has been altered to augen gneiss with the contained ilmenite altered to sphene. At the north end of the district, the rocks have been folded into a regional anticline with a medial syncline. Retrogression and mylonitization, predominantly Paleozoic in age, are widespread.

Factors affecting the origin of stratabound massive sulfide deposits of the Great Gossan Lead (GGL), southwestern Virginia

Field studies by J. E. Gair and J. F. Slack have identified many outcrops of banded amphibolite, interpreted to be metamorphosed mafic volcanic rock. The presence of the amphibolites along the strike of the GGL deposits suggests that volcanism took place contemporaneously with, and within at least 3 km of, the site of deposition of the GGL orebodies.

Geologic mapping by Gair and Slack, supplemented by petrographic studies by Gair, have identified the lithology of the host rocks and the post-depositional history of the ore bodies. Sulfide layers are interbedded with meta-arkose, metagraywacke, micaceous quartzite, quartz-mica-feldspar schist, and quartz-mica phyllite, locally graphitic. Sulfide and wall rock were tightly folded at the site of at least one large ore body after foliation had formed in some of the sedimentary rocks; at a nearby large ore body, sedimentary layers were broken apart into room-size blocks and smaller fragments, around which the sulfide flowed during deformation. The presence of the major ore bodies of the GGL may be a result of great thickening of originally thin sulfide layers at the sites of complex tight folding, disruption of sedimentary beds, and flowage of sulfide (now largely pyrrhotite) into spaces between and around the blocks of sedimentary rock.

Alteration associated with a fault zone in the Carolina slate belt, South Carolina

Conspicuously altered and deeply weathered Carolina slate belt rocks adjacent to a silicified and brecciated fault zone near Pageland, S.C., were studied by R. W. Luce and Henry Bell III for clues to the nature and history of widespread alteration associated with highly mineralized and ore-bearing rocks in the nearby Haile-Brewer area. Coarsely crystalline muscovite and silica metasomatism in the fault zone confirm a hydrothermal origin for at least part of the alteration. The paragenetic relations and sequence of events interpreted from the rocks in the fault zone include a period of acid leaching prior to regional metamorphism which seems to agree with other studies of altered rocks in the southeastern States reported in the literature.

Simultaneous crystallization and deformation in ophiolite complexes

The Vourinos (Greece), Troodos (Cyprus), and Canyon Mountain (Oregon) ophiolite complexes illustrate the effects of penetrative deformation at various stages in the accumulation and crystallization of peridotite and gabbro, according to T. P. Thayer. In the Vourinos Complex, only harzburgite has tectonic fabric. In the Troodos Complex, deformation increases downward from wehrlite through dunite into harzburgite. In the Canyon Mountain

Complex, the earliest identifiable deformation affected gabbro and obscured many petrologic relations between it and the earlier units; involvement of the gabbro, however, reveals large folds and faults. The presence of deformed and undeformed ultramafic dikes and pegmatites, and the absence of the early phases of deformation in gabbro in much of the complex, are interpreted as effects of intense deformation during deposition and crystallization of the lower part of a thick cumulate pile. Gabbroic augen gneiss in the Bay of Islands Complex in Newfoundland and widespread tight folding and foliation of gabbroic and ultramafic rocks together in the Zambales Complex in the Philippines are cited as additional evidence that tectonic fabrics related to hypersolidus and subsolidus deformation in ophiolitic rocks other than harzburgite are widespread.

Stratigraphic position of chromite deposits in selected ophiolite complexes

Because obviously cumulate podiform chromite deposits occur in supposedly residual harzburgite, it has been assumed that the chromite deposits were introduced into the harzburgite from the overlying olivine-rich cumulates. Two mechanisms for their introduction have been suggested, sinking of dense chromite masses or infolding.

In four ophiolite complexes, Vourinos (Greece), Troodos (Cyprus), Canyon Mountain (Oregon), and Josephine (Oregon and California), field relations are not compatible with sinking chromite bodies. First, each chromite deposit in harzburgite is surrounded by a dunite envelope. Dunite and harzburgite have about the same density (~3.3 g/cm^3). If chromite deposits will sink through harzburgite, they should also sink through their dunite envelopes. Second, many chromite deposits in these complexes are disseminated (less than 50 percent chromite) and have thick dunite envelopes. The aggregate density of the chromite and dunite is not much greater than harzburgite, so sinking would not occur.

Infolding of chromite is unlikely in three of the ophiolite complexes. For example, in Troodos, the cumulates are deformed and contain chromite, but the average composition of the chromite in the cumulates is significantly different from the chromite in the hazburgite. In Canyon Mountain, the cumulates are deformed but have no segregated chromite, so the process would have been remarkably selective, and, in Vourinos, the overlying cumulates were never folded.

Based on these observations, T. P. Thayer and B. R. Lipin conclude that chromite deposits neither sink into nor are folded in harzburgite, but rather, are indigenous to it.

MINERAL-RESOURCE INVESTIGATIONS OF WILDERNESS AREAS

The USGS and U.S. Bureau of Mines assess the mineral resource potential of areas included or considered for inclusion in the National Wilderness Preservation System.

Significant mineral potential in Elkhorn Wilderness Study Area, Montana

A mineral-assessment study shows the Elkhorn-Wilderness Study Area, about 354 km^2 just southeast of Helena, Mont., by W. R. Greenwood, S. D. Ludington, W. R. Miller, W. F. Hanna, and K. J. Wenrich-Verbeek, to be predominantly of moderate or high potential for porphyry-type copper and molybdenum deposits and precious- and base-metal deposits. The area may also have resources of uranium and thorium. This mineral assessment included chemical analysis of rocks, a detailed geochemical survey of stream sediments, a detailed aeromagnetic survey, and several aeroradiometric traverses. Three porphyry-type copper and molybdenum deposits that occur in Boulder batholith rocks on the west of the area have been explored by drilling. One of these, the Golconda, has a high potential for development. All of the Boulder batholith rocks in the study area have at least a moderate potential for porphyry deposits. The eastern part of the study area, underlain by Paleozoic and Mesozoic sedimentary rocks and Cretaceous volcanic rocks, has a moderate to high potential for precious- and base-metal vein deposits. Many such deposits have been mined from this eastern part in the past. Undeveloped extensions of known vein deposits and hidden veins are likely to be developed in the future.

Coal resources of Cranberry Wilderness Study Area, West Virginia

Reconnaissance geologic mapping and study of existing drill hole data in the Cranberry Wilderness Study Area in the Monongahela National Forest, Pocahontas and Webster Counties, West Virginia, have enabled C. R. Meissner and J. F. Windolph, Jr. (USGS), and P. C. Mory (U.S. Bureau of Mines) to calculate the coal resources (Meissner and others, 1978). About 100 million tons of prime low sulfur,

mostly low ash, bituminous coal may be present in five major and several minor beds in the study area. This coal is privately owned, although the U.S. Forest Service owns the surface rights. A geochemical survey based on stream sediment and rock samples did not find any evidence of metallic mineral resources.

Large submarginal iron resources in Virginia and West Virginia Wilderness Study Areas

Reconnaissance mapping and study of previous drilling data by F. G. Lesure (USGS) and B. B. Williams and M. L. Dunn (USBM) have resulted in the calculation of 1.75 billion metric tons of submarginal iron resources containing 250 to 350 million metric tons of iron in the Mill Creek, Peters Mountain, and Mountain Lake Wilderness Study Areas in Giles and Craig Counties, Virginia, and Monroe County, West Virginia (Lesure and others, 1978). The iron is in hematitic sandstone beds of the Rose Hill Formation of Silurian age. The iron content ranges from 10 to 30 percent and the phosphorus from 0.05 to 0.8 percent. The iron-rich sandstone beds range from 1 to 10 m in thickness and are as much as several kilometers long. They are scattered throughout an interlayered series of red and green shale and sandstone of lower iron grade that ranges in thickness from 45 to 60 m. Mining or quarrying of hematitic sandstone in areas of outcrop would be relatively inexpensive, but beneficiation methods are not yet adequate to permit economic production at existing prices.

Possible stratiform-copper occurrence in Devonian rocks in Virginia

Stream sediment and soil samples collected by F. G. Lesure and J. M. Motooka in the Ramseys Draft Wilderness Study Area, Augusta County, Virginia, suggest the presence of a low-grade stratiform copper occurrence in the Hampshire Formation of Late Devonian age. Although no mineralized rock is exposed, soil samples outline two copper-rich zones, 3 to 5 m thick, that have a grade of as much as 1,500 ppm copper. A strike length of 60 m and a down-dip dimension of 50 m are consistent with the size of mineralized area of that grade necessary to produce anomalous values of copper in the adjacent small drainage basins. Such small, low-grade stratiform deposits are not now economically important, but this is the first occurrence found in the Upper Devonian red-bed sequence south of known deposits in Pennsylvania.

GEOCHEMICAL AND GEOPHYSICAL TECHNIQUES IN RESOURCE ASSESSMENTS

GEOCHEMICAL-RECONNAISSANCE RESULTS

In the Sonoran Desert, Papago Indian Reservation, Arizona, G. A. Nowlan and W. H. Ficklin identified a cluster of water wells in the Baboquivari Mountains with molybdenum contents of 20 to 450 micrograms per liter (μg/L). Waters from the Reservation generally contain less than 10 μg/L of molybdenum. The cluster of anomalous wells occurs within a band of metavolcanic and metasedimentary rocks cutting across the mountain range and containing minor tungsten deposits.

On the Papago Indian Reservation, J. H. McCarthy, Jr., and G. A. Nowlan found anomalous amounts of copper, molybdenum, gold, silver, and several other metals in rock and stream-sediment samples. These anomalies delineated areas that have potential for new mineral deposits. Favorable geologic setting and aeromagnetic anomalies coincide with some of the indicated areas.

In the Silver City 1°×2° quadrangle, southwestern New Mexico, K. C. Watts, Jr., observed that detrital fluorite corresponded closely with many metal anomalies and, based on its distribution over known deposits, appear to reflect areas of fluorite mineralization. Ten areas containing fluorite mineralization were identified, and six of these were characterized by fluorite having violet coloration generally regarded as resulting from radiation damage. Of the six areas containing violet fluorite, uranium occurred in one, unidentified radioactive minerals were reported in another, and anomalous amounts of thorium were found in two other areas. Thus, violet-colored fluorite may be useful as a guide in locating areas of radioactive minerals.

In the Rolla 1°×2° quadrangle, Missouri, R. L. Erickson, E. L. Mosier, J. G. Viets, and S. C. King analyzed approximately 11,000 samples of whole rock and insoluble residues from 62 regionally spaced "barren" drill holes and found that the distribution of drill holes containing the highest amounts of lead, zinc, copper, nickel, cobalt, molybdenum, and silver (1) outlined known mineralized trends, (2) followed the limestone-dolomite interface in the Bonneterre Formation, (3) favored proximity to subsurface Precambrian "highs," and (4) could be projected to form an irregular band of mineralized ground encircling the St. Francois Mountains (Erickson, Mosier, and Viets, 1978). The distribution and abundance of lead and silver out-

lined best the known ore trends and appeared to be the best geochemical parameter for outlining broad target areas for exploration. The distribution and abundance of zinc, copper, nickel, and cobalt were more restricted than that of copper and lead, and the greatest amounts occurred in projections of known ore trends. These patterns suggest that the fluids that brought metal to the deposits were not of uniform composition throughout the southeast Missouri lead district.

Pyrite-marcasite concentrates from the Bonneterre Formation (principal ore host) are lead-rich, and the relative proportions of all trace metals in the concentrates are very similar to their proportions in the lead orebodies; whereas, concentrates from the underlying Lamotte Sandstone are copper rich and their zinc-nickel-cobalt contents are much higher than in Bonneterre concentrates. The relative proportions of all trace metals in the Lamotte concentrates are much different from their proportions in the lead orebodies.

These findings suggest multiple periods of movement of ore fluids in the southeast Missouri lead district. The metal-bearing fluids moving through solution channels in the Bonneterre Formation were lead rich, and those moving in the Lamotte Sandstone were copper-zinc-nickel-cobalt rich.

In the 18,000 km^2 Rolla 1°×2° quadrangle, Missouri, P. D. Proctor (University of Missouri, Rolla) found that anomalous heavy-metal contents of river waters, stream sediments, and selected aquatic plants spatially relate to present and former mining and milling areas. Nonmineralized drainage areas have lesser heavy metal contents and fewer anomalous values. In the Jack's Fork area, stream sediments from a mineralized area contained on the average 26 times more lead and 4 times more zinc than did sediments from a nonmineralized area. For these same areas, the metal content in solution in the stream waters is several orders of magnitude less than in the stream sediments. Steam algae yielded metal values similar to those of the stream sediments with which they are associated.

In the Iron River 1°×2° quadrangle, Michigan and Wisconsin, H. V. Alminas found up to 300 ppm copper in *B*-horizon soil samples and thus detected a known mineral deposit through lake-bed clays up to 60 m thick. The copper contents were enhanced by a factor of 20 by panning the heavy minerals from the soil and selectively extracting the iron- and manganese-oxide soil fractions using an oxalic acid leach.

In the Charlotte 1°×2° quadrangle, North and South Carolina, W. R. Griffitts found that heavy-mineral concentrates taken from stream beds contained substantial amounts of kyanite, rutile, staurolite, and minerals of tin and niobium, all of which had been recycled from older sedimentary formations. A little gold had apparently been recycled also.

Reconnaissance geochemical sampling by J. C. Antweiler in Central Region Wilderness Study Areas reaffirmed the importance of collecting more than one sample medium in a given area. Gold was detected in pan concentrates from the Blue Joint Wilderness Study Area, Ravalli County, Montana, but not from nearby Overwhich Creek. Fine-grained stream sediments collected at the same places had anomalous amounts of copper in the Overwhich Creek samples but not in the Blue Joint Creek samples. Using a single sample medium would have resulted in missing one of the anomalies.

Geochemical studies by H. D. King and W. D. Crim outline a number of possible new mineral occurrences in the Medfra and Lake Clark quadrangles, Alaska. Anomalously high tin, gold, and silver values in heavy-mineral concentrates delineated several previously unreported occurrences of mineralized rock in the western part of the Lake Clark quadrangle. Similarly, high copper values in heavy-mineral concentrates defined a number of new mineralized areas in the southeast and east-central parts of the Lake Clark quadrangle. Anomalous amounts of silver, arsenic, gold, bismuth, copper, lead, zinc, antimony, tin, and tungsten in heavy-mineral concentrates revealed mineralized areas in the Mystery Mountains, in the Sunshine Mountains, and in the Cloudy Mountains, all in the central and west-central part of the Medfra quadrangle.

GEOPHYSICAL EXPLORATION

A two-dimensional seismic-model study of the Patrick Draw Field, Washakie Basin, Wyoming, was conducted by R. C. Anderson and R. T. Ryder and showed that detecting the reservoir sand (Upper Cretaceous Almond Formation) with seismic data is difficult owing to acoustic contrasts and bed thickness. The likelihood that higher resolution seismic data would improve the results is not suggested by the model, and further work is required to determine what other acoustic measurements might be useful in exploring for Patrick Draw-type fields.

New data collected by R. J. Blakely at 180 gravity stations were combined with existing data to form

a suitable data base for ascertaining the deep structure of the Kalmiopsis Wilderness Area, Oregon, including the Josephine Periodotite body. This peridotite unit is massive and is in contact at its western edge with less dense rocks such as graywackes and volcanic rocks. The simple Bouguer anomaly showed little or no correlation with this western contact, which suggests that this part of the Josephine Peridotite is thin in vertical extent. This configuration supports geologic observations that this peridotite body was emplaced as a tectonic slice rather than as an intrusion.

LEAD ISOTOPES APPLIED TO MINERAL EXPLORATION

An assessment was made by B. R. Doe of the use of lead isotopes in mineral prospect evaluation of Cretaceous and Tertiary magmatothermal ore deposits in Arizona, Colorado, New Mexico, Utah, and a few selected examples from Idaho and Montana. Samples analyzed from all of the multi-billion dollar copper and molybdenum mines have values of $^{206}Pb/^{204}Pb$ less than 18.

Many of the largest lead-zinc-silver skarn-type deposits have $^{206}Pb/^{204}Pb$ values up to 18.6. The largest districts, with $^{206}Pb/^{204}Pb$ values between 18.6 and 19.1, have production in the range of $100-$200 million. No district is known to have a production approaching $100 million and a $^{206}Pb/^{204}Pb$ value greater than 19. The apparent correlation between maximum size of a deposit and the lead isotopic composition is of value in prospect evaluation. This measurement requires only one sample per prospect because the lead isotope composition is generally uniform within an individual deposit.

VOLATILE GASES USEFUL IN GEOCHEMICAL EXPLORATION

Using mass spectrometry and gas chromatography, M. E. Hinkle analyzed soil gases collected from the Long Valley geothermal area of California and from two areas of sulfide mineralization in Pinal County, Arizona. Anomalously high concentrations of helium coincided with known faults in the Long Valley area, and above-average amounts of sulfur compounds were detected over the Vekol copper deposit, southwest of Casa Grande, Ariz.

BIOGEOCHEMICAL INVESTIGATIONS

In culture experiments conducted during the summer of 1978, J. R. Watterson found that pigmented bacteria showed extreme sensitivity to environmental factors including temperature, pH, and metal concentrations. Specifically, chromobacterium violaceum produced a yellowish, diffusing pigment in the presence of 10 micrograms of molybdenum per gram of standard nutritive medium.

BOTANICAL INVESTIGATIONS

In several areas in central Montana, D. J. Grimes found *Eriogonum ovalifolium* growing over copper deposits and a high correlation between the distribution of this plant species and the copper content of the soil. Colonies of *Eriogonum ovalifolium* were associated with anomalous amounts of copper in soil overlying Precambrian sedimentary units, mafic sills, aplite dikes, quartz-calcite veins, and quartz monzonite porphyry intrusives. The distinctive foliage and growth habit of *Eriogonum ovalifolium* make it a potentially useful indicator plant for detecting copper deposits.

ANALYTICAL METHODOLOGY USEFUL IN GEOCHEMICAL EXPLORATION

Using ferric chloride and ammonium pyrrolidine dithiocarbamate as coprecipitants, A. E. Hubert and T. T. Chao determined parts-per-billion amounts of copper, lead, zinc, cobalt, nickel, cadmium, molybdenum, and uranium in a single natural water sample. The precipitated metals were deposited on a membrane filter for direct analysis by X-ray fluorescence.

Manganese in geological samples at concentrations above the crustal abundance interferes with the atomic absorption determination of cobalt, nickel, and copper in methods using sodium diethyldithiocarbamate chelation and solvent extraction. R. F. Sanzolone and T. T. Chao found that the interference disappeared completely when the extracted carbamates were allowed to stand for 24 hours. By setting aside sample solutions for 24 hours after the initial extraction, R. F. Sanzolone, T .T. Chao, and G. L. Crenshaw determined trace amounts of cobalt, nickel, and copper in a variety of geological materials, including iron- and manganese-rich samples and calcium-rich samples. As much as 50 percent Fe, 25 percent Mn or Ca, 20 percent Al, and 10 percent Na, K, or Mg in a given sample, present either individually or in various combinations, did not interfere with the determination of trace amounts of the other metals.

RESOURCE INFORMATION SYSTEMS AND ANALYSIS

RESOURCE INFORMATION SYSTEMS

Computerized Resources Information Bank

The number of records in the Computerized Resources Information Bank (CRIB) master file decreased to 45,243 during 1978, while the quality of records was increased as a result of intensive editing. Approximately 2,000 new records were received during the year.

Co-op arrangements continue with the Bureau of Land Management, the Forest Service, West Germany, the State Department, and South Dakota. Earlier co-ops were completed with useful results with Idaho, Montana, and Minnesota. Additional requests for CRIB co-ops have been received from Oregon and Nevada, and the agreement with the Tennessee Valley Authority was terminated.

In-house (USGS) CRIB participation increased markedly during 1978, mainly as a result of the CUSMAP and USGS statewide inventory programs; the latter now includes California, Oregon, Nevada, and Arizona.

Lead-zinc deposits of the world were studied by P. G. Schruben, and nickel-cobalt deposits of the world were studied by G. L. Shaffer using CRIB data. CRIB data also were used as contributory source material for four of the seven metal models used in the study of the mineral resource potential of Alaska by D. A. Singer. M. G. Johnson created a dynamic CRIB working file to study geologic-metallogenic correlations and relationships and to generate overlay maps showing these relations in space.

A Mineral Data System (MDS) Advisory Committee was established in September 1978 to foster ideas, methods, and support relating to CRIB. This committee, under the direction of J. A. Calkins, includes subcommittees for data validation and standards, applications, and information sources.

Geothermal resources file

GEOTHERM, the geothermal resources file, developed by J. A. Swanson, is a fully operational data base on geothermal resources, divided into three subfiles: geothermal fields, wells, and chemical analyses of geothermal waters. The file was used extensively in the USGS 1978 assessment of geothermal resources of the United States and for geothermometer calculations, stored heat and reservoir volume determinations map plots, and data display and publication. Presently, the file contains over 500 field records, 500 well records, and more than 4,000 chemical analyses records of warm-water wells and springs in the United States.

National Coal Resources Data System, Phase II

Phase II software is comprised of a set of interactive computer programs, developed by A. C. Olson, to aid the commodity geologist when dealing with irregularly spaced point-located field data, in analyzing, evaluating, and mapping resources. The data are processed by the program to produce structure, coal thickness, overburden, overburden-to-thickness ratio, and resource maps, as well as tables of resource tonnages in each reliability category.

Outcrop and political boundaries may be entered into the data set by means of the digitizer. Thickness, overburden, or chemical concentration boundaries may be generated by the software, in addition to combinations of different types of boundary conditions for constraining the resource computations. Resource maps are based on standard reliability-category distances from the point of field observations. Volume and tonnage values may be computed for each reliability category and for each set of boundary constraints.

All calculations and map displays can be done on an interactive graphics terminal. An option is provided for the creation of a plot tape to drive the offline plotter.

RESOURCE ANALYSIS

PROSPECTOR computer consultant

Based upon recent developments and testing, the PROSPECTOR rule-based computer consultant for mineral exploration shows great promise as a useful tool not only in mineral exploration but also in teaching and resource assessment. This method, developed by SRI International with J. M. Botbol as project monitor, depends upon a prior establishment of a set of rules that are used as a knowledge base. PROSPECTOR consists of a conversational dialogue between a geologist and the computer, and, from information provided by the geologist, PROSPECTOR computes degrees of similarity of the geologist's subject area with models included in the knowledge base. To establish each model, someone must quantify a consistent taxonomy that includes specification of occurrence, prior probabilities, and the probability that a given relation is of value if present and damaging if not present. In scope, the construction of a model is tantamount to writing a

professional paper but has the additional constraint of taxonomic quantification. In addition, the model is then immediately computer usable by a broad spectrum of users. The models can then be applied as teaching aids to students and project geologists who might be unfamiliar with the deposit types relevant to a given area. As information in a subject area is acquired, PROSPECTOR can be used to optimize the data-gathering program and quantify the components of the cost-benefit analysis that supports the program. With respect to resource appraisal, the procedure can be iterated for attributes of a group of areas (or cells within one area or both) resulting in specification of those areas with high resource potential.

Uranium resource appraisal and decision modeling

Decision modeling, formerly known as characteristic analysis, was developed by J. M. Botbol, R. W. Bowan, and R. B. McCammon (USGS) and Richard Sinding-Larsen (Norwegian Geological Survey) to create, to test, and to evaluate exploration and resource models based on geoscience data collected over large geographic areas. A computer program has been written that uses built-in tutorials to instruct the user at each stage of analysis. The user can save a model or a model component, for example, a region, cell, or a geologic variable, for later use, and a graphic overlay that might be displayed. Compound variable construction provides the capability to generate new variables as functions of existing variables. This is particularly useful in the designation of alteration and zoning patterns of orebodies. A unique feature of decision modeling is the ability to express the conditions necessary for an orebody in terms of mathematical logic. The statements for the necessary conditions are implemented on the computer as a logic circuit. For a given resource area, decision modeling can be used to estimate the favorability of occurrence of a particular deposit model. A resource estimate is then obtained by combining the probability of occurrence for different deposit models with their associated grade and tonnage characteristics.

Mineral resource assessment

An approach developed by W. D. Menzie II to assessing the mineral resources of a region is to (1) delineate areas permissive for the occurrence of deposits by type, (2) estimate relevant characteristics, such as grade and tonnage or contained metal, of each deposit type, and (3) estimate the number of deposits of each type that are likely to occur within the region (Singer, 1975). This approach was used to perform an assessment of the metalliferous mineral resources of central Alaska, at 1:1,000,000 scale (Eberlein and Menzie, 1978). For the regional assessment of Alaska's mineral resources, models of grades and tonnages, or contained metal, were built for 10 deposit types (Singer and others, 1978).

Models of grade and tonnage play an important role in this approach to mineral assessment; therefore, it is important to understand factors that relate to the variability and distribution of grade and tonnage. Regional variability in grades and tonnages, such as that demonstrated for nickel sulfide deposits associated with komatiitic rocks by M. P. Foose, W. D. Menzie II, D. A. Singer, and J. T. Hanley, is one such factor. Another factor that may influence the distribution of grades and tonnages is size-biased sampling. A preliminary method has been derived for removing the effects of size-biased sampling of podiform chromite deposits by W. D. Menzie II and D. A. Singer.

Observed frequency distributions of average grade, tonnage, and, in some cases, contained metal were found by D. A. Singer to be adequately represented by lognormal distributions for the following deposit types: porphyry copper, porphyry molybdenum, skarn copper, mafic volcanogenic sulfide, felsic and intermediate volcanogenic sulfide, nickel and copper sulfides associated with intrusive rocks, skarn tungsten, podiform chromite, mercury, and vein gold. For many of these deposit types, grades were found to be independent of tonnages (Singer, 1978). The grade-tonnage models represented by these frequency distributions combined with probabilistic estimates of the number of deposits by type and by tract were used in the mineral resource assessment of southern Alaska (MacKevett, Singer, and Holloway, 1978).

Copper-aluminum substitution model

A joint copper-aluminum model has been developed by M. S. Hamilton to assess the impact of higher energy prices and the depletion of high-quality ore deposits on copper and aluminum industry costs, substitution, and recycling potential. The estimates of the long-run supply elasticity for U.S. copper obtained in this study are considerably less than those computed by others in earlier years, indicating that large price increases are needed to increase domestic primary copper production substantially. Even the most pessimistic assumptions about bauxite producer-country royalty increases

have been found to have less impact on aluminum industry costs than substantial growth in energy prices (at 1974–77 rates). The incentive that higher energy prices give to increased recycling of aluminum has been found to be very substantial, but copper scrap reclamation was found to be little affected by such price increases.

Petroleum resource analysis

L. J. Drew determined that no major methodological barrier existed to expanding his discovery-process model, which is based on the area-of-influence concept, from two to three dimensions. The three-dimensional model was tested in the Midland Basin. The Arps Roberts discovery-process model, which was initially tested and found to produce very good predictions of future oil discovery in the Denver Basin, was modified for use in the far more geologically complex Permian Basin. With the modified model, predictions were made of the number and sizes of petroleum deposits remaining to be discovered in that basin and the rate at which they would be discovered in the future.

Major problems introduced into the exploration process in the Gulf of Mexico as a result of leasing procedures were resolved by modifying the discovery-process model to a form which produces a reasonable forecast of future discoveries from highly discontinuous data.

No evidence was found to indicate improvement in exploration efficiency either by vertical divestiture or by reducing major firms to regional units. The major conclusion of the Permian Basin study is that even if the price of oil should rise to $40 per barrel, or natural gas to $7.59 per MCF, the estimated potential reserves accruing from future discoveries represent little more than 3 years supply at the 1974 rate of production.

Revised calculations and recent data compiled by D. H. Root and E. D. Attanasi indicate that, in the non-Communist world outside the United States and Canada, the average quantity of crude oil discovered per exploratory well between 1970 and 1975 was 43 percent of the 1950–55 discovery rate instead of 56 percent, as earlier data indicated. Studies of the growth of oil and gas fields in the lower 48 States by D. H. Root showed that the growth which can be expected from oil and gas fields discovered before December 31, 1975, is less than 13 billion barrels of oil and 120 trillion cubic feet of natural gas.

Remote-access error-free computer timesharing

Two serious problems in computer timesharing were overcome through research by J. M. Botbol. These problems involve the frequent situation of being unable to gain telephone access to a computer from a remote location, such as in another country, and the general condition of telephone-line noise causing data-transmission errors. The problem of telephone access was solved by devising a means for the computer to call the terminal; the noise problem was solved by use of error-correction devices connected to a terminal and the computer to permit automatic retransmit queueing. As greater dependence on computer data storage and retrieval capabilities develops, the need for error-free and timely computer access becomes more critical. Thus, the results of the present work have far-reaching influence on the deployment of remote computer terminals and on the scope of collaborative efforts abroad. Given that a timeshare link is timely and reliable, future support commitments can be more accurately specified. This would be of immediate value in global mineral resource intelligence efforts and would serve to justify computer support services, personnel, and programs.

CHEMICAL RESOURCES

LITHIUM INVESTIGATIONS IN SEDIMENTARY AND VOLCANIC ROCKS

Origin of commercial lithium brines

Investigations of the chemistry and mineralogy of sediment and brine samples from bore holes in the Clayton Valley, Nevada, lithium brine field, by J. D. Vine, H. D. Downey, and A. R. Wanek, together with stratigraphic and geomorphic studies by J. R. Davis, provide additional evidence for the origin of this deposit. Previous studies show that the occurrence of lithium in amounts greater than a few parts per million is characteristic of evaporative concentration of water, while lithium-chlorine ratios >0.005 are characterisic of geothermal waters that have leached lithium from volcanic source rocks. The commercial lithium brine at Clayton Valley contains as much as several hundred ppm Li, but typical lithium-chlorine ratios of 0.002–0.003 are somewhat below that of geothermal springs that could have supplied the lithium. A reduction in the lithium-chlorine ratio could be explained if there was a transfer of lithium from brine to the sediments. Using the equilibrium constant for hectorite, $Na_{0.33}(Mg,Li)_3Si_4O_{10}(F,OH)_2$, recently calculated by W. E. Dibble, Jr., of Stanford University (written commun., Dec. 1978), the brine was found to be supersaturated with respect to this lithium clay.

This is regarded as evidence of the authigenic formation of hectorite in the clay fraction of Clayton Valley sediments that contain as much as 1,500 ppm Li. Brines with similar chemical characteristics occur in salars in the Andes of South America. Salar de Atacama, Chile, is currently under development (Comer, 1978), and salars in Bolivia show significant promise (Erickson, Vine, and Ballón, 1978). The volcanic setting of these deposits and the association between lithium and geothermal waters in the region are the subject of continued studies by J. R. Davis, R. L. Smith, S. L. Rettig, and K. A. Howard. The potentially large resources of lithium in brines provide assurance that there will be enough lithium for batteries for electric vehicles and for storage of off-peak power for utility nets.

Origin and distribution of lithium-rich clay deposits

The lithium clay mineral, hectorite, occurs in saline lake sediments where it may precipitate directly from waters containing high concentrations of SiO_2, Mg, F, and Li, or it may form by the alteration of volcanic sediments by reaction with alkaline saline waters. Hectorite comparable to that from the type locality in the Mojave Desert has been recognized in a number of nonmarine Tertiary rock units in the Basin and Range province. In the Lake Mead area, Nevada, exposures of the Horse Spring Formation of Oligocene and Miocene age at Lava Butte, Lovell Wash, White Basin, and Virgin Basin contain authigenic hectorite associated with dolomite, celestite, halite, and cristobalite, according to E. F. Brenner-Tourtelot and R. K. Glanzman (1978). Some of these deposits are closely associated with travertine spring mounds and stromatolitic algal structures interbedded with altered volcanic ash beds indicative of a shallow-water environment of deposition in saline waters and a possibility that some of the elements were introduced by thermal spring waters.

Clays similar to those described above have been identified in Tertiary lacustrine deposits in the Date Creek Basin near Wickenburg, Ariz., the Rio Grande rift zone near Socorro, N. Mex. (Brenner-Tourtelot and Machette, in press), a basin of unknown extent near Lincoln, Mont. (Brenner-Tourtelot, Meier, and Curtis, 1978), and in the moat-fill sediments of the McDermitt caldera complex near McDermitt, Nev. (Glanzman, Rytuba, and McCarthy, 1978). Lithium-enriched clays as much as 40 m thick occur in altered volcaniclastic sediments that are exposed for about 45 km along an arcuate belt of outcrop on the north and west sides of the McDermitt caldera, according to Glanzman and Rytuba (1978). Clays on the northern side of the caldera complex contain as much as 0.4 percent Li and resemble hectorite in their physical properties, whereas those on the west side of the complex contain as much as 0.7 percent Li and have different physical properties. Like hectorite, this previously unknown lithium clay mineral is dominantly a trioctahedral smectite. But unlike hectorite, the clay mineral contains significant amounts of aluminum and iron but little fluorine in the structure, and it does not disperse in water. Extraction tests by the U.S. Bureau of Mines confirm the different physical and chemical properties of the two clay minerals and indicate the feasibility of lithium recovery from both, according to D. C. Seidel (written commun., Dec. 1978).

While the high-alumina flint clays, such as those described from Missouri, Kentucky, and Pennsylvania by Tourtelot and Brenner-Tourtelot (1978), are known to contain as much as 0.5 percent Li, their distribution is unknown. Until more is known about their pattern of distribution, it is not possible to suggest how to search for commercial-size deposits.

Association of lithium with uranium

Lithium clays are associated with uranium deposits or occurrences at a number of localities in the western United States according to R. K. Glanzman and J. K. Otton (1979). Not only do lithium and uranium occur in the same sequence of mineralized rocks, but they may also be associated with mercury, beryllium, fluorine, or boron deposits in such different areas as the McDermitt caldera complex, Nevada and Oregon, the Spor Mountain district, Utah, the Date Creek Basin, Arizona, the Kramer Borate district, California, and the Henry Mountains district, Utah. The frequency of the association indicates that lithium-bearing ground waters might provide a useful hydrogeochemical method of searching for uranium deposits.

Autoradiographic method of lithium determination

Neutron-induced reactions in the lighter elements produce particles that can be recorded by a radioluxograph. J. R. Dooley, Jr., has successfully adapted this method to the preparation of an autoradiographic representation of the lithium distribution in a polished surface of spodumene-bearing pegmatite from Kings Mountain, North Carolina, using reactor-produced neutrons. This neutron induced radioluxograph (fig. 1) shows the lithium-bearing minerals in a manner analogous to the autoradiographs produced by natural radioactive

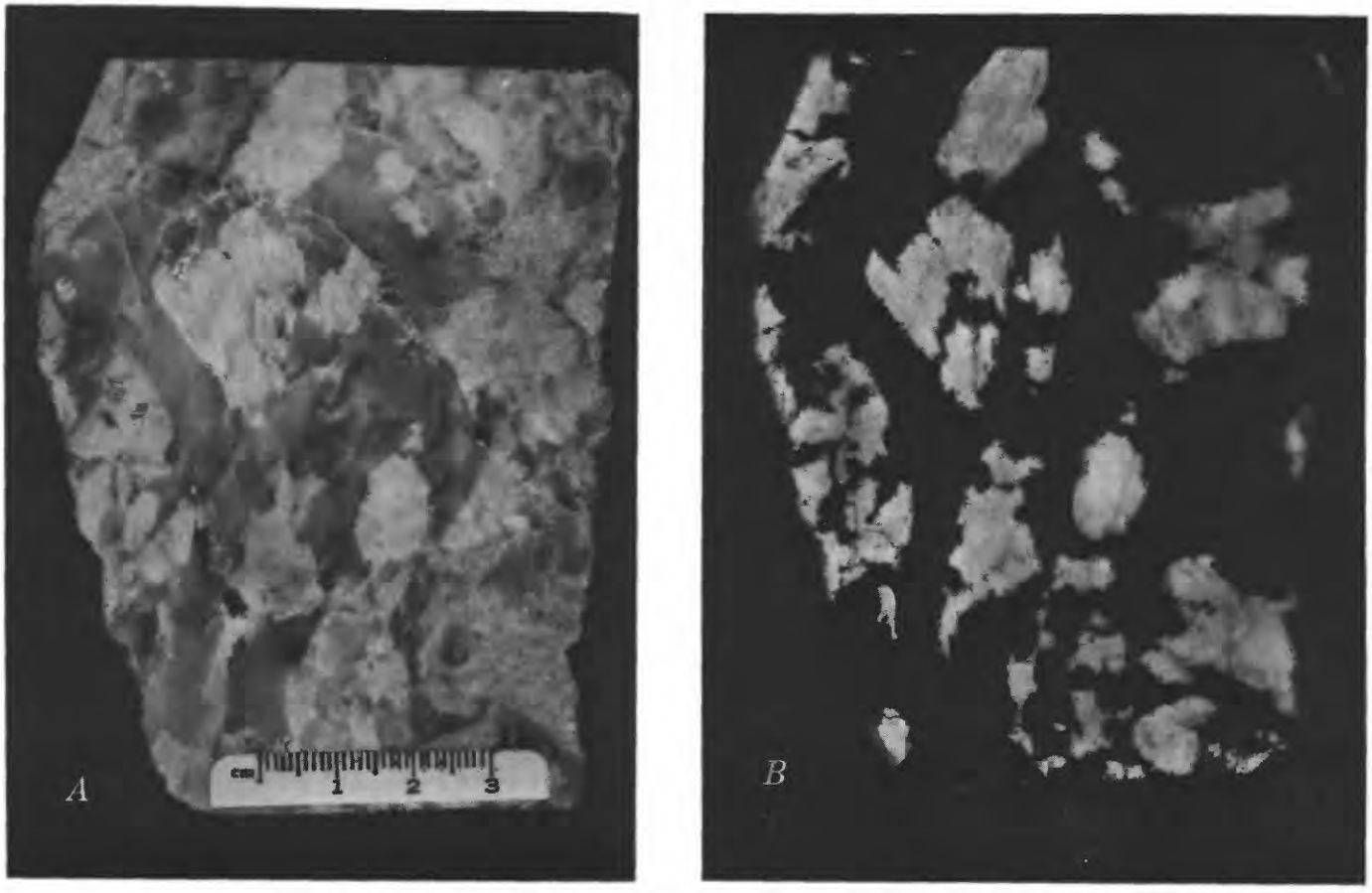

FIGURE 1.—Lithium distribution illustrated by a neutron-induced radioluxograph. *A*.—Photograph of polished surface of spodumene-bearing pegmatite. *B*.—Autoradiograph of *A* showing lithium-bearing spodumene in white as a photographic positive.

decay in uranium and thorium minerals. The positive print reproduced here shows the distribution of lithium minerals autoradiographically from the $^{6}Li(n,\alpha)\ ^{3}H$ nuclear reaction.

PHOSPHATE INVESTIGATION

Known extent of California phosphate deposit enlarged

The Cuyama Valley phosphate deposit is located along the southern edge of the Cuyama Valley in the foothills of the Sierra Madre Mountains that are a part of the Coast Ranges in Santa Barbara County, California. The phosphate-bearing rocks are in the Santa Margarita Formation, a marine unit of middle and late Miocene age, which ranges from 300 to 600 m thick in this area and is subdivided into two sandstone and two phosphatic mudstone members. The phosphatic members are brown to gray, weathering, laminated to medium-thick beds of phosphate, phosphatic mudstone, claystone, siltstone, and fine-grained sandstone. The beds of phosphate vary from nodular and size-graded pelletic to massively distributed fine-grained phosphate. The Santa Margarita Formation has been folded into northwest-trending anticlines and synclines by compression from the southwest. Throughout much of the area, formational attitudes are near vertical or overturned. The area is cut by northwest-trending faults parallel to the axes of the folds and by faults that cut obliquely across the limbs of folds. Geologic mapping, trenching, and sampling by A. E. Roberts extended the previous areal limits of the Cuyama Valley phosphate deposits from about 15 km^2 to nearly 40 km^2.

Florida phosphate resources enlarged by drilling

Drilling in eastern and southern Florida (DeSoto, Brevard, Clay, and Baker Counties) during 1978 indicates that phosphate resources are very large, aggregating billions of tons of material that can be recovered by using only minor modification of present mining and processing methods. According to J. B. Cathcart, phosphate thus recovered will be more costly and environmental problems may arise,

but resources here should be sufficient for many years into the future.

NOVACULITE IN NEVADA

The Arkansas Novaculite of Arkansas and Oklahoma and the Caballos Novaculite of Texas are well-known Paleozoic siliceous rock formations. In comparison with ordinary bedded chert, they are relatively thick bedded, coarse grained, and composed of pure intergranular quartz. K. B. Ketner reports the existence of a new novaculite locality among the Paleozoic eugeosynclinal rocks of northern Nevada. The Nevada novaculite strongly resembles petrographically both previously known novaculites. Like the Caballos, the Nevada novaculite lies concordantly on Upper Ordovician bedded chert. It is overlain by Middle Silurian sandstone.

MINERAL-FUEL INVESTIGATIONS

COAL ANALYSIS

The Coal Resources Investigations Program of the Geologic Division classifies the Nation's remaining coal resources into various categories based on geographic and geological distribution, physical and chemical characteristics, and recoverability. As part of this effort, personnel of the Division in 1978 mapped and assessed 4,200 km^2 of coal-bearing land in Colorado, Montana, New Mexico, Utah, Virginia, and Wyoming, and geologic sections were measured in the Crow Indian Reservation in Montana and the Wind River Indian Reservation in Wyoming. About 26,000 m of drilling was completed in the western coal basins to assess the quantity and quality of buried coal and to provide stratigraphic information. More than 1,000 channel and bench samples of coal were collected for chemical analysis from 20 States, in cooperation with 15 State geological surveys, the Conservation Division, the Bureau of Land Management, and the U.S. Bureau of Mines.

Computerization of the Nation's coal resources

About 7,000 records of coal resources and chemical analyses were added to the National Coal Resources Data System (NCRDS), bringing the total to nearly 93,000. The data base currently includes 31,000 coal resource tonnage records and 53,000 U.S. Bureau of Mines proximate and ultimate coal analyses, nearly all reported by coal bed and by location in counties and States. The NCRDS also contains 9,000 geodetically located drill-core records and chemical analyses, the latter including proximate, ultimate, major-, minor-, and trace-element constituents.

The NCRDS now has cooperative arrangements with eight State geological surveys for collection, correlation, transmission, entry, retrieval, manipulation, and display of drill hole, chemical analyses, and other relevant coal-resource-related data.

A basic computer program was developed by A. C. Olson to calculate coal resources from point-located information. Testing with actual data from selected areas in Colorado, Virginia, and Wyoming resulted in differences ranging from 1 to 15 percent between the machine and standard manual calculations; the variations appear to be largely dependent on the amount and distribution of data and the distances from point sources.

Participation in the interagency EMRIA program

The USGS is providing geological support to the Energy Minerals Rehabilitation Inventory and Analysis Program (EMRIA) of the Bureau of Land Management (BLM) by selecting representative reclamation study sites within several coal basins. USGS personnel obtain and examine samples of coal and other sedimentary rocks from cores drilled by BLM contractors and appraise coal quantity and quality, evaluate reclamation potential, and predict possible mining and environmental hazards. Studies were completed in 1978 in the following reclamation study areas: White Tail Butte, Campbell County, Wyoming; Hanging Woman, Big Horn County, Montana; Fish Creek, Routt County, Colorado; Pumpkin Creek, Powder River County, Montana; Kimbeto, San Juan County, New Mexico; and Bisti West, San Juan County, New Mexico.

FIELD STUDIES

Coal maps, 1:100,000 scale

The first of the new intermediate-scale coal maps (1:100,000 scale) were published in 1978, depicting structure contours and isopachs of coal, as well as isopachs of overburden, in the western half of the Recluse quadrangle, Campbell County, Wyoming (B. H. Kent and B. E. Munson, 1978 a,b); the area lies on the east flank of the Powder River basin. Of the total area under study (4,500 km^2) 2,800 km^2 are underlain by the Canyon coal bed and several associated splits and also by separately recognized coal beds. The authors estimated the coal resources in the Canyon coal and associated splits to be 25 billion t. The resources in the overlying and underlying coal beds were not estimated.

The Paleocene coal beds of the Recluse quadrangle appear to have been deposited in a geologically

unstable area that was the site of repeated temporally and spacially interconnected peat swamps. Each succeeding swamp covered somewhat a different part of the unstable area and was successively buried by random incursions of sediments that accumulated with erratic thicknesses. As a result, different parts of the mapped area, containing from one to four coal beds, posed problems in designing structure-contour and coal-isopach maps depicting such stratigraphic complications. Kent and Munson, therefore, divided the coal-bearing area into seven segments and compiled for each segment, (1) a structure map of the top of the coal-bearing zone, (2) a structure contour map of the base of the zone, and (3) a coal isopach map showing total coal thickness, disregarding intervening rock intervals. The resulting three maps, together with the isopach map of overburden, provide all pertinent geological information needed for industrial appraisal of coal resources in any given tract.

Coal beds in deltaic paleoenvironments

San Juan Basin, New Mexico.—The Upper Cretaceous sequence in the southwestern part of the San Juan Basin, New Mexico, consists from the base up of the Pictured Cliffs Sandstone, the coal-bearing Fruitland Formation, and the Kirtland Shale. Measurement of 200 new stratigraphic sections by R. M. Flores and mapping and study of new drilling by J. W. Mytton have led to reinterpretation of the stratigraphic development of these units. The Pictured Cliffs Sandstone, consisting of distributary-channel, delta-front, and beach-barrier lithofacies, appears to have accumulated on a prograding delta rather than, as formerly thought, in a beach-littoral zone. All evidence indicates that, as the delta continued to prograde during deposition of the Fruitland Formation, vegetative material accumulated in deltaic and back-barrier lagoonal swamps and was later converted to peat and coal. Coal derived from swamps in the deltaic environment is thick (1.2 m), laterally discontinuous, and cut by channel sandstones, whereas coal derived from back-barrier swamps is thin (0.45 m), laterally extensive, and contains abundant carbonaceous shale interbeds; all data indicate that the deltaic coals would be more suitable for economic development. The contact between the Fruitland and the overlying Kirtland was arbitrarily placed at the top of the highest coal zone containing prominent clinker. The Kirtland Shale contains only thin coal beds and is free of clinker.

Emery and Wasatch Plateau Basins, Utah.—Strata of the Ferron Sandstone Member of the Mancos Shale (upper Turonian Upper Cretaceous) in southern Castle Valley, Utah, accumulated in eastward-building deltas that existed along the western margin of the interior seaway. T. A. Ryer and J. D. Sanchez found a clear genetic relationship between the major coal beds and several cycles of delta progradation and destruction in the Ferron Sandstone Member. The thickest part of each major coal bed appears to lie just west of the landward pinchout of an associated delta-front sandstone body. This relation should prove useful in guiding coal exploration in other areas with similar depositional settings. J. M. Flores reported a similar setting in the nearby Wasatch Plateau coal basin where thick coal beds lie in the Blackhawk Formation, intertonguing on the landward side with the delta-front Star Point Sandstone.

Hams Fork Basin, Wyoming.—The Lazeart Sandstone, lowermost member of the coal-bearing Adaville Formation in the Hams Fork Basin of western Wyoming, was found by J. W. M'Gonigle to have prograded intermittently seaward and to rise stratigraphically toward the south. The overlying strata of the Adaville Formation record an upward transition from a lower delta plain to an upper delta plain. The Lazeart Sandstone Member contains coal beds 10 m thick and, in places, 30 m thick; whereas, the lower delta-plain sequence contains coal beds 2 m thick, and the upper delta-plain sequence contains coal beds from 4 to 6 m thick.

Rank and methane content of western coals

V. L. Freeman found that deeply buried coals in the Piceance Basin, Colorado, range in rank from high-volatile *B* bituminous to semianthracite. Some high-volatile *A* and medium-volatile bituminous coal may be of coking quality and suitable for use in the steel industry. Although not minable at present because of their depth of burial, coals of similar rank coking quality are being mined at equal or greater depths in western Europe.

As reported by Walter Danilchik, drilling in the Raton Mesa Basin, Colorado and New Mexico, has disclosed a large potential resource of methane in coal beds at depths between 450 and 600 m.

Estimates of coal resources

Southwestern Virginia.—C. R. Meissner and K. J. Englund, in mapping the geology and calculating the coal resources of the Honaker and Jewell Ridge quadrangles in southwestern Virginia, used newly available subsurface data and estimated the original

coal resources in 30 beds to be about 2 billion t, of which 150 million t have been mined. The remaining resources in these quadrangles average about 6 million t/km². Resources in the same area had been estimated previously by Brown and others (1952) to average 2.7 million t/km².

Douglas Creek arch area, Colorado.—Detailed geologic mapping by B. E. Barnum demonstrated that significant coal resources underlie the south-central Douglas Creek arch (T. 2 and T. 3 S., R. 101 and R. 102 W.) of northwestern Colorado. The coal is in intensely faulted rocks of the Mesaverde Group (Upper Cretaceous), occupying a stratigraphic interval from about 250 to 350 m above the Buck Tongue of the Mancos Shale. The coal-bearing unit contains a minimum of one discontinuous coal bed more than 1 m thick, and other beds locally are as much as 5 m thick. Most outcrops of thicker coal beds are burned, complicating stratigraphic interpretations. A similar unit of discontinuous coal beds crops out more than 30 km to the north, near Rangley; it can be correlated stratigraphically with the sequence in the Douglas Creek arch.

Weston SW quadrangle, Wyoming.—Robert Katock mapped the Weston SW quadrangle, Campbell County, Wyoming, an area underlain by two near-surface coal beds. The upper bed, cropping out in several hills in the southwestern part of the quadrangle, is at least 4.5 m thick, is overlain by as much as 30 m of overburden, and is estimated to contain resources of 14 million t. Except in the little Powder River and adjacent valleys, the lower bed generally is 1.5 m thick but in places is 3.6 m thick, and it is overlain by 100 to 200 m of overburden. Measured, indicated, and inferred resources of coal in the lower bed are estimated to be about 210 million t.

Gulf coast lignite.—Reserve estimates of gulf coast lignite as revealed in recent literature increased from 12 billion t in 1974 to 22 billion t in 1978, and current lignite resources, cited in the same sources, are estimated to be 100 billion t. According to J. E. Johnston, these revised estimates resulted from accelerated geologic mapping and in acquisition of subsurface data by State geological surveys and by private companies.

DATING, GEOCHEMISTRY, AND PETROLOGY OF PEAT, LIGNITE, AND COAL

Age of Everglades peat

By applying carbon-14 dating to cores from a stratigraphically controlled cross section of the south-central Everglades, Florida, Z. S. Altschuler and associates found that Holocene deposition began 5,500 years B.P. with a thin layer of fresh-water limestone. By 5,000 years B.P., sufficient plant cover had been established to permit accumulation of peat. The 1 m-thick Holocene deposits consist of two such cycles of fresh-water limestone succeeded by peat. Carbon-14 dating of the contact zones shows that peat accumulated at a rate of 2.65 cm/100 yr. This peat generally contains about 85 percent moisture; on a moisture-free basis, it has a fixed carbon content of 60 percent and a heat value of 22,100 to 23,300 J/g (9,500 to 10,000 Btu/lb).

Contaminants in coal

Detailed mapping and chemical analysis of the Upper Freeport coal bed in the mines of the Homer City area of Pennsylvania, under the direction of C. B. Cecil, indicates that the major, minor, and trace elements in the mineral matter of the coal are dominantly of plant origin. Calcite and pyrite are of chemical and of biochemical origin and quantitatively were controlled by the pH and Eh ambients in the Pennsylvanian swamps. Interpretation of geochemical analyses indicates that highly acidic fresh-water paleoenvironments in parts of the central Appalachian Basin resulted in accumulation of low-ash- and low-sulfur-bearing swamp vegetation that was later converted to coal, whereas slightly acidic to neutral pH paleoenvironments resulted in the accumulation of high-ash- and high-sulfur-bearing swamp vegetation, also later converted to coal.

Petrology of the Upper Freeport coal bed, Indiana County, Pennsylvania

E. C. T. Chao, J. A. Minkin, and C. L. Thompson conducted a detailed study on a 118-cm columnar sample collected from the Upper Freeport coal bed in the Helen Mine in Homer City, Pa. Petrographic analyses indicated that the bed consists of five major lithologic coal types. A carbonaceous shale parting, 85 to 92.5 cm below the top of the columnar sample, contains bands of vitrinite. Using an electron microprobe, Minkin, Chao, and Thompson (1979) found that kaolinite apparently is the dominant clay in the upper 50 cm of the sample; whereas, illite seems to be the dominant clay between the 50-cm level and the underlying shale parting. Illite, kaolinite, and mixed-layer clays occur in approximately equal proportions in the coal lying between the shale parting and the base of the coal bed.

Electron microprobe analyses also indicated that sulfur and chlorine are organically associated in

this coal sample. The organic sulfur content tends to be higher in the coal below the shale parting, whereas the chlorine content tends to be higher in the coal above the parting. The sulfur content in inertinite is about half that in vitrinite, and the sulfur content in exinite is about equal to that in vitrinite.

R. B. Finkelman, Minkin, and Thompson also used the electron microprobe to search for arsenic in the upper 43 cm of the columnar sample. A probe analysis of hundreds of pyrite grains in polished blocks indicated that arsenic is irregularly distributed within that zone and within individual pyrite grains. It was found that arsenic occurs only in pyrite grains lying in fractured coal, although not all such grains contain arsenic. The arsenic is concentrated in the outer rims of the pyrite grains or along microfractures within the grains; unfractured grains do not contain detectable amounts of the element (0.01 weight percent). Emplacement of arsenic apparently resulted from reactions between previously deposited pyrite and arsenic-bearing solutions.

Sphalerite in Interior Basin coals

J. C. Cobb (Illinois Geological Survey) examined sphalerite fracture fillings collected from 20 coal beds in four of the Interior province States. Microscopic examination of thin sections of sphalerite-bearing coal established that most fracture fillings consist of three-growth bands; the first formed and most characteristic is colorless sphalerite containing parallel, closely spaced purple lamellae. The second band is light yellow but in places contains lamellae differing slightly in color. The third band is orange iron-rich sphalerite. The recognition of widespread banded fracture fillings of sphalerite suggests that ground waters carrying zinc ions moved through much of this region and deposited zinc sulfide in fractured coal.

Partings in western coals

Conclusive mineralogic evidence confirming the volcanic origin of kaolinitic partings in western coals was obtained by optical petrographic analyses (Bohor, Pollastro, and Phillips, 1978). Such partings can now be used as isochronous markers to correlate coal beds. B. F. Bohor and his colleagues also found that the clay composition of these partings is a sensitive indicator of depositional environments, as confirmed by boron-illite analysis. Fission tracks of minerals in the partings radiometrically dates them to be slightly younger than the presumed geologic ages of their containing coals.

Hazardous elements in eastern coal resources

Peter Zubovic tabulated the minimum and maximum content of 16 hazardous elements in 1,600 coal samples collected east of the Mississippi River. Values as shown below are in parts per million except for sulfur, given in percent:

Element	*Maximum*	*Minimum*	*Element*	*Minimum*	*Maximum*
As	<.1	350	Ni	<1.0	530
Be	<.2	25	Pb	<.8	345
Cd	<.01	92	Sb	<.01	35
Co	<.7	930	Se	<.06	150
Cr	<1.8	230	U	<.2	20
Cu	<.8	275	V	<1.5	150
F	<20	460	Zn	1.3	7,000
Hg	<.002	3.2	S	.3	15

The maximum values for the contents of the following trace elements were in samples from northern Appalachian coals: Be, Co, Cr, Cu, Hg, Sb, Se, and U; the maximum content of the minor element S also was found in samples from the same area. Maximum contents of arsenic and fluorine were in the samples from southern Appalachian coals; however, the average fluorine content (60 and 61 ppm) was equally high in both segments of the Appalachian Basin. Maximum contents of Cd, Ni, Pb, V, and Zn are in samples from Eastern Interior region coals. Planned blending of coals from different regions could result in substantially reducing emissions of undesirable elements at any one coal burning facility.

Origin of methane in peat, coal, and eastern Devonian shale

It has been generally thought that loss of methoxyl groups ($-OCH_3$) from lignin in peat would lead to formation of marsh gas (CH_4). Breger, Krasnow, and Chandler (1978), analyzing three 1-m cores of Everglades peat, found that the methoxyl content of the upper half of each core remains essentially constant. It would appear, therefore, that attack on the cellulose by anaerobic, methanogenic bacteria provides the most satisfactory explanation for the origin of methane in the peat bogs. Such methane, if not lost to the atmosphere, could account for part of that gas normally found in coal beds. Inasmuch as much organic matter (kerogen) in eastern Devonian shale is actually coaly, the gas known to be associated with those shales probably was generated by the same type of microbiological attack on cellulose in the shale. In another study, Breger found that some lignite

and subbituminous coal samples from North Dakota still contain nearly 5 percent residual cellulose.

Borehole capture gamma-ray analysis

The fast- and thermal-neutron fluence rates from a 3.7-μg californium–252 neutron source in a simulated borehole have been measured as a function of the vertical distance between the source and the detector in the borehole sond (Senftle, Macy, and Mikesell, 1979). The instrument was tested in air, water, coal, and iron-ore concrete mix and dry-sand borehole media. Gamma-ray intensity measurements were made for specific spectral lines at low and high energies for the same range of source-to-detector distances in the iron ore concrete mix and in coal. Integral gamma-ray counts across the entire spectrum were also made at each source-to-detector distance. From these data, the specific neutron-damage rate and the critical count-rate criteria, it was shown that in an iron-ore concrete mix (low-hydrogen concentration) ^{252}Cf neutron sources of 2 to 40 μg are suitable. The source size required for optimum gamma-rate sensitivity depends on the energy of the gamma ray being measured. The results in a hydrogenous medium such as coal show that sources from 2 to 20 μg are suitable for obtaining the highest gamma ray sensitivity, again depending on the energy of the gamma ray being measured. A significant improvement in sensitivity can be achieved by using faster electronics in a hydrogenous medium; there is no improvement in iron ore.

OIL AND GAS RESOURCES

ALASKA

Origin of North Slope oil and gas

The Torok Formation, pebble shale unit, Kingak Shale, and Shublik Formation are potential oil and gas source rocks where immature and oil and gas source rocks where mature, according to L. B. Magoon III and G. E. Claypool. These rock units have generated oil and gas in the Colville trough, south of the Barrow high. Oil and mature gas (not low-temperature biogenic gas) are present on the Barrow high. Oil and gas have migrated from the Colville trough to the Barrow high. Along this migration route, stratigraphically trapped oil and gas fields may exist.

New information on age and petroleum potential of Lisburne Group (Carboniferous and Permian), North Slope

Exploratory drilling by the U.S. Navy and the USGS during the past 4 years in the National Petroleum Reserve in Alaska (NPRA) has expanded knowledge of the Lisburne Group and adjacent rock units, according to K. J. Bird. This new drilling includes eight Lisburne penetrations, which had not been completed in the earlier Pet-4 Navy drilling program. In the northeast part of NPRA, the Lisburne Group lies conformably on a thin sequence of the Endicott Group or with angular unconformity on a variety of basement rocks, including granite. The Lisburne, which ranges in thickness from 110 to 600 m, has a complex isopach pattern but shows general northward thinning. It appears to grade westward into red clastic beds in the area of the South Simpson and Topagoruk wells. The Lisburne consists predominantly of limestone (pellet and oolitic grainstone) with lesser amounts of dolomite, shale, and sandstone. Macrodolomite (crystal size $>30\mu$) is most common at the top of the Lisburne, and microdolomite (crystal size $<30\mu$) is most common near its base. A dolomite unit of middle Chesterian age is in the middle part of the Lisburne in the Prudhoe area, but in the NPRA it is recognized only in the Atigaru Point and West Fish Creek wells, where it lies at the base of the Lisburne. Microfossils indicate a Pennsylvanian age for most of the Lisburne Group. The base is as old as Late Mississippian in some wells, and the top is now known to be as young as Early Permian, based on the presence of the foraminifer *Protonodosaria* together with the hydrozoan(?) *Palaeoaplysina*. This is the first reported occurrence of this carbonate mound-building hydrozoan(?) in Alaska. *Palaeoaplysina* mounds in the Soviet Union contain oil. The reservoir potential of the Lisburne seen thus far appears to be less favorable than at Prudhoe Bay, mainly because of the lesser amounts of porous dolomite.

Petroleum potential of Lower Cretaceous deltaic sandstones, North Slope

Field work by A. C. Huffman, Jr., on the central and eastern parts of the North Slope during the 1977 and 1978 field seasons has revealed that the Nanushuk Group (Lower Cretaceous part) includes two separate deltas, a western or Corwin delta and a central or Umiat delta, separated by an interdeltaic area of sparse sandstone.

The Corwin delta is a dominantly fluvial delta, with a point source in the vicinity of the intersec-

tion of the Brooks Range and Lisburne Hills and a northeasterly direction of sediment transport. It is characterized by a low sand, high clay and mud content and was apparently deposited rapidly in the subsiding Colville trough. The sandstones exhibit low porosity and permeability caused by high percentages of clay matrix and calcite cementation. Organic geochemistry studies indicate deep burial and relatively high temperatures in the southern part of the delta. Coal beds, common in the delta-plain parts of the sequence, may attain thicknesses of more than 5 m.

The Umiat delta is also a dominantly fluvial delta with a point source in the vicinity of Analetuvik Pass in the Brooks Range. Sediment transport directions and sand isolith maps indicate three major lobes and a much broader shape, suggesting that sediments spread out onto a relatively shallow shelf. Sand percentages are much higher than those in the Corwin delta, and fairly thick units of porous and permeable sandstone are found throughout the area. Organic geochemistry studies indicate much shallower depths of burial and a better preserved palynomorph assemblage than in the western area.

Geochemical exploration for petroleum in a permafrost environment, North Slope

The petroleum exploration technique of surveying the concentration of helium in soil gas has been extended to a permafrost environment on the NPRA by A. A. Roberts and V. C. Dean. Helium surveys were conducted over a known gas reservoir, over nonproductive (background) areas, and over a petroleum prospect to be drilled in 1979. All samples of permafrost were taken at a depth of 0.75 m, hermetically sealed in aluminum cans, and later analyzed for helium content.

The survey over and around the South Barrow gas field revealed a high helium halo around the known productive areas, with all dry holes falling outside this halo. The results also suggested that two other areas in the vicinity of the South Barrow field may contain natural gas reservoirs. An examination of seismic data revealed the existence of three structures in these areas. A combination of this seismic work, geologic and geophysical studies indicating the existence of potential reservoir rocks, the existence of other gas reservoirs in the immediate vicinity indicating potential source rocks, and this near-surface geochemical study suggesting natural gas seepage to the surface make these three structures highly likely prospects for the discovery of more natural gas fields in the Barrow area.

A helium survey was also run over 1,300 km^2 south, east, and west of the J. W. Dalton test location at Pitt Point on the NPRA. No evidence of gas seepage from a possible reservoir there was observed. The lack of any surface manifestation here could be due to many factors including (1) lack of significant microseepage from an existent petroleum reservoir, (2) unlikely absence of significant concentrations of helium gas in the reservoir, (3) northward displacement of helium leakage beyond the study area, and (4) absence of a significant petroleum accumulation. This survey also revealed no pattern of high helium accumulation in the areas 27 km south and 24 km east or west of Pitt Point that would be indicative of microseepage from a petroleum reservoir. Thus, no evidence was found to support the existence of a significant petroleum reservoir in this prospect area.

The helium surveys also provided the first data on the expected background concentration of helium to be found in a silt or fine-grained sand permafrost. These data allow a more meaningful interpretation to be made of some samples previously collected over Prudhoe Bay and over some suspected petroleum accumulations in the Wildlife Range east of Prudhoe Bay. All samples in these areas were an order of magnitude higher than the new background samples. These very preliminary results suggest that this environmentally nondestructive petroleum exploration technique might be useful in helping to define possible petroleum prospects in the very fragile permafrost environment.

Petroleum geology of Cook Inlet Basin

Oil exploration commenced onshore adjacent to the lower Cook Inlet on the Iniskin Peninsula in 1900 and shifted with considerable success to the upper Cook Inlet from 1957 through 1965, only to return to the lower Cook Inlet in 1977 with the drilling of the COST well and the Federal OCS sale. Lower Cook Inlet COST well No. 1 was drilled to a total depth of 3,776 m. The well penetrated the tops of Upper Cretaceous, Lower Cretaceous, and Upper Jurassic strata at 832 m, 1,541 m, and 2,112 m, respectively. Basinwide unconformities are present in this well at the bases of the Tertiary, Upper Cretaceous, and Lower Cretaceous. Sandstone of potential reservoir quality occurs in the lower Tertiary and Cretaceous. All siltstones and shales that were geochemically analyzed are low (0–0.5 wt percent) in oil-prone organic matter, and only coals are high in humic organic matter. At

total depth, vitrinite readings reach a maximum average reflectance of 0.65. Indications of hydrocarbons present are slight.

The U.S. Bureau of Mines suggests that oils from the major fields of the Cook Inlet region, most of which produce from the Hemlock Conglomerate (Oligocene), probably have a common source. More detailed work by L. B. Magoon III and G. E. Claypool, including stable carbon isotope ratios, gasoline-range hydrocarbon distribution, and heavy hydrocarbon (C_{12+}) distribution, confirms this genetic relation among the major fields. In addition, oils from Jurassic rocks under the Iniskin Peninsula and from the Hemlock Conglomerate at the southwestern tip of the Kenai Peninsula are members of the same or a very similar oil family. The Middle Jurassic strata of the Iniskin Peninsula are moderately rich in organic carbon (0.5–1.5 percent) and yield shows of oil or gas in wells and surface seeps. Their extractable hydrocarbons are similar in chemical and isotopic composition to the Cook Inlet oils. Organic matter in Tertiary and Cretaceous rocks is judged to be thermally immature in all wells analyzed.

Oil reservoirs in the major producing fields are of Tertiary age and unconformably overlie Jurassic rocks, suggesting that the pre-Tertiary unconformity may be an important factor in exploration for new oil resources. The unconformable relation between reservoir rocks and likely Middle Jurassic source rocks also implies a delay in the generation and expulsion of oil from Jurassic until late Tertiary time when localized basin subsidence and thick sedimentary fill brought older deeper rocks to the temperature required for petroleum generation. Reservoir porosities, crude oil properties, oil field traps, and tectonic framework of the west flank oil fields provide evidence used to reconstruct a possible oil migration route. The oil route is inferred to commence deep in the truncated Middle Jurassic rocks and to pass through the porous West Foreland Formation in the McArthur River field area. The oil became stratigraphically trapped in the Hemlock Conglomerate and the lower part of the Tyonek Formation at the end of Miocene time. Pliocene deformation shut off this migration route and created localized structural traps, into which the oil moved by secondary migration to form the Middle Ground Shoal, McArthur River, and Trading Bay oil fields. Oil generation continued into the Pliocene, but this higher API gravity oil migrated along a different route to the Granite Point field.

ROCKY MOUNTAINS AND GREAT PLAINS

Facies relations of low-permeability Cretaceous reservoirs in the northern Great Plains

Major natural gas resources entrapped in low-permeability (tight) reservoirs at depths of less than 1,200 m in the northern Great Plains of Montana, North Dakota, South Dakota, and Wyoming have been evaluated by D. D. Rice and G. W. Shurr. Prospective reservoirs range in age from late Early Cretaceous to Late Cretaceous and include most of the sequence from the base of the Mowry Shale to the top of the Judith River Formation. To facilitate detailed examination, the sequence was divided into five intervals that consist of one or more formations and their correlatives, (1) Mowry Shale, (2) Belle Fourche Shale and Greenhorn Formation, (3) Carlile Shale, (4) Niobrara and Telegraph Creek Formations and Eagle Sandstone, and (5) Claggett Shale and Judith River Formation and their equivalents. Within any interval, different facies occur. These facies were identified on electric logs and tied to nearby outcrops and cores. Each facies contains distinct reservoir types, some of which are tight. The following six facies were identified and mapped for each interval: nonmarine rocks, coastal sandstones, shelf sandstones, siltstones, shales, and chalks. The siltstone and shale facies are grouped together at this time because conventional logs cannot distinguish between these two rock types, particularly where they are interbedded. For future evaluation of natural gas resources from low-permeability reservoirs, these two facies will have to be separated.

The most promising tight reservoirs are developed in the shelf sandstone, siltstone, and chalk facies. Reservoirs within these facies are particularly attractive because they are enveloped by thick sequences of shale, which serve both as a seal and a source for the gas. Where naturally fractured, these shales may also be gas-bearing reservoirs.

Geometry and history of petroleum-bearing sandstone units of early Late Cretaceous age in eastern Wyoming

Sandstone beds of early Late Cretaceous age locally serve as hydrocarbon reservoirs and have yielded major quantities of oil and gas in eastern Wyoming. The dimensions, age, and depositional environments of some of the sandstone bodies were interpreted by E. A. Merewether, W. A. Cobban, and E. T. Cavanaugh from outcrop descriptions, borehole logs, and paleontologic data. Sedimentary rocks of early Late Cretaceous age are included in

the Frontier Formation and the lower part of the overlying Cody Shale in most of eastern Wyoming. However, in the northeastern part of the Powder River basin near the Black Hills, the rocks are assigned to the Belle Fourche Shale, Greenhorn Formation, and Carlile Shale, in ascending order. These formations, largely of marine origin, range in age from Cenomanian to Santonian.

The Frontier Formation in eastern Wyoming is divided into as many as three members—the Belle Fourche Member (Cenomanian), an unnamed member (lower and middle Turonian), and the Wall Creek Member (upper Turonian and lower Coniacian), in ascending order. In the Powder River basin, shale, siltstone, and sandstone of the Belle Fourche Member grade eastward into shale of the Belle Fourche Shale and calcareous shale of the lower part of the Greenhorn Formation. In the same area, shale, siltstone, and sandstone of the unnamed member grade into calcareous shale and limestone in the upper part of the Greenhorn and into shale in the lower part of the Carlile (Pool Creek Member), and sandstone, siltstone, and shale of the Wall Creek grade into siltstone, shale, and sandstone of the Turner Sandy Member of the Carlile. Hiatuses occur at the tops of the Belle Fourche Member and an unnamed member of the Frontier and probably at the top of the Pool Creek Member of the Carlile.

Sandstone units in the Belle Fourche Member form broad, relatively thin, lobate bodies, which are more than 15 m thick on the southeast flank of the Bighorn Mountains and trend southward to a featheredge. Some of the bodies extend into the Hanna Basin. The sand apparently accumulated on a shallow shelf mainly as beaches, channel deposits, distributary mouth bars, and offshore bars, largely in response to southward-moving marine currents.

Deposition of the Belle Fourche Member probably was followed by regional uplift and erosion. The unnamed member was subsequently deposited and is locally preserved in the southwestern part of the Powder River basin, the eastern part of the Wind River basin, and the western part of the Hanna Basin. The basal sandstone of the unnamed member sharply overlies the Belle Fourche and is as much as 14 m thick in southern Natrona County. It probably accumulated in broad submarine channels in Carbon, Natrona, and Converse Counties.

Deposition of the unnamed member was followed by erosion during the early late Turonian and by deposition of the Wall Creek Member of the Frontier Formation and the Turner Sandy Member of the Carlile Shale later in the Turonian. In eastern Wyoming, the Wall Creek includes as many as three sandstone units, which generally are thickest (about 30 m) in southeastern Natrona County and southwestern Converse County. The two older sandstone bodies trend northeastward across the Powder River basin, from the northwestern part of the Laramie Mountains to the west flank of the Black Hills; they also occur in the Hanna, Laramie, and Denver basins. The uppermost sandstone is mainly in Natrona County and northwestern Carbon County. Evidently, these sandstone units accumulated on a shallow shelf mainly as channel deposits and nearshore bars in northeastern Wyoming and perhaps as offshore bars in southeastern Wyoming.

Stratigraphic relations of Mississippian and Pennsylvanian rocks and possible oil entrapment in western Wyoming

Carboniferous sequences that demonstrate irregular preservation of Upper Mississippian and Lower Pennsylvanian strata in northwestern Wyoming have been measured, described, and correlated by E. K. Maughan. Stratigraphic relations in Wyoming are similar to those established by Maughan and Roberts (1967) for equivalent rocks in Montana. The sequences, which comprise the equivalent of the Big Snowy Formation (Chesterian), the Amsden Formation (Morrowan to lower Atokan), and the Tensleep Sandstone (upper(?) Atokan and lower Des Moinesian to Virgilian) are bounded by unconformities of regional extent that were formed during intervals of differential uplift and erosion prior to deposition of each successive sequence. The Big Snowy Formation includes equivalents of the Kibbey, Otter, and Heath Formations. The Amsden Formation in most of the northwestern Wyoming comprises, in ascending order, the Darwin Sandstone, Horseshoe Shale, and Ranchester Limestone Members. The Darwin, which is interpreted as a littorial and dune-sand deposit with possible qualities of a good petroleum reservoir rock, intertongues northwestward into red beds (Kibbey equivalent) at the base of the Big Snowy Formation. The Horseshoe, contrary to its interpretation by Sando, Gordon, and Dutro (1975) as an eastward equivalent of the basal Chesterian (possibly upper Meramecian) red beds, is believed to unconformably overlie limestone beds of Chesterian age (the Heath equivalent or the Moffat Trail Limestone Member of the Amsden) at some localities in the western Wyoming thrust belt and to rest on older Mississippian strata at most localities east of the thrust belt. Therefore, search for possible oil reservoirs in the

Darwin Sandstone Member of the Amsden should be directed toward entrapment at the unconformity beneath the Horseshoe Shale Member in most of Wyoming or toward updip northwesterly facies pinch outs in the extreme western part of the State.

Depositional environments of gas-bearing Upper Cretaceous rocks in northwestern Colorado

Examination by L. W. Kiteley of exposures of Upper Cretaceous rocks in southern Moffat County, Colorado, has indicated that rocks of the Mesaverde Group were deposited in deltaic and interdeltaic environments. The Iles Formation of the Mesaverde Group thickens from west to east and contains lithologies representative of deposition in small distributaries, river mouth bars, extensive longshore bars, and adjacent coastal swamps. Changes in location of the strandline during the Late Cretaceous are represented by intertonguing of the Mancos Shale and overlying Mesaverde and of the Mesaverde and overlying Lewis Shale. Movements of the strandline, generally eastward and westward, probably were caused by changes in the sediment load and location of distributaries to the west and by basin subsidence and differential compaction. As many as five cycles of marine trangression and regression have been recognized in the upper part of the Mancos, the Mesaverde, and the lower part of the Lewis on the southern flank of the Sand Wash basin, as reported by Zapp and Cobban (1960). The western and landward terminus of four of the transgressions can be identified in measured sections in southern Moffat County.

In the Sand Wash basin of northwestern Colorado, 12 fields produce mainly gas and some oil from the Mancos-Mesaverde-Lewis sequence. Total cumulative production to October 1977 is 119 Bcf of gas and about 350,000 bbl of oil. Most of the petroleum is at depths of less than 2,440 m on the flanks of the basin. Reservoir rocks range in thickness from about 2.4 m to more than 91 m. Future discoveries can be expected in deep parts of the basin, where reservoir beds and source rocks are favorable.

Oil-bearing eolian sandstones, Colorado

Study of the Weber Sandstone (Pennsylvanian) by S. G. Fryberger in the vicinity of the Rangely oil field, northwestern Colorado, demonstrated that more porous and permeable eolian reservoirs of the Weber intercalate updip with less porous and permeable alluvial sediments of the Maroon Formation forming a stratigraphic trap within nonmarine rocks. Study of hydrocarbon-producing eolianites, such as the Lyons Sandstone (Permian) in the Colorado Front Range, further confirms the heterogenous behavior of eolian reservoirs noted in other Paleozoic eolianites such as those producing from the Tensleep and Weber Sandstones.

Sedimentation and petroleum potential of fluvial part of Mesaverde Group, Piceance Creek basin, Colorado

The fluvial part of the Mesaverde Group is a monotonous sequence of lenticular sandstone, mudstone, carbonaceous shale, and coal. It is considered to have the potential to produce natural gas, but before this potential can be realized, more needs to be learned about geometry and reservoir characteristics of the sand bodies in this relatively unstudied unit. From preliminary work, R. C. Johnson has suggested that the fluvial unit may be subdivided into two general facies—a channel and overbank facies and an overbank and paludal facies. In the channel and overbank facies, lenticular channel sandstones make up 50 to 80 percent of the unit. In the overbank and paludal facies, there are no major channel sandstones. In this facies, sandstone is a minor component, and it occurs as small lenticular bodies and thin fairly persistent sheet sandstones. The two facies commonly occur as individual units, 50 to 75 m thick. At some localities, however, the individual units attain thicknesses of 200 m or more. Such thicknesses indicate that the environment that produced these facies persisted in the same area for a long period of time.

The fluvial part of the Mesaverde Group was deposited in an environment that may be analogous to that of the Texas coastal plain. Rivers flow across the coastal plain for long periods of time in the same general area with only slight changes in channel position caused by meandering and meander cutoff. Areas between river channel systems are known as flood basins or backswamps and receive sediments only during major floods. Sediments build up in the vicinity of the channel, producing a topographic high that eventually causes a major shift in the position of the channel of as much as 10 km or more. This results in an abrupt change from backswamp deposition to channel deposition in the area of the new channel.

Influence of diagenesis on reservoir properties of some Upper Cretaceous sandstones, Uinta Basin, Utah

Examinations of core samples by X-ray diffraction, scanning electron microscopy (SEM), and in thin section by C. W. Keighin and J. K. Pitman

revealed significant diagenetic modifications that may influence the choice of drilling, logging, and producing techniques. Authigenic silica overgrowths on detrital quartz are common but are not a major cementing agent. Feldspars, although not abundant, are commonly selectively leached or replaced by illitic clays. Carbonates are generally abundant; they are commonly interstitial but also replace detrital quartz and feldspars. Chert and rock fragments are also abundant and generally have been extensively altered by dissolution, clay mineral formation (illite, chlorite, and kaolinite), and mechanical deformation. Compaction of ductile rock fragments reduced original intergranular porosity. Dissolution and leaching of rock fragments, however, produced a significant amount of intergranular and intragranular secondary porosity in some samples. Overall, dissolution and leaching exerted a greater influence on reservoir characteristics than did compaction or growth of authigenic minerals.

Cretaceous-Tertiary boundary in gas-bearing beds of southeastern Uinta Basin, Utah

The boundary between Cretaceous and Tertiary rocks in much of the southeastern part of the Uinta Basin had been tentatively placed by T. D. Fouch and W. B. Cashion at the disconformable contact between sandstone of the Tuscher Formation (Upper Cretaceous) and an overlying, heretofore undated, fluvial conglomeratic unit. In the area of the Book Cliffs, the conglomeratic rocks are overlain by Paleocene beds near the Green River and by Eocene units in the area of Westwater Canyon. D. J. Nichols has now identified Paleocene palynomorphs from the conglomeratic beds near Westwater Canyon. New analysis of stratigraphic relations indicate that there is a hiatus at the top of the conglomeratic unit as well as at its base.

The unnamed Paleocene conglomeratic beds and their lateral equivalents are traceable on borehole geophysical logs, which can be used to locate the Cretaceous-Tertiary boundary in the subsurface. The beds grade from conglomerate to beds composed dominantly of sandstone in much of the subsurface of the eastern Uinta Basin, where they are reservoirs for natural gas.

GREAT BASIN AND SOUTHWESTERN UNITED STATES

Mississippian source rocks in Utah and Idaho

Recent organic carbon, hydrocarbon, and maturation studies by C. A. Sandberg, D. R. Grogan, and T. J. Clisham provide additional evidence that the phosphatic shale member of the Deseret Limestone and equivalent Little Flat Formation was probably a source for petroleum that migrated eastward across the Cordilleran hingeline in northern and central Utah and southeastern Idaho. The phosphatic shale member consists mainly of interbedded organic-rich shale, phosphorite, and limestone and ranges in thickness from 2 to 22 m. Surface and shallow-depth (0.1–1.0 m) outcrop samples at Causey Reservoir, Ogden Canyon, and Old Laketown Canyon in northern Utah and at Dog Valley Mountain and Dog Valley Peak in central Utah have organic carbon yields of 1.50 to 7.95 (3.66 median) percent for shales, 0.67 to 5.11 (3.06 median) percent for phosphorites, and 0.40 to 3.17 (0.96 median) percent for limestones. These percentages are significantly greater than those obtained by sampling of the phosphatic member in previous years. Total hydrocarbon (light and heavy) analyses performed on phosphorites from Old Laketown Canyon and on rocks of several lithologies from Dog Valley Peak exhibit ranges of 175 to 2,167 ppm and 340 to 2,910 ppm, respectively. Color alteration index (CAI) values obtained from conodonts at four of the localities range from 1.5 to 3 and are within the limits of optimum thermal maturation for hydrocarbons. A CAI value of 4 from Ogden Canyon is believed to have been attained during Tertiary time after hydrocarbons were generated and had migrated. CAI values of 1.5 to 2 are in the optimum oil-generating range, and a CAI value of 3 is in the optimum gas-generating range (Epstein, Epstein, and Harris, 1977).

Regional source-rock studies must take into consideration that surface sampling almost invariably will produce organic carbon percentages that are much lower than those found at depth. For example, a phosphorite sample taken at the surface from the phosphatic member of the Deseret Limestone in the Eureka mining district, Utah, yielded 0.37 percent organic carbon, whereas organic carbon values between 6.7 and 13.3 percent from the same unit at the 1,600-ft level in a nearby mine were reported by Morris and Lovering (1961). Recent surface sampling demonstrates that outcrop characteristics govern the severity of organic carbon degradation.

Under certain conditions surface samples may yield organic carbon percentages closer to those found at depth.

- Weathering of organic carbon is minimal at outcrops or artificial cuts with nearly vertical

slopes where the beds dip gently and at outcrops where beds of any attitude have been deeply cut by recent erosion. Samples collected at outcrops such as these have yielded organic carbon percentages of 2.43 to 7.95 (5.46 median) for shales, 3.45 and 5.11 for two samples of phosphorite, and 0.40 and 3.17 for two samples of limestone.

- Greater weathering effects were observed in samples taken from outcrops with lower (<45°) slope angles where beds dip moderately to steeply (45°–75°). Samples from such outcrops generally had low organic carbon yields (0.5–1.0 percent) regardless of the depth of collection.
- Maximum weathering effects were found at outcrops with low slope angles (<25°) and steep dip angles (75°–90°). Samples from outcrops such as this are nearly depleted in organic carbon (<0.5 percent), and the hydrocarbons are severely degraded.

Petroleum source beds in Permian Phosphoria Formation, northeastern Great Basin

Limits of the organic-rich shale members of the Phosphoria Formation, determined by E. K. Maughan, indicate that their deposition took place in an area of about 700 km by 600 km. Maximum thickness of about 65 km is in northern Utah near Great Salt Lake. The southwestern limit of sapropelic accumulation now has been located approximately along a westward-trending line extending from Mount Nebo to Gold Hill, Utah, and from there northward through eastern Elko County, Nevada, where the organic-rich beds grade westward into cherty mudstone, siltstone, and carbonate rocks. In central Idaho, the eastern margin lies farther east, north of the Snake River Plain, than it does to the south. Pyrolitic evaluation of thermal maturity by G. E. Claypool for Great Basin samples of the Meade Peak Member of the Phosphoria showed that organic matter ranges from late post mature to metamorphosed, except in the southern Wasatch Mountains, where it is mature to early post mature. This evaluation indicates that considerable hydrocarbons could have been generated in the Meade Peak in the northeastern Great Basin. However, the hydrocarbons and the source beds probably were thermally degraded at most places in the Great Basin during the Tertiary.

Continuous lacustrine sedimentation of Paleogene source beds in the Great Basin

Late Cretaceous(?) and Paleogene continental sedimentary rocks were formed in a dynamic depositional system in which continually active Paleogene tectonism formed basins of internal drainage, according to T. D. Fouch. Although local unconformities are present, the age of fossils indicates a record of continuous lacustrine sedimentation in east-central Nevada, beginning perhaps in Late Cretaceous time and extending into the early Oligocene. Rocks formed in these lakes are rich in organic matter in the subsurface (Fouch, 1977) and are potential petroleum source beds. The areal extent of the lake or lakes is uncertain, but the distribution of fossils and lithofacies is perhaps more compatible with sedimentation in a series of separated lakes, many of which may have been temporarily connected.

The Sheep Pass Formation in Sheep Pass Canyon of the Egan Range is probably equivalent in age to the Flagstaff Member of the Green River Formation of Utah and to the upper part of the Newark Canyon Formation of Nevada. Beds mapped as Sheep Pass(?) Formation near Ely, Nev., probably are equivalent to parts of the Elko Formation of northeastern Nevada and to part of the Green River Formation stratigraphically near and above the Mahogany zone of Utah and Colorado.

Chesterian channels discovered in western Grand Canyon, Arizona

Pre-Supai valleys, more than 100 m deep, carved in the Redwall Limestone and filled with Upper Mississippian (Chesterian) strata, have been discovered in the western Grand Canyon. George Billingsly (Museum of Northern Arizona, Flagstaff) made the find while doing geologic mapping, and E. D. McKee (USGS) confirmed it. The age was determined by MacKenzie Gordon, Jr. (marine invertebrates), B. L. Skipp (Foraminifera), and R. B. Kosanke (plant material), all of the USGS.

Oil and gas resources of Permian basin, west Texas and southeastern New Mexico

Geologic assessments of undiscovered resources of oil and natural gas have been completed for the Permian basin by G. L. Dolton, S. E. Frezon, A. B. Coury, K. L. Varnes, Keith Robinson, R. B. Powers, E. W. Scott, R. W. Allen, and A. S. Khan. Assessments of undiscovered inplace quantities and their associated pool sizes were made by depth for each of the major productive units within the basin, Permian, Carboniferous, and lower Paleozoic rocks. Based on aggregations of the age-depth units, the estimates of undiscovered oil in place in the entire basin are 3.3 billion bbl at the 95-percent probability

level and 10.4 billion bbls at the 5-percent probability level. These estimates are 4 percent and 11 percent, respectively, of the known oil in place. The estimates of the total gas (non-associated, associated, and dissolved) in place are 12.9 trillion ft^3 at the 5-percent probability level and 33.8 trillion ft^3 at the 95-percent probability level. These estimates are 12 percent and 32 percent, respectively, of the total known gas in place. Estimates of pool size distributions indicate that undiscovered pools in the basin, on the average, will be significantly smaller than those discovered in the past.

CALIFORNIA

Petroleum potential of plate boundary

Petroleum potential of continental margins of a wrench-tectonic setting is generally higher than that of continental accretionary margins. Along the west margin of North America nearly 96 percent of all proven oil and gas is in Neogene strata situated in California along the transform boundary of the Pacific and North American plates, according to D. G. Howell, J. G. Vedder, and Hugh McLean. In other rocks along the west margin of North America, continental accretionary processes have prevailed, either with large additions of allochthonous terranes or with piecemeal enlargement involving subduction of trench sediments.

Maturation of organic matter and generation of petroleum in Tertiary oil basins

Accurate and early determination of the organic maturation or especially the prediction of maturation level would be very important prior to expensive offshore drilling. To help accomplish this, the vitrinite reflectance, rock temperature, and burial history of offshore California basins were investigated by N. H. Bostick. Five sites in the Los Angeles Basin and one in the Ventura Basin with 17 boreholes, reaching as deep as 5,800 m, and with 110 samples of conventional core, were studied. The rocks are late Miocene in age and younger. Their present temperatures are believed to be maximal in their postdepositional history. The determined gradients are 24°–35° C/km and 0.033 to 0.090 percent vitrinite reflectance per km.

GULF OF MEXICO AND FLORIDA

New appraisal of oil and gas resources, western Gulf of Mexico

A team of geologists, comprising B. M. Miller, R. S. Pike, E. W. Scott, R. B. Powers, A. S. Khan, B. T. Vietti, and K. H. Carlson, has completed a new assessment of the undiscovered offshore oil and gas resources of the western Gulf of Mexico. This area, which is commonly referred to as the clastic province, lies offshore from the States of Louisiana and Texas. In order to produce this new assessment, the team developed and applied experimental procedures for estimating the size and number of the remaining undiscovered oil and gas fields, with the assistance of R. J. Cassidy (USGS) and E. E. Remmenga (Colorado State University).

Origin of Cenozoic natural gas accumulations, western Gulf of Mexico

The western Gulf of Mexico has been estimated by D. D. Rice, R. B. Powers, and E. W. Scott to contain large resources of natural gas in Miocene, Pliocene, and Pleistocene rocks. Interpretation of chemical and isotopic analyses of natural gases from 47 fields suggests that the offshore province is gas prone for three reasons:

- Several Pleistocene accumulations are of apparent biogenic origin. This gas is characterized by enrichment of the light isotope C^{12} in methane (δC^{13} lighter than -55 percent) and by large amounts of methane ($C_1/C_{1-5}>0.99$).
- Many of the Miocene accumulations were generated during early stages of thermal cracking of liquid hydrocarbons. This type of gas is wetter than biogenic gas ($C_1/C_{1-5}>0.92$) and isotopically heavier (δC^{13} heavier than -43 percent).
- Many accumulations occur in thermally immature (with respect to oil generation) rocks in which hydrocarbons, particularly gases, have migrated vertically from deeper, more mature rocks. These gases are relatively dry (C_1/C_{1-5} generally greater than 0.90) with a wide range of carbon isotope values.

The gas occurrences can be related to the sedimentary history and tectonics of the area. The location, areal extent, and thickness of sediments in late Tertiary and Quaternary depocenters controlled the distribution of reservoir and source rocks and the depths of the maturity level for each rock series. Movement of a thick Mesozoic salt section, in conjunction with concurrent subsidence of the gulf basin and the influx of sediments, resulted in folding and faulting of Cenozoic rocks and the formation of structural traps. Regional growth faults, plus radial faults associated with salt diapirism, provided pathways for the migration of hydrocarbons.

Source rock potential, South Florida Basin, Florida

Studies of carbonate rocks in the South Florida Basin by J. G. Palacas, J. P. Baysinger, and C. M. Lubeck indicate that the best source rock potential, by virtue of organic richness and thermal maturation, is in the Sunniland Limestone. Possible source beds, 0.3 to 6 m thick and containing 0.4 to 12.2 percent organic carbon and 500 ppm or more hydrocarbons, are interbedded throughout the Sunniland. The greatest concentration of organic-rich rocks, containing as much as 12.2 percent organic carbon, commonly occurs in a zone as much as 6 m thick (often referred to as the "Rubble Zone") near the top of the "Lower" Sunniland Limestone.

Preliminary crude oil to source rock correlations suggest that oils in the uppermost carbonate reservoirs of the "Upper" Sunniland, particularly in West Felda and LeHigh Park fields, were derived in part, if not entirely, from "Upper" Sunniland carbonate source rocks. On the other hand, oils and oil shows in "Lower" Sunniland carbonate reservoirs were derived from "Lower" Sunniland source beds and possibly, in part, from organic-rich carbonate interbeds and partings in the underlying Punta Gorda Anhydrite.

Reservoir porosity in Sunniland Limestone (Lower Cretaceous), southern Florida

Petrographic analyses by R. B. Halley of limestone reservoir rocks in the Sunniland Limestone indicated that original depositional porosity is volumetrically the most abundant type of porosity. Other types of pores (secondary pores, intercrystalline pores in dolomite, and fracture pores) are also present but are not as widespread. These findings suggest that future exploration should focus on locations that were sites of accumulation of highly porous and permeable sediments during the Early Cretaceous. In addition, the variety of pore types identified in Sunniland oil reservoirs suggests the possibility of reservoirs in other settings, where porosity may have developed as a result of secondary grain dissolution, dolomitization, or fracturing, provided that suitable reservoir seals and source rocks are present.

APPALACHIAN BASIN

Gas generation in Devonian black shale

Chemical composition of natural gas produced from rocks of Middle to Late Devonian age in about 100 fields ranges systematically from wet (>10-percent ethane content) to dry (<2-percent ethane content) from west to east across the Appalachian Basin, according to G. E. Claypool and C. N. Threlkeld. Carbon isotope ratios of methane at 10 localities in the basin exhibit a parallel trend, with lighter methane ($\delta^{13}C = -54$ permil) in the east. Solid organic matter in upper Paleozoic rocks increases in degree of carbonization toward the east, reflecting deeper burial and higher geothermal temperatures. These trends indicate regional change in the degree of metamorphism of organic matter. Observed trends of coal rank were invoked by David White and others in the early 1900's to explain patterns of oil and gas occurrence in the Appalachian and similar basins.

In the Appalachian Basin, generation of natural gas in Middle to Upper Devonian rocks is largely a result of the thermochemical conversion of solid and liquid organic matter to methane. The conversion process is in its early stages in the western part of the basin but approaches completion in the eastern part. The amount of natural gas in rocks at a given locality is a function of the amount of organic matter present and the degree of conversion of organic matter to methane.

The degree of conversion of organic matter to gas was estimated for Devonian shale at four coring sites in Martin County, Kentucky, Mason and Lincoln Counties, West Virginia, and Wise County, Virginia. Based on estimates of original gas-generating capability and on remaining gas-generating potential (as determined by pyrolysis), the degree of conversion of organic matter to gas is 13, 13, 40, and 76 percent, respectively, at these four sites. For Upper Devonian rocks with >1 percent organic carbon, the average organic-carbon content is about 3 percent at several localities. Based on this and on pyrolytic gas yields, a uniform original gas-generating capacity of 3.1 standard m^3/m^3 was assumed for the black-shale facies throughout the Appalachian Basin. Based on a volume of Middle and Upper Devonian black shale of 5.38×10^{13} m^3 and assuming degrees of conversion of organic matter to gas (derived from patterns of natural gas composition) in different parts of the basin, the volume of gas generated in the Devonian black shale can be estimated. New information regarding black shale thickness, organic-matter content, or actual extent of gas-generating processes might significantly modify the estimate of the amount of gas generated, but the approach used in the calculation would not change.

Late Devonian black-shale sedimentation and possible gas exploration areas

Recent compilation of preliminary regional isopach maps of the Upper Devonian black shales of the Rhinestreet Shale Member of the West Falls Formation and the lower part of the Huron Member of the Ohio Shale and its equivalent, the Dunkirk Shale Member of the Perrysburg Formation, has shown thickness trends that may be significant in interpretation of sedimentation and location of possible exploration areas for gas in the Appalachian Basin. The regional isopach maps were compiled by J. B. Roen (USGS) from local studies supplied by R. G. Piotrowski (Pennsylvania Geological Survey) and by F. L. Majchszak and J. F. Schweitering (West Virginia Geological Survey), all under contract to the Department of Energy's Eastern Gas Shales Project. The interpretation of thickness trends derived from these maps indicates paleocurrent directions and a prodeltaic depositional pattern.

Thick areas of the Rhinestreet Shale Member are alined in a northeast-southwest linear belt extending from the southwest corner of New York southward along the Ohio-West Virginia State line. Each of the thick areas has a prominent elongation that trends west to northwest. These trends are indicative of a westerly paleocurrent direction and support data derived by other workers from cores and surface exposures. The Dunkirk-Huron thickness trends are similar to those of the Rhinestreet, except that they are more pronounced owing to a thicker black-shale sequence and that there are two northeast-southwest linear belts. The easternmost belt has subsidiary lobes that trend westward, again indicating a westerly paleocurrent direction. The westernmost linear belt of thick Dunkirk-Huron trend has no subsidiary lobes that would suggest a westerly paleocurrent direction. Instead, its configuration and thickness variation indicates a south-southwest direction. This approximate 90° change in direction may be due to longshore currents and to effects of the nearby Cincinnati arch on the black-shale sedimentation.

Combining the thickness trend patterns of the Rhinestreet and Dunkirk-Huron trend with the location of the Rome trough portion of the Eastern Interior aulacogen (Harris, 1978) indicates that the thick belts of black shale lie westward of the aulacogen. The thick trend of the older Rhinestreet is overstepped westward by the younger Dunkirk-Huron trend. This is indicative of a delta system prograding from east to west in the process of basin filling. This interpretation of westward progradation is supported by paleocurrent directions. The position of the thick black-shale belts west of the aulacogen suggests that this structural feature may have had some control on the sedimentation of these shales. The aulacogen acted as a sediment trap. The westward-flowing current velocity was slowed by the low trough area causing the heavier, coarse (silt and sand) sediments to settle out but allowing the lighter, finer grained sediments to continue westward. To the south, in West Virginia, thickness trends, although not pronounced, cross the aulacogen, indicating that this trough did not act as a sediment trap there as it did farther north. Harris (1978) documented the effects of the aulacogen on sedimentation of older rocks underlying the Middle and Upper Devonian and on sedimentation of Mississippian rocks. However, the relatively thin stratigraphic markers in the Upper Devonian change very little or not at all in thickness across the aulacogen. Consequently, it is difficult to document, except as mentioned here, the effects of the aulacogen on Late Devonian black-shale sedimentation. Perhaps over the aulacogen and along its margins, organic-rich black-shale source rocks may be interbedded with coarser clastic reservoir rocks, making the aulacogen a possible exploration area for gas.

Fracture reservoirs in Devonian black shale

Geographic position of the Big Sandy gas field relative to the trend of the bordering faults of the Rome trough indicates a relation may exist between the occurrence of fractured reservoirs and fault trends, according to L. D. Harris. This relation is particularly noticeable in the more recent extensions of the field in west-central West Virginia. The Rome trough, a major subsurface graben, is a fundamental part of the continental framework that trends northeastward for 800 km from central Kentucky to northern Pennsylvania. During the early development of the Rome trough in Cambrian and Early Ordovician time, movement along the border faults and sedimentation were concurrent, producing great changes in thickness of sediment from fault block to fault block within the trough. During the Middle and Late Ordovician, the border faults had limited recurrent movement. Consequently, the basin tended to change shape from a nearly vertical graben to a narrow canoe-shaped basin. Regional downwarping in the Silurian produced a broader oval basin. Silurian sediments accumulated in a lensatic mass with the thickest part centered over the trough. Subsidence of the trough had little effect on the

distribution of Devonian and Mississippian rocks. However, small recurrent movements along the border faults of the trough apparently occurred during and after deposition of these middle Paleozoic strata.

New method for computing organic carbon content of Devonian shale

The organic carbon content of Devonian shales of the Appalachian Basin is an important parameter for determining the natural gas resources of these rocks. J. W. Schmoker has developed a method for calculating organic-carbon content from formation-density logs. Analyses of logs from seven wells in Ohio, West Virginia, Virginia, and Kentucky were compared to laboratory core analyses, and the comparisons showed that organic content computed from density logs is as reliable and as accurate as that determined from core samples. The density-log method offers the advantage of continuous sampling of the heterogeneous shale section and is based on logs that are commonly run and readily available. Plots of gamma-ray intensity versus formation density were used to determine the applicability of the method at a given location and to identify individual intervals where the approach might not be valid. Available data indicate the density-log method can be used to calculate organic-carbon content in a large area of the western Appalachian Basin.

NEW EXPLORATION AND PRODUCTION TECHNIQUES

Primary migration of crude oil

New data gathered by L. C. Price and L. L. Rumen address the three principal criticisms of primary migration by molecular solution, (1) the low aqueous solubility of crude oil, (2) the assumed thermal destruction of hydrocarbons at moderate temperatures, and (3) the vast compositional differences between crude oil and hydrocarbons that are readily dissolved in water. These data demonstrate that gas-bearing waters between 300° and 350°C can carry enough crude oil to account for primary petroleum migration and that high temperatures and the presence of gas cause compositional equality between crude oils and the hydrocarbons that are dissolved in water. Moreover, organic geochemical data from deep wells suggest that hydrocarbons are thermally stable to higher temperatures than generally believed. Because many petroleum basins are currently not hot enough, either primary migration by molecular solution is not possible or these basins were in the past affected by heating events that caused migration. The possibility of primary petroleum migration by gaseous solution or bulk phase migration should also be considered.

Sources of organic matter in Devonian black shales

Gas chromatographic analysis of volatile products formed by pyrolysis of some black shales has demonstrated that the composition of pyrolysates can be related to the nature of the kerogen and to the precursor organisms, as recognized by visual microscopic examination. According to J. S. Leventhal, the kerogens from the Woodruff Formation and related black shales of the central Great Basin are derived predominantly from marine organisms such as *Tasmanites*. In contrast, the Chattanooga Shale and its equivalents in the Appalachian Basin contain both marine algal components and, in some cases, abundant vitrinite, a terrestrial component probably derived from *Callixylon*. Pyrolysis products from *Tasmanites*-rich shales are mainly n-alkanes and alkenes, with maxima at n-C_{12} and n-C_{17} and only small amounts of products with more than 21 carbon atoms. Pyrolysis products from vitrinite-rich shales are mainly substituted aromatics, such as would be expected from the degradation of lignin-type materials. Greater amounts of uranium were found to be associated with vitrinite-rich samples at several locations. Changes in the nature of pyrolysis products with depth in a single core can indicate changes in depositional environments with time, which affected mixing ratios of terrestrial and marine components.

Carbon isotopes as a correlation tool

A study by P. A. Scholle, based on samples from Mexico, the United States, England, the North Sea, Netherlands, France, Italy, and the North Atlantic DSDP, showed that carbon isotopic data on whole-rock chalk or pelagic limestone samples can be correlated with considerable confidence over distances of at least thousands of kilometers. These isotopic cycles appear to reflect changes in oceanic circulation patterns, which, in turn, may be related to global sea level and temperature fluctuations. The changes in circulation also appear to affect oxygenation of the ocean basins and thus the preservation of organic matter and the petroleum potential of marine sediment sections.

Aeromagnetic detection of diagenetic magnetite over oil fields

A recent study by T. J. Donovan, R. L. Forgey, and A. A. Roberts suggested that high-wave-num-

ber-magnetic anomalies measured as part of a low-altitude airborne magnetic survey over the Cement oil field, Oklahoma, reflect abundant near-surface magnetite (formed by the reduction of hydrated iron oxides) and (or) hematite. These iron minerals are believed to have formed as a direct result of petroleum microseepage.

Early fresh-water diagenesis produces limestone with favorable oil reservoir properties

Studies by E. A. Shinn, R. B. Halley, B. H. Lidz, J. H. Hudson, and D. M. Robbin showed that exposure of marine carbonate rocks to fresh water results in (1) conversion of unstable minerals to stable ones, (2) lithification through cementation, and (3) reorganization and preservation of large amounts of porosity. The resulting rock is a chemically stable porous limestone with blocky calcite cement, a common carbonate reservoir rock in the geologic record. The stable mineralogy and cement in these rocks will resist compaction and pressure solution in the subsurface, thus helping to preserve porosity and permeability at depth.

Effects of terrain on borehole gravity data

The effects of terrain upon gravity measurements in a borehole and upon formation density derived from borehole gravity data, as a function of depth in the well, terrain elevation, and radial distance to the terrain, were studied by J. W. Schmoker. The vertical attraction of gravity in a borehole, g_T, resulting from a terrain element, is small at the surface, reaches an absolute maximum at a depth (depending upon radial distance to a terrain element), and then decreases at greater depths. The effect of terrain upon calculated formation density, ρ_T, is proportional to the vertical derivative of g_T, is maximum at the surface, passes through zero where $|g_T|$ is greatest, and reaches a second extremum of opposite sign to the first and of much lower magnitude. Accuracy criteria for borehole gravity terrain corrections were developed and show that elevation requirements are most stringent for a combination of nearby terrain and near-surface gravity stations. The measurement of the free-air gradient of gravity, commonly made slightly above the ground surface, is extremely sensitive to topographic irregularities within about 300 m of the measurement point. Terrain 21.9 to 166.7 km from the well (Hammer's zone *M* through Hayford-Bowie's zone *o*) causes a ρ_T that is nearly constant with depth. At these distances, the terrain correction will be equivalent to a DC shift of about 0.053 g/cm^3/1,000 m of average elevation above or below the correction datum. The effect of all topography beyond 166.7 km upon ρ_T is not likely to exceed 0.01 g/cm^3.

Formation of conglomerates from submarine slides

Relatively few data have been published demonstrating that coarse-grained sediment-gravity flows can be generated from submarine slides and slumps. The genetic interrelations between slides and slide-generated deposits are important facets in understanding the petroleum geology of continental-slope, base-of-slope, and submarine-fan environments. Reservoir properties of deep-water conglomerate and sand are highly variable and are significantly influenced by their different modes of origin.

Data on submarine slides and slumps in a north-trending, seaward-prograding continental slope sequence that existed in central Nevada during early Paleozoic time were studied by H. E. Cook. On this slope, translational slides, which are as much as 400 m wide and 10 m thick, moved semilithified hemipelagic sediment. Once a slide was in motion, its transformation into conglomeratic mass flows began at its base and thin margins. Clast development progressed as the slide continued to move downslope until the base and margins attained a completely conglomeratic texture.

Conglomeratic debris-flow deposits generated by these slides occur in channels as much as 400 m wide and 12 m thick. Data indicate a downslope transition from debris flow to turbidity-current flow. Many conglomeratic turbidity-current flows on the lower slope probably originated as debris flows, which were, in turn, generated from slides higher on the slope. These turbidity-flow deposits occur in channels as much as 100 m wide and 2 m thick.

A further genetic link may exist between slides and slide-generated mass-flow deposits. The flow mechanics and the resulting reservoir properties in mass-flow deposits were influenced by the nature of the clasts generated by the slides. The size, shape, and original orientation of these slide-derived clasts, parameters which affect reservoir properties, were strongly controlled by the bedding characteristics, degree of induration, and style of deformation of the slides.

Prediction of oil and gas production from chalk reservoirs

Large areas of the Western Interior of the United States have been determined by P. A. Scholle to have a high potential for gas production from the Niobrara Formation. Some of this potential has been realized in the past few years in eastern Colo-

rado and western Kansas, but predictions based on burial depth-porosity relations of chalks throughout the world indicate that major parts of Nebraska and South Dakota, as well as parts of adjacent States to the west, may also have potential for such production. Deeper targets (chalks of Member of Carlile Shale Fairport and Greenhorn Limestone), which may also be prospective, have been identified in these areas as well. In the gulf coast region, some potential exists for North Sea-type oil production from overpressured offshore chalks where they are not too deeply buried. Fracture-related discoveries of oil or gas in chalks are likely to continue throughout the gulf coast and Western Interior regions, but this production probably will remain economically marginal.

OIL-SHALE RESOURCES

Geology and oil-shale resources of the Elko West and Elko East 7½-minute quadrangles, Elko County, Nevada

Geologic mapping of the Elko West and Elko East 7½-minute quadrangles, Elko County, Nevada, was completed by B. J. Solomon. Mapping revealed that oil shale occurs at the surface less than 8 km south and east of Elko, Nev. The oil shale occurs in the Elko Formation which is of Eocene and Oligocene(?) age and approximately 520 m thick near Elko. Assays of the Elko oil shale show oil yields of as much as 357 L/t, but the beds with high yields are thin and interbedded with strata that are barren or yield little oil.

Rocks of the Elko Formation overlie strata of Eocene age deposited in fluvial and lacustrine environments and are overlain by tuff, andesitic flows, and fluvial sedimentary rocks of Oligocene age. Tuffaceous material is sparse in the lower part of the Elko and underlying rocks but is abundant in the upper part of the Elko Formation. The Paleogene beds occur at the surface in northeast-trending ridges bounded by linear range-front faults. The ridges were probably uplifted during and after Miocene time in the period when basin-and-range structures were formed. Oil shale occurs in the Elko Formation in adjacent basins, but the shale is buried by younger Tertiary strata several hundred meters thick.

Quantitative mineralogy of Colorado oil shale

Chemical, X-ray diffraction, and fluorescence data were used by J. R. Dyni to determine the quantitative mineralogy of 279 samples from the Juhan 4-1 core hole, Piceance Creek basin, Colorado. The samples represent a cored sequence of nahcolite- and dawsonite-bearing oil shale 177 m thick in the Colorado oil-shale deposits. Arithmetic means in weight percent are nahcolite, 16.9; dawsonite, 9.5; dolomite, 22.4; calcite, 1.0; alkali feldspars, 20.6; quartz, 14.2; and kerogen, 18.8. The lack of clay minerals (small amounts of illite are in many samples), the high content of organic matter, and the presence of large amounts of uncommon minerals, including nahcolite and dawsonite, emphasize the unusual composition of these rocks. Quantitative mineralogy of the oil-shale deposits will aid in assessing the potential value of byproduct minerals and in determining energy requirements for retorting oil shale.

Comparison of spent shale and soil as sorbents for retort waste water

A study conducted by J. A. Leenheer and H. A. Stuber evaluated oil shale processed in a Tosco II retort and soil developed on oil shale from the Green River Formation as sorbents for organic solutes contained in retort waste water. The spent (processed) shale exhibited moderately high absorptive capacities for organic acids and absorbed about twice the amount of organic solutes absorbed by the soil. The soil showed almost no affinity for the organic acids contained in the waste water. Major amounts of organic matter were extracted from the oil by retort waste water, whereas only minor quantities of organic constituents were extracted from the spent shale. Retort waste water spilled or disposed on land surface will, therefore, transport much less organic solutes through spent shale material than through surface soils of the region.

Detailed geologic investigation of the Agency Draw Northeast quadrangle, east-central Uinta Basin, Utah

Geologic mapping, altimetry and plane tabling of control points for the structure contours, and the measurement of one stratigraphic section were completed by G. N. Pipiringos in the Agency Draw NE quadrangle. The Mahogany oil-shale bed is about 1.5 m thick and underlies an estimated 80 percent of the quadrangle, being absent only where it has been eroded along the main streams (Willow Creek and its tributaries, Sunday School Canyon and Main Canyon, and the east fork of Agency Draw). Near the southern edge of the map area, a thick sandstone bed occurs within the lower part of the Mahogany ledge in a stratigraphic interval commonly occupied by oil shale and marlstone. The

sandstone has a maximum thickness of 24 m in the quadrangle and forms a prominent vertical cliff in exposure on the west side of Willow Creek. It thins northeastward and grades laterally into a slope-forming sequence composed of siltstone and some marlstone. This abrupt facies change is a significant factor in evaluating oil-shale resources of the area.

NUCLEAR-FUEL RESOURCES

In 1974, the USGS uranium-thorium program took several new directions in response to the Nation's realization of the pending energy resource shortage. In a relatively short time many new research projects have developed critical information on uranium habitats and improved methods of exploration. The new program is designed to improve understanding of the nature and distribution of uranium and thorium resources of the entire United States. In studies of known uranium areas, modern concepts of stratigraphy, sedimentation, and igneous and metamorphic petrology, together with modern geochemical and geophysical methods, are being used to obtain new insights into uranium habitat. From these studies, it is anticipated that better geologic guides and exploration methods to aid industry in its vital economic role will result. As basic understanding is improved, an expansion of work into frontier provinces of the United States is occurring with the objective of discovering previously unrecognized analogs to known uranium habitats.

Studies of known uranium areas are increasingly being approached by scientific teams or task forces involving personnel of the Branch of Uranium and Thorium Resources and other cooperating branches. New looks at the major uranium districts studied and reported on long ago are yielding much detail not previously recognized. The integrated, multidisciplinary approach in uranium research is proving to be more scientifically productive. As the modern approaches are applied over the next 2 to 3 years, research will result in many topical reports enroute to a synthesis of uranium occurrence and origin. The following series of short reports summarize the most significant results of uranium-thorium-related research for FY 1978.

Uranium and thorium in granitic rocks of northeastern Washington

Northeastern Washington and northern Idaho is a uranium province in which many Cretaceous and Tertiary granitic plutons contain abnormal amounts of uranium. Investigations by J. T. Nash reveal that the mean uranium content of 108 samples of granitic rock is 8.8 ppm, more than twice normal for rocks of this composition. The mean thorium content, 20.3 ppm, and mean Th/U ratio, 3.19, are normal. The most uraniferous and fertile rocks are the peraluminus two-mica granitic suite, although not all two-mica plutons are enriched in uranium. The muscovite-bearing suite has a mean uranium content of 22.3 ppm, mean thorium content of 22.8 ppm, and mean Th/U ratio of 2.82. Porphyritic quartz monzonite of the Midnite mine, interpreted to be a two-mica granitic rock, is especially radioactive with mean uranium content of 14.7 ppm, mean thorium content of 32.1 ppm, and mean Th/U ratio of 2.72. Mean uranium and thorium contents of the two-mica granitic plutons are significantly different from those of the calcalkaline hornblende granitic suite, which are mean uranium content, 5.0 ppm; mean thorium content, 17.6; and mean Th/U ratio 3.78.

Occurrence of uranium and thorium in the muscovite and hornblende suites is systematically different. Many muscovite-bearing rocks are much more enriched in uranium (>15 ppm) than they are in thorium and have a relatively low Th/U correlation coefficient of $+0.409$. Many of the uraniferous muscovite-bearing rocks contain less than 20 ppm Th, probably a consequence of forming by anatexis of thorium-deficient sedimentary rocks. Uranium and thorium variation is much more regular in the hornblende suite, which has a Th/U correlation coefficient of $+0.780$. Uranium in the muscovite suite is held primarily in magnetite and biotite and possibly as minute uraninite grains, whereas in the hornblende suite uranium resides primarily in sphene, zircon, and allanite. Many muscovite-bearing plutons are considered fertile by two criteria, high uranium content and uranium residence in labile phases. The hornblende-bearing granitic plutons are not considered fertile, regardless of uranium content, because uranium resides in refractory phases.

Archean-Proterozoic boundary in Laramie Mountains in Wyoming may contain radioactive conglomerates

Upper Archean or lower Proterozoic metasedimentary rocks rest unconformably on Archean granitic and metamorphic basement in the Black Hills, South Dakota, in the northern Medicine Bow Mountains, Wyoming, and in the northern Sierra Madre, Wyoming. In each of these three localities, uraniferous metaconglomerates have been discovered directly on or immediately above the uncon-

formable contact. The Laramie Mountains lie between the Black Hills and the Medicine Bow Mountains and are crossed by the Archean-Proterozoic boundary. Precambrian metasedimentary rocks of the eastern Laramie Mountains have never been mapped except in reconnaissance fashion, and their distribution and stratigraphy are not well known. F. A. Hills examined these rocks during reconnaissance investigations of the eastern Laramie Mountains. From the Cooney Hills (approximately 41°57′ N., 105°7′ W.) at least as far north as Johnson Mountain (approximately 42°12′ N., 105°13′ W.), a distance of approximately 29 km, micaceous, dirty quartzite, quartz-rich phyllite or schist, and marble (all possibly early Proterozoic in age) crop out along the eastern edge of the Laramie Mountains on knobs and hill tops surrounded by Tertiary deposits. The contact between the Proterozoic metasedimentary rocks and the Archean granitic rocks along the eastern edge of the Laramie Mountains is covered by Tertiary sedimentary rocks, and it is not known whether the contact is an unconformity (as in the Black Hills, the Medicine Bow Mountains, and the Sierra Madre), a fault contact, or even an intrusive contact (which would be possible if the metasedimentary rocks are Archean rather than Proterozoic). The possibility exists that the Archean-Proterozoic boundary, where it occurs in the eastern Laramie Mountains, is overlain by uraniferous conglomerates of the Elliot Lake-Witwatersrand type.

Two-mica granite and the Mesoappalachian-Avalonian boundary in New Hampshire

A major northerly to northeasterly trending regional fault, interpreted by E. L. Boudette to be transcurrent and right lateral, separates two-mica granite belts of southeastern New Hampshire (Milford and Central belts) from the uranium mineralized (Lake Sunapee) belt on the west. This fault, called here the Canterbury fault, can be compared to the Dover fault of Newfoundland. This fault is probably the boundary between the Avalonian and Mesoappalachian tectono-stratigraphic zones. If so, a major reappraisal of the geology of central eastern New England is required.

J. A. Aleinikoff (1978) has dated two-mica granite near Milford, N.H., by zircon methods to be approximately 270 million years old. Two-mica granite of the Lake Sunapee belt is dated by whole-rock Rb-Sr methods to be approximately 330 million years old (Lyons and Livingston, 1977). The fault separating the two-mica granite belts could separate them into two entirely different irruptive sequences and preclude further attempts to correlate them. Important uranium distribution contrasts may also apply to the different sequences.

The two-mica granite of the Milford belt was apparently extracted from the "Massabesic Migmatite." Aleinikoff has also dated a volcanogenic protolith of the "Massabesic" by zircon methods. This rock yields an approximate depositional age of 650 million years, which is consistent with an Avalonian affiliation. The metamorphic prograde succession of the "Massabesic Migmatite" has been mapped by Boudette, who interprets the protoliths to be principally correlative with the Berwick Formation of Maine and New Hampshire and the Oakdale Formation of eastern Massachusetts. If this interpretation is correct, all of the rocks of the Merrimack synclinorium of Emerson are of Proterozoic Z age by implication. Thus, there very well could be two Merrimack synclinoria in New England, one of Precambrian Avalonian affiliation east of the Canterbury fault and another of Silurian and Devonian age to the west.

Thorium and uranium resources in Goodrich Quartzite upgraded

The Goodrich Quartzite in northwestern Michigan has long been considered a large, low-grade resource of thorium with the possibility of byproduct uranium production. Thorium occurs in detrital monazite with greatest concentrations in the coarser grained quartzite and in quartz-pebble conglomerate. Radiometric traverses by M. R. Brock, of the USGS, accompanied by R. C. Reed of the Michigan Geological Survey, across a thick deposit of boulder till located about 5 miles south of Ishpiming, Mich., showed the till to have a radiation level higher than other similar tills in the region. The anomalous radioactivity is contributed by abundant conglomeratic boulders of Goodrich Quartzite, most of which are significantly more radioactive than the previously studied outcrops of the Goodrich exposed a few miles to the north. The boulders, which comprise an estimated 5 percent of the till, are believed to be derived from a part of the Goodrich that lies concealed beneath glacial debris about 1.5 miles west of the village of Palmer. The abundance of Goodrich boulders suggests a sizable volume of conglomerate which contains a greater percentage of thorium and uranium than previously reported in samples from the outcrops in the region.

Paleogeography of the Jacobsville Sandstone, Michigan

The Jacobsville Sandstone of probable Proterozoic Z age has a basal pebble conglomerate only a few feet thick in the vicinity of Keweenaw Bay, Michigan. The pebbles are principally resistant quartz, quartzite, and iron formation with less resistant and less abundant pebbles of locally derived amphibolite, granite, and greenstone. Recent studies by J. O. K. Kalliokoski in areas further to the west, in outcrops north of Wakefield, and of drill cores from both east and west of Lake Gogebic disclose a much thicker basal conglomerate as well as much more conglomerate at higher stratigraphic levels within this very thick sandstone formation. The greater abundance of coarse quartz-rich conglomerates in the western area suggests that the paleogradient was steeper there than in the east. In both areas the detritus was derived from a deeply weathered source terrain.

For uranium resource evaluation purposes, the important feature is the evidence for deep weathering in the source area of the Jacobsville and the implied mobility of uranium in such oxidized weathered zones. Such mobile uranium is considered to be capable of producing ore-grade concentrations in the vicinity of suitable permeable structures and reductants. To date, several occurrences of uranium in fractures in underlying basement rocks have been found in the proximity of the base of the Jacobsville.

Paleocurrent studies contribute to uranium resource evaluation in upper peninsula of Michigan

Paleocurrent determinations by R. W. Ojakangas in the Proterozoic X and Y sedimentary rocks exposed in the western part of the upper peninsula of Michigan reveal bimodality in current directions in each of three quartzose units that served as the principal targets for study. Seventy-two determinations within the Sunday Quartzite (Proterozoic X) show the directions of transport to be mostly towards the northwest and southeast with the greatest contribution to the northwest. One hundred and two determinations on quartzose members in the Palms Formation (Proterozoic X) show paleocurrent directions were most pronounced towards the east and west, with the latter direction being the most prevalent. One hundred and five determinations were taken within the Bessemer Quartzite (Proterozoic Y) and east-north-east and west current directions prevailed, with the east-northeast component most common. These paleocurrent directions are important to the uranium resource evaluation in that they indicate the presence of a large volume of clastic debris contributed from anomalously radioactive granitic terrane that lies to the east and southeast of the study area. It is conceivable that the lower parts of the Proterozoic X strata may contain quartz-pebble conglomerates that are similar to, but probably somewhat younger than, those that constitute one of the world's largest reserves of uranium ore in the Elliott Lake and Blind River, Ontario, Canada, areas located about 200 miles east of this study area.

Geochemical expression of uranium in carbonate rocks, Pitch mine, Colorado

Recent evaluation of uranium zones at the Pitch mine, Saguache County, by Homestake Mining Company indicates that the orebody is in a zone of crushed and sheared Paleozoic rocks more than 100 m wide along the Chester reverse fault and that approximately one-half of uranium reserves occur in dolomite of the Mississippian Leadville Limestone. Mineralogical and geochemical investigatons of samples from drill core and open pit by J. T. Nash reveal that the most diagnostic near-surface characteristic of ore zones in dolomite is the presence of a thoroughly leached, limonitic gossan. Porous, ocher-colored altered carbonate rocks also occur to depths of more than 100 m in the ore zone. These leached rocks are depleted in Ca, Mg, and CO_2 and tend to be enriched in SiO_2, Pb, Zn, Mo, and Hg. Uranium probably was formerly present but has been leached relatively recently as indicated by gross disequilibrium in which radioactivity greatly exceeds chemical uranium. The leaching is attributed to acidic supergene fluids formed during the oxidation of approximately 1 percent pyrite formerly in the dolomites.

Pre-Belden unconformity in the Marshall Pass district, Colorado

In most of the area underlain by Paleozoic rocks in the Marshall Pass district, Colorado, J. C. Olson has determined that the Belden Shale of Pennsylvanian age lies unconformably on the Leadville Limestone of Mississippian age. The Paleozoic section is thick and is composed of formations of Cambrian, Ordovician, Devonian, Mississippian, and Pennsylvanian age. In the part of the district south and east of Marshall Creek, in the southeastern part of the Pahlone Peak quadrangle and the northern one-third of the Chester quadrangle, the Belden Shale was deposited unconformably on the Leadville Limestone only locally. In other places it is

in unconformable contact with Precambrian rocks or is faulted against them. The magnitude of this pre-Belden unconformity in the southeastern part of the district indicates considerable pre-Belden erosion, due presumably, to uplift along the north margin of the Uncompahgre Uplift.

Uranium ore in the Marshall Pass district occurs in the Leadville Limestone, Belden Shale, and Harding Sandstone, as well as in Precambrian rock. It is localized chiefly by faults. The position of the district on the north margin of the Uncompahgre Uplift may not have a direct bearing on the uranium mineralization, but it may be indirectly related to the structural features that helped localize the uranium deposits.

Regional geologic setting of the Cochetopa uranium district, Colorado

Regional mapping by J. C. Olson in and around the Cochetopa uranium district, Colorado, has shown that Proterozoic X granite and quartz monzonite, although largely covered by younger rocks, form an extensive batholithic mass southeast of the district. Several exposed parts of this granitic terrane are the Powderhorn Granite, the quartz monzonite of Cochetopa Creek, the granite of Wood Gulch, and the large quartz monzonite body in the Sargents-Monarch Pass area. This extensive granitic terrane is the setting in which the large Cochetopa Park caldera developed above an inferred batholith, in Tertiary time. Ashflow tuffs from several such calderas in the San Juan Mountains are possible source rocks for uranium through leaching. Northwest of the district, however, the northeast-trending Dubois Greenstone belt, comprising Proterozoic X volcanic rocks, related sedimentary rocks, and several bodies of syntectonic quartz diorite and quartz monzonite, is at least 20 km wide. Broadly speaking, the greenstone belt and related metasedimentary rocks to the northwest appear less likely to be source rocks for the uranium in the Cochetopa district than do the extensive granitic terrane to the south and east and ashflows from Tertiary calderas within it.

Uranium and thorium in Precambrian crystalline rocks of the Medicine Bow Mountains, north-central Colorado

Two hundred samples of Precambrian crystalline rocks collected by M. E. McCallum during the course of detailed mapping in the Colorado Medicine Bow Mountains were analyzed for uranium and thorium. Most of these samples are from the ±1.7 billion-years-old Rawah batholith, the uranium contents of which are generally less than 2 ppm and indicate a significant deficiency compared to other Precambrian plutons in the region which average approximately 5.0 ppm uranium (Phair and Gottfried, 1964). The Th contents of Rawah batholith samples average about 23 ppm, and these values are comparable to averages for other plutons in the area. The very low values of uranium in some samples may be a function of leaching associated with weathering processes; it is virtually impossible to obtain completely fresh samples at most exposures.

Uranium and thorium trend surfaces indicate relative enrichment of both elements to the northwest and southeast. These trends may reflect original compositional differences, increasing concentrations of faults, proximity to younger granitic plutons as in the north, or combination thereof. However, lower concentrations of uranium and thorium in the central portion of the Medicine Bow Mountains probably relate to the presence of a well-developed, moderately weathered erosion surface in that area.

Uranium studies in interior Alaska

Quartz porphyry intrusive bodies that are locally very radioactive were noted by T. P. Miller as occurring in three separate localities in the Bettles and Melozitna quadrangles in interior Alaska. These three localities are 32 to 161 km apart and occur near the contact between the Mesozoic Yukon-Koyukuk volcanogenic province and the Precambrian(?) and Paleozoic Kokrines-Hodzana metamorphic terrane. Purple fluorite is associated with strongly radioactive (3,000 counts/s total count) quartz porphyry at one locality, as is at least one secondary uranium mineral. The association of strongly radioactive quartz porphry in a particular geologic setting may have significance in outlining new exploration areas.

Genesis of the Schwartzwalder uranium deposit, Colorado

Studies by E. J. Young suggest a meteoric hydrothermal origin for the Schwartzwalder uranium deposit. The deposit occurs in Precambrian metamorphic rocks where fractures have provided conduits and open spaces for mineralization to occur. Nearby sedimentary rocks have provided a source of uranium. A meteoric hydrothermal origin seems likely for a number of reasons. First, pitchblende in the deposit is rich in molybdenum but very poor in thorium and rare earths. Such a composition is typical of sedimentary pitchblende. Second, unit-cell edges of the pitchblende (uraninite) of 5.42Å fit

sandstone and vein pitchblendes rather than pegmatitic (magmatic) uraninite. Third, amorphous carbon from sedimentary sources occurs in the fracture filling. Fourth, muscovite in the pitchblende-veined pegmatite host rock retains a Precambrian age according to K-Ar age determinations. The above determinations indicate a relatively low temperature for the ore solutions.

It appears that meteoric water, moving downdip along bedding planes in sedimentary strata tilted during Laramie tectonism, has leached uranium from the rocks and redeposited it in fractures and in the Golden fault zone. It is believed that intrusion of the Ralston dike of mafic monzonite 61.9 ± 2.5 million years ago introduced magmatic heat in and along the Golden fault zone and initiated convective flow of ground water through that zone and through other deep faults, such as the Rogers and Illinois. Parts of the Illinois fault and hanging wall faults west of the Illinois apparently were reactivated, and the wall rocks were brecciated in response to shearing. These brecciated zones and openings served as "depositional traps" for the pitchblende about 60 million years ago. Published radiometric ages of the Ralston dike (an unlikely source of uranium) and of the uranium ore are consistent with this postulated sequence of events.

Possible source of sand-size detritus, Tertiary Marfa Basin, Texas

Reconnaissance observations by M. W. Green and C. T. Pierson of clastic and volcaniclastic rocks in the "Vieja Group" of Tertiary age (DeFord, 1958, p. 13) exposed in the Mammoth uranium mine area (DeFord, 1958, fig. 1), Presidio County, Texas, suggest that there is a paucity of medium- to coarse-sand-size material in the sequence. The thick stratigraphic section exposed in the area of the Mammoth mine includes volcanic flows and ignimbrites as well as clastic rocks. The main rock types present are claystone, siltstone, and fine-grained sandstone; cobble and boulder conglomerates are present in lesser amounts.

Virtually no sand-size material was noted in the conglomerates, which are therefore interpreted to be lag conglomerates. The energy of the fluvial system that deposited the conglomerates apparently was high enough to have carried the sand-size fraction elsewhere.

Reconnaissance studies in the southeastern part of the Marfa Basin by Pierson and Green suggest that the sedimentary transport direction has a prominent south to north component in the Lajitas-Alpine area. If this same component were present in the Mammoth mine area, the sand-size material would probably have been carried into the Tertiary Marfa Basin, thereby possibly forming sandstone beds of sufficient porosity to be of interest as uranium host rocks.

Uranium in the Cutler Formation, Lisbon Valley, Utah

Uranium in the Cutler Formation in Lisbon Valley, Utah, is found only in small fluvial sandstone bodies that are interbedded with red shales and light-colored sandstone bodies of marine and eolian origin. The fluvial sandstones were deposited in small distributary streams that flowed across a flood plain, or tidal flat, close to sea level.

Studies by J. A. Campbell have shown that the elemental variation across the horizontal tabular ore, the petrology of ore and host rocks, and the diagenesis associated with the ore is different in the Cutler orebodies than in either Chinle or Morrison ore from the same area. No consistent pattern of elemental variation was found across the Cutler orebodies. Cutler ore consists of unidentified uranium minerals disseminated in a clay matrix. Ore implacement has not significantly modified the host rock. It occurred late in the diagenic history of the host rock. Estimates of the age of the Cutler ore, based on chemically determined ratios of uranium to lead, suggest that it is much younger than the host rock.

Disconformities in the Grants, New Mexico, mineral belt and their relationship to uranium occurrence

At least two major, regionally extensive, and numerous local intraformational disconformities are present in sedimentary rocks of Triassic, Jurassic, and Cretaceous age in the Grants mineral belt of the southern San Juan Basin of northwest New Mexico. These disconformities, some of which have been known for many years, have proven useful in stratigraphic correlation and in differentiating genetically related rock sequences in the mineral belt. In addition, two of these disconformities, one local and the other regional, are significantly associated with the distribution of sandstone-type uranium deposits in the Jurassic Morrison Formation and the overlying Cretaceous Dakota Sandstone.

M. W. Green's studies of the Westwater Canyon Sandstone Member and laterally equivalent beds in the Recapture Shale and Brushy Basin Shale Members of the Morrison Formation have shown that underlying Jurassic rocks are separated by an intraformational disconformity, which marks a ma-

jor change in depositional environment from predominantly sabkha-eolian dune to high energy fluviolacustrine within the Jurassic sequence. This disconformity is economically significant in that all of the large uranium deposits in rocks of Jurassic age in the mineral belt occur within fluvial sandstone facies of the Morrison above the disconformity. Recognition of this disconformity in outcrops and in the subsurface may prove important in delineation of exploration target areas and resource assessment in the San Juan Basin.

Uranium deposits in the basal part of the Dakota Sandstone are associated with the well-known regional, southward-beveling disconformity present at the lower boundary of the Dakota throughout the San Juan Basin and adjacent region. In the western part of the mineral belt, impermeable Brushy Basin shales have been truncated at this disconformity, and uranium-bearing ground waters from the Morrison Formation have migrated into basal organic-rich sandstone of the Dakota to produce several small- to medium-sized uranium deposits.

Cretaceous stratigraphic studies

Geologic mapping at a scale of 1:24,000 in the classical transgressive-regressive sequences of the Upper Cretaceous of the southern San Juan Basin by A. R. Kirk has led to a better understanding of the complex intertonguing of various facies. Stratigraphic studies and mapping of the lateral distribution of these facies suggest that a reinterpretation of the marine and nonmarine parts of the Crevasse Canyon Formation, the coastal barrier and offshore bar sands of the Gallup Sandstone, and various tongues of the offshore marine Mancos Shale and their correlatives in various subbasins will be necessary. Meetings and field conferences with interested geologists working with these units from the San Juan Basin and the Acoma and Gallup-Zuni subbasins, from the Geologic and Conservation Divisions of the USGS, the New Mexico Bureau of Mines and Mineral Resources, and various companies have led to a better understanding of the regional correlations within this interval and to marked progress in placing the various facies into a paleontological time framework (Kirk and others, 1978).

The Ruby Well No. 1 uranium mine, McKinley County, New Mexico

Primary uranium ore in the Ruby Well No. 1 mine, southern San Juan Basin, McKinley County, New Mexico, forms a narrow elongate body enclosed within a fluvial arkosic sandstone bed within the Brushy Basin Shale Member of the Morrison Formation (Upper Jurassic). The Ruby Well deposit is one of several uranium deposits alined west-northwest in the Smith Lake-Mariano Lake ore trend being studied by J. F. Robertson. The ore body, in plan view, is lenticular in shape, 1,500 m long, and about 180 m wide near the middle. It ranges from 0 to 8 m thick. In cross section, the orebody has a roughly C-shaped roll-front configuration, with the relatively thick and ragged convexity on the downdip northeast side. The upper and lower limbs of the roll extend and thin undip.

The host rock dips three degrees or less to northeast and contains planar cross bedding with dips dominantly to north and northeast. A few large-scale trough crossbeds in the sandstone plunge gently N. 60° E. in the probable direction of paleostream flow.

Ore distribution does not seem to be influenced by internal bedding structures in the host sandstone, but it does appear to be closely related to texture and permeability. Present studies indicate that the ore was deposited soon after Morrison deposition. Beginning in the Tertiary Period and extending to the present, oxidizing ground waters have attacked all margins of the deposit and taken uranium into solution. As would be expected in a classic roll-front model, the arkosic sandstone in the interior part of the roll is thoroughly altered. The sandstone exterior to and downdip from the deposit, however, is also intensively oxidized and leached, which is not the case in the classic roll-front model. This condition was undoubtedly caused by the later ground-water flow, which also markedly depleted pyrite and even secondary limonite and most of the chemical elements originally in the sandstone or associated with the ore. Most of the potash feldspar, still relatively fresh in primary ore, has been thoroughly altered to clay in the adjacent sandstone. No secondary redistribution of uranium is evident in the proximity of the deposit.

Geologic map of the Arroyo del Agua quadrangle, Rio Arriba County, New Mexico

Geologic mapping of the Arroyo del Agua 7½-minute quadrangle, Rio Arriba County, New Mexico, by J. L. Ridgley resulted in extension of the name Recapture Shale Member of the Morrison Formation into the Chama Basin from the adjacent San Juan Basin to the west. In this area, the Recapture includes the lower siltstone, fine-grained

sandstone, and claystone sequence in the Morrison Formation. In addition, a sequence of conglomeratic sandstone, sandstone, and mudstone previously included in the basal part of the Dakota Sandstone by Smith, Budding, and Pitrat (1961) and as an upper unit in the Morrison Formation by Woodward, Gibson, and McLelland (1976) has been mapped separately and tentatively correlated with the Burro Canyon Formation. The Burro Canyon Formation(?), as mapped, is the host rock for several small uranium deposits in the eastern part of the Chama Basin. Additional uranium deposits in the Burro Canyon Formation(?) probably occur in the northeast part of the basin. However, if present, they would occur at increased depths.

High-energy beds in the Dilco

R. E. Thaden demonstrated, by facies mapping of Cretaceous rocks along a north-south line of outcrop on the west side of the Chuska Mountains, western flank of the San Juan Basin, New Mexico, that the "Torrivio Sandstone Member" of Molenaar (1973) of the Gallup Sandstone is confined to the lower two-thirds of the Dilco Coal Member of the Crevasse Canyon Formation. The "Torrivio" consists of two zones of medium-grained to granule-size, cross-bedded, fluvial sandstone lenses interbedded with the normal paludal, probably deltaic, claystone, fine-grained sandstone, and coal of the Dilco. It channels underlying Dilco rocks, but was nowhere energetic enough to scour to the top of the underlying Gallup, which is of marine, probably largely lower shoreface, origin. The "Torrivio" lenses are shingled in a direction indicating northward progradation and therefore northward younging. Because the basin of deposition is known to be to the east, a strong eastward vector to the progradation, not observable on the outcrop, is implicit.

Uranium ore deposit controls in the Powder River basin

Uranium deposits near the axis of the Powder River basin are stratigraphically higher than those near the southern margin. Near the southern margin of the basin, ore deposits occur in the lowermost part of the Wasatch Formation. E. S. Santos found that, in places, this horizon in the subsurface near the basin axis contains a sandstone-mudstone ratio similar to that associated with ore deposits. The absence of ore deposits at this horizon near the basin axis is interpreted to indicate that, in addition to a facies control, there exists a depth-related control on ore-forming processes.

Depth limitation to uranium deposition, Powder River basin, Wyoming and Montana

Subsurface studies by H. W. Dodge, Jr., of gamma-ray logs in the Powder River basin, Wyoming and Montana, indicate a depth limit for deposition of uranium. This limit is approximately 762 m below present ground level in the southern part of the basin. In the northern part of the basin, a much shallower depth limit is possible. This suggests that uranium basins, in general, may have a depth control factor which should be considered important in the uranium-resource evaluation. Two possible reasons for this depth limitation in the Powder River basin are (1) the late introduction, during the Oligocene or later, of uranium-bearing fluids into susceptible, usually organic-rich, host rocks and (or) (2) regional and local hydrologic controls (both chemical and physical) which restricted downdip migration or at-depth reduction of uranium-bearing fluids.

Present-day stream valleys as guides to uranium deposits in Wyoming

D. A. Seeland made an attempt to locate major tributary streams to the Wind River of Eocene time in the Wind River basin in Wyoming. Overlays of maximum clast-size, sand-grain-regularity, sand-grain-elongation, and mean sand-grain-size maps were used to locate axes of basinward deflections in the isopleth data and areal concentrations of clasts or of particularly large clasts.

Several inflections in the isopleths along the Wind River Range are thought to locate the points where major streams issued from the range in Tertiary time. Similar inflections north of the Granite Mountains and south of the Owl Creek Mountains may have similar origins. These are thought to indicate major streams for two reasons. First, the larger streams draining a mountainous area should be incised more deeply and have a larger proportion of granitic debris than smaller ones, which would account for the presence of more elongate, less regular grains in the area of the basin into which these streams flow. Second, the postulated positions of these major streams are basinward of three of the largest drainages on the northeast flank of the Wind River Range—Dinwoody Creek, Bull Lake Creek, and North Popo Agie River. Remnants of an early Eocene alluvial fan are present at Dinwoody Creek. The Granite Mountains have been altered so much by post-Eocene collapse that there is no possibility of recognizing major stream courses within the once uplifted core area. However, the linear East

Canyon Conglomerate Bed of the Puddle Springs Arkose Member of the Wind River Formation probably represents the course of a major stream that drains the Granite Mountains. Crooks Gap is a remnant of a southward draining pre-collapse stream valley of the Granite Mountains. The Battle Spring Formation was deposited by the stream issuing from this major mountain valley. The size and shape data of this study suggest a major stream flowing north from the Granite Mountains about 50 km west of the Gas Hills. On the north side of the Wind River basin, a major tributary possibly entered about 20 km west of Lost Cabin near Copper Mountain, and another entered about 30 km northwest of Shoshoni.

The drainage patterns within the Wyoming basins have changed extensively since the Eocene. However, the persistence of major mountain drainages since then suggests that major present-day drainages may be guides to the thick, coarse-grained, arkosic Eocene sandstones that have been found to be the host-rock for all-important Wyoming uranium deposits.

Geologic setting for uranium deposits in the Date Creek basin, west-central Arizona

J. K. Otton has shown that uranium deposits in the Date Creek basin of west-central Arizona occur in fluvial-lacustrine beds of the Chapin Wash and Artillery Formations. These formations were originally thought to be Miocene and Eocene in age, respectively (Lasky and Webber, 1949); however, a recent age determination and new vertebrate fossil evidence show that the Artillery Formation is also Miocene in age, only slightly older than the Chapin Wash of probable early Miocene age. If so, then the deposits of the two formations represent a significant period of uranium mineralization in the middle Tertiary of western Arizona.

The Artillery Formation was deposited in a broad, shallow basin that extended farther to the west than the present Date Creek basin. In the type area two cycles of fluvial-lacustrine deposition have been recognized. The lacustrine facies in each cycle changes to fluvial facies to the west. Uranium occurs in discontinuous, tabular zones in carbonaceous siltstone and sandstone beds transitional between the fluvial and lacustrine facies in the lower cycle near Artillery Peak and south of adjacent Ester Basin. Similar beds in the upper cycle contain anomalous uranium, but deposits are not ore grade.

During deposition of the Chapin Wash Formation, a rapid increase in tectonic activity to the west of the basin caused lacustrine sedimentation to be restricted to the eastern end of the Date Creek basin. These lacustrine beds are rich in tuffaceous debris generally anomalous in uranium. A major uranium deposit occurs at the Anderson mine in lacustrine delta facies beds rich in organic detritus and in impure lignites deposited on the delta plain. The carbonaceous micaceous siltstones and impure lignites intertongue with green tuffaceous, locally silicified, siltstone, calcareous tuffaceous siltstone, limestone, and sandstone. Uranium was leached from tuffaceous debris by alkaline lake waters and shallow ground waters. It then migrated laterally to carbon-rich beds during the earliest stages of compaction and diagenesis of the host beds. With lowering Eh and pH, uranium coprecipitated with silica, precipitated as coffinite, or was absorbed by organic material.

Uranium potential of Cenozoic rocks of the Basin and Range province, Arizona

Emphasis of the study by H. W. Pierce (University of Arizona) is on Cenozoic sedimentary sequences that are older than late Cenozoic (post-15 m.y.) basin-fill. These older rocks, ranging from high- to low-energy continental deposits, have been deformed by folding, tilting, and faulting. Associated volcanic products, including ash beds, are common in these older sequences. In a broad northwesterly trending belt adjacent to the central Arizona Transition Zone, Cenozoic rocks are in contact with Precambrian crystalline rocks, including granites. Both the volcanic and granitic materials are considered ubiquitous uranium source rocks. In the pre-basin-fill sequences, preliminary indications are that uranium mineralization is associated with rare, but quantitatively important, carbonized plant debris, fresh-water fetid limestones, and high magnesian carbonate rocks.

Uranium and thorium in placer deposits

In field and laboratory studies of radioactive horizons along the east flank of the Deep Creek Range, Juab County, Utah, R. S. Zech, A. R. Wallace, and J. T. Nash have located anomalous radioactive zones in placer heavy mineral deposits within range-front alluvial fans. These deposits were derived from the Tertiary quartz monzonite rocks to the west. Heavy minerals have been further concentrated in parts of the alluvial fans that have been cut by Lake Bonneville shore line erosion and in the recent arroyos which drain wave-cut benches.

Preliminary analysis of grab samples indicates that uranium and thorium are contained in mona-

zite, sphene, zircon, and allanite. Heavy-mineral abundance in the recent and bench deposits is about five percent. Concentrations range from 20 to 170 ppm for uranium and about five times as much for thorium.

Uranium and thorium content in weathering profiles of the Catahoula Tuff, south Texas coastal plain

The amount and distribution of uranium and and thorium in samples taken from outcrops of the Catahoula Tuff depend on weathering and the proportion of volcanic detritus in the source material. The weathering process depends mainly on climate that ranges from semi-arid in about the southern one-half of the coastal plain to subhumid in the northern one-half. Volcanic material is the main constituent in the Catahoula Tuff of the southern one-half, but the amount of volcanic material in the northern one-half is questionable because none has been identified there. Four weathering profiles on the Catahoula in Duval, Karnes, Washington, and Saline Counties were studied by K. A. Dickinson and have different distributions of uranium, thorium, and other elements. Uranium decreases with depth in the southernmost profile and remains fairly constant in the three northern profiles. Thorium generally decreases with depth except in the Duval County profile. Thorium is probably high near the surface because of its concentration in resistate minerals. Uranium variations, on the other hand, are controlled more by the leaching process. Leaching of uranium seems to have occurred only in the southernmost, Duval County, profile as indicated by a high Th/U ratio at the base of the profile. The degree of uranium leaching and the original amount of uranium in the Catahoula are important parameters in evaluating uranium resources and exploration targets.

Epigenetic uranium mineralization, Alaska

Uranium averaged 12 ppm in two samples of Tertiary continental sedimentary rock collected by K. A. Dickinson and J. A. Campbell in Alaska. One sample was collected from Peters Creek and the other from Camp Creek in the Susitna Lowlands in the south-central part of the State. These samples, although far below uranium ore-grade, prove, for the first time, that epigenesis has resulted in uranium enrichment in Tertiary sedimentary rocks of Alaska. Both uranium samples were associated with reduction-oxidation interfaces and with siderite.

Uranium in central Colorado soil profiles

Preliminary studies of uranium, thorium, and potassium in soil and weathering profiles developed on Tertiary sedimentary rocks in the Denver area have been carried out by K. A. Dickinson. These studies show that uranium, thorium, and potassium decrease relatively with depth in auger holes up to 1.7 m deep. These diverse elements are believed to accumulate on or near the weathering surface in various resistate minerals. The data also show that the absolute amounts of uranium, thorium, and potassium in the soils increase toward the east, a probable result of the presence of older soil surfaces east of the Denver area. Data were obtained using a gamma-ray spectrometer with a 21.2 in^3 sodium iodide crystal. Each measurement was counted for 2 min, which gave a counting accuracy of about 10 percent. Measurements were made at 30-cm intervals.

Organo-clay complexes in uranium deposits

Iron and aluminum hydroxides on the surface of clay platelets may be the key to the formation of organo-clay complexes associated with tabular uranium deposits. In a model proposed by Christine Turner-Peterson (1977) to explain uranium mineralization in the Newark Basin, it is postulated that humic acids in uranium-bearing sandstones were derived from offshore lacustrine mudstones that interbed with the sandstones. During compaction, the alkaline pore waters (pH 8), containing humic acids and bisulfide, were expelled from the offshore muds into the nearshore sands, where slightly lower pH conditions (7–5) prevailed because of the influence of normal ground water.

Below pH 8, hydroxides on the surface of clay minerals are positively charged; above pH 8, they carry no charge. Organic anions, therefore, would have an attraction to clay surfaces only below pH 8. In the Newark Basin, iron and aluminum hydroxides on clays within the nearshore zone would have carried a positive charge, resulting in attraction for and precipitation of organic anions delivered by the pore fluids that were expelled from the lake muds.

Concomitant pyrite formation also involved the iron hydroxides. Bisulfide ions necessary for pyrite formation traveled along with the humic acids during compaction-induced lateral explusion of the pore fluids from the offshore muds. The humic-rich zone that formed in the nearshore zone subsequently fixed uranium from the ground water. This model accounts for the observed association of uranium, pyrite, humic matter, and clay clasts.

Organic acids on the move

A lacustrine humate model was recently proposed for some of the tabular sandstone-type uranium deposits in the Salt Wash Sandstone Member of the Morrison Formation (Upper Jurassic) of the Colorado Plateau (Peterson, 1977; Turner-Peterson and Peterson, 1978). This model suggests that humic and fulvic acids, generated in the muddy sediments of small lakes, were expelled by compaction or seepage into nearby sandstone beds where they were fixed as tabular humate deposits. Subsequently, uranium in ground water passing through the sandstone was concentrated by the humate into ore deposits. Because the mudstones play such an important role in this model, it would be helpful if evidence was found that the organic acids did, indeed, migrate out of them. Recent studies by Fred Peterson, R. H. Tschudy, and S. D. Van Loenen show that a fairly simple procedure run during routine lab processing for spores and pollen can be used as evidence supporting the idea that the organic acids were originally present in the lacustrine mudstones and subsequently left them.

Humic and fulvic acids can be recognized easily by the dark-brown-to-black stain they leave when a small sample of the rock is placed on filter paper and flooded with a dilute base. Approximately 95 percent of grey mudstone samples of Pennsylvanian, Cretaceous, Tertiary, and Quaternary age that yield palynomorphs (spores and pollen) also yield this stain. In contrast, Salt Wash lacustrine grey mudstones collected near ore deposits yield palynomorphs but consistently show either no stain or, rarely, a very light brown stain on the filter paper, indicating little or no humic and fulvic acids are present. Considering the unusually small quantities of these acids in Jurassic palynomorph-bearing mudstones compared to palynomorph-bearing mudstones of other systems, the best explanation is that the acids were originally present and were subsequently expelled. Although the degree of coloration varies somewhat owing to variations in the composition of the acids, it may be possible to quantify the procedure sufficiently for use in determining the favorability of a region for uranium mineralization by the processes involved in the lacustrine humate model.

Determination of precementation porosity and permeability in sandstones

Research by M. B. Sawyer, C. T. Pierson, A. S. Karma, and H. C. Granger suggests that it may be possible to calculate the precementation porosity and permeability of sandstones from textural studies of the cemented rock. Because the suitability of a sandstone as a uranium host rock is usually related to its porosity and permeability at the time of uranium deposition, a technique is being developed to predict what the porosity and permeability of a sandstone might have been shortly after deposition and prior to cementation. Using the image-analyzing computer and other physical methods, the postcementation porosity and permeability, the content of acid-soluble cement, the grain-size distribution, the grain-shape distribution, and the packing of a sandstone sample can be determined. A formula used by Manger, Cadigan, and Gates (1969) relates the postcementation permeability to the above listed parameters. Using this formula and knowing the amount of acid-soluble cement in the sample, preliminary results suggest that it may be possible to determine the precementation permeability. The precementation porosity can be calculated knowing the postcementation porosity and the amount of acid-soluble cement.

Some applications of thermoluminescence to uranium prospecting

C. S. Spirakis has shown that thermoluminescent-glow curves (plots of intensity of thermoluminescence versus temperature) of quartz and feldspar grains from the vicinity of a Wyoming roll-type deposit are suggestive that the mineralizing process produces a systematic change in thermoluminescence around these deposits. A comparison between glow curves of samples from locations which are believed to be former positions of the migrating roll front and glow curves of samples which were never mineralized indicates that the former areas of mineralization are characterized by an increase in higher temperature thermoluminescence relative to lower temperature thermoluminescence. The increased importance of higher temperature thermoluminescence in formerly mineralized samples can be detected with ratios of thermoluminescence from different temperature ranges or with glow curves. Both ratios and glow curves may be useful indicators of roll-type uranium deposits. A preliminary study of the thermoluminescence of quartz and feldspar grains in soils developed over uranium-mineralized veins suggests that glow curves might also be used as indicators of vein-type uranium deposits. Thermoluminescence may be particularly useful in locating veins that have been leached of uranium along their outcrops.

Uranium potential of Sierra Madre and Medicine Bow Mountains, Wyoming

Geologic studies by R. S. Houston, K. E. Karlstrom, and P. J. Graff indicate that pyritic, quartz-pebble conglomerate underlies large areas of the northwest Sierra Madre and northern and northeastern Medicine Bow Mountains, Wyoming. Study of unoxidized core samples from the One Mile Creek area in the Medicine Bow Mountains show that, at least locally, the conglomerate contains an order of magnitude rather than the 150 ppm uranium detected in surface samples. This suggests that the area is a good target for uranium exploration, but does not prove the existence of ore deposits. The conglomerate beds are in radioactive sericitic quartzite of both the "Phantom Lake group" and "Deep Lake group" (informal names) of the Sierra Madre and Medicine Bow Mountains. These metasedimentary rocks are believed to be Early Proterozoic in age and are bracketed between about 2,700 m.y. and 1,800 m.y. (Hills and others, 1968; Divis, 1976). The conglomerate is fluvial and is believed to have been deposited in braided streams. Veinlets containing up to 1,000 ppm uranium in granite that cuts metasedimentary succession suggest that uranium may have been mobilized and redeposited in faults and shear zones.

Obsidian, perlite, and felsite as sources of uranium: an experimental study

The relative rates of uranium removal from glassy and crystalline volcanic rocks have been experimentally determined by R. A. Zielinski. Well-characterized samples of rhyolitic obsidian, perlite, and felsite from a single lava flow were subjected to carefully controlled open-system leaching by alkaline oxidizing solutions. Pressure, temperature, flow rate, and solution composition were held constant in order to evaluate the relative importance of differences in surface area and crystallinity. Leachate solutions were continuously monitored for concentrations of dissolved uranium and selected additional elements (Si, Li, F, K), and the leached solids were recovered and examined for physical and chemical evidence of attack.

Uranium removal from crushed glassy samples is seen to proceed by a mechanism of glass dissolution in which uranium and silica are dissolved in approximately equal-weight fractions. Rates of release of uranium from glassy samples correlate positively with the surface area of the samples. Uranium removal from crushed felsite is controlled by the variable rates of attack of numerous uranium sites. Initial rapid loss of a small component of the total uranium from crushed felsite reflects selective dissolution of uranium-rich minerals or mobilization of uranium which is weakly bound to mineral surfaces or alteration products. After initial loss of readily soluble uranium, crushed felsite becomes a much less efficient source of uranium than equivalently treated glass.

Leaching results using crushed samples were combined with whole rock permeability measurements to explain the observed depletion of uranium in natural felsites as compared to coexisting obsidian. Permeability differences between massive, nonhydrated obsidian and felsite are apparently great enough to offset the greater time averaged solubility of glassy uranium sites.

Constraints on the genesis of uranium ores in the Midnite Mine, Washington, from geochronologic and lead-isotope investigations

The ores from the Midnite Mine, near Spokane, Wash., are localized in Precambrian metamorphic rocks near the contact with a Cretaceous granitic pluton that has a uranium-lead-zircon age of 76 m.y. Studies by K. R. Ludwig have shown that high-grade, unoxidized ores define a $^{207}Pb/^{204}Pb$–$^{235}U/^{204}Pb$ isochron age of 51 ± 1 m.y., which coincides with that of the overlying Sanpoil Volcanics. The apatite fission-track age of the Cretaceous pluton in the mine has not been reset, which indicates that the uranium ores could not have been formed during a high-temperature ($>150°C$ for $>10^6$ yr) hydrothermal process. It seems likely that the uranium ores were formed as the result of pervasive destruction and redistribution of an earlier low-grade protore by supergene fluids in the Eocene, possibly with thermal or hydrologic influence of the Eocene volcanic rocks and dikes.

Mineralogic residence of uranium in roll-type deposits

From petrographic and electron microprobe analysis of mineralized rock from three roll-type uranium deposits in Texas and from two in Wyoming, R. L. Reynolds has identified similarities and differences in the residence of uranium in deposits of different geologic settings.

In the fine-grained (<2 μm) fraction of each deposit, uranium is associated with clays and titanium-rich phases, both in part formed by in situ alteration of detrital rock fragments and the titanium-rich phases liberated commonly by the sulfidization of detrital iron-titanium oxide minerals.

In the Wyoming deposits, uranium also resides within petrographically observable (>5 μm) uraninite and in other opaque phases closely associated with vanadium and selenium. At present, such occurrences and elemental associations are not documented in any of the three Texas deposits.

The nature and process of uranium fixation, depositional environment and composition of the host rock, including presence or absence of organic debris, and solution geochemistry are among the many possible influences that may be responsible for the observed differences.

Identification of possible uranium province in central Wyoming through radio-element distribution in crystalline basement rocks

Detailed studies of granitic rocks from the Granite Mountains (Rosholt, Zartman, and Nkomo, 1973; Stuckless and Nkomo, 1978) and preliminary studies of some granitic samples from the Owl Creek Mountains (Nkomo and others, 1978) and Laramie Range (Nkomo and Rosholt, unpub. data) suggest that the region of central Wyoming has been a uranium province since Archean time. Thorium contents of Precambrian granites of this region are generally anomalously high as compared to contents cited as typical for granites (Rogers and Adams, 1969). Uranium contents of surface samples are generally not anomalously high, but isotopic evidence shows that most samples have lost much uranium during the Cenozoic. Most thorium-uranium ratios measured in the Granite Mountains are >5, but calculations based on radiogenic ^{208}Pb show that the thorium-uranium ratio would be <3 if uranium had not been lost. It is proposed that thorium contents of the crystalline basement rocks may be a better indicator of uranium province than uranium contents and that thorium-uranium ratios may be useful indicators of uranium loss. Finally, because the region of central Wyoming has been a uranium province for at least 2,600 m.y., deposits with ages of Archean to Holocene may be reasonably expected within and adjacent to this region.

Coffinite ores of the Tony M mine in Utah

Preliminary petrographic study by R. I. Grauch of a suite of samples that straddles a 0.5-m thick ore horizon in the Tony M mine in Utah indicates that most of the uranium is present as coffinite and is associated with organic material. The coffinite does not replace the organic material but fills pore spaces in the plant debris. In rare instances the cellular structure of the plant material is well preserved. However, most of the debris shows the effects of compaction perpendicular to bedding and was apparently extended parallel to bedding. Because the coffinite is restricted to cell spaces and because it mimics the convoluted structure attributed to the compaction of the organic material, it is suggested that the coffinite formed soon after deposition of the host organic material before and (or) after dewatering.

Computer modeling of ore-forming processes

During computer modeling studies by C. G. Warren and H. C. Granger of the genesis of uranium roll shapes, it was found that typical roll shapes could be produced by the following two unrelated processes: (1) channeled groundwater flow and (2) leakage of dissolved oxygen across the boundaries of the aquifer. Either process, if not moderated by the diffusion of oxygen, will create a highly discontinuous and irregular oxidation front. The regularity of the oxidation front is an indication of the importance of diffusion to the ore forming process. The numerical relation between shape and either flow or leakage theoretically offers a basis for calculating groundwater velocities.

Carbon-13/carbon-12 isotope fractionation of organic matter associated with uranium ores induced by alpha irradiation

Analyses by J. S. Leventhal of stable carbon isotopes from two sample suites from sandstone uranium (tabular) ores have shown interesting variations. The uranium ore sampled occurs in medium- to fine-grained nonmarine sandstones of the Upper Jurassic Westwater Canyon Sandstone Member of the Morrison Formation within the Grants mineral belt of northwest New Mexico. The ore is the trend or tabular type, where the ore forms blankets that are literally suspended in sandstone units. Individual orebodies range from a little less than 1 to 15 m thick, 5 m to somewhat more than 100 m wide, and 20 or 30 m to at least 1,000 m long. The richer parts of the ore commonly contain more than 1 percent uranium. The ore is intimately associated with structureless organic matter that is insoluble in organic solvents, weak acids, and bases. The ore and organic matter surround sand grains and fill interstices between grains. Five samples from each suite collected in a vertical traverse have an arrangement of one low-grade ore sample above, three ore samples, and another low grade ore sample below. The low-grade samples at the borders of the ore show $\delta^{13}C$ values of −22.7 to −26.4 per mil, which are typical of sedimentary organic matter. The

lightest values are similar to those reported for terrestrial kerogens and humic material. The ore samples have carbon isotopic values that range from −16.9 to −19.6 per mil, that is, approximately 5 to 8 per mil heavier than the low-grade samples. These values are not typical of sedimentary organic matter from the nonmarine environment and the organic material in these samples all appears to derive from an epigenetic introduction of originally soluble organic matter. Because the organic matter and uranium were deposited in Late Jurassic time, the uranium in equilibrium with its daughters has deposited a dose of 10^{11} rads, which was absorbed mainly in the intimately associated organic matter. The decay of each atom of uranium-238 to lead accounts for eight alpha particles, six beta particles, and associated gamma rays. Bond breaking by alpha radiation and alpha recoil of the nucleus are most effective in the immediate vicinity of the uranium atom, whereas bond breaking by beta and gamma radiation will be diffused over a much larger volume. The high linear energy transfer of the alpha radiation gives a high density of primary ionizations that are so close together that they may be considered as continuous. This energy transfer and ionization leads to many broken bonds, radicals, ions, and excited molecules in a small volume where preferential formation of carbon-13-deficient volatile products can occur to produce the observed isotope effect in the bulk organic material. It is also likely that the radiation acts to catalyze the "fixation" of the uranium ore in the organic matter by creation of chemically reactive reductants that reduce the soluble uranyl (VI) species to insoluble UO_2. The radiation also makes the organic material more refractory (less soluble and oxidizable), and it protects the uranium ore from remobilization or solution.

Scintillator used as fast neutron detector

F. E. Cecil (Colorado School of Mines) and others have measured the interaction length for the production by 3 and 14 MeV neutrons of the 57 keV nuclear gamma ray in NaI (Tl) scintillator. These interaction lengths ($0.008 \pm .001$ and $0.005 \pm /.001$ cm^{-1}, respectively) indicate that NaI (Tl) scintillator can be used as a high-efficiency fast neutron detector.

Uranium source potential estimated from radium and radon concentrations in flowing water

The concept of uranium source potential using uranium, radium, and radon in flowing water was proved feasible by R. A. Cadigan in a study using data from a hydrothermal springs area that lies along the Wasatch fault zone northeast of the Great Salt Lake in Utah. Radium and radon are more mobile in hydrothermal spring environments than are their parent nuclides. They are rapidly transported under pressure through fracture systems for distances as great as hundreds or thousands of meters. In the seven springs used in the study, radium values exceed the equilibrium amount with uranium by 4 to 25,000 times. Radon values exceed the equilibrium amount with radium by 11 to 2,100 times. Spring discharge values range from 400 to 13,600 L/min. The spring waters contain from 3 to 220 picocuries per liter (pCi/L) of radium and 500 to 6,500 pCi/L of radon. Radium in excess of equilibrium amounts is produced at the rate of about 2,200,000 pCi/min, and excess radon is produced at the rate of about 45,000,000 pCi/min by the seven springs. Calculated total uranium required in the hydrothermal conduit system to support such production of radium and radon is approximately 170,000 metric tons.

This use of quantitative exploration data does not define an exploration target, but it does identify the magnitude of the uranium sources in the area. Rate of movement of the spring waters and their hydrothermal nature suggests that they are migrating vertically along faults and joints. Whether or not the uranium can be extracted economically depends upon the degree of dispersal and depth of the uranium mineralization, both of which are unknown.

Radium and uranium in mineral springs

Analysis of data on radium, uranium, temperature, pH, and specific conductance for 116 mineral springs in 8 Western States (Arizona, California, Colorado, Idaho, Nevada, New Mexico, Utah, Wyoming) shows that a significant positive correlation exists between radium and conductance and that significant negative correlations exist between conductance and pH, radium and pH, and uranium and temperature. In other words, radium mobility relative to uranium is favored by water with high specific conductance, high temperature, and low pH.

The correlation between radium and conductance is probably due to the effort of total ionic strength on the solubility of salts, such as barium sulfate, with which radium can coprecipitate. The correlation between conductance and pH is probably related to the ionic composition of the waters. The combination of these two relationships yields a correlation between radium and pH. The correlation

between uranium and temperature may be related to the complexing of uranium with biocarbonate, which is more soluble in cold water.

The strongest correlation is between radium and conductance. By examining the ratio between these two parameters, one can see which springs have a radium concentration that is higher than can be accounted for by the relationships with conductance. Unmeasurable parameters, such as the presence of uranium-rich source rocks, may be affecting these radium concentrations.

Source for the anomalous uranium in surface waters of the Ojo Caliente area in New Mexico

Additional fieldwork by K. J. Wenrich-Verbeek in the Ojo Caliente-La Madera area of New Mexico has shed more light on the possible source of the anomalous uranium in waters of the numerous springs in the vicinities of Candad de la Cueva and La Madera. The Tertiary Santa Fe Formation and Quaternary surficial deposits of this area contain no apparent anomalous uranium concentrations; yet, overlying massive travertine deposits of Tertiary and Quaternary age contain gamma counts that are 3 to 6 times background. This suggests that the springs in this area have been bringing high-uranium waters to the surface since the beginning of deposition of the travertine. The source of the uranium appears to be the Precambrian rocks, which underly the Santa Fe in the area. Geologic evidence suggests that these uranium-bearing springs are coming up along contacts of the Ortega Quartzite of Precambrian age. Precambrian rocks north of La Madera in the Tusas Mountains, although riddled with uranium-bearing pegmatites, are the source of springs of low-uranium concentration. This suggests that the Precambrian rocks to the south contain uranium in more soluble form.

Helium detection for uranium exploration

Helium detection surveys conducted by G. M. Reimer and C .G. Bowles near Edgemont, S. Dak., near uranium deposits have shown anomalous helium concentrations in well waters. The waters are of reducing character and have low capacity to dissolve uranium from surrounding rocks, and so do not contain uranium in anomalous concentrations. Helium, a product of radioactive decay of uranium, however, is an inert gas unaffected chemically by the character of the water. Thus, helium in ground water may show the presence of nearby uranium when the uranium itself is not present in the same water. Helium analysis of waters is, therefore, an important addition to any geochemical exploration program. The helium data can reveal important information on areas that would be otherwise overlooked in exploring for uranium.

Value of radon measurements for uranium prospecting

Resurgence of uranium prospecting during the past decade has renewed interest in the measurement of radon-222, a gaseous decay product of uranium, to locate uranium deposits. Some advocates of radon measurements contend that radon anomalies in soil gas are the result of direct movement of radon from uranium orebodies more than 100 m below; such anomalies are thought by other people to be fortuitous. After a comprehensive review of publications bearing on radon movement in the ground, A. B. Tanner has concluded that a sufficient number of radon anomalies are associated with buried uranium deposits to imply a causal relation, but that the anomalies are more likely to be caused by movement of uranium and radium in ground water.

Relative uranium scavenging affects of organic matter, clays, and iron and manganese oxides

Present knowledge indicates that uranium is scavenged by organic material, clays, and iron and manganese oxides. Research by K. J. Wenrich-Verbeek into the associations of uranium in stream sediments suggests that the scavenging affect of organic material is many times more significant than that of iron and manganese oxides and clay. FeO, MnO, and Al_2O_3 do not show significant positive correlation with uranium in stream sediments. In fact, in the Ojo Caliente area of New Mexico, where organic carbon shows a highly significant correlation with uranium, Al_2O_3 shows a significant negative correlation; that is, samples which contain more clay have lower uranium concentrations. The correlation of FeO with uranium is somewhat greater than that of MnO or Al_2O_3, yet none of these three appears to contribute significantly to the uranium concentration in most stream sediments. Water samples collected in conjunction with all stream sediments also show interesting associations between uranium and some of the elements. Of all the trace elements, uranium is most frequently associated with arsenic in natural waters. It is possible that uranium is complexing in water with an arsenate anion. Although recent thermodynamic studies have shown that PO_4 significantly complexes with uranium (Langmuir, 1978), results from this project indicate that with the normally low PO_4 content of natural

waters and the consistent pH range of 6 to 9, the effect of PO_4 on uranium is almost negligible in most waters.

Relationship of modern ground-water chemistry to the origin and rereduction of a south Texas roll-front uranium deposit

Modern genetic models for roll-front uranium deposits demand that the ore-forming process involve incursion of oxygenated uranium-bearing ground water into reduced (pyrite- and (or) organic-bearing) rock. This process produces an altered tongue of rock updip from ore that contains ferric iron in the form of hematite or limonite. M. G. Goldhaber, in collaboration with R. L. Reynolds and R. O. Rye, has established from petrographic and stable-isotope studies on a deposit in Live Oak County, Texas, that the orebody has been secondarily rereduced such that the altered tongue now contains iron disulfide instead of iron oxide. This rereduced zone contains dominantly isotopically heavy pyrite, in contrast to ore and protore which contains isotopically light maracasite. Modern ground water at the stratigraphic level of the ore-host sandstone contains dissolved sulfide. The question thus arises whether the rereduction was caused by this modern sulfide. Accordingly, studies were carried out on the sulfate and sulfide content and isotopic composition of this ground water. Sulfate concentrations fall in the range 3 to 7 millimolar. The largest values occur adjacent to the Oakville fault, which is located on the downdip side of the deposit ahead of the roll. The isotopic ratio of this sulfate is very light near the fault (−17.2 per mil) and increases away from the fault. Sulfide is very light (−56 per mil) near the fault and likewise becomes heavier away from the fault (−39 per mil). These stable-isotope trends are best explained by near-surface processes involving oxidative weathering of iron disulfide to produce the light sulfate and subsequent bacterial reduction of this sulfate to isotopically light sulfide. The isotopic composition of the present day sulfide is grossly different from that of the iron disulfide in the altered tongue which, for the most part, is greater than 0 per mil. The rereduced iron disulfides are more closely matched by sulfide from the deep Edwards Limestone (Cretaceous) reef trend which underlies the deposit and has an isotopic value of +12 per mil. We postulate, therefore, that rereduction was caused by sulfide leaking up the Oakville fault from depth and moving out into the uranium host sand and that present day ground water chemistry is unrelated to this process.

Porous media model studies of sandstone-type uranium deposits

The penetration and precipitation of humic acid into a porous-media model saturated with aluminum potassium sulfate solution were studied under laboratory conditions by K. K. Sunada and F. G. Ethridge (Colorado State Univ.). In particular, the effects of variable flow rates, porous media layering, mudstone lenses (baffles), and density differences were evaluated. The aluminum and humic solutions were used only for convenience in studying precipitation reactions and ground-water flow patterns and not to simulate a specific ore-forming process.

It was found that a distinct band of precipitate formed parallel, as well as perpendicular, to the flow path at the interface between the two solutions. Results indicate that these precipitates fill pores and reduce hydraulic conductivity and that the deposits were larger where contact time between solutions was larger; for example, parallel to the flow path. Under conditions where the flow rate of humic acid was increased, the precipitate was dissolved back into solution and redeposited at a new interface. However, if the flow rate was decreased the original deposit remained and a new precipitate formed, thus providing two distinct precipitate zones. In experimental conditions characterized by multiple porous-media layers, the precipitate is richest in the more permeable layers, and flow lines converge toward these layers. Baffles used to simulate mudstone lenses caused changes in the flow configuration. Density differences between the solutions appear to have little effect on the distribution of the precipitate. Significant diffusion effects have not been observed because of the relatively high flow rates used in the experiments, as compared to flow rates in natural ground-water systems.

These initial experiments provide a visual record of the reactions between two solutions and information which may prove useful in predicting the shape and distribution of tabular as well as roll-front-type epigenetic sandstone uranium deposits. More importantly, they provide a means of assessing the relationship between such deposits and ground-water-flow patterns at the time of mineralization. Under the experimental conditions investigated, such as high flow rates, the most pronounced precipitates occur parallel to flow. Such conditions might be the case for some of the coarse-grained, highly permeable alluvial fan deposits of the Gas Hills district in Wyoming. In contrast, it is possible that under conditions of low-flow rates associated with finer grained, less permeable sandstone beds, the most

pronounced precipitates would occur at the base of the ore deposit.

Molybdenum in catclaw mimosa as a possible indicator of uranium

Results of a biogeochemical study by J. A. Erdman, J. M. McNeal, and C. T. Pierson at a uranium prospect on the eastern margin of the Marfa Basin, Texas, suggest that molybdenum may be a pathfinder element for uranium occurrences.

The stratigraphic sequence of Tertiary volcanic rocks at the study site consists of the tuffaceous "Pruett Formation" overlain by the dense, highly fractured "Crossen Formation" (a trachyte). The "Crossen" trachyte, in turn, is unconformably overlain by the "Sheep Canyon Formation," composed of a thick lacustrine unit and overlying dense basalt of variable thickness. At the Anderson Ranch prospect, uranium occurs in lignite interbedded with a lacustrine limestone (the lacustrine member of the "Sheep Canyon Formation" of Eocene(?) or late Eocene age).

Uranium concentrations in the fruit pods of *Mimosa biuncifers* (catclaw mimosa), an extremely thorny desert shrub, were mostly below the limits of detection (0.4 ppm in the ash). The only detectable levels occurred in samples from plants that grew on the "Crossen" trachyte. It was the molybdenum concentrations in the plant tissue, however, which provided the most useful data and showed the greatest contrast amount in the stratigraphic units. Molybdenum concentrations were lowest in plants sampled on the basalt, intermediate in those sampled on the lacustrine unit and the "Pruett Formation," and generally highest on the "Crossen Formation." Molybdenum levels in plants sampled from the trachyte were as much as 50 times (700 ppm) those in samples from the basalt. Associated with the high molybdenum were anomalous concentrations of selenium. A prominent set of fracture joints in the "Crossen" trachyte may have been filled by the uranium, molybdenum, and selenium that were leached from the overlying lacustrine source rock.

The main purpose of the study was to see whether this desert shrub might be used to locate uranium mineralization in the lacustrine unit concealed by the basalt. Molybdenum concentrations were uniformly low in all shrubs sampled from the basalt unit, even though the thickness ranged from about 6 to 40 m. Either the basalt was too impervious to root penetration or the root systems were shallower than anticipated. Despite this, catclaw mimosa appears to be responsive to mineralization at or very near the surface.

Geophysical study of gneiss domes and two-mica granites

An interpretation by J. W. Cady of gravity and aeromagnetic maps over the Omineca crystalline belt in northeastern Washington and southern British Columbia shows that individual gneiss domes are typically marked by local gravity highs and the high-grade gneiss terrain is marked by a regional gravity high. Gneiss domes and two-mica granites, both of which are suspected of being uranium source rocks, are marked by aeromagnetic lows, in contrast to the more magnetic hornblende-biotite granites. Crustal modeling, using gravity, refraction seismic, and geologic data, is permissive of the hypothesis that the core metamorphic complexes are the surface expression of a zone of dense infrastructure that makes up the top 20 km of the crust within the crystalline belt. A zone of steep gravity gradients lying close to the Purcell Trench probably marks the eastern border of the zone of dense infrastructure.

Thorium and rare-earth resources occur in disseminated deposits in the Bear Lodge Mountains in Wyoming

Studies by M. H. Staatz have recently shown that large, disseminated deposits of thorium and rare earths in the Bear Lodge Mountains occur in the core of the Bear Lodge dome. These deposits occur in a complex Tertiary phonolite-trachyte intrusive body where the central part of the dome has been altered and fractured. The fractures are filled with veinlets containing thorium and rare earth minerals. The altered area can be outlined by its contrast in radioactivity. Surface sampling within the area of highest radioactivity indicates the presence of three areas in which the thorium content exceeds 200 ppm. These three areas underlie 660,000, 790,000, and 770,000 m^2 and have an average ThO_2 content of approximately 0.023, 0.042, and 0.035 percent, respectively. Total rare-earth oxide content of these three areas is 0.75, 1.70, and 1.35 percent.

Thorium resources in the Wet Mountains of Colorado

A total of 202 samples collected by T. J. Armbrustmacher, from thorium-bearing veins and fracture zones in the Wet Mountain area of Colorado have been analyzed for radium equivalent uranium (RaeU) and thorium by gamma ray spectrometric measurements. The samples average 0.46 percent ThO_2, ranging from 0.00075 to 10.2 percent. The maximum RaeU value is 0.036 percent, but samples

usually contain less than 0.005 percent. The average thorium-uranium ratio is 64.

The total ThO_2 reserves of the Wet Mountains area is 66,700 tons. Probable potential resources are 91,900 short tons of ThO_2.

Cost analyses developed by the U.S. Bureau of Mines were done for 29 veins and fracture zones whose reserves and probable potential resources total at least 35,000 tons of ThO_2. Thoria could be produced from 13 of these veins at a cost of less than $30 per pound, in seven of them at a cost of $30–50 per pound, and the remaining at a cost greater than $50 per pound. The average grade of the veins and fracture zones containing ThO_2 producible at less than $30 per pound is 0.51 percent, and the average grade producible at $30–50 per pound is 0.11 percent ThO_2.

New thorium resource numbers calculated for vein-type occurrences

Recent thorium resource assessment studies of vein-type occurrences of ThO_2 by M. H. Staatz, T. J. Armbrustmacher, and J. C. Olson in seven mining districts in Idaho, Montana, Colorado, Wyoming, and California have shown 129,000 metric tons of ThO_2 in indicated reserves and 327,000 metric tons in inferred reserves. Eighty-seven percent of the reserves occurs in the Lemhi Pass district of Idaho and Montana and the Wet Mountains district of Colorado. Remaining reserves are present in veins of the Powderhorn district of Colorado, Hall Mountain and Diamond Creek districts in Idaho, Bear Mountains district of Wyoming, and the Mountain Pass area of California.

Veins constitute the highest grade thorium resource in the United States. Although over 300 thorium veins have been identified, most of the reserves in the two districts are contained in only 10 veins.

USGS quadrangle evaluation for Department of Energy

A major commitment was undertaken by the USGS in January 1978 in support of the Department of Energy National Uranium Resource Evaluation (NURE) program. Investigations aimed at evaluating the favorability of 42 NTMS 1° × 2° quadrangles for potential uranium deposits were begun. Work in 1978 included the completion of Phase I studies, including preparation of maps showing geology, uranium occurrences, and land status in the quadrangles, as well as annotated bibliographies. During the year, owing to a restructuring of the NURE program and establishment of new priorities and deadlines, work in 19 quadrangles was recessed, and the USGS effort was concentrated in the remaining 23 quadrangles. However, Phase-I products were completed for 38 of the original 42 quadrangles. As Phase-I planning and compilation work was finished, field evaluation studies were started on the second half of the year. Many uranium occurrences were visited in order to gather descriptive up-to-date information of the character and geology of the occurrences and to take samples for multielement geochemical analysis.

Uranium potential in Rio Grande rift basins

The presence of favorable lithofacies, uranium occurrences, and nearby uranium-rich volcanic source rocks suggests that the several Tertiary sedimentary basins alined along the Rio Grande rift in the Aztec, Albuquerque, and adjacent Socorro 2° NURE quadrangles are favorable uranium exploration target areas. Locally thick (up to 4,500 m ±) sequences of sedimentary volcaniclastic conglomerates, sandstones, and finer-grained rocks are present to serve as conduits and potential host rocks for uranium deposits. Locally these rocks are organic rich and contain scattered associated radioactive anomalies in outcrops. In conjunction with favorable parameters contained in the sedimentary units, a number of anomalous uranium occurrences in adjacent volcanic terrains attest to the availability of leachable uranium to serve as a source for sedimentary deposits.

Complex facies relationships, excessive drilling depths, and lack of sizeable discoveries in outcrop have, in the past, contributed to the lack of exploration activity within the rift basins.

Uranium resources in the Grandfather Mountain Window in North Carolina

Basement rocks exposed in the Grandfather Mountain, chiefly granitic gneiss and augen gneiss dated at 1,000 to 1,100 m.y., contain more than 15 uranium occurrences and numerous radioactive anomalies in veins and shears. The gneisses generally have radioactivity about four times normal for rocks of this composition. Interpretation by J. T. Nash of the uranium occurrences, widespread radioactivity, the Proterozoic age of the gneisses, and the presence of Proterozoic unconformity suggests that this area is favorable for uranium deposits, possibly of the unconformity-vein type. However, according to current geologic understanding of the area, there are several unclear or contradictory features when considered in the light of genetic models proposed for the large Australian and Canadian prototypes. First, the prototype deposits are in metasedimen-

tary sequences, whereas the gneisses here are considered to be metaplutonic (Bryant and Reed, 1970). However, the presence of graphitic zones and phyllonite of complex origin suggest that some of the gneiss could have a sedimentary protolith. Second, metacarbonate rocks are not known in the Grandfather Mountain area, but are important ingredients in the geology of the prototype deposits. Third, retrograde metamorphism is not as extensive as in the prototypes. Fourth, the known occurrences in the window can not be related with certainty to the unconformity. Large deposits might be present in areas with more graphite, more retrograde metamorphism, and spatially closer to the unconformity.

GEOTHERMAL RESOURCES

U.S. geothermal resource assessment updated

An updated geothermal resource assessment of the United States was prepared in cooperation with the U.S. Department of Energy (Muffler, 1979). The new assessment represents improvements in the estimates given in the first comprehensive national geothermal resource assessment (White and Williams, 1975). In general, the new assessment substantiates the basic rationale and overall conclusions of the first assessment. The total energies calculated are essentially the same, although substantially smaller energies were calculated for some of the larger hydrothermal convection systems. Both assessments distinguish between geothermal energy in the ground to a specified depth (resource base in the first assessment and accessible resource base in the new assessment) and the thermal energy that could be extracted and used at some reasonable future time (the resource).

The new assessment divides the accessible resource base into two broad types of geologic environment according to the dominant mode of heat transport, regional conductive environments and igneous-related systems. Thermal energies are given in 10^{18} joules (J); 10^{18} J $\approx 10^{15}$ Btu = 1 quad.

Diment and others (1975) estimated that in regions of conductive heat flow the amount of thermal energy stored at temperatures above mean annual surface temperature in the outer 10 km of the United States is about $8{,}000{,}000\times10^{18}$ cal ($33{,}000{,}000\times10^{18}$ J). According to J. H. Sass and A. H. Lachenbruch (1979), this figure would not be significantly changed if the 1975 calculations were repeated using the additional heat-flow data now available. The figure for regional conductive environments includes the thermal energy in geopressured basins, sedimentary basins at hydrostatic pressure, and hydrothermal convection systems unrelated to young igneous intrusions. This figure is an upper limit to any discussion of geothermal energy and cannot be used directly to estimate usable thermal energy.

R. L. Smith and H. R. Shaw (1975) estimated the thermal energy contained in young igneous systems to a depth of 10 km in the United States on the basis of a model of conductive cooling since a time represented by the age of the youngest silicic extrusion of each system. Smith and Shaw (1979) reevaluated this model in the light of recent studies of the effects of hydrothermal cooling in and around magma bodies and conclude that it is still valid. They estimated the thermal energy in evaluated young igneous systems to be $101{,}000\times10^{18}$ J, little changed from their 1975 estimate. The total thermal energy in both evaluated and unevaluated igneous systems was estimated to be at least an order of magnitude greater than the estimate for the evaluated systems, or approximately $1{,}000{,}000\times10^{18}$ J. It should be emphasized that these figures do not represent an inventory of measured thermal energy, but instead are estimates based on a model.

Resource estimates (Muffler, 1979) were made for two types of geothermal systems, (1) hydrothermal convection systems $\geqq$ 90°C to depths of 3 km and (2) geopressured fluids present in the northern Gulf of Mexico basin (onshore and offshore) to depths of 6.86 km.

C. A. Brook, R. H. Mariner, D. R. Mabey, J. R. Swanson, Marianne Guffanti, and L. J. P. Muffler (1979) made a detailed inventory of thermal energy to a depth of 3 km in identified hydrothermal convection systems with reservoir temperatures $\geqq$90°C and arrived at a figure of $1{,}650\times10^{18}$ J. The thermal energy in undiscovered hydrothermal convection systems to a depth of 3 km was estimated to be $8{,}000\times10^{18}$ J, giving a figure of $9{,}600\times10^{18}$ J for the total accessible resource base of hydrothermal convection systems $\geqq$ 90°C and a total resource of $2{,}400\times10^{18}$ J of thermal energy producible at the wellhead. For both identified and undiscovered systems having reservoir temperatures of 90° to 150°C, the total beneficial heat was estimated to be between 230 and 350×10^{18} J. For identified and undiscovered systems having reservoir temperatures greater than 150°C the electrical energy was calculated to be between 95,000 and 150,000 MWe for 30 years.

R. H. Wallace, Jr., T. F. Kraemer, R. E. Taylor, and J. B. Wesselman (1979) estimated the total thermal and dissolved methane energy contained in the geopressured fluids of the entire northern Gulf of Mexico basin, both onshore and offshore, to depths of 6.86 km to be $170{,}000 \times 10^{18}$ J. Their estimate, based on data from over 3,500 wells, in general subtantiates the preliminary estimate of Papadopulos and others (1975). Applying the recoverability analysis of Papadopulos and others (1975), Wallace and others (1979) estimated that the total recoverable energy from both the thermal and dissolved methane components ranges from 430×10^{18} J under plan 3 (controlled development with limited pressure reduction and subsidence) to $4{,}400 \times 10^{18}$ J under plan 2 (depletion of reservoir pressure).

The locations of other sedimentary basins of the United States where geopressured fluids are known or inferred to exist are shown; however, knowledge of these geopressured environments is scanty and no thermal estimate was made.

E. A. Samuel (1979) made a preliminary evaluation of low-temperature (less than 90°C) geothermal waters of the United States. A quantitative estimate of the low-temperature accessible resource base was not made because of inadequate and often conflicting data sets. However, areas favorable for discovery and development of low-temperature geothermal waters at depths less than 1 km are depicted on a map in text figures.

L. J. P. Muffler, (1979a) discussed the problem of assessing the accessible resource base for hot-dry-rock and concluded that it is not now possible to make such an evaluation because of insufficient available information on porosity, permeability, and other properties at depth.

World geothermal energy producers canvassed

Installed geothermal generating capacity of the world is about 1,500 MWe, and from 1941 to 1978 has been increasing at a rate of about 7 percent a year, equivalent to a 10-year doubling time. The United States capacity has increased more rapidly, from 0 in 1960 to 502 MWe in 1978, but is entirely from the huge vapor-dominated system, The Geysers, in California. D. E. White canvassed all present and future geothermal producers to determine firm commitments for increased capacity. If these "commitments" prove valid, 1,900 MWe of new capacity will be on line by 1982, representing a doubling of present capacity in only four years. Of special significance is the fact that world-wide efforts to use the hot-water systems are proving successful. Production from these systems is expected to surpass that of vapor-dominated systems by 1982.

Non-electrical uses of low-temperature geothermal energy (less than 150°C) is increasing rapidly, but individual uses tend to be small and diverse in nature.

Use of hydrogeologic mapping techniques in identifying potential geopressured-geothermal reservoirs

R. H. Wallace, Jr., R. E. Taylor, and J. B. Wesselman (1977) presented ten hydrogeologic maps and explanatory text to (1) facilitate the assessment of geopressured-geothermal energy resources, (2) aid in understanding the origin, migration, and accumulation of hydrocarbons, and (3) help in safely managing underground storage of liquid wastes in the Gulf Coast area. The maps show variations of selective fluid-pressure gradients, temperature, and salinity surfaces by depth contours for all or part of five counties in southern Texas. Techniques used were based primarily on data obtained from about 1,000 electrical logs. Analysis, interpretation, and presentation of these data were performed with the aid of computers and an automatic plotter. Pressure, temperature, and salinity maps reflect variations in physical and chemical characteristics of subsurface fluids, mainly water, with depth. These interpretations will aid in understanding hydrologic, hydrodynamic, and hydrochemical processes occurring in deep young sedimentary basins. The geologic framework, especially formation geometry, determines avenues and rates of fluid movement. Gross lithologic changes appear as broad upwarps or downwarps of the pressure, temperature, and salinity surface. Localized highs and lows on these surfaces near fault traces usually represent upward discharges of compaction effluents from greater depths. The hydrogeology of the system is best appraised by concurrent analysis of each parameter, as they are complexly interrelated.

Large, low-temperature geothermal resource in paleozoic rocks of South Dakota

Analysis of available data by L. W. Howells indicated that the Madison Group and other aquifers in Paleozoic strata constitute a large, low-temperature geothermal resource that underlies more than 100,000 km^2 of South Dakota. Throughout their extent in the State, except within 16 to 40 km of their respective outcrops in the Black Hills, aquifers in rocks of Paleozoic age contain water with a known temperature range of 35° to 121°C.

The total volume of water stored in these "hot-water" aquifers is estimated to be more than 10^9 m^3.

The amount of energy stored in these formations is estimated to exceed 6×10^{21} J.

The geochemistry of the water is important to possible development of these aquifers for geothermal energy. In the southern 40 percent of the State, water is of the calcium, magnesium-sulfate type and has a dissolved solids concentration of less than 1,200 mg/L. From this area and from near the Black Hills, the dissolved solids range from 1,200 mg/L of calcium, magnesium-sulfate-type water to more than 120,000 mg/L of sodium-chloride-type water near the North Dakota border in the Williston Basin.

Geothermal resource evaluation, Minarets Wilderness, California

Analysis by R. A. Bailey (1978) of presently available geological, geochemical, and geophysical data suggests that the Minarets Wilderness and adjacent roadless areas contain no significant geothermal resources.

The small size and dispersed distribution of Cenozoic volcanic centers within the area suggest that they did not have a substantial effect on the near-surface thermal regime, and their 3- to 9-million-year-old age suggests that the small thermal effect they may have had has since dissipated. The nearest large crustal heat sources, the magma chambers at Long Valley and Mono Craters east of the wilderness, are too distant to presently affect near-surface heat flow in the wilderness.

The thermal anomaly at nearby Devils Postpile, expressed by the hot springs at Reds Meadow and the moderately high-heat flow (3.75 mcal/cm^2/s) in drill hole DP (Lachenbruch and others, 1976), is probably related to small Holocene basalt centers east of the wilderness and is probably of limited extent. Chemical analyses of the Reds Meadow hot-springs waters suggest that they are mixed waters with a small hot-water component coming from depths in excess of 2 km. Geochemical equilibration temperatures of the hot-water component range from about 160°C to 65°C, depending on the chemical geothermometer used, but the lower temperatures are considered better estimates.

Geophysical studies indicate the presence of co-extensive gravity and aeromagnetic anomalies in the general vicinity of the Devils Postpile heat-flow anomaly, but they appear to have no geothermal significance. A small negative gravity residual is apparently related to a low-density Cretaceous granitic mass in the Sierran basement, and a negative aeromagnetic anomaly is produced by topographic effects related to the broad deep valley of the Middle Fork of the San Joaquin River; thus, the spatial coincidence of the geophysical anomalies is fortuitous.

REGIONAL GEOLOGIC INVESTIGATIONS

NEW ENGLAND AND THE ADIRONDACKS

A structural analysis of the Norumbega fault zone

D. R. Wones (USGS) and W. B. Thompson (Maine Geological Survey) have demonstrated that the Norumbega fault zone is 3 to 4 km wide, trends N. 45° to 60° E., contains at least three subparallel faults, and is continuous between Winterport and Grand Lake Stream, Maine (loc. 1). The system appears to be confined to the region underlain by the Vassalboro Formation (Ordovician? and Silurian). Conglomerates having a red sandstone matrix are present along the zone and are older than the faults. Faults are defined by abrupt changes in lithology associated with breccias and mylonites. Gneisses and granitic rocks adjacent to the fault contain planar mylonites, many of which trend N. 20° W., N. 60° W., or parallel the faults. Minor folds, drags in mylonite structures, and slickensides are evidence for a dextral northeast strain component, whereas minor offsets (1 mm–5 cm) along the N. 20° W. and N. 60° W. joints are sinistral. This suggests an east-west compressive principal stress. Four large (300 km^2 in area) plutons are truncated by the fault. All are coarse-grained, rich in K-feldspar, and difficult to distinguish where deformed. Fault-bounded medium-grained granite and syenite are in the zone. Reconstruction of the fault zone requires a minimum of 10 km of dextral offset. Maximum offset is unlimited in that all reconstructions leave one or more of the plutons incomplete. Bedding within the conglomerate and sandstone dips toward the faults and implies vertical offsets of several hundred meters. Glacially derived landforms appear undeformed along the fault zone. Vertical displacements of a few centimeters have been observed in glaciated pavements. Lateral displacements have not been observed in such pavements.

Early recumbent folding in Silurian turbidite section, Maine

Structural observations made by P. H. Osberg within the Silurian turbidite section exposed in the western part of the Bangor, Maine, 2-degree quadrangle (loc. 2) indicate (1) two sets of isoclinal

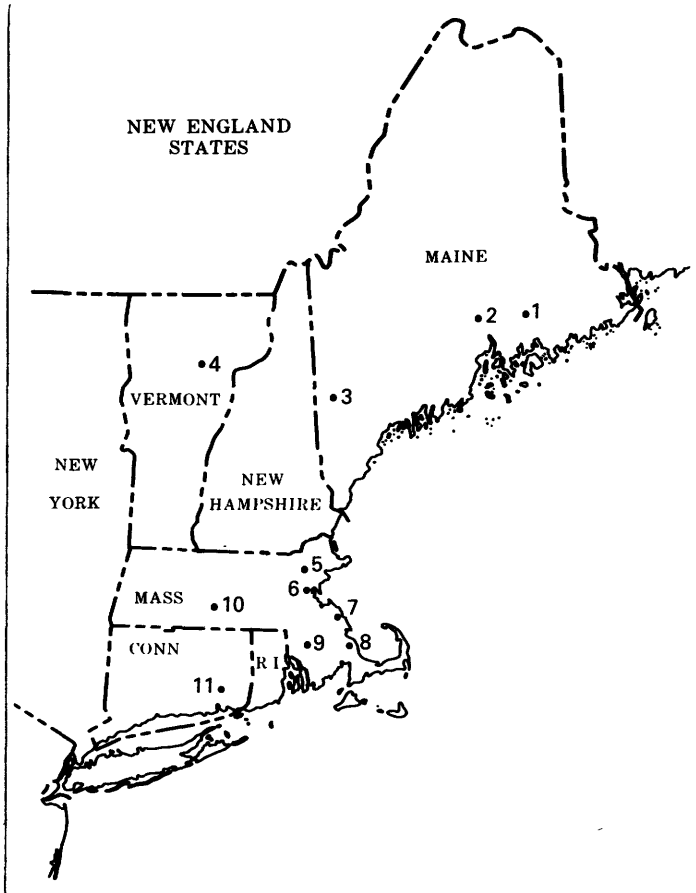

folds—one set plunging 55° to 85° and the second set plunging 0° to 20°, (2) folding of the steeply plunging set by the gently plunging set, (3) numerous localities where the stratigraphic information indicates that the gently plunging isoclinal folds face downward, (4) steeply plunging isoclinal folds consistently face upward where stratigraphic information is available, and (5) many displacements along bedding surfaces. Later fold phases and cleavages do not affect the mapped distribution of lithic units. On the basis of detailed observations, field mapping of isolated outcrops can be consistently synthesized into major recumbent folds that are folded by large upright, gently plunging, isoclinal folds. Such an interpretation preserves the lithic identity of the stratigraphic units and does

not require pronounced facies changes within the area of study.

A more complex Sebago batholith

Within the large mass of previously undifferentiated binary granite of the Sebago pluton in west-central Maine (loc. 3), N. L. Hatch, Jr., by means of reconnaissance mapping in the Fryeburg, Maine, 15-minute quadrangle, has distinguished two discrete rock groups. The first includes gray, generally medium-grained, faintly to well-foliated binary granite, binary pegmatite, and associated migmatite characteristic of the New Hampshire Plutonic Suite throughout much of central New England. The second group includes tan to pink, medium-grained non-foliated binary granite and pegmatite. The tan to pink rocks commonly crosscut the gray, but the gray have not been observed to cut the tan to pink. Both groups are cut by dikes associated with the Mesozoic White Mountain Plutonic-Volcanic Suite. The gray rocks are believed to have intruded during the Acadian orogeny; the age of the tan to pink rocks is unknown. Clearly, the Sebago batholith is a more complex body than previously thought.

Thrust faults in the ultramafic belt, Northern Vermont

R. S. Stanley reports that parts of the Hazens Notch, Ottauquechee, and Stowe Formations and the Belvidere Mountain Amphibolite of northern Vermont (loc. 4) have been subdivided into 25 or so mappable belts on the scale of 1:10,000. Many of these belts truncate on both sides of common surfaces and are interpreted as faults rather than unconformities or complex sedimentary facies changes. These surfaces are comparatively straight in some places but in others are deformed by at least two generations of mappable folds. Serpentinites and related talcose rocks are located along many of the discordant surfaces and hence appear to decorate faults as discontinuous slivers. Metagabbro intrusive rocks are restricted to lithically distinct thrust plates.

Mylonitization of the Salem Gabbro—Diorite intrusive complex

A. F. Shride reports that large areas within the Salem Gabbro—Diorite intrusive complex, eastern Massachusetts (loc. 5), are severely mylonitized. Because of this, many sheared plutonic rocks have been misidentified as metasedimentary and metavolcanic. These include parts or all of the Waltham Gneiss, the Westboro Quartzite, and the Marlboro, Woburn, and Kendal Green Formations and their recently renamed equivalents.

These mylonite zones, reported by Castle and others (1976) between the Bloody Bluff and Northern Boundary faults, north and west of Boston, are particularly abundant within a belt 4 to 10 km wide and at least 50 km long almost wholly occupied by various phases of the Salem Gabbro-Diorite intrusive complex. Within individual mylonite zones, centimeters to hundreds of meters in width, the original igneous textures of the diabases and fine- to coarse-grained gabbros that dominate the Salem and its felsic differentiates, abundant in the western part of the belt, have been totally destroyed.

Some rocks with an intense mylonitic foliation also exhibit an alternating light and dark layering and have been misidentified as unsheared gneisses. The varying amounts of felsic and mafic minerals in the original plutonic rocks and the degree of mylonitization greatly influence the final appearance.

Fault systems in the Boston Basin of Massachusetts

An analysis of faulting in the Boston Basin of Massachusetts (loc. 6) that combines structural information from rock tunnels and surface mapping has revealed a complex network of faults of several ages. C. A. Kaye found that numerous faults, identified in tunnels and, in some cases, spaced as closely as 150 m, cannot be recognized on the surface.

Two major sets of faults are recognized. The larger and older faults trend east to east-northeast and cut the Boston Basin into blocks, each of which is characterized by a specific stratigraphy and structure. These faults are offset by north- to northeast-trending faults, which are the youngest to have affected the area.

Narragansett Basin extends to Massachusetts coast

E. G. A. Weed, B. D. Stone, and D. W. Duty report that carbonaceous silty shale was recovered from 33 to 36 m in a hole drilled at elevation 17 m in Marshfield Hills, north of Plymouth, Mass. (loc. 7). A second hole, drilled at elevation 2 m along the North River in Norwell, recovered grayish pink sandstone from 9 to 12 m. According to P. C. Lyons, these rocks are typical of the Rhode Island Formation of Pennsylvanian age.

These findings suggest that the Narragansett Basin extends farther eastward than shown on Emerson's 1917 map of Massachusetts. Although no coal was encountered in these two holes, the rocks recovered strongly suggest the existence of a seaward continuation of the basin.

Readvance produces Ellisville moraine

G. J. Larson, working in the Plymouth, Manomet, and part of the Plympton quadrangles of Massachusetts (loc. 8), established that the Cape Cod Bay ice lobe readvanced over its own outwash to form the Ellisville moraine. By piecing together the detailed stratigraphy in sea-cliff exposures in the Manomet area and in deep excavations around Plymouth, Larson recognized the existence of a thin discontinuous sheet of basal till overlying thrust-faulted and sheared sediments through a broad area northwest of the moraine. Till fabric studies indicate a south-southwest direction of ice flow associated with the readvance sheet. In one deep exposure in the Monks Hill moraine, Larson noted that 6 feet of basal till and boulders overlie coarse fluvial and locally deltaic sands which in turn overlie coarse fluvial gravels on grade with surface gravels of the Wareham outwash plain to the south of the moraine.

Glacial Lake Taunton deposits

B. D. Stone reports that massive deltaic deposits in the Taunton Estuary east of North Dighton, Mass. (loc. 9), dammed up glacial meltwater in the northern part of the Taunton River basin. A major glacial lake, Lake Taunton, spread northward from the dam against the retreating ice margin. Delta topset-foreset elevations trace the level of the lake from about 16 m in elevation at North Dighton to 29 m in elevation in the southern part of the Brockton quadrangle, indicating postglacial rebound of about 0.8 m/km northward. Ice-contact deltas previously mapped in the Taunton, Bridgewater, and Brockton quadrangles by Hartshorn and by Chute indicate retreatal ice-margin positions in the lake trending nearly east-west. Similar ice-contact deltas mapped by J. D. Peper in the neighboring Norton quadrangle indicate ice-margin positions that are locally more nearly east-northeast. Melt-water streams that built outwash fans southward from the granite hills in Wrentham and Mansfield filled the shallow northern part of the lake with distal, fine-grained deltaic and lake-bottom sediments. In these distal deposits, fluvial beds are distinguished from subaqueous beds by their slightly coarser sand texture, by discontinuity of beds caused by cut and fill, as well as by the presence of planar cross-bedding associated with the formation of longitudinal bars in the braided glacial stream. Typical delta foreset beds of fine sand and silt occur in sets less than 3 m thick and contain laterally continuous ripple and plane-bed bedforms.

Retreat of ice left eastern upland of Massachusetts subject to deep freeze

F. D. Larsen, mapping in the Barre, Ludlow, and Springfield North quadrangles along the Quaboag-Chicopee drainages of central Massachusetts (loc. 10), established that the Chicopee Delta, graded to glacial Lake Hitchcock in the Connecticut Valley, is an ice-contact delta built by drainage from the Connecticut Valley ice lobe with a local source of material in the Pelham Hills, rather than an outwash delta built by melt-water flowing down the Chicopee River. The iron-stained late glacial gravels that form terraces along the midreach of drainage were traced by J. D. Peper and Larsen to ice-margin spillways on the east wall of the Connecticut Valley in the Ludlow quadrangle. The spillways are 12 to 18 m above the topset beds of the Chicopee Delta. This relationship indicates that the entire Quaboag drainage was largely deglaciated and had ceased to be a major source of melt-water deposits while ice still filled the Connecticut Valley in southern Massachusetts. Larsen found ice-wedge casts in outwash gravels, substantiating the existence of a severe periglacial climate in the deglaciated uplands.

A new look at the Chester syncline, eastern Connecticut

A detailed study of the geology around Chester, Conn. (loc. 11), has recently been undertaken by R. P. Wintsch to evaluate the evidence for the unusual, but generally accepted, interpretation that a southeast-trending thrust fault, the Honey Hill fault zone, terminates against the keel of a steeply eastward dipping isocline, the Chester syncline. According to this interpretation, biotite schist and gneiss of the Hebron Formation is flanked by biotite-muscovite schist and gneiss assigned to the Tatnic Hill Formation on the east limb and rocks of similar appearance assigned to the Brimfield Schist on the west limb. Plagioclase-hornblende gneisses that lie farthest from the axis on either limb are assigned to the Monson Gneiss.

The required symmetry on opposite sides of the narrow band of Hebron was not apparent in the field. A thick belt of hornblende-bearing gneisses and a band of calc-silicate-bearing granulite were mapped only on the east side, and anthophyllite-bearing rocks were found only on the west side. Biotite-muscovite schist is present only locally on both limbs. The Tatnic Hill Formation present on the Honey Hill fault zone could not be identified in the position of the syncline.

Detailed stratigraphy, therefore, does not support the existence of the Chester syncline. Instead, the local structure appears to be dominated by several high-angle north-northwest-trending faults showing a strong east-over-west sense of drag in outcrop. These faults commonly are cut by low-angle thrust faults of small displacement, continuations of the Honey Hill trend, that cut plagioclase gneisses, the Hebron Formation, and part of the Brimfield Schist before turning northward into the foliation along the western boundary of the Brimfield. This boundary probably marks a major structural discontinuity.

Differential deformation of the Grenville Complex and its basement in St. Lawrence County, New York

C. E. Brown reports that interpreting the regional geology in the important mineral-producing district of St. Lawrence County, New York, requires a better understanding of the geology of the domical alaskite bodies that appear to be basement highs below the Proterozoic Grenville Complex. Detailed mapping of the Hyde School body reveals a continuous sequence of lithologies that range from alaskite to diorite. Three stages of folding, including an early stage of nearly isoclinal folding, are recognized.

Although the domical bodies resemble each other, their structure bears little similarity to structure mapped in the overlying Grenville Complex that has a more intricate pattern of folds. Deformation of the Grenville that contains important zinc and talc deposits appears to be at least locally independent of the basement structure.

Deglaciation of central Connecticut

Compilation of Pleistocene geology in the upper Connecticut River basin by W. H. Langer and E. B. H. London, the lower Connecticut River basin by J. P. Schafer, and the Farmington and Quinnipiac River basins by J. R. Stone has shown that the last ice sheet retreated from central Connecticut in a systematic manner characterized by stagnation-zone retreat. The compilation illustrates the regional relationship between the broad topographic central lowland and the active glacier terminus and marginal zone of stagnant ice.

Most of the stratified sediments in the upper Connecticut River basin and the Farmington and Quinnipiac River basins are lacustrine and deltaic deposits. In the upper Connecticut River basin, sediments of glacial Lake Hitchcock predominate. This extensive and long-lived lake was dammed by older deltaic deposits that blocked the valley at Rocky Hill.

In the Farmington and Quinnipiac River basins, several lakes formed in front of the northward retreating ice margin in the Southington, Plainville, and Avon-Tariffville areas. Deltaic deposits in the valleys formed local dams that held in successively younger lakes to the north. The earliest of these dams clogged the present valley just north of the Quinnipiac gorge at South Meriden, resulting in the glacial lake of the Southington area.

Using the altitudes of deposits, local topography, and chronologic relationships between deposits, it has been possible to reconstruct the local and regional configuration of the ice margin. It extended as a lobe approximately 10 km south from the upland retreatal position into the upper Connecticut River lowland. A narrower lobe west of the Talcott Mountain ridge extended 10 to 12 km down the Farmington and Quinnipiac valleys.

In the lower Connecticut River basin, the ice lobe extended out of the lowland of Mesozoic rocks and into the eastern upland of crystalline rocks east of New Haven. Weaker lobation developed along the course of the lower Connecticut River where it cuts through the upland farther east. Deposits include small moraines formed along active ice margins, near-coastal deltaic deposits possibly built into a lake in Long Island Sound; numerous upland fluvial deposits; and deposits along the Connecticut River that dammed a temporary lake near Middletown, into which were built the Rocky Hill and Cromwell deltas that served as a dam for glacial Lake Hitchcock.

Geomorphology of New England

The New England States are largely highlands. The rocks in the highlands are similar to those that underlie the partly emerged and partly submerged piedmont to the southeast. Many of the rocks in the New England highlands are also similar to those that underlie the Piedmont province in the central and southern Appalachians where the relief over large areas is much less than in the highlands of New England. These comparisons made by C. S. Denny suggest that the New England highlands have been upwarped relative to the piedmont to the southeast. The uplift took place in the Miocene and may have continued into the Quaternary. Such a date is suggested by the presence of coarse clastic deposits in later Tertiary rocks of the submerged coastal plain of the New England coast. Large amounts of gravel and sand derived from sources to the northwest and to the north were deposited on the emerged coastal plain in New Jersey, Delaware, and Maryland be-

ginning in the Miocene, suggesting uplift of source areas to the north and northwest at that time. Estimates of rates of erosion based on sediment load in rivers and on volumes of sediments in the coastal plain suggest that if the New England highlands had not been uplifted in the late Cenozoic, the area should be largely a lowland.

The Oliverian domes, reevaluated

Reconnaissance of most of the Oliverian domes, trending along the core of the Bronson Hill anticlinorium through western New Hampshire, west-central Massachusetts, and Connecticut by G. W. Leo has shown that they comprise a large variety of core rocks with a wide range of composition, textures, and relations to mantling volcanic rocks. The Mascoma dome, regarded by Naylor (1969) as typical of the Oliverian domes, is useful as a model, but is not broadly representative of these bodies.

In general, the domes are ellipsoidal bodies of felsic to intermediate gneiss which are almost invariably mantled by rocks of the Ammonoosuc Volcanics (Middle Ordovician) and overlying units. The relationship between Oliverian core gneisses and Ammonoosuc Volcanics is different for different domes, unknown for some. "Oliverian" rocks intrude Ammonoosuc on the northeast side of the Whitefield Dome, in the Lebanon Dome, and the Glastonbury Dome (Massachusetts–Connecticut). Ammonoosuc unconformably overlies core gneisses of the Warwick Dome (Peter Robinson, Univ. of Massachusetts, person. commun.), but may be gradational with "stratified core gneiss" in the Mascoma Dome.

Naylor found that the Mascoma Dome consists of an inner, intrusive (unstratified) granite-granodiorite gneiss which intrudes stratified potassium-poor gneiss of probable volcaniclastic origin. Both unstratified and stratified gneiss were shown to have an Ordovician age (~450 m.y.), and the stratified gneiss appears to grade up into mantling Ammonoosuc Volcanics. Leo reports that the core rocks of the large Whitefield (or Jefferson) Dome are lithologically the most diverse. They include syenite, several texturally distinct but weakly foliated or unfoliated masses of granite and granodiorite, and the strongly foliated, locally quite mafic Whitefield Gneiss.

A chemical index of these lithologic variations is K_2O content, which shows a range from about 0.1 percent to 6 percent (in rocks with SiO_2 contents <70 percent). The K_2O content of the stratified core of the Mascoma Dome is low, typically less than 0.5 percent. Relatively potassium-poor gneiss in some other domes, such as the Jefferson, although distinct from the Ammonoosuc Volcanics, appears to be layered in some places but not in others. Elsewhere, such as in the "Baker Pond Gneiss," rocks that are both potassium poor and obviously layered, strongly resemble felsic Ammonoosuc Volcanics, leaving the identity of a "stratified core gneiss" in doubt. Still other domes, such as the Owl Head, seem to consist entirely of intrusive granite with a fine-grained potassic border phase. The Smarts Mountain Dome, by contrast, consists dominantly of massive and texturally homogeneous, but relatively fine-grained and friable rocks that suggests a metamorphosed tuff.

These various relations imply different ages of intrusion and (or) remobilization of rocks presently called Oliverian. Where mantling volcanic rocks can be shown to be related in space and time to the dome gneisses, the question arises whether the gneisses represent shallow intrusions into an extensive volcanic pile, which in turn, may be part of an Ordovician island arc.

APPALACHIAN HIGHLANDS AND THE COASTAL PLAINS

Late Alleghenian thrusting in New Jersey

Large and small klippen of Proterozoic and lower Paleozoic carbonate rocks have long been recognized in the Kittitinny Valley (loc. 1) of northern New Jersey (Baylor, Salisbury, and Kummel, 1914). Recent reconnaissance by A. A. Drake, Jr., has shown that most of these lie on rocks of the Martinsburg Formation, although the largest Proterozoic slab, Jenny Jump Mountain, lies on a variety of carbonate rocks of Ordovician age. The klippen within the Martinsburg terrane lie within troughs in the slaty cleavage and thus were emplaced subsequent to cleavage development. Cleavage in the areas of the klippen is marked by an extremely well-developed transport lineation, and the Martinsburg near the klippen boundaries is severely smeared and tectonically disrupted into autoclastic melanges.

The large Jenny Jump Mountain klippe transects several folds in the lower Paleozoic carbonate strata. These folds have the same trend (east-northeast) and style (upright to steeply inclined) as known late folds in the Kittitinny Valley (Drake, 1978).

Regionally, the rocks in this part of the Kittitinny Valley are in the brow and upper limb of a major nappe of Taconic age (Drake, 1970). The klippen material herein probably resulted from the dismemberment of a large thrust sheet composed of base-

ment and overlying carbonate rocks. The folds beneath the Jenny Jump Mountain klippe are superposed on the major Taconic structure and are thought to be of Alleghenian age (Drake, 1978). As yet, there is no consensus as to the age of the slaty cleavage, although cleavage in the commercial slate belt in Pennsylvania seems to be post-Taconic, probably Alleghenian in age (Epstein and Epstein, 1969; Lash, 1978). The thrusting that gave rise to the klippen is clearly a late geologic event and, on the basis of the available data, seems to have occurred during late Alleghenian deformation. Late Alleghenian thrusting has been documented in east-central Pennsylvania (MacLachlan, 1967). The most important aspect of the recognition of late Alleghenian thrusting in New Jersey is that basement rocks were moved. This observation presents some difficulties to the concept that the Alleghenian deformation was by gravity spreading (or sliding) and suggests that some revision of plate tectonic models may be needed.

Tectonic history of Shochary Ridge in Pennsylvania

Recent mapping in eastern Pennsylvania (loc. 2) by P. T. Lyttle and A. A. Drake, Jr., shows that the rocks of Shochary Ridge, a sequence of near-shore prodeltaic fossiliferous turbidite units, are in fault contact with the deep-water turbidite-flysch deposits of the Martinsburg Formation to the north and east and with several units of Hamburg klippe to the south. In both cases these faults are steep south-dipping upthrusts and are probably late Alleghenian in age. To the north, the Eckville fault, first noted by Behre (1933), brings the Shochary Ridge sequence over all three members of the Martinsburg Formation and thus marks an abrupt change from abundantly fossiliferous near-shore sediments to very sparsely fossiliferous deep-water sediments. The Eckville Fault also truncates at least two sets of folds in the Martinsburg, an early set of tight recumbent folds and a later set of open symmetric folds. To the south of Shochary Ridge, the Kistler Valley Fault brings rocks of the Hamburg klippe over the Shochary Ridge sequence and truncates an earlier, presumably Taconic, low-angle thrust fault in the klippe rocks. Thus, the classically held view that the northern boundary of the klippe is a low-angle thrust is incorrect.

Although the Eckville and Kistler Valley faults define the nature of the contacts of Shochary Ridge rocks, they are of minor significance in understanding the tectonic history and mass distribution of the three regionally important clastic sequences (the rocks of Shochary Ridge, the Martinsburg Formation, and the Hamburg klippe). The rocks of Shochary Ridge are anomalous in that they are much less structurally complex than the surrounding rocks. Detailed mapping in the Bushkill and Ramseyburg Members of the Martinsburg, paying close attention to the tops of units as shown by sedimentary structures and to the sense of rotation of folds, shows that these rocks are regionally overturned. Here, the Martinsburg is interpreted to be mantling a large nappe that has overridden both the rocks of Shochary Ridge and the Hamburg klippe. A pronounced elongation lineation in the rocks of Shochary Ridge and the Hamburg klippe in the Slatedale quadrangle is interpreted to be the result of nappe emplacement. Detailed mapping in the Hamburg klippe shows these rocks to be tectonically fragmented and mixed and cut by several low-angle thrust faults. In comparison, the asymmetric overturned syncline of Shochary Ridge, long recognized by many geologists, is a very simple structure.

Many earlier mappers in this region have assumed that the Shochary Ridge rocks are continuous with, and part of, the Martinsburg Formation. The presence of the Eckville fault does not eliminate the possibility that the Shochary Ridge rocks are a shallow-water lateral equivalent of the Martinsburg, but it is necessary to remember the complex tectonic history of the Martinsburg and the fact that the

Martinsburg was deposited considerably to the southeast of Shochary Ridge and not near its present structural position to the north and east of Shochary Ridge.

Thrust faulting indicated by relationship of Catskill and Pocono Formations in northeastern Pennsylvania

Geologic mapping by M. J. Bergin in the northern Anthracite field in northeastern Pennsylvania (loc. 3) indicates that the Susquehanna River between West Nanticoke and Shickshinny flows westward in a strike valley. The valley is floored along much of its course by the Catskill Formation of Devonian age rather than the Mauch Chunk Formation of Mississippian and Pennsylvanian age as shown on previous maps (Gray and others, 1960). The Pocono Formation of Mississippian age overlies the Catskill and crops out as a series of outliers on a dip slope on the highest parts of the ridge north of the river and in the lower part of a north-facing escarpment south of the river. The Mauch Chunk Formation and the overlying Pottsville Formation of Pennsylvanian age form the upper part of this escarpment.

Structural details have not yet been resolved; however, based on bedding attitude relationships, it is suggested that the Pocono, Mauch Chunk, and Pottsville Formations in the escarpment are allochthonous and have been thrust northward, possibly along a décollement within the Catskill Formation. North of the Susquehanna River the allochthonous rocks have been removed by erosion.

Paleozoic cataclastic deformation and low-grade metamorphism of Proterozoic rocks in the northern Virginia Blue Ridge

The Marshall and Rectortown quadrangles (loc. 4) on the eastern limb of the Blue Ridge anticlinorium in northern Virginia are underlain by older Proterozoic granitic rocks and younger Proterozoic metasedimentary (Fauquier Formation of Furcon, 1939) and metavolcanic (Catoctin Formation) rocks. According to G. H. Espenshade, these rocks were all uniformly metamorphosed to the greenschist facies, and a prominent cleavage (striking northeast and dipping southeast) was well developed in all rock types during a Paleozoic orogeny. The granitic rocks show a wide variety of cataclastic effects ranging from grain crushing along thin veinlets to thorough phyllonitization to quartz-sericite schist across widths of several meters. Folds have not been observed in the overlying layered Proterozoic rocks, but clasts in sedimentary conglomerates and in volcanic breccias are flattened parallel to cleavage. Deformation began before the start of metamorphism and continued, perhaps intermittently, until near the close of metamorphism as evidenced by some biotite, which is later than the cleavage.

Principal metamorphic minerals of the major lithologic types are as follows:

- *Metagranite, meta-arkose, and metasiltstone.*—Sericite, epidote, biotite, and quartz.
- *Metabasalt and metadiabase.*—Actinolite, epidote, chlorite, and albite; small amounts of biotite in some rock.
- *Siliceous marble.*—Calcite, dolomite, and tremolite.

In addition, sphene is a common accessory mineral in most rock types, and magnetite octahedra are abundant in some metasiltstone, schistose metabasalt, and phyllonitized granite (quartz-sericite schist).

Similar Paleozoic cataclastic deformation and low-grade metamorphism of older Proterozoic plutonic rocks have been described from several other places in the Blue Ridge anticlinorium. These effects are well developed in the Virginia Blue Ridge, about 100 km southwest of the Marshall quadrangle (Bartholomew, 1977; Gathright, Henika, and Sullivan, 1977) and about 300 km farther southwest in the North Carolina Blue Ridge (Bryant and Reed, 1970; Rankin, Espenshade, and Neuman, 1972; Rankin, Espenshade, and Shaw, 1973). It is likely that cataclastic deformation and low-grade regional metamorphism were very extensive during the Paleozoic in Proterozoic plutonic rocks of the Blue Ridge.

Flat Swamp Member of the Cid Formation extended

The Flat Swamp Member of the Cid Formation in the Carolina slate belt of central North Carolina was established by Stromquist and Sundelius (1969) as a major marker of mafic to felsic volcanic rocks that separates similar appearing mudstones in the Cid Formation below from the Floyd Church Member of the Millingport Formation above. They traced the Flat Swamp Member from its truncation by the Silver Hill fault near Lexington southward around a series of folds to an apparent pinchout on the west side of the Troy anticlinorium near Albemarle. D. J. Milton, while mapping in the Charlotte, N.C., 2-degree quadrangle (loc. 5) has found that the Flat Swamp does not pinch out but continues 70 km southwest, west, and finally north to another cutoff at the Silver Hill fault, 75 km from the northern one. Aerial radiometric surveys indicate the Floyd Church mudstones are more potassic than the Cid

mudstones. Accordingly, on the southeast side of the Troy anticlinorium, where the Flat Swamp is reduced to inconspicuous discontinuous beds, the contact between the Cid and the Floyd Church can be mapped by the contrast on radiometric maps as reliably as by field criteria.

Metamorphism and structural relationships in the Kings Mountain area of the Carolinas

Structural analysis by J. W. Horton, Jr., has revealed that the same four episodes of folding and related deformation occur in both the Kings Mountain and Inner Piedmont belts near the North Carolina-South Carolina State line (loc. 6). The structure of the central and eastern parts of the Kings Mountain belt is dominated by the north-plunging South Fork anticline of the earliest fold episode (F_1). The western part of the belt is dominated by the northeast-plunging Cherokee Falls synform of the second fold episode (F_2).

The nature of the boundary between the Kings Mountain and Inner Piedmont belts is an important consideration for regional tectonic models. This boundary is characterized by intense deformation related to the F_2 folding, but mylonitic and cataclastic rocks are lacking. Preliminary reconnaissance suggests that it may be possible to trace certain stratigraphic units across the boundary between the two belts near Blacksburg, S.C.

Regional metamorphism in the Kings Mountain belt and adjacent areas is typically of the Barrovian type (medium pressure). Metamorphic grade is lowest in the central part of the Kings Mountain belt, possibly as low as the biotite zone (greenschist facies). It increases eastward reaching the sillimanite-muscovite zone near the contact with granitic gneiss of High Shoals. It also increases westward, reaching the staurolite zone at the Inner Piedmont boundary and the sillimanite-muscovite zone in the Inner Piedmont. Metamorphic textures are consistent with a single progressive thermal metamorphic event that probably occurred between about 410 and 440 million years ago. The two major deformation events, D_1 and D_2, appear to be overlapped by this progressive thermal event, indicating that all are related to a single orogenic episode. Evidence for greenschist facies retrogressive metamorphism is also widespread in the area.

Thrust plates in the Blue Ridge

During geologic mapping in the Greenville (North Carolina, South Carolina, Georgia) 2-degree quadrangle (loc. 7), A. E. Nelson found that the Hayesville Thrust (D. W. Rankin, 1975; R. D. Hatcher, 1978) is a premetamorphic folded thrust separating two crystalline thrust plates, the Great Smoky plate to the northwest, which was overthrust by the Hayesville-Fries plate from the southeast. Closely associated with a part of the Hayesville-Fries thrust sole is an ultramafic complex containing amphibolite, talc schist, gabbro, serpentinite, and dunite as the principal rocks. This complex probably represents oceanic crust and mantle fragments or perhaps is part of an oceanic crust slab brought up along the Hayesville Thrust.

Erosion through the Hayesville-Fries plate has exposed two windows of Great Smoky plate rocks near Lake Chatuge in the northwest part of the quadrangle. The largest window, which is elliptical and whose longest dimension is 19 km, forms the core of an elongated dome-like structure. Ultramafic complex rocks in the Hayesville-Fries sole surround the window around the dome flanks, and paragneisses and schists of the Hayesville-Fries plate surround the ultramafic rocks farther out on the dome flanks. This same relationship applies to the smaller window as well. Hartley (1973) considered a part of these ultramafic rocks to be a sill. Northeast along the regional strike into the Knoxville quadrangle a series of various sized ultramafic masses are exposed in the Hayesville-Fries plate. It is suggested that they are related to the ultramafic rocks around the windows mentioned above, and together they may form part of a large oceanic-mantle slab caught up in and along a northeast-trending structural arch in the Hayesville-Fries plate.

Relationship between superimposed folding and geologic history in the Georgia Piedmont

Geologic mapping in the Georgia Piedmont, south and southeast of Atlanta (loc. 8), by M. W. Higgins has revealed five generations of folds and a major unconformity. The five generations of folds, informally named for localities where they are well exposed, are, from oldest to youngest, Buck Branch Klondike, Ellijah Mountain, Scott Creek, and Tara. Rocks beneath the unconformity have all five fold generations, whereas those rocks stratigraphically above it have only the last four. Buck Branch folds are generally tight to isoclinal, locally elastic, and are characterized by schistosity that parallels bedding and compositional layering, except in the hinge zones where it is axial planar. Klondike folds recumbently fold Buck Branch folds and are typified by an axial-plane schistosity. Ellijah Mountain

folds fold the nearly coaxial Buck Branch and Klondike folds. Scott Creek and Tara folds, which are generally gentle to open, are characterized by a widely spaced, joint-like axial-plane cleavage. All earlier generatons are folded by either Scott Creek or Tara folds; however, the relative chronology of these two late episodes is unknown.

These five fold generations and the unconformity between the first and second generations allow preliminary interpretation of the deformational and geologic history of a large part of the Georgia Piedmont. On the basis of tentative regional correlations, the unconformity is possibly the same as the one above the Knox Group and Newala Limestone in the Valley and Ridge Province and may be associated with the "Blountain" phase of the Taconic orogeny.

Cyclicity of Upper Cretaceous sedimentary rocks

The Upper Cretaceous rocks of the eastern Gulf Coastal Plain (loc. 9) are composed largely of siliciclastic sediments, which according to Juergen Reinhardt, were deposited in marginal marine and shelf environments. At the eastern margin of the basin (central Georgia) and in updip areas to the west, the deposits consist dominantly of fluvial feldspathic sand and kaolinitic clay which grade to open-shelf glauconitic sand, marl, and chalk both downdip and westward into the basin (central and western Alabama). Changes in the distribution of lithofacies are most notable in the marginal marine sediments; the sequences of lithofacies indicate that three major marine transgressions occurred during the Late Cretaceous.

Sedimentation apparently began during the Cenomanian along the Piedmont margin when the Tuscaloosa Formation was deposited. The overlying Eutaw Formation (Coniacian and Santonian) reflects the first marine transgression. This unit is composed dominantly of crossbedded quartz sand containing *Ophiomorpha* burrows, laminated carbonaceous silt to fine sand, and massive accumulations of *Ostrea cretacea* valves. The Eutaw sediments record the encroachment of a shallow sea onto an unconsolidated shoreline and the subsequent formation of a barrier-bar complex.

The second transgression took place during the early Campanian and "drowned" the Eutaw barrier system. The resulting Blufftown Formation consists largely of inner-shelf glauconitic sand and shelly marl. The overlying Cusseta Sand (lower Maestrichtian) represents the third transgression and "drowning" of the barrier-bar complex. After this third transgression, the Ripley Formation, an inner-shelf, massive glauconitic sand, was deposited.

The timing of marine transgressions was probably the major factor in determining the distribution of lithofacies during the Late Cretaceous in the eastern Gulf Coastal Plain. Local fluctuations in water depth, circulation, water chemistry, and sediment supply controlled the composition of lithofacies and the distribution of small-scale (<10 m thick) cycles within the basin. Controls on the large-scale (tens to hundreds of meters thick) cyclicity of transgressive and regressive phases of these Upper Cretaceous deposits were global and resulted in major changes in the world's water budget.

Quaternary deposits and soils of the central Susquehanna Valley in Pennsylvania

Recent geologic mapping in central Pennsylvania by D. E. Marchand has revealed a variety of glacial and nonglacial Quaternary deposits ranging in age from early Pleistocene to Holocene and has provided evidence for multiple pre-Wisconsinan glaciation. Surficial deposits in this area can be subdivided into at least six mappable units based on amount of weathering, soil development, degree of erosional dissection and preservation, superposition, and geographic distribution.

Pre-Wisconsinan till, ice contact stratified drift, fluvial deposits, loess, and colluvium occur beyond the Wisconsinan glacial border. Superposition, contrasting soil development, and degree of preservation indicate the existence of at least three drift units separated by buried soils; these are indicative of major interglacial weathering. Pre-Wisconsinan soils are much thicker and more strongly developed than post-Altonian soils. *B* horizon hues range up to 2.5 YR and chromas to 7 or 8. Clay content may exceed 50 percent, and free iron oxides range up to 8 percent or more. *B* horizons display very thick, continuous clay films. Fresh, unweathered parent material may lie at depths of 6 m or more.

Deposits mapped as Altonian encompass till, ice-contact sand and gravel, outwash, loess, and colluvium. Of these, only the till and ice-contact materials are extensively exposed, the outwash and loess having been severely eroded and the colluvium largely eroded or reworked during Woodfordian time. Altonian ice appears to have extended further south than the later Woodfordian border throughout most of central Pennsylvania, with lobes extending down both branches of the Susquehanna River valley. Post-Altonian relict soils have poorly to moderately developed argillic horizons 30 to 60

cm thick. Clay content of the *Bt* horizon is about 15 to 30 percent, and depth to fresh parent material is about 1.8 to 2.5 m. Soil structure is generally much weaker than in pre-Wisconsinan till soils.

Woodfordian deposits include till and ice-contact stratified drift deposits along the glacial border, outwash, loess and eolian sand downstream from the border, and extensive colluvial and alluvial deposits over the entire region. As many as six or seven outwash terraces can be recognized locally. Woodfordian deposits bear light-colored soils with textural *B* horizons and, in imperfectly drained areas, weak to moderately developed fragipans. Argillic horizons and stronger fragipans are developed in well-drained soils on colluvium which may be as young as Woodfordian. Soils on till, outwash, and eolian material lack argillic horizons. Clay content does not exceed about 20 percent, and fine iron oxides are generally less than 1.5 percent. Fresh, unweathered parent material typically lies within 120 to 150 cm of the surface.

Deposits of Holocene age include channel, point-bar, levee, and floodplain alluvial deposits along the Susquehanna River and its major tributaries. Holocene deposits and erosional surfaces bear weakly developed soils that show incipient *B* horizon development.

Warwoman lineament extention

The Warwoman lineament is a conspicuous geomorphic feature 40 km long which trends northeastward in northeastern Georgia to the South Carolina border. It has been termed a probable shear zone (Hatcher, 1973) and later was called a "photofault," not a fault (Hatcher, 1976), presumably because no field evidence has been found for offset. R. W. Luce and Henry Bell III believe that a small dunite body, now partially altered to talc and anthophyllite, which is located east and outside the Ellicott Rock Wilderness area, South Carolina, North Carolina, and Georgia, lies on an extension of the Warwoman lineament, 5 km from its previously known eastern termination. The presence of this ultramafic body, and another along it in Georgia, strongly indicates that the lineament was a zone of tectonism.

CENTRAL REGION

LAKE MICHIGAN

Geology of central Lake Michigan

Continuous seismic reflection profiles and bathymetry in central Lake Michigan provided information for maps on the thickness of unconsolidated sediment (primarily Pleistocene) and of the Paleozoic bedrock topography. According to R. J. Wold, the isopach map shows sediment thicknesses ranging from 183 m in a steep-walled northeast-trending erosional valley to less than 8 m over a mid-lake topographic high. The valley and the mid-lake high are the dominant topographic features of this part of the basin of Lake Michigan. A fault with a vertical displacement of about 100 m was recognized in Paleozoic rocks in the eastern part of the study area. The truncated edges of salt units in the Salina Formation trend through this area, and the faulting may be related to collapse caused by salt solutions along the erosional edge of the Salina. It is also possible that the fault persists downward into the Precambrian basement.

MICHIGAN

Revision in Proterozoic X stratigraphy in Marenisco-Watersmeet area, northern Michigan

Geologic mapping in the Marenisco-Watersmeet area, northern Michigan, by P. K. Sims and W. C. Prinz has shown that the stratigraphic sequence determined previously by Fritts (1969) needs revision. He concluded that the bedded rocks between the batholithic granitic rocks (called granite near Nelson Creek) east of the Gogebic Iron Range and the Wolf Lake Granite of Allen and Barrett (1915) north of Watersmeet composed a homoclinal succession of Proterozoic age at least 12,000 m thick. Instead, the bedded rocks are folded into a broad anticlinorium with flanking synclines and consist mainly of an older succession of metavolcanic and metagraywacke rocks of Archean age and a younger succession of metavolcanic and metagraywacke rocks of Proterozoic X age. Granitic rocks dated by Z. E. Peterman as being 2,700 million years old cut the older bedded succession. The younger succession constitutes the Marquette Range Supergroup in this part of the Lake Superior region. The unconformity at the base of the Marquette Range Supergroup can be observed directly in sec. 21, T. 46 N., R. 42 W., 10 km east of Marenisco.

In the area east of Marenisco, the Marquette Range Supergroup consists of a lower metavolcanic unit (450–1,800 m thick) and an upper thick metagraywacke unit. The metavolcanic rocks in strata near Blair Lake (Fritts, 1969) probably are correlative with the Emperor Volcanic Complex exposed in the eastern part of the Gogebic range; Fritts (1969) referred to the metagraywacke unit

near Marenisco as the Copps Formation and to the same unit north of Watersmeet as the strata near Paulding.

The mapping indicates that except for a northeast-trending erosional remnant in T.45 N., R.43 W., called strata near Banner Lake by Fritts (1969), rocks of the Chocolay Group are absent in the Marenisco-Watersmeet area. Also, economically significant deposits of iron ore apparently are missing.

MINNESOTA

Faulting in the Duluth Complex

Intense faulting and fracturing in the Harris Lake area, northeastern Minnesota, has been documented by M. P. Foose and R. W. Cooper. Faults are identified chiefly by the disruption of mappable layers within sequences of plagioclase and plagioclase-olivine cumulates in the Duluth Complex. Most layers grade from olivine-rich bottoms to plagioclase-rich tops and probably were deposited by density currents within the magma. Faults trend principally N. 35° E., N. 5° W., and N. 40° W. and outline block structures similar to those found in many rift environments. Recognition of the faults lends critical support to models that relate formation of the Duluth Complex to a period of regional rifting and also is an important contribution to understanding the apparently erratic distribution of important copper-nickel sulfides along the base of the Duluth Complex.

MISSISSIPPI EMBAYMENT

Post-Midwayan (Paleocene) uplift at margin of Mississippi embayment in northeastern Arkansas

Fieldwork west of Olyphant, Ark., in the 24-quadrangle Newport area (35°15′–36°00′ N. lat; 91°15′–91°45′ W. long) in northeastern Arkansas by E. E. Glick led to the discovery of outcrops of fossiliferous Tertiary chert resting on Paleozoic rocks at localities about 2 km west of the edge of the Mississippi embayment and as much as 150 m higher than the general level of the embayment. B. W. Blackwelder and L. W. Ward of the Paleontology and Stratigraphy Branch of the U. S. Geological Survey identified one species of Midwayan (Paleocene) fossil in the chert. This paleontological evidence, supplemented by the data from extensive fieldwork in the area, indicates that significant local uplifting took place over an area of about 750 km^2 in the south-central part of the Newport area sometime after the deposition of at least part of the Midway Group. This is later than the time of any other local uplifting of similar magnitude known in the central and upper parts of the Mississippi embayment.

The number of individual post-Midwayan uplifts throughout the Newport area, their position, and size were determined from subsurface data and from a reappraisal of field evidence gathered several years ago. Data from 25 stratigraphic test holes drilled in 1953 in the southeastern part of the Newport area indicate that a separate, smaller, probably post-Midwayan structure is buried by Quaternary sediments there. A third, much smaller, uplift or a pre-Late Cretaceous hill in the southwestern part of the area is ringed by Upper Cretaceous sediments. The total area involved by all three uplifts is nearly 950 km^2; the volume is about 52 km^3.

The geographic proximity of these uplifts to the concealed Newport pluton, which is recognized from geophysical data, suggests at least an indirect genetic relationship between the pluton and the uplifts. Field and subsurface evidence show no significant local uplifting well away from the pluton. The uplifts, which are only in part directly over the pluton, probably resulted from a late and relatively minor episode of the emplacement of the magma. One fact is quite evident from field data—the larger of the three uplifts is responsible for the abrupt offset or reentrant of the edge of the Mississippi embayment in the Newport area.

Age and mode of deposition of so-called "Lafayette formation" in northern Mississippi embayment

Continental deposits, informally known as the "Lafayette formation," are widespread in the northern Mississippi embayment. According to W. W. Olive, palynological and climatological data and lithologic, stratigraphic, and geomorphic relations indicate that the unit was deposited as a series of coalescing alluvial fans during the Pliocene and possibly the Miocene. Sedimentation was initiated by a marked increase in seasonal flow of major streams as a consequence of climatic change that accompanied a post-middle Miocene cooling trend which eventually led to Pleistocene glaciation. During the Pleistocene, the continental deposits were reworked in part and redeposited at four different levels which correspond with the Williana, Bentley, Montgomery, and Prairie terraces of Fisk (1938, p. 149–172). The gravel, including that of Pleistocene age, is offset at places by faults with displacement of as much as 1.5 m.

Ancient fault sets in northern Michigan

Recent mapping in the "Northern Complex," a block of Archean gneisses surrounded by Proterozoic X metasedimentary rocks in northern Michigan, has documented the existence of very old fault sets according to W. F. Cannon and J. S. Klasner. The gneisses, which are about 2.7 billion years old, are cut by numerous faults that produce major offsets of units within the complex; outside the complex there are smaller offsets and, in some cases, no offsets of flanking Proterozoic X rocks about 2.0 billion years old. Locally the faults caused minor offset of lower Keweenawan dikes about 1.1 billion years old. Hence, a major period of faulting occurred in the interval 2.7 to 2.0 billion years ago. These faults were reactivated probably during the Penokean orogeny about 1.9 billion years ago and after intrusion of lower Keweenawan dikes about 1.1 billion years ago.

A major fault is also suggested between the "Northern Complex" and the previously mapped "Southern Complex." Although both complexes are Archean gneisses, they differ appreciably in rock types, structural style, and structural trends. They can be traced to within a few kilometers of each other; however, the contact is buried beneath Proterozoic X rocks of the Marquette trough. The contact seems most likely to be a fault with large displacement to account for the juxtaposition of such different terranes.

ROCKY MOUNTAINS AND GREAT PLAINS

STRATIGRAPHIC STUDIES

A new Proterozoic Y stratigraphic unit, east-central Idaho

In east-central Idaho, the Swauger Formation, defined and described by Ross (1947) and further described and delineated by Ruppel (1975), has been the youngest unit so far known of a very thick Proterozoic Y section. In many places in the Lemhi Range the Swauger is overlain unconformably by the Wilbert Formation (Proterozoic Z) or by lower Paleozoic formations; elsewhere, its upper limit is a thrust fault, and locally it has been completely eroded before the deposition of younger strata.

Mapping by S. W. Hobbs in the Challis quadrangle and part of the May quadrangle at the northern end of the Lost River Range has identified a heterogeneous sequence of strata comprising quartzite, siltstone, and argillite at least 1,300 m thick in probable gradational contact above the Swauger. At three of the four known localities where the contact may be studied, a zone of brecciation, quartz veining, or narrow concealed interval suggests some structural disturbance. At all these, however, the disturbance does not appear to be a major fault, but could more reasonably result from structural adjustment between the very competent, thick-bedded Swauger quartzite and the far less competent, thin-bedded overlying unit. One completely exposed contact is unusually sharp in contrast to the other broadly gradational ones and shows no disturbance of any kind.

The best exposures of the post-Swauger Proterozoic strata occur at the east foot of the Pahsimeroi Mountains immediately south of Lawson Creek in the southwestern corner of the May quadrangle, Idaho. Here, over 1,300 m of strata are exposed in a westerly dipping sequence that starts in good recognizable Swauger at the mountain front and extends upward through the section to a cover of Challis Volcanics on the west side.

The lower several hundred meters of strata above the typical thick-bedded, fairly pure, light-to-medium, pinkish-gray Swauger quartzite is a somewhat thinner bedded, darker pink or purple quartzite that includes more frequent thin interbeds of dark-purple platy quartzite, silty flagstone, and laminae of deep-purplish-gray argillite. This part of the section is a transition zone that evolves upward into a series of beds approximately 450 m thick comprising heterogeneous mixture of generally dark purple, sub-platy to platy, impure, medium-fine-grained quartzite, thin-bedded siltstone, and deep purple argillite in various proportions. Feldspar is locally abundant in some of the quartzite beds. Thin films and laminae of dark purple or maroon argillite are abundant and in many places are the source beds for abundant mud-chip breccia. A 3- to 6-m-thick silicified shear and breccia zone on which there has been an unknown but probably not significant amount of movement separates the intermixed quartzite, siltstone, and argillite from a more homogeneous series of dark-purple or maroon thin-bedded impure fine sandstone, siltstone, and laminated argillite that comprises more than 500 m of the uppermost exposed section. The total thickness of the post-Swauger strata and nature of the upper contact is unknown.

Trilobite from the Silver Hill Formation

The Silver Hill Formation of southwestern Montana was named and described from the Philipsburg area by Emmons and Calkins (1913). Its age assignment, Middle Cambrian, apparently was not

based on fossils from the formation. Hanson (1952) cited *Glossopleura* from the middle limestone member of the Silver Hill of the Philipsburg area, but gave no reference. E-An Zen and J. T. Dutro, Jr. (1975), mapping in the Pioneer Mountains, Montana, correlated a formation having a lower member of siltstone and quartzite and an upper member of quartzose carbonate with the Silver Hill. Trace fossils have previously been described (Dutro, Zen, and Taylor, 1975), but nothing more definite was known. During the summer of 1978, M. E. Taylor, L. A. Wilson, and Zen discovered an *Albertella* within the upper part of the lower member of Zen's Silver Hill Formation from the east slope of Black Lion Mountain (Vipond Park quadrangle) at 2,950-m level. The fossil provided a date of early Middle Cambrian for this part of the formation. Because the Silver Hill, within the Pioneer Mountains, grades downward through interbedding and through gradual increase in size and proportion of clasts into an underlying sequence of cross-stratified conglomerate and sandstone, the latter (to be called the Black Lion Conglomerate) is to be assigned to the Lower Cambrian, but possibly includes some uppermost Proterozoic Z beds. The Black Lion Conglomerate is at least 500 m thick and maintains a uniform lithology. Its presence here, in part possibly overlying an ~1.9-billion-year-old basement gneiss complex, is a significant addition to the paleogeographic knowledge of the latest Proterozoic and earliest Paleozoic of the northern Rocky Mountain area.

Eastern extent of the Proterozoic Y Belt basin, Montana

Proterozoic Y Belt strata,exposed in the Big Snowy Mountains, central Montana, and described briefly by Reeves (1931), have been restudied and identified as the Newland Formation by M. W. Reynolds and D. A. Lindsey. Farther west the strata are in the lower part of the Belt Supergroup. Strata in the Big Snowy Mountains include even, very thin laminae of calcareous argillite and very thin-bedded micritic limestone characteristic of the Newland, and are interpreted to be dominantly of deep-water origin. The identification and facies of the rocks demonstrate that the northeastern and eastern margins of the lower part of the Belt depositional basin extended well beyond the present known distribution of the strata. Heretofore, the eastern lobe of Belt strata in west-central Montana has been termed the Belt or Helena embayment. The new studies demonstrate, however, that the lobe is not a narrow depositional embayment, but rather owes its configuration to post-belt pre-Middle Cambrian uplift and erosion within a basin that had a much wider northeastern and eastern areal extent.

Correlation of Eocene volcaniclastic rocks, southeastern Absaroka Range in northwestern Wyoming

Mapping investigations undertaken by T. M. Bown in the southeastern Absaroka Range in Hot Springs County, Wyoming, in 1977 and 1978 indicate that the volcanically derived Eocene rocks in this area are represented by three formations which are separated from each other by erosional or angular unconformities, the middle Eocene Aycross Formation (about 290 m thick), the middle and upper Eocene Tepee Trail Formation (about 425 m thick), and the upper Eocene Wiggins Formation (more than 180 m thick). Aycross and Tepee Trail terminology is extended from the type areas in the northwestern Wind River basin to the mapped area on the basis of lithologic equivalence, vertebrate faunas, and mappability. The names Aycross Formation and Tepee Trail Formation replace, respectively, the terms Pitchfork Formation and "Late Basic Breccia" that were variously applied to these rocks in the southeastern Absaroka Range by earlier workers; for example, Rouse, 1937; Hay, 1956; Wilson, 1963, 1964; and Rohrer, 1966.

In the mapped area, the breccia-poor Aycross Formation contains an early middle Eocene mammalian fauna that is now known from at least 56 species. This unit intertongues to the north with part of the breccia-rich Wapiti Formation (Nelson and Pierce, 1968) on Carter Mountain in Park County. The Wapiti Formation has also yielded a small early middle Eocene mammal fauna. Oil shale and tuffaceous green and brown clay shale in the lower part of the Aycross Formation record lacustrine deposition in the southwestern Bighorn Basin that is younger than the central basin Tatman Formation.

Rocks in the Wood River and Greybull River areas in Hot Springs and Park Counties that were mapped by Wilson (1963, 1964) as the lower part of the Wiggins Formation actually represent the lower beds of the Tepee Trail Formation. These rocks include the "Blue Point Conglomerate," which was named a member of the Wiggins Formation by Wilson (1963). True Wiggins strata are developed much farther west and at much higher altitudes than observed by Wilson and, in these outlying areas, much more closely resemble lithologies in the Wiggins Formation type section. On Carter Mountain in Park County, rocks of Wiggins lithology that lie immediately above the Trout Peak Trachyandesite

yield a late(?) middle Eocene fauna that most closely correlates in terms of age with Tepee Trail rocks elsewhere.

Archean and Proterozoic structural and stratigraphic details of the Hartville uplift in Wyoming

As a result of their work in the Hartville uplift of eastern Wyoming, G. L. Snyder and H. R. Dixon used surface exposures to erect a unified, internally consistent stratigraphy of Proterozoic metasedimentary and metavolcanic rocks. This stratigraphy consists of the following five units in stratigraphic order from top to bottom:

(1) Isolated exposures of very coarse muscovite schist, quartzite, and minor dolomite, probably above, perhaps part of unit 2, as much as 610 m thick.

(2) Intimately interlayered pure to chondroditic(?) dolomite, muscovitic schist, layered amphibolite, and siliceous calcareous marble, with top contact uncertain, and 305 to 610 m thick or more. thick or more.

(3) Granular biotite schist to muscovitic and sillimanitic schist with local amphibolite layers varies along strike from a unit a few hundred meters thick to at least 1,524 m thick.

(4) Greenstone to amphibolite has locally massive extrusives in lower two-thirds that contain at least two zones of pillow lavas and many amygdular and agglomeratic exposures. Finely laminated water-deposited amphibolites are interlayered with rare marbles and thin orthorhombic-amphibole gneisses. The unit is 30 m to at least 1,524 m thick.

(5) Dolomite, siliceous or tremolitic, massive to intimately interlayered with pelitic schist, quartzite, quartz-granule conglomerate, and calc-silicate pod-rock, especially near top. The bottom is not exposed, but the unit is likely more than 1,219 m thick.

Some of the obvious lenticularity is the result of original accumulation, whereas other thickening or thinning is apparently related to fold tectonism. The structure varies from homoclinal to isoclinal, but stratigraphic order is deducible internally from many excellent exposures of the following six sequence criteria: (1) crossbedding, (2) primary graded bedding in granule conglomerates and sands, (3) metamorphically reversed graded bedding in metashales, (4) algal stromatolites, (5) pillowed lavas, and (6) basal conglomerates.

New data on geology of Seminoe Mountains

The Seminoe Mountains are an eastward-trending range, uplifted on the north along the Seminoe fault. G. L. Snyder and H. R. Dixon, mapping in the eastern half of the Seminoes east of the North Platte River, showed that this fault separates Precambrian metamorphic rocks of the Seminoe Mountains on the south from massive unfoliated Precambrian granite and Paleozoic sedimentary rocks on the north. Within the Seminoes, the rock sequence from north to south is (1) dark-gray biotite gneiss with less abundant amphibolite and calc-silicate gneiss, (2) a white granite, varying from fine to coarse grained, interlayered amphibolite, and a thinly layered, medium-gray biotite-quartz diorite gneiss, (3) buff, weakly to unfoliated biotite granite, and (4) light-gray to pink weakly foliated, locally layered granite. Relative ages of units have not been established, but units 3 and 4 appear to be gradational. The various units are successively cut out to the east along the Seminoe fault, and only unit 4 is present at the eastern end of the range.

The unfoliated granite north of the fault is probably continuous with the granite of Lankin Dome of Peterman and Hildreth (1978), which was dated as 2,602±60 million years. The only metamorphic rocks observed north of the fault were small inclusions (>1 m diameter) in an exposure probably near the edge of the granite body. The granite is cut along the Seminoe fault to the east.

The Seminoe fault is well exposed along the north flank of the mountains. The trace of the fault is marked by intermittent exposures of mylonite, a few meters thick, and by a zone of cataclasis, tens of meters thick, on both sides of the fault. Undisturbed upper Miocene rocks were not observed overlapping the fault, but they do occur within a few meters of the fault and overlie cataclastic Precambrian rocks. Near the eastern end of the Seminoe range, the Paleozoic rocks on the north side of the fault are cataclastic and strongly slickensided. The youngest rock observed next to the fault is the Tensleep Formation of Pennsylvanian age. Thus, the latest movement on the Seminoe fault was prelate Miocene and post-Pennsylvanian.

Middle-Wisconsinan glacial lake in Scobey, Montana, area

Evidence of four glaciations around the high Glentana and Flaxville unglaciated areas in northeastern Montana has been found by R. B. Colton. The oldest evidence of glaciation (pre-Wisconsinan?) consists mostly of scattered erratics. The

next readvance of the ice is represented by patches of weathered till and some constructional topography; the surface of this till is characterized by a 130-km-long belt of ice-crack moraines. Large temporary lakes were held in by lobes of ice near Scobey and Glasgow. The third glaciation is represented by youthful moraines a few kilometers north of Scobey and east of Poplar. Very youthful swell-and-swale stagnation moraine and ice-contact stratified drift were left several kilometers north of Scobey and Plentywood and near Medicine Lake by the fourth readvance of the ice.

Mapping of thick terrace deposits along the Yellowstone River and its tributaries between Miles City and Fallon, Mont., indicates that deltas were formed at the mouths of several tributaries such as the Powder River, the Tongue River, and O'Fallon Creek. The glacial lake, in which the deltas formed, was held in by a lobe of ice that advanced up the valley of the Yellowstone River to Intake. The surfaces of the deltaic deposits have approximate altitudes of 800 m which agrees well with the inferred altitude of the lake spillway in North Dakota.

Trenches dug in volcanic ash deposits 9 km northeast of and 9 km southwest of Richland, Mont., show that they are as much as 13 m thick and are overlain by 1 to 2 m of bentonite.

More Archean rocks in Utah

The Farmington Canyon Complex, which forms the basement in north-central Utah, has been considered to be of Proterozoic X age based on K-Ar ages as great as 1,700 million years determined on hornblende. A Rb/Sr isochron determined by C. E. Hedge on samples of migmatite collected by B. H. Bryant from Weber Canyon, 20 km southeast of Ogden, Utah, shows that these rocks have a minimum age of 2,600 million years and could be as old as 2,900 million years. These data increase the area of Archean crust in the North American craton southwest of its previously known extent, especially if the basement rocks near Santaquin, 120 km south of Weber Canyon, are correlative with the Farmington Canyon Complex, as they appear to be.

Dissolution history, southeastern New Mexico

G. O. Bachman has further defined details of the dissolution history of subsurface salt and gypsum in southeastern New Mexico. A volcanic ash was found in the Gatuna Formation, which is tentatively correlated with "Pearlette Type O" ash (ca. 600,000 yr B.P.) (G. A. Izett, USGS, 1978, written commun.). This date is of considerable value for the timing of major events. The Mescalero caliche (informal term) overlies the Gatuna Formation and is generally a pedogenic deposit that began to form about 500,000 years ago.

Some broad karst features were formed before Gatuna time, and collapse sinks were active during Gatuna time. During most of "Mescalero" time the region was relatively quiescent. Since "Mescalero" time sulfate-bearing ground water has percolated through parts of the area. Dissolution, accompanied by karst development, is continuing today.

Visible and concealed geologic hazards in central Utah

I. J. Witkind reports that young faults and mass-wasting deposits are highly visible geologic hazards in central Utah. In many places, bedrock is broken by a large number of northeasterly trending, high-angle, normal faults that are probably of Pleistocene age. Several of the rock units, notably the North Horn Formation (Cretaceous and Paleocene) and the Flagstaff Limestone (Paleocene and Eocene), have supplied vast amounts of mass-wasting debris that clogs the valleys cut into both flanks of the Wasatch Plateau. East of the plateau most of the communities are distant from the valley mouths, but on the west, many are built near valley mouths. If the unstable mass-wasting deposits were to become saturated and then set in motion as a result of movement on one or more of the young faults, considerable property damage would be done to those towns.

Still another geologic hazard, one not so readily apparent, is in the area. A Jurassic unit, the Arapien Formation, contains huge amounts of evaporite—salt, gypsum, and calcite. These evaporite deposits apparently have flowed sporadically ever since they were deposited, and they have intensely deformed both the enclosing and the overlying strata. In one locality, semi-consolidated gravels, likely of Pleistocene age, have been bowed up into a vertical position by the evaporite deposits. These vertical beds are truncated and overlain by younger, horizontal, alluvial deposits that appear not to be warped, although detailed leveling records do not exist to determine whether warpage has occurred on a very small scale. The fact that the evaporite deposits have been active during the Pleistocene implies strongly that they are capable of moving today. Obviously, an abrupt movement on their part resulting in some shaking of the ground might set the mass-wasting deposits (if saturated) in motion.

It seems unlikely that the mass-wasting deposits would move very far from their present position

unless they were saturated, even if the ground were to be shaken vigorously. If much water were added to these deposits, however, either as a result of a rapid snowmelt or an unusually wet spring, the stability of these deposits would be lessened drastically, and it is possible that they might move even without any ground shaking.

In general, the potential for considerable damage exists in the area; the probability of such damage is small.

Pyritic alteration in the northern Keg Mountains, Utah

In the Delta 2-degree quadrangle, Utah, an unprospected zone of pyritic alteration containing anomalous trace concentrations of ore-stage base and precious metals was discovered by H. T. Morris in the northern Keg Mountains (Morris, 1978). Considerable interest in this area has been shown by exploration and mining companies. Claims were staked shortly after the announcement of its discovery, and currently the area is being studied in detail with the goal of selecting sites for diamond drill holes.

Tephrochronology

Tephrochronologic study by G. A. Izett of two volcanic ash beds interlayered in sediments of the Main Canyon Formation (Pleistocene and Pliocene) of Bright (1967) in Thatcher Basin in southeast Idaho indicates that the formation is much older than previously thought. The formation previously was assigned a late Pleistocene age (33,700–27,000 yr B.P.) based on seven carbon-14 ages. Of two of the ash beds in Bright's Main Canyon Formation, one correlates with the "Pearlette Type *B*" (2.0 m.y.) ash and the second with "Pearlette Type *O*" (0.6 m.y.) ash of the Great Plains. The correlation of the ashes in Bright's Main Canyon Formation with the "Pearlette Type *B* and *O*" ashes is based on similarities of (1) index of refraction of glass shards, (2) chemical composition of glass shards (major and trace elements), (3) chemical composition of phenocrysts of clinopyroxene, hornblende, magnetite, and ilmenite as determined using an electron microprobe, (4) phenocryst assemblage, and (5) paleomagnetic direction of the ashes. Zircon microphenocrysts of the ash in Bright's Main Canyon Formation that correlates with the "Pearlette Type *O*" yielded an age of 0.56 ± 0.18 million years (C. W. Naeser, USGS, written commun., 1978). The revision of the age assignment of the Bright's Main Canyon Formation indicated by the above data has important bearing on the geomorphic and tectonic history of Thatcher Basin relative to the history of Lake Bonneville.

An experimental technique for delineating areas best suited for mining of coal

An experimental method was developed for delineating those areas best suited for the surface mining of coal. A computer combined several resource and existing land-use maps into a single map that shows areas of low, intermediate, high, and very high suitability for mining. These map units were determined by adding separate evalution scores that had been assigned to the current use of land, plus five natural resources—ground water, surface water, soil, wildlife habitat, and scenic quality. Evaluation scores for these factors were arrived at by rating their suitability for one of the following purposes: agricutural use, importance or uniqueness to local ecological systems, or esthetic quality. It is assumed that in regions of widespread minable coal, areas having the most valuable natural resources should be mined last or not at all.

The Gap quadrangle, Wyoming, was chosen as an example of the method. This area is representative of a larger region in northeast Wyoming underlain by coal amenable to surface mining techniques. The quadrangle was divided into a grid having several thousand map cells. The factors found in the cells were individually evaluated and their scores totaled. The range in sums was subdivided into the four map units of the final map. These were printed as symbols by the computer to result in a map showing suitability for mining.

IGNEOUS STUDIES

Volcanic recurrence intervals and volcanic hazards in the eastern Snake River Plain in Idaho

Combining field mapping, radiocarbon and K-Ar age determinations, and statistical analyses, M. A. Kuntz, G. B. Dalrymple, and J. O. Kork have attempted to determine recurrence intervals of volcanism in selected areas of the eastern Snake River Plain for the purpose of evaluating volcanic hazards. In the Arco-Big Southern Butte area, volcanic recurrence intervals are on the order of one eruption per 3,000 years. Radioactive waste storage facilities of the Radioactive Waste Management Complex (RWMC) at the Idaho National Engineering Laboratory (INEL) are subject to potential volcanic hazards from volcanism in the Arco-Big Southern Butte area. The RWMC lies at the mouth of a funnel-shaped volcanic eruption basin; thus,

lava flows from distant vents have the possibility of being channeled into the storage area. Studies are currently underway to determine the K-Ar ages of approximately a dozen lava flows encountered in cored drill holes at the RWMC to determine the recurrence interval of flooding of the waste storage site by lava flows.

In a similar study, K-Ar dating of five basalt lava flows in cored drill holes at a proposed reactor site at INEL showed that the site had been covered by the flows over a period of about 350,000 years. The K-Ar age data indicate that the site has been covered by lava flows at irregular intervals from perhaps a few thousand to as much as 150,000 years, with an average recurrence interval between flows of approximately 50,000 years.

Field mapping of the Craters of the Moon lava field, Idaho

Field mapping of the Holocene Craters of the Moon lava field in south-central Idaho by M. A. Kuntz and D. C. Champion (USGS) and R. H. Lefebvre (Grand Valley State College) shows that a large part of the lava field was formed approximately 10,000±2,000 years ago, by tube-fed pahoehoe and as flows erupted from large spatter cones at the north end of the Great Rift. Several flows traveled as much as 45 km from their source vents. The older flows are covered by extensive younger flows, erupted about 2,000 to 2,400 years ago, also from large cinder cones at the north end of the Great Rift. Samples of organic soil were collected from beneath about 20 lava flows for radiocarbon age determinations; the data should provide the information necessary to provide an evolutionary model for the lava field. In addition, the age data will provide a framework for evaluation of the secular variation of the Earth's magnetic field during the last 12,000 years. The chemical and age data currently available suggest that lavas ranging from olivine tholeiite (~45 percent SiO_2) to ferrolatite (~63 percent SiO_2) were erupted nearly simultaneously from adjacent fissures in the Great Rift volcanic rift zone during several periods in the evolution of the lava field.

Structurally complex roots of a caldera near Questa, New Mexico

Reconnaissance mapping by P. W. Lipman of a little studied upper Tertiary volcanic field in the Sangre de Cristo Mountains near Questa, N. Mex., has led to recognition of a volcano-plutonic assemblage of remarkable structural complexity. This assemblage may reflect formation of an ash-flow caldera in an extensional tectonic environment, related to early growth of the Rio Grande rift. A single cooling unit of rhyolitic ash-flow tuff 1 km or more thick overlies a chaotically brecciated assemblage of intermediate-composition lavas and intermixed tuffs. This assemblage is cut by compositionally and texturally diverse high-level granitic intrusions (with published dates of 22-23 m.y.) analytically indistinguishable from a single date on the ash-flow tuff. Structural interpretation of this volcano-plutonic association, which may represent a caldera-fill assemblage, is complicated by repetition and rotation to near vertical dips along north-trending normal faults. These faults have displacements that are generally down on the west, a geometry similar to that of the Sangre de Cristo frontal fault system along the east boundary of the Rio Grande rift. Exposures along these fault slices and steep west slope of the mountain range appear to provide a vertical cross section of several kilometers through the interior of the caldera. This probable caldera is of economic interest because a large zone of major acid-sulfate alteration and molybdenum mineralization, which includes the open-pit Questa Mine, occurs along its south margin in the Red River area.

Initial strontium values of rocks from the Pioneer Mountains

Initial strontium (i-Sr) values of Cretaceous intrusive rocks of the Pioneer batholith, and of rocks within the Proterozoic X gneissic basement complex nearby, were determined by J. G. Arth in conjunction with the areal mapping and petrologic studies of E-an Zen. Arth found that the i-Sr values of the batholithic rocks fall into two groups, those at or near 0.7113 and those at or near 0.7138. Zen finds that these two groupings are compatible with an interpretation of the field relations, which shows these two groups to form two distinct intrusive series, even though on a Harker variation diagram the two groups are not distinguishable. Because the two groups yielded identical K-Ar ages by concordant hornblende and biotite determinations, they presumably coexisted as two distinct but contemporaneous magma bodies, and differentiation within each body could have given rise to various plutons within each series. The i-Sr values are much higher than those of the Boulder batholith (Tilling, 1973); the values are also sufficiently high as to suggest highly differentiated parent material such as sedimentary rocks, even though the rocks exhibit petrologic features suggestive of the I-series of igneous rocks according to the nomenclature of White and Chap-

pell (1977). On the other hand, the i-Sr values of the Proterozoic X gneiss and amphibolite are such that they could have given rise to the magmas of the Pioneer batholith in Late Cretaceous time. The distinctness of the magmas of the Pioneer region ceased to exist in the early Tertiary, for the volcanic rocks of this age from the Pioneer Mountains yielded i-Sr values that are the same as those of similar rocks from the area around the Boulder batholith.

Pliocene rhyolite in the Sevier Plateau, Utah

Past geologic mapping in southwestern Utah revealed that domes and lava flows of alkalic high-silica rhyolite, locally accompanied by subordinate volumes of alkalic basalt, are distributed along an east-trending structural feature named the Blue Ribbon lineament (Rowley and others, 1978). Rhyolite centers had been dated as old as 20 million years; they are younger toward the east along the lineament (Mehnert, Rowley, and Lipman, 1978). A large area of rhyolite at the eastern end of the lineament was studied in greater detail recently by P. D. Rowley and T. A. Steven, who found it to be younger than previously thought. The new mapping showed that the rhyolite occurs as a low-walled, poorly exposed crater of tuff and other airfall material intruded by a steep-sided lava dome or volcanic spine. A small basalt lava flow is in the inner wall of the crater, and clasts of basalt make up a significant volume of the airfall material of the crater wall. The resistent spine forms Phonolite Hill, a feature with 500 m of relief, which is in the bottom of the 1,200-m-deep Kingston Canyon, a largely antecedent canyon that cuts through the Sevier Plateau. Canyon cutting occurred during and after basin-range faulting, which uplifted the Sevier Plateau. The rhyolite postdates canyon cutting. H. H. Mehnert recently obtained a preliminary K-Ar age of 4.8 million years on obsidian from the margin of the spine. Rhyolite of similar lithology occurs as domes and flows north of Kingston Canyon, yet these rocks predate basin-range faulting and canyon cutting. They overlie basalt flows that probably are correlative with basalt that was dated at 12.6 million years (Damon, 1969). The rhyolites in Kingston Canyon thus seem to bracket the age of basin-range faulting in this area. Of perhaps greater importance, these rhyolites seem to contain anomalous amounts of uranium. The rhyolite of Phonolite Hill, in addition, may have potential for geothermal sources of energy.

Tertiary intrusions in the Cretaceous Idaho batholith

W. E. Hall and J. N. Batchelder have mapped into the southwestern corner of the Idaho batholith, Blane and Camas Counties, Idaho. The primary rock type in the Cretaceous batholith is biotite granodiorite. The measured magnetic susceptibilities of the batholith are very low, indicating a lack of magnetite. In general, the batholithic rocks are characterized by deep weathering, producing grus-covered slopes and subdued topography. Intruding the batholith are Tertiary dikes, sills, and stocks predominantly of biotite granite and granodiorite composition. These hypabyssal intrusions commonly are coarsely porphyritic. Their measured magnetic susceptibilities are approximately two orders of magnitude higher than the Idaho batholith and indicate the presence of magnetite. Unlike the batholith, the Tertiary rocks generally are unaltered and stand out in bold outcrops. Reconnaissance of the Atlanta lobe of the Idaho batholith during the 1977 and 1978 field seasons indicates that between Boise and the border of the batholith, approximately 30 percent of the area previously considered to be mainly Cretaceous in age is underlain by Tertiary intrusions. In many localities the crosscutting relations between the two units are strikingly visible.

Withington Creek caldera

The Withington Creek caldera, studied by David Lopez, is the first ash-flow tuff caldera recognized in a volcanic field satellitic to the Challis Volcanics of east-central Idaho. The caldera is about 13 km south-southeast of Salmon, Idaho, on the east flank of the Lemhi Range and is pear-shaped, measuring about 10 km by 6 km. The caldera margin is delineated on three sides by faults which separate rocks of the Yellowjacket Formation (Proterozoic Y) from massive rhyolite ash-flow tuff inside the caldera. The remainder of the margin is marked by a fault contact between thin, layered ash-flow tuff and andesite flows outside the caldera and the massive ash-flow tuff within the caldera. The rhyolite ash-flow tuff in the caldera is at least 600 m thick; beyond the caldera it is only 50 to 100 m thick.

TECTONIC AND GEOPHYSICAL STUDIES

Major tectonic zone across southern Colorado

A major and long-lived tectonic zone that extends west-northwest across almost all of southern Colorado has been identified by O. L. Tweto in conjunction with analysis of the new geologic map of Colo-

rado. Some elements of the tectonic zone have been referred to in the past as extensions of the Wichita-Amarillo tectonic zone of Oklahoma and Texas. Although the two zones may be related, they are not alined and, if projected, would be separated by 135 km. The tectonic zone in Colorado ends southeastward against a fault zone that extends southward nearly along the New Mexico-Oklahoma boundary. This fault zone may have been the means of transfer of movement from the Wichita-Amarillo zone to the Colorado zone.

In the subsurface of eastern Colorado, the tectonic zone is marked by faults along the northeast side of the buried late Paleozoic Apishapa uplift, by a line of truncation of pre-Pensylvanian Paleozoic rocks, by depositional wedgeouts of Pennsylvanian formations, and by overlap of Permian rocks onto Precambrian rocks. At the surface, it is marked by minor faults and monoclines in Cretaceous rocks. Near the crest of the buried Apishapa uplift is a belt of quartzites, phyllites, and volcanic rocks that overlie various older Precambrian rocks. These younger rocks may correspond to the undated "Tillman Metasedimentary Group" (Ham, Bennison, and Merritt, 1964), which lies beneath Lower and Middle Cambrian volcanic rocks in the Wichita Mountains of Oklahoma. Presence of these younger basement rocks on the upthrown side of the fault zone bordering the Apishapa uplift suggests an opposite displacement prior to the Late Cambrian.

In the Wet Mountains, the tectonic zone is expressed by west-northwest-trending faults, by alkalic and mafic plutons of Cambrian age, and by local swarms of lamprophyre dikes of presumed Cambrian age. Farther west, faults of the zone terminate the north-northwest-trending Sangre de Cristo Range and bound a deep graben of Neogene age. The same faults project toward a deeply eroded caldera and intrusive center at the southern end of the lower Oligocene batholith of the Mount Princeton Quartz Monzonite in the Sawatch Range. At about the longitude of the Sawatch Range, another segment of the tectonic zone begins in left echelon position to the south and continues west-northwestward to the Utah border. This segment is manifested by faults that show movements ranging from Precambrian to post-Oligocene in age, by the Early Cambrian or very late Precambrian alkalic-mafic intrusive center near Powderhorn, by the long Precambrian and Laramide Cimarron fault, by long diabase dikes of Late Cambrian age following faults of probable Precambrian origin in the Black Canyon of the Gunnison River, by diabase dikes of the same west-northwest trend in Unaweep Canyon on the Uncompahgre Plateau, and by mafic intrusive bodies at the Colorado-Utah boundary.

Major faults of the tectonic zone originated in Precambrian time, probably as strike-slip faults. One of the Precambrian faults in the Black Canyon of the Gunnison displaces vertical Precambrian rock units 5 to 6 km left laterally. Some post-Cambrian, possibly late Paleozoic, fault movements in the Wet Mountains were also strike-slip or nearly so, but most Phanerozoic movements seem to have been dip-slip. Faults in various segments of the tectonic zone moved independently at various times in the Phanerozoic, depending on conditions imposed by younger tectonic features of other trends.

Large-scale detachment faulting of Eocene volcanic rocks, southeastern Absaroka Range, Wyoming

Mapping studies in the southeastern Absaroka Range, Wyoming, in 1977 and 1978 led to the recognition by T. M. Bown of more than 70 erosional remnants of strongly deformed, allochthonous rocks that record a major episode of large-scale detachment faulting in Pliocene or Pleistocene time. These remnants are dispersed from the North Fork of Owl Creek in the south, to the Wood River in the north, and from Deer Creek on the west to Squaw Buttes on the east, indicating that the area affected by detachment faulting or overridden by detached masses comprises at least 1,200 km^2. Wilson (1975) has briefly described possible breakaway areas for related detached masses in the Wood River drainage, north of the mapped area.

Remnants of detached rocks and related displaced masses of volcaniclastic rock comprise four types: (1) thick masses of heterogeneous lithology, derived from lower and (or) middle parts of the middle and upper Eocene Tepee Trail Formation (up to 300 m of preserved rock), (2) thinner masses of essentially homogeneous green and brown volcanic wackes of uncertain stratigraphic derivation (150 m maximum preserved thickness), (3) slivers of volcaniclastic rock derived from the Aycross Formation that were rotated out of place beneath the plane of movement, and (4) lag blocks that have rolled or have been let down by erosion from topographically higher allochthonous rocks. Detached rocks of Tepee Trail lithology are intensely deformed but less so than the volcanic wackes, which often show plastic folding of beds. The allochthonous volcanic wackes invariably lie topographically beneath detached Tepee Trail beds, suggesting that they formed the bottom of the glide mass or represent

an earlier episode of detachment faulting. The first interpretation is favored because the greater deformation of the volcanic wackes is probably related to greater confining pressures that would have existed in the lower part of the mobile mass.

Field relations indicate that the faulting comprised four phases: (1) high-angle normal faulting that progressed to (2) low-angle normal faulting at depth, (3) erosion thrust faulting at the edge of the basinward-facing erosional scarp, and (4) gravity-glide faulting that was begun once the main body of the thrust sheet became detached from in situ rocks on the erosional scarp. The soles of the detachment faults were developed in the Tepee Train Formation in the breakaway area, but progressed downward to the Tepee Trail Formation-Aycross Formation erosional unconformity in more basinward areas. Within the mapped area, the glide planes of the detachment faults were developed on the upper badland unit of the Aycross Formation, a sequence composed principally of bentonitic mudstone.

Topographic considerations, the thicknesses of the detached masses, and the geographic positions of possible breakaway areas indicate that the detached sheets must have broken into several blocks shortly after detachment. The earthquake oscillation hypothesis of Pierce (1975) for movement of detached blocks related to the early to middle Eocene Heart Mountain dêcollement seems adequate to explain gravity-glide movement of blocks of volcanic rock in the mapped area. Normal faulting that occurred prior to detachment faulting may also have been caused by earthquakes or by a combination of earthquakes and compressive and tensional forces generated by late Tertiary or Pleistocene intrusive activity.

The topographic positions of the allochthonous remnants indicate that the gravity-glide sheets and (or) individual blocks crossed an area of considerable relief in some areas. Geomorphic relations suggest that this topography was developed during the present-day semiarid erosion cycle, probably in the late Pliocene or Pleistocene.

Summary of late Cenozoic history of the Wind River basin and adjacent uplands in Wyoming

H. W. Markewich and J. D. Love propose the following reconstruction of the late Cenozoic history of the Wind River basin and adjacent uplands in central Wyoming. By the end of Miocene deposition, the Wind River basin was completely filled, and the bordering pre-existing Laramide mountain ranges were partially to completely buried. This interval of deposition was followed by "epeirogenic uplift," with rapid excavation of the basin and exhumation of the surrounding mountains. Other events that accompanied this uplift were downfaulting of these mountains, regional warping within the basin, several episodes of glaciation, extensive modifications of previously established drainage patterns of major rivers, changes in paleo-climates, and development of a belt of sand dunes, now stabilized, which extends from the central Wind River basin eastward for 160 km into the southern Powder River basin.

After the end of Miocene deposition, the west-trending gentle Gas Hills-Riverton arch, 120 km or more in length, developed in the southern part of the basin. This arching caused the right-angle shift of Wind River from the central part of the basin northward across the still-buried Owl Creek Mountains and the beginning of the present cycle of degradation. Potassium-argon ages and correlation of ash deposits in and along the basin margin suggest that the rate of reexcavation of the basin by water and wind during the last 600,000 to 6 million years is about 0.3 m per 1,500 years.

The southern Absaroka Range was extensively modified by several episodes of glaciation during which ice moved southward and southeastward, impinging on northward- and eastward-moving ice from the Wind River Range. Other margins of the basin were not glaciated. Continued gentle uplift of the Gas Hills-Riverton arch caused northward migration of Wind River within the basin. The time of development of the sand dunes in the basin is probably, at least in part, late Pleistocene.

Tectonic style and history, north end of the Pioneer Mountains in Montana

In the northwestern part of the Vipond Park quadrangle and the adjacent Stine Mountain quadrangle to the west, flat-lying or gently dipping sedimentary rocks of Cambrian and Precambrian age are involved in an intricate pattern of faulting, according to the field observations of E-an Zen. A set of west-northwest-trending high-angle faults, commonly defined by parallel valleys, tilts the rocks of each block southward. On these faults the south side is upthrown relative to the north side. Rocks involved in most of the fault blocks are thin-bedded quartzite, siltstone, and shale that may be correlative with units in the upper part of the Missoula Group of the Belt Super-group, the upper member of the Middle Cambrian Silver Hill Formation (pre-upper units of the Silver Hill of the Paleozoic are missing in this tectonic setting), and the Middle and Upper Cambrian Hasmark and Red Lion Forma-

tions. This south-side-up fault set appears to lead southward, across the fault blocks, into the Lower Cambrian(?) rocks (to be called the Black Lion Coglomerate), and finally into a Proterozoic X gneiss and amphibolite basement complex; south of this complex spotty evidence suggests that the fault sense is reversed. These fault block are intersected by a set of north-northeast-trending high-angle faults (which parallel the range fronts that bound Tertiary basins) along which the rocks west of the faults are downthrown. A checkerboard outcrop pattern results. The most westerly fault block in this set is underlain by Precambrian quartzites. Zen interprets the relations to mean that the quartzites are contained in thrust sheets overlying younger, Paleozoic rocks. The leading edges of the thrusts have been obliterated by later high-angle faults that downdropped the rocks. The klippe of Precambrian quartzite at Morrison Hill (in the center of the Vipond Park quadrangle) is an erosional remnant of the same thrust sheet (or sheets) and outcrops of similar quartzite, now found scattered in intervening areas, are remnants of the proposed once-extensive thrust sheet. This thrust sheet of Precambrian rocks dominates the West Pioneer Mountains, and Zen (1977) has suggested that there these rocks overlie Paleozoic rocks in a tectonic situation closely similar to the relations inferred for the Medicine Lodge thrust system (Ruppel, 1978). A group of outcrops of sheared carbonate, lithically like the Pennsylvanian Amsden Formation, exist at the lower slopes or Ross Gulch in the West Pioneers at lower altitudes than the Precambrian quartzite that forms the mountains. These carbonate rocks were first discovered by Calbeck (1975); they could be part of the subjacent terrane. Similar relations, even more definitive, have been reported from elsewhere in the West Pioneers. Thus, the thrusts place Precambrian rocks on rocks of different ages in the area, ranging from early Paleozoic to Cretaceous; their relations show that considerable tectonic relief existed at the time, presumably reflecting the effects of considerable Laramide deformation. Petrologic study of intrusive rocks in the area indicate an episode of 70–75 million years intrusion at shallow level and an episode of 63 million years intrusion of granite containing liquidus muscovite, free of halogen, that presumably was deeper seated owing to the constraints of muscovite-quartz stability. The thrust sheets might have contributed to the tectonic load needed for the younger intrusive rocks; field relations clearly show these to be post-thrusting in age.

Younger-over-older thrust plates in southeastern Idaho

West of the Paris and Putnam faults (Bear River and Portneuf Ranges, Idaho), thrust plates of younger strata overlie older with as much as 7 km of stratigraphic units omitted, in contrast to eastern foreland thrusts of older over younger with about 6 km of stratigraphic units repeated. Folds in the western plates are broad, open, and upright in contrast to tight asymmetrical folds in eastern plates.

According to S. S. Oriel and L. B. Platt, three major thrust plates are recognized from extensive but incomplete mapping:

(1) An uppermost plate of Oquirrh strata (Pennsylvanian and Permian), with Manning Canyon Shale (Mississippian and Pennsylvania) locally below it, rests discordantly on middle Paleozoic units. This plate extends from the Albion Range 100 km east to the Bannock Range.

(2) A middle plate of mainly Ordovician to Middle Cambrian strata rests on Proterozoic Z quartzite and argillite of the Brigham Group in the Bannock Range between Pocatello and Utah. Ordovician strata in the Raft River and Albion Ranges rest on schist and quartzite of unknown age.

(3) A lower plate of mainly Proterozoic Z (Mutual and lower part of Camelback Mountain) quartzite overlies Proterozoic Z rocks of the Scout Mountain Member of the Pocatello Formation in the Bannock Range.

The middle plate locally overlaps the lower, placing Ordovician limestone directly on Scout Mountain strata. Scout Mountain rocks are more intensely sheared, mylonitized, and metamorphosed (greenschist) than any east of the Raft River Range.

The thrust plates are cut by younger basin-and-range faults marked by large apparent stratigraphic throw.

Muldoon Canyon thrust in south-central Idaho

The trace of the generally east-dipping and folded Muldoon Canyon thrust, first described by Nilsen (1977) at the head of Muldoon Canyon in the southern Pioneer Mountains, has been mapped from Muldoon Canyon south to the northern edge of the Snake River Plain (about 30 km) by B. A. Skipp and J. N. Batchelder, assisted by B. A. Watson. The thrust brings a western facies of the Copper Basin Formation, the Brockie subplate of Nilsen (1977), over an eastern facies of the same formation, the Scorpion subplate of Nilsen (1977), both structural elements within the Copper Basin allochthon

(Skipp, 1974; Skipp and Hall, 1975a, b; Skipp and Hait, 1977). Breccia and (or) barite are localized along the Muldoon Canyon thrust that cuts across and involves several facies at different stratigraphic levels. The thrust is cut by at least two northeast-trending normal faults.

The generally east-dipping Muldoon Canyon thrust probably connects with an unnamed west-dipping thrust mapped to the east. If this interpretation is correct, the Brockie subplate is a rootless remnant of a thrust sheet which is presently about 8 km wide and is high in the structural sequence of the Copper Basin allochthon (Nilsen, 1977; Skipp and Hait, 1977). The Brockie subplate is composed in part of very coarse-grained terrigenous turbidites formed in both inner- and middle-fan environments (Nilsen, 1977). These resistant rocks make up the rugged topographic spine of the southern Pioneer Mountains.

Bald Butte fault in the Helena area of Montana

New geologic data have been collected by R. G. Schmidt on the Bald Butte fault, a major deep-seated fracture in the zone of crustal discordance (Lewis and Clark line) that extends northwestward from Helena, Mont., across the Butte 2-degree quadrangle. Among the principal new discoveries are:

(1) Extension of the fault westward across the Continental Divide into Avon Valley (in the Avon quadrangle) where the fracture disappears beneath Tertiary strata.

(2) The alinement, magnitude, and structural characteristics of the fault are broadly similar to those displayed by a major fracture in the valley occupied by Nevada Lake (in the Nevada Lake quadrangle), which suggests continuity of these faults beneath Avon Valley.

(3) The occurrence of two large graben blocks on the south side of the fault, one between Threemile Creek and McKay Creek (in the Avon quadrangle) involving rocks of the Missoula Group of Proterozoic Y age, the other near Bald Butte (in the Elliston quadrangle) involving strata of Middle Cambrian age.

A prime characteristic of the Bald Butte fault is the large variation in stratigraphic throw along the fault within relatively short distances. For example, at Bald Butte, Cambrian strata on the south side of the fault are juxtaposed against the Empire Formation of the Ravalli Group of the Belt Supergroup, producing an apparent stratigraphic throw of more than 4,000 m, yet a few kilometers to the west the fault trace is confined to the Bonner Quartzite of the Missoula Group of the Belt Supergroup, and the apparent stratigraphic throw is 200 m or less. Similar variations occur along the fault farther west and to the southeast. These structural relations may indicate that the sense of movement on the Bald Butte fault was mainly strike slip.

Revised interpretation of thrust faults in the southern Flint Creek Range, western Montana

Geologic mapping by C. A. Wallace in the south part of the Flint Creek Range, western Montana, has resulted in a revised interpretation of some major structural elements that were described by Emmons and Calkins (1913), McGill (1959), Csejtey (1963), and Poulter (1956).

Thrust faults were mapped and named by earlier workers, but these apparent major faults are now considered to be of no greater tectonic significance than nearby unnamed thrust faults, and the practice of naming specific thrust faults is abandoned. Although thrust faults such as the Philipsburg, Georgetown, and Bungalow faults are locally distinctive because they superpose rocks of greatly different ages, these structures cannot be traced as discrete tectonic elements beyond the areas in which they were named. The reasons why these faults cannot be traced on a regional scale are:

(1) The thrust faults are composed of anastomosing strands that branch from the named faults and merge with other, unnamed thrust faults. The result is that the stratigraphic assemblages of rocks in contact along thrust faults are greatly, and this makes it difficult to trace major faults.

(2) Many thrust faults gently truncate bedding planes so that some structures have an older-over-younger characteristic at one locality and the same structure may have a younger-over-older characteristic at another locality.

(3) Numerous thrust faults were not mapped by previous investigators, and many of these faults have as much apparent stratigraphic separation as faults that were named.

Because of the nature of the thrust faults in this region, the major structural elements will have to be determined by comparative facies analysis to separate tectonically superposed facies assemblages.

A series of klippen has been identified in the south part of the Flint Creek Range. The zone of klippen extends for 20 km in an easterly direction from Cable Mountain on the west to Stucky Ridge on the

east. Csejtey (1963) described some of these klippen in the southeast part of the Flint Range, and now the zone has been extended westward to Cable Mountain by current mapping. The unifying characteristic of these klippen is that the unnamed middle member of the Mount Shields Formation tectonically overlies complexly folded and thrust-faulted Precambrian, Paleozoic, and lower Mesozoic strata. These klippen are thought to represent erosional remnants of a formerly continuous, flat-lying thrust sheet that had been transported from west-to-east.

Subsurface model for an area of the eastern Snake River Plain

The results from gravity, magnetic, resistivity, seismic refraction, and magnetotelluric surveys of the Idaho National Engineering Laboratory (INEL) on the Snake River Plain in eastern Idaho have been used by D. R. Mabey to develop a geologic model that is consistent with all the geophysical data, surface geology, and data from a 900-m-deep hole. The model indicates that the Cenozoic sedimentary and volcanic rocks overlying the Paleozoic sedimentary rocks thicken abruptly at the northwest edge of the Snake River Plain and are about 1.5 km thick within 3 km of the edge of the plain. The surface on the Paleozoic rocks may either dip steeply under the plain or be depressed by a series of step faults. Southeast from this zone of abrupt thickening, the Cenozoic rocks thicken slightly southeastward to about 10 km from the edge of the plain. Over this distance the Cenozoic rocks consist of an upper unit less than 1 km thick composed of basalt and sediments and a lower unit of either altered volcanic rocks or sediments. Paleozoic sedimentary rocks probably underlie the Cenozoic rocks. At this 10-km distance from the northwest edge of the plain, the geophysical data define a transitional zone parallel to the edge of the plain where major changes occur in both the Cenozoic rocks and the underlying older rocks. Southeast of this zone the upper Cenozoic unit thickens to about 1.5 km and is predominantly volcanic rocks. The lower unit continues at about the same thickness; the combined thickness of both units is about 2.5 km. The physical properties of the underlying rocks becomes complex, suggesting a structurally complex area where the Paleozoic sedimentary rocks may be overlain by about 2 km of older Tertiary volcanic rocks or Mesozoic sedimentary rocks.

Rio Grande rift, New Mexico

Compilations by L. E. Cordell of regional geophysical data show that the Rio Grande rift encompasses uplifts of the Southern Rocky Mountains and their southern extension, as well as fault blocks. Gravity gradients delineate major faults, which form a gridded or en echelon pattern over distances on the order of tens of kilometers. Aeromagnetic data shows these to be alined with basement structural grain—by inference, the Neogene-age rift faults zig-zag along preexisting basement cracks.

Structure of the Choteau 2-degree quadrangle, Montana

Geologic mapping by M. R. Mudge in the eastern part of the Choteau 2-degree quadrangle, Montana, revealed surface structures that are alined over the Scapegoat-Bannatyne trend—a northeasterly subsurface Precambrian structural alinement of numerous highs with as much as 425 m of relief that formed prior to Cambrian sedimentation. The trend is shown by a marked lineament on the Landsat photographs. The surface features alined along the trend are northeasterly trending normal faults and folds in Cretaceous rocks. They are east of the disturbed belt and therefore not related to the early Tertiary stresses that formed the northerly trending thrust faults and folds comprising the northern disturbed belt of Montana.

In the disturbed belt, the Scapegoat-Bannatyne trend is reflected by other structural discontinuities. The numerous thrust fault blocks with Paleozoic carbonate rocks that comprise the Sawtooth Range abruptly plunge to the southeast into a structurally low area reflected by the trend. Some structures on the trend change abruptly in strike from southeast to east for a few kilometers. In addition, an igneous plug, called Haystack Butte, intruded across the fault blocks near the trend. Further west in the mountains, northeasterly trending normal or strike-slip faults displace the major northwesterly trending thrust faults.

Data are insufficient to determine the nature of the trend in the subsurface. It probably is a fracture zone in the crystalline basement containing grabens and horsts.

BASIN AND RANGE REGION

MINERAL-RESOURCE STUDIES

Phosphate resources in Permian Phosphoria Formation of east-central Idaho

Geologic mapping and sampling by Peter Oberlindacher and R. D. Hovland of the Retort Phos-

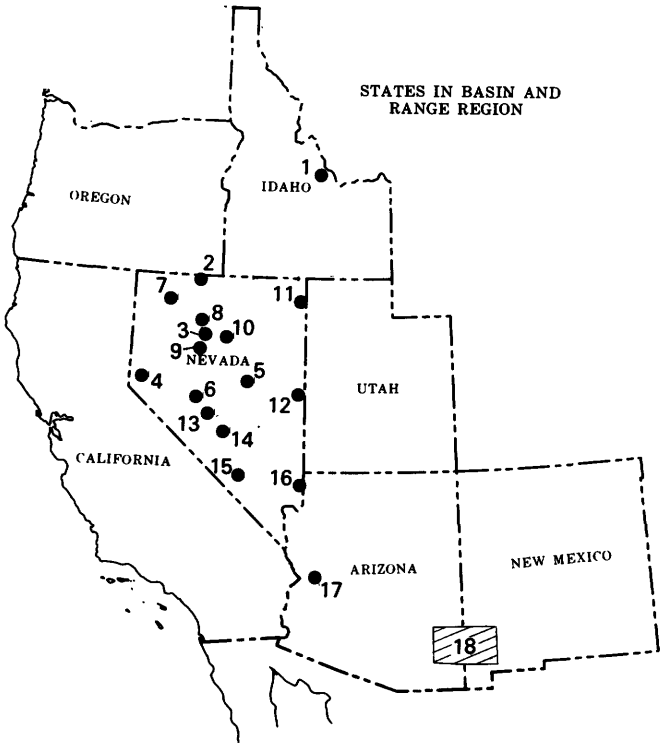

phatic Shale Member of the Permian Phosphoria Formation and associated rocks in the Hawley Creek area in the Beaverhead Mountains near Leadore, Lemhi County, Idaho (loc. 1), have revealed large resources of phosphate rock. Within the mapped area, the Retort has an average thickness of about 22 m over a linear outcrop distance of about 21 km. A trench across the Retort revealed a cumulative thickness of 2.7 m of medium-grade phosphate rock (>24 percent P_2O_5) and 10.2 m of low-grade phosphate rock (16 to 24 percent P_2O_5). Phosphate resources underlying less than 183 m of overburden, based on analyses of samples that represent about half of the Retort in the trench section, are about 73 million metric tons of medium-grade phosphate rock and about 280 million metric tons of low-grade phosphate rock.

Alteration aureoles in McDermitt caldera in Nevada and Oregon

J. J. Rytuba reported that mercury, uranium, and thorium deposits within tuffaceous sediments that were deposited in the McDermitt caldera complex, Humboldt County, Nevada, and Malheur County, Oregon (loc. 2), occur within areas of potassium feldspar alteration. The degree of cristobalite crystallinity, as measured by the d(101) spacing, indicates that a thermal gradient extended as much as 4 km away from each area of potassium feldspar alteration. Silicate mineralogy and cristobalite crystallinity define three previously unknown fossil geothermal areas within the caldera, and one of these areas is associated with significant uranium mineralization.

Big Mike sulfide deposit in northwestern Nevada

According to R. J. Roberts, the Big Mike volcanogenic massive copper-sulfide deposit in the Havallah Formation (upper Paleozoic), Pershing County, Nevada (loc. 3), consists of two contrasting mineral facies and origins that include early fine-grained laminated pyrite layers (0.01–0.10 mm) of syngenetic origin and coarse-grained pyrite and later copper sulfides of epigenetic origin. The coarse-grained pyrite (>0.20 to 1.0 mm) may have been initially syngenetic, but subsequently was recrystallized, fractured, and then replaced by chalcopyrite, bornite, djurleite, covellite, chalcocite, and sparse sphalerite. The inferred sequence of events was (1) early deposition of syngenetic pyrite in mudstone and chert on the sea floor, (2) burial by sedimentary and volcanic rocks, and (3) later addition of copper and zinc sulfides. These events may have taken place within a short time span, but the epigenetic phase was clearly separated in time from the syngenetic phase. The general term volcanogenic does not adequately describe the complex origin of these deposits; hence, special names should be used to identify clearly the early and late phases of sulfide formation in these contrasting environments. Deposits exhibiting similar characteristics in Saudi Arabia were considered by Roberts, Doe, and Delevaux (1976) to be of dual syngenetic and epigenetic origin, and this terminology also seems appropriate for the Big Mike deposit.

Age of Davidson Granodiorite and mineralization in Comstock Lode mining district of western Nevada

R. P. Ashley, M. L. Silberman, and J. R. O'Neil, in collaboration with staff members at the University of Nevada, have completed a study of the potassium-argon and fission-track ages stable-isotope relations of the Davidson Granodiorite in Storey County, Nevada (loc. 4). The granodiorite body, about 1 km^2 in outcrop area, intruded pyroxene andesites of the Miocene Alta Formation, the principle host rocks for silver- and gold-bearing veins in the Comstock Lode mining district. The Davidson Granodiorite was propylitically altered pervasively. Fission-track ages on zircon from two samples of the Davidson indicate that it was emplaced approximately 17 million years ago. Oxygen and hydrogen isotopic-ratio measurements on feldspars,

micas, and chloritized amphiboles separated from these and other samples of the granodiorite indicate that it was altered by a fluid of dominantly meteoric composition, similar to the fluids that mineralized the Comstock Lode (Taylor, 1973). Potassium-argon age determinations indicate that the granodiorite was altered between approximately 14 and 11 million years ago. These combined age and isotopic data provide the best estimates of the time interval during which hydrothermal activity affected the rocks in the Comstock Lode mining district. Previously reported K-Ar measurements on adularia, separated from gold- and silver-bearing quartz veins from two lode deposits, indicated that the vein mineralization occurred between 13.7 and 12.6 million years ago (Bonham, 1969; Whitebread, 1976). Our data, however, indicate that the hydrothermal system related to Comstock mineralization was active somewhat longer than indicated by dates on the veins.

Metals in Devonian marine strata in central Nevada

A kerogen-rich sequence of silicious mudstone, siltstone, and chert as much as 60 m thick in the southern Fish Creek Range, Eureka County, Nevada (loc. 5), has been evaluated by G. A. Desborough, F. G. Poole, R. K. Hose, and A. S. Radtke for its potential resources of vanadium, zinc, selenium, molybdenum, and syncrude oil content. These strata are part of a strongly deformed allochthonous mass of eugeosynclinal Devonian Woodruff Formation that overlies deformed allochthonous Mississippian siliceous rocks and relatively undeformed Mississippian flysch of Antler age. In fresh black rocks, the vanadium is syngenetic and occurs chiefly in organic matter; zinc occurs in sphalerite; selenium occurs in organic matter; molybdenum also is syngenetic and occurs both in molybdenite and in organic matter. Most fresh black rock is a low-grade oil shale and yields as much as 50 L/t of syncrude oil. Organic geochemical data indicate that the organic matter in the rock is thermally immature and has not been subjected to temperatures greater than 60°C since deposition in Devonian time. These marine strata are considered by Desborough and others (1979) to be a large low-grade metal and shale oil resource.

STRATIGRAPHIC AND STRUCTURAL STUDIES

Stratigraphy first, structure second

Structural interpretations can be no better than the stratigraphic data on which they are based. Recently, fossils collected by several geologists have required that ages of Paleozoic and Mesozoic volcanic and sedimentary sequences in several areas of western Nevada be drastically revised. Now, fossils collected by K. B. Ketner and identified by B. R. Wardlaw show that the ages of eugeosynclinal sequences in three additional areas must be modified. Limestone beds at Knickerbocker Wash in the southern Shoshone Mountains in Nye County, Nevada (loc. 6), previously assigned to the Pablo Formation and tentatively regarded as of Permian age, contain Middle to Late Pennsylvanian conodonts. Sedimentary rocks in a volcanic sequence between Bishop Canyon and Cherry Creek in the southern Pine Forest Range, Humboldt County, Nevada (loc. 7), previously mapped as Happy Creek Volcanics and thought to be of Permian age or older, contain limestone boulders that yielded Late Triassic conodonts. Siliceous rocks near the mouth of Clear Creek on the west side of the Sonoma Range in Humboldt and Pershing Counties, Nevada (loc. 8), originally identified as the Pumpernickel Formation (upper Paleozoic) and more recently as the Havallah Formation (Pennsylvanian and Permian), have yielded conodonts of Devonian and Mississippian age.

Ordovician Vinini Formation of northern Nevada

The Ordovician Vinini Formation of northern Nevada is a complexly deformed eugeosynclinal assemblage composed principally of black shale and bedded chert. Structural dismemberment, poor exposures, and monotonous uniformity of the shale and chert units heretofore have impeded efforts to establish a pre-deformational stratigraphic sequence. K. B. Ketner and R. J. Ross, Jr., recognized thin limestone and dolomite beds that, although a minor part of the dominantly siliceous sequence, are widespread in the Vinini. The carbonate beds are key units for the correlation and origin of the Vinini Formation because they are distinctive regional stratigraphic markers. Carbonate beds of early Early Ordovician age are mainly calcarenite deposits composed mostly of marine-current transported debris of the calcareous fossil *Nuia*, a probable algae; they differ from carbonate beds of late Early to earliest Middle Ordovician age, which are distinctive pelletal calcarenite deposits nearly free of *Nuia*. No carbonate rocks of middle Middle Ordovician age have been found in the Vinini; if rocks of this age are present, they likely are siliceous units. Carbonate rocks of latest Middle and Late Ordovician age are sooty micrites com-

posed of minute calcispheres and calcareous sponge spicules.

Paleozoic rocks in southern East Range, northwestern Nevada

According to D. H. Whitebread and M. L. Sorensen, rocks in the southern East Range, Pershing County, Nevada (loc. 9), formerly mapped as the "Leach" and Inskip Formations (upper Paleozoic), are instead part of the Cambrian Harmony and Ordovician Valmy Formations and the Pennsylvanian and Permian Havallah Formation. The Valmy Formation is separated from the Havallah by a steeply dipping thrust fault. The siliceous sedimentary and volcanic rocks of both units are considered potentially favorable for the occurrence of syngenetic-volcanogenic massive sulfide deposits because massive sulfide deposits occur in these formations elsewhere in Nevada.

Greenstone in Devonian Slaven Chert in north-central Nevada

Recent studies by D. L. Jones and C. T. Wrucke, Jr. (USGS), Brian Holdsworth (University of Keele, England), and C. A. Suczek (Western Washington University) have shown that rocks of Devonian age in the Roberts Mountains allochthon are more abundant than previously thought, and, that in the Shoshone Range, Lander County, Nevada (loc. 10), these rocks include greenstone in addition to abundant chert. Mapping and stratigraphic studies in the Shoshone Range reveal that greenstone forms as much as one-third of chert-greenstone sequences in which the associated chert contains radiolarians of post-Ordovician age. This chert-greenstone sequence now is considered as Devonian in age and assigned to the Slaven Chert rather than the Ordovician Valmy Formation as originally interpreted. These results, coupled with additional microfossil evidence that the chert-greenstone sequence in the Scott Canyon Formation at Battle Mountain is Devonian rather than Cambrian (Jones and others, 1978), emphasize the need for caution in assigning an age to undated greenstone and chert units in northern Nevada.

Triassic continental and marine rocks correlated by sedimentary features

Depositional cycles in Upper Triassic rocks of the Chinle Formation in east-central Utah resemble those observed in marine rocks of the Auld Lang Syne Group 500 km away in northwestern Nevada. Three successive, major influxes of fine-grained terrigenous clastic sediment from an eastern source are recorded in the Auld Lang Syne Group during late Late Triassic (Norian) to earliest Jurassic time according to N. J. Silberling. Studies of the Chinle Formation by R. D. Lupe suggest that these events may correspond to the three major fluviatile episodes of Chinle deposition. The suggested genetic relationship between these widely separated sedimentary sequences is supported by similarities in their composition. Extrapolation from the relatively well dated marine rocks in Nevada shows that the older age limit for the Chinle Formation in Utah may be Norian rather than Karnian, the usually accepted age.

Southward-directed thrusting of Mesozoic age in northeastern Nevada

Mapping by R. R. Coats northeast of Montello, Elko County, Nevada (loc. 11), disclosed a low-angle overthrust that probably moved southward as determined from mullion structures on the thrust surfaces. The lower plate consists of miogeosynclinal limestone beds of the Permian "Pequop Formation" (Steele, 1960), and the upper plate consists of eugeosynclinal bedded cherts of an undated and unnamed formation that are folded about north-trending axes. The north-trending fold axes in the bedded cherts represent an older structural event dominated by eastward-directed movements (Coats and Riva, 1976). Several nearby outcrops of greenstone and greenstone tuff, surrounded by alluvium, also exhibit northerly structural trends. Although these rocks have indeterminable relations to the upper and lower plates of the thrust, they are interpreted to be allochthonous in this area and to be a downfaulted part of the upper plate.

Calcium-poor quartzites in eastern Nevada

Chemical analyses of 18 samples of muscovite-bearing quartzite collected by D. E. Lee from Proterozoic Z and Lower Cambrian units, eastern White Pine County, Nevada (loc. 12), show they are almost devoid of CaO, even though their average SiO_2 content is less than 90 percent. They also contain only small amounts of Na_2O, and their average $K_2O:Na_2O$ ratio exceeds 20:1. This is in accord with the abundance of metamorphic muscovite, but nevertheless is unusual in clastic sedimentary rocks. Such a high $K_2O:Na_2O$ ratio is found mainly in some arkoses and argillites, and low contents of CaO in quartzite generally indicate very mature sands consisting almost entirely of SiO_2 (Pettijohn, 1963, table 2, figs. 2, 3).

The chemical data suggest that these sediments were derived from a deeply weathered crystalline

terrane composed mainly of quartz, weathered K-feldspar, and clay minerals. Stewart (1970) showed that the source of these sediments is to the east, and Stewart and Poole (1974, fig. 4) have found a suitable terrane in metamorphic rocks about 300 km away. The inferred paleoequator was nearby during Cambrian time (Smith, Briden, and Drewry, 1973, fig. 13), indicating a tropical climate in which ferromagnesian minerals and plagioclase would be rapidly destroyed and carried away. Potassium-argon radiometric data for five clastic micas from unmetamorphosed Lower Cambrian sedimentary rocks place the age of source rocks in the range 1,182 to 1,242 million years.

Age of type Pablo Formation in central Nevada

Age-diagnostic radiolarians have been obtained from chert units intercalated with submarine mafic lavas of the type Pablo Formation in Jett Canyon, southern Toiyabe Range, Nye County, Nevada (loc. 13). D. L. Jones identified Mississippian radiolarians in Pablo samples collected by F. G. Poole during detailed stratigraphic and structural studies in the southern Toiyabe Range. The type Pablo Formation is an allochthonous eugeosynclinal sequence that was considered by previous workers to be Permian in age. Regional studies suggest that emplacement of the allochthon in the Jett Canyon area probably occurred in Mesozoic time.

Ordovician rocks in Monitor Hills, south-central Nevada

Strongly deformed allochthonous transitional- and eugeosynclinal-assemblage chert, argillite, siltite, minor limestone, and quartzite of Ordovician age have been recognized by F. G. Poole in the Monitor Hills in west-central Nye County, Nevada (loc. 14). Discovery of Ordivician graptolites in part of the sequence indicates that Paleozoic rocks exposed in the Monitor Hills are not entirely (Middle and Upper Cambrian) Emigrant Formation as mapped previously by other workers. The lower Paleozoic rocks in the Monitor Hills are inferred from regional studies to be part of the Roberts Mountains allochthon.

Possible paleoseismic belt in Nevada Test Site region

Preliminary mapping, seismicity, and fault studies by W. J. Carr suggest that a seismic belt with moderate earthquake activity existed in southern Nye and westernmost Lincoln Counties, Nevada (loc. 15), in early to middle Quaternary time. The belt extended northeastward across the Amargosa Desert and southeastern Nevada Test Site and northward through Emigrant and Sand Spring Valleys. This possible paleoseismic belt coincides in a general way with a belt of Pliocene and Pleistocene basaltic lavas. Only one fault system in the seismic belt shows evidence of important late Pleistocene movement; however, low-level seismicity elsewhere in the belt indicate many other faults in the belt may be active.

Structure of southwestern Virgin Mountains, southeastern Nevada

R. K. Hose reports that the basement rocks in the southwestern Virgin Mountains, Clark County, Nevada (loc. 16), consist of deformed Precambrian gneiss and schist which are intruded by granite, mafic dikes, and pegmatite. This terrane is overlain by a nearly conformable sequence of Paleozoic and Triassic strata that total more than 2,700 m in thickness. Although the Virgin Mountains are in the Basin and Range province, stratigraphic units in the mountains are similar to those in the Colorado Plateau province to the east. The southwestern Virgin Mountains are a southwestward-dipping homoclinal block broken by many high-angle faults; rooted thrust faults occur along the western edge of the range. Also present are glide blocks presumed to be gravitationally emplaced on low-angle surfaces. Thrust faults of the Upper Cretaceous Sevier orogenic belt lie to the west and northwest of the Virgin Mountains but had only minor deformational effect on the southwestern Virgin Mountains.

Cenzoic events in west-central Arizona

In southernmost Mohave County, Arizona (loc. 17), southwest of a major structural discontinuity at the edge of the Colorado Plateau terrane, geologic mapping has enabled Ivo Lucchitta and N. H. Suneson to clarify a complex sequence of Cenozoic events and to assign ages to some of them with K-Ar dates. Tertiary(?) quartz-feldspar gneiss is separated by a thrust fault from overlying sedimentary and volcanic rocks, of which some are Tertiary and as young as 20 million years whereas others are low-grade metamorphic rocks of unknown age. Breccia that apparently was eroded from the upper plate during its movement is overlain by a basalt dated at 16.5 million years. The gneiss beneath the fault is, according to others, probably about 20 million years old. Hence, the main period of thrust faulting seems to have been not much more than 16.5 million years ago. Basin-and-range faulting was mostly later, for it tilted the 16.5-million-year-

old-basalt. Faulting virtually ended before eruption of 8-million-year-old basalts. High-potassium silicic intrusions, associated with still other basalts, were emplaced between about 15 and 10 million years ago during basin-and-range faulting; some of the silicic intrusions are in faults. Uranium minerals that have attracted exploration in the area probably are related to the silicic intrusions.

Ordovician Montoya Group extended westward in southeastern Arizona

Rocks mapped previously as El Paso Group in the Silver City, New Mexico-Arizona, 2-degree quadrangle (loc. 18), have been reported as nonfossiliferous to sparsely fossiliferous. J. E. Repetski and H. D. Drewes sampled these rocks for conodonts in the central part of the quadrangle, and preliminary study of the conodont faunas has clarified correlation of the rock units. The El Paso Group is nowhere younger than Early Ordovician, and its upper contact is unconformable owing to post-Early Ordovician erosion. In most areas of southeastern Arizona, Devonian rocks overlie the El Paso Group; however, the newly identified conodont faunas indicate that the Montoya Group (Middle and Upper Ordovician) extends farther west than was known previously. Late Ordovician conodonts were recovered from a section about 7 km east of the New Mexico-Arizona border in the Peloncillo Mountains in Hidalgo County, New Mexico, 10 km west of the previously reported western limit of Upper Ordovician rocks in this region (Hayes and Cone, 1975). Late Ordovician conodonts also were found in a section at Apache Pass, Cochise County, Arizona, which is located nearly 50 km west of the previously established western limit of Upper Ordovician rocks.

PACIFIC COAST REGION

CALIFORNIA

Plate tectonics of the western United States

The Mesozoic evolution of the western United States has been recognized for a decade as controlled primarily by interaction of lithosphere plates and particularly by subduction processes. As knowledge of the processes and products has increased, so has their comprehended complexity. W. B. Hamilton (1978) interpreted the plate-tectonic evolution of the region, evaluating geologic terrains in part by analogy with their counterparts in such active regions as Indonesia. Although the Cretaceous pattern was dominated by subduction of oceanic plates beneath North America, Triassic and Jurassic history records such "Andean" subduction as having operated only intermittently. The Triassic and Jurassic lithotectonic assemblages formed mostly in island arcs, separated from the continent by distances that reached at least 10,000 km, and aggregated by collisions both before and after they were added tectonically to the North American margin.

Melones fault North of Downieville

Mapping by A. M. Hietanen-Makela shows the Melones fault north of Downieville is 1.5 km farther west than shown on Chico sheet (Burnett and Jennings, 1962). The rocks on the west slope of Downie River are interbedded blastoclastic quartzite and schist similar to the Shoo Fly Formation east of the river.

The metamorphic rocks between the Melones fault and the Goodyear's Creek fault are lithologically similar to the Calaveras Formation to the west, but are intricately flow-folded and metamorphosed to a low-temperature and high-pressure facies as is typical of trench mélanges. Mineral assemblages in metavolcanic rocks include glaucophane, crossite, lawsonite, pumpellyite, and stilpnomelane, in addition to actinolite, chlorite, epidote, and albite, which are major constituents of chemically similar metavolcanic rocks within the Calaveras Formation west of the fault. A wedge-shaped slice of the Calaveras between the two faults was dragged down during the subduction to pressures of 5 to 6 kbar, but was forced back up before reaching temperatures higher than about 350°C. The deformation and recrystallization of the Calaveras Formation started during Paleozoic time, and the overprinted Jurassic Nevadan folding was mainly coaxial.

The metachert and phyllite along the North Yuba River west of the Ramshorn fault are less thoroughly recrystallized, are less deformed, and contain well-preserved radiolarians of Middle to Late Triassic and possibly of Early Jurassic age. The low-potassium island-arc-type metavolcanic Franklin Canyon Formation probably includes Paleozoic to Triassic rocks, the latter interbedded with the Triassic metasedimentary rocks on north side of North Yuba River. Conodonts in limestone interbedded with the metachert of the Calaveras Formation in the Onion Valley quadrangle yield Pennsylvanian to Permian age.

Root of the Sierra Nevada

Following an initial suggestion by geologist A. C. Lawson in 1936, geophysicists, notably P. Byerly

in 1938, J. P. Eaton in 1963 and 1966, Claus Prodehl in 1970, and D. S. Carder and his coworkers in 1970 and 1973, have examined and reexamined seismic evidence bearing on the depth of the crustal root of the Sierra Nevada in California. All but Carder and his coworkers have concluded that delays of P_n waves require a crustal root extending to depths of 40 km or more beneath the Sierra. Carder and his co-workers found that waves generated by explosions at the Nevada Test Site and identified as P_n arrived early at stations in the Sierra Nevada, leading them to conclude that the crust actually thins to <30 km beneath the high Sierra. L. C. Pakiser, Jr. (USGS), and James N. Brune (University of California-San Diego) have interpreted P_n waves generated by aftershocks of the September 1966 Truckee, Calif., earthquake (magnitude 5.75) and recorded by the California Institute of Technology in the Sierra Nevada. Stations at Woody, Isabella, and China Lake lie approximately on the arc of a circle 450 km south of Truckee. The P_n arrivals at Isabella are delayed 0.8 s with respect to those at Woody and China Lake, suggesting that the crust is about 11 km thicker at Isabella. P_n waves in the Sierra west of Tinemaha, about a second. The greatest P_n delay, in the high about a second. The greatest P_n delay, in the high Sierra west of Lone Pine, was 1.5 s, suggesting crustal thickening beneath the Sierra of about 21 km in relation to the foothills to the west and the basin ranges to the east. A crustal thickness of 50 km or more beneath the Sierra seems probable, implying that the waves identified as P_n by Carder and his co-workers actually bottomed within the crust rather than in the upper mantle.

Reflections from the Mohorovicic discontinuity of the seismic waves generated by explosions in Mono Lake, Calif., in 1970 confirm that the crustal thickness beneath the Sierra Nevada is 50 km or more.

Jurassic Granitic Rocks in the western Sierra Nevada

Recent geologic mapping by L. C. Calk and F. C. W. Dodge in the Lake Eleanor, California, 15-minute quadrangle and radiometric age dating of zircons by lead-uranium techniques by T. W. Stern indicate a Middle Jurassic intrusive sequence on the west side of the Sierra Nevada batholith. The Jawbone sequence, named after a prominent ridge north of the Tuolumne River, includes the large pyroxene diorite pluton 1 km east of Sonora, which has been redated at 164 million years, and at least two tonalite bodies, one dated at 163 million years and the other at 166 million years, within the main mass of the batholith. Recognition of this sequence on the west side of the Sierra Nevada, along with the known geographic locations of contemperaneous rocks on the east side of the Sierra, indicates Jurassic intrusions followed a general N. 45° W. trend in this region, whereas Cretaceous intrusions, which displaced the Jurassic granitoids in the central portion of the batholith, have a general N. 20° W. trend. The western Jurassic rocks share chemical affinities with their eastern counterparts; although generally containing 60 percent or less silica, they contain as much as 2.5 percent potash. Younger rocks of the western Sierra Nevada foothills have this K_2O content only at much higher SiO_2 values.

Paleozoic metasedimentary rocks in eastern Mojave Desert

Regionally metamorphosed Paleozoic strata have been identified by K. A. Howard and Paul Stone at several localities between the Providence Mountains and the Maria Mountains in California in terranes formerly regarded as Precambrian. These rocks form a cratonal sequence from Cambrian Tapeats Sandstone through Pennsylvanian and Permian Bird Spring Formation. The Paleozoic strata, along with the Precambrian basement, have been deformed by recumbent folding and thrust faulting. This deformation apparently represents a southward continuation of the Mesozoic Cordilleran fold and thrust belt onto the Paleozoic craton. Two-mica granite in the Old Woman Mountains is associated with the northwest limit of the belt of metamorphism.

Character of Peninsula Ranges batholith

In the area between its western wall, east of the city of San Diego, and the Elsinore fault zone, V. R. Todd found the Peninsular Ranges batholith between latitudes 33°00′ and 32°45′ to consist of at least a dozen large, irregularly shaped bodies of gabbro, which are rather uniformly spaced and are intimately mixed at their margins with the surrounding granitic plutons. Smaller satellite bodies and systems of mafic dikes, which cut all plutonic units, fringe the large gabbro bodies. Only small gabbro bodies (3–4 km along strike) occur east of a line about 10 km from the edge of the Laguna Mountains escarpment. Although gabbro is generally the oldest unit, intrusion of gabbroic and granitic magmas overlapped in time leading to a variety of complex contacts that show evidence of both tectonic and chemical mixing.

There is no field evidence for a genetic relationship between gabbroic and granitic magmas. What-

ever the source of the granitic magmas, there is evidence for a two-way branching differentiation at the present level of exposure, from quartz gabbro and pyroxene-biotite tonalite, to biotite-hornblende tonalite, to voluminous leucotonalite and granodiorite occurring east of 116°30′ long. and south of 32°45′ lat. and to small volumes of granodiorite and granite intimately mixed with the parent mafic tonalite. Although the leucotonalite is younger, these two derivative suites overlap in age. Highly deformed, deuterically altered granodiorite and tonalite form a shell around the mafic tonalite where it intruded prebatholithic metasedimentary rocks. This granodiorite is in part younger than the mafic tonalite and reacted with metasedimentary rocks to produce voluminous hybrid gneisses. The marginal granodiorite and hybrid rocks are found only in the eastern part of the Peninsular Ranges where metasedimentary clastic rocks are abundant.

Gabbroic and granitic plutons are variably deformed and recrystallized to gneissic textures, and are involved in syntectonic structures with prebatholithic rocks. The latter consists of relatively thick (~5 km) screens of metamorphosed clastic rocks with minor metavolcanic rock in the eastern part of the area and thinner (<0.5 km) screens with increasing metavolcanic content in the western part. Plutons occur as sheeted and lenticular bodies which are folded with screens on a scale of about 20 km^2. Broad structural trends swing from north-northwest in the eastern part of the area to west-northwest in the western part, with steep eastward and northward regional dips, respectively, describing a large-scale texture about a steeply-plunging northeast axis. The interior parts of large gabbro and tonalite plutons preserve relics of an earlier fabric, which appears to have been reoriented by deformation at metamorphic temperatures. Deformation had waned by the time of emplacement of the large leucotonalite pluton, but metamorphic temperatures persisted locally until 70 million years ago.

Slivers record past Garlock fault movements

Geologic mapping along the Garlock fault zone north of Mojave, Calif., by D. C. Ross has revealed a string of fault slivers of distinctive dioritic gneiss containing coarse haloed garnet crystals. The slivers were apparently "dropped off" as the parent dioritic gneiss terrane was pushed westward along the north side of the Garlock fault to its present position in the Tehachapi Mountains. A minimum of 40 km of left-lateral separation along the fault is recorded by these slivers. In addition, the easternmost dioritic gneiss sliver, discovered this year near Cinco, is along the range front east to where the most recent trace of the Garlock fault leaves the range front and trends off across Fremont Valley. This suggests that the Garlock fault bifurcates here into north and south branches, as it also does to the west in the Tehachapi Mountains.

Historic deformation in the Garlock fault-Slate Range area

The Garlock fault-Slate Range area, southeast California, is known from geologic evidence to have been tectonically active in very late Cenozoic time. Historic fault scarps are not known, but comparisons of successive surveys along five benchmark lines in the area by G. I. Smith and J. P. Church reveal systematic elevation changes, relative to one datum benchmark, which appear to mean that crustal deformation has occurred during this century. The observed changes are not likely to have been produced by surveying errors; successive surveys find the same senses of relative change, and the magnitude of change substantially exceed standards for leveling.

Most elevation change patterns can be explained as continued tectonic activity along known geological structures. The Garlock fault shows no activity southeast of the Slate Range but may be displaying creep west of that area. The Slate Range anticline and the Argus-Slate Range syncline, north of the Garlock fault, appear to be active and still forming where benchmark lines cross them. The Dome Mountain anticline and Pilot Knob Valley syncline, south of the fault, are also active.

Maximum rates of observed change were 3.45 cm in 2 months and 12.70 cm in 4 years. Surveys made decades apart, however, show rates that range only from 0.07 to 0.27 cm/yr. Short periods of rapid change therefore appear to be separated by long periods of no change (or reversals). The four benchmark lines that were resurveyed one or more times over periods ranging from 29 to 41 years had maximum elevation change rates of 0.01 to 0.02 cm/km/yr; this would produce 45° of tilting along a 1-km line in 5 to 10 million years.

Quaternary deposits and soils, Sierra Nevada Foothills

Six colluvial units and associated alluvial facies have been recognized by D. E. Marchand and J. W. Harden in the western Sierra Nevada foothills from superposition and comparative development of relict and buried soils. The deposits range from middle Pleistocene to modern in age. Properties distinguishing soils formed on these units include structure,

clay films, thin-section textures, clay content, bulk density, cation-exchange capacity, semiquantitative-clay mineralogy, organic carbon, and free iron-oxide content (dithionite method) of well-oxidized horizons. Many chemical properties such as pH, extractable cations, and free iron content of reduced horizons appear to change rapidly following burial and are generally not useful in characterizing buried soils. Soil interpretation is hampered by the presence of swelling clay in older soils and extensive reworking of clay, iron oxides, and weathered minerals from saprolite and old colluvial soils into younger colluvial deposits.

Radiocarbon dates indicate that the youngest colluvial/alluvial unit is late Holocene in age, and the next oldest unit is early Holocene or latest Wisconsinan. The latter unit can be correlated with the youngest part of the Modesto Formation (about 9,000–10,000 years old) and an older unit with the upper unit of the Riverbank Formation (about 140,000 years old) in the eastern San Joaquin Valley by physical continuity of deposits and soils. Other foothill units are tentatively correlated with the San Joaquin Valley using position in the sequence and soil development compared to that of the directly correlated foothill units.

Compared to soils about 9,000–10,000 years old in the eastern San Joaquin Valley and along the east side of the Sierra Nevada, soils of similar age in the foothills display stronger morphological development, more free iron oxides, higher B/A horizon clay ratios, lower pH, and usually higher clay contents. Soils appear to form faster in the foothills owing to higher precipitation in the mountains and to the finer grained texture and greater abundance of weatherable minerals in foothill parent materials compared with those in the Central Valley and east of the Sierra crest.

Absolute age of main marine terrace in Pacific Palisades

A cooperative effort instigated by J. T. McGill and tied to his geologic mapping has resulted in an amino-acid determination of the absolute age of the main late Pleistocene marine terrace in the Pacific Palisades area of Los Angeles. Fossils from an especially rich and well-known collection (Valentine, 1956) were made available for this purpose by Takeo Susuki, paleontologic curator of the University of California at Los Angeles Department of Earth and Planetary Sciences. The fossil locality, which has long been inaccessible, was in deposits immediately overlying the wave-cut platform near the head of Potrero Canyon, about 1.3 km from the present shoreline of Santa Monica Bay and at an elevation of about 73 m. The elevation of the nearest mapped point on the shoreline angle of the terrace is 76 m.

G. L. Kennedy, while on the staff of the Los Angeles County Museum of Natural History, selected several mollusk specimens from the collection for analysis by J. F. Wehmiller, University of Delaware. Wehmiller has determined amino-acid ratios for two samples of *Saxidomus nuttalli* and found that correlation with similar analyses of samples of this species from the first marine terrace at San Pedro (Palos Verdes Sand) permits a preliminary age assignment of 120,000 to 140,000 years. On the basis of the warm-water aspect of the fauna, Kennedy suggests the age may be about 125,000 years. If it is assumed that sea level at that time was 6 m above present sea level, the rate of uplift of the terrace at the nearby shoreline angle has averaged about 0.56 per 1,000 years.

Quaternary studies in the Los Angeles area

Modern techniques of basin analysis including soil stratigraphy, studies of stream profiles, photogeology, and regional geomorphic analyses provide data that have been interpreted by J. C. Tinsley III to reflect the structural and stratigraphic evolution of the Los Angeles basin during the Quaternary. Historic flood records and geologic and geomorphic mapping provided a sound basis for identifying the youngest sediments in a generally Holocene basin. Compared to earlier Holocene and Pleistocene deposits, modern sediments (less than 500 years old) generally have the highest susceptibility to liquefaction, other requisite factors being equal.

Potassium-argon ages of volcanic rocks in the Murrieta area of California

Geochronologic studies of volcanic rocks along the Elsinore fault zone near Murrieta, Calif., have been completed by J. L. Morton and D. M. Morton. Five K-Ar whole-rock ages were obtained, indicating two episodes of volcanism. Two samples of the "Santa Rosa Basalt" (Mann, 1955) from Mesa de Burro west of the fault zone yielded ages of 6.7 ± 0.2 and 7.4 ± 0.4 million years. An age of 6.8 ± 0.2 million years was obtained for a sample of the "Nigger Canyon Volcanics" (Mann, 1955) from within the fault zone. "Nigger Canyon Volcanics" from Vail Mountain east of the fault zone had been dated at 7.9 to 8.46 million years by Kennedy (1977, recalculated). Thus, Mann's "Nigger Canyon" and "Santa

Rosa" west of the fault zone appear to be the same age.

Basalt on Hogback Ridge east of the fault zone on the Perris surface of the Perris Block has been correlated by others, with Mann's "Santa Rosa." However, two samples from Hogback Ridge yielded ages of 10.4±0.3 million years and 10.8±0.3 million years, significantly older than Mann's "Santa Rosa" west of the fault zone.

Vanished alluvial-fan complex in the Riverside area

Fieldwork by D. M. Morton and J. C. Matti on the northern part of the Perris Block in southern California has lead to the discovery of exotic metamorphic and volcanic clasts that occur on basement highs of the Peninsular Ranges. At their highest elevation, 600 m in the Jurupa Mountains, the clasts occur about 416 m above the present valley floor. Farther south on the Block the clasts occur at 418 m elevation, about 236 m above the present valley floor. Clast compositions indicate a source area in the easternmost San Gabriel Mountains, Transverse Ranges. The clasts are interpreted as uncommon but widespread remnants of a vanished post-middle Miocene pre-upper Pleistocene alluvial-fan complex that once extended a minimum of 33 km southward from the San Gabriel Mountains. A buttress unconformity developed between the aggrading fan sediments and granitoid basement rocks of the Perris Block, and accumulation of the fan complex resulted in substantial burial of paleotopography on the northern part of the Block. Erosion and removal of distal parts of the old fan complex occurred prior to the late Pleistocene. During this event the Perris Block was uplifted and pre-fan paleotopography was exhumed.

Aggressive fan accumulation requires that eastern San Gabriel Mountains source areas were uplifted relative to the aggrading Perris Block. Subsequent degradation of the Perris Block requires that it in turn was elevated relative to the eastern San Gabriel Mountains, even though evidence suggests that the latter continued to rise. This relationship requires the existence of undetected east- to northeast-trending faults between the Jurupa Mountains and the southern boundary fault of the San Gabriel Mountains (Cucamonga Fault) and (or) a change in the rate of relative vertical movement between the Perris Block and the San Gabriel Mountains.

The stratigraphic and paleogeographic relationship between sediments of the vanished fan complex and other post-middle Miocene-pre-upper Pleistocene sedimentary units in this part of southern California is uncertain. A possible correlation exists between the vanished fan complex and Pliocene-Pleistocene sedimentary rocks that crop out in the San Timoteo Badlands (Matti and Morton, 1975). This correlation is suggested by several factors, (1) The San Timoteo sediments are a fan- and braided-river complex whose clasts also were derived from Transverse Range sources of San Gabriel Mountain type, (2) The San Timoteo sediments also substantially buried paleotopography on granitoid basement of Peninsular Range type, and (3) when postulated displacements of 25 to 27 km are restored on the San Jacinto fault zone, the known southern limits of perched exotic clasts on the Perris Block approximately coincide with the mapped southern limits of the San Timoteo sedimentary sequence. It is possible that the vanished fan complex and the San Timoteo sediments once were part of a widespread alluvial fan system that extended southward from the Transverse Ranges. Strike-slip displacement on the San Jacinto fault zone and vertical uplift of the Perris Block disrupted and obliterated most evidence for this regional fan system.

Environmental impacts of off-road vehicles

Physical and biological modifications brought about by vehicular use of natural terrain lead to highly accelerated erosion. Erosion rates have been monitored by H. G. Wilshire and J. K. Nakata by measurement of changes in gully dimensions, mass movements across a fence line on a sand dune destabilized by vehicular use, repeat measurement of mass losses from individual vehicle trails and hillslopes, and measurement of a grid of erosion pins. Data obtained indicate highly accelerated rates compared to natural erosion rates, with denudation rates as much as 60 times natural rates in areas of vehicular use that have been closed for 8 years. Major physical modifications and incomplete plant recovery persist in a Mojave Desert plant community disturbed by vehicular impacts 50 years ago.

OREGON

Large-scale nappes in southwest Oregon

J. A. Barker (USGS) and Francois Roure (Department of Structural Geology, University of Paris), by field mapping in the Gold Beach and Collier Butte quadrangles, documented that the Signal Hill-Carpenterville ultramafic mass consists of two distinctive, thrust-bounded units. Above is a dis-

membered ophiolite (the "Chetco River complex"), part of a huge, subhorizontal nappe, emplaced from east to west. Below is a serpentinite mélange, containing scarce blocks of high-grade glaucophane schist. The serpentinite mélange is part of the semi-autocthonous Dothan (Franciscan) Formation and is almost certainly an olistostrome within that unit.

WASHINGTON

Origin of malanges of the Olympic Peninsula

A reconstruction of the tectonic setting of western Washington by K. F. Fox, Jr., indicates that the northwestward transit of the Aja transform fault may be implicated in the formation of the enigmatic mélanges of the Olympic Peninsula. The core rocks of the Olympic Peninsula consist of mélange and broken formation, infaulted or imbricated with blocks of intact strata (Tabor and Cady, 1978). Rocks peripheral to the core consist of the oceanic tholeiitic basement of the Oregon-Washington borderland (Snavely, MacLeod and Wagner, 1968) with interfingering clastic deposits, overlain by bathyal deposits or shallow-water marine shelf deposits. The core rocks consist of bathyal marine turbidite deposits, and mélanges of the western core contain fossils, the youngest of whose reported ages is early or middle Miocene (Rau, 1975). Published K-Ar ages of the rocks of the eastern core suggest metamorphism after 29 million years ago and final cooling about 17 million years ago (Tabor, 1972).

Magnetic lineations of the northeastern Pacific step right laterally across the Aja fracture zone (Naugler and Wageman, 1973). From the age of these lineations, it appears that north of the Aja the spreading ridge system and coexisting subduction zone shrank, then vanished about 21.5 million years ago. The Aja transform fault then intersected the Queen Charlotte fault and the subduction zone to the south, and with continued right-lateral movement of the Pacific plate Charlotte fault and the subduction zone to the south, and with continued right-lateral movement of the Pacific plate, formed a Humboldt-type triple junction (Fox, 1976). That triple junction persisted through about 5.5 million years, then died about 16 million years ago as the ridge system south of the Aja stepped eastward and intersected the subduction zone. This timing coincides roughly with the problem K-Ar age (about 17 m.y. ago) of final cooling of the mélanges in the eastern core of the Olympics. To account for the structural fabric and geographic extent of the Olympic mélanges through the tectonism associated with this triple junction, it would have had to have been located immediately west of the Olympic Peninsula. If this spatial and temporal relation is valid, northwestward movement of the Pacific plate relative to the North American plate has averaged about 6 cm/yr at least since middle Miocene time, a rate comparable to accepted estimates of the rate of rotation of these plates averaged over the last 2 million years (Larsen, Menard, and Smith, 1968).

Clastic Dikes—A key to Tertiary regional stress fields in the northwest Olympic Peninsula

Numerous north- and northeast-trending vertical dikes of sandstone cut the well-bedded sequence of sandstone and siltstone of late Eocene to early Miocene age in the northwestern part of the Olympic Peninsula, Washington. Mapping by P. D. Snavely, Jr., and J. E. Pearl indicate these clastic dikes range in thickness from 1 cm to 1 m and are generally perpendicular to the strike of the strata. The clastic dikes were probably injected along fractures and small faults perpendicular to the direction of minimum compressional stress in a manner similar to that of basalt dikes (Nakamura, 1977). A regional stress field with generally north-south compression, therefore, is inferred during late Eocene to early middle Miocene time. North-south compression also is evidenced by west-trending and northward-dipping thrust faults that cut the Tertiary sequence. Downfolding of the deep linear west-trending basin of deposition that existed along the northern flank of the Olympic Mountains during late Eocene to middle Miocene time probably was produced in response to north-south compression.

Thrusting and lateral faulting, northwest Washington

Fragments of dismembered Middle and (or) Upper Jurassic ophiolite are widely distributed in the Cascade Range and San Juan Islands of northwest Washington. Structural position, lithology, and several age determinations suggest that rock bodies such as the Twin Sisters Dunite of Misch (1952); the intrusive rocks at Woods Creek, the ophiolite of the Fidalgo Formation of McLellan (1927), including the Cypress Island Peridotite as used by Brown, 1977, the klippen of the Index district, and the Ingalls complex as used by Frost (1975) form a cogenetic suite, which overrode a variety of terranes during Late Cretaceous low-angle thrusting.

The ophiolite was emplaced during the Late Cretaceous before deposition of the Chuckanut Formation, which unconformably overlies the klippe on

the north end of Lummi Island. Its emplacement is bracketed by middle Cretaceous (~100 m.y.) planktonic foraminifers occurring in structurally lower rocks on Lopez Island and the intrusion of the 88-million-year-old Mount Stuart Grandodiorite into the "Ingalls complex."

J. T. Whetten has identified the Roche Harbor terrane as a separate unit in the San Juan Islands. It is the lowest structural unit yet recognized and contains the most diverse association of rock types, with ages ranging from probably Precambrian to Middle Jurassic. All of the pre-Triassic rocks in the San Juans appear to be restricted to this terrane, including limestone-containing fossils with Tethyan faunal affinities.

Recognition of this terrane supports the interpretation that the San Juan Islands are not a single subduction complex, but, rather, an assemblage of rootless thrusts probably representing several subduction complexes and allows more precise correlating and mapping in the San Juan Islands and in the foothills of the Cascade Range to the east.

The Devils Mountain fault, previously found to be a major left-lateral fault linking thrust-bound terranes in the San Juan Islands with the western Cascade Range, is inferred from geophysical evidence to continue west to Vancouver Island where it may be the San Juan fault. The trace of the Devils Mountain fault parallels the traces of at least three other major faults to the south, (1) an unnamed fault a few kilometers south of the Devils Mountain fault, (2) the Leech River fault, and (3) the Calawah fault. Toward the west all of these faults appear to bend south and become thrusts. It is possible that a significant amount of the post-Eocene clockwise rotation of the Oregon-Washington coast range proposed by Simpson and Cox (1977) was accomplished by movement along these faults.

Postglacial isostatic uplift of the Puget lowland

Detailed study of the recessional history of the Puget Lobe of the Cordilleran Ice Sheet by R. M. Thorson provides important data on the pattern and amount of postglacial rebound. Outwash deltas that originally formed at the same altitude during formation of a sequence of proglacial lakes show a systematic increase in altitude toward the north. Uplifted marine muds, melt-water channels graded to former relative sea level, and marine deltas indicate the height of relative sea level during deglaciation. These independently derived data suggest that the Seattle and Port Townsend areas have been uplifted at least 75 m and 120 m, respectively, within the last 13,000 years.

Amino-acid dating of shell deposits at Willapa Bay

A new chemical technique for correlation and dating Quaternary sediments uses the property of amino acids to undergo changes in their geometric structures (racemization) with time. Extents of racemization of amino acids in fossil *Saxidomus* and *Ostrea* have been used to correlate and date shell deposits at Willapa Bay, Wash., by K. A. Kvenvolden, D. J. Blunt, and H. E. Clifton. Amino acids from *Saxidomus* show less variability in degree of racemization and, therefore, are of greater use in correlation and age estimation than are amino acids from *Ostrea*. Shell deposits of two different ages have been identified. One deposit is estimated to be about 110,000±30,000 years old and the other about 200,000±50,000 years old. These ages correspond to Stages 5 and 7 of the marine isotope record defined by Shackleton and Opdyke in 1973. These shell deposits likely were formed during two different high stands of sea level. The stratigraphic record at Willapa Bay is consistent with these ages and interpretations.

Historical changes of shoreline and wetland in Puget Sound region

Historical shoreline and wetland changes were studied for 11 major river deltas in the Puget Sound region by G. C. Bortleson, M. J. Charzastowski, and A. K. Helgerson. The study is based on comparison of maps made during 1854–99 and modern topographic maps.

The observed shoreline and wetland changes range from minor to significant in regard to land use, environmental impacts, and planning implications. The data provide documentation of (1) loss of subaerial and intertidal wetlands since white settlement, (2) shoreline modifications, (3) development patterns on wetland deposits, (4) progradation and erosion of the subaerial delta, and (5) migration of distributary stream channels.

Most of the river-mouth deltas show substantial loss of wetland habitat. Diking of marshes to develop farmlands accounts for the greatest loss of marsh. Three of the deltas show extensive loss of subaerial and intertidal wetlands due to landfill placement for commercial, industrial, and port facilities. Two of the deltas have changed stream course and have prograded significantly; the subaerial part of one delta has migrated seaward 1 to

1.5 km since 1887-88. Although extensive changes have occurred on the major deltas of Puget Sound, many of the deltas have some remaining wetlands and unmodified shoreline that if managed properly could retain the benefits of valuable fish and wildlife habitat.

Geology and limnology of the Alpine Lakes Wilderness Area

A wide variety of ice-related features, including moraines, rock glaciers, and protalus ramparts are preserved in the upper portions of many drainages in the Alpine Lakes Wilderness Area in the central Cascade Range in Washington. Reconnaissance study by D. P. Dethier of weathering characteristics on some of these features in the Enchantment Lakes and Necklace Valley areas suggests that the outer set of moraines associated with small alpine glaciers may be early Holocene rather than neoglacial as previously believed. Detailed studies of tephra deposits and relative weathering parameters are required to further evaluate this interpretation.

Low concentrations of nutrients and major ions characterize 45 lakes selected for reconaissance limnological studies in the Alpine Lakes Wilderness Area during 1978. Calculated flushing rates for most lakes are high enough so that pollution caused by recreational use is not likely to have a measurable effect on overall lake quality.

Tertiary history of the Straight Creek Fault and the Olympic-Wallowa Lineament

Studies of the Eocene and lower Oligocene(?) sedimentary and volcanic rocks by R. W. Tabor and V. A. Frizzell, Jr., along the Kachess Lake segments of the north-trending Straight Creek fault (Vance, 1957, p. 77; Misch, 1977, p. 37; Yeats, 1977, p. 274) indicate these sequences contain no fanglomerates indicative of fault movement during deposition. The fault consistently downdrops folded and faulted Naches Formation (upper Eocene and Oligocene?) to the west. But mildly deformed Eocene volcanic rocks (Stevens Ridge equivalents), which are abundant west of the fault, also occur in isolated areas east of the fault, suggesting that major relative uplift to the east has not occurred since the late Oligocene.

Where the fault intersects the northwest-trending Olympic Wallowa lineament (Raisz, 1945), the north-trending structures and upper Eocene rocks of the Naches swing to parallel the lineament. Stratigraphic throw across the fault in the area of intersection, where Naches arkose and rhyolite overlie the basalt of Frost Mountain appears to be markedly less than that farther north, suggesting that the fault does not continue much farther south beneath a cover of Miocene basalt. Lack of throughgoing lineament structures in the upper Eocene part of the Naches, including equivalents of the lower part of the Naches, the Mount Catherine Rhyolite as used by Grant (1942) and Guye Formation, along its trend to the northwest suggests that both the fault and Tertiary structures along the lineament terminate at or near their intersection. Also, the fault has strongly affected upper Eocene rocks, whereas faults and folds along the lineament mostly affect lower and middle Eocene rocks and their probable equivalents which suggests that activity along the Straight Creek fault continued later than any throughgoing faulting along the lineament.

Post-Miocene movement along both structures must be minimal or absent because the Snoqualmie Granodiorite (Miocene) and its satellite stocks cut faults in the Straight Creek zone and recrystallized cataclasites; the batholith is unmarked by structures paralleling and on strike with the lineament.

Late Miocene drainage patterns in southeast Washington

The distribution of intracanyon flows of the Columbia River Basalt Group indicates that drainage was toward the west across the Columbia Plateau in southeast Washington between about 14 and 6 million years B.P. D. A. Swanson and T. L. Wright have found that basalt flows erupted near the Washington-Idaho border flowed down valleys and canyons to a broad lowland that included, but possibly extended farther southwest than, the modern Pasco Basin. Three river courses of different ages can be outlined. First, the earliest 14 to 13(?) million years B.P., extended westward in a wide, shallow valley from the present site of the Uniontown plateau to the Othello area. It then turned southwestward, entering, and possibly crossing, the northern part of the Pasco Basin. This river appears to have been ancestral to the Snake River, which at that time apparently flowed northward across the present-day Lewiston Basin onto the Uniontown Plateau. Second, a deep paleocanyon of intermediate age containing flows 12.5 to 10.5 million years old closely follows the modern Snake River course from south of Asotin to Devil's Canyon. Here the ancestral river continued westward, rather than turning southwestward as does the present river, and entered Pasco Basin near Mesa. Third, the youngest ancient river course, outlined by a 6-million-year intracanyon flow, coincides exactly with

the modern Snake River westward from the Idaho border.

Reconstruction of the gradient of the youngest paleocanyon on the basis of elevations of flow remnants indicates a gradient comparable to that of the modern Snake; gradients of earlier drainages are marginally greater, possibly because of slight regional westward tilting that ended before 6 million years B.P. The maximum depth of the ancestral Snake River canyon 12.5 to 10.5 million years B.P. was at least 500 m, decreasing westward to zero at the mouth of the canyon. These depth figures provide an estimate of the minimum elevation of the plateau surface, as the canyon floor must have been above sea level, and are consistent with the variation in present elevations. Swanson and Wright conclude that, except for local areas of tectonism such as the Blue Mountains and Lewiston Basin, southeast Washington has remained remarkably stable over the past 12.5 million years, undergoing little elevation change and only modest westward tilting of a few tenths of a degree. This conclusion is consistent with the antiquity of the course of the Snake River, which throughout most of its length in Washington has remained in virtually the same location for the past 12.5 million years.

Stratigraphy of the Windermere Group

The Windermere Group makes up the uppermost Proterozoic Y and Z in northeastern Washington. It overlies the Belt Supergroup and is overlain by lowermost Cambrian quartzites. Recent mapping by F. K. Miller in the proposed Salmo-Priest Wilderness Area and earlier work in the Addy area to the southwest indicates the Windermere represents a complex period of deposition, uplift, and erosion.

At the U.S.-Canadian border, the Windermere Group is made up of, from oldest to youngest, Shedroof Conglomerate, 3,170 m; Leola Volcanics, 1,520 m; Monk Formation, 1,220 m; and Three Sisters Formation of Canadian usage, 2,470 m. Because of possible tectonic thickening, the thickness for the Shedroof is a maximum figure. The Gypsy Quartzite (Lower Cambrian) that unconformably overlies the Windermere is 1,700 m thick.

About 30 km along strike to the southwest, where the entire section is cut out by Cretaceous and Tertiary plutonic rocks, the thickness and stratigraphic relationships appear to be unchanged. About 15 km to the west, however, on the west side of a large fault of unknown attitude or displacement, the Three Sisters Formation is only 400 m thick, and the Gypsy Quartzite is 1,100 m thick. Full sections of the Shedroof, Leola, and Monk Formations are not exposed.

Where the Windermere again appears in the Addy area, 90 km to the southwest on the southwest side of the plutonic rocks, the Shedroof Conglomerate (called "Huckleberry Conglomerate") is only 500 m thick, the Leola Volcanics (called "Huckleberry Greenstone") are 1,240 m thick, and 1,070 m of Gypsy Quartzite (called Addy Quartzite) rests unconformably on the Leola, with no Three Sisters Formation present and only local 10- to 50-m remnants of Monk Formation preserved in pre-Gypsy structural lows.

ALASKA

Significant new scientific and economic geologic information has been obtained from many field and topical investigations conducted in Alaska during the past year. Discussions of the findings are grouped under six subdivisions corresponding to five of the six major geographic regions and a general statewide category. Outlines of the regions and locations of the study areas are shown on the accompanying index map of Alaska.

STATEWIDE

Alaska Mineral Resource Assessment Program

Impending transfer of lands in Alaska, 90 percent of which currently are under Federal management, will affect for generations the allocation, accessibility, and development of Alaska's vast lands and natural resources. There is therefore an urgent and growing demand by public and private interests for objective and timely information on Alaska's mineral endowment. To meet this demand, the USGS's Alaska Mineral Resource Assessment Program (AMRAP), administered by H. C. Berg, has two closely coordinated objectives designed specifically to furnish information for decisions about Alaska's lands.

One objective, based on a 1:250,000-scale (1°×3°) quadrangle format, is a systematic multidisciplinary assessment of Alaska's economic mineral potential for long-range planning and development. Assuming increased levels of staffing and funding, the deadline for this goal is 1984. The other objective, based on a 1:1,000,000-scale map format, is a statewide mineral appraisal for near-term Department of the Interior and Congressional decisions on classifica-

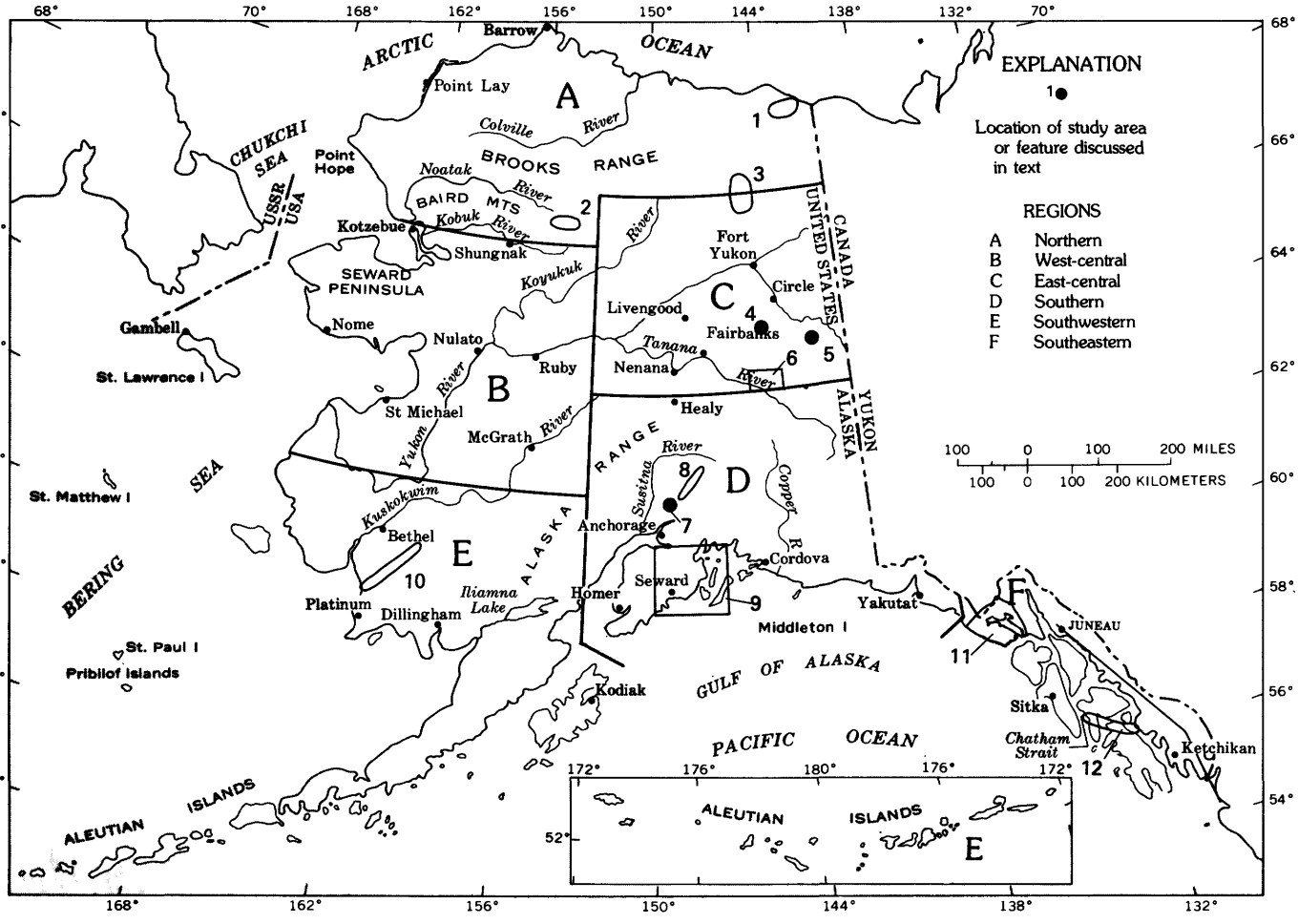

tion of Alaska's lands. This appraisal, informally termed RAMRAP (Regional Alaska Mineral Resource Assessment Program), was completed for mainland Alaska and published in January 1978. A RAMRAP-type investigation of southeastern Alaska was begun in 1978; the tentative deadline for completing this investigation is 1980.

The AMRAP long-range program is being carried out mainly by geologists and subprofessionals in the Alaskan Geology Branch, in collaboration with specialists from other branches and subactivities in the Geologic Division. In addition, several geoscientists from the Alaska Division of Geological and Geophysical Surveys and the University of Alaska are collaborators.

The RAMRAP studies comprised the compilation, synthesis, and publication of basic geological, geophysical, geochemical, and Earth satellite data, and of regional (1:1,000,000-scale) resource assessments for all of mainland Alaska. In October 1978, these assessments were used extensively to update environmental impact statements for approximately 40,500,000 ha of proposed National Interest Lands in Alaska. This update, urgently requested by the Department of the Interior, was completed within a 1-week deadline imposed by the Department, a deadline that would have been impossible to meet without the RAMRAP reports.

As of the end of 1978, field studies leading to multidisciplinary resource assessment have been completed in 20 quadrangles (1°×3°) on a 1:250,000 scale and are underway in 9 others. These quadrangles aggregate approximately 360,000 km². Mineral resource assessment folios have either been published or are in press or advanced preparation for 19 quadrangles encompassing about 250,000 km². More than 166 other AMRAP-sponsored topical research reports on the geology, geochemistry, geophysics, and mineral resources of Alaska and a new tectonic (tectonostratigraphic) map of southeastern Alaska have been published.

Studies of ore genesis or of other mineral-deposit research problems are underway or completed in eight Alaskan mining districts, (1) Aleutian

Peninsula porphyry copper district, (2) Kennecott sabhka copper deposits, (3) Willow Creek gold district, (4) Hope gold district, (5) Orange Hill porphyry copper deposit, (6) Bornite sabhka copper deposit, (7) Arctic Camp massive copper sulfide deposit, and (8) Eastern Alaska Range volcanogenic sulfide deposits.

Resources data summarized

Mineral resources are known in all major subdivisions of Alaska and have been described in reports issued during the last 80 years by the USGS, the U.S. Bureau of Mines, and various Territorial and State of Alaska agencies. E. H. Cobb has summarized the published (and open filed) references to mineral occurrences in 16 quadrangles (1:250,000 scale) in Alaska (Cobb, 1977, 1978a, b), thereby making readily available data from old out-of-print reports as well as from results of current investigations.

Review of Precambrian rocks of Alaska

G. D. Eberlein and M. A. Lamphere have reviewed the evidence for age and distribution of Precambrian rocks in Alaska. Ten widely separated areas in Alaska contain rocks of Precambrian or probable Precambrian age. The age assignment in four areas is based on radiometric dating; in the other six areas, stratigraphic evidence is used to infer a Precambrian age. The Alaskan Precambrian rocks are of Proterozoic Z age; there is no evidence at this time for an Archean age. The Tindir Group along the Yukon River in east-central Alaska, which is considered equivalent to parts of the Windermere, Belt, and Purcell "Supergroups" of Canada, is the only sequence of Proterozoic rocks in Alaska that can be definitely related to Proterozoic stratigraphic sections in other parts of the North American cordillera. The Neruokpuk Quartzite and underlying strata of eastern northern Alaska are Precambrian on the basis of stratigraphic evidence. The Tindir (?) Group along the Porcupine River in east-central Alaska, schist of the northeastern Kuskokwim Mountains in central Alaska, and low-grade metamorphic rocks in the Livengood-Crazy Mountains region of east-central Alaska are probably Proterozoic, although their precise ages are not known.

Tectonomagmatic events in the interval 1,100- to 600-million-year age are recorded in schist of the Yukon-Koyukuk region in central Alaska, in the Kanektok terrane of southwestern Alaska, in gneiss in the Seward Peninsula (west-central Alaska), and in trondhjemite intrusive into the Wales Group of southeastern Alaska. The Wales Group and the Kanektok terrane are allochthonous and appear to belong to exotic terranes accreted to the North American craton during Phanerozoic time.

Mineral deposits occur in several areas of Precambrian rocks, but many of these deposits were produced during Phanerozoic mineralization episodes. However, banded iron formation within the Tindir Group of the Yukon River region and certain volcanogenic, stratabound base-metal deposits within the Wales Group in southeastern Alaska are believed to have been formed during the Precambrian Era.

Reconstruction of Paleozoic continental margin in Alaska and accreted terranes

According to Michael Churkin, Jr., and Claire Carter, a belt of Paleozoic rocks in central Alaska grades southward from limestone and dolomite into highly deformed sequences of shale, chert, turbidite, and volcanic rocks; it represents a transition from carbonate shelf to continental slope and rise and ocean floor. South of this reconstructed continental margin lie a series of terranes of oceanic affinity (for example, Chulitna, Wrangell, Chugach) that have been successively accreted to the continent. Some terranes, like the Yukon-Tanana, have been metamorphosed. Reconstruction of a similar facies change in thrust slices along the Brooks Range suggests that another collision-deformed Paleozoic continental margin extends across arctic Alaska. Along the southern Brooks Range, terranes of schist, volcanic rocks, and ophiolite are accreted to the collapsed Paleozoic continental margin in a succession similar to that in central Alaska. The apparent termination of the continental margin in southwest Alaska near the Aniak-Thompson Creek fault, the presence of a similar continental margin along the trend of the Brooks Range, and oroclinal bends in the Cordillera of northern Yukon and the Brooks Range suggest that the continental and accreted microplate framework of southwestern Alaska was offset right laterally northeastward to the present-day Brooks Range.

Paleotectonic setting of the Carboniferous of Alaska

The Carboniferous of Alaska represents preserved segments of several plates, according to an analysis by J. T. Dutro, Jr., and D. L. Jones. Northern Alaska was the leading edge of an Arctic plate that moved south nearly 1,000 km, starting in early

Mesozoic time. Extreme western Alaska, including the Lisburne Peninsula, Cape York, and St. Lawrence Island, was part of an east Siberian region. East-central Alaska was the shelf edge and slope of the northwestern part of the North American platform. South-central Alaska was an arc or forearc trench at the northern edge of a paleo-Pacific plate. Southeastern Alaska consists of at least two fragments of the western edge of the North American plate that probably moved independently northwestward in post-Triassic time. These fragments may once have occupied positions west of present-day Oregon, California, or Baja California. Scattered outcrops of deep-water, radiolarian-bearing, laminated cherts and argillites in central and southwestern Alaska are possible remnants of the ancient North Pacific oceanic floor that have been preserved between plates converging from all sides.

Microplate tectonics

As interpreted by D. L. Jones and N. J. Silberling, recent geologic and paleomagnetic studies have shown that Alaska constitutes a gigantic mosaic of separate, allochthonous tectonic elements (microplates, blocks, and fragments) that originated to the south and accreted to North America during Mesozoic time. More than 30 discrete tectono-stratigraphic elements have been recognized to date, and further analysis undoubtedly will reveal more. The best known microplate (Wrangellia) occurs in southern Alaska and further south to at least Vancouver Island.

NORTHERN ALASKA

Geology of Alaska bordering Arctic Ocean

J. T. Dutro, Jr., summarized the geology of northern Alaska in terms of six major depositional episodes separated by major unconformities. The youngest of these (Holocene to Early Cretaceous) reflects postorogenic deposition in the Colville Trough north of the Brooks Range. The Jurassic to middle Permian episode records the last sediments of northern provenance, followed by preorogenic deep-water deposits in the region that was to become the Brooks Range. A predominantly shallow-water carbonate suite of facies characterizes the Carboniferous, after a northeastward transgression in the Early Mississippian. The Late Devonian included a period of complex marine deposition in the Frasnian, succeeded by a postorogenic clastic cycle in the Famennian. Platform carbonate rocks dominate the Early Devonian and Silurian sequence and are underlain by deep-water Ordovician and Cambrian units that include thin-bedded cherts, argillites, and volcanic rocks. The latest Proterozoic Z in the Demarcation Point quadrangle is represented by dominantly shallow-water, weakly metamorphosed sedimentary rocks, including quartzites, phyllites, and quartzose carbonates. The older Proterozoic includes quartz-mica schists, quartzites, and phyllitic strata.

Igneous activity can be assigned to five general orogenic periods, Taconian (about 450 m.y.), Acadian (about 380 m.y.), Sudetian (about 330 m.y.), late Kimmerian (about 160 m.y.), and early Alpine (about 80-90 m.y.).

The post-Paleozoic evolution of the Arctic Ocean basin could have involved southward movement of an Arctic plate which encountered a northward-moving Pacific plate during Jurassic time. Continued opening of the central Arctic Basin from Late Cretaceous to Holocene time may have resulted in underthrusting the Arctic margin of Alaska beneath the Brooks Range orogen.

Model for predicting offshore permafrost in the Beaufort Sea

During the height of the worldwide continental glaciation about 18,000 years ago, sea level was lowered. According to D. M. Hopkins and R. W. Hartz, the Bering Sea shelf was exposed seaward to about the present-day 90-m isobath. The position of the shoreline in the Beaufort Sea 18,000 years ago is not yet established but lay somewhere seaward of the 20-m isobath. The cover of ancient marine silt and clay became frozen as did the underlying gravel. The total thickness of bonded permafrost formed at any particular place depended partly upon the duration of exposure to subaerial temperatures, but thicknesses of several hundred meters were formed in most areas of the shelf landward of the present 20-m isobath.

The major rivers flowing north from the Brooks Range aggraded and formed outwash fans extending across much of the present-day coastal plain; the edges of most fans lay within a kilometer inland of or seaward of the present coast. Seaward from the edges of the fans, the rivers removed the ancient marine silt and clay to form broad, shallow valleys graded to the shoreline of the time. By analogy with the braided gravel floodplains of present-day North Slope rivers, the top of the ice-bonded layer lay at depths of several tens of meters beneath the river channels, but at depths of less

than a meter beneath uplands mantled with overconsolidated silt and clay.

When sea level began to rise, the shallow valleys were flooded early. In the absence of a cover of ancient, overconsolidated marine silt and clay, the cold but salty sea water gained ready access to the underlying gravel. Ice in the gravel was thawed rapidly and deeply by salt advection. Ultimately, these valleys began to collect Holocene marine sediments carried by currents from river mouths.

When the sea transgressed over the slightly higher plains away from the sea valleys, salt water was prevented from gaining access to the potentially porous gravel substrate by the mantle of tight overconsolidated clay. Consequently, thawing of ice in the shallow-bonded permafrost could progress only by the heat diffusion and silt diffusion. Water temperatures are below zero, and silt diffusion progresses only slowly. Consequently, thawing has progressed extremely slowly and only to very limited depths in most areas mantled by overconsolidated clay.

If this model is correct, deep permafrost is to be expected throughout the area of Holocene sediments shown by P. W. Barnes and Erk Reimnitz (Barnes and Reimnitz, 1974) as extending westward from the mouth of the Sagavanirktok River to a point northwest of Oliktok Point, where it is joined by another belt of Holocene sediments extending northward from the mouth of the Colville River to the shelf break. Similar belts of Holocene sediments and deep permafrost should be present in as-yet-undiscovered sea valleys extending from the Shaviovik and Canning Rivers, and these should be overconsolidated clay and shallow, potentially ice-rich permafrost in other parts of the Beaufort Sea.

Mesozoic radiometric ages in Precambrian rocks

Radiometric age determinations by M. L. Silberman, C. L. Connor, and J. L. Morton indicate an age no older than Triassic for a unique occurrence of volcaniclastic rocks overlain by Precambrian carbonate rocks in the central Demarcation Point quadrangle (index map, loc. 1). Potassium-argon age determinations of 188±7 m.y. on plagioclase clasts contradict field evidence for a simple depositional relationship with the overlying Precambrian carbonate rocks and indicate that the volcaniclastic sequence is not of Precambrian age.

New age of metaplutonic rocks in the Survey Pass quadrangle, Brooks Range

The phyllite, quartz-mica schist, and marble that make up the metamorphic belt of the southern Brooks Range appear, on the basis of fossil evidence, to be Devonian in the Survey Pass quadrangle. These rocks are intruded by the Arrigetch Peaks and Mount Igipak plutons (loc. 2), large intrusive bodies ranging in composition from alkali feldspar granite to tonalite and exhibiting well-developed cataclastic texture from later recrystallization. Previous workers (Turner, Forbes, and Mayfield, 1978) interpreted these plutons to be Cretaceous in age and to represent synkinematic intrusions accompanying a major Cretaceous metamorphic episode (defined on the basis of K-Ar ages) that affected the entire metamorphic belt. As part of the study of the geology of the Survey Pass quadrangle, M. L. Silberman (USGS) and Douglas Brookins (University of New Mexico) obtained a preliminary rubidium-strontium whole-rock isochron age of about 360 million years from six samples of granitic rocks from the two plutons. Initial strontium-isotope ratio of the system of approximately 0.712 suggests that these granites were derived in large part from crustal material. These preliminary data rule out a Cretaceous age for the granitic rocks.

EAST-CENTRAL ALASKA

Late Paleozoic fossils in ophiolite, northeastern Alaska

Brian Holdsworth and D. L. Jones have identified Mississippian radiolarians and Permian conodonts from cherts in the ophiolite sequences in the Arctic and Christian quadrangles (loc. 3). The fossils occur in a small isolated chert layer within the synformal Christian complex of mafic rocks (Reiser, Lanphere, and Brosgé, 1965) and at three localities in the nearly continuous unit of chert and shale that separates the synform of mafic rocks from the underlying Devonian(?) wacke and shale. Devonian spores and Paleozoic plants of probable Devonian age were previously identified from the wacke by R. A. Scott and S. H. Mamay.

The new fossil ages support the conclusion of Patton and others (1977) that the basalt-diabase-chert complexes of the Rampart belt are late Paleozoic in age while the younger radiometric ages of the igneous rocks represent the age of tectonic emplacement. The fact that the Mississippian is represented by radiolarian chert only 20 km southeast of outcrops where it is represented by Lisburne Group limestone and Kayak Shale in the typical Brooks Range sequence supports the conclusion that the ophiolite has been faulted against the Brooks Range rocks.

Hot Spring area, Circle quadrangle

T. E. C. Keith and H. L. Foster studied a small area on Big Windy Creek (loc. 4) in the northeast corner of the Circle A–2 quadrangle where several hot springs are on both sides of the Creek. The hot water comes through granitic rock near its northern contact with regionally metamorphosed rocks. Temperature of the water is about 58°C and pH is about 6.9. The water is very high in HCO_3 and Na. Water chemistry is quite different from that of Circle Hot Springs to the north and from Chena Hot Springs to the west. Small sinter terraces have been deposited by the thermal waters. The older sinter contains some carbonate and amorphous material; a thin layer of silica on the outer surface of the terraces indicates that water chemistry has not been constant.

Cumulate gabbro and pillow basalt associated with the Mount Sorenson ultramafic complex

T. E. C. Keith and H. L. Foster found a sequence of periodotite, cumulate gabbro, and pillow basalt with associated red chert on the north side of the Seventymile River on the boundary between the Charley River and Eagle quadrangles (loc. 5). This sequence appears to be a part of the ultramafic complex near Mount Sorenson (exposed to the west) that has been displaced to the southeast by faulting. The sequence appears to be dipping south. The presence of cumulate gabbro and pillow basalt (seen for the first time in the Mount Sorenson area) strengthens the evidence that the ultramafic complex is part of a dismembered ophiolite.

Preliminary Proterozoic lead ages on zircon from augen gneiss, Big Delta quadrangle

A study to determine the nature and age of the protolith of a large body (approximately 700 km^2) of augen gneiss (loc. 6) in the Big Delta quadrangle is presently being carried out by Cynthia Dusel-Bacon. The augen gneiss has undergone amphibolite facies metamorphism and contains large eyes of potassium feldspar ranging from 3 to 7 cm in longest dimension. Cataclasis and recrystallization have affected the gneiss, obscuring its original texture and making its history difficult to interpret. Uranium-thorium-lead dating of zircons is being done by T. W. Stern. The first sample run yielded discordant ages ($^{206}Pb/^{238}U$, 317.3 m.y.; $^{207}Pb/^{235}U$, 341.7 m.y.; $^{208}Pb/^{232}Th$, 332.4 m.y.; and $^{207}Pb/^{206}Pb$, 511.3 m.y.). These preliminary data suggest a Proterozoic Z age. Additional samples are being analyzed in an attempt to define a discordia.

A microprobe investigation of the zircon separate used for dating identified two inclusions of Al_2SiO_5. Inclusions of this composition indicate that the protolith may contain material from a source that has experienced a weathering cycle. One of the possible origins of the augen gneiss might be porphyritic granite derived from arkosic material shed off the Canadian shield.

The augen gneiss is part of the Yukon crystalline terrane, a metamorphic complex bordered by the Tintina fault to the north and the Denali fault to the south. Knowledge of the history of the augen gneiss will shed light on the origin and geologic history of this part of Alaska.

SOUTHERN ALASKA

Regional geochronology of the Willow Creek area

About 20 K-Ar determinations, part of a study by M. L. Silberman and Béla Csejtey, Jr., of the geochronology of plutonic granitic rocks, metamorphosed sedimentary rocks, and hydrothermal alteration and mineralization in the Willow Creek area (loc. 7), indicate that a major Paleocene metamorphic event affected many of the apparent ages. Preliminary results were reported by Silberman and others (1978). The oldest rock unit, a quartz-mica schist of probable Jurassic prograde metamorphic age, has been retrograded from the amphibolite facies and has been intruded by now-metamorphosed Cretaceous(?) ultramafic rocks. Plutonic granitic rocks with irregular propylitic alteration zones include Jurassic hornblende diorite and Upper Cretaceous tonalite and biotite granite. Aplite, pegmatite, and lamprophyre dikes intrude the tonalite. Gold-bearing quartz veins that contain sulfides and sulfosalts, have sericitic selvages, and contain disseminated muscovite, cut the schist and granitic rocks. Upper Cretaceous and Tertiary sedimentary rocks overlie the schist and granitic rocks.

Potassium-argon mineral ages for the rocks are 56 to 66 m.y. for the schist, 89 to 91 m.y. for the ultramafic rocks, 69 to 78 m.y. for the tonalite, 65 to 67 m.y. for the biotite granite, 66 to 67 m.y. for the dikes, 56 to 66 m.y. for the quartz veins, and 58 m.y. for propylitized tonalite. These data can best be interpreted as reflecting the effects of a metamorphic hydrothermal event of Paleocene age that has partially to totally reset the K-Ar ages of the schist, the granitic and ultramafic rocks, and the quartz veins. This event also produced the prophylitic alteration of the tonalite.

Trondhjemite in the Talkeetna Mountains, south-central Alaska

Reconnaissance geologic mapping, by Béla Csejtey, Jr., and W. H. Nelson, in the Talkeetna Mountains, south-central Alaska, discovered a large pluton (loc. 8) of trondhjemite, a unique rock type previously not known to occur in southern Alaska.

The trondhjemite pluton is a discordant, northeast-trending, elongate, epizonal body of fairly uniform lithology, occurring in the central Talkeetna Mountains. The pluton is approximately 120 km long with a maximum width of about 15 km, and has been intruded into Lower and Middle Jurassic plutonic and metamorphic rocks. Large portions of the pluton have been sheared and saussuritized. Typically, the trondhjemite is a light-gray, medium- to coarse-grained rock with a granitic texture. A faint flow foliation is locally developed. Major rock-forming minerals are plagioclase (oligoclase to sodic andesine), quartz, K-feldspar (as much as 10 percent by volume), and biotite, with subordinate amounts of muscovite and opaque minerals. Color index ranges from 3 to 9. Average oxide percentages by weight of seven trondhjemite analyses are SiO_2, 70.30; Al_2O_3, 16.74; K_2O, 5.07; CaO, 3.33. Three K-Ar age determinations from the northern half of the pluton by M. A. Lanphere (USGS) and by D. L. Turner (University of Alaska), including concordant ages on a mineral pair of muscovite and biotite, yielded very similar numbers indicating emplacement of the trondhjemite pluton between 145 and 150 million years ago. The trondhjemite is the youngest member of a group of Jurassic plutonic and metamorphic rocks in the Talkeetna Mountains.

Geophysical ore guides in south-central Alaska

J. E. Case reports that at least 75 percent of the granitic plutons in the Seward and Blying Sound quadrangles (loc. 9) are nonmagnetic and have little or no gravitational expression. The few granitic bodies that are magnetic are close to the mafic belt in Prince William Sound, perhaps indicating that the granitic magmas were contaminated at a late stage of emplacement by mafic materials. The granites of the Chugach terrane are thought to be anatectic (Hudson, Plafker, and Lanphere, 1977) and are largely devoid of significant mineral deposits. The lack of magnetic expression of most of these bodies may constitute a "negative" ore guide.

In comparison, many of the highly mineralized (Cu-Mo) plutons of the Alaska Peninsula, especially in the Chignik and Sutwik Island quadrangles, are thought to be related to subduction processes and have pronounced magnetic expression.

SOUTHWESTERN ALASKA

Exotic Precambrian rocks in southwestern Alaska

The metamorphic complex along the Kanektok River, an isolated 160-km belt of Precambrian gneisses and schists in southwestern Alaska, trends northeastward from Jacksmith Bay on the Bering Sea coast across the northwest corner of the Goodnews quadrangle into the Bethel quadrangle (Hoare and Coonrad, 1959, 1961) (loc. 10). The maximum exposed width is about 14 km, and geological and geophysical data suggest that it is not appreciably wider in the subsurface. According to J. M. Hoare and W. L. Coonrad, the complex apparently consists of recrystallized sedimentary, volcanic, and intrusive dioritic and granitic rocks metamorphosed to the upper greenschist and lower amphibolite facies. There is no apparent metamorphic gradation between these rocks and the Paleozoic and Mesozoic rocks that flank them on either side.

Both geological and geophysical data indicate that the Precambrian belt is thin and rootless. Geological observations suggest that it overlies Cretaceous sedimentary rocks. Interpretation of aeromagnetic data by Andrew Griscom suggests that the Cretaceous rocks, in turn, overlie magnetic rock at a depth of 1 to 2 km. The gravity data also attest to the rootless character of the metamorphic belt. There is no variation in the normal gravitational field where two gravity traverses cross the metamorphic belt. This implies that the crystalline rocks do not extend to any appreciable depth.

The origin of this displaced belt of Precambrian rocks is problematical. But the tectonic framework of southern Alaska and recent evidence of very large northwest transport in south-central Alaska (Jones, Silberling, and Hillhouse, 1977, p. 2565–2577; Hillhouse, 1977, p. 2578–2592) suggest that it probably originated far to the southeast. It may be a rifted fragment of the Precambrian shield in Canada, or it may have come from farther south.

SOUTHEASTERN ALASKA

Mineral resources and aeromagnetic studies of Glacier Bay National Monument

Completion of a joint USGS–USBM study of Glacier Bay National Monument (loc. 11) resulted in the identification of nine important mineral deposits with identified resources located in six areas considered to also have undiscovered hypothetical resources. The USGS authors, D. A. Brew, B. R. Johnson, and Donald Grybeck, also reported the identi-

fication of seven additional areas with important geochemical and (or) geophysical anomalies. The elements of greatest economic interest are nickel, molybdenum, copper, zinc, and gold. The following brief descriptions are based on both USGS and USBM information contained in the open-file report (Brew and Morrell, 1978).

The Pacific beach sands favorable area which has had past production of placer gold, contains both identified-inferred and undiscovered hypothetical resources of ilmenite and gold. It is unlikely that these low-grade resources are now or will be in the near future economically attractive, even though large tonnages are present.

The Crillon–La Perouse favorable area includes the Brady Glacier nickel-copper magmatic deposit, which contains about 80 million metric tons of identified-indicated resources with 0.53 percent nickel, 0.33 percent copper, and an unspecified amount of platinum-group metals and 80 million metric tons of identified-inferred resources of the same grade. In addition, the favorable area also is estimated to have another 80 million metric tons of undiscovered hypothetical resources of the same grade.

The Mount Fairweather favorable area is very poorly known, but the ore environment is similar to that of the Crillon–La Perouse, and 82 million metric tons of undiscovered speculative resources with 0.53 percent nickel and 0.33 percent copper are estimated to be present.

The Margerie Glacier favorable area includes the Margerie Glacier porphyry-copper deposit, which contains 145 million metric tons of identified-inferred resources with 0.2 percent copper, 0.27 g/t gold, 4.5 g/t silver, and 0.01 percent tungsten, and the Orange Point volcanogenic sulfide deposit, which contains 0.25 million metric tons of identified-inferred resources with 2.7 percent copper, 5.2 percent zinc, 1 g/t gold, and 34 g/t silver, as well as 0.47 million metric tons of identified inferred-resources containing 0.4 percent copper, 0.3 percent zinc, 0.2 g/t gold, and 12 g/t silver. In addition, the favorable area also is estimated to contain 0.9 million metric tons of undiscovered hypothetical resources with 1.5 percent copper and 2.0 percent zinc, and further unquantified, undiscovered speculative copper and zinc resources.

The Reid Inlet favorable area has had past production of gold from the Reid Inlet vein deposits, and is estimated to contain about 480 kg of undiscovered hypothetical resources.

The Rendu Glacier favorable area includes the "massive chalcopyrite" skarn deposit, which contains 0.004 million metric tons of identified-inferred resources with 0.5 percent tungsten, 4.0 percent copper, 240 g/t silver, and 5.2 g/t gold. The favorable area also has unquantified, undiscovered speculative copper and tungsten resources.

The Muir Inlet favorable area includes the Nunatak molybdenum porphyry deposit, which contains 7.4 million metric tons of identified-indicated resources with 0.06 percent molybdenum and 0.02 percent copper, and 124 million metric tons of identified-indicated resources with 0.04 percent molybdenum and 0.02 percent copper, as well as 8.3 million metric tons of identified-inferred resources with 0.06 percent molybdenum and 0.02 percent copper. The area also is estimated to have 90 million metric tons of undiscovered hypothetical resources with 0.15 to 0.20 percent molybdenum and unquantified, undiscovered speculative resources of copper and molybdenum.

The Casement Glacier favorable area also contains unquantified, undiscovered speculative molybdenum and copper resources, and part of the area has unquantified, undiscovered speculative copper-zinc resources in a volcanogenic environment.

The White Glacier favorable area also contains unquantified, undiscovered speculative zinc and copper resources in a volcanogenic environment.

These deposits and favorable areas are in the parts of the Monument that are best known geologically and geochemically. The presence of significant mineral resources in other areas cannot be ruled out. Glacier Bay National Monument is highly mineralized in comparison with most areas of similar size elsewhere in southeastern Alaska, and it is likely that it contains more deposits and favorable areas of the types described here and perhaps other types of deposits as well.

Andrew Griscom reports that aeromagnetic data plus physical-properties measurements (58 samples) indicate that granitic rocks of Cretaceous and Tertiary ages east of the Tarr Inlet suture zone (Brew and Morrell, 1978) are magnetic, while similar rocks west of the zone are not magnetic. The magnetic properties of these granitic rocks may thus have been determined by the crustal rocks in which the plutons formed or up through which the plutons moved. Additionally, the aeromagnetic data and measurements by C. S. Grommé on 94 samples show that the gabbro complexes of the Fairweather Range are generally rather magnetic except for the southern two-thirds of the "Crillon–La Perous complex," which is only very slightly magnetic and is also associated with a nickel-bearing sulfide deposit. The

association may be a guide for prospecting of the nonmagnetic gabbro masses in this region.

Mineral resources in Kuiu-Etolin Islands Tertiary volcanic and intrusive belt

Reconnaissance geologic mapping in the Petersburg and Port Alexander (1:250,000) quadrangles by D. A. Brew, H. C. Berg, R. P. Morrell, R. A. Sonnevil, J. D. Cathrall, S. J. Hunt, and Carl Huie has delineated a N. 70° W. trending Tertiary intrusive and volcanic belt that may contain molybdenum, tungsten, and uranium resources. The belt, which is discordant to regional structural trends and intrusive belts (including recognized Tertiary basins), extends eastward from an intermediate-composition granitic intrusive-volcanic complex on central Kuiu Island to beneath Sumner Strait and on to Zarembo and Etolin Islands (loc. 12). The belt on Zarembo consists of a dike-and-flow complex of intermediate-to-silicic composition with minor granitic intrusions and on Etolin of granitic intrusions. Age of the belt is established on the basis of fossils from sedimentary strata interlayered with flows and on comparisons of the lithic and structural character of the granitic bodies with dated bodies in the "Coast Range" plutonic complex. These latter bodies contain molybdenum and perhaps uranium resources. Very preliminary synthesis of available stream-sediment and bedrock geochemical data suggests that the belt contains anomalous concentrations of tungsten.

New analysis of paleomagnetic data from Alexander terrane

Research on Paleozoic rocks of southeastern Alaska initiated by C. S. Grommé (USGS) has been continued by Meridee Jones (USGS) and Rob Van der Voo (University of Michigan). Initial results suggested no displacement of the rocks of the Alexander terrane. Further analyses, however, indicate that inclinations and declinations of poles for sample groups of late Middle Ordovician, Late Ordovician, Devonian, Late Devonian, early and Late Carboniferous ages deviate from predicted values and that a better match can be obtained for a paleoposition of the terrane at about lat. 40° N., long. 120° W., which is in western Nevada or northeastern California, a location suggested earlier by Jones, Irwin, and Ovenshine (1972). In addition, the paleomagnetic results of Van der Voo and others require a post-Carboniferous 25° counterclockwise rotation of the terrane. Restoration of the counterclockwise rotation would alter the direction of major facies change from northwest to due north and complicate the comparison of Silurian facies belts between southern Alaska and California used by Jones and others in their treatment of the Alexander terrane as a displaced continental fragment.

Intrusive belts of southeastern Alaska

Compilations and synthesis of available published and unpublished data on the distribution, composition, and age of intrusive rocks in southeastern Alaska by D. A. Brew and R. P. Morrell have resulted in the recognition of 21 distinct intrusive belts or areas. These belts record a variety of magmatic and tectonic events from the Precambrian to the Tertiary. The table below summarizes the geographic distribution and ages of most of the belts. Ages given are based on isotopically dated samples and on field evidence and inference.

In addition to the belts in the table, there are five belts of mafic and (or) ultramafic intrusive rocks, as follows: (1) Yakobi-Fairweather belt of layered and nonlayered gabbros of Tertiary(?) or Cretaceous(?) age, (2) central Baranof belt of serpentinized peridotite and serpentinite of Mesozoic age, (3) central Chichagof belt of hornblende gabbros closely associated with the Glacier Bay-Chichagof belt of Cretaceous granitic rocks, (4) Duke Island-Klukwan belt of concentrically zoned mafic-ultramafic complexes (Taylor, 1967), and (5) "Coast Range" plutonic complex "belt" of peridotite, dunite, and gabbro (Grybeck and others, 1977).

REGIONAL STUDIES AND COMPILATIONS OF LARGE AREAS

Synthesis and analysis of Appalachian orogen

Better understanding of the early Paleozoic geology of the American Appalachians is being sought through geologic synthesis and analysis on both sides of the North Atlantic by American geologists, together with geologists from nine other countries of the North Atlantic region, as a part of the Caledonide Orogen Project of the International Geological Correlation Program (IGCP). One such synthesis that includes both the Canadian and American Appalachians is the Tectonic-Lithofacies map of the Appalachian orogen at 1:1,000,000 scale (Williams, 1978) based on recent work of many geologists including that of 15 members of the USGS. Analyses of several aspects of the geology of the orogen, by means of compilation of certain kinds of data at 1:1,000,000 scale, are under way by a

Age		*Location*	*Composition*
Tertiary	~20–25 m.y.(?)	Kuiu-Zarembo-Etolin Island	Intermediate to silicic intrusive and flow complex.
	~20–25 m.y.(?)	"Coast Range" plutonic complex	Granite, alkali granite.
	~30–45 m.y.	Glacier Bay-Baranof Island	Granodiorite.
	~45–50 m.y.	"Coast Range" plutonic complex	Do.
Tertiary or Cretaceous.	------	Yakutat-Glacier Bay	Do.
		"Coast Range" plutonic complex	Do.
Cretaceous	~80–100 m.y.	Revillagigedo Island-Stephens Passage.	Granodiorite porphyritic diorite.
	~100–110 m.y.	Glacier Bay-Chichagof Island	Granodiorite.
Cretaceous (?)	------	"Coast Range" plutonic complex sill.	Tonalite.
Cretaceous and (or) Jurassic.	------	Revillagigedo-Prince of Wales Island	Granodiorite.
Jurassic	~140–150 m.y.	Chilkat Mtns.-Baranof Island	Do.
		Bokan Mountain	Alkali granite, granite.
		Texas Creek	Granodiorite.
Late Paleozoic (?)	~280 m.y.	Yakutat	Diorite, quartz diorite.
Silurian and (or) Ordovician.	------	Southeastern Chichagof	Syenite, monzonite.
		Southeastern Prince of Wales Island	Quartz monzonite, granodiorite.
		Annette Island	Trondhjemite.
Precambrian	>700 m.y.	Southwestern Prince of Wales Island.	Do.

team of Federal, State, and university geologists coordinated by R. B. Neuman. Among these aspects is a Time-of-Deformation map of the U.S. Appalachians, compiled by a team of six geologists, led by P. H. Osberg (University of Maine, Orono) (See Dallmeyer and others, 1978), that shows by means of color coding the ages of eight kinds of structural features such as faults, folds, and foliations. The patterns of this map emphasize the differences between the northern Appalachians, where late Paleozoic deformation is of limited extent and early Paleozoic structures dominate, and the central and southern Appalachians, where late Paleozoic structures are pervasive.

WATER-RESOURCE INVESTIGATIONS

The mission of the USGS's Water Resources Division (fig. 2) is to provide, to interpret, and to apply the hydrologic information needed for the optimum use and management of the Nation's water resources. This is accomplished, in large part, through cooperative programs with other Federal and non-Federal agencies. The USGS also cooperates with the Department of State in providing scientific and technical assistance to international agencies.

The USGS conducts systematic investigations, surveys, and research on the occurrence, quality, quantity, distribution, use, movement, and value of the Nation's water resources. This work includes (1) investigations of floods and droughts and their magnitudes, frequencies, and relations to climate and physiographic factors, (2) evaluations of available waters in river basins and ground-water provinces, including assessments of water requirements for industrial, domestic, and agricultural purposes, (3) determinations of the chemical, physical, and biological characteristics of surface and ground water and the relation of water quality and suspended sediment load to various parts of the hydrologic cycle, and (4) studies of the interrelation of water supply with climate, topography, vegetation, soils, and urbanization.

One of the USGS's most important activities is disseminating water data and the results of investigations and research by means of reports, maps, computerized information services, and other forms of public release.

The USGS (1) coordinates the activities of Federal agencies in the acquisition of water data on streams, lakes, reservoirs, estuaries, and ground

FIGURE 2.—Index map of the conterminous United States showing areal subdivisions used in the discussion of water resources.

waters, (2) maintains a national network, (3) conducts special water-data-acquisition activities, and (4) maintains a central catalog of water information for use by Federal agencies and other interested parties.

Supportive basic and problem-oriented research is conducted in hydraulics, hydrology, and related fields of science to improve the scientific bases for investigations and measurement techniques and to provide sufficient information about hydrologic systems so that quantitative predictions of their responses to stress can be made.

During FY 1979, data on streamflow were collected at about 7,700 continuous record discharge stations and at about 9,750 lake- and reservoir-level sites and partial record streamflow stations. About 12,200 maps of flood-prone areas in all States and Puerto Rico have been completed to date, and about 825 pamphlets covering areas susceptible to flooding have been published in the past 5 years. Studies of the quality of surface water were expanded; there were approximately 6,820 water-quality stations in the United States and in outlying areas where surface water was analyzed by the USGS. Parameters measured include selected major cations and anions, specific conductance or dissolved solids, and pH. Other parameters, measured as needed, include trace elements, phosphorous and nitrogen compounds, detergents, pesticides, radioactivity, phenols, BOD, and coliform bacteria. Streamflow and water temperature records were collected at more than 4,050 water-quality stations. Sediment data were obtained at almost 1,380 locations.

Annually, about 500 USGS scientists report participation in areal water-resource studies and research on hydrologic principles, processes, and techniques. There are 1,818 active water-resource projects; 426 of the studies in progress are classed as research projects. Of the current water-resource studies, 116 are related to urban hydrology problems, 177 are energy-related projects, and 54 are related to water use.

In FY 1979, 684 areal appraisal studies were carried out. Maximum and mean areas of the studies were about 1.5×10^6 and $.067 \times 10^6$ km^2, respectively. Total areal appraisal funding was nearly $42 million. Ground-water studies have been made or are currently in progress at some degree of intensity for all of the Nation. Long-term continuing measurements of ground-water levels were made in about 28,000 wells, and periodic measurements in connection with investigations of ground water were made in many thousands of other wells. Studies of saline-water aquifers, particularly as a medium for disposal of waste products, are becoming increasingly important, as are hydrologic principles and analytic and predictive methodologies for determining the flow of pollutants in ground-water systems. Land subsidence caused by ground-water depletion and the possibilities for induced ground-water recharge and practicality of subsurface disposal of wastes are under investigation. Ground-water supplies for energy development and the effects of coal mining activities on both ground and surface water resources are being intensively studied.

During FY 1979, the use of computers continued to increase in research studies of hydrologic systems, in expanding data storage systems, and in quantifying many aspects of water-resource studies. Records of about 320,000 station-years of streamflow acquired at about 17,600 regular streamflow stations are stored on magnetic tape, and data on about 580,000 wells and springs have been entered in a new automated system for storage and retrieval of ground-water data. Digital computer techniques are used to some extent in almost all of the research projects, and new techniques and programs are being developed continually.

NORTHEASTERN REGION

In July 1978, severe flooding occurred in parts of southeastern Minnesota and central and southwestern Wisconsin. The peak discharge of 864 m^3/s at the gaging station on the South Fork Zumbro River near Rochester, Minn., on July 6, 1978, was the largest observed there since 1908 and was greater than that of a 100-year flood. Damage was reported to be especially severe in Rochester where several thousand residents were evacuated, at least nine people were killed, and many were reported missing. The National Weather Service reported that 147 mm of rain fell in 5 hours at Rochester. On July 7, 1978, about 56 km southwest of Rochester, the Cedar River flooded in and near Austin, Minn., and the peak discharge of 289 m^3/s at the gaging station near Austin was the largest observed in 39 years of record. Ten days later, however, this discharge was exceeded by a record-breaking flood peak of 351 m^3/s.

Flooding was also severe in the Kickapoo River basin in west-central and southwestern Wisconsin. Sixteen counties were declared eligible for Federal disaster assistance, and total losses were estimated at $53 million. The National Weather Service reported rainfall of as much as 152 mm in about 20

hours. The flow of the Kickapoo River at LaFarge, Viola, and Steuben of 382, 387, and 481 m^3/s, respectively, was greater than that expected on an average of every 100 years.

Two major changes in the field of water quality have begun in the northeastern region. (1) Water-quality activities are being adjusted in areas where coal is mined in order to obtain the data needed for mining permits and to evaluate the impact of mining on water quality. (2) The number of investigations to assess the occurrence and movement of organic compounds in ground-water systems is increasing, particularly where water is used for public supply.

A 4-year study of aquifers (collectively known as the Cambrian-Ordovician aquifer) in a six-State region of the northern Midwest has begun. Parts of Illinois, Indiana, Iowa, Minnesota, Missouri, and Wisconsin are included. The study is designed to evaluate potential aquifer response to regional ground-water development. Specific objectives include:

- Describing geologic, hydrologic, and chemical characteristics of the aquifer systems.
- Determining past and present ground-water withdrawals and estimation of future withdrawals.
- Developing digital models to simulate hydrologic systems and to estimate effects on the systems caused by various stresses.
- Evaluating present hydrologic data monitoring and designing a new system to monitor future water use, water levels, and water quality.

REGIONAL STUDIES

Allen Sinnott and E. M. Cushing (1979) completed an appraisal of the ground-water resources of the mid-Atlantic region, which includes parts of Maryland, Massachusetts, New York, Pennsylvania, Vermont, Virginia, and West Virginia and all of Delaware, New Jersey, and the District of Columbia. They reported that the ground water occurs in three main geologic terranes: (1) unconsolidated deposits in the Coastal Plain seaward of the Fall Line, (2) hard consolidated sedimentary rocks and crystalline igneous and metamorphic rocks in the remainder of the region, and (3) unconsolidated sand, gravel, and other deposits of glacial origin that overlie the older rocks extensively in the glaciated northern part of the region.

Natural discharge from all the aquifers is estimated to be 146 million m^3/d ; in addition, 530 to 1,325 billion m^3 is held in dynamic aquifer storage.

ILLINOIS

Time-of-travel measured in Peoria Pool of the Illinois River

Flourescent dye was used to measure time-of-travel along a 116-km reach of the Illinois River from Starved Rock Lock and Dam to Peoria Lock and Dam. At a discharge of 170 m^3/s, the velocity averaged 0.8 km/h. A 27-km reach of the river, from Chillicothe to Peoria, consists of a lake with an average width of 1.6 km. The dye did not disperse into the shallow parts of the lake, but it remained in the 122-m-wide navigation channel. The study will be repeated at a discharge of 340 m^3/s.

Sludge irrigation hydrology

In Fulton County, Illinois, where a strip-mined area is being reclaimed by recontouring and by applying liquified sewage sludge as a soil conditioner, water quality varied greatly between mined and unmined land. However, no significant differences in water quality were observed in geologically similar materials, regardless of their proximity to fields where sludge was applied, according to R. F. Fuentes and G. L. Patterson.

Water levels in shallow aquifers fluctuated more in undisturbed glacial drift than in strip-mine spoil, and also fluctuated more as the distance from local discharge points increased. Depth to water was generally greater in the spoil than in the drift.

Discharge hydrographs of streams in the mined area showed delayed responses to precipitation caused by water being temporarily stored in interconnected small lakes left from mining operations.

INDIANA

Effects of seepage from fly-ash settling ponds and construction dewatering on ground-water levels at the Indiana Dunes National Lakeshore

Part of the Indiana Dunes National Lakeshore shares a common boundary with land of the Northern Indiana Public Service Company (NIPSCO). This area is underlain by unconsolidated deposits approximately 55 m thick. According to William Meyer and Patrick Tucci (1978), NIPSCO accumulates fly ash in settling ponds from which seepage has raised ground-water levels approximately 5 m under the ponds and more than 3 m within the lakeshore. Construction activities at a new NIPSCO nuclear powerplant included pumping ground water to dewater the construction site, and a slurry wall was installed around the site to prevent lowering of ground-water levels within the lakeshore. Plans call

for continuous pumping through at least December 1979.

A multilayered digital flow model was constructed to simulate the area's ground-water system. The model was used to demonstrate the effects of seepage from the fly-ash ponds on ground-water levels. The model indicated a decline of 1 m or less in the upper sand unit and 2 m or less in the lower sand unit within the lakeshore, owing to pumping from the construction site (Meyer and Tucci, 1978).

Saline ground water near Vincennes well field

In July 1976, the Vincennes Water Department expanded its well field by installing two new wells in the glacial outwash aquifer about 100 m west of the older wells. One of the new wells was within and the other was near an area underlain by saline water at the base of the outwash aquifer. During a 2-year study, R. J. Shedlock observed that the pumping of different combinations of the five older wells had little effect on the shape of the saline plume and the average chloride concentration of the municipal water supply, both of which have been stable since 1976. These observations encouraged the water department to use the new wells.

On December 22, 1978, the new well within the saline area was connected to the system at a pumping rate of 30 L/s. The well initially yielded water with a chloride concentration of 450 mg/L, which raised the chloride concentration of the municipal water to 150 mg/L. After 12 days, the chloride concentration had decreased to 195 mg/L in the new well and to 54 mg/L in the municipal water. The new well was intercepting the leading edge of the saline plume, and the chloride concentration of its water was decreasing as the saline water between the new well and the older wells was being flushed from the aquifer. The test indicated that the chloride concentration of the municipal water should eventually approach its average for 1976–78 after the new wells are put into full service.

Irrigation and ground water in Newton and Jasper Counties

M. P. Bergeron reported that effects of seasonal irrigation pumping are being investigated in limestone and sand and gravel aquifers in Newton and Jasper Counties in northwestern Indiana. The limestone aquifer, which consists mainly of Silurian and Devonian limestone, is confined by a continuous clay unit. The sand and gravel unit above the clay constitutes a water-table aquifer. Virtually all irrigation pumpage is derived from the limestone aquifer. During the irrigation season, water-level declines of nearly 12 m have been observed near limestone wells. Some local residents claimed that domestic wells in the sand and gravel aquifer go dry because of this pumping, but preliminary investigations indicated that the wells go dry because of seasonal water-level fluctuations.

Evaluation of ground water in Elkhart County

A preliminary evaluation of ground water in northwestern Elkhart County, Indiana, was made by T. E. Imbrigiotta, Angel Martin, Jr., and D. C. Gillies. An extensive test-drilling program provided stratigraphic information that supplemented drillers' logs for the 2,700-m^2 study area. Most of Elkhart is underlain by a 65- to 85-m-thick layer of sand and gravel on top of blue shale bedrock; however, at the industrial landfill northwest of Elkhart, no areally continuous clay layers were found. A preliminary water-level map indicated that ground-water flow through the landfill area is from north to south.

Background water quality of the shallowest aquifer was established by analyses of water samples from the completed network of observation wells. The samples were a calcium bicarbonate type, and samples from a few rural areas had high nitrate concentrations (>10 mg/L as nitrogen). Sampling also showed that water in the shallow aquifer immediately south of the industrial landfill was high in sodium, chloride, sulfate, iron, boron, and dissolved organic carbon. The concentration attenuates with depth and does not seem to be areally extensive.

Availability of ground water in the upper White River basin

Five digital models are being developed by W. W. Lapham, L. D. Arihood, and J. P. Reussow to simulate ground-water flow in the West Fork White River basin, upstream from Marion County, Indiana. These models will be calibrated with data collected over the past 3 years and will then be used to predict the effects of large-scale pumping.

Final mapping of the unconsolidated sediments resulted in the delineation of seven thin discontinuous sand and gravel aquifers and an extensive alluvial system in the southern half of the study area. These aquifers, as well as the alluvial system and the permeable limestone underlying the drift, will be modeled. Data indicated that the top 45 m of the limestone is permeable.

Specific-capacity tests of USGS wells showed that hydraulic conductivities of the sand and gravel aquifers ranged from 9.1 to 810 m/d and averaged approximately 160 m/d.

Flow model of the unconsolidated aquifers near Logansport

A digital flow model of the ground-water system near Logansport in Cass County, Indiana, was developed and calibrated by D. C. Gillies. The principal aquifer simulated was the sand-and-gravel deposit at or near the bottom of the buried preglacial Teays Valley. The transmissivity of this semiconfined aquifer ranges from zero along the valley walls to approximately 3,000 m^2/d along the axis of the buried valley. Model simulations demonstrated that ground water flowing in the Teays Valley is derived primarily from recharge within the study area and discharges to local streams, mainly to the Eel River and Crooked Creek.

The model was also used to demonstrate the hydrologic effects of ground-water development. A withdrawal rate of 440 L/s from the deep sand-and-gravel aquifer near Crooked Creek was simulated. Model-derived drawdowns in the deep aquifer ranged from less than 2 m at a distance of 23 km from the simulated well field to 11 m in the immediate vicinity of the simulated wells. Model results indicated that this pumping will reduce the dry-weather streamflow of Crooked Creek by approximately 20 percent.

MARYLAND

Drilling phase of modeling project completed

A drilling program was undertaken to better define the Cretaceous Potomac Group on Maryland's upper Eastern Shore. According to R. J. Mandle, six wells were drilled to bedrock—one each at Cecilton (444.4 m), in Cecil County, and Still Pond (350.8 m), Kennedyville (509.6 m), Massey (666 m), Fairlee (469.3 m), and Rock Hall (558.3 m), in Kent County. Brackish water (1,000 m/L chloride) was penetrated at Still Pond, Kennedyville, Massey, and Fairlee. The presence of brackish water at these locations can be directly related to topography and freshwater heads on the western shore of the Chesapeake Bay, this conclusion is in agreement with the findings of William Back (1966).

MASSACHUSETTS

Water quality in the Blackstone River basin

In the part of the Blackstone River basin in Massachusetts, water supply is less of a problem than water quality. Sand-and-gravel aquifers capable of providing municipal supplies are fairly widespread along valleys. However, the quality of water of the Blackstone River and its principal tributaries and the quality of ground water near the river is affected by waste discharges.

Historic data and samples of water from headwater sites above sources of contamination indicated that the original water of the basin was of the calcium bicarbonate type and had a chloride concentration of about 3 mg/L and a hardness of 20 mg/L. Sodium and chloride content are now greater in public water supplies. Only 1 of the 40 public supply well samples yielded water that had 3 mg/L or less of chloride; half had more than 30 mg/L. Half of the municipal-supply wells contained 1.2 mg/L or more of nitrate (as N) compared with a possible original content of about 0.1 mg/L of nitrate (as N). Median value of hardness of water is now 33 mg/L.

High manganese and iron content is a persistent problem in water from many municipal wells. About 40 percent of the sampled well contained more than 0.05 mg/L of manganese, and 10 percent had more than 0.3 mg/L of iron, the maximum limits recommended by EPA for public drinking water supplies. The iron and manganese deposits on well screens gradually reduce well yields, thus necessitating reconditioning of well screens.

MICHIGAN

Ground water in Marquette County

Ground water in Marquette County, Michigan, is derived from bedrock aquifers and aquifers in glacial deposits. In the northern and southeastern parts of the county, most water is obtained from bedrock at depths of less than 30 m. In the central part, ground water is generally derived from glacial deposits through wells as deep as 75 m.

Well yields in many parts of the county are unpredictable, even by test drilling. Wells in glacial deposits yield 0.1 to 19 L/s, and wells in bedrock yield as much as 12 L/s. Some shallow wells yield small quantities of water and often go dry during periods of drought. Wells in Precambrian igneous and metamorphic rocks yield little or no water.

Water resources of the Marquette Iron Range area

N. G. Grannemann reported that average annual surface-water discharge in the Marquette Iron Range area is about 20 m^3/s, and 10-year 7-day low-flow for the 1,580-km^2 study area is about 5 m^3/s. Surface water is used primarily for iron-ore concentration and pelletization.

Glacial outwash under water-table conditions constitutes the area's principal aquifers. The areal extent of outwash that is 30 m or more in saturated thickness is about 200 km^2. Ground water is used primarily for public supplies in small communities.

Surface water and ground water are generally of good chemical quality. Dissolved-solids concentration in surface water averages less than 120 mg/L, and in ground water it averages 107 mg/L and ranges from 26 to 352 mg/L. About 60 percent of the ground water is moderately hard. Iron concentration of water in glacial deposits averages 2,060 μg/L and ranges from 0 to 26,000 μg/L.

Model study of Michigan coal deposit

A seven-layered three-dimension digital model was used by J. R. Stark and M. G. McDonald to study ground-water constraints to coal mining in Michigan and to establish baseline conditions against which future changes caused by mining can be judged. The 51.8-km^2 study area in Bay County includes a 1-m thick coalbed approximately 45 m below land surface; it is an area typical of most coal-deposit areas in Michigan.

Hydraulic characteristics were estimated by matching model results with drawdowns observed during two aquifer tests. Preliminary results indicated that mine seepage could be controlled by maintaining reasonable pumping rates (<2 m^3/s for a mining area of 10 km^3). However, dewatering would produce significant water-level declines in aquifers near such a mine.

MINNESOTA

Design for a ground-water-quality monitoring network

A network for monitoring the quality of water in the 13 principal aquifers in Minnesota was designed by M. F. Holt, and 350 wells and springs were selected for sampling. The network is based on point sampling and point, areal, and site-specific monitoring. Wells were selected for all but the site-specific element.

The system was designed to obtain baseline data throughout the State on concentrations of major cations and anions, minor constituents, trace metals, and selected organic compounds.

Shallow aquifers in southwestern Minnesota

Several shallow aquifers have considerable potential in Cottonwood, Jackson, Lincoln, Murray, Nobles, Pipestone, Redwood, and Rock Counties in southwestern Minnesota, according to D. G. Adolphson. The area contains five major and two minor alluvial outwash aquifers. Major aquifers will yield 30 to 60 L/s, and minor aquifers will yield 5 to 30 L/s to wells. Augering 400 test holes showed that the outwash ranges in thickness from 5 to 25 m. The depth to water in 22 observation wells ranged from 2 to 4 m below land surface.

Effect of copper and nickel mining on surface and ground water in northeastern Minnesota

D. I. Siegel and D. W. Erickson reported that streams in the copper-nickel mining area of northeastern Minnesota have similar flow characteristics, except where they are extensively regulated because of mining operations. Base flow during winter accounts for less than 11 percent of annual discharge. About 60 percent of annual discharge occurs during April, May, and June. Storage of overland runoff in headwater wetlands and inchannel lakes is reflected in breaks in slope above the 90 percentile point on flow-duration curves for the Kawishiwi and Shagawa Rivers. Flood peaks are smaller and the period of overland runoff is longer for the Kawishiwi and Shagawa Rivers than they are for rivers in the St. Louis River watershed, which has less surface-water storage.

Ground water is contained in local surficial materials. Hydraulic conductivities ranged from 3 to 1,050 m/d for sand-and-gravel aquifers and from 10^{-2} to 10^{-6} m/d for till and peat. Average concentrations of major constituents in water in till were about twice those in sand and gravel. Seasonally, concentrations of major constituents in surficial ground water did not significantly change. Water in surficial materials is generally of the calcium–magnesium–bicarbonate type. Oxidation of copper and nickel sulfide minerals increased the sulfate content of water in aquifers in and immediately south of the mineralized contact zone between the Precambrian Duluth Complex and older rocks.

Appraisal of ground water in central Minnesota

Preliminary test drilling by C. F. Myette in Todd and parts of Cass and Morrison Counties, Minnesota, indicated that surficial sand and gravel deposits form a long irregularly shaped area of approximately 650 km^2 along the Eagle Creek, Crow Wing, and Long Prairie Rivers. The outwash is continuous for nearly 65 km and ranges in thickness from 8 m at the north end near Pillager to 30 m at the south end near Round Prairie. Widths range from 2 km near Round Prairie to nearly 7 km at

Pillager. Three aquifer tests indicated that wells tapping the aquifers locally yield as much as 60 L/s.

Ground-water appraisal of sand-plain areas

Pumping tests of irrigation wells indicated that the hydraulic conductivity of the unconfined drift aquifer in Benton, Sherburne, Stearns, and Wright Counties in Minnesota is commonly from 90 to 180 m/d. Saturated thickness is greatest (24 m) in outwash-filled buried valleys in eastern and western Sherburne County and 30 m in the Maine Prairie area of Stearns County. G. F. Lindholm reported that water levels were measured in 240 irrigation wells in March 1978, when hydrologic stress was minimal. Measurements were repeated in selected wells in May and September, before and after the irrigation season. Discharge of major streams were measured at the time ground-water levels were obtained to determine ground-water contribution to streamflow. Streamflow pickup in the Elk and St. Francis Rivers ranged from 28 to 84 L/s per river mile during high base-flow conditions in May. A digital-flow model is being used to study the ground-water system in Sherburne County and in the Maine Prairie area of Stearns County.

Use of surficial aquifers increasing in Minnesota

H. W. Anderson, Jr., identified 10 sand-plain areas in Minnesota for detailed studies, contingent on the availability of ground water and the development of irrigation supplies. Wells in the Pelican River, Bagley, Pomme de Terre River, Lake Emily, Brainerd, Litchfield, Onanegozie, Anoka, Stillwater, and Rosemont sand plains may yield as much as 300 L/s. Ground water is being developed for irrigation in each of the areas at an accelerated rate.

Water balance of Williams Lake, north-central Minnesota

According to D. I. Siegel and T. C. Winter, water-level measurements in 18 piezometers indicated that the water table around Williams Lake in north-central Minnesota ranges from 1.2 m below land surface adjacent to the lakeshore to about 30 m on the northern and eastern margins of the lake watershed. Water levels in a piezometer nest 15 m northwest of the lake showed, on August 20, 1978, an upward potentiometric gradient between confined sand and gravel lenses to overlying sandy, surficial till. This contrasts with a downward potentiometric gradient between the till units on the eastern margin of the watershed on the same date.

Spread of contaminants through multiaquifer wells in southeastern Minnesota

M. F. Hult reported that multiaquifer wells in southeastern Minnesota can permit water to flow from contaminated near-surface aquifers to underlying aquifers. In Fillmore County, a flow of 3.8 L/s was measured in a 150-m test well that connects the upper carbonate and the St. Peter aquifers. Geophysical logging of four abandoned wells that also connect the aquifers indicated that such wells are unstable because the intervening Middle Ordovician Decorah Shale tends to collapse. Partly cased or lined wells, such as the test well, however, can permit a sustained flow. The measured rate of flow was an order of magnitude less than that predicted on the basis of aquifer characteristics because entrainment of air and sediment in water moving down the well tends to plug the lower aquifer adjacent to the well bore.

Water-quality monitoring in Voyageurs National Park

Water samples were collected by G. A. Payne at 11 sites in three lakes in Voyageurs National Park, northeastern Minnesota, as part of a continuing monitoring program. Results of analyses of samples collected in March and August 1977 showed that water in the lakes was soft and dilute. Dissolved solids, however, were appreciably higher in Black Bay and Kabetogama Lake than in Rainy and Sand Point Lakes. Specific conductance ranged from 32 to 111 μmho/cm at 25°C. Differences in water quality were further shown by algal cell counts that ranged from 2,100 cells/mL in Rainy Lake to 210,000 cells/mL in Black Bay. Secchi-disk transparencies of 2.9 in Rainy Lake and 0.6 in Black Bay reflected the differences in cell count. Blue-green algae were the dominant phytoplankton in most of the samples.

Water quality established before highway construction

Seven lakes in the Minneapolis-St. Paul metropolitan area were sampled to determine water quality before construction of highways. According to G. A. Payne, results of measurements and chemical analyses showed that the lakes are shallow, unstratified, and nutrient enriched. Considerable seasonal variations in dissolved solids, nutrient, and dissolved oxygen concentration were observed. Oxygen depletion and high nutrient concentrations were characteristic conditions under ice cover in winter. Blue-green algal blooms typically occurred soon after ice breakup and persisted until late fall.

Two-dimensional model of the Buffalo aquifer

An evaluation of the water-supply potential of the western part of the Buffalo watershed in Clay and Wilkin Counties is being completed by R. J. Wolf. The aquifer is a major source of water for irrigation and for the city of Moorhead. The narrow elongated aquifer, 1.5 to 4 km wide and 48 km long, is roughly diamond shaped in cross section. Test drilling revealed that the aquifer is as thick as 60 m along the narrow troughlike bottom. This deep part of the aquifer is generally composed of highly permeable sand and gravel, and wells locally yield as much as 60 L/s. The aquifer is overlain by fine-grained glacial lake sediments and underlain by clayey till. Water is under both confined and unconfined conditions and, for the most part, is not directly connected hydraulically either to the Buffalo River or to the South Branch Buffalo River. Vertical hydraulic conductivity values from core samples of the overlying lake sediments range from 1.8×10^{-5} to 4.3×10^{-2} $(m^3/d)/m^2$. Analysis of the natural flow system, aided by a digital computer model, indicated that vertical leakage from the overlying sediments is important to the water-supply potential of the aquifer. Chemical analyses of water samples collected from 20 wells showed that the water is hard and mostly of the calcium-magnesium-bicarbonate and magnesium sulfate type. Specific conductance ranged from 500 to 2,300 μmho/cm at 25°C. Current development has not affected water levels significantly except locally near the pumping center in the northern part of the aquifer. The model will define present water levels and storage in the aquifer and predict the long-term response of the aquifer to selected proposed development patterns.

MINNESOTA AND WISCONSIN

Streamflow was measured and suspended-sediment samples were collected from March 1976 to September 1977 in Elim Creek, Skunk Creek below Elim Creek, and Deer Creek, which are tributaries to the Upper Nemadji River in northeastern Minnesota. E. G. Giacomini reported that annual mean discharged ranged from 0.012 to 0.108 m^3/s, and daily mean discharge ranged from 0 to 2,577 m^3/s. The daily mean suspended sediment concentration ranged from 0 to 2.400 mg/L, the daily mean suspended sediment load ranged from 0 to 824 t, and the suspended sediment yield ranged from 15 to 318 t/km^2. Observation of particle-sized distributions showed that suspended material during storms is 63 percent clay, 31 percent silt, and 6 percent sand. These data do not represent long-term trends because precipitation during this period was considerably below normal.

Water-quality data collected by G. A. Payne on Skunk and Deer Creeks, northeastern Minnesota, showed significant increases in concentrations of phosphorus, nitrogen, and bacteria in runoff water from spring snowmelt and summer storms. Small increases in discharge above base-flow conditions were concurrent with large increases in concentration of some constituents, particularly nitrogen and phosphorus. In contrast, during snowmelt runoff, dissolved solids were reduced by more than 50 percent to concentrations of 100 mg/L. Although both creeks are in the Red Clay area and have similar drainage areas, Deer Creek typically has 25 percent higher bicarbonate concentrations under low-flow conditions. A concentration of 0.01 g/L of the pesticide, *2,4,5*–T, was found in one water sample from Skunk Creek.

R. J. Wolf reported a potential for upward movement of ground water in the Skunk Creek valley in northeastern Minnesota. Vertical pressure differences, shown by a vertical flow section across the valley, indicated downward or lateral movement of ground water in upland areas and upward movement near the valley bottom. Therefore, fissures, joints, or slippage planes that extend below the water table in the area of upward ground-water movement could serve as avenues for ground water to wet and possibly lubricate slippage planes in the overlying clay in the slump areas. Hydrographs showed that the directions of ground-water flow may be reversed seasonally in response to recharge. In addition to movement from below, continuous water-level recorders showed that recharge from rainfall or snowmelt quickly reaches depths of 5.5 m in the red clay, thus wetting the slippage planes in the hillside slump areas from above.

NEW HAMPSHIRE

Ground-water resources of the Lamprey River basin

The principal aquifers in the Lamprey River basin are composed of glaciofluvial deposits. J. E. Cotton reported that in the lower part of the main river valley (downstream from the center of Epping) such aquifers commonly consist of small coarse-grained ice-contact deposits. Most of the main valley in this area is underlain by less productive fine-grained estuarine sediments associated with marine invasion during late glacial time. Within the Lamprey River valley upstream from the center of Epping

and in some tributary valleys, glaciofluvial sand and gravel beds offer the best potential for developing ground-water supplies. Such development would be slight in some areas, however, because of the relative thinness of the saturated section.

NEW JERSEY

Impact of land-use changes on water resources

According to T. V. Fusillo, suburban development of Winslow Cross affected surface- and ground-water resources of the area. Developing 25 percent of a 4.25-km^2 rural drainage area caused the peak discharge from a 4.3-cm 10-hour rainfall to increase from 0.48 m^3/s before development to 1.18 m^3/s after development. Installing a stormwater detention basin below the developed area reduced the peak discharge to 0.56 m^3/s for a 4.3-cm 12-hour storm.

Sediment loads increased significantly during construction but decreased to levels approaching preconstruction conditions after construction because of a stormwater detention basin.

BOD, total nitrogen, and total phosphorus loads were lower in streams draining developed basins, whereas concentrations of lead, dieldrin, and DDT in the bottom material were higher in developed basins.

Pumping did not seem to significantly affect water levels in the aquifer. Some degradation in ground-water quality was noted in the vicinity of the infiltration ponds of the sewage-treatment plant, where high nitrogen levels were found. A change in treatment, however, reduced the nitrogen level.

NEW YORK

The role of the unsaturated zone in artificial recharge

R. C. Prill, E. T. Oaksford, and J. E. Potori reported that ponding tests, where a tertiary-treated effluent was being recharged through unsaturated glacial deposits, showed that basin management can have considerable influence on the effectiveness of the unsaturated zone for polishing the effluent. When the basin was operated at infiltration rates between 0.7 and 1.4 m/h, the effluent moved through a 7-m unsaturated section essentially unaltered. When the basin was operated at rates between 0.05 and 0.20 m/h, significant changes occurred as the effluent moved through the system. The most noticeable change was the removal of suspended solids. During normal plant operation, when the content of suspended solids was between 5 and 15 mg/L, about half the solids were removed. When the content of suspended solids was higher because of inadequate plant performance, the proportion removed was also higher. Nitrogen measurements made when the ammonium content of the effluent was high showed that, except during winter, conversion to nitrate occurred as effluent moved through the unsaturated section. Tests showed that polio virus that was added to the effluent was almost completely removed.

Transducers in the unsaturated zone provided accurate measurements of pressure head for an operating temperature range of 4° to 30°C. The transducers, which are sensitive for a pressurehead range of ±750 mm of water, provided readings within ±10 mm of manometer readings.

Hydrogeology of artificial-recharge site

According to D. A. Aronson, information obtained by drilling numerous observation and injection wells at the Meadowbrook Artificial Recharge Project site in central Nassau County indicated that the upper glacial aquifer is thinner in this area than had been estimated. Color and textural differences among core samples indicated that the generally poorly defined Pleistocene-Cretaceous contact is clearly distinguishable at the site. Palynological and lithologic studies showed that the Pleistocene-Cretaceous boundary ranges from less than 18 m to more than 27 m in depth at the site.

Apparently, DO content of ground water does not vary significantly from the water table to a depth of 61 m, thus indicating that the upper Magothy aquifer is well oxygenated.

Pumping tests at four injection wells showed that the Pleistocene-Cretaceous deposits 20 to 30 m below land surface have a hydraulic conductivity of 0.85 m/d.

Transport of PCB's in the Hudson River

J. T. Turk and R. J. Archer reported that the transport of PCB's in the Hudson River was monitored at four sites. No PCB's (<0.1 ppb) were detected in water-column samples from the Glens Falls station, although PCB's were commonly detected at the three downstream stations. PCB concentrations varied substantially both with flow and river reach. Highest PCB concentrations (>1 ppb) were associated with high flows (approximately 10^6 L/s), and the lowest were associated with medium discharges of 2×10^5 to 6×10^5 L/s. In flows lower than 10^5 L/s at Schuylerville, Stillwater, and Waterford, PCB concentrations seemed to increase with flow, thereby indicating dilution of a relatively constant load.

OHIO

Subsurface mines as a water source

J. O. Helgesen and T. M. Crouch reported that a group of abandoned underground coal mines near Cambridge is being evaluated as a potential source of water for industrial use. These 13 mines comprise an area of 43 km^2, within which about half of the coal has been removed. The mines lie below local stream-base level and are flooded and under artesian pressure. A stream adjacent to the study area is the major discharge area for most water moving through the mines. Pumping tests helped to determine the degree of mine interconnection, hydraulic connection with streams, and water quality. A 29-day pumping test at 0.126 m^3/s in 40 observation wells showed interconnection of nine mines and drawdowns of about one-third of available artesian head. Water-level declines in wells completed in overlying and near-stream alluvium indicated some connection to the mines. Time-drawdown response of the mines showed no trend toward steady state.

Most water in the mines is of the sodium bicarbonate type. Dissolved solids concentrations ranged from 250 to 7,500 mg/L, and the pH of most samples was between 6.5 and 7.6. During the pumping test, specific conductance of the discharge increased steadily from 750 to 1,800 μmho/cm.

PENNSYLVANIA

Water-supply capability of shale in south-central Pennsylvania

A. E. Becher reported that a preliminary evaluation of data indicated a median yield of 1.9 L/s from wells in the Ordovician Martinsburg Shale of Franklin County. About 2 percent of the wells provide less water than is adequate for household needs, and more than 20 percent of the wells are capable of yielding in excess of 6.3 L/s. Water quality is good, although, locally, ground water contains large amounts of iron and manganese.

Low-flow frequency of ungaged streams

H. N. Flippo, Jr., used multiple regression methods to derive regional equations for estimating low-flow frequency characteristics on unregulated streams. A newly developed geologic index, which is a refinement of the infiltration index used by J. T. Armbruster (1976), permitted derivation of useful regression equations. For example, throughout 80 percent of Pennsylvania the 7-day, 10-year, low-flow discharge can be estimated by means of regional equations that have standard regression errors of less than 40 percent. The other independent variables in the equations are drainage area and precipitation.

VERMONT

Ground-water quality

According to R. E. Willey, results of an investigation of ground-water quality and pollution problems in Vermont indicated that potable water can be obtained almost anywhere in the State. Natural ground-water quality problems included objectionable concentration of hardness, iron or manganese, sulfur taste or smell, and, rarely, dissolved gases. Instances of iron or manganese exceeding recommended Vermont State Health Department limits were widespread and not unusual.

Ground-water quality problems resulting from man's activities seemed to be scattered and site-specific. Some of the problems were excessive concentrations of bacteriologic agents, sodium or chloride, nitrate, and toxic or hazardous materials. Among the principal causes of these problems were (1) improper well construction or spring improvement, (2) inadequate isolation of water-supply sources, (3) excessive or improper use or storage of highway deicing materials, (4) inadequate design of waste-disposal facilities, and (5) improper handling or accidental spilling of toxic or hazardous materials.

VIRGINIA

Ground-water reconnaissance of the Blue Ridge Parkway

H. T. Hopkins began a reconnaissance of the geohydrology along the Blue Ridge Parkway in western Virginia. Springs along the parkway occur at the contact of saprolite with underlying bedrock, yields ranged from <0.1 to >1.3 L/s, and dissolved solids were generally <75 mg/L. Well yields ranged from <0.3 to >1.6 L/s. The highest yields were from drilled wells generally <91 m deep in small valleys. Water moves primarily along joints and fractures in the underlying rocks.

Chemical quality of ground water in Fairfax County

Results of a study by J. D. Larson (1978) indicated that ground water in Fairfax County is generally of good chemical quality. Three geologic provinces are tapped: coastal plain sediments, Piedmont crystalline rocks, and Triassic sedimentary rocks. Water quality was marginal in two areas; an area in the Coastal Plain sediments had sodium chloride concentrations of more than 250 mg/L, and

an area of Triassic sedimentary rocks had sulfate concentrations of more than 250 mg/L. Data obtained from the Triassic rock area indicated that water of marginal quality is found only in wells >200 m deep. Isolated areas of Piedmont rocks and Coastal Plain sediments contained water with iron concentrations large enough to stain laundry and utensils.

Potentiometric surface of Cretaceous aquifer, Atlantic Coastal Plain

J. F. Harsh and H. T. Hopkins reported that water levels in wells penetrating the undifferentiated Cretaceous aquifer in the coastal plain of Virginia were measured in January and February 1978. At that time, water levels ranged from 56 m below sea level at Franklin in Southampton County to 18 m above sea level near the Fall Line. Water levels in the area have been declining for many years as a result of a gradual increase in withdrawals for municipal and industrial use. The principal industrial development is in the Franklin-Smithfield-West Point area where withdrawals averaged 1.6 m^3/s in 1977.

Relation of highway construction to water quality

Interstate Highway 77 is being constructed through the drainage basin above the Wytheville National Fish Hatchery. Boiling Spring and West Spring supply all of the water used by the hatchery, and any degradation of quality or supply would jeopardize the operation. W. E. Hendrick, Jr., reported that continuous recorders were used to monitor the flow and turbidity of the two springs, and water-quality samples are being collected four times per year during construction. In addition, the flow of Glade Creek, which is crossed by the highway, is being measured. Preliminary analyses showed no effect from construction on the quality or quantity of water from the two springs.

Ground-water resources, James City County

According to J. F. Harsh, coastal plain sediments were investigated as a possible alternate source of water supply to surface-water sources in James City County, Virginia. Subsurface correlation indicated that these sediments can be separated into four water-yielding units that range in age from Quaternary to Cretaceous or older (P. M. Brown, J. A. Miller, and F. M. Swain, 1972). These aquifers are hydraulically interconnected to some extent and comprise a leaky aquifer system. The most productive and consistent source of water is the undifferentiated Cretaceous aquifer.

In June and July 1978, when ground-water withdrawals were high, water levels in the undifferentiated Cretaceous aquifer were below sea level in about half of the county; water levels ranged from 42 m below sea level at Williamsburg in the southern part to 6 m below sea level in the northwestern part.

WISCONSIN

Hydrology of the Mole Lake Indian Reservation area in Forest County

R. A. Lidwin is studying the Mole Lake Indian Reservation area in Forest County, Wisconsin, to determine effects of developing a large copper-zinc deposit. Nearby water sources may be contaminated from mining and processing the deposit.

Both quantity and quality of surface and ground water are being studied, especially Swamp Creek and Rice Lake because they are most likely to be affected by development. The benthic macroinvertebrate and periphytic diatom communities of Swamp Creek are being studied as is the aquatic vegetation of Rice Lake, with particular emphasis on wild rice. The dominant macrophyte in Rice Lake is wild rice *(Zizania aquatica)*, and water lilies (*Nymphaeacea*) and pondweeds (*Potamogeton zosteriformis*) are abundant.

Contamination potential of the Silurian dolomite aquifer in eastern Wisconsin

Several parts of Wisconsin's 14-county area bordering Lake Michigan have a potential for contaminating the Silurian dolomite aquifer, according to M. G. Sherrill (1979). Much of the water supply for the area is from the Silurian dolomite aquifer. Most water movement in the rocks is through interconnected joints and solution zones. Because of the rapidity of its movement, water in the aquifer is susceptible to contamination by water percolating downward from the surface. It is most susceptible where the aquifer is jointed at or near the land surface, where it is overlain by a relatively thin cover of very permeable material or where the water table is close to the land surface.

Wisconsin wetlands affect streamflow and sediment yields

According to R. P. Novitzki, analyses of streamflow characteristics in Wisconsin river basins with different percentages of lake and wetland area indicated that peak flood flows are 80 percent lower, springtime streamflow is 40 percent higher, and fall

baseflow is 40 percent lower in basins with 40-percent lake and wetland area than in basins with no lake or wetland area. Sediment yields in the north-central third of the State are also 90 percent lower in basins with 40-percent lake and wetland area than in basins with no lake and wetland area.

Wisconsin's wetlands occur in depressions and on slopes and may be in contact with ground water, or they may be totally surface-water supported. Depression wetlands retain water, but slope wetlands allow water to drain away. Ground-water wetlands may receive continuous ground-water inflow, but surface-water wetlands receive sporadic inflow. The plant community reflects the various hydrologic characteristics of differing wetland sites. This conclusion is based on data on 14 wetland study sites, supplemented by data on another 219 wetlands.

SOUTHEASTERN REGION

Throughout the southeastern region, the collection of hydrologic data and the pursuit of problem-oriented projects, especially those related to the environment, continued during the past year. A regional study of the Tertiary southeastern limestone aquifer, a major source of ground water in the region, got under way.

A procedure for relating streamflow depletion to geology led to the development of regression equations for estimating the 7-day, 2-year and 7-day, 10-year low flows of Alabama streams. The equations should be of great value in determining streamflow available for water supply and dilution of effluent discharged to streams.

Saltwater encroachment into coastal aquifers is a problem in many coastal areas of the Southeast. In Florida, surface electrical resistivity surveys proved to be a valuable tool in determining the approximate position of the freshwater-saltwater interface in shallow coastal aquifers.

Crystalline rocks of the Piedmont of Georgia have long been considered poor sources of ground water. However, ongoing studies, using downhole sonic-televiewer pictures, have shown that large low-angle fractures 70 to 200 mm in height are present in the crystalline rocks. Tests of wells indicated that the fractures are extensive laterally and will yield as much as 30 L/s.

Clearing of swampland for large-scale agriculture is still underway on the Albermarle-Pamlico Peninsula of North Carolina. Major changes in water quality have been observed in runoff from land that was formerly swampland but that is now under cultivation.

In North Carolina, the data on the State's observation well network of 460 coastal plain wells were reviewed. Nearly 30 percent of the wells did not provide water-level data of sufficient accuracy to meet the needs of the program. The review also showed that data from 20 percent of the wells was redundant and that less frequent measurements of 40 percent of the wells would still provide adequate water-level data for evaluation. The evaluation has enabled North Carolina to expand the network coverage with less manpower .

ALABAMA

Regionalization of low flow in Alabama streams

A procedure for relating geology to low flow in Alabama streams resulted in the development of regression equations for estimating the 7-day, 2-year and 7-day, 10-year low flows. The relation of geology to low flow was described at continuous record gaging stations by the number of days required for one log cycle of streamflow depletion, according to R. H. Bingham (1979). These streamflow recession indexes, in days per log cycle, were compared with lithology, and areas with similar features were delineated on a regional basis Statewide. The standard error of estimate is 40 percent for the 7-day, 2-year low-flow equation and 44 percent for the 7-day, 10-year low-flow equation using a streamflow recession index, drainage area, and mean annual precipitation as independent variables. Each equation applies Statewide to all natural flow streams; the equations do not apply to streams where flow is significantly altered by activities of man.

FLORIDA

Hydrologic resources of the Ochlockonee River basin area

An investigation conducted by C. A. Pascale and J. R. Wagner showed that the Ochlockonee River basin area of northwestern Florida receives an average of 1,450 mm/yr of rainfall. Much of the rainfall that is not lost to evaporation enters the surficial sand aquifer and seeps to streams or enters the water-bearing zone of the upper confining unit and the Floridan aquifer. The water-bearing zone of the upper confining unit is important for rural domestic supplies, storage of water, and recharge to the Floridan aquifer, which is the principal source of municipal supplies.

The potentiometric surface of the upper part of the Floridan aquifer was about 15 m higher in southwestern Gadsden County and about 3 m higher in southeastern Gadsden County than the potentiometric surfaces of the middle and lower parts of the aquifer in these respective areas. Saline water occurs at relatively shallow depths within the Floridan aquifer and ground-water quality (C. A. Pascale, J. R. Wagner, and J. E. Sohm, 1978) generally deteriorates with depth and duration of pumping.

Average daily stream discharge is about 3.8×10^6 m^3. Stream discharge diminishes quickly during periods of drought, and streams are not reliable sources of water without storage. The chemical quality of the water in most streams is acceptable for most uses.

Surface resistivity used to locate the saltwater-freshwater interface

An electrical resistivity survey was conducted by J. D. Fretwall in the springs area of western Citrus County, as part of a saltwater-freshwater interface study encompassing most of coastal southwestern Florida. Results of the survey correlated well with available hydrologic data. Depths to the interface, based on measurements at electrical sounding sites, were found to be similar to depths obtained from nearby chloride monitor wells and by applying the Ghyben-Herzberg principal. On the basis of this study, Fretwell concluded that surface electrical resistivity measurements can provide information on the most beneficial placement of monitor wells and can be used to establish a baseline from which movement of an interface can be detected.

Water availability in St. Johns County

A study to provide information on the availability of potable water from the shallow-aquifer system in St. Johns County is being conducted by the USGS in cooperation with St. Johns County. According to E. C. Hayes, preliminary data from test wells drilled at three locations indicated that the aquifers and confining beds are discontinuous. Aquifers in test wells drilled to the top of the Miocene Hawthorn Formation (approximately 30 m) were located at depths ranging from 7 to 20 m. Yields to wells ranged from 24.5 to 229 m^3/d. Information from the test wells indicated that a possible source of good-quality water adequate for public supply occurs in the vicinity of Tillman Ridge.

Potential of contamination increased by ground-water pumpage in Lee County

F. A. Watkins reported that preliminary maps of the potentiometric surface of the lower and upper water-bearing units of the Hawthorn Formation showed that there is a potential for upward movement of saline water from the lower bearing unit into the upper freshwater-bearing unit. Under natural or relatively undisturbed conditions, there is a head differential of about 6 m; but in areas where the upper water-bearing unit is heavily pumped, the upward potential may be increased to as much as 30 m of head. Thus, the potential for upward movement of saline water and the contamination of freshwater is greatest where pumpage is greatest.

Test well probes hydrogeology beneath Tampa Bay

An observation well was drilled in Hillsborough Bay near Tampa to determine whether freshwater existed in the aquifer beneath the bay and to determine the head relation between the aquifer and the bay. The well was finished in the Oligocene Suwannee Limestone at a depth of 54 m. Seven specific capacity tests, conducted by W. C. Sinclair during and after construction, indicated that the lower section of Miocene Tampa Limestone (between depths of 21 and 40 m) is relatively impermeable, whereas the upper part of the Tampa and the part of the underlying Suwannee Limestone penetrated are relatively permeable. Chloride concentration of water from the Tampa and Suwannee Limestones is about 16,000 mg/L, about the same as the average concentration of chloride of Tampa Bay water at the site. A recorder installed on the well indicated that the water level in the well responds to tidal loading in synchronization with the tide gage at McKay Bay, but with only 35 percent of the magnitude of tidal fluctuation. Water level, corrected for density, was about one-tenth of a meter below mean sea level.

Water quality of the Hillsborough River

The effect of point sources of pollutants on the water quality of the Hillsborough River is being assessed by using a USGS water-quality model. According to C. L. Goetz, results of water-quality sampling showed that three waste sources having 5-day BOD of 15 mg/L, 2 mg/L, and 2 mg/L can be easily assimilated by the river. The average stream BOD is 0.6 mg/L. A potential water-quality problem in the Hillsborough River is the introduction of ammonia-rich wastewater. However, the

quantity of wastewater currently is small, and the stream is able to quickly convert the ammonia to nitrate and to eventually remove the nitrate through natural processes. The forward reaction rate for conversion of ammonia to nitrate was found to be very high (about 7). Runoff from urban areas has caused increased BOD, organic nitrogen, and total organic carbon concentrations and decreased sulfate concentrations.

Leaky confined conditions at Pensacola well

According to Henry Trapp, Jr., a test of Pensacola's Dunaway well indicated that the main producing zone of the sand-and-gravel aquifer acts as a leaky confined aquifer under prolonged pumping. The test was begun March 30, 1978, and measurements continued through July 10, 1978, with the Dunaway well pumping 0.11 to 0.13 m^3/s. The cone of depression reached an observation well 2.01 km away within 1 day, and reached steady-state conditions in 8 to 12 days. An observation well 79 m from the pumped well and in the same zone had about 4.7 m of drawdown, while a twinned shallow well had >0.3 m drawdown. Calculated values of transmissivity clustered around 1,100 m^2/d, storage coefficent was 5×10^{-5} to 3×10^{-4}, and vertical hydraulic conductivity of the confining bed was about .003 m/d. The test confirmed conclusions drawn from monthly observation well data.

Geohydrological assessment of a landfill in Pinellas County

A Pinellas County landfill is located about 3 km west of old Tampa Bay on a flat coastal area with a high water table. Mario Fernandez, Jr., reported that the area is underlain by three types of sediments: (1) A surficial layer of fine to very fine sand and shell, about 6 m thick, (2) a marl or calcareous clay bed, about 3 m thick, and (3) a bluish-gray to blue-green clay, about 14 m thick. These sediments and the underlying limestone form three geohydrologic units: a 6-m-thick surficial aquifer composed of the fine-sand shell, a 17-m-thick confining bed composed of marl and clay, and the Floridan aquifer composed of limestone and containing about 55 m of freshwater.

The rate of downward migration of leachate from the landfill through the confining bed is about 1 mm/yr, thus precluding probable danger of Florida aquifer contamination. Quality of water from a Floridan aquifer well located within the landfill was similar to that of wells drilled into the same strata 16 km to the west, thus indicating that little or no vertical migration of leachate has occurred. Wells located downgradient from the landfill indicate that leachate is moving away from the site through the surficial aquifer. Peaks in graphs of specific conductance, chloride, ammonia-nitrogen, and COD, and a flow-rate analysis indicated the possibility of slug-flow of leachate from the trenches.

Water quality of the Floridan aquifer, Manatee County

Water in the Floridan aquifer in Manatee County is generally more mineralized than water from the surficial or minor artesian aquifers, according to D. P. Brown. Also, the mineral content of ground water generally increases with depth and increases from the northeastern part of the county toward the west (coastal area) and south.

Concentrations of total dissolved solids range from about 300 mg/L in the northeastern part of the county to about 2,500 mg/L in the western (coastal) part. Concentrations of chloride are less 250 mg/L except near the coast, where saltwater intrusion has occurred. In eastern and southeastern Manatee County, concentrations of chloride are generally less than 50 mg/L. Concentrations of sulfate range from about 5 to 900 mg/L, generally increasing with depth and increasing from the northeastern part of the county toward the west and south. Relatively high concentrations of sulfate (more than 250 mg/L) occur in the western and southern parts of the county.

Deep cavernous zone in the Floridan aquifer

During test drilling at Jacksonville, a 24-m cavity in the deep zone of the Floridan aquifer was encountered. According to G. W. Leve, the cavity was first penetrated at a depth of 215 m below sea level in the Eocene Lake City Limestone and extended to a depth of 239 m. The lateral extent of the cavity was too large to be determined by downhole logging and television traverses. Smaller cavities have been recorded at about the same depth in other wells in Jacksonville, which is an indication of a relatively extensive cavernous zone in the aquifer.

Saltwater intrusion in the city of Cape Coral

D. J. Fitzpatrick used ground-water quality analyses and domestic well inventories in the city of Cape Coral to locate areas of saltwater intrusion in the upper part of the Hawthorn Formation. A major source of this saltwater contamination in areas adjacent to tidal water bodies is from the

downward leakage of saline water from the water-table aquifer through improperly sealed or corroded well casings (D. H. Boggess, T. M. Missimer, and T. H. O'Donnell, 1977).

Water analyses from an observation well network tapping the upper Hawthorn aquifer showed dissolved solids concentrations ranging from 381 to 2,400 mg/L. The chloride concentration of the water ranged from 80 to 1,100 mg/L. Most of the high chloride concentrations occurred in observation wells in the western and southern parts of Cape Coral.

Over half of the 350 domestic wells inventoried in Cape Coral yielded water with chloride concentrations of more than 250 mg/L, which is the maximum acceptable limit of chlorides in drinking water.

Water quality in Everglades National Park

An analysis of water-quality conditions in Everglades National Park between 1959 and 1977 showed marked seasonal changes for most chemical and physical parameters. According to B. G. Waller, these changes were due to evapotranspiration of ponded water, changes in the redox potential at the water-sediment interface, and an increase in metabolic activities in a smaller volume of water during the dry season (November to May). During the remainder of the year, most of the parameters stabilized throughout the system. Long-term increases in concentrations of major inorganic ions, total dissolved solids, iron, and color in the Shark River Slough were attributed to changing water-management practices to the north of the park. Low concentrations of residues of chlorinated hydrocarbon insecticides were detected in bottom material at every sampling station in the park. The quality of water in Taylor Slough and the Big Cypress Swamp had not changed since sampling began.

Sewage-effluent disposal by spray irrigation

Long-term hydrologic effects of sewage-effluent spraying by the city of Tallahassee were studied by L. J. Slack (1975) and, more recently, by M. C. Yurewicz. Secondary treated sewage effluent has been applied at varying rates on sandy soil since 1966 at the Thomas P. Smith Wastewater Renovation Plant, southwest of Tallahassee. In December 1977, the spray-irrigation field was increased from 16.2 ha to 49.8 ha. In February 1978, spraying was abated during installation of a sprinkler network. Water from a well open to the upper Floridan aquifer in the spray field subsequently exhibited an approximately 62-percent decrease in nitrate nitrogen, along with decreases in specific conductance, sodium, and chloride.

Water samples collected from selected wells in March, August, and September 1978 indicated that the ground-water quality does not exceed the maximum contaminant level for inorganic chemicals as established by EPA for the National Interim Primary Drinking Water Regulations. Analyses of ground-water samples showed no detectable amounts of the organochlorine insecticides, PCN, and PCB.

Natural sulfate contamination of the Santa Fe River

J. D. Hunn (1978) reported that sulfate concentrations in the Santa Fe River near High Springs are above the average for Florida streams. The sulfate source is natural discharge of ground water from the Floridan aquifer. The Santa Fe River, under average- and low-flow conditions, goes underground at O'Leno State Park and emerges near High Springs, about 5 km downstream, gaining both in discharge and sulfate concentration. During a low-flow period in April 1977, river discharge at O'Leno State Park was 3.6 m^3/s, with a sulfate concentration of 30 mg/L. The discharge of the river emerging near High Springs was 8.1 m^3/s with a sulfate concentration of 70 mg/L.

The Biscayne aquifer

The Biscayne aquifer of southeastern Florida is one of the most productive aquifers in the United States, but, because of its shallow depth and proximity to the sea, it is susceptible to pollution from surface sources and to encroachment of seawater. According to Howard Klein and J. E. Hull (1978), pollutants can enter the Biscayne aquifer by direct infiltration from the land surface or controlled canals, septic tanks or other drain fields, drainage wells, and solid waste dumps. Pollutants usually are found only in the upper 10 m of the aquifer as dilution, dispersion, and adsorption tend to reduce concentrations.

The Miami-Dade Water and Sewage Authority has proposed developing of the Three Square Mile well field several kilometers inland of Miami to avoid the danger of saltwater encroachment. Klein and R. A. Miller reported that a digital model of the proposed well field showed that if a line of 15 wells spaced 215 m apart in the Biscayne aquifer were pumped at a total rate of 6.5 m^3/s, the water-level drawdown at the center of pumpage would be about 4 m after 210 days assuming no recharge from rainfall or infiltration of water from canals.

Water loss in the flood diversion link between the Hillsborough River and the Tampa Bypass Canal

The first flood-diversion link between the Hillsborough River and the Tampa Bypass Canal was completed in late 1978 when the earthen dam plug between Structure *S*–161 and the river was removed to allow flood waters to be diverted from flood-prone urban Tampa areas. During excavation of the plug, S. E. Henderson determined that water from the river entered the underlying Floridan aquifer through a confining bed breach caused by canal excavation. Henderson's investigation showed that there was no return flow from the aquifer to the canal below Structure *S*–161. Although water is lost to the aquifer, there should be no significant losses of river water to the sea when water levels in the canal above Structure *S*–161 are maintained at river level.

Shallow aquifers replacing deep artesian aquifers as Hendry County water supply

Hydrologic studies in Hendry County in the mid-1950's showed that deep artesian wells producing poor-quality water from the Floridan aquifer provided a large part of the ground water used in the area (Klein, Schroeder, and Lichtler, 1963). According to J. E. Fish, Carmen Causaras, and T. H. O'Donnell, test drilling and a recent well inventory showed that shallow aquifers are now used extensively; 77 percent of the known wells currently in use have depths of no more than 30 m. Many deep artesian wells have been plugged or are seldom used. The shallow aquifers usually contain good-quality water. However, in the northwestern part of the county where the poor-quality Floridan aquifer had been used extensively, the water-table aquifer was badly contaminated.

GEORGIA

Water-bearing openings in crystalline rocks found to be horizontal fractures

As part of a ground-water investigation of the greater Atlanta region, C. W. Cressler and C. J. Thurmond are studying the nature of water-bearing openings in crystalline rocks. Sonic televiewer pictures of well bores showed that water enters high-yielding wells from horizontal or nearly horizontal fractures 70 to 200 mm in height. This contradicts the general belief that wells in crystalline rocks obtain water from steeply inclined fractures and openings along joint and foliation planes that are recharged by water stored in saprolite near a well. Many high-yielding wells on hills, ridges, and steep slopes in the study area appear to have only low-yield potential. During drilling, these wells characteristically remained dry at 90- to 215-m depths, well below the floors of adjacent valleys. Yields of 2.5 to 30 L/s can be obtained from one or two horizontal openings several centimeters in height, thus indicating that the water-bearing openings are low-angle fractures similar to those observed on the televiewer. Wells commonly are hundreds of meters from valleys or other likely sources of recharge, which indicates that the fractures have wide areal extent and are independent of local topography.

Saltwater encroachment in a carbonate aquifer system at Brunswick

Ground water is being pumped at a rate of about 400,000 m^3/d from a carbonate aquifer system of Tertiary age in Brunswick. The resulting decline in artesian pressure has led to saltwater encroachment, according to H. E. Gill, G. D. Mitchell, and Robert Bisdorf. Contamination of the aquifer by saltwater was first reported in 1939, but the source of the saltwater was uncertain.

An 830-m test well on Colonels Island near Brunswick indicated that the primary source of intruding saltwater is the lower part of the Tertiary carbonate sequence. The freshwater-saltwater interface occurs in a cavernous zone between depths of 655 and 658 m, below which chloride concentrations increase to a maxium of 20,000 mg/L at a depth of 830 m. The decline in artesian head resulting from heavy pumpage allows saltwater from the lower zones to migrate upward through solution-enlarged fractures from cavernous zones in the carbonate sequence.

Direct-current surface resistivity studies conducted in the Brunswick area also indicated that the source of saltwater is the lower part of the Tertiary carbonate sequence. Vertical electrical soundings at 80 stations were effective in locating the top of the carbonate system and in delineating the zones of saltwater to depths of 1,000 m.

NORTH CAROLINA

Chemical characteristics of unpolluted streams

C. E. Simmons used stream-quality data collected periodically at 59 small streams in North Carolina to define the chemical characteristics of unpolluted streams during periods of extreme low flow and storm runoff. The streams have drainage areas ranging from 0.8 to 44 km^2, they have no known

point sources of pollution, and they are generally representative of baseline conditions. Many of the study basins are almost totally forested. During periods of low flow, concentrations of most major dissolved constituents were at maximum levels and appeared to be directly related to geochemical characteristics of the stream basins. Major dissolved constituents were generally at minimum concentrations during the height of stormflow, and in some instances the quality of the streamwater approached that of precipitation. In the State's Coastal Plain region, concentrations of dissolved solids during low flows were often 5 or more times greater than those during stormflow. Levels of nitrogen and phosphorus increased slightly during stormflow but remained relatively constant in most streams regardless of flow conditions. Mean concentrations of total nitrogen ranged from about 0.2 to 0.6 mg/L, and total phosphorus ranged from 0.01 to 0.03 mg/L. Concentrations of minor elements were well below maximum levels recommended for drinking water.

Hydrology of Chicod Creek basin

Extensive channelization of the Chicod Creek basin, a 155-km^2 watershed in the central Coastal Plain region of eastern North Carolina, is scheduled to begin in 1980. C. E. Simmons used data from four stream and eight observation well sites, in operation since 1976, to define hydrologic characteristics of the basin prior to channel construction.

Water-quality analyses showed that during base runoff, concentrations of major dissolved constituents in surface water were in close agreement with values obtained from shallow wells, thereby indicating that the surficial aquifer was the major source of base runoff. Concentrations of Kjeldahl nitrogen, total nitrogen, and total phosphorus in Chicod Creek were at least five times greater than levels determined for baseline streams in undeveloped basins nearby. The high nutrient levels appeared to be related directly to farming, poultry, and livestock activities in the basin. Small amounts of DDT and dieldrin (0.01 and 0.02 μg/L, respectively) were found in stormflows; however, no pesticides were detected in low flows. Maximum concentrations of minor elements occurred during stormflows but did not exceed maximum limits recommended for drinking water.

Hydrologic effects of land clearing and drainage, Albemarle-Pamlico Peninsula

A cooperative study with the North Carolina Department of Natural Resources and Community Development is underway to determine the hydrologic effects of land clearing and drainage on the 5,200-km^2 Albemarle-Pamlico Peninsula in eastern North Carolina. The rapid development of the peninsula provides an opportunity to compare the hydrology of cleared and uncleared areas and to observe changes in hydrologic characteristics and water quality during the conversion of areas from their natural state to their ultimate developed state.

A 120-km^2 area of swamp forest that was cleared and is now being intensivly farmed is being monitored for water quality and discharge. The data are to be compared with data from two uncleared swamp areas.

According to C. C. Daniel III, water from the swamp areas is characteristically dark brown, low in nutrients and dissolved solids, and quite acid; pH values as low as 2.5 were measured during 1978. Specific conductance of the swamp water is usually less than 150 μmho and averages about 70 μmho. On the other hand, pH of the water from farmlands is usually around 6.5, and specific conductance during 1978 ranged from 125 to 550 μmho. The higher specific conductance values were observed near the end of a protracted dry period in late fall. The farm-drainage water at that time was a calcium–magnesium–bicarbonate type and was probably influenced by agricultural lime applied to the acidic organic soils.

Freshwater availability on offshore barrier islands

Fresh ground water in the Cape Lookout National Seashore occurs in an unconfined aquifer, in an upper confined aquifer, and in a lower confined aquifer. The freshwater lenses in the unconfined aquifer are subject to periodic saltwater contamination by overwash during storms, and periods ranging from weeks to months are needed to reestablish the freshwater lens, depending on the amount of rainfall, according to M. D. Winner, Jr. (1978). The best places to develop freshwater from the unconfined aquifer are in the high dunes of Shackleford Banks and at Cape Lookout where overwash rarely occurs. The upper confined aquifer is known to contain freshwater only in the vicinity of Drum Inlet, whereas all of the lower confined aquifer south of Drum Inlet contains freshwater. Freshwater yields of as much as 32 L/s are available from individual wells tapping the lower confined aquifer.

Water-level measurements in observation wells

According to M. D. Winner, Jr., a review of records of approximately 460 coastal plain wells of

the federally and State-operated observation well networks in North Carolina indicated that nearly 30 percent of the observation wells were not providing water-level data of sufficient accuracy to warrant their continuation in the network; a little more than 20 percent of the wells provided good data, but those data were redundant. Less frequent measurement of almost 40 percent of the wells would still provide data adequate for the network objectives. Winner found that the network in the coastal plain area had a number of gaps in coverage for some aquifers. Additional observation wells were proposed for those areas.

TENNESSEE

Channel characteristics identify losing stream reaches

E. F. Hollyday and P. L. Goddard reported that attempts to locate high-yield wells in carbonate regions in Tennessee were most successful when wells were drilled near losing stream reaches. (A losing stream reach is one whose channel is above a water table.) During seasons of high precipitation, overland runoff can cause a losing stream reach to appear to have a base-flow component; therefore, channel characteristics rather than a sequence of discharge measurements should be used to identify losing reaches.

Investigations showed that, in carbonate regions of Tennessee, the channels of losing stream reaches are characterized by banks that are steep and higher than the streambed is wide large amounts of flood trash in the center of the channel, tightly compacted and poorly sorted bed and bank material, and trees or grass in the center of the channel. On the other hand, streams with a base-flow component have gently sloping grassy banks, very little visible flood trash in the channel, and sorted loose bed and bank material.

Locating successful well sites in Jefferson County

E. F. Hollyday and P. L. Goddard found that usable ground water in quantities as great as 13 L/s per well was available from carbonate rocks that discharged to four large springs in Jefferson County. Water occurring in the study area flows across strike from topographic highs in the northwest to lows in the southeast through solution openings along bedding planes and joints. This flow is intercepted by beds of high permeability in the middle of the Cambrian and Ordovician Knox Group and is routed along strike to springs.

At Riley Spring, the average production of four wells was 6 L/s. More than half of the section is limestone; the rest is dolomite and dolomite-cemented quartz siltstone. Water-bearing zones occur as deep as 120 m. An aquifer test revealed a no-flow boundary and no communication between the wells and the spring. Three test holes at Moore's Spring encountered only mud and solid rock in a sinkhole trending across both the flow of water and strike of the rock.

The most productive wells are near a large spring, near a dry stream, and near the Copper Ridge Dolomite-Chepultepec Dolomite contact in the Knox Group.

CENTRAL REGION

Hydrologic activities in the central region in 1978 strongly emphasized studies related to energy development. Establish programs for the collection and publication of diverse water-resources data continued. Intensive hydrologic investigations related to coal development continued in Colorado, Montana, New Mexico, North Dakota, Oklahoma, Utah, and Wyoming and were begun in coal areas of Kansas and Missouri; studies related to oil shale in Colorado, Utah, and Wyoming continued at a reduced level of intensity. Water-resource studies of uranium-mining areas of New Mexico were continued. Hydrologic studies of small basins that are representative of potential surface coal mining areas were given continuing attention. Results of these studies are expected to be applied to leasing decisions, environment impact statements, mining plan formulation, and specifications for reclamation of mining areas.

An investigation of special significance to coal development is an evaluation of the water-yielding potential of the Mississippian Madison Limestone—an important deeply buried aquifer underlying large areas in the Powder River basin in Montana, North Dakota, South Dakota, and Wyoming. The third deep exploratory well was drilled through the Madison Limestone, and hydraulic testing was completed.

Digital model analyses are being used for coal and oil shale areas where surface-water supplies are inadequate; the models evaluate availability of ground water and indicate impacts of accelerated energy production on future water resources of the mining areas. A preliminary model analysis was made of potentially available water from deep and intermediate-depth aquifers in the Missouri River basin,

and productivity of wells that might tap those sources for supplementing surface-water supplies during early years of accelerated energy production.

Central region research activities continued to be varied and complex. Sediment research in the central region is directed toward surface mining effects, channel changes, bedload transport and sampling, and estuarine sediment movement. Estuarine studies are being made on both the Pacific and Atlantic coasts. Particular emphasis is being placed on sediment transport and geomorphologic processes. An intensive historical study of channel changes in the Platte River of Nebraska was undertaken to aid in the management of a section of the river as habitat for the sandhill crane and the whooping crane. In the East Fork River of Wyoming, an intensive multidiscipline sediment study is underway to evaluate channel changes, sediment transport, and bedload movement as these factors are affected by spring runoff.

Chemical and geochemical studies in the central region included a geochemical survey of water in coalfields, organic determination and definition of waters from oil shale retorting, studies of organic polyelectrolites, and the removal of dissolved organic material by use of selective resins. Such work is a continuation of studies to determine the types and quantities of organic materials in natural waters. Organic fouling of reverse-osmosis membranes used in the desalting process is being investigated. Geochemical kinetic studies, modeling of the chemical changes of water, and transuranium research studies also are underway.

At the Nevada Test Site, intensive investigations of the feasibility of high-level radioactive waste disposal continued. Also, studies in the Paradox Basin of Colorado and Utah to determine the hydrologic conditions that might affect the use of the deeply buried evaporites for waste disposal and related studies in deep evaporite deposit basins of New Mexico and salt dome provinces of Louisiana and Texas continued.

Methods development for laboratory and field application as well as for increased sensitivity has become a new research endeavor in the central region. Present emphasis is on the analysis of metals and organic compounds, including pesticides.

Hydraulic modeling continued to be a major factor in central region research. Studies of the relation of lakes to ground water are underway in Connecticut and Minnesota, and other sites are being evaluated for possible inclusion in the study. Precipitation-runoff modeling research, initially aimed at predicting the effects of surface mining, have received increased emphasis. Work continued in the development of modeling techniques for the prediction of solute transport in ground water and of modified runoff and sediment transport from areas undergoing surface mining in several hydrologic regimes. Development of techniques also continued for estimating numerical values for parameters and boundary-condition values for ground-water systems and research in sediment transport, channel-geometry changes, and fluvial processes.

Studies of artificial recharge to aquifers by spreading ponds continued in El Paso County, Colorado and near Lubbock, Tex. An investigation of the feasibility of artificial recharge to an alluvial aquifer by means of naturally filtered river water in an injection well continued in south-central Nebraska.

Studies of regional aquifer systems continued in the Madison Limestone and associated deep aquifer systems in the northern Great Plains of Montana, North Dakota, South Dakota, and Wyoming, and in the High Plains Tertiary Ogallala aquifer and associated systems of Colorado, Kansas, Nebraska, New Mexico, Oklahoma, South Dakota, Texas, and Wyoming. Also, a study of southwestern alluvial basins in New Mexico and adjacent parts of Colorado and Texas was started. In all of these areas, aquifer system boundaries and characteristics are being intensively studied to determine storage capacity and natural discharge and withdrawals, sources and amounts of recharge, anticipated yields of wells, and effects of pumping on supplies and water quality. The studies will also determine the history of past ground-water development and the effect on the aquifer of future development under various assumptions as to rates and points of withdrawal. Mathematical models of the flow system in the northern Great Plains are being prepared.

Field investigations of the hydrology of geothermal systems are continuing in Colorado and Montana. Also, development and testing of instruments, tools, and interpretative techniques for use in the extreme heat of geothermal systems and in possible areas suitable for deep disposal of radioactive and chemical wastes is continuing.

Intensive water-quality studies continued in the coal areas of the central region, especially in parts of Colorado, Montana, New Mexico, North Dakota, Utah, and Wyoming. A study in the Tongue River drainage of Montana focused on interpretation of water-quality data from a short-term data base; chemical, physical, and biological data were collected and interpreted. In other States, attempts are being

made to predict how ground- and surface-water systems will have been affected after mining activities have ceased.

Lake studies were broadened to include modeling of phosphorus in several reservoirs in Colorado. In addition, a nutrient-primary productivity study is underway in Koocanusa Reservoir, Montana. In Kansas and Oklahoma, limnological studies of strip mine lakes are underway.

Surface-water activities continued to be an important part of the regional program. Additions to gaging-station networks were made in coal-development areas in Montana, New Mexico, North Dakota, Oklahoma, and Wyoming. Most of these new stations were constructed and operated on behalf of the USGS under Government contracts with private engineering firms. The stations were installed to monitor streamflow conditions in coal-development areas and to document changes resulting from mining operations.

Mapping of flood-prone areas continued in several States in the region. HUD type–15 flood-insurance studies for specific cities continued; however, the program is approaching completion, and few new areas were included.

Flood-frequency studies were completed for St. Louis County, Missouri, for related small streams in Oklahoma, for urban development in the Walnut Creek basin in Iowa, and for small streams in Louisiana. Additional flood-frequency studies are underway in several States.

A major study is being made of the relationship of channel geometry to streamflow characteristics in the Missouri River basin.

MULTISTATE STUDIES

Third test well completed in the Madison Aquifer

As part of a regional evaluation of the geology, hydrology, and geochemistry of the Madison aquifer, Madison Limestone test well 3 was bottomed 14.6 m below the top of the Precambrian rocks at 2,187 m below land surface on November 16, 1978. The well is in sec. 35, T. 2 N., R. 27 E., Yellowstone County, Montana.

E. M. Cushing reported that 20 cores were taken from selected intervals ranging in age from Late Cretaceous to Precambrian. Core recovery was 159 m out of 181 m attempted. Twelve drill-stem tests were attempted in formations ranging in age from Cretaceous to Precambrian. Geophysical logs available included dual induction laterolog, sidewall neutron porosity, borehole compensated sonic, compensated formation density, temperature, and caliper. The well casing was perforated at two water-bearing zones in the Madison Limestone, one from 1,334 to 1,328 m and the other from 1,323 to 1,317 m below land surface. Two cement plugs were placed in the bottom of the well, one from 2,187 to 2,114 m and the other from 1,900 m below land surface, to block upward leakage of the highly saline water in the lower geologic units.

Water from the two zones open in the well had a specific conductance of 2,900 μmho. The rate of flow was 3.2 L/s. The shut-in pressure was not determined because of extremely cold weather at the well site. However, the shut-in pressure on a preliminary test of a water zone at the top of the Madison was 3,172 kPa above land surface. The temperature of water measured at the end of a 120-m discharge pipe on the land surface was 48°C.

Historical perspective of the South Platte River

G. P. Williams reported that the channel of the South Platte River from Kersey, Colo., to North Platte, Nebr., is only about one-ninth as wide, on the average, as it was about 100 years ago. This drastic reduction (nearly 90 percent) in width has been accompanied by an increase in vegetation. The vegetation occupies that part of the former channel that now carries no water. Mean annual discharges and annual peak discharges have not changed significantly at Kersey and Julesburg, Colo., since measurements began in the early 1900's. At North Platte, both of these discharges have decreased considerably since around the turn of the century.

COLORADO

Effects of a cattle feedlot on ground-water quality

In the South Platte River valley of Colorado, animal waste in a cattle feedlot with a stocking rate of 90,000 head of cattle per cycle has not had a noticeable effect on ground-water quality, according to R. G. Borman. Nineteen observation wells in and near the feedlot were monitored from 1974, during construction and stocking of the feedlot, to June 1978. Only one well downgradient from a runoff-detention pond has shown an upward trend in chlorides that can be related to the feedlot operation.

Water from a lysimeter installed at a depth of 1.5 m in the unsaturated zone beneath the pens had high concentrations of chloride and nitrate. Water from a lysimeter at the same location and installed at a depth of 6.1 m did not contain high concentrations of chloride or nitrate.

Dawson aquifer model converted

P. J. Emmons converted a 1974 digital simulation model of the Dawson aquifer (R. K. Livingston, J. M. Klein, and D. L. Bingham, 1976) to the USGS two-dimensional finite-difference aquifer simulation model (P. C. Trescott, G. F. Pinder, and S. P. Larson, 1976). The modeled part of the Dawson aquifer, which underlies approximately 2,200 km^2 of the northern half of El Paso County, Colorado, consists of an arkosic conglomerate to sandstone with discontinuous layers of silty claystone, shale, and lignitic coal. For modeling purposes, the aquifer was considered to be a single unconfined unit with a hydraulic conductivity of 5.5×10^{-7} m/s and a specific yield of 0.15. The 1974 water-table altitude configuration was considered to represent steady-state conditions of the aquifer. Water-level measurements made annually since 1974 in approximately 50 wells completed in the Dawson aquifer indicated that the water table has not changed.

Ground-water resources of Crowley County

The occurrence and chemical characteristics of ground water in Crowley County were studied by B. J. Ryan, D. L. Cain, and P. J. Emmons. The county is in a semiarid region, and sources of surface-water supplies are limited to the Arkansas River. Most ground-water supplies for stock, domestic, and municipal uses are obtained from wells completed in shallow unconsolidated aquifers. Well yields are generally less than 0.3 L/s. Analyses of water samples collected from 18 shallow wells showed that dissolved solids and sulfate concentrations exceeded the Colorado Department of Health's recommended limits for drinking water in 15 wells, the limit for fluoride was exceeded in water from 5 wells, and the limit for nitrate was exceeded in water from 3 wells.

Depth to the top of the Cretaceous Dakota Sandstone ranges from about 300 to 1,000 m and has been a factor in preventing widespread development of the aquifer; only five wells in the county have been completed in the Dakota Sandstone. A specific capacity of 0.07 (L/s)/m was determined during an aquifer test of a well that is 600 m deep and has a yield of 0.92 L/s. Few water-quality data for the Dakota Sandstone in Crowley County are available. During the aquifer test, the water temperature was 31°C, and the specific conductance was 1,410 μmho/cm at 25°C.

Hydrology of coal spoil piles near Hayden

The chemical quality of water percolating through spoil piles at the Seneca coal mine near Hayden is being investigated by R. S. Williams, Jr., as part of a study to determine the effects of the spoil piles on the hydrologic system and to determine the reclamation potential of the spoil piles. Water samples for chemical analysis are collected from five tank-type lysimeters ($2.4 \times 3.0 \times 2.4$ m) that have been filled with material from spoil piles in the immediate area. Water collected in the lysimeters during 1978 had a specific conductance of about 4,000 μmho/cm at 25°C and contained about 500 mg/L of calcium, 400 mg/L of magnesium, 20 mg/L of potassium, 2,500 mg/L of sulfate, 20 μg/L of iron, and 200 μg/L of selenium.

IOWA

Study to determine hydrology of sandstone aquifers in the coal-bearing Pennsylvanian strata

J. W. Cagle's studies of a nine-county 11,888-km^2 area in southern Iowa indicated that several sandstone aquifers are present within the Pennsylvanian (Cherokee Shale) strata. The sandstone aquifers comprise one of the few usable sources of ground water in a primarily rural agricultural region that has a history of water-availability and water-quality problems. Preliminary results of the study indicated that (1) individual sandstone units are not continuous over large areas, (2) sandstone units that are identifiable as aquifers in one locality may not be water bearing at another site, and (3) sandstone aquifers probably will not be affected by strip mining.

Effects of urbanization on flood-flow characteristics of Walnut Creek basin

O. G. Lara (1978) used a rainfall runoff digital model to determine the probable impact of urbanization on flood-frequency characteristics of the Walnut Creek basin near Des Moines. Long-term rainfall data, recorded at two stations near the basin, were used as the basic input to the calibrated model to generate annual peak discharges for the basin in its present state of development and to generate annual peak discharges for the basin corresponding to selected stages of urbanization. In this study, urbanization is measured by the percent of impervious area in the basin. The results of the model indicated, for example, that the present magnitude of the 100-year flood could increase by 39 percent if the impervious area in the basin reaches a 50-percent level;

likewise, the present magnitude of the 2-year flood could increase by 81 percent.

Water quality of Iowa's coal region

A preliminary investigation of the surface-water quality of Iowa's coal region was conducted by L. J. Slack. Based on three sets of samples (during high, average, and low streamflow) collected in the White Breast, English, and Cedar Creek basins in south-central Iowa, the prevalent water type is calcium bicarbonate with occasional high magnesium and sulfate concentrations. Turbidity generally increased with increasing discharge while specific conductance generally decreased with increasing discharge. No other parameters showed a trend versus streamflow, and no parameters showed a trend versus season.

Test drilling of aquifers in northwestern Iowa

A cooperative geology and water-resources investigation of northwestern Iowa is being conducted by the USGS and the Iowa Geological Survey. According to K. D. Wahl, test drilling by the Iowa Geological Survey and private land owners has provided new stratigraphic and hydrologic data for an area where little information was available previously.

Most of the test holes penetrated the full thickness of Cretaceous rocks in the area and also penetrated a sufficient thickness of the Paleozoic rocks to make stratigraphic determinations possible.

The thickness of sandstone aquifers in the Cretaceous seems to be related to the buried topography of the underlying Paleozoic surface. The thicker sandstone aquifers occur in low areas of the Paleozoic surface which results in a greater total thickness of the Cretaceous. Several test wells indicated that the Paleozoic rocks may be water bearing; however, testing for yield and chemical quality has not been completed. Preliminary data indicated that the chemical quality of water in the Cretaceous may be related to that in the underlying Paleozoic units.

KANSAS

Changes in historic patterns of a stream-aquifer system

Analyses of time variations in Arkansas River gains and losses between the Kansas–Colorado State line and Syracuse, Kans., were made by using historic streamflow, canal diversions, and return data. Results showed no net channel loss in years prior to 1965, but losses occurred in 9 of the years from 1965–78. In 1976, the Arkansas River lost 46 percent of its flow between the State line and Syracuse, a distance of about 29 km. The average annual gain in flow from 1951–64 was about 10 percent (14,000 m^3), and the average annual loss from 1965–78 was about 5 percent.

R. A. Barker reported that time distribution of river gains or losses are consistent with water-level trends. The direction of the ground-water gradient, which historically sloped from the aquifer to the stream, was reversed in recent years. This change probably resulted from increased pumpage, decreasing streamflow at the State line, and successive years of below-normal precipitation.

Chemical quality of ground water in Kansas

According to C. D. Albert, approximately 450 wells were sampled as a part of network evaluations. Chemical analyses showed that ground-water quality in Kansas is highly variable and reflects the lithologic differences in geologic formations. Data analyses revealed that in wide areas, nitrate, chloride, sulfate, fluoride, and some trace elements, particularly selenium and cadmium, exceed the maximum limits recommended by the USPHS for drinking water. Other constituents and trace elements in amounts that exceed drinking-water limits occur sporadically across the State.

Hydrologic conditions in the *Equus* beds region

The aquifer in the area of the city of Wichita's well field is heavily stressed by municipal, industrial, and agricultural withdrawals. In this approximately 300-km^2 area of the *Equus* beds region, pumpage is about 62 million m^3/yr. J. M. McNellis and T. N. Gross reported that analyses of historical and current water levels indicated that, prior to 1940, the water-bearing layers above and below the clay of the Pleistocene Sappa Formation were in dynamic equilibrium. Subsequent differential stressing of the layers resulted in two distinct aquifers and in a significant head loss in the lower aquifer.

Seepage runs on the streams draining the *Equus* beds region indicated that the tributaries recharge the upper aquifer; however, the main stem of the Little Arkansas River continues to be a gaining stream. Salinity surveys showed that several streams in the region continue to have high salinities resulting from past pollution by oilfield brines.

LOUISIANA

Index to ground-water monitor wells in Louisiana

S. L. Marshall (1978) compiled a computer index that provides information on the availability of re-

cords for water-level and water-quality monitoring wells in Louisiana.

The index currently lists 3,177 water wells, active and inactive, for which data have been collected periodically and maintained by the USGS. A continuing program for the collection of ground-water data was begun in Louisiana in 1936, and currently about 780 wells are monitored routinely. Of these, 177 wells are sampled for chemical quality. The computer listing, in tabular format, provides the station identification number, location, owner, depth, geohydrologic unit, type of data, current status or frequency, and period of record. Maps showing the location of the observation wells by parish (county) are also available. Most of the wells in the index have been monitored at intervals ranging from monthly to every 5 years. However, for some, weekly or continuous recorder measurements of water level are available.

Plans call for maintaining the computer file on a current basis and periodically publishing an updated version of the index. The data storage system will facilitate production of other types of tables, in addition to the standard index.

Saltwater encroachment at Baton Rouge

Saltwater encroachment was detected in two major aquifers of the Baton Rouge area and is probably occurring in several other aquifers. C. D. Whiteman, Jr., reported that, at present pumping rates, salty water in the "600-foot" sand may reach important well fields in the Baton Rouge industrial district in about 40 years. Salty water in the "1,500-foot" sand may reach an important public supply well field in about 30 years. Saltwater encroachment is indicated by rising chloride concentrations in water from monitor wells in the "800-foot" and "2,000-foot" sands, but salty water has not yet reached additional monitor or production wells.

Saltwater encroachment is probably occurring in the "2,800-foot" sand but has not been detected by the existing monitoring network. A recent monitor well installed near the base of the "2,800-foot" sand north of the industrial district showed that the aquifer contains freshwater to its base at a depth of 893 m below land surface, thus indicating that the northern limit of salty water in the "2,800-foot" sand is at least 2 km farther south and the danger of encroachment to nearby public supply wells is less than had been thought previously.

MISSOURI

Deep wells in Audrain County

L. F. Emmett reported that 23 deep wells have been installed in Audrain County during the past 3 years. The wells, each of which yields 4,400 to 5,500 m^3/d, produce water from the Cambrian-Ordovician aquifer. Because a freshwater-saltwater boundary extends through northern Audrain County, a study was made, in cooperation with the Missouri Division of Geology and Land Survey, to determine the effects of pumping on the quality of the water in the aquifer.

Countywide water-level measurements made in November 1978 showed that pumping from three deep municipal wells in Mexico had lowered water levels locally in the deep aquifer; however, deterioration of water quality had not occurred. Pumping for irrigation had not caused a significant lowering of water levels, and there had not been a detectable change in the chemical quality of the water in the aquifer.

Technique for estimating the magnitude and frequency of floods in St. Louis County

D. W. Spencer and T. W. Alexander (1978) used equations and nomographs to estimate peak flood discharges having recurrence intervals up to 100 years in rural and urban areas of St. Louis County. Drainage area and impermeability, which are basin characteristics significant at the 5-percent probability level, were used as independent variables in the equations. Drainage area can be measured from maps, and percentage of impermeability can be measured from aerial photographs or estimated from land-use projections. The equations were based on an analysis of hydrologic data collected at 30 continuous record gaging stations; drainage area ranged from 2.1 to 101 km^2, and area of impermeability ranged from 1 to 32 percent.

MONTANA

Saline-seep development in Hailstone basin

Saline seeps are agricultural areas which were once productive but are now less productive owing to seepage of saline ground water into the areas. Factors contributing to saline-seep formation were examined at Hailstone basin; B. D. Lewis investigated hydrologic factors, such as characteristics of the ground-water system and geologic framework. The ground-water system in Hailstone basin is shallow, perched, and locally recharged. Abatement of the saline-seep problem may be accomplished by

water management in the local recharge areas; intensive planting of crops that require large quantities of water appears to be the most practical method.

Regional scale aquifers investigated in Montana

W. R. Hotchkiss reported that the Montana Northern Great Plans Regional Aquifer System Analysis, a multidiscipline study in eastern Montana, was initiated during the year. R. D. Feltis interpreted geophysical logs to delineate 20 aquifer units, and G. W. Levings examined all hydrologic data and interpreted drill-stem tests from wildcat test holes. A well inventory yielded data on 413 wells, of which 290 were sampled for chemical analyses. Concentrations of sulfate, chloride, and dissolved residue and pH of 64 samples ranged from 0 to 3,545 mg/L, 3 to 1,226 mg/L, 509 to 5,910 mg/L, and 6.8 to 9.3, respectively.

Ground-water resources of part of the Flathead Indian Reservation

A Quaternary glacial deposits aquifer was tested at nine well sites as part of a ground-water study of part of the Flathead Indian Reservation. A. J. Boettcher reported that the transmissivity of this artesian aquifer ranges from 6.5 to 150 m^2/d. The wide range is due to the discontinuous nature of the aquifer. In some areas where wells flow for a 2-week period, wells that are 2.4 km distant cease flowing.

Geohydrology of the Helena Valley

As a result of urbanization in the Helena Valley, the Lewis and Clark County Commissioners are concerned about the quality of water in a shallow aquifer. Fifty-two wells were drilled during the summer of 1978, according to A. J. Boettcher. These wells, some of which are near septic systems, were drilled as deep as 20 m. During a 1-year study, the water was sampled quarterly to determine water quality, water levels were monitored weekly, and geophysical methods were used to determine the lithology of the valley.

Hydrology of Prairie Dog Creek

A detailed study of the hydrology of the Prairie Dog Creek drainage, between Decker and Birney on the west side of the Tongue River, was begun in May 1978. The study is one of a series of studies for BLM on the baseline (premining) hydrology of areas expected to be mined for coal in southeastern Montana. N. E. McClymonds reported that the Wall coal bed, one of the numerous coal seams in the Tongue River Member of the Fort Union Formation (Paleocene), is from 15 to 18 m thick under the western part of the area; it crops out along the sides of the drainage at the low eastern part and where it has been burned to clinker. The Wall coal and an overlying sandstone, which is as much as 36 m thick, are the main aquifers in the drainage. Pumping tests indicated that yields of 0.3 L/s to wells are near the maximum limit for these aquifers. Four test holes drilling in the alluvial aquifer along Prairie Dog Creek yielded less than 0.06 L/s.

Preliminary water-quality data from the coal aquifers of the area indicated that the water contained moderate to high concentrations of dissolved solids (specific conductance, 1,450–5,100 μmho/cm) generally dominated by sodium and bicarbonate ions.

Hydrogeology of the Fort Union coal region

The surficial hydrogeology of the Fort Union Coal Region in eastern Montana was determined by J. D. Stoner and B. D. Lewis. Boundaries of the hydrogeologic units delineated indicated prominent changes in the ability of the rocks to transmit water. Aquifer boundaries usually correlated closely to those of stratigraphic origin. The aquifers comprise most of the hydrogeologic units that crop out in the study area. The Tongue River aquifer crops out in more than half of the area, but the Fox Hills-lower Hell Creek aquifer has the greatest surface and subsurface area.

Seepage runs in Federal coal-lease areas

K. R. Wilke reported that seepage runs were made on 11 streams in southeastern Montana in August and October 1978 to provide information for the monitoring of ground and surface water in Federal coal-lease areas. The work, done by Morrison-Maierle, Inc., under contract to the USGS, was coordinated with similar work being done in Wyoming.

Streamflow and water-quality data were collected from the Powder, Little Powder, and Tongue Rivers and Mizpah, Pumpkin, Otter, Hanging Woman, Rosebud, Armells, Sarpy, and Tullock Creeks. The data will be used in conjunction with thermal-infrared imagery of the Tongue and Powder Rivers to compute estimates of ground-water discharge and recharge to streams and to approximate evapotranspiration rates.

NEW MEXICO

Aquifer near Capulin

An evaluation of the water-supply potential of a 70-km^2 area within a closed basin near Capulin was

made by D. L. Hart, Jr., and Christian Smith. Lava flows from Capulin Mountain caused the basin's ancestral drainage to be closed by as much as 60 m of alluvial deposits. Six test holes were drilled to determine the potential well yield from the alluvial deposits and the volcanic cinders of Quaternary age and the Dakota Sandstone of Cretaceous age. The alluvial deposits have the potential to yield 6.3 to 15.8 L/s in areas where the saturated thickness of the deposits ranges from 30 to 53 m. The volcanic cinders may produce as much as 126 L/s where their saturated thickness is 7 to 9 m; however, their areal extent is limited to about 8 to 10 km^2. The Dakota Sandstone in this area generally yields less than 1.6 L/s. Analyses of nine water samples from these aquifers showed the dissolved-solids concentration to be less than 500 mg/L.

Hydrology of coal areas in northwestern New Mexico

Streamflow records of newly established gaging stations on ephemeral streams in the coal areas of northwestern New Mexico indicated that about one-half of the precipitation and most of the surface runoff is produced during July through October from localized short-duration thunderstorms; flow occurs at some time on about 36 days each year. Preliminary results of studies by H. R. Hejl indicated that unit-runoff volumes and suspended sediment concentrations increase as the percent of shale outcrop (badlands) of a watershed increases. These volumes and concentrations may be predictable when 30 percent or more of a watershed is shale outcrop.

A single-stage sediment sampler developed specifically for sampling surface runoff in the coal areas is being statistically evaluated. Suspended sediment concentrations in the ephemeral streams ranged up to 250,000 mg/L.

Transmissivity of the strippable coal seam in the Cretaceous Fruitland Formation ranged from 0.1 to 4 m^2/d, which is several times higher than in either the overburden or the sandstone layer below. The coal seam is usually saturated downdip of intersecting arroyo streambeds.

Projected ground-water pumpage from uranium mines in northwestern New Mexico

F. P. Lyford and P. F. Frenzel used a three-dimensional digital model to predict dewatering rates, effects on water levels in the Jurassic Morrison Formation, and effects on surface flows to the year 2000 for three projected levels of development of uranium mines in northwestern New Mexico.

Mines that are currently operating or that are scheduled for future operation (a maximum of 33 in 1985) will produce 7.1×10^8 m^3 of water from the Morrison Formation by the year 2000. The maximum dewatering rate will be about 1.0 m^3/s in 1985, with drawdowns of 600 m or more expected near the deepest mines.

A maximum of 72 mines in 1985 would produce about 1.6×10^9 m^3 of water by 2000; the maximum dewatering rate would be about 2.6 m^3/s with drawdowns of 1,200 m or more near the deepest mines. A maximum of 105 mines in 1985 would produce nearly 2.5×10^9 m^3 of water by 2000; the maximum dewatering rate would be about 3.3 m^3/s with drawdowns of 1,200 m or more near the deepest mines.

By the year 2000, dewatering of uranium mines and other ground-water developments would reduce flow in the San Juan River by less than .001 m^3/s, and flow toward the Rio Grande Valley might be reduced by .015 m^3/s.

Ground-water conditions in the vicinity of Elephant Butte Irrigation District well field

The Elephant Butte Irrigation District's well field is located in the Mesilla Valley, southwest of Las Cruces. The five district wells range in depth from 112.8 to 209.1 m and have average yields of about 130 to 190 L/s. The casings of these wells are perforated in the Santa Fe Group of Miocene to middle Pleistocene age. The aquifer consists mostly of alternating and interfingering layers of fine- to medium-grained sand and clay. Overlying the Santa Fe Group is the flood-plain alluvium of Holocene age, which consists of clay, sand, and gravel. About 25 privately owned deep irrigation wells occur in the vicinity of the well field.

According to C. A. Wilson, R. R. White, and R. G. Roybal, a zone of slightly saline water (1,000–3,000 mg/L dissolved solids) occurs from the water table to depths of about 40 to 50 m. Underlying this zone is a much thicker zone of good-quality water (<1,000 mg/L dissolved solids). A water sample taken between depths of 358.7 and 363.6 m contained 354 mg/L dissolved solids. The district's wells have cemented surface casings that extend through the slightly saline water zone.

The Santa Fe Group in the well-field area behaves as a leaky confined aquifer. Transmissivities range from about 660 to 1,960 m^2/d; the storage coefficient ranges from .0002 to .0006. The average hydraulic conductivity is 18 m/d.

As pumpage of all irrigation wells tapping the Santa Fe Group continues, the quality of the water

produced will deteriorate slowly owing to downward movement of ground water from the slightly saline water zone.

Ground-water resources of the lower Rio Grande Valley area of New Mexico

According to C. A. Wilson, R. R. White, and R. G. Roybal, water supplies for the lower Rio Grande Valley area are obtained from surface water of the Rio Grande and from ground water occurring in the valley-fill sediments. The Rincon and Mesilla Valleys, which occupy the flood plain of the Rio Grande, are agricultural areas extensively irrigated by water from the Rio Grande. Ground water provides supplemental irrigation water and water for municipal and industrial supplies. Total ground-water pumpage in the lower Rio Grande Valley area in 1975 was estimated to be 128 hm^3, mostly in the Mesilla and Rincon Valleys.

Major aquifers in the area are the Santa Fe Group of Miocene to middle Pleistocene age and the flood-plain alluvium of Holocene age. The alluvium consists of clay, silt, sand, and gravel. The much thicker Santa Fe Group consists of alternating and interfingering layers of sand and clay. Ground water is unconfined in the flood-plain alluvium and may be unconfined or confined in the Santa Fe. The hydraulic conductivity ranges from 1.3 to 27 m/d for the Santa Fe.

Ground water in the flood-plain alluvium is usually slightly saline (1,000–3,000 mg/L dissolved solids). In the Santa Fe Group in the Mesilla Valley, Southern Jornada, and La Mesa areas, most water is fresh (<1,000 mg/L dissolved solids). Slightly saline water is found in the Santa Fe in the Northern Jornada area and along the eastern margin of the Mesilla Valley. About 60,000 hm^3 of freshwater was estimated to be available to wells.

NORTH DAKOTA

Major factors controlling sediment runoff in Park River watershed

A reconnaissance of the Park River watershed by D. J. Ackerman indicated that gradient and ground-water seepage are major factors controlling water quality of the streams. Most sediment transport originates on a shale escarpment where the stream gradient is 4 to 5.5 m/km. In this reach, sand-sized particles are transported. In lower reaches, where gradients are <0.4 m/km, only fine silt- and clay-sized particles are transported.

During summer, base-flow stream salinities are strongly influenced by the contribution of saline ground water.

Ground-water availability and quality in Billings, Golden Valley, and Slope Counties

L. O. Anna reported that the major aquifers in Billings, Golden Valley, and Slope Counties are the Fox Hills–lower Hell Creek system, the upper Hell Creek–lower Ludlow system, and aquifers in the Tongue River and Sentinel Butte Members of the Paleocene Fort Union Formation. Yields up to 19 L/s can be expected from the Fox Hills–lower Hell Creek system, the most dependable supply. The water is generally a sodium bicarbonate type.

Major deflections in the potentiometric surface are evident in the area of flowing wells along the Little Missouri River.

Results of test drilling in Bottineau and Rolette Counties

According to C. A. Armstrong, the first phase of test drilling in Bottineau and Rolette Counties indicated that the Cretaceous Hell Creek Formation does not surround the North Dakota part of the Turtle Mountains as is presently indicated on the bedrock geologic map of North Dakota (Carlson, 1969). The Cannonball Formation (North Dakota usage) directly overlies either the Fox Hills Formation or the Pierre Formation.

Hydrology of Wibaux-Beach deposit

The first of two phases of drilling and observation well construction were completed in 1978. W. F. Horak found that the Harmon lignite bed of the Tongue River Member of the Fort Union Formation was water bearing at most locations. The lower part of the Tongue River is a good aquifer, but the sand section occurs inconsistently. Potentiometric data for both aquifers indicated a northward flow gradient with downward vertical leakage. Dissolved solids content of the waters ranged from about 400 to 2,000 mg/L. The water was generally a sodium bicarbonate-sulfate type and had a low iron content.

Outwash plain in Logan County

R. L. Klausing reported that test drilling in north-central Logan County showed a surficial outwash aquifer with an areal extent of about 78 km^2. The aquifer consists of sand-and-gravel deposits that have an average saturated thickness of about 8 m.

Glaciofluvial aquifers in McIntosh County

R. L. Klausing reported that test drilling in McIntosh County revealed the presence of two aquifer systems capable of yielding 32 to 63 L/s to wells. The aquifer systems are composed of buried valley, buried outwash, and surficial outwash deposits.

Major aquifers in buried valleys

According to P. G. Randich, test drilling disclosed that four buried valleys underlie the glacial Lake Souris area in McHenry County. All of these buried valleys were incised in the underlying bedrock and were formed by glacial ice-front streams. These buried valleys contain the most productive aquifer systems in the county.

Test drilling in Sheridan County penetrated buried Pleistocene valleys. These valleys are cut into Upper Cretaceous bedrock under the Coteau du Missouri. Sand-and-gravel aquifers up to 122 m thick were found in some of the buried valleys. These and other Pleistocene aquifer systems are expected to produce large volumes of water, but most of Sheridan County is underlain only by Upper Cretaceous sandstone aquifer systems.

SOUTH DAKOTA

Pumping test of a Niobrara Marl aquifer in northeastern Aurora County

L. J. Hamilton reported that drawdown exceeded 5 m over an area of 10 km^2 after 5 days of pumping 75 L/s of water from the Cretaceous Niobrara Marl aquifer in northeastern Aurora County. The extensive drawdown was due to slow recharge and a low artesian storage coefficient of about 0.0001. However, transmissivity was estimated to be 3,000 to 5,000 m^2/d, which is unusually high for a marl. The high transmissivity appears to be caused by fault-fracturing of the marl, according to L. S. Hedges (South Dakota Geological Survey).

Saline ground water in Clark County

The concentration of dissolved solids in 100 water samples from six glacial sand-and-gravel aquifers in Clark County, northeastern South Dakota, ranged from 270 to 3,380 mg/L. L. J. Hamilton reported that most of the water was saline and very hard—hardness ranged from 190 to 1,800 mg/L. Generally, the shallowest aquifer yielded a calcium bicarbonate-type water that had an average dissolved solids concentration of 600 mg/L and an average hardness of 500 mg/L. The underlying aquifers yielded a calcium or sodium sulfate-type water that had average concentrations of dissolved solids ranging from 1,300 to 2,000 mg/L and average hardness ranging from 900 to 1,100 mg/L. Most of the dissolved solids probably were leached from the 15- to 150-m thickness of glacial till that overlies the aquifers.

Potential for radioactive waste disposal in Pierre Shale

W. S. Keys reported that a suite of logs of several test holes in the Cretaceous Pierre Shale in South Dakota were completed. The holes were drilled to investigate shale as a potential host for a high-level radioactive waste repository. Preliminary interpretation of these logs suggested the presence of some natural fractures and a much greater variation in lithology than was apparent from the examination of core.

TEXAS

Ground water in Jasper aquifer

The Jasper aquifer, which is one of several highly productive aquifers on the Texas Coastal Plain and which has been mapped from the Sabine River to the Rio Grande, has been only slightly affected by pumping stresses. According to E. T. Baker, Jr., analyses of water-level trends from hydrographs showed that the stresses are relatively small and are mostly localized in municipal well fields; consequently, water-level declines are small. On a regional basis, the aquifer shows only a small response to this local pumping.

The lack of adequate historical water-level data, together with the fact that water-level declines in the aquifer are small, will preclude verification of a digital model against potentiometric head declines for various time periods. However, by using available data, it will be possible to calibrate the model on a steady-state basis so that the model can be made to simulate predevelopment heads in the aquifer.

UTAH

Navajo Sandstone, an important aquifer in southwestern Utah

R. M. Cordova determined that the Navajo Sandstone of Jurassic and Triassic(?) age is the most important aquifer in the Kanab area of southwestern Utah. The Navajo underlies a large area (compared to the area's other aquifers) where development of ground water by wells is economically feasible; most of the existing public supply and irrigation wells in the Kanab area tap the Navajo. Ground water from the Navajo, which is of better chemical quality than water from other aquifers in

the area, commonly contains <500 mg/L dissolved solids.

Springs in the northern Wasatch Plateau

Numerous springs in the Huntington and Cottonwood Creeks drainages in the northern Wasatch Plateau of central Utah were studied and sampled by T. W. Danielson. With few exceptions, the springs sampled discharge from the Blackhawk Formation of Cretaceous age.

Most of the springs occur at high elevations where recharge is supplied by snowmelt, and most are located within a relatively short distance of the recharge area. On East Mountain, discharge from springs decreases markedly through the summer and fall; November discharges are commonly one-half or less of those in July.

In general, all perennial springs with discharges greater than about 5 L/s appeared to be located along joints, fractures, or major faults. Water from these springs generally discharges near the contact between the Starpoint Sandstone and the Mancos Shale, both of Cretaceous age.

Most spring discharge is of good chemical quality, with specific conductances less than 800 μmho/cm. The water from all of the springs is of calcium bicarbonate type, and water discharging from springs in formations of Cretaceous and Tertiary age is very similar in chemical composition.

Sources of water discharged from Fish Springs

J. S. Gates and S. A. Kruer estimated that the 32 million m^3 of water flowing annually from Fish Springs in west-central Utah discharges from carbonate rocks of Paleozoic age along fault zones. Probably the water, most of which flows to Fish Springs Flat from Snake Valley, entered the aquifer around the flanks of the Deep Creek Range about 30 to 40 km west of the springs.

Navajo Sandstone a source of ground water for future energy-related development

The Navajo Sandstone, a major aquifer in arid southeastern Utah, is a probable source of water for energy-related development. J. W. Hood and T. W. Danielson estimated that recharge to the Triassic (?) and Jurassic Navajo Sandstone in the area between the Henry Mountains and the San Rafael Swell is only 6.2 hm^3/yr, or about 0.006 percent of the estimated 110,000 hm^3 of water stored in the aquifer. Most of the recharge occurs along Waterpocket Fold and in the highlands at the western edge of the area.

Although there is no appreciable recharge to the Navajo in the San Rafael Swell and average hydraulic conductivity of the aquifer is only about 0.3 m/d, withdrawal of water from the Navajo Sandstone is feasible. Small withdrawals for stock and domestic uses would have little effect on the hydrologic system. Large withdrawals would greatly lower water levels and might cause degradation of the chemical quality of the water. For an assumed 36-year period of withdrawal of 25 hm^3/yr from a hypothetical well field near Caineville, the amount of recoverable water in the aquifer would diminish no more than 0.7 percent; drawdown in the well field would be at least 335 m. Large-scale development would cause a measurable decrease of streamflow in the Dirty Devil River and cessation of the flow of some springs, but its effect on the flow of the Colorado River into Lake Powell would be minimal.

Digital model of ground-water flow in Tooele Valley

A. C. Razem, using a two-dimensional digital model of the principal aquifer in Tooele Valley, predicted that if current average annual withdrawal of water from wells were increased from 37.2 hm^3 to 74.4 hm^3, water levels in the valley would decline from less than 3 m in the northern half of the valley to more than 9 m in the southeastern part of the valley. Water-level declines of 3 to 6 m would occur in most of the area where ground water is presently heavily pumped. If average annual well discharge were to remain at 37.2 hm^3 over most of the valley, water levels would decline less than 1.5 m, and, in part of the Erda irrigation area, water levels would decline 1.5 to 3 m.

WESTERN REGION

In 1978, heavy snowfalls and rains brought an end to 2 years of drought in most of the western region. In California, streamflow for the entire State was well above normal; the Kings River flowed 10 times its normal rate in September. The contents of 10 major reservoirs in northern California dramatically increased, from 32 percent of average at the beginning of the water year to 122 percent of average at the end of the water year. Above-normal streamflows were also recorded in Alaska, Arizona, Idaho, Nevada, Oregon, and Washington. Streamflow in Hawaii was extremely low during the first half of the year but increased sharply from June to September.

Heavy rains not only brought an end to the drought but also caused severe damage and loss of life in Arizona and southern California. In parts of southern Ventura County and northern Los Angeles County, California, where more than 50 indirect measurements were made, rainfall totals reached 203 mm on February 10. High water during the storm period between February 7–11 resulted in significant flooding south of the San Francisco Bay region. Particularly hard-hit were the Arroyo Seco and Big Sur drainage basins in the Los Padres National Forest of California, where forest fires destroyed most of the vegetative cover in the summer of 1977. Peak discharge in the Arroyo Seco on February 7 was estimated to be 1,210 m^3/s, about twice the previous maximum discharge which was recorded in December 1966.

Results of a cooperative study with the U.S. Bureau of Reclamation and the Arizona Department of Transportation showed that ground-water levels have been declining rapidly in parts of Maricopa and Pinal Counties, Arizona, and that, southeast of Phoenix, 310 km^2 of land has subsided more than 2 m.

ALASKA

Geohydrology of the Delta-Clearwater area

By using data from a hydrologic model, D. E. Wilcox formulated the thesis that the aquifer transmitting water to the spring-fed Clearwater Creek–Clearwater Lake system is recharged, at least in part, by seepage losses from the Tanana River to the east of the springs. A test of this thesis on October 15, 1978, showed that the hydraulic gradient west of the Tanana River, 29 km above the mouth of the Gerstle River, sloped northwesterly at about 0.85 m/km, and the water level in a well approximately 30 m west of the Tanana River was 9.02 m below the water surface in the river. These findings indicated that the Tanana River in this area is perched and has seepage losses to the aquifer during at least part of the year.

Geohydrology of the Fairbanks North Star Borough

The geohydrologic study of the Fairbanks North Star Borough is a continuing program designed to provide basic hydrologic data for land-use planning. Since its start in 1975, the program has been expanded to include outlying areas. According to A. P. Kromhardt, the most recently canvassed area was the Chena Ridge area southwest of Fairbanks. Although some homeowners in that area reported water-level declines in their wells, the majority reported no noticeable changes in water yield. Water wells from the Chena Ridge area had total arsenic concentrations ranging from 0 to 6 $\mu g/L$, well below the USPHS recommended maximum of 50 $\mu g/L$. Nitrate concentrations exceeding the USPHS recommended maximum of 10 mg/L were found in samples from two wells. The source and extent of nitrate in ground water around Fairbanks is still relatively unknown. Water levels in a deep observation well on a ridge directly north of Fairbanks continued to decline at a rate of about 1.5 m/yr. It has not been determined whether this drop is due to a decrease in precipitation or an increase in the number of wells tapping the aquifer.

Hydrology and water quality of the Keta River basin

In 1978, G. O. Balding collected water-discharge, suspended sediment, and water-quality data at seven sites on streams east of Ketchikan to delineate hydrologic conditions in an area with known molybdenum development potential. Recording stations were installed on White Creek and Keta River near Ketchikan to obtain continuous records of stream discharge, specific conductance, and water temperature. For White Creek, the mean daily unit discharge ranged from 20.6 to 293 $(L/s)/km^2$, conductivity ranged from 27 to 72 μm, temperature ranged from 0.0° to 8.5°C, and pH ranged from 6.0 to 6.4. Measured suspended sediment concentrations ranged from 0 to 1 mg/L. For Keta River, the mean daily unit discharge ranged from 11.2 to 1,410 $(L/s)/km^2$, conductivity ranged from 9 to 36 μm, temperature ranged from about 0.0° to 14.5°C, pH ranged from 6.0 to 6.4, and measured suspended sediment concentrations ranged from 0 to 23 mg/L.

During a ground-water reconnaissance, L. L. Dearborn and G. O. Balding collected down-hole geophysical and water-quality data in two coreholes in the area. Data consisted of thermal, natural gamma, and gamma-gamma logs. Flow velocities were measured by using a brine injector. One of the two coreholes was discharging ground water at the surface. The initial discharge rate of 0.9 L/s eventually dropped to 0.1 L/s.

The thermal log of the flowing corehole indicated three distinct deflections in the thermal gradient. On the natural gamma and gamma-gamma logs, zones of relatively less density than those immediately above and below indicated fracture zones and coincided with the deflections on the geothermal log. Subsequent brine-injection measurements near

those deflection points indicated that ground-water-flow velocities ranged from 0.03 to more than 0.10 m/s.

There were no deflections on the geothermal log for the nondischarging corehole, even though the gamma-gamma log indicated two possible fracture zones. Subsequent brine-injection measurements confirmed the expected static conditions.

Specific conductance ranged from 185 μm in the nonflowing corehole to 1,200 μm in the flowing corehole. Water-quality analyses showed that water from the nonflowing corehole was a $Ca(HCO_3)_2$ type, whereas that from the flowing corehole was a $CaSO_4$ type.

ARIZONA

The results of a cooperative study with the U.S. Bureau of Reclamation and the Arizona Department of Transportation indicated that about 310 km^2 of land southeast of Phoenix has subsided more than 2 m since 1952. The study covers an 11,650-km^2 area of Maricopa and Pinal Counties in south-central Arizona. R. L. Laney (R. L. Laney, R. H. Raymond, and C. C. Winikka, 1978) reported that, since 1915, ground-water withdrawals have totaled more than 134,400 hm^3, which is much more than could be replaced by natural recharge. As a result, ground-water levels in the study area have been declining since 1923; the most rapid declines have occurred since the 1940's—in some areas, declines were as much as 122 m. The greatest subsidence occurred in the Eloy and Stanfield areas where surface elevations have decreased as much as 3.7 m since 1952. In the area of greatest subsidence, the underground storage capacity was estimated to have been reduced more than 617 hm^3.

Potential flood and debris hazards at Willow Beach

Significant hazards to life and property exist at Willow Beach, a recreation site on the eastern side of Lake Mohave. According to Otto Moosburner, floods equal to or greater than the 25-year recurrence interval flood could overtop the diked channels along Willow Beach Wash and Jumbo Wash. High-flow velocities in the channels and the overflow areas could wash away people and property and impact damage to stationary objects could be caused by floating manmade objects and sediment.

CALIFORNIA

Availability of water for irrigational use, Santa Rosa Indian Reservation

Anthony Buono, W. R. Moyle, Jr., and Patricia Dana reported that an investigation of the availability of water for irrigation to supplement the 305-mm average annual precipitation indicated that only limited quantities of water can be withdrawn from the ground-water system in the Santa Rosa Indian Reservation. The aquifer consists of saturated sections of the unconsolidated alluvium of Holocene age and partly consolidated nonmarine sandstone and siltstone of Pleistocene age (Bautista Formation of local usage). Damming of surface water that is normally lost from the area (1.8 hm^3/yr) could supply part of the water needed to supplement ground water.

Indian Wells Valley water-level predictions

Ground-water pumpage in Indian Wells Valley, a virtually closed basin in the Mojave Desert of southern California, has increased gradually since 1945 and now exceeds the long-term mean annual recharge. In order to aid in the understanding and management of the ground-water basin, a USGS digital ground-water model was modified to reflect current conditions in the basin, including areal distribution and rates of ground-water pumpage.

The results of the present simulation for the period 1969–76 verified the original model, according to M. J. Mallory; calculated heads for 1976 agreed well with observed heads, thereby indicating a good calibration of the original model. A predictive simulation for the period 1977–2020 used pumpage values that predicted increases of about 19 to 32 hm^3/yr. The pumpage used in the present simulations reflects a slightly slower growth rate and a more concentrated pattern of development than that of the original model. Predicted drawdowns for 1983 were less extensive, but locally more severe, than those predicted earlier.

The model simulation suggested that by the year 2020 reversal of the hydraulic gradient between China Lake Playa and the city of Ridgecrest could result in the flow of poor-quality water from the China Lake Playa southward into areas of water withdrawals.

Computation of tidal river discharge

R. N. Oltmann reported that the multiple-reach method of characteristics one-dimensional flow-simulation model developed by Chintù Lai has been successfully used on a 17.3-km tide-affected reach of the Sacramento River since February 1976. The model was used to provide the streamflow record for the Sacramento River at the Sacramento stream-gaging station, which is at the upstream end of the

reach. The model's reach was recently extended 16.9 km downstream from Freeport, which is the downstream end of the 17.3-km reach, to Hood in order to provide flow-characteristics data at sites farther downstream into the San Francisco Bay system. The reach is uniform throughout its 34.3-km length; therefore, the model was applied as a single-reach model and not as a multiple-reach model. The model was calibrated by comparing model-computed 15-min discharge data with discharge measurements at both ends of the reach. The Sacramento-to-Freeport model, which was also calibrated by using discharge-measurement data but only at the upstream end, was verified numerous times throughout the entire discharge range. As yet, the Sacramento-to-Hood model has not been verified.

History of flooding in Butte Basin between 1878 and 1978

J. C. Blodgett studied the effects of flooding in Butte Basin and the Sacramento River between 1878 and 1978. The study area includes the Sacramento Valley between Chico and Meridian. Blodgett investigated such aspects of flood control as a history of levee and bypass construction, occurrence and location of levee failures, problems of backwater at Colusa Weir, and improvement in flow capacity of Butte Slough; other data included annual peak stages and discharges at gaging stations, staff gages, crest-stage gages, and miscellaneous points and discharge-measurement data and cross-section data for selected locations in Butte Basin.

There are indications that the channel of the Sacramento River in the study area had degraded about 0.5 m between 1946–78, and flow efficiency of Butte Slough had improved over 25 percent between 1940–74. At the upstream end of the study area, data have been assembled relating channel hydraulic and geologic conditions to the location and amount of overflow to Butte Basin. Following construction of Shasta Dam and other upstream impoundments, the average duration of flooding in the basin dropped from 99 to about 47 d/yr. Since 1970, however, the amount of overflow to Butte Basin, as a percentage of the total flow, has increased 4 percent, apparently the result of upstream channel and flood-plain changes that allow more water to leave the Sacramento River. At the latitude of Butte City, there has been a shift since 1970 in the distribution of left-bank overflow from the west toward the eastern part of the flood plain.

IDAHO

Ground-water-quality assessment, northern Idaho

D. J. Parliman reported that 116 water samples were collected from five major aquifers in northern Idaho to obtain 1978 water-quality data. The aquifers are comprised of unconsolidated alluvium, glacial-fluvial deposits, jointed basalt, batholithic granite, and undifferentiated metamorphic rocks.

Recharge to the aquifers is principally from precipitation in adjacent mountains and, in places, leakage from rivers and lakes. The most productive aquifers occur in thick unconsolidated alluvial and glacial deposits. Water quality is generally excellent in northern Idaho; recharge water with low mineral concentrations passes rapidly through the unconsolidated sand and gravel. However, water-quality problems do occur locally.

Concentrations of dissolved trace elements (Cd, Cu, Pb, and Zn) are high (2–3,600 μg/L) in the Coeur d'Alene mining district, where heavy-metals mining and smelting have been in operation for more than 100 years. Concentrations of dissolved solids (28–773 mg/L), hardness (14–610 mg/L), and dissolved iron (0–13,000 μg/L) are locally high throughout northern Idaho, but they are regionally high in the Kootenai River valley. Nitrate concentrations are high (0–25 mg/L) in the thick glacial aquifer of southern Rathdrum Prairie because of septic tank drainfield seepage in the Coeur d'Alene urban area.

Hydrology of Rathdrum Prairie aquifer

The Rathdrum Prairie aquifer in northern Idaho is of glaciofluvial origin and consists of highly permeable sand, gravel, and boulders. H. R. Seitz constructed a finite element model to define the flow system in the aquifer. Model calibration runs showed that T (transmissivity) values in parts of the aquifer are as high as 5×10^5 m^2/d. Most of the lakes are perched above the regional water table and are sources of recharge to the aquifer. Lake-budget determinations indicated that recharge to the aquifer from individual lakes ranges from 0.3 to 7 m^3/s.

Hydrologic conditions in Rockland Valley

Concern that continued development of ground-water resources for irrigation may lead to a decrease in limited surface-water supplies already appropriated for irrigation resulted in a 2-year study focusing on ground-water—surface-water relationships in Rockland Valley.

H. W. Young reported that an inventory of about 150 wells in the valley showed that ground water occurs chiefly under water-table conditions. The major aquifers are comprised of sand and gravel that make up the valley fill.

A seepage study indicated that Rock Creek gains from ground-water discharge throughout most of the valley. Lack of definable stream channels heading in the surrounding mountains indicated that much of the annual snowmelt seeps into the ground, thus leaving little for overland runoff.

NEVADA

Development of a relation for steady-state dumping rate in Eagle Valley

A current ground-water modeling study has revealed that available ground-water and surface-water resources of Eagle Valley are substantially less than was previously thought. The interrelation between runoff, recharge from argicultural and municipal use, use of sewage effluent for irrigation, and discharge through pumping and natural ground-water discharge has been expressed in a water-budget equation. According to F. E. Arteaga and T. J. Durbin, this mathematical expression was used to point out management alternatives. For example, allowable steady-state pumpage decreases with the conversion of surface water from agricultural to municipal usage because of loss of irrigation return flow.

OREGON

High arsenic concentrations in ground-water samples from northern Malheur County

Five of 14 ground-water samples collected from widely separated wells and springs in northern Malheur County during the fall of 1978 yielded water that contained dissolved arsenic in concentrations that exceeded 50 μg/L, the maximum concentration allowable for drinking water (U.S. Environmental Protection Agency, 1975). According to J. B. Gonthier and C. A. Collins, each of the wells and springs containing high concentrations of arsenic provides water supplies for range stock. The arsenic concentrations in the 14 samples ranged from 1 to 320 μg/L; in the five samples containing excessive arsenic, concentrations ranged from 120 to 320 μg/L. Part of the Ironsides area is a known geothermal resource area, and it is likely that the source of the arsenic is related to the effects of deep-seated geothermal activity on the area's ground-water flow system.

Iron distribution and geochemistry in a coastal dunes aquifer at Coos Bay

Detailed studies of iron distribution were made at two cross sections perpendicular to the coast by using permanently installed profile samplers (screened tubes) spaced vertically every 1.2 to 1.5 m to depths of 15 m. According to J. E. Luzier, high ferrous iron concentrations (20–56 mg/L) seem to be generated in vegetated areas of the deflation plain that are subject to inundation during the wet season. These high iron concentrations persist to about 12 or 15 m below msl (mean sea level). Piezometers at greater depths (30–43 m below msl) revealed iron concentrations of less than 1 mg/L. Increases of pH with depth ranged from about 5 at the water table to about 9 at the base of the aquifer (49 m below msl). Field measurements of alkalinity also increased with depth, ranging from about 10 mg/L near the water table to about 600 mg/L near the base of the aquifer.

The presence of relatively low iron concentrations in the lower part of the aquifer suggested that the system may be self-cleansing with respect to iron; for example, increasing pH and alkalinity with depth cause the ferrous iron to precipitate as iron hydroxide or as siderite. The distribution and geochemistry of the iron suggested that further development of the dunes aquifer is possible by extracting water from wells screened near the base of the aquifer.

Irrigation return flow from pastures and orchards in Bear Creek basin, Jackson County

A comparison of the quality of inflow and outflow water from irrigated plots of pastures and orchards in Bear Creek basin showed that (1) pastures contributed indicator bacteria (more bacteria generally left a plot in the return flow than entered with the inflow), (2) pastures removed suspended sediment, turbidity-causing particles, and dissolved nitrite plus nitrate nitrogen from the water so that return flow was generally cleaner than water delivered for irrigation, and (3) orchard return flows had at least twice the concentration of indicator bacteria, suspended sediment, and dissolved nitrite plus nitrate nitrogen as did orchard inflows. The methods of irrigation most commonly used are rill and furrow for orchards and flooding for pastures. S. W. McKenzie reported that the use of irrigation return-flow water for irrigating pastures would help to reduce the high suspended sediment and nitrogen concentrations in a receiving stream such as Bear Creek.

A preliminary evaluation of dissolved-oxygen depletion in the South Santiam River

The first year of intensive assessment of dissolved-oxygen (DO) in the South Santiam River basin was completed in 1978. Preliminary estimates by Frank Rinella indicated that point-source loadings of ammonia through the process of nitrification accounted for 79 percent of the DO depletion in the 31.7-km stretch of river from Waterloo to the mouth of the South Santiam River. Nonpoint loadings of ammonia and carbonaceous loadings from point and nonpoint sources made up the remaining 21 percent of river DO depletion. The total oxygen depletion is approximately 4,700 kg/d of oxygen removed, resulting in a net decrease of 10-percent DO saturation in the river.

Wide range of conditions represented in western Oregon flood-frequency analysis

A flood-freqency analysis of western Oregon showed a wide range in basin and hydrologic characteristics. According to D. D. Harris, L. L. Hubbard, and L. E. Hubbard, the analysis made by using the log-Pearson type III method and regional skew coefficients was based on a regression analysis of data from 230 gaging stations. Drainage areas used in the analysis range from 0.54 to 18,900 km^2, the area of lakes and ponds ranges from 0 to 19 percent of the drainage area, and forest cover ranges from 2 to 100 percent of the drainage area. In the drainage basins sampled in western Oregon, the greatest 24-hour, 2-year recurrence-interval precipitation ranged from 36 to 157 mm; annual precipitation ranges from as low as 510 mm in some interior valleys to as much as 5,000 mm in isolated mountains of the Coast Range. High flows along the Coast Range are generated primarily from rainstorms, whereas floods in the Cascade Range are caused by snowmelt and direct rainfall runoff.

Hydrological system of the Bend-Redmond area

Ground water in the main zone of saturation in the Bend-Redmond area occurs from more than 180 m to less than 75 m below land surface, and flow in this system is from the south and southwest toward the north. The area is underlain by thick units of Tertiary and Quarternary age, faulted and interbedded basaltic lava flows, pyroclastic deposits, and sediments. According to J. B. Gonthier, a downward component of flow apparently is present in this deep system because static water levels in wells penetrating it become increasingly deeper with increasing well depths. Several wells, each capable of yielding in excess of 63 L/s, were developed in the main zone of saturation in basalt, pyroclastic deposits, or sediments at widely separated localities. These well data suggest that the system is highly permeable and that large quantities of ground water can be developed from deep wells in much of the area.

A zone of perched ground water is generally present beneath an area of several square kilometers north of Bend. The perched zone occurs about 45 to 85 m below the land surface and is tapped by numerous wells for domestic and stock supplies. This perched ground water is recharged by local precipitation, seepage from the Deschutes River, excess irrigation water, and canal seepage.

WASHINGTON

Seawater intrusion along the Washington coast

As part of a reexamination of seawater intrusion along the Washington coast, approximately 1,300 water samples were collected from wells in 14 counties. According to N. P. Dion and S. S. Sumioka, wells selected for sampling were generally within about 2 km of the coast and were finished below mean sea level. The water samples were analyzed for specific conductance and chloride concentration. Preliminary results showed that specific conductance and chloride concentrations of samples taken in 1978 were slightly lower than those of samples taken from the same wells about 10 years ago.

Water-resource investigations on Indian reservations in Washington

Preliminary calculations by B. W. Drost indicated that average water-level declines of 0.76 m/yr from 1975–78 in the Tulalip tribal well field near Everett were due to abnormally low natural recharge and pumpage. Continued pumpage at the 1978 rate with the well field in its present form would probably result in a 15-to 20-year life span for the well field.

J. A. Skrivan developed and calibrated a finite-difference ground-water-flow model of the aquifer system in the Toppenish Creek basin on the Yakima Indian Reservation in south-central Washington. The aquifer system consists of (1) unconfined young valley fill, (2) old valley fill and shallow basalt, (3) primary basalt, and (4) deep basalt. Calibrated transmissivities for the confined aquifers ranged from less than 0.001 to 0.04 m^2/s in the center of the basin, with storage coefficients of 0.0004 to 0.006. The leakance of the confining beds between aquifers reached 0.05×10^{-10} (m/s)/m. Transient state calibration was based on the period 1955–72,

during which time pumpage increased about tenfold. The 1971–72 average annual pumpage was about 24.7 hm^3. A simulation showed that declines caused by pumpage from 1950–60 were as much as 18 m in the primary basalt aquifer.

The temporal distribution of streamflow on the Makah Indian Reservation in Clallam County is closely related to the amount and distribution of rainfall. According to N. P. Dion and K. L. Walters, during a year of average precipitation, about three-quarters of the streamflow can be expected to occur during the 6-month period, October–March. The chemical quality of water in streams is generally suitable for domestic purposes. Ground water is known to occur only in sand and gravel layers that underlie the lowlands of the reservation. Although individual wells are capable of yielding as much as 4 L/s, several wells in the study area have been abandoned because of high chloride concentrations in the water.

Flood elevations for the Sooes River

J. N. Bartells determined possible tide-infiuenced water-surface elevations at the site of a proposed fish hatchery on the Sooes River in northwestern Washington. Frequency relationships were developed for both river discharge and tidal elevation, and water-surface elevations were then determined for various combinations of these two parameters.

Assuming that the mean-tide elevation occurs in conjunction with any discharge, water-surface elevations were related to a specific probability without actually determining the probability of a particular discharge of tide elevation happening concurrently. The determined elevations will aid in the most cost-efficient design of flood protection for the new hatchery.

SPECIAL WATER-RESOURCE PROGRAMS

DATA COORDINATION, ACQUISITION, AND STORAGE

OFFICE OF WATER-DATA COORDINATION

During FY 1979, progress made in several major activities and publications of the Office of Water-Data Coordination (OWDC) included the "Catalog of Information on Water Data," the "National Handbook of Recommended Methods for Water-Data Acquisition," State hydrologic unit maps, a field coordination program, and advisory committees.

In cooperation with NAWDEX, the computer file of the "Catalog of Information on Water Data" was updated through 1978, and a national index was prepared and presented in 21 volumes, one volume for each of the 21 Water Resources Council (WRC) regions. In addition to information on station activities, information on areal investigations and miscellaneous activities was added to each of the volumes.

The preparation of a directory of water-data acquisition activities in coal-producing areas of the United States was completed. The directory, a special index to the "Catalog of Information on Water Data," was prepared to assist those involved in the development, management, and regulation of the Nation's coal resources by providing information on the availability of water data.

The "National Handbook of Recommended Methods for Water-Data Acquisition," which is nearing completion, includes chapters on sediment, physical and chemical quality of water, soil moisture, basin characteristics, snow and ice, and hydrometeorological observations. Chapters on surface and ground water are now in the final stages of review preparatory to printing. The handbook will include 12 chapters covering almost all phases of hydrology, and an appendix will provide information on metric units, conversion factors, precision of metric measurements, and metric conversion of equipment.

In accordance with recommendations made at meetings of the Advisory Committee on Water Data for Public Use (ACWDPU) and the Interagency Advisory Committee on Water Data (IACWD), two technical working groups were established to assist in the preparation of the national handbook. These are the Working Group on Water-Data Handling and Exchange and the Working Group on Water-Use Data.

Two maps that show national hydrologic units were prepared. One map (scale, 1:7,500,000) shows all regional, subregional, and accounting unit boundaries. Another map (scale, 1:2,500,000) shows approximately 2,150 cataloging units as well as the boundaries shown on the smaller scale map.

OWDC prepared a USGS nontechnical pamphlet describing State hydrologic unit maps and their varied uses. The publication shows part of a four-color map with its map legend and gives addressess where the hydrologic unit maps can be obtained.

Digitization of all hydrologic unit boundaries at a scale of 1:500,000 was completed, thus permitting (1) computation of all drainage-basin areas, (2) computer plotting of boundaries at various scales,

and (3) computer conversion of locations from latitude and longitude coordinates into locations by hydrologic unit code.

The report, "Plans for Water Data Acquisition by Federal Agencies Through Fiscal Year 1980" was prepared and distributed. The report consists of statements from 36 Federal agencies summarizing their water-data programs through FY 1980 and gives information on current and planned activities and on anticipated future water-data needs.

The OWDC field coordination and planning cycle for FY 1980 and 1981 was completed. The scope of the cycle was essentially the same as that for the previous cycle except that reporting on areal investigations and on miscellaneous activities was added. The procedure was for the first time tied directly to the Master Water-Data Index of NAWDEX, which now constitutes the base file of the "Catalog of Information on Water Data for Station Activities."

WATER-DATA STORAGE SYSTEM

The National Water Data Storage and Retrieval System (WATSTORE) is a large-scale computerized system developed to process and disseminate water-resource data collected by the USGS. Representative WATSTORE products are computer-printed tables and graphs, statistical analyses, digital plots, and data in machine-readable form. The computer system consists of a central computer located in Reston, Va., and remote terminal facilities in nearly every State.

The Daily Values File, which contains data on daily discharge, includes about 17,600 regular streamflow stations. Hydrologic data collected by satellites are processed, and the results are stored in this file. These data are compatible with a variety of statistical programs for analysis on the basis of calendar years, water years, climatic years, or any other period desired.

The Ground-Water Site-Inventory File contains hydrologic, geologic, and well-inventory data on more than 580,000 ground-water sites. To facilitate file management, the data base is divided into four files, each of which corresponds to one of four water-resource areas.

The Peak Flow File, which contains nearly 400,000 measurements of annual maximum-streamflow and gage-height values at surface-water sites, was revised so that it is more compatible with other files in the system. The new Peak Flow File enables partial peak data to be stored, eliminates duplication of station header data, improves input and output formats, and increases retrieval capabilities.

Newly acquired access to the Taxonomic Biological Data File of the Central Laboratory System provides users with additional methods for obtaining statistical analyses and publication tables.

Minicomputers are being used in some States to maintain local files; to reproduce maps, plots, and other graphics; to model local hydrologic systems; and to process or preedit some data before they are included in WATSTORE.

NATIONAL WATER DATA EXCHANGE

The National Water Data Exchange (NAWDEX), a national confederation of water-oriented organizations cooperating to improve access to water data, continued to expand, and, in December 1978, the number of member organizations had increased to a total of 128. Membership is voluntary and open to any water-oriented organization that wishes to participate in the NAWDEX endeavor to provide a greater array of information about water data and sources of water data. There are no dues or fees for membership.

A nationwide network of 54 Local Assistance Centers in 45 States and Puerto Rico responded to nearly 70,000 requests for data and information in FY 1978. The 54 centers, along with the NAWDEX Program Office located in the National Center in Reston, Va., provide an extensive telecommunication network for access to the NAWDEX computerized data bases. Most of the centers have direct access to the National Water Data Storage and Retrieval (WATSTORE) system of the USGS, and they provide referral services to data systems maintained by NAWDEX members. The Program Office in Reston also has direct access to the Storage and Retrieval (STORET) system of the Environmental Protection Agency (EPA).

Over 600 organizations have been registered in the computerized Water Data Sources Directory (WDSD), which identifies organizations that have available water data, locations within these organizations from which data can be obtained, types of data available, the geographic areas in which the data are collected, the media in which the data are available, and alternate sources for acquiring an organization's data. A data dictionary entitled "Definitions of Components of the Water Data Sources Directory Maintained by the National Water Data Exchange" was published in 1978. This dictionary contains a systems description and definition of each data component in the WDSD.

The Master Water Data Index (MWDI) is the computerized NAWDEX data base that identifies individual sites for which water data are available, the locations of these sites, organizations collecting these data, hydrologic disciplines represented by the data, periods of record for which data are available, major parameters for which data are available, frequency of measurement of these parameters, and media in which the data are available. Over 127,000 sites for 50 data-collecting organizations were added to the MWDI in 1978. This increase was due primarily to the completion of annual indexing updates of data in the STORET system of EPA and the WATSTORE system of the USGS. More than 300,000 sites have been indexed in the MWDI for over 370 organizations. A data dictionary entitled "Definitions of Components of the Master Water Data Index Maintained by the National Water Data Exchange" was published in 1978. This dictionary also contains a systems description and definition of each data component contained in the MWDI.

The first annual membership conference of the National Water Data Exchange was held in Denver, Colo., May 9–11, 1978. The 83 participants represented 47 member organizations and 15 nonmember organizations. Four working panels convened during the conference provided significant input in the areas of program administration, management, and coordination; methods for the handling and exchange of water data; water-data indexing and technical systems development; and request, response, and service activities.

URBAN WATER PROGRAM

The objective of the USGS urban water program is to provide generalized relationships for estimating (1) hydrologic changes owing to urbanization and (2) hydrologic conditions under urbanization. In order to fully meet these objectives, an adequate data base is necessary. D. J. Lystrom (1978) reported that the USGS, in cooperation with EPA, is developing a consistent and accessible urban hydrology data base.

Data-management system

L. D. Wilson, W. H. Doyle, Jr., and R. A. Miller (1978) reported that storm-water data were collected at four urban watersheds in Broward and Dade Counties in Florida. A supporting system of 20 FORTRAN computer programs was developed to edit, store, retrieve, and publish 1-minute time-interval rainfall, runoff, and water-quality data for up to 100 storms at each site.

Modeling of urban storm-water processes

D. R. Dawdy, J. C. Schaake, Jr., and W. M. Alley (1978) reported that an urban rainfall-runoff model was developed and documented. The model uses kinematic wave theory for routing flows over contributing areas and through a branched system of pipes and (or) natural channels to a watershed outlet.

The STORM (storage, treatment, overflow, and runoff) model, developed by the U.S. Army Corps of Engineers, was selected from existing models and adapted to use available data to compute runoff from the Houston, Tex., area and to compute the loads and concentrations of BOD, dissolved solids, total phosphorus, total organic carbon, total nitrogen, and fecal coliform bacteria. According to K. M. Waddell, B. C. Massey, and M. E. Jennings, the model was calibrated for eight sites in the Houston area. Differences between observed and computed concentrations for the calibration water year ranged from −21 to +8 percent for dissolved solids, −56 to +31 percent for total organic carbon, 0 to +83 percent for BOD, −13 to +50 percent for total nitrogen, −40 to +133 percent for total phosphorus, and −33 to +140 percent for fecal coliform bacteria. Errors for discharge ranged from −9 to +5 percent.

Loads of nutrients, total residue, COD, lead, and zinc from two urban basins in southern Florida were represented by linear regression models. According to R. A. Miller, H. C. Mattraw, and M. E. Jennings (1978), 45 independent variables representing prior rainfall history, rainfall intensity, depth of rainfall, peak discharge, antecedent dry period, season of the year, and various cross products were tested for statistical significance. Loads for 32 measured periods of storm runoff from a single-family residential area and 42 measured periods of storm runoff from a six-lane divided highway were used in the analysis. Mattraw and Miller determined that peak discharge, rainfall depth, and cross products of rainfall depth and antecedent dry hours appeared most commonly in the regression models.

Flood frequency

According to M. A. Lopez, the USGS urban basin rainfall-runoff model, RRURBAN1, was calibrated by using data from the gaging station on Allen Creek near Largo, Fla. The 4.87-km^2 watershed has 70-percent residential and 30-percent commercial land use. About 36 percent of the area is impervious, which is typical of urban areas near Tampa Bay. Rainfall data for 1905–52 were used to simulate annual peak discharges for the Allen Creek gage.

The log-Pearson type III frequency curve values for the T-year interval peak discharges were compared to the peaks computed by the Rational method. The urban basin model predicted a 5-year peak discharge of 12.4 m^3/s as compared to 24.5 m^3/s predicted by the Rational method. For a 100-year recurrence interval, the urban basin model predicted a peak discharge of 49.4 m^3/s as compared to 48.3 m^3/s predicted by the Rational method.

Land-use changes associated with urbanization increased peak discharges in northeastern Illinois by factors ranging up to 3.2, according to H. E. Allen. Equations were developed to estimate flood magnitudes at ungaged sites in northeastern Illinois for recurrence intervals ranging from 2 to 500 years.

Urban water quality

M. L. Maderak's and R. M. Slade's preliminary evaluations of surface-water data for the Austin, Tex., area indicated that man's activities influence the quantity and quality of storm runoff from this area. Fecal coliform bacteria in water samples from selected drainage basins varied from 0 to more than 50,000 colonies per 100 ml. In general, bacteria concentrations were highest in areas with substantial urban development.

Chemical and bacterial analyses of water from 50 wells sampled by M. E. Dorsey indicated that dissolved solids concentrations ranged from 271 to 8,240 mg/L, nitrate (as N) concentrations were less than 10 mg/L for all samples, and fecal coliform bacteria concentrations were less than 2 colonies per 100 ml in over 90 percent of the samples.

WATER USE

In 1978, the principal USGS water-use activity was the establishment of a National Water-Use Data Program. One objective of the program is to have a cooperative program with each of the States so that more precise data will be available in computer storage for compiling USGS reports on water use (Murray and Reeves, 1977). By midyear, about 35 cooperative agreements had been established, and agreements with all of the 50 States and Puerto Rico were scheduled for completion before mid-1979. To obtain information on how to operate the program most efficiently, prototype programs were established in Connecticut, Kansas, and Virginia.

Prototype water-use data systems in Connecticut, Kansas, and Virginia

The purpose of the Connecticut Water-Use Data System program, a cooperative program between the State of Connecticut and the USGS, is to complement Connecticut's Statewide water-resources planning efforts by providing the water-resources community with information that can be used for a better understanding of the present and projected demands on Connecticut's water resources and that will provide aggregated water-use data to the National Water-Use Data System. F. P. Haeni reported that during 1977, the first year of the program, a working group composed of the USGS, CACI, Inc., and State agency representatives defined the functional and data requirements for the system. Subsequently, CACI, Inc., under contract to the USGS, used this information to design a system and prepare a project plan for Connecticut. The plan was implemented in January 1979 by the designation of a program manager by the State of Connecticut. Concurrently, CACI, Inc., is designing the physical data base for Connecticut's water-use program. Collection of field data will begin later in the year and continue as the system is developed and fully implemented.

The Kansas Water-Use Data System is a cooperative program between the Division of Water Resources (DWR), Kansas State Board of Agriculture, and the USGS. The DWR, which is charged with administering the water appropriation laws of Kansas and is necessarily very concerned with water use within the State, works closely with State planning agencies and water-resources research groups. According to C. H. Baker, Jr., the State water-use data base design formulated by CACI, Inc., was adapted to the needs of the State by the State Division of Computer Services. Target date for beginning the entry of data into the State data base is July 1979 and the data management system is expected to be fully operational by 1980. In addition to creating the State-level data base, the DWR expanded its well-audit program, which provides information on the validity and accuracy of ground-water-use data. Eventually, the audit program will be expanded to include surface-water diversions.

H. T. Hopkins reported that a task force including USGS and State agency representatives was set up to establish the Virginia Water-Use Data System. About 50 people from private and public organizations were interviewed by the task force to determine what types of water-use data were available and what data are needed. CACI, Inc., used the task-force information to prepare a prototype water-use data system that included a dictionary with a general description of each data element to be collected and stored. Preliminary investigations of software

and hardware that will interface with the National Water-Use Data System were begun.

Water use in southwestern Florida in 1977

A. D. Duerr reported that in 1977 approximately 27 billion m^3/d of water was used in southwestern Florida. About 5.7 billion m^3 of this was fresh water, of which about 70 percent was from ground-water sources. The largest use of water was for thermoelectric power generation, 23.1 billion m^3/d, of which about 95 percent was saline water. Water used for irrigation, the next largest use, was 1.7 billion m^3/d. Industrial, public supply, and rural water use amounted to 1.6 billion, 0.9 billion, and 0.2 billion m^3/d, respectively.

Methods of estimating ground-water withdrawals for irrigation

One of the most difficult problems in an analysis of the aquifer system in western Kansas is to determine accurately the quantity of water that is pumped for irrigation use. Reported values of annual withdrawals generally were 10 to 15 percent lower than measured quantities. Estimated withdrawals based on measured power consumption rates were unreliable for extrapolation from one well to another.

C. H. Baker reported that adequate results may be obtained by a statistical sampling of measured discharges from metered wells, by calculating an average power consumption coefficient for wells pumped by natural gas engines, and by using reported values of water applied to selected crops in zones of similar precipitation. Recently designed running-time and discharge-totaling meters were installed at selected well sites to monitor discharge rates, total withdrawals, and power consumption.

Relation of ground-water pumping for irrigation to energy use

Increasing demands on ground water for irrigation are causing greater use of natural gas for energy in the High Plains area. Local management districts determined that about 15,000 wells pumped 6.5 billion m^3 of ground water during 1977 to irrigate 10,000 km^2 of cropland. An estimate based on records of local companies indicated that 1.05 million m^3 of gas were used to supply power for 80 percent of those wells.

E. D. Gutentag reported that water and gas are easily accessible, but inflated costs have caused much concern over the rapid depletion of both resources. The demand for ground water far exceeds natural recharge, and water levels are declining an average of 0.3 to 0.6 m/yr. Although the aquifer system may have 250 to 300 billion m^3 of water in storage, future irrigation development may depend mostly on the availability and cost of energy.

Digital model predicts effects of powerplant water use on lake levels and river flow in Wisconsin

A powerplant that consumes 1,130 dm^3/s of water from Lake Koshkonong, southeastern Wisconsin, would lower the lake level about 130 mm in a dry year, according to W. R. Krug. A smaller powerplant consuming 280 dm^3/s would lower the lake by <38 mm under the same conditions.

A digital streamflow model was developed to simulate flow in the Rock River and levels of Lake Koshkonong. The model uses 44 years of streamflow records for the Rock River and major tributaries and predicts water levels in Lake Koshkonong and streamflow at the Indianford dam for natural conditions and for four different magnitudes of water use by a powerplant. It was determined that during normal conditions, powerplant water use would have very little effect on lake levels, but, during long dry spells, powerplant withdrawals would increase the natural drop in water levels.

NATIONAL WATER QUALITY PROGRAMS

National Stream Quality Accounting Network completed

The National Stream Quality Accounting Network (NASQAN), the only national program for uniformly measuring the quality of the major rivers of the United States, was fully implemented by the USGS during FY 1979. NASQAN, which was started with 50 stations in early 1973, reached full design size of 525 stations with the addition of the final 80 stations in the spring and summer of 1979. Locations of NASQAN stations are determined according to the hydrologic subdivision of the United States developed by the U.S. Water Resources Council (WRC). The WRC system includes 21 regions, 222 subregions, and 349 accounting units. There is at least one NASQAN station in each accounting unit, and many of the complex units, such as those in coastal areas, have multiple stations.

Data from NASQAN are published annually, by State, in USGS water-data reports and in special annual summaries of national patterns of water quality at NASQAN stations. The data also are available through the USGS computerized data system, WATSTORE, and through STORET, the data system operated by EPA. NASQAN data are used by many State, Federal, and private organizations,

and have been summarized in annual reports of the Council on Environmental Quality since 1975. With more than 5 years of data now available for many NASQAN stations, the next step in the operation of the network is detailed studies to analyze data for evidence of changes or trends in the quality of the Nation's rivers.

River Quality Assessment Program

The USGS River Quality Assessment Program was initiated in FY 1973 in response to growing concern over the paucity of reliable water-quality data and assessment methods as vital inputs in rational water- and land-use planning. Objectives of the program include:

- The identification of causal relationships for existing river quality conditions and problems.
- The development of new analytical tools and methodologies for assessing the impact of alternative water-resource and land-use planning strategies on present and future river quality conditions.
- The demonstration of these techniques coupled with active efforts to transfer new technologies to local, State, and regional land-use planners and decisionmakers.

Sites for assessment studies are selected based on their representativeness of water quality problems and situations that might be encountered nationwide. Since every river basin is unique in some respects, efforts are made to focus methodology studies on common or basic problems that would maximize the transferability of techniques in future applications. These include:

- Point vs. nonpoint sources of pollution, especially urban runoff.
- Distribution, transport, and disposition of toxic substances.
- Effects on the quality of biota.
- Occurrence and distribution of pathogens.
- Effects of instream structures.
- Eutrophication.
- Distribution, transport, and fate of sediments.
- Nuisance growth of aquatic organisms.
- Influence of ground water.

The first intensive river-quality assessment was conducted for the Willamette River in Oregon. Original plans called for the conduct of an additional 11 river-basin assessments and two follow-up studies. The program is scheduled to terminate in FY 1985. Sites for the seven assessments that have been selected are the Willamette River (Oreg.), the Chattahoochie River (Ga.), the Yampa River (Colo.), the Patoma River (Va.), the Apalachicola (Fla.), the Carson and Truckee Rivers (Nev. and Calif.), and the Schuylkill River (Pa.).

THE REGIONAL AQUIFER-SYSTEM ANALYSIS PROGRAM

Water withdrawals from the Nation's ground-water reserves are expected to greatly increase during the next decade. Factors contributing to these increases include sharply increased irrigation, increased water needs for energy production, greater water demands by expanding cities, fewer new surface reservoirs because of environmental constraints, and the desire to establish drought-resistant water-supply systems. The impacts of increased withdrawals are regional in scope, and an ability to predict and understand these regional impacts is essential for effective water management. To address this need, the USGS's Water Resources Division has established a program of Federally funded regional ground-water studies—the Regional Aquifer-System Analysis Program.

As the term is used here, a regional aquifer system is any areally extensive set of aquifers having a link in some way. The link may be a direct hydraulic connection among the aquifers so that pumpage from one has an influence throughout the entire set; the link may be an external hydraulic connection, as in the case of a number of aquifers joined to a single stream system; the link may be economic in the sense that aquifers form a common source of supply to some element of the economy; or the link may simply be the nature of aquifers in that they share so many characteristics, which makes it efficient to study an entire set in a single exercise.

A number of aquifer systems have been identified for study under this program. Although each study will be designed to fit the particular problems of the study area, the general approach will be to develop an aquifer system computer simulation that will be supported by more detailed simulations of local or subregional problem areas.

These simulations will be an aid to understanding the natural (prepumping) flow regime and changes caused by human activities and will provide basic information required for water management such as hydraulic effects of future pumpage, artificial recharge, and waste disposal. In some studies, certain associated effects can be simulated, such as land

subsidence, seawater transgression, or costs of pumping.

Simulations will be based on existing data and on new data required to fill critical gaps in the available information. In some cases, collection of new data will require extensive field operations.

Information will be assembled on the quality of water throughout each aquifer system by bringing together all existing information and by collecting field data required to fill the gaps. An effort will be made to interpret water-quality information in terms of the original flow pattern and the changes that have occurred in response to development, as inferred from hydraulic simulations. By using water-quality data in conjunction with predicted flow patterns derived from hydraulic models, insight may be gained into future water-quality problems.

The regional studies are expected to complement the more detailed local studies. Each regional analysis should provide a geologic, hydraulic, and geochemical framework for local investigations. In terms of simulation, the regional model will offer a method of evaluating boundary flows, both lateral and vertical, for local models. In terms of water quality, an understanding of the regional flow pattern and the geochemical processes occurring along the flow path should provide a background for the study of local water chemistry.

Each study is expected to produce a series of reports—beginning with summaries of data as they are assembled and culminating in interpretive reports that include the results of predictive simulations.

The 10-year program will use advances in investigative technology that occur during the period of investigation. The average time for completion of each study will be approximately 4 years. Studies of the High Plains, the northern Great Plains, and the Central Valley of California began in FY 1978, and studies of the southeastern carbonate aquifers, the northern Midwest sandstone aquifers, and the southwestern alluvial basins began in FY 1979.

MARINE GEOLOGY AND COASTAL HYDROLOGY

COASTAL AND MARINE GEOLOGY

ATLANTIC CONTINENTAL MARGIN

Further studies of two classic geologic sites of Massachusetts

In 1889, 10 years after it was founded, the USGS published two reports within a series of papers on "coastal and marine geology" by N. S. Shaler (1889). One report was titled "The Geology of Cape Ann, Massachusetts," and the other "The Geology of Nantucket." Since then the two areas have continued to attract geologic attention, and, with application of new techniques and approaches, studies of deposits at both places continue to offer increased insight to the glacial history of New England. During 1978, R. N. Oldale and Diane Eskanasy included the two islands in their studies of coastal and offshore Massachusetts, a cooperative effort funded jointly by the USGS and the State.

Off Cape Ann, Eskanasy and Oldale used a sparker reflection profiler to study internal structures of a submerged Wisconsinan end moraine. The records for a transverse track show folded strata within the moraine and undeformed beds beneath it. Eskanasy and Oldale infer that both deformed and undeformed beds belong to the Presumpscot Formation of Bloom (1959, 1960), a late glacial morainal deposit, and consider the moraine itself to be a glaciotectonic feature caused by a minor readvance of the Woodfordian ice. The moraine appears analogous to a subaerial end moraine of the Kennebunkport readvance described by Bloom (1959, 1960).

On examining the Sankaty Sand of Nantucket, Oldale and Eskanasy found a glacial drift complex consisting of a basal till, varved clays and glaciolacustrine silt, and delta foreset beds beneath the lower part of the Sankaty Sand of Sangamon age (Gustavson, 1976). The complex therefore constitutes the first clearly established association of pre-Sangamon glacial deposits in New England. Oldale and Eskanasy interpret the upper part of the Sankaty Sand to be a basal conglomerate of upper Wisconsinan drift.

Holocene submergence of the southern New England inner Continental Shelf

In studies related to the foregoing, R. N. Oldale and C. J. O'Hara have combined recently determined radiocarbon dates on shells and peat from southeastern Massachusetts with previously published dates to construct a new sea-level rise curve for the inner Continental Shelf of southern New England and northern Georges Bank. The curve begins with a sea level at about 70 m below its present position 12,000 years ago. From that time to approximately 10,000 years ago, sea level rose at a rate of 1.7 m/100 yr. Between 10,000 and 6,000 years B.P., the rate declined gradually to 0.3 m/100 yr and then remained steady until 2,000 years ago. Since then, sea level has been rising about 0.1 m/100 yr according to Redfield and Rubin (1962).

Trace metals of Boston Harbor sediments

The concentrations of trace metals (Zn, V, Cd, Ni, Ca, Pb, As, Sb, and Hg) in surface sediments of Boston Harbor in Massachusetts reflect an increasing flux of these metals within wastes from the adjacent industrialized area. M. H. Bothner found that, in one part of the harbor, concentrations of the various trace metals rise above background levels at a nearly uniform 40-cm depth in the sediments. Preliminary lead-210 data indicate an approximate date of 1900 for this horizon and a subsequent sedimentation rate of nearly 0.5 cm/yr.

Trace metals and an area of possible sediment accumulation on the North Atlantic Continental Shelf

Bradford Butman has extended his observations of currents and movement of bottom sediments westward from Georges Bank in one of the two directions of apparent sediment escape from the imperfect clockwise circulation around the bank (Geological Survey Research 1978, p. 146). Preliminary results of his observations offer the possibility of an area south of Martha's Vineyard in Massachusetts serving as a potential sink for accumulation of fine material that has been winnowed from the bank and transported westward over the shelf.

In a study of trace metal concentrations in sediment cores, M. H. Bothner, E. C. Spiker, R. G. Johnson, and W. M. Ferrebee have obtained preliminary carbon-14 and lead-210 data that also suggest present accumulation of fine-grained sediments in the area south of Martha's Vineyard. This area lies within a region in which all sediments were formerly thought to be relict deposits and, therefore, additional tests have been undertaken to assess plausibility of the suggestion. If proven to be a site of modern deposition, the area will have special significance as the only major site on the Continental Shelf off the Northeastern United States where sediments and associated pollutants introduced by offshore development could be expected to accumulate.

An ancestral Hudson River valley of the Continental Shelf off New Jersey

Using seismic reflection profiles of the Continental Shelf off New Jersey, H. J. Knebel has identified a large buried channel that branches from the existing Hudson shelf valley off northern New Jersey and extends southward at least 80 km. Like the channel of the present Hudson shelf valley, the buried channel has a flat bottom, a width of 2 to 17 km, and relief of 3 to 15 m. Fill of this apparent ancestral pathway of the Hudson River across the shelf consists of heterogeneous fluvial deposits capped by an additional 10 to 30 m of sediments. Vibracore samples of the upper part of the sedimentary fill consist of interbedded marine sand and mud layers. Radiocarbon ages, micropaleontologic analyses and geotechnical properties of these samples indicate formation and filling of the valley more than 28,000 years ago and subsequent subaerial exposure during at least one sea-level regression. The profile and cores provide the first unequivocal subbottom evidence for flow of the ancestral Hudson River to the south of the existing valley and across an exposed continental shelf during the Pleistocene.

Observations from a submersible of slumps on the upper continental slope south of Georges Bank

R. A. Slater and J. M. Aaron used a research submersible to make direct observations of slumped and unslumped areas on the upper continental slope south of Georges Bank, in order to gain added information on submarine mass movement of sediments. In this area, slump scars were found to have steep slopes (20° to 45°), clay outcrops, and many burrows and depressions inhabited by a variety of megabenthic crustaceans and fish. Below the scars, the seafloor has a stepped topography with reverse slopes and hummocks. In contrast, the seafloor of unslumped areas has smooth gentle slopes (5° to 8°) and sparse faunas.

Reefs and hardgrounds of the Georgia Bight

V. J. Henry, M. M. Ball, and Peter Popenoe have analyzed sidescan sonar profiles and vibracores to identify and determine the nature of "reefs and hardgrounds" on the Continental Shelf off Georgia, South Carolina, and Florida. Except for shelf-edge reefs, the patchy distribution of these features is currently unpredictable. The "hardgrounds" are low and moderate relief features that provide attachment for marine organisms and apparently are related to one or more near-surface acoustically hard layers that crop out in low areas formed by erosion or nondeposition. Exposures of the hard layer are less common near shore, probably because the overlying Quaternary sediments have greater thickness and the layers have been partly removed by stream channeling during periods of lowered sea level. The hard layers also are less common off Georgia than to the south off Florida and to the north off South Carolina.

The shelf-edge reefs form a well-defined ridge or group of ridges that usually have high relief and are located in water depths of 20 to 110 m near the initial break in slope at the edge of the Continental Shelf. These reefs are present from Cape Hatteras to Fort Lauderdale and, where dredged off Georgia, consist of well-lithified oolitic conglomerates. From a submersible, the shelf-edge reef appears to be composed of slablike tabular blocks that lie flat or at an angle to the bottom and are broken by many joints. Organisms, including alcyonarians, ascidians, and numerous sponge species, encrust the blocks completely and provide a habitat for a large variety of reef fish and crustaceans, including spiny lobsters. The submersible observations support a hypothesis of Macintyre and Milliman (1970) in which the reefs are considered relict ridges or dunes (beachrock) formed during the Holocene transgression.

In a complementary contract study, O. J. Pilkey of Duke University used seismic-reflection data to select a number of targets on the Continental Shelf and inner Blake Plateau for dredging and for piston and box coring from the R/V EASTWARD during April 1978. In addition, a number of steep erosional escarpments were chosen for rock dredging in an attempt to determine reasons for their high angles of repose. All rock-dredge hauls of these features con-

tained pieces of manganese or phosphorite pavements, suggesting a nearly uninterrupted coating of the escarpments. Dredge hauls and cores of raised bottom features at average water depths of about 650 m contained living deep-water corals, which verify the presence of sensitive living environments atop the ubiquitous coral mounds on the Blake Plateau beneath the Gulf Stream. An almost impenetrable lag gravel pavement obstructed attempts to core a slump feature.

M. H. Bothner determined trace-metal concentrations in 30 samples from five cores of Continental Shelf sediments collected in the course of the foregoing studies. Several samples from the upper 3 cm of box cores represent undisturbed surficial sediment in which recent additions of trace metals from anthropogenic sources might be anticipated. Results of the determinations provided values that are generally low compared to average crustal abundances for the trace metals and offer essentially no evidence for present-day input of increased amounts.

Stratigraphy and structure of the Atlantic continental margin

Increasing amounts of geophysical and subsurface data continue to enhance the base that is available for the analysis and interpretation of the deep structure, geological relations, and associated resource potentials of the Atlantic continental margin. In order to obtain a clearer picture of the basement on which sediments of the shelf, slope, and rise were deposited, J. A. Grow constructed eight isostatic profiles and two gravity models from the large amounts of data that he and C. O. Bowin (Woods Hole Oceanographic Institution) (GS Research 1978, p. 144) had used to prepare a 10 mGal free-air gravity map of the margin between Maine and Florida. The profiles and models indicate thick oceanic crust beneath the East Coast Magnetic Anomaly, thin continental crust beneath the major sedimentary basins of the Continental Shelf, and a transitional zone of variable width between.

In a complementary study using multichannel seismic data, Grow, R. E. Mattick, and J. S. Schlee noted the existence of a linear acoustic basement ridge, which limits penetration of sound waves to depths of 6 km and less below sea level, has widths of 25 to 75 km, and separates basins of the continental rise from those beneath the shelf. The landward edge of the ridge coincides with the East Coast Magnetic Anomaly and, following the gravity interpretation, is attributed to a thick accumulation of oceanic crustal material, with its height accentuated by construction of reefs, faulting, or other processes.

Origin of the East Coast Magnetic Anomaly

The East Coast Magnetic Anomaly is a linear magnetic high that can be traced along the U.S. continental margin from Georges Bank to the Blake Spur fracture zone off Charleston, S.C., where it branches and changes character. The anomaly is bounded to the west by magnetic patterns typical of continental areas and to the east by a magnetic quiet zone that is thought to be underlain by oceanic crust of Jurassic age on the basis of linear 10 to 30 nT magnetic anomalies that parallel seafloor trends to the east. Since identification as a significant feature in 1954, many proposals have been advanced to explain its origin.

J. C. Behrendt is using digital high-sensitivity aeromagnetic survey data collected during 1974 to 1976 in a continuing study of the East Coast Magnetic Anomaly. Calculations during an early stage of this study suggested the presence of a magnetic basement ridge at depths of 6 to 8 km beneath the anomaly (Klitgord and Behrendt, 1978). The source of the anomaly may therefore be attributed to a combination of a basement ridge, which is composed of basaltic rocks (corresponding to seismic layer 2 of the seafloor) and causes short wavelength fluctuations, and an edge effect involving the contrast between thick, flat-lying nonmagnetic sedimentary successions overlying continental rock types and a thinner sedimentary sequence above a more magnetic oceanic or transitional crust.

The horizontal magnetic gradient is steepest on the northwest flank of the anomaly between Georges Bank and Cape Hatteras and on the southeast flank to the south of Cape Hatteras. Behrendt attributes the steepest gradient to the edge effect and has used it to map the boundary of the ridge-oceanic crust. He infers that a linear relationship between amplitude and gradient on the northwest flank of the anomaly to the north of Cape Hatteras results from a variable intensity of magnetization in the basement ridge at a relatively constant depth.

Behrendt also has calculated a general theoretical model for a number of profiles across the basement magnetic ridge using Werner depths for the structure and inversion techniques to obtain best fits for intensity and direction of magnetization. With differing magnetizations, the model fits the anomaly for highest amplitude (approximately 700 nT) south of Georges Bank, lowest amplitude (approximately

150 nT) southeast of the Baltimore Canyon Trough, and the portion of the anomaly south of Cape Hatteras where the steepest gradient is on the southeast flank.

K. D. Klitgord has used the aeromagnetic data described above, together with multichannel seismic reflection data, to compare basin and platform locations on the North American and African continental margins. For a reconstruction of the Atlantic at about 175 million years ago, the results are indicative of a strong influence of initial rifting at sites of basin formation. Details of the initial early Jurassic rift pattern are evident in the depth to magnetic basement maps, and nearly all initial minor (approximately 10–30 km) and major offsets connect with fracture zones in adjacent oceanic crust.

Stratigraphic test wells on the Outer Continental Shelf

Using a logging format, P. A. Scholle, H. L. Krivoy, and J. L. Hennessy (1978) have summarized information for one of the stratigraphic test wells drilled by industry off New Jersey (COST No. B-2). A comparable set of logs for another well located in the southeast Georgia embayment has been completed. The logs include data that permit chrono- and litho-stratigraphic identification of seismic reflecting units, and, together with successes and lack of successes in industry's exploratory program, they provide a greatly enhanced base for assessing the geologic environment and associated oil and gas resource potentials. For the Baltimore Canyon region east of New Jersey, the combination of exploration failures, well data, and geophysical records has transferred petroleum interests eastward from large structures beneath the shelf to an area of faulting near the edge of the shelf and to the acoustic basement ridge and associated reefs (Mattick and others, 1978) which underlie the continental slope and are interpreted to have formed the edge of the continental platform during Mesozoic time.

R. E. Mattick suggests a possible analogy between the marginal reefs beneath the slope and the carbonate reef trends of the Edwards Limestone of Texas and the El Abra-Tamaulipas Formation of the Mexican Golden Lane relative to location of potential petroleum reservoirs and relations between potential reservoirs and seals.

W. P. Dillon envisions the following geologic history for the southeastern U.S. continental margin on the basis of geophysical data for the basement and a combination of a deep-penetration seismic profile off Jacksonville, Fla., and information from the stratigraphic test well off Georgia.

Rifting of continental crust with erosion of highlands and sediment deposition in fault basins initiated margin development during the Triassic. In Early Jurassic time, 185 to 175 million years ago, igneous intrusion and extrusion provided mafic materials that mixed with sediments from adjacent uplands to produce the transitional basement beneath the present Blake Plateau. As marine waters invaded, reefs formed on fault-block highs. A reorganization of plate movements about 175 million years ago resulted in a 200-km eastward jump of the rifting and seafloor spreading axis. Then about 140 million years ago a reef began to develop at the site of the present Blake Escarpment. It bounded a broad reef platform and grew upward nearly 2 km before it died in Berriasian time and was replaced by another reef that took over its function as a sediment dam and was located 70 km to the west. Until this later reef died at the end of the Early Cretaceous, the outer Blake Plateau was the site of carbonate bank development; to the west, sediment deposition became increasingly terrigenous. Throughout Late Cretaceous and Paleocene time, the Plateau and Outer Continental Shelf areas remained sites of moderate-depth, quiet-water deposition of chalk and terrigenous mud. Later, the upper Paleocene sediments were eroded vigorously, presumably by the onset of post-Paleocene Gulf Stream flow across the inner Blake Plateau. The present continental shelf results from sedimentary accumulation limited seaward by the flank of the Gulf Stream.

Organic geochemistry of a stratigraphic test well, southeast Georgia embayment

In an evaluation of petroleum source-rock potentials of lithologic units sampled in drilling the stratigraphic test well in the southeast Georgia embayment (COST GE No. 1 Well), R. E. Miller, D. M. Schultz, G. E. Claypool, and M. A. Smith found evidence of significant contamination of well cuttings by drilling mud additives and possible diesel fuel in the upper 6,000 ft of the hole. The degree to which the mud additive influenced the extractable $C_{15}+$ hydrocarbons, thermal pyrolysis maturity, and richness characteristics could result in a misleading evaluation of true source-rock potentials in marine clays of the 3,000- to 6,000-ft interval. Below 6,000 ft, however, the amounts of contamination by mud additives were significantly less,and the maturity indicators exhibit a consistent gradual increase with depth. The Lower Cretaceous sedimentary rocks from 5,950 to 8,900 ft have larger amounts of hydrogen deficient kerogens, with pyrolytic hydrocarbon-

to-organic carbon ratios of 10 percent or less and other geochemical properties indicative of very poor source beds for liquid petroleum hydrocarbons. Vitrinite reflectance values of R_0 0.6 percent and kerogen color alteration values of 2+, considered necessary for the onset of petroleum or natural gas generation at geologically significant rates, are approached at sample depths of about 9,000 ft. Below 9,000 ft, however, the sediments have low contents of organic matter and poor hydrogen quality of the kerogen and, therefore, probably have little or no source-rock potential.

GULF OF MEXICO

Cooperative study of the Texas inner Continental Shelf

Since late 1975 when they launched a joint systematic study of the geology and biology of the submerged territorial lands, which extend to a distance of 3 leagues (10.3 m) off Texas, the USGS, through its office at Corpus Christi, and the Texas Bureau of Economic Geology at the University of Texas have collected about 4,000 nautical miles of high resolution seismic reflection profiles and 6,600 bottom samples. The profiles were obtained along tracks that are generally about 1 mile apart and the bottom samples on a 1-mile grid spacing. C. W. Holmes and E. A. Martin have made a preliminary study of this material, noted indications of sand deficiencies on the northern Texas shelf in areas where shoreline erosion has been severe, and found evidence that the Willamar fault zone of the southern Texas coastal plain crosses obliquely onto the Continental Shelf to form part of an extensive offshore fault system.

Turbidity structures in Corpus Christi Bay, Texas

On the basis of synoptic in situ measurements of light transmissivity and suspended sediment concentrations, G. L. Shideler was able to establish a time sequence for six turbidity structures along the longitudinal trend of Corpus Christi Bay and its tidal inlet. The observed bay turbidity structures were highly variable in time and space, ranging from a vertically homogeneous water column to a well-stratified column that had an increasing turbidity gradient with depth. Wind appeared to be the dominant forcing agent of turbidity toward the bayhead sector where it generated waves for bottom-sediment resuspension and regulated fluvial sediment influx from the Nueces River. Tidal forcing effects from Aransas Pass inlet appeared to be the dominant controls of turbidity toward the baymouth sector. Discharge characteristics of the Nueces River and mean density of the bay's water column had no discernible influence on the observed bay turbidity structures.

Late Tertiary tectonics event in the southwestern Gulf of Mexico

In a continuing study of the geologic framework of the Gulf of Mexico, R. G. Martin has assembled and analyzed evidence for a late Tertiary episode of widespread tectonic activity within the southwestern part of the Gulf. Here the continental slope of the Golfo de Campeche is a region of knolls and open basins underlain by diapiric and nondiapiric masses of probable salt. Most salt, or saltlike, structures underlie the western and uppermost parts of the slope and the adjacent shelf and suggest continuity between the Sigsbee Knolls structures of the abyssal plains beneath the central gulf and the onshore isthmian salt basin structures in the Mexican states of Tabasco and Campeche.

Although it is similar topographically to the continental slope of the northern gulf and has comparable internal salt structures, the Golfo de Campeche includes numerous broad, linear hillocks composed of thick sections of continental slope and abyssal plain strata that have been uplifted, folded, and faulted by tectonic events which apparently were unrelated to salt mobility. Stratigraphic evidence from Deep Sea Drilling Project (DSDP) boreholes in the Sigsbee Knolls, Sigsbee Plain, and east Mexico slope indicate late Pliocene and early Pleistocene ages for the youngest strata involved in the deformation. Fold-axis orientations and evidence of reverse (thrust) faulting suggest that compressional forces rather than uplift and salt instrusion were the primary cause of deformation. Salt emplacement on the slope apparently resulted from both quasi-continuous diapiric movement beginning soon after Middle Jurassic deposition and Pliocene and Pleistocene tectonic mobilization and flow into anticlinal cores.

Support for a late Tertiary episode of deformation in the Golfo de Campeche Slope province includes post-Miocene left-lateral faulting transverse to Laramide trends in the Chiapas foldbelt to the south, continental rifting and associated late Tertiary and Quaternary volcanism across Mexico to the west, abundant evidence for late Pliocene folding to form ridges of the Mexican slope to the west and northwest, and data indicative of late Cenozoic east-west spreading in the Cayman Trench to the east.

Seasonal drift patterns off the Texas coast

G. W. Hill has prepared a series of maps summarizing the speeds and directions of coastal current drift along the Texas coast determined through 7 years of observing ballasted surface drift bottles and Woodhead-type plastic seabed drifters. The maps illustrate a yearly cycle of water movement parallel to the coast controlled by seasonal winds. Some areas are characterized by complex convergences and a stratified water column, whereas others have simpler longshore trends. Atypical winds can alter significantly the usual drift pattern of any season.

Vector patterns obtained by summation of all drift observations for each release point suggest a net southward onshore surface drift off the north and north-central Texas coast, and northward off the south Texas coast, separated by a region of westward (onshore) movement off the south-central coast. Average bottom drift is to the south for the entire study area without a preferred onshore-offshore direction. Overall drift velocities were greater at the surface than near the seafloor.

Effects of cyclic loading on underconsolidated sediments

In a continuing study of the effects of storm waves and other cyclic loading events on the rapidly deposited, underconsolidated sediments of the Mississippi Delta region, L. E. Garrison and his associates implanted a set of accelerometers at depths of a meter below the seafloor to measure sediment movement and several piezometers at various depths between 3 and 16 m to measure sediment pore pressures. Measurements were recorded by these instruments and others over a 6-month period in the winter of 1975–76 and a 12-month period from November 1976 to December 1977. Results demonstrate conclusively a direct effect of storm waves on sediment strength, principally by driving pore pressures above ambient pore pressures that normally exceed hydrostatic pressures in the underconsolidated sediments.

The effects of the cyclic loading were especially noticeable during a winter storm in February 1977 when pore pressures rose 2.4 psi above ambient levels at the 3-m depth and 5.0 psi at 15 m. Again during Hurricane Anita in September 1977, pore pressure at 15 m increased by 6.5 psi. At elevated levels such as these, the effective stress in the sediment, defined as the difference between total stress and pore pressure, approaches zero, at which point shear strength also becomes zero and failure occurs. An accelerometer recording of a sudden reorientation (tilt) during the hurricane indicates that actual failure probably took place at this time. When recovered, the accelerometer vessel was found 5 m below its original depth of burial. These observations on reactions of the metastable water-gas pressures within sediment pores help substantiate the caution that must be applied in characterizing the foundation properties of sediments on the basis of static tests alone.

PACIFIC CONTINENTAL MARGIN

CALIFORNIA TO WASHINGTON

The introduction of an early USGS Bulletin begins—"One of the most novel and interesting sights along the coast of Santa Barbara County is that of the derricks marking the location of the oil wells which start down from wharves over the Pacific Ocean at Summerland." (Arnold, 1907). Drilled between 1896 and 1900, these wells provided the Nation's first offshore oil and gas.

An earlier USGS Bulletin entitled "Earthquakes in California in 1889" (Keeler, 1890) marked the initial report of an activity that now constitutes an important service of the Geological Survey—to monitor and provide information on earthquakes, one of the potentially devastating natural hazards for man. Followed by another bulletin outlining results of one of the most definitive studies on the causes and effects of the San Francisco earthquake and fire of 1906 (Gilbert and others, 1907), the USGS achieved worldwide recognition as a leader in research on earthquakes and their potential impacts.

Offshore oil and gas and potential earthquake hazards provide two of the principal foci of today's marine geologic investigations off the western and Alaskan coasts of the United States. Another principal focus, sedimentary processes, encompasses subjects that are closely related. Geographically, the submerged borderland off southern California continues to attract much attention—attention that has progressed from little more than dreams of potential subsurface oil pools at the turn of the century when G. H. Eldridge of the Survey first examined the Summerland District (Arnold, 1907, p. 7) to detailed examination of subsurface stratigraphy, structure, and sedimentary processes that are permitted now by advances in offshore exploration and development techniques.

Geologic framework of the southern California borderland

Based on a synthesis of stratigraphic and structural information and analogies with correlative

rocks throughout mainland California, J. G. Vedder and D. G. Howell conclude that the Jurassic and younger rocks of the California borderland are indicative of nearly continuous continental margin activity. Two types of basement rocks are juxtaposed, (1) Upper Jurassic(?) through lower Tertiary(?) melange and blue-schist of a subduction or accretionary complex, overthrust by (2) Upper Jurassic ophiolitic, arc-volcanogenic, and forearc sedimentary rocks. The distribution of basement within the overriding plate implies east-west foreshortening. Spatial relations of upper and lower plate rocks suggest northwest-directed dislocation of basement blocks beneath the borderland.

Thick wedges of clastic sediments composed largely of turbidites accumulated in forearc basins during Cretaceous and early Tertiary time. Restricted middle Cretaceous and late Paleocene hiatuses and concurrent lapses in regional magmatism may represent times of transform faulting that interrupted subduction. Ridge and basin topography began to emerge in middle Tertiary time as a result of wrench tectonics within the pliant intersection of the Pacific and North American plates. Tholeitic to calc-alkaline volcanism accompanied the early developmental stages of typical borderland features. In late Tertiary time, diminishing volcanic activity and concurrent crustal cooling may have caused subsidence with encroaching seas and deepening basins. Intense deformation that included rapid local uplift of several structural blocks and continued strike-slip faulting marked early Quaternary time.

Environmental geology of the southern California borderland

H. G. Greene, S. H. Clarke, Jr., and M. E. Field have made preliminary analyses of side-scan sonar records, sediment cores, and more than 3,500 km of high resolution seismic tracklines obtained during May 1978 on a cruise off southern California from Los Angeles to San Diego, over the San Nicholas platform and northwestward across Rodriguez Seamount and Arguello Canyon to the west of Points Conception and Arguello. Results suggest a need for a new tectonic model that provides for an apparent offshore tie between the Newport-Inglewood fault zone of the Los Angeles area and the Rose Canyon fault zone of San Diego and for a southeastward extension of the Palos Verdes Hill fault zone to a possible connection with a seismically active, newly-named La Jolla fault zone. Strike-slip movement within these two nearly parallel fault systems has produced compressional and dilational structures that trend obliquely across the intervening 20- to 30-m fault block. La Jolla Canyon, which is a graben of five distinct down-stepped fault blocks, provides an example of the dilational structures. Scripps Canyon at its head marks an offset caused by right-lateral movement along the Rose Canyon fault.

To the north, Greene, Clarke, and Field found levees flanking the downslope portions of the more than six heads of Arguello Canyon that notch the outer edge of the Continental Shelf. These levees suggest down-canyon transport of sediment volumes that at times were greater than canyon capacities. A fault zone on the east side of Santa Lucia Bank, north of Arguello Canyon, was traced southeastward along the slope and around Point Conception to an intersection with faults of the northeast San Miguel platform. The trace of this zone suggests a curving of offshore structures around the tip of the Transverse Ranges rather than truncation by a merging into the range structures.

Sediment transport on the San Pedro shelf, California

Based on preliminary analyses of side-scan sonar records and other data, D. A. Cacchione and D. E. Drake report great spatial variability in the nature of bedforms on the San Pedro shelf near Los Angeles and in the amounts of suspended sediment in the overlying waters. In general, well developed oscillation ripples characterize the seafloor at water depths of 20 m and less. Current energy "levels," which decrease with depth, become sufficiently low at 40 to 50 m to permit marine organisms to erase evidence of ripples and other bedforms. A unique type of cross-ripple pattern at depths of about 20 to 25 m are the result of a mechanism that is not yet understood.

Cacchione and Drake also find that, in general, concentrations of suspended sediments on the San Pedro shelf decrease seaward. Some evidence suggests seaward movement of these particulates along preferential routes. Internal waves appear to be among the relevant active processes. Definitive conclusions on processes, however, require added information on storm and winter regimes to complement that of their fair-weather data sets.

Late Miocene paleogeography of the Santa Cruz region in California

To gain a better understanding of the geologic history involved in formation of San Francisco Bay and the surrounding region, R. L. Phillips has devoted particular attention to a sequence of upper

Miocene marine transgressive sedimentary rocks in the Santa Cruz Mountains, which provide evidence of a past seaway connection between the Pacific Ocean and the San Joaquin Basin to the east. The sequence forms an east-west trending belt, which is about 8 km wide, consists of coarse dominantly crossbedded clastic rocks, and occupies the preserved remnant of this seaway. The deposits, a part of the Santa Margarita Formation, are characterized by repeated channeling, extensive lag gravels, unidirectional large-scale crossbed sets, and giant crossbeds. Paleocurrent data obtained from crossbeds indicate dominant west-southwestward sediment transport. Mudstone and siltstone overlying a sharp contact with the coarse clastic channel-fill sequence reflect termination of strong tidal flow as a result of lateral channel migration and an increase in water depths. Through palinspastic reconstruction along the San Andreas Fault, the channel-fill sequence to the west of the fault adjoins a marine basin to the east of the fault south of Coalinga, California.

San Francisco Bay

Beginning with a contribution to the Geological Survey's 15th Annual Report (Lawson, 1895), the San Francisco Bay region has remained a center of attention. This attention was intensified by the Great 1906 San Francisco Earthquake and Fire and the establishment of a geological research center at Menlo Park during the 1950's. The Bay itself is subject to a variety of both natural and man-induced impacts, some of which are difficult to distinguish from one another. This, together with its proximity to the research center, has made it a natural laboratory for increasingly detailed studies of its properties and for testing new marine geologic instruments and techniques of study.

F. H. Nichols has shown that strong seasonal and annual variations in Sacramento River flow that affect San Francisco Bay salinity, coupled with intermittent but intense biotic and abiotic disturbances of surficial sediments, contribute to nonpredictable fluctuations in the benthos. These natural fluctuations tend to mask those resulting from man's activities, as, for example, the effects of waste disposal on nearby organisms. Because the benthos is the commonly used indicator of environmental quality in coastal waters, our ability to determine and subsequently control the human impacts through routine water-quality programs will remain greatly inhibited until ways to predict the fluctuations are found.

Using routine periodic sampling of the very common circumarctic mollusk *Macoma balthica*, in conjunction with growth experiments, J. E. Cloern and F. H. Nichols (1978) developed a new model for the growth of animals by incorporating a seasonally varying coefficient in the classic von Bertalanffy model to provide greater realism. The model, which applies to many long-lived animals including fish, permits rapid interpretation of size-frequency data from field samples, which in turn are used to estimate the turnover rate of organic matter on the seabed of San Francisco Bay.

D. M. Rubin and D. S. McCulloch placed a rotating side-scan sonar, which they developed, on the floor of San Francisco Bay in order to monitor changes of bottom configuration through an 8-month interval. At the site, 400 m north of Fort Mason, sand waves with heights of 60 cm and wavelengths of 15 m migrate at average rates of ¼ cm/d. The result of the first long term observations and measurements of bedform movement at a single site, this migration rate will form a basis for comparison of data now being collected within other environments.

In a related study, D. M. Rubin and R. E. Hunter have established an equation to relate the thickness of a stratum deposited by a migrating bedform climbing at a small angle to a shape factor for the bedform, the bedform height, the rate of sediment transport, and the change in the sediment transport rate per bedform wavelength. Application of the equation to the Navajo Sandstone of northeastern Arizona permits reconstruction of a depositional terrain in which the original height of the dunes is inferred to have been many times that of the preserved sets of cross-strata.

Petroleum potential of central and northern California Outer Continental Shelf

On the basis of currently available information, D. S. McCulloch infers a low hydrocarbon potential for the basins off central and northern California. Here the principal targets for petroleum exploration are five relatively shallow late Tertiary basins. Sediment thicknesses appear to preclude attainment of hydrocarbon generating temperatures; the presence of coarse clastic sections and well-developed source beds within the basins is doubtful. Production from adjacent onshore geologic analogs has been inconsequential except in the southernmost Santa Maria Basin where most is from fracture porosity and involves considerable development. Prospective needs for similar offshore development and attendant low yield rates per well detract fur-

ther from the petroleum potential of the Outer Continental Shelf area.

Geologic hazards of the northern California-Oregon Outer Continental Shelf and slope

S. H. Clarke Jr., and M. E. Field undertook a preliminary review of information obtained in the course of a geologic reconnaissance to determine the nature and extent of potential geologic hazards to petroleum development on the Continental Shelf and upper slope in the Coos Bay basin off the Oregon coast and Eel River basin off northern California. Several active faults (that is, faults that offset the seafloor or displace Quaternary sediments) of large apparent displacement have been mapped on the inner shelf off Coos Bay and in the southern Eel River basin west of Eureka, Calif. A history of earthquakes of magnitude 5.0 and greater substantiate the recency of movements in the latter area.

Potentially unstable seafloor conditions, indicated by evidence of submarine slides and accumulation of unconsolidated sediment, are present locally at the heads of submarine canyons and on the upper continental slope of both basins. They appear to pose the greatest threat on slopes seaward of the inner shelf (plateau slope) of the southern Eel River basin where unstable conditions prevade an area of more than 150 km^2 and locally may extend to depths exceeding 300 m. The Outer Continental Shelves of both basins have been mapped and they contain very young features and are thought to be piercement structures associated with shale flowage and diapirism comparable to that reported previously from the Continental Shelf of the Pacific Northwest. Faulting and other seafloor movement accompanying formation of these structures could be hazardous to offshore installations, if flowage occurs within a conducive time scale.

Stratigraphic and tectonic framework, Oregon-Washington continental margin

Based on interpretation of multichannel seismic profiles across the continental margin of central Oregon near lat. N. 40°44′, P. D. Snavely, Jr., has identified a deep marginal basin with as much as 6,000 m of Tertiary sedimentary rocks beneath the inner shelf and above an acoustic basement of upper Eocene volcanic rocks. A middle Miocene pillow lava flow and a basalt sill, each about 30 m thick where mapped onshore in the Coast Range, can be traced seaward on the profiles for more than 15 km to and beyond the Standard-Union, Nautilus No. 1 offshore test well (Braislin and others 1971; Snavely, Pearl, and Lander, 1977). An upper Eocene to middle Miocene succession can also be traced westward from the shore to the test well where, however, the lithofacies is finer grained than in onshore outcrops.

The Outer Continental Shelf and upper continental slope are characterized structurally by imbricate landward dipping thrust faults, some of which are folded. Here, the acoustic basement consists most probably of an upper Oligocene to middle Miocene wedge of melange and broken formation similar to the "Hoh" rock assemblage mapped by Rau (1975) along the west coast of the Olympic Peninsula.

The lower continental slope consists of broadly folded and uplifted abyssal plain turbidite deposits of Pliocene and Pleistocene age, cut by thrust faults that dip eastward at low angles and are bounded upslope by small perched basins filled with Pleistocene(?) and Holocene sediments. The thrust faults are probably caused by underthrusting of oceanic crust, which forms acoustic basement on profiles to the west of the continental slope. The upper surface of the oceanic crust dips gently eastward and can be traced landward beneath the middle slope. About 3,500 m of Pliocene and Pleistocene sediments overlie it on the abyssal plain at the base of the lower slope. The underthrust model of the central Oregon continental margin, as interpreted from the multichannel seismic profiles, agrees generally with that proposed by Sealy and others (1974) and supported by the stratigraphic studies of Kulm and Fowler (1974).

Using high-resolution profiles, Snavely was also able to trace the left-lateral Calawah tear fault across the Washington-Vancouver Island shelf for more than 50 km seaward of the northwestern part of the Olympic Peninsula where the fault forms the north boundary of the "core rocks." Along the Calawah fault trace, the offset seafloor sediments include horst and graben structures, some of which have bathymetric expression. Where mapped on land in the Cape Flattery area, the Calawah fault cuts Holocene stream terrace deposits and upper Pleistocene drift, supporting the offshore evidence of recent movement.

Pleistocene terraces at Willapa Bay, Washington

Based on her analyses, Gretchen Luepke has established general correspondence of the basic heavy mineral assemblages within sands from Pleistocene terraces bordering the eastern shore of Willapa Bay and those of modern bay sediments. Mixed ortho-

pyroxene-amphibole-clinopyroxene assemblages denote a Columbia River source whereas clinopyroxene-rich assemblages characterize sources provided by rivers that drain from the east and southeast. The mixed assemblages also indicate marine conditions and longshore transport, including tides, and, therefore, terraces and modern bay sediments deposited in intertidal and subtidal environments usually contain them. Terraces and modern bay sediments of fluvial environments may have the clinopyroxene-rich assemblages, but more commonly contain mixed suites suggesting either tidal influences or derivation from older marine sediments cut by the streams.

Sediment transport processes on the Monterey Deep-Sea Fan

In their continuing study of the Monterey Deep-Sea Fan, W. R. Normark and G. R. Hess made detailed studies of two areas, a 30-km^2 area of abyssal-depth sediment waves and a large mass-flow deposit. The sediment waves are associated with a levee of the Monterey Fan and, assuming a two-layer model for water circulation, are products of low velocity (10 cm/s), low concentration turbidity flows about 100 to 800 m thick. Gravity cores from the central part of the mass-flow deposit show that its upper 2 to 5 m consists of 20 to 35 cm of gray-green mud overlying a highly cohesive mudball conglomerate with well rounded to angular mud clasts and sparse matrix. The continental slope off Point Sur, California, is the likely source for this deposit.

ALASKAN CONTINENTAL MARGIN

Discovery of potential source rocks for petroleum, eastern Gulf of Alaska

As co-chief scientists of a cruise along the continental slope in the eastern Gulf of Alaska, George Plafker and P. R. Carlson directed a seafloor dredging program that has provided samples of a previously unknown Eocene sedimentary sequence containing argillaceous lithologies with favorable source-rock potential for petroleum. The potential source rocks were obtained from water depths between 2,640 and 1,270 m and consist of moderately indurated dark-brown shales and claystones that are commonly glauconitic and pyritic and less commonly concretionary or laminated. They have extremely abundant foraminiferal and siliceous microfaunas, numerous large fish scales, and carbonized plant fragments. The argillaceous fragments of the dredge hauls were accompanied by pieces of palagonitized green and black basaltic glass, light-greenish gray, waxy, slightly calcareous siltstone, grayish-green medium-grained, quartzo-felspathic sandstone, glauconitic sandstone, and carbonaceous sandstone. Abundant slickensides on fracture surfaces within the dredge samples indicate shearing of the sequence.

On the basis of coccoliths, J. D. Bukry assigns an Eocene age to the sequence and an early Eocene age (*Discoaster lodoensis* Zone) to at least a part of it. The coccoliths indicate deposition in warm water at depths ranging from shallow to bathyal.

G. E. Claypool reports preliminary determinations of organic carbon values of 1 percent to as high as 1.64 percent from the argillaceous fragments obtained from three dredge hauls. The organic matter, though thermally mature, is hydrogen deficient, favoring a gas rather than liquid hydrocarbon source potential for units represented by the samples. The deficiency, however, may reflect a hydrogen loss associated with seafloor weathering. In any case, the dredge samples differ markedly from those of coeval units that crop out on land and consist of hard, complexly deformed, coal-bearing continental and nearshore marine rock types that appear to have little or no petroleum potential.

Neoglacial sedimentation in Glacier Bay, Alaska

P. R. Carlson and B. F. Molnia are able to distinguish at least two stratigraphic units above the crystalline and metasedimentary rocks on high resolution profiles of Glacier Bay, an area of deglaciation within the past 200 years. The lower unit appears to include ice-contact, glacial-fluvial and glacial-marine deposits as it is characterized by common irregular, discontinuous hummocky reflectors typical of till and by scattered sediment masses with parallel reflectors that suggest stratified drift. The upper unit is distinguished by even, continuous parallel reflectors that suggest deposits of glacial flour carried into the fjords by glacial melt waters. Some layers may be products of deposition from density flows caused by slumping, especially near the active ice front.

The thickest deposit of neoglacial sediment was found in the lower West Arm of Glacier Bay, is about 200 m thick, and has been accumulating since 1860, providing an accumulation rate of 1.7 m/yr. In upper Johns Hopkins Inlet, sediments collected in depression on the fjord floor have thicknesses exceeding 160 m and accumulation rates as high as 2.3 m/yr. Muir Inlet, which has been lengthened by a 45 km retreat of the Muir Glacier in the last 120

years, has as much as 115 m of neoglacial sediment in the central deepest part of its channel. In the portion of upper Muir Inlet where the terminus of Muir Glacier was located between 1961 and 1964, the bedrock basin contains a maximum of 60 m of sediment, indicating accumulation at a rate of 4.3 m/yr. Not all stable ice-front positions have thick sedimentary bodies, however, as almost no sediment exists adjacent to Riggs Glacier, a tributary of Muir Glacier with an ice-front that has changed little since 1960. And this contrasts with the more than 100 m of sediment in front of McBride Glacier, another tributary with a similar ice-front history. Carlson and Molnia conclude that no correlations can now be made between the time since beginning of ice retreat, rate of retreat, or thickness of accumulated sediment. They note further, however, that in areas of glaciation, such as Glacier Bay, thicknesses of recent sediment are generally great and rates of accumulation high compared to thicknesses and rates of other types of marine deposition both within and outside the areas.

Comparison of sedimentation in Yakutat and Icy Bays, Alaska

In studies related to the foregoing, P. R. Carlson and B. F. Molnia have also used high resolution seismic profiles to compare sediment accumulation in two rather recently deglaciated bays that border the eastern Gulf of Alaska farther north. Yakutat Bay, a fjord that was last filled by Hubbard Glacier about 600 years ago, has glacially scoured bedrock walls and a series of three irregular marginal ridges. Each moraine has intramorainal basins that are as much as 500 m across and contain several meters of modern sediment. Deep basins separating the moraines are filling rapidly with clayey silt. In the upper bay, as much as 140 m of this modern rock flour has accumulated in about 200 years, amounting to a deposition rate of 70 cm/yr.

In comparison, deglaciation of Icy Bay began in the early 1900's and continues today with rapid retreat of Guyot, Yahtse, and Tyndall Glaciers (approximately 40 km in 70 years). Icy Bay also contains discrete depositional basins separated by glacially scoured bedrock sills and recessional moraines. A basin behind the bay-mouth moraine was filled with a maximum of 75 m of sediment between 1922 and 1976—an accumulation rate of about 1.4 m/yr. Near the present ice margin, the seismic profiles show basins with more than 40 m of unconsolidated glacial flour and, thereby, a more rapid rate of accumulation than in either Yakutat Bay or Lower Icy Bay.

Sedimentation in coastal embayments of the northern Gulf of Alaska

Using an approach that differs from the foregoing, B. F. Molnia has compared old maps and aerial photographs to demonstrate that during the past 2 centuries, glacial-fluvial, glacial-marine, and littoral sedimentation filled completely at least three major embayments along the northern Gulf of Alaska coastline and caused significant shoaling in Icy, Yakutat, and Controller Bays. Vancouver's Icy Bay, a former embayment to the east of modern Icy Bay with an area of about 50 km^2 and maximum depth of 25 m, was filled with about .5 km^3 of sediment between 1794 and the 1830's. Tsviat Bay and Kaliakh Bay, with areas of roughly 65 km^2 and 30 km^2 in 1913, were filled prior to 1941. Icy Bay, which is still enlarging through glacier retreat, and Yakutat Bay have sedimentation rates as high as 2 m/yr. The lower basin of Icy Bay, with an area of about 480 km^2, has received more than 4.8 km^3 of sediment in the 54 years between 1922 and 1976. This volume provides an average basinwide sediment thickness of 10 m and a maximum new sediment thickness exceeding 75 m. Controller Bay covering about 800 km^2 has also shoaled significantly since the middle of the 18th century; Russian charts of the 1840's indicate water depths of 10 to 20 m at present mudflat sites.

Depositional regimens within the embayments have changed rapidly. Tsviat and Vancouver Bay are undergoing shoreline erosion today with sediment transported alongshore from Vancouver's Bay contributing to deposition in the lower basin of Icy Bay. Changes in the glacial regimen cause fluctuations in sediment yield and, thereby, control deposition and erosion within the coastal embayments. If climate does not change excessively during the next few centuries, Icy Bay, Controller Bay, and parts of Yakutat Bay will probably fill. With major climatic shifts, however, the future of the Gulf of Alaska coastline is uncertain.

Holocene sediment volume on the northeast Gulf of Alaska Continental Shelf and the sediment contribution of present-day rivers

B. F. Molnia, P. R. Carlson, and W. P. Levy calculated a volume of 300 km^3 for the Holocene sediment on the northeast Gulf of Alaska Continental Shelf by planimetering an isopach map of surface sediments (Carlson and Molnia, 1976) between Yakutat Bay and Montague Island. If uniformly distributed over the 55,885 km^2 of the entire shelf, this sediment would have a thickness of about 54 m. The

distribution, however, is not uniform. West of Kayak Island, 38 percent of the 3,300 km^2 shelf area has no Holocene sediment, and the remainder has an average Holocene sediment thickness of 65.5 m, providing an overall average of 40.8 m. East of Kayak Island, corresponding amounts for the 25,600 km^2 shelf are 23 percent bare, 90.2 m average thickness elsewhere, and overall average thickness of 69.1 m.

East of Kayak Island, much of the uncovered surface is at the shelf edge in water depths near 200 m, seaward of the growing wedge of Holocene sediment. This contrasts with the western area where most of the uncovered surface has water depths of 100 m or less. Here Holocene sediment apparently has been scoured and resuspended by strong bottom currents and storm waves that prevent accumulation and presumably transport it beyond the shelf break.

Suspended sediment contents have been measured for most rivers and streams draining into the Gulf of Alaska. Variation is great with discharged amounts depending on the time of year, on whether a particular stream drains the coastal plain or is fed glacially, on the quality of runoff, and on other factors. Sediment yields from the Malaspina Glacier drainage systems and the Copper River, two of the major sediment sources, are calculated at .095 km^3/yr and .053 km^3/yr, respectively; together these sources appear to contribute between one-third and one-half of the sediment input to the Gulf of Alaska. If these rates are projected back for the 10,000 to 12,000 years since deglaciation of the shelf, the Copper River and Malaspina systems could account for about 1,480 km^3–1,780 km^3, or one-half to two-thirds, of the sediment now on the shelf. If other sources, including the Bering Glacier and Alsek River systems, are assumed to contribute nearly equal amounts, one can account for all Holocene sediment on the northeast Gulf of Alaska shelf. If these other sources yield more sediment, or if the inputs of the Malaspina and Copper River systems are lower now than in the past, then substantial quantities of sediment must have bypassed the shelf.

Seismic profiles which show Holocene sediment on the slope and ERTS images of suspended sediment plumes that project into Prince William Sound, around Montague Island, and westward beyond the edge of the Continental Shelf provide evidence of modern sediment bypassing the shelf. In addition, fjords such as Icy Bay, Yakutat Bay, Glacier Bay, and the lower Copper River and its delta system trap much sediment.

Movement of bedforms in the lower Cook Inlet, Alaska

Movement of sand over the bottom of lower Cook Inlet has definite tidal controls and may be influenced by storms. To gain added knowledge concerning the nature and causes of this movement, especially as it relates to potential oil and gas activities within the area, A. H. Bouma and M. A. Hampton investigated several types of bedforms beneath the inlet waters including ripples, sand waves, sand ridges, dunes, and sand ribbons. Some of the lower Cook Inlet sand waves have heights exceeding 12 m and wavelengths of more than 900 m.

Bouma and Hampton found that bottom motion is very complex and influenced by local microtopography, that the yearly amount of sand transport is small compared to the volume of the large bedforms, and that bedform migration is difficult to establish for all but the small features. Bottom water velocities, observed during July and August 1978, reached sufficient force to move significant amounts of sand only during the final few hours of each tide at times of spring tide conditions.

Volcanic ash in surficial sediments of the Kodiak shelf, western Gulf of Alaska

Surficial sediments of the Kodiak shelf contain various amounts of volcanic ash from the 1912 eruption of Katmai Volcano in Alaska. The present distribution of the ash differs from the original depositional pattern and has a relationship to the physiography that may be attributed chiefly to redistribution by ocean currents. A. H. Bouma and M. A. Hampton have used the present distribution, in conjunction with grain-size distributions, as indicators of present-day sediment dispersal patterns on the shelf. These patterns confirm shallow banks on the shelf as sites of winnowing by currents, and broad traverse troughs, together with local shallow depressions, as sites of deposition. By implication, the depositional sites also mark storage areas for potential bottom-borne pollutants. The amounts of volcanic ash influence the engineering behavior of the sediments, with enrichment causing looser packing and larger internal friction angles.

Gas-charged sediment areas in the northern Gulf of Alaska

In analyses of high-resolution seismic profiles of continental shelf areas in the northern Gulf of Alaska, B. F. Molnia, P. R. Carlson, and K. A. Kvenvolden identified Holocene sediments with acoustic properties that differ from those of correlative deposits found in other areas of the gulf. Reflector ter-

minations with acoustic turbidity for the entire 30 to 80 m of penetration characterize profiles of these sediments. In three areas—the Copper River prodelta, southeast of Kayak Island, and south of the Dangerous River—subsurface reflectors are expressed as velocity "pull-downs" that do not conform to the smooth seafloor. At a fourth site, east of the Alsek River, the seafloor is undulatory and has as much as 10 m of relief. The reflector terminations and offsets suggest the possible presence of gas-filled pore spaces that result in uneven absorption of acoustic energy.

Potential sources of gas in the Holocene sediments, which are accumulating at rates of from 4.5 to 10 m/1,000 years in the four areas, include decay of trapped organic material and seepage from deeper sources. To check the alternatives, gas contents within gravity and piston cores from the four areas have been determined. In 2 to 7 m cores from the area of anomalous acoustic returns on the Copper River prodelta, measured concentrations of hydrocarbons were only slightly higher than those of nearby areas without anomalies.

Southeast of Kayak Island, however, the gas content of surface sediment was very high and increased with depth. Methane, with concentrations reaching 2.2×10^7 nL/L of wet sediment, was the dominant gas and was probably from biologic sources. An increase in higher molecular-weight hydrocarbons was also noted for the cores from this area.

Upper Jurassic shallow-water sandstones of the Bering Sea continental margin

M. S. Marlowe, A. K. Cooper, Hugh McLean, J. R. Hein, and D. W. Scholl report the recovery of shallow-water arkosic sandstones of Late Jurassic age by dredging nine sites where acoustic basement forms the seafloor at water depths of 1,500 to 2,800 m along the Beringian continental margin between the Pribilof Islands and eastern Siberia. Preliminary lithologic and petrographic examination of the feldspathic sandstones indicates their equivalence to units in the Naknek Formation of southern Alaska and the Alaska Peninsula. The megafossil *Buchia rugosa* of one dredge haul also indicates deposition in a neritic or shallow-water environment. Other samples of the dredge hauls consist of diatomaceous mudstone and sandstone that overlie the Jurassic basement rocks and are as old as early Oligocene.

The Jurassic samples come from a basement complex that can be traced on multichannel seismic-reflection profiles from near the tip of the Alaska Peninsula northwestward to Siberia, a distance of almost 1,250 km. Prior to recovery of the samples, predicted models for the basement beneath the continental margin included a complex of deformed Mesozoic trench and deep-water slope deposits that had been accreted to the margin by oblique convergence between the Kula (?) and North American plates or, alternatively, a complex of disrupted fragments of Mesozoic slope sediments deposited along a transform or strike-slip boundary separating the plates. The dredge samples represent a belt of Upper Jurassic shallow-water sandstones between southwest Alaska and Siberia; their occurrence forces rejection of these alternatives and substitution of a model involving early Tertiary collapse and subsequent burial of the belt. Collapse along the margin exceeded 4 km locally, with subsidence of the Mesozoic basement complex amounting to 10 km and more at some places on the Outer Continental Shelf.

Sources of surficial sediment, southern Bering Sea

Using Q-mode factor analyses, W. E. Dean, Jr., has examined the distribution patterns of 58 textural and compositional variables of sediment on the Outer Continental Shelf of the southern Bering Sea (Gardner and others, 1978) and has related them to sediment sources on the Alaska mainland, the Aleutian Islands, and the Pribilof Ridge. The analyses permit the identification of three dominant sediment associations that result from the mixing of distinctive inputs from each source area by both present and past sedimentary processes.

The most significant sediment contribution, providing a coarse-grained background association over most of the shelf, is from the Alaska mainland and has a felsic composition. This background association contains relatively high concentrations of silicon, barium, rubidium, quartz, garnet, epidote, metamorphic rock fragments, k-feldspar, and illite. The second most important input, superimposed on the felsic background, derives from the andesitic terrain of the Aleutian Islands. An association with these mafic sediments as the dominant component has relatively high amounts of Na, Ca, Ti, Sr, V, Mn, Cu, Fe, Al, Co, Zn, Y, Yb, Ga, volcanic rock fragments, glass, clinopyroxene, smectite, and vermiculite. A local basaltic association derived from the Pribilof Islands is treated as a subset of the Aleutian andesite association. Fine-grained sediments of the Saint George Basin compose the third major association which has relatively high concentrations of C, S, U, Li, B, Z, Ga, Hg, silt, and clay.

Sediments of the Aleutian andesite association are concentrated within a band or "plume" that extends northwestward along the continental slope from Unimak Pass to Saint George Basin between the 100- and 200-meter isobaths and has steep gradients of characteristic properties to those of other associations. Today, bottom currents lack sufficient capacity to move even clay-size particles within the "plume," and the Bering Submarine Canyon forms a barrier to transport of sediment from the Aleutian Islands to the Outer Continental Shelf and slope. Dean, therefore, concludes that the distribution pattern for the Aleutian association is probably relict and results from movement of sediment during lowered sea levels of the Pleistocene.

Manganese-rich sediment from the Aleutian Basin, southern Bering Sea

Cores from five sites in the central portion of the Aleutian Basin of the southern Bering Sea contain a layer of brown oxidized sediment intercalated between green diatom oozes. W. E. Dean, Jr., determined that this layer has significantly less C and Fe and more Mn, Mo, Ba, Co, and Ni than the underlying and overlying reduced sediments. The differences are greatest for manganese, which is almost two orders of magnitude higher, and molybdenum, which is about 3 times higher, in the brown oxidized layer. Preliminary results of organic carbon and grain-size analyses suggest the possibility of a past interval of increased oxygen in the bottom waters resulting in precipitation of manganese oxides and absorbed trace metals (Mo, Co, Ba, and Ni) and caused by decreased organic productivity and (or) increased bottom-water circulation following the maximum glaciation of the late Wisconsinan.

Bottom boundary layers and sediment transport, Norton Sound in Alaska

D. A. Cacchione and D. E. Drake continued deploying GEOPROBES to gather added data on currents, suspended sediments, and other bottom conditions of use in analyzing the temporal and spatial variability of sediment transport on the prodelta of the Yukon during both the ice-free summer and ice-covered winter seasons. Using data of two long-term records, they were able to demonstrate tidal control of sediment transport during fairweather periods. In particular, critical shear stresses are reached during spring tide periods, resulting in small amounts of silt resuspension and bedload transport. However, most sand and coarse silt movement across the prodelta takes place during a few late summer-early winter storms when surface waves entering Norton Sound from the west generate bed shear stresses that greatly exceed threshold levels. One 3-day storm of moderate intensity in September 1977 caused more sediment transport than that of a 2-month nonstorm period.

Surprisingly, suspended sediment transport in winter (February 1978) is nearly equal to that of fairweather summer periods, despite the ice-cover reduction of wave effects and negligible input of new sediment from the frozen Yukon River. In their preliminary interpretation, Cacchione and Drake attribute winter resuspension and northward movement of silt and clay deposited on the prodelta the previous summer to astronomical tidal currents which may, in fact, be slightly stronger in the winter.

Crustal structure, abyssal basins, and Continental Shelf beneath the Bering Sea

During the 1978 field season, A. K. Cooper, J. R. Childs, and Audrey Parker prepared more than 250 sonobuoys, donated by the U.S. Navy, for deployment and use in conjunction with multichannel seismic data to resolve the thicknesses of shallow sedimentary layers and determine configurations of the deeper crustal layers along the west coast and Alaskan continental margins. Based on preliminary interpretation of the wide-angle reflection and refraction sonobuoy records for the Bering Sea, for example, Cooper, Childs, and Parker conclude that the velocity structures of the crust beneath the abyssal Aleutian basins resemble an oceanic crustal section and that those beneath the adjacent continental shelves differ and indicate thick (7–10 km) sedimentary basins overlying a typical continental crustal section.

Seafloor thermogenic gas seep, Norton Sound

Building on a 1976 discovery of assumed thermogenic hydrocarbon gases in the water column south of Nome, Alaska, and 1977 identification of a seafloor source area (Geological Survey Research, 1978, p. 155–156), C. H. Nelson, K. A. Kvenvolden, and D. R. Thor delineated and undertook detailed studies of the specific source area during the 1978 summer field season. Records of sparker and uniboom traverses across this area have two important features: (1) a series of subparallel, northwest-trending faults that displace both near-surface sediments and the underlying basement rocks and (2) near-surface acoustic anomalies that have character-

istic sharp terminations of subbottom seismic reflectors and acoustic turbidity. Like those in Holocene sediments of the northern Gulf of Alaska Continental Shelf, reported above, the anomalies are attributed to the inability of seismic signals to penetrate high-impedence, near-surface gas-charged sediments.

Side-scan sonar, 12-kHz, and 200-kHz records for the seep site have classical linear and "V" shaped return signals from the water column above the regions of acoustic anomalies. These return signals are interpreted to be gas bubble trains emanating from the seafloor throughout a 2-km^2 area. Video of underwater television drift stations over the seep site displayed gas-bubble trains originating from conical craters with seafloor diameters of 2 to 5 cm.

A vibracore sample from the most active part of the seep area exhibited gas charging and had gas cavities and expansion voids as much as 30 cm long. Gas in the cores was dominantly carbon dioxide and methane, but also included gasoline-range hydrocarbons in concentrations that were significantly higher than background values. Low methane to ethane-plus-propane ratios (<10) and the heavier hydrocarbons are indicative of a subsurface thermocatalytic origin at possible depth of 2 to 5 km. The gases have apparently migrated up faults that act as conduits to the surface. A rapid rate of vibracore penetration compared to rates at sites without acoustic anomalies indicates a reduced near-surface bearing capacity that may pose a potential hazard for structures footed in the gas-charged sediment.

Wave-generated sand and gravel ribbons in the Bering Sea

R. E. Hunter directs attention to ribbon-shaped textural segregations of sand and gravel that may be distinguished on side-scan sonar records of inner shelf areas near Nome and Port Clarence, northeastern Bering Sea. Unlike ribbons of other seas that generally have been attributed to tidal and non-wave currents, these have features that suggest generation by waves. For example, some coarse sand and fine gravel ribbons have ripples with sizes spacing ½ to 2 m and symmetrical forms indicative of generation by waves. The ripples have orientations that typically lie at near right angles to those of the ribbons and where orientations of these ripples change as a result of wave refraction in shoaling water, ribbon orientations change accordingly. Where wave ripples of variable sizes and trends have developed at differing times in sediments of divergent grain size, the textural segregations have rather irregular patterns, but their longer and straighter margins tend to be oriented roughly perpendicular to the average ripple trend.

ISLAND POSSESSIONS AND TERRITORIES

Sedimentation patterns on the Puerto Rico insular shelf

The intricate patterns and relationships of biogenic calcareous sediments and terrigenous siliceous sediments on the insular shelf of Puerto Rico have become clearer through cooperative marine geologic mapping by the USGS and Puerto Rico Department of Natural Resources. According to J. V. A. Trumbull, the prevailing westward-moving oceanic currents of the Puerto Rico area cause biogenic sediments to predominate at the eastern end of the island and to a lesser degree along the north and south coasts. Most island drainage is to the north, resulting in widespread distribution of terrigenous sediments along the north coast with sands at and near the shore and muds at the outer edge of the shelf. Terrigenous sediments dominate the nearshore shelf off the west coast where the large amounts prevent the proliferation of organisms and thereby reduce the availability of a biogenic component.

Potential sand resources of the northeast Puerto Rico shelf

In addition to clarifying patterns of sediment distribution, described above, the cooperative marine geologic mapping of the Puerto Rico insular shelf continues to disclose areas having potentially mineable sand resources. J. V. A. Trumbull reports the identification and delineation of a large area of clean biogenic sand in the Luquillo area off the east end of the north coast. Here the composition and grain sizes of the offshore sands differ from those of nearby beaches and apparently come from coral-algal reefs to the east. Although both beach and offshore sands have predominantly biogenic origins, Trumbull tentatively concludes that they are sedimentologically separate and that mining of the offshore sand would not be injurious to the shoreline.

Sand deposits of the Virgin Island platform

The depletion of onshore sand resources in the Virgin Islands has led to the initiation in 1977 of a search for offshore sources, bypassing potential beach and nearshore sources that are of fundamental importance to the island economy. The offshore search involves three phases of activity: (1) an initial broad survey of the shelf, (2) detailed inves-

tigations of identified target areas, and (3) a study of sediment dynamics. Conducted by C. W. Holmes, the initial survey provided seven target areas. Subsequent detailed examination of three of these target areas resulted in location of two significant deposits of sand. One, a "double" deposit off the southwest coast of Saint Thomas, has an estimated 30×10^6 m^3 of fine sand (0.3–0.5 mm). The second, a deposit in the central area near Buck Island, contains an estimated 12×10^6 m^3 of slightly coarser sand. Textures of the sands are very close to those of beach sands which have been used in the past for construction.

Reef limestones of the Palau Islands, Trust Territory of the Pacific Islands

Based on re-examination of photographs and other information concerning the Palau Islands in the western Pacific Ocean, Gilbert Corwin concludes that in order to explain morphologies of the existing coral reefs and reef-limestone islands, one must add a factor of essentially continuous tectonic motion to the processes of coral reef development proposed by Charles Darwin, R. A. Daly, and others. At Urukthapel in the south-central part of the island group, axial ridges of Miocene reef limestones with summit elevations exceeding 200 m have flanking terraces and terrace remnants that appear to be composed of successively younger limestones as one descends the steep slopes to the shore. This inverted stratigraphy of oldest at the top and most recent at the base is explained best by a geologic history that involves a change from subsidence to uplift during the late Miocene and at least two major cycles of sea-level fluctuations serving as controls of subsequent reef growth. Lower axial ridges and broader flanking terraces of the islands to the southwest of Urukthapel reflect lower rates and amounts of uplift. Broad barrier reefs on the north and west sides of the island group lie within regions of continuing subsidence. Future studies to investigate the differential tectonic movements will focus on the relationship between the axial and flanking island and reef limestones and should provide valuable information on late Neogene and Quaternary datum planes and events of the western Pacific region.

DEEP-SEA RELIEF, SEDIMENTS, AND MINERAL DEPOSITS

Manganese nodules from three equatorial North Pacific test sites

Using box cores and bottom photographs, D. Z. Piper and J. L. Bischoff estimated the morphology, abundance, and composition of manganese nodules at three of NOAA's Deep Ocean Mining Environmental Study (DOMES) sites in the North Pacific Ocean. They observed two morphologic nodule populations. One consists of small smooth nodules which have a sharply defined range of mean sizes from about 1.5 to 3.0 cm. The other is composed of larger granular nodules which have mean sizes that exceed 4.5 cm and commonly have a poorly defined size range. The latter population is restricted to channels between abyssal hills at DOMES site C, but not at sites A and B.

Nodule abundance apparently relates to associated sediment stratigraphy. It is high (5 kg/m^2) in areas where the uppermost layer of acoustically transparent sediment is less than approximately 20 m thick. This acoustic unit of the three test sites may correlate with the "Red Ooze Unit" of the Clipperton Oceanic Formation. Nodule compositions seem to relate in a rather complex manner to compositions of the hydrogenous components of the fine-grained sediment fraction.

Mixing of equatorial Pacific siliceous clays

J. L. Bischoff and D. Z. Piper report a direct correlation between the bulk chemical compositions of surficial siliceous clays from the equatorial Pacific and the proportionate amounts of Quaternary and Tertiary clays that are mixed to form them as indicated by micropaleontological analyses. Sediments with little or no Tertiary material have low MgO/Al_2O_3, high K_2O/Al_2O_3, low MnO, and low P_2O_5 values. Clays composed chiefly of reworked Tertiary material may have higher MgO/Al_2O_3 and P_2O_5 values that may reflect greater maturity. High MnO values in such sediment are not generally to be expected owing to postulated remobilization of manganese during low temperature diagenesis. MnO concentrations of manganese nodules that are associated with the siliceous clays and may represent final diagenetic products do not seem to relate in any obvious way to the MnO values of the sediment or to the degree of Quaternary and Tertiary sediment mixing.

Paleoenvironment of Cretaceous silicoflagellates north of Baffin Island

J. D. Bukry has examined Maestrichtian silicoflagellates from siliceous mudstone samples provided by the Canadian Geological Survey and collected from Bylot Island, north of Baffin Island in the Canadian Arctic. He reports a *Lyramula furcula* Zone assemblage that contains common *Lyramula furcula* and sparse *Vallacerta* sp. aff. *V. tumidula*

and *Corbisema* sp. aff. *C. geometrica,* a species array similar to assemblages found in the Moreno Shale of California and cores from DSDP Site 275 south of New Zealand. These three arrays, with *L. furcula* dominant, differ from the only other known Arctic Maestrichtian silicoflagellate assemblage, which was found in a core from latitude 85° N and has dominant *Vallacerta siderea.* The similarities and differences suggest closer affinity of the Bylot Island silicoflagellates with those of the Pacific Basin and constitute evidence supporting isolation of the Arctic Basin during the Maestrichtian.

Planktonic microfossils and the lower-middle Miocene boundary in the California borderland

The base of the type Langhian Stage at Cessole, Italy, has been used as the stratotype for the base of the middle Miocene (Ewing and others, 1969, App. I; Ryan and others, 1974). Some authors (for example, Berggren, 1972), however, have used the first appearance of *Orbulina,* a planktonic foraminifer genus, to define the lower-middle Miocene boundary. Following the stratotype concept, the international subseries boundary would fall within the *Helicosphaera ampliaperta* Zone of the coccoliths (Bramlette and Wilcoxon, 1967). J. D. Bukry and J. K. Crouch report 13 records of the *H. ampliaperta* Zone for microfossil-rich drill cores from the California Continental Borderland. Provincial stages identified by benthic foraminifers from these samples are Saucesian, Relizian, and Luisian. Thus, according to the coccolith zones, the provincial stages in the California Continental Borderland do not provide a consistent means for correlation with international subseries boundaries.

Deep-tow studies of the East Pacific Rise off Mexico

In support of planned submersible diving operations to study the East Pacific Rise, W. R. Normark, G. R. Hess, and their associates compiled base topographic (Normark and others, 1978) and geologic maps of the crustal region to the west of Mexico near latitude 21° N, using deep-tow soundings, side-scan sonar records, and bottom photographs. Within the map area, the crest has an axial zone that is generally 1 to 2 km wide and in which young pillow lavas and some flow basalts have been extruded. Extensional zones with numerous faults and fissures bound this axial zone of extrusion.

Since completing the base geologic maps, Normark and Hess have improved it by incorporating the results of direct observations made during 11 dives of the French submersible CYANA within the mapped area. Among observations were those of most recent volcanic activity, which have taken place within a crestal band that is narrower than the originally identified axial extrusion zone and locally only 500 m wide.

MARINE GEOLOGIC PROCESSES

Composition and source of petroleum

In order to identify sources of petroleum found within coastal environments, W. E. Reed and I. R. Kaplan of the University of California at Los Angeles have undertaken a contract study to develop a set of criteria for distinguishing (fingerprinting) petroleum and its sources. Emphasis has been devoted to determining the distribution of aromatic hydrocarbons within crude and seep oils and the nature of the seawater-soluble components of these oils. To date, each oil appears to have a distinctive distribution of aromatic hydrocarbon compounds that is independent of stratigraphic controls. Molecular compositions of the aromatic compounds in seep oils differ substantially from those of crude oils with preliminary evidence suggesting formation of some components in seeps during contact with the marine environment. Exposure to sunlight markedly increases the proportion of seawater-soluble aromatic constituents from crude oils with the composition and other properties of sunlight-exposed seawater extracts differing from those of dark controls.

Diagenetic laumontite—a low-temperature paleothermometer

The alteration of feldspathic and volcanogenic sandstones with coincident formation of the calcium zeolite, laumontite, is known to involve critical combinations of temperature, fluid pressure, framework composition, and pore-fluid composition. T. H. McCulloh, B. D. Ruppel, M. L. Holmes, and R. J. Lantz have found that as a consequence of the interplay among these factors, alteration with formation of laumontite can probably take place at any depth, from the surface to at least 7 km, and through an extreme temperature range, from about 30°C to 200°C and more. If fluid pressure can be determined, the shallowest occurrence of laumontite thereby provides a gauge of temperature or, in fossils systems, paleotemperature. As such, the presence of this mineral in sandstones interbedded with petroleum source rocks has a high potential for answering important questions about source-rock maturation and hydrocarbon migration.

Coral reefs and man's influence on them

Like tree rings, coral bands provide a record of both natural and human impacts on the environment. In one example, E. A. Shinn, J. H. Hudson, and Barbara Lidz have established a coral chronology for changes in Carbon-14 activity that extends back to the year 1620 and reflects clearly the effects of burning fossil fuels since the beginning of the industrial revolution and atomic testing from 1960 to the present. In a different but related example, they use coral band widths within a large study area as an index of coral health, on the assumption that unhealthy or stressed corals grow less rapidly than healthy ones. Their preliminary analysis suggests little change in annual growth rates during the past 50 years in a south Florida area that man has stressed harshly.

Papa'u Seamont, a submarine landslide deposit off the Island of Hawaii

Papa'u Seamount on the south submarine slope of Kilauea Volcano is a large landslide deposit about 19 km long, 6 km wide, and as much as 1 km thick. with a volume of about 39 km^3. J. G. Moore and L. C. Calk (USGS) and D. J. Fornari (Lamont-Doherty Geological Observatory, Columbia University) have investigated the landslide using dredge hauls, remote camera photographs, and submersible observations. Their results indicate that the landslide consists primarily of unconsolidated angular glassy basalt sand with scattered basalt blocks up to 1 m in size; no lava flows were observed. Sulfur contents of basalt glass from several places on and near the sand-rubble deposit are low (240 ppm), indicative of onland eruption of all the clastic basaltic material. Fornari, Moore, and Calk conclude that the Papa'u sand-rubble deposit was emplaced during a single flow event fed from a large nearshore bank of clastic basaltic material that in turn had formed as lava flows from the summit area of Kilauea Volcano disintegrated on entering the sea. The current eruptive outputs of the volcano suggest that the material in the submarine sand-rubble flow represents about 6,000 years of accumulations and that the landslide occurred several thousand years ago.

Results of this study support the concept that the sulfur content of fresh basalt glass serves as a reliable criterion for distinguishing subaerially erupted basalts that have lost sulfur by degassing from submarine-erupted basalts that have retained sulfur because ambient hydrostatic pressures have suppressed degassing (Moore and Schilling, 1973).

ESTUARINE AND COASTAL HYDROLOGY

GULF COAST

Tidal circulation in Tampa Bay, Florida

Two-dimensional digital model studies of tidal-water motion in Tampa Bay, Florida, by C. R. Goodwin indicated the presence of residual tidal currents throughout the bay. Residual currents were detected in the model by time-integration of water transport during a tidal cycle. These residual currents tend to form complex circulation patterns, which are thought to play an important role in the distribution and flushing of dissolved and suspended material in the bay.

Modeling attempts to modify selected parts of the overall circulation pattern of Tampa Bay to induce greater local flushing rates were marginally successful. Creation of large islands from dredged material and selective removal of previously deposited material improved circulation characteristics in some areas but not in others. Apparently, residual currents and resulting circulation patterns are the result of many interacting elements that are not well understood. Temporal and spatial distribution of friction and inertia in the tidal-flow system are thought to be the controlling hydraulic elements. These elements, however, are in turn influenced by the shape of the tidal forcing function, estuary dimensions, bottom configuration, bottom friction, freshwater inflow, and degree of stratification.

In general, it appeared that greater tidal circulation may be induced by promoting asymmetrical distributions of inertia and friction in estuaries. This can be accomplished temporally by using curved channels so that ebb-flow directions along a channel are not simply a 180° reversal of flood-flow directions. Asymmetrical spatial distributions of friction and inertia can be created by development of tidal-flow sections with adjacent deep and shallow areas. This causes an inertially dominated flow to develop in a deep area, and a frictionally dominated flow to form in a shallow area. A shallow area responds more rapidly than a deep area to changes in tidal-stage gradients that produce shear currents during tidal "slack" periods. Shearing action induces greater water interchange than would occur in a comparable section of uniform depth, thus contributing to greater residual currents and greater tidal circulation.

ATLANTIC COAST

Factors influencing seasonal distributions of biochemically reactive substances in the Potomac River

D. H. Peterson and T. J. Conomos completed a preliminary synthesis of the results of their Potomac River studies during 1977–78. Analyses of the major sources and sinks of O, C, N, and Si indicated that, during winter, the river is typically the dominant factor influencing water chemistry. During summer, however, waste inputs (primarily from the Blue Plains sewage-treatment facility), phytoplankton production-consumption processes, exchanges with the river bottom, atmospheric exchanges, and exchanges with Chesapeake Bay must be considered.

The study provided the first 24-hour quantitative (in situ) observations of photosynthetic activity in relation to light. Results suggested that the general spatial pattern of phytoplankton is primarily the result of light limitation and that dissolved silica is an extremely important factor in the phytoplankton-eutrophication problem.

Notwithstanding the preliminary nature of this study, an important frame of reference was provided for other more detailed and specialized studies of the Potomac system.

Studies of benthic fauna in the Potomac River Estuary

R. L. Cory and P. V. Dresler are investigating the seasonal and spatial variability of the Potomac River Estuary's benthic fauna. Grab samples of 0.15 m^2 are taken three times a year at 59 locations in seven transects located in the lower, middle, and upper estuary, and 10 stations are sampled in the Wicomico River, a major tributary of the Potomac. Sampling began in November 1977 and will be concluded in August 1979. Average numbers of animals per square meter per transect were least (350/m^2) at river mile 13, greatest (5,649/m^2) in the transition zone at river mile 68, and intermediate in the tidal river (3,000/m^2) at river miles 73 and 89. Animal distributions were patchy at each transect area; individual samples ranged from 37 to 1,581/m^2.

Excluding insect larvae and oligochaete worms, over 60 species were identified; there were 20 to 25 different species per transect. In the estuary at river mile 13, marine annelid worms comprised 75 percent and molluscs comprised about 20 percent of the population. At river mile 23, molluscs were 50 percent and marine worms were about 40 percent of the total population. In the transition zone at river mile 46, crustacean amphipods comprised 45 percent and marine worms comprised 50 percent of the population; while at river mile 68, amphipods increased to 70 percent and oligochaete worms were 25 percent of the population. In the tidal river at river mile 73, oligochaete worms and insect larvae comprised 70 percent and amphipods comprised 25 percent of the population. Oligochaetes increased to 90 percent of the total population at river mile 89.

The presence of the Asian clam *Corbicula manilensis* in the Potomac River Estuary was documented for the first time, and, although it is not yet considered a problem, this invader had already reached densities of 667 clams/m^2 at river mile 89.

PACIFIC COAST

Movement and equilibrium of bedforms in central San Francisco Bay, California

D. M. Rubin and D. S. McCulloch reported that the sand-covered floor of central San Francisco Bay is molded by tidal currents into a series of bedforms, each of which is stable through a discrete range of tidal velocity, grain size, and water depth. Many of the bedforms are moved in each tide cycle and do not require storms, floods, or abnormal flow conditions to be active. The net direction of bottom-sediment transport has been deduced from bedform asymmetry. The geometry of the central part of the bay exerts considerable control on the sediment transport pattern. Tidal flows accelerate as they pass through the narrow Golden Gate and produce ebb and flood jets that transport sediment away from the Golden Gate. Lower velocity flows that occur between the shoreline and the jets are ebb dominant within the bay and flood dominant outside the Golden Gate; these flows transport sediment toward the Golden Gate.

In the central part of the bay, where many of the bedforms are active in every tide cycle, sediment turnover, which is important in organic and inorganic exchange between the sediment and the water column, results largely from bedform migration. This rigorous hydraulic regime also acts to reduce biological turnover by benthic organisms by producing an environment more suited to animals that extract nutrients from the water column and surface and suspended sediment rather than from buried sediment.

History, landforms, and vegetation of San Francisco Bay tidal marshes

Brian Atwater reconstructed the history of the tidal marshes of the San Francisco Bay system and

is studying man-made changes in these marshes. It was determined that man has levied or filled all but approximately 85 km^2 of the original 2,200 m^2 of these marshes during the past 125 years. Concurrently, human activities caused delivery of enormous quantities of sediment to the bay system and slackening of tidal currents in sloughs, thereby contributing to the creation of nearly 75 km^2 of marsh, about half of which remains pristine. Plains situated near high-tide levels are the most extensive landforms of both historic and modern marshes. Tides rather than upland tributaries created most sloughs around the bay system, but riverine floods erected natural levees that confined tidal water in the delta. Tidal marshes around San Francisco Bay typically contain 13 or 14 species of vascular plants characteristic of salt marshes; they are dominated by common pickleweed *(Salicornia pacifica)* and California cordgrass *(Spartina foliosa)*. In the delta, tidal marshes support between 20 and 28 species characteristic of freshwater marshes and are dominated by tules and bulrushes (*Scirpus* spp.) cattails (*Typha* spp.), and common reed *(Phragmites communis)*. These contrasting communities overlap around San Pablo Bay, Carquinez Strait, and Suisun Bay. Damage to tules and bulrushes during the drought of 1976–77 confirmed that intolerance to salt causes these plants to diminish in numbers toward San Francisco Bay. The decreasing numbers of California cordgrass and common pickleweed toward the delta, alternatively, may result from unsuccessful competition against tules, bulrushes, and other species. If export equals one-quarter of net aboveground productivity, then vascular plants of the tidal marshes collectively contribute about 10 billion grams of carbon per year to other parts of the estuary.

Natural and anthropogenic influences on benthic-community structure in San Francisco Bay

According to F. H. Nichols, a study of data collected in the San Francisco Bay estuary over the last 65 years showed that numbers of macrofaunal species are greatest in the marine environment of the central region near San Francisco and decrease toward the north and south. This distribution has traditionally been attributed to differences in absolute values of salinity and sediment texture. Recent USGS studies of both the benthos and the physicochemical environment near the substrate suggested that species distribution is more related to temporal variation in salinity and to intermittent disturbance of bottom sediments by storm-generated and seasonal wind waves and by the seasonally alternating high and low river inflow. Physical disturbance of the substrate apparently contributes to a state of nonequilibrium in the benthic community, especially in the shallow reaches; the community, dominated by colonizers, reflects an early stage of species succession. Some of the most successful species under these conditions are those introduced from other estuaries.

Maximum values of total benthic biomass, in contrast to numbers of species, were found in the southern part of the bay, thus probably reflecting reduced salinity variability, somewhat greater stability of subtidal sediments, and large quantities of food (high sewage-waste loadings, high concentrations of suspended particulate matter, and moderate to high standing stock of primary producers) resulting from shallow depth and the absence of strong water circulation. High biomass can also be attributed to the successful establishment of several large and abundant introduced species that thrive in the southern part of the bay.

Although waste once was an apparent cause of reduction of numbers of species, the effect of waste disposal on the benthos is now often masked by natural perturbations resulting from biotic and abiotic disturbances of surficial sediments and by inhomogeneous distribution of the animals. Anthropogenic influences on benthic-community structure other than that resulting from the introduction of exotic species will become increasingly difficult to quantify and therefore to predict. Future changes in the biota may be expected with continued reduction in freshwater flow into the estuary.

Temporal dynamics of copper, zinc, and silver related to freshwater discharge in southern San Francisco Bay

Significant contamination of the tellnid clam *Macoma balthica* by copper and silver was observed by S. N. Luoma and D. J. Cain at stations in southern San Francisco Bay. The degree of contamination appeared to be greatly influenced by the discharge of freshwater into the southern part of the bay. Local runoff appeared to be an important source of the contaminants, especially in the summer and fall. Freshwater discharge, either from local sources or from the Sacramento-San Joaquin Delta, also provided the force that flushed biologically available copper and silver from the southern part of the bay, and the degree of this flushing force appeared to determine the magnitude of annual peak in copper and silver concentrations in the clam. A metal-discharge

index that combines an indirect estimate of annual metal loading (derived from cumulative rainfall) and the inverse of freshwater discharge at the delta, explained 60 to 80 percent of the temporal variance in the silver and copper concentrations of *M. balthica*. The index represents a first step toward quantitatively predicting the effect of any reduction in freshwater discharge into the bay on silver and copper contamination in the southern part of the bay. Significant differences between temporal variations in zinc concentrations in clams and variations in copper and silver concentrations suggested that not all contaminants have similar effects in southern San Francisco Bay.

Population biology and production of *Gemma gemma* in San Francisco Bay

Populations of *Gemma gemma* at three intertidal elevations in San Francisco Bay were studied by J. K. Thompson to determine population structure, stability, and production, and to compare these to previous descriptions of *G. gemma* on the east coast. Thompson found that in San Francisco Bay, *G. gemma* live about 2¼ years, attain sexual maturity in 1 year, have 3 to 4 broods per lifetime, and release juveniles from May through November. Although San Francisco Bay females have more broods per lifetime, a reduction in the number of juveniles per brood in the late brooding season may mean that there are no more recruits per season in San Francisco Bay than on the east coast. There were fewer species in the *G. gemma* community in San Francisco Bay than in east coast communities; however, this did not appear to affect the relative success of *G. gemma*—competition between *Macoma balthica* and *G. gemma* at a nearshore station may have resulted in a smaller *G. gemma* population. Annual production at the three stations was estimated at 1.9, 11.0, and 10.6 g ash-free dry weight/m^2, which is high compared to production values for other estuarine animals.

Plankton dynamics in San Francisco Bay

As an expansion of ongoing studies of chemical-biological processes in San Francisco Bay, J. E. Cloern initiated new approaches to the study of phytoplankton dynamics, including documentation of changes in species composition, size composition, and three-dimensional spatial distribution of algal populations over an annual cycle. These field studies demonstrated that microflagellates (smaller than about 15 μ) contribute a substantial part of the total phytoplankton biomass in the San Francisco Bay system, particularly in the southern part. Diatoms became dominant only in the northern part of San Francisco Bay during summer, and their large summer population densities were apparently the result of physical entrapment by estuarine circulation coupled with rapid population growth in lateral shallows, where light availability is not limiting. An empirical model of algal photosynthetic growth rate (Cloern 1978) substantiates the hypothesis that the shoals are areas of net algal population growth, whereas the deeper, turbid, central channel is a net sink.

Simultaneous studies of zooplankton dynamics demonstrated that the southern part of the bay supports a very large zooplankton biomass that is dominated by the copepod *Acartia clausi* year-round and includes rotifers and ciliates during spring. Zooplankton composition in the northern reach is more diverse because of the longitudinal salinity gradient there.

Sources and sinks of oxygen, carbon, nitrogen, and silica in San Francisco Bay

Studies by D. H. Peterson showed that the distributions of biologically reactive dissolved oxygen, carbon, nitrogen, and silicon (OCNSi) in the main channels of northern San Francisco Bay are related to winter and summer variations in the dynamics of the estuary. At moderate or higher (>500 m^3/s) river flow, OCNSi distributions in the estuary frequently are nearly conservative. Thus, during high river-discharge periods, the relative effects of additional estuarine sources and sinks (waste inputs, phytoplankton production, and remineralization, or atmospheric- and benthic-exchange processes) appear to be minimal. At such river flows replacement time for estuarine water is on the order of weeks, whereas the OCNSi replacement (turnover) times owing to additional sources and sinks are longer. The turnover time of NH_3-N, however, is shorter. The river and ocean are probably not major sources of NH_3 to the estuary.

Marked departures from near-conservative OCNSi distributions occur during low river flow (<200 m^3/s) when the magnitudes of the local sources and sinks may exceed river and ocean inputs. As an overview, however, several processes seem to control these distributions at comparable rates and no one factor dominates. Dissolved oxygen is typically 5 to 10 percent below saturation concentrations; dissolved carbon dioxide is 150 to 200 percent above

saturation concentrations and in approximate balance with oxygen consumption; phytoplankton production keeps pace with waste inputs of nitrogen; and dissolved silica is maintained above concentrations that would be limiting for phytoplankton growth.

Distributions of carbon and stable-carbon isotopes in waters and sediments of San Francisco Bay

According to Elliott Spiker and L. E. Schemel, distributions of $P(CO_2)$ and $\delta^{13}C$ of dissolved inorganic carbon (ΣCO_2) in San Francisco Bay indicated that the bay is a source of CO_2 to the atmosphere and to the ocean during low river-discharge conditions. The $P(CO_2)$ decreased from values as high as four times the atmospheric level at the confluence of the Sacramento and San Joaquin Rivers to near or below atmospheric level seaward of the Golden Gate. The $\delta^{13}C$ (ΣCO_2) was lowest in the Sacramento River (about -10.0 permil), increasing to marine values in the Gulf of the Farallones (about $+2$ permil). At the Golden Gate, values were about 2 permil less than those seaward, thus indicating that at least 10 percent of the ΣCO_2 was of biogenic origin and were the result of respiration and decomposition. In the southern part of the bay, alkalinity and $P(CO_2)$ levels increased southward while $\delta^{13}C$ (ΣCO_2) and salinity decreased. Municipal waste discharged into southern San Francisco Bay is the probable source of the excess biogenic CO_2.

Apparent depletions of $P(CO_2)$ in northern San Francisco Bay coincided with increases of chlorophyll *a*, particulate organic carbon (POC), and $\delta^{13}C$ (ΣCO_2). The $\delta^{13}C$ (POC) values during March 1977 approached those predicted for in situ algal production, thus suggesting that an estimated 80 to 90 percent of the POC was produced in the seaward part of northern San Francisco Bay. In situ algal production was an important source of POC in the river. However, in the turbidity maximum less than two-thirds of the POC appeared to be riverborne; at least one-third was produced in situ, resuspended from bottom sediment, or transported landward from the estuary by circulation. *Spartina* salt-marsh grass was not identified by $\delta^{13}C$ as a significant source of detritus in the bay. The $\delta^{13}C$ of sediment total organic carbon (TOC) indicated that riverine carbon from the Sacramento-San Joaquin Rivers is diluted by estuarine and marine carbon in the bay. The $\delta^{13}C$ of suspended POC and sediment TOC approached marine values seaward of the Golden Gate.

MANAGEMENT OF NATURAL RESOURCES ON FEDERAL AND INDIAN LANDS

The Conservation Division is responsible for carrying out the USGS's role in managing the mineral and potential water-resource development sites on Federal and Indian lands, including the Outer Continental Shelf; that includes, in particular, the conservation and evaluation of the leasable mineral resources and waterpower or reservoir site potential of these areas and the development of the leasable mineral resources. Primary functions are (1) mapping and evaluation of mineral lands, (2) delineation and preservation of potential public-land reservoir and waterpower sites, (3) promotion of orderly development, conservation, and proper use of mineral resources on Federal lands under lease, (4) supervision of mineral operations in a manner that will assure protection of the environment and the realization of a fair value from the sale of leases and that will obtain satisfactory royalties on mineral production, and (5) cooperation with other agencies in the management of Federal mineral and water resources.

CLASSIFICATION AND EVALUATION OF MINERAL LANDS

The organic act creating the USGS gave the Director the responsibility of classifying and evaluating the mineral resources of public-domain lands. There are about 101 million ha of land for which estimates of the magnitude of leasable mineral occurrences have been only partially made. Such appraisals are needed so that the rights to valuable minerals can be retained in the event that the land surface is disposed of and so that the extent of U.S. mineral resources can be determined. Estimates are based on data acquired through field mapping and the study of available geologic reports, in addition to spot checks and investigations made in response to the needs of other Government agencies. As an aid in this assessment of certain minerals, guidelines have been prepared setting forth limits of thickness, quality, depth, and extent of a mineral occurrence that are necessary before land is considered mineral land.

CLASSIFIED LAND

Mineral-land classification complements the leasing provisions of the mineral leasing laws by reserving to the Government, in disposals of public land, the title to energy resources such as coal, oil, gas, oil shale, asphalt, and bituminous rock and fertilizer and industrial minerals such as phosphate, potassium, sodium minerals, and sulfur.

The reserved minerals on public lands are subject to development by private industry under the provisions of the Mineral Leasing Act of 1920. All minerals in acquired lands and on the Outer Continental Shelf are subject to development under comparable acts.

As a result of USGS investigations, large areas of Federal land have been formally classified as mineral land. At the end of calendar year 1978, more than 17 million ha of land had been formally classified, and an additional 948 million ha had been designated prospectively valuable for a leasable mineral.

Lands Classified

Commodity	During Calendar Year 1978		Total at end of Calendar Year 1978	
	Formerly Classified (ha)	Prospectively Valuable (ha)	Formerly Classified (ha)	Prospectively Valuable (ha)
Asphaltic minerals	0	0	0	7,262,766
Coal	391,465	0	17,390,662	142,040,102
Geothermal resources	0	40,470	0	41,802,102
Oil and gas	0	0	1,714	595,321,498
Oil shale	0	34,707	0	5,849,963
Phosphate	29,512	−7,365	216,436	12,403,324
Potassium	0	−7,138	0	35,676,410
Sodium	0	0	254,536	108,303,594

KNOWN GEOLOGIC STRUCTURES OF PRODUCING OIL AND GAS FIELDS

Under the provisions of the Mineral Leasing Act of 1920, the Secretary of the Interior is authorized to grant to any applicant qualified under the act a noncompetitive lease to prospect for oil and gas on

any part of the mineral estate of the United States that is not within any Known Geologic Structure (KGS) of a producing oil or gas field. Lands within such known structures are competitively leased to the highest bidder. During calendar year 1978, 205,456 ha of onshore Federal land were classified as KGS lands, either as new KGS's or as additions to previously established KGS's. The total acreage in KGS's at the end of the year was over 7.5 million ha.

Onshore oil and gas lease sales

During calendar year 1978, there were 23 lease sales for oil and gas on Federal lands. A total of 27,355 ha were sold for $7,717,059. The sale held in New Mexico on February 21, 1978, was exceptional in that one tract received a high bid of $244,787 with the total of $2,380,121 for bonus bids in the sale. The highest bid per acre was received on two very small tracts in Kern County, California, on January 25, 1978, which were sold for $4,556 per acre. The second highest bid per acre was $1,025 for a 120 acre tract at a sale in Wyoming, February 15, 1978. The average bid price per acre has increased from $62 in 1976 to $135 in 1978 despite the decreasing number of lease sales and acreage offered.

KNOWN GEOTHERMAL RESOURCE AREAS

The Geothermal Steam Act of 1970 provides for development by private industry of federally owned geothermal resources through competitive and noncompetitive leasing. During calendar year 1978, 1,492 ha was included in Known Geothermal Resources Areas (KGRA), and 1,312 ha was deleted, which brought the total to 1,347,918 ha.

KNOWN RECOVERABLE COAL RESOURCE AREAS

The Federal Coal Leasing Amendment Act of 1976 provides for the development by private industry of federally owned coal lands by private industry through competitive lease and authorizes the Secretary of the Interior to designate Known Recoverable Coal Resource Areas (KRCRA). During calendar year 1978, 210,306 ha of coal land was included in KRCRA's and brought the total to 7,760,842 ha. Contract drilling in support of coal land classification during 1978 totaled 84,823 m for 618 holes completed, at an average depth drilled of 137 m/hole.

COAL RESOURCE OCCURRENCE/COAL DEVELOPMENT POTENTIAL (CRO/CDP) REPORTS

During calendar year 1978, 90 CRO/CDP reports were placed in open file. About 400 reports are expected to be released in open file by the end of calendar year 1979.

During calendar year 1978, 234 additional quadrangles were contracted in Colorado, North Dakota, New Mexico, Utah, and Wyoming. During calendar year 1979, quadrangle reports will be contracted in Alabama and Oklahoma.

KNOWN LEASING AREAS FOR POTASSIUM, PHOSPHATE, AND SODIUM

During calendar year 1978, known phosphate leasing areas were increased by 7,365 ha for a total of 40,470 ha. Net additions of 46,391 ha to the known sodium leasing area (KSLA) resulted in a total of 162,906 ha classified for competitive leasing. Potassium known leasing acreage increased by 7,244 ha to 181,789 ha.

WATERPOWER CLASSIFICATION—PRESERVATION OF RESERVOIR SITES

Suitable sites for water-resource development are valuable natural resources that should be protected to assure that they will be available when they are needed. The waterpower classification program is conducted to identify, evaluate, and protect from disposal and injurious uses those Federal lands located in sites having significant potential for future development. USGS engineers review maps, aerial photographs, and streamflow records to determine potential dam and reservoir sites. Topographic, engineering, and geologic studies are made of the identified sites to determine whether the potential value warrants formal classification of the affected Federal lands. These resource studies provide the land administering agencies with information that is basic to management decisions and effective land use planning. Previous classifications are reviewed as additional data become available and as funds permit. If the sites are no longer considered suitable for development, the classification of the affected Federal lands is recommended for revocation. If the lands are not reserved for other purposes, they are returned to the unencumbered public domain for possible disposition or other use. During calendar year 1978, about 3,400 ha of previously classified lands in two Western States were released, and reviews of classifications were conducted in river basins in Alaska and six Western States.

To assure consideration of potential reservoir and waterpower sites in the preparation of land use plans, information concerning such sites was fur-

nished to the Bureau of Land Management and the U.S. Forest Service for several planning units in Western States and Alaska.

SUPERVISION OF MINERAL LEASING

Supervision of competitive and noncompetitive leasing activities for the development and recovery of leasable minerals in deposits on Federal and Indian lands is a function of the USGS, delegated by the Secretary of the Interior. It includes (1) geologic and engineering examination of applied-for lands to determine whether a lease or a permit is appropriately applicable, (2) approval of operating plans, (3) inspection of operations to insure compliance with regulations and approved methods, and (4) verification of production and the collection of royalties (see table 2).

Before recommending a lease or a permit, USGS engineers and geologists consider its possible effects on the environment. Of major concern are the esthetic value of scenic and historic sites, the preservation of fish and wildlife and their breeding areas, and the prevention of land erosion, flooding, air pollution, and the release of toxic chemicals and dangerous materials. Consideration is also given to the amount and kind of mining land reclamation that will be required.

For the first time, Federal OCS leases were offered for sale on the basis of cash bonus bidding with a fixed sliding scale royalty rate. As in the traditional cash bonus bidding with a fixed royalty rate, the leases are awarded on the basis of a cash bonus bid, but the royalty rates are determined by the amount of production.

MANAGEMENT OF OIL AND GAS RESOURCES ON THE OUTER CONTINENTAL SHELF

The Outer Continental Shelf (OCS) Lands Act of 1953 authorizes the Secretary of the Interior to issue oil and gas leases on a competitive basis in the submerged lands of the OCS. The functions of the USGS, delegated by the Secretary of the Interior, include (1) tract selection and evaluation to insure orderly resource development, protection of the marine environment, and receipt of a fair market value, (2) approval of exploration plans and development and production plans, (3) inspection of operations to insure compliance with regulations and approved methods, and (4) verification of production and the collection of royalties.

OCS lease sales for oil and gas

Four OCS oil and gas lease sales were held in calendar year 1978. One sale was held in March for leases in the South Atlantic, and three sales were held for leases in the Gulf of Mexico in April, October, and December. A summary of the results of these individual lease sales is is presented in table 3. For the entire Federal OCS, 586 tracts totaling 1,271,026 ha were offered for lease. High bids of $1,767,042,064 were accepted on 249 tracts totaling 525,005 ha.

TABLE 2.—*Mineral Production, Value, and Royalty for Calendar Year 1978*

[Conversions: Barrels—7.3=Tonnes; MCF×28.32=Thousand cubic meters; Gallons×3.785=Liters; Tons×.90718486=Tonnes.]

Lands	Oil (Tonnes)	Gas (Thousand Cubic Meters)	Gas Liquids (Liters)	Other[1] (Tonnes)	Value (Dollars)	Value (Dollars)
Public	21,205,935	28,625,125,259	887,379,230	67,392,246	2,362,019,771	297,722,511
Acquired	650,025	948,760,922	(23,365,975)	631,951	66,376,892	11,009,129
Indian	3,325,793	3,159,344,423	190,558,505	23,302,762	346,852,323	50,237,457
Military	43,223	589,396,916	60,650,757	—	16,624,271	2,746,582
Outer Continental Shelf	40,036,307	124,184,924,064	2,720,551,445	—	7,096,500,055	1,150,346,082
TOTAL	65,261,283	157,507,551,584	3,835,773,962	91,326,959	9,888,373,312	1,512,061,761

[1] All minerals except petroleum products; includes coal, potassium, and sodium minerals, etc.

TABLE 3.—*Summary of CY 1978*

Sale No.	Area-Date	OCS Oil and Gas Lease Sales No. of Tracts Offered	Hectares	No. of Tracts Offered	Hectares	Total Bonus
43	South Atlantic 3/28/78					
	Total	224	516,096	43	99,072	$100,743,443
	Sliding-scale royalty	80	184,320	31	71,424	67,885,374
	Cash bonus	144	331,776	12	27,648	32,858,069
45	Central and Western Gulf of Mexico 4/25/78					
	Total	145	287,223	90	177,567	$733,656,893
	Sliding-scale royalty	16	30,897	10	17,833	79,850,250
	Cash bonus	129	256,326	80	159,729	653,806,643
65	Eastern Gulf of Mexico 10/31/78					
	Total	89	207,089	35	81,464	$ 61,176,730
	Sliding-scale royalty	22	51,284	10	23,311	15,287,117
	Cash bonus	67	155,805	25	58,153	45,889,613
51	Central and Western Gulf of Mexico 12/19/78					
	Total	128	260,618	81	166,902	$871,464,998
	Sliding-scale royalty	59	121,761	36	75,243	425,149,273
	Cash bonus	69	138,857	45	91,659	446,315,725

GEOLOGIC AND HYDROLOGIC PRINCIPLES, PROCESSES, AND TECHNIQUES

GEOPHYSICS

ROCK MAGNETISM

Paleomagnetic poles and polarity zonation in the Proterozoic Belt Supergroup

The Belt Supergroup is a thick sequence of sedimentary rocks in Idaho and western Montana. Radiometric age determinations indicate that these rocks range from 850 to 1,450 million years old, but owing to the lack of fossils, detailed geologic analysis of the supergroup has been difficult. D. P. Elston and S. L. Bressler have conducted a paleomagnetic investigation of the Belt rocks with the objectives of providing stratigraphic correlations and determining the extent of large-scale structural displacements. The lower and middle parts of the Belt Supergroup all have normal magnetic polarity, whereas reversed and normal polarity zones of various lengths are found in the upper part of the supergroup (the Missoula Group). This pattern is similar to the polarities observed in the Grand Canyon Supergroup of northern Arizona, which has been shown by radiometric dating to be approximately the same age as the Belt rocks. In marked contrast to the Grand Canyon Supergroup and the coeval Keweenawan Supergroup of the Lake Superior region, only little apparent motion of the paleomagnetic pole is recorded in the Belt rocks. This may be interpreted to mean that the rocks of the Belt basin were not involved in the large movements of the North American crustal plate that the Keweenawan and Grand Canyon paleomagnetic data have indicated. Within the Belt rocks, paleomagnetic poles for correlative stratigraphic units in the eastern and western parts of the outcrop area show distinct differences in an east-west direction. These differences result from structural rotations and translations along the late Mesozoic and early Cenozoic thrust faults that occur across the Belt basin.

Paleomagnetic method for determining burning rates of ancient coal seam fires

D. E. Watson has developed a technique for estimating the rates of burning of natural fires in coal seams. Oriented samples of clinker were collected over a distance of 225 m along a quarry near the Wyodak Mine in Gillette, Wyo. The samples were collected along the same direction that the fire had burned. The direction of stable natural remanent magnetization in the clinker samples show gradual changes in inclination and declination that are similar to geomagnetic secular variation. By comparing these changes with known secular variation curves, it was estimated that the time during which the burn front had progressed 225 m was approximately 300 years, or in other words the burning progressed roughly 1 m/yr.

Magnetostratigraphy of lower Tertiary rocks in the Powder River basin

D. P. Elston and S. L. Bressler have found that the natural remanent magnetization in sedimentary rocks of the upper part of the Fort Union (Paleocene) and lower part of the Wasatch (Eocene) Formations in Wyoming and Montana is stable and of detrital origin and that the magnetic carrier is magnetite. This fact has enabled them to establish and correlate geomagnetic polarity zones within the Powder River basin. The paleomagnetic correlations confirm previous correlations made by surface and subsurface mapping of coal beds. Comparison of a composite polarity zonation for the Powder River basin strata with the known polarity time scale has shown that the upper part of the Fort Union Formation is late Montian to late Thanetian (late middle to late Paleocene) in age. The length of the hiatus represented by the unconformity separating the Fort Union and Wasatch Formations appears to be about 1 million years.

Paleomagnetism of the Clear Lake Volcanics, California

Paleomagnetic data by E. A. Mankinen and C. S. Grommé, along with K-Ar ages and geologic mapping by J. M. Donnelly and B. C. Hearn, Jr., in the Clear Lake volcanic field, show that the Jaramillo normal polarity event lasted from 0.97 to 0.90 million years B.P. These data also show that much

of Mt. Hannah and vicinity near the center of the volcanic field formed quite rapidly about 0.90 million years ago. The period of time involved probably was no longer than a few hundred years and may have been as short as a few tens of years. Intermediate virtual geomagnetic pole (VGP) positions recorded in Clear Lake lavas erupted at the polarity boundaries of the Jaramillo event and the earlier Cobb Mountain event are very similar and fall remarkably close to the Brunhes-Matuyama polarity transition VGP path as recorded in sediments from Lake Tecopa, Calif. Because the Earth's transitional field has previously been shown to be not dipolar, the recurrence of similar intermediate directions over this time interval shows that the drifting nondipole field must also decay during a reversal. The present data suggest that the transitional field recorded at any given locality may be influenced by some quasi-stationary feature of the nondipole field that is regional in extent.

Paleozoic and Triassic paleomagnetism of the Alexander terrane, southeastern Alaska

Most of southeastern Alaska lies within the Alexander terrane, a distinctive belt of Paleozoic and lower Mesozoic rocks that extends from the Yukon-Alaska border to the southern tip of Prince of Wales Island. C. S. Grommé, G. D. Eberlein, Michael Churkin, Jr., and Meridee Jones (USGS), collaborating with Rob Van der Voo (University of Michigan), have obtained a series of paleomagnetic poles from Paleozoic rocks of the southwestern part of the Alexander terrane, ranging in age from Middle Ordovician to Middle Pennsylvanian. When compared with paleolatitudes predicted from the coeval paleomagnetic data for stable central North America, the paleomagnetic latitudes for this part of the Alexander terrane turn out to be anomalously low, indicating a 1,500 km northward displacement of the terrane since late Carboniferous time. Additional paleomagnetic results have been obtained by J. W. Hillhouse and C. S. Grommé from the Hound Island Volcanics of Triassic age in Keku Strait, which are the youngest rocks of the southern part of the Alexander terrane. The pole position for these basalts is at lat. 23° N. and long. 189° W., and the corresponding paleolatitude is not significantly different from that predicted by Triassic paleomagnetic data from central North America. These data therefore show that the northward drift of the Alexander terrane had been completed by Late Triassic time. The pole position for the Hound Island Volcanics is anomalous, however, and is interpreted to mean that the region immediately surrounding Keku Strait was rotated approximately 100 degrees counterclockwise at some time since the Late Triassic.

Geomagnetic secular variation during Halocene time

An extensive series of paleomagnetic direction and intensity measurements has been completed by D. E. Champion on a collection of 35 basalt flows with radiocarbon ages ranging from historic to 11,900 years B.P. These lava flows occur in Oregon, Idaho, Colorado, and Arizona. Because the ages are nonuniformly distributed, the detailed parts of the paleomagnetic record are in the time intervals 0 to 4,100 years B.P. and 5,800 to 6,900 years B.P. in these intervals the geomagnetic field behaved in a manner similar to the historic records from geomagnetic observatories. The paleointensity determinations were done using the Thellier method. The variations of intensity and direction of the paleomagnetic field have similar characteristic periods, suggesting that both are due in similar proportions to the dipole and nondipole parts of the geomagnetic field. When these new paleointensity data are combined with similar published data from other parts of the world, the geomagnetic dipole moment is seen to have varied through nearly one cycle of a quasi-sinusoid with a period of about 8,000 years and an amplitude range from 6×10^{22} to 11×10^{22} Am^2. This variation is almost exactly coincident with the known variation in radiocarbon activity in the Earth's atmosphere, which adds further confirmation to the theory that radiocarbon production changes have resulted mainly from changes in the strength of the Earth's magnetic field.

GEOMAGNETISM

Geomagnetic secular change

The current rates of secular change in the United States emphasize the necessity of updating magnetic charts and models as frequently as every 5 years. According to E. B. Fabiano, data from the magnetic observatory in Fredericksburg, Va., now indicate a rate of change of −142T/yr in the vertical intensity in contrast with a rate of −87nT/yr presently indicated on the 1975 magnetic chart of the United States. This current rate of change of vertical intensity exceeds that ever recorded in this region since observatory operations began in 1901. Also, significant shifts in the rate of annual change of declination at U.S. magnetic observatories have

been recorded at Newport, Wash. (from −4.8 min/yr to −8.3 min/yr), and at Sitka, Alaska (from −1.5 min/yr to −6.1 min/yr). The unpredictability of these shifts clearly indicates the importance of a balanced network of magnetic observatories for a continuous monitoring of the secular change.

Electromagnetic refraction in the mantle and secular change

L. R. Alldredge has noted that, because of the large decrease in conductivity in the mantle in going from the core-mantle interface to the surface, the electromagnetic wave velocity increases very rapidly as waves propagate outward from the interface. This velocity increase with radius causes extreme refraction of electromagnetic waves proceeding outward from the core, so that only those waves leaving the core within a fraction of a degree from vertical will ever reach the surface; others will be internally refracted back to the core. This effect greatly complicates the description of secular variation at the surface.

Magnetic variations from external sources

Analysis of observatory annual means by J. C. Cain (USGS) and Takesi Yukutake (University of Tokyo) has revealed that external field variations contain a double solar-cycle period that is related to the frequency of magnetic storms. Also, there is an induced component of the solar-cycle variation, as well as an internal variation, unrelated to the external variation, having a period of a little more than 6 years.

L. R. Alldredge and C. O. Stearns (USGS), together with Masahisa Sugiura (NASA), have determined the external first-order spherical harmonic coefficients directly from observatory data without first filtering to remove all but the solar cycle. The resulting values of the first-degree zonal term clearly show the solar-cycle effect and correlate very well with several geophysical indices. The absolute values of these zonal terms, as a function of time, agree very well with expected results, provided solar-wind effects are considered.

Improved selection of geomagnetically quiet-day levels

Three groups of indices were studied by W. H. Campbell as indicators for quiet-day geomagnetic field level determinations: one was the *AE* index, the other two were the positive and negative value groups of the *D*st index. Two selections of the quietest days were made to provide at least 19 and 30 chosen days per year. These selections required the correspondence of equivalent fractional portions of the distribution of days in which all hourly values of indices were below specified levels. A comparison of lists of those days for the years 1958 to 1974 with the 5-d/mo selection derived from the geomagnetic-activity index, *Kp*, shows that for the same total number of quiet days per year only about one-third to one-half of the low-*Kp* days would be quiet by *AE*- and *D*st-index standards. Use of the quiet *AE*-*D*st days provides an improvement in the determination of the regular secular, annual, and semiannual changes of the Earth's magnetic field.

Magnetic stations for the International Magnetospheric Study (IMS)

In cooperation with the National Science Foundation and NOAA, the USGS developed the instrumentation for the North American network of ground magnetometer stations. According to R. W. Kuberry, 16 microprocessor-controlled, fluxgate magnetometer systems assembled and tested by the USGS were deployed by three universities, the Canadian Department of Energy Mines and Resources, and the USGS. In addition, 11 satellite-telemetry systems were interfaced into existing magnetic stations and observatories. The instrumentation system developed for this program represents a major advancement in the collection of geomagnetic data from remote locations. The implementation of satellite telemetry has provided the first real time data from a network of magnetometer stations located on meridional chains specifically selected for the detailed study of geomagnetic substorm and storm phenomena.

Representation of geomagnetic field by local functions

L. R. Alldredge has shown that the 606,000 grid-point values in the Nevada grid aeromagnetic-anomaly map could be replaced by 123,000 double-Fourier and trend coefficients without appreciable loss of accuracy. In addition to saving storage space, the use of such analytical expressions for anomaly maps would help in identification of erroneous data points, would provide a general picture of directional trends in the field, and would give an estimate of the depth to the magnetic sources for each basic cell used in the Fourier representation.

PETROPHYSICS

Nonlinear complex resistivity

G. R. Olhoeft continued the development of nonlinear complex resistivity techniques. The measure-

ment process was redesigned to be simpler and completely automatic. Mathematical studies of nonlinear processes resulted in providing four distinct measures of nonlinearity in a general system:

- The transfer function relating the system stimulus and response is a function of the amplitude of the stimulus.
- The response of the system contains harmonics that were not present in the stimulus of the system.
- Stimuli from differently shaped waveforms (sinewave versus squarewave) yield responses that are characterized by different transfer functions.
- The real and imaginary parts of the transfer functions have a frequency dependence that does not obey the Kramers-Kronig relations (a Hilbert transform).

All four types or measures of nonlinearity were experimentally observed. The last measure of nonlinearity is particularly pronounced in clay minerals. A new application of the nonlinear complex resistivity technique is its use as a laboratory tool to study the kinetics of chemical reactions. As the nonlinear response is particularly sensitive to specific reactions, it is possible to use the frequency dependence of the nonlinear response to measure reaction rates. The power of the technique is its use in observing reactions inside environmental chambers and pressure vessels where the reactions would otherwise have to be inferred.

Electrical properties of geothermal materials

G. R. Olhoeft (USGS) and Hikmet Ucok (Univ. of California, Los Angeles) completed a series of electrical resistivity measurements of geothermal brines over a temperature range from ambient to 673 K, with concentrations up to 24 weight percent, and while being subjected to hydrostatic pressure. A three-dimensional regression of the data to fit a model has produced a predictive set of equations with an accuracy of ± 2 percent, which is an order of magnitude better than reported in the literature. Basalt and sandstones have also been investigated with various solutions filling the pores. The results confirm the previous data showing the significant influence of pore-wall alteration on electrical properties (Olhoeft, 1977). G. R. Olhoeft and G. R. Johnson performed in-situ electrical measurements at the Kilauea Caldera in Hawaii using a 100-MHz center-frequency impulse radar. The measured electrical properties were very similar to those determined in laboratory studies, but a significant new advance was the discovery that radar can successfully probe basalt to depths of 20 m, with fractional meter resolution. The radar system produced high-quality profiles that allowed mapping of the lateral and vertical extent of interbedded lava flows, hidden faults, and lava tubes. Vertical resolution was 0.3 m, and lateral resolution was 0.1 m.

Impulse radar for geologic mapping

G. R. Olhoeft and G. R. Johnson demonstrated the use of a 100-MHz center-frequency impulse radar as a technique to map near-surface geological structure with very high resolution. The radar system was used in the permafrost terrain of the Arctic coastal plain of Alaska to monitor the degradation of permafrost around manmade structures, to map the thaw bulb around the Trans-Alaska Pipeline, and to map general geological structures with fractional-meter resolution to depths of about 10 m. Around the Kilauea Caldera, the radar achieved 0.3 m vertical resolution to depths of 20 m and 0.1-m lateral resolution in mapping interbedded lava flows, hidden faults, lava tubes, and related features. The radar system may also be used in a common-depth-point sounding mode of operation to measure electrical properties in situ over large volumes of material. It was used to determine the dielectric properties for the calibration of depth on the profile records, and it was also used to study in situ electrical properties and their variations in space. Thus far, common-depth-point techniques worked successfully in granite at the Chelmsford Quarry in Massachusetts, in basalt in Hawaii, and in freshwater lake ice, permafrost, and first-year sea ice in Alaska.

Electrical conductivity of pyroxenes

J. S. Huebner and L. B. Wiggins (USGS) and A. G. Duba (Lawrence Livermore Laboratory) measured the electrical conductivity of three natural orthopyroxene single crystals in the laboratory. The measurements showed that three crystals are more than one-half order of magnitude more electrically conducting over the temperature range 850° C to 1,200° C, than previously measured crystals. Small concentrations (1 to 2 percent) of Al_2O_3 plus Cr_2O_3 present in these crystals may be responsible for their relatively high conductivity. The new conductivity values for pyroxene are responsible for the relatively large bulk conductivity calculated for (polymineralic) lunar-mantle assemblages. The results permit a somewhat cooler lunar temperature profile that previously proposed from electromagnetic sounding observations. Such lower profiles,

several hundred degrees Celsius below the solidus, are quite consistent with seismic data for the lunar mantle.

Rheology of rocks and rock-forming minerals

S. H. Kirby has studied the rheology of pyroxenites at intermediate temperatures (400° C to 900° C) and over a wide range of pressures (100 MPa to 2,000 MPa). Triaxial tests carried out on rock aggregates of orthopyroxene and clinopyroxene indicate that the intrinsic plastic strength at high pressure is remarkably insensitive to temperature and strain rate and can be approximated by a perfectly plastic rheology with yield stress of about 14 kbar. At lower pressure, the flow stress is very sensitive to confining pressure, a phenomenon thought to be caused by the contributions of microfracturing.

In studying the creep of hydrolytically weakened synthetic quartz, Kirby found that crystals compressed perpendicular to $(10\bar{1}0)$ deformed by duplex $\{10\bar{1}0\}$ $\langle a \rangle$ slip at creep rates considerably lower than earlier experiments on crystals oriented to promote $(2\bar{1}\bar{1}0)$ (c) slip and showed no incubation stage as found in the earlier tests. The temperature effects on creep rates are different for the two directions of creep compression, and this casts doubt on a single mechanism controlling creep rates for both orientations.

Detailed lithology near coal seams indicated by borehole and hole-to-hole logging

J. H. Scott and J. J. Daniels successfully tested borehole and hole-to-hole geophysical techniques for detecting and mapping lithologic features, such as sandstone lenses and calcium-carbonate cementation in rock overlying coal beds in the Illinois Basin. They showed that detection of these features prior to mining makes it possible to plan and design mines for more efficient and more complete recovery of the coal resource.

Physical-property changes associated with roll-front uranium deposits

A study by J. J. Daniels of borehole geophysical data in a Utah channel deposit, in the Shinarump Member of the Chinle Formation, indicated changes in physical properties near the ore deposit that are similar to those seen in roll-front environments. These physical-property changes include variations in resistivity, induced polarization, density, and magnetic susceptibility responses. Variations in resistivity and induced polarization geophysical well-log responses near sedimentary uranium deposits can also be detected with hole-to-hole measurements.

Borehole magnetic susceptibility probe detects low-level anomalies

J. H. Scott and J. J. Daniels have made improvements in the sensitivity and temperature stability of a borehole magnetic-susceptibility measurement system that make it possible to detect weak but significant anomalies in sedimentary rock in the vicinity of uranium deposits. The magnetic susceptibility of low anomalies often indicate that magnetic minerals, such as magnetite and maghemite, have been oxidized to weakly magnetic minerals, such as limonite and hematite. Oxidizing conditions also occur where ground-water geochemistry is favorable for dissolving uranium minerals and transporting them to locations where reducing conditions prevail and cause precipitation. Thus, the detection of low-level magnetic anomalies can be used as a guide for uranium exploration in areas where ground-water transport is the mechanism by which uranium is concentrated in minable deposits.

Development of hole-to-hole and deep-penetrating electrical and acoustic borehole-geophysical systems

J. J. Daniels made borehole geophysical field studies at the Waste Isolation Pilot Plant (WIPP) Site in New Mexico that indicate that the contrast between the high-resistivity evaporite deposits and the low-resistivity borehole fluid makes it difficult to obtain geologically significant electrical well logs. However, hole-to-hole measurements at the WIPP Site yielded resistivity-response values that were close to the true resistivity values that were made on core samples in the laboratory. Analysis of induced-polarization (IP) well logs at the Nevada Test Site showed a large IP-response contrast between welded and zeolitic tuffs. An acoustic-velocity contrast of approximately 2-to-1 is present between salt and salt interbeds in the Paradox Basin in Utah. Hole-to-hole electrical and acoustical measurements can be used to determine the continuity of geologic units between boreholes.

Visible and near-infrared spectra of rocks from a chromite-rich area in Oregon

G. R. Hunt measured the reflection spectra of a suite of ultramafic rocks collected by J. C. Wynn in chromium-rich areas in southwest Oregon and northwest California. The spectra show that features owing to the presence of chromium are entirely absent, but that the massive chromite sam-

ples are distinguishable from all others on the basis of spectral features produced by absorptions in the ferrous ions located in unique tetrahedral sites afforded by the chromite spinel structure. Chromite samples are also distinguishable by their lack of specific absorption near 1.0μm, normally caused by ferrous ions located in octahedral sites; absorption in the 1.0μm region is the typical situation found in ultramafic and mafic rocks. The potential usefulness for remote-sensing purposes of this unusual spectral regime was suggested.

Near-infrared spectra of alteration minerals and the potential for use in remote-sensing applications

Near-infrared bidirectional reflection spectra from 1.3 to 2.4μm of particulate samples of minerals that commonly occur in hydrothermally altered rocks and soils were recorded by G. R. Hunt at a sufficiently high spectral resolution to allow the features to appear at very near their natural or true bandwidths. The features that appear near 1.4, 1.76, and 2.2μm are sufficiently characteristic to be of particular value for analytical work, and, in addition, those near 2.2μm are shown to be both accessible and appropriate for remote-sensing applications, especially for discriminating between altered and unaltered areas. Atmospheric transmission spectra recorded by Hunt in Denver, Colo., also revealed that the 1.762μm minimum in the alteration mineral alunite is accessible through the atmosphere and could be particularly useful for remote-sensing activities. The major instrumental effects that alter the appearance and degrade the quality of spectral data are the lack of resolution and recording times that are too fast to allow for full instrumental response.

Altered-rock spectra in the visible and near infrared

G. R. Hunt recorded visible and near-infrared spectra of a large suite of hydrothermally altered rock samples that were collected and characterized by R. P. Ashley. The features displayed in the spectra are caused by both electronic and vibrational processes in the individual mineral constituents of the rocks. Electronic transitions in the iron-bearing constituents produce diagnostic minima near 0.43, 0.65, 0.85, and 0.93μm, which can be related to particular minerals. Vibrational transitions in clay and water-bearing mineral constituents produce characteristic single and multiple features over limited spectral ranges near 1.4, 1.76, 1.9, 2.2, and 2.35μm. The most abundant feature-producing minerals in the altered rocks were hematite, geothite, and alunite, while others frequently present were jarosite, kaolinite, potassium micas, pyrophyllite, montmorillonite, diaspore, and gypsum. The feasibility of employing the visible and near-infrared regions, particularly the region near 2.2μm, for detecting the presence of alteration by remote-sensing techniques was confirmed, as was the usefulness of the near infrared as a rapid and reliable technique for detecting and identifying the presence of clay minerals in rocks.

APPLIED GEOPHYSICAL TECHNIQUES

Magnetization directions from magnetic anomalies

In order to determine the direction of magnetization of a body with only minor knowledge about shape or distribution of magnetization, R. J. Blakely and R. W. Simpson, Jr., have developed a technique that uses the phase of a two-dimensional Fourier transform of the associated magnetic anomaly. The algorithm operates by (1) calculating the phase of the Fourier transforms, (2) transforming to a vertical field, (3) using least squares along the wavenumber axes to locate the centroid of the body, (4) moving the origin to the centroid, and (5) applying least squares throughout a quadrant of a wavenumber domain to obtain the inclination and declination. The only requisite assumption is that the distribution of the intensity of magnetization on any horizontal plane through the body be symmetric about a point, a condition met by a wide variety of sources. The method compares favorably with conventional inverse techniques requiring knowledge about the distribution of magnetization. As an application of the method, a circular aeromagnetic anomaly over Estero Bay in central California was studied. This negative anomaly is offshore from a line of late Oligocene hypabyssal intrusions that extends from Morro Rock to Islay Hill of San Luis Obispo County, California. On the assumption that the offshore anomaly is produced by an intrusion similar to those onshore, the calculated direction has an inclination of $-51°$ and a declination of 243°. This direction suggests that the buried intrusion was formed during a reversed period of the Oligocene and has since rotated clockwise, as suggested for the onshore intrusions by Greenhaus and Cox (1978).

Model for magnetic-anomaly inversion

A generalized model consisting of a number of contiguous bodies has been developed by B. K. Bhattacharyya for inversion of magnetic anomalies. The

magnetized region creating anomalous magnetic fields in an area of observation is broken up into several units having different magnetizations. The iterative method developed for inversion of magnetic data determines the optimum orientation of the units with respect to geographic north. The top and bottom surfaces of each of the units are adjusted in the least-squares sense to minimize the difference between observed and calculated field values. At the conclusion of the iterations, a three-dimensional distribution of magnetization is generated to delineate the magnetized region responsible for the observed anomalous magnetic field.

Vector aeromagnetic data

Theoretical research by B. K. Bhattacharyya on the usefulness of vector aeromagnetic data indicates that the following parameters of the causative body can be computed with reasonable accuracy with the data over an area: (1) magnetization vector associated with the body and (2) the geometry of the body by analysis of the data or by drawing lines of force.

Field tests of real-time magnetotelluric systems

Final tests of a microcomputer-based real-time magnetotelluric system were completed by W. D. Stanley confirming that soundings to depths of 20 km in geothermal areas may be accomplished in 1 hour using a two-man crew. The approximate increase in number of soundings per day using the real-time system over the normal method is a factor of 3. In addition, surveys can be more intelligently executed because the real-time system provides Earth models immediately upon acquisition of field data at the sounding site.

Calculation of resistivities of two-dimensional structures

A new method was developed by A. A. R. Zohdy for the extremely rapid computation of electrical-resistivity sounding or profiling over completely generalized two-dimensional structures. Preliminary tests of the method against responses for simple models computed by tedious methods, such as the image method (from the Russian literature), the finite element method, and scaled-model experiments, have yielded good to excellent results. Using programmable pocket calculators, computations with the present method can be made for up to five horizontal boundaries and two vertical boundaries. The method is based on computations made with convolution for horizontal boundaries and convolution or numerical integration using Gauss-LaGuerre coefficients for vertical boundaries. Further testing and generalization of the method are underway.

Calculation of self-potential anomalies

An analysis of the self-potential anomaly associated with a vertical contact has been completed by D. V. Fitterman. Expressions for a rectangular patch source, which are easily computed, were derived. The anomalies have an antisymmetric pattern across the contact. The magnetic field associated with this current system was computed by using an extension of a theorem of Heaviside. The main component of magnetic field was found to be parallel to the contact and to be of an observable magnitude. This result has application to the problem of tectomagnetic anomalies.

Electromagnetic response of inhomogeneous overburden

A large slab having variable conductance was constructed for use in scale-model electromagnetic studies by F. C. Frischknecht and C. L. Tippens. Scale-model slingram measurements were made above the overburden alone, above the overburden plus a highly conductive model orebody, and above overburden and orebody plus host rock, the latter simulated by brine. For the cases studied, the anomaly of the model orebody is clearly recognizable at low frequencies but is lost in the "geologic noise" caused by the overburden at high frequencies. In addition to causing an offset in the response, the host rock causes some enhancement of the quadrature anomaly of the orebody at high frequencies. The use of an inhomogeneous overburden should be a very effective means for studying the relative effectiveness of various electrical methods in environments where the geologic noise level is high.

Electromagnetic soundings at Randsberg Known Geothermal Resource Area (KGRA)

Frequency- and time-domain electromagnetic soundings were made by W. L. Anderson (1978) and J. P. Kauahikaua (1979) at the Randsberg KGRA, Calif., to compare the two approaches and to test newly developed inversion programs. The measurements were made by using a grounded-wire source 1,528 m in length. Amplitude and phase measurements were made in the range 1 to 2,000 Hz; transient measurements were made with a resolution of 200 samples per second. Good fits to a

one-dimensional model were found by inversion for all of the frequency domain soundings except for one near the steam well. Most of the time domain results also fit layered Earth models reasonably well, although shallow layers were not resolved as well as by the frequency soundings. As used in this experiment, the time-domain method had a greater depth of investigation and was faster than the frequency domain method. The most important feature in the geoelectrical section is a good conductor which occurs at relatively shallow depths near the steam well and becomes progressively deeper away from the well.

Geophysical studies of a uranium deposit in southern Utah

Ground geophysical surveys and petrophysical measurements of drill-core samples from a channel-controlled uranium deposit in southern Utah by B. D. Smith and V. J. Flanigan have led to the following conclusions. First, the association of pyrite with the uranium mineralization produces pronounced variations in the electrical properties of samples. This variation has been mapped also by large-scale, Induced-Polarization (IP), complex resistivity surface surveys. The location and trend of IP anomalies correlate well with the uranium mineralization. Second, the overall magnetic susceptibility of the Triassic sedimentary rocks is very small. There is, on a small scale (sample size), inverse correlation between uranium mineralization and magnetic susceptibility. The magnetic field surveys produce no simple magnetic anomaly associated with the uranium mineralization. However, there are trends in the magnetic anomalies that correlate with paleosedimentary trends. Slingram, turam, and VLF electromagnetic surveys produce anomalies that generally trend with paleosedimentary features. Distinct anomalies may be caused by sequences of mudstone lenses higher in the geologic section than the uranium mineralization. For this particular geological setting, IP and magnetic surveys appear to have the best potential for uranium exploration where the deposits are within 60 to 80 m of the surface.

Electrical and magnetic studies of Belt green beds

Electrical and magnetic surveys were made over Montana green beds of the Belt Supergroup at the Blacktail Mountain drilling site by B. D. Smith. The results suggest that induced polarization surveys can be used to define potential areas of copper mineralization in the green beds. The contoured electromagnetic and magnetic data show trends that are discordant to local lithologic trends, indicating that petrophysical variations (for example, resistivity) are not concordant to formation boundaries. The implications of this observation are not clear at this time; perhaps the geochemical trends are also discordant with formation boundaries.

Airborn pulse sounding of Alaskan glaciers

R. D. Watts and D. L. Wright made the first known airborne soundings of temperate glacier ice. More than 500 km of profile data were obtained over the Columbia, Guyat, Yahtse, Tyndall, and Hubbard glaciers using a system designed by the USGS and Colorado State University. The system uses 100-m-long transmitting and receiving antennas trailed from the wing tips of the Survey's Fairchild-Heli-Porter slow-takeoff-and-landing (STOL) aircraft. The results were monitored by use of an oscilloscope and camera and also recorded on tape. Bottom reflections from depths as great as 600 m can be recognized directly in the data. The data will be processed to enhance reflections from greater depths and to help separate reflections from the bottom of the glacier and sides of the valley.

Geophysics applied to permafrost on Mars

G. R. Olhoeft has studied the applicability of using the nonlinear, complex resistivity technique together with impulse-sounding radar to study the properties and occurrence of permafrost on Mars (G. R. Olhoeft, 1976, 1978). Laboratory and field studies in Alaska have shown that the impulse radar may be used to map structural features in permafrost and basalt to depths of 10 m with fractional-meter resolution. The radar techniques are relatively insensitive to geochemical parameters but are very sensitive in mapping changes in bulk density and the content and state of water. The nonlinear complex resistivity technique is most sensitive to specific chemical parameters, such as, the presence or absence of oxidation-reduction reactions versus ion-exchange processes and the kinetics and rates of the reactions. Because of the presence of small amounts of unfrozen water to very low temperature in permafrost containing clay minerals, the nonlinear complex resistivity will respond to the geochemistry of the water-rock system as long as there are a few adsorbed layers of water present and the temperature is above 233 K. Depending upon the amount of colloidal, claylike materials and the

amount of water present, it may be possible to go to lower temperatures.

Resistivity soundings in Florida

Seventy-eight Schlumberger soundings totalling 100 km in length were made by A. A. R. Zohdy and R. J. Bisdorf along several profiles near Venice, Parrish, and Homosassa, Fla., for the purpose of studying the extent of seawater intrusion in limestone aquifers on the western coast of Florida. Seven computer-generated geoelectric cross sections of interpreted true resistivity were produced, the longest of which is about 30 km in length. The freshwater-saltwater interface was clearly depicted on several of these profiles, and the depth to the interface ranged from about 20 m to about 300 m. Near Parrish and Homosassa, the low-resistivity (1–5 ohm-m, near Homosassa, and 10–30 ohm-m, near Parrish) layer representing saltwater-saturated sediments and limestone was found to extend to distances of 10 to 12 km inland from the coastline. Near Homosassa, at a distance of about 3 km from the coastline, a high-resistivity layer of 50 to 100 ohm-m exists at a depth of 300 to 500 m. This layer may represent a second freshwater aquifer or limestone of very low porosity but saturated with saltwater.

Geophysical studies over subsidence fissures

Earth fissures associated with ground-water withdrawal near Picacho, Ariz., were studied by R. C. Jachens using surface geophysical techniques. Gravity and ground magnetic surveys were used to infer the basement configuration beneath six areas in which earth fissures exist. In five of the six areas, fissures were found to lie above basement ridges or marked changes in the slope of the basement surface.

The effects of differential subsidence caused by water-table decline and compaction of the underlying sediments were examined for two of the areas by means of the finite element method. Sediment thicknesses inferred from the geophysical data and one-dimensional consolidation theory (Terzaghi and Peck, 1948) were used to generate displacement boundary conditions. In both cases, the model results show that the fissured areas are characterized by large values of horizontal extensional strain. For an area underlain by a basement ridge reaching within 200 m of the surface, the finite element model yielded a maximum horizontal extensional strain located within about 80 m of the fissure. For an area underlain by a basement shelf, the finite element model yielded a maximum horizontal extensional strain located within 20 m of the fissure.

Gravity map of California

A preliminary gravity map of California was compiled under the direction of H. W. Oliver (USGS) and R. H. Chapman (California Division of Mines and Geology) at scale 1:750,000, accompanied by a 200-page interpretive text. The map shows that Bouguer anomalies in California range from about −280 mGal in Long Valley to about +30 mGal along several sections of the California coastline. They increase further on the offshore islands to as much as +80 mGal. The Bouguer anomalies correlate generally with regional elevation averaged to a radius of 41 km, indicating that the various mountain ranges are in regional isostatic balance. Locally, a number of anomalies up to ±50 mGal reveal buried ophiolites under the Great Valley, structural basins within the Great Valley Basin and Range and the Mojave Desert provinces, buried faults throughout the State—particularly those in southern California—and the depth extent of low-density plutons in the Sierra Nevada, Coast Ranges, and Peninsular Ranges. Offshore data indicate numerous sedimentary basins and the offshore extension of many faults.

Southern California high-precision gravity networks

High-precision gravity surveys were conducted by R. C. Jachens (USGS) and W. E. Strange (National Geodetic Survey) in March 1978 for purposes of studying long-term crustal movements. The USGS, National Geodetic Survey, and the Defense Mapping Agency jointly participated in this program. Gravity was measured at bench marks approximately every 3.2 km along lines that were leveled during the same period as part of the southern California releveling program. Approximately 4,000 km of lines were surveyed. Gravity also was measured at sites located on roughly a 15-km × 15-km regional grid covering the same area. All surveys were tied to a primary reference station at Riverside, Calif., and also were tied to the U.S. National Gravity Base Net (Schwimmer and Rice, 1969) and the California Gravity Base Station Network (Chapman, 1966).

Gravity at each station was measured twice with at least three gravimeters, and all stations are recoverable both in terms of location and reading orientation. All gravimeters used for this work were standardized over the same detailed calibration range.

This work has resulted in an extensive high-precision gravity datum against which past and future gravity observations may be compared. The concurrent gravity and leveling data should provide a good foundation for future studies of crustal deformation in this tectonically active region.

GEOCHEMISTRY, MINERALOGY, PETROLOGY

EXPERIMENTAL AND THEORETICAL GEOCHEMISTRY

Unary and binary multisystem nets for $n+k$ ($k \leq 6$) phases

E-an Zen has studied the geometric properties of unary $n+k$ ($k \leq 6$) phase multisystems, and, in collaboration with E. H. Roseboom, Jr., studied the binary $n+4$ phase multisystem. These systems are qualitatively different from $n+3$ phase multisystems in the same sense that $n+2$ phase invariant systems differ from $n+3$ phase multisystems. One geometric expression of the difference is that whereas for $n+3$ multisystems all invariant points, indifferent crossings, univariant lines, and divariant fields permitted by the combinatorial rule can be uniquely represented in two-dimensional maps (such as p-T diagrams), and that their complete representation is possible as closed nets; this is no longer true in $n+4$ or more complex multisystems. The governing principle is Euler's theorem of polyhedra which states that topologically simply connected polyhedra obey the relation: number of vertices+number of faces=number of edges+2; the numbers are respectively identified with (invariant points + indifferent crossings), divariant fields, and univariant lines (or line segments defined by indifferent crossings). The $n+3$ multisystem nets exactly obey the theorem, and all more complex systems, if fully portrayed, would violate it. As a rule, no p-T type diagram can be drawn for such multisystems that exhibit each and all geometric elements once; only subnets can be drawn. However, by considering the geometric possibilities of intersection of free energy surfaces of individual phases, it was shown that the number of topologically distinct arrangements for binary $n+4$ multisystems are surprisingly few and that each of these does obey Euler's theorem. Each apparently forms a topologic group containing internal transformability, including the existence of an Identity transform. For unary $n+k$ multisystems, the solutions are obtained by simple geometric considerations. Although the strictures of Euler's theorem still apply, the unique composition makes the problem straightforward. Thus for $k=4$, there is just one geometrically distinct type of net. For $k=5$, there are two; for $k=6$, there are five distinct types of nets. Even though no single net can encompass all the geometric (that is, phase-assemblage) possibilities, enumeration of the permissible nets allows prediction of equilibria; thus, these nets should be useful petrographic tools.

Radio-telemetered volcanic gas monitoring in Hawaii

Motoaki Sato and K. A. McGee have established two radio-telemetered gas monitoring stations on Hawaiian volcanoes. One station, powered by a solar panel, was set up at a gas vent in the 1975 fissure of Makuoweoweo crater of Mauna Loa. Gas and temperature data are transmitted to a receiver located at the southwest rim of the crater by using an FM analog transmitter and then multiplexed to the existing, seismic, telemetry network to be telemetered to the Hawaiian Volcano Observatory. The other station was established at a sulfur-rich fumarole in the 1974 fissure of the summit caldera of Kilauea. The analog data are directly radioed to the observatory from the site. The two stations have produced valuable data, and further improvement of the monitoring system is contemplated.

Thermochemistry of maturation of fossil fuels

Maturation of fossil fuels is a process involving dehydration, decarbonation, and demethanation. Motoaki Sato has made thermochemical studies of common organic compounds which show that at diagenetic temperatures these reactions, if coupled with lengthening of carbon chains or condensation of aromatic rings, release energy rather than require an energy input. In other words, maturization of fossil fuels will occur spontaneously, given enough time. It has also been shown that so-called "hydrogenation" of unsaturated compounds in fossil fuels could also occur spontaneously by intra- and inter-molecular hydrogen trasfer, when coupled with the lengthening of carbon chains of lipids or condensation of aromatic rings.

MINERALOGIC STUDIES AND CRYSTAL CHEMISTRY

Crystal structures of alkali-iron copper sulfide minerals erdite, $NaFeS_2 \cdot 2H_2O$

As part of the crystal chemical study by R. C. Erd and J. R. Clark of the new suite of alkali-iron sulfide minerals obtained from Coyote Peak, Calif., by G. K. Czamanske, the structure of erdite has been solved by J. A. Konnert. The monoclinic structure is closely related to the known structure of

synthetic $KFeS_2$. The iron atoms form FeS_4 tetrahedra that link, by sharing opposite edges, into infinite chains, thus accounting for the soft, fibrous character of the crystals. The Fe-S bond length is 2.25Å, and the iron valency is 3. The water molecules are loosely bound in the structure, coordinated to sodium atoms at an average distance of 2.41Å.

Rasvumite, KFe_2S_3

The crystal structure of rasvumite, KFe_2S_3, has been solved by J. R. Clark (USGS) and G. E. Brown (Stanford University). The mineral is orthorhombic and isostructural with synthetic $BaFe_2S_3$ (Hong and Steinfink, 1972), both having, parallel to *c*, double chains of edge-sharing Fe-S tetrahedra. In rasvumite, the average Fe-S distance is 2.26Å, and the close Fe-Fe approaches are 2.71Å. Because these chains can accommodate the presence of either divalent barium cations or univalent potassium cations, the electronic states of iron and sulfur within the chains must vary. In rasvumite, the average iron valency is 2.5. The potassium cations in rasvumite are coordinated by 10 sulfur atoms at an average K-S distance of 3.52Å. These coordination polyhedra share edges to form double chains parallel to *c* that cross link via corner sharing in the *a* direction to produce a framework of polyhedra.

Bartonite, $K_6Fe_{20}S_{27}$

The crystal structure of the new mineral bartonite from Coyote Peak, Calif., has been solved and refined by J. R. Clark and H. T. Evans, Jr. The structure contains pentlanditelike clusters, each resulting from edge sharing among eight Fe-S tetrahedra. The clusters are linked into a framework by corner sharing. The average distances within a cluster are: Fe-S, 2.29Å; Fe-Fe 2.7Å. Potassium cations fit into the available cavities, each potassium cation being coordinated by nine sulfur atoms at an average K–S distance of 3.364Å. The basic structure is closely related to that of the cubic djerfisherite ($K_6Fe_{24}S_{26}Cl$) (Dmitrieva and Ilyukhin, 1976; Tani, 1977), differing only in the stacking sequence of the Fe_8S_{14} clusters, which shifts the symmetry from cubic to body-centered tetragonal. With sulfur replacing chlorine, the structure analysis implies an analogous composition, but electron microprobe analyses by G. K. Czamanske and density measurements by R. C. Erd indicate a considerable deficiency of iron. This deficiency can be accounted for only by random vacancies in the iron sites in the structure, to give a formula $K_6Fe_{20}\square_4S_{27}$. Thus, the average valency of Fe is 2.4.

Djurleite and chalcocite, Cu_xS

The solution of the crystal structure of djurleite, $Cu_{1.94}S$, during this period by H. T. Evans, Jr., represents a significant advance in our continuing crystal chemical study of the copper-rich sulfides. This mineral is closely related to chalcocite, Cu_2S, together with which it forms a common ore mineral for copper. The structure of chalcocite was solved in this laboratory several years ago (Evans, 1971), revealing a structure based on 24 copper and 12 sulfur atoms, all different, with copper mainly in threefold, triangular coordination with sulfur. The details of that structure are still under study, especially in connection with the newly discovered djurleite crystal structure. The latter is also monoclinic and is based on 94 independent atoms, 62 copper and 32 sulfur. Of the 62 copper atoms, 52 are in triangular coordination with sulfur, 9 in highly distorted tetrahedral coordination, and one is in twofold, linear coordination. New, detailed study of the chalcocite structure shows that of the 24 kinds of copper atoms, two are partly displaced from triangular coordination into twofold, linear coordination. Aside from the general features cited above, no extensive analogies between the two structures are yet apparent.

MINERALS AND ENVIRONMENTAL HEALTH

The asbestos minerals and cancer incidence

Mineral commodities such as chrysotile, amosite, anthophyllite, and crocidolite asbestos, hematite, chromite, beryl, bertrandite, nickel sulfide, and serpentine are now considered by many to be potential carcinogens. In addition, other minerals containing cadmium, chromium, beryllium, arsenic, or nickel and silicate minerals that possess a fibrous, acicular, or elongate habit may, in due course, also be assumed to cause human cancer. Because there appears to be a lack of good quantitative data on the extent of exposure to a carcinogen and the probability of getting cancer, many health authorities assume that even a minimal exposure is dangerous. Thus, regulatory agencies are proposing a "lowest feasible limit" to human exposure to possible cancer-producing agents. The necessity for the USGS to assess our important mineral commodities in relation to health is apparent. In this regard Malcolm Ross has undertaken a study of the relationships between exposure to various fibrous minerals, particularly the commercial forms of asbestos, and human cancer.

Mesothelioma, a cancer of the pleura and peritoneum, occurs in excess of that found in the general male population (about one death in 1,000) only in asbestos "trades" workers (shipyard insulation, textiles, and construction). The cancer also occurs in South African and Australian crocidolite miners and in workers who installed crocidolite filters in gas masks during WWII. Lung cancer is seldom found in nonsmoking asbestos "trades" workers. Regression analysis of mortalities resulting from lung cancer and mesothelioma for 11 large groups of asbestos "trades" workers shows that a linear relationship exists between the percent incidence of these two diseases; 79 percent of the variance (r^{-2}) of lung cancer is accounted for by mesothelioma. A large part of the remaining 21 percent variance can be accounted for by intergroup differences in smoking statistics. Cancer mortalities are also noted for adult male populations of six nations and for six "asbestos" mining-factory populations not exposed to crocidolite. The very low incidence of mesothelioma in these groups show that they do not have the cancer risk experienced by those in the "trades"; their lung-cancer incidence is generally accounted for by smoking habits alone. Cancer risk to those in the "trades" is attributed to exposure to both smoke and crocidolite. There is no evidence that the mineral dust levels presently maintained in responsibly operated mines of North America cause increased incidence of lung cancer or mesothelioma, including those mines that process rock containing the so-called commercial forms of asbestos: anthophyllite, tremolite, actinolite, cummingtonite, grunerite, and chrysotile.

VOLCANIC ROCKS AND PROCESSES

HAWAIIAN VOLCANO STUDIES

Kilauea Volcano quiescent during FY 1978

Hawaii's volcanoes remained quiet during the period October 1977 through September 1978, providing needed time for studies of the products from Kilauea's most recent eruption, which lasted from September 13 to October 1, 1977. During this eruption, lava was emitted from a system of new fissures about 7 km long between Kalalua and Puu Kauka along the central section of Kilauea's east rift zone. A substantial amount of summit deflation accompanied the eruption. Mapping of the new flows indicates that approximately $35\times10^6 m^3$ of lava covering about 8 km^2 erupted. The lava contained appreciable plagioclase phenocrysts and very minor amounts of clinopyroxene and olivine. This unusual (for Hawaii) mineralogy, plus data from 12 wet-chemical analyses, indicates that the magma was differentiated. The lava composition remained nearly constant throughout the entire eruption, suggesting that all the erupted lava had been stored within reservoirs in the rift zone and that none of the magma involved in the large summit deflation reached the surface.

Although Kilauea has been quiescent since October 1977, surveillance and monitoring has continued as usual. About 130,000 microearthquakes were detected by the seismic network and classified according to general source areas beneath Kilauea. Nearly 3,000 of these events, having magnitudes of 1 to 4.5, were analyzed for location, focal depth, and magnitude.

The posteruptive seismic activity was considered to be typical: earthquake counts being initially high in the summit, south flank, and east rift zone of Kilauea and gradually decreasing during the ensuing weeks to very low counts in November 1977. During this posteruptive decrease in seismicity, Kilauea's summit continued gradually to deflate. Late in 1977, inflation resumed, and seismicity gradually increased. Throughout 1978, moderate inflation continued nearly continuously, and simultaneously seismicity also increased.

Synthesis of seismic, geodetic, electrical self-potential, and gravimeter observations for the period November 1975 through September 1977 has provided new insights into the magma budget at Kilauea volcano. The 7.2 magnitude earthquake, which struck Hawaii in November 1975, apparently created 40 to $90\times10^6 m^3$ of void space within Kilauea's intermediate magma reservoir. This space was filled by magma prior to June 1976 when the first of four intrusions into the east rift zone occurred. This suggests a magma supply rate to the summit reservoir of 6 to $13\times10^6 m^3$/mo, consistent with the rate of $9\times10^6 m^3$/mo proposed by Swanson (1972). Roughly $150\times10^6 m^3$ of magma from the summit reservoir migrated into the east rift zone between June 1976 and September 1977. This magma presumably filled new fractures created by subsidence of Kilauea's south flank during the November 1975 earthquake. Roughly $35\times10^6 m^3$ of magma eventually reached the surface along the east rift zone in September 1977 near a center of inflation first identified by tilt observation in May 1976. The total volume of magma supplied by Kilauea volcano from its mantle source during November 1975 to September 1977 ($280\times10^6 m^3$ maximum)

was apparently partitioned as follows: (a) 40 to $90\times10^6 m^3$ to refill newly created void space within the summit magma chamber, (b) $150\times10^6 m^3$ to occupy new volume within the east rift zone; (c) $35\times10^6 m^3$ extruded, and (d) $55\times10^6 m^3$ responsible for net uplift of the eruptive zone. These results suggest that quantitative modeling of Kilauea's magma budget may now be feasible, given adequate geophysical surveillance of the summit region and rift zones.

Mauna Loa continues slow inflation

During the 3 years since Mauna Loa's summit eruption of July 1975, bore-hole and short-base water tilt meters, together with periodic geodimeter measurements, show that the volcano is inflating continuously but at a very slow irregular rate. For several weeks during a slightly accelerated episode of inflation in late 1977, increased fuming from the vents of the 1975 eruption cast a visible pall over the summit area. A time-lapse camera was installed to monitor this activity, but the fuming has since diminished. The lack of seismic activity accompanying this slow inflation, although anomalous and somewhat puzzling, suggests that renewed volcanicity is probably not imminent.

Mantle structure of Hawaiian volcanoes investigated

The velocity structure of the crust and mantle underlying the island of Hawaii was investigated by W. L. Ellsworth and D. P. Hill, using an iterative three-dimensional modeling technique which employs geometric ray-tracing in heterogeneous media and determines high-resolution image of crust and mantle structure to depths in excess of 150 km. Crustal structure is dominated by the presence of high-velocity dikes and sills in the summit complexes and radial rift zones of the five shield volcanoes. Mantle structure in the lithosphere indicates that a low-velocity region with typical horizontal dimensions of 50 km underlies the island. The velocity contrast between the low-velocity region and encircling high velocities at the same depth averages 3 to 4 percent. This contrast increases markedly in the asthenosphere to about 10 percent. The most intense low-velocity regions below 100 km lie east of Hawaii and coincide with the axis of the Hawaiian Island chain as extrapolated from the older islands. Structural relationships indicated by the three-dimensional velocity models support other geophysical and geochemical evidence that Hawaiian tholeiitic basalts are derived from a source region below the lithosphere and originate from depths at least as great as 150 km. Because the most intense low-velocity regions in the asthenosphere are not associated with any overlying volcanism and lie ahead of the island chain along the direction of chain growth, these results are difficult to reconcile with fracture-propagation models for linear island chains. They more directly support the hotspot or plume hypothesis.

Global correlation of magma ascent and earthquake energy

H. R. Shaw has compared the volumetric moments calculated from magma ascent rates for Hawaii and the Earth with volumetric moments calculated from earthquake energy for Hawaii and the Earth. The ratio of seismic moments, averaged over 14 years for Hawaii and about 40 years for Earth, is 2×10^{-3}; the ratio of average annual rates of magma ascent for both is about 3×10^{-3} based on an estimate of 30 km^3/yr total magma ascent (including both intrusive and extrusive fractions). Because the estimated seismic moment in Hawaii for the 14-year period also agrees with the total volume of magma supply during that period, Shaw concludes that a rough balance exists both locally and globally in the volume rate of magma ascent and the average energy release of earthquakes. If correct, this implies that earthquake energy arises from gravitational energy release and that the average secular rate of release is measured by the rate of magma generation and ascent.

Molokai petrologic studies

Trace element studies by M. H. Beeson (USGS) and D. A. Clague (Middlebury College, VT) shed further light on the origin of the Kalaupapa section on East Molokai described by Beeson (1976). Potassium-barium ratios of the transitional lavas are uniformly different from those of the alkalic lavas. Because the Kalaupapa flows do not contain sanidine or other phenocrysts with appreciable potassium or barium contents, the contrasting potassium-barium ratios in alkalic and transitional basalts are believed to reflect differences in the mantle sources for the two lava types. If the alkalic and transitional lavas are derived from different sources, then alkalic and transitional lavas cannot be part of the same subsection. Thus, the eight subsections defined by Beeson (1976) on the basis of major-element composition expand to 12 subsections based on potassium-barium ratios and trace-element composition.

Although the potassium-barium and trace-element data appear to weaken the batch concept by requiring more subsections, they can be viewed as

strengthening the concept by requiring the different lava types to be alternately supplied to the surface with little or no mixing. In any event, magma generation (or its supply to the surface) appears to be a discontinuous rather than continuous process, with each batch probably being generated or supplied alternately from different levels in the mantle.

Age and strontium isotopic composition of the Honolulu Volcanics

Potassium-argon ages measured by M. A. Lanphere and G. B. Dalrymple on basalts from 12 vents of the Honolulu Volcanics suggest that these basalts of the posterosional stage of volcanism were erupted between about 0.6 and 0.3 million years ago. The reproducibility of argon measurements for basalts from six of the vents is poor, and, for some, the calculated K-Ar ages are older than the younger age limit of the underlying Koolau Volcanics. The data indicate that at least some of the Honolulu basalts contain variable amounts of excess radiogenic ^{40}Ar that probably was contributed to the basaltic liquid from ultramafic xenoliths.

Ratios for $^{87}Sr/^{86}Sr$ of 14 Honolulu basalts and 8 Koolau basalts have weighted mean values of 0.70331 ± 0.00004 and 0.70379 ± 0.00006, respectively. These data clearly demonstrate the heterogeneity of the mantle source regions for basalt beneath Oahu. The data also indicate that the time-integrated rubidium-strontium ratio in the source region for the Honolulu basalts was lower, or had a less-differentiated source, than in the source region for the Koolau basalts.

Age of Black Point dike, Oahu and Yarmouth Interglaciation

The Black Point basaltic dike cuts the Kaena Limestone of probable Yarmouth age on the southeast slope of Diamond Head, Oahu, Hawaii. G. B. Dalrymple (USGS) and Harold Stearns (Honolulu, Oahu) have determined that the dike, a nepheline basanite, has a potassium-argon age of 0.41 ± 0.04 m.y. and was probably emplaced at the time of eruption of the Black Point Basalt, which has a potassium-argon age of 0.48 ± 0.08 m.y. The Kaena Limestone is the most extensive Pleistocene reef deposit formed in Hawaii during any of the high eustatic stands of the sea. The Kaena shoreline was about 30 m above present sea level. The dike was intruded into the limestone after the reef deposits had been exposed above sea level long enough to have been covered with slope wash and trees. Our date is consistent with a previously published uranium series date of 0.6 ± 0.1 m.y. on coral from the Kaena Limestone. The data suggest that the Yarmouth Interglaciation ended about 0.5 million years ago.

HAWAIIAN ISLAND—EMPEROR SEAMOUNT STUDIES

Age of Emperor Seamounts confirms hot-spot hypothesis

Conventional potassium-argon, $^{40}Ar/^{39}Ar$ total fusion, and $^{40}Ar/^{39}Ar$ incremental heating data on hawaiite and tholeiitic basalt samples from Ojin (Site 430), alkalic basalt samples from Nintoku (Site 432), and alkalic and tholeiitic basalt samples from Suiko (Site 433) Seamounts in the Emperor Seamount chain give the following best ages for these volcanoes: Ojin $= 55.2 \pm 0.7$ m.y., Nintoku $= 56.2 \pm 0.6$ m.y., and Suiko $= 64.7 \pm 1.1$ m.y. These new data obtained by G. B. Dalrymple and M. A. Lanphere (USGS) and D. A. Clague (Middlebury College) bring the number of dated volcanoes to 26 in the Hawaiian-Emperor volcanic chain. The new dates prove that the age progression from Kilauea Volcano on Hawaii (0 m.y.) through the Hawaiian-Emperor bend ($\sim$43 m.y.) to Koku Seamount (48.1 m.y.) in the southernmost Emperor Seamounts continues more than halfway along the Emperor chain to Suiko Seamount.

The age versus distance data for the Hawaiian-Emperor chain are completely consistent with the kinematic hot-spot hypothesis, which predicts that the volcanoes are progressively older westward and northward from the active volcanoes of Kilauea and Mauna Loa. The data are consistent with an average volcanic propagation velocity of either 8 cm/yr from Suiko to Kiuauea, or of 6 cm/yr from Suiko to Midway followed by 9 cm/yr from Midway to Kilauea, but it appears that the change in direction that formed the Hawaiian-Emperor bend probably was not acompanied by a major change in velocity.

Minimum age of Mieji Seamount

G. B. Dalrymple and M. A. Lanphere (USGS), working with James Natland of the Deep Sea Drilling Project (DSDP), completed conventional potassium-argon and $^{40}Ar/^{39}Ar$ age data on altered basalts from DSDP Hole 192A on Meiji Seamount, Emperor Seamount chain. The results indicate a minimum age for the volcano of 61.9 ± 5.0 m.y. The potassium-argon data are consistent with the early Maestrichtian Age of the overlying sediments, but the minimum age does not provide either a positive or negative test of the hot-spot hypothesis, which predicts that Meiji is older than Emperor

volcanoes to the south. The most prominent alteration in the Meiji basalts is potassium metasomatism, particularly of feldspar phenocrysts. Calculations based on the potassium-argon apparent ages of feldspar separates from the Meiji basalts show that more than half of the potassium metasomatism occurred within the last 25 million years or so and that, if the potassium replacement rate has been constant, the alteration did not begin for 10 to 20 m.y. after the volcano formed. The extensive metasomatism may have started only after Meiji had been covered by the sediment blanket that now obscures the volcanic form of the seamount.

Age and composition of Jingu Seamount

Incremental heating experiments of $^{40}Ar/^{39}Ar$ by G. B. Dalrymple (USGS) and Michael Garcia (University of Hawaii) on three samples dredged from Jingu Seamount in the Southern Emperor Seamount chain indicate that Jingu is 55.4 ± 0.9 million years old and is thus older than the Hawaiian-Emperor bend (43 m.y.) and younger than the two dated Emperor Seamounts to the north (55–56 m.y.) Major oxide chemistry and petrography show that the samples are similar to hawaiites and mugearites from the Hawaiian Islands. Groundmass plagioclase compositions (An_{40-47}) indicate that the three samples are probably mugearites. These results suggest that Jingu is a Hawaiian-type volcano and that the ages of the Emperor volcanoes become progressively older from south to north as predicted by the hotspot hypothesis.

Rubidium-strontium systematics of Hawaiian-Emperor Seamount chain basalts

Strontium isotope measurements by M. A. Lanphere and G. B. Dalrymple (USGS) and D. A. Clague (Middlebury College) on 70 samples of basalt from the Hawaiian Islands and Emperor Seamount chain yield $^{87}Sr/^{86}Sr$ ratios that range from about 0.7032 to 0.7040. Tholeiites and alkalic basalts from the same volcano yield strontium compositions that agree within analytical uncertainty. These data are consistent with derivation of both tholeiitic and alkalic basalt liquids from a source region having approximately the same rubidium-strontium ratio and strontium isotopic composition. Along the Hawaiian Islands, from Kilauea Volcano to the Hawaiian-Emperor bend, the $^{87}Sr/^{86}Sr$ ratios range from about 0.7036 to 0.7040. However, in the Emperor Seamounts north of the bend $^{87}Sr/^{86}Sr$ ratios drop abruptly to between about 0.7032 and 0.7035. This shift in isotopic composition coincides with a major change in sea-floor spreading direction of the Pacific plate.

CENOZOIC VOLCANISM IN WESTERN UNITED STATES

Magma sources and tectonic setting of Clear Lake Volcanics, California

Basaltic lavas of the Clear Lake Volcanics were probably derived from more than one mantle source area, based on their major-, trace-, and rare-earth element (REE) geochemistry and strontium isotopic composition, according to B. C. Hearn, Jr., J. M. Donnelly, F. E. Goff, Kiyoto Futa, and C. E. Hedge. Northward progression of Coast Range volcanism suggests a genetic relation either to a mantle hot spot or to propagation of the San Andreas transform fault system or to heating of a subducted oceanic slab. REE patterns cast doubt on a derivation by partial melting of subducted oceanic crust, and volcanic loci are too near the coast to be analogous to the present subduction-related Cascade volcanic chain. The data seems most compatible with the hot spot model, with superimposed effect of leaky transform faults, but northward migration of volcanism implies southward motion of the North American plate, rather than west-southwest plate motion as inferred from the Yellowstone hot spot. The Clear Lake hot spot appears to be linked to motion of the Pacific plate, or a sliver of it, and thus may imply that part of the Pacific plate is moving beneath the North American plate.

Upper Cenozoic rhyolites of the southern Sierra Nevada, California

Four upper Cenozoic rhyolite domes occur on the Kern Plateau of the southern Sierra Nevada within 40 km of the Coso geothermal area. The Sierra Nevada domes include Monache, Templeton, and Little Templeton Mountains, dated by $^{40}Ar/^{39}Ar$ and potassium-argon at about 2.4 m.y., and an unnamed dome between the Monache and Templeton domes that is dated by potassium-argon at 0.185 ± 0.015 m.y.

Results of detailed mineralogic and geochemical studies by C. R. Bacon and W. A. Duffield suggest that the 2.4-million-year-old rhyolites erupted from deep crustal sources, whereas the youngest rhyolite was probably derived by relatively shallow differentiation of somewhat less-silicic magma. The rhyolite of Monache Mountain contains the unusual phenocryst assemblage almandine + fayalite + biotite + plagioclase. Four lines of evidence show that the garnets are indeed phenocrysts: (1) crys-

tals are euhedral, virtually unzoned, and have growth-related striations on faces, (2) inclusions of apatite and zircon in almandine, fayalite, and biotite have minor element contents within the range of microphenocrysts in the groundmass, (3) both almandine and fayalite commonly contain blebs of pyrrhotite in their cores, and (4) tiny inclusions of silicate glass are present within apatite needles included in almandine. Consideration of experimental and thermodynamic data and mineral compositions indicates that phenocrysts equilibrated at 980±50°C, 10.5±3.0 kbar total pressure, and at oxygen fugacity below the fayalite-magnetite-quartz buffer, approximately equivalent to that defined by the breakdown of graphite to form CO_2.

Pliocene (3.6 m.y.) and Pleistocene mafic volcanic rocks occur on the Kern Plateau near the Sierra Nevada rhyolite domes. These and the rhyolites are coeval with mafic and silicic volcanic rocks 40 km southeast in the Coso volcanic field. Their generation and eruption may reflect intense tectonic extension at the margin of the Basin and Range province and concomitant relaxation of compressive stress in a west-northwest direction allowing melt to reach the surface.

The youngest of the Sierra domes is a high-silica rhyolite. Conceivably, a small geothermal system may exist within granitic basement rocks nearby.

Origin of voids in volcanic bedrock at Teton damsite, Idaho

Detailed analysis by G. F. Embree (USGS) and G. G. Oberhansley (Brigham Young Univ.) of secondary flow structures in the Huckleberry Ridge Tuff (1.9 m.y.) between Ashton and the Teton River, Fremont County, Idaho, suggests that the tuff was remobilized after it came to rest and developed normal compaction fabric, but before it completely cooled. The orientation of major structures, including large (20–100 m) amplitude folds, suggests that the secondary flowage was the result of doming of the ash-flow sheet during precollapse tumescence of a 15- to 20-km-diameter Pleistocene caldera. The south rim and moat of this caldera are defined by an arcuate scarp and a depression known as Hog Hollow, located 2 km north of the confluence of Teton River and Canyon Creek.

The Huckleberry Ridge Tuff, which has its source in Yellowstone caldera, is about 100 m thick in Teton Canyon. When secondary flowage occurred, the lower quarter to third of the sheet was still quite hot and mobile; thus it responded to doming by viscous flow as evidenced by well-developed foliation and recumbant isoclinal flow folds. The middle part of the sheet, which was slightly cooler, contains subhorizontal zones of closely spaced, imbricate, low-angle joints or shears that probably behaved as miniature detachments. The upper third of the unit, which was considerably cooler and more brittle, developed columnar joints as well as low-angle joints. Flowage in the lower viscous part of the sheet caused the more brittle upper part to pull apart forming large blocks separated by open fissures and voids a few centimeters to a meter or more wide.

At the Teton damsite, about 6 km southwest of the "Hog Hollow" caldera rim, the dominant set of open joints strikes northwest (Prostka, 1977) normal to the inferred direction of flow off the precaldera dome. Thus it appears that the numerous open fissures and voids in the volcanic bedrock at the Teton damsite were caused by secondary flowage of the Huckleberry Ridge Tuff about 1.9 million years ago, and this flowage was related to tumescence of the nearby "Hog Hollow" caldera.

Latest eruptions at Newberry Volcano in Oregon

The latest eruptions at Newberry Volcano in central Oregon produced a pumice fall, ash flow, and obsidian flow that erupted near the southern margin of the summit caldera. The pumice fall (Carbon-14 age 1720±250, 1550±120 years) occurs in a narrow 8-km-wide lobe that extends as much as 60 km N. 80° E. from its apparent source, at or very near the vent for the "Big Obsidian Flow." Isopachs based on 150 thickness measurements by N. S. MacLeod (USGS) and D. R. Sherrod (Oregon State University) show that the fall is 4 m thick at 3.5 km from the vent, 3 m at 5 km, 2 m at 9 km, and 1 m at 25 km and that the 0.25 m isopach extends to about 60 km. The total volume of ash is about 0.3^3 km^3 or 0.06 km^3 equivalent dense rock. The ash flow (Carbon-14 age 2054±230, 1390±200, 1270±60 years) covers an area of about 5 km^2 mostly north of the vent. Its volume is poorly constrained but is probably about 0.01 km^3 or 0.002 km^3 equivalent dense rock. Pumiceous and ash-rich mudflows extend 1 to 2 km south from the caldera rim down canyons of the upper flank of the volcano. They overlie the pumice fall and probably resulted from remobilization of thick near-vent tephra deposits on oversteepened slopes. The "Big Obsidian Flow," and an associated domal protrusion which marks its vent, formed during the concluding phase of the eruption sequence. The flow covers an area of about

3 km², is typically 10 to 35 km thick at its margins, and has a volume of about 0.1 km³. The pumice fall, ash flow, and obsidian flow are virtually aphyric and chemically similar. They are interpreted to be the products of degassing and extrusion of rhyolitic magma during one eruptive cycle. They are the youngest of numerous small rhyolitic eruptive events within Newberry Caldera that postdate the 6,700-year-old "Mount Mazama ash" of Crater Lake, also recognized within the caldera.

Source areas and distribution of Columbia River Basalt Group in Washington

D. A. Swanson and T. L. Wright conclude that known volcanism on the Columbia Plateau began and ended in the southeast part of the province, although NNW feeder dikes for flows of intermediate age occur throughout the eastern two-thirds of the plateau. The oldest flows, the Imnaha Basalt (~17–16 m.y.), were erupted in the southeast and confined there by rugged prebasalt topography. The most voluminous formation, the Grande Ronde Basalt (~16–14.5 m.y.) of the Yakima Basalt Subgroup, was fed by dikes distributed across the eastern half of the plateau; flows cover most of the plateau because of gentle topography and broad source area. The Picture Gorge Basalt, coeval with part of the Grande Ronde, was erupted from dikes in north-central Oregon and is virtually confined to the John Day Basin. Vent areas for major units in the Wanapum Basalt (~14.5–13.5 m.y.) shifted 150 km eastward with time, from the Walla Walla area of the Frenchman Springs Member of the Wanapum Basalt of the Yakima Basalt Subgroup to the Orofino area, Idaho, of the Priest Rapids Member of the Wanapum; flow distributions reflect the changing source areas. All later eruptions, producing flows in the Saddle Mountains Basalt (~13.5–6 m.y.) of the Yakima Basalt Subgroup, apparently occurred in the southeast part of the province, except for those that fed its Ice Harbor Member (8.5 m.y.) near the center of the Columbia Plateau. Some Saddle Mountains flows advanced far westward despite their eastern sources and were channelled by drainages leading to the subsiding center of the plateau. Continuing tectonism during Saddle Mountains time further influenced flow distribution. The fact that volcanism returned to the southeast part of the province and continued there episodically for about 7 million years despite changing tectonic conditions suggests a fundamental heat source or crustal flaw in this area.

Chemical and petrographic subdivision of Precambrian rhyolites in Missouri

A review of the exposed Precambrian rocks of Missouri by W. P. Pratt, based on recent detailed and reconnaissance mapping, shows that widespread volcanic rocks, previously characterized as rhyolites and felsites, can be subdivided into three megascopically distinct petrographic assemblages having relatively simple gross stratigraphic relations (Pratt and others, 1979). The oldest assemblage, which is predominant in the southern and central Saint Francois Mountains, consists of quartz latites and soda-rhyolites (classification of Rittmann, 1952) distinguished by albite-twinned albite phenocrysts. This assemblage is overlain by a second rhyolite assemblage in which "chess-board" albite as well as albite-twinned albite phenocrysts occur in notable amounts. The third and youngest assemblage consists of alkali-rhyolites characteristically containing perthite or microperthite phenocrysts. It makes up most of the Saint Francois Mountains north of about lat. 37°27′ N. and also the Eminence Mountains, where they are unusually rich in potassium. All three assemblages include abundant ash-flow tuffs; remnants of one ash-flow tuff unit are exposed locally over an area of about 1,160 km² and may be as much as 2 km thick. Some evidence suggests that these units erupted from several calderas, but their outlines have not yet been clearly defined.

STUDIES OF VOLCANIC EJECTA AND GASES

Water-extractable trace metals in volcanic eruption clouds

D. B. Smith and R. A. Zielinski participated in a project conducted by the National Center for Atmospheric Research to study volcanic eruption clouds. Aircraft-mounted filter samplers were used to collect the aerosol fraction of the eruption clouds of three active Guatemalan volcanoes (Fuego, Pacaya, and Santiaguito). The samplers contained three filters in series. The first was a Fluoropore filter with a nominal pore size of 0.5 microns for removing particulates from the eruption cloud. The second and third were Whatman filters treated with tetrabutyl ammonium hydroxide to preferentially retain acidic volatiles contained in the cloud. The mass of air sampled by the filters ranged from 0.15 to 6.6 kg. For each, volcano samples were collected at increasing distances from the vent. After sample collection, each filter was extracted with 60 ml of water. Splits were filtered and analyzed for 18 metals by inductively coupled plasma-optical emis-

sion spectrometry. Fluoride and chloride were analyzed by specific ion electrode. Uranium was determined by fission track methods.

The elements Zn, Cu, Pb, Cd, Co, Cl, and F are consistently enriched in the water-soluble extracts of the aerosol relative to bulk ash by factors ranging from ten to a few thousand. The results pertain to the mobility of elements during and shortly after a volcanic eruption and have economic and environmental applications.

PLUTONIC ROCKS AND MAGMATIC PROCESSES

New data on the age of the Independence dike swarm in eastern California

Radiometric dating of zircons by the lead-uranium method by James Chen (University of California, Santa Barbara) has yielded concordant ages of 148 m.y. on three silicic dikes of the regionally important Independence dike swarm that extends for more than 250 km in eastern California. These lead-uranium ages probably indicate the time of intrusion of the entire dike swarm. Ages older than 148 m.y. were also obtained by the lead-uranium method on 11 plutons that are cut by the dikes, and a younger age was determined on one pluton that cuts the dike swarm—these data support the indicated age of the dike swarm. Additional lead-uranium analyses of rare zircons in mafic dikes of the swarm yielded discordant, inordinately old ages that suggest entrapment of Precambrian zircons in the dike magma at depth.

Analysis of these new age data suggests to J. G. Moore that the regional fracture system intruded by the dikes was produced by a crustal extension event that occurred after the Late Jurassic Nevadan orogeny when subduction beneath the Sierra Nevada foothill belt jumped westward, and subduction of Franciscan rocks along the Coast Range thrust was initiated.

Age of Archean events in the Big Horn Mountains of Wyoming

Field mapping of Archean gneisses in the Lake Helen quadrangle of the southwestern Big Horn Mountains, Wyo., by Fred Barker has documented two major rock-forming events. In the older event, migmatitic, banded trondhjemitic, and tonalitic gneiss was formed. This rock contains from 1 to 5 percent lenses of metabasalt, either as smeared-out dikes or inclusions, and was metamorphosed to the upper amphibolitic facies and partially melted to produce 5-to-10-percent dikes of pegmatite. Isotopic dating of zircons in the trondhjemitic gneiss by the lead-uranium method by T. W. Stern and M. F. Newell and whole-rock rubidium-strontium determinations on the gneiss by J. G. Arth gave ages of 2,972±180 and 3,007±88 m.y., respectively. In the younger event, small lenticular bodies of quartz diorite, tonalite, granodiorite, and granite were synkinematically intruded. Rubidium-strontium dating of these rocks by Arth confirmed the 2,800 m.y. age determined by earlier workers. A pluton of foliated trondhjemite (45 km^2), emplaced before the major plutonism of the younger event, may be a precursor of that event, however. The trondhjemitic rocks of both events are high in Al_2O_3 (14.6 to 16.3 percent) and depleted in heavy rare earths. The intrusive rocks of the younger event are calc-alkaline and have color indices of 10 to 20 for all types except granite.

METAMORPHIC ROCKS AND PROCESSES

Mineral equilibria of slightly calcic pelitic schists in Barrovian regional metamorphism

Many pelitic schists, which have undergone Barrovian-type metamorphism, have a garnet almandine-rich-chlorite association in the presence of muscovite and quartz, whereas others have a biotite-chloritoid assemblage. It has been thought that the biotite-chloritoid assemblage is a higher grade equivalent of the garnet-chlorite assemblage, because a balanced reaction can be written showing the release of H_2O upon formation of biotite+chloritoid. However, the biotite-chloritoid pair is found in coexistence with chlorite and garnet in many schists in southwest Massachusetts, and the areal distribution of the assemblage suggests that univariancy is not an adequate explanation. Microprobe studies show that the garnet invariably contains calcium in significant amounts; calcium is not zoned and rim depleted as is manganese. E-an Zen proposes that calcium in garnet pulls the phase out of the AFM plane of projection into the ACFM volume. Thus garnet-chlorite-chloritoid-biotite in the presence of quartz, muscovite, and plagioclase is a stable, pseudodivariant assemblage. Two of the bounding facies of this four-phase assemblage, respectively without biotite and without chloritoid, are both univariant and are commonly found. With higher calcium content in the rock, hornblende can be added to either three-phase assemblage. Epidote is a common mineral in these rocks, and, below the garnet zone, it is an important calcium-bearing phase. Its abundance drops abruptly with the appearance of garnet, but even in the staurolite zone

it is common in minor quantities and actively participates in reactions such as garnet+chlorite+muscovite→epidote+staurolite+biotite+H_2O. Thus, the success of analyzing mineral assemblages of schists with chlorite+garnet assemblages may be the result of the assemblages being saturated with calcium.

GEOCHEMISTRY OF WATER

The primary objectives of geochemical studies in hydrogeology are to increase the understanding of (1) hydrochemical processes that control the chemical character of water and the mineralogic changes in sediments and rocks, (2) physics of flow systems by application of geochemical principles, (3) rates of chemical reactions and transport of physical and chemical masses within the geohydrologic system, and (4) concomitant chemical changes between water and sediments.

WATER-ROCK INTERACTIONS

Isotopes indicate rain-soil interaction

Comparisons of deuterium and tritium concentrations in rainfall and the resulting storm runoff in the Mattole River basin in northwestern California indicated that extensive contact between rainwater and soils can occur during periods of heavy precipitation and rapid runoff. V. C. Kennedy and T. A. Wyerman found that the deuterium and tritium content of stream water changed relatively little even when discharge increased more than 50 times because of rainfall that had markedly different concentrations of these isotopes. The apparent explanation for these interactions is that rain displaced prestorm water and (or) reacted with soils that changed its isotopic composition.

HYDROCHEMISTRY OF VOLCANIC AQUIFERS

Leaching profiles in volcanic glasses

A. H. Truesdell (1966) and A. F. White (1979) suggested that the vitric tuffs underlying many areas of the western United States significantly affect the quality of ground water in these areas. Present research by White and H. C. Claassen is aimed at understanding the kinetic mechanisms and rates of hydrolysis and dissolution of volcanic glasses under experimentally controlled pH, temperature, and ionic concentrations similar to those of ground water. Concentration profiles produced by cation diffusion of glasses during reaction were studied by repeatedly reacting glass surfaces with dilute hydrofluoric acid. Specific gravity, chemical composition, and surface-area data permitted quantitative description of the diffusion profiles as a function of time, pH, and solution ionic composition. The leached zones of selected hydrated glasses appeared to increase in thickness during the first 300 hours of reaction at near neutral pH. Over longer time periods, steady-state thickness (~75Å) corresponded to equilibration of the rates of surface-layer dissolution and ion diffusion.

Kinetic model

The hydrologic system of the Rainier Mesa in Nevada consists of a partially saturated divitrified tuff which overlies a vitric tuff that ranges from saturated to partially saturated. Studies by White and Claassen (1977) showed that reactions taking place within the vitric tuff are primarily responsible for the observed water chemistry. Kinetic modeling of the water composition by H. C. Claassen and A. F. White consisted of the following steps: (1) estimating initial carbon dioxide availability, (2) determining the reaction step interval, (3) estimating the reaction rate constants for each species as a function of pH, and (4) determining the mass transferred to solution for each species. Because montmorillonite was present in the aquifer, the model allowed the mineral to precipitate.

Matching ground-water composition with the model results yielded a unique value for the ratio of aquifer surface area to ground-water volume. Values for this ratio are required to model ground-water transport of pollutants.

EVALUATION OF BRINES

Closed-basin lake systems

A general scheme for the evaluation of mechanisms controlling the major solutes during the geochemical evolution of closed-basin brines was formulated and applied by B. F. Jones (USGS) and H. P. Euster (Johns Hopkins University) to data from closed-basin lake systems in the western United States and Canada and the Magadi Basin of Kenya. The pronounced chemical fractionations that take place between dilute and concentrated brines were recognized by referencing individual solute concentrations to chloride or minor constituents conserved in solution over a wide range of salinity. The mechanisms identified (other than

mineral precipitation) included selective dissolution of efflorescent crusts and sediment coating, sorption on active surfaces, degassing, and redox reactions. Only mineral precipitation has been tested by computer simulation; the other processes vary considerably in importance from basin to basin because of differences in flow patterns, availability and nature of reactive surfaces, solids-solution ratios, and residence time of the fluids.

Bolivian Altiplano salars

Analyses and interpretation of brine data from the Bolivian Altiplano salars by S. L. Rettig and B. F. Jones (USGS) and Francois Risacher (Office of Overseas Scientific and Technical Research) (ORSTOM) developed interpretive techniques, based on referencing solutes to bromide and density to predict brine evolution trends, mineral controls on solution composition, most favorable locales for resource exploration, and re-solution of deposits in other areas. These techniques were used successfully to determine major solute accumulation from the Pleistocene lake system, including Lake Titicaca, in Bolivia, and the economically significant input of lithium and boron from the rhyolitic terrane of the Rio Grande de Lipez to the south.

Geopressured zones

Y. K. Kharaka reported that detailed chemical and isotopic analyses of 120 formation-water samples from 25 oil and gas fields in coastal Texas and Louisiana (Y. K. Kharaka, W. W. Carothers, and P. M. Brown, 1978) showed that (1) the salinity of water in the geopressured zone ranges from about 10,000 to 270,000 mg/L dissolved solids and may be higher or lower than the salinity of water in the normally pressured zone, (2) the waters are of marine connate type, and (3) samples with salinities lower than about 10,000 mg/L do not represent the true salinity of formation water because of dilution by condensed water vapor produced with natural gas.

Organic acid anions and $\delta^{13}C$ values of HCO_3 in 95 samples from oil and gas fields in Texas and California indicated that decarboxylation of these acid anions may produce natural gas and CO_2 in formation waters, diagenetic carbonate materials, and petroleum.

Lignite decomposition

Soil-gas probes were installed at six locations in and near an active lignite mine at Gascoyne, N. Dak., as part of a study of the influence of strip mining on the geochemistry of ground water. D. W. Fisher and D. C. Thorstenson found significant differences relative to the atmosphere in soil-gas oxygen and carbon dioxide at four of the six sites. The four sites (two in reclaimed spoils and two at undisturbed locations) were characterized by the presence of some lignite above the water table. At depths greater than about 10 m, only trace amounts of oxygen remained in soil gas, whereas carbon dioxide contents ranged from 11 to 26 percent by volume, thus suggesting an active generation of carbon dioxide by reaction between lignite and atmospheric oxygen. At the two remaining sites (both undisturbed) no significant amounts of lignite occurred above the water table. Oxygen depletion was slight and carbon dioxide content was less than 2 percent of the soil gases in these locations.

The $\delta^{13}C$ values of seven samples of the low oxygen, high carbon dioxide soil gases ranged from -12 to -23 per mil. Carbon-14 analyses of six of these gases showed about 2 percent modern carbon from the undisturbed sites and 10 to 20 percent modern carbon in the spoils. The isotope data indicated that much of the subsurface carbon dioxide from these sites is derived from lignite. There were significant vertical and lateral variations in the carbon-isotope ratios of the soil gases. The causes of these variations have not been determined.

Clay-humic complexes

A procedure devised by R. W. Wershaw and D. J. Pinckney for the isolation, fractionation, and characterization of clay-humic complexes showed that amino acids and proteins bind humic materials to clay mineral particles. Soil organic polyelectrolytes (humic substances) exist in soils and sediments in a free state and as complexes with clay minerals and metal oxides. Clay-humic complexes are generally much more abundant than metal oxide-humic complexes. Athough it has long been recognized that clay-humic complexes are major components in most soils and sediments and that they influence the chemical and physical properties of soils and sediments that contain them, methods for the isolation and characterization of these complexes have not been well developed.

Stability of polysulfides

J. D. Hem reported that thermodynamic calculations describing the redox chemistry of sulfur in aqueous systems (Nriagu and Hem, 1978) showed

that disproportions can lead to an extensive array of dissolved species, especially in sulfur-rich reduced systems; these may include such species as polysulfides, thionates, and thiosulfate as well as the usually predominant sulfides. Some of these anions form complexes with metal cations and increase the solubility of a metal. Conditions favorable for these effects occur in some geothermal systems but are probably rare in other ground-water systems.

STATISTICAL GEOCHEMISTRY AND PETROLOGY

Universal data transformation

A universal log transformation, $z=\ln[bx/(b-x)]$, has been proposed by H. J. de Wijs (Harris, 1977, pt. III, p. 1–12) for normalizing assay data, where z is the transformed value, x is the original value, and the parameter b is the theoretical upper limit for the assay value. For example, in a chalcopyrite ore b is equal to 34.5, the percentage concentration of copper in the pure mineral. A. T. Miesch has examined the possible utility of this transformation in geochemical investigations of rocks and soil rather than ores. De Wijs has shown that it has the advantage over other log transformations in that it may be applied to negatively skewed, symmetrical, and positively skewed data. In geochemical studies of rocks and soils, however, the theoretical upper concentration limit, b, is generally far greater than the maximum observed concentration, and the transformation in this situation is unsuccessful. Alternatively, b was estimated by incrementing upwards from the maximum observed concentration until the skewness in the transformed values reached a minimum in absolute value. The results of the study showed that skewness and kurtosis of the universal transformed values were closer to those of the normal distribution than those transformed by $z-\ln(x-a)$ or $z=\ln(a-x)$ in about one-half of the comparisons, but that they were far worse in enough comparisons to discourage one from using the new transformation routinely.

EXTENDED Q-MODE FACTOR ANALYSIS

It is generally recognized that in Q-mode factor analysis of geochemical and petrologic data, based on a cosine-theta similarity matrix (Imbrie and Purdy, 1962), the variables must be scaled in order to give them equal weight. This is most commonly done by either dividing each variable through by its maximum value or by expressing each value as a proportion of the total range of the variable. Neither of these transformations, however, leads to scaled data with equal means and variances. A. T. Miesch has found it advantageous to scale each variable to have a mean of 0.5 and a standard deviation of s, where s is as large as possible without causing the appearance of negative values in the scaled data. It has also been shown that the common method of interpreting eigenvalues in Q-mode factor analysis is grossly misleading. If the sum of the first m eigenvalues of the cosine-theta matrix, or its equivalent, is equal to 90 percent of the trace of the matrix, for example, it is commonly concluded that m factors (end-members in a compositional system) will account for 90 percent of the variance in the data. This conclusion should refer to the data in their scaled and row-normalized form, not the original data that entered the analysis. The extended form of Q-mode factor analysis described by Miesch (1976a, b) provides estimates of the variance accounted for in the original data; these estimates are always much closer to those derived from the eigenvalues of the correlation matrix than to those from the cosine-theta matrix and are always a great deal more conservative.

Application to volcanic rocks of Antarctica

The methods of extended Q-mode factor analysis were applied to a study of differentiation processes that formed the volcanic rocks of Ross Island and vicinity, Antarctica, in a cooperative study by J. S. Stuckless, A. T. Miesch, S. S. Goldich, and P. W. Weiblen (1978; in press). The results showed that the compositional variations among 48 of the 49 lavas could have been caused largely by fractional crystallization within the magma chamber. It is shown further that the compositions of the crystallized phases must have changed abruptly when the differentiation process was about three-fourths complete and that about 87 percent of the initial magma crystallized before the last eruption occurred. Variation among the early lavas can be accounted for by differential separation of pyroxene, olivine, iron-titanium oxide, and ilmenite. Variation among the younger lavas can be accounted for by differential separation of plagioclase, pyroxene, hornblende, iron-titanium oxide, apatite, and, at the very late stages, anorthoclase. The model accounts for more than 94 percent of the variance in all of the major oxides and 49 to 95 percent of the variance in 17 minor constituents.

Application of granitic rocks of the Granite Mountains, Wyoming

J. S. Stuckless, A. T. Miesch, and H. T. Millard, Jr., used extended *Q*-mode factor methods to examine chemical variations among 38 chemical constituents in 49 samples from the Granite Mountains in Wyoming. It was found that in the 29 unaltered samples known to be part of the major intrusion, four of the constituents vary with almost complete independence of the others; these are H_2O, CO_2, UO_2, and Cs_2O. Other constituents that vary somewhat independently of the others are Cl, F, Fe_2O_3, FeO, MnO, and Rb_2O. Fe_2O_3 and FeO, however, vary closely with other constituents when expressed as total iron oxide (FeO). The concentrations of H_2O, CO_2, UO_2, and, to lesser degrees, those of CL, F, and the iron oxides, are interpreted to have been controlled by recent near-surface alteration. Most of the variation in 33 constituents, including 11 rare-earth elements, can be accounted for by a process wherein one group of materials is added to a parent magma and another group is subtracted. Each group of material varied in composition within a two-end-member compositional series. Thus, the model contains five end members. An approximation of the original analytical data was derived by mathematically mixing the five end-member compositions in the derived mixing proportions. The constituent means for the computed data are essentially the same as those for the original data, and the correlations between the computed and original data range from 0.80 to 0.97 for the 33 constituents. The rare-earth patterns derived from the computed data are also close to those constructed from the original data, especially for the lighter rare-earth elements.

ISOTOPE AND NUCLEAR GEOCHEMISTRY

ISOTOPE TRACER STUDIES

Extreme fractionation of $^{234}U/^{238}U$ isotopes within a Missouri aquifer

Isotopic fractionation between ^{234}U and ^{238}U as great as 1,600 percent was measured by B. J. Szabo in spring waters of the Western Ozark Highland in Missouri. The artesian springs, located in the Pomme de Terre River Valley of southern Benton and northern Hickory Counties, include Trolinger, Nigger, Phillips, Koch, and Boney Spring. The bedrock is mainly Lower Ordovician limestone. The uranium and thorium concentrations of all but Boney Spring are 0.2 ppb and <0.1 ppb, respectively; Boney Spring shows 0.5 ppb and <0.2 ppb, respectively. The activity ratios of $^{234}U/^{238}U$ in Trolinger, Nigger, Phillips, Koch, and Boney Spring are 16.0, 15.2, 13.0, 7.6, and 7.2, respectively. Typical values of $^{234}U/^{238}U$ ratios in surface waters range from 0.8 to 2.5. The previously reported ratios in underground waters vary from 0.6 to 12.2. The extreme fractionation is probably the result of ^{238}U decay within the rock. Alpha recoil propels some of the ^{234}Th daughters across the rock-water interface, followed by rapid decay of ^{234}Th to ^{234}U. Because this is a time-dependent process, the $^{234}U/^{238}U$ ratios may provide a means of measuring the residence time of confined groundwaters in aquifers.

Strontium and lead isotopic composition in volcanic rocks from Peru and New Hebrides—genesis of calc-alkaline lava

Mitsunobu Tatsumoto (USGS) and J. R. Lancelot, Louis Briqueu, and B. Westphal (University of Sciences et Techniques du Languedoc, Montpellier, France) performed strontium (at USTL) and lead (at USGS, Denver) isotope analyses on Pliocene and Quaternary calc-alkaline lavas of two active plate margins where an oceanic slab is being subducted under another oceanic slab.

In New Hebrides, lead isotopic compositions of calc-alkaline lavas (mostly andesites) fall in the field of midocean ridge basalts (MORB). Spilitized MORB fall in the same field. Strontium isotope ratios ($^{87}Sr/^{86}Sr = 0.70238 \pm 0.00020$) are homogenous for the calc-alkaline lavas and in agreement with previous results obtained for rocks of subduction zones where a continental crust is not involved. Lead and strontium ratios and trace-element data suggest that calc-alkaline rocks of this island arc were derived by partial melting of altered MORB from the subducted oceanic slab. Furthermore, the data support the incorporation of sediments (1 to 2 percent) during partial melting (Tatsumoto, 1969; Kay and others, 1978), but the lead isotopic data for this young island arc system appear to limit possible source materials of these sediments to the arc itself.

In southern Peru, the Barrosso and Arequipa volcanic fields were studied (andesite, dacite, rhyolite). Measured $^{87}Sr/^{86}Sr$ of 0.70511 to 0.70735 agrees with previous results of James and others (1976), but a plot of $^{87}Sr/^{86}Sr$ versus $1/(^{86}Sr)$ indicates that enrichment of radiogenic ^{87}Sr occurred during the fractional crystallization of the calc-alkaline liquid. Similar trends were observed in $^{87}Sr/^{86}Sr$ versus rubidium-strontium diagrams by James and others (1976) who interpreted them as

apparent isochrons resulting from inhomogeneities in the source region. An interpretation involving contamination by radiogenic strontium from the continental crust is more satisfactory, but the proposed binary mixing model does not involve a simple mass-mixing of the two components. This model is confirmed by samarium-neodymium studies (DePaola and Wasserburg, 1977; Ben Othman and others, in press) and anomalous lead isotopic compositions. Both tracers clearly indicate the influence of an old continental material on the calc-alkaline magma.

Neodymium isotopic composition of kimberlites

The Sm-Nd systematics of six kimberlites from South Africa, India, and the Colorado-Wyoming border, whose eruption ages range from 90 to 1,300 m.y., were studied by Mitsunobu Tatsumoto (USGS) and A. R. Basu (Colorado School of Mines). The study also included granular and sheared garnet lherzolite inclusions in kimberlite from the Bultfontein pipe in South Africa.

In the garnet lherzolites, samarium and neodymium concentrations are highest in clinopyroxene, intermediate in garnet, and lowest in phlogopite. The initial $^{143}Nd/^{144}Nd$ ratios (at the time of pipe emplacement) are the same for garnet and clinopyroxene, in both sheared and granular lherzolite. The ratio of phlogopite is higher and that of host kimberlite the highest.

The isotopic equilibration of coexisting garnet and clinopyroxene supports the assumption of chemical equilibrium in the estimation of temperatures and pressures on the basis of major element partitioning. The difference in neodymium-isotopic composition of phlogopite and coexisting clinopyroxene and garnet is probably due to contamination from the host kimberlite. The lower initial $^{143}Nd/^{144}Nd$ values in isotopically unaltered minerals in lherzolite compared with kimberlite suggests that the mantle represented by the xenoliths has a lower Sm/Nd ratio and a rare-earth-element (REE) pattern enriched in light REE, such as those of alkalic basalts. The data support the conclusion of petrologic studies that the inclusions are not cognate, but originate deeper in the mantle where the Sm/Nd ratio is larger than that of the inclusions.

The initial $^{143}Nd/^{144}Nd$ ratios of the six kimberlites fall on the $^{143}Nd/^{144}Nd$ growth line for basaltic achondrite, Juvinas, for the time of pipe emplacement. Thus the kimberlite source is chondritic in REE abundances and has remained so for 4.56 billion years. Uranium-lead and rubidium-strontium systematics in mantle-derived kimberlites reveal that the kimberlite source region has a higher uranium-lead and a lower rubidium-strontium ratio than chondrites. This difference may reflect entry of lead and rubidium, along with sulfur and potassium, into the core during core-mantle differentiation

Origin and history of the adcumulate eucrite, Moama

The cumulate eucrite, Moama, was analyzed for rare-earth elements (REE), uranium, thorium, and lead concentrations and neodymium and lead isotopic compositions by D. M. Unruh and Mitsunobu Tatsumoto (USGS) and Jean Hamet (Colorado School of Mines) and N. Nakamura (Kobe Univ., Japan). A Sm-Nd age of 4.59 ± 0.05 (2σ) b.y. and an initial $^{143}Nd/^{144}Nd$ ratio of 0.50684 ± 0.00008 were obtained.

Moama contains the lowest total trivalent-REE abundances, the largest positive eucrite anomaly, and the most fractionated REE abundance pattern (light REE depleted) of any eucrite. These observations support the hypothesis that Moama is a cumulate and was not derived by partial melting of a chondritic source. The REE data suggest that Moama was derived by about 1 to 5 percent fractional crystallization from a liquid with REE contents similar to Juvinas, or by about 20-to-30-percent fractional crystallization from a Sioux County-like liquid, and support the hypothesis that the cumulate meteorites —Moama, Serra de Magé, and Moore County— may be derived from the same parent liquid by fractional crystallization of pigeonite and plagioclase in peritectic proportions.

Most of the lead in Moama is of terrestrial origin, of *B*-type composition (U depleted relative to Pb). This demonstrates that large amounts of *B*-type lead contamination in meteorites can exist. Other meteorites (for example, Toluca) that show anomalously young second-stage lead-lead ages should be reexamined to determine if the ages are significant and date asteroidal collisions and if these meteorites contain significant terrestrial lead contamination.

Implications from Luna 24 to U-Pb evolution in the lunar mantle

Uranium, thorium, and lead analyses were performed by D. M. Unruh and Mitsunobu Tatsumoto on mineral separates from a 12-mg aliquot of Luna 24 sample 24170 in an attempt to determine the age of the basalt and uranium-lead evolution in the Mare Crisium area. The lead in the Luna 24 separates is nonradiogenic ($^{206}Pb/^{204}Pb$ ~22–50) compared to other lunar basalts ($^{206}Pb/^{204}Pb \geq 300$).

This may reflect terrestrial contamination; however, terrestrial contamination alone will not account for all of the trends suggested by the data. The Luna 24 basalt had a rather complex postcrystallizational history. A 0.5±0.5-billion-year-old disturbance to the U-Pb system is suggested by the U-Pb data (if the disturbance represents a single event). Some separates also appear to be "contaminated" by Luna 24 soil-type lead. Three-stage U-Pb evolution model calculations indicate that crystal cumulates in the source area of the Luna 24 basalt evolved under a very low $^{238}U/^{204}Pb$ environment (~12–15) relative to Apollo mare basalts. The calculations may reflect a laterally heterogeneous lunar magma ocean, U-Pb fractionation during cumulate formation (primary differentiation), and (or) lack of potassium, rare-earth elements and phosphorous addition to the Luna 24 basalt. In spite of the calculated low initial $^{238}U/^{204}Pb$ ratios, the data are consistent with the hypothesis that the moon originally accreted as a volatile-depleted body. The low observed $^{238}U/^{204}Pb$ ratios are roughly compatible with a crude relationship between the potassium content and the $^{238}U/^{204}Pb$ ratio observed in Apollo mare basalts.

STABLE ISOTOPES

Strontium isotopes and minor-element geochemistry of alkaline rocks, Wet Mountain, Colorado

C. E. Hedge and T. J. Armbrustmacher have found that strontium isotopes and minor-element geochemistry of the alkaline rocks of the Wet Mountains indicate a complex petrogenesis. The McClure Mountain Complex was emplaced about 530 million years ago. The data suggest that at least three different magmas were involved. The gabbros and hornblende syenites have similar initial Sr^{87}/Sr^{86} ratios (≈0.7045), but their respective rare-earth patterns seem to preclude any possible genetic relationship between the two rock types. The nepheline syenites, from the McClure Mountain Complex, have lower initial Sr^{87}/Sr^{86} ratios (≈0.7038) than the hornblende syenites or the gabbros.

The complex at Democrat Creek is slightly younger (510 m.y.) than the McClure Mountains Complex and has distinctly different geochemical characteristics. Rubidium, strontium, and the light rare-earth elements are lower in the syenites at Democrat Creek, and so are the initial Sr^{87}/Sr^{86} ratios (0.7030).

Lower Archean gneiss from Wyoming

A minimum age of 3,200 m.y. has been obtained on zircon from a tonalitic gneiss from the Granite Mountains of central Wyoming in a study by R. E. Zartman and J. S. Stacey. The rock is a medium-gray, fine- to medium-grained, foliated tonalite that occurs at the west end of the Granite Mountains where it forms part of a metamorphic complex that includes migmatite, amphibolite, and biotite schist. Previous Rb-Sr whole-rock dating gave an isochron corresponding to an age of 2,860±80 m.y. with an $^{87}Sr/^{86}Sr$ intercept of 0.7048±0.0012 (Peterman and Hildreth, 1978). The Rb-Sr age agrees with an earlier Pb-Pb whole-rock age of 2,910 m.y. reported by Nkomo and Rosholt (1972). The Rb-Sr age was interpreted as the time of major metamorphism, and the high initial Sr-isotope ratio prompted the suggestion that the protoliths of these rocks may have been considerably older by 300 to 400 m.y.

Data for the zircons show a moderate discordance with $^{206}Pb/^{238}U$, $^{207}Pb/^{235}U$, and $^{207}Pb/^{206}Pb$ ages being 2,430, 2,870, and 3,200 m.y., respectively, for the 100- to 150-mesh fraction. Data for a coarser fraction (50–100 mesh) are not significantly different. Although the pattern of discordance cannot be determined from these data, the 3,200 m.y. Pb-Pb age is considered to be a minimum value for the age of the zircons. This age is among the oldest reported for gneisses of the Wyoming age province and further illustrates the long and complex history contained in the rocks of this major Archean craton. This age also adds credence to the empirical observation that the oldest units in ancient high-grade complexes are commonly gray, foliated, tonalitic gneisses. Whether the central part of the Wyoming age province contains gneisses akin to the very ancient rocks of southern Minnesota, northern Michigan, Labrador, and Greenland is uncertain, but the probability may be increasing.

Light-stable isotope and fluid-inclusion studies of the East Tintic district in Utah

J. N. Batchelder, J. R. O'Neil, and H. T. Morris conducted a light-stable isotope and fluid-inclusion study of quartz, barite, and galena from the East Tintic mining district in Utah. Fluid inclusions in barite have homogenization temperatures of 300°C to 390°C. No salinities could be obtained. Fluid inclusions in quartz have temperatures of homogenization from 185°C to 325°C and salinities generally less than 1 percent but locally up to 3.5 equivalent weight percent NaCl. The calculated $\delta^{18}O$ values of water in equilibrium with quartz range from −10.0 to +1.5 per mil. The δD values of water in fluid inclusions in quartz range from −131 to −98 per mil.

Fluid-inclusion water in galena has $\delta^{18}O$ values of −16.6 to −5.4 per mil and δD values of −121 to −84 per mil. Values of $\delta^{34}S$ for the galenas range from −3.5 to +0.6 per mil.

A technique was developed to scrutinize inclusion fluids in cleaved galena. Upon cleaving, the fluids from the inclusions "blew out" leaving behind evaporite halos on the surface around the cavity. Quantitative analyses were performed using an X-ray energy dispersive analyzer and halite and sylvite were identified in the halos but not in the cavities. However, daughter minerals of tetrahedrite, chalcopyrite, argentiferous tetrahedrite, and a silver-antimonide were identified in the cavities.

These data indicate that galena was likely deposited from a saline-brine (<23 equivalent weight percent NaCl) composed of approximately equal proportions of magmatic and meteoric waters. Quartz, on the other hand, although intimately related to galena texturally, was deposited entirely by fluids of meteoric origin that were enriched in ^{18}O through exchange with the wall rock.

Sulfur isotope studies at Creede, Colorado

P. B. Barton, R. O. Rye, and P. M. Bethke have conducted a sulfur isotope study of the ores at Creede, Colo. Analyses of 67 sulfides and 26 barites show a narrow range of $\delta^{34}S$ values for individual sulfide minerals (−1.2±2.2 per mil for sphalerite) but a very large range of values for barite (19.8 to 33.8 per mil). Systematic sampling of two samples of growth-banded sphalerite from widely spaced localities representing only a small percentage of the paragenesis shows small, but systematic variations that correlate with variations in temperature and salinity of associated fluid inclusions. Late-stage pyrite is significantly heavier than earlier stage pyrite. No gross changes with location within the district are evident. Two pyrites from different localities yielded very anomalous and puzzling $\delta^{34}S$ values of about 41 and 47 per mil.

Except for short-lived perturbations, the chemistry of the hydrothermal system responsible for the ore deposits was sufficiently oxidizing that sulfate was probably 100 times as abundant as sulfide in the ore fluid, yet the ores themselves contain equal amounts of sulfide and sulfate. Sulfate-sulfide sulfur isotope relationships and detailed sulfur isotope data on sphalerite indicate that the sulfur isotope systematics of the hydrothermal system were not governed by equilibrium exchange reactions; rather, they were governed by mixing of reduced and oxidized fluids in an oxidizing environment. Consideration of possible sources and bulk sulfur isotopic composition for the district as a whole favor strongly, but do not prove, a magmaticlike sulfur near 0 per mil derived from either local volcanic rocks or magmatic emanations.

ADVANCES IN GEOCHRONOMETRY

Dating of the Climax Stock; Nevada Test Site

Five samples from the Climax Stock, Nevada Test Site, have been dated by C. W. Naeser using the fission-track method. Apatite from four surface outcrop localities have an average age of 101±3.2 m.y. A fifth sample of apatite is discordant and has an apparent age of 79±7 m.y. This sample was separated from a piece of core taken at a depth of 536 m. The Climax Stock was therefore emplaced at a shallow level in the crust (approximatey 3 km) and has not been significantly buried or uplifted since then.

Marysvale volcanic chronology

In the Marysvale area, Utah (Richfield 2° quad.), H. H. Mehnert, working with C. G. Cunningham and T. A. Stevens, has provided a chronology for a sequence of volcanic events. Volcanic activity began in this area about 30 million years ago and several units were erupted during a brief period from 30 to 26 million years ago. A later cycle of siliceous volcanism occurred between 21 and 17 million years ago. Mineralization apparently took place at several times, but a major period was 14 million years ago.

Potassium-argon ages of Mesozoic mafic rocks of the Pensacola Mountains

Results of a study by A. B. Ford and R. W. Kistler indicate that the Dufek intrusion is the same age as sills of tholeiitic diabase in the Pensacola Mountains and as the main Early to Middle Jurassic episode of Ferrar-type magmatism of the Transantarctic Mountains. Plagioclases from widely separated stratigraphic levels in the Dufek intrusion yield ages of about 172 m.y. Pyroxene dates from the Dufek intrusion are considerably younger, probably as a result of argon loss related to inversion and exsolution in these minerals. Pyroxenes in the sills are optically homogeneous and yield dates slightly older than their coexisting plagioclase. The best age for the sills is considered to be 180 m.y. This date is from a concordant plagiocase-pyroxene mineral pair from a specimen collected several

meters from the top of one of the sills. The sills show close similarity in chemistry and $^{87}Sr/^{86}Sr$ with the Ferrar Group of the Transantarctic Mountains.

Corrections for marine shell radiocarbon dates

Corrections for radiocarbon dates on marine mollusk shells from the Pacific coast have been determined by S. W. Robinson using analysis of modern shells collected prior to nuclear weapons testing. Without correction marine shells yield radiocarbon ages that are too old because of the depletion of carbon-14 in marine bicarbonate. On the Atlantic coast this effect is about 290 years, but, along the Pacific, coastal upwelling brings even older water to the surface. Our results give a correction of 800 years for the Northern Puget Sound and the coasts of Washington and Oregon and 680 years for the California coast.

Thermoluminescence properties of soil carbonate

A preliminary investigation of the thermoluminescence properties of four calcic soils from the Rio Grande Rift, N.M., by R. J. May has shown that thermoluminescence (TL) dating of soil carbonate may be feasible. The four samples represent well-documented calcic horizons whose stratigraphic relationships are known and for which ages inferred from estimated soil formation rates have been established. Recently determined uranium series disequilibrium dates for three out of the four samples agree in general with the soil formation ages and confirm the relative stratigraphic position of the four units. The youngest unit is about 5,000 years old, and the oldest is approximately 400,000 years old. The normalized TL ratios for these units stack in the right order, and the ratios differ from one another by an amount that agrees closely with the differences in age between the units based on the independent age data.

GEOTHERMAL SYSTEMS

Transient pressure analysis in vapor-dominated geothermal systems

A. F. Moench continued theoretical investigations of pressure behavior in vapor-dominated geothermal systems with numerical studies of radial steam flow through porous fissures (Moench, 1979). Results showed that thermal conduction from blocks of impermeable rocks bounding narrow fissures should have a significant influence upon transient-pressure buildup in geothermal steam wells.

In another numerical study using an approach similar to the above, Moench and W. N. Herkelrath (1979) showed that the phenomenon of vapor-pressure lowering, which occurs at low-liquid saturations, has a profound influence upon transient-pressure buildup. With vapor-pressure lowering, it appears that transient-pressure behavior is similar to that expected for noncondensable gases.

Experimental work by Herkelrath on steam flow in porous materials revealed a significant delay in pressure response. This delay is attributed to condensation within the sample even though the steam is superheated (Herkelrath and Moench, 1979). Numerical studies are underway to simulate the experimental results.

Variometer array used to detect electrical conductors and telluric currents in the crust

J. N. Towie reported that interpretation of a geomagnetic array survey across the eastern Sierran Front in the vicinity of the Coso Range, Calif., suggests that there is an electrically conductive path to the east of the Sierra Nevada batholith extending from north-central Oregon to southern California. In the north, this path may consist of a conductive basement beneath the volcanic plateaus of southern Oregon. To the south, the conductive path supports other evidence of the general high conductivity of the Basin and Range province. A secondary electrical conductor was found to be associated with the Coso Range.

Towie also recorded simultaneous observations of geomagnetic field variations across the Rio Grande Rift at approximately lat.35° N. Several instances of current channeling were interpreted to indicate a concentration of telluric current flow beneath the rift. The close spacing of geomagnetic observations in this study allows good lateral resolution of this current concentration which extends from the western margin of the rift to well beneath the Pedernal uplift on the east.

Field procedure and data reduction (with HP 97–67) for total field resistivity surveys

A report by A. A. R. Zohdy (1978) described a field procedure and data-reduction methods for bipole-dipole total-field resistivity surveys. The report includes detailed descriptions of (1) crew requirements and equipment, (2) recommended field procedure, (3) data acquisition procedure, (4) data reduction and program description, (5) theory, and (6) HP 97–67 program listings.

The given programs allow instant in-the-field computation of simple total field, primary field, and complete total-field apparent resistivities, as well as the azimuth of the primary field and the measured field referred to geographic north.

Electrical techniques for geothermal exploration

D. B. Hoover reported that for rapid reconnaissance of geothermal areas a combination of audiomagnetotelluric resistivity mapping and *E*-field ratio telluric traverses has proven effective for delineating the shallow- to medium-depth extents of anomalous conductors. These combined techniques can be applied rather quickly in the field and qualitative interpretations made in a minimum of time.

Method for extrapolating the viscosity of geothermal brines derived

NaCl has been shown to be usable as a model for the viscosity of geothermal brines. Using the viscosity of an NaCl solution having the same equivalent concentration as the geothermal brine yields viscosities that are ±1 percent of those that are observed. This is in contrast to errors in excess of 70 percent based on using the viscosity of pure water for a brine such as the Salton Sea. R. W. Potter II and M. A. Clynne derived a correlation method that allows the existing data for NaCl, which is largely confined to 0°C–150°C, to be extrapolated to temperatures of geothermal interest.

Magnesium correction determined for sodium-potassium-calcium geothermometer

All well-documented high-temperature (>175°C) waters encountered in wells drilled into active hydrothermal systems have low concentrations of magnesium relative to the other dissolved cations. However, many low-temperature geothermal waters have high concentrations of magnesium relative to other dissolved cations. The usefulness of the Na-K-Ca geothermometer for magnesium-rich waters is doubtful because many low-temperature, magnesium-rich waters yield estimated temperatures well above 150°C. R. O. Fournier and R. W. Potter II found that the Na-K-Ca geothermometer can be applied to magnesium-rich waters if a temperature correction is made to compensate for high-magnesium concentrations. Graphs and equations are now available (Fournier and Potter, 1978) that can be used to determine temperature corrections when given waters have Na-K-Ca calculated temperatures >70°C and values of R <50, where $R=\{Mg/(Mg+Ca\ K)\}\times 100$ in equivalents. Waters with values of R >50 probably come from relatively cool aquifers with temperatures about equal to the measured spring temperature, irrespective of much higher calculated Na-K-Ca temperatures.

Teleseismic *P*-wave study at the Battle Mountain heat-flow high, Nevada, shows a deep, high-velocity intrusion present

Preliminary results from teleseismic *P*-wave residual studies over the Battle Mountain High, Nev., by H. M. Iyer and S. M. Green show the presence of a deep, high-velocity intrusion in the upper mantle. Detailed analysis of the data is required to delineate the shape of the intrusion, its depth, and the velocity contrast inside it. Even though it is not clear how the intrusive body is related to the high-heat flow in the region, the results demonstrate the power of the teleseismic technique to detect velocity anomalies in the upper mantle.

Conductive heat flow in the Randsburg area in California

The Randsburg Known Geothermal Resource Area (KGRA) forms part of a NNW-trending series of hydrothermal convective systems stretching from the Northern Gulf of California to the Susanville area in northern California. J. H. Sass reported that heat flows were determined from 14 holes between 100 and 150 m deep; 8 in granitic rocks, 4 in volcanic rocks, and 2 in alluvium. Heat flows range from 1.1 to 8.3 heat-flow units (HFU) (Sass and others, 1978). Heat-flow contours suggest an anomaly comparable in areal extent to the Coso Thermal anomaly (Combs, 1976) but with a much smaller area of very high heat flow (>8 HFU).

A hydrothermal system near Ennis, Montana

Six test holes recently drilled to a maximum depth of 133 m in valley fill near Ennis, Mont., partially delineate a shallow hydrothermal reservoir that extends at least 1 km northward from Ennis hot spring (temperature 83°C). One test hole penetrated about 80 m of saturated sediment at a uniform temperature of about 88°C from a depth of about 20 m to the bottom of the hole. Water temperatures in most of the test holes and nearby domestic wells were higher than in the surrounding groundwater and increased with depth. Higher concentrations of sodium and fluoride characterize the warmer waters.

R. B. Leonard suggested that the water was heated during deep circulation through fractures associated with faults in the crystalline rock that presumably underlies the valley fill. Subsurface tem-

peratures estimated from the chemical composition of the hottest water range from 109°C (chalcedony) to 167°C (Na-K-Ca). Preliminary results of ongoing geophysical studies and penetration of highly permeable zones by the test holes justify deeper drilling to describe the nature and extent of the reservoir.

Intermediate-temperature geothermal waters found in the Verde Valley, Arizona

Verde Hot Springs, which is at the south end of the Verde Valley, has long been known for its thermal qualities. P. P. Ross and C. D. Farrar reported that water samples from wells and springs in the valley indicate two anomalously high temperature areas where Na-K-Ca geotemperatures range from 70°C to 125°C, and SiO_2 geotemperatures range from 79°C to 135°C. The high boron and fluoride concentrations reinforce the distribution pattern of geotemperatures indicated by the two geochemical thermometers. The water temperatures place the geothermal reservoir in the intermediate category for convective hydrothermal systems.

Evaluation of the geothermal potential of the INEL area in Idaho, with deep Schlumberger soundings

Fifty-eight deep Schlumberger soundings were made to study the geothermal potential of the Idaho National Engineering Laboratory (INEL) area on the Snake River Plain in Idaho. Twenty-nine of these soundings were expanded to (AB/2) electrode spacings of 7.3 km that allowed the detection of a high-resistivity electric basement at depths estimated to range from 2 to 5 km. A. A. R. Zohdy prepared five geoelectric sections that depict six primary geoelectric units: (1) wind blown soil of 10–30 ohm-m and a thickness of 0–10 m, (2) dry basalt of ≥1,000 ohm-m and a thickness of 70–300 m, (3) freshwater basalt of 200–600 ohm-m and a thickness of 200–2,000 m, (4) low-resistivity material interpreted to be sedimentary rocks of 7–45 ohm-m and a thickness of 500–2,000 m, (5) silicic volcanic rocks with resistivities of 45–200 ohm-m and thickness of ≥500–2,000 m, and (6) highly resistive ≥500 ohm-m pre-Tertiary basement rocks of very large thickness (several kilometers). A probable presence of a NE-SW-striking major fault was pointed out by the interpretation of the electrical soundings, which supports earlier gravity interpretations. The presence of this fault coupled with the presence of an extensive low-resistivity layer enhances the possibilities for a geothermal resource in the INEL area. The proposed drilling of a 3-km well near the fault zone should also yield significant information on the nature of the low-resistivity layer and the type of the underlying high-resistivity basement rocks.

Seismic refraction at Idaho National Engineering Laboratory, eastern Snake River Plain

A seismic-refraction profile was made across the northwestern boundary of the Snake River Plain at the Idaho National Engineering Laboratory near Arco, Idaho. Interpretation of the results by H. D. Ackermann show that the boundary is marked by a 2,500 m drop in the elevation of the basement rocks from the Arco hills that bound the area. This displacement takes place over a distance of approximately 4 km and can be interpreted either as a fault or a steep downwarp. Eastward onto the plain, the basement undulates slightly for at least 25 km to the eastern end of the survey. A horstlike basement displacement of approximately 150 m was interpreted at a distance of about 10 km from the edge of the plain. This displacement has associated with it a decrease in basement velocity from about 5.5 to 4.9 km/sec. The site for a deep geothermal test well was selected near the western edge of this feature on the basis of results from the seismic and other geotechnical surveys.

Geothermometry applied to Hot Springs in Western United States

N. L. Nehring, E. D. Roberts, and Grace Kaczanowski analyzed over 140 water samples from hot spring systems of the Western United States for sulfate isotope geothermometer temperatures to estimate the geothermal energy contained in these systems. The following selected results give temperatures in degrees Celsius calculated for the most reasonable cooling process: (1) Oregon-Alvord, 207–270; Neal, 190–200; Crumps, 180–200; Breitenbush, 175–200; Vale, 160–190; and Klamath Falls, 135–196; (2) Idaho-Raft River, 142; Weiser, 210–230; and Bruneau-Grandview, 95–131; (3) California-Long Valley, 240 or 269 with calc ^{18}O; Lassen, 300, Morgan-Growler, 235; Coso, 283, old 400-ft well; Kelly 180–200; Seyforth, 185–200; and Clear Lake, 120–190; (4) Nevada-Steamboat Springs, 210–230, Desert Peak, 200–230; West Pinto, 200–230; Lee, 240–280; Leach, 160; Kyle, 150; Sulfur, 150; Smith Creek, 140; Boulder, 130; Utah-Thermo, 135–145; Roosevelt, 270, drillhole, 220, warm seep; and (6) Alaska-Geyser Bight, 282. Other systems tested generally indicated lower temperatures. The sulfate isotope temperatures were generally in good

agreement of a little higher than silica and Na-K-Ca temperatures. For several warm springs (50°C–80°C), SO_4 indicated temperatures were equal to orifice temperatures.

Drill holes give a deeper view into eastern Snake River Plain, Idaho

The USGS and the U.S. Department of Energy sited and supervised the drilling of three intermediate-depth exploration core holes on the eastern Snake River Plain, Idaho (ESRP). These wells provide information about stratigraphic levels not previously penetrated in the ESRP; previous wells reached maximum depths of 500 m. The wells were drilled to investigate the geological relations in three different types of volcanic terrane in the ESRP: (1) a region of rhyolite domes (Well 1), (2) a volcanic rift zone (Well 2–2A), and (3) a caldera (Well 3).

Drill hole 1, logged by D. J. Doherty, is located approximately 2 km southwest of East Butte in Butte County (NE¼ of sec. 22, T. 2 N., R. 32 E.) and was cored to a total depth of 610 m. The top 119 m consists of several olivine-bearing basalt lava flows. These basalts overlie approximately 400 m of devitrified, granular, flow-banded, crystal-poor rhyolite lava flows. The rhyolites rest on vesicular-to-amygdaloidal, porphyritic basalts. Hydrothermal-alteration products are abundant in the rhyolites and lower basalts, especially along joints and fractures in the bottom 396 m of the hole. The 400-m rhyolite section in Well 1 is believed to represent part of a rhyolite dome, possibly the edge of the East Butte dome or the edge of an unnamed dome exposed approximately 1 km southwest of the well.

Drill hole 2–2A, logged also by Doherty, is located 8 km southeast of the southern tip of the Lemhi Range in Bingham County (NE¼, sec. 15, T. 5 N., R. 31 E.) and was cored to a depth of 914 m through alternating layers of basalt and clay-rich lake sediments. Eight different sediment intervals were cored ranging from 10 to 131 m; the lower 610 m of the hole show evidence of hydrothermal alteration of both basalts and sediments. Four thin vitric, rhyolitic air-fall ash beds were penetrated at depths of 324, 779, 896, and 899 m. An 11-m-thick, welded rhyolitic ash-flow tuff consisting of two flow units was found at a depth of 768 m. The rock types encountered in Well 2–2A reflect the variety of geological environments that have affected this region of the eastern Snake River Plain during the last several million years.

Core from drill hole 3 was logged by G. F. Embree (USGS) and M. D. Lovell (Ricks College). This hole is located at the southwest corner of Sugar City, Madison County (SW¼, sec. 4, T. 6 N., R. 40 E. of Boise Meridian) and was cored to a total depth of 697 m. The uppermost 134 m consist predominantly of interlayered basalts and gravels with one rhyolitic interval at 96–110 m that contains the 2-million-year-old Huckleberry Ridge Tuff. These basalts and gravels overlie at least 563 m of rhyolitic lava flows, ash-flow and air-fall tuffs, and a few thin beds of tuffaceous sediment. This thick section of rhyolitic rocks suggests a caldera-fill sequence and supports the conclusion drawn from previous mapping and geophysical surveys that a large Pliocene caldera complex is centered in the Rexburg-Sugar City area.

Correlation of cyclic sediments between Raft River geothermal wells

S. S. Oriel and H. R. Covington made detailed examination of cuttings, core, and borehole geophysical data from the first three deep geothermal wells drilled in the Raft River basin, Idaho, and identified three cycles of tuffaceous sediments within the Cenozoic basin fill. The cyclic deposition is characterized by an almost pure tuff grading upward to nontuffaceous silts and sands. The importance of this discovery is that this type of deposition can be expected to be widespread within the Raft River basin, and it will aid greatly in determining casing points and distance from the geothermal resource in future wells.

Seismicity studies of the Mount Hood, Oregon, area

Seismicity, *P*-delay, and crustal structure studies in the region of Mount Hood, Ore., were made by C. S. Weaver, S. M. Green, and H. M. Iyer. During the study period only six local earthquakes were recorded, all located under the volcano.

Teleseismic residuals were faster by 0.5 s to the west of Mount Hood. No anomalous delays were associated with the volcano itself.

The crustal model for the region, estimated using construction and quarry blasts, seemed to consist of a 3.7 km/s surface layer overlying a 5.7 km/s crust. Travel paths through the volcano did not show any anomalous travel time.

Crustal structure beneath Kilauea Volcano

A seismic refraction line established in November 1976 off the southeast coast of Hawaii was interpreted by J. J. Zucca and D. P. Hill for crustal

structure. Analysis of Pn arrival times on land indicate that the summit and rift zone areas of Kilauea and Mauna Loa contain a core of high-density, high-velocity material compared to the surrounding shield areas. Estimates of this velocity difference from other studies combined with Zucca's and Hill's data suggest these differences extend down to the top of the ancient sea floor. Analysis of the data from two University of Hawaii ocean-bottom seismometers, located on the south flank of Kilauea during the experiment, indicates that the old oceanic crust has uniform thickness in the study area and dips at roughly 4° toward the island. A dip value of 4° is consistent with the fault-plane solution for the 1975 Kalapana earthquake, admitting the possibility that the fault may have broken along the ancient sea floor-volcanic pile contact.

A proposed source mechanism for Kilauean self-potential anomalies

The large-magnitude self-potential anomalies that are characteristic of thermal areas in Kilauea, Hawaii, were evaluated by C. J. Zablocki for consistency with a previously assumed source mechanism (Zablocki, 1978) that is hydrogeologically reasonable and consistent with all observations. The basic hypothesis is that the sources are streaming potentials resulting from the descent of meteoric water through the vadose zone. The surface anomalies arise from the potential-derived currents that flow from the source in the vadose zone, through the saturated zone (that is, at and below the water table), up the conductive thermal zone, and then back to the source in the cool, flanking lavas.

Changes in Yellowstone seismicity patterns observed

A. M. Pitt reported that a notable change in the pattern of Yellowstone seismic activity occurred during 1977 and 1978. The persistent activity in the north-central caldera and north and west of the caldera declined to a low level during the second quarter of 1977. Activity in the southern and eastern caldera increased in the latter part of 1977. Earthquake swarms occurred in a diffuse pattern south and east of Old Faithful and in a north-trending zone extending across Yellowstone Lake and the eastern resurgent dome within the caldera. The earthquake reached a maximum of M 3.5; over 100 events were felt.

Releveling of 1923 level lines in 1975 and 1976 revealed a general uplift of about 1 m of the Yellowstone caldera relative to the Absaroka Range to the east. The steepest gradient of this uplift occurs along the north edge of Yellowstone Lake. Additional seismograph stations will be used to study the possible relationship between the edge of the uplift and the coincident trend of current high-seismic activity.

Yellowstone seismometer net detects geothermal seismic noise

High-resolution frequency-wave number analysis of seismic noise data, collected using the two closely spaced arrays of seismometers near the Norris Geyser Basin in Yellowstone National Park by D. H. Oppenheimer and H. M. Iyer, show seismic noise in the frequency range of 2 to 8 Hz radiating from the geyser basin. Velocities in different frequency bands vary from 1 to 2.5 km/s, with no clear relationship between frequency and velocity. It appears that the noise propagates as surface waves. The possibility of the presence of body-wave radiation, however, cannot be ruled out. The above results show that a highly active convection system, such as the Norris Geyser Basin, does generate seismic noise. But for practical use of seismic noise as an exploration tool, it will be necessary to estabish the relative contributions of noise generated at the surface that is due to hot springs, fumaroles, and geysers and of noise generated at depth that is due to turbulent transport of hot water and steam.

Analcime a notable concentrator of cesium in Yellowstone Geyser Basins

T. E. C. Keith reported that quantitative emission spectrographic analyses for lithium, scandium, and rubidium in samples from Y–7, Y–8, and Y–13 drill holes of Yellowstone Park by R. E. Mays showed that analcime-rich zones have concentrated cesium from upflowing thermal waters, with cesium values as high as 750 ppm. Alternating zones of clinoptilolite-rich sediments are low in cesium, and rhyolite underlying the sediments is low in cesium. Analysis of an analcime, separated by L. J. P. Muffler from Y–1 drill hole and not previously published, shows 2,600 ppm cesium. Those analcimes are probably "cesian analcimes" according to the definition by Cerný (1974, p. 334). Although an analysis of a pure analcime without inclusions for deriving an accurate formula is not available, X-ray powder data and chemistry indicate that the pollucite component is probably less than 20 percent. Clearly, however, hydrothermal analcimes are potent concentrators of cesium.

Limits of hot-water geothermal system in the Geysers-Clear Lake geothermal area

J. M. Donnelly, F. E. Goff, and N. L. Nehring used the association of thermal waters with sulfur fuming and with Clear Lake Volcanics to draw limits for the hot-water geothermal system northeast of The Geysers steam field. They found that the system extends out to Chalk Mountain, about 8 km northeast of Clear Lake. A separate system appears to exist around Wilbur Springs, about 20 km east of Clear Lake, where thermal waters, mercury deposits, and active sulfur fuming are in close proximity to an early basalt of the Clear Lake Volcanics. In the area northeast of Clear Lake, application of geothermometers to the thermal waters is difficult. The Na-K-Ca geothermometer was found by Goff and Donnelly (1978) to be independent of P_{CO_2}, but strongly influenced by salinity, which is in part controlled by the bedrock type in the Clear Lake area.

Apparent stress changes at The Geysers

C. G. Bufe, S. M. Marks, and M. C. Stickney documented large temporal changes in focal plane mechanisms of earthquakes at The Geysers, Calif. In August–September 1977 and during the previous 2 years, the predominant mode of faulting at The Geysers was strike slip. This was true throughout the range of focal depths (0–5 km) of Geysers earthquakes. Since the end of September 1977, the dominant mechanism has been normal faulting. This change in stress orientation followed the occurrence on September 22 of a magnitude 3.7 strike-slip event, the largest earthquake to be located at The Geysers to date. The change can be explained as a reduction in northeasterly compression such that the vertical (lithostatic) compression, which was the intermediate stress, is now the principal compression. This interpretation is supported by the observation that very shallow depth (<2 km) earthquakes at The Geysers continue to be strike slip. The majority of earthquakes are deeper (2–4 km) and have focal mechanisms that indicate normal faulting. The reduction in northeasterly compression may be a local response to the September 22 earthquake, because strike-slip faulting continues to predominate at all depths along the Maacama fault 10 km south of The Geysers. However, some regional reduction in cross-fault compression may be inferred from the greatly increased level of earthquake activity in the surrounding region that began with a swarm at Alexander Valley in September 1977. In addition to moderate earthquakes along the Maacama system at Ukiah and Willits, a very unusual sequence of earthquakes occurred near the San Andreas fault at Fort Ross. The Geysers may be more sensitive to stress changes than the surrounding region. This sensitivity may result from fluid withdrawal and injection or may be inherent in a steam reservoir.

Magma body postulated under Clear Lake Volcanics from teleseismic *P* wave delays

Detailed analysis of teleseismic *P* delays in The Geysers-Clear Lake region by H. M. Iyer, D. H. Oppenheimer, and Tim Hitchcock, shows the presence of low-velocity bodies under the volcanic zone centered in Mount Hannah and under the geothermal production zone at The Geysers. Maximum velocity decrease from normal in these areas is estimated to be of the order of 25 percent. It is postulated that a magma chamber under the Clear Lake Volcanics, with a highly molten core under Mount Hannah, and a highly fractured steam reservoir at The Geysers are responsible for the observed *P* delays.

Low-velocity body lies under Coso Hot Springs

P. A. Reasenberg reported that preliminary results of a teleseismic *P*-delay study undertaken in the Coso geothermal area, California, indicate a low-velocity body centered 5 to 15 km beneath Coso Hot Springs and Devils Kitchen. Size and velocity contrast for this body could not be uniquely determined by simple ray tracing. Formal inversion of the residual data was made using the linear block inversion method developed by Aki and others. The three-dimensional velocity structure thus modeled is characterized by a deep, broad, north-south-trending zone of slightly lowered velocity ($\Delta V/V \sim 2$ to 4 percent; depth 20–30 km) under Sugarloaf Mountain-Devils Kitchen, paralleling the eastern Sierra Nevada front. In addition, a small, isolated, low-velocity body ($\Delta V/V \sim 4$ to 8 percent) is observed directly below Devils Kitchen, from 5- to 15-km depth, not much more than 5 km across. The deep, north-south-trending feature is probably associated with the Sierra Nevada root lying directly to the west, but may also be associated with the rhyolitic volcanic belt lying above it. The location of a body under Devils Kitchen coincides with the center of a heat-flow anomaly observed by Combs, a seismic noise high located by Teledyne-Geotech, and recent surface hydrothermal activity.

Geothermal well logged at Roosevelt Hot Springs in Utah

The borehole geophysics research project succeeded in running the following geophysical logs

in a geothermal production well at Roosevelt Hot Springs, Utah: temperature, acoustic televiewer, acoustic caliper, mechanical caliper, and gamma spectra. This was the first time that several of these logs had been made at temperatures greater than 200°C. Because of cable problems, the maximum temperature recorded was 238°C, but other evidence indicates that considerably higher temperatures were encountered in the well. Interpretation of these logs by W. S. Keys provided the location and orientation of hot-water-producing natural fractures and a drilling-induced hydraulic fracture. Similar techniques have been successfully applied to the characterization of hot-water-producing fractures in the Raft River geothermal reservoir, Utah.

Thermal-conduction mechanisms in rocks and minerals

Grain-to-grain thermal conduction in rocks is represented by a proportionality between the thermal conductivity and solidity squared; analogously, electrical conductivity in rocks is proportional to porosity squared, known as Archie's Law. Furthermore, in electrical conduction, dead-end cracks and isolated voids account for the porosity-squared relationship, as demonstrated experimentally by resistor-network simulations; similarly, the solidity-squared thermal relation is substantiated by the difference between crystalline intrinsic and observed thermal conductivity, caused by the isolation of grains by microfractures and cracks. By the Boltzmann equation, four mechanisms of thermal conductivity in single-crystal minerals were found by E. C. Robertson to be additive and activated with temperature.

Heat production in the southern Rocky Mountains, Colorado

George Phair converted results of uranium, thorium, and potassium determinations on 634 Precambrian igneous and metamorphic rocks, distributed throughout the southern Rocky Mountains and adjacent parts of the Colorado Plateau in Colorado, to heat production values (1.0 HPU$=1\times10^{-13}$ cal/cm^3/s). Of the samples analyzed, 379 were igneous, collected from 41 different plutons; 255 were metamorphic, collected from 22 different areas. Most of the samples were also analyzed for lead in the ppm range. About two-thirds of the data were collected in the Front Range, a distribution that reflects the large areas of outcrop of Precambrian rocks in that region relative to all others. The analytical results were expressed as areal averages.

The overall picture is one of generally decreasing heat production in igneous and metamorphic areas that is alike in all directions away from the broad regional highs in the central Front Range. Within parts of the central Front Range underlain by three batholiths of Silver Plume Granite, areal heat production averages close to 15.0 HPU, and the associated metamorphic rocks average close to 6.7 HPU. The high rates of heat production in the central Front Range result in high measured surface heat flows in the range of 1.9 to 2.4 HFU as determined by several investigators; one locality close to the center of the thorium-rich Silver Plume batholith ran as high as 3.0 HFU. Such high regional heat flows provide a marked exception to the hypothesis of Polyak and Smirnov (1974) which states that heat flow decreases as the age of the tectonism that produced the rocks increases. According to Chapman and Pollack's (1977) plot of Polyak and Smirnov's data, the high-heat flows typical of the Proterozoic Y and X rocks in the central Front Range (1,400–1,700 m.y.) fall in the range of those representative of the youngest ages of tectonophysics (0–100 m.y.).

Viscosity of ionic substaces

J. P. Kestin (Brown University) completed a detailed study of the effect of pressure on the viscosity of aqueous NaCl solutions in the range 20°C to 150°C and the concentration range 0 to 5.4 molal. The viscosity was measured by the oscillating-disk method in the pressure range 0 to 30 MPa at six concentrations along a large number of isotherms with an estimated uncertainty of ±0.5 percent. These are the first measurements of the viscosity of NaCl solutions over an extended range of pressure, temperature, and concentration. The experimental data were correlated in terms of pressure, temperature, and concentration. New experimental data on the viscosity of aqueous KCl solutions were also acquired. The data cover the temperature range 25°C to 150°C, the pressure range 0 to 30 MPa, and the concentration range 0 to 4.4 molal. The viscosity and density have been correlated as a function of pressure, temperature, and concentration.

Surface self-potential distributions as indicators of subsurface geothermal activity

H. F. Morrison (University of California, Berkeley) developed a computer program to calculate the surface potentials generated by an arbitrary distribution of current sources and sinks in a half-space. Some examples of self-potential anomalies generated by electrical activity along fault zones were assembled. A more sophisticated program was

then written to include the effect on the potential field of a vertical contact separating regions of different resistivities. Plotting routines have been incorporated into the program to give profiles and contour maps of calculated potential fields.

High helium isotope ratios associated with geothermal fluids

Harmon Craig (University of California, San Diego) found that helium isotope ratios ($^3He/^4He$) in Lassen and Yellowstone National Park volcanic gases show large ^3He enrichments relative to atmospheric and crustal helium indicating the presence of a dominant mantle-helium component. The ratios in Lassen helium are up to 8 times atmospheric and are thus isotopically similar to helium in island-arc and other continental-margin orogenic areas. At Yellowstone, however, the isotopic helium ratio in the eastern part of Yellowstone caldera is 15.6 times atmospheric, similar to the ratio from Kilauea, Iceland, and the Ethiopian rift. These high ratios, 15 times atmospheric or greater, may be distinctively associated with deep-mantle plumes under hot spots, whereas ratios about 10 times atmospheric characterize mantle helium in basalt glasses at the crests of midocean spreading axes, and ratios about 8 times atmospheric characterize helium extracted from basalts by hydrothermal circulation (Red Sea brines, Galapagos Rift hot-water plumes, East Pacific Rise bottom water, Guaymas Basin in the Gulf of California). At convergent plate margins such as Lassen, the ratio is 6 to 8 in geothermal fluids. Low ratios are found along the San Andreas fault in California, except from the Salton Sea south where ratios range to more than 6. These values approach those observed at other tectonic-plate boundaries, including the Guaymas Basin where dissolved helium at the ridge crest shows a ratio of 7.9. The association of high ^3He and high heat flow in the Imperial Valley and the Guaymas Basin suggests that active spreading is localized along this plate boundary and that processes such as hydrothermal convection that increase heat flow also favor transport of helium from the mantle. The presence of "Kilauea-type" helium at Yellowstone indicates that, at least in certain areas, the continental crust is essentially transparent to mantle volatiles.

Gravity variation at microgal level

The superconducting gravimeter, developed at the University of California, San Diego, has an intrinsic noise level below that of environmental influences on gravity. Observed environmental noise is below that of the best conventional gravimeters by as much as an order of magnitude. At the lowest frequencies the uncompensated drift of the superconducting device is less than 60 μGal/yr, and independent means for measuring and subtracting the drift are built into the instrument. Conventional instruments usually show that amount of drift in a few days.

J. M. Goodkind (University of California, San Diego) reported that the first unambiguous observation of slow variations of gravity at the microgal level was accomplished using two superconducting gravimeters in a vault built in Pinon Flat, Calif. After 3 year's observation, it was determined that gravity at Pinon Flat can vary by as much as 10 μGal over a 3 to 5 month period. Thus, in order to extract longer period trends and to correlate gravity with variations in water-extraction rate, at least a 1-year record will be required.

Magnetotelluric method for geothermal prospecting

G. V. Keller and A. A. Kaufman (Colorado School of Mines) completed a review of the extensive Russian and other literature on magnetotelluric methods for exploration. Two particularly interesting research possibilities were (1) the measurement of magnetic gradients in place of electric field components to provide a contactless magnetotelluric sounding approach and (2) the possibility that the principal directions for the resistivity tensor measured with magnetotelluric method can be determined from properties of the magnetotelluric sounding curves that are not now used.

Transient temperature inversions in geothermal boreholes

R. P. Lowell (Georgia Institute of Technology) analyzed transient temperature inversions resulting from drilling-fluid losses in thin horizontal fractures and thick permeable formations. For thin fractures, the results indicate that the temperature disturbance exists over a region approximately 20 m high along the borehole wall. Such a disturbance may decay by conduction on the same time scale as normal drilling disturbances. Rapid relaxation of a temperature inversion in a thick porous formation suggests that the return to equilibrium takes place by means of fluid flow in the porous formation. The rate of return allows one to estimate the fluid velocity, which, for the data available from an Icelandic borehole, was approximately 5.6×10^{-7} m/s.

Crustal thinning in northwest Nevada

K. F. Priestly (University of Nevada, Reno) used body wave travel-time data and surface-wave

dispersion data to refine the structural details of the crust and upper mantle within the Great Basin of Nevada and western Utah. North-trending apparent P_n velocity data from a test at the Nevada Test Site were compiled into an apparent P_n velocity contour map. Assuming the upper mantle compressional wave velocity lies near 7.8 km/s, and using P_n interval-velocity data for other azimuths from earthquakes and chemical explosions, a crustal-thickness contour map was derived for the central and northern Great Basin. Crustal thickness varies from greater than 40 km southeast of Reno to 19 km in northwest Nevada.

Relationship between the silica geothermometer and known regional heat flow

C. A. Swanberg (New Mexico State University) applied the silica geothermometer to over 70,000 nonthermal ground waters from the United States and found a correlation between the average silica geotemperatures for a region (T SiO_2 in °C) and the known regional heat flow (q in mW m^{-2}) of the form: T $SiO_2 = mq + b$, where m and b are constants determined to be 0.67°C m^2 mW^{-1} and 13.2°C, respectively. The physical significance of "b" is the mean annual air temperature. The slope "m" is related to the minimum average depth to which the ground water may circulate. This minimum depth is estimated to be between 1.4 and 2.0 km, depending on the rock type. A preliminary heat-flow map, based on the above equation, was prepared using the T SiO_2 for new estimates of regional heat flow where conventional data are lacking. Anomalously high local silica geothermometer values indicate potential geothermal areas.

Heat-flow map for State of Idaho

D. D. Blackwell (Southern Methodist University) completed compilation of heat-flow data for the State of Idaho. All available data were placed in a relatively comprehensive data format for overall analysis. Over 400 data points were included in this data set. A heat-flow map of Idaho, at the scale of 1:1,000,000, was prepared using these data. Various interpretive maps were also prepared, including a map of heat flow averaged by ½° in 1° squares.

Intermediate-period seismic studies in Yellowstone Caldera

D. M. Boore (Stanford University) analyzed intermediate-period seismic data from Yellowstone National Park and determined azimuthally dependent increases of S wave travel times ranging from 0.1 to 2 seconds. The measured Rayleigh wave phase velocities were about 3.2 km/s at 27-s period and 2.0 km/s at 7-s period; these values are significantly lower than phase velocities measured in other tectonically active regions of the world and should provide valuable constraints on the physical properties of the crust beneath Yellowstone.

Two-dimensional inversion of seismic attenuation observations at Coso Hot Springs Known Geothermal Resource Area

More than 60 teleseismic events, recorded by a 16-element vertical component telemetered seismograph array installed by the USGS in the Coso Hot Springs Known Geothermal Resources Area (KGRA), were analyzed by R. W. Ward (University of Texas, Dallas) to determine the lateral variation of seismic attenuation using the reduced spectral ratio technique. Teleseismic events from the southeast and northwest, observed at a five-station linear array, were used to infer a two-dimensional (2-D) Q-1 model across the center of the geothermal system. A constrained generalized linear inversion algorithm was used to infer the Q-1 model. The model contains 15 cells that have boundaries at depths of 5, 20, and 33 km, and Q variation from 32 to 890. The zone of high attenuation dips from the surface between Coso Hot Springs and Airport Lake toward the northwest beneath Devil's Kitchen. The generalized inversion technique for a tenuation observation was extended from two-dimensional to three-dimensional models.

SEDIMENTOLOGY

Sedimentology is the study of sediments and the processes by which they were formed and includes the detachment, entrainment, transportation, deposition, and consolidation of rock particles of all sizes. Usually these actions occur in water or air.

Sedimentological processes are of great economic importance to the Nation. For example, inorganic and organic particles can carry significant quantities of sorbed toxic metals, pesticides, herbicides, and other organic constituents, all of which can pollute the environment and accelerate the eutrophication of lakes and reservoirs. Sediment affects land conservation; rehabilitating strip-mined areas; flooding caused by channel aggradation; damage to urban areas (parks, homesites, streets); loss of topsoil; and silting of streams, lakes, reservoirs, canals, and navigational arteries.

USGS scientists study sedimentology in various ways, including basic research on pertinent physical principles, applied research directed toward site-specific problems, and instrumentation development. Many USGS projects involving sedimentology also apply to related topics, such as water-resource investigations, economic geology, marine geology, engineering geology, and regional stratigraphic studies.

Sediment transport

T. L. Katzer and J. P. Bennett used a calibrated sediment-transport model of the East Fork Carson River of Nevada to predict sediment transport and bed scour and fill for flow conditions other than those of the calibration period. The model includes an unsteady, nonuniform flow component, simulated bedloads and suspended-loads and their interactions, and bed-armoring and bed-elevation changes. The model was calibrated by using 1978 spring streamflow and sediment data collected over a 50-day period in a 16.5-km reach of the river. Predicted total sediment load entering the study reach was about 13 percent lower than measured values, and predicted outflow was about 8 percent lower. Simulated bed-scour and fill at selected sites varied as much as 0.6 m and generally compared favorably with observed values.

W. W. Emmett calibrated a Helley-Smith bedload sampler on the East Fork River of Wyoming by comparing the results given by the Helley-Smith sampler to results obtained by using an open slot on the streambed where trapped sediment was continually excavated by a conveyor-belt apparatus. For sediment-particle sizes between 0.50 and 16 mm, the Helley-Smith bedload sampler had a near-perfect sediment-trapping efficiency. For particle sizes smaller than 0.50 mm, the Helley-Smith sampler trapped suspended load as well as bedload and was therefore "over-efficient." For particle sizes larger than about 16 mm, the Helley-Smith sampler had a low sediment-trapping efficiency, but this may be related to the paucity of coarse particles in transport during the calibration tests, rather than a reflection of actual low sediment-trapping efficiency for large-size particles.

R. P. Williams selected six sites on a 28-km reach of the North Fork Teton River of Idaho to study sediment transport and channel change by subreach. Despite continued levee construction during 1977, sediment rates and channel changes were less than expected. From April 1 to September 30, 1977, total river discharge at the Teton Island Bridge site (farthest upstream site) was 1,390 m^3/s, and total sediment transported was 3,960 t, whereas from April 1 to September 30, 1978, total river discharge was 2,740 m^3/s, and total sediment transported was 10,110 t. Total suspended-sediment discharge ranged from 6,990 to 14,900 t at the six measuring sites, and total bedload discharge ranged from 83 to 7,040 t during a base period of 460 days.

M. L. Jones and H. R. Seitz reported that bedload measured by a Helley-Smith sampler averaged about 5 to 6 percent of the total load in the Snake River near Lewiston, Idaho, and about 4 percent of the total load in the Clearwater River near Lewiston, from 1972–76. Individual measurements made during 1978 showed that bedload varied between about 5 and 9 percent of the total load in the Snake River and remained at about 4 percent in the Clearwater River. Data indicated sediment transport in both rivers was less than average in 1978. A total of about 840,000 t of sediment passed the Lewiston area in 1978 compared to a high of about 5.5 million t in 1974.

W. P. Carey measured suspended-sediment loads in the New River of Tennessee in an area that has undergone strip mining. At the New River at New River gage (drainage area 990 km^2), suspended loads during the 1977 and 1978 water years were 545 and 500 t/km^2 of drainage area, respectively. Over 90 percent of this suspended sediment was silt and clay-size material. The load also consisted of about 29 mg of suspended iron per gram of suspended sediment. Thus, about 15,000 and 14,000 t of suspended iron were discharged from the basin in water years 1977 and 1978, respectively. Manganese and nickel were also present in the suspended load, though in lesser amounts than iron. Besides carrying a large load of sorbed metals, the suspended load imparted an aesthetically displeasing appearance to the water. The displeasing appearance is of particular importance because of a proposed recreation area immediately downstream of the confluence of New River and Clear Fork.

Channel changes

Severe channel erosion is occurring in Pheasant Branch within the city of Middleton, Dane County, Wisconsin, a rapidly urbanizing area, according to a preliminary evaluation by R. S. Grant and G. L. Goddard. Accelerated degradation is occurring in the entire Pheasant Branch drainage basin because the channel was straightened in the 1930's for a drain-

age program. Comparison of a 1977 channel survey with a 1971 survey showed that the 1977 channel was 1 to 2 m deeper at some sites in the urban study reach. In one segment within the urban reach, channel width increased from about 11 to 16 m,and channel cross-sectional area increased about 90 percent. Six erosion-control structures in the urban reach appeared to have had some benefit in controlling head-cutting in the channel.

In his 1977–78 study of the North Fork Teton River of Idaho, R. P. Williams found minimal channel change in the upper 13 km of the 28-km study reach. However, significant lateral erosion and deposition in the lower 15 km suggested that subreaches shortened by manmade channel alinements may begin to meander in the near future. Additional channel instability may be triggered by future deposition of coarse sediment at several upstream diversions.

Sedimentation in lakes and streams

A study by W. J. Herb indicated that Lake Bernard Frank, a Public Law 566 impoundment in Montgomery County, Maryland, trapped about 96 percent of the 123,000 t of sediment entering the impoundment from 1968 to 1976. Total sediment outflow was measured as 5,400 t immediately downstream from the impoundment. Total sediment inflow was estimated by using a combination of measured suspended-sediment loads plus loads estimated by using empirical bedload equations, suspended-sediment transport curves, and a land-use per land-cover sediment-yield relationship. Sediment inflow per unit volume of runoff decreased during the last several years of the study as a result of onsite sediment controls in urban construction areas and a reduction in the total construction area. Sediment accumulation in Lake Bernard Frank was estimated to be 125,000 m^3 or 39 percent of the original sediment-pool capacity. If average runoff conditions and recent sediment yields continue, the sediment pool will be filled in 27 years.

R. S. Grant, S. J. Field, and D. J. Graczyk, on the basis of a preliminary evaluation of data for Trout Creek in Wisconsin, concluded that a flood-control dam on this stream has reduced flood discharges significantly but has trapped only a minor amount of sediment. From February 1, 1976, to January 31, 1977, only 6 percent of inflowing sediment was trapped behind the dam. Sediment reaching the impoundment during high-runoff periods was merely detained, then released slowly throughout the year. Sediment concentrations downstream of the dam were about four times higher than upstream from the reservoir during the 4 months after the only significant runoff in 1976. Streambed material from the dam to the mouth of the creek was much finer than that found in the creek's upstream reach. The fine material probably was deposited during long periods of sediment release from the impoundment when stream discharge and velocity were not adequate to keep it in suspension.

D. E. Burkham (1978) investigated the probable causes for the deterioration of trout habitat in Hot Creek downstream from the Hot Creek Fish Hatchery in California. The accumulation of fine-grained sediment is a phenomenon that probably occurs naturally in the problem reach. Fluctuation in the weather probably is the basic cause of the deposition that has occurred since about 1970. Man's activities and the Hot Creek Fish Hatchery may have contributed to the problem; the significance of these factors, however, was magnified because of drought conditions from 1975 to 1977.

Eolian processes

J. F. McCauley, M. J. Grolier, and C. S. Breed conducted field studies of eolian processes and landforms in deserts of Southwestern United States, Iran, the Western Desert of Egypt, and the coastal deserts of Peru. Their studies indicated that the importance of wind erosion as a geologic process has been seriously underestimated. Effects of wind erosion were evident on surfaces ranging from relatively soft sediments to crystalline basement rocks. Yardangs on a plateau formed on dense, crystalline Thebes Limestone of Eocene age in the Western Desert of Egypt probably have the widest areal extent and include some of the largest wind-erosion features of any known yardang field on Earth. The development of yardangs in marbles confirmed the authors' hypothesis that wind erosion produces large-scale modifications of surfaces composed of very hard rocks, as well as of soft sediment and rocks of lesser competencies.

Curve-fitting techniques

According to W. R. Osterkamp, J. M. McNellis, and P. R. Jordan, regression analysis is a useful curve-fitting technique, but often it is misapplied to geomorphic data sets. When error components can be identified for both variables, the statistical technique of structural analysis is preferred. If regression results are available, conversion to a structural analysis can be made either manually or by com-

puter. By using computer-generated data, the investigators constructed curves that related variation between regression and structural analyses to the range of data of the independent variable. The data have imposed errors and a slope of the linear relation that simulates gradient-discharge relations of rivers. The empirically developed curves can be used to determine the need for structural analysis of real geomorphic data.

GLACIOLOGY

USGS research on glaciology covers a broad spectrum of basic and applied topics ranging from the mechanics of glacier surges to the prediction of snowmelt runoff. Basic studies on snow and glacier hydrology are emphasized, but some research projects are directed toward increasing the knowledge of climate trends and potential glaciological hazards. In 1978, research was specifically concentrated on the Columbia Glacier, which may soon retreat drastically and produce large numbers of icebergs, and on current international programs for prediction of runoff from glaciers and for a world glacier inventory.

Snowmelt-runoff prediction models

W. V. Tangborn developed an operational hydrometeorological streamflow-prediction model that allows hydroelectric-power utilities, irrigation districts, and municipal water-supply companies to forecast and manage snowmelt runoff water more efficiently. The method requires existing streamflow and weather-station data only. The accuracy of forecasting seasonal runoff by using the model appears to be superior to other existing operational methods in areas of Arizona, California, Montana, and Washington where it has been tested.

A model to predict short-term snowmelt runoff by using synoptic observations of precipitation, runoff, and temperature was tested in mountain drainages in Arizona, California, Montana, and Washington. W. V. Tangborn reported that this model is an extension of the seasonal hydrometeorological model in that it incorporates a method to estimate snow ablation and gives ranges of streamflow projections based on forecasts of precipitation and temperature during the prediction season. Ablation is estimated by combining daily mean temperature with the range in daily temperatures, which is shown to be related to cloud cover (and thus to radiation). The snowmelt model is being calibrated for operational use by Puget Sound Power and Light for hydroelectric-power reservoir management in the Baker River drainage basin of Washington.

Glacier ice and water balances

A program for measurement of ice and water balances has been underway since 1957 at South Cascade Glacier in Washington State. Hydrological and meteorological results for most of this 20-year program were compiled on computer files by R. M. Krimmel, W. V. Tangborn, W. G. Sikonia, and M. F. Meier. Analysis programs were developed to calculate mass balances as a function of altitude for the glacier and nonglacier areas of a glacier basin, and the contribution of snow to the glacier by avalanching and drifting, for each year and as functions of altitude within the basin. The mass loss of South Cascade Glacier during the International Hydrological Decade, 1965–74, was 1.4 m (water equivalent). The minimum mass during the 1957–77 period was in the fall of 1970; from 1970 to 1977 the glacier gained 1.6 m. The mass in 1970 was the minimum during the past 100 years and perhaps for the last 5,000 years.

Ice and water balances of Maclure Glacier of California, South Cascade Glacier of Washington, and Wolverine and Gulkana Glaciers of Alaska were compared for the period 1966–77 by M. F. Meier, L. R. Mayo, D. C. Trabant, and R. M. Krimmel. Mean snow balances for the individual glaciers ranged between 0.99 and 3.02 m. Mean annual runoff at the highest altitude and highest latitude glaciers was only 1.13 and 1.96 m, respectively; runoff averaged 3.80 m at the intermediate South Cascade Glacier, and its year-to-year variability was very low (only 0.32 m). Temporal variations in mass balance did not correlate well between glaciers, except that South Cascade and Wolverine Glaciers showed a crude inverse relation, probably stemming from variations in the mean position of storm tracks as they passed over the Pacific coast of North America during the accumulation season.

Glacier inventories

The total area of glaciers in the 12 principal mountain systems of Alaska was estimated at 74,700 km^2 by Austin Post and M. F. Meier. The area of glaciers in individual mountain massifs was measured by correcting the glacier outlines on 1:250,000-scale maps and using recent aerial photographs for control. This method could not be used for the Seward Peninsula or the Kilbuk-Wood River Mountains because of in-

adequacy of maps and photographs. The mountain regions containing the greatest areas of glacier ice include the Chugach Mountains (21,600 km^2), Alaska Range (13,900 km^2), St. Elias Mountains (11,800 km^2), and Coast Mountains (10,500 km^2). Individual glacier inventories in regions such as these will be very difficult because some glaciers are bounded in part by obscure or constantly changing ice divides, some consist of variously-named component areas, and some span political boundaries.

Austin Post inventoried glaciers in the Brooks Range of Alaska by using preliminary copies of 1:63,360-scale topographic maps; glacier margins were checked or reinterpreted by comparing the maps with aerial photographs. In this study, 1,001 glaciers were identified and measured; the area of exposed ice was 647 km^2, and the total area (exposed plus moraine-covered ice) was 723 km^2. Individual glaciers ranged in area from 0.03 to 16.8 km^2, with a mean area of 7.23 km^2.

Columbia Glacier, Alaska

Columbia Glacier may become unstable and retreat rapidly and thereby cause an increase in the calving of icebergs (Austin Post, 1975). M. F. Meier reported that a program was begun by the Columbia Glacier Team (M. F. Meier and others, 1978) to determine the glacier's stability and to predict its future behavior. Hydrographic soundings showed that the glacier terminates against a compact moraine; water depths over this shoal do not exceed 23 m at low tide. Seventeen new geodetic-survey stations were established, and new survey procedures were devised to tie together a 38-station network and to survey stakes on the glacier. A new method was devised to use aerial photography to map the surface-ice velocity, strain rate, and acceleration field on the lower glacier. An airborne, radio-echo sounding system to measure ice thickness was developed. Estimates of ice thickness, velocity, and discharge were used in preliminary one-dimensional models, which were run until steady state was achieved. The preliminary data did not indicate that the present thickness distribution was a steady-state one. A simple stability model for the terminus was devised, and development of more complex and realistic models was begun.

Surface-ice velocity, thickness change, and snow and ice balance were measured at 57 stakes throughout the 1,100 km^2 of Columbia Glacier according to L. R. Mayo and D. C. Trabant (USGS), Rod March (University of Alaska), and Wilfried Haeberli (Federal Institute of Technology, Zürich). At the highest stake, 2,540 m above sea level and 65 km from the terminus, 10 m of snow (5.2 m water equivalent) accumulated during the 1977–78 measurement year, and little melting and almost no liquid precipitation occurred. Surface velocity measured at this station was only 88 m/yr, and ice thickness was 760 m. At the average equilibrium line (approximately 700 m altitude) the ice was nearly 1 km thick and surface velocity near the centerline ranged from 600 to more than 1,000 m/yr. In this area, 37 km from the terminus, the bottom of the ice is near or below sea level. Should drastic retreat begin, the newly exposed fiord could extend as far inland as the present equilibrium zone of the glacier.

The lowest stake on the flow centerline was 5 km from the calving face at about 200 m altitude. The ice thickness at this point was about 600 m and the surface velocity was 900 m/yr. There was a net loss of 5.4 m of ice owing to ablation, but the nonequilibrium ice flux through this area resulted in a surface lowering of 8.6 m.

A detailed bathymetric map was compiled by the USGS research vessel *Growler* during the spring and summer of 1977 (Austin Post, 1978). Very little information on the bathymetry of the area was available prior to the study. Especially during summer and fall months, large quantities of glacier ice in the form of brash and small to medium sized icebergs (up to 100 m or more long) were discharged from Columbia Glacier. The rate of discharge fluctuated greatly from day to day. Iceberg frequency was greatest in Columbia Bay and the waters north of Glacier Island, which, on occasion, were so encumbered with ice as to render the area inaccessible to shipping. Less frequently, dangerous bergs drifted into Prince William Sound east and west of Glacier Island.

Periodic aerial photographs provided data on seasonal changes in the terminal position, thickness, and flow of Columbia Glacier, according to W. G. Sikonia and Austin Post. Very large embayments formed during the summer and fall seasons from 1975 to 1978, and by January 1979 the glacier had retreated from Heather Island on which it had terminated since at least 1890. Largely owing to ice loss by embayment formation, the glacier area was reduced by more than 1 km^2 between July 27, 1974, and January 6, 1979. Embayment formation resulted from localized rapid iceberg calving; the calving rate correlated well with the rate of runoff. Glacier flow varied seasonally and synchronously over at least the lower 17 km of the glacier; superimposed on this seasonal variation were large accelerations in the flow

near the terminus following embayment formation. Surface speed near the center line at about 5 km from the terminus increased from an average of 1.9 m/d between 1977 and 1978. In the lowest 15 km of the glacier, the average surface level was lowered about 9 m between 1957 and 1974, whereas from 1974 to 1978 the average lowering was about 13 m. These data demonstrate that the lower glacier was reduced in mass both by retreat and thinning which had not been fully compensated by more rapid flow of ice from the upper glacier. These losses are the greatest yet recorded for Columbia Glacier.

CLIMATE

U.S. Geological Survey scientists have long realized the importance of climate to the other earth sciences and vice versa, and many studies have been completed over the years. However, within the USGS these studies have always been done under the sponsorship of other programs, and climate has rarely been a top priority. During the past year, in recognition of the pressing need to understand climatic changes and how they may affect society, the USGS initiated a formal program of climate-related studies that is being coordinated by G. I. Smith, with funding beginning in October 1978.

As part of the preparation for a climate program, a three-part circular was released describing the relations of the earth sciences to climate research and the past and projected USGS roles in such work. Part A (Smith, 1978a) reviewed the need for intensified climate research and the roles and methods of earth science research that apply to climate research, as well as summarizing the types of evidence available, the periods of time for which these types are useful, and the geographic and temporal scales involved in climatic changes; also included were lists of academic, governmental, and international organizations active in climate research.

Part B (Smith, 1978b) gave a description of much of the current climate-related research within the USGS. The work was classified into five categories: (1) present climate-related processes and indices that provide baseline data for climatic interpretation, (2) geologically short-term changes in climate, (3) geologically longer term climate changes, (4) areal distributions of past climates, and (5) dating and correlation methods. The report gave rationales and some results for about 50 selected projects and presented a selected bibliography of several hundred climate-related papers published by USGS authors since 1964.

Part C (Howard and Smith, 1978) presented the USGS Climate Plan, and specified the goals, approaches, and tasks for five program elements: (1) consequences of climate variation on land and water resources, (2) recurrence of climate variations that affect land and water resources, (3) understanding climate change, (4) research related to monitoring climate, and (5) data management.

Light-stable isotopes applied to paleoclimatology

Irving Friedman and K. J. Murata, in studies of isotopic fractionation of carbon and oxygen in Miocene calcites and dolomites from California, found an abrupt increase in the amount of ^{18}O in middle Miocene dolomites. They interpret this as a result of the enrichment of the oceans in ^{18}O when isotopically lighter water was preferentially removed from the oceans during the initial stages of Antarctic ice sheet formation.

Early Holocene history of Lake Bonneville

In Utah, W. E. Scott has reviewed several localities that have been interpreted as evidence for a high stand of Lake Bonneville less than 10,000 radiocarbon years ago. He concludes that the evidence for such a high stand is not compelling and that some of the critical deposits that were earlier interpreted as lacustrine are actually of alluvial origin. Other misinterpretations may be attributed to the use of carbonate rocks for radiocarbon dating and to the effects of landslides on some stratigraphic sections.

Sierra Nevada Holocene lake records

Cores were collected from two climatically sensitive lakes in the Sierra Nevada during August 1978. A 2.8-m core from Siesta Lake, Yosemite National Park, was collected by D. P. Adam, and a 5-m core from Upper Echo Lake in Eldorado County was collected by Adam and J. D. Sims. Both cores contain abundant pollen, diatoms, cladocera, chrysomonad cysts, and sponge spicules, which should indicate the sequences of past environments. But, even though both lakes are the first settling basins downstream from neoglacial moraines, neither core contains an obvious record of variations in glacially generated clastic sedimentation; apparently, the upstream neoglacial glaciers were not large enough to erode effectively and produce rock flour in their melt water.

The Siesta Lake core also contains two tephra layers, and other work in the area suggests that these layers may be useful in dating neoglacial moraines in the Yosemite region. The core also contains deformed sedimentary structures that probably record

Holocene earthquakes. "Mazama(?) ash" was found near the bottom of the Upper Echo Lake core. Volcanic-ash shards are disseminated widely throughout both cores, although there were presumably only a few actual ashfalls.

Chrysomonad cysts as a paleoecological tool

In California, D. P. Adam and Albert Mahood (California Academy of Sciences) have found abundant chrysomonad cysts in numerous upper Pleistocene, Holocene, and modern samples and have photographed many different forms using a scanning electron microscope. Although these cysts have been known for many years, both as fossils and as modern forms, they are so small (2.5–30 μm) that much of their morphology could not be resolved using optical microscopes. Scanning electron microscopy has provided a much more detailed description of the cysts, and they should be useful paleoecological tools once their modern distributions become better known.

San Joaquin Valley windstorm, December 20, 1977

H. G. Wilshire, J. K. Nakata, C. M. Sakamoto, and Rosemary Aquino (USGS) and Bernard Hallet (Stanford University) have determined that more than 25 million metric tons of soil were removed from about 600 km^2 of grazing lands by the December 20, 1977, windstorm in the southern San Joaquin Valley. Comparable soil losses were probably sustained in adjacent agricultural lands. Soil losses reached 15 cm in the high mountain areas, 60 cm in the foothills of the Tehachapi and San Emigdio Mountains, and reportedly as much as 1.3 m from agricultural lands.

Material was blown at least as far as the northern end of the Great Valley. At Davis, Calif., dust fallout of about 1 g/m^2 was reported. Fungal spores in the dust caused a dramatic increase in the incidence of coccidiomycosis ("valley fever") in north-central California. Material moved by the wind was as large as nearly 10 cm across; the average diameters of sand grains lodged in telephone poles, 2.4 m, 1.6 m, and 0.8 m above the ground, were 2.5 mm, 3.2 mm, and 4.9 mm, respectively. Material transported by surface creep formed gravel ripples with particles more than 5 cm across. Deflation of rocky alluvial fan soils left remarkably coarse and extensive lag gravel surfaces in only 24 hours. Deposits of blown material commonly filled drainage channels to depths of more than 2 m. The wind-denuded hillslopes and debris-choked drainages greatly exacerbated the destructive effects of heavy rainstorms that followed the windstorm.

The principal factors contributing to the severity of the storm's impact were drought, overgrazing, and the general lack of windbreaks in the agricultural land.

Ice-age pollen record from coastal California

D. P. Adam (USGS) and Roger Byrne and Edgar Luther (University of California at Berkeley) have analyzed a pollen record from a landslide pond in northern coastal Santa Cruz County that covers the time interval between about 30,000 and 4,000 years ago. They found that the grand fir (*Abies grandis*) grew in the area between about 24,000 and 12,300 years ago, far south of its present southern limit. Because of the buffering effect of the ocean, climatic changes in the immediate vicinity of the coast were lower in amplitude than those recorded further inland, but the presence of this tree indicates a southward migration of the favorable climatic belt by at least 150 km.

Central Valley Quaternary studies

Geologic mapping and stratigraphic studies of Quaternary deposits, from Fresno to Sacramento in the Central Valley of California, by D. E. Marchand, are being integrated with studies of estuarine and fluvial environments and deposits in the Sacramento-San Joaquin delta by B. F. Atwater and investigations of Quaternary deposits and soils in the western Sierra Nevada foothills by Marchand and J. W. Harden. Cyclical Pleistocene climatic changes appear to have produced cyclical geologic responses in a variety of environments. A tentative model of the geologic events that occur during a climatic cycle, based on the late Wisconsinan-Holocene record, includes the following seven phases:

(1) Full scale glaciation in the Sierra Nevada crest and contemporaneous deposition of gravels in incised river channels graded to a bedrock notch in Carquinez Straits, simultaneous deposition of fluvial lacustrine silt and clay in the closed Tulare and Buena Vista Lake basins of the southern San Joaquin Valley, continued lacustrine deposition in the closed basins (through phase 4), and soil formation on exposed surfaces.

(2) Glacial retreat in the mountains and glacial outwash deposition in the eastern San Joaquin Valley that filled the channels and caused widespread upward-coarsening aggradation and fan building.

(3) Incision of the major rivers draining glaciated basins as a result of reduced load as glaciation ceased while base level remained low because sea

level had not yet risen to its present position and soil formation had started on outwash fans.

(4) Sheetlike colluviation in the western foothills, overloading nonglacial streams and causing alluviation along their courses in the foothills and out into the Central Valley, and eolian reworking of glacial outwash fans into low dunes.

(5) Further minor incision of major rivers and foothill streams and the beginning of soil formation on all exposed deposits.

(6) Sea-level rise, deposition of peaty estuarine deposits burying the fan toes and some of the dunes, and continued soil formation.

(7) Minor alluviation along all stream channels, deposition of channel, levee, and thin overbank deposits, and continued soil formation, estuarine deposition, and ephemeral lacustrine deposition.

These lead finally back to the first phase—the onset of new glaciation, lowering of sea level, incision of streams to a lowered base level, and a new cycle.

Phases 1, 6, and 7 were probably of long duration; phases 2–5 occurred within a short timespan, perhaps a few thousand years. Multiple and episodic colluviation in the foothills may have been produced by a combination of moisture and vegetational changes associated with the change from glacial to interglacial climate in this region.

Studies of soils formed on deposits about 9,000 to 14,000 years old indicate that soils tend to form more rapidly in the Sierra Nevada foothills than in the eastern Sierra slope and in the Central Valley. This contrast in rates of soil formation is attributed to a combination of climatic and parent-material factors.

Wind as a geologic agent in desert climates

The role of the wind as an agent of erosion, transportation, and deposition is a relatively neglected and misunderstood aspect of geology, and better understanding of the geologic capabilities of the wind and its role with time are essential to the Survey's Climate Program. Unfortunately, critical measurements, such as the velocity, direction, and periodicity, are almost totally lacking for key localities where the wind is known to contribute to shaping the ground surface; data available from the National Weather Service generally lack geologically important details. A few years ago, electronic microprocessors became available that can accept, store, process, and transmit, by satellite, data from arrays of field sensors mounted on remote data collection platforms (DCP's). A prototype remote meteorological station has since been acquired, mounted on a DCP, and is currently being tested on the USGS grounds at Flagstaff, Ariz. It measures wind speed and direction, pressure, humidity, air temperature, and precipitation at ½-hour intervals, transmits the data every 3 hours to the GOES-1 geostationary satellite for relay at Suitland, Md., National Environmental Satellite Service (NESS), and thence to the USGS Computer Center at Flagstaff where computer programs are currently being tested and modified. The station will be reprogrammed shortly to acquire data at more frequent intervals, with emphasis on frequency of peak gusts and ambient atmospheric pressure. After testing, stations will be placed in key sites ranging from the high, cold deserts in northern Arizona to the low, hot deserts in the southern and western parts of the State. Systematic collection of quantitative meteorological data from the DCP's will be combined with geologic data from site studies.

This project, staffed by J. F. McCauley, C. S. Breed, M. J. Grolier, A. W. Ward, Jr., and D. A. MacKinnon, has as its goals (1) to assess the role of the wind as a geologic agent, (2) to analyze the rates and extent of wind erosion in various types of deserts, (3) to determine the response of lithologies ranging from soft sediments to crystalline rocks to eolian processes, and (4) to provide a high resolution quantitative data base that can lead to better understanding of desert processes and the possible effects of past and future climate changes in deserts.

GROUND-WATER HYDROLOGY

In 1979, ground-water hydrology research continued to emphasize a better understanding of ground-water systems and the development of new techniques to improve the management of ground water as an increasingly important national resource.

Digital-modeling techniques were improved and their applications were made more flexible. Methodology for assessing the reliability and significance of aquifer parameters, computed by using field data reflecting steady state conditions, was improved. A model was developed to simulate flow in a two-aquifer system in which the aquifers interact by leakage through an intermediate confining layer. This model offers flexibility in simulating regions of complex geometry. A digital model developed to study a regional three-dimensional ground-water system provided results that were comparable in accuracy to those of the electric-analog model simuation.

Tracer techniques were used in artificial recharge studies in Nebraska and Texas to estimate dispersivities, and several inorganic, organic, and particulate tracers were compared. Infiltration rates of treated-sewage effluent were determined for sugarcane irrigation in Puerto Rico.

Problems concerning subsurface waste-disposal and storage continued to be intensively studied. The potentiometric surface was defined for the Arbuckle Group, parts of which are used for disposal of large volumes of brine and industrial waste in Kansas. Tests of the hydraulic properties of Cretaceous shale in the Midwest indicated that the degree of fracturing is an important consideration in assessing fluid movement within this widespread lithologic unit.

The use of aquifers for cyclic storage of thermal energy is an area of increasing interest. Winter cold-water storage and subsequent summer retrieval for air conditioning at Kennedy Airport in New York were shown to be feasible.

A series of assessments to provide broad-scale analyses of the quantity and quality of ground water in each of the Nation's 21 water-resources regions is nearing completion. These summary appraisals of ground-water resources are being published in the USGS Professional Paper 813 series; 17 of the 21 regional appraisals are now available.

AQUIFER-MODEL STUDIES

Evaluation of aquifer parameters

R. L. Cooley developed and improved a regression-based model of steady-state ground-water flow that uses as input the types of information generally collected in the field—water levels, permeability as determined from pumping tests or analyses of drillers' logs, measurements of spring discharge, and similar types of information. The model calculates the optimum value for hydrologic parameters (transmissivities or permeabilities, hydraulic conductance of confining beds, recharges or discharges, and boundary conditions), the predicted head distribution, and various measures of error. "Ridge regression," a stabilizing algorithm, significantly improved model results and expanded the number of problems to which the model is applicable. This methodology is being applied to a regional analysis of the Madison Limestone aquifer.

Model of a two-aquifer system

M. J. Mallory (1979) documented theoretical development and operational instructions for a finite-element model simulating flow in a two-aquifer system in which the aquifers are coupled by leakage through an intermediate confining layer. The model uses the Galerkin finite-element method to numerically approximate equations of ground-water flow. Resulting simultaneous equations are solved by a point-successive over-relaxation procedure. This method has flexibility for modeling regions of complex geometry. Documentation includes a source-program listing, instructions for the input-data format, sample input data, and an example of the model output. The program includes subroutines for graphical presentation of results.

Simulation of multiaquifer system along Arkansas River valley, southwestern Kansas

A model of the hydrologic system in the Arkansas River valley was calibrated to simulate hydraulic relationships among three principal aquifer zones and the Arkansas River under predevelopment conditions. According to R. A. Barker and C. G. Sauer, the model indicated that the three-layer system is interconnected to the extent that stream depletion over a long time period is the same, regardless of which zone is pumped. Simulated responses were consistent with recent water-level changes caused by variations of streamflow and pumping rates. Rates of stream depletion computed by the model compared favorably with those determined in a separate analysis.

Multiaquifer model, Kent County, Delaware

A quasi-three-dimensional model that includes effects of confining-bed storage was designed by P. P. Leahy to simulate the response of the Piney Point and Cheswold aquifers to generally increasing ground-water withdrawals. The model included the Magothy, Piney Point, Cheswold, and unconfined aquifers and will be used utimately to predict water levels resulting from alternative management plans. Calibration using historical pumpage was accomplished with steady-state and transient simulations. A steady-state simulation of apparent equilibrium conditions existing prior to the early 1950's was used to determine aquifer transmissivities and vertical hydraulic conductivities of the confining beds. The transient model simulated pumpage from 1952 to 1977 and was used to refine estimates of the storage coefficient and specific storage of aquifers and confining beds.

Calibration of the model showed that (1) the transmissivity of the Cheswold aquifer ranges from 690 m^2/d to less than 90 m^2/d in the Dover area, (2)

the vertical hydraulic conductivity of the confining bed separating the Cheswold from the overlying unconfined aquifer ranges from 1.2×10^{-4} m/d to 3.7×10^{-4} m/d—the area having the higher vertical conductivity corresponds to an area of substantial vertical leakage northwest of Dover as was suggested by the results of an earlier study (R. H. Johnston and P. F. Leahy, 1977); and (3) the hydraulic properties of the Piney Point aquifer and the overlying confining bed determined through calibration of the multilayer model were in agreement with the results of a single-layer two-dimensional model of the Piney Point aquifer (Leahy, 1979).

Model study of the Chicot and Evangeline aquifers, Texas gulf coast

A model study of the Chicot and Evangeline aquifers in a 13,400-km^2 area between the Trinity and Saline Rivers of Texas had good results when compared to computed and observed water-level declines for the periods 1900–40, 1941–62, 1963–70, and 1971–75, according to W. R. Meyer, J. E. Carr, Carole Loskot, and W. M. Sandeen. During the simulation period (1900–75), 19 percent of the water pumped was derived from aquifer storage; 30 percent was derived from clay storage (56 percent from claybeds in the Chicot aquifer and 44 percent from claybeds in the Evangeline aquifer); and 51 percent was derived from recharge from precipitation, return flow from irrigation, and seepage from streams. Over the same time interval, simulated subsidence near the city of Orange, Tex., was 0.17 m, compared with measured subsidence of 0.15 m.

Application of a numerical model in simulating water-level changes in the Floridan aquifer

A numerical model developed by P. C. Trescott, G. F. Pinder, and S. P. Larson (1976) was used by L. R. Hayes and Douglas Barr to simulate water-level changes in the upper Floridan aquifer in response to withdrawals. Calibration of the model to steady-state and transient conditions showed that the model is most sensitive to pumpage and aquifer transmissivity. Differences between observed and simulated head values were generally less than 2 m.

The apparent transmissivity of the upper limestone of the Floridan aquifer ranged from 56 to 2,800 m^2/d in seven aquifer tests in Okaloosa and Walton Counties, according to Hayes and Barr. Thickness and structural contour maps of the aquifer and associated confining beds showed that this variation is a function of changes in thickness of the aquifer. Brine-injection tests showed that intraborehole flow that occurred during aquifer tests influenced the water levels in some observation wells; consequently, the calculated transmissivity values may be higher than the actual values.

RECHARGE STUDIES

Tracer studies at sites in Nebraska and Texas

A series of tracer tests to estimate dispersivity values at a recharge facility near Aurora, Neb., were reported by E. G. Lappala. The aquifer at the site is unconsolidated Pleistocene sand and gravel with a transmissivity of about 2,700 m^2/d and a storage coefficient of about 0.10. Bromide and four fluorocarbons were used as tracers. Dispersivities were determined by matching observed bromide data to analytical and finite-difference solutions of the dispersion-convection equation in radial coordinates. The best matches were obtained at an observation well 3.2 m from the injection well, by using an effective flow-zone thickness (effective porosity times flow-zone thickness) ranging from 2.4 to 4.5 m and dispersivities ranging from 0.15 to 0.30 m. Matches to data from more distant observation wells gave dispersivities from 0.20 to 0.30 m. No increase of dispersivity with distance from the injection well was observed.

Lappala reported that tracer tests similar to those in Nebraska were performed in the Ogallala aquifer at a site near Stanton, Tex. The aquifer has a thickness of 12 m and is composed of sand and gravel with calcium carbonate cementation and numerous clay lenses; transmissivity is about 215 m^2/d, and the apparent storage coefficient from pumping tests is about 0.002. Bromide and boron were used as tracers to estimate dispersivities. Observed tracer breakthrough curves were matched with finite-difference solutions of the dispersion-convection equation in radial coordinates. The thickness of the sampled flow zone was estimated from single-point resistivity logs, and the flow rate into each zone was estimated by flow-meter surveys in the injection well. Because of the resulting approximations, it was not possible to determine the effective porosity. A value of 0.2 was used for all numerical solutions, and the flow-zone thickness was adjusted to match the data. Resulting dispersivities ranged from 0.4 m at the observation well 2 m from the injection well to about 1.5 m at the observation well 5 m distant. Although there was no apparent increase in dispersivities between the wells 5 m

and 10 m from the injection well, data were insufficient to define a quantitative relationship between dispersivity and distance.

Geochemical aspects of injection tests at the Texas site were studied by R. L. Bassett. The tests defined the flow field and allowed comparisons of inorganic tracers (chloride, iodide, bromide, fluoride, and boron), fluorocarbon tracers, several organic tracers, and a particulate tracer (yeast). The purposes of the study were to investigate techniques for successfully recharging surface water into the Ogallala aquifer, to develop general equations that describe the partitioning of aqueous chemical species between the ground water and the porous media, and to develop models that simulate the transport chemistry.

Conversion of a three-dimensional analog model to a three-dimensional digital model

T. E. Reilly and A. W. Harbaugh converted a regional analog model of ground-water flow in Long Island, N.Y. (R. T. Getzen, 1977), to a three-dimensional finite-difference digital model, a change that allows greater flexibility in solving water-management problems and that uses the increasing capabilities of digital computers. The digital model uses the three-dimensional ground-water flow program of the USGS (P. C. Trescott, 1975). Both models use the same hydraulic coefficients, and the results compare favorably.

Treated sewage effluent used for sugarcane irrigation

J. R. Diaz reported that when secondary treated-sewage effluent was used for sugarcane irrigation at Fort Allen on the southern coast of Puerto Rico, the rates of vertical percolation through the unsaturated zone were 0.025 and 0.244 m/d for application rates of 140 and 203 mm/wk, respectively. The unsaturated zone ranged in thickness from 7.0 to 7.6 m and was composed of interbedded clay, silt, and sand, with thin layers of fine gravel. A hydrologic budget for a specific year of project operation indicated that 40 to 45 percent of the applied effluent reached the water table, 35 percent was added to soil moisture, and 20 percent evaporated from bare moist soil or was transpired by sugarcane plants.

Potentiometric surface—Arbuckle Group

The Arbuckle Group, which occurs at great depths throughout Kansas, includes units comprising an important hydrocarbon reservoir in central and south-central Kansas that is used for disposal of large volumes of brine and industrial waste. According to A. J. Gogel, the configuration of the potentiometric surface of the Arbuckle Group indicated that the main direction of ground-water flow is from the central Kansas uplift in west-central Kansas toward the southeastern part of the State. Sandstone units within the group in this area form an important freshwater aquifer extending into adjacent parts of Arkansas, Missouri, and Oklahoma. Another direction of flow may be south from the central Kansas uplift toward the Anadarko Basin in Oklahoma.

DISPOSAL AND STORAGE STUDIES

Hydraulic properties of Cretaceous shale

R. G. Wolff evaluated the hydraulic properties of Cretaceous shale units in the Midwest to determine the feasibility of storing waste in the shales. Results of the study indicated that the porous-media permeability is very small and that fractures probably play a major role in fluid movement.

Aquifer storage of chilled water for air conditioning at Kennedy Airport, New York

Julian Soren reported that four test wells were drilled in a north-south-trending buried valley at Kennedy Airport to evaluate the confined Jameco aquifer for winter cold-water storage and summer retrieval of the cold water for cooling the passenger terminal. The air conditioning will require about 23 million cubic meters of water cooled to about 3°C. Geologic mapping and test drilling showed that the dimensions of the aquifer are such that storage of this magnitude could be accommodated within the airport boundaries. The aquifer in the channel-thalweg area is mainly gravelly sand, with little silt or clay, and has a hydraulic conductivity probably in excess of 80 m/d.

SUMMARY APPRAISALS OF THE NATION'S GROUND-WATER RESOURCES

A series of assessments, initiated in 1970, to provide broad-scale analyses of the quantity and quality of ground water in each of the Nation's 21 water-resources regions (as defined by the Water Resources Council) is nearing completion. These assessments have demonstrated that ground water is a large, important, and manageable resource that should have a significant role in regional water development. The completed series of assessments will constitute a national ground-water compendium for

the guidance of planning agencies and all others concerned with the Nation's water supply.

The analyses include appraisals of the significance of the ground-water resource to regional water supply, the quantities of ground water available, the quality of ground water, the present and potential problems associated with ground-water use, and additional information needed for planning and efficient development of ground water.

These summary appraisals are being published in the USGS Professional Paper 813 series, and the following 17 of the 21 regional appraisals are available: Bloyd, R. M., Jr., 1974, 1975; Price, Don, and Arnow, Ted, 1974; West, S. W., and Brondhurst, W. L., 1975; Thomas, A. E., and Phoenix, D. A., 1976; Baker, E. T., and Wall, J. R., 1976; Eakin, T. E., Price, Don, and Harrill, J. R., 1976; Bedinger, M. S., and Sniegocki, R. T., 1976; Sinnott, Allen, and Cushing, E. M., 1978; Weist, W. J., Jr., 1978; Reeder, H. O., 1978; Zurawski, Ann, 1978; Takasaki, K. J., 1978; Terry, J. E., Hosman, R. L., and Bryant, C. T., 1979; Cederstrom, D. J., Boswell, E. H., and Tarver, G. R., 1979; Taylor, O. J., 1978; Zenone, Chester, and Anderson, G. S., 1978.

MISCELLANEOUS STUDIES

Lithology of the Edwards aquifer

Core drilling in the Edwards aquifer in the Austin, Tex., area revealed significant lithologic differences between the transitional and freshwater zones of the aquifer, according to M. L. Maderak and R. M. Slade. The transitional zone consists of chalky limestone, light gray crystalline to dolomitic limestone, and buff dolomite in the top half of the section. The bottom half consists of gray dolomitic limestone, gray shaly limestone, and dark-gray, organic-rich carbonates with traces of petroleum. Secondary porosity is fairly well developed near the top of the aquifer but is poorly developed in the bottom half. Porosity and permeability decrease with depth, whereas salinity increases with depth. The freshwater zone consists of light-gray limestone to buff dolomite that is highly fractured and vuggy. Secondary porosity has greatly increased the overall transmissivity of the zone. In general, freshwater-zone areas that have well developed secondary porosity are near areas of recharge and contain water with a dissolved-solids concentration of less than 300 mg/L.

SURFACE-WATER HYDROLOGY

The objectives of research in surface-water hydrology are to develop improved techniques for estimating the magnitude and variability of streamflow in time and space, both under natural and man-modified conditions, to understand the flow process in stream channels and estuaries, and to define the rate of movement and the dissipation of pollutants in streams.

Model development

The first phase of development of a hydrologic modeling system to assess the impacts of land-use and climatic changes on the hydrology of small drainage basins was completed by G. H. Leavesley and R. W. Lichty. The USGS rainfall-runoff model (D. R. Dawdy, R. W. Lichty, and J. M. Bergmann, 1972), the USGS distributed routing rainfall-runoff model (D. R. Dawdy, J. C. Shaake, Jr., and W. M. Alley, 1978), and a distributed parameter snowmelt-runoff model (G. H. Leavesley and W. D. Striffler, 1979) were combined to develop the system. It is modular in design with each module representing one component of the hydrologic cycle. A library of compatible and interchangeable modules provides flexibility for handling variations in climate and hydrology in different regions of the United States. Model structure is designed around the concept of partitioning a basin into hydrologic response units based on slope, aspect, altitude, soils, and vegetation characteristics.

R. W. Lichty is investigating the feasibility of using data derived from rainfall-simulator plot experiments (G. C. Lusby, 1977) to estimate the model system parameters that define infiltration, overland flow, and sediment detachment and transport characteristics of individual hydrologic response units. Initial evaluation of the data indicated that the plot studies provide reasonable estimates of parameter values but that additional soil-moisture data will be required to explain and reduce the variance of these estimates. Calibration using replicate plot experiments offers a potential means of assessing the impacts of changing land-use patterns on surface runoff and sediment yield.

The various sources of error and uncertainty encountered in applying the USGS rainfall-runoff model (D. R. Dawdy, R. W. Lichty, and J. M. Bergmann, 1972) were investigated by B. M. Troutman. Optimal techniques for parameter estimation were considered, and joint confidence intervals for the model parameters were constructed by using a model-sensitivity analysis to obtain variances and correlations of the estimates. Errors caused by spatial variability of rainfall were studied by using a stochastic areal rainfall model. This study is the

first phase of the development of a theory of errors for the full hydrologic modeling system.

L. G. Saindon completed a procedure to enter hydrologic and climatic data recorded on magnetic cassette tapes into the USGS WATSTORE computer files. The procedure includes a program that converts the input data to a format suitable for use with standard USGS computer programs.

In order to increase flexibility and allow for testing and analysis of alternate algorithms, K. M. Hammett and J. F. Turner made several modifications in the Georgia Tech Watershed Simulator (GTWS) computer program. Main program logic was not altered, but conceptual procedures for hydrologic phenomena were isolated into individual subroutines. The streamflow-routing procedure was modified to allow for calibration of individual subwatersheds through a comparison of upstream and downstream discharge hydrographs. Small-scale sensitivity analyses of input parameters indicated an extremely complex multidimensional response surface. It is believed that analysis of the response surface can be simplified by deleting or selecting alternate algorithms for some hydrologic phenomena.

A numerical streamflow-prediction model that uses only daily values of runoff and low-altitude precipitation was tested and implemented on the Salt and Verde Rivers in Arizona. W. V. Tangborn reported that retrospective seasonal (March 1–May 31) predictions of snowmelt runoff for the past 18 years demonstrated a reduction in the standard error of prediction over existing methods by 50 percent for those streams. Application of the hydrometeorological model for short-term runoff predictions during severe flooding in February and March 1978 also assisted the Salt River Project in reservoir management.

J. E. Miller and M. E. Jennings further developed and tested the USGS steady-state water-quality model. The model includes components for determining nitrification, fecal and total coliforms, anoxic conditions, and orthophosphate-phosphorus; it also can be used to predict DO concentrations, ultimate carbonaceous and nitrogenous BOD, and concentrations of three conservative constituents. The revised model was calibrated and verified by using four independent sets of data collected on the Chattahoochee River near Atlanta, Ga., during approximately steady-state flows. Model calibration requires extensive data; the magnitudes of all important water-quality reactions must be defined (J. E. Miller and M. E. Jennings, 1978).

A Lagrangian temperature model developed by H. E. Jobson was modified by D. J. Schultz to simulate the transport of rhodamine-WT dye through an open channel under steady-flow conditions. The model allows for diffusion of the dye into flocculent material at the bottom of the channel. This conservative transport model was further modified to allow for volatilization of dispersants as a first-order process.

Chintu Lai determined important characteristics of models for numerical simulation of hydrodynamic phenomena by digital computer and prepared guidelines for model development (Chintu Lai, R. W. Schaffranek, and R. A. Baltzer, 1978). Lai (1978) also delineated sources of computer programs and numerical models in hydraulics.

Open-channel hydraulics

Nobuhiro Yotsukura developed a completely nondimensional method of describing the steady-state distribution of conservative solutes in meandering nonuniform open channels. It is based on the closed-form solutions of Yotsukura-Sayre-Cobb stream tube equation, which is a two-dimensional convection-diffusion equation in which a natural coordinate system is used (Nobuhiro Yotsukura and E. D. Cobb, 1972; Nobuhiro Yotsukura and W. W. Sayre, 1976). Examinations of extensive sets of tracer data from natural streams showed that the revised mixing-distance equation can be used not only for estimating mixing distances but also for determining transverse mixing coefficients in a meandering width-varying natural channel, provided the flow and solute input rates are both steady. The method is useful for unified definitions of a mixing zone downstream of an industrial- or domestic-waste effluent site as well as for studying the mixing of large tributary waters with different constituent concentrations. The nondimensional transverse mixing coefficients (Elder's coefficient) observed in the Amazon River of Brazil and MacKenzie and Liard Rivers of Canada are less than unity when averaged over 100 to 400-km distances.

R. E. Rathbun developed equations for estimating the amounts of tracer gas and rhodamine-WT dye needed for measuring the reaeration coefficient of a stream by using the modified-tracer technique. The amounts of gas and dye needed depend on length of a reach, mean water velocity, water discharge, longitudinal dispersion coefficient, and length of time over which the tracers are injected. The amount

of tracer gas needed also depends on the tracer-gas process.

D. E. Troutman determined the measurement of reaeration coefficients in a 10-km reach of Canadaigua Outlet from Canadaigua Lake outflow to Littleville, N.Y., by using the modified-tracer technique (R. E. Rathbun, D. J. Schultz, and D. W. Stephens, 1975; R. E. Rathbun and R. S. Grant, 1978). The measured coefficients in hydraulically differing stream reaches compared favorably with those measured previously by using radioactive-tracer techniques (Tsiuoglou and others, 1974). The results indicated a direct relationship between stream-reaeration capacity and stream discharge under the flow regimes studied.

C. A. Thomas reported that discharges greater than 570 m^3/s at the gaging station on Snake River at Hells Canyon Dam seemed too large when compared with discharge measurements made at upstream and downstream sites. The Hells Canyon measuring section is in loose volcanic boulders, flow is rapid, and observable surges or "boils" move past the section. Because of the turbulence, the Price current meter and the 68-kg sounding weight moved about considerably when they were suspended from the sounding cable; this movement resulted in an overregistering of velocity. There were no appreciable differences in measured velocities when an Ott meter was used. However, when a 136-kg sounding weight was used, travel of the weight and meter was noticeably damped, depth soundings were more precise, and measured velocities were significantly lower. The discharge record at Hells Canyon can be improved by use of the larger sounding weight for discharge measurements.

Hydrologic studies

Floods caused by intense rainfall were reported to have occurred on seven small streams, all above 2,300 m elevation, in Colorado. The peak discharges were computed from surveys of channels and high-water marks. Geomorphic and sedimentologic reconnaissances by R. D. Jarrett indicated that the flows had large fluid strength and were laminar; that is, they were debris flows. Evidence consisted of coarse, lobate, poorly sorted gravel deposits with well-defined levees, and terminal lobes bordering the deposits. The largest boulders were deposited on levees bordering the deposits. Although boulders as large as 50 to 80 cm were transported, small trees on debris fans were not severely scarred, and some small willows diverted flow. Downstream high-water marks and gaging-station records indicated that only a small percentage of the computed flows at the sites was water, thus confirming evidence found on the reaches. The distinction between debris flows and flood flows is important because indirect methods of measuring peak discharges are not valid for measuring debris flows; indiscriminate use of indirect methods may lead to unrealistically large estimates of possible maximum floods on streams at high elevations in the Rocky Mountains of Colorado. Furthermore, because of sparse data on rainfall in mountainous regions, peak discharges computed by indirect methods have been used to estimate rainfall; such rainfall estimates are reasonable only to the extent that computed peak discharges are reasonable. Apparently, debris flows in mountain channels not only occur because of large amounts of rainfall but also occur when there are moderate amounts of rainfall in areas with steep slopes and an accumulation of poorly sorted channel debris.

J. E. Costa (1978) investigated the feasibility of using geomorphic and stratigraphic evidence to decipher the flood hydrology of small, foothill streams in Colorado. The techniques developed are viable alternatives to the classical engineering interpretation of high outliers on the low-probability end of the flood-frequency curve. In foothill streams with drainage areas of less than 12 km^2, geomorphic evidence of flood discharges greater than 100 $(m^3/s)/km^2$ persists for approximately 100 years. The geomorphic evidence includes large streamlined gravel bars preserved on narrow flood plains of mountain streams, isolated lichen-free boulders (commonly larger than 1 m in diameter) scattered across a flood plain in wide stretches of a valley, and valley morphology in which a small, deep stream channel is inset into a much larger flood channel.

Stratigraphic evidence of prehistoric catastrophic floods was found in four small watersheds that had experienced historic catastrophic floods. Gravel deposits preserved in the valley fill are very poorly sorted, are imbricated, and have erosional basal contacts. All of the gravel deposits contain charcoal fragments, some of which were collected for radiocarbon dating. Magnitudes of prehistoric floods whose evidence is preserved in the valley fills can be compared with magnitudes of historic catastrophic floods in the basin by comparing size analyses of gravel deposits. For example, on the basis of the maximum sizes of gravel deposited, it was determined that the 1938 flood in Cold Spring Gulch was the largest flood in the history of the valley fill, which probably dates from mid- to late-Holocene time.

W. J. Herb developed equations for estimating monthly and annual mean flows of Pennsylvania streams from drainage-basin characteristics. The 98 regression equations were based on streamflow and basin characteristics of 294 gaged basins in Delaware, Maryland, New Jersey, New York, Ohio, Pennsylvania, and West Virginia. Basin characteristics included drainage area, average annual potential evapotranspiration, mean basin elevation, basin storage, stream distance to the drainage divide, and an index of monthly precipitation excess. Standard errors of estimate for monthly mean flows ranged from 5 to 41 percent; those for June through November were lowest. Standard errors for annual mean flows ranged from 8 to 12 percent.

N. B. Carmony and R. M. Turner (USGS) (1978) and D. E. Brown (Arizona Game and Fish Department) prepared a map showing the perennial streams and wetlands of Arizona. The map shows (1) three categories of perennial streams (unregulated, regulated, and those of effluent or wastewater); (2) important wetlands in two size classes; (3) three categories of base-flow volume (for unregulated, regulated, and those of effluent or wastewater); nially in historic times but that are no longer perennial; (5) former wetlands; and (6) fish populations at selected altitudes.

PALEONTOLOGY

Research by paleontologists of the USGS involves biostratigraphic, paleoecologic, taxonomic, and phylogenetic studies in a wide variety of plant and animal groups. The results of this research are applied to specific geologic problems related to the USGS program of geologic mapping, to resource investigating, and to providing a biostratigraphic framework for synthesis of the geologic history of North America and the surrounding oceans. Some of the significant results of paleontological research attained during the past year, many of them as yet unpublished, are summarized in this section by major geologic age and area. Many additional paleontologic studies are carried out by paleontologists of the USGS in cooperation with USGS colleagues. The results of these investigations are ordinarily reported under the section "Geological, Geophysical, and Mineral-Resource Investigations."

MESOZOIC AND CENOZOIC STUDIES

Quaternary paleolimnology of Lake Valencia, Venezuela

Diatom analyses by J. P. Bradbury of a 7.43-cm core of profundal sediments in Lake Valencia, Venezuela, reveal two floral assemblages that provide a paleolimnologic and paleoclimatic history of this large tropical lake. The core is barren of diatoms below 4.92 m, but the sediments contain ostracode (*Cyprinotus salinus*) from 5.0 to 5.93 m, which suggests that during this period Lake Valencia was comparatively shallow and saline.

The first diatom zone (3.49–4.92 m) is characterized by planktic diatoms that either tolerate or prefer brackish water. Initially this assemblage is represented by *Chaetoceras muelleri* Lemmermann, a widely distributed diatom in brackish lakes and coastal regions. In succeeding levels of this zone, *C. muelleri* is replaced by *Cyclotella* sp., probably *Cyclotella* aff. *C. striata* (Kützing) Grunow, a common brackish-water species. These planktic, brackish-water diatom assemblages occur in that portion of the core that contains discrete laminae of aragonite. Aragonite precipitates from modern brackish-water lakes (salinity, 10 per mil or higher) in which the Mg : Ca ratio is >12.

In the second upper zone (0–3.49 m), the fossil diatom assemblages resemble the modern diatom communities of Lake Valencia and indicate a transition from brackish water to alkaline, eutrophic water. *Melosira granulata* (Ehrenberg) Ralfs, *Nitzschia amphibia* Grunow, *Fragilaria construens* (Ehrenberg) Grunow, and *F. brevistriata* Grunow dominate at various levels. The *Fragilaria* species currently dominate in the shallow-water areas of Lake Valencia, and their appearance in the profundal sediments suggests either periodic lower lake levels in the past or greater sediment transport from the littoral zone of the lake.

The transition from a brackish-water, planktic diatom flora to freshwater diatom floras of both planktic and benthic habitats suggests a major climatic change that ended a past endorheic phase of Lake Valencia. The radiocarbon chronology in the upper part of the core indicates that this change probably occurred 9,000 years ago. Apparently, the Holocene climate of tropical Venezuela was characterized by greater effective moisture than the late Pleistocene climate of this area. This research has important implications for the study of recent climatic changes in the United States.

Shoreline datum planes in the Southeastern United States

Paleoshorelines in the Atlantic Coastal Plain were dated by integrating biostratigraphic, radiometric, geomorphic, and paleoecologic data. The following outline by B. W. Blackwelder, T. M. Cronin, and T. A. Ager of the geologic history of the Southeast-

ern United States is based on use of these postulated paleoshorelines and associated marine deposits as datum planes:

- Extensive inundation of the Coastal Plain during the early Pliocene (5.0–3.5 m.y. ago). Formation of the Orangeburg Scarp and deposition of the Yorktown and Raysor Formations.
- Regression at the close of the early Pliocene and extinction of the molluscan genera *Planicardium, Chesapecten,* and *Ecphora.*
- More than 30 m of differential uplift of the western part of the Coastal Plain from lat. 34°30′N. to lat. 35°N. during the middle Pliocene.
- Late Pliocene (2.6–2.1 m.y. ago) transgression about half as extensive as that of the early Pliocene. A Cape Hatteras-like prominence was located approximately 175 km west of the present-day Cape Hatteras.
- Regression at the close of the Pliocene. Disappearance of the *Glycymeris subovata* molluscan lineage and a significant change in the ostracode fauna. Differential uplift of about 8 to 15 m in the middle portion of the present Coastal Plain from between lat. 33°30′N. to lat. 35°30′N.
- Early Pleistocene (1.8–1.0 m.y. ago) transgression almost as extensive as that of the late Pliocene.
- Early Pleistocene regression and differential uplift in the Cape Fear Arch region.
- Early late Pleistocene transgression (0.6–0.4 m.y. ago) with deposition localized in northeastern South Carolina where shallow back-barrier deposits lie at elevations of 12 m. First appearance of the molluscan genus *Lunarca* and numerous extant ostracode species in the Atlantic Coastal Plain.
- Regression and extinction of the *Argopecten eboreus* molluscan lineage.
- Latest Pleistocene (120,000 to 60,000 yr B.P.) with the present coastline at elevations of 6 to 8 m.

Late Cenozoic vertebrate biochronology

Continued studies of the meadow mice and their relatives in North America by C. A. Repenning have produced a biochronology for continental sediments over the past 5 million years that is nothing short of spectacular in comparison to the usual precision of vertebrate paleontology. Three mammalian ages are usually recognized over this timespan, but the study of the microtid rodents has clearly identified 10 definable "meadow-mouse" ages, the longest about 800,000 years in duration and the shortest about 175,000 years in duration. Average time resolution throughout the entire 5 million years obviously is about ±0.25 m.y., but in many cases it is much more precise. This is a resolution that competes realistically with that of potassium-argon age determinations.

Although no effort has yet been spent in refining the biochronology of other mammals by application of the "meadow-mouse ages," it is very apparent that this will be possible in some groups, especially in the complex rodent groups whose very complexity has discouraged biohistorical reconstruction. A better understanding of the ranges of larger mammals is also emerging. But most promising is the possibility of establishing a biochronology based on the very diverse and widely dispersed freshwater invertebrates. Freshwater ostracodes and diatoms were selected for study because they are not endemic to specific drainage basins but, instead, are widely scattered across the continent on birds' feet or even by the wind. They are ecologically very sensitive and thus offer the further advantage of detecting minor changes in climate.

In part supported by funds from the Reactor Hazards Program, fieldwork was conducted in March, June, and July to collect diatoms and ostracods from known dated localities in the western States of Arizona, California, Oregon, Washington, Idaho, Utah, and Wyoming, as well as in the state of Chihuahua, Mexico. Diatom floras and (or) ostracod faunas were successfully collected from all known localities and from a number of new meadow-mouse localities that were discovered in the process. Most remarkable from the standpoint of vertebrate paleontology, the stratigraphic succession of 6 of the 10 "meadow-mouse stages" in the earlier part of the biochronology was established through the combination of three overlapping sections. To insure close correlation between sections, nearly all of the fieldwork was done in association with paleomagnetic investigators from Lamount-Doherty Geological Observatory, N.Y.

Miocene sporomorphs from Massachusetts

Sporomorphs (spores and pollen) from three localities in eastern Massachusetts were examined by N. O. Frederiksen. Units and localities are (1) three unnamed Neogene formations exposed at Gay Head, Martha's Vineyard, (2) dark-gray clayey silt, exposed in Third Cliff, Scituate, Plymouth County, and (3) dark-gray clayey silt exposed in

gravel pits at Marshfield Center, Plymouth County. All of the samples were supplied by C. A. Kaye, who has been studying the stratigraphy and correlation of the units. Palynological examination shows that the lowermost of the three Neogene units at Gay Head, a greensand, is very different from the two overlying units because it contains a rich assemblage of temperate forest taxa, pollen of the genera *Sciadopitys* and *Pterocarya,* which no longer live in North America, and reworked Paleogene pollen and spores, mainly from the lower Eocene. This unit has been dated with vertebrate fossils by F. C. Whitmore, Jr., as probably late early Miocene to early middle Miocene in age. Samples from the Tertiary strata at Marshfield Center and Scituate Third Cliff have the same assemblage as the lowermost Neogene unit at Gay Head and thus are now known to be Miocene in age. No Eocene strata exist in eastern Massachusetts as far as can be determined with sporomorphs.

Sedimentary environments in the Neogene of the central Atlantic Coastal Plain

The analysis of sedimentary patterns by T. G. Gibson both from surface and subsurface sections, combined with accompanying biostratigraphic and paleoenvironmental data from macro- and microfossils, has given a better understanding of the regional depositional system in the Miocene and Pliocene strata of the central Atlantic Coastal Plain. Clastic deposition was the dominant mode in the early and middle Miocene in the northern part of this area. The influx of deltaic sediments into northeastern Maryland during the middle Miocene caused periodic restriction of the open marine environment and resulted in brackish environments to the west and southwest of the delta. To the south at this time (southern Virginia and North Carolina) chemical and biogenic deposits including carbonates, diatomites, and phosphorites dominated. A series of marine transgressions and regressions continued through the later Miocene and Pliocene, primarily in the southern area, and was accompanied by increasing clastic sedimentation.

Vertebrate faunas of Gay Head, Martha's Vineyard, Massachusetts

The northernmost exposure of Coastal Plain Tertiary deposits on the east coast of North America is in the Gay Head Cliffs on the island of Martha's Vineyard in Massachusetts. Fossil vertebrates were first reported from the cliffs by Charles Lyell in 1845. Lyell's specimens have been lost, but specimens are still available that are collected there as long ago as 1870. In recent years C. A. Kaye and F. C. Whitmore, Jr., have collected from the cliffs, and numerous amateur collectors have kindly made their specimens available for study. C. E. Ray and R. W. Purdy of the Smithsonian Institution have collaborated in the study of the collections.

Miocene and Pleistocene vertebrates were collected from the cliffs. The Miocene fauna consist of sharks, bony fish, seals, sea cows, primitive whales, primitive mastodonts, and camels, all of which are found in the greensand of Gay Head. Most significant for dating the greensand are the mastodont *Gomphotherium* cf. *G. productum* (Cope) and the primitive cetacean *Squalodon* cf. *S. atlanticus* (Leidy). *Squalodon atlanticus* and the closely related species *S. calvertensis* occur in the upper part of the Kirkwood Formation of New Jersey and in the Calvert Formation, Zones 5 through 12, of Maryland. This places the species in the late early Miocene or early middle Miocene, which is the latest occurrence of *Squalodon* in North America. In Europe, *Squalodon* occurs as late as the Tortonian and possibly the Messinian (late Miocene).

Mastodonts of the *Gomphotherium* group first appear in Europe during the late Burdigalian (late early Miocene). In North America, the earliest occurrence of *Gomphotherium* is in the Coldspring fauna (middle Barstovian: early middle Miocene) in the upper part of the Fleming Formation of Texas. The latest occurrence of *Gomphotherium productum* of the size range of the Gay Head specimen is in the Tesuque Formation, Santa Fe Group, of New Mexico, which is assigned a Valentinian or Clarendonian (late middle Miocene) age. It appears that *Gomphotherium,* the first mastodont to reach the Western Hemisphere, arrived in North America somewhat later than its first appearance in Europe and spread rapidly to the east coast, for the Gay Head occurrence is as old as the earliest record of *Gomphotherium* in the Western United States.

On the basis of the vertebrate fauna, the greensand of Gay Head is of early middle Miocene age.

The Aquinnah Conglomerate at Gay Head contains reworked Miocene bones, including many whale remains and the molar of the rhinoceros *Diceratherium.* The Pleistocene age of the Aquinnah is established by the presence of an astragalus (ankle bone) of *Equus.* This is from a large horse, of a size common in the Pleistocene, occasionally found in the Pliocene of the West and unknown in beds of earlier age.

Reproduction by glochidium larva in an Eocene nonmarine bivalve

Modern Unionacean (freshwater) bivalves have evolved a complex life cycle, using fish as an intermediate host to parasitic larvae. After fertilization within the shell of the female bivalve, eggs enter a portion of the female's gills. At an advanced developmental stage, the larvae are forcefully ejected into the water. The emergent larva, termed the glochidium, has a small (05–0.5 mm), bivalved, calcium carbonate shell. The glochidia quickly clasp onto superficial tissues (gills, fins) of passing fish by adduction (rapid closing) of the valves. Many Unionacean bivalves infest a variety of fish, but some require a particular species of fish for completion of their life cycle. The glochidia become an irritant and are soon encapsulated by a thin layer of flesh, at which time they become parasitic on the fish and metamorphose into juvenile bivalves, normally within 14 to 36 days. The juvenile bivalves are subsequently sloughed off the fish and drop to the bottom to form new populations.

The calcified glochidium larval shell of the early Eocene freshwater bivalve *Plesielliptio littoralacustris* n. sp. has been identified by J. H. Hanley. Recognition of the glochidium represents the first documentation of mode of reproduction in preQuaternary Unionacean bivalves. The glochidium indicates that the life cycle of this species included a parasitic stage on a fish as in living Unionacean bivalves and substantiates adaptation for dispersal of larvae by fish in the early Eocene. *Plesielliptio littoralacustris* inhabited the shallow, nearshore lacustrine environment in Eocene Lake Gosiute during deposition of the Luman Tongue and Tipton Shale Member of the Green River Formation in southwestern Wyoming. The high mobility of fish provided an excellent mechanism for geologically "instantaneous" dispersal of *P. littoralacustris* larvae within Lake Gosiute and adjacent drainage systems. Because of its potentially broad geographic distribution, *P. littoralacustris* may be useful in early Eocene nonmarine biostratigraphy in the Green River, Piceance Creek, and Uinta Basins.

Early Tertiary flora found in New Mexico

The discovery of a new paleobotanical locality in the Nacimiento Formation of the San Juan Basin, N. Mex., resulted from the close cooperation of J. A. Wolfe with the Laboratory of Paleontology at the University of Arizona. The locality contains the first early Paleocene (Dragonian) flora known from this State. The flora is bracketed by mammalian faunas, and it is also correlated with magnetostratigraphy. The plants are well preserved and appear to have the cuticle preserved—a rare phenomenon in deposits of such antiquity. The state of preservation is expected to be a significant factor in the interpretation of early angiosperm evaluation, and it is of major importance to the understanding of floral criteria used to recognize the Cretaceous-Tertiary transition.

Dinoflagellates helpful in North Slope biostratigraphy

The paucity of mega- and microfossils in the past has impeded the progress of Albian and Cenomanian biostratigraphy on the North Slope of Alaska. Although foraminifers generally have been helpful, other fossil groups have not occurred in sufficient numbers to be consistently useful.

During the last fiscal year, diverse and often well preserved dinoflagellate and acritarch assemblages were studied by F. E. May in palynological residues from several cored wells and outcrop samples from the North Slope. These are proving to be particularly useful in Albian to Cenomanian strata of the Nanushuk Group. Two published reports on these findings suggest that a dinoflagellate zonation is possible, correlating outcrop sections with subsurface sections. Thus far, approximately 80 species of fossil dinoflagellates and acritarchs have been reported as a result of this study from four wells and one type section, and particular biostratigraphic distributions of these microfossils are evident. The middle to upper Albian portion of the section is characterized by *Spinidinium vestitum, Luxadinium propatulum,* new genus W, *Pseuduceratium expolitum,* and *Muderongia asymmetrica.* The lower Cenomanian portion of the section is characterized by a previously unpublished assemblage of small peridinioid cysts that appear to be unique to this part of the section.

Biostratigraphy of Cretaceous nonmarine mollusks from the Western Interior of North America

J. H. Hanley (USGS), E. G. Kauffman (U.S. National Museum), and L. S. Russell (Royal Ontario Museum, Canada) have completed a survey of the biostratigraphy of Cretaceous nonmarine mollusks from the Western Interior of the United States. Mollusks are the most abundant element of Cretaceous freshwater and terrestrial macrofaunas, and more than 260 species have been described from the Western Interior. Virtually all species have been plotted on a range chart relative to a modern lithostratigraphic framework.

Several problems affect the application of nonmarine mollusks to zonation and correlation of the Western Interior Cretaceous: (1) inadequate collecting from geographic areas and stratigraphic intervals, (2) poor understanding of taxonomy and morphologic variability relative to species concepts in living forms, (3) provinciality of mollusks, and (4) conservative evolution and long species ranges. Inferred mechanisms for rapid, widespread, geographic dispersal and tolerance for high-stress environmental conditions, however, enhance their biostratigraphic potential. The "index fossil" concept of biostratigraphy cannot be applied to a refined nonmarine zonation. Rather, techniques of assemblage zone biostratigraphy provide a mechanism by which even long-ranging species might contribute to a refined zonation.

Most species are restricted to one stage or less in time. Few nonmarine mollusks are recorded from times of major marine transgressions into the Western Interior. Major radiations of nonmarine mollusks occurred during the Aptian-Albian and Campanian-Maestrichtian Stage intervals, prior to and after the principal period of marine flooding (late Albian to early Campanian). The distinct taxonomic character of molluscan assemblages between these intervals indicates they are separated by a major evolutionary break. The Albian to Maestrichtian increase in genus- and species-level diversity at least partially reflects increasing radiation and niche partitioning of mollusk-dominated "paleocommunities" through the Cretaceous.

PALEOZOIC STUDIES

The Late Devonian and Early Mississippian ostracode genus *Pseudoleperditia*

The marine ostracode genus *Pseudoleperditia* (Schneider, 1956) was considered to be a stratigraphic marker for lower Tournaisian limestones in Belgium, Nevada, and Russia because the three known species were considered to be synonyms of each other. I. G. Sohn examined the types of the Belgian species and described a new species from the Gilmore City Limestone (Lower Mississippian) in Iowa. He concluded that there are five named and at least three undescribed species of *Pseudoleperditia* in Europe and North America. The stratigraphic range of the genus is from the Upper Devonian (Frasnian) through Lower Mississippian (lower Tournaisian); consequently, correlation has to be based on the species level. The habitat of the genus has been inferred to be deep subtidal. The new species from Iowa, however, is interpreted by Sohn to have been transported and deposited in a lagoon by seasonal storms and that *P. poolei* Sohn, 1969, was not transported because adult specimens are associated with very young growth stages. Thus, species of *Pseudoleperditia* have potential biostratigraphic utility in areas of limestone deposition.

Eight lateral biofacies within a single Upper Devonian conodont zone

Three new shallow-water biofacies—the pandorinellinid, scaphignathid, and clydagnathid biofacies—were recognized in the *Polygnathus styriacus* conodont zone by C. A. Sandberg (USGS) and Professor Dr. Willi Ziegler (Philipps-Universität, Marburg, West Germany). These augment the five biofacies of the same zone (including one shallow-water biofacies, the patrognathid) that were identified by Sandberg (1976). Thus, eight different biofacies, representing settings ranging from shallow peritidal to offshore pelagic, are now recognized within a single Upper Devonian (upper Famennian) conodont zone. The shallow-water clydagnathid, pandorinellinid, scaphignathid, and patrognathid biofacies are each dominated by a different conodont genus and have few faunal elements in common with the four deeper water biofacies. The four shallow-water genera—*Pandorinellina, Scaphignathus, Clydagnathus,* and *Patrognathus*—on which the shallow-water biofacies are based, are all phyletically related within the long-ranging *Pandorinellina* stock. Previously, the genus *Pandorinellina* was known only from the Lower Devonian (mainly Emsian), Middle Devonian (Eifelian), and lower Upper Devonian (lower Frasnian), but it now has been found in Upper Devonian (Famennian) zones above and below the *P. styriacus* zone as well as in several Lower Mississippian (Kinderhookian) zones. Thus *Pandorinellina* was the ancestor of the other three Late Devonian shallow-water genera, two of which (*Patrognathus* and *Clydagnathus*) range into the early Carboniferous. Recognition of the diversity of faunas within a single zone will help provide better interregional and intercontinental correlations of Upper Devonian and lower Carboniferous rocks.

Devonian coral biostratigraphy

W. A. Oliver, Jr. (USGS), and A. E. H. Pedder (Geological Survey of Canada, Calgary) have completed an analysis of the stratigraphic value of Devonian rugose corals. The geographic and stratigraphic distribution of over 300 genera were plotted using 15 non-American geographic areas (plus 8

Western Hemisphere areas analyzed earlier) and 6 stages. Principal conclusions are that (1) corals are of negligible value in worldwide correlation and of limited value in intercontinental correlation, but that within more restricted areas their value is considerable, (2) corals are more sensitive indicators of biogeographic provincialism and environment than any other group of stratigraphically studied fossils thus far analyzed, and (3) corals have a large, but unrealized, potential in community analysis.

Corals clearly show an increase in the number of faunal provinces through Early Devonian time to a maximum of eight or nine, then a decrease through the Middle Devonian to three or four, and the virtual disappearance of provinces during the Late Devonian.

Lower-Middle Ordovician boundary in the north-central Appalachian Basin

Analysis of conodont faunas by A. G. Harris and L. D. Harris across the Lower Middle Ordovician boundary in south-central Pennsylvania shows that the boundary lies at least 215 m below the top of the Beekmantown Group dolomites and that deposition was continuous through this interval. The same depositional patterns and faunas succession also occur in the upper part of the Beekmantown Group from Maryland to the Harrisonburg, Va., area. Farther north in Pennsylvania, however, in Blair and Huntingdon Counties, latest Early Ordovician conodont faunas are succeeded by middle Whiterockian faunas 215 m below the top of the Beekmantown Group (earliest Whiterockian conodont faunas are missing). Moreover, at Tyrone, Pa., a chert-pebble conglomerate occurs at this same stratigraphic level. The Early Middle Ordovician unconformity in north-central Pennsylvania is of much smaller magnitude than that in eastern Pennsylvania and New Jersey or in southern Virginia and Tennessee.

The characterization and stratigraphic position of the Lower Middle Ordovician boundary in the central Appalachian Basin are crucial to the search for metallic-mineral and hydrocarbon deposits because the porosity zone developed at or near the Early Middle Ordovician unconformity has served as a host for metallic-mineral deposits as well as a reservoir for hydrocarbons. Conodonts and some lithostratigraphic evidence indicate that in part of central Pennsylvania an unconformity does occur between Lower and Middle Ordovician rocks, but that this boundary lies within the dolomite of the upper part of the Beekmantown Group and not, as previously thought, at the contact of Beekmantown dolomite with the overlying Middle Ordovician limestone.

Cambrian primitive mollusks

John Pojeta, Jr., J. E. Repetski, and Juergen Reinhardt (USGS) and Ed Landing (University of Waterloo, Canada) have added significant new stratigraphic information to the Cambrian record of some mollusks belonging to the classes Rostroconchia and Pelecypoda. The rostroconch *Ribeiria* has now been identified from Acadian-age rocks in New Brunswick, Canada, on the basis of a specimen at the Royal Ontario Museum, Toronto, Canada. This specimen shows that typical ribeiriids occur in Middle Cambrian rocks, where they are transitional between the Early Cambrian genus *Heraultipegma* and a diverse fauna of Late Cambrian ribeirioids.

In the upper Franconian or Trempealeauan part of the Frederick Limestone of Maryland, several shells, which are symmetrical around the commissural plane and have shapes that are known in two subclasses of pelecypods, have been found in acid residues. They occur with a much larger fauna of inarticulate brachiopods. This discovery, combined with new information from the Middle Cambrian of New Zealand (provided by D. T. MacKinnon, University of Canterbury, New Zealand) and the occurrence of *Fordilla* in Lower Cambrian rocks, suggests that pelecypods were part of the world's biota throughout most of Cambrian time. One reason for Cambrian pelecypods not being better known is their small size. All known specimens are less than 5 mm long and most are around 1 mm long.

PRECAMBRIAN STUDIES

Ediacarian (?) age fossils from Saudi Arabia

The first fossils to be recorded from the Arabian shield were found by P. E. Cloud, Jr. (USGS), and Karen Morrison and S. M. Awramik (University of California at Santa Barbara) in rocks of the Muraykhah Formation, Jubaylah Group, collected in northern Saudi Arabia by D. G. Hadley. Microbial species associated with cryptalgalaminates and an unusual form of the stromatolite *Conophyton* include two size classes of simple spheroidal nannofossils and the distinctive coiled filaments of a blue-green alga that is similar to *Obruchevella parva* Reitlinger from the Tinnovsk Suite of Yudomian

(Ediacarian) Age in eastern Siberia. A very latest Proterozoic to early Phanerozoic affinity is implied, perhaps close to biotas that elsewhere have been dated as about 680 million years old. A rubidium-strontium whole-rock age of 540 million years obtained in associated basalts, therefore, may be too young. The Jubaylah Group is localized along ancient depressions associated with the Najd set of apparently contemporaneous left-lateral faults, trending northwestward parallel to present-day plate boundaries. Faulting of the Arabian Shield area associated with early continental fracturing and plate motions may, therefore, be very old.

PLANT ECOLOGY

Flood related movement of scree

Movement of some screes on Massanutten Mountain in Virginia is indicated through ring analysis of trees growing on or near the scree. Preliminary results by C. R. Hupp indicate that parts of a continous scree move periodically and movements are correlated with high streamflow. Trees in the path of moving rock are often scarred or tilted. Scars are dated by examining cross sections of trees. Reaction wood formation permits dating of severe tilts. Rock movement downslope appears to have occurred no less than three times in the last 25 years.

Analysis of streamside tree forms below the scree record flood stages on Passage Creek and correlate with existing streamflow records. Further study should significantly extend the flood record for the stream.

Severity of droughts estimated from tree rings

Widths of tree rings were used by L. J. Puckett to estimate a 230-year record of drought severity in northern Virginia. Cores were extracted from eastern hemlock, *Tsuga canadensis* (L.) Carr., at three locations in northern Virginia, and growth increments were converted to indices. Growth was positively correlated with precipitation and negatively correlated with temperature during the May-July growing season.

Standardized indices of growth were calibrated with the indices of July drought severity. Greatest improvement in calibration was made by extracting principle components of individual tree growth indices thereby accounting for 64 percent of variance in regression. Comparison of the results with a 279-year reconstruction from New York showed considerable agreement between low-frequency climatic trends, suggesting that network collections throughout the East may yield information about widespread drought.

Plant societies along a bajada in southern Arizona

The mathematical analysis of spatial or seasonal changes in vegetation is useful. This approch was found by T. E. A. van Hylckama and R. M. Turner to let them compare changes in vegetation from different climates and environments (van Hylckama, 1978).

One such approach is by the use of similarity indices, expressed as $2W/(A+B)$ in which A and B are the number of species in two vegetation plots and W is the number of species growing in both plots. A matrix of these indices can be constructed. Analysis of this provides one (or more) dimensional ordinations (Mueller-Dombois and Ehrenberg, 1974).

Ten plots, at elevations between 850 and 1,400 m above sea level, were studied. Woody and succulent perennial plants were counted. Grasses and forbs were not included. This record was made to explain differences in infiltration and evapotranspiration rates and in soil-moisture content on a westerly exposed slope of the Santa Rita Mountains near Tucson, Arizona.

The ordination in one dimension showed a similar index in vegetation differences. Small differences exist between plots at close elevations, but large differences exist between extreme elevations. The noticeable change in vegetation is thus mathematically verified.

CHEMICAL, PHYSICAL, AND BIOLOGICAL CHARACTERISTICS OF WATER

Water-quality trend analysis

Efforts to evaluate 20-year trends in water-quality data on the Neuse River in North Carolina necessitated the development of techniques to eliminate the effects of discharge on concentrations of dissolved materials in the stream. C. C. Daniel III and D. A. Harned devised two methods of water-quality trend analyses; one is a method of statistically weighting observed concentrations on the basis of the discharge-frequency distribution resulting in weighted average annual concentrations of dissolved constituents, and the other is a method of calculating total annual loads from regression-synthesized daily concentrations normalized to a central value of dis-

charge. Both techniques were applied to Neuse River data and produced similar results, thereby indicating what the water quality of the stream would have been each year if average discharge had been the same for each year.

Changes in concentrations of several dissolved constituents in the French Broad River indicated that pollution loads increased from 1958–67 and decreased from 1974–77. H. B. Wilder and M. S. Weiner found that these changes in concentrations correlate well with changes in manufacturing in the river basin.

Relation between pH and fishkills in Oyster Creek, New Jersey

Trout-stocking operations in Oyster Creek in southern New Jersey have been unsuccessful due to the occurrence of fishkills following rainstorms. T. V. Fusillo and J. C. Schornick found a relationship between the occurrence of fishkills and decreases in pH which occur during runoff periods. The runoff flushes acid water (pH 3.5–3.9) from surrounding swamp areas into the poorly buffered creek, thereby causing a rapid pH drop in the creek. Low pH, in combination with high iron concentrations normally found in the stream, are lethal to trout populations. Low pH levels found in the swamp water results from several physical and chemical processes, including hydrolysis of iron and aluminum, oxidation of sulfides, and production of carbon dioxide and humic acids during the decomposition of organic matter.

Large pH decreases in Oyster Creek occurred only during large storm events; however, no direct relationship between stream discharge and pH was found. The length of time between storm events and pH of the swamp prior to a storm were significant factors in the magnitude of the decrease in pH.

Chemical mass-transfer model of spring water

By using a chemical mass-transfer model, B. A. Kimball made quantitative predictions about a sequence of chemical reactions that accounts for most of the observed changes in water chemistry as ground water circulates from recharge areas to springs in the southeastern Uinta Basin of Utah. Weathering reactions of calcite, dolomite, plagioclase, K-feldspar, and pyrite with CO_2-charged water were evaluated as a function of reaction progress. This group of minerals includes most of the material involved in weathering of carbonate rocks and arkosic sandstone, both of which occur in the Green River Formation of Tertiary age. The predicted sequence includes saturation with kaolinite and calcite during early stages of reaction and saturation with an expandable clay and dolomite during later stages. During early stages, most of the dissolved solids are produced by weathering of calcite only. After calcite is in equilibrium with ground water, weathering of feldspar minerals becomes an important influence on the solution chemistry. The effect of combining carbonate minerals with feldspar minerals in a weathering system is to increase the amount of dissolved solids produced and to decrease the amount of clay minerals formed. The solution chemistry changes as different dissolved solids are precipitated as product minerals. The general change is from a calcium bicarbonate water to a calcium-magnesium-sodium-bicarbonate-sulfate water.

The mass-transfer predictions resemble both the observed variations in chemical character of the spring water and the observed occurrence of precipitated minerals in soils and streambed material in the southeastern Uinta Basin. This suggests that the mass-transfer model might be used to study weathering in other complex lithologic settings.

Geochemical processes at mining areas in North Dakota

D. C. Thorstenson studied the geochemical processes at a lignite mine near Gascoyne, N.Dak. Temperature profiles were obtained from about 40 shallow wells in and around the mine after initial work had suggested the possibility of estimating rates of lignite oxidation in spoils by temperature profile anomalies. The detailed study suggested that surface effects, such as variability in vegetative cover, overshadow the subsurface thermal effects and that, at Gascoyne, this technique will not provide lignite oxidation rates. Mineralogical analyses from approximately 60 samples (core and highwall) showed that carbonates and gypsum generally occur near the surface. A zone of sulfide concretions is present in the silts above the lignite; the concretions are oxidized at shallow depths. The mineralogy, water chemistry, and distribution of gases in the unsaturated zone all appear to be a complex function of the relative depths below land surface of the lignite and the water table.

M. E. Crawley reported that X-ray diffraction analyses of samples from the upper part of the Sentinel Butte formation in the Beulah Trench area, a potential lignite mining area of North Dakota, indicated that the major mineral species present are quartz, feldspars, and the clay minerals. Calcite concentrations average about 3 percent, while dolomite concentrations average 4 percent. Gypsum is rare,

occurring only in shales and lignite. The clay minerals are predominantly smectite and illite. Kaolinite was detected in only three samples. Small amounts of pyrite are also present.

Under normal precipitation conditions, water rich in dissolved oxygen causes oxidation of pyrite in near-surface sediments. This generates H^+ and SO_4^{-2} ions. The resulting slightly acidic water dissolves the carbonate minerals. As this occurs, the H^+ content decreases; the pH, Ca^{+2}, and HCO_3^- increase. These reactions occur in the near-surface sediments. Because of infrequent recharge events, pore water usually undergoes concentration because of evapotranspiration and results in precipitation of calcite and gypsum.

Results of soluble salt analyses indicated that sodium is the most predominant cation and that sodium concentrations of leachates increase with depth. Exchangeable cation analyses indicated a similar trend in increasing sodium concentrations with depth.

Column studies of waste-water infiltration

Infiltration of reclaimed waste water was studied in four columns packed with soil taken from the horizon of the basin floors at the Cedar Creek, N.Y., artificial recharge site. According to M. S. Garber, the columns were subjected to constant application of highly treated, reclaimed sewage effluent for a period of 2 weeks at the USGS laboratory located at the Bay Park Sewage Treatment Plant in Nassau County, New York. Water supplied to two of the columns was filtered through a 3-μm foam plastic filter; water supplied to the remaining two columns was not pretreated. Break-point chlorination was provided in the effluent supplied to one filtered and one unfiltered column. The remaining two columns were unchlorinated. Four test conditions were thus established and results could be analyzed by cross correlation. The experiment was designed in this manner in order to examine qualitatively the effects on surficial clogging caused by bacterial and physical sources, either together or singly.

Results showed that greatest total flow by far was through the column receiving filtered, unchlorinated water, and the least total flow was through the column receiving unfiltered, unchlorinated water. Intestingly, chlorination or filtration alone yielded about the same total flow. At the end of 10 days, flow in all columns was less than 3mL/min. No significant change in bacterial count was observed in the unchlorinated columns. Growth appeared to have occurred in the chlorinated columns.

Land conservation related to water quality

Concern over agriculture's role in water pollution may be unjustified in some areas of Michigan, according to results of a 4-year study of the upper St. Joseph River basin by T. R. Cummings. Chemical and physical characteristics of water were determined and related to land use in 21 drainage areas that comprise the 373-km^2 basin. Runoff ranged from 0.002 to 0.044 (m^3/s)/km^2; both the higher and lower values were largely the result of naturally occurring interbasin and intrabasin transfers of water.

Suspended-sediment concentrations were low throughout the basin, rarely exceeding 100 mg/L. Mean concentrations at four daily sampling stations on the major tributaries and on the St. Joseph River ranged from 9.7 to 38 mg/L. The maximum sediment yield was 204 (kg/ha)/yr. Deposition of sediment in 5 of the 21 areas resulted in a net loss of sediment transported.

Nitrogen and phosphorus concentrations did not vary greatly from site to site. Mean concentrations of total nitrogen at downstream sites on major tributaries and on the St. Joseph River ranged from 1.5 to 1.8 mg/L. About 90 percent of all nitrogen and 66 percent of all phosphorus are transported in solution. Land use principally for agriculture has a mean total nitrogen yield of 5.5 (kg/ha)/yr and a mean total phosphorus yield of 0.15 kg/ha. A comparison of total nitrogen and total phosphorus yields with the type of agricultural use showed few relationships; nitrogen yield, however, seemed to decrease as the percentage of land in row crop and small grain increased. A relation between the amount of fertilizer applied to land and the amount in streams could not be demonstrated.

Only about 6 percent of the total nitrogen and about 1 percent of the total phosphorus added to the land in animal wastes, in precipitation, and applied as fertilizer, are transported from the basin by the St. Joseph River. It was estimated that almost three times as much nitrogen and twice as much phosphorous fall in precipitation on the basin as are transported from the basin by runoff. In general, land conservation practices of the past seem to have been effective in minimizing erosion and leaching of soils in the basin.

Biochemical activity following subsurface waste injection

G. G. Ehrlich and E. M. Godsy studied the consequences of injecting nitrate-containing wastes into a limestone aquifer such as the Floridan aquifer. Two waste-injection systems were studied. One sys-

tem, at West Palm Beach, Fla., is used for injecting nitrified secondary sewage effluent. The other, near Pensacola, Fla., involves injection effluent from an acrylonitrile polymer plant. In both systems, vigorous biochemical denitrification (reduction of nitrate to gaseous nitrogen) occurs in the injection zone. A single bacterium capable of denitrifying the acrylonitrile-based waste was isolated in pure culture. Methanogenic bacteria, which are present in significant numbers in the undisturbed aquifer adjacent to the waste-injection zones, were absent from the areas where denitrification was occurring.

The acrylonitrile-based liquid was deficient in phosphate. Phosphate to meet biosynthetic needs was apparently derived from phosphorite, a phosphorous-containing mineral in the formation.

Effect of nitrification on the oxygen balance of the upper Chattahoochee River in Georgia

T. A. Ehlke (1978) reported that oxygen consumption, as a result of nitrification, and carbonaceous bacterial oxidation were compared in a 108-km reach of the Chattahoochee River of Georgia. Nitrogenous and carbonaceous oxygen consumption were separated by using an inhibitor of nitrofication, 1-allyl-2-thiourea. The comparison was conducted in a laboratory by using samples collected from the water column. Nitrification accounted for 38 to 52 percent of the total oxygen consumption.

Nitrifying bacteria were enumerated from the same reach of the river. The density of *Nitrosomonas* ranged from 10 to 1,000/mL in the water column and 100 to 100,000/g of benthic sediment. The *Nitrobacter* population ranged from 10 to 100/mL in the water column and 100 to 1,000/g in the benthic sediment. The concentration of ammonium, nitrite, and nitrate nitrogen was determined from water samples collected throughout the study reach. The average rate of ammonium disappearance and of nitrate appearance was 0.02 (mg/L)/h of flow time.

Trace-metal form and bioavailability in estuarine sediments

Field studies of San Francisco Bay by S. N. Luoma showed variations with time in concentrations of the toxic metals, Co, Ag, and Zn found in clams and sediments. Metal concentrations in the clams increased with the onset of rainfall in the early winter (and the associated discharge of urban runoff) in each of 3 years. Concentrations peaked in midwinter and declined to a minimum by midsummer. Freshwater flow into the estuary from major river systems appeared to cleanse bioavailable copper and silver from San Francisco Bay. The highest silver and copper concentrations ever observed in a tellenid clam occurred during the period of lowest river discharge into the Bay and were followed by a substantial "die-off" of the affected clam population.

Partial chemical extractions and statistical methods were employed to illustrate the partitioning of trace metals among different sorption sinks in oxidized sediments from 20 estuaries. Oxides of iron, oxides of manganese, and organic materials (especially humic substances) all adsorbed some fraction of the six metals studied. Dominance by any single sink varied with the physicochemical characteristics of the sediment. Earlier work suggested sorption to iron oxides reduced the biological availability of lead. Statistical studies of metal form suggested that the bioavailability of lead was greatly enhanced by lead sorption to oxides of manganese, a process that predominates only in environments with a high ratio of lead to iron and low concentrations of organic carbon.

Volatile and semivolatile organics in the Lower Mississippi River in Louisiana

Eight volatile organic compounds were detected in samples from five locations in the Mississippi River between St. Francisville and Belle Chasse, La., from 1976 to 1978, according to F. C. Wells. The volatile organics appeared to be evenly distributed in this reach of river. Benzene, toluene, and chloroform were detected in samples from all five locations; however, concentrations of these compounds did not exceed 11 μg/L. Fourteen semivolatile organic compounds were identified in water samples from the river, and an additional six compounds were isolated but could not be positively identified by mass-spectrometer analysis. Concentrations of the semivolatile organics recovered from the river were generally less than 5 μg/L. The most frequently detected semivolatile organics were the phthalate compounds.

Analysis of duplicate river samples and duplicate standard samples submitted to two laboratories indicated that the methodology recommended by EPA for the identification of volatile organic priority pollutants yields good semiquantitative results. However, for semivolatile organics, results of duplicate river samples and duplicate standard samples submitted for quality-control purposes revealed relatively low recovery rates for base-neutral compounds. Both laboratories experienced extremely low recovery or no recovery of compounds in the acid-

neutral standard sample, thus indicating a failure in the methodology used for semivolatile analysis.

Bacterial growth kinetics with acetone as a substrate

D. J. Shultz used a continuous culture apparatus (chemostat) to study the kinetics of bacterial growth on an acetone substrate. Departure from Monod kinetics was found to be caused by bacterial growth. Experiments without bacterial growth indicate that suspended bacteria grow according to Monod kinetics.

Adsorption of ketones in water

D. W. Stephens determined there was no adsorption of acetone in concentrations ranging from 30 mg/L to 158 mg/L, at 20°C, and within a pH range of 6.57 to 11.42 by montmorillonite or kaolinite clays (particle size, <50 μm) in sterile distilled water or sterile buffered water during a 500-hr test period.

Natural sediment (organically rich sand and clay) which was autoclaved also failed to adsorb acetone (105 mg/L) or tertiary butyl alcohol (39 mg/L) over a 500-hr period at 20°C and a pH of 7.26

Sorption of acetone by a naturally occurring aquatic mold was investigated both in the presence and in the absence of bacteriostatic levels of antibiotics. No uptake or acetone occurred within the effective antibody period of 2 weeks. After that time, bacterial degradation of the acetone occurred. In the absence of antibiotics, bacterially induced losses of 10 percent per day occurred.

No sorption of ketones from an aqueous mixture containing 30 mg/L of acetone, 5 mg/L of 2-pentanone, 5 mg/L of 3-pentanone, and 2 mg/L of methylisobutyl ketone by a naturally occurring algal mat of *Spyrogyra* and *Cladophora* treated with bacteriostatic antibiotics at 20°C was noted over a 100-hour time period.

Compilation of carbon–14 data

L. J. Schroder, R. L. Emerson, and W. A. Beetem (1978) compiled carbon–14 data for Alaska, California. Colorado, Nevada, and Wyoming. The carbon–14 samples were collected in support of underground nuclear-waste disposal or detonations financed by the Nevada Operations Office, U.S. Energy Research and Development Agency. All of the samples collected in Colorado that had total alkalinities exceeding 1,000 mg/L had positive $\delta^{13}C$ values. All $\delta^{13}C$ values for the Nevada samples were negative, which is a departure from earlier results obtained for the same general area. Duplicate samples were obtained from one well and the results of the check samples agreed with the originals.

RELATION BETWEEN SURFACE WATER AND GROUND WATER

Ground-water flow near lakes

T. C. Winter (1979) showed that complex geologic conditions can greatly influence lake seepage. In many geologic settings, lakes in surficial geologic units are separated from deep extensive aquifers by confining beds. Steady-state numerical simulation of such a setting, for a given water-table configuration, showed that the interaction of lakes and ground water is greatly affected by the continuity of the confining bed. If the confining bed is continuous and has a vertical hydraulic conductivity three orders of magnitude less than the upper geologic unit, the lake is not affected by the presence of the deep unit even if a head difference between the two aquifers is as great as 6 m. The location and extent of discontinuities in the confining bed, relative to the lake, have an important effect on seepage. If the discontinuity is directly below the lake and is half the diameter of the lake, a vertical head difference of as little as 1 m is sufficient to cause outseepage from the lake. If the diameter of the discontinuity is only one-fourth the diameter of the lake and the head difference is less than 0.6 m, outseepage from the lake will not occur.

According to D. E. Troutman and N. E. Peters, three small lakes of different pH, alkalinity, and buffering capacity are currently under study in a geologically similar area of the Adirondack region of New York. Quantitative estimates from a reconnaissance study, in which six seepage meters (Lee, 1977) were located in each lake during summer base flows, indicated that more than 50 percent of the total outflow discharge at Panther Lake, the lake with highest alkalinity (5 mg/L as $CaCO_3$), is attributable to ground-water seepage through the lake bed. A 25-percent value was reported for Woods Lake, the lake with lowest alkalinity (0 mg/L as $CaCO_3$). Less than 5 percent was recorded at Sagamore Lake, the lake with intermediate alkalinity (0.5 mg/L as $CaCO_3$) and a significantly larger drainage area. Measurements of pH from water samples collected during these seepage-meter studies indicated that ground-water quality differs significantly from lake-outflow quality and, under baseflow conditions, may alter lake alkalinity and lake chemistry. These quantitative differences in percent

of ground-water contribution to Woods and Panther Lakes correlate directly with increased chemical loadings.

Lake budget in Minnesota

The 1978 water budget of Eagle Lake near Willmar in central Minnesota was determined by C. F. Myette to support a nutrient-budget study being made by the University of Minnesota at Morris, Minn. Emphasis in the water budget was placed on measurements of seepage and head. Seepage measurements were made at 140 sites around the periphery of the lake. Seepage into the lake was greatest in sand and gravel deposits at the northwestern end of the lake, and seepage from the lake was greatest through lake sediments near the outlet at the southern end of the lake. Flow of ground water, calculated as a residual in the water budget, compared favorably with calculations of flow based on a flow-net analysis using hydraulic conductivities derived from well logs and the head distribution derived from water-level measurements in an observation-well network.

Maintaining lake levels by using ground water

Cedar Lake, a kettle lake in Wisconsin with no surface inlet or outlet, was studied in detail by R. S. McLeod to evaluate the feasibility of maintaining lake levels in the glaciated area of eastern Wisconsin by supplementary pumping of ground water. The general hydrogeology of the area around the lake was defined, and a water budget was prepared to quantify the components of the hydrologic system of Cedar Lake. Inflow to the lake from October 1974 to September 1976 averaged approximately 1,143 mm/yr—711 mm precipitation, 51 mm ground-water seepage, and 381 mm overland flow. Outflow from the lake for the same period averaged 1,245 mm/yr—787 mm evaporation and 458 mm ground-water seepage. A volume of water sufficient to raise the lake level 1,194 mm was pumped from the shallow aquifer system into Cedar Lake between February 1, and September 30, 1977. Approximately 90 percent of pumped water was either recycled from the lake to the well or otherwise lost as seepage from the lake.

Streamflow augmentation

A stream in a highly suburbanized part of southeastern Nassau County, New York, was augmented during a 24-hr period to test the response of the stream-aquifer system. Water from a public supply was routed to the stream at a rate of 0.6 m^3/s. Dennis Sulam reported that the effects of this augmentation were (1) an immediate response of stream stage and ground-water levels near the stream channel, (2) a decrease in ground-water seepage to the stream caused by the increased stream stage, (3) an increase in discharge at the gaging station located 3 km downstream from the augmentation site, and (4) the occurrence of maximum increases in stream stage and ground-water levels between 2 and 5 hours after augmentation began.

Stream-aquifer model of north-central Kansas

Modeling of three principal stream-aquifer systems in north-central Kansas is nearly complete. These systems extend from an upstream reservoir to the terminus of a valley-wide irrigation system. L. E. Stullken reported that preliminary results from a two-dimensional model reproduced streamflow gains and losses documented by seepage runs made prior to irrigation development from the valley aquifers. Seepage runs were made on Prairie Dog Creek prior to activation of a surface-water irrigation system. During each run, the lower half of the reach consistently gained flow, and some sections in the upper half of the reach lost flow in response to heavy municipal demands. The net gain over the entire reach ranged from 0.05 to 0.09 m^3/s. The model calculated an increase of 0.10 m^3/s with gain-loss increments similar to those measured in the seepage runs.

Hydrology of Ozark basins in Missouri

According to E. J. Harvey, a study of hydrology in three Missouri Ozark basins and an analysis of hydrologic methodology for carbonate terranes showed that there are intricate relationships between ground water and surface water. These relationships can best be determined by using a number of study methods. The measurement of streamflow, in conjunction with geologic mapping, is one of the most important tools for investigating the hydrology of carbonate terranes. Current and historic ground-water level data are also essential. One of the most effective ways to determine the relationships between ground water and surface water is to construct basin profiles by using ground-water levels and streamflow data in conjunction with topographic, geologic, and structural information.

EVAPORATION AND TRANSPIRATION

Evaporation from water surfaces and the combined evaporation and transpiration from vegetated land surfaces play a major role in hydrology; they return about 70 percent of the incident precipitation in the conterminous United States to the atmosphere. Moreover, evapotranspiration from a given area can be substantially altered by land-use changes, such as irrigation development, reforestation, drainage of wetlands, and urbanization. Consequently, knowledge of evapotranspiration under various land-use and climatic conditions is needed for planning purposes.

Most of the significant results of evaporation and transpiration studies in 1978 were related to methods of estimating evaporation and evapotranspiration at selected sites by using climatic data.

Relationship of evaporation to windspeed for an open channel

Evaporation from ponds and lakes is frequently estimated from windspeed, water-surface temperature, and air-humidity data by the Dalton equation:

$$E = f(u)\,(e_o - e_a),$$

where E = evaporation rate, L/T; that is, length/time such as m/yr;

$f(u)$ = an empirical wind speed function that includes a proportionality coefficient which depends on the size and shape of the surface-water body, the units of length, mass, and time used, and many other factors, L^2T/M;

e_o = saturation vapor pressure of air at a temperature equal to that of the water surface, M/LT^2;

and e_a = vapor pressure of the air above the water, M/LT^2.

H. E. Jobson (1979) extended the use of the Dalton equation to estimate evaporation from open channels; the estimate was based on a study of the thermal balance of the 26-km-long concrete-lined San Diego Aqueduct, a canal in southern California. The appropriate wind function was determined by calibration of a model of the thermal balance of the canal. Coefficients for the wind function were determined as those giving the best match between the computed and measured thermal balance of the canal by using data obtained during a 28-day period. The coefficients were verified by comparing computed thermal balances to measured thermal balances that were based on data obtained during 113 days but that did not include data used for calibration. These data verified that the derived wind function provides reliable estimates of the canal evaporation.

The wind-function coefficients applicable to the San Diego Aqueduct are similar to those commonly obtained from lake-evaporation studies. However, they indicate that evaporation from the canal is greater at low windspeeds than that from a lake. Annual evaporation of 2.08 m/yr was computed; this is about 91 percent of the annual evaporation from nearby class-A evaporation pans.

Selecting an equation for computing potential evapotranspiration in an arid area

Potential evapotranspiration, defined as the evapotranspiration that would occur if water were never in short supply, is a climate-related factor useful for predicting actual evapotranspiration under various conditions. Consequently, a great number of equations have been proposed for estimating potential evapotranspiration from climatic data. T. E. A. van Hylckama, R. M. Turner, and O. M. Grosz have tested three such equations by using soil-moisture and precipitation data obtained from a study undertaken along a bajada on the western slope of the Santa Rita Mountains near Tucson, Ariz. Because deep percolation generally is insignificant beneath desert soils, soil-moisture depletion during a rain-free period represents actual evapotranspiration during that period. Potential evapotranspiration, computed from three different equations, was used in a model to predict soil-moisture depletion on the bajada. Moisture depletion predicted by use of the Penman (1956) method correlated with the measured values with a coefficient (r) of 0.66 ± 0.07; values predicted by using the Budyko (1948) model correlated with a coefficient of 0.72 ± 0.03, and surprisingly, a purely empirical model described by Olivier (1961) gave the highest coefficient of 0.73 ± 0.03. Although all correlation coefficient values were significant at the 1 percent level, correlation between measured and computed values was significantly higher for the Olivier equation than for the Penman equation.

These data suggested that the Olivier method is the most useful method tested in the Tucson area. However, other models may be preferable in other climatic areas. In particular, the success of the Olivier method in the Tucson area may result because the method is based mainly on studies of arid African lands having climates similar to that of southern Arizona.

LIMNOLOGY AND POTAMOLOGY

Although the term "limnology" originally applied only to the study of lakes, its current usage also applies to the study of streams and rivers. The term "potamology" is more restrictive; it applies only to river investigations. Limnology is the study of the sources and nature of freshwaters, the motion and changing conditions of freshwaters, and the organisms supported by freshwaters.

Invertebrate drift in a meadow and a canyon reach of a mountain stream

The influence of mesoscale environmental factors on drift of stream invertebrates was studied in adjacent third-order reaches of Little Boulder Creek, Idaho, a tributary of the East Fork Salmon River. Drift-net collections were made hourly for 24 hours, and the samples were then compared for presence and relative abundance of taxa. Site 1, with a channel slope of 5.08 m/km, is a meadow stream with bed material of sand and coarse gravel. Site 2, 2.5 km downstream from site 1, has a slope of 30.48 m/km; the bed material of this section is gravel and cobble with scattered boulders. The drift net sampled 3.5 and 2.2 percent of the total flow at sites 1 and 2, respectively.

S. S. Hahn, L. J. Tilley, and K. V. Slack reported that total numbers of aquatic invertebrates, exclusive of the family Chironomidae for which data were not available at this time, were similar at the two sites. Rates of drift (individuals/m^3) varied according to time of day; a large increase in drift rates occurred at dusk. Drift rates decreased after dawn, and the lowest drift rates coincided with the period of maximum solar radiation. More taxa were collected at night than during daylight hours. However, no sample contained more than one-third of the 90 taxa found. Drift collections from site 1, the more poollike habitat, contained more *Baetis* mayflies and fewer *Ephemerella* and *Epeorus* mayflies than did site 2, the more rifflelike habitat, and site 1 contained fewer *Rhyacophila* and *Parapsyche* caddisflies but more *Psychoglypha* caddisflies, Tipulidae, and many more Copepoda than did site 2. Mayflies were relatively more abundant at site 1, whereas stoneflies were more abundant at site 2.

Water-quality effects of underground coal mining

Water-quality measurements made near an abandoned coal mine in western Washington were used by F. A. Packard, L. A. Fuste, and M. O. Fretwell to design a monitoring program for small streams likely to receive drainage from new areas of underground coal-mine development. During low flows, changes in quality of the mixing zone of the receiving stream included ferric hydroxide deposition; increased hardness, alkalinity, sulfate, and dissolved solids; and slight decreases in dissolved oxygen saturation and pH. There was an accompanying decrease in diversity of benthic invertebrates. However, at the point where complete mixing of mine effluent into streamflow occurred, no significant change in invertebrate diversity was detected, and chemical changes were largely confined to moderate increases in dissolved solids, alkalinity, sulfate, hardness, and total iron. Correlation analyses showed caddisflies of the family Glossosomatidae and mayflies of the subfamily Heptageniinae to be most sensitive to the mine drainage and the family Cypridae to be least sensitive. Among taxa found to be tolerant to the drainage were the stoneflies *Brachyptera* sp., *Nemoura* sp., and *Hastaperla* sp., Chironomidae (dipterans), and Atractideidae (water mites). Regression analysis indicated that temperature, net acidity, and total iron were constituents associated with significant changes in the biological community.

Biotic and abiotic uptake of added nitrate and phosphate in a northern California stream

Nitrate and phosphate were added to a northern California coastal forest stream so that the uptake of these nutrients as a function of time and nutrient concentration could be studied. Nitrate was added during a 4-hour period, and 1 week later orthophosphate was added during a 3-hour period. Sampling was done 310 m below the injection point. According to M. J. Sebetich, V. C. Kennedy, S. M. Zand, R. J. Avanzino, and G. W. Zellweger, almost 100 percent of the nitrate was removed from the leading edge of the added solute, but, following that, over the concentration range 40 to 560 $\mu g/L\ NO_3-N$, removal was nearly constant at 24$\mu g/L$ per 100 $\mu g/L\ NO_3-N$ added. Nitrate was not desorbed back into the water, and its loss was attributed to uptake by periphyton. Relatively little orthophosphate was lost from the leading edge of the added solute, although there was a proportionally greater loss with increasing orthophosphate concentration. Some desorption of orthophosphate occurred after the termination of injection. The dissimilarity in the uptake of added nitrate and phosphate may be due to differing rates of reaction with the biota and to a different degree of interaction with the abiotic component of the stream solids.

Observations on the diurnal variation in orthophosphate uptake by periphyton showed a well-defined tendency toward a minimum in the afternoon and a maximum in the evening. This trend was observed under baseline conditions, when orthophosphate averaged about 5 $\mu g/L$ PO_4-P and also when added orthophosphate raised the level to about 90 $\mu g/L$ PO_4-P. The variation in phosphorous uptake contrasted with that of nitrate, which was greatest during afternoon hours and sharply lower during evening hours.

Algal stromatolites (oncolites), Onondaga Lake, New York

Onondaga Lake in New York is a moderately saline, eutrophic lake characterized by water rich in calcium, sodium, chloride, and bicarbonate. Large quantitites of calcium carbonate that are precipitated in the lake result from input of excess of calcium from calcium chloride wastes produced by soda-ash manufacturing. Beaches along the leeward (northeastern) shore of the lake are composed almost entirely of oncolites that range from a few millimeters to several centimeters in maximum dimension. Offshore, in 1 to 2 m of water, the oncolites are composed mainly of low-magnesium calcite, but dissolution of the carbonate with dilute acid results in a mass of blue-green algal filaments of the same approximate size and shape as the original oncolite. According to W. E. Dean, scanning electron micrograms (SEM) revealed that the oncolites grow by trapping and binding sediment particles (mainly calcium carbonate) by mucilaginous sheaths of blue-green algae and later cementation by calcite. SEM observations further revealed that the most common nucleus is the hollow stem and cortication tubules of the calcareous green alga *Chara* (stonewart). *Chara* is not found in Onondaga Lake today although it is very common in other hard-water lakes in central New York State. *Chara* most likely was eliminated by the markedly increased salinity of the lake that resulted from the introduction of soda-ash manufacturing on the lakeshores around 1880. This suggests that growth of the oncolites began at least 100 years ago.

Limnological characteristics of small Montana reservoirs

Limnological data were collected for 12 multiple-use reservoirs in northern Valley County, Montana. Surface areas of these reservoirs ranged from 0.5 to 28.3 ha, and they were 1.2 to 6.5 m in mean depth. Temperature profiles made by R. F. Ferreira during 1978 indicated that the reservoirs remain mixed through the summer months. Specific conductance values in the 12 reservoirs ranged from 62 to 1,600 μmho/cm; pH generally was above 7.0 and increased in some reservoirs to values greater than 9.0 in late summer when algal populations were at their greatest densities. Shallow reservoirs were more turbid than the deep reservoirs, due to relative ease of mixing by moderate winds. The turbid waters frequently were high in iron and other metals. Ice covers on the reservoirs in March 1978 were about 1 m. The shallow reservoirs were anaerobic under ice, whereas a few of the deep reservoirs had saturation concentrations of dissolved oxygen. Specific conductance values were approximately three times higher during winter months than during summer months.

A reconnaissance of biological and chemical characteristics of selected Ohio lakes

Fourteen Ohio lakes were sampled by C. G. Angelo, R. L. Robin (USGS), and John Younger (Ohio Environmental Protection Agency) during the spring and summer of 1978. Measurements included profiles of temperature, dissolved oxygen, pH, and specific conductance; biological and trace organic constituents; major and minor inorganic constituents; and physical and chemical data associated with major inflows. Dissolved-oxygen saturation ranged from 170 percent in Nettles Lake to zero percent in the bottom waters of all lakes with stable thermal gradients. The BOD_5 ranged from 0.4 mg/L in Lake Hope to more than 20 mg/L in West Fork Mills Creek Lake. Anaerobic zones were frequently characterized by hydrogen sulfide and high concentrations of ammonia. Seasonal thermal gradients developed in most lakes that were more than 6 m deep.

The water of all lakes was hard or moderately hard. Specific conductance ranged from 103 to 3,000 μmho/cm. Pesticide and trace-element concentrations did not exceed limits established by the Ohio Environmental Protection Agency. All fecal-coliform counts were below State limits. Blue-green algae (Cyanophyta) dominated the phytoplankton communities of 8 lakes in the spring and 14 lakes during summer months. Estimated discharge-weighted mean concentrations for nitrite+nitrate and total phosphorus in 19 inflow samples were 1.28 mg/L nitrogen and 0.14 mg/L phosphorus, respectively.

Chemistry and hydrology of Winter Haven chain of lakes

W. C. Sinclair reported that a reconnaissance during the spring of 1976 of water quality of the 14 navigable lakes in the Winter Haven chain (Flor-

ida) showed that most of the lakes had high nutrient concentrations. Lakes Lulu and Shipp were the most enriched—a result of surface runoff from residential, agricultural, and urban areas and many years of contamination by municipal- and industrial-waste effluents. Stage during May 1976 of the Chain of Lakes, as measured on Lake Howard, was the lowest recorded in 31 years. Stage hydrographs of Lake Howard, representative of the chain, and Lake Otis, the nearest isolated lake with a reasonably long record, were compared with other hydrologic measurements. Linear-regression analyses of lake stage versus cumulative precipitation indicated that deficient rainfall was the dominant factor in decline of lake levels in the area.

Water quality of selected reservoirs in Texas

Periodically since 1961, the USGS, in cooperation with State, local, and Federal agencies has conducted comprehensive water-quality surveys of selected reservoirs in Texas, according to H. B. Mendieta. During the 1978 water year, 51 surveys were made on 17 reservoirs. A review of the nutrient data showed that inorganic nitrogen and total phosphorus concentrations of these reservoir waters are both usually less than a few tenths of a milligram per liter (expressed as the element). Under reducing conditions in the hypolimnion of stratified lakes, inorganic nitrogen and total phosphorus concentrations can both reach 1 to 6 mg/L. Livingston Reservoir on the Trinity River has the highest nutrient concentrations of the lakes surveyed. Phytoplankton sampling at selected sites in 11 of the reservoirs was initiated during 1978.

Water quality of Tulpehocken Creek, Pennsylvania, prior to impoundment of Blue Marsh Lake

Impoundment of Tulpehocken Creek, Berks County, Pennsylvania, by Blue Marsh Dam generated much speculation on the likely rate of eutrophication and ultimate usefulness of the 390-ha impoundment. Of primary concern were phosphorus and nitrogen loadings from the watershed. According to J. L. Baker, monthly analyses over a 5-year period indicated that annual phosphorus and inorganic nitrogen loadings are 76 and 381 kg/km^2, respectively. These amounts far exceed loadings measured at other Pennsylvania lakes classified as eutrophic.

Sources of nutrients in Lake Waramaug, Connecticut

K. P. Kulp reported that nutrients enter Lake Waramaug, Connecticut, primarily via surface-water inflows to the northeastern part of the lake. Bacteriological determinations of surface-water inflow indicated frequent high levels of fecal contamination, primarily from nonhuman sources. Precipitation analyses showed relatively high concentrations of nutrients, particularly in May, late August, and September. Ground water and lake seepage did not appear to contribute significant quantities of nutrients. Lake sediments contained high concentrations of nutrients, particularly bed material from the deep basins.

NEW HYDROLOGIC INSTRUMENTS AND TECHNIQUES

A complex system for recirculating sediment in transport as bedload was designed and constructed as an attachment to an existing concrete flume at the University of Minnesota's St. Anthony Falls Hydraulic Laboratory in accordance with specifications developed by D. W. Hubbell, H. H. Stevens, Jr., J. V. Skinner, and J. P. Beverage. The system is being used by the research team to calibrate bedload samplers. The system accommodates bedload particles that range in size from about 2 to 64 mm and are transported at rates from near 0 to 7.44 (kg/s)/m of flume width. Bed material placed in the flume is transported as bedload along the channel by flow, diverted from the Mississippi River, downstream to a slot in the floor of the flume. At that point, the bedload particles fall through the slot, but the water (up to 7.1 m^3/s) flows out the end of the flume and back to the river. Weigh pans beneath the slot catch the sediment and increasingly load cells, which support the pans, as the material accumulates. Whenever a pan fills, doors in the bottom of the pan automatically open and the sediment is recirculated to the head of the flume. A data-acquisition system designed by the research team continuously monitors and records bedload discharge. So far, only 6.5-mm bed material has been used in the research. Calibration data on Helley-Smith type samplers indicated that the ratio of the entrance to exit area of the nozzle appreciably affects sampling efficiency. The data also dramatically show the extreme cyclic variability of bedload-transport rates.

Winchell Smith and S. H. Hoffard began an investigation in August 1978 to determine if modern acoustic transducers could reliably transmit and receive signals over a 4,100-m path across Suisun Bay at Chipps Island, California. Signals could be

attenuated or refracted by salinity and temperature gradients and suspended solids in this wide tidal reach. Also, the effect of aquatic growth on the functioning of the transducers was unknown.

Approximately 2 months of testing indicated that the aquatic growth, predominantly a species of small barnacles, has little effect on signal transmission and reception. About 98 percent of the signals received from transducers at depths of 3 m or more below the surface appeared to be of adequate strength. About 90 percent of the signals received at transducer depths 1 to 2 m below the surface appeared adequate. Periods of weak signal strength have not yet been clearly correlated with physical characteristics of the water.

SEA-ICE STUDIES

W. J. Campbell reported that the first set of a series of aircraft remote-sensing missions was flown over Arctic regions in October and November 1978 by the NASA Convair-990 *Galileo II* flying laboratory. These flights were part of the Polar Ice Program for the Seasat 1 and Nimbus 7 satellites, which were launched previously. The *Galileo II* carried active- and passive-microwave instruments that simulated those onboard the satellites. The flights were coordinated with satellite passes whenever possible. Sea-ice data were obtained for the Bering, Beaufort, East Greenland, Barents, and Norwegian Seas, the Baffin Bay, for ice sheets in Greenland, and for the polar ocean front in the Norwegian and Barents Seas, as part of a joint Norwegian-American experiment. Flights were also coordinated with "surface-truth" experiments in the Barents and Norwegian Seas (Norway), Pond Inlet and Beaufort Sea (Canada), and data buoys in the Bering Sea (United States). Data obtained by means of remote-sensing flights will provide invaluable aid in the validation, interpretation, and application of active- and passive-microwave data collected by the Seasat 1 and Nimbus 7 satellites in the Arctic regions.

W. J. Campbell (USGS), R. O. Ramseier (Department of Environment, Canada), and Per Gloersen and H. J. Zwally (NASA-Goddard Space Flight Center) produced an 11-minute film of Arctic sea-ice variations from time-lapse passive microwave imagery. The film consists of a series of color-enhanced brightness temperature images from the electronically scanning microwave radiometer (ESMR) onboard Nimbus 5. It shows the seasonal variation of sea-ice morphology and concentration and many aspects of short-term and long-term changes in ice structure and motion that are not noticable on individual images. An analysis of the film indicated that the interannual variability of the Arctic ice-cover structure and extent is more pronounced than was previously shown by non-synoptic data. Along the ice edge, complex wave forms appear and migrate at speeds as great as 100 km/wk in areas of high meteorological activity. One of the most important discoveries was that large areas of low ice concentration occur within the Arctic pack throughout the year. It had been believed that the concentration of the main pack near the Pole was essentially 100 percent, but there are actually areas where concentrations are as low as 50 percent.

Erk Reimnitz and D. K. Maurer reported that data collected over a 6-year period and observations from vessels and aircraft showed that ice dynamics, the occurrence of major ice features, and overall ice zonation on the Beaufort Sea shelf are strongly influenced by ice interaction with shoals. This was seen in the correspondence of a belt of charted shoals with the outer edge of the fast-ice zone. Recognition of this relationship led to the concept of a stamukhi zone—a midshelf belt of grounded pressure ridges and hummock fields on shoals sheltering the inner shelf. It also led to the recent discovery and survey of a shoal 17 km long and up to 10 m high, on the poorly charted shelf near the Prudhoe Bay oilfield. This feature, Stamukhi Shoal, lies next to charted shoals that apparently no longer exist, and it may have formed as a result of ice-related processes. A series of Landsat images representing views of sea ice during several winters and summers shows a striking correlation between ice features and the west end of Stamukhi Shoal as it was when surveyed in 1977.

Gravel, a resource required for building roads to petroleum-producing areas of the Arctic shelf, probably is a major component of the shoal. However, Stamukhi Shoal helps protect the inner shelf and coast from ice pressure and helps determine the extent of fast ice and, thereby, the extent of areas where petroleum can be readily developed. Thus, it appears that mining the shoal's gravel would be inadvisable.

In early May 1978, W. Barnes, Erk Reimnitz, L. J. Toimil, and H. R. Hill studied fast ice in the Prudhoe Bay region of Alaska to determine the relationships of under-ice morphology and seabed morphology, tidal currents, and variations in snow thickness in order to learn (1) how oil spilled below

the ice in winter would be contained by the ice canopy and (2) how an oil-containment capability would vary with environmental conditions.

At three sites representing three different environments—protected shallow bay, narrow tidal channel, and deep open lagoon—trenches were cut through the ice parallel and perpendicular to the northeast-southwest-trending snowdrift pattern of sastrugi. Along these trenches, snow depth, ice thickness, and ice draft were measured, and an upward-directed side-scanning sonar examined the undersurface in a 25-m-wide zone.

Snow depth correlated with ice thickness—ice was thin where an insulating snow canopy was thick—and the areal pattern reinforced the correlation. Elongate subice ridge-and-trough patterns, with relief up to 30 cm, paralleled the surface sastrugi pattern on a wavelength of 10 to 20 m. Underwater observations indicated that a smaller set of depressions (5 cm or less in depth) paralleled the ice-crystal fabric. Under-ice morphology did not correlate with water depth, oceanographic environment, or sediment character.

The saturation vapor pressure of water vapor in the atmosphere is an important variable in many meteorological processes that are essential parameters in sea-ice dynamics studies. In the modeling of meteorological processes, the numerical approximation of the dependence of saturation vapor pressure of water on temperature is a necessary step. L. A. Rasmussen developed a series of coefficients for saturation pressure with respect to a liquid water surface for the temperature intervals [−50°C, +50°C] and [0°C, +50°C] and, with respect to an ice surface for the temperature interval, [−50°C, 0°C]. The order of accuracy of this method is the same as the accuracy of some other recently published functions, but the method requires less computer time.

ANALYTICAL METHODS

ANALYTICAL CHEMISTRY

Spectrophotometric determination of tungsten in rocks

A spectrophotometric method for the determination of tungsten in silicate rocks was developed by P. J. Aruscavage and E. Y. Campbell. Tungsten was determined in rocks by a spectrophotometric procedure that measures the absorbance of the tungsten-dithiol complex. After the samples were dissolved in $HClO_4$ and HF, the tungsten was isolated by extraction of the tungsten-dithiol into isoamyl acetate and back extracted into citric acid. The absorbance was measured after reextraction into isoamyl acetate. The determination of 0.1 ppm tungsten in 500 mg sample can be made routinely. Tungsten was determined in 11 USGS standard rocks with a relative error of 10 percent or better.

The measurement of uranium content in metallic ores, sediments, and water

Current interest in uranium exploration has sparked a major effort to develop new or improve existing analytical methodology. According to F. N. Ward, exploration geologists may choose conventional fluorimetry, neutron activation—delayed neutron counting, X-ray fluorescence, laser-induced fluorescence, and nuclear-fission track techniques for the determination of uranium (Ward and Bondar, 1978). The choice will be governed by several considerations, sensitivity, sample media, turn-around time, and cost. Both conventional fluorimetry and laser-induced fluorimetry can be adapted to field use with commercially available instrumentation.

EMISSION SPECTROSCOPY

Induction coupled plasma spectroscopy

A procedure has been developed by J. M. Motooka, E. L. Mosier, S. J. Sutley, and J. G. Viets for the simultaneous determination of Ag, Au, Bi, Cd, Cu, Pb, and Zn in geologic materials by induction coupled plasma optical emission spectroscopy. The process involved a selective extraction technique that effectively eliminated common problems encountered by major elements. Direct spectral interferences, matrix and interelemental effects caused by Al, Ca, Fe, K, Mg, Mn, and Na were substantially reduced and trace metals critical to a mineral evaluation were enhanced to a more precise detection level by concentration in the organic phase. The technique allows for a greater degree of confidence in the analysis by minimizing correction factors and elements that introduce adverse effects. Variable matrix samples having multiple major elements present in wide concentration ranges are, for exploration purposes, better suited to selective extraction techniques. The precision and accuracy of the procedure far exceed that which is required for exploration geochemical purposes.

Emission spectrographic analysis for trace elements in basalts from core holes near Charleston, South Carolina

Spectrographic determinations completed by C. S. Annell on selected basalt samples from Clubhouse

Crossroads core holes no. 2 and no. 3 (CCC no. 2 and CCC no. 3), near Charleston, S.C., suggest differences in the trace-element geochemistry of these basalts. Major-element chemistry is largely similar to basalts from CCC no. 1 which was a quartz-normative tholeiite. However, at least 3 or 4 meters of CCC no. 3 consists of olivine-bearing basalt, with quartz-normative tholeiite of different chemistry above and below it. Visual examination of CCC no. 3 by David Gottfried and M. I. Byerly points to different degrees of alteration and texture which could be further characterized by chemical and physical tests.

NEUTRON ACTIVATION

Neutron activation of geologic materials

An automated instrumental neutron-activation analysis (INAA) system has been developed by J. J. Rowe, P. A. Baedecker, and J. W. Morgan at Reston, Va. A similar system has been developed by H. T. Millard, Jr., at Lakewood, Colo. Complex gamma-ray spectra were converted to elemental concentrations on the MULTICS computer. The INAA systems were applied to the determination of 22 to 26 elements in more than 4,500 samples at the two laboratories for a variety of geochemical investigations.

Morgan has developed radiochemical separation procedures for individual or groups of isotopes in order to extend the INAA detection limits for the analysis of ultramafic rocks or special mineral samples. The INAA system in Reston has been used to analyze samples as small as 5μg.

X-RAY FLUORESCENCE

Loss-On-Fusion method for determining volatiles in geochemical samples

A Loss-On-Fusion (LOF) method for the determination of volatiles in rocks has been developed by V. G. Mossotti and B. S. King (1978). The method is unique in that it used data obtained by the lithium-tetraborate fusion procedure during the preparation of fused sample glass discs prior to X-ray fluorescence (XRF) major element analysis. The difference between the weight of the sample and flux prior to fusion and the weight of the resulting fused sample glass disc is directly correlatable to the volatile content (total water and CO_2) of the rock samples. When appropriate, the total sulfur content is determined by an alternative XRF procedure. The Loss-On-Fusion method requires no additional analytical time and can save up to $1,600 per 40 samples over the cost of conventional wet chemical procedures. This LOF method may be preferred for geological investigations where the specific H_2O^+, H_2O^-, and CO_2 content are not critical to the analysis. The LOF method has been found to be accurate within 1 to 2 percent of the total volatile content in a wide variety of rock types.

ANALYSIS OF WATER

Metallic constituents

An automated, continuous flow-through procedure to determine tin in water and streambed materials was developed by G. S. Pyen and M. J. Fishman. Sample solutions of streambed materials were prepared by a standard USGS extraction procedure involving digestion with a dilute mineral acid. The interferences from most trace elements were eliminated by addition of EDTA (ethylenediaminetetraacetic acid). Sodium borohydride was added to the sample stream to form tin hydride, which was then stripped from the solution with the aid of nitrogen and decomposed at 850°C in a tube furnace located in the optical path of an atomic absorption spectrophotometer. Twenty samples per hour can be analyzed; the detection limits are 1 μg/L and 0.1 μg/g for water samples and streambed materials, respectively.

J. E. Bonelli and H. E. Taylor discovered a significant interference from iron on the trace determination of copper in natural waters by differential-pulse anodic-stripping voltammetry. This interference is caused by the diffusion-controlled voltammetric reduction peak of Fe (III), which is unresolved from the stripping peak of copper. Concentrations of 1 mg/L of iron cause a 100-percent error when determining 10 μg/L of copper. An instrumental correction technique was developed to permit quantitative determination of copper.

Bonelli and Taylor also developed techniques for the determination of thallium by differential-pulse anodic-stripping voltammetry at both a hanging mercury drop electrode and a mercury thin-film electrode. High sensitivities at a comparable analysis time can be achieved by the mercury thin film, and detection limits on the order of 10 ng/L can easily be obtained.

J. R. Garbarino and H. E. Taylor developed a pneumatic nebulizer for use with an induction-coupled plasma-emission spectrometer, based on a modified Babington design. The primary advantage of the nebulizer is its ability to aspirate water sam-

ples containing appreciable amounts of suspended matter. Comparison studies showed that the nebulizer offers equivalent precision and sensitivity to the more conventional cross-flow pneumatic nebulizer.

G. W. Johnson and R. K. Skogerboe (Colorado State University) and H. E. Taylor (USGS) developed a d.c. argon-plasma atomic-emission spectrometric method for the quantitative determination of 20 major and trace elements. A comparison of two-electrode and three-electrode systems showed that a significant improvement in reproducibility and a decrease of spectral background are achieved by the latter.

Anionic constituents

Samples of pore waters were analyzed for chloride, fluoride, nitrate, bromide, and sulfate by G. S. Pyen and M. J. Fishman using an ion chromatographic technique. Fluoride, nitrate, bromide, and sulfate were determined simultaneously, but chloride was determined singly because of its extremely high concentration (approximately 20,000 mg/L). Chloride, nitrate, and sulfate were also determined independently by automated colorimetric procedures. Results obtained by both techniques showed good agreement. To determine the validity of bromide results, samples were spiked with 1 to 3 milligrams of bromide per liter. Recoveries ranged from 97 to 103 percent. Several replicate analyses were made to evaluate precision. The relative standard deviations for fluoride, chloride, and sulfate were approximately 4, 2, and 2 percent, respectively. The concentrations ranged from 0.78 to 2.02 mg of fluoride per liter, 1.7 to 119 mg of chloride per liter, and 15.1 to 146 mg of sulfate per liter. At 0.53, 5.3, and 1.27 mg of NO_3-N per liter, the relative standard deviations were 1.9, 2.7, and 3.9 percent, respectively.

Organic constituents

Routine determinations of individual phenolic compounds in water at concentration levels on the order of 1 μg/L require preconcentration if gas or liquid chromatography is used for analysis. M. C. Goldberg and E. R. Weiner developed a method that uses continuous liquid-liquid extractors to concentrate 14 phenolic compounds from water into dichloromethane, followed by Kuderna-Danish evaporative concentration. The extractors can extract 18 L of sample in 3 hours. Two additional hours are required for solvent concentration, resulting in overall concentration factors of about 1,000. Overall extraction and concentration efficiencies for the compounds examined ranged from 23.1 to 87.1 percent. Concentration efficiencies for several phenols were also determined for a batch method that is suitable for extracting and concentrating phenols from sediments. Overall concentration efficiencies for the batch method ranged from 18.9 to 73.8 percent.

A semiquantitative method was developed by W. E. Pereira and B. A. Hughes for the determination of 19 volatile organic priority pollutants in water by gas chromatography-computerized quadrupole mass spectrometry. The method involves sparging a 5-mL water sample with helium. The volatile organics were trapped on a porous polymer adsorbent, backflushed with helium, and then thermally desorbed from the porous polymer trap onto a gas chromatography column. The volatile organics were then separated by gas chromatography and detected by mass spectrometry. The organics were identified by means of their relative retention times, and their mass spectra were characterized by using a "reverse library" search routine. The individual volatile organics were quantitated by an internal standard method, using dibromoethane-d_4 as the internal standard. The method is semiautomated, and the results are generated in the form of a quantitation and identification report. The method is applicable to the analysis of ground and surface waters. The lower limit of detection for each component is 5 μg/L.

D. Y. Tai used a gas chromatographic technique with direct aqueous injection to determine acetone, methyl ethyl ketone, 2-pentanone, 3-pentanone, and methyl isobutyl ketone in water samples with concentrations ranging from 5 to 75 mg/L. Column material was 80/100 Carbopack C (with 0.2 percent Carbowax); the column was constructed of special nickel alloy tubing. Good separation and sharp peaks were obtained with temperature programming from 80° to 130°C at 10°/min.

Experiments with rhodamine-WT dye, acetone, and t-butyl alcohol showed a distinct color change in the dye from a dark red to a bright orange when these three substances were injected together into a small stream. To investigate this effect, Tai also conducted controlled experiments in the presence of sunlight and found that the dye did not affect the concentrations of acetone or t-butyl alcohol and that the acetone and t-butyl alcohol did not affect the fluorescene of the dye. Stream sediment had no effect on the measured concentrations.

D. W. Stephens determined that dilute standard solutions of adenosine triphosphate (ATP) may be frozen for at least 4 months with no loss in activity. However, after thawing, an 18-percent decrease in

ATP peak area occurs within 2 hours, followed by a 5-percent decrease in the next 2 hours. Loss is believed to be due either to overextension of the buffering capacity of the enzyme-buffer complex by dilution or to hydrolysis of the ATP standard solution after thawing. Comparison of standards prepared in a pH 7.7 buffer, in a pH 10.7 buffer of recrystallized sodium phosphate, and in a pH 10.7 buffer prepared in reagent-grade sodium phosphate showed no differences among the buffer systems when the standard solutions were analyzed promptly after preparation and also showed no significant difference among the systems when the frozen standards were analyzed 6 days later but within 1.5 hours of thawing.

Stephens also investigated three different reagents as means of extracting ATP from sediments; the reagents investigated were (1) boiling tris buffer, (2) nitric acid, and (3) trisodium phosphate-chloroform. The third reagent system gave the best recovery and provided the greatest sensitivity; however, because of the many handling steps involved in the extraction, an internal spike of ATP was required to identify losses. ATP concentrations in a local biologically active stream sediment ranged from 1,000 to 1,600 ng of ATP/g dry sediment.

Errors in gross radioactivity measurements

Periodic measurements of gross radioactivity are being widely used in the United States to indicate quality of community water systems with respect to radioactivity. Analytical requirements for making these measurements are defined by the U.S. Environmental Protection Agency in Title 40, Part 141, "Interim Primary Drinking Water Regulations," in the July 9, 1978, *Federal Register*.

Americium-241 apparently is being used by an increasing number of laboratories as an alternative gross-alpha-activity calibration standard in place of the uranium standard required by Federal regulations. Higher alpha-counting efficiencies obtained when using americium-241 as a calibration standard result in gross-alpha-activity analyses differences of up to 100 percent when compared to duplicate sample analyses based on a uranium standard. Studies by V. J. Janzer (1979) demonstrated that the use of americium-241 as an alternative gross-alpha calibration standard, in effect, doubles the federally specified maximum contaminant. This problem exists because of widespread nonconformance and confusion regarding federally mandated standards for gross-alpha radioactivity calibration, measurement, and reporting.

Analytical precision for inorganic determinations

In order to provide documented precision data for inorganic determinations, L. C. Friedman compiled and statistically analyzed interlaboratory data from the USGS Water Resource Division's Standard Reference Water Sample Program and intralaboratory and interlaboratory data from the division's laboratories at Denver, Colo., Albany, N.Y., and Atlanta, Ga. The precision data so acquired provide the basis for regular continuing evaluation of the routine performances of the Water Resources Division and cooperating State and contractor laboratories.

GEOLOGY AND HYDROLOGY APPLIED TO HAZARD ASSESSMENT AND ENVIRONMENT

EARTHQUAKE STUDIES

SEISMICITY

Operations and special investigations

The National Earthquake Information Service (NEIS) in Golden, Colo., occupies an esteemed position within the international scientific community. It is the foremost source of data on recent earthquake activity around the world. Last year, as part of its program to monitor global seismicity, the NEIS determined the location and magnitude of approximately 6,000 earthquakes. Of these, approximately 1,500 were large enough to cause damage in populated areas. The NEIS program to monitor earthquakes throughout the world can be viewed as an information-gathering and analysis procedure. Input data in the form of arrival times and amplitudes recorded at cooperative seismograph stations throughout the world are sent to Golden where they are machine processed to obtain output composed of earthquake origin times, locations, magnitudes, and associated station observations. These results are then disseminated to seismologists, engineers, government agencies, and other interested parties throughout the world.

According to W. J. Person, the NEIS early alert service, which operates on a 24-hour basis, issued 54 earthquake bulletins last year. These bulletins concern potentially destructive shocks overseas or somewhat smaller U.S. quakes that may have caused damage. Because of the breakdown in communications following a major earthquake, these bulletins often provide disaster relief organizations, public safety agencies, and the news media with the only factual information available for a considerable period of time after the shock.

Through cooperation with universities and other agencies and the installation of new equipment, an effort has been made to lower the detection threshold of U.S. earthquakes in areas not covered on regional and local networks. M. A. Carlson reports that signals from 55 stations are telemetered to the Golden, Colo., recording center of the U.S. seismograph network. The network, which now extends from coast to coast and border to border, gives NEIS the capability of responding rapidly to earthquakes within the conterminous United States.

In conjunction with four university seismological centers and the Delaware Geological Survey, the USGS established a network to investigate the Northeastern United States. P. W. Pomeroy coordinated operation of this network, which now consists of about 85 seismic stations. Origin times, locations, and magnitudes of all events within this regional network are published in the "Bulletin of Seismicity of the Northeastern United States."

The NEIS carried out surveys of the damage done by and felt areas of 118 earthquakes in the conterminous United States during 1978, according to C. W. Stover. These intensity surveys, which permit recent instrumentally recorded shocks to be compared with historic earthquakes, are valuable in engineering seismology and risk analysis. The basic data needed to delineate the severity and extent of ground shaking accompanying an earthquake are obtained from a postal questionnaire canvass carried out by means of modern data-processing techniques. The results of the questionnaire canvass and maps showing the areal distribution of intensities are published in the quarterly circular "Earthquakes in the United States."

The Albuquerque Seismological Laboratory (ASL) has become a recognized leader in efforts to upgrade instrument and recording systems used at seismograph stations. The ASL continued to provide the technical and logistical support necessary to keep the Worldwide Standardized Seismograph Network (WWSSN) operational. At present, this 15-year-old network is composed of 85 foreign stations and 31 domestic stations. Each observatory consists of matched, three-component, long-period, and short-period instruments. Paper seismograms recorded at the stations are sent to Golden for quality control and forwarded to the National Oceanic and Atmospheric Administration (NOAA) data center at

Boulder, Colo., for film reduction. Researchers from all over the world may order exact copies of the WWSSN records from NOAA at moderate cost.

According to H. M. Butler, the ASL is well underway in the installation of a Global Digital Seismograph Network, which eventually will consist of at least 35 observatories. Among these are 13 Seismic Research Observatories (SRO) with advanced seismograph systems consisting of shallow borehole seismometers coupled to state-of-the-art electronics and recording packages. With the addition of SRO recording systems, five High-Gain Long-Period Observatories have been modified to Abbreviated Seismic Research Observatories. In addition, equipment has been purchased to add digital recording capability to about 15 stations of the Worldwide Standardized Seismograph Network. The Global Digital Seismograph Network data tapes will be processed at the ASL and converted to network day tapes for distribution to research seismologists.

C. J. Langer reports good agreement between the hypocenters computed with local network data and those determined with calibrated teleseismic data for the larger aftershocks of the Peru earthquake of October 3, 1974 ($m_s=7.8$). Langer operated a network of portable stations along the coast adjacent to the aftershock region for a period of three weeks following the main shock. Composite focal mechanisms of the aftershocks, in the vicinity of Chilca and southwestward, indicate a strong component of right-lateral strike slip along a northeast-trending nodal plane. This implies a more complex rupture process than the dominantly underthrust motion previously reported.

W. J. Spence and C. J. Langer (1978) have identified clusters of aftershocks in the sequence following the Peru earthquake of October 3, 1974. They note an oscillation of aftershocks between subzones of the aftershock area.

New or revised Modified Mercalli (MM) intensity maps have been prepared for 110 earthquakes in the United States, according to S. T. Algermissen. The maximum MM intensities assigned to most of the larger earthquakes in the Eastern United States through 1975 have been reviewed. In addition, many errors found in standard catalogues in earthquake origin times and locations have been corrected.

J. N. Jordan (USGS) and Maximiliano Martinez (Centro de Investigaciones Geotecnicas) completed a study of the seismic history of El Salvador. They found many cases in which the instrumentally determined hypocenters do not coincide with the maximum intensity region. The mislocation errors are more then a degree for some earthquakes. They urge caution in the use of unevaluated data bases for seismic risk or other studies that rely on accurate locations.

The Office of Earthquake Studies, in liaison with the National Research Council, Panel on National, Regional, and Local Seismograph Networks, has investigated the feasibility of establishing and operating a national digital seismograph network. Initial plans call for the addition of digital recording capability to five WWSSN observatories. Preparation of a Panel Report is in progress.

Seismic network studies

J. C. Lahr and C. D. Stephens have investigated the seismicity of southeastern Alaska using both locally recorded and teleseismically recorded data. The Devils Canyon and Watana damsite area is of special concern because it lies within a region of high seismicity. Most of the current earthquake activity in the damsite area seems to be occurring at shallow depths or in the so-called Benioff zone within the underthrusting Pacific plate, rather than on the surface of contact between the Pacific and North American plates. The accuracy of the hypocenter computation with data from the present USGS network is not sufficient to associate the shallow earthquakes with individual faults in the area. A local network of seismic stations in the region of the damsites is prerequisite to the identification of active faults in the area and to the monitoring of induced seismicity, according to Lahr and Stephens. In addition to the naturally occurring earthquake activity in the region, there is also the hazard that filling of a reservoir may trigger potentially damaging earthquakes.

Stephens and Lahr are continuing to investigate the seismic activity along the eastern Gulf of Alaska. Using data from the USGS network of stations, they have located more than 500 earthquakes that have occurred in the region during the past 4 years. Areas of concentrated shallow activity have been identified beneath and northeast of Icy Bay and onshore northeast of Kayak Island. Areas of earlier activity beneath Pamplona Ridge and south of Yakatat Bay are now relatively quiet seismically. Based on the occurrence of earthquakes with local magnitudes greater than 3.3, offshore and onshore seismic activities are comparable, although many more earthquakes are located onshore than offshore. During the first 10 months of 1978, at least 41 earthquakes with magnitudes of 4 or greater occurred in southern Alaska, but only three of these occurred east of Kayak Island.

Using data from the Rio Grande seismic network, L. H. Jaksha has identified three zones of shallow, low-magnitude earthquake activity near Albuquerque, N. Mex. Both normal and strike-slip fault mechanisms have been observed. Apparent *P*n velocities of about 8.0 to 8.1 km/s have been obtained along unreversed profiles in the Rio Grande Rift. The M discontinuity appears to dip both to the north and east in this part of New Mexico. W. J. Spence and Jaksha (1978) inverted teleseismic *P*-wave delay data from a 24-element seismograph network to estimate *P*-wave velocity structure in the mantle beneath the central Rio Grande rift. They estimate that the upper 180 km of the mantle beneath the rift has a *P*-wave velocity about 5 percent lower than that beneath the adjacent High Plains province. This velocity anomaly increases to about 7 percent in the upper mantle beneath the Valles caldera and beneath the Mogollon Datil volcanic field.

According to C. J. Langer, the spatial distribution of hypocenters near Puerto Rico computed for the time interval June 1, 1977, and January 1, 1978, shows less scattering than indicated by locations made from data recorded prior to June 1, 1977. These results are, in part, a reflection of a more careful and uniform method of data analysis than was previously used in the determination of hypocentral locations. Of particular interest is a well-defined concentration of hypocenters in the vicinity of lat. 19.2° N. and long. 66.5° W., which appears to occur along a short segment of the boundary of the inclined seismic zone on the south side of the Puerto Rico trench. There are also several on-island clusters of earthquakes that may be related to mapped surface faults. Linear zones of hypocenters extend oceanward to the northeast, northwest, and southeast of the island. The zones to the northeast and northwest appear to represent a complex mode of faulting within the Puerto Rico-Virgin Islands platform. The zone to the southeast may be associated with the extension of a mapped on-island strike-slip fault that strikes east-southeast.

Using the data recorded by the South Carolina seismographic network, C. J. Langer reported that earthquakes located define two distinct source regions that occupy areas in the vicinity of Summerville-Middleton Place and near Bowman, S.C. Middleton Place is approximately 15 km northwest of Charleston and about midway between the centers of the highest intensity zones of the 1886 Charleston earthquake. The earthquake epicenters located in this region since 1974 define a linear north-northwest-trending zone approximately 25 km long and 10 km wide. The seismicity is especially associated with the northeastern edge of gravity and magnetic anomalies that have been interpreted as a mafic intrusive. The area near Bowman (about 100 km northwest of Charleston) has been known to be seismically active only for the past decade and has continued to exhibit a low level of seismicity since the installation of the seismograph network.

According to J. W. Dewey, all nine regionally or teleseismically recorded earthquakes that occurred through 1976 within 100 km of Charleston, S.C., have been relocated to lie within or very near two small zones of seismic activity defined by the recently installed South Carolina network. These zones are the Middleton Place zone, thought to be the source of the destructive 1886 Charleston earthquake, and the Bowman zone, located about 50 km northwest of the Middleton Place zone. The fact that these zones, identified on the basis of microearthquakes, also account for all the regionally or teleseismically recorded earthquakes from the Charleston area, supports the hypothesis that significant seismic activity in the Charleston area is restricted by some mechanism to occur in relatively few source regions, rather than randomly throughout a broad zone of the coastal plain. Four of the relocated earthquakes had previously been mislocated by more than 50 km—the mislocated shocks had suggested structural trends that now appear to be spurious.

A. M. Rogers reports that data from the Kermit, Tex., seismograph array show that earthquakes are occurring in the Central Basin Platform (CBP) and in the Delaware Basin, possibly in association with inferred pre-Permian faults that bound the CBP on the west and east. The earthquakes seem to occur largely at depths shallower than the crystalline basement. Some events appear to occur at depths where no faulting has been inferred, but the majority of earthquakes are located at oil-producing depths where secondary recovery is employed, and none of the best located events occur outside this zone if consideration is given to the standard errors in focal depth measurements.

Although the time of the first earthquakes in the region is not known, the first felt event was in 1966, and there is no reason to suspect that earthquakes would not have been felt before that time. This time coincides with a rapid increase in the number of injection projects and the coincidental increase in the injection pressures that began in the early 1960's and peaked around 1968. These weak correlations suggest a causal relation between the earthquakes and hydrocarbon production that could be related to

increased fluid pressures along faults. Verification of this model for CBP earthquakes, however, will require improved earthquake locations that can be used to identify injection wells associated with the earthquakes, clearly defined focal mechanisms, and a record of the increase in reservoir pressures with time.

Seismic data bases

With encouragement from the International Association of Seismology and Physics of the Earth's Interior, W. H. K. Lee organized and maintains a bibliographic data base and retrieval system for current earthquake literature. Monthly indexes of current earthquake literature are distributed.

A. C. Tarr reports that a newly designed master U.S. earthquake catalog was created in the past year to fill a long-standing need of earthquake hazards and reactor hazards research projects for an accurate, comprehensive, and complete earthquake data base. By employing the principles of relational database management systems and USGS computers, it is now possible to store and retrieve virtually all significant parameters computed for and associated with U.S. earthquakes, large and small, from 1534 to the present. The data base is currently populated by several national and regional catalogs, but current effort is concentrated on the earthquake catalog of the Southeastern United States, where limitations on the data are being examined.

EARTHQUAKE MECHANICS AND PREDICTION STUDIES

SEISMICITY

During the past year, refinements were made in the inversion of *P*-arrival times recorded by microearthquake networks and in seismic ray tracing of heterogeneous media. W. H. K. Lee adapted the method of singular value decomposition to a generalized inversion scheme and applied the adaptive finite difference techniques to two-point seismic ray tracing. More work will be required, however, to implement these methods for earthquake prediction purposes.

D. P. Hill and W. L. Ellsworth used a 96-sensor microearthquake recording array in their seismic study of the creep-active central segment of the San Andreas. The study area encompassed the 15-km portion of the fault lying within Dry Lake Valley, Little Rabbit Valley, and Rabbit Valley (about 50 km southeast of Hollister, Calif.). Preliminary results from the array conclusively demonstrated that the seismicity associated with this segment lies directly below the geologically mapped zone of recent movement. Routine earthquake locations reported in the USGS bulletins are therefore systematically mislocated to the west of their true positions by 2 to 3 km in this region. Simple estimates of the compressional and shear wave velocities along the fault zone indicated that both compressional and shear wave velocities are very low. Near surface velocities, as determined by a short, reversed refraction profile, were not unusually low and suggest that anomalously low velocities extend into the source region of the deeper earthquakes (8 to 12 km). Within the region there are also pronounced variations in the degree to which body waves are attenuated. At present, the physical mechanism responsible for these gross variations remains unresolved. The most plausible candidate hypothesis is the difference in thickness and lithology of sedimentary rocks and (or) intrinsic properties of the fault zone.

A. G. Lindh, D. A. Lockner, and W. H. K. Lee reexamined the seismic data recorded prior to the last two earthquakes of magnitude 5 that occurred along the San Andreas fault in central California. Based on these data, significant velocity changes were reported to precede the two earthquakes. In both cases the anomalies were based on an increase of 0.2 seconds in traveltime residuals from small regional earthquakes at one or more nearby seismic stations. A detailed reexamination of the data showed that the changes were probably caused by differences in the depth and magnitude of the source earthquakes during the "anomalous" periods and were unrelated to any premonitory property changes. Additional data from sources chosen to minimize such problems revealed that traveltimes before the two earthquakes of magnitude 5 were stable to within a few hundredths of a second for rays that passed within a few kilometers of the hypocenters. Given the great latitude that can be exercised in the selection of data after the fact to define premonitory changes, such anomalies may not be of any significance unless it is explicitly shown that they are not due to some other change in the sources used or signals measured (Lindh, Lockner, and Lee, 1978b).

Laboratory studies of wave velocity in saturated Franciscan rocks were conducted by R. M. Stewart. Compressional and shear wave velocities were measured simultaneously in a typical Franciscan metagraywacke while fluid pressure was held 100 and 500 bars below confining pressure. Similar measurements were made in the dry rock. Results revealed

that an effective pressure rule applied to both compressional and shear wave velocity in the saturated rock; that is, wave velocity varied linearly with the difference between confining pressure and pore pressure. The change of wave velocity in the sample upon saturation was less than that in crystalline rocks of comparable total porosity and similar to that in unmetamorphosed sandstones of much greater porosity.

FORESHOCK STUDIES

W. H. Bakun, R. M. Stewart, and C. G. Bufe examined the high-frequency body-wave radiation from two foreshocks of the January 15, 1973, $M_L=4.1$ earthquake on the Cienega Road section of the San Andreas fault (20 km south of Hollister, Calif.). Their study resulted in the documentation of the unambiguous signature of directed rupture propagation (Bakun, Stewart, and Bufe, 1977, 1978). According to W. H. Bakun and T. V. McEvilly (University of California at Berkeley), seismic waves radiated by normal Parkfield earthquakes and foreshocks and aftershocks of the 1966 Parkfield and 1975 Oroville, Calif., earthquakes suggest that foreshock radiation is neither a universally higher nor lower frequency than comparable aftershocks or normal earthquakes (Bakun and McEvilly, 1978). The Parkfield and Oroville studies were consistent with the Cienega Road earthquake results. If foreshocks can be discriminated on the basis of the frequency content of body-wave radiation, then a network of broad-band seismographs surrounding the epicentral region will be necessary to sort out the three-dimensional pattern of high- and low-frequency body-wave radiation.

The ratio of compressional and shear wave amplitudes from the foreshocks and aftershocks of three recent California earthquakes which displayed a characteristic change at the time of the main events was evident. However, since this ratio is extremely sensitive to small changes in the orientation of the fault plane, a small systematic change in stress or fault configuration in the source region may be inferred. The results obtained by A. G. Lindh, G. S. Fuis, and C. E. Mantis (1978) suggest an approach to the recognition of foreshocks based on simple measurements of the amplitudes of seismic waves.

SEISMIC GAPS

Nicaragua

D. H. Harlow's work focused on two recent moderate-sized earthquakes originating on the subduction zone that dips northeastward beneath the Pacific coast of Nicaragua. The earthquakes occurred on May 31 ($M_b=5.6$), and July 20 ($M_b=5.8$), 1978. These earthquakes are the largest recorded in the 3½-year operation of the Nicaraguan seismograph network. Subduction zone earthquakes of similar magnitude had not occurred in this region during the previous 8 years. In addition, the earthquakes are located on the opposite edges of a seismically quiet area of the subduction zone. The quiet area has a width of 50 km along the strike of the subduction zone and extends from a depth of 10 to 15 km at the Middle American Trench to a depth of 70 km near the Nicaraguan coastline.

The relationship of the two recent earthquakes to the area of relative seismic inactivity is of interest because similar distributions of seismicity are observed prior to mainshocks. These observations indicate that, in addition to the relative seismic quiescence of a rupture zone before an earthquake, prior seismicity often occurs at the edges of the rupture zone of the main event. The level of this prior activity increases with the approach of the mainshock. The significance of this seismically quiet area is further enhanced because it is part of a larger seismic gap off the coast of El Salvador and western Nicaragua that is considered a good candidate for a magnitude 7 or larger earthquake. The recurrence interval for large earthquakes in Central America is roughly 50 years. A series of large earthquakes ruptured the larger gap, including the smaller gap shown by the Nicaraguan seismic data, between 1915 and 1926.

Despite the seismicity patterns shown by the present results and the likelihood of an earthquake suggested by historical data, it is not possible to predict when an earthquake will occur in western Nicaragua.

Peru

Using relocated hypocenters of teleseismically recorded earthquakes, J. W. Dewey and W. J. Spence considered the seismicity of the central Peruvian coastal zone for 1964 to 1974. Application of the seismic gap concept in the region is complicated by the existence of two distinct zones of shallow (hypocenter <70 km) earthquake activity inland of and parallel to the axis of the Peru trench. The interface thrust (IT) zone includes the major thrust-fault earthquakes of 1966 and 1974. The coastal plate interior (CPI) zone includes the major normal fault earthquake of 1970 and is centered about 50 km inland and 30 km deeper than the interface thrust zone. Within any currently aseismic seg-

ment of the central Peruvian subduction zone, there may therefore be a seismic gap corresponding to each of the two prominent zones of shallow earthquake activity. It is not clear that the occurrence of a major earthquake in one of the two gaps lessens the danger of a major earthquake in the other gap. On the positive side, recognition of the existence of the two zones may facilitate detection of unusual seismic activity precursory to a great earthquake in one of the two zones.

Other conclusions on the seismicity of coastal Peru affect the application of the seismic gap concept to this region. The aftershock distribution of the 1966 earthquake suggests an uncertainty of ±50 km in the estimation of fault length from the distribution of teleseismically recorded aftershocks. The fault ruptures of the major interface-thrust earthquakes of 1966 and 1974 apparently did not extend to the Peru trench but left unruptured, long regions of 50- to 75-km width immediately inland from the trench axis.

GRAVITY SURVEYS

The USGS, National Geodetic Survey, and the Defense Mapping Agency conducted high-precision gravity surveys in southern California from January through March 1978. Gravity was measured at bench marks spaced approximately every 2 km along lines leveled during the same period as part of the southern California leveling program. R. C. Jachens and W. E. Strange (National Geodetic Survey) reported that the surveys resulted in an extensive high-precision gravity datum against which past and future gravity observations may be compared. The concurrent gravity and leveling data should provide a good foundation for future studies of crustal deformation in this tectonically active region.

In Alaska, repeated tide-gauge and first-order leveling measurements showed that two areas are being uplifted at rates of nearly half a meter per decade. Reoccupation of gravity base stations in both these areas, however, suggests that gravity changes accompanying the uplifts are significantly smaller than would be caused by such movement along a vertical free-air gradient. According to D. F. Barnes, the data indicate a process in which significant rock masses are added beneath the gravity stations and are perhaps most easily explained as uplift caused by elastic compression of the underlying rocks. Preliminary results of this type were reported last year for an area south of Anchorage where the uplift can logically be associated with deformation following the 1964 earthquake. More recent measurements have strengthened these data and their tectonic interpretation. For example, recent gravity data from Glacier Bay, where the uplift was once associated with retreat of glacier ice, suggest a similar tectonic explanation.

CRUSTAL DEFORMATION

The current pattern of straining across the locked and creep-active segments of the San Andreas fault zone in central and southern California were delineated from geodetic measurements. W. R. Thatcher (1978a) reported that deformation is broadly distributed across the southern locked zone with only a broad maximum in shear strain centered over the San Andreas and significant strain extending 50 km or more from this fault. In contrast, relative motion on the 170-km long creeping segment is strongly concentrated near the fault, with only very minor deformation of the crustal blocks adjacent to the San Andreas.

J. C. Savage, W. H. Prescott, Michael Lisowski, and N. E. King measured strain accumulation at seven sites in southern California in the interval 1972 to 1978. Their findings revealed a remarkably consistent uniaxial north-south contraction of about 0.3 ppm/yr. An expected east-west extension was absent. The strain field was inferred from repeated precise distance measurements. No systematic error (such as an isotropic dilatation) was identified in the measuring system, although a negative dilatational strain in almost all strain networks was observed. It is likely that the negative dilatation is a real effect and that strain in southern California is indeed a uniaxial north-south contraction.

In cooperation with L. Slater (University of Washington), Louis Pelselnick and R. O. Burford conducted a preliminary analysis of interferometric distance measurements near the Calaveras fault trace in Hollister, Calif. Instrument readings giving the change in distance from the transmitter at Park Hill to nine reflectors located in a radial pattern from the transmitter showed relatively large changes for seven of the reflectors in the spring of 1977. Analysis of the data indicated that a displacemen of about 4.9 mm in a south-southeast direction occured on the east side of the main trace of the Calaveras fault. The result was obtained from a least-squares solution for the displacement of the transmitter site, assuming fixed reflector positions. A second least-squares solution was obtained using seven simultaneous equations, omitting the data for those two reflectors that did not indicate cor-

responding large distance changes. The solutions and residuals obtained in both cases were about the same, $x \simeq 2$ mm east and $y \simeq 4.5$ mm south. The root-means-square residual is about 1 mm, with only two reflectors showing residuals as large as 2 mm. The assumption in the model is satisfactory inasmuch as variations of 2 mm in the data were not considered significant. The calculated displacement event is consistent with the occurrence of right-lateral slip on the Calaveras fault.

Strength of the San Andreas

M. D. Zoback used a hydraulic fracturing technique to measure stress in a profile of wells within the western Mojave Desert near Palmdale, Calif. The data show a marked increase in horizontal shear stress with distance from the San Andreas fault. The magnitudes of the shear stresses, the manner of the change of shear stress with distance from the fault, and the lack of anomalous heat flow near the fault can be explained by models in which shear stress on the fault increases linearly with depth to values of about 200 bars at depths of 15 to 20 km. If such models are correct, a nearly total release of tectonic stress may occur during earthquakes.

New heat flow results from southern California

A. H. Lachenbruch, J. H. Sass, and S. P. Galanis, Jr. (1978), made a preliminary analysis of heat-flow data from 40 new sites in granitic rock in the region extending from the San Andreas and Garlock faults eastward to Arizona. Little or no correlation was found between heat flow and radioactive heat production. Within the Mojave tectonic block, heat flow is relatively uniform with a mean value of about 1.6 HFU ($\sim$70 w/m^2). Such values persist up to and across the San Andreas fault—the southwest boundary of the block. Toward the east, the heat flow rises sharply along a north-northwest-trending boundary that coincides with the easterly limit of active seismicity and a change from predominantly strike-slip to normal faulting. The average heat flow east of this boundary is about 2.1 HFU (90 w/m^2), similar to the average for the Great Basin. Additional measurements are needed to help distinguish among thermo-tectonic, magmatic, and regional hydrologic effects.

Numerical modeling

W. R. Thatcher (USGS) and J. B. Rundle (Scandia) applied the plate-tectonic model of a strong elastic lithosphere overlying a relatively weak visco-elastic asthenosphere to his study of earthquake-related deformation occurring at subduction zones. Coseismic thrust faulting in the plate was found to induce time-dependent stress relaxation in the asthenosphere. This phenomenon is reflected in aseismic surface deformation (principally downwarping) that persists during the time interval between major earthquakes. The predicted deformation matches well the steady coastal subsidence observed landwards of major seismically active subduction zones and demonstrates the importance of including the effect of the asthenosphere in realistically modeling crustal movements at convergent plate boundaries.

The flexure profile of the Kurile trench-Hokkaido rise system was fitted numerically to observational accuracy by an elastic, time-dependent plastic plate model. Hsi-Ping Liu derived the elastic part of the constitutive relation from seismology (relaxed moduli = 50 percent of the seismic values) and the strain rate dependent plastic part from dunite deformation data extrapolated to the appropriate loading rates. The numerical fit of the flexure profile depends on a number of parameters, such as the rock flow law parameters, the temperature distribution inside the lithosphere, and the state of prestress of the plate before it enters into the subduction zone. Two examples of fitting, one with Kirby-Raleigh flow law parameters and one with Carter-Ave'Lallement flow law parameters, are given. Because the solution of the problem is nonunique, conclusions regarding the values of the individual parameters cannot be drawn from the flexure profile alone.

FAULT STABILITY

W. D. Stuart's theoretical analysis of two- and three-dimensional strain-softening models for earthquake instability revealed that in all cases accelerating fault slippage near the inferred earthquake focus occurs prior to the instability. In the Earth, this increasing fault-slip rate should cause increasing deformation rates near the epicentral area and possibly ground breakage at the fault trace. Since the models admit both stable (fault-creep episode) and unstable (earthquake) modes, inversion of geodetic data may allow the likelihood of an earthquake to be estimated.

J. H. Dieterich conducted laboratory studies to determine the mechanism of slip instability. Signals from an array of strain gauges and displacement transducers adjacent to a simulated fault in a large granite block were recorded over a frequency range

of 0 to 50 Khz. During unstable slip, fault displacements often showed sharp onset and simple linear increase with time. In such events, the magnitude of the slip velocity correlates with the dynamic stress drop, giving ~1 cm/s slip velocity per 1 bar stress drop. This result agrees with simple theoretical models for the earthquake source and is the first direct confirmation of that prediction. Some experimental events showed a more complex character consisting of two or three distinct phases with differing slip velocities. For all events, shear strain adjacent to the fault plotted against fault slip showed a displacement weakening of friction over a characteristic displacement of 3–6 μM at the onset of instability. This supports previously reported experimental observations indicating that the characteristic displacement is proportional to surface roughness and that the weakening and potential for instability arise because of time dependency of friction.

In the theoretical and field studies conducted by D. D. Pollard and Paul Segall, a fault is seen as a set of echelon fractures, rather than as a single, continuous break. Observations over a wide range of length scales demonstrate the ubiquity of such echelon fault patterns. These patterns may develop when a planar fault breaks down at its periphery into discrete segments that propagate into a new orientation. Field examples from granitic rocks of the Sierra Nevada illustrate echelon patterns and the nature of rock deformation between segments where tension gashes and secondary faults are observed. Theoretical model studies demonstrate a difference in stability between a single fracture and a set of discrete, en echelon breaks.

EARTHQUAKE PRECURSORS

Magnetic studies

M. J. Johnston and colleagues studied the local variations in the magnetic field at several sites along the San Andreas fault. Their findings revealed no apparent magnetic field change for earthquakes with $M_L/<4$, although magnetic changes were observed for a $M_L/>5$ earthquake. No magnetic changes occurred with creep events.

According to J. A. Steppe, linear regression of magnetic-field values from one site against those from several other sites can be used to reduce noise in tectonomagnetic observations at periods greater than a day. For total-field data from central California, this method provided a reduction in the noise level, compared with two-site differences, of roughly a factor of two on the average. The effectiveness of the method, however, varies considerably from site to site.

Tilt

C. E. Mortensen's analysis of an extensive set of tiltmeter data provides a general insight into their characteristics from a broad range of periods for a wide variety of site conditions. These data were processed to account for spurious signal sources ranging from instrument adjustments and malfunctions to telemetry and automatic processing errors. Preliminary findings indicate that secular tilt rate may be inversely related to distance from the fault. Long-term secular tilt rates range from ½ μrad/yr to 50 (or more) μrad/yr. Typical values range between 5 to 20 μrad/yr.

Radon and water level

The radon content of soil gas was monitored at more than 100 stations along active faults in California, Hawaii, and Alaska. Chi-Yu King reported that recorded radon emanation in central California showed significant temporal variations (decrease followed by increase, each by about a factor of 2) at the time of five local earthquakes of magnitude 4.0 and larger, starting mostly a few months before the events. The spatial extent of the anomaly areas is large—tens of kilometers along the strikes of the faults. The anomalies occurred in three different seasons and are apparently not due to seasonal effects. Radon emanation recorded in Hawaii showed increases at the time of increasing seismic and volcanic activities. Anomalous radon emanation was also recorded in Santa Barbara for a 10-month period prior to the magnitude 5.1 earthquake of August 13, 1978. The pattern of this anomaly (increase followed by decrease) differed from the central California anomalies and can be attributed to a difference in earthquake focal mechanisms (thrust instead of strike slip).

Water-level data were affected by nontectonic activities and did not show significant premonitory changes. On the other hand, changes in water quality were observed at the time of several larger earthquakes.

EARTHQUAKE SWARMS

In the Imperial Valley, Calif., several dozen swarms followed a 10-year period of relative quiescence after the Heber earthquake of May 1940 (M_L=6.7). C. E. Johnson and G. S. Fuis analyzed these swarms using the master event approach and

a location program similar to HYPO71 (Lee and Lahr, 1975). The relocated swarms were generally confined to a narrow zone extending from south of the Mexican border to a point beneath the Salton Sea. Similarly, recent data obtained since the installation of the Imperial Valley network of seismic stations in 1973 indicate that swarms roughly outline the Imperial and Brawley faults, when viewed together. When studied in detail, however, most swarms appear to be associated primarily with transverse structures not evident at the surface. Migrations of seismicity both along the Brawley fault and along transverse structures are evident in the January 1975 swarm (Johnson and Hadley, 1976) and the November-December 1976 swarms (Fuis and Schnapp, 1977). Detailed studies of the October and November 1977 swarms northeast of El Centro reveal that both are on structures transverse to the Imperial fault and that swarms in these two locations have generally been paired in time since 1973 (C. E. Johnson, unpublished manuscript).

Between November 1976 and November 1977, a swarm of small earthquakes ($M_L \leq 3$) occurred on or near the San Andreas fault near Palmdale, Calif. According to K. C. McNally and others from Caltech, the swarm was the first observed along this section of the San Andreas since cataloging of instrumental data began in 1932. The activity followed partial subsidence of the 35-cm vertical crustal uplift along the "locked" segment of the San Andreas fault. The swarm events displayed characteristics previously observed for some foreshock sequences such as tight clustering of hypocenters and time-dependent rotations of stress axes inferred from focal mechanisms. However, because of the present lack of understanding of the processes that precede earthquake faulting, the implications of the swarm for future large earthquakes on the San Andreas fault are unknown (McNally and others, 1978).

THE THESSALONIKI EARTHQUAKE

On June 20, 1978, a magnitude 6.5 earthquake occurred in an agricultural valley between Lakes Koronia and Volvi in northern Greece, 30 km east of the major port of Thessaloniki (Bufe and others, 1978). Data from a Thessaloniki accelerograph (maximum acceleration of 0.15 g) suggest that the June 20 earthquake was a complex rupture consisting of two or more events within a few seconds. A 10-km-long zone of discontinuous, right-stepping ruptures extends across the valley on a west-northwest trend through the villages of Stivos and Skolari. A second zone of ground rupture was mapped along the southern margin of the valley. The mapped ruptures lie along the faulted boundary between the Rhodope massif to the north and the intensely deformed Vardar "root" zone to the south.

Focal plane solutions for the initial main shock, the May 23, 1978, magnitude 5.8 foreshock (Papazachos and others, 1978), and the aftershocks located under Lake Koronia (using data from a 10-station USGS network of portable seismographs) are consistent with left-lateral strike slip along a fault trending west-northwest and dipping steeply to the north. Inferred principal stress orientations are east-west compression and north-south extension, similar to those for the 1963 Skopje, Yugoslavia, earthquake.

Although many reinforced masonry structures suffered total collapse in the epicentral region, casualties were light because the people left their dwellings during the sequence of foreshocks which began on May 8. In Thessaloniki, significant damage was limited to a few structures, with 38 killed in the collapse of an eight-story reinforced concrete apartment building.

EARTHQUAKE HAZARDS STUDIES

Active faults, seismotectonic framework, and earthquake potential

Geological and geophysical investigations in areas of known or suspected seismicity have continued to increase understanding of faulting, fault activity, and earthquake potential in many areas of the United States.

Northern California

The Chico monocline, studied by E. J. Helley, D. S. Harwood, and M. P. Doukas, is a northwest-trending flexure between Chico and Red Bluff, Calif., that approximately separates Quaternary clastic deposits of the northeastern Sacramento Valley from Pliocene volcanic rocks of the Tuscan Formation. Along most of the monocline, a dense network of near-vertical, northwest-trending, anastomosing faults defines a zone 1 to 3 km wide. Vertical separation on fault segments along this zone ranges from 0 to 35 m; movement is dominantly west side down. The maximum vertical separation observed is on a fault segment in the vicinity of Deer Creek that offsets a distinctive micaceous tuff in the Tuscan Formation. This tuff is disconformably overlain by a 1.08 ± 0.16-million-year-old basalt that is offset about 3 m on the north rim of Deer Creek Canyon. Just west of the northern part of the monocline lineaments, sag

ponds, scarps, and anomalous contacts of sediments of the post-Red Bluff Formation suggest faulting in alluvium that is younger than 0.5 million years old.

Ground cracks occurred in early August 1978 during a swarm of magnitude 4 earthquakes near the southern end of the Cascade Range in northern California. The cracks, examined by W. P. Irwin, are 26 km east of the summit of Mount Shasta and are in the general region of the earthquake epicenters. They form an irregular zone generally 4 or 5 m wide in rocks mapped as Quaternary basalt and can be traced discontinuously for more than a kilometer in a northerly direction. Scarps 0.1 to 0.5 m high were formed by vertical displacement of the ground along some of the cracks. They generally face inward and define a shallow, irregular, grabenlike trough. The ground cracks are interpreted by some investigators to be the surficial expression of movement along a regional tectonic fault. According to Irwin, however, the amount of ground breakage and depth of collapse seem excessive for magnitude 4 earthquakes. He considers the possibility that rather than a tectonic origin, the cracks and subsidence resulted from the collapse of the roof of a concealed lava tube, the collapse being triggered by the earthquakes.

Two strike-slip fault zones east of Cape Mendocino in northern California are interpreted by D. G. Herd as the apparent northward continuation of a northwest-trending line of large en echelon, recently active right-slip fault zones that bifurcates from and parallels the San Andreas fault zone north from Hollister. This line of faults, the Hayward-Lake Mountain fault system, extends past Arcata onto the Continental Shelf southwest of Crescent City. The Hayward-Lake Mountain fault system defines the Humboldt plate, a small northwest-elongate sliver of the North American Continent bounded on the west by the San Andreas fault zone and to the north by the Gorda plate. This newly recognized plate is converging northwestward against the Gorda plate, which is being thrust beneath it. Herd further stated that steps between en echelon member fault zones in the Hayward-Lake Mountain fault system suggest that the line of faults is of such recent age that there has been insufficient time to integrate the fault zones into a surficially connected break. The fault system may have resulted from a recent and still continuing structural realinement of the North American plate boundary near the Mendocino triple junction.

Aeromagnetic anomalies east of the San Andreas fault in the southern San Francisco Bay region, California, are associated either with steeply dipping serpentinite bodies along strike-slip faults or with more gently dipping and folded sheets of serpentinite along thrust faults. Correlation of these anomalies by W. F. Hanna and E. E. Brabb with epicenters for the 1949–1974 period indicates that some of the linear anomalies are interrupted in areas of intense earthquake activity, as if the magnetic material is in the initial phase of intrusion along the fault zone. An alternative explanation is that the serpentinite acts as a lubricant in relieving stress along the fault zone and where serpentinite is absent the rocks are failing and are associated with many small earthquakes.

According to Andrew Griscom, interpretation of aeromagnetic maps of the northern San Francisco Bay region shows that nearly all magnetic anomalies here are caused by serpentinite masses. Such serpentinite masses tend to occur along certain of the major active or recently active faults such as the Rodgers Creek, Green Valley, Hayward, Concord, and Collayomi fault zones. Belts and areas of significant seismicity, in general, correlate with aeromagnetic highs believed to be caused by these serpentinite masses. The serpentinite may lubricate these faults, permitting active seismicity and perhaps creep, thus avoiding stress build-up and resultant major earthquakes. Conversely, the San Andreas fault in this area, which generated a major earthquake in 1906, lacks significant magnetic anomalies (serpentinite) and also lacks significant seismicity today.

Tectonic uplift rates along the west coast of the United States are generally so low (<0.5 mm/yr) that wave erosion is able to maintain a wave-cut platform at or near present sea level. However, K. R. Lajoie found that near Cape Mendocino in northern California and along the Santa Barbara coast in southern California tectonic uplift rates are sufficiently high to elevate Holocene marine terraces (less than 5,000 years old) above modern sea level where they are protected from wave erosion and can be mapped and dated today. These areas of high rates of tectonic uplift coincide with regions of compressional tectonics, as opposed to lateral tectonics, which are most common along coastal California. In southern California the region of rapid tectonic uplift coincides with the western terminus of the southern California uplift recorded in geodetic data.

Southern California

According to R. F. Yerkes and W. H. K. Lee, the magnitude 5.1 Santa Barbara earthquake of August

13, 1978, occurred 4 km south of Santa Barbara, Calif., at a depth of 12.5 km in the northeast Santa Barbara Channel, part of the western Transverse Ranges geomorphic-structural province. A fairly well constrained fault-plane solution of the main shock and distribution of the aftershocks indicate that reverse-left-oblique slip occurred on a west-northwest-trending, north-dipping reverse fault(s) and that subsurface rupture propagated northwest from the main shock toward the shoreline at Goleta, 15 km west of Santa Barbara. The fault-plane solution and aftershock pattern closely fit the model of regional deformation (near-horizontal compressive stress directed about N 25° E. toward the big bend of the San Andreas fault).

Studies by A. M. Sarna-Wojcicki and several coworkers indicate that an east-trending, south-dipping, high-angle reverse fault is exposed in Javon Canyon northwest of Pitas Point in the western Transverse Ranges of southern California. The fault offsets terrace alluvium graded to an uplifted marine terrace platform that has been dated by carbon-14 at 2,500 years B.P. Throw on the fault is 3.3 m. Three superposed colluvial debris aprons derived from the collapse of the hanging wall interfinger with stream terrace alluvium and record three displacements over the last 2,500 years. One km to the east, the fault offsets a 45,000-year-old marine terrace platform (dated by amino-acid racemization and uranium-series methods) by 49 m, in the same sense. The two offsets give displacement rates of 1.1 and 1.6 mm/yr.

Sarna-Wojcicki and coworkers also found that the fault cuts across the west-plunging axis of the Ventura Avenue anticline, an elongate, east-trending, doubly plunging structure. The anticline is bounded on the north by the Red Mountain fault, an east-trending, north-dipping, seismically active reverse fault. Measured rates of offset on the Red Mountain and associated faults, derived from offsets of dated marine terrace platforms near the plunging northwest part of the anticline, range from 0.5 to 1.6 mm/yr, whereas long-term vertical separation rates across this fault, estimated from subsurface data north of the central part of the anticline, are as high as 13 mm/yr over the last 0.5 million years. Regional tectonic uplift rates, from uplift of dated marine terrace platforms, increase systematically from the northwest (3 mm/yr) to the structural high of the anticline (10 mm/yr), decreasing again to the southeast, on the south limb. Deformation, as expressed by faulting and regional uplift, has continued at about the same rate over the last 45,000 years.

Geologic structures exposed in two trenches across the Garlock fault in the playa of Koehn Lake in southern California show a history of late Quaternary displacements and probable earthquakes. The trenches, studied by D. B. Burke and M. M. Clark, are within 700 m of an offshore gravel bar formed during a pluvial high stand of the lake in an area where the zone of Holocene displacement is less than 35 m wide. Faulting has offset the bar 80 m left laterally and the playa surface 0.5 to 1 m vertically. Both trenches expose alluvial and shallow lake sediments above a massive deep-lake clay. The clay, presumably deposited during the last high lake stand, contains ostracods dated by carbon-14 at 14,700±130 years. Most displacement of the sediments concentrates on three principal strands in the fault zone. The trench nearest the bar exposes an anticline in the fault zone that has a central diapir of the massive clay. Unconformities, disturbed bedding, and truncated secondary faults in and near the anticline indicate a minimum of 9 to 17 tectonic events after the high stand of the lake. Although the age of individual events is unknown, the interval between events is about 1,700 years for 9 events and 900 years for 17 events. Assuming the offshore bar and massive clay to be contemporary and about 15,000 years old, local maximum mean left slip would be about 9 m each for 9 events and 5 m each for 17 events.

Study of active faults and folds and Quaternary deposits in the Antelope Valley-western Mojave Desert region of southern California by Burke indicates that generally north-south crustal shortening over the region is accommodated in four structural domains. Episodically active folds and thrust faults on the north flank of the San Gabriel Mountains border a closed irregular syncline containing perhaps 2 km of upper Pliocene and Quaternary fill beneath Antelope Valley. Unsystematic differential warping or folding, over distances of several kilometers in the basin, is 1 mm/yr. Folding decreases to the northeast, and regional horizontal strain is distributed among numerous small strike-slip faults: left-lateral faults trend similar to the Garlock fault, right-lateral faults are transitional to larger active faults of the Helendale-Calico (central Mojave) trend. Cenozoic volcanic rocks on crustal slices between faults of the central Mojave Desert system give anomalous geomagnetic directions that suggest counterclockwise rotation during late Cenozoic offsets of about 30°, substantial north-south crustal shortening, and partial accommodation by continued flexure of the central Transverse Ranges.

S. H. Wood and M. E. Wilson analyzed lake-level measurements taken over the last 25 years on the Salton Sea in southern California and derived rates of tectonic tilt by determining the difference of lake levels recorded at two points. The history of vertical deformation was marked by down-to-southeast tilting having a maximum differential elevation change of 110 mm along a 38-km separation of water-level staff gages. A reversal in tilt direction occurred in late 1972. There is good agreement between vertical deformation recorded by these water-level records and the geodetic leveling data used to define the southern California uplift in this area.

Examination by R. V. Sharp of vertical and oblique aerial views of portions of the 1940 Imperial Valley earthquake surface rupture permits a fairly accurate reconstruction of the detailed geometry and distribution of slip on the Imperial fault of southern California. The compilation reveals that the rupture trace was not a linear single break as depicted on many maps, but instead consisted of a number of en echelon separate breaks. The maximum displacement occurred about 1 km northwest of the All-American Canal where the initial slip, plus an unknown amount of afterslip, totaled about 6.3 m, one of the larger historic strike-slip displacements known. The vertical airphotos show crop rows offset along a 14-km length of the fault trace, and they provide an unusually good record of short-distance variability of fault slip.

Trenches examined by Sharp that cut across the Imperial fault at the international boundary exposed the two 1940 fault ruptures that are known to have extended into Mexico. In addition to fixing the location of the breaks in a sector where little surficial evidence of the 1940 rupture has survived, the trenches showed that no fault strands other than those that moved in 1940 exist, at least within 2.5 m of the ground surface. A cross-cutting channel was found near the main fault strand, and its truncation of a particular stratum was picked as a linear feature to be followed into and out of the fault break. A system of trenches and pits was cut to expose the two intersections of the linear feature with the fault surface (the "piercing points"). The offset on the fault strand was found to be 3.7 m, in close agreement with observations of slip at the international boundary in 1940. Although this evidence suggests that the channel deposits encountered in the trench have experienced only a single episode of fault movement, that of 1940, other stratigraphic features in the prechannel section suggest that at least one other and possibly several more episodes of movement have occurred along the Imperial fault since 770 years B.P.

Western United States excluding California

Geologic mapping by H. D. Gower in the Puget Sound region in Washington shows that the surface expression of the Seattle-Bremerton structure, a suspected major Quaternary fault defined by a large east-west gravity anomaly, is located north of where it had previously been inferred. Overturned Oligocene volcaniclastic strata north of Issaquah and steeply dipping Oligocene and Quaternary(?) strata in Eastgate mark the location of this structure east of Seattle.

Geomorphic evidence, noted by R. C. Bucknam during mapping along a 20-km-long section of surface faulting on the Wasatch Front near Mona, Utah, indicates that the segment has undergone repeated movement in late Quaternary time. A charcoal sample from the scarp face dated by the carbon-14 method at 4,580±250 years gives a maximum age for the youngest event. Comparison of photographs of the scarp taken in 1903 with its present appearance suggests that the scarp formed more than several hundred years ago.

Bucknam also compiled a map of fault scarps formed on unconsolidated sediments in western Utah and made studies of the scarps' morphology to determine their ages. On a regional basis, there is good agreement between the observed numbers of dated fault scarps of approximate Holocene age and the expected number of earthquakes in the magnitude range 7.0 to 7.6 obtained from analysis of historic seismicity data. Though the numbers agree well, some Holocene fault scarps are found in areas that appear to have been virtually aseismic in historic time, indicating a lack of uniform spatial association between Holocene faulting and historic seismicity. Nevertheless, there is broad regional agreement in number and distribution of Holocene faults displaying historical seismicity.

Geologic studies in Beaver Valley, Utah, by R. E. Anderson revealed recurrent Quaternary faulting and stratal tilting events. Sediments that accumulated in a closed-basin environment include at least three layers of tephra; these layers are exposed at numerous localities as a result of stratal repetition produced by erosional truncation of the faulted and tilted layers. A preliminary typing of one of the tephra layers by G. A. Izett indicates correlation with the "Pearlett B" ash that has been dated at about 1.9 m.y. These tilted strata are overlain by mafic lava dated by the potassium-argon method at

0.59±0.16 m.y. by H. H. Mehnert. They are also overlain by a bed of pumice dated by the fission-track method at about 0.64±0.22 m.y. by C. W. Naeser. Overlying the lava and pumice is a widespread pediment surface that has a mature calcic soil developed on it. The surface and its soils are cut by at least 50 northerly trending faults, which have indicated vertical displacements of as much as 25 m and possibly as much as 70 m, and by northeasterly faults. Terrace surfaces that are progressively younger than the pediment surface are offset by fewer faults with smaller displacements and have soils of lesser development formed on them. The youngest surfaces, which are probably Holocene, are not faulted and have no apparent calcic soil formed on them.

The Espanola Basin in north-central New Mexico has been generally portrayed as a graben between the Nacimiento uplift to the west and the Sangre de Cristo uplift to the east. However, recent mapping by E. H. Baltz, Jr., indicates that the basin has a general synclinal shape that has been modified only moderately by Pliocene and Pleistocene normal faults. Stratigraphic data indicate that the bounding uplifts rose and were tilted toward the basin in Eocene, Oligocene, and Miocene time. Major faults at the west margin of the Nacimiento uplift and the eastern margin of the Sangre de Cristo uplift are reverse faults that dip toward the basin. These data seem to indicate that, prior to 7 or 8 million years ago, the deformation in this segment of the Rio Grande rift was mainly compressional, as was the preceding Laramide deformation. Late Pliocene and Pleistocene normal faulting seem to have caused only a small amount of east-west extension, which may be less than the amount of crustal shortening caused by the preceding compression. Therefore, it seems likely that this segment of the rift exhibits a partly "locked," relict condition; if this is so, it may explain the low seismicity of the Espanola Basin as contrasted to the higher seismicity and numerous large, young normal faults of the Albuquerque-Belen Basin to the south where a larger amount of east-west extension occurred.

Eastern United States

Investigations by D. P. Russ of sand-blow dikes and faults exposed in an exploratory trench across Reelfoot scarp in northwestern Tennessee suggest that the dikes and faults formed simultaneously during strong earthquakes. Parallelism of the convex topographic profile of Reelfoot scarp with the convex profile of gently folded sediments in trench walls shows that the greater part of the scarp is the product of monoclinal flexing that took place during the uplift of the adjacent Tiptonville dome. The relationships among the faults, folds, and sand-blow dikes support the contention that Tiptonville dome and Reelfoot scarp formed during earthquakes and were not produced aseismically. A 0.5-m-wide zone of eastward-dipping normal faults exposed in the trench near the base of Reelfoot scarp overlies, in a parallel fashion, subsurface faults detected by Vibroseis reflection profiling, thus suggesting that the surficial faults are tectonic and deep seated. These faults represent the first instance where Mississippi embayment earthquakes can be associated with surficial tectonic faults. Geologic evidence indicates that not more than 0.5 m of the 3-m offset mapped on these faults could have occurred during the 1811–12 New Madrid earthquakes.

In the upper Mississippi embayment region of Missouri, Illinois, Indiana, Arkansas, and Tennessee, major geological or tectonic structures inferred from the analyses of gravity and aeromagnetic data by T. G. Hildenbrand and others (1977) include (1) several mafic/ultramafic intrusive bodies, (2) a northeast-trending, parallel-sided depression of basement rocks that is believed to be a Proterozoic Z to early Paleozoic rift, and (3) transverse shear zones striking normal to the axis of the proposed rift. These implied structures have a geometry that suggests that they are responsible for the generation or control of seismicity. An area of present-day seismicity and the estimated region of principal historical activity trend along the axis of the rift zone. Moreover, a map of calculated depths to magnetic basement indicates several kilometers of vertical movement has occurred along the rift axis. Normal faulting is commonplace within extensional features such as rifts and may account for this large offset in the basement. The axial seismicity pattern and vertical offset suggest that the rift is presently active or that stress is concentrated along a zone weakened by normal faulting during the active periods of rifting.

C. M. Wentworth, Jr., examined the literature and current fieldwork of others that indicated the presence of abundant, poorly understood reverse faults that offset Upper Cretaceous to Pleistocene deposits along the eastern seaboard of the United States. Most of these faults trend northeastward and thus represent northwest-southeast shortening as well as varied local upthrow and downthrow. Where well studied, the Stafford fault zone in Virginia (Mixon and Newell, 1977) and the Belair fault zone in

Georgia (Prowell and O'Connell, 1978) show evidence of progressive offset through Late Cretaceous and Cenozoic time. Map patterns suggest that early Mesozoic extensional faults, where properly oriented, formed the locus for much of this movement. Thus the geologic record suggests that the Atlantic seaboard has undergone continued or sporadic compression approximately parallel to the northwesterly Atlantic spreading direction. Some seismologic evidence, particularly that indicating modern reverse movement of the early Mesozoic Ramapo fault zone in northern New Jersey (Aggarwal and Sykes, 1978), suggests modern continuation of this process.

N. M. Ratcliffe successfully recovered core from two vertical drill holes alined normal to the N. 45° E. trend of the Ramapo fault in southern New York. The drill holes penetrate Triassic and Jurassic(?) basalt flows and bottom in cataclastic gneiss of the footwall block. One-hundred-percent recovery of the rock adjacent to the fault was obtained, and the fault contact was preserved intact. Observations of the fault in the cores and calculations from depth of penetration indicate a 60° SE. dip for the Ramapo fault at this locality and show that the slip is mostly oblique and largely down to southeast. The core data also show a close correspondence to the proposed southeast surfaces and strengthen the conclusion of Aggarwal and Sykes (1978) that reactivation of Triassic and Jurassic faults may be responsible for the current seismicity in the New York-New Jersey area along the Ramapo trend.

Magnetic contour maps, compiled from a high-sensitivity aeromagnetic survey by J. C. Behrendt, suggest a lineation that can be correlated with the projection of the Blake Spur fracture zone as mapped in the western Atlantic from magnetic and seismic data. The lineation has a trend of about S. 53° E., where it crosses the coast about 20 km southwest of Charleston, S.C. The lineation truncates the East Coast Magnetic Anomaly (ECMA) at about 31° 10′ N., 77° 40′ W. If the lineation represents a track and projection into the continent of the Blake Spur fracture zone, its relevance to the Charleston earthquake problem is not easily understood. If the crust landward of the ECMA is continental, then any structure associated with the lineation predates the initial opening of the Atlantic and the trace of the transform fault marked by the oceanic Blake Spur fracture zone. Certainly it would not be unusual for preexisting structures or zones of weakness to localize a developing fracture zone at the time of initial rifting. Possibly the present-day seismicity in the Charleston area is the result of the reactivation of the same zone of weakness.

Earthquake source mechanisms

J. P. B. Fletcher reports that multiple near-field recordings of the $M=4.7$ Oroville, Calif., aftershock of August 6, 1975, permit a significant advance on several fronts. Ten three-component records were recovered within the distance range $R \leq 15$ km from the hypocenter, allowing a more rigorous interpretation of seismic phases in terms of the effects associated with the earthquake source, the propagation path, and the near-surface site geology. For the first time, source parameters such as moment (4×10^{23} dyne-cm), source radius (0.75 km), and stress drop (422 bars) were determined from averages of eight to nine independent observations, rather than the more usual one to three observations. Refinement in the technique for the accurate calculation of ground displacements, together with large data set, resulted in a marked decrease in the error associated with the stress drop so that it has a level of precision nearly the same as that for the moment. The high stress drop reported is unusual and significant, both in the debate on the physical understanding of stress drops determined from seismic waves and on the level of tectonic stress in the upper part of the Earth's lithosphere.

D. J. Andrews has proposed a stochastic model of faulting in which slip and stress changes in an earthquake are assumed to consist of a smooth coherent part and an incoherent part that is more important at shorter wavelengths. In the broad band of wavelengths between the rupture length and the grain size of the medium, it is assumed that the incoherent component has no characteristic length or time scale. Its spectrum is given by a power law. It is assumed that the coherent component of stress change (negative in the center of a slip patch and positive around the border) has, on the average, a negative correlation with the initial stress function. The difference between stress and sliding friction tends to become smoother at the length scale of the rupture but rougher at smaller length scales. A large earthquake establishes irregularities that determine the size of future smaller earthquakes. All earthquakes with rupture dimension less than the thickness of the brittle region are aftershocks. The fault stress spectrum that is consistent with earthquake stress drops being independent of size is also consistent with an omega-squared far-field displacement spectrum. The slope of the number-moment distribution of earthquakes

($\log N = a - b \log Mo$) is restricted to the range ($2/3 < b < 1$) with the lower end of the range being favored.

Ground motion

From analysis of the patterns of damages in major past earthquakes, particularly the 1906 California earthquake, R. D. Nason concludes that the Modified Mercalli intensity scale of 1931 should be revised if it is to be a precise and consistent scale for measuring earthquake shaking. The scale, as currently defined, misinterprets damage caused by ground failure, such as bent railroad tracks, as being due to some sort of very violent seismic shaking. The mechanisms causing ground failures such as liquefaction and compaction have only become understood since 1964. It is not surprising that they were misinterpreted in the early intensity scales.

A. F. Espinosa and L. F. Zambresky estimated the attentuation of particle velocity as a function of distance from the Modified Mercalli intensity ratings for ten of the most important historical earthquakes that have occurred in the conterminous United States. The levels of the estimated horizontal particle-velocity curves differ as a function of the magnitudes and regions in which these earthquakes occurred.

R. K. McGuire reports that the duration of strong shaking does not appear to be a useful parameter in statistically predicting the damage that can be caused by ground motion, at least when using conventional definitions of duration, simple structural models to assess potential building damage, and a magnitude-distance description of the earthquake. Duration is important in explaining the reason for observed damage, but with the available set of California strong motion data, we cannot predict the duration with any certainty for future events.

Strain-dependent shear moduli of San Francisco Bay mud were studied in the laboratory by K. H. Stokoe and P. F. Lodde (1978) (University of Texas) using a resonant column apparatus. The low-amplitude shear modulus (defined as a shearing strain less than 0.001 percent), G_{max}, continually increases with time at a constant confining pressure. Increases in G_{max} as large as 25 percent per log cycle of time are observed. Increases in shear modulus with time are also found at shearing strain amplitudes as large as 0.1 percent, and these are similar to those for G_{max}. The increase in high-amplitude shear moduli with time indicates that field moduli determined by the arithmetic-increase procedure, $G_{field} = G_{lab} + G_{max\ field} - G_{max\ lab}$, represent a reasonable upper bound for in-situ strain-dependent shear moduli.

The distribution of intensities mapped in metropolitan Guatemala City, Guatemala, for the destructive February 1976 earthquake can serve as the basis for seismic zonation of the area, according to A. F. Espinosa. The intensity ratings obtained in the field after the earthquake reveal an intensity amplification along the Continental Divide, which trends in a northwest-southeast direction. Response spectra for different damping coefficients are constructed for four different levels of ground shaking in Guatemala City. The information recorded on a seismoscope in the city is used to constrain the level of ground motion for a given intensity rating. The spectral response curves obtained by Espinosa, Asturias, and Quesada (1978) can be used by engineers to determine the upper and lower bounds of ground motion to be expected in Guatemala City for an earthquake of similar magnitude ($M_S = 7.5$).

Ground motion produced by the 1971 San Fernando earthquake was compared by A. M. Rogers and W. W. Hays (1978a) to that acompanying nuclear explosions at the distant Nevada Test Site, using recordings of both events at several common stations in the San Fernando Valley-Pasadena area of California. Similar trends in ground response were observed for both sources. Observed differences in the nuclear and earthquake ratios are tentatively explained by changes in wave propagation at the rock sites because of the proximity of the earthquake source relative to the nuclear source. The known dispersion in such observations, however, would also account for significant portions of the observed variations.

Another study by Rogers and Hays (1978b) comparing ground response in Long Beach, Calif., Las Vegas, Nev., and Salt Lake City, Utah, led to an improved understanding of the effects of geologic lithology and structure on ground motion. This study shows that large variations can occur in the ground-motion response of alluvium and other Quaternary sediments. These variations are caused primarily by lateral changes in the lithology and depth of the sediments. Sediments with similar lithologic descriptions (for example, in Salt Lake City and Long Beach) may have different response characteristics depending on the degree of consolidation and (or) water content. High water content produces low shear velocities and high ground response; greater consolidation produces high shear velocities and low ground response. The short-period spectral ratios of motion recorded at different sites are most

strongly affected by near-surface shear velocities. Although material damping may also play a role, this effect was distinctly observed only in Long Beach. The long-period spectral ratios are primarily controlled by the thickness of unconsolidated and semiconsolidated sediments, but may also be affected by depth to basement. Detailed accounts of these results are given by Rogers and Hays (1978a, b).

Shear-wave velocities measured at 59 sites in the San Francisco Bay region of California by J. F. Gibbs, T. E. Fumal, and E. F. Roth have been compared to site amplifications determined from ground motions generated by nuclear explosions and to intensities from the 1906 San Francisco earthquake. The resulting empirical relations will be useful for making improved quantitative estimates of variations in ground shaking on a regional scale for seismic zonation of the San Francisco Bay region. Moreover, the seismic velocity relations will permit the extrapolation of some of these data to other regions. Seismic-wave velocities in the San Francisco Bay region have been compared with several readily determined physical properties of the geologic materials. Shear-wave velocity was found to correlate with these properties more strongly than *P*-wave velocity. Correlations obtained suggest a classification scheme useful in defining seismically distinct units. Six seismically distinct units have been determined for the sedimentary deposits. Classification of these units are based on geotechnical parameters such as texture (grain size), standard penetration resistance, and depth. Seven seismically distinct units have been determined for bedrock materials based on hardness, fracture spacing, and lithology.

Recordings of ground motions from nuclear explosions at 27 sites in the Salt Lake City area of Utah show the characteristics of the ground shaking hazard in the area. W. W. Hays found that the ground response at sites in the Jordan River valley underlain by thick, water-saturated, fine-grained clay and sands is significantly greater than that for sites underlain by rock or thin, unsaturated gravels and sands. The enhanced levels of ground response (factors of 8 to 10) occur over the entire spectrum rather than being centered around a narrow band of frequencies. Site-specific physical-properties data are needed to determine the parameters that control the ground response. Some 47,350 single-family dwellings with an estimated value of $1.1 billion are exposed to the earthquake threat in corporate Salt Lake City.

Ground shaking hazard and risk

According to S. T. Algermissen, consideration of parameter variability in the probabilistic estimation significantly increases the ground motion. For example, assuming log normal distributions for attenuation of ground acceleration and for fault rupture length in the hazard calculation may increase maximum values of ground acceleration (for an extreme probability of 90 percent and an exposure time of 50 years) by two to three times.

Estimation of earthquake losses in the San Francisco Bay area by S. T. Algermissen (USGS) and K. V. Steinbrugge (Insurance Services Office) indicates that, in the event of a large earthquake on the San Andreas fault, losses will range from about 4 to 24 percent of the replacement cost of the building, depending upon the class of construction (Algermissen and Steinbrugge, 1978). Long-term annual losses are of the order of 0.1 to 1.6 percent of replacement value, depending upon class of construction.

In the course of work on seismic hazard maps of the U.S. Outer Continental Shelf (OCS), seismic source region maps have been prepared by D. M. Perkins and others for western California, Oregon, and Washington, the adjacent OCS, and the Atlantic seaboard and OCS. In California, the source zones were based almost entirely on Holocene faulting, with some additional contribution from Pleistocene faulting and geologic texture. In the Pacific Northwest, evidence of Holocene faulting is almost entirely missing. Zones were based on correlations between historical seismicity and geologic provinces; most seismicity is found in the vicinity of Quaternary basins and volcanic rocks, although there are some extensions into regions of Tertiary intrusive rocks. In western Washington, source zone boundaries could be associated with steep gradients, as shown by Bouguer anomaly maps. In the Atlantic seaboard, both large-scale and small-scale zones were produced, with the intention of combining these zones as alternative hypotheses, using appropriate weights, in the construction of a risk map. The small-scale zones were based on Triassic and Jurassic basin provinces. The large-scale zones were partitions of the small-scale zones in regions where higher levels of seismicity could be associated with structures transverse to the Triassic and Jurassic basins. These transverse structures may be onshore extensions of offshore seamount chains or bathymetric discontinuities associated with Atlantic transform faults.

Earthquake investigations

A magnitude 6.5 earthquake occurred on June 20, 1978, in an agricultural valley between Lake Langadha and Lake Volvi, 30 km east of Thessaloniki, Greece. R. F. Yerkes, C. G. Bufe, and R. P. Maley report that the main shock was preceded by a series of foreshocks, one on May 23 of M=5.8 and two on June 12 of M=4.8 and 5.2. An aftershock of M=5 occurred on July 4, 1978. The four largest events of the May–July 1978 sequence were alined with a 10-km zone of right-stepping en echelon ruptures that trends N. 55°–60° W. between the two lakes; their fault-plane solutions are consistent with left-reverse-oblique slip along that zone. Other effects of the earthquakes include localized ejection features and landslides.

In Thessaloniki, 50 people were killed, 38 by collapse of an eight-story, reinforced concrete-frame apartment building; columns of a nearby structure were damaged near ground level. Both buildings were in a small area near the shore. Cracking and crushing of hollow tile commonly used as walls in medium-rise reinforced concrete-frame buildings and fall of parapets and cornices was fairly widespread. In the epicentral area, damage was concentrated in villages along and near the rupture zones. Many unreinforced brick or stone buildings collapsed or performed poorly at distances of 200–300 m from the zones. Although none of the common reinforced concrete-frame structures collapsed, those on or within about 20 m of the rupture zones were severely damaged by fracturing of slabs, offsetting of columns, and crushing of wall tile.

The epicentral area is known to be one of recurrent earthquakes. One of M=6.9 in 1932 reportedly was associated with surface rupture in a village (Stivos) that was traversed by both ruptures of the 1978 sequence. Detailed maps of the rupture zones thus would aid in avoiding or designing for them. The restricted distribution of severe damage in Thessaloniki suggests a correlation with unusual foundation conditions of limited extent, such as loose fill over pre-existing foundations. A detailed map of such near-surface characteristics would assist in identifying areas susceptible to abnormally intense ground shaking during future earthquakes.

ENGINEERING GEOLOGY

Engineering geologic map of the United States

A computer method was devised for producing color-separation negatives as part of the procedure of preparing an engineering geologic map of the conterminous United States, according to Dorothy Radbruch-Hall. Six maps (landslides, karst, steep slopes, volcanic hazards, standing water, seismic probability) were prepared by this method. They in turn were used in different combinations by the computer to produce three other maps: an engineering geology map, a map showing areas covered by the six component maps, and a map showing where construction might cause direct or indirect damage to the physical environment. In addition, all color proofs were prepared by the computer.

Research in geologic hazards

Reconnaissance of the proposed Devils Canyon and Watana damsites, Alaska, and reservoir areas for geologic hazards was completed by Reuben Kachadoorian. Known or inferred faults were examined, and no evidence of recent or active movement was found. The reconnaissance did reveal, however, recent movement of surficial deposits that occurred as a result of mass wasting, and possibly by seismic shaking and minor displacements of bedrock along joints.

Landslides have occurred in these places in the past, and the likelihood of future slides is enhanced if the reservoirs are constructed. Unconsolidated glacial debris, alluvium, and Tertiary-age sediments that occur below the altitudes of the proposed reservoir levels may slump and slide into the water when they are inundated. Some of these sediments may be permanently frozen and may be ice-rich locally; this condition could increase the probability of slumping and sliding when the sediments thaw as a result of the water being impounded behind the dams.

Research in rock mechanics

As part of a continuing study of residual rock stresses, two theoretical models for the development of such stress as a result of cooling of rock bodies were developed by W. Z. Savage. The first describes the "locking in" of stresses between grains in an igneous rock, and the second describes the locking in of stresses between rock masses. Application of the grain-to-grain model and the rock-mass model leads to predicted residual stresses and strains that are in reasonable agreement with field measurements made at Barre, Vt., in the Barre Granite and surrounding metasedimentary rocks.

Long-term laboratory experiments to determine the nature of stored strain energy and its significance to engineering practice continued under the direction of T. C. Nichols, Jr. Cores with a diameter

of 15 cm were systematically sawed and recored into smaller pieces. The resulting strains on old surfaces, as well as the newly cut surfaces, were monitored over periods of months. The strains were monitored by strain-gaging techniques and holographic interferometry, a very precise technique that measures deformations by comparing distances traveled by fixed-source laser light waves to the undeformed and deformed surfaces.

Results showed that holographic interferometry measurements did not agree with strain-gage measurements in monitoring long-term deformations on rock samples. The holography measurements, however, were in closer agreement with strain-gage measurements made on old surfaces than with those made on newly cut surfaces.

Also, it was found that the exposure of the cut surfaces to water allowed absorption of moisture in the pore spaces that caused long-term deformations. The deformations recovered when the surfaces were allowed to dry and the absorbed pore-space moisture was lost.

Research in soils engineering

T. L. Youd and D. K. Keefer made onsite investigations following the November 23, 1977, San Juan, Argentina, earthquake. These investigations revealed rather extensive liquefaction over an area of about 6,000 km^2, and further revealed that liquefaction was a major source of earthquake-caused property damage. Five specific sites of liquefaction-induced damage were investigated in detail, and exploratory holes were augered to determine the character of the soils. At two sites on level ground, blocks of relatively stiff surface materials, as wide as 200 m and thicker than 6 m, were detached from the surrounding soils and oscillated back and forth in a horizontal direction over the liquefied layer. This movement caused sand boils to be concentrated at the margins of the blocks and caused considerable damage. This investigation provided the opportunity for was the first documentation of such ground-failure movements on level ground.

At the other three sites, liquefaction led to loss of strength and bearing capacity under buildings and tanks. Several of these structures settled and tipped while others suffered severe differential settlements. As a result of subsurface pore-water pressures associated with the liquefaction process, water vented to the surface along well casings at two places; resulting erosion formed large cavities at the tops of the well casings under a pump and a pump house, and the two structures subsequently tilted and fell into the cavities.

Analyses of data collected during the field investigations indicate:

- The areal distribution of liquefaction was consistent with that of previous earthquakes. The furthest distance from the epicenter to an effect of liquefaction from this earthquake was 260 km, which is the greatest distance yet recorded for an M=7.4 earthquake but only marginally more than would be predicted from the worldwide trend.
- Nearly all of the sediments that liquefied during the earthquake were in Holocene flood plain and playa deposits, types of deposits proven to be very susceptible to liquefaction during other earthquakes.
- Densities of five core samples obtained from silt and sand sediments that likely liquefied during the earthquake ranged from 1.35 to 1.55 gm/cm^3, indicating loosely packed sediments.
- Measurements of sediment and water depths in a house into which sand boils erupted showed that 12.0 m^3 of sand and water came up into the house, yielding a ratio of water to sand of 3.3 by volume and 1.3 by weight. This was the first time it had been possible to determine such ratios.

Geophysical techniques were applied as a possible in-situ test for for liquefaction potential in the Salt Lake Valley, Utah, area by C. H. Miller. Compressional wave velocities and electrical resistivities were measured through a selected area of fine-grained lake deposits, both before and after detonation of a small amount of explosives. The explosive was buried in the sediments at the center of the geophysical arrays, and the velocities and resistivities were measured by surface instrumentation. Preliminary comparison of the nonexplosive and explosive velocities reveal that velocities were modified throughout a larger volume of sediment than is usual near the explosion but also revealed that resistivities may be only little changed. These changes in compressional wave velocities may be caused by liquefaction and change in physical characteristics in saturated fine-grained lake sediments.

Standard Penetration Test data provided by the U.S. Army Corps of Engineers were examined as part of an effort to determine the liquefaction potential of an area between Marked Tree, Ark., and New Madrid, Mo. A consistent pattern was observed

in the tests, according to S. F. Obermeier. Blow counts that reflect high porosity and low density are commonly reported from the base of a clayey stratum at the surface to a depth of about 9 m in sand, where the counts abruptly increase significantly to suggest low porosity and high density. These higher counts usually continue to depths of about 18 to 24 m, the bottom of the holes. Saturated sand with low blow counts would liquefy during an MM VII earthquake, whereas sands with the higher counts would not liquefy. One can assume on that basis that in the event of an MM VII earthquake, ground response to liquefaction could cause damage throughout the area.

Research in permafrost engineering

An integral part of the Geological Survey's evaluation of the petroleum potential of the National Petroleum Reserve in Alaska is the drilling of two holes at Inigok and Tunalik. This required the construction of all-year support airfields capable of handling large C–130 (Hercules) aircraft. Design and construction problems for the two airfields were compounded by permafrost and by the constraints that they be built in the winter and in accordance with environmental requirements. According to Reuben Kachadoorian, it is unlikely that the construction of such large all-year airfields in the winter on permafrost terrain had been done previously.

In cooperation with the Corps of Engineers (Cold Regions Research Engineering Laboratory and the Waterways Experiment Station), a new concept was developed to construct the airfields. A base course of local borrow material (sand at Inigok and gravel at Tunalik) was overlain by styrofoam insulation (7.5 cm at Inigok and 5 cm at Tunalik). This, in turn, was overlain by 48 cm of gravel to protect the insulation from the C–130 traffic. The airstrips were monitored by thermocouples, and the data show that this new concept was a success.

This new technique used in building the large year-around airfields is not only a significant contribution to Arctic construction, it also (1) minimizes the amount of gravel required to place airstrips or other structures on permafrost terrain (heretofore, all large airstrips underlain by permafrost were constructed in the summer and required up to 25 m of gravel fill), (2) minimizes the environmental effects of such construction, and (3) insures a substantial financial saving in construction of airfields and other similar structures subject to permafrost-related problems.

LANDSLIDE HAZARDS

In 1978, the USGS conducted more landslide studies with greater diversity than ever before. Landslides have been recognized for many years as both an important landscape-forming process and a costly economic problem in the United States. However, the associated costs and the extent of landsliding in the United States now are better understood as a result of recently completed studies. Inventories of landslides in the Appalachian Plateau, Rocky Mountains, and northern Great Plains delineated extensive areas of failed slopes. A nationwide study of the distribution of failed slopes and areas susceptible to failure by Radbruch-Hall and others (1976) found significant landslide problems in virtually every State of the United States.

F. A. Taylor and R. W. Fleming studied the cost of damages by landslides in Los Angeles and the San Francisco Bay area, California, and Allegheny County, Pennsylvania. Only documented costs were used to develop damage estimates, and the damage totals were minimum figures. By reducing figures to account for differences in year-to-year climate and adjusting to a per capita basis, the data from different regions could be compared. For example, intense rainstorms in the Los Angeles area that led to severe landslide activity occurred about once every 4 years during the past 30 years. Therefore, average annual cost of damage was assumed to be one-fourth the cost of damage in a year of severe storms. Minimum per capita costs for the city of Los Angeles, the San Francisco Bay area, and Allegheny County ranged from about $1.25 to $4.35 annually. The total annual cost of landsliding for the three areas is more than $46 million.

In a nationwide assessment of damages, R. L. Schuster of the USGS concluded that the total annual cost of damages from landslides in the United States was in excess of $1 billion (Schuster and Krizek, 1978). In an independent assessment of damages for the National Academy of Sciences, R. H. Jahns, Stanford University, found that damages caused by landslides and subsidence during the period 1925 to 1975 was at least $75 billion. This estimate was more than three times the estimate of combined damages from floods, hurricanes, tornadoes, and earthquakes during the same period (Jahns, 1978).

Areal and regional studies

Soil slides in southwestern North Dakota.—D. E. Trimble found extensive landsliding in the ungla-

ciated areas of the Missouri Plateau. The most common form of landslide was 15 to 30 m across and generally less than that downslope. Individual slides contained low scarps at the line of separation between failed masses, and a long smooth slope contained perhaps 5 to 10 scarps.

One of the landslide areas in Stark County, North Dakota, was studied in detail in a trench that extended from the base to near the top of the slope. The study established that the landslides were not earthflow features, as had been thought, but were soil slides. Thin plates or pads of soil, 18 cm to about 1 m thick, apparently failed on the top of the B-horizon in the soil and slid a short distance. Failure apparently took place when the soil was saturated and the lower permeability of the B-horizon promoted development of seepage forces parallel to the slope. This, combined with increased weight and perhaps reduction in strength, caused failure of the thin plates of soil. In cross section, the soil slides appeared to be miniature décollements.

Landslide activity in the Pacific Palisades area of Los Angeles, California, in 1978.—A reexamination of the Pacific Palisades area by J. T. McGill following the near-record 1977–78 seasonal (July 1–June 30) rainfall in Los Angeles, Calif., revealed extensive fresh slope failures and provided a basis for comparison with effects of the highly damaging winter 1969 storms.

Landslide effects of the 1977–78 rains were similar to but not as great as those of the 1968–69 storms, although the seasonal rainfall total at Los Angeles civic center in 1977–78 was 84.94 cm as compared to 69.77 cm for 1968–69 (the average for 101 years of record is about 38 cm). The lessening of landslide effects probably was due partly to the time pattern of rainfall and partly to remedial and preventive measures taken by the Los Angeles Department of Public Works after the landsliding in 1969. In 1968–69, the rainfall was mostly concentrated in a few intense storms in the months of January and February, and it was preceded by 3 years of above average precipitation. In 1977–78, on the other hand, the rainfall mostly occurred over a period of about 3½ months, and it was preceded by 3 years of below average rainfall (indeed, only 1 year had been appreciably above average since 1969). The remedial and preventive measures consisted primarily of installation of soldier beams (piling), timber bulkheads, and associated drainage devices at or immediately upslope from the heads of landslides where necessary to restore and protect public roads that had been damaged. This work, much of which took place between 1969 and 1971, was generally effective in preventing further damage to those roads in 1977–78.

The principal types of landslides were new small thin debris slides, debris flows and mudflows, and renewed movement of preexisting, large, deep-seated slumps. The debris slides and flows occurred mainly on the steep walls of the major canyons, on both natural and artificially modified slopes. Evidence of at least 84 discrete debris slides and flows was observed. In addition, several extensive areas containing numerous long, narrow scars of the soil-slip-variety debris slides were noted. The thin failures apparently moved rapidly, and most of them probably took place during brief periods of especially heavy rainfall in February and early March. Greater than average precipitation in December and January had set the stage for this response. The debris slides and flows caused only local generally minor damage to residences and fortunately no injuries or fatalities. (Elsewhere in the Los Angeles region, two deaths were attributed to debris flows or "mudslides.") Several historic and prehistoric deep-seated slumps, mainly along the palisades fronting the ocean, experienced a renewal of activity. Their movements have been slow and small but damaging, especially to roads, and some movements apparently continued into the summer months.

Other types of landslides were more limited in number but locally very troublesome. Two of the most extensive enlargements of preexisting landslides in the area were block glides on bedding in seaward-dipping shales in the central palisades. One of these slides severely damaged a residence, and the other threatened part of a trailer park. A soil-fall from the high eastern palisades caused the only reported injuries when a car traveling on the Pacific Coast Highway was engulfed. That failure did not occur until April and apparently was triggered by seepage of ground water.

Landslide investigations in the Appalachian Plateau.—Landslide studies by W. E. Davies and his associates showed that, depending on location, 50 to 90 percent of slopes in the Appalachian Plateaus contain hummocks and lobes characteristic of old landslides. About 5 percent of the slopes have scars and other features indicative of recent or active landslides. Almost all of the recent or active landslides are old landslides reactivated naturally or through the work of humans. The landslides are so numerous and widespread that this form of mass

wastage was probably the dominant process of erosion on the plateaus.

Analysis of the deposits involved in Appalachian Plateau landslides indicated that illite is the dominant clay mineral and that montmorillonite is generally absent or very scarce.

Large-scale gravitational slope movement in Colorado.—Dorothy Radbruch-Hall and D. J. Varnes studied large-scale gravitational slope movements ("Sackung") in Colorado. Field investigations in 1978 showed that such slope movements are abundant in the Williams Fork Mountains. Previous reconnaissance identified numerous areas in other Colorado mountain ranges where large-scale slope movements occurred. Study of exposures near large-scale slope movement in the Sawatch Range indicated that movement is probably controlled by pronounced jointing both parallel and normal to the direction of movement. Study of a thin section of an oriented specimen taken from Bald Eagle Mountain showed that internal microfractures in the rock were parallel to jointing and probably influenced both the formation of joint systems and large-scale rock movement.

Topical studies of landslides

Properties of saprolite as related to slope stability.—In a study of the properties of saprolite that control slope stability, S. F. Obermeier compared shear strength data with inclinations of natural slopes in colluvium derived from saprolite. He found that, for the Piedmont of Fairfax County, Virginia, critical slope angles for creep approximated the angles predicted from triaxial strength data obtained in the laboratory.

In a related study, Obermeier examined the characteristics of joints in saprolite in two different physical situations. Joints in saprolite buried beneath Coastal Plain sediments of Fairfax County were coated with clay, which was washed into the joints from the overlying sediments. These clay coatings reduce the overall strength of the saprolite. However, in the Piedmont, the joints in saprolite are commonly cemented with oxides and organic materials or have no weak coatings.

High-resolution sensing techniques for slope-stability studies.—R. B. Johnson conducted the USGS portion of a joint study with the National Bureau of Standards to develop high-resolution sensing techniques for slope-stability studies. The purpose of the study was to examine and test innovative approaches to detect and resolve buried subsurface features. The physical characteristics of a site in granite near Denver, Colo., were documented by mapping, drilling, and laboratory testing of samples. Frequency-modulated continuous wave (FM–CW) radar scanned the documented site and accurately located features such as pegmatites and joints to a depth of 6.8 m.

Earthquake-induced landslides

Lateral-spreading landslide near Ogden, Utah.—An area comprising about 13 km^2 between Ogden and North Ogden, Utah, underlain by what may be a previously unrecognized slide resulting from liquefaction, was investigated by R. D. Miller as part of surficial geologic studies along the Wasatch Front, Utah. An area near Farmington, about 32 km south of this site,was identified by Van Horn (1975) as a large slide caused by lateral spreading as a result of liquefaction. Mounds or small hills, 1–10 m high, separated by nearly flat surfaces characterize both localities. The surficial materials in both places are silt and clay, but characteristically they contain thin layers of sand at depth. If the area near Ogden is a liquefaction-caused failure, the entire low-lying area underlain by fine-grained materials along the east shore of the Great Salt Lake may also be susceptible to such failure, especially as a result of a large earthquake.

Landslides near Kemmerer, Wyoming.—Surficial geologic mapping around Kemmerer, Wyo., by A. B. Gibbons led to the tentative conclusion that main episodes of movement of abundant and widespread landslides were triggered by earthquakes. Landslide deposits in the eastern edge of the Basin and Range province, Fossil Basin, and the western edge of the Green River basin differ in abundance and age. Slides in the Basin and Range and the Fossil Basin moved all the way to the valley floors. Those in the Green River basin are older and typically found as eroded remnants capping pedestals of undisturbed rock above the valley floor. The Wasatch Formation is found in both the Green River and Fossil Basins and is similar in appearance in both areas. Yet, there are innumerable landslide deposits in the Fossil Basin and only a few landslides in the west part of the Green River basin.

The eastern edge of the Basin and Range province is a belt of definite seismic activity, and two normal faults are present that have offset modern topography. Slide activity was confined to the western part of the mapped areas even though conditions to the east appeared identical, suggesting that

an influential variable was missing. Seismicity was the tentative choice.

Landslides caused by historic earthquakes.—D. K. Keefer completed a preliminary analysis of slope failures in 15 historic earthquakes. The number of slope failures triggered by an earthquake was found to be strongly dependent on earthquake magnitude. The predominant types of slope failures were falls and shallow slides in rock; avalanches, falls, and shallow slides in soil; lateral spreads; cut-slope failures; and slumps and block sides in rock and soil. Other types of slope failures occur less frequently during earthquakes but have high inherent potentials for causing loss of life and property. These include rock avalanches, lateral spreads, wet flows, subaqueous landslides, and liquefaction-induced failures in artificial fills. Certain geologic environments with high susceptibilities to earthquake-induced slope failure were also identified on a preliminary basis.

Landslides caused by recent earthquakes.—E. L. Harp and G. F. Wieczorek prepared a map depicting the concentration of landslides on canyon slopes for the Guatemala City, Guatemala area (fig. 3), using information from the 1976 earthquake investigation. Further investigation and analyses indicated that the zones of high and severe landslides concentration shown on this map reflect physical site conditions (such as lithology and topography) and are, therefore, areas of high susceptibility to seismic-induced landslides in future earthquakes.

Preliminary data gathered from fieldwork and grain-size analyses of soil samples from Guatemala suggested that the thickness and percentage of clay present in the soil governs its susceptibility to forming soil debris slides under seismic conditions. It is likely that the clay fraction inhibits the formation of disaggregating debris slides in thick soils with high clay contents. Laboratory analyses, still in progress, may have application to areas in this country, such as southern California, where thousands of debris slides, similar to those in Guatemala, occurred in response to the 1971 San Fernando earthquake.

Correlations of rockfall occurrence with lithology in several major and moderate earthquakes indicated that, for most well-cemented rocks, the fracture or joint spacing, orientation, and proximity to steep slopes greater than 35° are the most important parameters determining the susceptibility of a rock mass to seismic induced rockfalls. For weakly cemented rocks, fractures and joint spacing are not as important in controlling their seismic deformation. The cohesion of many such rocks is low enough that seismic shaking produces additional

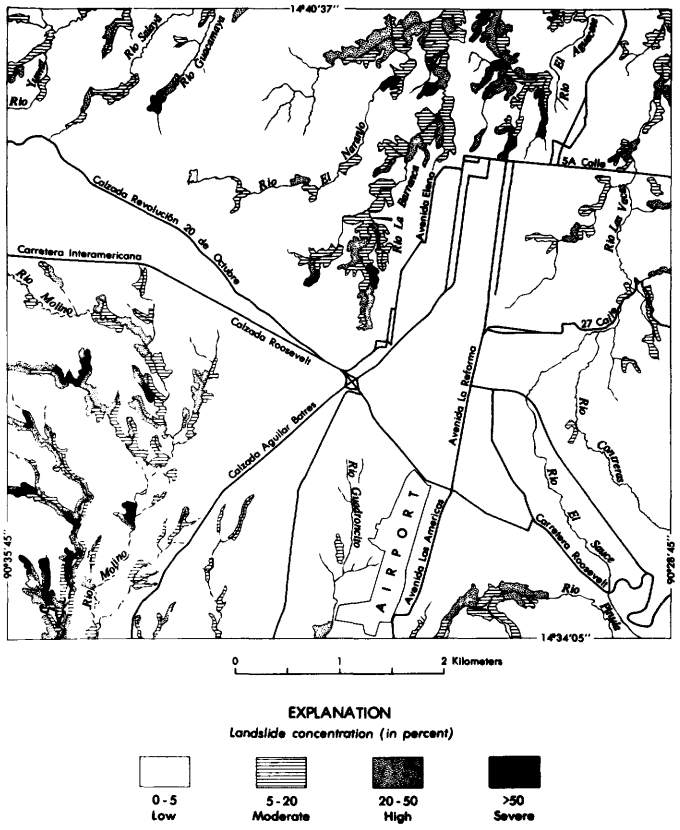

FIGURE 3.—Landslide concentration map for Guatemala City area. (From Harp and others, 1978.)

fractures through previously intact rock. Although most weakly cemented materials tend not to form steep natural slopes, materials such as volcanic pumice tuffs commonly form nearly vertical slopes several hundred meters in height and are essentially uncemented. These materials have a high internal friction, a result of the shape and interlocking nature of individual particles, and thus are stable under static conditions. However, the low tensile strength of the rocks is apparently responsible for their extreme seismic instability, as evidenced by the extensive rockfall occurrence in such deposits in Guatemala.

Reconnaissance of ground failure in Miyagi Prefecture, Japan, by E. L. Harp and D. K. Keefer established that several thousand landslides were triggered in response to the M=7.5 earthquake. Most were small rockfalls and rockslides originating in steep roadcuts and natural slopes of Mesozoic metamorphic rocks and Miocene volcanic deposits. The largest rockfalls (several thousand square meters volume) were in Miocene tuff breccia. The largest of these damaged four houses located at the base of the failed slope. Several houses and roads were also affected by rotational slumps and settlement in loosely compacted artificial fills. A housing development in Sendai experienced the largest of these, about 30,000 m^3 volume. In all, seismic-induced landslides accounted for 2 houses

destroyed and 13 damaged. The main factors governing landslide occurrence appeared to be the presence of weakly cemented and (or) extensively jointed rocks exposed in steep slopes, in the case of rockfalls, and loosely compacted artificial fill, in the case of rotational slumps.

Landslides from the M=5.1 earthquake that occurred on August 13, 1978, near Santa Barbara, Calif., were mainly small rockfalls and rockslides from steep roadcuts. One large (100 m^3) rockfall in conglomerates of the Sespe Formation closed California Highway 154 near San Marcos Pass in the Santa Ynez Range for 30 hours. Weakly cemented and heavily fractured sandstones in the Coldwater Sandstone also produced rockfalls and slides in the Santa Ynez Range. Other small rockfalls occurred along the coastal cliffs near Santa Barbara in the Monterey and Sisquoc shales. Seismic-induced settlement of a railroad embankment west of Santa Barbara near Ellwood was responsible for a train derailment occurring 7 minutes after the earthquake. Harp and Wieczorek concluded that the landslide occurrence from this moderate earthquake indicated that steep slopes in weakly cemented and extensively fractured rocks were the most susceptible to seismic-induced failure. Most of the steep slopes in these rocks are roadcuts, and the same areas will likely sustain failures in future earthquakes of magnitude 5 or greater in the Santa Barbara Channel area.

Correlation between ground failure and seismic intensity.—Analysis of data resulting from field investigations after the 1976 Guatemala earthquake (M=7.5) by R. C. Wilson indicates that the onset of earthquake-induced ground failures, either liquefaction or landsliding, occurs at a much lower shaking intensity than described in the Modified Mercalli Intensity Scale (MM). According to both the 1931 and 1956 versions of the MM scale, significant ground failures do not occur unless the shaking intensity equals or exceeds MM IX. Estimates of shaking intensity from the 1976 Guatemala earthquake were based primarily on observations of structural damage, especially to adobe dwellings. An attempt was also made to separate shaking damage from damage resulting from ground failures in the foundation. According to the 1956 version of the Scale, damage to adobe structures begins at MM VI, serious damage occurs at MM VII, and collapse begins at MM VIII. Although adobe stuctures were destroyed or seriously damaged over a wide area during this earthquake, there were a number of localities with severe ground failures, either liquefaction-induced lateral spreads or slope failures on steep pumice slopes; yet, relatively little shaking damage was done to nearby adobe structures. It appears, therefore, that seismic-induced ground failures may occur at shaking intensities of MM VI and perhaps as low as MM V.

Subsequent field investigations of ground failure effects in the Santa Barbara, Calif., earthquake of August 13, 1978, by Wilson also supported the conclusion that the onset of ground failures occurs at shaking intensities of MM VI or less. Rockfalls from roadcuts occurred up to 30 km from the epicenter of this M=5.1 earthquake.

REACTOR HAZARDS

The Geological Survey continued its program of research to elucidate various tectonic features and geologic processes that are potential hazards to the siting of nuclear reactors. Most of these research projects have already been described in the appropriate chapter under "Regional Geologic Investigations," and the following discussion, therefore, reports results of only a few projects in this progam.

Charleston, South Carolina

Interrelated investigations in the Charleston, S.C., area are directed to development of an understanding of the source mechanism of the damaging earthquake that occurred August 31, 1886. Active projects included field mapping, subsurface studies, and geophysical studies.

Auger drilling and shallow seismic reflection profiles provided a basis for studying the distribution of Tertiary sediments in the Charleston area. According to G. S. Gohn and B. B. Higgins, the Cooper Formation (Eocene and Oligocene) has been divided informally into three members: an upper member composed of calcareous phosphatic muddy sand, a middle member composed of clayey fossiliferous limestone, and a lower member that consists of clayey fine-grained limestone. The three members are separated by erosional unconformities marked by phosphatic or glauconitic lag deposits. The geometry of the channel deposits that characterizes the upper two members produces a wide variation in the thicknesses of the members throughout the study area. Dimensions of channels are as wide as 4 km and over 30 m in depth. A preliminary comparison of the distribution of the Cooper members with distribution patterns and geometries of younger deposits in the Charleston area suggests that structural control of depositional trends may have occurred during much of the Tertiary.

Joseph Liddicoat (Lamont-Doherty Geological Observatory), working in conjunction with geologists and paleontologists of the USGS, has found two sedimentary units deposited during the present

Brunhes normal polarity epoch and one unit deposited during the Matuyama reversed polarity epoch (0.7 to 2.5 m.y. ago).

According to R. E. Weems and E. M. Lemon, Jr., two Tertiary stratigraphic units above the Cooper Formation (Eocene and Oligocene), one late Oligocene and one middle Pliocene in age, are recognized in the Charleston area. Further investigation of these units may provide a record of late Tertiary differential tectonic movements that may have affected the area. The presence of Miocene beds could not be confirmed, and Miocene beds, if present, are certainly not widespread. Although large *Carcharodon* (shark) teeth found in Pleistocene lag gravels attest to the former presence of such Miocene beds, the teeth may have become totally reworked into later units.

H. D. Ackerman has designed a means of interpreting seismic refraction data using interactive computer methods. This method uses information from previous studies that indicate that perturbations in refraction arrival time curves are as often due to lateral changes in rock properties as they are to structure. Inversion schemes presently in common use demand determination of the average velocity of a refracting horizon before using this velocity to calculate depth and structure. If the refracting horizon is subject to significant lateral velocity changes, these schemes cannot produce a model that satisfies the data. The new method requires reversed data and permits both lateral velocity change and change in depth of the refracting horizon. It results in a model that, if inverted back to arrival times, satisfies the initial arrival time data.

A combination of depth estimates based upon magnetic source and seismic refraction data has been used by J. D. Phillips to define the geophysical basement in the Charleston area. A basement ridge with 1 km of relief is seen to be northwest of Charleston. The ridge is located under a regional magnetic and gravity high and has a minimum depth of 1.1 km. Present seismic activity is concentrated along a line extending northwest from Charleston that crosses this ridge and is greatest under the ridge. North and east of the ridge, the depth to basement is 2 km. This depth is maintained to the limits of the study area. The regional magnetic high north of the ridge may be caused by shallowing of basement, or it may be related to a thick volcanic sequence extending from depths of approximately 500 m to 1 km. Both the basement ridge and the basement under the northern volcanic province are intruded by mafic plutons. Between these areas, the basement does not exhibit strong magnetic contrasts.

Paleomagnetic analysis by D. L. Campbell of basalt cores from the Clubhouse Crossroads coreholes near Charleston indicated a possible southeast dip of the basalt flow. This evidence fits well with the velocity model of the "basalt" horizon calculated for the area to the northeast of the coreholes. One possible interpretation is that the dipping basalts may have been partly to entirely eroded away there, so that velocity signals of the underlying well-indurated sediments are discernable.

Over 60 km of deep seismic reflection profiles were run across the Middleton Place-Summerville epicentral zone by the Consortium for Continental Reflection Profiling under joint sponsorship of the National Sciences Foundation, the Nuclear Regulatory Commission, and the USGS. Prominent reflectors are the top of the basalt in the vicinity of Clubhouse coreholes 1–3, crystalline basement, and at several intracrustal depths. At least one fault clearly offsets the basalt with a displacement of about 50 m.

Piedmont tectonic features in Virginia

Reconnaisance mapping by Louis Pavlides southwestward of the fault zone delineated in the Richardsville quadrangle by K. E. Wier (1977) indicates this zone may be regionally extensive and important in the Piedmont of Virginia. Along its trace, the fault zone contains serpentine and amphibolite as blocks within schist. Highly magnetic polydeformed mica schist (Candler Formation) occurs on its northwest side, and weakly magnetic less deformed schist occurs on its southeast side. The fault zone has been traced southwest to the northeast margin of the Ellisville pluton which truncates it. South of the Ellisville pluton, the fault zone may be defined by a thin belt of amphibolitic rocks, and it may extend into the "Shores Melange" of Brown exposed along the James River. Major movement on the fault is earlier than intrusion of the Ellisville pluton.

Although sense of movement direction and inclination of the fault zone are unknown, the zone may be a thrust upon which much of the Piedmont block to the southeast has been transported northwestward.

Basin structure in Culpeper, Virginia

Recent investigations by R. P. Volckmann and W. L. Newell show that both the eastern and western margins of the Culpeper Triassic and Jurassic basin consist of high-angle faults. The eastern margin consists of a series of faults, and it appears to have experienced left-lateral as well as vertical displacement. In contrast, the western margin con-

sists of one principal east- to southeast-dipping normal fault, which is offset at widely spaced intervals and shows no evidence of other than vertical displacement. The lack of evidence for lateral displacement on the western fault suggests that the eastern faults occurred earlier than the western fault, in reaction to a different set of tectonic conditions.

The suggestion of R. C. Lindholm (1978) that Triassic border faults owe their trends to foliation attitudes in pre-Triassic crystalline rocks is not supported by this investigation. Foliation in the Piedmont rocks of the eastern margin is only locally parallel to the eastern border faults. The western border fault is more or less parallel to the strike of foliation in rocks of the Blue Ridge but cuts across the dip of the foliation at a steep angle. In addition, the western fault truncates Blue Ridge formation boundaries along strike at an acute angle.

Structure of the Coastal Plain, Virginia

W. L. Newell reports that reconnaissance mapping of upper Miocene and Pliocene near-shore marine sediments, which underlie the uplands of northern tidewater Virginia, indicates that three cycles of regressive sequences can be distinguished and related (in ascending order) to the St. Marys Formation (Miocene) of Maryland, the St. Marys Formation (Miocene) of Virginia, and the Yorktown Formation (Pliocene) of Maryland and Virginia. Each regressive sequence is unconformable upon facies of preexisting cycles.

Mapping indicates that the Yorktown Formation caps the upland crests and extends to the Coastal Plain margin. Upland fluvial gravels along the Coastal Plain margin are laterally continuous with near-shore marine sediments that trend downdip into shelf deposits that bear faunal assemblages of the Yorktown Formation. Aeromagnetic gravity data and structure contours drawn on the base of the Yorktown Formation delineate a northeasterly trending monocline. The distribution of near-shore marine and shelf deposits across the monocline suggests structural control during deposition.

Active faults in Houston, Texas

Thousands of residential, commercial, and industrial structures in the Houston metropolitan area of Texas have suffered moderate to severe damage by virtue of their location on or near active faults. Examples of damage include broken and offset foundations, infiltration of water and sediment into broken sewer lines, rupture of small natural gas and water-supply pipes, distortion of railroad tracks, and offset of airport runways. Gradient changes in streams and drainage ditches, noted in numerous areas, can be detrimental to flood-control efforts in an area where natural gradients are very low and flood incidence is already high. Market values of land and improvements will change as public awareness of faulting grows. Large-scale fault maps of selected areas seem certain to influence future deveopment of the Houston metropolitan area.

E. R. Verbeek states that high-resolution shallow seismic lines across selected faults demonstrate that scarps mapped at the surface represent only the most recent displacements on faults that persist to depths in excess of several hundred meters and show evidence of continued Quaternary movement. Most faults and their associated surface scarps are related either to salt domes or regional growth faults of Tertiary age; the faults are thus natural rather than man-induced geologic features. The abundant evidence that most offset of the present land surface has taken place only within the last few decades supports the hypothesis that withdrawal of subsurface fluids from unconsolidated sediments has served to accelerate movement along faults.

Foothill fault system in Sierra Nevada, California

Offsets along the Foothills fault system in California studied by D. E. Stuart-Alexander indicate normal faulting, but, in the Auburn area, strike-slip movement may be locally important. Horizontal movement is consistent with fault-plane solutions made by Eaton and Simirenko (1978) for two localities in the western Sierran foothills. Although no surface displacements occurred, fault-plane solutions for both localities indicated strike-slip movement at depth. The report describes predominantly normal movement during an earlier earthquake at one of these localities and at a third locality.

Lineament studies in the San Joaquin Valley, California

Seismic reflection studies by J. A. Bartlow of lineaments in Cenozoic deposits in two areas of the eastern San Joaquin Valley show no displacement of reflectors exceeding the resolving power of the data (~15 m at 300-m depth). The basement surface at 1,200–1,500 m below the ground surface shows some irregularities, possibly erosional basement topography, but no recognizable fault displacement. Near one lineament, a zone of apparent disruption of the reflectors could be interpreted as a west-dipping fault zone of very small displacement.

In a second area about 19 km east of Merced, the eastern margin of the valley is defined by a system of northwest-trending lineaments along which the base of the Tertiary is offset several tens

of meters down to the west. Short detailed gravity profiles by Andrew Griscom across the lineaments provided no clear-cut evidence of basement offset under Cenozoic cover.

HYDROLOGIC ASPECTS OF ENERGY

Geochemistry of geopressured geothermal waters in coastal Louisiana and Texas

According to Y. K. Kharaka, P. M. Brown, and W. W. Carothers (1978), detailed chemical and isotopic analyses of 120 formation water samples from 25 oil and gas fields in coastal Texas and Louisiana showed that (1) salinity of water in the geopressured zone ranges from about 10,000 to 270,000 mg/L of dissolved solids, (2) samples from many gas wells indicate low salinities that are not representative of the true salinity of formation water because of dilution by condensed water vapor produced with natural gas, and (3) concentrations of problem components (H_2S, SiO_2, Hg, and As) are low, whereas concentrations of toxic components (boron, ammonia, and others) are moderately high. Subsurface injection probably will be the only acceptable method of disposing of spent geothermal waters because of high salinities and relatively high concentrations of toxic contaminants in the waters.

Coal hydrology and geochemical studies in the Powder River basin, Montana and Wyoming

According to B. D. Lewis and W. R. Hotchkiss, the shallow hydrogeologic system of the Powder River basin in Montana and Wyoming, for digital modeling purposes, is composed of five distinct units—three aquifers separated by two extensive confining units—bounded at the base by the Bearpaw Shale.

R. W. Lee identified active geochemical phenomena in shallow ground water in the northern Powder River basin in southeastern Montana. Very localized shallow flow systems are superimposed on a chemically distinct regional flow system. The shallow system develops a sodium sulfate quality high in dissolved solids (3,000 mg/L) with cation exchange of calcium and magnesium for sodium on clays and pyrite oxidation and gypsum dissolution supplying sulfate, as the major chemical phenomena. The deeper system (and some reducing coals) achieves a sodium bicarbonate quality by cation exchange and bacterially induced sulfate reduction. Solution thermodynamic calculations indicated generally high saturation levels of ground-water solutions with respect to calcite and sodium feldspars, whose presence was supported by mineralogical investigations. The slow breakdown of sodium feldspars apparently explains the seemingly continuous supply of sodium for cation exchange to the ground water.

Data collection for base-flow studies of perennial streams in southeastern Montana was completed for the 1977 and 1978 water years. Generally, inflows to the streams from ground water consisted of sodium sulfate-type waters. Both Tongue River and Rosebud Creek showed significant gains from ground-water discharge, while gains in Otter Creek were intermittent and the creek lost most of its flow at its mouth. The large base flow from the dam on Tongue River limited interpretations of flow and quality data.

Chemical-quality studies conducted by J. R. Knapton showed that surface-water-quality characteristics of streamflow are influenced by the mode of contribution to the stream; for example, runoff or base flow . While the base-flow component is associated with high concentrations of major ions dominated by sodium and sulfate, the surface-runoff component, which presumably has had no residence time in the ground-water system but has had extensive contact with soil and vegetation, is characterized by low concentrations of major dissolved ions and is generally dominated by calcium or magnesium cations and bicarbonate anions.

Highly fractured lignite at the Gascoyne mine in Bowman County, North Dakota

According to M. G. Croft, D. W. Fisher, M. E. Crawley, and D. C. Thorstenson, a three-dimensional ground-water flow model of the Gascoyne lignite mine in Bowman County, North Dakota, indicated that the Harmon lignite bed and the underlying sandstone of the Tongue River Member of the Fort Union Formation (Paleocene) have high hydraulic conductivity (K) beneath several major stream valleys. These valleys parallel major regional lineaments that probably are fracture zones. Fractured sandstone and lignite have K values >61 m/d. In interstream areas, lignite and sandstone have K values of about 0.3 m/d and 0.6 m/d, respectively. Specific yield of lignite at the Gascoyne mine is 0.01.

Geochemical studies indicated that when mining operations expose sulfide minerals in the lignite to weathering, oxidation reactions release sulfate and hydrogen ions. The weathering products are rapidly transported to the water table where the acidity is neutralized by dissolution of carbonate materials. Bulk X-ray analysis indicated that overburden material contains significant amounts of calcium sulfate that are returned to mine pits containing water. Calcium is then exchanged for sodium on clay min-

erals, thereby resulting in a sodium sulfate-bicarbonate ground water. Dissolved solids concentrations of >10,000 mg/L and sulfate concentrations of 6,500 mg/L were found in water samples from mine lakes, ground water, and streams draining the mine.

Vertical ground-water movement in abandoned mine shafts in Pennsylvania

Boreholes and mine shafts in the Western Middle Anthracite Field of Pennsylvania were logged by borehole geophysical equipment. D. J. Growitz reported that thermal profiles of standing water in many of the wells showed zones of little to no temperature change, an indication of vertical movement. Subsequent brine testing confirmed internal movement at most sites. Velocities as high as 33 m/min and internal flows of up to 10 L/s were measured in the boreholes. The highest velocity measured in any shaft was 0.88 m/min. Large flows of water probably are associated with the relatively low velocities in the shafts owing to large cross-sectional areas of the shafts. Flows in shafts could not be calculated because of lack of data on their cross-sectional areas.

Potential effects of stripping coal from the Ferron Sandstone aquifer, Utah

The Ferron Sandstone Member of the Mancos Shale of Cretaceous age is a source of both ground water and strippable coal in south-central Utah. D. J. Morrissey and G. C. Lines reported that an aquifer test in the outcrop area of the Ferron indicated significant directional differences in the aquifer's hydraulic conductivity, both radially and vertically, that are believed to be due to fracturing.

Tests, by means of expandable packers in open holes, indicated that potentiometric surface and quality of water varies with depth in the Ferron. In one test hole 1.5 km from the Ferron outcrop, the potentiometric surface in the aquifer increased 43 m, and specific conductance of water decreased 575 μmho/cm with an increase in depth of only 23 m.

Areal differences in the potentiometric surface nearby Emery, Utah, indicated that water moves updip through the aquifer from the Wasatch Plateau toward the Ferron outcrop. Most water that recharges the aquifer in the outcrop area is either consumed by phreatophytes or discharged to streams that cross the outcrop.

In order to evaluate the potential leaching characteristics of spoil piles resulting from strip mining of coal, leaching experiments were made by R. H. Fuller. Material for these leaching experiments came from cores drilled near Emery, Utah, in an area of potential strip mining. In the experiments, water was allowed to equilibrate with core material, either by circulating through a column of core material or by constantly shaking a water-core material mixture. Preliminary results indicated that the core material contains easily soluble salts that are quickly leached by a first flush of water. Subsequent leachings slowly remove less soluble salts.

Dissolved sulfate loads, an index of mining activity

By using available historical water-quality data, S. M. Rogers found dissolved sulfate in terms of kilograms per day per square kilometer to be the most reliable chemical parameter to evaluate the effects of past mining activities on stream quality in the coal fields of southwestern Virginia. Stream conditions were evaluated by synoptic sampling and field measurement of stream quality at selected sites during low flow. These data permit regional ranking of unit low-flow discharge and of unit dissolved sulfate loads contributed by subbasin areas.

GEOLOGY AND HYDROLOGY RELATED TO NATIONAL SECURITY

The USGS, through interagency agreements with the U.S. Department of Energy (DOE) and the Department of Defense (DOD), investigates the geologic, geophysical, and hydrologic environment of each site within the Nevada Test Site (NTS) where underground nuclear explosions are conducted. In addition, the USGS compiles geologic and hydrologic information pertaining to underground nuclear explosions conducted within the USSR. Geologic and hydrologic data are needed to assess the safety, engineering feasibility, and environmental effects of nuclear explosions. The USGS does research on specialized techniques needed to acquire geophysical and hydrologic data at nuclear explosion sites; some of the results of this research are summarized as follows.

Geologic and geophysical investigations at the NTS in support of the Los Alamos Scientific Laboratory (LASL), the Lawrence Livermore Laboratory (LLL), the Sandia Laboratories (SL), and the Defense Nuclear Agency (DNA) have continued to develop a clearer understanding of Quaternary alluvium, Tertiary volcanic rocks, and Paleozoic car-

bonate and clastic rocks and their structural setup in the Great Basin. Interdisciplinary communication within the USGS is the key to this clearer understanding. Isopach maps of the alluvium and of the Cenozoic rocks under Yucca Flat in eastern NTS have been updated by A. T. Fernald and D. L. Healey, on the basis of new drillhole information. Interpretation of magnetic anomalies in Yucca Flat, by G. D. Bath, has delineated near-surface structures, and gravity work by D. L. Healey describes the configuration of the tuff-Paleozoic interface. Postnuclear test surface effects, described and mapped by F. M. Byers, Jr., P. P. Orkild, and E. C. Jenkins, show near-surface structures and stress-strain relationships at or near test sites.

G. E. Brethauer and colleagues have initiated use of the Geologic Retrieval and Synopsis Program (GRASP) system for the compilation of data from Pahute Mesa and selected areas of Yucca Flat. This program is designed for use in predicting material properties by extrapolation and interpolation from the data base, thus effecting substantial savings by reducing the collection of geologic and geophysical data for new sites.

The effect of invasion of borehole walls in drill holes in Yucca Flat is a continuing study being conducted by D. C. Muller. Results of the study indicate that higher than true densities are recorded by the gamma-gamma density log where invasion occurred. Density logs run several times, over an extended period of time, show a gradual decrease in densities with time from cessation of drilling activities. Densities never decrease to a level equal to the true density but always remain at a higher level. The conclusion from these observations is that a residue of fluid and solids remains in the borehole wallrock spaces after much of the fluid and some solids have dissipated. D. C. Muller has also coordinated an experiment using vertical seismic profiling techniques. The objective of the experiment was to provide an accurate method of determining the distance to the tuff-Paleozoic interface within a drilled site without damaging the site. Air guns on the bottom of the drill hole and on the surface were compared with surface Vibroseis as signal generators for vertical seismic profiling. Data indicate that distance to the Paleozoic surface and possibly local configurations of the surface can be obtained with this type of exploration. In addition, the air-gun source is a suitable method for borehole velocity surveys.

R. D. Carroll has examined the relationship of the time of collapse of cavities formed by nuclear explosions and the shear and compressional velocity of the surrounding rock. The collapse times for 18 tunnel events in tuff were compared with velocity data obtained from refraction spreads in the initial 67 m from the working point in the tunnel driven to emplace the device. Collapse times ranged from instantaneous to 3,734 minutes. The data suggest a compressional velocity threshold of about 2,440 m/s below which collapse is early or instantaneous and above which the data are scattered. This conclusion is tempered by the fact that,where no collapse time is recorded (no seismic recording of collapse observed from about 30 seconds, when amplifiers come out of saturation, to several days), the collapse time is defaulted to instantaneous because collapse has been subsequently observed on reentry mining. There is a body of opinion, however, that finds it difficult to accept cavity collapse in such short time frames. Thus, there is an uncertainty in the collapse mechanics and the seismic signatures therefrom,and further investigation is necessary.

The Special Projects Branch completed a series of maps of the NTS for the Data Exchange working group, in connection with the Threshold Test Ban Treaty. The maps include the surface distribution of the various rock types, the altitude of the buried surface of rocks of Paleozoic age, and the altitude of the water table.

Jack Rachlin, W. J. Dempsey, S. M. Bonham, and Salih Faizi have continued studies on underground nuclear explosion sites in the USSR. Data compiled for geologic maps and stratigraphic sections, combined with information provided by the Soviets, has been included in computational analyses and compared with data obtained from experience in the United States.

A crack approximately 135 m long opened in April 1978 near the northwest end of the 1969 crack in Yucca Lake at NTS. The crack is of hairline width except on the southern 25 to 30 m, where erosion from inflowing water has opened it to about 1 cm in width. Significant inflow of water to the fissure has been observed by G. C. Doty and W. A. Evert, but attempts to channel and measure it have been abandoned because of the instability of the playa soil.

Doty, C. L. Washington, and L. E. Wollitz are currently instrumenting subsidence sinks above nuclear explosion sites to determine the effectiveness of observed inflow and ponding in inducing recharge and leaching of radioactive debris.

As suggested by Truesdell (1966), A. F. White (1979), and others, the vitric tuffs underlying many areas of the western U.S. significantly affect the

ground-water quality in these areas. Present research is aimed at understanding the kinetic mechanisms and rates of hydrolysis and dissolution of volcanic glasses under experimentally controlled pH, temperature, and ionic concentrations similar to ground-water conditions. The concentration profiles produced by cation diffusion out of the glass during reaction are studied by repeatedly reacting glass surfaces with dilute hydrofluoric acid. Specific gravity, chemical composition, and surface-area data permit quantitative description of the diffusion profiles as a function of time, pH, and solution ionic composition. The leached zones of selected hydrated glasses appear to increase in thickness during the first 300 hours of reaction at near-neutral pH. At longer times, steady-state thickness (~75Å) is reached corresponding to equilibration of the rates of surface-layer dissolution and ion diffusion.

The Rainier Mesa, Nev., hydrologic system consists of a fractionally saturated devitrified tuff that overlies a vitric tuff ranging from saturated to fractionally saturated. Previous studies (White and Claassen, 1977) showed that reaction of the vitric tuff is primarily responsible for the observed water quality. Kinetic modeling of this water composition by Claassen and White consisted of the following steps: (1) estimation of initial carbon dioxide availability, (2) determination of the reaction step interval, (3) estimation of the reaction rate constants for each species as a function of pH, and (4) determination of the mass transferred to solution for each species. The presence of montmorillonite in the aquifer required that the model allow for precipitation of this species.

Matching the ground-water composition with the model results yields a unique value for the ratio of aquifer surface area to ground-water volume (Claassen and White, 1979). Values for this ratio are necessary to realistically model ground-water transport of pollutants.

By the end of 1978, about 702 million gallons of water had been pumped from a satellite well 100 m from an expended underground nuclear test. Pumping has been maintained for almost 3 years in an effort to draw radionuclides from the cavity region produced by the Cambric nuclear explosion, detonated in 1965 about 80 m below the water table. Tritium concentrations began to rise above natural background in early 1978 and have reached about 8×10^5 pCi/L. The USGS project, headed by D. D. Gonzales, works cooperatively with the Los Alamos and Lawrence Livermore scientific laboratories and with the Desert Research Institute in this experiment.

The reentry hole into the cavity created by the Almendro nuclear explosion on Pahute Mesa was logged to determine the feasibility of perforating the casing near the detonation point. Measurements collected by D. D. Gonzales show that temperatures at these levels are 175°C, which is 40°C too high to safely perforate the lower portions of the casing. Caliper logs verified the integrity of the casing, and water levels were detected at a depth of 731 m, which is still 36 m below the preexplosion water table 5 years after the explosion.

RADIOACTIVE WASTES AND THE GEOLOGIC AND HYDROLOGIC ENVIRONMENTS

Research related to the quest for radioactive waste repositories in geologic formations and the assessment of environmental effects of existing repositories continued in 1978. The search for repositories is concerned with the disposal of high-level and transuranic wastes. High-level wastes include fission products that initially have a high level of beta and gamma radiation and a high rate of heat generation; they also include transuranic elements with a long toxic life. Transuranic waste contains long-lived alpha emitters at concentrations >10 nCi/g and generates little or no heat. Studies of existing repositories involve low-level wastes, which consist in part of miscellaneous solid materials that have become contaminated through use, and products of reactors and fuel reprocessiong plants.

Investigations of some existing low-level radioactive waste disposal sites were financed in part by the U.S. Department of Energy (DOE). Regional studies to identify potential repositories in geologic formations, investigations of the Waste Isolation Pilot Plant site in New Mexico, and most geophysical and geochemical research were supported by DOE funds.

The USGS started a research program in 1978 to complement and augment the DOE program for geologic disposal of high-level radioactive waste. In general, the USGS program is designed to provide concepts, methods, data, and analytical results that can be used by Federal agencies having operational and regulatory responsibilities for radioactive waste disposal. A primary objective of the program is to identify regions whose geologic and hydrologic characteristics embody relatively independent multiple

natural barriers to the movement of waste radionuclides. The program includes general research as well as studies of areas that, because of their geologic and hydrologic characteristics, appear to be suitable radioactive waste repositories.

STUDIES OF LOW-LEVEL RADIOACTIVE WASTE DISPOSAL SITES

Waste tritium migration in ground water, Cook County, Illinois

Tritium from one of the world's first low-level radioactive waste burial sites at Palos Hills Preserve, Cook County, Illinois, moved in ground water to nearby canals, according to M. G. Sherrill. Preliminary calculations indicated a traveltime of about 60 months from the burial site to a public well.

Two- and three-dimensional ground-water flow models of the site, developed by J. C. Olimpio, indicated that the water moved as much as 760 m in a period of 4 years. Sensitivity tests of the three-dimensional model showed that water movement is particularly influenced by leakage from an upper till aquifer to a lower dolomite aquifer and by hydrologic properties of the lower aquifer.

Tritium migration at Barnwell, South Carolina

Tritium, apparently from buried radioactive waste, was found in a well about 3 m from the edge of a trench at a commercial low-level radioactive waste burial site near Barnwell, S.C., according to J. M. Cahill. High levels of dissolved organic carbon were found in water from that well and in another well 8 m from a trench provided further evidence of waste-solute migration.

Subsurface waste nuclide migration at Maxey Flats storage site near Morehead, Kentucky

Analyses of water samples from wells drilled in a radioactive waste storage site near Morehead, Ky., suggested that tritium, cobalt–60, and other unidentified waste isotopes have migrated at least 10 m laterally from nearby burial trenches, according to H. H. Zehner. The migration appeared to be through a thin fractured sandstone bed. A computer model of the ground-water flow system at this site, developed by D. W. Pollock and H. H. Zehner, has aided in the analysis of the complex geohydrology.

Tritium tracer tests successful at Oak Ridge National Laboratory in Tennessee

Tritium tracer tests were used successfully near radioactive waste burial areas at Oak Ridge National Laboratory (ORNL) in Tennessee by D. A. Webster to determine directions and rates of shallow ground-water flow. The degree of anisotropy and the role of secondary permeability in controlling ground-water flow in weathered bedded rocks were defined at this site.

Webster's studies at another ORNL burial site showed that raising the ground surface with permeable earthfill apparently allows more precipitation to infiltrate, which, in turn, causes the water table to rise into the filled burial trenches. This, combined with the resulting steeper head gradients, increases the potential for waste migration.

Tunnel aids investigation near Sheffield, Illinois

A 1.8-m-diameter tunnel under construction at radioactive waste burial trenches near Sheffield, Ill., enabled J. B. Foster and J. R. Erickson to collect soil and ground-water samples directly beneath the trenches; apparently, tritium had migrated 1 to 2 m below one trench. Wells drilled near this trench indicated that lateral migration of tritium was as much as 30 m.

REGIONAL STUDIES

Geohydrology of salt domes in northeastern Texas

The geohydrology of Keechi, Mount Sylvan, Oakwood, and Palestine salt domes, in Anderson, Smith, Leon and Freestone, and Anderson Counties, respectively, was investigated by J. E. Carr and S. J. Halasz. These domes were selected for study by DOE as part of an evaluation of the potential of gulf coast salt domes as repositories for the disposal of high-level radioactive waste. Regional mapping of the potentiometric surface of the Carrizo-Wilcox aquifer showed that ground water flows southeast across all four domes. Limited water-level and water-quality data indicated that recharge occurs where the Carrizo-Wilcox aquifer crops out at Keechi salt dome and probably at the Palestine salt dome.

There is a potential for dissolution at all four domes, but a comparison of chemical analyses of water from wells in the region with those of water from wells near the domes showed only two wells with possibly abnormally high chloride concentrations and none with abnormally high dissolved solids concentrations. Mapping of dissolved solids within the basal Wilcox sands, based on analyses of electric logs, showed subsurface saline plumes at all four domes.

A survey of Lake Duggey, which overlies the Palestine dome, indicated a maximum lake depth of

about 5.7 m and a relatively uniform specific conductance distribution of about 6,600 μmho/cm at 25°C.

Additional geohydrologic information will be required to make a reliable assessment of the hydrologic stability of these domes.

Geohydrology of three Mississippi salt domes

Three salt domes in southern Mississippi (Richton and Cypress Creek domes in Perry County and Lampton dome in Marion County) were selected for study by DOE as part of an evaluation of the potential of gulf coast salt domes as repositories for the disposal of radioactive wastes. The shallowest and largest of the three domes is Richton dome. Depth to the salt stock is 220 m, and, at a depth of 900 m, the cross-sectional area of the dome is about 16 km^2. In a study of the ground-water hydrology in the area of these domes, C. A. Spiers found that the base of freshwater above the domes is as much as 190 m higher than the regional position of the base of freshwater and that concentrations of chloride in water wells near two of the domes are higher than those in other wells in the area. Chloride concentration exceeded 150 mg/L in water from wells near Richton dome and in water from wells east of Cypress Creek dome, whereas chloride concentrations in water from wells elsewhere in the salt basin were generally less than 25 mg/L.

Lineaments related to subsurface geology in Salina Salt Basin, New York and Pennsylvania

Studies of the potential of the Salina Salt Basin, New York and Pennsylvania, as an environment for radioactive waste repositories have indicated that salt-bearing beds are extensively folded and faulted.

M. H. Podwysocki, H. A. Pohn, M. D. Krohn, J. S. Phillips, and L. C. Rowan reported that analysis of subsurface data and Landsat images shows a correlation between lineaments and structure in south-central New York and north-central Pennsylvania. At the surface, Middle and Upper Devonian clastic rocks, in broad open folds trending east-northeast, are transected by NNW-trending lineaments. In the subsurface, units above the Salina Group (Upper Silurian) parallel the surface folds, whereas units below show no folds. Isopach maps of the uppermost Salina units reveal a large rectilinear block of salt-bearing rock, whose lateral boundaries are parallel and normal to the fold axes. Basement-controlled faulting contemporaneous with deposition during the early Paleozoic and thin-skinned thrusting in the late Paleozoic are two postulated mechanisms for the formation of this block.

Both mechanisms probably acted; basement features at the basin margins induced zones of weakness that were used later in the main period of deformation during the Allegheny orogeny.

Evidence supporting basement control is (1) high magnetic contrasts in the basement at the west edge of the block, (2) NNW-trending horsts and grabens, generally below the salt, but in some places reaching the surface, and (3) change in sense of movement from pre- to post-Ordovician time along a fault on the west edge of Lake Cayuga, New York. Evidence supporting thickening of the blocks owing to thrust-faulting is (1) seismic, well-log, and mine data showing thrust faults originating in the salt, (2) deformed fossils along the east and west margins of the block, and (3) fold axes that commonly change plunge and strike near the west margin of the block. A structure contour map suggests that the block acted as a unit regionally but was broken into many small blocks locally by tear faults.

Thickness of bedded salt in northeastern Ohio

S. E. Norris reported that the salt-bearing beds of the Salina Formation in a 650-km^2 area near Lake Erie, in eastern Lake, northwestern Ashtabula, and northeastern Geauga Counties, Ohio, are less than 915 m deep and range in aggregate thickness from about 90 m in the northern part of the area to more than 137 m in the southern part. The aggregate thickness of salt, exclusive of the intervening rocks, also increases southward, from about 30 m to more than 60 m. The thickest salt bed, the F–1–A salt (Rickard, 1969) is 10.7 to 11.6 m thick in northeastern Geauga and southeastern Lake Counties.

Complexity of structure and hydrology of Eleana Formation confirmed at Syncline Ridge, Nevada Test Site

Detailed geophysical investigation of argillite in the Eleana Formation in the vicinity of Syncline Ridge on the Nevada Test Site, reported by D. B. Hoover, have indicated even greater structural complexity than indicated in earlier studies. Data from a wide range of geophysical surveys combined with earlier drill-hole information revealed major faulting parallel to a synclinal axis in the area studied. This block of the Eleana has now been ruled out as a potential site of a repository for radioactive waste.

Hydrologic conditions in the Syncline Ridge block are also complex. J. E. Wier, Jr., and J. N. Hodson (Fenix and Scisson, Inc.) reported that hydraulic heads measured by shut-in pressure techniques in

the upper parts of the section are smaller than those measured at depth. Extremely low transmissivity was measured in the fine-grained beds tested. A strike-slip fault trending east-west through the study area constitutes a major barrier to ground-water flow. The difference in water level across this fault is on the order of several tens of meters.

Paradox Basin, Utah, explored for high-level waste repository location

USGS exploration in the Paradox Basin, Utah, in 1978 included monitoring the drilling of three DOE test wells on the Salt Valley anticline, Grand County, Utah, and regional hydrologic and geophysical investigations.

R. J. Hite coordinated these activities and monitored the drilling program. He reported that the deepest hole (DOE No. 3) was cored almost continuously from 42.7 m to its total depth at 1,242 m. Core recovery in the caprock was poor, especially in intervals of dolomitic siltstone. This rock type has a tendency to disaggregate when wetted by the drilling fluid. From 171 to about 436 m, this hole penetrated an uninterrupted interval of halite. Below 436 m, the hole intersected numerous steeply dipping interbeds of anhydrite, dolomite, and black shale. Folding and reverse faulting of these interbeds resulted in the hole penetrating the same bed several times. All cores from the interbeds were observed to bleed gas and oil when first removed from the core barrel. However, drill stem tests of the interbed intervals showed that hydrocarbons were present only in low volumes. Attempts to correlate the interbeds intersected in DOE No. 3 with established regional stratigraphy of the Paradox Member of the Middle Pennsylvanian Hermosa Formation have so far been unsuccessful. Although the Salt Valley anticline is known to contain numerous potash deposits, only two thin and low-grade deposits of carnallite were found in DOE No. 3. Two shallower holes (DOE No. 1 and No. 2) did not encounter any potash interbeds.

According to F. E. Rush, the following tentative conclusions can be drawn from the drill holes about the hydrology of Salt Valley anticline:

- The Paradox Member interbeds that were penetrated are very low in permeability.
- The salt beds penetrated are virtually impermeable.
- The caprock does not have enough permeability to be utilized as an aquifer, but it does have enough permeability to allow some ground-water circulation.
- Water salinity is stratified, with concentrations increasing downward within the saturated part of the caprock.

Electromagnetic, electrical, gravity, and seismic surveys were carried out in the vicinity of the drill holes. Two types of loop-loop electromagnetic surveys were performed, high-frequency Slingram and Extremely Low Frequency (ELF). R. D. Watts reported that the Slingram detected considerable variation in the near-surface electrical conductivity. The variation is most likely due to variations in the water content of the near-surface rock. The surface rock is the insoluble residue from dissolution of the salt and is quite inhomogeneous. The deep-looking ELF survey detected the presence of the salt, with no indication of a highly conductive layer just above it. This supports the idea that there is no continuous aquifer in contact with the crest of the diapir. H. D. Ackerman reported that the seismic data clearly defined the top of the salt body. It appears to have depth variations on the order of tens of meters, with a systematic dip of the top of the salt body to the northeast. A possible foundered block of sandstone(?) was identified, but there was inadequate information to determine whether it penetrated the salt mass.

J. D. Friedman and S. L. Simpson (1978) compiled a lineament map of the northern Paradox Basin at a scale of 1:400,000, using computer-enhanced Landsat images. The map shows numerous previously unmapped northeast-trending lineaments between the Green River and Yellowcat Dome; confirmatory detail on the structural control of major segments of the Colorado, Gunnison, and Dolores Rivers; and new evidence for late Phanerozoic reactivation of Precambrian basement structures. Lineament trends appear to be compatible with the postulated Colorado River lineament zone, with geophysical potential field anomalies, and with a NNE-trending basement fault pattern. Combined Landsat, geologic, and geophysical field evidence for this interpretation includes the sinuosity of the composite Salt Valley anticline, the transection of the Moab-Spanish Valley anticline on its southeastern end by NE-striking faults, and possible transection of the Moab diapir. Similarly, NE-trending lineaments in Cottonwood Canyon and elsewhere are interpreted as manifestations of structures associated with northeasterly trends in the magnetic and gravity fields of the La Sal Mountains region. Other long northwesterly lineaments near the western termination of the Ryan Creek fault zone may be associated

with the fault zone separating the Uncompahgre uplift from the Paradox Basin.

WASTE ISOLATION PILOT PLANT SITE, SOUTHEASTERN NEW MEXICO

Dissolution history of evaporite beds defined

G. O. Bachman continued to define details of the dissolution history of subsurface salt and gypsum in the region explored for the Waste Isolation Pilot Plant (WIPP) site. A volcanic ash was found in the Gatuna Formation which G. A. Izett considers to be equivalent to Pearlette type "O" (ca. 600,000 years B.P.). This date is of considerable value for the timing of major events. The Mescalero caliche overlies the Gatuna and is generally a pedogenic deposit that began to form about 500,000 years ago.

Some broad karst features were formed before Gatuna time, and collapse sinks were active during Gatuna time. During most of Mescalero time the region was relatively quiescent. Since Mescalero time, sulfate-bearing ground water has percolated through parts of the region. Dissolution, accompanied by karst development, is continuing today.

Hydrologic testing of strata associated with Permian bedded salt

Hydrologic investigations of the WIPP site continued with the drilling of hydrocomplexes at three new locations. A hydrocomplex is composed of a cluster of three holes at each location, each hole extending to and completed in a different water-bearing zone. The holes range in depth from 126 m to 328 m and tap the Magenta and Culebra Dolomite Members in the Permian Rustler Formation and the contact between the Rustler and the underlying Salado Formations. Testing of the formations of low yield has necessitated developing specialized techniques and the use of inflatable packers and pressure transducer systems.

J. W. Mercer found that the transmissivity of most water-bearing beds above and below the salt in the Salado Formation is very low. Preliminary analyses of data from the new hydrologic test wells resulted in the following values of transmissivity (m^2/d):

Test Well	H4	H5	H6
Magenta Dolomite Member	5×10^{-2}	2×10^{-2}	3×10^{-2}
Culebra Dolomite Member	8×10^{-2}	3×10^{-2}	—
Rustler-Salado contact zone	4.6×10^{-6}	—	—

Computer model of gamma spectra in boreholes

Ulrich Schimschal developed a computer model that simulates the response of a well-logging probe used to record gamma spectra in boreholes. For each spectral component, the model allows for variations in borehole size, bed thickness, and porosity. The purpose of this model is to permit the quantitative analysis of borehole gamma spectra for radioisotopes that have migrated from waste-disposal sites and to provide information on lithology and ground-water migration from areas where natural radioisotopes occur.

Development of a borehole neutron generator

According to W. S. Keys, a borehole neutron generator was assembled and successfully tested in a laboratory. An output of 10^8 neutrons/s was obtained from a probe less than 10 cm in diameter. Although more work is needed to develop it into a field-logging probe, the generator has potential for both borehole neutron activation analyses and pulsed neutron logging, capabilities that could be used to obtain accurate subsurface porosity data.

GEOPHYSICS

Effects of heat-induced fluid flow near a buried canister of high-level radioactive waste

The heat from a canister of high-level radioactive waste buried in geologic media will result in fluid expansion and (or) the formation of steam, which will drive fluid away from the canister. C. R. Faust and J. W. Mercer applied a numerical model for heat transport in water- and (or) steam-saturated media to several hypothetical problems for a variety of geologic settings. The model is based on the assumption of an ideal porous medium, but it was modified to include fluid-pressure-dependent permeabilities, which were thought to be important in fractured media. In the model, canisters were assumed to be 3.0 m in length, spaced on 16.5-m centers, and to generate more than 1 kW of heat. The surrounding medium had a relatively high porosity (larger than a few percent). For geologic media of moderately low permeability (10^{-12}–10^{-17} m^2), induced ground-water flow resulted. In materials of low permeability ($<10^{-18}$ m^2), high fluid pressures resulted; these pressures could cause hydraulic fracturing of the surrounding rocks. The effects of fluid-pressure-dependent permeability were not highly significant.

Computer programs to relate acoustic waveforms and fracture permeability in boreholes

F. L. Paillet developed a computer program to determine the relationship between digitized acoustic waveforms in a borehole and fracture permeability. Programs have been written for identifying modes of wave propagation in boreholes through the exact solution of the wave equation (as a function of lithology and the frequency content of the source) and for plotting logs of amplitude and frequency attenuation across fracture intervals identified on the acoustic televiewer log. Preliminary results suggested that amplitude variation in tube waves can provide information on the extent of hydraulic connection between the borehole fluid and a fracture system.

Borehole geophysical logs of granitic rocks in Manitoba, Canada

W. S. Keys made a series of geophysical logs of three test holes in granitic rocks at the Whiteshell Nuclear Reactor Establishment, Manitoba, Canada. The holes were drilled to investigate igneous rocks as possible host media for disposal of high-level radioactive waste. Interpretation of the logs indicated the unanticipated occurrence of water-transmitting fractures at depths greater than 396 m. Resistivity logs indicated that water below the deeper fracture zones was saline; the electrical conductivity of the water was greater than that of the shallower water by a factor of 30.

An electronics circuit, developed by A. E. Hess, was used to produce an acoustic amplitude log that provided additional evidence of the existence of open fractures.

T. A. Taylor used recently developed computer software to crossplot digitized logs from these holes. Crossplotting is the plotting by computer of logged measurements at equivalent depths, for each of several pairs of log types, in order to infer lithologic characteristics. The crossplots demonstrated that various igneous rock types can be distinguished by using this method of interpreting conventional geophysical logs.

GEOCHEMISTRY

Computer programs simulate distribution of aqueous uranium species

D. L. Parkhurst, D. C. Thorstenson, and L. N. Plummer reported that work continued on the development of the computer program PHREDX for computing aqueous speciation and mineral solution and precipitation for chemical reactions in hydrogeochemical systems.

As a result of previous work by F. J. Pearson, Jr., who used the program to model geochemical processes in the Edwards Limestone aquifer of Texas, PHREDX was adapted to model the distribution of aqueous uranium species as a function of pH and Eh. Pearson also modified WATEQF (L. N. Plummer, B. F. Jones, and A. H. Truesdell, 1976) to determine distribution of uranium species; the resulting program, WATEQU, is now available for use.

Feedback effects analyzed in salt dissolution

The potential for salt dissolution is an important factor in assessing the long term risk related to the isolation of radioactive waste from the biosphere in a mined repository in salt. H. R. Shaw made use of the simulation language DYNAMO (Campbell and others, 1978, Chapter B Appendix) to analyze dissolution times under a variety of conditions. Factors that were varied in the simulations were thermal loading, porosity of backfill material, fluid flow rates, and faulting frequency for a hypothetical repository in a halite member of an evaporite sequence, at a depth of about 600 m, separated from sandstone aquifers by shale interbeds. Included in the analysis were feedback relationships between rate of salt removal and propagation of openings.

The simulations showed that times for extensive salt dissolution ranged from as little as a thousand years to more than a million years, given a triggering mechanism to start dissolution. The time ranges for dissolution are independent of the nature of the triggering mechanism and depend principally on fluid flow rates. The influence of the various factors varies with time, so it is not possible to predict long-term feedback effects on the basis of rates calculated for the initial stages of dissolution.

Tritium removed from tritiated water by bacteria

When certain strains of *Pseudomonas sp.* are grown in tritiated water, they transfer the tritium as tritiated water (HTO) into the cell and incorporate it as part of a polysaccharide complex that forms a slime layer around the bacteria. Experimental findings indicate that the radioactivity of the tritium per milligram of hydrogen in the slime layer is significantly higher than that in the medium. F. A. Sisler and J. L. Zeliber, Jr., suggested that a biological concentration technique might be an economically feasible method to remove environmen-

tally objectionable tritium from wastewater produced at nuclear facility sites.

FLOODS

Three major categories of flood studies by the USGS are (1) measurement of stage and discharge, (2) definition of the relation between the magnitude of floods and their frequency of occurrence, and (3) delineation of the extent of inundation of floodplains by specific floods or by floods having specific recurrence intervals.

OUTSTANDING FLOODS

Flood in northeastern Georgia resulting from failure of dam on Toccoa Creek

The Kelly Barnes Dam on Toccoa Creek, 4 km northwest of Toccoa, Ga., failed at about 1:30 a.m. on November 6, 1977, after a 4-day rainfall of 183 mm. Thirty-nine deaths and $2.8 million in damages resulted.

C. L. Sanders and V. B. Sauer reported that high-water marks and valley cross sections were surveyed over a 7-km reach downstream from the dam to document the disaster. Topographic maps were made of the lakebed and broken dam.

Kelly Barnes Dam was constructed in 1937 on a 12-km^2 drainage basin and incorporated an 1899 rock-crib dam which was built for power generation. The earth dam, 122 m long and 12 m high at the break, impounded about 0.8 million m^3 when it failed.

Upstream from Kelly Barnes Lake, a computed discharge of 23,500 L/s indicated a recurrence interval of about 10 years. The outflow attenuated from 680,000 L/s to 104,000 L/s 8.7 km downstream at Georgia Highway 184. Main channel depths varied from 4.6 to 6.4 m.

Profiles with and without the unbroken dam in place were estimated by computer modeling using postflood cross sections. Sediment size ranged from less than 0.062 mm to greater than 256 mm.

Changes in valley environment caused by floods of December 1977, Mount Rainier, Washington

Areas in the vicinity of Mount Rainier, Washington, severely damaged by floods in December 1977, were examined by R. S. Sigafoos in September 1978. Detailed studies of many of the areas by Sigafoos and E. L. Hendricks (1961, 1972) indicated that catastrophic floods probably produce massive changes in valley environments. Some of the areas were so changed by erosion and deposition during the December 1977 floods that they were not recognizable. The brief reconnaissance study showed that this alpine region, which includes many vacation cabins, is subject to frequent major environmental changes.

Flood of July 1978 in Kickapoo River basin, Wisconsin

P. E. Hughes reported that intense rainfalls early in July resulted in severe flooding in the Kickapoo River basin in southwestern Wisconsin. The Kickapoo River valley between Norwalk and Wauzeka, an area 193 km in length that contains nine incorporated communities, was inundated. The drainage area upstream from the mouth at Wauzeka is 1,991 m^3.

Recurrence intervals of peak flows approximated 100 years. Peak discharges at gaging stations at La Farge and Steuben, 406 m^3/s and 440 m^3/s, respectively, were the greatest since 1938. Antecedent meteorological conditions, extent of inundation, water-surface profiles, and impact of the flood on the valley system are under investigation, in cooperation with the Wisconsin Department of Natural Resources and the Wisconsin Geological and Natural History Survey.

Countermeasures for hydraulic problems at bridges

J. C. Brice and J. C. Blodgett developed guidelines to assist design, maintenance, and construction engineers in selecting measures that can be used to reduce bridge losses attributable to scour and bank erosion. These guidelines are based on case histories of 224 bridge sites in the United States and Canada, on interviews with bridge engineers in 34 States, and on a survey of published works on countermeasures. Each case history includes data on bridge, geomorphic, and flow factors; a chronological account of relevant events at the site; and an evaluation of hydraulic problems and countermeasures. Problems at piers occurred at 100 sites, and problems at abutments occurred at 80 sites. Problems are attributed to local scour at 50 sites, to general scour at 55 sites, and to lateral stream erosion at 105 sites. Performance ratings are given for rigid and flexible revetment, for flow-control measures (spurs, dikes, spur dikes, check dams, jack fields), and for measures incorporated into the bridge. Streams are classified for engineering purposes into five major types, each having characteristics of lateral stability and behavior that need to be taken into account in the design of bridges and countermeasures. Hydraulic analyses were carried out for flood conditions at 60

bridges, for which values of flow, bridge, and geomorphic factors were tabulated.

Evaluation of dam-break flood-wave models

L. F. Land is conducting research to evaluate selected computer models for the simulation of flood waves resulting from a dam failure. The objective is the selection, development, and documentation of a general-purpose dam-break flood-wave model for field use.

The extreme magnitude of a flood resulting from a dam failure, often producing a peak discharge of 10 to 25 times that of a 100-year flood, requires a model that can handle a wide variation and a very high rate of change in discharges. It also appears that dams are often located on creeks or rivers where supercritical flow is common. The results to date indicated that a modified Puls routing method may be the most practical model for steep streams with complex geometry. For streams on moderate slopes and with simple geometry, a nonlinear implicit finite-difference model of the Saint-Venant equations probably is the most practical method.

Analysis of flood-data network for regional information

The techniques for analyzing hydrologic data networks that were outlined by M. E. Moss and M. R. Karlinger (1974) were used by G. D. Tasker and Moss (unpub. data, 1978) to analyze a flood-data network in northwestern Arizona. This case study showed how the standard error of the regression model is expected to change as a function of the number of stations operated over a specified planning horizon. The results will be useful to network managers who must decide whether to discontinue data collection at the present sites or to shift data-collection activities to new or additional sites.

FLOOD-FREQUENCY STUDIES

Flood hydrology of foothill streams in Colorado

Preliminary results of a flood-frequency analysis of mixed population flood records in Colorado by R. C. Christensen and J. L. Ebling indicated that the composite flood-frequency relation, formed by the statistical combination of separate snowmelt and rainfall annual flood arrays fitted to the log Pearson type III distribution, provides a significantly better fit of the higher peaks than the flood-frequency relation based on the mixed annual flood array.

Long-term gaging station records for Colorado streams such as Bear Creek, Clear Creek, North and South Saint Vrain Creeks, South Boulder Creek, and the Big Thompson River were used to develop annual arrays for mixed, snowmelt, and rainfall floods. After fitting the separate annual flood arrays to the log Pearson type III distribution, it was noted that the mixed flood-frequency relations had large positive skew coefficients—sometimes greater than one, the snowmelt flood-frequency relations conformed to the typical pattern of high mountain streams having slightly negative skews, and the rainfall flood-frequency relations approximated the plains streams having near-zero skews. The snowmelt and rainfall relations were combined by the formula:

$$P(\text{composite}) = P(\text{snowmelt}) + P(\text{rainfall}) - P(\text{snowmelt} \times \text{rainfall}),$$

where P = probability of occurrence. For each station, the resulting composite relation was graphically compared with the other relations. Generally, the composite and rainfall relations were nearly identical for recurrence intervals greater than 10 years and gave a better fit of the higher peaks than the mixed flood-frequency relation.

To conveniently handle the annual flood data for more than 100 stations, data storage and retrieval files for the snowmelt and rainfall flood arrays were created on the Survey's IBM 370/155 computer in Reston, Va.

Flood-stage frequency relations of lakes in Florida

M. A. Lopez developed regional flood-stage frequency relations by multiple regression analyses, based on log Pearson type III distribution, of the change in volume between annual maximum stage and average stage for 16 gaged lakes in Polk County, Florida, and adjoining areas. The 10-, 50-, 100-, and 500-year changes in volume were regressed against watershed parameters of drainage area, surface area at average stage, and difference between lake volume at average stage and at the stage of zero outflow. Standard errors of estimates ranged from ±32 percent to ±42 percent. The error in elevation ranged from ±0.1 to ±0.8 m. The regional analyses were used at ungaged natural lakes having drainage areas of more than 10.4 km^2.

Flood-stage frequency relations for ungaged lakes, ponds, and depressions having drainage areas of less than 10.4 km^2, strip mining pits, and interconnected lakes were determined by using a combined Soil Conservation Service hydrograph inflow model (U.S. Department of Agriculture, 1972) and a storage routing model. The model computes the change in the stage of a single lake or up to five interconnected lakes, where culvert outflow is dependent on

head change between lakes, channel or embankment outflow, and leakage to the underlying aquifer.

Flood profiles of Skunk River and tributaries in Iowa

A. J. Heinitz and S. W. Wiitala (1978) compared heights of major floods with heights of 50-year floods along the Skunk River and its tributaries downstream from Ames, Iowa. Magnitude and frequency of floods, stages, and water-surface profiles were determined for a 10,400-km^2 area that included the Skunk River, South Skunk River, and downstream reaches of Squaw Creek (13.2 km), Indian Creek (18.7 km), North Skunk River (134.0 km), Cedar Creek (89.8 km), and Big Creek (34.9 km).

Magnitude and frequency of peak discharges on small streams in Louisiana

A. S. Lowe developed techniques for estimating magnitude and frequency of peak discharges on small streams in Louisiana. Drainage area, main-channel slope, and annual precipitation were used as independent variables to define Statewide regression equations for estimating the magnitude of peak discharges with recurrence intervals ranging from 2 to 100 years. Nonlinear regression equations are applicable for watersheds that drain less than 26 km^2, have main-channel slopes between 0.94 and 18.9 m/km, and are not affected by regulation.

Flood magnitude and frequency in three regions of Massachusetts

Peak-discharge estimating techniques for rural ungaged streams in Massachusetts were improved by using three, rather than two, State hydrologic regions, according to S. W. Wandle, Jr. Average standard error of estimate for the 0.02 exceedance-probability peak discharge was 46, 42, and 36 percent, respectively, in the eastern region (coastal river basins), western region (river basins west of the Connecticut River), and central region (remaining basins east of the Connecticut River). Flood peaks with 0.5 through 0.01 exceedance probabilities are very much related to drainage area and main-channel slope in the eastern region. The significant independent variables in the central region are drainage area and a storage factor, and, in the western region, they are drainage area, main-channel slope, and a temperature index.

The standard errors were reduced an average of 8 percent over those previously defined (S. W. Wandle, Jr., 1977). This was attributed to the identification of three hydrologic regions, improvement in the sample of flood peaks with additional adjustments for high outliers, and the inclusion of synthetic flood peaks at nine sites. The synthetic flood-peak discharges were generated from the USGS rainfall-runoff model calibrated to sites with drainage areas between 1.27 and 19.5 km^2 and time of discharge concentration (TC) between 1.3 and 14.4 hours. Final flood-frequency curves at the model sites were computed from a weighted average of the synthetic frequency curve and the observed winter frequency curve.

Flood-frequency relations for small streams in Nevada

The 10- to 100-year flood magnitudes for 71 uncontrolled drainage basins less than 260 km^2 in area were regressed against basin and climatic characteristics. According to Otto Moosburner, preliminary results indicated that floods of different recurrence intervals are proportional to drainage basin size and are inversely proportional to basin altitude and basin latitude. Standard errors of estimate are about 0.4 log units, typical of those for other regions in the semiarid Southwest.

Magnitude and frequency of floods on unregulated rural streams in New York

T. J. Zembrzuski, Jr., and Bernard Dunn developed techniques for estimating the magnitude and frequency of floods at ungaged sites on unregulated, rural streams in New York (excluding Long Island). The frequency-discharge data and basin characteristics of 220 stream-gaging stations in New York and adjacent States were used in multiple linear-regression analyses to develop equations for floods with 2- to 100-year recurrence intervals. Separate equations were developed for northern, southeastern, and western New York. Standard errors of estimate of the 100-year flood ranged from 32.9 percent in the southeastern region to 42.8 percent in the western region. Drainage area is the independent variable needed in all equations; other variables needed, depending on region, are main-channel slope, storage index, and mean annual precipitation.

FLOOD MAPPING

Flood-prone areas in Helena, Montana

R. J. Omang and Charles Parrett completed comprehensive studies of the hydrology and hydraulics along Last Chance Gulch which flows through Helena, Mont., and Prickly Pear Creek which flows northward through east Helena. Magnitude and

frequency of annual peak streamflows were analyzed, and areas inundated by 100-year floods were delineated on maps. The 100-year flood for Prickly Pear Creek was 360 m^3/s. The 100-year flood for Last Chance Gulch was 84 m^3/s at the upstream end of the study reach and 88 m^3/s at the downstream end.

Maps of flood-prone areas

Areas inundated by the 100-year flood are outlined on topographic maps as part of the National Progam for Managing Flood Losses. According to G. W. Edelen, Jr., nearly 13,000 such maps have been completed for all States, the District of Columbia, and Puerto Rico. The objectives of this activity are to rapidly inform cities and towns of the general extent of their potential flood problems and to identify areas of potential flooding downstream from dams or reservoirs where structural failure could result in extensive loss of life and catastrophic flood damages.

Flood-hazard maps are used extensively to meet local planning needs and to meet the objectives of the National Flood Insurance Act of 1968, the National Disaster Protection Act of 1973, and Executive Order 11988.

An investigation to define simple but reliable techniques for estimating the magnitude and frequency of future floods at ungaged sites, based on an evaluation of flood-producing (basin) characteristics at about 10,000 sites, is in progress.

Inundation maps of urban areas

Maps showing areas inundated by major floods, flood profiles, discharge-frequency relationships, and stage-frequency relationships were published during the current year as Hydrologic Investigations Atlases for Johnston Station, Magee, Summit, and Waldrup, Miss. (B. E. Colson, C. O. Ming, and G. J. Arcement, 1978 a,b,c,d,e), and Libuse and Olive Branch, La. (G. J. Arcement, B. E. Colson, and C. O. Ming, 1978 a,b).

EFFECTS OF POLLUTANTS ON WATER QUALITY

PCB transport in the upper Hudson River

Comparisons of 23 Hudson River water samples with 23 samples of treated river water indicated that the Waterford, N.Y., treatment plant removes 97-percent of PCB and 94 percent of iron from water, according to N. E. Peters. Only 14 of the 23 raw water samples contained detectable PCB concentrations, and only one of these had a concentration higher than the suggested maximum of 1 $\mu g/L$. The samples were also analyzed for iron and lead concentrations. Although treatment was less effective for lead (57 percent removal) than for PCB's, all samples of treated water contained lead concentrations below the recommended maximum of 50 $\mu g/L$. Iron concentrations in all but one sample of the treated water were below the recommended maximum level of 300 $\mu g/L$.

Organic compounds in ground water

Minnesota.—M. F. Hult reported that geophysical logging of a visibly contaminated multiaquifer well at a coal-tar distillation and wood preservative plant in St. Louis Park, Minn., showed that contaminated water is flowing down the well bore into the Prairie du Chien-Jordan aquifer at a rate of approximately 6 L/s. M. E. Schoenberg found that at least 25 multiaquifer wells have been drilled on and near the site and that all four major aquifers in the Minneapolis-St. Paul metropolitan area may have been affected by organic compounds derived from coal tar. As early as 1932, a municipal well completed in the Prairie du Chien-Jordan aquifer was abandoned because the water tasted of coal tar. Test drilling indicated that organic compounds have moved at least 1,200 m from the site through glacial drift to a buried bedrock valley and into the St. Peter aquifer. Chemical analyses of cores of contaminated drift suggested that the rate of movement of the individual compounds that compose coal tar varies widely. Compounds with a high solubility in water, such as napthalene (solubility = 30 mg/L), are moving from the site at greater concentrations than compounds such as pyrene (solubility = 0.13 mg/L) and chryzene (solubility = 0.0018 mg/L).

New York.—According to R. A. Schroeder, several organic compounds on EPA's list of priority pollutants have been found in ground water throughout New York State. Semiquantitative analyses using gas chromatography–mass spectrometry (GCMS) techniques were conducted on water from shallow water-table aquifers at about 50 locations Some commonly used industrial solvents, such as methylene chloride and toluene, appeared to be present above detection limits of 0.1 $\mu g/L$ at virtually all sites. These and other organic chemicals occurred at elevated concentrations of 1 to 100 $\mu g/L$ at locations where the ground water is recharged by a contaminated stream and where there

is evidence of surface storage of organic chemicals, in barrels or in landfills, for example.

Subsurface storage of liquid industrial waste

R. W. Hull, C. A. Pascale, and C. M. Martin (1977, 1978) are continuing an investigation of two underground waste-injection systems in western Florida, one near Pensacola and the other near Milton, in which liquid industrial wastes are injected into a confined saline limestone aquifer of low transmissivity. In 1978, 4 million m^3 of acidic industrial waste were injected at the site near Pensacola, and 0.8 million m^3 of treated industrial waste were injected at the site near Milton. Injection rates and wellhead injection pressures had changed little since 1977. Monitor wells at the two sites indicated no chemical changes in aquifers overlying the injection zone. Monitor wells in the injection zone, however, showed significant increases in alkalinity and in concentrations of dissolved organic carbon, methane, and carbon dioxide. Alkalinity (as bicarbonate) had increased from 270 to 933 mg/L since 1973 at a monitor well 2 km south of the Pensacola site. Similar increases were detected in the injection zone at the Milton site.

Preliminary analyses indicated that the plume of sewage-affected ground water is characterized by the presence of ammonia, MBAS (detergents), and boron and by concentrations of dissolved solids that are as much as 5 times greater than background levels. Ongoing exploration has shown that the contaminated water extends more than 2,440 m downgradient from the disposal site. At 610 m downgradient from the disposal site, the plume is at least 760 m wide and more than 30 m thick.

Ammonia concentrations in ground-water samples from as far as 1,220 m south of the disposal site have exceeded 9 mg/L. MBAS levels as high as 0.8 mg/L, boron levels as high as 0.34 mg/L, and specific conductances exceeding 400 μmho/cm were found in ground water from 350 to 2,440 m south of the disposal site. Background levels of ammonia, MBAS, and boron in the study area generally were less than 0.05, 0.00, and 0.05 mg/L, respectively. Specific conductance of natural ground water in the study area usually was less than 80 μmho/cm.

Effects of mining on water quality

Colorado.—During an investigation of movement of metals in ground water, D. B. Grove, L. F. Konikow, and R. W. Miller found concentrations of hexavalent chromium greater than 50 μg/L in ground and surface waters near the city of Telluride, Colo. Water containing more than 50 μg/L of chromium is generally considered unfit for human consumption, but samples collected during October 1978 from wells that were intended to be part of the city's water supply contained more than 200 μg/L of chromium. The chromate is believed to be related to the discharge of mill-processing wastes into the alluvium aquifer draining the valley.

Idaho.—L. L. Thatcher reported that 11 trace elements, including the toxic trace elements selenium, cadmium, and arsenic, were determined by neutron activation analyses in spring runoff from the Blackfoot River basin of southeastern Idaho. In addition, the presence of radium and radon was determined by radioactivity count. These data are indicative of the environmental impact of expanded phosphate mining. Although trace-element concentrations were high in runoff from ore faces, concentrations of selenium, cadmium, and arsenic diminished to less than 10 μg/L in the Blackfoot River.

Illinois.—Discharge hydrographs for streams in unmined control basins in Illinois have higher and sharper peaks than hydrographs for streams draining strip mined land, according to T. P. Brabets. Base flow, however, remains higher in the streams which drain the strip mined land. Sulfate concentrations and specific conductance, indicators of dissolved solids concentrations, are higher in water draining from the mined land than from unmined land. However, geologic differences between locations are apparently important in determining concentrations. In western Illinois, sulfate concentrations ranged from 200 to 1,000 mg/L in water from mined land and from 35 to 55 mg/L in water from unmined land. In southern Illinois, sulfate concentrations were as high as 2,700 mg/L in water from mined land and as high as 280 mg/L in water from unmined land. Specific conductance ranged from 500 to 800 μmho/cm for water from unmined land compared to 1,000 to 4,200 μmho/cm for water from mined land.

Kansas.—A. M. Diaz and C. D. Albert reported that results of data analyses of streams draining coal mined areas in Kansas showed excellent correlations between specific conductance and dissolved constituents such as calcium, magnesium, sulfate, and dissolved solids. Data from continuous monitor records of specific conductance can be correlated with concentrations of selected dissolved constituents to give regression equations that are useful for predicting concentrations and loads.

Subsurface storage of liquid wastes in Florida

G. G. Ehrlich, E. M. Godsy, C. A. Pascale, and John Vecchioli reported that extensive chemical transformations were occurring because industrial waste liquid was injected at the Milton, Fla., site. The major reaction identified involved reduction of nitrate to elemental nitrogen and concomitant oxidation of organic constituents to carbon dioxide and ammonia. Data from a backflow test of the injection well and from sampling of a monitor well 312 m from the injection well indicated that these bacteria-mediated alterations begin immediately after injection and are virtually completed within a distance of 100 m from the injection well. Based on the concentration breakthrough curve for sodium thiocyanate at the 312-m monitor well, a dispersivity of 10 m was calculated for the injection zone.

Ground-water contamination by secondary treated wastewater

A plume of sewage-affected ground water emanating from rapid-infiltration sand beds at the sewage-treatment facility on Otis Air Force Base, Cape Cod, Mass., is being mapped by D. R. LeBlanc. It was estimated that more than 22 hm^3 of secondary-treated wastewater has been discharged to the sand beds since the plant began operation in 1941. The water-table aquifer, which is recharged by the infiltrated wastewater, consists of unconsolidated sand and gravel and is estimated to be 76 to 107 m thick. The water table in this aquifer slopes to the south at approximately 1.5 m/km.

Aluminum, iron, and manganese were abundant in area streams. Suspended-metals concentrations correlated well with suspended-sediment concentrations. Bottom materials also contained significant amounts of Al, Mn, Zn, Sr, Ni, and Pb.

Caloosahatchee River assessment

According to B. F. McPherson, water quality in the Caloosahatchee River, Lee County, Florida, is affected by runoff of agricultural and urban chemicals, inflow from flowing artesian wells and shallow ground water seepage, and saltwater intrusion caused by boat lockages at the seaward lock and dam. Severe algal blooms occur during the early part of the rainy season and pose a particular threat because the river is used directly as a source of drinking water.

Insecticides in Louisiana oxbow lake beds

Seven oxbow lakes in the northeastern and central parts of Louisiana, which were once a part of the Mississippi River, were sampled and analyzed for pesticides in bed material. The results showed relatively high levels of DDT and related compounds in bottom material from five of the oxbow lakes. According to H. L. Leone, Jr., concentrations of DDT-related compounds exceeded 100 $\mu g/kg$ in bed material collected from Lake Saint Joseph and Lake Bruin. Bed material from Lake Providence, Lake Saint John, and Lake Concordia contained concentrations greater than 20 $\mu g/kg$. These lakes, which drain primarily agricultural areas, serve as major fishing areas for both sport and commercial fishermen. Because of high levels of pesticides in tissues of fish from Lake Providence, the lake was recently closed to commercial fishermen.

Nutrient content of ground water

Lake Cochituate, an urban recreational lake in eastern Massachusetts, has for years been subjected to high nutrient loads and is in a eutrophic-to-hypereutrophic state. In a cooperative study with the Massachusetts Division of Water Pollution Control, F. B. Gay and B. P. Hansen are estimating the quantities of nutrients, nitrogen, and phosphorus entering the lake from both surface- and ground-water sources.

Nineteen wells were installed at seven sites close to and around the lake to determine the concentrations and loads of nutrients carried into the lake by ground water. Results of chemical analyses of water collected from these wells indicated that relatively high concentrations of nitrate nitrogen (9.4 to 14.0 mg/L) occur in ground water at four of the seven sites. These high nitrate nitrogen values (10 mg/L is the limit recommended by EPA for public drinking-water) are from ground water located in unsewered or partly sewered urban areas, thus suggesting contamination from septic tanks, cesspools, and lawn fertilizers.

Orthophosphate and total phosphorus concentrations were low—less than 0.04 mg/L. However, the low phosphorus values, particularly that of orthophosphate, indicated absorption on soil particles or on sediment particles within the aquifer. Dissolved potassium at these sites ranged from 2.0 to 2.8 mg/L which was above background levels of 1.3 mg/L in ground-water samples collected in less urbanized areas of the Lake Cochituate watershed, thereby further suggesting contamination from sewage and lawn fertilizers.

ENVIRONMENTAL GEOCHEMISTRY

Geochemical survey of the Western Energy Regions

Five years of work in the coal-bearing regions of the Northern Great Plains and Rocky Mountains have resulted in the establishment of broad-scale geochemical baselines in 37 near-surface materials (U.S. Geological Survey, 1976; 1977; 1978). These results are based on field collections of regional scope in the northern Great Plains, the Powder River basin in Montana and Wyoming, the Bighorn and Wind River basins in Wyoming, the San Juan basin in New Mexico, and the oil-shale region of Colorado and Utah. The materials studied include bedrock formations, stream sediments, ground water, soils, and plants. Collectively, these studies define and quantify the regional geochemical background in the Western Energy Regions. Such background or baseline information is used to assess the impact of resources development, mainly coal, in the West.

A broad spectrum of topical studies have been undertaken, many of which were first perceived while doing the regional surveys and many of which used the baselines developed in the regional studies. Much of this work has focused on two broad problem areas: (1) geochemical change in vegetation and soil resulting from powerplant operations or strip-mine reclamation and (2) availability of elements in soils to native plants and in rock materials that may become plant-growth media in areas of mine-spoil reclamation. Major findings from studies of vegetation and soil chemistry in the immediate vicinity of three coal-fired powerplants in Wyoming and New Mexico indicate that (1) soils are a poor pollution-monitoring media, (2) certain element increases in vegetation near powerplants are related to blown soil-dust contamination from construction, mining operation and activities, and flyash handling, and (3) the elements S, Se, Cu, Pb, Zn, and Sr are viewed as potential stack emittants. A major conclusion from other studies of vegetation chemistry is that reclaimed surface-mined lands in the northern Great Plains coal region may induce appreciable departures from normal in the chemical composition of agriculturally important plants. The potential for the development of molybdenosis in cattle, a copper-deficiency disease, is of particular concern, as is the general increase in a phosphorus deficiency of forage plants. Yet the concentrations of other essential elements, such as zinc, seem to be enhanced.

In the first phase of the "availability" studies, three native plant materials and six chemical extracts on two soil horizons were used in order to evaluate the usefulness of these extracts in predicting soil-plant element transfers. One of the extracts, DTPA, was used to extract three different soil preparations or fractions and has been found to be the most useful predictor of the concentration of selected elements in plants in the northern Great Plains coal region. A substantially larger data base, using native plants and DTPA extracts of soils from the San Juan Basin in New Mexico, is currently being examined. These broad regional assessments of element availability will be complemented by site-specific studies of phase two. As part of the second-phase work, dominant revegetation species were collected along with topsoil and spoil materials at 12 surface coal mines in five western States. The availability of elements in topsoil and spoil to selected grasses, legumes, and shrubs will be evaluated using DTPA as an extractant. The data should provide some insight as to whether or not broad-based regulations, which detail the levels of extractable elements in spoil materials as being potentially deleterious to revegetation, are realistic.

LAND SUBSIDENCE

Pattern of land-surface subsidence changing in the Houston-Galveston area, Texas

According to R. K. Gabrysch, a shift of groundwater withdrawals from the eastern to the western part of the Houston-Galveston, Tex., area is causing accelerated declines in water levels in the western part of the area, whereas water levels are continuing to rise in the southern part of Harris County, Tex. Extensometer records indicated an increased subsidence rate in the western part of the area and a decreased rate in the southern part of the area. An extensometer in the western part of Harris County showed that 3.5 cm of subsidence occurred in 1977, and 3.9 cm occurred in 1978. During 1964–73, the average rate of subsidence was about 3.4 cm/yr. Extensometers in the vicinity of the Johnson Space Center in southern Harris County showed a subsidence of 2.7 cm in 1977, 1.7 cm in 1978 until October 5, and an increase of 1.4 cm between October 15, 1978, and January 3, 1979. During 1964–73, the average rate of subsidence was about 6 cm/yr.

The extensometer records and piezometer measurements indicated that water-level recoveries (de-

creases in stress) are sufficient to halt subsidence in the southern part of Harris County in the near future. However, analyses were complicated by the wide range of stress changes, by the compressibility of clay in a vertical direction, by the effect of shrinking and swelling of the near-surface clay on the extensometer records, and by the short period of record. Redetermination of elevations throughout the area will be completed early in 1979.

Earth fissures form in alluvial deposits that overlie buried bedrock irregularities

Preliminary results of an investigation of land subsidence and earth fissures along the proposed Salt-Gila aqueduct of the Central Arizona Project indicated that earth fissures in the alluvial deposits develop at locations that overlie bedrock irregularities. According to R. L. Laney, Chester Zenone, and L. W. Pankratz, seismic-refraction surveys and borehole data showed that earth fissures form in alluvial deposits that overlie bedrock protuberances, points of rapid change in slope of the bedrock surface, and areas where the bedrock dips steeply. Bedrock is at a depth of less than 305 m beneath most fissures and consists of granitic intrusive and metamorphic rocks and (or) a structurally competent conglomerate-basalt-mudstone unit. The preliminary data will be used to predict the areas of susceptibility for the development of earth fissures along the aqueduct alinement.

Lands above underground coal mines should be developed with caution

Results of coal mine subsidence studies in the Powder River basin, Wyoming (C. R. Dunrud and F. W. Osterwald, 1978, p. 59–67), reveal that the land surface above shallow underground mine workings should not be developed for residential or industrial use unless precautions are taken. The precautions should insure that either the mine workings are located and stabilized or that surface structures are designed to withstand deformation caused by subsidence depressions, pits, tension cracks, and compression features.

Subsidence depressions, cracks, and compression features occur above modern coal mines as much as 600 m below the surface, where much of the coal bed is removed (Dunrud, 1976, p. 8–38). However, the most damaging and hazardous subsidence effects occur above old, abandoned mines where large amounts of coal remain adjacent to unstable openings, and the mine overburden thickness is less than about 10 to 15 times the thickness of coal mined. In these areas, subsidence pits (sinkholes) may occur suddenly and without warning many decades after the mines are abandoned.

According to USGS studies, the pits form either by piping failure of surficial material above tension cracks in bedrock or, more commonly, from the upward migration of underground mine cavities by successive collapse of the cavity roofs (Dunrud and Osterwald, 1978, p. 26–33). The pits form by en masse failure of the near-surface material when the cavities have migrated to within a few meters of ground surface. The time required for surface collapse to occur depends on such factors as (1) overburden thickness and strength, (2) extent of the mined-out area, and (3) quantity of available ground water and surface water. Cyclic wetting and drying of rock units above mine cavities, which may be quasi-stable under dry conditions, promotes roof collapse and also tends to reduce the porosity and volume of the caved debris on the cavity floors.

The subsidence pits often occur suddenly and without warning, particularly the pits above unstable mine workings, where coal adjacent to the workings is strong enough to temporarily support the weight of the overburden and thus prevent minor subsidence depression from forming at the surface. In the Powder River basin, subsidence pits caused by either piping failure of surficial material above open cracks in bedrock or by plug failure above mine openings may be deeper than the original height of the mine workings because the collapsed material (1) spreads laterally into adjacent mine cavities, particularly in water-filled cavities, (2) is transported by water into mine cavities, and (or) (3) compacts more than the original material owing to wetting, drying, and dynamic loading.

Results of subsidence studies by the USGS in the Somerset mining area, Colorado, reveal that development above underground mines should be preceded by careful planning to avoid future problems caused by the local lowering of the ground surface (Dunrud, 1976, p. 38). Development above old, abandoned, shallow mines, such as in parts of the Boulder-Weld County coal field in Colorado where the overburden is less than 10 to 15 times the height of the mine workings and a substantial amount of coal remains underground, should not be developed until subsurface investigations delineate the cavities, and they either are proven to be stable or are stabilized by backfilling or grouting.

Fires are another serious problem in abandoned mines or abandoned parts of active mines, particularly where large amounts of coal were left un-

mined (Dunrud and Osterwald, 1978, p. 187–190). Air and water can enter the mine workings through subsidence cracks or pits through improperly sealed mine openings and cause spontaneous combustion of the unmined coal. Once started, the fires can spread into adjacent mine areas creating more subsidence, which in turn causes more depressions, pits, or cracks.

Mechanisms of ground failure associated with ground-water withdrawal

Two mechanisms of ground failure associated with ground-water withdrawal are indicated by field studies in Arizona and California. Geodetic data, based on closely spaced benchmarks, indicate that some earth fissures are caused by horizontal tensional strains generated by localized differential compaction. The zones of differential compaction investigated were tens of meters wide. Surface faulting can result when the zone of differential compaction becomes narrower. The subsurface conditions conducive to this localization of differential compaction include differences of thickness of compressible material and preexisting faults acting as partial ground-water barriers (Holzer and others, 1977; Holzer, 1978). Other earth fissures are more satisfactorily explained by horizontal contractions within the zone desaturated by water-table declines (Holzer and Davis, 1976). Fissures formed by this mechanism typically form polygonal patterns.

Subsidence of peatland varies with depositional environment

Regional differences in the rate of subsidence in peaty farmlands of the Sacramento-San Joaquin Delta in California correlate with differences between sedimentary facies of Holocene tidal-marsh deposits. Average rates as high as 7.5 cm/yr have been measured by soil scientists in reclaimed lands distant from the Sacramento River. Close to the river and its distributaries, however, average rates reach only 1–5 cm/yr. The difference in rate is related to organic content of sediment which, in turn, reflects depositional environment; marshes transitional with alluvial flood basins and natural levees trapped more mineral sediment than marshlands distant from the river.

Land subsidence and collapse over soluble rocks

J. R. Ege has initiated a study on the mechanisms and geologic controls of subsidence of the land surface above carbonate and evaporite rocks. Review of the literature, contacts with researchers, and field observations confirmed that subsidence of the land surface above soluble rocks does constitute a geologic hazard in rural, urban, and industrial areas. In carbonate karst regions of the Central and Southeastern States, sinkholes form when ground-surface materials collapse into underlying voids. A major triggering mechanism is fluctuating ground-water levels, caused either by natural hydrologic cycles or by man-induced disturbances such as ground-water pumping or surface-water diversion. J. G. Newton (1976) reported this type of sinkhole problem in Alabama.

Ground collapse has occurred on properties of companies engaged in salt-brining operations. Consequently, the Salt Mining Research Institute, an industry research group, is studying subsidence processes also.

HAZARDS INFORMATION AND WARNINGS

Information from USGS scientists on hazardous conditions or processes is being used in a program for Hazards Warning, Preparedness, and Technical Assistance that was formally initiated in 1977 (U.S. Geological Survey, Federal Register, 1977). The Governors of all States and Territories were informed of this program and asked to designate representaives to work with the USGS to develop procedures for communicating information on hazards and to develop information on preparedness for, and the avoidance and mitigation of these hazards. Contacts were also made with some 75 Federal agencies that have facilities, programs, or activities that may be affected by geologic-related hazards. To date, meetings have been held with the Governors' designated contacts, the State Geologists, and representatives from appropriate Federal agencies in 24 States.

Early in 1977, USGS notified officials in Billings, Mont., of a potentially hazardous rockfall. Later in 1977, a newly released map (A. M. Sarna-Wojcicki and others, 1976) that delineates the trace of an active fault that passes through the city of Ventura, Calif., was brought to the attention of the appropriate State, local, and Federal authorities.

Information developed by T. L. Holzer (1978) was sent to the Governor's designee in Nevada concerning potential hazards from continued fissuring and potential surface faulting in the Las Vegas Valley area. As part of the technical assistance aspects of this program, Holzer is collaborating with personnel of the Nevada Bureau of Mines and

Geology and the Nevada Highway Department in monitoring horizontally and vertically controlled survey lines and water-well levels in the area to better quantify the amount, type, and location of subsidence areas.

Reuben Kachadoorian (USGS) and W. H. Slater (Alaska Department of Transportation) (1978) reported on a large landslide near Kodiak, Alaska. The slide, portions of which appear to be active, is situated above a recently constructed containerized-cargo loading facility and poses a potential threat to that facility, as well as to a highway that connects the city of Kodiak with the airport. In the report, Kachadoorian and Slater discussed the potential for a sudden failure of the landslide mass that could generate a wave comparable to the tsunami that damaged Kodiak during the 1964 Alaskan earthquake. The information was communicated to the Governor's designee for Alaska and other appropriate officials. Survey personnel subsequently participated in meetings with State and local officials to advise and assist them in developing procedures for determining the severity of the hazard and planning mitigation procedures. A Geotechnical Advisory Panel, which includes representatives from USGS, the State Division of Geological and Geophysical Surveys, the City and the Borough of Kodiak and their consultants, the State Highway Department, and the U.S. Army Corps of Engineers, was established to identify data needs and design followup studies to better define the hazard.

A report by C. D. Miller (1978) describes the likely nature of future volcanic eruptions and the potential hazards to people and property in the vicinity of Mount Shasta, Calif. Subsequent to the release of this report, a series of earthquake events in the vicinity of Mount Shasta were recorded and monitored by the California Division of Mines and Geology and the USGS. A copy of this report and a letter describing the uncertainty of the relationship of the seismic events to possible eruptive activity of the volcano was sent to the Governors' designee and other appropriate officials.

Reports from studies of potential hazards from future eruptions of Mount Baker and Mount Saint Helens volcanoes in Washington (J. H. Hyde and D. R. Crandall, 1978; D. R. Crandall and D. R. Mullineaux, 1978) were sent to the Governor's designee and other appropriate officials. The reports describe the nature and extent of likely eruptive events at each volcano and the accompanying maps show areas likely to be affected by future eruptions. The USGS's volcano hazards research in the Cascades will serve as a continuing source of technical information and advice for State and local jurisdictions.

D. M. Morton and R. H. Campbell (1978) described landslides and mudflows in the Wrightwood, Calif., area that are parts of a composite cycle of landslide activity characterized by three recognizable stages. In general, the stages are (1) massive slides on the sidewalls and heads of canyons, (2) smaller slides involving the toes and lower slopes of the first-stage slides, and (3) slides and mudflows originating in the second-stage deposits. The three stages are independent, occur in sequence, and are of different duration. Mudflows developed in the third stage of the cycle have been costly to the residents of Wrightwood in the past. Morton and Campbell currently are advising State and local officials on the potential hazards from future landslides and mudflows in this area.

ASTROGEOLOGY

PLANETARY INVESTIGATIONS

The Viking Mars Mission

During fiscal year 1978 the Viking Orbiters acquired a vast amount of new photographic and other scientific data on Mars, most of which is now under analysis. Of particular interest to the geologist are color and stereo coverage of most of the surface at resolutions of approximately 500 m and extremely high resolution coverage (<8 m) of selected areas. The pictures reveal that the surface has formed through a complex interplay of volcanic, aeolian, fluvial, glacial, and tectonic activity. The new pictures are particularly rich in land forms suggestive of permafrost and glacial conditions and of pervasive mass wasting. The pictures are being organized into mosaics and cataloged to make them available to the scientific community at large. A number of USGS scientists have continued to analyze and interpret the new Viking data. M. H. Carr, Harold Masursky, and L. A. Soderblom were continually involved in Viking Orbiter mission operations while H. J. Moore, Jr., and E. C. Morris were engaged in similar mission operations for the Viking lander spacecrafts.

The two Viking landers have operated successfully on Mars since landing on July 20, 1976, and September 3, 1976. The surface samplers were parked and turned off in early May 1978 after establishing an outstanding record of operations in space. Lander cameras will continue to operate into 1979 on a limited schedule. The surface samplers and cameras have provided a wealth of information that is being analyzed to define the physical properties of martian surface materials (Moore and others, 1978a,b).

Shortly after Viking 1 landed on the surface of Mars, attempts were made by members of the Viking flight team to locate the lander on the surface of the planet by correlating topographic features in the lander pictures with similar features in the Viking Orbiter pictures. Tracking data initially indicated Lander 1 was at lat. 22.48±0.02° N. and long. 48.00±0.07° W. (aerographic coordinates). Only two features in the Lander 1 pictures were considered large enough to be recognized in the orbiter pictures. Since these first attempts at locating the Viking 1 lander, radio science experiments have increased the accuracy of the lander location and narrowed the possible search region for correlating orbiter and lander features. With the help of these new tracking data, surface features in the lander pictures were used to determine a unique Viking 1 lander location on the orbiter pictures. The location is estimated to be accurate to within 200 m. The new location is at lat. 22.487° N. and long. 48.041° W. (Morris and others, 1978).

Priestly Toulmin III, H. J. Rose, Jr., and R. P. Christian (USGS), in conjunction with B. C. Clark (Martin Marietta Aerospace), A. K. Baird (Pomona College), K. Keil (University of New Mexico), and other members of the Viking Inorganic Chemical Analysis Team (ICAT), report the acquisition and analysis of two additional samples of martian surface materials by the Viking landers and by the onboard X-ray-fluorescence spectrometers. The results generally confirm those previously reported. Bromine has definitely been identified in some samples previously interpreted as cemented by water-soluble salts, strengthening that inference.

The Pioneer Venus Mission

A preliminary base map has been constructed of the Earth-facing hemisphere of Venus from Earth-based radar images; landing locations for the USSR spacecraft Venera 8, 9, and 10 are shown. Details of mission operations and planning for the nominal and extended missions have been worked out by the Orbiter Mission Operations Planning Committee chaired by Harold Masursky. Reduced radar altimetry, radar reflectivity, and support spacecraft data are being sent directly from the Massachusetts Institute of Technology to the USGS in Flagstaff, Ariz., for analysis and use in compiling Venus maps.

The Pioneer-Venus Orbiter spacecraft was launched successfully in May and was inserted into

Venus orbit on December 4, 1978. Low-resolution radar images and radar altimetry data are currently being acquired between 75° N. and 50° S. latitudes along the subspacecraft tracks spaced 150 km apart at the Equator. During the extended mission, the ground tracks will be adjusted to obtain coverage at a spacing of 75 km at the Equator. The coarse radar images and altimetry traces, combined with high- and low-resolution Earth-based radar images of Venus, will allow the construction of mosaics and topographic maps despite cloud cover. These maps, combined with gravity and magnetic data obtained by the orbiting spacecraft, will increase our knowledge of the surface expression of geologic features. Such clues to possible volcanic, tectonic impact, and aeolian processes that have operated on Venus lead to a better understanding of those on Earth, a planet with nearly identical density and diameter. Harold Masursky is a member of the Pioneer-Venus radar team and an interdisciplinary scientist. He is working with other USGS and non-Survey scientists in analyzing the radar data and preparing topographic and radar reflectivity maps of the planet.

The Voyager Mission

The two Voyager spacecraft will encounter Jupiter and its Galilean satellites in the spring of 1979. Therefore, in fiscal year 1978 final preparations were made to prepare sequences for imaging the satellites of Jupiter and to process the data on the ground. Primary activities have included (1) completing and testing the Voyager Image Processing System, which is expected to process some 45,000 images in about 1 year, (2) redesigning and simplifying the entire encounter sequence because of a failure on the second spacecraft, (3) completing detailed plans to accomplish computer mosaicking of black and white and color imaging sequence of the satellites, and (4) adding eight scientists, four from the USGS, to the Voyager Imaging Science Team to prepare for the science analysis tasks during fiscal years 1979 and 1980. The new USGS scientists are E. M. Shoemaker, M. H. Carr, J. M. Boyce, and J. F. McCauley. L. A. Soderblom and Harold Masursky have been team members for several years. During fiscal year 1978, Soderblom continued to serve as a member of the team, as chairman of the team's data processing working group, and as deputy team leader.

On March 5, 1979, the Voyager 1 spacecraft will fly past Jupiter and its satellites, making close approaches to three of the satellites. Io, Ganymede, and Callisto will be imaged over a wide range of phase angles in both color and black and white at resolutions between 1 and 3 km. Also, the satellites Europa and Amalthea will be imaged at far encounter at a resolution of about 10 km. Of these five satellites, two are larger than our Moon and two are larger than the planet Mercury. The imaging data will be used for visual interpretation and the surface histories, as well as to prepare color or spectral albedo maps to characterize the distribution of materials on their surfaces. On July 9, 1979, Voyager 2 will make a similar pass through the Jovian system, again passing close to three of the satellites. The hemispheres of Callisto and Ganymede that were not imaged by Voyager 1 will be imaged by Voyager 2, providing coverage of about 80 percent of those bodies at resolutions between 1 and 3 km. Also, Europa, slightly larger than our Moon, will be imaged at a resolution of about 5 km. The Jovian system is important to planetary research because its satellites revolve about Jupiter in regular orbits as do the planets around the Sun. The satellites exhibit regular trends, such as decreasing density and increasing mass and volume, with increasing distance from Jupiter. Because they have identical bombardment histories (taking into account effects of Jupiter's gravity), it should be possible to compare the evolutionary histories of a collection of bodies, which range from rocky satellites to large ice balls.

The Galileo Mission

L. A. Soderblom, Harold Masursky, and H. H. Kieffer are members of a team to design and support a near-infrared mapping spectrometer (NIMS) to be flown on the upcoming Galileo mission to Jupiter that is to be launched in 1982. This instrument will map the mineral distribution of the surfaces of the satellites of Jupiter at spatial resolution of 5 to 30 km. The mineralogical provinces will be related to geologic provinces on the satellites that are delineated by a multispectral, high-resolution imaging camera. Image and composition data will be correlated wtih magnetics and gravity. The Galileo project also will provide support for activities associated with the planning of the Solid State Imaging System on the Galileo spacecraft. M. H. Carr reports that activities during 1978 included (1) evaluation of the proposed camera, (2) evaluation of proposed increases in capability, such as addition of wide-angle camera and large tape recorder, and (3) examination of typical satellite tour to assess potential science returns.

Fluvial history of Mars

M. H. Carr (1979) reports that many large martian channels arise full scale from discrete areas of chaotic terrain. Estimates of peak discharge based on channel dimensions range from 10^6 to 10^8 m^3/s. He proposes that the large channels were eroded by water released rapidly, under great pressure, from deeply buried aquifers. Early in the planet's history, the old cratered terrain was probably highly permeable to depths of several kilometers as a result of its volcanic origin and intense brecciation by meteorite impact. Extensive dissection of the old cratered terrain by fine channels suggests that warmer climatic conditions prevailed at one time and fluvial action was widespread. Much of the water that cut the fine channels was probably removed from surface circulations and entered the ground-water system. Subsequent global cooling wrapped the ground water under a thick permafrost layer and formed a system of confined aquifers. Thickening of the permafrost and warping of the surface created high pore pressures within the aquifers, particularly in low areas. Episodic breakout of water from the aquifers could have been triggered either by impact or by the pore pressure reaching the lithostatic pressure. The rate of outflow would have depended on the aquifer thickness and permeability, its depth of burial, and the diameter of the region over which water had access to the surface. Plausible values give discharges that range from 10^5 to 10^7 m^3/s. Outflow from the aquifer probably caused undermining of the adjacent areas and collapse of the surface to form chaos. Flow ceased when the aquifer was depleted or when the hydraulic gradient around the chaos, and, thus, the flow was so reduced that the flow could freeze. The process could be repeated if the aquifer were recharged.

One of the largest fluvial channels on Mars, the Valles Marineris, empties into the Chryse Basin on which the Viking 1 lander spacecraft touched down in the summer of 1976. Most workers agree that the large channels that descend into the Chryse Basin from the south and southwest have at least been modified by fluvial action. Harold Masursky suggests that questions concerning the evolution of the martian atmosphere, and the possible presence of life in the past, are intimately tied to the channel and volcanic history of the planet; the Chryse Basin may be the most promising area on the planet in which to investigate these questions. From recently acquired Viking high-resolution stereoscopic photography of the Chryse Basin and Valles Marineris regions of Mars, Masursky is (1) attempting to date the channeling, (2) estimating the volume of water that has traversed these channelways, and (3) estimating the volume of collapsed terrain that may represent melted subsurface ice that provided the water. To aid in this research, topographic contour maps of the Tithonium Chasma and Ius Chasma regions of Mars have been made at 1:500,000 scale. Numerous crater counts have been completed on a large number of channels of probable fluvial origin.

Mass wasting and periglacial processes on Mars

B. K. Lucchitta has been studying larger landslide deposits in the Valles Marineris on Mars (Lucchitta, 1978a,b). The study is based on a detailed investigation of Viking pictures in the region of the martian equatorial troughs. The pictures were analyzed stereoscopically, where possible, and the outlines of landslides mapped on enlargements of the orthophoto mosaic subquadrangles of the Coprates (MC–18) and the Margaritifer Sinus (MC–19) quadrangles of Mars. The detailed morphologic study was supplemented by crater counts and, where topographic maps were available, by an estimate of the volume of the deposit and calculations of the potential energy of the landslides.

The study showed that most large landslide deposits in wide trough sections have slump blocks near their heads and vast longitudinally grooved aprons towards their toes. In narrow trough sections, the deposits appear compressed into transversely ridged material throughout. Small landslide deposits tend to have smooth aprons that issue from walls without visible scars.

Many of the prominent slide deposits may be of similar age because they appear to be of similar freshness, though a few are degraded. Major faulting preceded most landsliding, but some minor faulting continued afterwards. Most landslides occurred after the trough walls were dissected by gullies and tributary canyons, but a few of these erosional features developed after the sliding took place. The emplacement of the landslides approximately coincided with major late eruptive activity on the Tharsis volcanoes as shown by a density of 570 ± 130 craters $>1 km/10^6 km^2$ (combined landslide deposit). An active tectonic period, probably acompanied by quakes, is indicated by the coincidence of faulting and volcanism.

Many martian landslides are larger than terrestrial ones because of the unusual height of the fault scarps on which they formed. These scarps may

have risen as high as 7 km locally because of the absence of both degradation by fluvial erosion and concomitant infilling of adjacent lows. The efficiency of the martian landslides is high; they are equivalent to known terrestrial slides with regard to efficiency versus size. The trough walls were probably highly instable owing to their great height and steep gradient, and free water may have saturated pores of poorly cemented breccia materials only about 1 km behind and below the ice-cemented free face and top surface. A quake may have initiated collapse, followed by large-scale breaking of bonds in the breccia cement and eventual wholesale liquefaction of the material of the entire lower wall section.

D. H. Scott (1978) reports that lava flows cover many areas in the northern lowland plains of Mars and embay older rocks of the highlands bordering the plains to the south. In places, the flows extend close to the highland front and have extended 400 km or more into the older residual surface left by the southward retreat of the plateau. Remnants of this older surface occur as islands above the lava-covered plains. Several hundred million years probably elapsed between the retreat of the highland surface and extrusion in the lowlands of lava that in places embays the present boundary escarpment. Viking images allow the subdivision of the lava flows of the lowland plains into several distinct lithologic units.

Volcanic deposits on Mars

G. G. Schaber and D. H. Scott are continuing to investigate the distribution and relative stratigraphy of numerous lava flows characterizing the Tharsis region of Mars. Some 14 separate eruptive periods occurred in this region. Crater density determinations indicate the volcanic activity extended over several billion years. Six major eruptive events are recognized on Arsia Mons Volcano; most flows emanated from fissure vents radial to the summit caldera, and individual flows were traced as far as 400 km. Maximum flow lengths within each eruptive sequence may reach 1,000 km. The youngest recognized eruption of flood-basalt type lavas occurred in the topographic depression surrounding the basal scarp of the Olympus Mons volcanic shield, which is the largest on Mars. Measurement of individual flow-scarp heights by D. W. G. Arthur indicate flow thicknesses between 5 and 20 m on steeper flank slopes and between 20 and 50 m on flatter terrain. On slopes of lower gradient, martian flows are comparable in their dimensions to some flows in Mare Imbrium on the Moon (Schaber and others, 1978).

H. J. Moore, Jr., has reported that yield strengths of lava flows (excluding pahoehoe) on Earth, Mars, and the Moon can be calculated using remote measurements of their thickness, widths, and levee widths (Moore and others, 1978c). Using the Bingham plastic model, yield strengths of lava flows on Earth appear to be related to both chemical composition and topographic gradient. For a given topographic gradient, silicic flows tend to have larger yield strengths than mafic flows. Yield strengths of martian and lunar flows suggest they are more akin to basalts than they are to trachytes and rhyolites.

C. A. Hodges has investigated the geologic and climatic environments of Iceland as they may approximate conditions on Mars. Especially distinctive are the table mountains that formed by subglacial eruption (Van Bemmelen, 1955; Sigvaldsson, 1968; and others). These are steep-sided pedestals of pillow lava and palagonized tuffs and breccias, overlain by subaerial flows, some of which developed into shield volcanoes. Similar cratered mesas and plateaus, especially those concentrated north of lat. 40° N., may be the martian equivalents of table mountains. If the interpretation is valid, the north polar cap of Mars must have been more extensive than at present during times of active volcanism, allowing analogous ice-magma interactions.

Eolian features on Mars

C. S. Breed and J. F. McCauley have continued their classification of martian windforms (Breed and others, 1978). The windforms recognized on Mars are remarkably similar in size, shape, and distribution pattern to those on Earth. These features include both barchanoid and longitudinal dunes, yardangs, grooved and fluted terrains, deflation pits, and eolian sheets and streaks. The present differences in wind-transport regimes on the two planets should result in different spacings and heights of dunes on Mars. Theoretical work indicates that saltation paths on Mars should be 50 times longer, under present atmospheric conditions, than they are on Earth. The finding of close similarities between the two classic types of dunes on both planets suggests that the martian dunes are relict or fossil forms that date from an earlier era on Mars when its atmosphere was more like Earth's (Ward, 1978).

J. F. McCauley, M. J. Grolier, and C. S. Breed report that field investigations of eolian processes and landforms in deserts of the Southwestern United States, Iran, the Western Desert of Egypt, and the coastal deserts of Peru indicate that the importance of wind erosion as a geologic process has been seriously understimated (McCauley, Breed, and Grolier, 1978). Effects of wind erosion are evident on surfaces ranging from relatively soft sediments to crystalline basement rocks. A vast field of yardangs was identified in the Western Desert of Egypt. These yardangs were eroded by wind in the plateau formed on dense, crystalline Thebes Limestone of Eocene age. The Egyptian yardangs probably have the widest areal extent and include some of the largest wind erosion features of any known yardang field on Earth. The development of yardangs in marble confirms the hypothesis that wind erosion produced large-scale modifications of surfaces composed of very hard rocks, as well as of rocks of lesser competencies.

Image chronology on Mars

Based on the areal density of small bowl-shaped craters in the size range of 2 to 10 km on Mars, L. A. Soderblom, C. D. Condit, and D. A. Johnson have subdivided regional plains on Mars and established their relative ages. They then used models of the impact-cratering rate for Mars over geologic time to establish approximate absolute chronologies for the martian surface units. Their primary conclusion is that the evolution of volcanic rocks on Mars has taken place at a rather steady but slow rate throughout geologic time; the major volcanic constructs in the Tharsis region appear to be as young as about 100 million years, but some may be as old as two billion years. The volcanic plains, which form the planar surfaces between large craters and the martian highlands, probably date back to the early postaccretional history, near 3.5 to 5 billion years ago.

Geologic mapping of Mercury

H. E. Holt reports that geologic mapping of the surface of the planet Mercury is continuing. It is based on the photographic and physical data returned by Mariner 10 during three flybys of the planet in 1974–75. These 1:5,000,000-scale maps will depict the stratigraphy and structure of the surface materials from which the sequence and nature of events that have affected the planetary surface are being derived (Holt, 1978; McCauley and others, 1978b).

The photogeologic studies reveal that, compared to the Moon, the mercurian surface has a deficiency of craters in the 30- to 60-km diameter range and fewer basins larger than 240 km in diameter. Fields of secondary craters occur much closer to their primary crater source, covering only one-fifth of comparable lunar secondary crater field areas. The erosive effect of these secondary swarms is significant, but the secondary craters themselves are well preserved. The oldest geologic unit, intercrater plains, extends over one-third of the planetary surface imaged thus far, and the unit appears to be volcanic deposits emplaced during the later stages of the heavy bombardment period, obliterating most of the preexisting craters. A younger outpouring of volcanic rocks produced smooth plains peripheral to the large Caloris Basin and in many more localized areas. These plains lack volcanic features common to the Moon, for example, domes, sinuous rilles, and well-defined flow fronts.

Geologic maps and summary texts materials are in the review process for the Kuiper (H–6), Tolstoj (H–8), Discovery (H–11), Bach (H–15), and Victoria (H–2) quadrangles. Quadrangles H–1 and H–3 are 75 percent completed, and preliminary geologic maps are compiled for quadrangles H–7 and H–12.

Planetary cartography and photogrammetry

R. M. Batson and associates have completed planimetric mapping of Mercury at a scale of 1:15,000,000 and of Mars at a scale of 1:5,000,000. Controlled photomosaics of Viking images are being compiled at a scale of 1:2,000,000.

The 1:15,000,000-scale map of Mercury consists of two shaded-relief renditions; one rendition has albedo patterns superposed. The 1:5,000,000-scale map of Mars consists of 30 sheets showing shaded relief derived primarily from Mariner 9 data and 15 shaded-relief sheets that have albedo-pattern overprints derived from Mariner 9 data. Six of the shaded-relief versions incorporate some Viking data, and one of the shaded-relief versions, originally compiled from Mariner 9 information, has been revised to incorporate Viking data. Work has begun on a new series of photomosaics of Viking Orbiter pictures at 1:2,000,000 scale. Sixteen sheets were completed during fiscal 1978.

Harold Masursky reports that the Viking landing-site series of maps is now complete with the publication of two controlled mosaics of the Chryse Planitia region of Mars, which includes the landing site of the Viking 1 spacecraft. Chryse Planitia,

one of the lowest areas of Mars, appears to have been the catchment basin for several large martian channel systems. The sinuous channel Bahram Vallis, and the smaller dendritic channels Vedra and Maumee Valles, cut the highlands of Lunae Planum to the west of the Chryse lowland plain. The four largest martian channels, Ares, Tiu, Simud, and Shalbatana Valles, rise in the southern highlands region of these map areas. Notched mare ridges, tear-shaped "islands," and braided and scoured areas indicate that the surface has been modified by fluvial erosion near the landing site, which is as much as 300 km from the channel source areas.

In 1978, the design of the cartographic data reduction scheme for the Voyager mission was completed. Harold Masursky reports that this design includes geometric transformation and enhancement of images by digital processing, establishment of geodetic control nets using data provided by Merton Davies (Rand Corporation), generation of controlled mosaics, and production of selected shaded-relief bases of the Galilean satellites of Jupiter. The primary goal of the Voyager mission is to generate topographic and geologic maps of five satellites of Jupiter based on $\simeq$1,500 images that will be acquired by the cameras of Voyagers 1 and 2 from March through June 1979.

S. S. C. Wu reports completion of a detailed topographic map of the Tithonium Chasma and Ius Chasma canyons located west of Tharsis Mons on Mars. This contour map shows the canyon to be deeper than 6 km and the slope of the canyon walls to vary from 20° to 28°. The map represents only a small portion of the martian equatorial canyon-system complex that extends more than 4,800 km from the region of the Tharsis uplift north and east to empty into the Chryse Planitia.

Radar investigations

Analysis of terrain roughness using radar backscatter data was continued by G. G. Schaber in support of the Venus Orbiting Imaging Radar (VOIR) mission planned for 1984 and the Shuttle Imaging Radar (SIR–A) experiment planned for 1980. The major areas of detailed investigation were Death Valley, Calif., and San Francisco Peaks in north-central Arizona.

Radar research during fiscal year 78 was concentrated on completion of a long-term study of Death Valley, Calif., using airborne radar imagery and spectral data to determine terrain microroughness statistics. Roughness statistics, such as mean relief, relief variance, mean slope, correlation length, and variance in the spectral frequency of relief, were correlated with digitized X-band (3-cm wavelength) and L-band (25-cm wavelength) radar images and calibrated radar cross-section values. Excellent correlation was found between these data sets. At present, W. E. Brown, Jr. (Jet Propulsion Laboratory), is modifying a Bragg-Rice scattering model and deriving algorithms to fit the detailed surface-roughness data for Death Valley saltpan and gravel surfaces. This technique has been used to successfully predict the covariance spectrum of relief in Death Valley with the use of measured radar cross section values and vice versa. SeaSat radar images of Death Valley are currently being analyzed.

Schaber reports that the extremely blocky basaltic andesite of the SP lava flow in north-central Arizona was significantly brighter on direct polarization K-band (0.86-cm wavelength) than on cross-polarized images taken simultaneously. The opposite was true for the longer wavelength (25 cm) L-band radar image data, where the cross-polarized returns from SP flow are brighter than the direct-polarized images. This effect was explained by Bragg-scattering models for rough surfaces. Two distinct types of surface relief on SP flow, one extremely blocky, the other subdued in relief (by ash and soil), were found to be well discriminated on the visible and thermal wavelengths images but to be separated only on the longer wavelength, L-band radar image data. The inability of the K- and X-band (3-cm wavelength) radars to portray the differences in roughness between the two SP flow surfaces is attributed to the radar-frequency dependence of the surface-relief scale, representing the transition between quasi-specular and primarily diffuse backscatter (Schaber and others, 1979).

G. R. Olhoeft, B. E. Schaefer, and G. R. Johnson have completed a series of experimental measurements to determine the relative importance of surface and volume scattering properties at radar wavelengths. The experiments were performed on Ottawa sand between 26 and 37 GHz in a microwave anechoic vacuum chamber. Both surface and volume scattering processes were found to be important in radar scattering. Measurements were performed in both the backward and forward directions (backscatter reflection and forward scatter transmission). In surface scattering, the following were found to be important variables: coherence, spacing, depth, and orientation of scatterers, as well as the angle between the antenna and the

surface, between the dominant direction of spatially coherent scatterers and the antenna E-field, and the orientation and height of the antenna relative to surface peaks and troughs in the scatterer pattern. Volume scattering was more complicated as the process was sensitive to the same variables as surface scattering, but there was also the additional complication of an interaction between the surface and volume scatterers, depending upon the depth of burial of the volume scatterers. The major conclusion is that both volume and surface scattering processes must be included in any interpretation of Earth-based or orbital microwave measurements of the surface of the Moon and planets.

Quantitative morphology of volcanoes

R. J. Pike, Jr. (1978), has shown that statistical models establish standard shapes for 20 classes of terrestrial volcanoes and provide analogs for comparison with extraterrestrial landforms. Geometric means of edifice dimensions and their ratios quantify the prevailing classification of cratered volcanoes. There are two systematic progressions of topographic form—one involving edifices that have small craters relative to size of the volcanic pile and the other involving edifices that have comparatively large craters. The continuum of pyroclastic cones, cinder cones, tuff rings, and maar reflects variable conditions (water content, for example) in the eruptive environment. The shape-continuum of caldera-bearing volcanoes from tholeiitic-basalt shield to calcalkalic ash-flow plain arises from differences in magma chemistry. According to a multivariate analysis of averaged edifice variables, the 20 classes cluster in 8 geometric groups, each of which implies a correspondingly unique process or combination of processes for forming cratered volcanoes on Earth and perhaps on other planets as well: lava shields, stratocones with summit craters, stratocones with calderas, cauldron-centered ash-flow plains, small pyroclastic cones erupted in a largely dry environment, maars, table mountains, and domes.

LUNAR INVESTIGATIONS

Basin and crater studies

In collaboration with V. R. Oberbeck and H. R. Aggarwal (Ames Research Center), D. E. Wilhelms has determined separate size-frequency distributions for primary impact craters 4.5 to 260 km in diameter formed in four time intervals and for secondary impact craters of two basins (Wilhelms and others, 1978). Each of the primary distributions differs from the others and from the secondary distributions. Each distribution has a complex form in which small craters are deficient relative to extrapolations of power functions characteristic of large craters. The sample of the pre-Nectarian primary craters is most pronounced in this respect and approximates a log-normal form. Distributions of successively younger primary populations are closer to the log-log form. Differential obliteration by younger deposits is not the cause of the disparities in distributions; such disparities may reflect changes with time in the production populations of the craters and in the objects that produced them. Many craters previously thought to be small members of the older primary populations were identified as basin secondaries, which outnumber primaries in sizes smaller than 20 km in diameter. The basin secondaries resemble secondaries of smaller craters in morphology, spatial distribution relative to their source, and slope of size-frequency distributions.

The first detailed study of the Strangways Impact Structure, Northern Territory, Australia, was made by an Australian-U.S.-Canadian team, and D. J. Milton, a team member, was primarily responsible for the geologic mapping. The structure consists of a core of uplifted granitic gneiss about 5 km in radius surrounded by a collar of upturned and overturned strata generally about 5 km wide, but nearly flat-lying overturned flaps extend locally as far as 12 km from the center. The core-collar pattern resembles that of the flaps of the Vredefort Dome, South Africa, while the flaps may be analogs of the rim flaps of such craters as Meteor Crater, Ariz., or may be features of the crater floor not recognized elsewhere. The exposed core is brecciated and commonly highly shocked and in places covered by a thin layer of impact-melted rock (Ferguson and others, 1979).

D. J. Roddy is continuing his work on combining field, laboratory, and theoretical data bases for both large-scale impact and man-made explosion craters and laboratory impact and explosion craters as a long-term effort to examine shock-wave cratering mechanics, their structural effects in rocks, and related shock metamorphism. The work is supported jointly by the Defense Nuclear Agency, Department of Defense, NASA, and the USGS.

A set of preimpact conditions, postimpact initial dimensions, and new measurements of orientations of structural features of Meteor Crater, Ariz., were presented by Roddy (1978) in numerical formats

intended to provide quantitative data for computer cratering codes, scaling relationships, and cratering analog studies. A range of energies for the formation of Meteor Crater was estimated by both diameter and volume scaling from nuclear and high-energy (HE) explosion crater data; the best average estimate is probably about 1.62×10^{23} ergs (3.95 megatons) derived from nuclear-energy volume scaling. The equivalent kinetic energy determined from explosion scaling and three assumed impact velocities (15, 25, 42 km/s) permits bounding calculations of the dimensions of the Canyon Diablo meteorite, including representative estimates of the impact area covered by a potentially fragmenting body.

Roddy (1978) also described new measurements of orientations of selected pre- and postimpact structural features including the regional joint system, faults in the crater walls, and straight segments and diagonals of the crater walls. These measurements document previous qualitative observations that jointing appears to strongly influence the orientation of both the crater faults and straight-wall segments; each group of fault directions is approximately parallel to one of six measured joint bearings.

Volcanism and tectonism studies

B. K. Lucchitta and J. A. Watkins (1978) investigated straight and arcuate lunar rilles that can be confidently regarded as structural grabens in order to date their formation. They studied the grabens on lunar orbiter photographs, measured their extent in individual geologic units, determined the age of the mare on which they are superposed, investigated their relation to basins, and established their trends. Results indicate that (1) most preserved grabens formed considerably later than the impacts that formed the basins, (2) the grabens are bounded by faults that are reactivated along older basin concentric and radial structures and lunar grid directions, (3) graben formation stopped about 3.6 ± 0.2 billion years ago and postdates early mare emplacement but precedes the eruption of lavas that cover vast areas of the nearside of the Moon, and (4) graben formation reflects a tensional stress field that was obtained during part of early lunar history. The stress field may have been lunar wide or local and associated with basins or a combination of the two.

D. H. Scott completed studies on lunar sinuous rilles and their relation to structural deformation of mare surfaces and the tectonic significance of large topographic irregularties within Mare Serenitatis (Scott, Watkins, and Diaz, 1978). The attitudes of sinuous rilles proved to be good indicators of deformation subsequent to their formation. Surface topography of Mare Serenitatis compared with the slopes of subsurface radar reflectors and stratigraphic relations of mare basalt units indicates that subsidence, faulting, and possible folding preceded the broad doming of Mare Serenitatis.

Lunar and Planetary Geoscience Consortium

L. A. Soderblom (USGS) reports that during 1978 processing of new multispectral images (0.35 to 1.0 microns) of the Moon (acquired about 1° in phase angle as the Moon emerged from an eclipse) have been completed in collaboration with D. L. Matson and T. V. Johnson of the Jet Propulsion Laboratory (JPL). Also completed are global frontside colorimetric maps of phase-angle-color variations from composites of the above image data and generation of new gamma-ray maps of Fe, Ti, Mg, and K concentrations from data supplied by J. R. Arnold (University of California, San Diego), M. J. Bielefeld (Computer Sciences Corp., Silver Springs, Md.) and A. E. Metzger (JPL). The initial stages have been completed by D. E. Wilhelms in assembling new color data and consortium remote-sensing data to produce a new lunar maria map. R. J. Pike (USGS) reports that he has begun analysis of data supplied by the Geoscience Consortium file including lunar gravity, color, laser altimetry, albedo, and bistatic radar. Generation of new, improved X-ray fluorescence maps by P. E. Clark (USGS), using Earth-orbiting SOLRAD data for control, has resulted in a variety of new correlations between gamma-ray and X-ray data (Clark and others, 1978). B. R. Lichtenstein (University of Arizona) and others (1978) report correlations between new Apollo orbital magnetometer maps with a new map of Explorer 35 bow shock measurements and with electron reflection data. M. J. Bielefeld and others (1977) report consortium file correlations between lunar color, gamma-ray, Ti, Fe, and X-ray data. Numerous color maps showing various correlations of lunar data sets were produced as frontispieces for the Ninth Lunar and Planetary Science Conference Proceedings.

A major program system to digitize and manipulate map data has been developed. The system has routines to edit raw data from line-digitizing systems and to put the line data into raster format.

Other routines are available to interpolate elevation values between contour lines to make terrain data sets in raster format, to assign attribute codes to units in line maps that have been digitized, to fill these units with specified colors and patterns, and to output black-and-white color separation plates for preparation of press-ready halftones (thus eliminating the necessity for preparing peel coats). Routines were also developed for transforming digitized maps from one projection to another without introducing distortions like stairstep effects into the lines and for using a line digitizer to edit digitized data collected with a scanning digitizer, thus eliminating tedious tracing of each line on a map. The latter technique is operational but not yet competitive with conventional methods.

Consortium of Apollo 17 breccias

After the Apollo 17 mission in 1972, a consortium of investigators in 12 different fields studied two especially significant lunar breccias, samples 73215 and 73255. These rocks were chosen for concentrated and coordinated study because superficial examination suggested that (1) they formed as aggregates of melt and clasts produced during the Serenitatis basin-forming impact, (2) they cooled rapidly after aggregation, and (3) they were never significantly reheated. Thus, it appeared that consortium studies of the breccias and the clasts they contain might yield several important kinds of information: the date of the Serenitatis event; the processes of ejecta formation, transport, deposition, and consolidation that operated in basin-forming events; and the nature of the lunar crust prior to formation of the major basins.

The work of the consortium from 1973 to the present has indeed upheld the early tentative suppositions concerning the processes of breccia genesis, and the research is currently yielding information of the sort predicted. O. B. James has directed all aspects of the consortium research and carried out the investigations of sample petrology. The following are the most important results of the studies carried out by James in fiscal year 1978. Studies of clasts extracted from breccia 73215 are providing data on the lithology and chemistry of the early lunar crust. Detailed petrologic studies have been made of a clast of pink spinel-bearing troctolitic basalt. This rock is an example of an important class of highlands rocks, the spinel troctolites. Major-, minor-, and trace-element analyses and sederophile and volatile element analyses have been made by other consortium members (Blanchard and others, 1977; Morgan and others, 1976). The petrologic studies (James and Hedenquist, 1978a) have shown that at the earliest stage for which evidence remains the parent rock of the clast was a troctolitic melt. This melt crystallized rapidly, probably at or near the lunar surface, to form a fine-grained basaltic-textured rock. Later the rock was minutely granulated, but islands of basalt were preserved virtually undeformed. The granulated areas recrystallized; this recrystallization was at quite high temperatures because a small amount of melt was formed. Later the rock was again fragmented, perhaps more than once. The last significant event in the history of the clast was its incorporation in the 73215 breccia. The granulation and fragmentation episodes to which this rock was subjected were most likely induced by impact events. The high temperature recrystallization is not yet understood; the shock-induced heating related to the impact granulation would not have generated the temperature required for recrystallization so that an additional, as yet unexplained, source of heat seems necessary. Genesis of the original troctolitic melt is also somewhat of an enigma, but it seems most likely that this melt represents an impact melt of a preexisting highlands rock; the bulk composition suggests that the preexisting parental rock was a pyroxene-bearing troctolite, possibly an igneous cumulate. Work is now in progress on several other troctolitic basalt clasts to attempt to resolve some of the questions remaining concerning genesis and history of these rocks and their relations to other highlands rocks.

Petrologic studies of breccia 73255 (James and Hedenquist, 1978b; James and others, 1978) have clearly demonstrated that this rock is a consolidated aggregate of impact melt and fragmented rock formed during the South Serenitatis basin-forming impact. The breccia has retained its shape and internal structures produced by the breccia-forming event; thus, studies of the rock structures are providing valuable data concerning the processes of ejecta transport and consolidation that operated in major lunar impacts. The sample is a first-sized oblate spheroid consisting mostly of gray aphanitic rock. It has a large ovoid core in which the aphanite is nonvesicular and a distinct rind in which the aphanite is vesicular. Slightly vesicular aphanites form globular particles and lenses at the core-rind boundary, and small particles of cryptocrystalline aphanite are found within other types of aphanite. All these aphanites form distinct bodies with sharp contacts, and many have rounded outlines. The

petrologic data demonstrates that all these different types of aphanite formed as fragment-laden melts during a single very large impact, by a process of mechanical mixing of superheated impact melt and relatively cold fragments of granulated rock. The mixing probably took place in the radially flowing melt sheet that lined the floor of the crater in which the melts formed. Melt constituted about 70 percent by volume of the original fragment-melt mixtures, and the major-element composition of the melt was identical in virtually all the aphanites. It appears that the different types of aphanite formed from distinct masses of fragment-laden melt that had slightly different physical properties and may also have differed in content of volatiles. The rock-forming process appears to have been one of mixing of globs and splashes of these melts and may have occurred upon breakup of the melt sheet during its ejection from the crater cavity.

Transmission electron microscopy (TEM) studies have been made of a single matrix sample from breccia 73255. The groundmasses in three types of aphanite in the sample were examined in detail, and the thermal and deformational histories of three clasts were investigated (Nord and James, 1978a,b). The studies confirm that the groundmasses crystallized from a silicate melt; the crystallization was apparently quite rapid, and plagioclase and pigeonite were the major minerals that formed. The three clasts that were studied show the effects of a wide range of shock deformation prior to being incorporated in the breccia—one was unshocked, one was partly vitrified, and one was almost completely vitrified. TEM studies indicate that (1) all the clasts were heated to $>990°C$ when the breccia formed, (2) the bulk breccia cooled rapidly after it formed, at least in the temperature interval between the temperature of clast-melt equilibration, to some temperature below 600°C, and (3) there was no significant postconsolidation shock (to pressures >25 kb) or reheating (to temperatures $>600°C$) of the bulk breccia after it formed. The results of this study are extremely important for interpretation of the isotopic data. The TEM work indicates that isotopic exchange between clasts and enclosing melt at the time of breccia formation should have been minimal, and many clasts should retain considerable isotopic information on the chronology of events prior to their incorporation in 73255. The TEM work also indicates that the ^{40}Ar–^{39}Ar age of the aphanite samples, 3.88 b.y. (Jessberger and others, 1978), cannot reflect any event after breccia formation, so this date most likely is the date of the breccia-forming impact.

The laser ^{40}Ar–^{39}Ar dating method has been used to study two clasts from breccia 73215 (Eichorn and others, 1978). The first clast is of black aphanite lithologically similar to the matrix, but occurring as a fragment within granulated feldspathic clast material which is in turn enclosed by matrix. The laser results establish that the date of formation of this "clast" aphanite is the same as that of the matrix, so that the "clast" is not a fragment of older breccia but is cogenetic with the matrix. The second clast is of an anorthosite-norite-troctolite suite anorthositic gabbro. The laser results show a pattern of variation of radiogenic argon contents in plagioclase grains that can be ascribed to partial outgassing of the clast when it was incorporated in the breccia; the centers of the largest grains show the oldest ages, the smallest grains and material at grain boundaries show the youngest ages, and intermediate-size grains show intermediate ages. The oldest age obtained sets a lower limit of 4.26 b.y. on the date of an episode of high-temperature melting/recrystallization that affected the parent rock of the clast. The Rb-Sr data for the same clast (Compston and others, 1977) provide an upper limit on the date of this event at 4.45 b.y. An additional laser dating study, of a clast of potassium-rich feldspar from breccia 73215, sets a lower limit of 4.00 b.y. on the date of igneous crystallization of the "granitic" parent rock of this clast. The Rb-Sr data (Compston and others, 1977) set an upper limit of $\sim$4.05 b.y. on crystallization of the parent rock, thus establishing that it was a relatively "young" highlands rock. This age determination is the first reliable date for crystallization of a lunar "granitic" melt.

Extraterrestrial oxygen fugacities

On the basis of his theoretical studies, Motoaki Sato has concluded that carbon probably played a major role in the redox reactions occurring within planetary bodies, as carbon has a large redox capacity because of its low atomic weight and high valency numbers. Sato has found that, along the geothermal gradient, carbon becomes more reducing with increasing depth in the Earth's mantle and at the core-mantle boundary it can precipitate a metallic phase. Similar relations exist in Venus, Mercury, and Mars, but not in the Moon. The pressure-temperature condition for the core region of the Moon is such that carbon is not capable of

forming a metallic phase, a conclusion that is compatible with the low density of the lunar interior. Sato has proposed a mechanism of the core formation in which carbon dissolves in a low-melting, heavy FeS-FeO melt that sinks to the core region, precipitates a metallic phase at this depth, and ascends as a light liquid similar to carbonatite magma (Sato, 1978).

REMOTE SENSING AND ADVANCED TECHNIQUES

EARTH RESOURCES OBSERVATION SYSTEMS PROGRAM

The Earth Resources Observation Systems (EROS) program supports and coordinates research in applications of remote sensing technology and conducts demonstrations of these applications within Bureaus and Offices of the Department of the Interior. The EROS Data Center (EDC) in Sioux Falls, S. Dak., is the principal archive for and distributor of data collected by USGS and NASA research aircraft and by Landsat, Skylab, Apollo, and Gemini spacecraft. The Center's other major functions are assistance and training in the use of remotely sensed data and development and demonstration of remote-sensing technology.

Scientists and other members of the Data Analysis Laboratory staff at EDC cooperate with Federal and State user agencies in demonstration projects to apply reliable remote-sensing techniques to resource management problems. The cost-effectiveness and usefulness of the techniques are assessed and documented, and the user agency personnel gain experience in carrying out the procedures.

Research in the applications of remote-sensing data is also conducted by scientists in the EROS program office in Reston, Va., and a field office in Flagstaff, Ariz.

DATA ANALYSIS LABORATORY

INTEGRATION OF REMOTELY SENSED DATA WITH OTHER DATA

Significant results were reported by F. A. Waltz and C. A. Nelson (Technicolor Graphic Services, Inc.) in the development of techniques that combine Landsat data with digital data from other sources, such as digital terrain tapes, topographic data, and geophysical data.

W. G. Rohde used principal components and canonical analysis to enhance the classification of data into land-cover types.

CORRECTION OF LANDSAT IMAGES

D. D. Greenlee and C. M. Trautwein (Technicolor Graphic Services, Inc.) developed a technique to correct Landsat multispectral scanner (MSS) data for nonuniform illumination of the Earth's surface caused by variations in terrain. The method was used in an analysis of types of land cover in an area near Nabesna, Alaska, where there is considerable topographic relief and a low Sun angle. Brightness values related to incident solar flux were normalized to simulate horizontal Lambertian reflector equivalents by applying atmospheric correction algorithms to digitized topographic data from the Defense Mapping Agency, registered to the MSS data display. By reducing the effect of shadows, this technique permits a more accurate delineation of types of land cover from an analysis of spectral relation.

WATER DEPTH FROM LANDSAT IMAGES

A technique to calculate water depth from Landsat MSS data was reported by W. L. Bauer (Technicolor Graphic Services, Inc.). Developed from work done at the Environmental Research Institute of Michigan by Fabian C. Polcyn (1976), the method uses visible wavelength data from MSS bands 4 and 5 for water penetration and near-infrared data from MSS band 7 for discrimination between water and land.

MONITORING THE ENVIRONMENT

COOPERATIVE PROJECTS WITH THE BUREAU OF LAND MANAGEMENT

The Bureau of Land Management (BLM), NASA, and EDC are cooperating in a demonstration project to evaluate the usefulness of Landsat film products, computer-compatible tapes, and aerial photographs at several scales for mapping and inventorying wildland vegetation. W. G. Rohde, W. A. Miller, and C. A. Nelson (Technicolor Graphic Services, Inc.) used digital analysis techniques to classify Landsat data of Alaska into nine land cover categories. The overall classification accuracy was 84.5±4.2 percent

at the 0.95 probability level. According to Rohde (1978), stratifying the project area into broad vegetation classes and allocating primary sample units for the estimation of areas improved the accuracy of vegetation classification with Landsat data.

W. G. Rohde, W. A. Miller, M. E. Engel, K. G. Bonner, and Elizabeth Hertz (Technicolor Graphic Services, Inc.) used digital terrain data (elevation, slope, and aspect) to stratify Landsat data to improve the accuracy of classification of vegetation at a test site in northern Arizona. The relation of terrain to vegetation was defined by more than 9,000 photograph points and map data. Vegetation map overlays produced from interpretation of Landsat data were equivalent in detail to the Level II (Anderson and others, 1976) vegetation maps in the Bureau of Land Management Unit Resource Analysis. A Landsat image base showing landforms and drainage patterns in a regional perspective was used to interpret the vegetation overlays. The vegetation map overlays made from interpretation of 1:120,000-scale color-infrared aerial photographs were found to be useful in general management decision making for large areas. Vegetation maps made from larger-scale photographs were found to be more appropriate for application to site-specific management problems.

COOPERATIVE PROJECTS WITH THE NATIONAL PARK SERVICE

D. T. Lauer (USGS) and W. J. Todd, D. G. Gehring, C. M. Trautwein, C. A. Sheehan, and W. H. Anderson (Technicolor Graphic Services, Inc.) completed a cooperative demonstration project with the National Park Service to meet specific information requirements for planning development, resource management, and visitor use of park lands. Basic geologic information, location of water sources, surveys of range conditions, assessment of fire hazards, and analysis of vegetation types were derived from data collected by Landsat and aircraft over the 514,000-ha Lake Mead National Recreation Area. A regional study of the geology and hydrology of the area was made by manual interpretation of enhanced Landsat imagery at a scale of 1:250,000. Woodland, shrub, and desert vegetation classes were delineated, and their relation to sedimentary, metamorphic, and igneous terrains was analyzed, using computer-assisted methods to interpret 1:250,000-scale Landsat data. Analyses of geologic and vegetation resources in five sites were made from computer-enhanced Landsat data and standard aerial photographs. Cost evaluations showed that the regional geologic study was performed at a cost of 4.16 cents per hectare, and the vegetation and terrain classification at 15.6 cents per hectare. The costs of the analysis using enhanced Landsat data and aerial photographs ranged from 8.98 cents per hectare for a 119,000-ha area to 82.6 cents per hectare for a 2,266-ha area.

COOPERATIVE PROJECTS WITH THE U.S. FISH AND WILDLIFE SERVICE

L. R. Pettinger (Technicolor Graphic Services, Inc.), Adrian Farmer, and Mel Schamberger (U.S. Fish and Wildlife Service) investigated high-altitude color-infrared aerial photographs as a potential source of data for the Fish and Wildlife Service Habitat Evaluation Procedure project (Pettinger and others, 1979). The purpose of the project was to determine whether the use of standardized techniques of collecting and interpreting aerial photographs would increase the efficiency of assessing the impact of resource development projects on fish and wildlife.

The number of habitat units for elk and sage grouse that might be lost by the proposed development of a phosphate surface mine in Caribou County, Idaho, were determined at two sites. Three vegetation community types, coniferous forest, upland deciduous forest, and sagebrush/perennial grass, were delineated on high-altitude color-infrared photographs of the area at a scale of approximately 1:24,000. Parameters were measured for each habitat unit within each vegetative community. The image characteristics associated with each habitat parameter were studied, and a subjective determination was made regarding the applicability of the aerial photographs for measuring each parameter.

More than half of the parameters for elk and sage grouse habitats could be successfully measured by photointerpretation. Those parameters not interpretable from aerial photographs were measured by traditional field techniques.

The habitat units threatened by mining activity were calculated for each species on both sites, and the relative value of each site for each species was assessed.

This project, though limited to two species in an upland environment, indicated that high-altitude color-infrared aerial photographs can be used effectively to quantify and evaluate wildlife habitat.

COOPERATIVE PROJECTS WITH THE MINE SAFETY AND HEALTH ADMINISTRATION

In a cooperative program with the EROS Data Center Data Analysis Laboratory, R. K. Rinkenberger (Mine Safety and Health Administration (MSHA), Department of Labor, formerly, the Mining Enforcement and Safety Administration, U.S. Department of the Interior) developed techniques of image analysis to evaluate mine ground stability. Data from computer-compatible tapes (CCT's) of Landsat scenes of areas containing underground coal, limestone, and salt mines and surface coal pits in New York, Kentucky, New Mexico, Wyoming, Utah, and Colorado were enhanced on the General Electric Image 100 image analysis system. The ground stability at these sites was previously evaluated by the Ground Support Branch of MSHA in Denver, Colo., using conventional methods of image analysis, including an analog scanning system. Computer enhancement routines, such as linear and nonlinear stretch, principal components analysis, overview, and ratioing of the CCT data, were found to be promising for extending the capabilities of image interpretation for predicting ground hazard areas.

The procedures developed were documented by Rinkenberger (1979) for use in a series of workshops offered at EDC to instruct personnel from MSHA and the mining industry in remote sensing technology relating to an evaluation of the stability of mined ground.

COOPERATIVE PROJECTS WITH THE BUREAU OF RECLAMATION

Sierra Cooperative Pilot Project.—With the support of the EROS program, Olin H. Foehner (Bureau of Reclamation) reported on satellite monitoring of cloud-top temperatures over the Sierra Nevada, California, as part of the Sierra Cooperative Pilot Project (SCPP), a major winter precipitation enhancement research project. Digital data from the Geostationary Operational Environmental Satellite (GOES) were collected for three intensive case studies of winter storms affecting the central Sierra Nevada. Analyses of these storms showed detailed mesoscale convective band structure during the storms and variations in infrared cloud top temperatures of the bands. Because of these mesoscale variations, detailed observation and analysis of winter storms are necessary to detect the natural variability in scale and to discriminate between natural effects and the effects owing to seeding.

The Automatic Environmental Surface Observation Platform (AESOP) was developed to provide near real-time hydrometeorological data from remote sites to the SCPP. Donald Rottner (Bureau of Reclamation) led an EROS-supported project to test two AESOP's, installed for the winter season at Blue Canyon and the Central Sierra Snow Laboratory, both in the Sierra Nevada (Rottner and Price, 1978). The stations measured pressure, temperature, dew point temperature, average wind speed and direction, and precipitation. Surface data were relayed on the hour by GOES to Wallops Island, Va., then automatically relayed to the World Weather Building, Camp Springs, Md., to the National Meteoroloigcal Center, Suitland, Md., and finally to the Bureau of Reclamation's Engineering and Research Center, Denver, Colo. In Denver, the data were merged with National Weather Service and Federal Aviation Administration hourly surface data and made available within 10 minutes after the hourly observation was taken. Both AESOP's were reliable in the sometimes severe Sierra Nevada environment, and the observations were comparable with measurements taken at manned stations.

Resource inventory of Grand Valley, Colorado.—A computer-assisted analysis of Landsat data to inventory the resources of Grand Valley in western Colorado was funded by the U.S. Geological Survey and performed for the Bureau of Reclamation by contract with the University of California at Berkeley. Predominantly agricultural, urban, and industrial lands (49,000 ha) were classified into crop versus noncrop groups with an accuracy of 85 percent and into 13 land use categories with an accuracy of 63 percent (DeGloria, 1979). With advice and consultation from the EDC Data Analysis Laboratory, the Bureau of Reclamation is installing an interactive digital image analysis system to establish an in-house capability to continue and expand the work.

IMPACT OF SURFACE MINING

L. R. Pettinger (Technicolor Graphic Services, Inc.) used interactive digital analysis of Landsat images to produce maps of vegetation and land cover in the Blackfoot River watershed in southeastern Idaho. These maps were compared with vegetation maps from a draft environmental impact statement (EIS) describing the effects of the expansion of phosphate strip mining in the watershed. The maps based on the digital analysis were also compared with vegetation maps based on an interpretation of aerial photographs.

Two levels of resource classes (Anderson and others, 1976) were identified in this project: (1)

generalized (Level I) classes, such as forest and wetland, and (2) detailed (Levels II and III) classes, such as conifer forest, aspen forest, wet meadow, and riparian hardwoods. Training set statistics were developed using a modified clustering approach. Discrimination between resource classes with similar spectral signatures was improved by stratification that separated upland areas from lowland areas.

Agreement of the digital classification and the manual classification of aerial photographs was 83.0±2.1 percent at the 0.95 probability level in the case of generalized classes (corresponding to the EIS vegetation classes) and 52.2±2.1 percent in the case of detailed classes determined from pixel-sized plots.

D. M. Carneggie found Landsat data valuable for detecting changes in surface mines located in large areas where aerial photographs were not available. Digital Landsat data, acquired on several dates and photographically enlarged to scales ranging from 1:50,000 to 1:15,000, were manually interpreted to detect changes associated with phosphate surface mining. Digital techniques of interpreting multidate Landsat data were also useful in detecting change. Ratioing the data from two Landsat scenes produced a new image on which changed areas were conspicously displayed. Aerial photographs or ground surveys were used to identify the type of change.

COOPERATIVE PROJECTS WITH STATES

Pacific Northwest Regional Commission

D. R. Hood (Technicolor Graphic Services, Inc.) reported that the Pacific Northwest Regional Commission, NASA, and USGS have completed a five-phase project designed to determine the usefulness of Landsat data for regional resource inventory, planning, and management in the States of Idaho, Oregon, and Washington (Gaydos, 1978; Gaydos and Newland, 1978; Gaydos and others, 1979; Hedrick, 1979). The goal of the program was to establish a self-sustaining capability for Landsat data analysis on an operational basis in the three States. Approximately 90 people from 45 State, regional, and local units of government were involved in the project.

Washington Department of Natural Resources

G. R. Johnson and E. W. Barthmaier (Technicolor Graphic Services, Inc.) cooperated with the State of Washington Department of Natural Resources in a project to demonstrate the application of digital image processing techniques for classification of forest lands using Landsat MSS data.

Forest resource information from Washington's Gridded Resource Inventory Data Systems (GRIDS) was entered into a digital image processing computer. The forest resource data included cover type group, species composition, and stand age, size, and density information, as well as terrain data for more than 2,200 plots in each of two townships in western Washington. Landsat data of the two townships were geometrically corrected to State base maps and merged with the forest resources data from GRIDS.

Unsupervised clustering procedures were applied to the Landsat data to determine, by comparison to the forest resource data, which resource groups could be identified with MSS data. Training statistics are being developed for these resource groups, and the maximum likelihood algorithm is being evaluated as a classification method and compared to the canonical analysis and minimum distance algorithm.

Suwannee River Water Management District, Florida

J. R. Lucas (Technicolor Graphic Services, Inc.) cooperated with the Suwannee River Management District of Florida to develop an operational method to collect, store, and retrieve data on water used for irrigation. The data are required for long-term management of northern Florida's water resources. An agricultural inventory was conducted in a study area in which the cultivation and irrigation practices were typical of northern Florida. Both digital and photographic Landsat data of the area were obtained for the 4 seasons of 1977. Acreages for croplands calculated by interpreting photo-optically enhanced Landsat color imagery at a scale of 1:125,000 were compared to acreages computed from Landsat digital tapes to determine the consistency of the two analysis procedures. Irrigated corn acreage identified on the June 1977 image was estimated to be 80 percent accurate when compared to ground survey data. Accurate identification of irrigated cropland was found to depend on the analyst's familiarity with the study area and the availability of reliable field data. Other types of crops and ground cover were successfully identified at varying accuracy levels. The use of Landsat data was determined to be quicker and less expensive than a ground reconnaissance in providing data on a repetitive basis for an irrigation water use model.

FOREST DEFOLIATION

Landsat digital data were used effectively for mapping the areal extent of hardwood-forest canopy defoliation by the gypsy moth (*Porthetria dispar*) in a project completed by G. R. Johnson (Technicolor Graphic Services, Inc.). Accuracy of the maps was estimated using a stratified random sample of 541 individual pixels. The sample was designed to provide an estimate at the 0.95 probability level of the proportions of pixels correctly classified within a nonforest class, three classes of tree defoliation, and a nondefoliated tree class. The estimate was designed to be within ±10 percent of the true proportion in each class and ±5 percent of the true proportion in all classes. Classification of sampled points was also verified by comparison with aerial photographs of the area.

The results showed that Landsat data are not useful for discriminating between degrees of defoliation, but that the data can be used successfully to map the areal extent of hardwood canopy defoliation.

CAPE COD, MASSACHUSETTS

R. S. Williams, Jr., used a Landsat 3 RBV image to study the breach in Monomoy Island, off of Cape Cod, Mass., resulting from the severe storm of February 6–7, 1978. The 30-m image resolution (compared to about 80 m for the MSS) and planimetric precision of the Landsat 3 RBV permitted an accurate assessment of changes in coastal morphology.

Williams also reported that the Landsat 3 RBV image of Cape Cod showed geometric fidelity and terrain detail superior to the MSS image when enlarged to a scale of 1:125,000 for use as a base for a geologic map.

TARGETING, INVENTORYING, AND MONITORING GROUND-WATER RESOURCES

J. R. Lucas and D. J. Stetz (Technicolor Graphic Services, Inc.) are assessing the capabilities of Landsat MSS data for targeting areas probably underlain by ground water at shallow depths in glaciated terrains of the upper Midwestern United States. Landscape features produced by continental glaciation are so large that they require a regional scale for analysis and interpretation. Patterns delineated on springtime Landsat images of test areas in eastern South Dakota and southeastern Wisconsin were found to be related to continental glaciation. Glacial features characterized by high content of sand and gravel are considered potential sites for ground water exploration because of the permeable nature of these deposits. A procedure was developed for mapping the patterns using conventional techniques of photointerpretation. Linear and curvilinear features, drainage patterns, and land cover types were analyzed on Landsat imagery at a scale of 1:500,000. Comparison of these image patterns with published hydrologic and geomorphic data indicate that the patterns are related to preglacial buried valleys and other glacial landforms. Additional field data are required before specific patterns can be identified as indicating the sites of potential ground-water reservoirs.

Arcuate features in southwestern Minnesota mapped by J. V. Taranik (USGS), J. R. Lucas, and C. A. Sheehan (Technicolor Graphic Services, Inc.) from a springtime mosaic of 55 Landsat images coincide with glacial deposits mapped by personnel of the Minnesota Geological Survey. These deposits consist of well-sorted, porous, and permeable outwash sands and gravels. These deposits constitute a major target for the exploration and development of ground water resources. Approximately 900 high-altitude color-infrared photographs at a scale of 1:80,000 were acquired of the Des Moines lobe by the Iowa Geological Survey in the spring of 1978. Geologists from EDC and the Iowa Geological Survey are cooperating in the analysis of these photographs and in the collection of ground-based data on Wisconsinan glacial deposits.

STUDYING THE GLOBAL ENVIRONMENT

MONITORING DESERTIFICATION

C. J. Robinove developed a system for monitoring changes in the albedo of land in arid and semiarid regions (Robinove and Chavez, 1979). The albedo of each Landsat picture element in each of two scenes of the same area acquired at different times is calculated. The scenes are geometrically registered to each other, and the difference in albedo is calculated for each picture element. Resulting maps show areas where albedo has decreased or increased. This change may be correlated with increased or decreased growth of vegetation, increased erosion, or other changes caused by weather fluctuations or man's impact on the land. In a test site in western Utah, the average area darkened in a 5-year period indicates that vegetation may be more extensive at present than in the past and that "greening" rather than desertification is occurring.

SATELLITE IMAGE ATLAS OF GLACIERS

A project was begun by R. S. Williams, Jr., and J. G. Ferrigno to produce a satellite image atlas of glaciers. Preliminary results of the research include:

- Landsat images of many outlet glaciers in Greenland, Iceland, and Svalbard show termini in positions different from those shown on existing maps (Ferrigno and Williams, 1979).
- Subtle surface features of the inland ice of Greenland, which appear to be related to subglacial topography, are visible on winter Landsat images enhanced by illumination at a low Sun angle.
- Some aspects of ablation facies, for example, exposed glacial ice, exposed superposed ice, saturated snow zone, and superposed meltwater ponds, can be delineated on late summer Landsat images of Greenland and Iceland.
- Melting snow can be differentiated from the permanent ice cover shown in different spectral bands of the Landsat images taken at particular seasons.
- Digital enhancement of Landsat images may aid in differentiating rock-covered terrain from debris-covered ice.
- Specially processed images from the National Oceanic and Atmospheric Administration (NOAA) satellite can be used to supplement Landsat images of glaciers and to provide coverage of arctic and antarctic regions beyond the orbit of Landsat.

INTEGRATED TERRAIN MAPPING

Mapping land using digital images to categorize land capability was shown to be feasible by C. J. Rovinove (1979) working in Queensland, Australia, and C. F. Hutchinson (1978) working in the Mojave Desert, California. Statistical analysis of Landsat images was used to group terrain into categories, each a unique combination of geomorphic features, soil and vegetation, that relate to land capability management.

TARGETING MINERAL EXPLORATION

MINERAL EXPLORATION AT CLAUNCH, NEW MEXICO

W. A. Fischer and D. G. Orr (USGS) and D. D. Greenlee (Technicolor Graphic Services, Inc.) continued the investigation of five playa lakes in an area northwest of Vaughn, N. Mex. Initial geochemical analyses of the muds within the lakes showed abnormally high concentrations of strontium and lesser, but possibly significant, concentrations of rare earths and uranium and vanadium. These analyses show a striking parallelism of concentrations of elements among the playas despite the fact that each playa occurs in a different geologic setting. The parallelism suggests that the lakes are interconnected in the subsurface and that ground-water flow patterns are the key to understanding the distribution of minerals in the area. Similarities have been noted between the geomorphological setting of the Vaughn area and that of the Yeelirrie uranium district (one of the largest in the world) in Australia.

Aerial surveys were conducted with the Fraunhofer Line Discriminator (FLD) over four of the five playas under study. Because the luminescence intensities in the playas were the highest ever recorded by the FLD, the geochemical sampling program was extended. Previously acquired magnetic data and recently acquired gravity data are being prepared for three-dimensional viewing to aid in the understanding of the basement configuration and how it affects ground-water flow.

PETROLEUM IN NORTHWESTERN COLORADO

J. V. Taranik (USGS) and Patrick Anderson (Technicolor Graphic Services, Inc.) analyzed Landsat data, aerial photographs, and geophysical data of northwestern Colorado to compile geological information useful in petroleum exploration and development. Landsat images taken at different seasons were compared to determine the optimal times of illumination and the condition of land cover needed to analyze landscape patterns. Landform and drainage patterns were best displayed on imagery taken in late November, and June data were best for land cover. Analysis of land cover patterns alone produced no useful geological information, but the presence of major structural folds and faults could be determined from an analysis of land cover and landforms combined. Anticlinal structures were considered primary targets for wildcat exploration, and fractured shales in synclines were ranked as secondary targets. Large faults indicated possible sites for structurally entrapped petroleum in porous and permeable reservoir rocks of basins. Joints and fractures in exposed reservoir rocks were judged to be important in secondary recovery programs because these structures can channel water during injection.

PORPHYRY COPPER IN ARIZONA

J. V. Taranik (USGS) and C. M. Trautwein (Technicolor Graphic Services, Inc.) developed a procedure by using combined Landsat and geophysi-

cal data to target ground-based geochemical exploration for porphyry copper deposits in the Tucson area of Arizona. Linear features and the contact between exposed bedrock and valley fill alluvium were drawn on a Landsat image. Aeromagnetic data reduced to contoured values of residual magnetic intensity were registered to the Landsat image at a scale of 1:1,000,000, and areas having anomalous values of magnetic intensity were noted in the valley fill alluvium. Ground-based gravity data, reduced to contoured Bouguer gravity values, were registered to the Landsat image and aeromagnetic data. Areas were identified where anomalously high values of gravity in valley fill alluvium coincided with anomalous values of magnetic intensity.

Displacements of alluvium and basement were inferred where alinement determined from reduced geophysical data coincided with linear features delineated on Landsat images.

COPPER AND MOLYBDENUM IN NABESNA, ALASKA

Trautwein and Taranik also developed a model for the copper and molybdenum minerals in Nabesna, Alaska, from a systematic analysis and interpretation of Landsat image data. Image data were adjusted to compensate for atmospheric Rayleigh scatter and water vapor absorption (Taranik, 1978a). Objective aspects of image analysis and interpretation were carefully separated from subjective considerations in developing geologic interpretations. Landsat brightness values were converted to reflectance values, which were then compared to the reflectance values observed for landscape cover in which limonitic alteration is dominant. Only a few of a total of 262,144 pixels were found to contain reflectance values indicating altered rock cover. Most landscape areas having alteration were covered by vegetation and unconsolidated rock. Therefore, exploration models could not be successfully developed from analysis of cover types alone.

An exploration model for copper and molybdenum minerals in the Nabesna area was developed from key surficial attributes of a geological model constructed by an analysis of Landsat data. These attributes included surface expression of faults coupled with the occurrence of granitic intrusions in metasedimentary rock sequences.

Of the computer processing techniques used to enhance landform and cover patterns (Taranik, 1978b), linear contrast stretching was the most successful.

DATA FROM AIRBORNE INSTRUMENTS

FRAUNHOFER LINE DISCRIMINATOR EXPERIMENTS

The FLD is an electro-optical device that permits detection of solar-stimulated luminescence several orders of magnitude below the intensity detectable with the human eye. The luminescent dye rhodamine WT is used as a sensitivity standard for measuring the detectivity of FLD target materials. The airborne FLD routinely detects materials whose luminescence intensity is equivalent to 0.1 parts per billion (ppb) rhodamine dye in distilled water.

R. D. Watson and A. F. Theisen conducted an investigation with cooperators from the U.S. Department of Agriculture and the Environmental Protection Agency to determine the correlation of drought-stressed citrus trees with luminescence. The work was conducted at the experimental citrus tree farm of the University of Arizona near Phoenix. Luminescence measurements were made with an FLD operating in an imaging mode and suspended over the trees on an 18-m track. An image of the reflectance and luminescence of each tree was acquired. Measurements of moisture potential, leaf resistivity (stomatal openings), neutron soil moisture to a depth of 1 m, air temperature, leaf temperature, and relative humidity were also acquired for each tree and its surrounding environment. Data reduced from approximately 28,000 FLD readings indicated a detectable difference in luminescence between the stressed and unstressed citrus trees. After watering of the unstressed trees, a definite diurnal pattern developed in which the maximum contrast in luminescence between the stressed and unstressed citrus trees occurred in the afternoon.

With the cooperation of scientists from the University of California at Santa Barbara, Watson and Theisen measured the luminescence of 13 species of phytoplankton with a laboratory fluorescence spectrometer operating at 656.3 nanometers in a water-cooled front surface mode. Each species was grown in three media: sea water, sea water plus silicon, and sea water enriched with nutrients. Corrections for the source-detector, sunlight, and depth were programmed into a 6800 microprocessor and automatically applied during each measurement. The luminescence of 10 species at concentrations to be expected in the open ocean (1.0 μg/L) exceeded the minimum level detectable with the airborne FLD. Luminescence of the other three species was detectable at concentrations of 2.0 to 5.0 μg/L.

A luminescence image of the Alpine Mill and the surrounding Pinenut Mountains in Nevada was

acquired with an airborne FLD operating at a wavelength of 656.3 nm. At a site just north of the Mill, a known molybdenum geochemical anomaly was readily discerned on the image. High luminescence was also observed around Divide mine, once an active tungsten mine, approximately 2.0 km north of the Alpine Mill. Sheelite, present in the soil in this area, has a luminescence of approximately seven times the minimum detectable with the FLD. Soil samples are being analyzed to determine if the sheelite and other minerals are contributing to the luminescence anomalies.

The luminescence of several samples of playa deposits from western Nevada was measured on a laboratory fluorescence spectrometer at the 486.1-nm, 589.0-nm, and 656.3-nm Fraunhofer wavelengths. The samples were from Garfield Flat, where ground water moves downward through underlying units, and Fourmile Flat, where ground water is drawn to the surface by capillary action. Measurements were normalized to a rhodamine WT standard and expressed in ppb rhodamine WT dye equivalence for comparison with measurements made by a FLD having a minimum luminescence detectivity of 0.1 ppb. In general, the halite samples showed greater luminescence (1.2 to 1.98 ppb) at all three wavelengths than mud and silty clay (0.22 to 0.49 and 0.19 to 0.40 ppb, respectively). These materials could also be seen on a luminescence image acquired by the airborne FLD. A luminescence anomaly noted on the image of the south edge of Garfield Flat may be due to a sheelite deposit upslope from the playa.

A laboratory fluorescence spectrometer was used to measure the luminescence of selected samples of uranium-bearing and non-uranium-bearing sandstones from Lisbon Valley, Moab, Utah. Luminescence was highest in the 486.1-nm and 589.0-nm Fraunhofer wavelengths. Values from mineralized outcrops exceeded the background luminescence by one order of magnitude. The FLD imaging system, operating at 486.1 and 589.0 nm, was then flown over Lisbon Valley and the surrounding area. Outcrops of the Mossback Member of the Chinle Formation, the principal ore-bearing unit of the area, and uranium and copper workings were readily identified on the images obtained by the FLD. Assistance was provided by Preston Neisen of Atlas Minerals, Moab, Utah.

APPLICATIONS TO GEOLOGIC STUDIES

Lineament studies help characterize waste disposal study areas

M. H. Podwysocki, H. A. Pohn, M. D. Krohn, J. D. Phillips, and L. C. Rowan note that an analysis of subsurface data and Landsat images shows a correlation between lineaments and structure in south-central New York and north-central Pennsylvania. At the surface, Middle and Upper Devonian clastic rocks, in broad open folds trending east-northeast, are transected by NNW-trending lineaments. In the subsurface, units above the Salina Group (Upper Silurian) parallel the surface folds, whereas units below appear to be planar. Isopach maps of the uppermost Salina units reveal a large rectilinear block of salt-bearing rock, whose boundaries are parallel and normal to the surface fold axes. Basement-controlled faulting and deposition in the early Paleozoic and thin-skinned thrusting in the late Paleozoic are postulated mechanisms for the formation of this block. Evidence supporting basement control includes (1) high magnetic contrasts in the basement at the west edge of the blocks, (2) NNW-trending horsts and grabens, generally below the salt, but occasionally reaching the surface, and (3) changes in sense of movement through pre- and post-Ordovician time along a fault at the west edge of Lake Cayuga, New York. Evidence supporting a thrust-fault origin for the block includes (1) seismic, well-log, and mine data, which show thrust faults originating in the salt, (2) deformed fossils along the east and west margins of the block, and (3) fold axes that commonly change both plunge and strike near the west margin of the block. A structure-contour map of the block surface suggests that the block acted as a single entity regionally but was broken into many small blocks locally by tear faults.

The first stage of a remote-sensing project on the Paradox Basin, Utah-Colorado, part of the USGS radioactive waste-emplacement program, consisted of a review and selection of the best available satellite scanner images to use in geomorphologic and tectonic investigations of the region. High-quality Landsat images in several spectral bands (E–2260–17124 and E–5165–17030), taken under low sun angle on October 9 and 10, 1975, were processed via computer for planimetric rectification, histogram analysis, linear transformation of radiance values, and edge enhancement.

A lineament map of the northern Paradox Basin was subsequently compiled at a scale of 1:400,000

by J. D. Friedman and S. L. Simpson, who used the enhanced Landsat base. Numerous previously unmapped NE-trending lineaments between the Green River and Yellowcat Dome, confirmatory detail on the structural control of major segments of the Colorado, Gunnison, and Dolores Rivers, and new evidence for late Phanerozoic reactivation of Precambrian basement structures are among the new contributions to the tectonics of the region.

Lineament trends appear to be compatible with the postulated Colorado lineament zone, with geophysical potential field anomalies, and with a NNE-trending basement fault pattern. Combined Landsat, geologic, and geophysical field evidence for this interpretation includes the sinuousity of the composite Salt Valley anticline, the transection of the Moab-Spanish Valley anticline on its southeastern end by NE-striking faults, and possible transection(?) of the Moab diapir. Similarly, NE-trending lineaments in Cottonwood Canyon and elsewhere are interpreted as manifestations of structures associated with northeasterly trends in the magnetic and gravity fields of the La Sal Mountains region. Other long northwesterly lineaments near the western termination of the Ryan Creek fault zone may be associated with the fault zone separating the Uncompahgre horst uplift from the Paradox Basin.

Regional structures interpreted from Landsat data

A linear features map was prepared by photointerpretation of processed Landsat images of the Rolla, Missouri-Illinois, 2-degree sheet and vicinity by D. H. Knepper, Jr. The linear feature data were statistically analyzed for preferred orientation, and the spatial distribution of preferred trend intervals was evaluated from contour maps of linear feature density. An x-shaped concentration of linear features near the center of the Rolla sheet suggested to Knepper the possible presence of two adjacent circular features aligned northeast-southwest in the basement rock. Examination of available gravity and aeromagnetic maps confirmed the presence of these features. The northeastern circular feature is about 50 km in diameter and covers the region of the central Saint Francis Mountains of southeast Missouri; it has escaped previous detection because its expression in the gravity data is suppressed by a strong northwest-trending gravity gradient. The magnetic expression is equally subtle. The southwestern circular feature, although somewhat smaller, is strongly expressed on the gravity data of the Spring Valley area in the southwest corner of the Rolla sheet; no magnetic data are available for this area. These two circular features, plus a third discovered by L. E. Cordell in the northeast corner of the Rolla sheet, are alined along a northeast-trending line parallel to the Mississippi Embayment rift zone to the southeast. Three strong gravity gradients discovered by T. G. Hildenbrand and others strike northwestward out of the rift zone, and each intersects one of the circular features. It is believed that the circular features originated during Precambrian volcano-tectonic activity and have influenced subsequent geologic events in the region. Most importantly, the distribution of mineralization in the lead belts of southeast Missouri show good correlation with the rims of the central and northeastern circular features; the southwestern circular feature is too deeply buried to expose a similar correlation. It is not yet known whether the possible mineralization controls are in the nature of a metal source or a structural/topographic effect on the subsequent accumulation of favorable sedimentary strata. Both types of controls may have been operational.

Further refinement in thermal-inertia mapping

The theoretical basis for the relationship between absolute thermal inertia and "relative" thermal inertia was examined by Kenneth Watson and S. H. Miller. The analysis produced a much more accurate nonlinear approximation as compared with those produced by the proportional and the linear forms. For a limited set of site parameters, the standard deviation associated with predicting thermal inertia using the proportional form was approximately 175 TIU, where 1 TIU $=1[w(s^{1/2}m^{-2}k^{-1})]$; with the linear form it was approximately 15 TIU, and with the new nonlinear form it was approximately 2 TIU. Other input data sets gave comparable results. They conclude that the new nonlinear approximation provides a very precise fit and will be appropriate for high-resolution aircraft and ground studies. The linear form will probably be accurate enough for most satellite and aircraft data analysis, but the proportional fit will only be satisfactory where high thermal-inertia differences are present.

A new, more efficient method of calculating with Laplace transform solution for surface temperature was developed by Watson and Miller on the Honeywell computer. Three surface temperature algorithms, including the new Laplace Transform algorithm, were numerically compared by determining the relative and absolute uncertainty each introduces into a thermal-inertia map. The relative

thermal-inertia error of the Jaeger model is 0.5 percent as compared to the exact solution. The relative uncertainties in thermal inertia for the finite difference and the Fourier series are approximately 5 percent for both.

The absolute error introduced into a thermal-inertia map by each of the three surface-temperature algorithms was determined using a limited but representative data set. For low thermal-inertia values (500 TIU), the absolute error using the Jaeger solution was approximately 1 TIU; the finite difference solution gave an absolute error of approximately 10 TIU; the linear Fourier series solution gave an error of approximately 150 TIU. For large thermal-inertia values (4,000 TIU), the absolute errors for the Jaeger, finite difference, and Fourier series solutions were 5, 250, and 50 TIU, respectively. The finite difference solution is more accurate than that of the Fourier series at low thermal inertias and vice versa at high thermal inertias. This improved accuracy means that greater reliance can be placed on the selection of the appropriate algorithm.

Visible and near-infrared multispectral aircraft images used to distinguish altered rocks

Multispectral scanner aircraft images of the East Tintic Mountains, Utah, were used by L. C. Rowan to evaluate various ratio image data and to map several altered rock types consisting of calcareous, siliceous, and argillaceous sedimentary and volcanic rocks, in a relatively vegetated area. Study of field spectra guided selection of the .48/1.6 μm ratio image to show intensity variations in the Fe^{3+} bands, the 2.2/1.6 μm image to express the differences in the OH band, and the .73/1.0 μm image to display the distribution of vegetative cover. In the East Tintic Mountains CRC image, both non-limonitic and limonitic argillized and silicified rocks are distinctive because of the general lack of Fe^{3+} bands in the non-limoniti rocks and the presence of OH bands in both of the latter rock types. However, discrimination between the argillized and silicified rocks is not possible in this image. Also, hydrothermal dolomite and calcitized and chloritized volcanic rock are not distinguishable because they are spectrally similar to most of the unaltered rocks. Limonitic unaltered rocks, except for the Tintic Quartzite, are consistently separable from all of the altered rocks; the Tintic Quartzite has a prominent 2.2 μm band related to detrital muscovite. Significantly, the shales and carbonate rocks here generally lack intense absorption features and, therefore, are not confused with the altered rocks.

Experimental data to help design the space shuttle radar system

Multifrequency-and-multipolarization, airborne-radar image data of a 70,000 year old lava flow in north-central Arizona were compared by G. G. Schaber to surface and aerial photography, Landsat and airborne thermal infrared imagery, surface geology, and surface roughness statistics. The extremely blocky, basaltic-andesite of the SP lava flow was found to be significantly brighter on direct-polarization K-band (0.9 cm wavelength) radar images than on cross-polarization images taken simultaneously. The opposite situation was found for the longer wavelength (25 cm) L-band radar images, where the cross-polarized returns from SP flow are brighter than the direct-polarized image data. This effect is explained by Bragg scattering models for rough surfaces.

Two distinct types of surface relief on SP flow, one extremely blocky, the other subdued in roughness, are clearly discriminated in the visible and thermal wavelength images; among the radar images, surface relief is discriminated only in the longer wavelength (L-band) radar image data. The inability of the K- and X-band (3-cm wavelength) radars to depict the differences in roughness between the two SP flow surfaces is attributed to the very short wavelengths of these bands (on the order of millimeters); radar scattering is intense in these bands for all but very fine-grained smooth surfaces.

Evaluation of geothermal heat flux models

A new model for geothermal heat flux mapping using discrete scanner measurements was developed by Kenneth Watson. This model makes direct use of measured flux values instead of surface temperatures which are inferred from flux measurements. By means of this heat flux model the absolute uncertainties in estimating the geothermal heat flux were determined for three algorithms: Laplace transform, linear Fourier series, and finite difference. For a limited representative set of site parameters, the standard deviation of predicting heat flux using the Laplace transform algorithm was approximately 6 HFU; where 1 HFU$=4.19\times 10^{-2}$w/m^2, Using the finite difference it was approximately 50 HFU, and using the linear Fourier series it was approximately 225 HFU. Thus, only the Laplace transform algorithm is appropriate for most geothermal studies.

Interpretation of aerial gamma-ray data from the northern part of the Boulder batholith

Aerial gamma-ray data were obtained over the northern part of the Boulder batholith in Jeerson County, Montana (Duval, Pitkin, and Macke, 1978). The gamma-ray spectrometer used was calibrated at the Department of Energy calibration pads in Grand Junction, Colo., so that the data could be presented in parts per million (ppm) of equivalent uranium (eU), ppm of equivalent thorium (eTh), and percent potassium (K). Based upon the geologic map of the area, almost all of the data were obtained over the geologic unit known as the Butte Quartz monzonite. The radiometric values measured were in the ranges 11–27 ppm eTh, 6–13 ppm eU, and 1.8–3.1 percent K. These values agree reasonably well with the ranges of 12–19 ppm Th, 2–7 ppm U, and 1.8–3.7 percent K given by Tilling and Gottfried (1969) for chemical analyses of rock samples. Using the criteria that values of eU greater than 11 ppm or the combination of the ratio eU/eTh greater than 0.56 and eU/K greater than 4.6 define anomalous areas, a number of anomalies were identified. These anomalies are interpreted as areas with potential uranium mineralization. Some of the stronger anomalies are associated with alaskite intrusives.

The radiometric data also revealed several areas of the Butte Quartz monzonite that are each relatively uniform in their radiometric character but significantly different from each other. Some of these areas coincide with a fine-grained subdivision of the Butte Quartz monzonite mapped by Becraft, Pinckney, and Rosenblum (1963). Other areas coincide with areas of the Butte Quartz monzonite where numerous small dikes of alaskite and related felsic rocks are present (Smedes, 1966). Because the radiometric characteristics of these areas are distinctive, a detailed aerial gamma-ray survey could be used to further define the extent and occurrence of the above subdivisions and, perhaps, to identify areas not previously recognized.

APPLICATIONS TO HYDROLOGIC STUDIES

In 1978, the USGS's Water Resources Division evaluated three satellite data relay systems—Landsat, GOES, and Comsat. One or more of these systems will be selected for water-resource investigations. Other studies included (1) the use of principal components transforms of Landsat image data to enhance surface-water features, (2) the development of an algorithm to geometrically correct radar imagery for aircraft flight-path curvature, (3) operational use of remote sensor data for ground-water exploration, (4) preliminary determination of the significance of saturated soils in Coastal Plain sediments, and (5) remote-sensing research in wetlands.

Tests of hydrologic-data relay systems

Landsat and GOES data relay systems were evaluated in Florida. Instrument and system reliability was tested in the Tampa Bay area by J. F. Turner and W. M. Woodham. Performance was based on accurate transmissions of data from field sites via satellite and land lines to USGS computer terminals. During 8-month and 17-month test periods, an average of three out of a possible six data messages was received from two Landsat transmitters. At least one data message was successfully relayed on 88 percent of the days. Similarly, an average of seven out of eight daily messages was received from one GOES transmitter, and at least one data message was received on 96 percent of the days.

Two problems in the GOES data-relay system were reported by E. H. Cordes for the southern Florida area. Timer errors and malfunctions, which occurred in 7 of 10 installations, required immediate corrections, regardless of other work plans. Also, the field technicians did not possess the skills required to service and repair transmitters. An evaluation of system performance showed that at least one correct data message was received from each site on 77 to 97 percent of the days.

The final data-relay evaluation, performed over an 8-month period by Comsat General Corporation under contract to the USGS and the Canadian government, used Canada's Telesat communications satellite and transmitters at five sites in Pennsylvania, five sites in Oregon, and one site in Virginia. According to W. G. Shope, Jr., the test showed that a reliable data transmitter can be developed for use on remote sites, and satellite relay of environmental data can coexist with other commercial applications, such as telephone and television. Minor problems involving power supplies, transmitters, and land-line links were quickly resolved or reduced. During the final 3 months of the test, correct data messages were received 100 percent of the time from all operating transmitters.

Enhancement of surface-water features by principal-components transform of Landsat data

Principal-components transform, an advanced statistical procedure, uses the rotation of eigenvectors to create uncorrelated data matrices from original, correlated data sets. Landsat-image data are correlated; an object that is dark on a band-4 image is usually dark on a band-5, -6, or -7 image. The spectral rotation of these data by digital processing creates four new images. Nearly all of the original variance is explained by the first and second component images; small differences in spectral reflectance that are obscure in the original data usually can be seen in the second and third component images; noise and random differences in spectral reflectance tend to be confined to the third and fourth component images. The practical advantage of a principal-components transform is that hydrologically significant information can be concentrated in one or two of the component images.

Surface water appears dark on all of the four Landsat-band images, and small differences in color and turbidity are obscure. In some cases, small differences in spectral reflectances of surface waters can be discriminated by contrast increases or by digitally scaling (translating) the data. Recent research by G. K. Moore (USGS) and J. R. Lucas (Technicolor Graphic Services, Inc.) showed that a principal-components transform of the data is a useful technique for enhancement and discrimination of surface-water features.

Geometric correction of flight-path curvature in SLAR imagery

SLAR imagery often contains geometic distortions caused by aircraft roll, pitch, yaw, altitude or ground-speed changes and flight-path curvature. Modern instrument systems correct some of these distortions mechanically and with electronic algorithms. The largest remaining errors are caused by flight-path curvature and ground-speed changes. A new correction method, developed by C. H. Ling (1978), requires identification of a few points on both the image and a corresponding map. The algorithm then employs a quasi-circular function passing through these points to convert image coordinates to map coordinates. Although it was developed specifically for correction of flight-path curvature, the algorithm also produces a good correction for ground-speed changes. The curvature error for a 130-km flight path over the Alaskan coast was as much as 2.8 km, but the new algorithm reduced this error to about 0.2 km.

Ground-water information on Landsat imagery

Recent tests by G. K. Moore showed that procedures to obtain ground-water information from Landsat images are ready for operational use. Data selection, image enhancement and analysis, image interpretation, and geologic and hydrologic interpretations provide information on surface and near-surface lithologies, structure, and ground-water occurrence and chemical quality in a variety of geologic terranes.

Significance of saturated soils in coastal plains

Saturated soils appear gray to nearly black on Landsat band-7 images. A series of 13 images of an area near Tupelo, Miss. (made between October 1975 and April 1976), showed a wide variation in area covered by dark soil tones near streams and rivers. Formerly it was believed that changes in saturated-soil areas were related to amounts of streamflow; however, tests by G. K. Moore showed that areas of saturated soil apparently expand in response to rises in a water table and increases in areas of seeps and springs where ground water is discharged. Thus, it is probable that the sizes of these areas are related to the amount of ground water in streamflow.

Wetland studies

The methods used to identify and map vegetation of the Great Dismal Swamp of Virginia and North Carolina by using color-infrared photographs were documented by Patricia Gammon and Virginia Carter (1979).

An evaluation of the accuracy of Landsat digital data for wetland vegetation classification and mapping is presently being conducted in the Great Dismal Swamp. Eight classification maps at two levels of detail have been completed. Each map is being evaluated for accuracy by comparing randomly located 10×10 pixel blocks on Landsat data with the same blocks located on orthophotoquads and interpreted from color-infrared photographs.

LAND USE AND ENVIRONMENTAL IMPACT

MULTIDISCIPLINARY STUDIES IN SUPPORT OF LAND-USE PLANNING AND DECISIONMAKING

In recent years, planners, developers, and public officials have begun to appreciate more fully the utility and predictive power of earth-science information in day-to-day decisions. Costly blunders such as placing homes in floodplains, hospitals on earthquake faults, or waste disposal facilities where they contaminate water supplies, can be avoided by appropriate application of this information.

Much of the earth-science information required to evaluate impacts of alternative uses of the land and to facilitate related planning and decisionmaking is derived from more than one of the USGS core disciplines—geology, hydrology, cartography, and geography. During the last few years increased emphasis has been given to multidisciplinary studies that provide specialized and interpretive data that can be understood and used by planners and decisionmakers who may have little or no training in the earth sciences. The research described in the following sections is indicative of the broad range and variety of earth-science information applicable to land-use planning.

Historical changes of shorelines and wetland at river deltas, Puget Sound region, Washington

Historical shoreline and wetland changes were studied for 11 major river deltas in the Puget Sound region. The study, by G. C. Bortleson, M. J. Chrzastowski, and A. K. Helgerson, is based on comparison of maps made during the period 1854–99 with modern topographic maps.

The observed shoreline and wetland changes range from minor to significant in regard to land use, environmental impacts, and planning implications. The data provide documentation of (1) loss of subaerial and intertidal wetlands since modern settlement, (2) shoreline modifications, (3) development patterns on wetland deposits, (4) progradation and erosion of the subaerial delta, and (5) migration of distributary stream channels.

Most of the river deltas showed substantial loss of wetland habitat. Diking of marshes to develop farmlands caused the greatest loss of marsh. Three of the deltas showed extensive loss of subaerial and intertidal wetlands caused by landfill placement for commercial, industrial, and port facilities. Two of the deltas changed stream course and prograded significantly; the subaerial part of one delta migrated seaward 1 to 1.5 km since 1887–88. Although extensive changes occurred on the major deltas of Puget Sound, many of the deltas have some remaining wetlands and unmodified shoreline that, if managed properly, could retain a valuable fish and wildlife habitat.

Geology and limnology for resource planning and management, Alpine Lakes Wilderness Area, Washington

In a cooperative study with the U.S. Forest Service to develop earth-science information to assist in planning and management, D. P. Dethier has found that a wide variety of ice-related features, including moraines, rock glaciers, and protalus ramparts, are preserved in the upper portions of many drainages in the Alpine Lakes Wilderness Area, central Cascade Range, Washington. Reconnaissance study of weathering characteristics on some of these features in the Enchantment Lakes and Necklace Valley areas suggested that the outer set of moraines associated with small alpine glaciers may be of early Holocene age rather than Neoglacial as previously believed. Detailed studies of tephra deposits and relative weathering parameters are required to further evaluate this interpretation. The basic geologic information, however, already is being used by Forest Service personnel as an aid to interpreting their soil-resource inventory. Together, the geologic and soils information provides a basis for most of the Forest Service's resource capability and suitability analyses of the Wilderness Area.

Low concentrations of nutrients and major ions characterized 45 lakes selected for reconnaissance limnological studies in the Alpine Lakes Wilderness Area during 1978. The flushing rates calculated for most lakes were high; consequently, pollution from

recreational use is not considered as a potential threat to overall lake water quality.

Ancestral Potomac River deposits in Fairfax County, Virginia

Porous sand and gravel beds comprise a significant part of the non-consolidated deposits that occupy an abandoned Pleistocene channel of the ancestral Potomac River in Fairfax County south of Washington, D.C., according to A. J. Froelich, R. H. Johnston, and W. H. Langer (1978). The deposits lie from 3 to >30 m below sea level adjacent to the Potomac estuary. These newly discovered deposits, which occur beneath and adjacent to fresh water in the Potomac, are of interest as a potential source of supply for a riverbed infiltration system. Such a system involves pumping a well to create a cone of depression that intersects the riverbed and induces flow from the river through the aquifer to the well. Critical factors, which are to be assessed before this new and potentially significant adjunct to the local water supply is proved, include (1) the permeability of the aquifer, (2) the possible inhibiting or plugging effect of mud, silt, and clay that lies between the river bottom and the aquifer, and (3) the effectiveness of the aquifer to filter out contaminents present in the estuary.

Computer-composite hydrogeologic maps for Fairfax County, Virginia

Hydrogeologic derivative maps of Fairfax County, Virginia, have been produced by a computer-composite mapping technique developed by R. H. Johnston and J. N. VanDriel (1978, 1979). One map, which shows the susceptibility of the Coastal Plain aquifers to pollution, is a combination of four factor maps showing aquifer occurrence, hydraulic gradient, clay thickness, and lithology. A second composite map, showing the potential yields of water wells, was made by combining maps showing lithology, topography, Landsat lineaments, overburden thickness, bedrock highs, and surface materials.

Computer-composite mapping made it possible to combine these source maps to present information which is difficult or impossible to produce by any other method. Both maps are being used by citizens and planners to aid the protection of existing ground-water resources and to evaluate the feasibility of increased ground-water use in Fairfax County.

Methane gas from landfill deposits in Denver area of Colorado

Methane gas produced by decaying organic matter in landfills is rapidly becoming a major safety hazard in the Denver metropolitan area. Methane escaping from landfills caused several gas explosions, which resulted in at least two fatalities and several severe burn cases. Many of the landfills, which also pose contamination threats to the shallow ground-water table and foundation and land surface subsidence threats to future land uses, are shown on geologic maps resulting from engineering geology studies by R. M. Lindvall. A regional map showing landfills in the greater Denver area was prepared by L. A. McBroome and W. R. Hansen (1978) as a part of the Front Range Urban Corridor project. These maps are being used by local government organizations in land-use planning studies.

Mountain soils mapping in Front Range Urban Corridor, Colorado

A reconnaissance method for mapping the ratio of soils to bedrock has been developed by K. L. Pierce and P. W. Schmidt for the mountainous part of the Front Range Urban Corridor in Colorado. Rapid population growth in this area of varied crystalline bedrock has fostered the need for soils maps suitable for broad-scale land-use planning.

The objectives of the mountain soils project were to outline the relative distribution and ratio of soil to bedrock to a depth of 2 m and to present this information in a format easily understood and usable by the nongeologist. Twenty-one soils maps at a scale of 1:24,000 have been completed. Five simple map units were used throughout the project area; each unit has distinct land-use capabilities that are outlined in a tabular text accompanying each map.

Regional agencies use of earth-science products from the San Francisco Bay Regional Study

A critical evaluation of regional agency use of the 100 earth-science products prepared as part of the USGS-HUD San Francisco Bay Region Environment and Resources Planning Study (SFBRS) was completed by W. J. Kockelman (1979).

Inventories of seven selected regional agencies having various regional planning and plan implementation assignments, such as bay conservation and development, coastal zone conservation, metropolitan transportation, and water-quality control were conducted. The inventories were designed not only to document applications of SFBRS products but also to evaluate the extent of those applications

and to suggest ways to achieve greater and more effective use of earth-science information.

From the inventories and responses to interviews, Kockelman concluded that the selected regional agencies in the San Francisco Bay region are familiar with, make frequent use of, and will continue to use SFBRS products for a wide range of regional planning and decisionmaking activities.

Fifteen selected examples of applications of the products to various regional planning and decisionmaking activities are discussed and illustrated by Kockelman (1979, p. 53–111). Some of the activities selected are:

- Forecasting locations of maximum earthquake damage.
- Preparing natural process and landscape relationship inventories to be used in assessing the consequence of transportation projects.
- Identifying potential waste-disposal sites.
- Evaluating transportation corridors related to land use and natural hazards.
- Regulating coastal bluff and cliff development based on erosion potential.
- Marsh protection planning based on geologic materials and processes.
- Open-space planning based on natural resources and hazards.
- Water-quality control planning based on San Francisco Bay circulation studies.
- Determining legal boundaries and area of jurisdiction for regulating bayshore development.
- Preparing environmental impact reports.
- Implementing computer-based information systems containing most SFBRS products.

LAND USE AND LAND COVER MAPS AND DATA AND OTHER GEOGRAPHIC STUDIES

Land use and land cover mapping and data compilation and related research being done by the Geography Program of the USGS is divided into the following major activities:

- Release to the open file of land use and land cover maps and associated maps at scales of 1:250,000 and at 1:100,000 for selected areas.
- Experimentation with and demonstration of land use and land cover mapping at scales larger than 1:100,000 for specific applications.
- Experimentation with Landsat multispectral data for consistent mapping results and measurement of spatial and temporal changes in land use and land cover.
- Research on and development of a Geographic Information Retrieval and Analysis System (GIRAS) for handling land use and land cover data in conjunction with environmental, socioeconomic, demographic, and other data.
- Analytical and interpretative studies on land use patterns, problems, and trends.

Land use and land cover and associated maps

The land use and land cover mapping and data compilation being conducted by the Geography Program began in fiscal year 1975 to provide systematic and comprehensive mapping and analysis of land use and land cover on a nationwide basis. The Geography Program provides program development, specifications, quality control, accuracy checks, and consultation, although the basic compilation of land use and land cover maps is done in the Topographic Division's Mapping Centers.

Land use and land cover maps are being compiled at a scale of approximately 1:125,000. Associated maps showing hydrologic units, counties, and census county subdivisions are also being compiled for each land use and land cover map produced. Federal land ownership maps are compiled on request for States involved in cooperative cost-sharing agreements with USGS. State land ownership is shown when such information is made available by the appropriate cooperating State agency. The land use and land cover maps and accompanying associated maps are keyed to the standard topographic map series at 1:250,000 scale and, for selected areas, to the new base maps being prepared at 1:100,000 scale by the Topographic Division. By September 1978, land use and land cover data had been compiled for 202 quadrangles, and 103 quadrangles were in production. The total area mapped at that time was about 2,590,000 km^2 (1 million mi^2) (fig. 4).

These compiled maps include 100 percent of the Atlantic coastal areas, 98 percent of the coastal area of the Gulf of Mexico, and 50 percent of the coasts of California, Oregon, and Washington and other areas such as the Western coal areas (covered by the Dickinson, Ekalaka, Glendive, Gillette, Hardin, Newcastle, and Miles City 1:250,000-scale sheets) in Montana, North Dakota, and Wyoming.

Land use and land cover data are categorized according to the classification system presented in USGS Professional Paper 964 (Anderson and others, 1976). Specifications for compilation of these

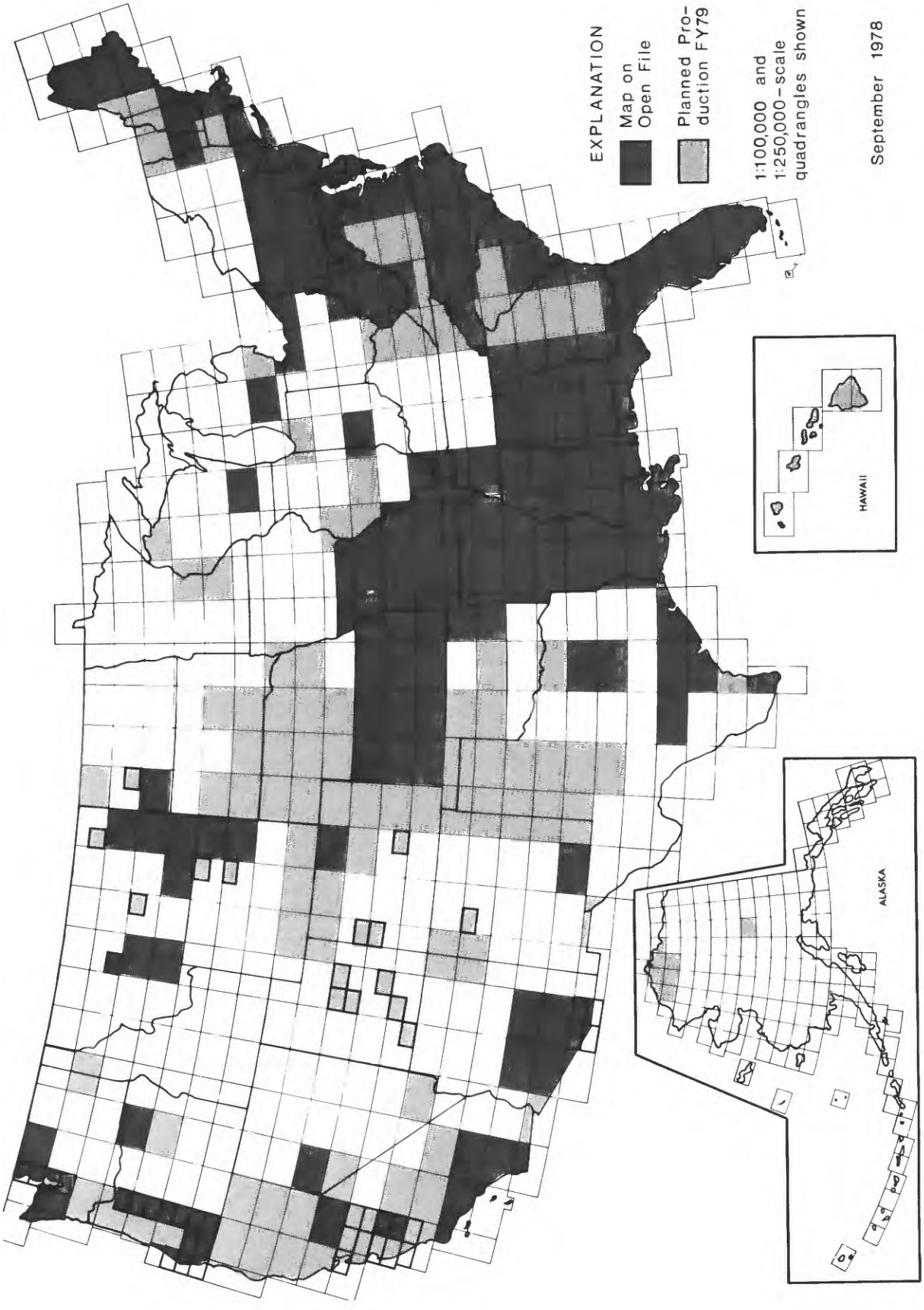

FIGURE 4.—Status of land use and land cover mapping as of October 1978.

maps were issued in USGS open-file report 77–555 (Loelkes, 1977). The minimum mapping unit for urban or built-up uses, water areas, confined feeding operations, other agricultural land, and strip mines, quarries, and gravel pits is 4 ha. All other categories are delineated with a minimum unit of 16 ha. Federal land holdings are shown for tracts of 16 ha or larger.

The first color-coded land use and land cover map of Kansas City in Missouri and Kansas has been published (USGS, 1978). Level I land use categories are presented in a color-coded format based on a modified version of the World Land Use Survey color scheme. Level II land use categories are denoted by two-digit numerals such as "21," which signifies cropland and pasture. This is the first of a projected group of maps of selected areas of the United States to be published in full color to illustrate land use and land cover patterns.

Land use maps and associated maps, initially available as black-and-white products at 1:250,000 scale, are placed on open file at the USGS Mapping Centers. Enlargements to scales such as 1:125,000 can be requested from the Mapping Centers. When an enlargement is made, however, the positional accuracy of the base map on which the land use and land cover data have been plotted still remains that of the 1:250,000-scale map. The maps can be used for many purposes in the scale range of 1:100,000 to 1:250,000.

Land use and land cover maps and associated maps are being digitized in a polygon format. Polygons can be converted to grid cells of varying sizes to derive land use and land cover statistical data.

After the land use and land cover data and other map overlays are digitized, computerized graphic displays and statistical data on current land use and land cover are available for use in conjunction with other data. Statistical data are compiled for counties, for areas of Federal ownership, by river basins and subbasins, and by statistical units such as census tracts or other census county subdivisions.

Cooperative land use mapping and data projects

Cooperative agreements between the USGS and State and county agencies have provided land use and land cover and associated maps for the following States: Alabama, Arkansas, Florida, Georgia, Kansas, Louisiana, Missouri, North Carolina, Pennsylvania, and West Virginia and for the county of San Mateo, California. The San Mateo County project produced 18 Level III land use and land cover maps on a 1:24,000 scale.

Land use and land cover maps for the State of Hawaii are presently being compiled under a cooperative agreement. Digital data on magnetic tape were delivered to Arkansas, Florida, Kansas, and Louisiana.

Land use and land cover change mapping of urban areas

The operational and developmental activities of the Geography Program are generating both standard and prototype products in three forms: maps, statistics, and computer tapes. The map products can be either in polygon or in digital format. Recent technological advances were applied directly in the preparation of prototype thematic land use and land cover map products. Examples of such maps are a pair of digital land cover maps of the Washington, D.C., urban area, prepared for reproduction by a tape-driven laser plotter. These maps were published as Miscellaneous Investigations maps I–858–E and I–858–F (Gaydos and Wray, 1978a; 1978b). Area summaries, another immediate byproduct of computer assisted classification, are listed on the maps.

A land use and land cover map of the Atlanta, Ga., metropolitan region at a scale of 1:100,000 (USGS, 1976), compiled by conventional aerial photograph interpretation, was chosen to demonstrate the use of laser scanning and plotting equipment to prepare a polygon-style thematic map for publication. The scan-digitizing method also provides area measurement summaries of the land cover classes.

These automated thematic mapping techniques help to (1) expedite the preparation and distribution of operational land use and land cover information in all three forms (maps, statistics, and computer tapes), (2) permit interactive viewing of the analysis by video display, and (3) make it feasible to prepare more current statistical and other thematic maps for future editions of the "National Atlas of the United States of America."

Central Atlantic Regional Ecological Test Site

The Central Atlantic Regional Ecological Test Site (CARETS) project, a 5-year demonstration project for introducing data from Landsat and high-altitude aircraft sensors into regional land use planning and management, was concluded with completion of the final summary report, which is being reviewed. This demonstration project was carried out by means of an environmental information systems model by which land use maps were prepared

from remotely sensed data. The maps were digitized, processed, and linked to other environmental and social data sets and to environmental consequences such as air pollution, stream runoff, local climate, and coastal erosion. A related report dealing with air quality implications of land use was published as USGS Professional Paper 1099–B (Reed and Lewis, 1978). A method for coding and reformatting computerized land use data tapes was devised, and tapes were prepared for release to the public. The establishment of a network of regional land resource information centers throughout the country for coordinating the use of remotely sensed data in environmental planning and management and for setting priorities for future land use data collection, dissemination, and analysis is recommended in the final report for this project.

Landsat used to map vegetation in Alaska

Using Landsat digital data, the Geography Program has mapped vegetation in the 100,000-km^2 National Petroleum Reserve–Alaska (NPR–A). Multispectral scanner data from 10 Landsat scenes were analyzed using EDITOR software and the ILLIAC IV parallel processing computer at NASA Ames Research Center, Moffett Field, Calif. Then each spectral class that was determined through the computer analysis was identified with a specific class of vegetation by using an interactive color display system.

Recent high-altitude, color-infrared photographs and other information, collected during a Bureau of Land Management sponsored field trip, were used to establish a uniform classification system of 10 classes that would consistently characterize vegetation over the NPR–A by using Landsat digital data. The vegetation classification obtained from Landsat was generalized and edited to match this classification system. This land cover map of the NPR–A was prepared as an uncontrolled color mosaic at a scale of 1:500,000 for preliminary evaluation by agencies interested in the region.

A 1978 field trip, conducted with the cooperation of the Geologic Division, verified the reliability of the preliminary map and provided additional information for the final map and statistical products.

Land use map accuracy determination

Accuracy analyses were made for the land use and land cover maps at the scales of 1:24,000 and 1:100,000 for the greater Atlantic, Ga., region and land use and land cover maps at 1:24,000, 1:100,000, and 1:250,000 scales of the Central Atlantic region (Fitzpatrick-Lins, 1978a). Land use change maps for the period 1970–72, prepared from high-resolution, high-altitude aerial photographs of the Central Atlantic Regional Ecological Test Site (CARETS), were also analyzed (Fitzpatrick-Lins, 1978b, 1978c). The Atlanta study demonstrated an accuracy of 90 percent at 1:100,000 scale and 87 percent at the 1:24,000 scale. The accuracy of the interpretations was consistent from category to category mapped. The findings of this study have emphasized the necessity for quality control checks both during and after map compilation and have contributed to the development of quality-control procedures for the nationwide mapping of land use and land cover currently being carried out by the USGS.

Statistical design of sampling techniques

A computer program to perform statistical sample design to select test points for the accuracy evaluation of land use and land cover maps was developed in 1978 by Dr. H. S. Ling, a National Urban League Summer Fellow in the USGS from South Carolina State College. Initial sample selection is based upon a systematic, stratified, unalined sampling technique. Dr. Ling's analysis includes selection of the minimum-sample size necessary to statistically validate the accuracy of a given category of land use and land cover classification. For the underrepresented categories, the computer program selects the remaining needed sample points in a random manner from all classified polygons in the given category. In addition, the computer program performs all of the post-field test analysis that had previously required long, tedious computation. Tables of reduced data have been prepared to assist the Geography Program staff in the accuracy analysis of the land use and land cover maps.

Statistical comparisons of land use mapping at 1:24,000 and 1:100,000 scales

Maps of the greater Atlanta region of Georgia completed in 1976 were compared for costs and information differences at scales of 1:24,000 and 1:100,000 (Fitzpatrick-Lins, 1978a). Both maps were compiled at Level II using the USGS land use and land cover classification system (Anderson and others, 1976) and the mapping specifications in USGS open-file report 77–555 (Loelkes, 1977), except for the 1-ha minimum mapping unit used for the 1:24,000-scale maps. M. J. Chambers found that there was no statistically significant difference between land use and land cover information mapped

at the 1:24,000 scale and the 1:100,000 scale (Fitzpatrick-Lins and Chambers, 1977). Land use and land cover polygons in the 61,000-ha study area in north Atlanta were measured with an electric planimeter, and the results were yielded through Chi-square analysis for significance.

Costs incurred in the mapping of the same area at a scale of 1:24,000 were 16 times greater than for the same area at a scale of 1:100,000. The fact that no statistically significant difference in category acreage totals was found between the scales of 1:24,000 and 1:100,000 will aid when making decisions relating to scales to be used in an inventory of land uses, how much information is required at different map scales, and differences in costs and benefits for land use maps at different scales.

Land use change detection and map update

Extensive research into the various aspects of land use and land cover change detection has been conducted as a first step toward the establishment of an operational program of map update. A comprehensive evaluation was completed by V. A. Milazzo of alternative considerations in five general areas of land use change detection related to land use and land cover map update: remote sensing sources, map bases, areas of update, frequencies of update, change detection procedures, and data presentation formats. The advantages and limitations of each consideration within this framework with respect to such factors as cost, time efficiency, accuracy, data comparability, and product usability were documented. In order to facilitate application of this general research, several studies dealing with more specific aspects of change detection and land use map update have been undertaken.

To determine how frequently land use and land cover map update may be needed in a dynamic urban setting, an analysis was conducted of the land use changes in an 880-km^2 area of Phoenix, Ariz. Land use changes that occurred between base year 1972 and 4 years prior (1970, 1967, 1963, 1954) were derived by comparing the base-year map with aerial photographs in each of the given years. Evaluation of the changes showed that by routinely monitoring the change activity within select "index" land use categories, an update interval could be established based upon the degree of change activity. Quantitative analysis of the changes in the Phoenix study area revealed that residential land use could be used as an index category for determining map update frequency. The degree of land use change activity within the residential category indicated an optimum map update cycle of 3 to 4 years.

In a second study conducted by D. B. Gallagher, land use and land cover changes were analyzed as part of a study of the impact of phosphate mining on the landscape in a three-county area in southeastern Idaho. Significant change activities observed in the Idaho study area included (1) the conversion of forest, farmland, and rangeland to intensive mining and industrial uses, (2) the accumulation of massive amounts of tailings at the phosphate processing plants, (3) the construction of schools, hospitals, and other public service oriented facilities, and (4) the proliferation of mobile homes in the region's urban centers. Knowledge of such land use and land cover change trends is vital to planners and resource managers for the successful future management of the area's land resources.

A final area of investigation dealt with the Pilot Test (formerly the Applications System Verification and Transfer project) conducted jointly with NASA. The primary objective of this project is to test the operational feasibility and effectiveness of using Landsat digital data for change detection and update of the land use and land cover maps and data being produced by the USGS.

Land use and land cover patterns and changes were analyzed in several test sites in Louisiana. These test sites were selected to represent various types of changes and conditions including (1) forested bottomland being cleared for crops or pasture, (2) forest and agricultural land being cleared for urban development, (3) wetlands being converted to urban or built-up uses, and (4) forested and agricultural uplands undergoing relatively little change.

In the first phase, the main objective was to determine what types of changes had actually taken place in the test sites. Recent aerial photographs of the test sites were compared with the original source material used to compile the existing land use and land cover maps. In the second phase, Landsat digital analysis techniques were developed to determine changes from sequential sets of Landsat data. Then these techniques were tested and the results evaluated to determine how well land use change data derived from Landsat computer classification could be used to update the land use and land cover maps. The results showed that Landsat digital analysis techniques were adequate for identifying land use changes in areas where there were substantial changes and where change occurred over large areas. The same techniques were inade-

quate, however, in areas where there was a small percentage of change and where change occurred over small areas. In addition, numerous areas of "false change" were identified from the Landsat analysis. The difficulties encountered suggest that Landsat classification accuracy and digital analysis techniques must be improved prior to application in an operational program for land use change detection and map update.

Interrelation of census and USGS land use data

Duval County, Florida, containing the Jacksonville metropolitan area, was selected for an experiment to interface Geological Survey land use and land cover data with Bureau of the Census population and related demographic data using a computer. The residential population density patterns determined for the study area were shown to be more useful to researchers than the usual population density patterns prepared for urban areas.

Development of Atlantic-Gulf Barrier Islands

Land use and land cover change measurements on most of the barrier islands along the Atlantic and gulf coasts were prepared for the Heritage Conservation and Recreation Service. Measurements for the period 1945–55 were prepared from aerial photographs taken during those years and compared with land use and land cover measurements prepared in 1978. Urbanization and other types of development were tabulated as an aid in recreation planning.

Geographic information systems software development

The Geography Program continued research and development work on a Geographic Information Retrieval and Analysis System (GIRAS) to extend and improve its capability for computer-aided storage, editing, manipulation, and retrieval of a geographic data base for land resource planning and management as well as for analysis of land use patterns, trends, and problems. The system includes (1) contract and in-house digitization of land use and land cover maps and other environmental data, (2) editing and correction of the geographic data base, and (3) manipulation and retrieval of those data in order to perform area measurements, map compositing analyses, and statistical and other computer-aided operations.

Through the end of fiscal year 1978, land use and land cover map sets covering about 1,295,000 km^2 (500,000 mi^2) of the 48 contiguous States were digitized under commercial contract and edited with the GIRAS system.

USGS Professional Paper 1059 (Mitchell and others, 1977), reprinted in 1978, provides a general system description of the facilities and procedures of GIRAS I, the batch-oriented geographic information retrieval and analysis system operational in the Geography Program. In addition to a detailed description of the data structure being used in GIRAS I, the Professional Paper describes procedures for data capture and editing, data retrieval, data manipulation, and data output and establishes the design features for GIRAS II.

The Geographic Information Systems Branch established a training course in the use of its software to assist in the technology transfer process. Representatives from the State of Missouri and the University of Arkansas attended the course and began to implement the software on their own computers. The Branch received an average of 20 inquiries per month about digital data and software from both present and potential users. Additional contacts included 7 from international sources, 6 from States, and 17 from other Federal agencies.

Research on public response to geologic hazards

A project for monitoring public response to geologic hazards information concerning earthquakes, volcanoes, landslides, subsidence, glaciers, and related phenomena has been carried out by USGS for several years. R. H. Alexander of the Geography Program served as USGS contact person for socioeconomic research on pubic acceptance and use of the hazard information. This phase of the project included coordination with Federal, State, and local Government users or producers of such information, which was facilitated through workshops and through a network of contacts provided by the Natural Hazards Research and Applications Information Center, University of Colorado, Boulder. Preliminary public response to hazard notifications in five Western United States sites was monitored, and considerable local concern over the negative economic impact of the notifications was noted. Results of the study indicated that public response to geologic hazards related information could be improved by having more thorough documentation of the impacts of notification and greater efforts to increase local understanding and awareness of geologic hazards and by using more appropriate warning systems, preparedness programs, and land use planning.

ENVIRONMENTAL IMPACT STUDIES

Subsidence of reclaimed coal mine spoils, Colstrip, Montana

Precise leveling surveys and ground and aerial inspections were conducted to determine the nature and practical effects of surface lowering caused by consolidation of reclaimed spoils at the Rosebud mine, Colstrip, Montana. In spoils 30 to 40 years old, lowering of spoil surfaces occurring since 1968 average 0.1 m and is of no practical effect. In spoils rehandled to form fill in 1968, surface lowering approached 0.25 m and is caused by failure of excessively steep side slopes and by compaction in response to saturation. Surface lowering in spoil areas emplaced since 1971 is as great as 0.6 m in areas of about 1×2 m. Compaction of the redistributed topsoil following saturation is the apparent cause.

Mode of deformation of Rosebud coal—Colstrip, Montana

Cylindrical specimens of subbituminous B Rosebud coal from Colstrip, Mont., were experimentally deformed at room temperature, at a strain rate of 1×10^{-5} s^{-1} and at a confining pressure of up to 1,054 kg/cm^2. Specimens were then made into thin sections and examined. Three modes of deformation were observed and found to depend on confining pressure. At confining pressures up to 70.3 kg/cm^2, the coal failed by brittle fracture along surfaces subparallel to the compression axis. At confining pressures of 105.5 to 632.8 kg/cm^2, the coal exhibited behavior that was transitional between brittle and ductile and failed by shearing along one or more surfaces inclined to the compression axis. At confining pressures of 703.1 kg/cm^2 or greater, the coal exhibited ductile deformation.

INTERNATIONAL COOPERATION IN THE EARTH SCIENCES

Although the USGS is primarily concerned with surveys, investigations, and research within the territorial limits of the United States, it has also been involved in activities abroad for almost 40 years, partly on behalf of other U.S. agencies and programs, and partly in cooperative research to extend and complement its own domestic program. Most USGS activities abroad have involved scientific and technical assistance to counterpart agencies of other governments and to international organizations, in support of the U.S. Foreign Assistance Program. Other activities can be categorized as cooperation and research on subjects of mutual interest to the USGS and counterpart agencies and representation and participation in international commissions, working groups, and meetings.

SCIENTIFIC AND TECHNICAL ASSISTANCE

In nearly 4 decades of assistance activities, the USGS has provided a wide range of services in more than 80 countries to strengthen counterpart earth science agencies and programs, to help identify and assess resources, and to study geologic hazards or other phenomena. All such assistance is at the request of, and funded by, other agencies or governments. The scope of such assistance and the countries involved have changed over the years to meet the more urgent needs of the developing countries and the priorities of the U.S. Foreign Assistance Program. In earlier years, the assistance was concerned mainly with general mapping, resource identification, and training, whereas in later years the assistance has been concerned more with studies of specific resources and environmental and hazard problems, or with the introduction of new earth-science techniques.

Assistance in studying energy resources

During 1978, increased concern about energy resources for the future led to the development of an assistance program involving the identification and assessment of such resources. Under the Nuclear Non-proliferation Act of 1978 and on behalf of the U.S. Department of Energy (DOE), the USGS participated in studies of energy resources options in Egypt and Peru. The work consisted of preparing preliminary summaries of resources information based on literature search, followed by studies of unpublished data, and on limited field inspections in host countries by a team of specialists in petroleum geology, coal, uranium, geothermal energy, and water. In cooperation with counterpart scientists, they compiled all available nonproprietary information and appraised the energy potential so that the information could be used to evaluate future energy options in the host countries. Results are discussed under "Summary by Country."

In another phase of cooperation in energy, F. E. Senftle was requested to chair an International Atomic Energy Agency (IAEA) consultants' meeting in Cairo, Egypt. Attendees were from Austria, Belgium, the United Kingdom, and Egypt. Senftle reported on two borehole gamma-ray spectrometers used for mineral exploration. Specific examples of their use for coal and uranium were given. The consultants recommended the development of nuclear techniques for mineral exploration, mining, and processing and initiation of an interregional training course on these subjects.

G. H. Davis served as a lecturer for the Seminar on Isotope Techniques in Water Resources Development in the African Region. The seminar was sponsored by IAEA, UNESCO, and the World Meteorological Organization.

G. D. Debuchananne advised both IAEA and the Nuclear Energy Agency of the Organization for Economic Cooperation and Development on land burial of radioactive waste.

As part of the agreement between DOE and the Mexican Comision Federal de Electricidad for cooperation in the expansion of the Cerro Prieto geothermal field, the USGS was assigned the responsibility for establishing a regional triangulation network to monitor crustal strain. Cerro Prieto is an extension of the Imperial Valley, California,

where the United States is exploring for geothermal steam. The triangulation network will provide a base line to monitor both subsidence and horizontal movement during future development. Monumented stations, whose positions were established by a series of extremely precise measurements, were installed. The network started from a base station on the United States-Mexico border and extended 50 km south across the Cerro Prieto field. The instrument used to perform the measurements, the geodolite, used a reflected laser beam to determine distances. High accuracy was obtained by applying precise corrections for meteorological conditions at the time and place of measurement. The meteorological data for these corrections were obtained by flying a fixed-wing aircraft along the line of measurement at the time the measurement was being made and by making the measurement on two different occasions. The regional net as established consists of 12 stations, each occupied twice, with a total of 87 lines (distances) measured. The work was done by R. W. Ruthven, K. W. Gatson, W. A. Olson, Jr., K. L. Walthall, and N. D. Scheetz.

As part of the same program, A. H. Truesdell, F. J. Pearson, Jr., T. B. Coplen, and G. S. Laurin collected steam and water samples from wells and springs. Analyses for stable and radioisotopic constituents will be made in an effort to determine the age and origin of geothermal fluids and possible recharge sources and rates.

Red Sea Commission

A study of remote sensing applications to environmental pollution and marine resources studies in the Red Sea was made by S. J. Gawarecki for the joint Saudi Arabia-Sudan Red Sea Commission. The study considered the use of orbital, suborital, and submarine remote-sensing techniques to investigate the Red Sea heavy-metal area prior to and during proposed dredge-mining operations and to determine possible applications to other Red Sea resources.

Gawarecki found that Landsat multispectral scanner (MSS) bands 4 (green-yellow) and 5 (orange-red), especially in the high gain mode, would be very useful in defining turbidity patterns in the dredging environment, as would be the return beam vidicon (RBV) image from Landsat 3. Bands 6 (red-near IR) and 7 (near IR), which show the high reflectivity of chlorophyll-bearing phytoplankton at the surface, should prove useful in fishery studies and, together with other bands, provide clues to current patterns.

The Heat Capacity Mapping Mission satellite, the Coastal Zone Color Scanner in the Nimbus 7 satellite, and a variety of airborne sensors can be useful. Conventional color and color infrared photography, supplemented by thermal infrared scanning to establish temperature-color relationships, may be used for monitoring the dredging operations. Shipborne sensors including echo-sounding profilers and mid-scan sonar (Sound Navigation and Ranging) are the main tools for submarine mapping, and a new underwater fluorometric system is available to continuously monitor dissolved hydrocarbons from an oil spill.

Assistance to intergovernmental organizations

F. H. Wang has been assisting in the work of the United Nations Committee for Co-ordination of Joint Prospecting for Mineral Resources in Asian Offshore Areas, which is an intergovernmental body composed of 11 countries in East and Southeast Asia. Programs are primarily concerned with search for hydrocarbons and mineral resources in offshore and oceanic areas, related geoscientific studies, and research and training programs for the benefit of developing countries. Reconnaissance geological and geophysical surveys have been carried out over the vast shelf areas of this region. Most of the member countries in Asia have now advanced in intensive petroleum exploration and development. Recent offshore petroleum production in several countries already constitutes an increasing segment of their national economies and has also significantly contributed to the energy needs of the world. With participation of many scientists and research institutions in the United States, supported by the National Science Foundation under the International Decade of Ocean Exploration and other programs, a program of Studies of East Asia Tectonics and Resources is being undertaken to intensify and extend geological and geophysical surveys and research into oceanic regions and across the shelf and coastal areas; particular emphasis is placed on multidisciplinary research along six key transects across the oceanic trenches and island arcs.

R. P. Maley was detailed to UNESCO to advise on the selection of strong motion accelerographs and on training of local personnel in the operation and maintenance of these instruments. He assisted in the establishment of an UNDP accelerograph network in the Philippines, Indonesia, Hong Kong, Thailand, Malaysia, and Singapore. Eight UNDP and two Philippine Atmospheric, Geophysical, and

Astronomical Services Administration (PAGASA) accelerographs were installed in the Metro Manila Area, and one PAGASA accelerograph was installed at Bagac, Bataan. In Indonesia, seven UNDP accelerographs were installed. Accelerographs belonging to the Indonesia Meteorological and Geophysical Institute were repaired and relocated at Lembang, Java, and Padang and Medan, Sumatra. Three Royal Observatory accelerographs were placed on Hong Kong Island and at Kowloon and New Territories on the Mainland. Maley assisted Thailand in planning for a five-instrument network in 1978–79, located one accelerograph at Petaling Jaya, just outside Kuala Lumpur, Malaysia, and assisted Singapore in the planning for a modest strong-motion program to be implemented in 1978.

Participant training and technology transfer

Technical assistance programs are a means of transferring technological expertise to developing nations. Some programs consist largely of training of participants either in-country or in the United States, others range from consultation or advisory to the implementation of highly technical resource analyses. Most of the USGS cooperative assistance programs are sponsored by the Agency for International Development, U.S. Department of State, at the request of the host government and in accord with the Foreign Assistance Act. The types of activities are varied, depending on the needs of the particular country, and are summarized in table 4. During this report period, USGS scientists undertook 240 formal assignments in 40 countries. During the same period, 210 earth scientists and engineers from 60 countries pursued academic, observation, or intern training in the United States (see table 4).

Since the beginning of USGS technical assistance in 1940, more than 2,750 technical and administrative documents authored by or closely supervised by USGS personnel have been issued. During 1978, 29 administrative documents were prepared, and 60 reports and (or) maps were released (see table 5).

Training through workshops, seminars, and field courses continues to be a small but important phase of the USGS's international activities. S. J. Gawarecki and L. C. Huff led eight Saudi Arabian geologists on a 5-week geologic field methods course in Colorado, Arizona, and New Mexico in July and August 1979. The course included formal classroom sessions at the USGS Denver headquarters, visits to selected classic igneous, metamorphic, and sedimentary rock localities and different types of ore deposits, and attendance at the Annual Meeting of the International Association on the Genesis of Ore Deposits.

CENTO training program

The USGS, under the auspices of the Agency for International Development, has provided leadership for summer-long field courses in mapping and appraisal of mineral deposits in the CENTO region (Turkey, Iran, and Pakistan) since 1966. More than 170 graduate geologists and mining engineers have participated in the training. Several comprehensive mine reports have been published, and exploration suggestions that resulted from the groups' studies have led to major ore discoveries. The 10th CENTO training program, under the direction of E. H. Bailey, was conducted July–September 1978, at the Sizma mercury mines in Central Turkey. Those assisting in the instruction were J. W. Barnes, University College of Swansea, U.K.; M. P. Nackowski, University of Utah, U.S.A.; Tarek Tugal, MTA, Turkey; M. Momenzadeh, Geologic Survey of Iran; and Z. Ahmad, Geological Survey of Pakistan. Fourteen graduate geologists from the CENTO region took part in the course.

As part of the training, the group made a detailed geologic and topographic map of 2 km^2 of the Sizma mines, a reconnaissance geologic map of the 150-km^2 district, and a geochemical survey of the district and mapped the underground workings of the Medrese mine. Maps and exploration suggestions were given to the mine operators upon completion of the field study. Also discussed with the operators was the discovery of a large area of active surface subsidence directly above the major area of underground ore extraction.

SCIENTIFIC COOPERATION AND RESEARCH

Inasmuch as many geologic phenomena of concern in the United States must be studied in other countries in order to be properly understood, the USGS has carried out cooperative studies and exchanges of information with counterpart agencies and scientists in a number of countries. Most of these are short-term activities dealing with specific phenomena or resources. The USGS has entered into scientific exchange agreements with a number of countries, including Poland, Yugoslavia, Federal Republic of Germany, France, Morocco, and Mexico, where frequent exchange or joint investigations make such agreements desirable. In

TABLE 4.—*Technical assistance to other countries provided by the USGS during FY 1978*

Country	USGS personnel assigned to other countries			Scientists from other countries trained in United States	
	Number	Type	Type of activity[1]	Number	Field of training
Latin America					
Argentina	1	Hydrologist	B, D	1	Earthquake Studies
Bolivia	4	Geologist	B, D		
	1	Hydrologist	B, D		
Brazil	2	Hydrologist	B, D	2	Theoretical and Applied Graphics
	1	Geologist	A, D		
Chile	2	Geologist	B, D	6	Remote Sensing
				1	Uranium Ore Analysis
				1	Map Compilation
Colombia	4	Geologist	A, B, D	1	Map Compilation
Costa Rica	--			4	Remote Sensing
Ecuador	2	Geologist	B, D	--	
El Salvador	--			4	Remote Sensing
Guatemala	--			4	Remote Sensing
Guyana	--			--	
Honduras	--			4	Remote Sensing
Mexico	2	Research Chemist	A, D	--	
	6	Hydrologist	A, D	--	
	3	Remote Sensing Specialist	A, D	--	
	2	Geologist	D	--	
Nicaragua	--			2	Remote Sensing
				1	Hydrologist
Peru	8	Geologist	A, C, D	--	
	1	Hydrologist	A, C, D	--	
Venezuela	1	Hydrologist	A, C	1	Remote Sensing
	4	Geologist	A, C	--	
Africa					
Algeria	--			2	Remote Sensing
Central African Republic	--			2	Seismic Research
Congo				2	Remote Sensing
Djibouti	1	Hydrologist	D	--	
Egypt	12	Geologist	A, B, D	4	Remote Sensing
	3	Geophysicist	A, B, D	3	Hydrology
	1	Hydrologist	A, B, D	1	Cartography
	1	Cartographer	A, B, D	--	
Ethiopia	--			1	Hydrogeochemistry
Ghana	--			2	Remote Sensing
				1	Sediment Samples/Hydrology
Kenya	1	Geologist	A, B	--	
	1	Cartographer	A, D	--	
	2	Technical advisor	A, B	--	
Lesotho	--			--	
Libya	--			2	Remote Sensing
Malawi	--			1	Remote Sensing
Mali	--			1	Topographic/Photo Interpretation
Mauritania	--			1	Remote Sensing
Morocco	--			1	Remote Sensing
Nigeria	--			2	Remote Sensing
				1	Coal Resources
Senegal	--			--	
Sierra Leone	--			1	Remote Sensing
Sudan	1	Geologist	D	2	Remote Sensing
Swaziland	--			2	Remote Sensing
Tunisia	1	Consultant	A, B, D	1	Remote Sensing
	1	Computer Scientist	A, B, D	--	
	1	Geologist	A, B, D	--	
	1	Geographer	A, B, D	--	
	1	Remote Sensing Specialist	D	--	
Near East and South Asia					
CENTO/Turkey	1	Geologist	D	--	
India	1	Geologist	A	8	Remote Sensing
				1	Geochemistry/Geothermal Fluids
				2	Photographic Technology
				1	Hydrology
				1	Analytical Chemistry
				1	Isotope Geology
				1	Hydrochemistry

TABLE 4.—*Technical assistance to other countries provided by the USGS during FY 1978*—Continued

Country	USGS personnel assigned to other countries			Scientists from other countries trained in United States	
	Number	Type	Type of activity[1]	Number	Field of training
Near East and South Asia—Continued					
Iran	2	Geologist	A, B, D	3	Remote Sensing
	5	Remote Sensing Specialist	A, D	1	Seismic Research
Israel	--			1	Remote Sensing
Jordan	2	Geophysicist	A, C, D	2	Remote Sensing
	1	Non-Metallic Specialist	A, C, D	--	
	1	Exploration Geochemist	A, C, D	--	
	8	Geologist	A, C, D	--	
	2	Hydrologist	D	--	
Korea	--			1	Data Bank System
				1	Engineering Geology
Pakistan	2	Geologist	A, D	1	Uranium Geology
	2	Hydrologist	C, D	3	Hydrology
Qatar	--			--	
Saudi Arabia	2	Hydrologist	A, B	6	English/Geologic Mapping
	6	Technical Advisor	A, B	3	English
		Geologic Cartographer	A, B	2	Geologic Mapping
	17	Geologist	A, C	1	Geologic Printing
	3	Administrator	A, D	2	Surveying
	4	Water Resource Specialist	A, B	2	Business Administration
				3	Computer Science
	2	Management Specialist	A, B	1	Cartography/Publications/Printing
	1	Chemist	A, D	3	Analytical Techniques
	13	Geophysicist	A, D	1	Analytical Chemistry
	7	Physical Science Technician	A, C	2	Supply/Warehousing
	1	Electronic Technician	A, C	1	Cartography
	3	Contract Specialist	A, C	11	Remote Sensing
	1	Cartographer	A, D	1	Health Physics
	3	Geochronologist	A, D	--	
	7	Publications Specialist	A, D	--	
	5	Computer Specialist	A, D	--	
Syria	1		A, D	--	
Turkey	2	Hydrologist	A, D	1	Natural Resources Data
	6	Geologist	A, D	1	Seismology
	1	Publications Specialist	A, D	1	Geophysics
	1	Photo. Consultant	A, D	1	Remote Sensing
Yemen	2	Geologist	A, D	1	Hydrology
	1	Hydrologist	A, D	1	Surveying Equipment and Techniques
Far East and Pacific					
Australia	--			3	Remote Sensing
				1	Isotope Geology
				1	Tectonic Map Compilation
Burma	--			1	Geochemical Exploration
China, Republic of	--			3	Remote Sensing
Fiji	1	Geologist	A, B, D	--	
Indonesia	4	Geologist	A, D	3	Remote Sensing
	1	Hydrologist	D		
Japan	1	Advisor	B, D	1	Acidic Volcanic Rocks
				1	Uranium Minerals
				1	Tectono Physics
				1	Natural Zeolites
				1	Isotope Geology
				1	Sedimentology
				1	Geochronology
				--	Remote Sensing
Korea	3	Geologist	C, D	--	
Malaysia	2	Petroleum Geologist	A, D	--	
	1	Petroleum Engineer	A, D	--	
New Zealand	1	Hydrologist	A, D	--	
Philippine Islands	1	Advisor	A, D	--	
	1	Hydrologist	A, D	--	
	1	Geologist	A, D	--	
	1	Remote Sensing Specialist	A, D	--	
Southeast Asia	1	Geologist	D	--	
Thailand	3	Geologist	A, D	2	Remote Sensing
	1	Remote Sensing Specialist	A, D		

TABLE 4.—*Technical assistance to other countries provided by the USGS during FY 1978*—Continued

Country	USGS personnel assigned to other countries			Scientists from other countries trained in United States	
	Number	Type	Type of activity[1]	Number	Field of training
Europe					
Austria	2	Geologist	D	--	
France	9	Geologist	D	1	Remote Sensing
				1	Paleomagnetism
				1	Geomorphology
	1	Hydrologist	D	1	Orthophotography
Germany (West)	6	Geologist	A	3	Remote Sensing
	1	Conservation Specialist	D	1	Organic Geochemistry
Greece	--			1	Remote Sensing
Italy	2	Hydrologist	D	4	Remote Sensing
				1	Strong Motion Data Analysis
				1	Isotope Geology
Netherlands	--			2	Remote Sensing
New Zealand	--			1	Seismic Research
Norway	--			2	Seismic Research
Poland	--			4	Remote Sensing
Portugal	1	Geologist	D	2	Civil and Environmental Hydrology
Romania	1	Geologist	A, D	1	Remote Sensing
Spain	--			1	Remote Sensing
Switzerland	--			2	Remote Sensing
				1	Experimental Petrology
				1	Glaciology
United Kingdom/ Great Britain	3	Geologist	D	2	Paleontology
	2	Cartographer	D	1	Paleobotany
U.S.S.R.	--			1	Sedimentary Deposits and Paleontology
Yugoslavia	--			1	Remote Sensing
				1	Seismology
Other					
Canada	--			2	Remote Sensing
				2	Isotope Geology
				1	Hydrology
Haiti	--			2	Remote Sensing
Trinidad and Tabago	--			4	Photolithography
				1	Administrator of Mapping Agency

[1] A, Broad program of assistance in developing or strengthening earth-science institutions and cadres; B, broad program of geologic mapping and appraisal of resources; C, special studies of hydrologic phenomena or resources; D, short-range advisory help on geologic or hydrologic problems and resources.

TABLE 5.—*Technical and administrative documents issued during the period October 1977 through October 1978 as a result of USGS technical and scientific cooperation programs*

Country	Reports or maps prepared			
	Project and administrative reports	Approved for publication by counterpart agencies or USGS	Published	
			In technical journals	By USGS
Brazil	--	--	--	1
Cambodia	--	--	--	1
Circumpacific	--	1	--	1
Colombia	--	--	--	1
Ecuador	--	--	--	1
Egypt	4	--	--	1
Indonesia	1	2	--	1
Israel	--	--	--	1
Jordan	4	--	--	--
Kenya	--	--	--	1
Libya	--	--	--	1
Liberia	--	--	--	2
Malaysia	1	--	--	--
Nigeria	--	--	2	1
Oman	--	1	--	--
Pakistan	2	--	--	--
Peru	3	--	1	--
Poland	--	1	--	--
Saudi Arabia	9	22	20	15
Taiwan	--	--	1	--
Turkey	1	1	--	--
Viet Nam	--	--	--	1
Yemen	1	5	--	2
General	3	7	1	4
TOTAL	29	40	25	35

addition, the USGS is participating extensively in two international programs of major dimensions, the International Geological Correlation Program and the Circum-Pacific Energy and Mineral Resources Program.

International Geological Correlation Program

The International Geological Correlation Program (IGCP) is a cooperative effort of the International Union of Geological Sciences and UNESCO. This program encourages international research on fundamental geological problems and techniques relating to the identification and assessment of earth resources and the improvement of man's environment. The program operates through a 15-member Board and, currently, 66 countries participate through IGCP National Committees. Daniel Merriam of Syracuse University is chairman of the U.S National Committee for IGCP, Lynn Hoover is the Secretary, and Gilbert Corwin serves as editor-compiler of IGCP publications.

In 1978, a review and evaluation of the IGCP Program was prepared by J. A. Reinemund of the USGS together with Professor Janet Watson of the United Kingdom (Reinemund and Watson, 1978), who were members of the IGCP Board. Their review covered the 62 projects in the IGCP Program prior to 1978 and evaluated achievements in four categories: improved techniques, methods, and standards; better knowledge of geological processes, correlations, and concepts; more effective protection and use of the environment; and more efficient identification and assessment of resources. USGS geologists are involved in IGCP projects in each of these four categories, which encompass various aspects of research underway in the Survey's domestic program. Four IGCP projects are led by USGS scientists, and, of 27 U.S. working groups for IGCP projects, 11 are chaired by USGS personnel.

The four projects led by USGS scientists are Project 30, Circum-Pacific plutonism headed by P. C. Bateman; Project 98, Standards for computer applications in resource studies, headed by A. L. Clark; Project 115, siliceous deposits of the Pacific region, headed by J. R. Hein; and Project 143, remote sensing and mineral exploration, headed by W. D. Carter.

Project 30 has identified systematic changes in the chemistry of granite batholiths away from continental margins in North America and Australia that do not apply in Asia. The seventh meeting of the working group consisted of field trips across the main structural belts of the inner zone of Southwest Japan and South Korea to study the relation of batholiths to tectonics, volcanism, and ore deposits. On the basis of patterns of deformation and compositional zoning examined in the field, it is believed that mineralization related to these batholiths is largely a result of remobilization and concentration of minerals from surrounding rocks.

Project 98 is concerned with perfecting and broadening the application of computerized systems to the study and assessment of resources and development of methods of collecting, storing, and retrieving data relating to resource studies. The project is coordinating its efforts with the International Commission on Storage and Retrieval for Geologic Data for monitoring standards and computer applications. This provides assurance that all data standards and computer applications are coordinated internationally.

The project held a workshop in connection with the annual meeting at Taita, Kenya, to develop the criteria whereby resource-assessment methods are coordinated internationally. A. L. Clark, A. H. Chidester, and S. M. Cargill from the USGS participated. Proceedings of two international meetings have been published (Cargill and Clark, 1977;

1978). As a result of these conferences, Project 98 will be able to focus specifically on the application of resource-assessment techniques to problems of global assessment, primarily emphasizing specific programs for developing countries.

Project 98 and Project 156 jointly held an international Phosphate Resource Data Base workshop at the Resources Systems Institute of the East-West Center; sponsors were the USGS, the two IGCP Projects, and Resources Systems Institution. As part of Project 156, R. P. Sheldon leads the U.S. Working Group for Phosphorites of the Proterozoic-Cambrian. This activity collects phosphate data for analysis of phosphogenic provinces, depositional environments in geologic time, and the relation between phosphate deposition and plate tectonics. The first international meeting of Project 156 was held in Australia. At Ardmore, in the Georgina Basin Middle Cambrian rocks, evidence for hypersaline deposits underlying the Beetle Creek Formation (the main phosphate-bearing formation) was examined.

J. A. Barron is chairman of the Subgroup on Paleontology of Project 115, siliceous deposits of the Pacific region. These deposits are commonly associated with accumulations of hydrocarbons, iron, manganese, and phosphates; they may be thick and cover large areas of the sea floor. R. E. Garrison is chairman of the Neogene Siliceous Deposits subgroup.

Project 143 contributes to the rapidly evolving technology of multispectral satellite imagery by testing on a global basis and under many different climatic conditions. New technologies are disseminated to help mineral-exploration geologists search for mineral and energy resources. Analysis of computer-enhanced imagery has revealed relationships between visible lineament patterns and localization of mineral deposits.

Other significant IGCP research involving U.S. Geological Survey personnel includes, for example, working groups on the Caledonian orogen, headed by R. B. Neuman; ophiolites, headed by R. G. Coleman; Caledonian stratabound sulfides, headed by J. E. Gair; and sulfide deposits in mafic and ultramafic rocks, headed by G. K. Czamanske.

Circum-Pacific Energy and Mineral Resources Program

The USGS supported activities of the non-profit Circum-Pacific Council for Energy and Mineral Resources, which are directed toward a better understanding of the energy and mineral resources potential in the Pacific region. A major part of this support involved the coordination and guidance of the Circum-Pacific Map Project. U.S. Geological Survey geologists continued to coordinate the 5 panels of working geologists of the map project, who are compiling a series of geologic, tectonic, and resources maps covering the entire Pacific region. Contributions are also made by U.S. Geological personnel directly to the panels, principally those of the northeast and northwest quadrants.

Geographic maps at a scale of 1:10,000,000, showing topographic and bathymetric features in five parts of the Pacific region, and a geographic map at a scale of 1:20,000,000, covering the entire region, have been published and are now available from the American Association of Petroleum Geologists. Geologic, tectonic, resources, and geodynamics maps are being compiled.

Mineral data for much of North America compiled by the map project have been digitized and can be plotted on base maps whose projections are part of the computerized automated map (CAM) program. Mineral data entered in the data bank include deposit location, mineral elements of each deposit, relative size of deposit, and geologic type of each deposit. The data can be selectively retrieved (for example, disseminated copper deposits of Canada) and computer plotted so that the data will become a valuable data source when completed. A bibliography of about 20,000 reports on energy resources and phosphate deposits in the northeast circumpacific region was completed and reviewed.

U.S. Geological Survey personnel also had active roles in organizing the second Circum-Pacific Energy and Mineral Resources Conference, July 30–August 4, 1978, in Honolulu and in conducting sedimentary basin analysis, geologic hazards, and remote-sensing workshops in connection with the conference.

At the conference, the Landslide Workshop given by E. E. Brabb, T. H. Nilsen, and W. J. Kockelman on August 4, 1978, was well attended; participants came from Australia, Hong Kong, Japan, Malaysia, New Zealand, Philippines, Singapore, Thailand, and the United States.

Resource Attache Program

A major responsibility of the Department of the Interior is to appraise the present and future supplies of mineral and energy raw materials in relation to the Nation's requirements. To help meet the need for data on reserves and resources in foreign countries, the U.S. Bureau of Mines and the USGS are cooperating with the Department of State in a Resources Attache and Reporting Pro-

gram. Some Attaches have petroleum reporting as their principal responsibility, but cover other minerals as time permits. The program is expanding and will include at least 20 Regional Resources Attaches; 10 have already been assigned to Belgium, Australia, Venezuela, Indonesia, South Africa, Bolivia, Mexico, India, Brazil, and Japan. Also, information is received from many part-time minerals-reporting officers in other countries.

INTERNATIONAL COMMISSIONS AND REPRESENTATION

The USGS is active in the Commission for the Geological Map of the World, a commission affiliated with the International Union of Geological Sciences. The Commission is composed of representatives from more than 100 adhering geological surveys; through its subcommissions, the Commission sponsors or encourages the publication of many kinds of small-scale geological maps: tectonic, metallogenic, metamorphic belt, environmental, and hydrogeological. Other subcommissions sponsor and coordinate compilations of small-scale geological maps of continents and regions of the Earth's crust, such as Africa, the Middle East, South America, and South and East Asia. The Geological Survey has been represented on the Commission for more than 10 years by D. M. Kinney, Vice President for North America, and by P. W. Guild, President of the Subcommission for the Metallogenic Map of the World. At the biennial meeting in March 1978, G. E. Tolbert was elected Co-Secretary of the Metallogenic Subcommission. All three are members of the Bureau (executive committee) that determines policy between biennial meetings.

The Fourth International Conference on Cosmochronology, Geochronology, and Isotope Geology was held at Snowmass, Colo., co-sponsored by the USGS, National Academy of Sciences, Geochemical Society, Lunar Science Institute, International Union of Geological Sciences, and Carnegie Institution of Washington, D.C. About 400 attendees gathered from 27 countries.

U.S. Geological Survey scientists participate in a large number of international conferences, committees, seminars, and programs, in some cases being the only U.S. delegates or representatives. G. H. Davis attended the first meeting of the International Hydrological Program (IHP) working group 5.7 on Hydrological Problems Arising from Development of Energy Resources. Davis was elected Chairman. The working group updated a preliminary report of which Davis was the principal author, who approved it for publication by UNESCO.

The Association of Geoscientists for International Development (AGID) held its annual Council meeting in Caracas, Venezuela, in conjunction with the AGID Symposium on Mineral Exploration in Tropical Rain Forests, and its training course on the same subject, and with the Fifth Venezuelan Geological Congress and the First Ibero-Latin American Geophysical Congress. L. A. Heindl attended as Editor of the AGID Newsletter and member of the Council.

The International Hydrological Program Working Group on Investigation of the Effects of Thermal Discharges met in Oak Ridge, Tenn. The session was invited to Oak Ridge by Dr. C. C. Contont, Oak Ridge National Laboratory, who represents the Man and the Biosphere Program and its interests, which are parallel to those of the working group. The group's objective was to complete the rough draft of its assigned report on Thermal Pollution. L. A. Heindl joined the working group to offer the welcome of the U.S. National Committee on Scientific Hydrology and to attain first-hand knowledge of the state of the report.

The 12th International Symposium on Remote Sensing of the Environment, conducted by the Environmental Research Institute of Michigan and the Philippines National Resources Management Center in Manila, was attended by 500 participants from 52 countries. Representatives from the USGS were W. A. Fischer, T. M. Sousa, W. D. Carter, J. O. Morgan, and G. K. Moore. All the reports on national programs in remote sensing showed progress and growing conviction that Landsat is a uniquely useful and low-cost tool.

In response to an invitation from the Organization of American States (OAS), A. F. Espinosa and G. E. Erickson attended the Geological Risk Seminar held in Caracas, Venezuela, and presented invited papers. This seminar was organized by the Venezuelan Geological Survey, Fundacion Venozolana de Investigaciones Sismologicas, the OAS, and the Colegio de Ingenieros de Venezuela. Ericksen and Espinosa chaired two different sessions and participated in a round table discussion with scientists from Europe, Central and South America, Japan, India, and the U.S.A. Approximately 250 people attended the sessions.

R. L. Wesson attended a meeting of the Preparatory Committee of Experts on Earthquake Predic-

tion in France, and C. F. Knudson was an invited reporter for the Central American Conference on Earthquake Prediction in France.

J. C. Savage was detailed to UNESCO and served as U.S. delegate to the advisory meeting and seminar on Earthquake Prediction at Trieste, Italy. The seminar was part of a course in theoretical geophysics given at the International Center for Theoretical Physics, and it was more oriented toward review than toward technical presentations of the most recent advances. Leaders in earthquake prediction—Japan, U.S.S.R., U.S.A., and Italy—attended.

S. H. Patterson attended the 1978 Conference Pour L'etude des Argiles, and D. F. Davidson was the U.S. Delegate to the 16th Meeting of the Central Treaty Organization Minerals Advisory Board. E. A. Noble participated in the International Atomic Energy Advisory Group meeting on Uranium Geology of Latin America.

P. W. Richards attended the meeting of the Committee for Coordination of Joint Prospecting for Mineral Resources in South Pacific Offshore Areas in Port Moresby, Papua New Guinea, as U.S. member of the Technical Assistance Group. Seven member countries (Cook Islands, Fiji, New Zealand, Papua New Guinea, Solomon Islands, Tonga, and West Samoa) were represented. Five supporting countries were represented.

P. D. Snavely, Jr., was a delegate of the 5th Joint Meeting of the U.S.-Japan Marine Geology Panel; R. W. Rowland was a U.S. delegate of the U.N. Conference on the Law of the Sea. V. E. McKelvey was invited to attend the Executive Committee meeting, Union of Geological Sciences.

Harold Masursky presented an invited paper for the Canadian Aeronautics and Space Administration. Gary Galino was the keynote speaker at a seminar of the Argentina National Space Research Commission. Personnel assigned to the USGS's Saudi Arabian cooperative program participated in the Arabian-Nubian Shield Symposium, which was sponsored by the Institute of Applied Geology. G. F. Brown and R. O. Jackson presented the keynote speech, and four other papers were presented by USGS authors.

Examples of other international meetings in which the USGS took part are the International Magnetics Conference, International Atomic Energy Agency, International Society for Photogrammetry, International Symposium on Isotope Hydrology, International Workshop on Strong Motion Arrays, U.S.-Japan Panel on Wind and Seismic Events, International Geodynamics Conference, and Intergovernmental Oceanography Commission Association for the Caribbean.

C. R. Showen, a member of the Expert Working Group Meeting on Water Resources Data Systems convened by the Economic and Social Commission for Asia and the Pacific and UNESCO (Bangkok, Thailand, April 4–10, 1978), presented a paper titled "Developing an Automated Water Resource Data System."

L. M. Sutphin was a panelist at the International Conference and Exhibition, Training, and Education for the Water Well Industry, sponsored by the National Water Well Association of Australia (Singapore, October 29–November 1, 1978).

G. D. DeBuchannane participated in a meeting of the Radioactive Waste Management Committee of the Organization for Economic Cooperation and Development (Paris, September 18–20, 1978).

INTERNATIONAL HYDROLOGICAL PROGRAM

About 90 countries and several international organizations participated in the International Hydrological Program (IHP) launched by the United Nations Educational, Scientific and Cultural Organization (UNESCO) in 1972. The international guidance and supervision of the program is under the Intergovernmental Council comprising 30 member countries elected every 2 years. The United States was not a member of the Council during 1977–78, but was elected to membership for 1979–80.

The major activities of the IHP are (1) the scientific program, including studies of the hydrological cycle, assessment of water resources, and evaluation of the influence of man's activities on water regimes, (2) the promotion of education and training in hydrology, (3) the enhancement of exchange of information, (4) support of technical assistance programs, and (5) the enlargement of regional cooperation.

Participation of the United States in the IHP is guided by the U.S. National Committee on Scientific Hydrology (USNC/SH) which consists of the Chief Hydrologist of the USGS, J. S. Cragwall, Jr., who has served as chairman since 1975, and representatives of eight other Federal agencies and six nongovernmental organizations. The Associate Chief Hydrologist, O. M. Hackett, is the alternate chairman. L. A. Heindl was the executive secretary of the committee from 1975 to 1978. The USGS Office of International Hydrology serves as the Secretariat of USNC/SH.

SUMMARY BY COUNTRY

AFGHANISTAN-IRAN-TURKEY

The National Geographic-Smithsonian Pyrotechnological Expedition of 1968, in cooperation with the governments of Afghanistan, Iran, and Turkey, made samples of sediments available to the USGS for chemical analysis. The original purpose for collecting the samples was to determine whether tin was present in amounts indicative of sources for tin ores used in antiquity for the manufacture of bronze. J. A. Domenico, W. C. Overstreet, A. E. Hubert, and R. B. Tripp undertook the chemical and mineralogical study of the samples and the interpretation of the results on a time-permitting basis. Tin was found to be a minor element commonly associated with copper ores at mineralized areas known to have been worked in antiquity. The relation may have historical significance in the context of the development of bronze. The results of the analyses also permitted an evaluation to be made of the regional potential for other elements of industrial use; gold, base metals, ferroalloy metals, beryllium, rare earths, and barium.

The most notable areas for tin represented by the samples are near Mirzaka, near Meshed, Shir Kuh, Notanz, Nodus, and Talmesi in Iran and the shore of the Black Sea just west of Trabzon in Turkey.

In Afghanistan an array of anomalous elements at the known gold placers around Mirzaka and along the Anguri River signals the presence of complex ore deposits. These elements are Ag, As, Au, Bi, Cd, Cu, Hg, In, Mo, Pb, Sb, Sn, Tl, W, and Zn. This assemblage may indicate a Carlin-type gold deposit in which the rocks are enriched in micro-sized particles of gold. Other localities in Afghanistan shown by the results of the analyses to be anomalously rich in valuable metals and to merit further geochemical exploration are (1) a reach of the Panjshir River for Be, Pb, Zn, Cr, and Ni, (2) an area near Bamian for Be, (3) the Siakhak village area for Au and Cu, (4) around Qala-i-Asad and Shah Agha for Pb, An, Au, and W, and (5) the vicinity of Siakhak, Shahjui, Qala-i-Asad, and Shah Agha for the rare earths and Th.

In Iran, the pluton of granodiorite porphyry near Sar Cheshmeh shows as a strong geochemical anomaly for copper and molybdenum in the samples collected in 1968. Investigations by the Geological Survey of Iran, already under way in 1968, have subsequently proved a huge porphyry copper deposit at this locality. Samples from a granitic area near Meshed are persistently enriched in Be, Sn, and Ba, and they are locally enriched in Au, La, Nb, and Y. This area deserves a thorough geochemical survey for beryl and nonberyl sources of Be, for fluorite, and for the ores of Nb, Sn, Ba, the rare earths, and Th. Other localities that merit exploration on the basis of these data are (1) between Tabas and Deyhuk, as well as east and south of Naiband, for Ba and An, (2) a locality about midway between Kerman and Sirdjan for Ba, La, Sr, and Zn, (3) the Meskani copper mine area for Hg, Pb, Ni, and Cu, (4) the Talmesi copper mine area for Ba, Co, Hg, Sr, and Zn, (5) a pluton of granodiorite north of Natanz for tungsten and base metals, (6) the vicinity of Zendjan for auriferous polymetallic sulfide deposits, (7) gold in the gorge 15 km east of Miyaneh, and (8) an area near Nodus for Au, Cu, Pb, An, Mo, Nb, and, possibly U.

In Turkey, the Harrit River basin appears to be a suitable target for geochemical exploration for gold and for low-temperature hydrothermal deposits of Cu, Pb, An, Hg, and Ba.

BOLIVIA

In continuation of a cooperative program with the Servicio Geologico de Bolivia, field study of the Salar de Uyuni, a large salt pan, indicates the presence of large amounts of lithium- and potassium-rich brine. The amount of recoverable lithium may be greater than the estimated resources of 660,000 tonnes in the United States, which is presently the world's largest producer. The lithium deposits are being studied by S. L. Rettig, J. R. Davis, R. L. Smith, K. A. Smith, and G. E. Ericksen. These reserves of lithium, together with brines in salt pans in northwest Argentina and northern Chile, may be of such magnitude as to stimulate research for new uses of lithium, particularly in high-energy storage batteries. The probable source of much of the lithium is ash flow tuffs. Only 2 of 10 large calderas studied were previously known. It is now believed that the widespread ash flow tuffs in the Central Andes originate from calderas, rather than being related to fissure eruptions.

BRAZIL

J. A. Leenheer, detailed to the Organization of American States, participated with the Brazilian Instituto Nacional de Pesquisas da Amazonia in sampling and analyzing tropical waters of the Amazon-Rio Negro systems near Manaus. The hu-

mic acids responsible for the "black water" coloration of the Rio Negro river system were investigated as to their origin, concentration, chemical and physical characteristics, and resultant environmental effects. The primary source of "black water" was found to be ground-water drainage from a transitional soil between podsol sands and latosol clays. The light absorbance spectrum and acid-base characteristics of black-water humic acids indicated a relatively simple mixture of compounds when compared to humic acids obtained from surface waters in temperate regions. Dissolved humic acids reduce the pH of the Rio Negro to pH 4–5 so that suspended sediment added by the Rio Branco is acid flocculated; this has resulted in the formation of the clay islands of the Analvihanas archipelago of the lower Rio Negro.

DJIBOUTI

L. A. Heindl visited Djibouti in July and August 1978 to delineate areas for ground-water development. New water supplies are necessary for the development of agriculture and other industries.

EGYPT

The USGS, under USAID sponsorship, is collaborating with the Egyptian Geological Survey and Mining Authority (GSE) to augment GSE's capability for carrying out a national resources assessment. The USGS project has directed compilation of two geologic maps, upgraded techniques of mineral resource identification such as geochemical and geophysical exploration, and assisted in establishing analytical laboratory facilities, use of remote sensing in geologic studies, and the use of modern methods of data processing.

The USGS participated in a DOE-funded project of energy resource assessment for Egypt. Based on some of the findings, the following studies have been recommended to Egypt:

- Most oil reserves are in the Gulf of Suez Basin where 20 producing fields are present. Commercial oil discoveries have also been made in the Western Desert. Proved gas reserves occur in the Delta Basin, the Western Desert, and the Gulf of Suez Basin. The area of promising petroleum prospects in Egypt totals more than 600,000 km^2, of which only 230,000 km^2 have received more than a cursory examination. According to J. C. Maher and A. A. Fouda, the Gulf of Suez Basin holds the most immediate prospects for replacing and increasing petroleum reserves, whereas the most promising frontier regions are the relatively unexplored broad expanses of the Western Desert, the Nile Delta Basin, Nile Basin, and northern Sinai along with adjacent offshore tracts. The Red Sea area holds moderate possibilities, perhaps mostly as a gas province.
- Coal deposits with small, but seemingly economic, reserves have been defined in the areas of the Maghara anticline, Ayun Musa, and Wadi Thora, all on the Sinai Peninsula. Based on his investigations, W. W. Olive reported that the Maghara deposits of Middle Jurassic age has the greatest potential for economic development. It is estimated to contain, in beds more than 0.65 m thick, reserves of 51.8×10^6 t, of which 35.6×10^6 t are recoverable by mainly underground mining. The coal is comparable to Western United States subbituminous C rank and contains on the average from 4.9 to 7.5 percent ash and 2.6 to 3.5 percent sulfur.

  Coal beds ranging from 5 to 120 cm in thickness have been penetrated at depths between 400 and 600 m below the surface in tests drilled for oil near Ayun Musa about 14 km southeast of Suez. The coal in core samples analyzed contained 8.9 to 30.8 percent ash, 1.3 to 4.9 percent sulfur, and 8,512 cal/g calorific value. Because these lenticular coal beds occur in an artesian aquifer zone with high pressure, economic development of the coal is questionable.

  A coal bed attains a maximum thickness of 80 cm along an outcrop distance of 17 km in rocks of Carboniferous age at Wadi Thora, about 25 km east of the harbor of Abu Zenima. Reserves within an area of 1.5 km^2 that has been explored by holes drilled to depths of 50 m are estimated to be 1.5×10^6 t. Resources for a larger adjacent area are projected to be 60×10^6 t. Analyses of the coal samples show 25–59 percent ash and 0.56–9.08 percent sulfur. Near-surface coal beds west of the Gulf of Suez are considered to be too thin for economic development and coal beds reported in oil test wells in the Western Desert areas are too thin, too deep, and too remote to be economically important at present.
- Olive also reports that no estimate has been made for the oil-shale resources in Egypt because of the lack of data. Shale beds, as much as 1.5 m thick that contain disseminated car-

bonaceous matter, a petroliferous odor, C:H values of 6.9–7.9, a high sulfur content, and capable of yielding a very low-grade type of fuel, have been reported from the Galalah Kebleih-Bahariya area, the Buda area, and the Qusseir area.

- Neither uranium nor thorium is being produced in Egypt at present. Assay data and exploration are insufficient to calculate reserve estimates. L. R. Page found that known deposits occur in (1) black sands of the Nile Delta and the Mediterranian Sea Coast, (2) siliceous fluorite-hematite veins in the El Missikat and Eredyia area some 80 km west of Safaga on the Red Sea, (3) fractures of contacts where bostonite dikes have intruded shale, sandstone, and conglomerate in the El Atshan area of the Western Desert, and (4) association with silicified fault zones and silicified logs in thin cross-bedded sandstone and shale in the Qatrani area of the desert. Analyses show that the uranium content of phosphate ores of the Western Desert ranges from 50 to 2,000 ppm. Economically recoverable uranium might be produced by chemical treatment of the phosphate ore. Geological conditions similar to those at known deposits favor the finding of additional uranium deposits in many parts of Egypt. More than 7,000 radiometric anomalies have been identified by airborne surveys of large areas of Egypt (200,000 km^2), but on-the-ground investigations have been conducted at only about 50 of the areas.
- A. A. R. Zohdy concludes from his studies that the potential for geothermal energy in Egypt is good, but no investigations directly aimed at exploration of geothermal energy have been made. The geothermal potential is evidenced by the presence of warm springs, by moderately high temperatures in deep water wells, and by geologically young volcanism. In order of decreasing importance the potential areas include (1) the east and west sides of the Gulf of Suez where springs reported to have temperatures as high as 75°C occur near Hammam Feroun, Ayun Musa, and El Sukhara, (2) a 30-km-wide area along the west coast of the Red Sea that also contains hot springs, (3) the Western Desert near Kharga, Dakhla and Farafra Oases, and El-Rasr where temperatures as high as 43°C were reported in wells drilled to depths of 1,200 m, (4) the area between Cairo and Suez, especially near Gabal El-Ahmar where there is evidence of extinct geysers, and (5) miscellaneous indications in the Helwan, Eswan, Qatrani, and Faiyum areas.
- Most of Egypt's hydroelectric power potential has already been developed along the Nile. Some additional capacity could be attained by installing a second generating station at Aswan, by installing turbines on three existing barrages, and by installing new barrages equipped with turbines. These additions, however, would be allowed only if they do not interfere with irrigation which is now strictly controlled. Small amounts of hydropower could be produced by development of the Qattara Depression in the Western Desert of Egypt and by construction of pumped storage facilities at several places such as Galala el Bahariya and Gebel Ataqua, south of Suez on the Red Sea.
- Egypt is deficient in nearly all energy-related mineral resources—those minerals needed in the exploitation of energy-related sources.

GUATEMALA

A symposium on the results of studies of the February 1976 earthquake in Guatemala, organized by A. F. Espinosa and Raul Husid, was held in mid-May 1978 in Guatemala City. The Guatemalan earthquake has been of special interest because many of the modern buildings in Guatemala are similar in construction to buildings in cities of California.

HUNGARY

As a result of a visit to geological and geophysical institutions in Hungary, including the Hungarian Academy of Sciences, M. F. Kane, S. M. Lang, P. G. Teleki, and W. J. Spence concluded that USGS scientists can benefit from studies of unique geologic conditions in Hungary, in part because of the painstaking detailed work of Hungarian scientists in several subject areas. They are advanced in deep-well logging in high-temperature formations, investigations of the Earth's crust and upper mantle, methods of mineral prospecting, geo-electric exploration methods, paleomagnetic correlation, seismic research on coal, and geothermal water. The visit was made at the request of the Hungarian Government and is expected to implement a cooperative research program.

INDIA

G. K. Moore attended a remote-sensing workshop held at Hyderabad, India, in April 1978. The work-

shop was jointly sponsored by the U.S. National Science Foundation and the Indian National Remote Sensing Agency as an activity of the Joint Indo-United States Subcommission on Science and Technology.

INDONESIA

J. M. Knott served as Sediment Specialist at the Institute of Hydraulic Engineering in Bandung. On assignment to the United Nations Development Program, he evaluated the sediment program of the Hydrochemistry Branch of the Institute; observed and commented on sediment problems in Java; trained Indonesian personnel in collection, analysis, interpretation, and publication of sediment data; and made recommendations on improvement of methods, equipment needs, and future sediment investigations.

Tectonics of the Indonesian region

The integration by W. B. Hamilton of onshore geologic data with offshore geophysical information from Indonesia and surrounding regions has led to completion of a multicolor tectonic map (Hamilton, 1978) and a book (Hamilton, 1979) depicting the plate-tectonic evolution of this exceedingly complex and active region. The project was undertaken both for its high scientific interest and, with the partial support of the Agency for International Development of the U.S. Department of State, for its value in guiding exploration for fuels and minerals. Much was learned about the behavior of island areas, which reverse subduction polarity, go dead, or collide with each other and with continents with subsequent breakthrough of new subductive systems. Mature island arcs commonly are composite products of several subduction systems, rather than products of single, little-varying systems. The many small lithosphere plates of western Melanesia record prograde and ball-bearing motions in the oblique-convergence zone between the giant Pacific and Australian-Indian plates. Projection into the future of the major plate motions indicates that the complex arcs of the Indonesian-Philippine region likely will be compressed into a continuous, broad mountain zone between the Asian and Australian continents. Comparison of the components of Phanerozoic orogenic terrains that are now parts of the continents with their active analogs indicates that the evolution of the old terrains has been far more complex than has yet been recognized generally.

Energy resources

First-phase investigation by USGS researchers under the energy-resources assessment program for developing countries funded by DOE confirm that Indonesia is well endowed with sources of energy including oil, gas, coal, geothermal, hydropower, and possibly radioactive materials. Almost 90 percent of Indonesia's total energy now comes from oil and about 8 percent from natural gas. As a world oil producer, Indonesia ranks about 12th, providing 2.5 percent of the world's total production. Other sources of energy must be explored and developed in order for Indonesia to meet future increased domestic energy needs and also maintain the export of petroleum that now represents 70 percent of the nation's export products. The potential for discovery of additional large petroleum reerves is excellent, for about 99 percent of present total production comes from only 6 of 28 known Tertiary basins. Prospects for additional oil and gas developments are increased by recent discoveries in offshore areas and in carbonate and deltaic reservoirs.

A considerable quantity of coal exists in Indonesia, perhaps as much as 680×10^6 t of resources in rocks of Tertiary age.

The coal is ranked as lignite, subbituminous, and bituminous with volatile matter between 30 and 40 percent, calorific values between 5,000 and 8,000 cal/g, ash content generally less than 5 percent, sulfur content generally less than 1 percent, and in some cases a marginal to moderate coking characteristic. Exploration efforts have concentrated on coal beds already being mined or readily accessible. Coal-bearing rocks with high potential for coal development underlie large parts of Sumatra, Java, Kalimantar, Sulawesi, and Irian Jaya; isolated known deposits are separated by large unexplored areas that certainly contain considerable quantities of coal which have not been included in present resource estimates.

Hydrocarbons other than oil, gas, and coal are not being exploited for energy purposes in Indonesia; however, asphalt-impregnated limestone having a bitumen content ranging between 2 and 46 percent is produced from the open pit mine on the island of Butan off the southeast coast of Sulawesi. The rock is used for surfacing roads, and, though not used as a source of energy, it replaces asphalt that could be used.

Indonesia has been so little explored for radioactive energy source materials that a realistic appraisal of potential resources is impossible on such

meager data. Uranium-rich rock has been reported from west Kalimantan, and other promising uranium localities have been investigated in south Sumatra, southwest Sumatra, and another area in Kalimantan. Environments favorable for the occurrence of uranium are prevalent in different parts of the country; potential sources might include disseminated or locally concentrated mineralization in sedimentary environments, association with tin in intragranitic veins, association with veins in alkalic granitic stocks, and association with porphyry copper deposits.

Being the most active volcanic province in the world, Indonesia has high potential for producing energy from geothermal sources. Potential areas for development are related either to volcanic activity or to nearsurface granitic intrusions. Indonesia has more than 500 volcanoes spread throughout the islands, from Sumatra eastward to Ceram and northward across Halmahera and Sulawesi; 177 of the volcanoes have been active since 1600. Eight-eight of nearly 100 sulfatara and fumerole fields are associated with active volcanoes; the others are related to intrusive masses. Geothermal areas related to granitic intrusions occur in Sulawesi, Java, and Kalimantan. Exploration for geothermal energy began as early as 1926 in the Kawah Kamojang field southwest of Jakarta. Since then interest has been restimulated many times through domestic programs and outside aid. More than 100 geothermal areas with energy potential have been identified, mainly on Java, Sumatra, and Sulawesi; 25 area have been recommended to receive additional study; and two areas, the Kawah Kamojang and the Dieng Plateau (also on Java) have undergone drilling, geological, geochemical, and hydrological exploratory investigations. A 30-megawatt generating plant is now planned at the Kawah Kamojang locality.

Indonesia has a large potential for development of hydroelectric power facilities; however, the resources and the need are not in proximity. Only about 1.5 percent of the total hydropower potential of the islands has been developed. Most all of this development, which began as early as 1925 and is still continuing, has been on Java (the most highly industrialized and populous island), so that now some 50 percent of that island's installed electrical capacity is based on hydropower. Most additional development of hydropower facilities is planned also for Java because of its need for electric energy now. However, the Indonesian Government plans to develop resources in Bali and Lombok (the next most densely populated islands after Java) and to develop river basins in Sumatra, Kalimantan, and Sulawesi that will serve as rice-producing areas and immigration centers for movement of population from Java, Bali, and Lombok.

IRAN

D. G. Orr, R. E. Beck, W. H. Anderson, and G. K. Moore presented a basic training course in applications of remote sensing in resources investigations and mapping at the Iranian Remote Sensing Center in Tehran, with assistance from Iranian personnel.

ISRAEL

Z. S. Altschuler served as an invited consultant to the Geological Survey of Israel to review their programs for phosphate, uranium, and peat. The phosphate is in shallow-water semi-restricted hypersaline deposits, intercalated with chert and chalk. Peat deposits, which have been studied only slightly, are exceedingly thick in the Huleh Valley, north of the Sea of Galilee. The peat is impure, containing 50 percent ash and 5–10 percent sulfur. Because the peat occurs immediately above the major source for irrigation water, the environmental problems of development would be immense.

S. P. Sauer visited Israel to explore the causes and effects of changes in the water level of the Dead Sea. Sauer (1978) found a close relationship between the water level of the Dead Sea and accumulated departure from the mean of long-term rainfall until 1964. Since 1964 the abstraction of water for irrigation in the Jordan River basin has also affected the water level of the Dead Sea.

B. F. Jones lectured at the Bath-Sheva Seminar on Saline Lakes and Natural Brines, at the invitation of the Bath-Sheva de Rothschild Foundation for Advancement of Science and the Weizman Institute of Science.

JAPAN

C. M. Wentworth, Jr., together with E. L. Harp and D. K. Keefer, visited Tokoyo and the Sendai area in Japan to determine the geologic effects of the M=7.5 earthquake of June 12, 1978, off Miyagi. A well-organized series of briefings and a tour of the microseismal area were provided by the Japan Ministry of Construction. Saturated river channel sands and hydraulic fill liquified locally, with resulting damage to river dike and harbor facilities. A small number of rockfalls occurred on

steep cut slopes and many hillside fills failed, most of the deaths resulted from toppling of reinforced block walls. Shaking damage to buildings appeared greater on Holocene delta deposits than on adjacent terrace deposits, and may have been controlled by the delta plain facies as well.

JORDAN

J. R. Jones participated in the Jordanian National Water Symposium (Amman, March 19–22, 1978) which was primarily concerned with development of a national master water plan.

C. R. Showen was detailed to UNESCO as an advisor on computorization of the entire hydrologic system of Jordan.

S. P. Sauer visited Jordan to explore the causes and effects of changes in the water level of the Dead Sea. Sauer (1978) found a close correlation between the water level and the Dead Sea and accumulated departure from the mean of long-term rainfall until 1964. Since 1964 the abstraction of water for irrigation in the Jordan River basin has also affected the water level of the Dead Sea.

Copper ore has been mined since early historic times in Jordan in the rift valley between the Dead Sea and the Gulf of Aqaba. The excellent engineering and workmanship in the extensive mine galleries and shafts in the Wadi Feinan area attest to the skill of the miners and indicate a culture having relatively advanced technology. The people responsible for the mining activity are not known, nor is the time in which it took place known with any certainty. During the course of field studies undertaken as part of a cooperative program with the Natural Resources Authority of Jordan and sponsored by AID, an effort was made to establish the age of the mining activity, which in turn might indicate the culture responsible. For this purpose, slag was collected from several extensive slag heaps that had accumulated from smelting, presumably during the time of the major mining activity. The slag was broken open, and charcoal that was used in the smelting process was recovered. This was dated by the radiocarbon method, and the ages of the two largest slag heaps were determined as 2,400 years B.P. and 3,000 years B.P., respectively. These ages are both pre-Roman and pre-Nabataen, the two cultures known to possess the level of knowledge and skill required for such mining as was done here. This, therefore, indicates that another earlier culture existed in this area that had developed a technology previously thought to be possessed only by the Nabataens and later the Romans.

KENYA

During December 1977 and February 1978, T. L. Loesch was detailed to the U.N. Development Program in Nairobi, Kenya, to assist the Central Bureau of Statistics (CBS) in census cartography for its 1979 census of population and housing in Kenya. He set up a geographical identification code for all places in Kenya to be used in compiling and analyzing census reports. In the field, boundaries were checked, new roads plotted, and housing units counted. The type, scale, and number of maps needed were determined and recommended to CBS. Where housing unit count estimates are not available, Loesch worked out a system of enumerating by means of area maps.

The departure of N. E. McClymonds in December of 1977 ended 9 years of AID-sponsored resident technical assistance in water resources studies by the USGS to the Government of Kenya. The difficulties of obtaining water in the Northeastern Province were documented, some relatively favorable areas delineated, and the episodic nature of ground-water recharge suggested.

LIBERIA

On October 13, 1977, William W. S. Bull, Counselor, Liberian Embassy, Washington, was presented with a set of geologic maps of his country by J. R. Balsley, Assistant Director of the USGS. The ceremony was held at the National Center, USGS, at Reston, Va., and marked a milestone in that Liberia is the first African country covered by geologic mapping at a scale of 1:250,000. The mapping and publication were undertaken through a cooperative program between the Liberian Geological Survey and the USGS, sponsored by AID.

MEXICO

The USGS is cooperating with the U.S. Department of Energy and the Mexican Commission Federal de Electricidad in a program for research, development, and demonstration of applications of geothermal energy, centered on the Cerro Prieto geothermal field in the Mexicali Valley (a continuation of the Imperial Valley of California) where geothermal energy is being produced commercially. B. E. Lofgren participated in the establishment of a local network of precise horizontal-control points to monitor the horizontal component of ground movement in the area.

A USGS team joined by members of the Consejo de Recursos Minerales was involved in field work

in parts of a 300 km² study area around Ranch Rodeo, Mexico, approximately 40 km southwest of Nogales, Ariz. The work is sponsored by the National Science Foundation. Geochemical analyses of stream sediment samples showed a series of interesting anomalies of lead and molybdenum south of Las Planchas Canyon, Mexico. The major source of these metals was found to be crystals of wulfenite, which are naturally concentrated in lenses of heavy minerals in some arroyos. Upstream from these concentrations the wulfenite was found to fill fractures in the country rock over a zone several meters wide. An as yet unidentified lead mineral occurs in beds higher in the section and may be the source of lead for the wulfenite. Thirty-one audiomagnetotelluric stations were occupied in the Las Planchas area, and preliminary interpretation of the distribution resistivities suggests an intrusive system that has not been deeply eroded. An unaltered intrusive body surrounded by an alteration halo is postulated. The alteration halo correlates with geochemical anomalies in lead and molybdenum.

J. G. Frisken, R. L. Turner, and J. W. Rozelle finished the reconnaissance sampling in the Correo study area, Mexico, constructed base maps, and sampled the anomalous lead zone and the Tio Flaco parts of the area. Preliminary geologic investigations of the Tio Flaco area revealed widespread copper staining associated with sericite and tourmaline, as well as local faults west of Tio Flaco, and porphyritic intrusive rocks perhaps related to the mineralization.

Direccion General de Estudios del Territorio Nacional (DETENAL), Mexico's topographic and natural resources mapping agency, has begun a program of small-scale (1:250,000 and 1:1,000,000) resources mapping for the entire country to complement their continuing large-scale (1:50,000) mapping program. To complete the small-scale mapping within a 2-year period, the survey was based on the manual analysis of Landsat satellite images. To develop a team of interpreters who can interpret this imagery, personnel from the EROS Data Center (EDC) presented a 2-week training course in Landsat applications at the DETENAL headquarters in Mexico City, April 3–14, 1978. EDC personnel included L. R. Pettinger, W. C. Draeger, and J. R. Lucas. The following subjects were covered during the course: review of remote-sensing fundamentals related to Landsat imagery; applications of Landsat system and data characteristics; principles of manual interpretation of Landsat imagery; application of Landsat analysis to geology, hydrology, agriculture, natural vegetation, and land use; multidisciplinary analysis of Landsat imagery of Mexico; and a field trip to the Cuernevaca area to verify interpretations. The training course emphasized alternative methodologies that DENTENAL might consider to implement in its resources-mapping program.

A field tour of the Correo area, where the USGS and the Consejo de Recursos Minerales are conducting a joint mineral exploration research program, partly funded by the NSF, was conducted April 28–30, 1978, by P. K. Theobald, Jr., G. L. Raines, and M. D. Kleinkopf. Attending were Kenneth Watson, L. C. Rowan, A. H. Chidester, F. C. Frischknecht, M. F. Kane, and J. J. Hemley and members of NSF and CRM.

OMAN

The largest known ophiolite in the world, the Oman Semail Ophiolite in the Sultanate of Oman, is the best exposed ancient (Cenomanian) fragment of oceanic crust. It is part of the Middle East Alpine Mountain chain that forms the southern part of the "Peri-Arabian Ophiolite Crescent." It was investigated in cooperation with the Government of Oman and NSF by R. G. Coleman.

The ophiolite consists of individual thrust plates whose internal structure suggests interplate independence during tectonic emplacement. Internal low-angle thrust faults have led to tectonic repetition of the ophiolite sequence and, in some places, to overturning of the section. The imbricate thrusting within the ophiolite, combined with strong deformation along its leading edge, but only mild deformation at its trailing edge, suggests emplacement by gravity sliding.

Mélange units at the base of the Semail Ophiolite are overlain by serpentinized peridotites constituting 60 percent of the outcrop area of the ophiolite. Harzburgite with discordant bodies of dunite is the most abundant original rock of the peridotite. Chromite bodies are at the top of and within these dunite masses. A transition zone, exhibiting cumulate igneous textures, overlies the harzburgite and dunite. This transitional zone grades upward into layers of gabbro and lastly into massive gabbro exhibiting few layers. Small and scattered plagiogranite bodies, representing the end-product of progressive differentiation, are found at the top of the gabbro. The contact between the gabbro and plagiogranite with the over-

lying sheeted diabase dikes marks a major unconformity. The sheeted dikes are fine grained and have the ophitic texture of sodic andesine (An_{30-40}) and augite ($Fe_9Mg_{45.5}Ca_{45.5}$).

The pillow lavas of the Semail Ophiolite rest on the sheeted dikes and are the least abundant rock type (3 percent). The pillow lavas and sheeted dikes have undergone thermal metamorphism, which produced zeolite and greenschist assemblages. Petrologic reconstruction shows that the ophiolite formation was polygenetic and that these processes probably took place at a spreading center in the Tethys Sea.

Through intense exploration by Prospection (Oman), Ltd., more than 150 massive sulfide-copper prospects were discovered throughout the vast thickness of the Semail Ophiolite, but the sulfide deposits, formed in the pillow lavas close to the top, contain the largest tonnages of ore. Some of these large deposits are associated with a central fault, whereas others lie along northwest-trending faults related to younger tectonics. Numerous small copper prospects are present along the contact between the cumulate gabbro and cumulate peridotite. This relationship and the high-nickel content of ancient slags in the prospects strongly suggest that these sulfides are related to the cumulate gabbros—a situation similar to that of the sulfide deposits of the Duluth Gabbro, U.S.A. The massive sulfides consist mainly of pyrite and chalcopyrite as the main ore minerals, with late chalcopyrite accompanied by sphalerite in fractures. Minor amounts of bornite and chalcocite have been observed in drill cores.

The low-grade hydrothermal metamorphism of the pillow lavas and sheeted dikes can be related to hot circulating ocean water produced by high heat flow near a spreading center. The copper-bearing massive sulfides in Cyprus are thought also to have formed as a result of oceanic hydrothermal process.

NEW ZEALAND

As part of a cooperative program sponsored by the National Science Foundation, P. C. Trescott (USGS) and F. G. Donaldson (New Zealand Department of Scientific and Industrial Research) applied computer models to simulated ground-water flow in an area of the northern Canterbury Plains of New Zealand.

PAKISTAN

H. M. Babcock and S. P. Larson worked with the staff of the Master Planning and Review Division of the Water and Power Development Authority of Pakistan. They lectured and conducted discussion sessions with midmanagement staff on ground-water modeling, aquifer management, water-data collection and storage, and design and development of water wells.

Under a program funded by DOE, U.S. Geological Survey scientists have evaluated the conventional sources of energy in Pakistan through a compilation of the literature as an initial phase of the program to assess energy resources of developing countries. They conclude that although its energy sources include oil, natural gas, coal, uranium, and hydropower, Pakistan is, in terms of indiginous energy, among the least favored nations of the world. Except for petroleum, Pakistan currently supplies all its energy needs from domestic sources, but more than 50 percent of the requirement in rural areas is met by noncommercial sources such as firewood, dung, and agricultural waste materials. Pakistan produces about 10 to 15 percent of its petroleum requirements; the oil is produced from five fields in the Potwar Basin of northeastern Pakistan. Through completion of additional development wells in these fields and with the expected development of the recently discovered Dhodak oilfield about 320 km to the south, Pakistan anticipates self-sufficiency in oil in the early 1980's. Natural gas is produced at two fields, the Sui and Mori, in south-central Pakistan. Nine other fields scattered in this same general area and southward to Karachi are known to contain substantial additional reserves of natural gas, but are not yet producing. Natural gas is used for electric power generation, in fertilizer and cement plants, in other miscellaneous industries, and in commercial and domestic establishments. The sources of oil and gas in Pakistan are sedimentary rocks of Paleozoic, Mesozoic, and Tertiary ages in structural traps within regional basins. Large areas of potentially petroliferous sedimentary rocks as yet remain to be explored. With continued exploration and the use of the latest technologies in drilling, logging, and seismic equipment, important new discoveries of oil and gas are likely.

Pakistan's coal is lignitic to bituminous in rank and has high contents of ash, sulfur, and moisture. About 90 percent of the coal produced is used in brick kilns; the remainder is used for electric power

generation (5 percent) and by industrial and domestic consumers. The coal beds are in sedimentary sequences ranging in age from Jurassic to Miocene. Economically significant coal is produced from beds ranging from 0.3 to 3.0 m in thickness at mines in seven different areas designated as coalfields. In addition, coal is known in 15 other areas, but the extent of the coal beds and the size of the resources have not yet been determined, even though a minor amount of mining has been done in a few of the areas. Estimated coal resources of Pakistan total about 549×10^6 t, probably a very conservative figure. Resources will surely be added as exploration in the known coal fields extends the coal-bearing sequence both laterally and to greater depths than were previously evaluated. Resources will also be increased as the other 15 coal areas are evaluated; even though resources in these areas may seem small, exploration and evaluation of the coal might prove significantly large quantities in one or more, or perhaps in a locality unreported as yet.

Low-grade oil shale, which is readily accessible for exploration, is associated with salt at mines in the Salt Range. Large oil-shale deposits are rumored to lie along the Afghanistan border. Pakistan reports an export of several thousands of tons of tar sands annually, but according to the U.S. Bureau of Mines, the figures probably represent residue from oil refineries within the nation rather than excavations from naturally occurring material.

Uraniferous deposits were discovered in 1959 by airborne radiometric survey in the foothills of the Suliman Range of central Pakistan. Minable grade ore in lenses as much as 90 m long and 2.5 m thick has been delineated in the principle deposit, Baghal Char. Both oxidized and unoxidized mineralization are present. Six other areas of uranium mineralization occur south of the Baghal Char area within a distance of 105 km. In all areas, including the Baghal Char, the uranium mineralization is confined to sedimentary rocks near the base of the Middle Member of the Silwalik Formation that ranges in age from middle Miocene to early Pleistocene. The possibility for finding additional deposits of uranium ore are good because this formation is one of the most widespread sedimentary units in Pakistan and crops out in or underlies large areas in the western and northern parts of the country. Pakistan has a single 125–MW nuclear powerplant that supplies electricity to Karachi and, based on the anticipated development of the uranium deposits, has scheduled light nuclear powerplants for construction during the 1980's.

No references have been found which mention present-day volcanic activity in Pakistan. Hot spring deposits, presumably of Holocene age, are present in the Chagai district of Baluchistan, western Pakistan. Nothing is known of the possibility of offshore hot springs. Tectonically active zones, such as the Kirthar tectonic zone, are likely sites for near-surface geothermal energy sources. The possibility of finding and using geothermal energy needs further in-country study.

The development of Pakistan's water resources for irrigated agriculture has been substantial, but in terms of potential, the development for hydroelectric power has been relatively small (about 16 percent of the identified power potential and 4 percent of the total identified and unidentified potential). The nine hydroelectric facilities already completed or under development and all potential sites worthy of consideration are confined to the Indus River basin, in fact, to the northern two-thirds of that basin, because waters in the eastern rivers, Ravi, Beas, and Sultey, have been allocated to India and the southern third of the Indus Basin is a broad, open plain with only limited sites on which to construct hydroelectric facilities. Eighteen sites that are receiving appraisal, reconnaissance, or feasibility studies are included in the identified potential for hydroelectric power generation. The unidentified potential for hydroelectric power includes some 175 damsites in Pakistan.

PEOPLE'S REPUBLIC OF CHINA

During 1978, under the U.S. Committee on Scholarly Communication, contacts between scientists of USGS and those of the People's Republic of China (PRC) were considerably expanded. Delegates from both countries met at international meetings on remote sensing at Manila, Philippines; ore deposits at Snowbird, Utah; geochemistry at Snowmass, Colo.; and surface-water hydrology in China. PRC scientists participated with USGS personnel in several international organizations, in particular the IUGS stratigraphic subcommissions and IGCP projects. R. J. Ross, Jr., headed a group of Ordovician stratigraphers on a visit to China, and PRC scientists participated in the Project 156 workshop on Precambrian-Cambrian phosphorites in Australia and in a field conference on Upper Precambrian correlation problems in the Western United States. Exchanges included a 12-member U.S. delegation on earthquake engineering (USGS members were R. B. Matthiesen and R. E. Wallace); a PRC

marine-science delegation which visited U.S. facilities at Reston, Va., and Woods Hole, Mass., and another on geography visited Reston, Va., and Denver, Colo.

Direct government-to-government exchanges also became a reality. In January 1978, a 19-member delegation from the Petroleum Corporation of the PRC was hosted by DOE on a 25-day visit to the United States; some of this delegation spent part of 2 days at briefings at the USGS National Center, and demonstrated considerable interest and competence, particularly in lacustrine-basin environments.

In June-August 1978, E. C. T. Chao of the USGS spent 9 weeks traveling in China and visiting a wide diversity of facilities. His chief host was the State Geological Bureau, a 380,000-man organization whose direct responsibility was geologic mapping and mineral resource exploration. Considerable discussion focused on future potential exchanges with the USGS.

In early July 1978, H. W. Menard, Director, USGS, visited Peking as part of the 14-member delegation of U.S. science administrators. He met with Chinese scientists from the State Geological Bureau and the State Seismological Bureau. Subsequently, USGS forwarded proposals to PRC for cooperative programs in three categories: (1) exchange of scientists and geological information, (2) energy resources, and (3) seismology and earthquake prediction.

In October 1978, Secretary Schlesinger led an energy-related delegation to Peking, which included B. M. Miller of the USGS. The Ministry of Petroleum agreed, among other items, on future PRC geoscientist training in resource appraisal techniques at the USGS and on visits of U.S. scientists to the PRC oil-shale facilities. Thus, by the end of the year following normalization of relationships between the United States and PRC, the stage was set for formal agreement on a broad range of initiatives between the USGS and the appropriate PRC counterpart organizations.

In exchange, in mid-July 1978, geophysicists responsible for the PRC remote-sensing program in the State Geological Bureau visited the USGS at Sioux Falls, S. Dak., and Reston, Va.

In exchange, in October 1978, a 13-member delegation from the PRC Institute of Petroleum Exploration and Development visited the USGS at Reston, Va., Denver, Colo., and Sioux Falls, S. Dak. They were particularly interested in new developments in sedimentology, remote sensing, computer techniques, and integrated methods of petroleum resources appraisal.

PERU

Recommendations for third phase studies funded by DOE have also been made to Peru based on the following:

(1) Peru depends principally on petroleum and hydropower for its energy needs. These meet present requirements but improved standard of living and growth of industry in the future will demand greatly increased supplies of energy.

(2) Peru has recently become self sufficient in petroleum, which is its principle source of energy. Production of petroleum has been mainly from onshore and offshore basins of the coastal belt province, especially in northwestern Peru where production began in 1874. The sharp increase in production of petroleum in recent years has resulted from the belated development of fields in the Amazon region, even though discoveries there date from 1937. R. E. Mattick and K. A. Yenne estimate that Peru's identified oil reserves are $1{,}095\times10^6$ bbl and undiscovered recoverable oil resources are an additional $2{,}060\times10^6$ bbl ($1{,}490\times10^6$ bbl in structural traps of basins in the Amazon region and 570×10^6 bbl in traps on the continental shelf and onshore basins). Substantial additional discovered resources may exist in deep waters beyond the continental shelf and in stratigraphic traps in basins of the Amazon region. Natural gas is produced chiefly from one area, the Talara, in northwestern Peru; most Amazon basin fields have water drive so that gas production is small. Prospects to increase natural gas production are not favorable. In general, Peru probably has a large potential for additional petroleum development. With advancement of deep-water exploration and production technologies and seismic exploration tools, new fields may be found along the coastal belt in northwest Peru. The Amazon basins, however, offer the best long-term prospects for increased production in Peru, but exploration and development of new fields there will be difficult, expensive, and time-consuming because of the remoteness of the area and its inhospitable environment.

(3) Eleven separate coalfields are known in Peru. Little or no coal is currently being produced, and only a few fields have histories of significant mining. According to W. W. Olive and R. G. Hobbs who investigated the coal deposits in association with Peruvian specialists, the minable coal beds (more than 0.6 m thick) are (1) included in Upper

Jurassic and Lower Cretaceous sedimentary rock sequences that have been intensely folded and faulted and intruded by igneous rocks, (2) as much as 6.0 m thick, but average about 1.5 m thick, (3) subbituminous to anthracite in rank, with about two-thirds of the coal areas reported to be anthracite, (4) generally low to moderate in sulfur content, low to high in ash content, and moderately high in heating values, and (5) in some areas of coking quality suitable for lead-smelting furnaces or, when mixed with strongly coking coal, suitable for blast furnaces in steel mills. Peru's coal reserves have been estimated as $1{,}060 \times 10^6$ t of which 142×10^6 t were classified as "measured" and "estimated" (Escudero, 1977). Future energy shortages and domestic power needs warrant additional development of Peru's coal resources. Four coal fields appear to offer the most potential for immediate development; the Alto Chicama and Santa Valley in northern Peru and the Oyon-Gazuna and Jatunhuasi in central Peru. The Oyon area holds the best prospects for development of coking coal.

(4) The geothermal energy resources of Peru are poorly known because of the lack of prior investigations. Thermal gradients in South America are generally high along the Andes, so, because the Andes occupy much of Peru, the geothermal resources may be large. Geothermal resources are indicated by emergence of hot springs at many places in northern and central Peru in a narrow belt within the Cordillera Occidental and by large areas of recent and active volcanism in southern Peru. R. O. Fournier, in collaboration with Peruvian scientists, recommends that a program of geochemical exploration be undertaken in the area of fumarole activity near Cajamarea in northern Peru and in the volcanic areas of southern Peru and that a geologic mapping program be expanded to delineate volcanoes, faults, and hydrothermally altered rocks. Results of these programs would determine locations for drilling test wells to evaluate the geothermal resources. S. L. Schoff evaluated Peru's water resources in relation to potential energy supplies.

(5) Exploration for uranium resources in Peru has been neither comprehensive nor intensive and has lacked modern airborne radiometric surveys. Peruvian geologists have made local investigations in readily accessible areas of the country only. No economic deposits have yet been found. Peru is not located in a generally recognized uranium province; however, E. A. Noble in conjunction with Peruvian scientists points out that the foothills of the Eastern Cordillera and the adjoining jungle area extending toward the Brazilian Shield are a geological continuation of the known uranium province similarly situated in Argentina and would be a favorable area in which to search for uranium through aeroradiometric reconnaissance and geologic, geochemical, and geophysical mapping and analytical programs.

(6) Neither oil shale nor tar sand deposits have been reported in Peru. R. L. Miller in discussion with Peruvian geologists concludes that this fact may be due to the lack of data rather than a lack of deposits, but development of either industry is not likely in the near future.

POLAND

Research studies have been undertaken by Helmuth Wedow, Jr., E. W. Roedder, and R. E. Zartman as part of a cooperative USGS project with the Polish Geological Institute under the Special Foreign Currency Program (P.L. 480). Principal counterpart scienstists are Jadwiga Pawlowska and Czesław Haranczyk. The investigations concern the lead-zinc deposits of the Upper Silesian region. The deposits are situated in the Lower Muschelkalk of Middle Triassic age. These rocks are a part of the Cracow-Silesian monocline and are underlain by older Triassic and Permian strata that in turn are unconformable on a basement of folded and partly metamorphosed Carboniferous and older Paleozoic rocks. The monocline is the top part of a broad, northwest-trending horst that has been repeatedly uplifted relative to basins to the northeast and southwest, since the region was cratonized in the Early Permian.

The studies indicate that the lower Muschelkalk strata were deposited in a tidal-flat environment and are marked by anomalous concentrations of as much as 0.2 percent zinc and lead. Diagenesis of Muschelkalk carbonate strata further concentrated the metals in the primary sediments to form the first generation of disseminated, fine-grained bedded sulfides. In even later stages, epigenetic ores were concentrated into a relatively few ore zones, the main control of which seems to be the transition facies between primary limestone and early diagenetic dolomite.

From these studies it has been generally, although not unanimously, concluded that the Zn-Pb karst ore concentrations are not directly related geochemically to other sulfide deposits in older rocks in the basement. Instead, they were formed by four main peri-

ods of influx of highly saline paleobrines in a sequence that extends from Triassic through Quaternary time. One influx in Liassic time during the initial formation of the Alpine geosyncline was the most influential. These infiltration stages thus probably correspond to several stages of brecciation and karst development.

SAUDI ARABIA

Water-resources advisory services

Four USGS hydrologists worked with the Water Resources Development Department of the Saudi Arabian Ministry of Agriculture and Water. Major areas of progress in 1978 were the activation of a computorized data-storage bank and the estimation of stream discharge by measurements of channel geometry. S. S. Papadopulos conducted a seminar in Riyadh on digital ground-water modeling in April 1978.

Study of Precambrian formations

An informal lithostratigraphic lexicon for the Arabian shield was prepared by F. H. Fitch, a consultant to the USGS project, and published by the Directorate General for Mineral Resources.

Study of silicic plutonic rocks

D. B. Stoeser and J. E. Elliott continued a study of granitic rocks in the Hail and Tathlith areas. In addition samples of quartz diorite from the Wadi Tarib batholith were collected for rubidium-strontium dating. Petrographic study of rocks of the Tathlith alkaline granite province continued.

Mineral belt studies

C. M. Conway completed fieldwork on the Habawnah mineral belt project and on the Al Masane mapping project. Several hundred samples were collected from gossans throughout the northern part of the mineral belt in the Wadi Wassat, Malahah, and Wadi Husn quadrangles. An east-west zone across the northerly trending mineral belt was mapped at scale 1:25,000 between the Dhanar-Hagira area and Wadi Qatan in a successful attempt to further elucidate the distribution of silicate rock and gossan types and to decipher the major stratigraphic and structural elements of this portion of the mineral belt. All rock types were extensively sampled to enable petrographic study, trace element analysis, and petrogenetic studies. J. E. Elliott and D. B. Stoeser completed field investigation and sampling of granitic rock near Hail. Several low-level beryllium, molybdenum, niobium, tin, yttrium, lanthanum, and fluorine anomalies are associated with some plutons of younger granite. Cassiterite was identified in a sample from a granite stock in the Wadi Wassat quadrangle. The granite had previously been known to have an anomalous tin content.

Mining geophysics

H. R. Blank, Jr., and J. C. Wynn are analyzing contract airborne electromagnetic surveys made in 1977. In the Wadi Bidah, Masane, Shuwas, and Kamal areas, 15 anomalies have been selected for investigation. Some anomalies undoubtedly are related to graphite rocks, but one anomaly having a strike length of several kilometers is produced by a previously unknown 2- to 5-meter-thick bed containing disseminated nickeliferous sulfides. Most anomalies do appear to be associated with indications of alteration.

Airborne EM anomalies from the 1977 Saudi Arabian Shield INPUT survey were assessed with geological reconnaissance and ground geophysical follow-up. This assessment showed that many known prospects and ancient mines are related because they lie on a common buried conductor. Some of these conductors are many kilometers long, are associated with shear zones, and are covered in many places with younger volcanics. In other places, anomalies classed as "bedrock-good" were associated with only weak gossans, and showed no evidence of previous mining. There is a good probability, therefore, that economic mineralization might be found that was missed by ancient miners. Some of the ground follow-up EM and SP results are highly encouraging, and, if geochemical results prove favorable, drilling targets can be identified.

Seismic profile

Analysis of the data collected from the seismic profile from the Red Sea across the Arabian Shield continued. Data obtained from shots at six points have been analyzed and tentative conclusions are:

- The crust along the profile consists of two discrete homogeneous isotropic layers, an upper one having a compressional velocity near 6.0 km/s and a lower one having a velocity near 6.7 km/s.
- The boundary between crust and mantle (Mohorovicic discontinuity) is sharp.
- Velocity within each layer does not increase with depth.

- No "hidden" low velocity layers are present.
- Delays due to surface inhomogeneities of altitude differences are negligible.
- For most of the line the thickness of the upper crustal layer is consistent and averages about 23 km, and total crustal thickness is computed to be 35 to 45 km, averaging 40 km; for the southernmost part of the line the upper layer thins to about 9 km, and total crustal thickness is about 15 km.

Geophysical laboratory

The first determinations of electrical conductivity and chargeability were made by M. E. Gettings and M. Bassari (Directorate General of Mineral Resources, DGMR), on 25 specimens from Mahd adh Dhahab. Four new specimens from a previously sampled granite intrusion near Hamdah were collected and are expected to improve the statistical validity of a paleomagnetic pole position that has been determined by Karl Kellogg for the intrusion, dated at 665 m.y. B.P.

For the Mahd adh Dhahab specimens, paleomagnetic results show a normal, an antinormal, and a transitional direction of magnetization. These positions are not yet corrected for tilt of the volcanic host formations, but appear to be adequately stable and to represent additional paleomagnetic pole positions for the late Precambrian of the Arabian Shield.

Geochronology

Rubidium-strontium measurements on gneisses from east of Umm adh Dhamar were completed by R. J. Fleck in Menlo Park. Results are consistent with earlier data from rocks in the southern part of the Arabian Shield; diorite units are more than 800 million years old, and initial Sr 87/Sr 86 ratios are below 0.703.

Evaporite studies

L. F. Rooney reports that in exploring Sabkhah Hazawaza by drilling, in one drill hole, brines containing about 2000 mg/L of potassium were encountered.

Regional gravity studies

M. G. Gettings, assisted by Mohammad Uthman (DGMR), completed the gravity survey of the coastal plains and escarpment from Jidda to Al Qunfudhah. Only one block in the southeastern part of the Arabian shield remains to be surveyed. Gettings and M. Donzeau (French Bureau de Recherches Géologiques et Minières) made a crustal model from a gravimetric profile derived from existing regional coverage along the seismic-refraction line and from the preliminary results of part of the refraction survey. They found that a low density and, therefore, probably hot mantle must underlie the western part of the Arabian shield in order to account for the gravity and seismic results, assuming isostatic equilibrium.

Regional magnetic studies

M. Bazzari (DGMR) and G. E. Andreasen prepared a manual of circular aeromagnetic anomalies based on 1:500,000-scale geologic maps for inclusion in a 1:2,000,000-scale study of Arabian Shield magnetic data.

Remote sensing

Several computer-based classification and image-enhancement techniques that use Landsat multispectral scanner (MSS) data were compared to evaluate usefulness for geologic mapping in the low-latitude deserts of western Saudi Arabia. Two areas were studied by G. F. Brown (USGS) and W. H. Blodget (NASA), one near the Yemen border in a rugged terrain that is undergoing fluvial erosion and an area in northwest Arabian where the rainfall is less than 5 mm and surface reflectances are influenced more by wind scour and desert varnish. It was found that discrimination of various rock surfaces was improved by Landsat data manipulated by a variety of computer algorithms, of which the most effective is the simultaneous use of two differently computer-enhanced Landsat MSS color-composite images. These are the ramp-cumulative distribution function (CDF) contrast stretch and the ratio-contrast stretch, the latter using MSS band ratios 4/5, 5/6, and 6/7, projected respectively through blue, green, and red filters. The contrast-stretched imagery increased the separation of low spectral values of picture elements in the display at the expense of the brighter rocks in the complex structures of the shield where the rocks have low but differing reflectances. Structural elements are particularly well accentuated in the ramp-contrast stretch imagery, whereas the ratio-contrast stretch provides best capability for rock discrimination. Data from high-sun-angle (summer) images provide significantly better discrimination than low-sun-angles images (winter) which show more detailed structural information.

Various factors influencing the spectral response of individual rock classes such as extent of weathering and soil development, eolian sand blasting, desert varnish, shape and age of pediments, and abundance of vegetative cover must be considered. With due allowance for these factors, it proved possible to separate various granitoid outcrops in greater detail than had hitherto been possible by using aerial photographs and ground reconnaissance. Some color differences have yet to be explained by more detailed geologic mapping. Of particular merit was the discovery of a unique color for gossan and lateritic regolith. By use of the imagery, known gossan was extended over long distances. Also, carbonaceous schists were distinctly separable from other schists in areas where the contact was difficult to locate on the ground and impossible to locate on aerial photographs.

Water-personnel development

Water-resources advisory services were provided to, and field operations were conducted on behalf of, the Water Resources Development Department (WRDD), Ministry of Agriculture and Water, under the auspices of the United States-Saudi Arabian Joint Commission on Economic Cooperation. G. C. Tibbitts, Jr., is the Senior Water Resources Specialist of the four-member USGS team assigned to the operation. R. L. Wait, W. J. Shampine, and D. O. Moore were the other USGS participants.

The USGS specialists supervised or reviewed some aspects of consulting services being provided to WRDD and assisted in developing specifications. A good beginning was made in computerizing the processing, storage, and retrieval of hydrologic data. It was estimated that at least 3,000,000 punch cards would be used. Considerable progress was made in estimation of stream discharge from analysis of channel geometry. In addition, the stream-gaging network was strengthened. The completion of data on water quality continued. In support of the program, S. S. Papadopulos presented a seminar on digital modeling of ground-water systems.

TURKEY

F. A. Kohout served as consultant, lecturer, and advisor to the Devlet Su Isleri (DSI) with the objective of strengthening DSI's ground-water investigations capability.

As a part of the initial phase of the program to assess energy resources of developing countries, USGS scientists evaluated the conventional sources of energy in Turkey through a literature study. They concluded that Turkey suffers a deficiency in primary energy raw materials even though all types that are of special interest in today's world occur within its borders. Turkey produces only about 65 percent of its required energy.

The energy minerals petroleum, coal, lignite, and asphaltite are currently produced in Turkey. Hydropower, wood, and plant and animal waste are also used as energy sources. Turkish long-range plans call for future use of bituminous shale (1981), geothermal resources (1982), and radioactive materials (1987) for energy sources. About 98.5 percent of Turkey's oil production has been from fields in the Arabian Platform and Southern Foothills areas in the southeastern part of the country near the border with Iraq. Potential oil production of this area is considered to be high, and it still receives about 88 percent of drilling activity and 80 percent of the geological and geophysical exploration. Coarse clastics, porous sandstone, reefal limestone, and evaporite sequences occur in numerous basins that are likely prospects to contain petroliferous accumulations; the Adana, Hatay, and Iskenderun Basins along the Mediterranean coast near the Syrian border, the Antalya basin along the north coast of the Mediterranean; the Thrace Basin near the border with Greece; and the Heymana-Polatli, Salt Lake, Cankiri, Sivas, Van, and Erzurum Basins, west to east across the interior of the country. The northern foothills and northern folded belt contain thick sedimentary sequences that are modified by complex structural features, but proper exploration methods may locate oil-productive areas. The southern folded belt displays a high degree of tectonicism and volcanic characteristics in the sedimentary rocks, but shows of oil have been reported in test wells. Offshore areas of Turkey are also being explored for possible petroleum development.

Turkey produced 4.6×10^6 t of coal and 10.5×10^6 of lignite in 1976. The principal coal-bearing and coal-producing area is the Zonguldak field on the Black Sea coast in northwestern Turkey. Lignite-bearing and producing areas are scattered throughout most of the country; the most significant deposits are in the northwest near the border of Greece and in the west-central part near Edremit and Eskisehim. Coals in the Zonguldak field are in rocks of Carboniferous age that have been intensely folded and faulted. The coal is bituminous and anthracite in rank and has an average ash content of 14 percent, sulfur content less than 1 percent, and a calorific value of about 7,000 kcal/kg. Approxi-

mately 134×10^6 t are classified as coking coal. Total estimated coal resources in Turkey are $1,276 \times 10^6$ t of which 186×10^6 t are reserves. Total lignite resources are estimated to be $5,607 \times 10^6$ t, including the $1,882 \times 10^6$ t classified as reserves. The lignite is found in beds as much as 3 m thick in rocks of Permian, Jurassic, Cretaceous, Eocene, Oligocene, Miocene, and Pliocene ages.

Organic-rich shales are reported in the Zonguldak coal region near Ankara, Manisa, and Mersin and at several widely distributed areas associated with lignite in western and southcentral Turkey. A total reserve of $5,000 \times 10^6$ t of bituminous shale has been estimated for six localities. Deposits of asphaltite in the Siirt-Sirnak and Mardin-Silopi regions of southeast Turkey contain 52×10^6 t of reserves. Asphaltite also occurs near Odiyamon and Kilis in the south-central part of the country and near Finike on the Mediterranean coast in the southwestern part. Approximately 443×10^3 tons of asphaltites were produced in 1976. Plans call for additional exploration and evaluation to increase production of asphaltite and to begin using bituminous shale for energy generation in 1981.

Hydropower potential for Turkey has been estimated at 72×10^9 kWh based on measurements of stream flow at 500 stations in 15 river basins. Present yearly output from the 18 hydroelectric plants now operating is $8,829 \times 10^6$ kWh. When completed, seven more plants now under construction will approximately double present output by 1985.

Some 600 thermal springs have been reported in Turkey. Their distribution is countrywide, with a general increase in concentration from east to west. The springs, especially in the western part of the country, are commonly along young faults at boundaries of grabens. In southwestern Turkey the springs are associated with the Menderes graben. A few areas of hot springs are associated with the young volcanoes, Kula, Erciyes, Nemrut, and Suphan. Temperatures of surface waters in the springs range from 29° C to 100° C; reservoir temperatures range from 132° C to 490° C in drill holes. A 15-megawatt geothermal station that will begin generating in 1982 is being built at Saraykoy. National objectives are to develop geothermal sources for space heating and electrical power generation to yield a potential of 1,240 MW.

Uranium mineralization is reported at two localities near the Black Sea coast in northeastern Turkey, at nine localities in western Turkey, and at three localities in the Thrace Basin near the border with Greece. Magmatic, metamorphic, and sedimentary types of deposits are present; reserves of 4,089 tons of U_3O_8 are estimated. Several million tons of uranium ore have been reported at depths of 1 to 2 km in the Black Sea region. In the sedimentary deposits of the western part of the country, uranium is secondarily emplaced in association with silicates, opal, limonite, phosphorite, tuff, gypsum, clay, siltstone, sandstone, and gravel of Neogene age. An ore-processing plant in the area is capable of producing yellow cake containing 70 to 80 percent U_3O_8. Turkey plans to intensify uranium exploration and use so that it will have nuclear power in use by 1987 in order to meet the deficit that is foreseen by the year 2000 for electrical power generation by other fuels.

Palladium, platinum, and rhodium

The Kizildag and Guleman areas, Turkey, and the Faryab and Esfandagheh-Agdasht areas, Iran, have produced chromite from ophiolite complexes consisting of harzburgite tectonite and dunite tectonite containing chromitite, pyroxenite, wehrlite, and gabbro. Forty-six samples from these complexes were analyzed in order to investigate the possibility of platinum-group metals being present that could be produced as byproducts. The results, however, indicate concentrations of palladium, platinum, and rhodium ranging to 46 ppb, 55 ppb, and 24 ppb, respectively. The concentration levels and ratios of these metals are similar to other alpine ultramafic bodies that have been analyzed by modern analytical techniques. Ten samples from massive sulfide deposits in the Gunes and Erigani-Maden areas, Turkey, and the Sheikh Ali mine, Iran, were analyzed also. The results of the analysis suggests a low potential for byproduct palladium, platinum, and rhodium production in these ophiolite-associated massive sulfide deposits.

Computer modeling

A computer-assisted model of Black Sea paleohydrochemistry has shown that during most of the period since about 300,000 years ago, the Black Sea Basin was characterized by a dominant fresh and slightly brackish environment, interrupted by short, sharp marine influxes. Prior to that time, the Black Sea was the site of hypersaline conditions like Great Salt Lake, and rock salt was deposited in enlarged coastal limans or brine lagoons around the periphery of the Black Sea. The computer-iterative technique lends itself well to input of geological and paleontologic information.

Results of previous programs

During March 13 and 14, 1978, A. L. Dilonardo and J. A. Reinemund visited the Mineral Research and Exploration Institute of Turkey (MTA), in regard to cooperative activities involving MTA and the USGS. A number of projects of mutual interest were identified. A tour was arranged of MTA's publications facilities and operations to show the results of the completed USGS training and assistance programs provided under a previous AID-funded project. Dilonardo found that MTA is fully and effectively using all personnel and equipment. MTA is, in fact, a model of successful transfer of technology and organization in the publications field.

VENEZUELA

M. E. Moss and J. M. Landwehr participated in a symposium on hydrology and water resources with emphasis on stochastic hydrology and network design. The symposium was sponsored by the University of Simon Bolivar.

ANTARCTIC PROGRAMS

During the 1978–79 austral summer, three groups of USGS personnel carried out geologic and geophysical field studies on the Dufek intrusion, a large stratiform gabbroic and granophyric body in the Pensacola Mountains (see index map). One group, led by A. B. Ford, did detailed mapping, measured stratigraphic sections, and sampled the intrusion in the Dufek Massif and Forrestal Range. A second group, led by A. W. England, made a detailed gravity survey and measured ice thicknesses by radar soundings along a 60-km line across the intrusion; and at one location they made a resistivity depth profile (induction sounding) to a depth of 5 km in an effort to locate the base of the intrusion. The third group consisted of J. C. Behrendt who made an aeromagnetic survey of most of the intrusion using a C–130 aircraft. Stateside work consisted of the compilation of geologic maps and of X-ray diffractometer, paleomagnetic, and petrologic studies on rock samples and data collected during the field season of 1977–78 in the Orville Coast-eastern Ellsworth Land (see index map). Similar studies were made on rock cores obtained in the Dry Valleys area (see index map) as part of the Dry Valley Drilling Project.

Potassium-argon geochronology of Mesozoic mafic rocks of the Pensacola Mountains

Results of a cooperative study by A. B. Ford and R. W. Kistler indicate that the Dufek intrusion is about the same age as sills of tholeiitic diabase in the Pensacola Mountains and is approximately coeval with the main Early to Middle Jurassic episode of Ferrar-type magmatism of the Transantarctic Mountains. Dating of plagioclases from widely separated stratigraphic levels in the Dufek intrusion yields closely grouped ages that average about 172 m.y. Pyroxene dates from the Dufek intrusion are considerably younger, possibly resulting from argon loss related to inversion and exsolution. Pyroxenes in the sills are optically homogeneous and yield dates slightly older than their coexisting plagioclases. The sills show close similarity in chemistry and $^{87}Sr/^{86}Sr$ ratios with the Ferrar Group of the Transantarctic Mountains. The best age estimate for the sills is considered to be 180 m.y.

Geologic field study of the Dufek Intrusion

During the 1978–79 summer, a field party consisting of A. B. Ford, R. L. Reynolds, S. J. Boyer, and Carl Huie carried out 1:25,000-scale geologic mapping and detailed sampling of the layered gabbroic Dufek intrusion of Jurassic age in the northern Pensacola Mountains (Ford, 1976). The work led to major reinterpretation of late-stage plutonic events in the consolidation of this differentiated igneous complex. Earlier laboratory studies show that iron-magnesium ratios in pyroxenes increase

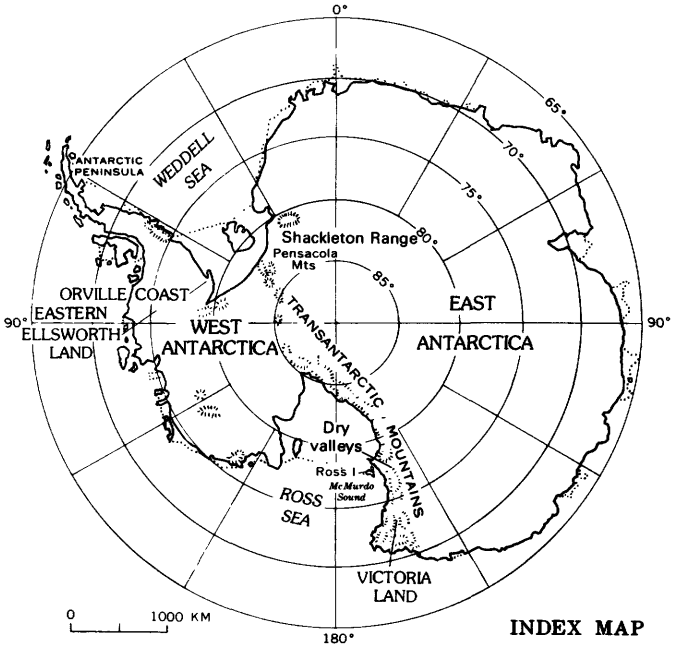

INDEX MAP

progressively upward in the layered sequence except for a strong reversal about 1 km below the top of the body (Himmelberg and Ford, 1976). Preliminary interpretation of field relations found in the 1978–79 season suggest that this reversal is related to a major influx of comparatively little-differentiated magma near the top of the gabbroic sequence. Gabbroic cumulates that formed from the added magma lie with angular discordance on more steeply dipping subjacent cumulates. The discordant contact is marked by the presence of a sedimentary breccia-like layer of inclusion-rich gabbro that is probably related to emplacement of the new magma. Strong loppolithic subsidence preceded the late-state emplacement of magma and may be related to magma withdrawal from below.

Magnetic correlation of Upper Cenozoic Dry Valley Drilling Project cores

Zonations of magnetic polarity and susceptibility have been established by D. P. Elston for four drill cores obtained from sediments in Taylor Valley, Antarctica, as part of the Dry Valley Drilling Project. The magnetic polarity was used to define time-stratigraphic zones, whereas the magnetic susceptibility was used to define rock-stratigraphic zones. The time and rock correlation derived from the data greatly enhance the geologic history of Taylor Valley and the McMurdo Sound region of Antarctica. According to preliminary correlation with the polarity time scale, deposition of the sediments was less than about 10 million years ago. Zones of magnetic susceptibility slightly transgress time, and increasing susceptibility upward in the cores corresponds to the introduction of clasts of volcanic rocks derived from the McMurdo Sound area. These volcanic rocks were carried by an ice sheet that moved southward up the fjord that now is Taylor Valley, in a direction that is reversed to the normal continental ice flow.

Structural geology and paleomagnetism of the Orville Coast area

The Orville Coast area and adjacent eastern Ellsworth Land, mapped during the 1977–78 field season, consists of a thick folded sequence of Middle and Upper Jurassic sedimentary rocks (Latady Formation) and interbedded volcanic rocks that are intruded by Upper Cretaceous calc-alkaline plutons (Rowley, 1978). Recent compilation of the structural and paleomagnetic data by K. S. Kellogg shows that the area resembles other parts of the southern Antarctic Peninsula. The Latady Formation is everywhere openly to isoclinally folded, and the rocks display a well-developed axial-plane cleavage. Many folds are asymmetric, and some are overturned, with axial planes dipping steeply to the north or northwest, and the structures indicate yielding toward the south. Fold axes are horizontal to gently plunging. Strikes of the beds reflect an oroclinal bend from about N. 50° E. in the northeastern Orville Coast and about east in the central and western Orville Coast to about N. 75° W. in eastern Ellsworth Land. A paleomagnetic analysis of Upper Cretaceous plutons and dikes shows that the mean paleomagnetic declination of these rocks is rotated about 51° clockwise relative to rocks of similar age from elsewhere in the Antarctic Peninsula. The oroclinal bend thus formed after most intrusive activity ceased.

Numerous high-angle faults of apparent small strike-slip displacement cut the Latady. The strikes of the faults define two conjugate sets that formed during the folding. En echelon thrust faults indicate at least local overthrusting toward the south. Extension joints strike normal to the fold axes. In contrast, joints and dikes in the plutonic rock are randomly oriented and affirm the contact relations that indicate post-tectonic plutonism.

Mineralogy of surface encrustations in the Orville Coast area

Small white, pale-yellow, green, and blue encrustations are common on the surfaces of rock exposures in the Orville Coast area. Most encrustations are no closer than 25 km to the coast, and, because of ice shelves that extend out from the coast, the encrustations are rarely closer than 150 km to open ocean. An X-ray study by W. R. Vennum (Sonoma State University) of samples collected throughout the Orville Coast area shows that the white encrustations are dominantly gypsum and calcite and include subordinate aragonite, thenardite, thomsonite, and epsomite(?). Yellow encrustations consist of carphosiderite, alunite, natrojarosite, fibroferrite, and copiapite(?). Green and blue encrustations consist of atacamite, antlerite, brochanite, plancheite, and azurite(?). All the encrustations result from an extremely slow rate of rock weathering. A small amount of water melts from ice and snow on the rock surfaces by sun insolation for brief periods on a few days during the austral summer. This water briefly permeates into fractures to a shallow depth in the rock, reacts slightly with the rock, again rises to the surface by capillary action, and evaporates to form the white mineral crusts. The yellow crusts form from the oxidation of pyrite that occurs disseminated in the sedimentary and plutonic bedrock.

The green and blue crusts form from the oxidation of copper sulfides under conditions of low acidity. Natrojarosite, fibroferrite, alunite, brochantite, and plancheite have not been reported previously from Antarctica.

Former more extensive glacial ice in the Orville Coast area

Field studies and compilation of data by P. E. Carrara indicate that glacial ice in the Orville Coast area and eastern Ellsworth Land was formerly more than 450 m thicker than at present. Evidence of the higher ice level consists of glacial erratics, polish, and striations on all rock summits visited. Because no areas were found that had not been glaciated, the figure of 450 m clearly is a minimum. The ice thus formerly covered all mountain ranges and nunataks. Striation directions indicate that the former ice sheet flowed southward over the Sweeney and Hauberg Mountains; to the east, in the vicinity of the Wilkins Mountains, the regional flow was to the southeast (S. 50° E.) over the range; to the west, in the Behrendt and Merrick Mountains, the regional flow was to the southwest (S. 35° W.). Projection back from these regional flow directions indicates an ice sheet center about 75 km north of the Sweeney Mountains, near the present divide of the Antarctic Peninsula. This expanded ice sheet is thought to represent the general expansion of West Antarctic ice during the last worldwide glacial period. The region of the present Weddell Sea was probably occupied by a large ice sheet, similar to that of the Ross Sea region whose collapse has been correlated with the worldwide rise in sea level about 18,000 years ago.

TOPOGRAPHIC SURVEYS AND MAPPING

FIELD SURVEYING

SURVEYING FROM THE AIR USING INERTIAL TECHNOLOGY

Since 1974 the Geological Survey has been studying the concept of measuring accurate terrain profiles from low-flying aircraft using a laser altimeter and inertial guidance technology—the Aerial Profiling of Terrain (APT) project. The desired accuracy of 15 cm vertically and 61 cm horizontally can be achieved for extended missions if positional updates are provided at 3-min time intervals. The project has progressed from a developmental phase, through completion of system design, to initial fabrication of a prototype system.

The APT airborne instruments include a laser profiler, a TV camera, an inertial measuring unit (IMU), a laser tracker, an onboard computer, and a magnetic tape recorder. The airborne computer interacts continuously with the sensors by directing their actions and performing the necessary computations for initial alinement and calibration, for navigation to survey site, and for execution of profile surveys. The laser tracking instrument provides update data by measuring distances and directions to ground reflectors. In addition, the computer feeds data to the onboard magnetic tape recorder to be used later for final smoothing computations.

The IMU and laser tracker furnish the high-accuracy three-coordinate position datum that enables the laser profiler to measure the terrain elevation. Inside the IMU is the stable platform which incorporates three gyros, three pendulous gyro-integrating accelerometers, and associated electronics. Outside the stable platform are three servodriven gimbals under control of the gyros. These gimbals (azimuth, pitch, and roll) isolate the stable platform from aircraft angular motions. The tracker assembly mounts directly to the base of the support structure which surrounds the IMU gimbals and provides a rigid physical connection between the stable platform and the tracker pointing axes.

All data collected by remote sensors must be referenced to a coordinate system before it becomes of value to most users. The first use of the APT system is the collection of terrain profile data for USGS resource analysis and mapping programs. Of greater significance than this application is the inertial technology associated with the system and its capability as a precise three-coordinate reference platform for guiding many of the remote sensors commonly used today. The APT aircraft could easily be fitted with an aerial camera, side-looking radar, magnetometer, or infrared scanner, and the IMU-tracker system could provide precise x, y, and z coordinates for the sensor focal point. Reference data of this precision can increase the usefulness of a number of sensors and reduce the data-reduction requirements associated with nearly all sensors.

The USGS plans to continue with the APT program through 1982 until the operational prototype is completed and flight-tested. Further activities will be based on the results of actual field tests of the prototype system. Costs to date have been approximately $5 million. The fabrication and assembly phase began in October 1978 and is scheduled for completion in 1981.

INERTIAL SURVEYING WITH SPAN MARK

The Camden, Tex., area was selected for testing the SPAN MARK inertial surveying system for establishing horizontal and vertical mapping control along paved highways. The system, mounted in a four-wheel-drive van, surveyed 638 control points during a 15-d period; the survey involved measuring 1,093 km of double-run survey lines. The initial trunk lines, running between established geodetic triangulation stations, averaged 34 km in length, with the longest line 61 km. The largest error found was 0.76 m, well within the maximum allowed. The vertical accuracy of the system was carefully monitored, and 39 test points were established. The standard error of the 39 test points was 0.14 m. The largest error, 0.37 m, was located where the net appeared weak because of greater spread than normal in the SPAN MARK elevations. This area of less accurate elevations was caused by greater spacing between vertical ties than the normal 14 km. The

vertical accuracy was sufficient for the production of 10-ft contour-interval maps.

PHOTOGRAMMETRY

ARBITRARY-PHOTOCOORDINATE PASS POINTS

Pass points used to orient stereomodels in map compilation are usually selected as discrete objects or points on the ground that appear in each image. The Geological Survey is testing the feasibility of using arbitrary photocoordinate positions as pass points, rather than discrete points marked on the photographs. The most recent test used the TA3/P1 stereocomparator, but the procedure is designed for use with three analytical stereoplotters now on order.

The three analytical plotters should be comparable in accuracy to the TA3/P1, and, like that of the TA3/P1, the software will include options for frame or panoramic photographs with or without reseaus, interior and relative orientation routines, point editing, and output of either photocoordinates or stage coordinates. Advantages of these analytical plotters over other conventional instruments include (1) high-speed measurement of points under computer control, (2) computer-maintained stereomodeling which lessens the amount of parallax and associated eye fatigue, (3) point-editing for blunder detection, and (4) image-refinement during the measurement operations. In addition, the three new analytical stereoplotters are designed for use both as comparators and as map compilation instruments.

The pass-point test project was measured on 50 unmarked photographs in four strips. The project had been processed previously by measuring marked points on a monocomparator, and these results were available for comparison. The triangulation results of the two methods were not significantly different, indicating that the elimination of point marking prior to point measurement is a main advantage of the procedure.

MAPPING FROM HIGH-RESOLUTION HIGH-ALTITUDE PANCHROMATIC PHOTOGRAPHS

The relative imagery characteristics of Kodak 2402 and high-resolution SO–022 panchromatic films, exposed in a standard mapping camera at high altitudes, have been investigated. Results indicate that the resolution on Kodak SO–022 film was only slightly higher than on 2402 film using photographs taken at 40,000 ft (12,200 m) above mean terrain with a 6-in.-focal-length camera. Based on reading resolution targets on the ground in 24 exposures, the 2402 film averaged 20 lines/mm resolution and the SO–022 film averaged 26 lines/mm. These resolution measurements were made on diapositives prepared on Cronar CT–7 film and observed in a Kern PG–2 plotting instrument using 16-power magnification.

The anticipated image motion at an altitude of 40,000 ft (12,200 m) with an airspeed of 400 knots was 7 ft (2 m) ground scale during a 0.01-s exposure. No appreciable difference in resolution was observed between a target oriented along the flightline and one oriented across the flightline. This indicates that, for high-altitude photographs, image motion was not a predominate factor in resolution problems.

Both geometric accuracy and the ability to photoidentify and plot required map detail fell slightly short of meeting map accuracy standards. Enough promise does exist, however, to continue the search for a high-resolution film/camera combination that will satisfy mapping requirements using high-altitude photographs.

BUILDING DLG–2 DIGITAL FILES DIRECTLY FROM STEREOMODELS

Techniques were developed for collecting digital data during stereocompilation using an analog stereoplotter equipped with digital data collection hardware and a file-building strategy for digital line graph–2 (DLG–2) data files. The DLG–2 files consist of line map information edited to add attribute codes and to remove visible errors and inconsistencies. The procedure used had three phases: (1) data collection, (2) data processing, and (3) interactive editing.

The technique was tested on a mapping project for Iowa. The Packwood SE, Iowa, quadrangle was planned for a 10-ft contour interval using 11,500-ft (3,505-m) compilation photographs. Digital data for the planimetry and the contours were collected from stereomodels utilizing a Kern PG–2 stereoplotter fitted with an Altek AC–189 three-axis digitizer. Both header and coordinate data were recorded on magnetic tape for each feature traced in the stereomodel. All stereomodels were scaled and leveled before digitization, using four to six model control points. Data were collected in an arbitrary-machine-coordinate system and later transformed to State plane coordinates through the set of model control points. Depending on the complexity of a model, 1 to 1.25 man-hours per model are added to

the normal compilation time for digitizing from the stereomodel.

The project has shown that stereomodel digitization and the subsequent interactive editing of these data are within the state-of-the-art and appear to be feasible in the plains area of the Midwest. As a result of this work, flexible procedures for digitizing and editing stereomodel data have been adopted, and these procedures are being tested in digitizing four quadrangles.

NUMERICAL ORIENTATION OF KELSH K–100 PLOTTER

Orientation parameters for the Kelsh K–100 plotters, computed from the direct geodetic constraint method of analytical aerotriangulation, are being used in stereocompilation at the USGS. The output data include the air base in ground feet and millimeters at model scale, elevation differences between the two exposure stations in feet and millimeters at model scale, and angular tilts for each exposure.

Initial results of numerical orientation with this method are favorable. Residuals on control points after initial setting of the orientation parameters are on the order of 10 ft (3 m) both horizontally and vertically at a 1:6,000 model scale. A time savings of 5 to 15 min is achieved in the orientation of each model.

Twenty-four Kelsh plotters have been fitted with aluminum photographic-film millimeter scales for the setting of BZ and BX data. Graduated level trivets have been designed and fabricated to provide for direct setting of the angular tilts for each exposure.

POINT-TRANSFER EYE TEST

Prior investigation into the ability of operators of point-transfer devices to accurately transfer a marked location from one diapositive to another revealed that their eyes are subject to biases that can usually be removed with proper examination and lens prescriptions. Because the point-transfer procedure is the largest error source in monocomparator aerotriangulation, all employees operating point-transfer instruments are periodically tested.

To expedite the testing procedure, a Wang 720C program was written to allow the person being tested to compute his own test results. The program card-deck input includes camera and comparator calibration data, the fiducial and test-point coordinates of the master test plate, and the fiducial and test-point coordinates of the subject's marked plate. The printed output consists of calibrated coordinates, observed coordinates, and residuals of the fiducials; transformed test-point coordinates; test-point residuals; and the average and root-mean-square errors in the x and y directions.

PLANIMETRIC COMPILATION FROM ORTHOPHOTOGRAPHS

The USGS has developed and put into operation an economical method of using orthophotographs in the topographic mapping process. For each new mapping project at 1:24,000 or 1:25,000 scale, two levels of photography are exposed—high altitude for producing an orthophoto base and low altitude for compiling contours. Aerotriangulation with the high-altitude photographs requires much less horizontal ground control than is needed for lower altitude photographs.

Using a Gestalt Photo Mapper, each high-altitude photograph is transformed into an orthophotograph covering a 7½-min quadrangle area. The orthophotograph image is registered to a base sheet containing the graticule and grid and is then printed on scribe-coat material.

By reference to field-annotated photographs, all planimetric features that can be seen clearly on the image base are scribed in final form directly on the image. Several image bases are used so that the features can be color-separated for printing. Each color separation is overprinted on the other bases in a prescribed sequence so that precise register is maintained throughout the process.

The stereomodels formed from the lower altitude photographs are fitted and scaled to the map by reference to discrete image points on the orthophotograph base. Contours and other map features not clearly visible on the image are compiled from the stereomodels. The contours are scribed in final form on a separate base, and the other stereocompiled features are transferred and scribed on the appropriate bases. The completed scribed drawings are used to prepare color-composite proofs and printing pressplates.

The photobase mapping process reduces the cost and time required to produce standard topographic maps by eliminating aerotriangulation of the low-altitude photographs and by avoiding the preparation of manuscript copy prior to color-separation scribing. A companion orthophotoquad may be prepared as a byproduct of the process.

PHOTOGRAMMETRIC ARCHIVAL STORAGE SYSTEM

By aerotriangulation, horizontal and vertical pass points are established for controlling stereomodels in map compilation. Input to the aerotriangulation consists of ground coordinates of control points and photocoordinates of discrete points measured on precise comparators or model coordinates measured on digitizing stereoplotters. The observations are refined to remove known systematic errors, and ground coordinates of pass points are computed.

An average photograph contains 15 to 20 points, and the data for a single point may exist in four or five coordinate systems. The storage of this data and its later retrieval quickly become a massive and time-consuming function.

Current research efforts are directed toward designing and testing a computer-based system of storage of aerotriangulation data. It is envisioned that each mapping center would have a file for its own area of interest and would have access to the files from other mapping centers.

Each data-bank record, or card image, will contain items such as identification of the point, coordinates, type of coordinate system, evaluation of coordinate accuracy, and retrieval codes. The records could be retrieved according to location, type, State, or any other item in the record. During the next year, extensive testing of the data bank is planned.

IMAGE CONTROL TARGETS

For evaluating image quality for resolution, tone reproduction, and flare characteristics, 42 image control targets (ICT) have been developed and produced. The ICT is a precision-engineered composite-type target that includes a sophisticated array of features that makes it useful for uniformly evaluating performance aspects of photo-optical instruments or entire photo-optical systems used in the map production process. These features include five USAF 1951 resolution targets (1 to 102 cycles/mm), two gray-scale step tablets, four different background densities, and two Siemens stars.

Each ICT is supplied with a diffuse density calibration sheet and is calibrated using National Bureau of Standards step-tablet values. The basic procedure is to use the ICT as input in place of the original aerial negative in testing individual instruments or entire systems and then to measure the output for comparison and evaluation of performance.

"NATURAL" COLOR IMAGE MAPS FROM COLOR INFRARED FILM

Experimental color image maps of the Canadian border have been printed from pressplates made from two black and white aerial negatives which were simultaneously exposed in like cameras on panchromatic film and infrared film with yellow and red filters. The reproductions were printed both as color infrared images, which would be the expected color result from any imagery made at the infrared end of the spectrum, and as pseudonatural color imagery in which the high infrared response vegetation was printed in green. The results were very favorable.

Experiments in making the same type of black and white separate plates from original color infrared film have shown that pressplates can be made which will also produce pseudonatural color while retaining the advantages of infrared haze penetration and water delineations. The use of the color infrared film as input for the pressplates eliminates the need for the two-camera system required with the use of two black and white films.

DIGITAL CARTOGRAPHY

Computers have been incorporated into nearly all phases of map production, and cartographers have taken advantage of this evolution to enhance many of their production procedures. With the modern digital cartographic equipment now available, it is possible to reorganize many phases of map production to allow greater flexibility in mapping techniques and products.

In conventional map compilation operations, a topographic map manuscript is the work base for the various mapmaking phases. Map data are drawn in ink or pencil on a mylar base and then scribed with proper symbology to provide the manuscripts used to produce lithographic-quality color separates. The corresponding digital data stored on magnetic tape or disks can be the sole medium.

The USGS has been investigating integration of digital mapping hardware and techniques into its cartographic mapping operations for several years. New equipment permits the use of stereomodel digital-data capture, interactive editing, and cartographic machine-plotting techniques for the production of conventional map color separates.

Data collected from the online digitizing of stereomodels can be used not only for producing final-scribe map bases, but also for establishing digital

topographic data bases for map revision and data dissemination. The process involves online acquisition, formatting, filtering, and interactive editing of the topographic map data. The edited data can be plotted in final scribe copy, along with enhancements needed to produce color-separated bases.

DIGITAL DATA EDITING SYSTEM

Many interactive editing functions are performed on the digital map data; for example, line clipping, extending, and smoothing eliminate discontinuities at stereomodel joins within a quadrangle. Internal editing includes any separate-to-separate feature correlation needed for color composite register, such as registering contour reentrants with drains, offsetting buildings from roads to avoid conflict of symbology, and registering multifeature intersections. Other types of data editing include line smoothing, feature redigitizing, and placement of names and other text. The amount of editing required for each separate depends upon the amount of map detail that is required for the final scribing process. Many of the separates—such as transportation, drainage, and culture—require little smoothing of the data and are interactively edited to essentially a finished manuscript. In contrast, the contour separate requires so much interactive editing that it must be processed differently. The contour data are first edited to remove gross blunders and then machine-scribed on a mylar manuscript that is returned to the compiler for final manual edit.

Edited mylar plots are generated by a digital map production system and given to a final scriber for touchup, eliminating the need for rescribing of the raw cartographic data by the initial map compiler. Comparison of separates produced by final scribing and plots of edited digitized separates revealed that content and register were identical for all color separates except the contour sheets. An additional advantage of the interactive data acquisition process is that digital representation of the cartographic features in a 7½-min quadrangle can be stored on a magnetic tape or disk for future processing in map revision, data structuring, and map data-base construction.

The cost and time advantage of digital interactive compilation over manual scribing have not been established. Research is continuing to evaluate these aspects and to establish and develop a digital data base that will provide additional products and greater flexibility.

DIGITAL PROFILE RECORDING AND OUTPUT SYSTEM

The Digital Profile Recording and Output System (DPROS) semiautomatically digitizes and records elevation profile data from a stereomodel and automatically produces orthophotographs from these data. Currently, either a Zeiss C–8 stereoplotter or a Kelsh plotter with manual profiler is used in the recording operation and a Zeiss GZ–1 orthoprinter is used in the exposing operation. A T–64 Orthophotoscope is being altered and tested to determine the feasibility of also using this instrument as a profiling medium.

Tests are underway to determine the feasibility of interpolating the digital elevation profiles between scans to permit the orthoprinter to expose at smaller scan widths. This procedure would reduce image mismatches between scans caused by terrain slopes.

DIGITAL READOUT AND REFERENCE SYSTEM FOR CARTOGRAPHIC CAMERA

Two cartographic cameras were fitted with digital readout systems having precision rack and pinion drives for rotary encoders. The racks are 0.1-in. pitch, and the system can be read to 0.001 in. on the display. A single rack is used for both the copyboard and the lens board carriages.

In addition to the racks, precise level assemblies were attached to the copyboard and the lens board carriages. These levels employ dial gages which permit measurement of the deflection from a vertical plane to 0.0005 in. This combination of measurement and corrections for deflection permits accurate calibration of all interchangeable lenses and should result in much improved accuracy in photographic reproduction.

COORDINATE TRANSFORMATION SYSTEM

The USGS is investigating the feasibility of using a multiple microcomputer data processor to transform sets of digital cartographic data from one coordinate system to another. Currently, time-consuming transformation programs are run on mainframe computers at high expense.

Preliminary design of the Coordinate Transformation System (CTS) has been completed as a high-speed direct-memory-access interconnection scheme between a front-end processor minicomputer and remote microcomputer modules. After the network interconnect details are resolved, hardware

will be assembled and performance measured and optimized.

A twofold design approach was used in an effort to improve system speed. Design was started on programming the computer control unit to perform more rapidly the multiple precision arithmetic instructions now performed using slow software. Also, design was started on a high-speed hardware arithmetic processor that will perform the multiple precision floating-point instructions. Both of these methods for increasing program speed will be evaluated based upon cost-performance criteria. A performance evaluation will be made of a computer network consisting of three microcomputer modules and the front-end processor.

SATELLITE TECHNOLOGY

LANDSAT 3 RETURN BEAM VIDICON IMAGES

Landsat 3, launched on March 5, 1978, carries longer focal length return beam vidicon (RBV) cameras that provide substantially improved resolution and geometric fidelity as compared with the RBV's of earlier Landsats. Preliminary evaluation of the RBV images revealed that, while the normally produced images were lacking in image quality, specially processed images were excellent. When the new NASA digital Image Processing Facility (IPF) and the EROS Digital Image Processing System (EDIPS) become fully operational, normal image quality is expected to be much better.

In an investigation on Landsat 3 RBV images, four RBV scenes of the Upper Chesapeake Bay were analyzed for geometric quality. Control points were identified on 1:24,000-scale topographic maps, and the RBV images of these points were measured on a comparator. A direct similarity transformation from image coordinates to UTM ground coordinates yielded a root-mean-square error of approximately 90 m. A more accurate central-perspective fit of the image coordinates to space-rectangular ground coordinates reduced the error to approximately 40 m.

SATELLITE IMAGE MAPS

Lunar and planetary mapping

A project is underway to produce 1:250,000-scale lunar orthophotographs from high-oblique Apollo mapping camera photographs. The NASA Lunar and Planetary Photography and Cartography Committee requested USGS support in extending orthophotocoverage into additional lunar areas covered by oblique photographs to complement the maps produced by the Defense Mapping Agency (DMA) from vertically oriented Apollo photographs.

The use of high-oblique photographs required an in-house capability to rectify photographs with a 40-degree tilt and scales ranging from approximately 1:370,000 to 1:530,000 at 2× enlargement. All control data for the project were furnished by DMA. Attempts to rectify the photographs on the T–64 Orthophotoscope, following initial rectification to a lunar control base on the E–4 rectifier, were unsuccessful due to the excessive tilt. Rectification on the Gestalt Photo Mapper (GPM–2) was also unsuccessful due to the amount of tilt involved and lack of sufficient contrast on the photographs necessary for automatic correlation between models. The problem of tilt may be overcome in the future when new software being formulated for the GPM–2 becomes operational, but the lack of contrast inherent in the original Apollo photographs may continue to present difficulties in electronic correlation.

Further rectification experiments are being conducted on the Wild OR–1 orthophoto system using digital profile data provided by the DMA as input. Results obtained on the OR–1 will be instrumental in determining current USGS capabilities for rectifying high-oblique Apollo photographs to produce 1:250,000-scale lunar orthophotomaps.

Temporal mapping with Landsat data

A 1:500,000-scale color image map of Chesapeake Bay and vicinity, winter 1976–77, was printed using three Landsat 1 scenes. The map portrays the area under the most severe winter conditions on record and is a true temporal map, as well as a historical portrayal of thematic data. The entire Chesapeake Bay was imaged in a 50-s period on February 7, 1977. On the following day the western part of the Bay and the Potomac River were imaged, and the changes that occurred in the ice within 24 h were recorded.

Enhancement of the imagery at the EROS Data Center introduced digital one-dimensional (scanline) clipping and stretching to accentuate the various ice conditions. Edge enhancement was also used to increase contrast.

Upper Chesapeake Bay

A third edition of the Upper Chesapeake Bay color image map was printed at 1:250,000 scale using a precision-processed edge-enhanced image digitally processed by IBM Corporation. The larger scale map shows more color contrast and informa-

tion and improved geometric accuracy as compared with the two previous editions. The first edition was produced by conventional photograph processing, and the second used an image that had been precision processed by digital methods. Since all three editions contain the same basic data (the Landsat 1 image recorded October 11, 1972), valid comparison of results is possible, and the advancement in image processing techniques is evident. An estimated 100 percent increase in both information content and geometric accuracy has been achieved through improved processing.

An accuracy test of the map as printed is significant because the root-mean-square error is only 61 m. This indicates that Landsat data, when properly processed and referenced to ground control, can be printed in multicolor image form to meet U.S. National Map Accuracy Standards for 1:250,000 scale.

Wenatchee, Washington

The use of Landsat images for theme extraction of open water, vegetation, and natural shaded relief was tested on the 1:250,000-scale Wenatchee, Wash., quadrangle map. The vegetation and natural-shaded-relief data and the image map background were combined with the line map data. However, it was found that the time of year and Sun angle of the image need to be carefully selected for a complete water plate. This map was selected by the Commission on Cartography of the Pan American Institute of Geography and History (PAIGH) as the standard model for preparation of the PAIGH 1:250,000-scale unified Hemispheric Mapping Series for areas where no topographic coverage is available.

SPACE OBLIQUE MERCATOR PROJECTION

In 1974, a proposal was made for a new map projection—the Space Oblique Mercator (SOM) projection—that would permit continuous mapping of satellite imagery, particularly Landsat. Until 1974 no map projection had been devised to show the satellite groundtrack continually true to scale for an orbiting satellite combined with a rotating Earth. In 1977, as a result of a contract with John Junkins, University of Virginia, at Charlottesville, a complex set of universal equations that can be applied to noncircular orbits and other general cases was developed. At the same time, an independent investigator, John P. Snyder, Madison, N.J., developed simpler equations defined specifically for Landsat. Since then, Snyder has refined and improved the equations, and they can be applied to other polar-orbiting satellites. Snyder's equations have been programmed in FORTRAN language on the USGS IBM-370 computer, and copies of the program and documentation are available. Copies have been distributed to other government agencies, some commercial firms, and several foreign organizations. When fully adopted, Landsat processing based on the SOM projection will expedite the automated production of image maps.

CARTOGRAPHIC EQUIPMENT

MICRODOTTER

The negative-scribing technique, which has been adopted by many Government agencies and commercial mapmakers as a means to substantially reduce the time required in preparing printing negatives, has been continually improved by the development of new and dependable scribing instruments. One of these instruments is the electric microdotter used in scribing miniature dots for cartographic symbols on coated polyester plastic film. The USGS designed, improved, and patented this instrument.

The microdotter has a manually operated actuator for moving the drive motor and needle-chuck assembly into contact with the plastic film surface coating. With the downward movement of the actuator, a snap-action switch automatically turns the motor on to rotate the cutter needle. An adjustable depth limiter allows the cutter to penetrate only the opaque surface material and not the transparent base material. Additional features include a rechargeable power source with an adapter-charger, a magnifier, and a needle guard.

COMPUTER TECHNOLOGY

The Computer Center Division (CCD) continued to provide staff advice to the Director on all matters relating to ADP. The CCD provided computational resources, data processing, systems analysis and design services, and interactive time-sharing services and assisted in the acquisition of computer hardware, software, and telecommunication services to enable USGS scientists to meet their informational and computational needs.

TIME SHARING

The time-sharing needs of the USGS are being supported by the three Honeywell Multics computers located in Denver, Colo., Menlo Park, Calif., and Reston, Va. Each system provides high-speed magnetic core memory for 2 million characters of information, bulk store memory for 8 million characters of information, and 1.2 billion characters of disk storage. To allow USGS scientists to access one or more of these computers, the contract with TYMNET, Inc. (a worldwide data communications network), was renewed.

TYMNET provides highly reliable connections from many varieties of terminals located in all major metropolitan areas. Approximately 1,400 users are registered on one or more of the three Multics computers systems and are averaging more than 21,000 interactive sessions per month.

BATCH COMPUTING

The batch computing facilities provided by the CCD continue to be at an overload condition. Action continued on the project to replace the batch computers at Reston, Va., but the procurement has taken longer in the acquisition cycle than originally anticipated. To help alleviate this problem, an extension of the Telecommunications Services Program contract to American Management Systems for the RE–3 resource was necessary, and the conversion of a significant subset of user programs from the IBM 370/155s was completed.

COMPUTER MANAGED MEETINGS

A package of computer programs called CONTINUUM was developed to provide a facility for computer-managed meetings. The facility allows participants to be disconnected in both space and time but still permits interaction and rapid feedback whenever participants happen to be connected in time. Several meeting participants may "speak" simultaneously without confusion. Participants may come and go freely from one meeting to another without interrupting or interfering with speakers. The facility has been found to be particularly useful to managers and members of working committees and has overcome many of the communication problems related to geographic and time-zone separation. CONTINUUM is available on the Denver, Colo., Menlo Park, Calif., and Reston, Va., Multics computers.

U.S. GEOLOGICAL SURVEY PUBLICATIONS

PUBLICATIONS PROGRAM

Books and maps

Results of research and investigations conducted by the USGS are made available to the public through professional papers, bulletins, water-supply papers, circulars, miscellaneous reports, and several map and atlas series, most of which are published by the USGS. Books are printed by the Government Printing Office, and maps are printed by the USGS; both books and maps are sold by the USGS.

All books, maps other than topographic quadrangle maps, and related USGS publications are listed in the catalogs "Publications of the Geological Survey, 1879–1961" and "Publications of the Geological Survey, 1962–1970" and in yearly supplements, available on request, that keep the catalogs up to date.

New publications, including topographic quadrangle maps, are announced monthly in "New Publications of the Geological Survey." A free subscription to this list can be obtained on application to the *U.S. Geological Survey, 329 National Center, Reston, VA 22092.*

State list of publications on hydrology and geology

"Geologic and Water-Supply Reports and Maps, [State]," a series of booklets, provides a ready reference to these publications on a State basis. The booklets also list libraries in the subject State where USGS reports and maps can be consulted; these booklets are available free on request to the USGS.

Surface-water, quality-of-water, and ground-water-level records

Surface-water records through water year 1970 were published in a series of water-supply papers titled "Surface-Water Supply of the United States"; through water year 1960, each volume covered a single year, but the period 1961–70 was covered by two 5-year volumes (1961–65 and 1966–70).

Quality-of-water records through water year 1970 were published in an annual series of water-supply papers titled "Quality of Surface Waters of the United States."

Both surface-water and quality-of-water records for water years 1971–74 were published in a series of annual reports titled "Water Resources Data for [States]." Some of these reports contained both types of data in the same volume, but others were separated into two parts, "Part 1: Surface-Water Records" and "Part 2: Water-Quality Records." Limited numbers of these reports were printed, as they were intended for local distribution only. Since the data in these reports will not be republished in the water-supply paper series, reports will be sold by the National Technical Information Service.

Records of ground-water levels in selected observation wells through calendar year 1974 were published in the series of water-supply papers titled "Ground-Water Levels in the United States." Through 1955, each volume covered a single year, but, during 1956–74, most volumes covered 5 years.

Starting with water year 1975, records for surface water, quality of water, and levels of ground-water-observation wells are all published under one cover in a series of annual reports issued on a State-boundary basis. Reports for water year 1975 and subsequent water years appear in a series of reports entitled "Water-Resources Data for [State]"; these reports are sold by the *National Technical Information Service, U.S. Department of Commerce, Springfield, VA 22161.*

State hydrologic unit maps

State hydrologic unit maps, which are overprints of the 1:500,000-scale State base maps, show culture in black, water features in blue, hydrologic subdivision boundaries and codes in red, and political (FIPS county) codes in green. The Alaska State map is at 1:2,500,000 scale, and the Puerto Rico map is at 1:240,000 scale. All river basins having drainage areas greater than 700 mi^2 (except for Alaska) are delineated on the maps. The hydrologic boundaries depict water-resources regions, water-resources subregions, National Water-Data Network accounting units, and cataloging units of the

USGS "Catalog of Information on Water Data." These maps are available for every State and Puerto Rico.

State water-resources investigations folders

A series of folders entitled "Water-Resources Investigations in [State]" is a project of the Water Resources Division to inform the public about its current programs in the 50 States and Puerto Rico, the U.S. Virgin Islands, Guam, and American Somoa. As the programs change, the folders are revised. The folders are free on request as follows: for areas east of the Mississippi River, including Minnesota, Puerto Rico, and the Virgin Islands—*Branch of Distribution, U.S. Geological Survey, 1200 South Eads Street, Arlington, VA 22202,* and for areas west of the Mississippi, including Alaska, Hawai, Louisiana, Guam, and American Samoa—*Branch of Distribution, U.S. Geological Survey, Box 25286, Federal Center, Denver, CO 80225.*

Open-file reports

Open file reports, which consist of manuscript reports, maps, and other preliminary material, are made available for public consultation and use. Reports and maps released only in the open files are listed monthly in "New Publications of the Geological Survey," which also lists places of availability for consultation. Most open-file reports are placed in one or more of the three USGS libraries: Room 4A100, National Center, 12201 Sunrise Valley Drive, Reston, VA 22092; 1526 Cole Boulevard at West Colfax Avenue, Golden, Colo. (mailing address: Stop 914, Box 25046, Federal Center, Denver, CO 80225); and 345 Middlefield Road, Menlo Park, CA 94025. Other depositories may include one or more of the USGS offices listed on p. 349 and interested State agencies. Some open-file reports are superseded later by formally printed publications.

Microfiche and (or) paper copies of most open-file reports can be purchased from the *Open-File Services Section, Branch of Distribution, U.S. Geological Survey, Box 25425, Federal Center, Denver, CO 80225.*

Earthquake publications

The "Earthquake Information Bulletin" is published bimonthly by the USGS to provide information on earthquakes and seismological activities of interest to both general and specialized readers. Each issue also lists a worldwide summary of felt earthquakes and a State seismic history.

The USGS National Earthquake Information Service locates most earthquakes above magnitude 5.0 on a worldwide basis. The "Earthquake Data Report," a bimonthly publication, provides a chronological summary of location and magnitude data for each located earthquake and contains station arrival times, individual distances, azimuths, and traveltime residuals. "Earthquakes in the United States" is published quarterly as a USGS circular. The circulars provide detailed felt and intensity data as well as isoseismal maps for U.S. earthquakes.

"United States Earthquakes [year]" is published jointly by the NOAA and the USGS. This annual sourcebook on earthquakes occurring in the United States gives location, magnitude, and intensity data. Other information such as strong-motion data fluctuations in well-water levels, tsunami data, and a list of principal earthquakes of the world is also given.

PUBLICATIONS ISSUED

During FY 1979, the USGS published 5,597 maps comprising some 16,874,864 copies:

Kind of map printed	*Number*
Topographic	4,793
Geologic and hydrologic	512
Maps for inclusions in book reports	30
Miscellaneous (including maps for other agencies)	262
Total	5,597

In addition, six issues of the "Earthquake Information Bulletin," 169 technical book reports, and 186 leaflets and maps of flood-prone areas were published.

At the beginning of FY 1979, more than 103.8 million copies of maps and 2.3 million copies of book reports were on hand in the USGS distribution centers. During the year, 9,302,500 copies of maps, including 498,125 index maps, were distributed. Approximately 6.6 million maps were sold, and $5,486,090 was deposited to Miscellaneous Receipts in the U.S. Treasury.

The USGS also distributed 351,872 copies of technical book reports, without charge and for official use, and 1,375,943 copies of booklets, free of charge, chiefly to the general public; 312,000 copies of the monthly publications announcements and 257,800 copies of a sheet showing topographic map symbols were sent out.

The following table compares USGS map and book distribution (including map indexes and booklets, but excluding map-symbol sheets and monthly announcements) during FY 1978 and FY 1979:

Number of maps and books distributed

Publication	Fiscal year 1978	Fiscal year 1979	Change (percent)
Maps	9,321,340	9,800,625	5.1
Books	215,918	351,901	63.0
Popular publications	1,483,793	1,375,943	−7.3
Total	11,021,051	11,528,469	4.6

HOW TO OBTAIN PUBLICATIONS

OVER THE COUNTER

Book reports

Book reports (professional papers, bulletins, water-supply papers, "Topographic Instructions," "Techniques of Water-Resources Investigations," and some miscellaneous reports) can be purchased from the *Branch of Distribution, U.S. Geological Survey, 1200 South Eads Street, Arlington, VA 22202,* and from the USGS Public Inquiries Offices listed below under "Maps and Charts" (authorized agents of the Superintendent of Documents).

Some book publications that can no longer be obtained from the Superintendent of Documents are available for purchase from the above authorized agents of the Superintendent of Documents.

Maps and charts

Maps and charts can be purchased at the following USGS offices:

Branch of Distribution:

1200 South Eads St.,
Arlington, Va.

Building 41, Federal Center,
Denver, Colo.

Alaska Distribution Section:

Federal Building–Box 12,
101 Twelfth Ave.,
Fairbanks, Alaska

National Cartographic Information Center:

1400 Independence Rd.,
Rolla, Mo.

Public Inquiries Offices:

Rm. 108, Skyline Bldg.,
508 2d Ave.,
Anchorage, Alaska

Rm. 7638, Federal Bldg.,
300 North Los Angeles St.,
Los Angeles, Calif.

Rm. 122, Bldg. 3,
345 Middlefield Rd.,
Menlo Park, Calif.

Rm. 504, Customhouse,
555 Battery St.,
San Francisco, Calif.

Rm. 169, Federal Bldg.,
1961 Stout St.,
Denver, Colo.

Rm. 1028, General Services Bldg.,
19th and F Sts., NW.,
Washington, D.C.

Rm. 1C45, Federal Bldg.,
1100 Commerce St.,
Dallas, Tex.

Rm. 8105, Federal Bldg.,
125 South State St.,
Salt Lake City, Utah

Rm. 1C402, National Center,
12201 Sunrise Valley Dr.,
Reston, Va.

Rm. 678, U.S. Courthouse,
West 920 Riverside Ave.,
Spokane, Wash.

USGS maps are also sold by some 1,792 commercial dealers throughout the United States. Prices charged are generally higher than those charged by USGS offices.

Indexes showing topographic maps published for each State, Puerto Rico, the U.S. Virgin Islands, Guam, American Samoa, and Antarctica are available free on request. Publication of revised indexes

to topographic mapping is announced in the monthly "New Publications of the Geological Survey." Each index also lists special and U.S. maps, as well as USGS offices and commercial dealers from which maps can be purchased.

Maps, charts, folios, and atlases that are out of print can no longer be obtained from any official source. They may be consulted at many libraries, and some can be purchased from second-hand book dealers.

BY MAIL

Book reports

Technical book reports and some miscellaneous reports can be ordered from the *Branch of Distribution, U.S. Geological Survey, 1200 South Eads Street, Arlington, VA 22202.* Prepayment is required and should be made by check or money order in U.S. funds payable to the U.S. Geological Survey. Postage stamps are not accepted; please do not send cash. On orders of 100 copies or more of the same report sent to the same address, a 25-percent discount is allowed. Circulars, publications of general interest (such as leaflets, pamphlets, and booklets), and some miscellaneous reports can be obtained free from the Branch of Distribution.

Maps and charts

Maps and charts, including folios and hydrologic atlases, are sold by the USGS. Address orders for maps of areas east of the Mississippi River, including Minnesota, Puerto Rico, and the U.S. Virgin Islands, to *Branch of Distribution, U.S. Geological Survey, 1200 South Eads Street, Arlington, VA 22202,* and for maps of areas west of the Mississippi River, including Alaska, Hawaii, Louisiana, Guam, and American Samoa, to *Branch of Distribution, U.S. Geological Survey, Box 25286, Federal Center, Denver, CO 80225.* Residents of Alaska can also order maps of their State from the *Alaska Distribution Section, U.S. Geological Survey, Federal Building–Box 12, 101 Twelfth Avenue, Fairbanks, AK 99701.*

Prepayment is required. Remittances should be by check or money order in U.S. funds payable to the U.S. Geological Survey. On an order amounting to $300 or more at the list price, a 30-percent discount is allowed. Prices are quoted in lists of publications and in indexes to topographic mapping for individual States. Prices include the cost of surface transportation.

Earthquake Information Bulletin

Subscriptions to the "Earthquake Information Bulletin" are by application to the *Superintendent of Documents, Government Printing Office, Washington, DC 20402.* Payment is by check payable to the Superintendent of Documents or by charge to your deposit account number. Single issues can be purchased from the *Branch of Distribution, U.S. Geological Survey, 1200 South Eads Street, Arlington, VA 22202.*

National Technical Information Service

Some USGS reports, including computer programs, data and information supplemental to map or book publications, and data files, are released through the National Technical Information Service (NTIS). These reports, available either in paper copies or microfiche or sometimes on magnetic tapes, can be purchased only from the *National Technical Information Service, U.S. Department of Commerce, Springfield, VA 22161.* USGS reports that are released through NTIS, together with their NTIS order numbers and prices, are announced in the monthly "New Publications of the Geological Survey."

REFERENCES CITED

Aggerwal, Y. P., and Sykes, L. R., 1978, Earthquakes, faults, and nuclear power plants in southern New York and northern New Jersey: Science, v. 200, p. 425–429.

Aleinikoff, J. N., 1978, Structure, Petrology, and U-ThOPb geochronology in the Milford 15-minute quadrangle, N.H.: Ph. D. Dissert., Darmouth College, 247 p.

Algermissen, S. T., and Steinbrugge, K. V., 1978, Earthquakes losses to buildings in the San Francisco Bay area: Second International Conference on Microzonation for Safer Construction, San Francisco, Calif., 1978, Proc., 13 p.

Allen, R. C., and Barrett, L. P., 1915, Contributions to the pre-Cambrian geology of northern Michigan and Wisconsin: Mich. Geol. and Biol. Survey, Publication 18, Geol. Series 15, p. 13–164.

Anderson, J. A., Hardy, E. E., Roach, J. T., and Witner, R. E., 1976, A land use and land cover classification system for use with remote sensor data: U.S. Geol. Survey Prof. Paper 964, 28 p.

Anderson, W. L., 1978, Interpretation of electromagnetic extra-low-frequency soundings in the Randsburg, California, known geothermal resource area: U.S. Geol. Survey open-file rept. 78–562, 22 p.

Arcement, G. J., Colson, B. E., and Ming, C. O., 1978a, Backwater at bridges and densely-wooded flood plains, Flagon Bayou near Libuse, Louisiana: U.S. Geol. Survey Hydrologic Investigations Atlas HA–604, 5 sheets, scale 1:4,000.

——— 1978b, Backwater at bridges and densely-wooded flood plains, Comite River near Olive Branch, Louisiana: U.S. Geol. Survey Hydrologic Investigations Atlas, HA–602, 3 sheets, scale 1:2,000.

Armbruster, J. T., 1976, Technical manual for estimating low-flow frequency characteristics of streams in the Susquehanna River basin: U.S. Geol. Survey Water Resources Investigations 76–51, 51 p.

Arnold, Ralph, 1907, Geology and oil resources of the Summerland District, Santa Barbara County, California: U.S. Geol. Survey Bull. 321, 93 p.

Back, William, 1966, Hydrochemical facies and ground-water flow patterns in northern part of Atlantic Coastal Plain: U.S. Geol. Survey Prof. Paper 498–A, 8 p.

Bailey, R. A., 1979, Geothermal resource evaluation, Minarets Wilderness and adjacent areas: Chapter D *in* Mineral Resources of the Minarets Wilderness and adjacent areas, Madera and Mono Counties, Calif., USGS open-file rept. no. 79–1472, 196 p.

Baker, E. T., and Wall, J. R., 1976, Summary appraisals of the Nation's ground-water resources–Texas-Gulf region: U.S. Geol. Survey Prof. Paper 813–F, 29 p.

Bakun, W. H., and McEvilly, T. V., 1978, Are foreshocks different? Evidence from Parkfield and Oroville (abs.): Earthquake Notes, v. 49, no. 1, p. 61.

——— 1978, Are foreshocks distinctive? Evidence from the 1966 Parkfield and 1975 Oroville, California, sequences: Seismological Soc. of America Bull., v. 69.

Bakun, W. H., Stewart, R. M., and Bufe, C. G., 1977, Unilateral rupture propagation of foreshocks (abs.): EOS, American Geophys. Union Transactions, v. 58, no. 12, p. 1193.

——— 1978, Directivity in the high-frequency radiation of small earthquakes: Seismological Soc. of American Bull., v. 68, p. 1253–1263.

Barnes, P. W., and Reimnitz, Erk, 1974, Sedimentary processes on Arctic shelves off the northern coast of Alaska, *in* Reed, J. S., and Sater, J. E., eds., The coast and shelf of the Beaufort Sea: Arctic Institute of North America, p. 439–476.

Bartholomew, M. J., 1977, Geology of the Greenfield and Sherando quadrangles, Virginia: Va. Division of Mineral Resources Pub. 4, 43 p.

Batson, R. M., 1978, Planetary mapping with the airbrush: Sky and Telescope, v. 55, no. 2, p. 109–112.

Bayley, W. S., Salisbury, R. D., and Kummel, H. B., 1914, Raritan, N.J.: U.S. Geol. Survey Geol. Atlas, Folio 191.

Becraft, G. E., Pinckney, D. M., and Rosenblum, S., 1963, Geology and mineral deposits of the Jefferson City quadrangle, Jefferson and Lewis and Clark Counties, Montana, U.S. Geol. Survey Prof. Paper 428, 101 p.

Bedinger, M. S., and Sniegocki, R. T., 1976, Summary appraisals of the Nation's ground-water resources–Arkansas-White-Red region: U.S. Geol. Survey Prof. Paper 813–H, 31 p.

Beeson, M. H., 1976, Petrology, mineralogy, and geochemistry of the East Molokai Volcanic Series, Hawaii: U.S. Geol. Survey Prof. Paper 961, 53 p.

Behre, C. H., Jr., 1933, Slate in Pennsylvania: Pa. Geol. Survey, Fourth Series, Bull. M16, 400 p.

Ben Othman, D., Allegre, C. J., Polve, M., and Richard, P., 1979, Nd-Sr isotope correlation in mantle material and geodynamics: Earth and Planet. Sci. Lett., no. 209; p. E976.

Berggren, W. A., 1972, A Cenozoic time-scale–some implications for regional geology and paleobiogeography: Lethaia, v. 5, p. 195–215.

Bielefeld, M. J., Andre, C. G., Eliason, Eric, Clark, P. E., Adler, Isidore, and Trombka, J. I., 1977, Imaging of the lunar surface chemistry from orbital x-ray data: Proc. 8th Lunar Science Conf., p. 901–908.

Bingham, R. H., 1979, Low-flow characteristics of Alabama streams: U.S. Geol. Survey open-file rept. 79–208, 49 p. [In press.]

Blanchard, D. P., Jacobs, J. W., and Brannon, J. C., 1977, Chemistry of ANT-suite and felsite clasts from consortium breccia 73215, and of gabbroic anorthosite 79215: Proc. 8th Lunar Science Conf., p. 2507–2524.

Bloom, A. L., 1959, Late Pleistocene changes of sea level in Southwestern Maine: New Haven, Connecticut, Yale University, Department of Geology, 143 p.

——— 1960, Late Pleistocene changes in sea level in southwestern Maine: Department of Economic Development, Augusta, Maine, 143. p.

Bloyd, R. M., Jr., 1974, Summary appraisals of the Nation's ground-water resources–Ohio region: U.S. Geol. Survey Prof. Paper 813–A, 41 p.

——— 1975, Summary appraisals of the Nation's ground-water resources–Upper Mississippi region: U.S. Geol. Survey Prof. Paper 813–B, 22 p.

Boggess, D. H. Missimer, T. M., and O'Donnell, T. H., 1977, Saline-water intrusion related to well construction in Lee County, Florida: U.S. Geol. Survey Water-Resources Investigation 77–33, 29 p.

Bohor, B. F., Pollastro, R. M., and Phillips, R. E., 1978, Mineralogic evidence for the volcanic origin of kaolinitic partings (tonstein) in Upper Cretaceous and Tertiary coals of the Rocky Mountain region: *in* Programs and abstracts, 15th Ann. Clay Mins. Soc., 27th Ann. Clay Mins. Conf., Oct. 8–12, Bloomington, Ind., p. 47.

Bonham, H. F., Jr., 1969, Geology and mineral deposits of Washoe and Storey Counties, Nevada: Nev. Bureau of Mines and Geol. Bull. 70, 140 p.

Boyer, R. E., 1962, Petrology and structure of the Southern Wet Mountains, Colorado: Geol. Soc. America Bull., v. 73, no. 9, p. 1047-1070.

Braislin, D. B., Hastings, D. D., and Snavely, P. D., Jr., 1971, Petroleum potential of western Oregon and Washington, *in* Cram, I.A., ed., Possible future petroleum provinces of North America: American Association of Petroleum Geologists Memoir 15, p. 229-238.

Bramlette, M. N., and Wilcoxon, J. A., 1967, Middle Tertiary calcareous nannoplankton of the Cipero Section, Trinidad, W.I.: Tulane Studies in Geology, v. 5, p. 93-131.

Breed, C. S., Ward, A. W., and McCauley, J. F., 1978, Windform patterns on Earth and on Mars – implications for similarities of eolian processes on two planets, *in* Reports of Planetary Geology Program, 1977-1978: NASA Tech. Memo. TM 79729, p. 228-229.

Breger, I. A., Krasnow, M., and Chandler, J. C., 1978, Peat from the Everglades of Florida: A study of the origin of coal and natural gas: 10th Intl. Cong. Sedimentology, Jerusalem, July, Abstracts, v. 1, p. 85-86.

Brenner-Tourtelot, E. F., and Glanzman, R. K., 1978, Lithium-bearing rocks of the Horse Spring Formation, Clark County, Nevada: Energy, v. 3, p. 255-262.

Brenner-Tourtelot, E. F., and Machette, M. N., 1979, Lithium in the Popotosa Formation, Socorro County, New Mexico, as related to the mineralogy and geochemistry: U.S. Geol. Survey open-file rept. 79-839, 27 p.

Brenner-Tourtelot, E. F., Meier, A. L., and Curtis, C. A., 1978, Lithium in rocks from the Lincoln area, Montana, and nearby basins: U.S. Geol. Survey open-file rept. 78-430, 22 p.

Brew, D. A., and Morrell, R. P., 1978, Tarr Inlet suture zone, Glacier Bay National Monument, Alaska, *in* Johnson, K. M., ed., The U.S. Geol. Survey in Alaska – accomplishments during 1977: U.S. Geol. Survey Circ. 772-B, p. B90-B92.

Bright, R. C., 1967, Late Pleistocene stratigraphy in Thatcher Basin, southeastern Idaho: Tebiwa, v. 10, no. 1, p. 1-7.

Brook, C. A., Mariner, R. H., Mabey, D. R., Swanson, J. R., Guffanti, Marianne, and Muffler, L. J. P., 1979, Hydrothermal convection systems with reservoir temperatures ® 90° *in* U.S. Geol. Survey Circ. 790, p. 18-85.

Brown, Andrew, Berryhill, H. L., Jr., Taylor, D. A., and Trumball, J. V. A., 1952, Coal resources of Virginia: U.S. Geol. Survey Circ. 171, 57 p.

Brown, D. E., Carmony, N. B., and Turner, R. M., compilers, 1978, Drainage map of Arizona showing perennial streams and some important wetlands: Ariz. Game and Fish Department, 1 sheet, scale 1:1,000,000.

Brown, E. H., 1977, Ophiolite on Fidalgo Island, Washington: Oreg. Department of Geol. and Min. Resources Bull. 95, p. 67-73.

Brown, P. M., Miller, J. A., and Swain, F. M., 1972, Structural and stratigraphic framework and spatial distribution of permeability of Atlantic Coastal Plain, North Carolina to New York: U.S. Geol. Survey Prof. Paper 796, 79 p.

Bryant, Bruce, and Reed, J. C., Jr., 1970, Geology of the Grandfather Mountain window and vicinity, North Carolina and Tennessee: U.S. Geol. Survey Prof. Paper 615, 190 p.

Budyko, M. I., 1948, Evaporation under natural conditions – Israel Program for Scientific Translations, trans.: U.S. Dept. of Commerce, Office of Technical Services, 120 p.

Bufe, C. G., Maley, R. P., Carver, D. L., and Henrisey, R. F., 1978, The May-July 1978 earthquake sequence near Thessaloniki, Greece (abs): EOS, American Geophysical Union Transactions, v. 59, no. 12, p. 1127.

Burkham, D. E., 1978, Sedimentation in Hot Creek in vicinity of Hot Creek Fish Hatchery, Mono County, California: U.S. Geol. Survey open-file rept. 78-661, 11 p.

Burnett, J. L., and Jennings, C. W., 1962, Geologic map of California (Chico sheet): Calif. Division of Mines and Geol., scale 1:250,000.

Calbeck, J. M., 1975, Geology of the central Wise River valley, Pioneer Mountains, Beaverhead County, Montana: Univ. of Mont. M.S. thesis, 89 p.

Campbell, J. E., Dillion, R. T., Tierney, M. S., Helton, J., Davis, H. T., Pearson, F. J., and Shaw, H. R., 1978, Risk methodology for geological disposal of radioactive waste-interim report. SAND 78-0029 (NUREG No. CR-0458), 264 p.

Cargill, S. M., and Clark, A. L., eds., 1977, Papers presented at IGCP Project 98, Leon, Norway, on resource/reserve assessment methods: Mathematical Geology, v. 9, no. 3 (special issue) 337 p.

——— 1978, Papers presented at IGCP Project 98, Taita Hills Conference: IAMG Jour. v. 10, no. 4-5.

Carlson, C. G., compiler, 1969, Bedrock geologic map of North Dakota: N. Dak. Geol. Survey Misc. Map 10, scale 1:1,000,000.

Carlson, P. R., and Molnia, B. F., 1975, Preliminary isopachous map of Holocene sediments, northern Gulf of Alaska: U.S. Geol. Survey open-file rept. 75-507.

Carr, M. H., 1979, Formation of Martian flood features by release of water from confined aquifers: Jour. Geophys. Research. [In press.]

Castle, R. O., Dixon, H. R., Grew, E. S., Griscom, A., and Zeitz, I., 1976, Structural dislocations in eastern Massachusetts: U.S. Geol. Survey Bull. 1410, 39 p.

Cederstrom, D. J., Boswell, E. H., and Tarver, G. R., 1979, Summary appraisals of the Nation's ground-water resources – South Atlantic Gulf region: U.S. Geol. Survey Prof. Paper 813-0, 35 p.

Cerny, P., 1974, The present status of the analcime-pollucite series: Canadian Mineralogist, v. 12, p. 334-341.

Chapman, D. S., and Pollack, H. N., 1977, Heat flow production in Zambia – evidence for lithosphere thinning in Central Africa. Tectonophysics, v. 4, p. 79-100.

Chapman, R. H., 1966, Gravity base station network: Calif. Division of Mines and Geol., Special Rept. 90, 49 p.

Claassen, Hans C., and White, A. F., 1979, Application of geochemical kinetic data to ground-water systems, pt. 1: A tuffaceous-rock system in southern Nevada: American Chemical Society, Symposium Series, book 93, chap. 34, p. 771-793.

Clark, P. E., Eliason, Eric, Andre, C. G., and Adler, Isidore, 1978, A new color correlation method applied to XRF Al/Si ratios and other lunar remote sensing data: Proc. 9th Lunar and Planet. Sci. Conf., p. 3015-3027.

Clayton, D. N., and Miller, R., 1977: Geologic studies of the southern continuation of the Straight Creek Fault, Snoqualmie area, Washington: Washington Public Power Supply System, WNP ¼, 31 p.

Cloern, J. E., 1978, Empirical model of *Skeletonema costatum* photosynthetic rate, with applications in the San Francisco Bay estuary: Advances in Water Resources, v. 1, p. 267-274.

Cloern, J. E., and Nichols, F. H., 1978, A von Bertalanffy growth model with a seasonally varying coefficient: Fisheries Research Board of Canada Jour., v. 35, p. 1479-1482.

Coats, R. R., and Riva, J. F., 1976, Eastward obduction of early Paleozoic eugeosynclinal sediments, and early Mesozoic transverse thrusting resulting from southward movement of a compressed Paleozoic sedimentary pile, northeastern Great Basin, Nevada, U.S.A. (abs.): 25th, International Geol. Congress, 1976, v. 1, no. 25, p. 80.

Cobb, E. H., 1977, Summary of references to mineral occurrences (other than mineral fuels and construction materials) in the Eagle

quadrangle, Alaska: U.S. Geol. Survey open-file rept. 77-845, 122 p.

——— 1978a, Summary of references to mineral occurrences (other than mineral fuels and construction materials) in the Nome quadrangle, Alaska: U.S. Geol. Survey open-file rept. 78-93, 213 p.

——— 1978b, Summary of references to mineral occurrences (other than mineral fuels and construction materials) in the Beaver, Bettles, and Medfra quadrangles, Alaska: U.S. Geol. Survey open-file rept. 78-94, 55 p.

——— 1978c, Summary of references to mineral occurrences (other than mineral fuels and construction materials) in the Solomon quadrangle, Alaska: U.S. Geol. Survey open-file rept. 78-181, 185 p.

——— 1978d, Summary of references to mineral occurrences (other than mineral fuels and construction materials) in the Mount Fairweather quadrangle, Alaska: U.S. Geol. Survey open-file rept. 78-316, 128 p.

——— 1978e, Summary of references to mineral occurrences (other than mineral fuels and construction materials) in the Juneau quadrangle, Alaska: U.S. Geol. Survey open-file rept. 78-374, 155 p.

——— 1978f, Summary of references to mineral occurrences (other than mineral fuels and construction materials) in the Sitka quadrangle, Alaska: U.S. Geol. Survey open-file rept. 78-450, 123 p.

——— 1978g, Summary of references to mineral occurrences (other than mineral fuels and construction materials) in the Sumdum and Taku River quadrangles, Alaska: U.S. Geol. Survey open-file rept. 78-698, 64 p.

——— 1978h, Summary of references to mineral occurrences (other than mineral fuels and construction materials) in the Port Alexander quadrangle, Alaska: U.S. Geol. Survey open-file rept. 78-787, 32 p.

———1978i, Summary of references to mineral occurrences (other than mineral fuels and construction materials) in the Dixon Entrance quadrangle, Alaska: U.S. Geol. Survey open-file rept. 78-863, 33 p.

——— 1978j, Summary of references to mineral occurrences (other than mineral fuels and construction materials) in the Craig quadrangle, Alaska: U.S. Geol. Survey open-file rept. 78-869, 261 p.

——— 1978k, Summary of references to mineral occurrences (other than mineral fuels and construction materials) in the Petersburg quadrangle, Alaska: U.S. Geol. Survey open-file rept. 78-870, 52 p.

——— 1978l, Summary of references to mineral occurrences (other than mineral fuels and construction materials) in the Bradfield Canal quadrangle, Alaska: U.S. Geol. Survey open-file rept. 78-922, 97 p.

Colson, B. E., Ming, C. O., and Arcement, G. J., 1978a, Backwater at bridges and densely-wooded flood plains, Bogue Chitto near Johnston Station, Mississippi: U.S. Geol. Survey Hydrologic Investigations Atlas HA-591, 5 sheets, scale 1:8,000.

——— 1978b, Backwater at bridges and densely-wooded flood plains, Okatoma Creek east of Magee, Mississippi: U.S. Geol. Survey Hydrologic Investigations Atlas HA-595, 3 sheets, scale 1:4,000.

——— 1978c, Backwater at bridges and densely-wooded flood plains, Okatoma Creek near Magee, Mississippi: U.S. Geol. Survey Hydrologic Investigations Atlas HA-596, 3 sheets, scale 1:4,000.

——— 1978d, Backwater at bridges and densely-wooded flood plains, Bogue Chitto near Summit, Mississippi: U.S. Geol. Survey Hydrologic Investigations Atlas HA-592, 4 sheets, scale 1:8,000.

——— 1978e, Backwater at bridges and densely-wooded flood plains, Tallahala Creek at Waldrup, Mississippi: U.S. Geol. Survey Hydrologic Investigation Atlas HA-590, 9 sheets, scale 1:4,000.

Combs, J., 1976, Heat flow determinations in the Coso geothermal area, California: Technical Report No. 3, ERDA Prime Contract E(45-1)-1830, 24 p.

Comer, E. P., 1978, The lithium industry today: Energy, v. 3, p. 237-240.

Compston, W., Foster, J. J., and Gray, C. M., 1977, Rb-Sr systematics in clasts and aphanites from consortium breccia 73215: Proc. 8th Lunar Science Conf. p. 2525-2549.

Costa, J. E., 1978, Holocene stratigraphy in flood-frequency analysis: Water Resources Research, v. 14, p. 626-632.

Crandell, D. R., and Mullineaux, D. R., 1978, Potential hazards from future eruptions of Mount St. Helens Volcano, Washington: U.S. Geol. Survey Bull. 1383-C, 26 p.

Csejtey, B., 1963, Geology of the southeast flank of the Flint Creek Range, western Montana: Princeton Univ. unpublished Ph. D. dissertation, Princeton, N.J., 175 p.

Cunningham, C. G., and Steven, T. A., 1978, Preliminary structural and mineralogical analysis of the Deer Trail Mountain-Alunite Ridge mining area, Utah: U.S. Geol. Survey open-file rept. 78-314, 1 pl.

Dallmeyer, D. R., Drake, A. A., Dunn, D. E., Hall, L. M., Tull, J. F., and Osberg, P. H., 1978, Time-of-deformation map of the Appalachian orogen (abs.): Geol. Soc. Am., Abst. with programs, v. 10, no. 2, p. 38 and v. 10, no. 4, p. 166.

Damon, P. E., 1969, Correlation and chronology of ore deposits and volcanic rocks: Tucson, Ariz. Univ., Geochronology Laboratory, USAEC Contact AT (11-1)-689, Annual Progess Rept. 000-689-120, p. 48-51.

Davis, J. R., and Vine, J. D., 1979, Stratigraphic and tectonic setting of the lithium brine field, Clayton Valley, Nevada: *in* Newman, G. W., ed., Guidebook, 1979 field conference, Basin and Range Province, sponsored by Rocky Mountain Assn. Geologists and the Utah Geological Association, Oct. 1979.

Dawdy, D. R., Lichty, R. W., and Bergmann, J. M., 1972, A rainfall-runoff simulation model for estimation of flood peaks for small drainage basins: U.S. Geol. Survey Prof. Paper 506-B, 28 p.

Dawdy, D. R., Schaake, J. C., Jr., and Alley, W. M., 1978, User's guide for a distributed routing rainfall-runoff model: U.S. Geol. Survey Water Resources Investigations 78-90, 146 p.

DeFord, R. K., 1958, Tertiary formations of the Rim Rock country, Trans-Pecos, Texas: Bur. of Economic Geology, Univ. of Texas, Rept. of Investigations, no. 36, 37 p.

DeGloria, S. D., 1979, Computer-assisted analysis of Landsat data for resource inventory-Grand Valley demonstration: University of California at Berkeley, 22 p.

DePaolo, D. J., and Wasserburg, G. J., 1977, The sources of island arcs as indicated by Nd and Sr isotopic studies: Geophys. Res. Lett., v. 4, p. 465.

Desborough, G. A., Poole, F. G., Hose, R. K., and Radtke, A. S., 1979, Metals in Devonian kerogenous marine strata at Gibellini and Bisoni properties in southern Fish Creek Range, Eureka County, Nevada: U.S. Geol. Survey open-file rept. 79-530, 31 p.

Diment, W. H., Urban, T. C., Sass, J. H., Marshall, B. V., Munroe, R. J., and Lachenbruch, A. H., 1975, Temperatures and heat contents based on conductive transport: *in* U.S. Geol. Survey Circ. 726, p. 84-103.

Divis, A. F., 1976, Geology and geochemistry of Sierra Madre Range, Wyoming: Colo. School of Mines Quarterly, v. 71, no. 3, 127 p.

Dmitrieva, M. T., and Ilyukhin, V. V., 1976, Crystal structure of djerfisherite [sic.]: Sov. Physics Dokl., v. 20, p. 469-470.

Donnelly, J. M., Goff, F. E., and Nehring, N. L., 1979, Geothermal potential northeast of Clear Lake, California: Proceedings of Geothermal Seminar-78, Sacramento, California.

Drake, A. A., Jr., 1970, Structural geology of the Reading Prong, *in* Fisher, G. W., and others, eds.: Studies in Appalachian geology, central and southern, N.Y., Wiley Interscience, p. 271-291.

——— 1978, The Lyon Station–Paulins Kill nappe–the frontal structure of the Musconetcong nappe system in eastern Pennsylvania and New Jersey: U.S. Geol. Survey Prof. Paper 1023, 20 p.

Dunrud, C. R., 1976, Some engineering geologic factors controlling coal mine subsidence in Utah and Colorado: U.S. Geol. Survey Prof. Paper 969, 39 p.

Dunrud, C. R., and Osterwald, F. W., 1978, Coal mine subsidence near Sheridan, Wyoming: Bull. of the Assoc. of Engineering Geologists, v. XV, no. 2, p. 175–190.

——— 1978, Effects of coal mine subsidence in the western Powder River basin, Wyoming: U.S. Geol. Survey open-file rept. 78–473, p. 59–67.

Dutro, J. T., Jr., Zen, E-an, and Taylor, M. E., 1975, Middle Cambrian in the Pioneer Mountains, southwest Montana: Geol. Soc. of America Abs. with Programs v. 7, no. 7, p. 1062.

Duval, J. S., Pitkin, J. A., and Macke, D. L., 1978, Aerial gamma-ray survey in the northern part of the Boulder batholith, Jefferson County, Montana: U.S. Geol. Survey open-file rept. 78–180, 16 p.

Eakin, T. E., Price, Don, and Harrill, J. R., 1976, Summary appraisals of the Nation's ground-water resources–Great Basin region: U.S. Geol. Survey Prof. Paper 813–G, 37 p.

Eaton, J. P., and Simirenko, Marie, 1978, Report on microearthquake monitoring in the vicinity of Auburn Dam, July 1977–June 1978: Administrative rept. to U.S. Bureau of Reclamation, 24. p.

Eberlein, G. S., and Menzie, W. D., 1978, Maps and tables describing areas of metalliferous mineral potential of Central Alaska, U.S. Geol. Survey open-file rept. 78–1–D, 2 sheets, 43 p., scale 1:1,000,000.

Ehlke, T. A., 1978, The effect of nitrification on the oxygen balance of the upper Chattahoochee River, Georgia: U.S. Geol. Survey Water Resources Investigations 79–10, 19 p.

Eichhorn, G., James, O. B., Schaeffer, O. A., and Müller, H. W., 1978, Laser ^{39}Ar–^{40}Ar dating of two clasts from consortium breccia 73215: Proc. Ninth Lunar and Planet. Sci. Conf., p. 855–876.

Emmons, W. H., and Calkins, F. C., 1913, Geology and ore deposits of the Philipsburg quadrangle, Montana: U.S. Geol. Survey Prof. Paper 78, 271 p.

Elston, D. P., Purucker, M. E., Bressler, S. L., and Spall, Henry, 1978, Polarity zonations, magnetic intensities, and the correlation of Miocene and Pliocene DVDP cores, Taylor Valley, Antarctica (Abs.): DVDP Seminar–III, Tokyo, Japan, June 5–10, 1978, Bull. No. 8, National Institute of Polar Research, Tokyo.

Epstein, A. G., Epstein, J. B., and Harris, L. D., 1977, Conodont color alteration–an index to organic metamorphism: U.S. Geol. Survey Prof. Paper 995, 27 p., 9 pls.

Epstein, J. B., and Epstein, A. G., 1969, Geology of the Valley and Ridge Province between Delaware Water Gap and Lehigh Gap, Pa., *in* Subitzky, Seymour, ed: Geology of selected areas in N. J. and eastern Pa., New Brunswick, Rutgers Univ., p. 132–205.

Ericksen, G. E., Vine, J. D., and Ballon, A. R., 1978, Chemical composition and distribution of lithium-rich brines in Salar de Uyuni and nearby salars, southwestern Bolivia: Energy v. 3, p. 355–363.

Erickson, R. L., Mosier, E. L., and Viets, J. G., 1978, Generalized geologic and summary geochemical maps of the Rolla 1° x 2° quadrangle, Missouri: U.S. Geol. Survey Misc. Field Studies Map MF–1004–A, scale 1:250,000.

Espinosa, A. F., Asturias, J., and Quesada, A., 1978, Applying the lessons learned in the 1976 Guatemalan earthquake to earthquake hazard and zoning problems in Guatemala: International Symposium on the February 4, 1976, Guatemalan Earthquake and the Process of Reconstruction, Proc., v. 1, p. 1–91.

Evans, H. T., Jr., 1971, Crystal structure of low chalcocite: Nature Phys. Sci. 232, p. 69–70.

Ewing, Maurice, Worzel, J. L., Beall, A.O., Berggren, W. A., Bukry, J. D., Burk, C. A., Fischer, A. G., and Pessagno, E. A., Jr., 1969, Appendix I–Time stratigraphic framework: Deep Sea Drilling Project Initial Repts. v. 1, p. 643–651.

Ferguson, J., Brett, Rolin, Milton, D. J., Dence, M. R., Simonds, C. H., and Taylor, S. R., 1979, Strangways cryptoexplosion structure, Northern Territory, Australia–preliminary results (abs.): Meteoritics, v. 13, no. 4, 459 p.

Ferrigno, J. G., and Williams, R. S., Jr., 1979, Satellite image atlas of glaciers: International Workshop on World Glacier Inventory, Riederalp, Switzerland, 1978, Proc.

Fisk, H. N., 1938, Geology of Grant and LaSalle Parishes: La. Department of Conservation, Geol. Bull. 10, 246 p.

Fitzpatrick-Lins, Katherine, 1978a, Accuracy of selected land use and land cover maps in greater Atlanta region, Georgia: U.S. Geol. Survey Jour. of Research, v. 6, no. 2, p. 169–173.

——— 1978b, Accuracy and consistency comparisons of land use and land cover maps made from high-altitude photographs and Landsat multispectral imagery: U.S. Geol. Survey Jour. of Research, v. 6, no. 1, 23–40.

———1978c, An evaluation of errors in mapping land use changes for the Central Atlantic Regional Ecological Test Site: U.S. Geol. Survey Jour. of Research, v. 6, no. 3, p. 339–346.

Fitzpatrick-Lins, Katherine, and Chambers, M. J., 1977, Determination of accuracy and information content of land use and land cover maps at different scales: Remote Sensing of the Electromagnetic Spectrum (RSEMS), Univeristy of Nebraska, v. 4, no. 4, p. 41–48.

Ford, A. B., 1976, Stratigraphy of the layered gabbroic Dufek intrusion, Antarctica: U.S. Geol. Survey Bull. 1405–D, 36 p.

Fouch, T. D., 1977, Sheep Pass (Cretaceous? to Eocene) and associated closed-basin deposits (Eocene and Oligocene?) in east-central Nevada–implications for petroleum exploration (abs.): American Assoc. of Petroleum Geologists Bull., V. 61, no. 8, p. 1378.

Fournier, R. O., and Potter, R. W., II, 1978, A magnesium correction for the Na-K-Ca chemical geothermometer: U.S. Geol. Survey open-file rept. 78–986, 24 p.

Fox, K. F., Jr., 1976, Melanges in the Franciscan Complex, a product of triple junction tectonics: Geology, v. 4, p. 737–740.

Friedman, J. D., and Simpson, S. L., 1978, Landsat investigations of the northern Paradox Basin, Utah and Colorado–implications for radioactive waste emplacement, pt. I–Lineaments and alinements: U.S. Geol. Survey open-file rept. 78–900, 49 p.

Fritts, C. E., 1969, Bedrock geologic map of the Marenisco-Watersmeet area, Gogebic and Ontowagon Counties, Michigan: U.S. Geol. Survey Misc. Geologic Investigations Map I–576, 5 p. text, scale 1:48,000.

Froelich, A. J., Johnston, R. H., and Langer, W. H., 1978, Preliminary report on the Ancestral Potomac River deposits in Fairfax County, Virginia, and their potential hydrogeologic significance: U.S. Geol. Survey open-file rept. 78–544, scale 1:48,000.

Frost, B. R., 1975, Contact metamorphism of serpentinite, chloritic blackwall, and rodingite at Paddy-Go-Easy Pass, central Cascades, Washington: Jour. of Petrology, v. 16, no. 2, p. 272–313.

Furcon, A. S., 1939, Geology and mineral resources of the Warrenton quadrangle, Virginia: Va. Geol. Survey Bull. 54, 94 p.

Fuis, G., and Schnapp, M., 1977, The November–December 1976 earthquake swarms in northern Imperial Valley, California–Seismicity on the Brawley fault and related structures: EOS, American Geophys. Union Transactions, v. 58, p. 1188.

Gammon, Patricia, and Carter, Virginia, 1979, Vegetative communities of the Great Dismal Swamp: Identification and mapping

with seasonal color-infrared photographs: Photogrammetric Engineering and Remote Sensing, v. 45, no. 1, p. 87–97.

Gardner, J. V., Vallier, T. L., and Dean, W. E., 1978, Grain size, total carbon, mineralogy, and inorganic geochemical data from surface sediments of the southern Bering Sea Outer Continental Shelf: U.S Geol. Survey open-file rept. 78–923, 32 p.

Gathright, T. M. II, Henika, W. S., and Sullivan, J. L. III, 1977, Geology of the Waynesboro East and Waynesboro West quadrangles, Virginia: Va. Division of Min. Resources Publication 3, 53 p.

Gaydos, Leonard, and Newland, W. L., 1978, Inventory of land use and land cover of the Puget Sound region using Landsat digital data: U.S. Geol. Survey Jour. of Research, v. 6, no. 6, p. 807–814.

Gaydos, Leonard, Newland, W. L., Thehim, G. P., and Ennes, R. A., 1979, Using Landsat digital data for mapping land cover written urban regions in the Pacific Northwest [abs]: Assoc. of American Geographers Ann. Mtg., 74th, New Orleans, La., 1978, Proc.

Gaydos, Leonard, and Wray, J. R., 1978a, Land cover from Landsat, 1973, with census tracts, Washington urban area, D.C., Md., and Va.: U.S. Geol. Survey Investigations Map I–858–F, scale 1:100,000.

——— 1978b, Land cover from Landsat, 1973, with place names, Washington urban area, D.C., Md., and Va.: U.S. Geol. Survey Misc. Investigations Map I–858–E, scale 1:100,000.

Getzen, R. T., 1977, Analog-model analysis of regional three-dimensional flow in the ground-water reservoir of Long Island, New York: U.S. Geol. Survey Prof. Paper 982, 49 p.

Gilbert, G. K., Humphrey, R. L., Sewell, J. S., and Soule, Frank, 1907, The San Francisco earthquake and fire of April 18, 1906, and their effects on structures and structural materials: U.S. Geol. Survey Bull. 324, 170 p.

Glanzman, R. K., and Otton, J. K., 1979, Geochemical association of lithium and uranium (abs.): Proceedings of the assoc. exploration geochemists, Tucson regional symposium, April 9–10, 1979.

Glanzman, R. K., and Rytuba, J. J., 1978, Zeolite-clay mineral zonation of volcaniclastic sediments within the McDermitt caldera complex of Nevada and Oregon (Abs.): Program and abstracts for the 27th Annual Clay Min. Conf. Ind. Univ., Bloomington, Ind., p. 32.

Glanzman, R. K., Rytuba, J. J., and McCarthy, J. H., 1978, Lithium in the McDermitt caldera, Nevada and Oregon: Energy, v. 3, p. 347–353.

Goff, F. E., and Donnelly, J. M., 1978, The influence of P_{CO_2}, salinity, and bedrock type on the Na-K-Ca geothermometer as applied in the Clear Lake geothermal region, California: Geothermal Resources Council, Transactions, v. 2, p. 211–214.

Gottfried, D., Annell, C. S., and Schwarz, L. J., 1977, Geochemistry of subsurface basalt from the deep corehold (Clubhouse Crossroads Corehole 1) near Charleston, South Carolina – magma type and tetonic implications: U.S. Geol. Survey Prof. Paper 1028, Studies Related to the Charleston, S. C., earthquake of 1886 – a preliminary report, D. W. Rankin, ed., p. 91–113.

Grant, A. R., 1969, Chemical and physical controls for base metal deposition in the Cascade Range of Washington: Washington Div. of Mines and Geology, Bull. 58, 107 p.

Gray, Carlyle, and others, 1960, Geological map of Pennsylvania: Pennsylvania Geol. Survey, 4th series, scale 1:250,000.

Greenhaus, M., and Cox, A., 1978, Paleomagnetic results from the Morro Rock-Islay Hill complex of central coast California – significant rotation of small crustal blocks (abs.): American Geophys. Union Trans., v. 59, p. 270–271.

Grybeck, Donald, Brew, D. A., Johnson, B. R., and Nutt, C. J., 1977, Ultramafic rocks in part of the Coast Range batholithic complex, southeastern Alaska, *in* Blean, K. M., ed., The United States Geological Survey in Alaska – accomplishments during 1976: U.S. Geol. Survey Circ. 751–B, p. B82–B85.

Gustavson, T. C., 1976, Paleotemperature analysis of the marine Pleistocene of Long Island, New York, and Nantucket Island, Massachusetts: Geol. Soc. of America Bull., v. 87, no. 1, p. 1–8.

Ham, W. E., Dennison, R. E., and Merritt, C. A., 1964, Basement rocks and structural evolution of southern Oklahoma: Okla. Geol. Survey Bull. 95, 302 p.

Hamilton, Warren, 1978a, Tectonic map of the Indonesian region: U.S. Geol. Survey Misc. Investigation Map I–875–D, scale 1:5,000,000.

——— 1978b, Mesozoic tectonics of the Western United States: Pacific Section, Society of Economic Paleontologists and Mineralogists, Pacific Coast Paleogeography Symposium 2, p. 33–70.

——— 1979, Tectonics of the Indonesian region: U.S. Geol. Survey Prof. Paper 1078, 345 p.

Hanson, A. M., 1952, Cambrian stratigraphy in southwestern Montana: Mont. Bureau of Mines and Geology Memoir 33, 46 p.

Harp, E. L., Wieczorek, G. F., and Wilson, R. C., 1978, Earthquake-induced landslides from the February 4, 1976, Guatemala earthquake and their implications for landslides hazard reduction: International Symposium on the February 4, 1976, Guatemalan Earthquake and the Reconstruction Process, Guatemala City, Proc.

Harris, D. P., 1977, Quantitative methods for the appraisal of mineral resources: U.S. Energy Research and Development Administration, Grand Junction Office, Contract Nos. AT–05–05–1–16344 and E(05–1)–1665, 836 p.

Harris, L. D., 1978, The eastern interior aulacogen and its relation to Devonian shale-gas production: U.S. Dept. Energy Reprints, Second Eastern Gas Shales Symposium, Morgantown, W. Va., v. 2.

Hartley, M. C. III, 1973, Ultramafic and related rocks in the vicinity of Lake Chatuge: Ga. Department of Natural Resources, Earth and Water Div. of the Geol. Survey of Ga. Bull. 85, 61 p.

Hatcher, R. D., Jr., 1973, Basement versus cover rocks in the Blue Ridge of northeast Georgia, northwestern South Carolina, and adjacent North Carolina: American Jour. of Science, v. 273, p. 671–685.

——— 1976, Introduction to the geology of the eastern Blue Ridge of the Carolinas and nearby Georgia: S.C. Division of Geol., Carolina Geol. Soc. Guidebook, 53 p.

——— 1978, Tectonics of the Western Piedmont and Blue Ridge, Southern Appalachians Review and Speculation: American Jour. of Science, v. 278, p. 276–304.

Hay, R. L., 1956, Pitchfork Formation, detrital facies of Early Basic breccia, Absaroka Range, Wyoming: A.A.P.G. Bull. v. 40, no. 8, p. 1863–1898.

Hayes, P. T., and Cone, G. C., 1975, Cambrian and Ordovician rocks of southern Arizona and New Mexico and westernmost Texas: U.S. Geol. Survey Prof. Paper 873, 98 p.

Hedrick, W. E., 1979, Pacific Northwest Regional Commission's Land Resource Inventory Demonstration project: Canadian Symposium on Remote Sensing, Fifth, Victoria, B. C., Canada, 1978.

Heinitz, A. J., and Wiitala, S. W., 1978, Floods in the Skunk River basin, Iowa: U.S. Geol. Survey open-file rept. 79–272, 80 p.

Herkelrath, W. N., and Moench, A. F., 1979, Laboratory investigations of steam pressure transient behavior in porous materials *in* Kruger, Paul, and Ramey, H. J., Jr., eds., Proceedings of the Fourth Workshop on Geothermal Reservoir Engineering, Stanford, Calif., Stanford Geothermal Program, p. 54–59.

Hildenbrand, T. G., Kane, M. F., and Stauder, W. S. J., 1977 Magnetic and gravity anomaly in the northern Mississippi embayment and their spatial relation to seismicity: U.S. Geol. Survey Misc. Field Studies Map MF–914. 1:1,000,000 scale.

Hillhouse, J. W., 1977, Paleomagnetism of the Triassic Nikolai greenstone, McCarthy quadrangle, Alaska: Canadian Jour. of Earth Sciences, v. 14, p. 2578-2592.

Hills, F. A., Gast, P. W., Houston, R. S., and Swainbank, I. G., 1968, Precambrian geochronology of the Medicine Bow Mountains of southeastern Wyoming: Geol. Soc. of America Bull. v. 79, no. 12, p. 1757-1783.

Himmelberg, G. R., and Ford, A. B., 1976, Pyroxenes of the Dufek intrusion, Antarctica: Jour. Petrology, v. 17, no. 2, p. 219-243.

Hoare, J. M., and Coonrad, W. L., 1959, Geology of the Bethel quadrangle, Alaska: U.S. Geol. Survey Misc. Geol. Investigations Map I-285, 1:250,000 scale.

——— 1961, Geologic map of the Goodnews quadrangle, Alaska: U.S. Geol. Survey Misc. Geol. Investigations Map I-339, 1:250,000 scale.

Hodges, C. A., 1978, Basaltic ring structures of the Columbia plateau: Geol. Soc. of America Bull. v. 89, p. 1281-1289.

Hodges, C. A., and Moore, H. J., 1978, Tablemountains of Mars (abs.), *in* Lunar and Planet. Sci. IX, p. 523-525.

Holt, H. E., 1978, Mercury geologic mapping, *in* Reports of Planetary Geology Program, 1977-1978, NASA Technical Memorandum TM-79729, p. 327.

Holzer, T. L., 1978, Documentation of potential for surface faulting related to ground-water withdrawal in Las Vegas Valley, Nevada: U.S. Geol. Survey open-file rept. 78-79, 12 p.

——— 1978, Surface faulting probably related to ground-water withdrawal, San Joaquin Valley, Calif. (abs.): Geol. Soc. of America Abst. with Programs, v. 10, no. 7, p. 424.

Holzer, T. L., and Davis, S. N., 1976, Earth fissures associated with water-table declines [abs.]: Geol. Soc. of America Abst. with Programs, v. 8, no. 6, p, 923-924.

Holzer, T. L., Davis, S. N., and Lofgren, B. E., 1977, Active surface faulting caused by ground-water extraction near Picacho, Arizona [abs.]: Geol. Soc. of American Abst. with Programs, v. 9, no. 4, p. 437.

Hong, H. Y., and Steinfink, H., 1972, The crystal chemistry of phases in the Ba-Fe-S and Se systems: Jour. Solid State Chem., v. 5, p. 93-104 (1972).

Howard, K. A., and Smith, G. I., 1978, Climate variation and its effects on our land and water, Part C. Geol. Survey Climate Plan: U.S. Geol. Survey Circ. 776-C, 15 p.

Hudson, Travis, Plafker, George, and Lanphere, M. A., 1977, Intrusive rocks of the Yakutat-St. Elias area, south-central Alaska: U.S. Geol. Survey Jour. of Research, v. 5, no. 2, p. 155-172.

Hunn, J. D., 1978, Natural sulfate contamination of the Santa Fe River [abs.]: American Water Resources Assoc. 1978 Conference, Nov. 6-10, Lake Buena Vista, Florida.

Hutchinson, C. F., 1978, The digital use of Landsat for integrated land resource survey: A study in the eastern Mojave Desert, California: Ph.D. dissertation, University of California at Riverside, June 1978, 265 p.

Hyde, J. H., and Crandell, D. R., 1978, Postglacial volcanic deposits at Mount Baker, Washington, and potential hazards from future eruptions: U.S. Geol. Survey Prof. Paper 1022-C, 17 p.

Imbrie, John, and Purdy, E. G., 1962, Classification of modern modern Bahamian carbonate sediments, *in* Classification of carbonate rocks: Am. Assoc. Petroleum Geol. Mem. 1, p. 253-272.

Jahns, R. H., 1978, Landslides, chapter 5 *in* Geophysical Predictions: National Academy of Sciences, p. 58-65.

James, D. E., Brooks, C., and Cuyubamba, A., 1976, Andean Cenozoic volcanism; magma genesis in the light of strontium isotopic composition and trace-element geochemistry: Geol. Soc. of Amer. Bull., v. 87, p. 592.

James, O. B., and Hedenquist, J. W., 1978a, Spinel-bearing troto-litic basalt 73215, 170: Texture, mineralogy and history (abs.), *in* Lunar and Planet. Sci. IX, p. 588-590.

James, O. B., and Hedenquist, J. W., 1978b, Consortium breccia 73255: Petrology of aphanitic lithologies (abs.), *in* Lunar and Planet. Sci. IX, p. 585-587.

James, O. B., Hedenquist, J. W., Blanchard, D. P., Budahn, J. R., and Compston, W., 1978, Consortium breccia 73255: petrology, major- and trace- element chemistry, and Rb-Sr systematics of aphanitic lithologies: Proc. 9th Lunar and Planet. Sci. Con., p. 789-820.

Janzer, V. J., 1979, Discordant gross radioactivity measurements of natural and treated water: American Soc. for Testing & Materials Conf. on Effluent and Environmental Radiation Surveillance, Johnson, VT., 1978, Proc.

Jessberger, E. K., Staudacher, T., Dominik, B., and Kirsten, T., 1978, Argon-argon ages of aphanite samples from consortium breccia 73255: Proc. 9th Lunar and Planet. Sci. Conf., p. 841-854.

Jobson, H. E., 1979, Thermal modeling of flow in the San Diego Aqueduct, California, and its relation to evaporation: U.S. Geol. Survey Prof. Paper 1122, 24 p.

Johnson, C. E., and Hadley, D. M., 1976, Tectonic implications of the Brawley earthquake swarm, Imperial Valley, California, January 1975: Seismological Soc. of America Bull. v. 66, p. 1133-1144.

Johnston, R. H., and Leahy, P. P., 1977, Combined use of digital aquifer models and field base-flow data to identify recharge-leakage areas of artesian aquifers: U.S. Geol. Survey Jour. of Research, v. 5, p. 491-496.

Johnston, R. H., and VanDriel, J. N., 1978, Susceptibility of coastal plain aquifers to contamination, Fairfax County, Virginia – a computer composite map: U.S. Geol. Survey open-file rept. 78-265, scale 1:48,000.

——— 1979, Potential yields of water wells in bedrock aquifers of Fairfax County, Virginia – a computer composite map: U.S. Geological Survey open-file rept. 79-525, scale 1:48,000.

Jones, D. L., Irwin, W. P., and Ovenshine, A. T., 1972, Southeastern Alaska – a displaced continental fragment? U.S. Geol. Survey Prof. Paper 800-B, p. B211-B217.

Jones, D. L., Silberling, N. J., and Hillhouse, 1977, Wrangellia – a displaced terrane in northwestern North America: Canadian Jour. of Earth Sciences, v. 14, p. 2565-2577.

Jones, D. L., Wrucke, C. T., Holdsworth, Brian, and Suczek, C. A., 1978, Revised ages of chert in the Roberts Mountains allochthon, northern Nevada (abs.): Geol. Soc. of America Abs. with Programs, v. 10, no. 3, p. 111.

Jones, Meridee, Van der Voo, Rob, Churkin, Michael, Jr., and Eberlein, G. D., 1977, Paleozoic paleomagnetic results from the Alexander terrane of southeastern Alaska: American Geophys. Union, Dec. 1977, San Francisco, Calif., program.

Kachadoorian, Ruben, and Slater, W. H., 1978, Pillar Mountain landslide, Kodiak, Alaska: U.S. Geol. Survey open-file rept. 78-217, 21 p.

Kauahikaua, J. P., 1979, Interpretation of time-domain electromagnetic soundings in the Randsburg, California, known geothermal resource area: U.S. Geol. Survey, open-file rept. 079-244.

Kay, R. W., Sun, S. S., and Lee-Hu, C. N., 1978, Pb and Sr isotopes in volcanic rocks from the Aleutian Islands and Pribilof Islands, Alaska: Geochim. Cosmochim. Acta, v. 42, p. 263.

Keeler, J. E., 1890, Earthquakes in California in 1889: U.S. Geol. Survey Bull. 68, 25 p.

Kennedy, N. P., 1977, Recency and character of faulting along the Elsinore fault zone in southern Riverside County, California: Cal. Div. Mines and Geol. Spec. Rept. 131.

Kent, B. H., and Munson, B. E., 1978b, Isopach maps of the Canyon and associated coal beds, western half of the Recluse

1° × ½° quadrangle, Campbell County, Wyo.: U.S. Geol. Survey Coal Investigations Map C-81B, scale 1:100,000.

——— 1978a, Structure contour maps of the Canyon and associated coal beds, western half of the Recluse 1x½ quadrangle, Campbell County, Wyo.: U.S. Geol. Survey Coal Investigations Map C-81-A, scale 1:100,000.

Kharaka, Y. K., Brown, P. M., and Carothers, W. W., 1978, Chemistry of waters in the geopressured zone from coastal Louisiana – implications for the geothermal development: Geothermal Resources Council Ann. Meeting, Hilo, Hawaii, July 25-28, 1978, Transactions, v. 2, p. 371-374.

Kicktenstein, B. R., Coleman, P. J., Jr., and Russell, C. T., 1978, A comparison of contour maps derived from independent methods of measuring lunar magnetic fields: Proc. of Lunar and Planet. Sci. Conf. IX, p. 3079-3092.

Kirk, A. R., Huffman, A. C., Jr., Zech, R. S., Robertson, J. F., and Jackson, T. J., 1978, Review of the history of usage of the Gallup Sandstone and related units, Southern San Juan Basin, New Mexico: U.S. Geol. Survey open-file rept. 78-1055, 51 p.

Klein, Howard, and Hull, J. E., 1978, Biscayne aquifer of southeast Florida: U.S. Geol. Survey Water Resources Investigations 78-107, 52 p.

Klein, Howard, Schroeder, M. C., and Lichtler, W. F., 1963, Geology and ground-water resources of Glades and Hendry Counties, Florida: Fl. Geol. Survey Rep. of Investigations 37, 101 p.

Klitgord, K. D., and Behrendt, J. C., 1979, Basin structure of the U.S. Atlantic Continental Margin, *in* Watkins, J. S., and others, eds., Geophysical investigations of continental slope and rises: American Assoc. of Petroleum Geol. Memoir 29, p. 85-112.

Kickelman, W. J., 1979, Use of U.S. Geological Survey earth-science products by selected regional agencies in the San Francisco Bay region, California: U.S. Geol. Survey open-file rept. 79-221, 173 p.

Krug, W. R., 1979, Simulation of streamflow of Rock River at Lake Koshkonong, Wisconsin, to determine effects of withdrawal of powerplant-cooling water: U.S. Geol. Survey open-file rept. 79-253, 43 p.

Kulm, L. D., and Fowler, G. A., 1974, Oregon Continental Margin structure and stratigraphy – A test of the imbricate thrust model, *in* Burk, C. A., and Drake, C. L., eds., The geology of continental margins: N.Y., Springer-Verlag, p. 261-283.

Lachenbruch, A. H., Sass, J. H., and Galanis, S. P., Jr., 1978, New heat-flow results from southern California: EOS, v. 59, no. 12, p. 1051.

Lachenbruch, A. H., Sass, J. H., Munroe, R. J., and Moses, T. H., Jr., 1976, Geothermal setting and simple heat conduction models for Long Valley caldera: Jour. Geophys. Res., v. 81, p. 769-784.

Lai, Chintu, ed., 1978, Bibliographic sources of computer programs and numerical models in hydraulics: American Soc. of Civil Engineers, The Hydraulics Division, Task Committee on Computational Hydraulics. Seminar on Computational Hydraulics, 26th Ann. Specialty Conf., Univ. of Maryland, College Park, Md., Aug. 9-11, 1978, 13 p.

Lai, Chintu, Schaffranek, R. W., and Baltzer, R. A., 1978, An operational system for implementing simulation models, a case study: American Soc. of Civil Engineers, Hydraulics Division, Seminar on Computational Hydraulics, 26th Ann. Hydraulics Specialty Conf., Univ. of MD, College Park, MD, Aug. 9-11, 1978, Proc. p. 415-454.

Laney, R. L., Raymond, R. H., and Winikka, C. C., 1978, Maps showing water-level declines, land subsidence, and earth fissures in south-central Arizona: U.S. Geol. Survey Water Resources Investigations 78-83, 2 maps.

Langmuir, Donald, 1978, U solution-mineral equilibria at low temperatures with application to sedimentary ore deposits: Jour. of Geochemical Exploration, v. 42, p. 547-569.

Lara, O. G., 1978, Effects of urban development on the flood-flow characteristics of the Walnut Creek basin, Des Moines metropolitan area, Iowa: U.S. Geol. Survey Water Resources Investigations 78-11, 31 p.

Larson, J. D., 1978, Chemical quality of ground water, Fairfax County, Virginia: U.S. Geol. Survey open-file map 78-268, 2 sheets, 3 tables, scale 1:48,000.

Larson, R. L., Menard, H. W., and Smith, S. M., 1968, Gulf of California, a result of ocean-floor spreading and transform faulting: Science, v. 161, p. 781-784.

Lash, G. G., 1978, The structure and stratigraphy of the Pen Argyl Member of the Martinsburg Formations in Lehigh and Berks Counties, Pa.: Unpublished manuscript thesis, Lehigh Univ., 213 p.

Lasky, S. G., and Webber, B. N., 1949, Manganese resources of the Artillery Mountains region, Mohave County, Arizona: U.S. Geol. Survey Bull. 961, 86 p.

Lawson, A. C., 1895, Sketch of the geology of the San Francisco Peninsula: U.S. Geol. Survey 15th Ann. Rept. 1893-1894, p. 399-476.

Leahy, P. P., 1979, Digital model of the Piney Point aquifer in Kent County, Delaware: Delaware Geol. Survey Rept. of Investigations no. 29, 98 p. [In press.]

Leavesley, G. H., and Striffler, W. D., 1979, A mountain watershed simulation model: U.S. Army Cold Regions Research and Engineering Laboratory, Workshop on Modeling of Snow Cover Runoff, Hanover, N.H., Sept. 1978, Proc.

Lee, D. R., 1977, A device for measuring seepage flux in lakes and estuaries: Limnology and oceanography, v. 22, p. 140-147.

Lee, W. H. K., and Lahr, J. C., 1975, HYPO71 (Revised) – A computer program for determining hypocenter, magnitude, and first-motion pattern of local earthquakes: U.S. Geol. Survey. open-file rept. 75-311, 113 p.

Lesure, F. G., Williams, B. B., and Dunn, M. L., 1979, Mineral resources of the Mill Creek, Mountain Lake, and Peters Mountain Wilderness Study Areas, Craig and Giles Counties, Virginia and Monroe County, West Virginia: U.S. Geol. Survey open-file rept. 78-1076, 74 p.

Lindh, A. G., Fuis, G. S., and Mantis, C. E., 1978, Seismic amplitude measurements suggest foreshocks have different focal mechanisms than aftershocks: Science, v. 201, p. 56-59.

Lindh, A. G., Lockner, D. A., and Lee, W. H. K., 1978a, Velocity anomalies – an alternative explanation: Seismological Soc. of America Bull., v. 68, no. 3, p. 721-734.

Lindholm, R. C., 1978, Triassic-Jurassic faulting in eastern North America – a model based on pre-Triassic structures: Geol. Soc. of Amer., Geology, v. 6, p. 365-368.

Ling, C. H., Rasmussen, L. A., and Campbell, W. J., 1978, Flight-path curvature distortion in side-looking airborne radar imagery: Photogrammetric Engineering and Remote Sensing, v. 44, no. 10, p. 1255-1260.

Livingston, R. K., Klein, J. M., and Bingham, D. L., 1976, Water resources of El Paso County, Colorado: Colo. Water Conservation Board, Water Resources Circ. 32, 85 p.

Loelkes, G. L., Jr., 1977, Specifications for land use and land cover and associated maps: U.S. Geol. Survey open-file rept. 77-555, 51 p.

Loucks, R. R., and McCallum, M. E., 1978, Platinum-group minerals in the New Rambler copper-nickel deposit, Wyoming [abs., in Russian]: Program for XI General Mtg. of the Internat. Mineralogical Assoc., Novosibirsk, U.S.S.R.

Love, J. D., Antweiler, J. C., and Mosier, E. L., 1978, A new look at the origin and volume of the Dickie Springs–Oregon Gulch placer gold at the south end of the Wind River Mountains, *in* Resources of the Wind River Basin, Wyoming: Wyo. Geol. Assoc. Guidebook, 20th Ann. Field Conf.: p. 379-391.

Lucchitta, B. K., 1978a, Morphology of Chasma Valles, Mars: U.S. Geol. Survey, Jour. of Research, v. 6, no. 4, p. 651–662.

——— 1978b, A large landslide on Mars: Geol. Soc. of America Bull., v. 89, no. 11, p. 1601–1609.

Lucchitta, B. K., and Watkins, J. A., 1978, Age of graben systems on the Moon: Proc. 9th Lunar and Planet. Sci. Conf. p. 3459–3472.

Lusby, Gregg C., 1977, Determination of runoff and sediment yield by rainfall simulation, *in* Toy, T. J., ed., Erosion: Research techniques, erodibility, and sediment delivery: Norwich, England, Geo Abstracts Ltd., p. 19–30.

Lyons, J. B., and Livingston, O. E., 1977, Rb–Sr date of the New Hampshire plutonic series: Bull. Geol. Soc. Amer., v. 88, p. 1808–1812.

Lystrom, D. J., 1978, Data needs in urban hydrology: *in* Whipple, William, Jr., Water problems of urbanizing areas, American Soc. of Civil Engineers, p. 90–99.

McBroom, L. A., and Hansen, W. R., 1978, Map showing artificial fills in the greater Denver area, Colorado, exclusive of engineered embankments: U.S. Geol. Survey open-file rept. 78–878, scale 1:100,000.

McCallum, M. E., Loucks, R. R., Carlson, R. R., Cooley, E. F., and Doerge, T. A., 1976, Platinum metals associated with hydrothermal copper ores of the New Rambler mine, Medicine Bow Mountains, Wyoming: Economic Geology, v. 71, p. 1429–1450.

McCauley, J. F., Breed, C. S., and Grolier, M. J., 1978, Eolian erosion studies, *in* Reports of Planetary Geology Program, 1977–1978: NASA Technical Memorandum TM 79729, p. 75–78.

McCauley, J. F., Guest, J. E., Trask, N. J., Schaber, G. G., Greeley, Ronald, and Holt, H. E., 1978, Stratigraphy of the Caloris Basin, Mercury, *in* Reports of Planetary Geology Program, 1977–1978: NASA Technical Memorandum TM 79729, p. 75–78.

McGill, G. E., 1959, Geologic map of the northwest flank of the Flint Creek Range, western Montana: Mont. Bureau Mines and Geology, Special Pub. 18 (Geologic Map 3).

McLellan, R. D., 1927, The geology of the San Juan Islands: Washington, Univ., Pub. in Geology, v. 2, 185 p.

McNalley, K. C., Kanamori, H., Pechmann, J. C., and Fuis, G., 1978, Earthquake swarm along the San Andreas fault near Palmdale, southern California, 1976 to 1977: Science, v. 201, p. 814–817.

Macdonald, G. A., 1968, Composition and origin of Hawaiian lavas: Geol. Soc. America Memoir 116, p. 477–522.

Macintyre, I. G., and Milliman, J. D., 1970, Physiographic features on the outer shelf and upper slope, Atlantic Continental Margin, southeastern United States: Geol. Soc. of America Bull., v. 81, p. 2577–2598.

MacKevett, E. M., Jr., Singer, D. A., and Holloway, C. D., 1978, Maps and tables describing metalliferous mineral resource potential of southern Alaska: U.S. Geol. Survey open-file rept. 78–1–E, 2 sheets, 45 p., scale 1:100,000.

MacLachlan, D. B., 1967, Structure and stratigraphy of the limestones and dolomites of Dauphin County, Pa.: Pa. Geol. Survey, 4th Series, General Geol. Report 44, 169 p.

Mallory, Michael J., 1979, Documentation of a finite-element two-layer model for simulation of ground-water flow: USGS Water Resources Investigations 79–18, 347 p.

Manger, G. E., Cadigan, R. A., and Gates, G. L., 1969, Irmay's saturation factor as an indication of an immobile fraction of pore water in saturated permeable sandstone: Jour. Sed. Petrology, v. 39, no. 1, p. 12–17.

Mann, J. G., Jr., 1955, Geology of a portion of the Elsinore fault zone, California: Calif. Department of Natural Resources, Div. of Mines Special Rept. 43, 22 p.

Marshall, S. L., 1978, Index to water-resources records data for Louisiana–ground-water records: Louisiana Dept. of Transportation and Development, Office of Public Works, Water Resources Basic Records Rept. 9, 176 p.

Matti, J. C., and Morton, D. M., 1975, Geologic history of the San Timoteo Badlands, southern California (abs.): Geol. Soc. of America Abst. with Programs, v. 7, no. 3, Cordilleran Section meetings, p. 344.

Mattick, R. E., Girard, O. W., Jr., Scholle, P. A., and Grow, J. A., 1978, Petroleum potential of U.S. Atlantic slope, rise and abyssal plain: American Assoc. of Petroleum Geologists Bull., v. 62, no. 4, p. 592–608.

Maughan, E. K., and Roberts, A. E., 1967, Big Snowy and Amsden Groups and the Mississippian-Pennsylvania boundary in Montana: U.S. Geol. Survey Prof. Paper 554–B, p. B1–B27.

Mehnert, H. H., Rowley, P. D., and Lipman, P. W., 1978, K–Ar ages and geothermal implications of young rhyolites in west-central Utah: Isochron/West, no. 21, p. 3–7.

Meier, M. F., Post, Austin, Brown, C. S., Frank David, Hodge, S. M., Mayo, L. R., Rasmussen, L. A., Senear, E. A., Sikonia, W. G., Trabant, D. C., and Watts, R. D., 1978, Columbia Glacier progress report–Dec. 1977: U.S. Geol. Survey open-file rept. 78–264, 56 p.

Meissner, C. R., Jr., and others, 1978 Mineral resources of the Cranberry Wilderness Study Area, Pocahontas and Webster Counties, West Virginia: U.S. Geol. Survey open-file rept. 78–142, 49 p.

Meyer, William, and Tucci, Patrick, 1978, Effects of seepage from fly-ash settling ponds and construction dewatering on groundwater levels in the Cowles Unit, Indiana Dunes National Lakeshore, Indiana: U.S. Geol. Survey Water Resources Investigations 78–138, 95 p.

Miesch, A. T., 1976a, *Q*-mode factor analysis of geochemical and petrologic data matrices with constant row-sums: U.S. Geol. Survey Prof. Paper 574–G, 47 p.

——— 1976b, Interactive computer programs for petrologic modeling with extended *Q*-mode factor analysis: Computers & Geosciences, v. 2, no. 4, p. 439–492.

Miller, C. D., 1978, Potential hazards from future eruptions in the vicinity of Mount Shasta volcano, northern California: U.S. Geol. Survey open-file rept. 78–827, 36 p.

Miller, J. E., and Jennings, M. E., 1978, Modeling nitrogen, oxygen, Chattahoochee River, Georgia: American Society Civil Engineers Preprint, Oct. 1978, ASCE National Convention, 18 p.

Miller, R. A., Mattraw, H. C., and Jennings, M. E., 1978, Statistical modeling of urban storm-water processes, Broward County, Florida, *in* International Symposium on Urban Storm-Water Management, July 24–27, 1978, Proceedings: Lexington, Ky., Univ. of Ky., p. 269–274.

Minkin, J. A., Chao, E. C. T., and Thompson, C. L., 1979, Distribution of elements in macerals and minerals–determination by eletron microprobe: American Chemical Soc., Div. of Fuel Chem. Preprints, v. 24, no. 1, p. 242–249.

Misch, P. H., 1952, Geology of the northern Cascades of Washington: The Mountaineer, v. 45, no. 12, p. 4–22.

Misch, Peter, 1977, Dextral displacements at some major strike slip faults in the North Cascades (abst.): Geol. Assoc. of Canada Program with Abs., v. 2, p. 37.

Mixon, R. B., and Newell, W. L., 1977, The Stafford fault system–structures documenting Cretaceous and Tertiary deformation along the fall line in northeastern Virginia: Geology, v. 5, p. 437–440.

Moench, A. F., 1979, The effect of thermal conduction upon pressure drawdown and buildup in fissured, vapordominated geothermal reservoirs *in* Kruger, Paul, and Ramey, H. J., Jr., eds., Proceedings of the Fourth Workshop on Geothermal Reservoir Engineering, Stanford, Calif.: Stanford Geothermal Program, p. 112–117.

Moench, A. F., and Herkelrath, W. N., 1978, The effect of vapor-pressure lowering upon pressure drawdown and buildup in geothermal steam wells: Transactions, Geothermal Resources Council, v. 2, p. 465–467.

Molenaar, C. M., 1973, Sedimentary facies and correlation of the Gallup Sandstone and associated formations, northwestern New Mexico, *in* Fassett, J. E., ed., Cretaceous and Tertiary rocks of the southern Colorado Plateau: Four Corners Geol. Soc. Memoir, p. 85–110.

Moore, H. J., Liebes, S., Jr., Crouch, D. S., and Clark, L. V., 1978, Rock pushing and sampling under rocks on Mars: U.S. Geol. Survey Prof. Paper 1081, 21 p.

Moore, H. J., Arthur, D. W. G., and Schaber, G. G., 1978, Yield strengths of flows on the Earth, Mars, and Moon: Proc. 9th Lunar and Planetary Science Conf., p. 3351–3378.

Moore, H. J., Spitzer, C. R., Cates, P., Bradford, K., Scott, R. F., Hutton, R. E., and Shorthill, R. W., 1978, Surface materials of the Viking landing sites–extended mission (abs.), *in* Reports of Planetary Geology Program, 1977–1978: NASA Technical Memorandum TM 79729, p. 301–302.

Moore, J. G., and Schilling, J. G., 1973, Vesicles, water, and sulfer in Reykjanes Ridge basalts: Contributions in Mineralogy and Petrology, v. 41, p. 105–118.

Morgan, J. W., Gros, J., Takahashi, H., and Hertogen, J., 1976, Lunar breccia 73215–siderophile and volatile trace elements: Proc. 7th Lunar Science Conf. p. 2189–2199.

Morris, E. C., Jones, K., and Berger, J. P., 1978, Location of Viking 1 Lander on the surface of Mars: Icarus, 34, p. 548–555.

Morris, H. T., 1978, Unprospected zone of pyritic alteration in west-central Utah: U.S. Geol. Survey open-file rept. 78–791, 8 p., 1 map.

Morris, H. T., and Lovering, T. S., 1961, Stratigraphy of the East Tintic Mountains, Utah: U.S. Geol. Survey Prof. Paper 361, 145 p.

Morton, D. M., and Campbell, R. H., 1978, Cyclic landsliding at Wrightwood, southern California–a preliminary report: U.S. Geol. Survey open-file rept. 78–1079, 23 p.

Moss, M. E., and Karlinger, M. R., 1974, Surface-water network design by regression analysis simulation: Water Resources Research, vol. 10, no. 3, p. 427–433.

Mossotti, V. G., and King, B. S., 1978, Loss-on-fusion method for the determination of volatiles in geochemical materials: National ACS Meeting, Miami, Fla., Sept. 1978, p. 467–2945.

Muffler, L. J. P., 1979a, Summary *in* U.S. Geol. Survey Circ. 790, p. 156–163.

Muffler, L. J. P. ed., 1979, Assessment of geothermal resources of the United States–1978: U.S. Geol. Survey Circ. 790, 163 p.

Murray, C. R., and Reeves, E. B., 1977, Estimated use of water in the United States in 1975: U.S. Geol. Survey Circ. 765, 39 p.

Nakamura, K., 1977, Volcanoes as possible indicators of tectonic stress orientation; principle and proposal: Jour. of Volcanology and Geothermal Resources, v. 2, no. 1, p. 1–16.

Nash, J. T., 1972, Fluid-inclusion studies of some gold deposits in Nevada: U.S. Geol. Survey Research 1972, Prof. Paper 800–C, p. C15-C19.

Naugler, F. P., and Wageman, J. M., 1973, Gulf of Alaska–magnetic anomalies, fracture zones and plate interaction: Geol. Soc. of American Bull., v. 84, p. 1575–1584.

Naylor, R. S., 1969, Age and origin of the Oliverian domes, central-western New Hampshire: Geol. Soc. America Bull., v. 80, p. 405–428.

Nelson, W. H., and Pierce, W. B., 1968, Wapiti Formation and Trout Peak Trachyandesite, northwestern Wyoming: U.S. Geol. Survey Bull. no. 1254–H, p. 1–11.

Newton, J. G., 1976, Early detection and correction of sinkhole problems in Alabama with a preliminary evaluation of remote sensing application: Alabama Highway Department Rept. 73, 83 p.

Nilsen, T. H., 1977, Paleogeography of Mississippian turbidites in south-central Idaho, *in* Stewart, J. H., Stevens, C. H., and Fritsche, A. E., eds., Paleozoic paleogeography of the Western United States: Soc. Economic Paleontologists and Mineralogists, Pacific Section, Pacific Coast Paleogeography Symposium 1, p. 275–299.

Nkomo, I. T., and Rosholt, J. N., 1972, A lead-isotope age and U-Pb discordance of Precambrian gneiss from Granite Mountains, Wyoming: U.S. Geol. Survey Prof. Paper 800–C, p. C169–C177.

——— 1972, Uranium-thorium-lead systematics in Precambrian gneiss from Wyoming: Geol. Survey Research 1972, Chapter A, pg. A120.

Nkomo, I. T., Stuckless, J. S., Thaden, R. E., and Rosholt, J. N., 1978, Petrology and uranium mobility of an early Precambrian granite from the Owl Creek Mountains, Wyoming, *in* Wyo. Geol. Assn. Guidebook 30th Annual Field Conf., Symposium on Resources of the Wind River Basin; p. 335–348.

Nord, G. L., Jr., and James, O. B., 1978a, Consortium breccia 73255–Electron petrography of aphanitic lithologies and anorthite clasts: Proc. 9th Lunar and Planet. Sci. Conf., p. 814–816.

——— 1978b, Consortium breccia 73255–thermal and deformational history of bulk breccia and clasts, as determined by electron petrography: Proc. 9th Lunar and Planet. Sci. Conf., p. 821–839.

Normark, W. R., Alpha, T. R., Hess, G. R., Lichtman, G. S., and Gutmacher, C. E., 1978, Map showing the crest of the East Pacific Rise near the mouth of the Gulf of California, scale 1:18,000: U.S. Geol. Survey open-file rept. 78–350, 1 sheet.

Novitzki, R. P., 1979, An introduction to Wisconsin wetlands–plants, hydrology, and soils: Wis. Geol. and Natural History Survey Educational Series 22, 19 p., 15 figs. [In press.]

Olhoeft, G. R., 1976, Effects of water on the electrical properties of planetary regoliths: Colloquim on Water in Planetary Regoliths, Oct. 5–7, 1976, Hanover, N.H., Dartmouth College, p. 139–142.

——— 1977, Electrical properties of water-saturated basalt; preliminary results to 506K: U.S. Geol. Survey open-file rept. 77–688, 8 p.

——— 1978, Nonlinear complex resistivity as a technique to study the state and chemistry of ground water: Second Colloquim on Planetary Water and Polar Processes, Oct. 16.18, 1978, U. S. Army CRREL, p. 9–11.

Olivier, Henry, 1961, Irrigation and climate: London, Edward Arnold Publishers, Ltd., 250 p.

Pakiser, L. C., and Brune, N. N., 1978, Root of the Sierra Nevada (abs.): EOS, Transactions, American Geophysical Union, v. 59, no. 12, December 1978, p. 1135.

Papazachos, B. C., Mountrokis, D., Psilovikos, A., and Leventakis, G., 1978, Surface fault traces and fault plane solutions of the May-June 1978 major shocks in the Thessaloniki area, Greece, *in* European catastrophic earthquake, Tectonophysics, v. 53, no. 3–4, p. 171–183.

Papadopulos, S. S., Wallace, R. H., Jr., Wesselman, J. B., and Taylor, R. E., 1975, Assessment of onshore geopressured-geothermal resources in the northern Gulf of Mexico basin *in* U.S. Geol. Survey Circ. 726, p. 125–146.

Pascale, C. A., and Martin, J. B., 1977, Hydrologic monitoring of waste injection wells near Pensacola, Florida, March 1970–March 1977: U.S. Geol. Survey Water Resources Investigations 78–27, 61 p.

——— 1978, Hydrologic monitoring of waste-injection wells near Pensacola, Florida, March 1970–December 1977: U.S. Geol. Survey open-file rept. 78–355, 78 p.

Pascale, C. A., Wagner, J. R., and Sohm, J. E., 1978, Hydrologic, geologic, and water-quality data, Ochlockonee River basin area, Florida: U.S. Geol. Survey Water Resources Investigations 78–97, 515 p.

Patton, W. W., Jr., Tailleur, I. L., Brosgé, W. P., and Lanphere, M. A., 1977, Preliminary report on the ophiolites of northern and western Alaska, *in* Coleman, R. G., and Irwin, W. P., eds., North American ophiolites: Oreg. State Department of Geology and Mineral Industries Bull. 95, p. 51-57.

Penman, H. L., 1956, Evaporation: An introductory survey: Netherland Jour. of Agricultural Sci., v. 4, p. 9-29.

Peterman, Z. E., and Hildreth, R. A., 1978, Reconnaissance geology and geochronology of the Precambrian of the Granite Mountains, Wyoming: U.S. Geol. Survey Prof. Paper 1055, 22 p.

Pettijohn, F. J., 1963, Chemical composition of sandstones – excluding carbonate and volcanic sands, Chapter S, Data of geochemistry, 6th ed.: U.S. Geol. Survey Prof. Paper 440-S, 21 p.

Peterson, Fred, 1977, Uranium deposits related to depositional environments in the Morrison Formation (Upper Jurassic), Henry Mountains mineral belt of southern Utah; *in* Campbell, J. A., short papers of the U.S. Geol. Survey Uranium-Thorium Symposium, 1977: U.S. Geol. Survey Circ. 753, p. 45-47.

Peterson, L. R., and Meyer, Gerald, 1977, Hydrologic reconnaissance evaluation of the Federal Capital Territory and Surrounding areas, Nigeria: U.S. Geological Survey open-file rept. 77-596, 30 p.

Pettinger, L. R., Schamberger, Mel, and Farmer, Adrian, Quantitative wildlife habitat evaluation using high-altitude color infrared aerial photographs: W. T. Pecora Memorial Symposium, Fourth Sioux Falls, South Dakota, 1978, Proc.

Phair, George, and Gottfried, D., 1964, Colorado Front Range, Colorado, U.S.A., as a uranium and thorium province *in* Natural radiation environment, Adams, J. A. S. and Lawder, W. M., eds: Chicago Press, p. 7-38.

Pierce, W. G., 1975, Principal features of the Heart Mountain fault and the mechanism problem: Wyo. Geol. Assoc. 27th Annual Field Conf. Guidebook, p. 139-148.

Pike, R. J., Jr., 1978, Volcanoes on the inner planets: Some preliminary comparisons of gross topography: Proc. 9th Lunar and Planet. Sci. Conf., p. 3239-3273.

Plummer, L. N., Jones, B. F., and Truesdell, A. H., 1976, WATEQF – a FORTRAN IV version of WATEQ, a computer program for calculating chemical equilibrium of natural waters: U.S. Geol. Survey Water Resources Investigations 76-13, 66 p.

Polcyn, F. C., 1976, NASA/Cousteau ocean bathymetry experiment: NASA-CR-ERIM 118500-I-F, 127 p.

Polyak, B. G., and Smirnow, Y. B., 1974, Relationship between terrestrial heat flow and the tectonics of continents: Geotectonics, v. 4, p. 204-213.

Post, Austin, 1975, Preliminary hydrography and historic terminal changes of Columbia Glacier, Alaska: U.S. Geol. Survey Hydrologic Investigations Atlas HA-559, 3 sheets, scale 1:10,000.

——— 1978, Interim bathymetry of Columbia Glacier and approaches, Alaska: U.S. Geological Survey open-file rept. 78-449, 1 sheet, scale 1:20,000.

Poulter, G. J., 1956, Geologic map and sections of the Georgetown thrust area, Granite and Deer Lodge Counties, Montana: Mont. Bureau Mines and Geology, Geologic Map 1.

Pratt, W. P., Anderson, R. E., Berry, A. W., Jr., Bickford, M. E., Kisvarsanyi, E. B., and Sides, J. R., 1979, Geologic map of exposed Precambrian rocks, Rolla 1° × 2° quadrangle, Missouri: U.S. Geol. Survey Map MF-1001-C, scale 1:250,000.

Price, Don, and Arnow, Ted, 1974, Summary appraisals of the Nation's ground-water resources – Upper Colorado region: U.S. Geol. Survey Prof. Paper 813-C, 40 p.

Prostka, H. J., 1977, Joints, fissures, and voids in rhyolite welded ash-flow tuff at Teton damsite, Idaho: U.S. Geol. Survey open-file rept. 77-211, 14 p.

——— 1977, Joints, fissures, and voids in rhyolite welded ash-flow tuff at Teton damsite, Idaho, *in* Failure of Teton Dam, a report of findings by U.S. Department of Interior, Teton Dam Failure Review Group, April 1977, p. B-65 to B-64.

Prowell, D. C., and O'Conner, B. J., 1978, Belair fault zone – evidence for Tertiary fault displacement in eastern Georgia: Geology, v. 6, p. 681-684.

Radbruch-Hall, D. H., and others, 1976, Landslide overview, conterminous United States: U.S. Geol. Survey Misc. Field Studies Map MF-771, scale 1:7,500,000.

Raisz, E., 1945, The olympic Wallowa lineament: American Jour. of Science, v. 243A, p. 479-485.

Rankin, D. W., 1975, The continental margin of eastern North America in the southern Appalachians – the opening and closing of the Proto-Atlantic Ocean: American Jour. of Science, v. 275a, p. 298-336.

Rankin, D. W., Espenshade, G. H., and Neuman, R. B., 1972, Geologic map of the west half of the Winston-Salem quadrangle, N.C., Va., Tenn.: U.S. Geol. Survey Misc. Geol. Investigations Map I-709-A, scale 1:250,000.

Rankin, D. W., Espenshade, G. H., and Shaw, K. W., 1973, Stratigraphy and structure of the metamorphic belt in northwestern North Carolina and southwestern Virginia – A study from the Blue Ridge across the Brevard fault zone to the Sauratown Mountains anticlinorium: American Jour. of Science, Cooper v. 273-A, p. 1-40.

Rathbun, R. E. and Grant, R. S., 1978, Comparison of the radioactive and modified techniques for measurement of stream reaeration coefficients: U.S. Geol. Survey Water Resources Investigations, 78-68, 57 p.

Rathbun, R. E., Schultz, D. J., and Stephens, D. W., 1975, Preliminary experiments with a modified tracer technique for measuring stream reaeration coefficients: U.S. Geol. Survey open-file rept. 75-256, 36 p.

Rau, W. W., 1975, Geologic map of the Destruction Island and Taholah quadrangles: Wash. Department of Natural Resources, Div. of Geology and Earth Resources, Geologic Map GM-13, scale 1:62,500.

Redfield, A. C., and Rubin, Meyer, 1962, The age of salt-marsh peat and its relation to recent changes in sea level at Barnstable, Massachusetts: National Academy of Science Proc., v. 48, p. 1728-1735.

Reed, W. E., and Lewis, J. E., 1978, land use and land cover information and air-quality planning: U.S. Geol. Survey Prof. Paper 1099-B, 43 p.

Reeder, H. O., 1978, Summary appraisals of the Nation's ground-water resources – Souris-Red-Rainy region: U.S. Geol. Survey Prof. Paper 813-K, 25. p.

Reeves, Frank, 1931, Geology of the Big Snowy Mountains: U.S. Geol. Survey Prof. Paper 165, p. 135-149.

Reinemund, J. A., and Watson, J. V., 1978, Achievements of the International Geological Correlation Program as related to human needs: UNESCO Nature and Resources, v., XIV, no. 2, April-June 1978, p. 2-13.

Reiser, H. N., Lanphere, M. A., and Brosgé, W. P., 1965, Jurassic age of a mafic igneous complex, Christian quadrangle, Alaska: U.S. Geol. Survey Prof. Paper 525-C, p. C68-C71.

Rickard, L. V., 1969, Stratigraphy of the Upper Silurian Salina group, New York, Pennsylvania, Ohio, Ontario: N. Y. State Museum and Scientific Service Map and Chart Series 12, 57 p., 14 pls.

Rinkenberger, R. K., 1979, Operational application of remote sensing technology for predicting mine ground hazard areas: International Conference on Basement Tectonics, Third, Durango, Colo. 1978, Proc.

Rittman, A., 1952, Nomenclature of volcanic rocks: Bull. Volcanol., Ser. II, Tome XII, p. 75-102.

Roberts, R. J., Doe, B. R., and Delevaux, M. H., 1976, Genesis of Precambrian sulfide deposits, Kingdom of Saudi Arabia (abs.): Internat. Geol. Congress, 25th, 1976, v. 1, no. 25, p. 183.

Robinove, C. J., 1979, Integrated terrain mapping with digital Landsat images in Queensland, Australia: U.S. Geol. Survey Prof. Paper 1102, 39 p.

Robinove, C. J., and Chavez, P. S., Jr., 1979, Landsat albedo monitoring method for an arid region: American Association for the Advancement of Science International Arid Lands Conference on Plant Resources, Lubbock, Tex., 1978, Proceedings.

Roddy, D. J., 1978, Pre-impact geologic conditions, physical properties, energy calculations, meteorite and initial crater dimensions and orientations of joints, faults and walls at Meteor Crater, Arizona: Proc. 9th Lunar and Planet. Sci. Conf., p. 3891–3930.

Rogers, A. M., and Hays, W. W., 1978a, Preliminary evaluation of site transfer functions developed from earthquakes and nuclear explosions: Second International Conf. on Microzonation, San Francisco, Calif., Proc. 11 p.

——— 1978b, Ground response studies in three western United States cities: 6th Symposium on Earthquake Engineering, Univ. of Roorkee, Roorkee, India, Proc. 5 p.

Rogers, J. J. W., and Adams, J. A. S., 1969, Thorium, *in* K. H. Wedephol, ed., Handbook of Geochemistry, v. 2, no. 4, Springer-Verlag, Berlin, p. 90-1 to 90-0.

Rohde, W. G., 1978, Improving land cover classification by image stratification of Landsat data: International Symposium on Remote Sensing of Environment, 12th, Manila, Philippines, 1978, Proc., v. 1, p. 729–741.

Rohrer, W. L., 1966, Geology of the Adam Weiss Peak quadrangle, Hot Springs and Park Counties, Wyoming: U.S. Geol. Survey Bull. 1241-A, p. 1–39.

Rosholt, J. N., Zartman, R. E., and Nkomo, I. T., 1973, Lead isotope systematics and uranium depletion in the Granite Mountains, Wyoming: Geol. Soc. of America Bull., v. 84, p. 989–1002.

Ross, C. P., 1947, Geology of the Borah Peak quadrangle, Idaho: Geol. Soc. of America Bull., v. 58, no. 12, p. 1097–1099.

Rottner, Donald, and Price, G. R., 1978, Testing of satellite unlinked remote surface weather station in the Sierra Nevada: Conference on Sierra Nevada Meteorology, South Lake Tahoe, Calif., American Meteorological Soc., 1978, Preprints, p. 19–22.

Rouse, J. T., 1937, Genesis and structural relationships of the Absaroka volcanic rocks, Wyoming: Geol. Soc. of America Bull., v. 48, p. 1257–1296.

Rowley, P. D., 1978, Geologic Studies in Orville Coast and eastern Ellsworth Land, Antarctic Peninsula: Antarctic Jour. of the U.S., v. 13, no. 4.

Rowley, P. D., Lipman, P. W., Mehnert, H. H., Lindsey, D. A., and Anderson, J. J., 1978, Blue Ribbon lineament, an east-trending structural zone within the Pioche mineral belt of southwestern Utah and eastern Nevada: U.S. Geol. Survey Jour. of Research, v. 6, no. 2, p. 175–192.

Ruppel, E. T., 1975, Precambrian and Lower Ordovician rocks in east-central Idaho: U.S. Geol. Survey Prof. Paper 889, p. 12–14.

——— 1978, Medicine Lodge thrust system, east-central Idaho and southwest Montana: U.S. Geol. Survey Prof. Paper 1031, 23 p.

Ryan, W. B. F., Cita, M. B., Dreyfus-Rawson, M., Burckle, L. H., and Saito, T., 1974, A paleomagnetic assignment of Neogene stage boundaries and the development of isochronous datum planes between the Mediterranean, Pacific, and Indian Oceans in order to investigate the response of the world ocean to the Mediterranean "salinity crisis": Revista Italiana di Paleontologia, v. 80, p. 631–688.

Samuel, E. A., 1979, Occurrence of low-temperature geothermal waters in the United States *in* U.S. Geol. Survey Circ. 790, p. 86–131.

Sandberg, C. A., 1976, Conodont biofacies of Late Devonian *Polygnathus styriacus* Zone in western United States, *in* Barnes, C. R., ed., Conodont paleoecology: Geol. Assoc. Canada Spec. Paper 15, p. 171–186.

Sanders, C. L., and Sauer, V. B., 1979, Kelly Barnes Dam flood of November 6, 1977, near Taccoa, Georgia: U.S. Geol. Survey Hydrologic Investigations Atlas HA-613. [In press.]

Sando, W. J., Gordon, Mackenzie, Jr., and Dutro, J. T., Jr., 1975, Stratigraphy and geologic history of the Amsden Formation (Mississippian and Pennsylvania) of Wyoming: U.S. Geol. Survey Prof. Paper 848-A, p. A1–A83.

Sarna-Wojcicki, A. M., Williams, K. M., and Yerkes, R. F., 1976, Geology of the Ventura Fault, Ventura County, California: U.S. Geol. Survey Misc. Field Studies Map MF-781, scale 1:6,000.

Sass, J. H., Galanis, S. P., Jr., Marshall, B. V., Lachenbruch, A. H., Munroe, R. J., and Moses, T. H., Jr., 1978, Conductive heat flow in the Randsburg area, California: U.S. Geol. Survey open-file rept. 78-756, 45 p.

Sass, J. H., and Lachenbruch, A. H., 1979, Heat flow and conduction-dominated thermal regimes *in* U.S. Geol. Survey Cir. 790, p. 8–11.

Sato, Motoaki, 1978, A possible role of carbon in characterizing the oxidation state of a planetary interior and orginating a metallic core: Proc. 9th Lunar and Planet. Sci. Conf., p. 990–992.

Sauer, S. P., 1978, Recent and projected changes in Dead Sea level and effects on mineral production from the Sea: U.S. Geol. Survey open-file rept. 78-176, 43 p., 5 figs., 1 table.

Schaber, G. G., Elachi, Charles, and Farr, Tom, 1979, Radar images of SP lava flow in north-central Arizona: Jour. Remote Sensing of Environment, v. 9, no. 2, p. 149–170.

Schaber, G. G., Horstman, K. C., and Dial, A. L., 1978, Lava flow materials in the Tharsis region of Mars: Proc. 9th Lunar and Planet. Sci. Conf., p. 3433–3458.

Scholle, P. A., Krivoy, H. L., and Hennessy, J. L., 1978, Summary chart of geological data from the COST No. B-2 well, U.S. Mid-Atlantic Outer Continental Shelf: U.S. Geol. Survey Oil and Gas Investigations Chart OC-79.

Schroder, L. J., Emerson, R. L., and Beetem, W. A., 1978, U.S. Geol. Survey, Denver, Colorado, radiocarbon dates II: Radiocarbon, American Jour. of Sci. v. 20, no. 2, p. 200–209.

Schuster, R. L., and Krizek, R. J., eds., 1978, Landslides–analyses and control: Washington, D.C., Transportation Research Board Special Rept. 176, Natl. Acad. of Sci., 234 p.

Schwimmer, P. M., and Rice, D. A., 1969, U.S. National Gravity Base Net: American Geophys. Union Trans., v. 50, no. 10, p. 527.

Scott, D. H., 1978, Mars, highlands-lowlands–Viking contributions to the Mariner relative age studies: Icarus, v. 34, p. 479–485.

Scott, D. H., Watkins, J. A., and Diaz, J. M., 1978, Regional deformation on mare surfaces: Proc. 9th Lunar and Planet. Sci. Conf., p. 3527–3539.

Seely, D. R., Vail, P. R., and Walton, G. G., 1974, Trench slope model, *in* Burk, C. A., and Drake, C. L., eds., The Geology of Continental Margins: New York, Springer-Verlag, p. 249–260.

Senftle, F. E., Macy, R. I., and Mikesell, J. L., 1979, Determination of the optimum-size californium-252 neutron source for borehold capture gamma-ray analysis: Nuclear Instruments and Methods, v. 158, no. 1, p. 293–302.

Sheler, N. S., 1889a, The geology of Cape Ann, Mass.: U.S. Geol. Survey 9th Ann. Rept., 1887-88, p. 529–611.

——— 1889b, The geology of Nantucket: U.S. Geol. Survey Bull. 53, 55 p.

Sherrill, M. G., 1979, Contamination potential in the Silurian dolomite aquifer, eastern Wisconsin: Water Resources Investigations 78-108, 2 sheets.

Sigafoos, R. S., and Hendricks, E. L., 1961, Botanical evidence of the modern history of Nisqually Glacier, Washington: U.S. Geol. Survey Prof. Paper 387-A, p. A1–20.

——— 1972, Recent activity of glaciers of Mount Rainier, Washington: U.S. Geol. Survey Prof. Paper 387-B, p. B1-24.

Sigvaldsson, G. E., 1968, Structure and products of subaquatic volcanoes in Iceland: Contributions Mineralogy and Petrology, v. 18, p. 1-16.

Silberman, M. L., O'Leary, R. M., Csejtey, Béla, Jr., Smith, J. G., and Connor, C. L., 1978, Geochemical anomalies and isotopic ages in the Willow Creek mining district, southwestern Talkeetna Mountains, Alaska: U.S. Geol. Survey open-file rept. 78-233, 32 p.

Simpson, R. W., and Cox, Allan, 1977, Paleomagnetic rotation of the Oregon Coast Range: Geology, v. 5, p. 585-589.

Singer, D. A., 1975, Mineral Resource Models and the Alaskan Mineral Resource Assessment Program–in Vogely, W. A., Ed., Mineral Materials Modeling: Resources for the Future, Baltimore, p. 370-382.

——— 1978, Properties of mineral resources and information requirements for assessment: Proceedings of Conf. on Techniques of Broad Mineral Appraisal NSF. [In press.]

Singer, D. A., Menzie, W. D., and DeYoung, J. H., Jr., 1978, Regional Mineral Resource Assessment in Alaska–a case study: Proceedings of International Conf. on Computer Mapping for Resource Analysis, COGEODATA, p. 265-272.

Sinnott, Allen, and Cushing, E. M., 1978, Summary appraisals of the Nation's ground-water resources–Mid Atlantic region: U.S. Geol. Survey Prof. Paper 813-I, 32 p.

Skipp, Betty, 1974, Copper Basin allochthon in central Idaho: U.S. Geol. Survey Prof. Paper 900, p.34-35.

Skipp, Betty, and Hait, M. H., Jr., 1977, Allochthons along the the northeast margin of the Snake River Plain, Idaho: 29th Ann. Field Conf., Wyo. Geol. Assoc. Guidebook, p. 499-515.

Skipp, Betty, and Hall, W. E., 1975a, Structure and Paleozoic stratigraphy of a complex of thrust plates in the Fish Creek Reservoir area, south-central Idaho: U.S. Geol. Survey Jour. of Research, v. 3, no. 6, p. 671-689.

Skipp, Betty, and Hall, W. E., 1975b, Paleozoic rocks adrift in south-central Idaho: Geol. Soc. of America Abs. with Programs, v. 7, no. 5, p. 641-642.

Slack, L. J., 1975, Hydrologic environmental effects of sprayed-sewage effluent, Tallahassee, Florida: U.S. Geol. Survey Water Resources Investigations 55-75, 73 p.

Smedes, H. W., 1966, Geology and igneous petrology of the northern Elkhorn Mountains, Jefferson and Broadwater Counties, Montana: U.S. Geol. Survey Prof. Paper 510, 115 p.

Smith, A. G., Briden, J. C., and Drewry, G. E., 1973, Phanerozoic world maps, Special papers in palaeontology, no. 12, *in* Hughes, N. F., ed., organisms and continents through time: A symposium volume of 23 papers, The Palaeontological Association, London, England.

Smith, C. T., Budding, A. J., and Pitrat, C. W., 1961, Geology of the southeastern part of the Chama Basin: N. Mex. Bur. Mines and Mineral Res. Bull. 75, 57 p.

Smith, G. I., 1978a, Climate variation and its effects on our land and water, pt. A, Earth Science in Climate Research: 2 U.S. Geol. Survey Circ. 776-A, 15 p.

——— 1978b, Climate variation and its effects on our land and water, pt. B., Current research by the Geol. Survey: U.S. Geol. Survey Circ. 776-B, 52 p.

Smith, R. L., and Shaw, H. R., 1975, Igneous-related geothermal systems *in* U.S. Geol. Survey Circ. 726, p. 58-83.

——— 1979, Igneous-related geothermal systems *in* U.S. Geol. Survey Circ. 790, p. 12-17.

Snavely, P. D., Jr., MacLeod, N. S., and Wagner, H. C., 1968, Tholeiitic and alkalic basalts of the Eocene Siletz River Volcanics, Oregon Coast Range: American Jour. of Sci., v. 266, p. 454-481.

Snavely, P. D., Jr., Pearl, J. E., and Lander, D. L., 1977, Interim report on petroleum resources potential and geologic hazards in the Outer Continental Shelf–Oregon and Washington Tertiary Province: U.S. Geol. Survey open-file rept. 77-282, 64 p.

Soderblom, L. A., Edwards, K., Eliason, E. M., Sanchez, E. M., and Charette, M. P., 1978, Global color variations on the Martian surface: Icarus, v. 34, p. 446-464.

Soil Conservation Service, 1972, National engineering handbook: U.S. Department of Agriculture, sec. 4, chap. 18, Hydrology, 29 p.

Spence, W., and Jaksha, L. H., 1978, Teleseismic P-wave delays across the central Rio Grande Rift: Programs and abstracts, 1978 International Symposium on the Rio Grande Rift, Oct. 8-17, 1978, Los Alamos Scientific Laboratory, Los Alamos, N. Mex., p. 93-94.

Spence, W., and Langer, C. J., 1978, A notable space-time distribution for the 1974 Peru aftershocks: 73rd Seis. Soc. Am. Ann. Mtg., Sparks, Nev., Earthquake Notes, 49, 53-54.

Spencer, D. W., and Alexander T. W., 1978, Technique for estimating the magnitude and frequency of floods in St. Louis County, Missouri: U.S. Geol. Survey Water Resources Investigations 78-139, 23 p.

Steele, Grant, 1960, Pennsylvania-Permian stratigraphy of east-central Nevada and adjacent Utah, *in* Geology of east-central Nevada: Intermountain Assoc. of Petroleum Geologists, 11th Ann. Field Conf., 1960 Guidebook, p. 91-113.

Stewart, J. H., 1970, Upper Precambrian and Lower Cambrian strata in the southern Great Basin, California and Nevada: U.S. Geol. Survey Prof. Paper 620, 206 p.

Stewart, J. H., and Poole, F. G., 1974, Lower Paleozoic an uppermost Precambrian Cordilleran miogeocline, Great Basin, Western United States, *in* Dickinson, W. R., ed., Tectonics and sedimentation: Soc. of Economic Paleontologists and Mineralogists, Special Pub. 22, p. 28-57.

Stokoe, K. H., and Lodde, P. F., 1978, Dynamic response of San Francisco Bay mud: Proc. Geotech. Engineering Div. Speciality Conf. on Earthquake Engineering and Soil Dynamics, ASCE, Pasadena, Calif., June, p. 940-959.

Stromquist, A. A., and Sundelius, H. W., 1969, Stratigraphy of the Albemarle Group of the Carolina slate belt in central North Carolina: U.S. Geol. Survey Bull. 1274-B, 22 p.

Stuckless, J. S., Miesch, A. T., Goldich, S. S., and Weiblen, P. W., 1978, A petrochemical model for the genesis of the volcanic rocks from Ross Island and vicinity, Antarctica: DVDP (Dry Valley Drilling Project) Bull., v. 8, p. 81-89.

——— 1979, A *Q*-mode factor model for the petrogenesis of the volcanic rocks from Ross Island and vicinity, Antarctica: American Geophys. Union Mem., Antarctica Research Series, v. 33.

Stuckless, J. S., and Nkomo, I. T., 1978, Uranium-lead isotope systematics in uraniferous alkali-rich granites from the Granite Mountains, Wyoming–implications for uranium source rocks: Econ. Geol., v. 73, p. 427-441.

Swanson, D. A., 1972, Magma supply rate of Kilauea Volcano, 1952-1971: Science, v. 175, p. 169-170.

Tabor, R. W., 1972, Age of the Olympic metamorphism–K-Ar dating of low-grade metamorphic rocks: Geol. Soc. of America Bull. v. 83, p. 1805-1816.

Tabor, R. W., and Cady, W. M., 1978, The structure of the Olympia Mountains, Washington–analysis of a subduction zone: U.S. Geol. Survey Prof. Paper 1033, 38 p.

Takasaki, K. J., 1978, Summary appraisals of the Nation's ground-water resources–Hawaii region: U.S. Geol. Survey Prof. Paper 813-M, 29 p.

Tani, B. S., 1977, x-ray study of $K_6LiFe_{24}S_{26}Cl$, a djerfisherite-like compound: American Mineralogist, v. 62, p. 819-823.

Tanner, A. B., 1979, Radon migration in the ground–a supplementary review: U.S. Geol. Survey open-file rept. 78-1050, 61 p.

Taranik, J. V., 1978a, Characteristics of the Landsat multispectral data system: U.S. Geol. Survey open-file rept. 78-187, 76 p.

——— 1978b, Principles of computer processing of Landsat data for geologic applications: U.S. Geol. Survey open-file rept. 78-117, 98 p.

Tatsumoto, Mitsunobu, 1969, Lead isotopes in volcanic rocks and possible ocean-floor thrusting beneath island arcs: Earth and Planet. Sci. Letters, v. 6, p. 369.

Taylor, H. P., Jr., 1967, The zoned ultramafic complexes of southeastern Alaska, *in* Wylie, P. J., ed., Ultramafic and related rocks: N. Y., John Wiley and Sons, p. 97-121.

——— 1973, O^{18}/O^{16} evidence for meteoric-hydrothermal alteration and ore deposition in the Tonopah, Comstock Lode, and Goldfield mining districts, Nevada: Economic Geol., v. 68, no. 6, p. 747-764.

Taylor, O. J., 1978, Summary appraisals of the Nation's ground-water resources–Missouri Basin region: U.S. Geol. Survey Prof. Paper 813-Q, 41 p.

Terry, J. E., Hosman, R. L., and Bryant, C. T., 1979, Summary appraisals of the Nation's ground-water resources–Lower Mississippi region: U.S. Geol. Survey Prof. Paper 813-N, 41 p.

Terzaghi, K., and Peck, R. B., 1948, Soil mechanics in engineering practic: N. Y., Wiley, 566 p.

Thatcher, W., 1979a, Horizontal crustal deformation from historic geodetic measurements in southern California: Jour. of Geophys. Research, v. 84, p. 2351-2370.

———1979b, Systematic inversion of geodetic data in central California: Jour. of Geophysical Research, v. 84, p. 2283-2295.

Thomas, H. E., and Phoenix, D. A., 1976, Summary appraisals of the Nation's ground-water resources–California region: U.S. Geol. Survey Prof. Paper 813-E, 51 p.

Thurber, H. K., and others, 1979 Mineral resources of the Minarets Wilderness and adjacent areas, Madera and Mono Counties, California: U.S. Geol. Survey open-file rept. no. 79-1472, 195 p.

Tilling, R. I., 1973, Boulder batholith, Montana–a product of two contemporaneous but chemically distinct magma series: Geol. Soc. of America Bull. v. 84, p. 3879-3900.

Tilling, R. I., and Gottfried, D., 1979, Distribution of thorium, uranium, and potassium in igneous rocks of the Boulder batholith region, Montana, and its bearing on radiogenic heat production and heat flow: U.S. Geol. Survey Prof. Paper 614-E, p. E1-E29.

Tourtelot, H. A., and Brenner-Tourtelot, E. F., 1978, Lithium, a preliminary survey of its mineral occurrence in flint clay and related rock types in the United States: Energy, v. 3, p. 263-272.

Trescott, P. C., 1975, Documentation of finite-difference model for simulation of three dimensional ground-water flow: U.S. Geol. Survey open-file rept. 75-438, 32 p.

Trescott, P. C., Pinder, G. F., and Larson, S. P., 1976, Finite-difference model for aquifer simulation in two dimensions with results of numerical experiments: U.S. Geol. Survey Techniques of Water Resources Investigations, bk. 7, 116 p.

Trusdell, A. H., 1966, Ion exchange of natural glasses by the electrode method: American Mineralogist, v. 51, nos. 1 and 2, p. 110-122.

Tsiuoglou, E. C., Standard Engineering Corp. and Environment Oce Corp., 1974, The reaeration capacity of Canandaigua Outlet, Canandaigua to Clifton Springs: N. Y. State Dept. of Environmental Conservation, Basin Planning Unit, Project Rept. C-5402, 79 p.

Turner, D. L., Forbes, R. B., and Mayfield, C. F., 1978, K-Ar geochronology of the Survey Pass, Ambler River and eastern Baird Mountains quadrangles, southwestern Brooks Range, Alaska: U.S. Geol. Survey open-file rept. 78-254, 41 p.

Turner-Peterson, C. E., 1977, Uranium mineralization during early burial, Newark basin, Pennsylvania-New Jersey, *in* Campbell, J. A., ed., Short paper of the U.S. Geol. Survey Uranium-Thorium Symposium, 1977, U.S. Geol. Survey Circ. 753, p. 3-4.

Turner-Peterson, C. E., and Peterson, Fred, 1978, Uranium in sedimentary rocks, with emphasis on facies control in sandstone-type deposits: U.S. Geol. Survey open-file rept. 78-359, 15 p.

U.S. Environmental Protection Agency, 1975, National interim primary drinking water regulations: Federal Register, v. 40, no. 248, p. 50566-59588.

U.S. Geological Survey, 1976, Geochemical survey of western energy regions (formerly Geochemical survey of western coal regions), Third Annual Progress Report, July, 1976: U.S. Geol. Survey open-file rept. 76-729, 138 p.

——— 1976, Land use and land cover Greater Atlanta region: U.S. Geological Survey open-file rept. 76-127, scale 1:100,000.

——— 1977, Geochemical survey of the western energy regions, Fourth Annual Progress Report: U.S. Geol. Survey open-file rept. 77-872, 207 p.

——— 1977, Warning and preparedness for geologic-related hazards–proposed procedures: Federal Register, April 12, 1977, pt. III, p. 19292-19296.

——— 1978, Geochemical survey of the western energy regions, Fifth Annual Progress Report: U.S. Geol. Survey open-file rept. 78-1105, 194 p.

——— 1978, Land use and land cover, Kansas City, Missouri; Kansas, 1973: U.S. Geol. Survey Misc. Investigations Map I-1117, scale 1:250,000, color.

——— 1978, Marine geology and coastal hydrology *in* Geological Survey Research 1978: U.S. Geol. Survey Prof. Paper 1100, 464 p.

Valentine, J. W., 1956, Upper Pleistocene mollusca from Potrero Canyon, Pacific Palisades, California: San Diego Society of Natural History Trans., v. 12, no. 10, p. 181-205.

Van Alstine, R. E., 1976, Continental rifts and lineaments associated with major fluorspar districts: Economic Geol., v. 71, no. 6, p. 977-987.

Van Bemmelen, R. W., 1955, Tablemountains of Northern Iceland: E. J. Brill, Leiden, 217 p.

Vance, J. A., 1957, The geology of the Sauk River area in the northern Cascades of Washington: Univ. of Wash. Ph. D. thesis, 312 p.

Van Horn, Richard, 1975, Largest known landslide of its type in the United States–a failure by lateral spreading in Davis County, Utah: Utah Geol., v. 2, no. 1, p. 82-87.

Wallace, R. H., Jr., Kraemer, T. F., Taylor, R. E., and Wesselman, J. B., 1979, Assessment of geopressured-geothermal resources in the northern Gulf of Mexico basin *in* U.S. Geol. Survey Circ. 790, p. 132-155.

Wallace, R. H., JR., Taylor, R. E., and Wesselman, J. B., 1977, Use of hydrogeologic mapping techniques in identifying potential geopressured-geothermal reservoirs in the lower Rio Grande embayment, Texas, *in* Third geopressured-geothermal energy conference, Nov. 16-18, 1977, University Southwestern Louisiana, Lafayette, La. Proc., v. 1, p. GI-1-88.

Wandle, S. W., Jr., 1977, Estimating the magnitude and frequency of floods on natural-flow streams in Massachusetts: U.S. Geol. Survey Water Resources Investigations 77-39, 26 p.

Ward, A. W., 1978, Windforms and wind trends on Mars: An evaluation of martian surficial geology from Mariner 9 and Viking spacecraft television images: Ph. D. thesis, Univ. of Wash., Seattle, Wash., 201 p.

Ward, F. N., and Bondar, W. F., 1978, Analytical methodology in the search for metallic ores: Proc. Canadian Geoscience Council Explo 77, Ottawa, Canada, Oct. 16-21, 1977.

Weist, W. J., Jr., 1978, Summary appraisals of the Nation's ground-water resources–Great Lakes region: U.S. Geol. Survey Prof. Paper 813-J, 30 p.

West, S. W., and Broadhurst, W. L., 1975, Summary appraisals of the Nation's ground-water resources–Rio Grande region: U.S. Geol. Survey Prof. Paper 813-D, 39 p.

White, A. F., 1979, Geochemistry of ground water associated with tuffaceous rocks, Oasis Valley, Nevada: U.S. Geol. Survey Prof. Paper 712-E, 25 p.

White, A. F., and Claassen, H. C., 1977, Kinetic model for the dissolution of a rhyolitic glass (abs.): Geol. Soc. of America Abst. with Programs, v. 9, no. 7, p. 1223.

White, A. J. R., and Chappell, B. W., 1977, Ultrametamorphism and granitoid genesis: Tectonophysics, v. 43, p. 7-22.

White, D. E., and Williams, D. L., 1975, Assessment of geothermal resources of the United States–1975: U.S. Geol. Survey Circ. 726, 155p.

Whitebread, D. H., 1976, Alteration and geochemistry of Tertiary volcanic rocks in parts of the Virginia City quadrangle, Nevada: U.S. Geol. Survey Prof. Paper 936, 43 p.

Wier, K. E., 1977, Preliminary geology of the Richardsville and a portion of the Midland quadrangles, Fauquier, Culpeper, and Stafford Counties, Virginia: U.S. Geol Survey open-file rept. 77-699.

Wilhelms, D. E., Oberbeck, V. R., and Aggarwal, H. R., 1978, Size-frequency distributions of primary and secondary lunar impact craters: Proc. 9th Lunar and Planet Sci. Conf., p. 3735-3762.

Williams, Harold (compiler), 1978, Tectonic lithofacies map of the Appalachian orogen: Memorial Univ. of Newfoundland, St. John's, map no. 1, scale 1:1,000,000.

Wilson, L. D., Doyle, W. H., Jr., and Miller, R. A., 1978, Urban storm-water data management system, Broward County, Florida, *in* Internat. Symposium on Urban Storm-Water Management, July 24-27, 1978, Proceedings: Univ. of Ky., Lexington, p. 263-268.

Wilson, W. H., 1963, Correlation of volcanic rock units in the southern Absaroka Mountains, Wyoming: Univ. of Wyo. Contrib. Geol., v. 2, p. 13-20.

——— 1964, Geologic reconnaissance of the southern Absaroka Mountains, northwest Wyoming; pt. 1, The Wood River–Greybull River Area: Univ. of Wyo. Contrib. Geol., v. 3, p. 60-77.

——— 1975, Detachment faulting in volcanic rocks, Wood River area, Park County, Wyoming: Wyo. Geol. Assoc. 27th Ann. Field Conf. Guidebook, p. 167-171.

Winner, M. D., 1978, Ground-water resources of the Cape Lookout National Seashore, North Carolina: U.S. Geol. Survey Water Resources Investigations 78-52, 49 p.

Winter, T. C., 1978, Numerical simulation of steady state three-dimensional flow near lakes: Water Resources Research, v. 14, no. 2, p. 245-254.

Woodward, L. A., Gibson, G. G., McLelland, Douglas, 1976, Geology of Gallina quadrangle, Rio Arriba County, New Mexico: New Mexico Bur. Mines and Mineral Res. Geol. Map 39.

Wu, S. S. C., 1978, Mars synthetic topographic mapping: Icarus, v. 33, no. 3, p. 417-440.

Yeats, R. S., 1977, Structure, stratigraphy, plutonism, and volcanism of the Central Cascades, Washington *in* Geological Society of America Annual Meeting Guidebook, Geological excursions in the Pacific northwest, Seattle, Washington: Western Wash. Univ., Bellingham, Wash., p. 265-275.

Yotsukura, Nobuhiro, and Cobb, E. D., 1972, Transverse diffusion of solutes in natural streams: U.S. Geol. Survey Prof. Paper 582-C, 19 p.

Yotsukura, Nobuhiro, and Sayre, W. W., 1976, Transverse mixing in natural channels: Water Resources Research, v. 12, no. 4, p. 695-704.

Zablocki, C. J., 1978, Streaming potentials resulting from the descent of meteoric water–a possible source mechanism for Kilauean self-potential anomalies: Geothermal Resources Council, 1978 Ann. Meeting, Hilo, Hawaii, Trans. v. 2, sec. 2, p. 747-748.

Zapp, A. D., and Cobban, W. A., 1960, Some late Cretaceous strandlines in northwestern Colorado and northeastern Utah: U.S. Geol. Survey Prof. Paper 400-B, p. 246-249.

Zen, E-an, 1977, Some regional tectonic problems inferred from the Pioneer Mountains, Montana: Geol. Soc. of America Abst. with Programs, v. 9, no. 6, p. 779-780.

Zen, E-an, and Dutro, J. T., Jr., 1975, Upper Precambrian–Lower Cambrian sedimentary sequence, Pioneer Mountains, southwest Montana: Geol. Soc. of America Abst. with Programs v. 7, no. 7, p. 1327.

Zenone, Chester, and Anderson, G. S., 1978, Summary appraisals of the Nation's ground-water resources–Alaska: U.S. Geol. Survey Prof. Paper 813-P, 28 p.

Zohdy, A. A. R., 1978, Field procedure and data reduction methods (with Hewlett-Packard 97-67 programs) for total field resistivity surveys: U.S. Geol. Survey open-file rept. 78-424, 35 p.

Zurawski, Ann, 1978, Summary appraisals of the Nation's ground-water resources–Tennessee region: U.S. Geol. Survey Prof. Paper 813-L, 35 p.

INVESTIGATIONS IN PROGRESS IN THE GEOLOGICAL SURVEY

Investigations in progress during fiscal year 1979 are listed below together with the names and headquarters of the individuals in charge of each. Headquarters at main centers are indicated by NC for the National Center in Reston, Va., D for Denver, Colo., and M for Menlo Park, Calif. The lowercase letter after the name of the project leader shows the Division technical responsibility: c, Conservation Division; l, Land Information and Analysis; w, Water Resources Division; no letter, Geologic Division.

The projects are classified by principal topic. Most geologic-mapping projects involve special studies of stratigraphy, petrology, geologic structure, or mineral deposits but are listed only under "Geologic mapping" unless a special topic or commodity is the primary justification for the project. A reader interested in investigations of volcanology, for example, should look under the heading "Geologic Mapping" for projects in areas of volcanic rocks, as well as under the heading "Volcanology." Likewise, most water-resource investigations involve special studies of several aspects of hydrology and geology but are listed only under "Water Resources" unless a special topic—such as floods or sedimentation—is the primary justification for the project.

Areal geologic mapping is subdivided into mapping at scales smaller than 1:62,500 (for example, 1:250,000) and mapping at scales of 1:62,500 or larger (for example, 1:24,000).

Abstracts. *See* Bibliographies and abstracts.

Aluminum:
- Resources of the United States (S. H. Patterson, NC)

Analytical chemistry:
- Activation analysis (J. J. Rowe, NC)
- Analytical methods:
  - Textural automatic image analyzer research (M. B. Sawyer, D)
  - Water chemistry (M. J. Fishman, w. D)
- Analytical services and research (J. I. Dinnin, NC; Claude Huffman, Jr., D; C. O. Ingamells, M)
- Mineral deposits, characteristic analysis (J. M. Botbol, NC)
- Organic geochemistry and infrared analysis (I. A. Berger, NC)
- Organic polyelectrolytes in water (R. L. Wershaw, w, D)
- Plant laboratory (T. F. Harms, D)
- Radioactivation and radiochemistry (H. T. Millard, D)
- Rock chemical analysis:
  - General (D. R. Norton, D)
  - Rapid (Leonard Shapiro, NC)
- Services (L. B. Riley, D)
- Trace analysis methods, research (F. N. Ward, D)
- Ultratrace analysis (H. T. Millard, D)
- X-ray spectrometer for Viking lander (Priestley Toulmin III, NC)
- *See also* Spectroscopy.

Arctic engineering geology (Reuben Kachadoorian, M)

Artificial recharge:
- Artificial recharge methods (W. F. Lichtler, w, Lincoln, Nebr.)
- Artificial recharge research (E. P. Weeks, w, Lubbock, Tex.)
- Beaver-Badger Creeks recharge (A. W. Burns, w, D)
- Chemical reactions mineral surfaces (J. D. Hem, w, M)
- Columbia River basalt recharge (M. R. Karlinger, w, Tacoma, Wash.)
- Column-basin studies (Murray Garber, w, Syosset, N.Y.)
- Deepwell waste injection (C. A. Pascale, w, Tallahassee, Fla.)
- Fort Allen recharge (J. R. Diaz, w, Fort Buchanan, P.R.)
- Fresh water in saline aquifers (F. W. Meyer, w, Miami, Fla.)
- Heat storage (D. R. Cline, w, Tacoma, Wash.)
- Injection wells, Santa Rosa County (C. A. Pascale, w, Tallahassee, Fla.)

Artificial recharge—Continued
- Lee County freshwater injection (F. W. Meyer, w, Miami, Fla.)
- Nassau County recharge (T. M. Robison, w, Syosset, N. Y.)
- Recharge feasibility factors (J. Rubin, w, M)
- Recharge, Peace-Alafia basins (R. W. Coble, w, Tampa, Fla.)
- Salina hydrology (R. M. Waller, w, Ithaca, N.Y.)
- Subsurface storage, waste heat (J. D. Bredehoeft, w, NC)
- Supplemental recharge by storm basins (D. A. Aronson, w, Syosset, N. Y.)

Barite:
- Geology, geochemistry, and resources of barite (D. A. Brobst, NC)

Base metals. *See* base-metal names.

Bibliographies and abstracts:
- Luna bibliography (J. H. Freeberg, M)
- Outer Continental Shelf onshore impact assessment (M. L. Pattison, l, NC)

Borates:
- California (N):
  - Furnace Creek area (J. F. McAllister)
  - Searles Lake area (G. I. Smith)

Chromite. *See* Ferro-alloy metals.

Clays:
- Georgia, kaolin investigations (S. H. Patterson, NC)

Climatic changes:
- California, Quaternary (D. P. Adam, M)

Coal:
- Geochemistry of United States coal (V. E. Swanson, D)
- National Coal Resources Data System (M. D. Carter, NC)
- *States:*
  - Bering River coal field (C, Anchorage)
  - Cape Beaufort-Corwin Bluff coal field (J. E. Callahan, c, Casper, Wyo.)
  - Nenana (Clyde Wahrhaftig, M)
  - Shallow geophysical logging for coal-National Petroleum Reserve in Alaska (J. E. Callahan, c, Anchorage)

Coal—Continued

States:

Arizona, collection of coal samples for analysis (R. T. Moore, Tucson; V. E. Swanson, D)

Colorado (c, D, except as otherwise noted):
- Buckhorn Lakes quadrangle (R. G. Dickinson)
- Citadel Plateau (G. A. Izett)
- Collection of coal samples and coal resource data in Colorado and entry of data into the USGS National Coal Resources Data System (D. K. Murray; M. D. Carter, NC)
- Courthouse Mountain quadrangle (R. G. Dickinson)
- Denver basin, tertiary coal zone (P. E. Soister)
- Disappointment Valley, eastern (D. E. Ward, D)
- Douglas Creek Arch area (B. E. Barnum)
- Geology and energy resources of the Paonia and Crested Butte coal fields (D. L. Gaskill)
- Grand Mesa coal field (G. P. Eager)
- North Park area (D. J. Madden)
- Savery quadrangle (C. S. V. Barclay)
- Smizer Gulch and Rough Gulch quadrangles (W. J. Hail, D)
- Washboard Rock quadrangle (R. G. Dickinson)
- Watkins and Watkins SE quadrangles (P. E. Soister)

Idaho, collection of coal samples in Idaho (C. R. Knowles, Moscow; V. E. Swanson, D)

Illinois, preparation of Illinois coal resource and chemical data for entry into the USGS National Coal Resources Data System (H. J. Gluskoter, Urbana; M. D. Carter, NC)

Kentucky (D):
- Adams quadrangle (D. E. Ward)
- Blaine quadrangle (C. L. Pillmore)
- Louisa quadrangle (R. M. Flores)
- Richardson quadrangle (P. T. Hayes)
- Sitka quadrangle (P. T. Hayes)

Missouri, coal data collection and transfer to the National Coal Resources Data System (C. E. Robertson, Rolla; M. D. Carter, NC)

Montana:
- Birney SW quadrangle (S. Volz, c, Casper, Wyo.)
- Black Butte quadrangle (W. L. Rohrer, c, Casper,Wyo.)
- Coal mechanics in northern Powder River basin (J. M. White, c, Billings)
- Collection of coal samples in Montana (R. E. Matson, Butte; V. E. Swanson, D)
- Decker quadrangle (B. E. Law, c, D)
- Girard field (M. A. Soule, c, Billings)
- Half Moon Hill quadrangle (V. Neirmeir, c, Casper, Wyo.)
- Holmes Ranch quadrangle (N. E. Micklich, c, Casper, Wyo.)
- Jordan quadrangle (G. D. Mowat, c, Billings)
- Kirby quadrangle (c, Casper, Wyo.)
- McCone County lignite (H. C. Taylor, c, Billings)
- Monarch quadrangle (B. E. Barnum, c, D)
- Pearl School quadrangle (G. L. Galyardt, c, Casper, Wyo.)
- Sidney coal field (J. C. Harksen, c, Billings)
- Spring Gulch guadrangle (N. E. Micklich, c, Casper, Wyo.)
- Subsidence of spoil piles, Colstrip (R. A. Farrow, D; J. M. White, c, Billings)
- Taintor Desert quadrangle (S. Volz), c, Casper, Wyo.)
- Tongue River Dam quadrangle (N. E. Micklich, c, Casper, Wyo.)

Nevada, collection of coal samples in Nevada (J. A. Schilling, Reno; V. E. Swanson, D)

Coal—Continued

States—Continued

New Mexico:
- Alamosa Mesa West quadrangle (D. B. Umshler, c, Roswell)
- Collection of coal samples in New Mexico (F. E. Kottlowski, Socorro; V. E. Swanson, D)
- Gallup East quadrangle (E. D. Patterson, c, Roswell)
- Gallup West quadrangle (J. E. Fassett, c, Farmington)
- Manuelito quadrangle (J. E. Fassett, c, Farmington)
- Ojo Encino Mesa quadrangle (D. B. Umshler, c, Roswell)
- Pueblo Alto Trading Post quadrangle (R. W. Jentgen, c, Farmington)
- Samson Lake quadrangle (J. E. Fassett, c, Farmington)
- Star Lake quadrangle (J. E. Fassett, c, Farmington)
- Tanner Lake quadrangle (D. B. Umshler, c, Roswell)
- Twin Butte quadrangle (M. L. Millgate, c, Farmington)
- Western Raton field (C. L. Pillmore, D)

North Dakota (c, Billings, Mont., except as otherwise noted):
- Adams, Bowman, and Slope Counties lignite resources (R. C. Lewis)
- Clark Butte 15-minute quadrangle (G. D. Mowat)
- North Almont quadrangle (H. L. Smith, c, D)
- West-central North Dakota lignite resources (E. A. Rehbein)
- Williston area lignite resources (J. M. Spencer)

Oklahoma (c, Tulsa, except as otherwise noted):
- Blocker quadrangle (E. H. Hare, Jr.)
- Collection of coal samples in Oklahoma (S. A. Friedman, Norman; V. E. Swanson, D)
- Hackett quadrangle (E. H. Hare, Jr.)
- Panama quadrangle (E. H. Hare, Jr.)
- Spiro quadrangle (E. H. Hare, Jr.)

Pennsylvania (NC, except as otherwise noted):
- Collection of coal samples for analysis (W. E. Edmunds, Pennsylvania State Geological Survey, Harrisburg; M. J. Bergin)
- Northern anthracite field (M. J. Bergin)
- Southern anthracite field (G. H. Wood, Jr.)

Utah (c, D, except as otherwise noted):
- Basin Canyon quadrangle (Fred Peterson)
- Blackburn Canyon quadrangle (Fred Peterson)
- Butler Valley quadrangle (W. E. Bowers)
- Canaan Peak quadrangle (W. E. Bowers)
- East-of-the-Navajo quadrangle (H. D. Zeller)
- Fourmile Bench quadrangle (W. E. Bowers)
- Geology and coal resources of Wasatch Plateau coalfield (L. F. Blanchard)
- Geology and energy resources of the Emery coal field (G. M. Edson)
- Horse Flat quadrangle (H. D. Zeller)
- Horse Mountain quadrangle (W. E. Bowers)
- Jessen Butte quadrangle (E. M. Schell, c, Casper, Wyo.)
- Needle Eye Point quadrangle (H. D. Zeller)
- Pete's Cove quadrangle (H. D. Zeller)
- Ship Mountain Point quadrangle (H. D. Zeller)
- Sunset Flat quadrangle (H. D. Zeller)

Virginia and West Virginia, central Appalachian Basin (K. J. Englund, NC)

Washington:
- Coal resources of Washington (W. H. Lee, c, M)
- Collection of coal samples for analysis (V. E. Livingston, Jr., Olympia; V. E. Swanson, D)

West Virginia:
- Formatting coal data for National Coal Resources Data System (M. C. Behling, Morgantown; M. D. Carter, NC)

Coal—Continued
States—Continued
West Virginia—Continued
Louisa quadrangle (C. W. Connor, D)
Wyoming (c, D, except as otherwise noted(:
Acme quadrangle (B. E. Barnum)
Appel Butte quadrangle (G. L. Galyardt)
Bailey Lake quadrangle (M. L. Schroeder)
Beaver Creek Hills quadrangle (c, Casper)
Betty Reservoir NE quadrangle (N. McKinnie, c, Casper)
Browns Hill quadrangle (C. S. V. Barclay)
Cottonwood Rim quadrangle (C. S. V. Barclay)
Coyote Draw quadrangle (G. L. Galyardt)
Deer Creek quadrangle (M. L. Schroeder)
Eagle Rock quadrangle (S. P. Buck, c, Casper)
Fortin Draw quadrangle (B. E. Law)
Four Bar-J Ranch quadrangle (G. L. Galyardt)
Gillette East quadrangle (B. E. Law)
Greenhill quadrangle (S. P. Buck, c, Casper)
Grieve Reservoir quadrangle (C. S. V. Barclay)
Hilight quadrangle (W. J. Purdon, c, Casper)
Hultz Draw quadrangle (c, Casper)
Kemmerer area (M. L. Schroeder)
Ketchum Buttes quadrangle (C. S. V. Barclay)
Little Thunder Reservoir quadrangle (G. S. Martin, c, Casper)
Monarch quadrangle (B. E. Barnum)
Moyer Springs quadrangle (B. E. Law)
Neil Butte quadrangle (S. P. Buck c, Casper)
North Star School NE quadrangle (S. P. Buck, c, Casper)
North Star School NW quadrangle (S. P. Buck, c, Casper)
North Star School SE quadrangle (L. Jefferies, c, Casper)
North Star School SW quadrangle (L. Jefferies, c, Casper)
Open A Ranch quadrangle (G. C. Martin, c, Casper)
Oriva quadrangle (B. E. Law)
Pickle Pass quadrangle (M. L. Schroeder)
Pine Mountain-Oil Mountain area (G. J. Kerns, c, Casper)
Piney Canyon NW quadrangle (G. C. Martin, c, Casper)
Piney Canyon SW quadrangle (L. Wackwitz, c, Casper)
Rawlins coal field (C. S. V. Barclay)
Reid Canyon (G. J. Kerns, c, Casper)
Reno Junction quadrangle (L. Jefferies, c, Casper)
Reno Reservoir quadrangle (G. C. Martin, c, Casper)
Rock Springs uplift (P. J. LaPoint)
Rough Creek quadrangle (S. P. Buck, c, Casper)
Savery quadrangle (C. S. V. Barclay)
Sheridan Pass quadrangle (W. L. Rohrer, c)
Sheridan quadrangle (E. I. Winger, c, Casper)
Square Top Butte quadrangle (G. J. Kerns, c, Casper)
Teckla quadrangle (J. E. Goolsby, c, Casper)
Teckla SW quadrangle (J. E. Goolsby, c, Casper)
The Gap quadrangle (G. L. Galyardt)
Tullis quadrangle (C. S. V. Barclay)
Turnercrest NE quadrangle (G. C. Martin, c, Casper)
Weston SW quadrangle (R. W. Jones, c, Casper)

Construction and terrain problems:
Areal slope stability analysis, San Francisco Bay region (S. D. Ellen, M)
Electronics instrumentation research for engineering geology (J. B. Bennetti, D)
Engineering geology laboratory (R. A. Farrow, D)
Fissuring-subsidence research (T. L. Holzer, M)
Geotechnical measurements and services (H., W. Olsen, D)
Reactor hazards research (K. L. Pierce, D)

Construction and terrain problems—Continued
Reactor site investigations (R. H. Morris, D)
Research in rock mechanics (F. T. Lee, D)
Sino-Soviet terrain (L. D. Bonham, l, NC)
Soil engineering research (T. L. Youd, M)
Special intelligence (L. D. Bonham, l, NC)
Volcanic hazards (D. R. Crandell, D)
States:
California (M, except as otherwise noted):
Geologic environmental maps for land use planning (E. H. Pampeyan)
Geology and slope stability, western Santa Monica Mountains (R. H. Campbell)
Los Angeles County Cooperative (R. H. Campbell)
Pacific Palisades landslide area, Los Angeles (J. T. McGill, D)
California and Colorado, regional stability studies (D. H. Radruch-Hall, M)
Colorado (D):
Coal mine deformation studies, Somerset mining district (C. R. Dunrud)
Engineering geology-mapping research, Denver region (H. E. Simpson)
Massachusetts, sea-cliff erosion studies (C. A. Kaye, Boston)
Nevada:
Geologic and geomechanical investigations (J. R. Ege, D)
Seismic engineering program (K. W. King, Las Vegas)
Surface effects of nuclear explosions (R. P. Snyder, D)
Utah, coal-mine bumps (F. W. Osterwald, D)
See also Urban geology; Land use and environmental impact; Urban hydrology.

Copper:
United States and world resources (D. P. Cox, NC)
States:
Alaska, southwest Brooks Range (I. L. Tailleur, M)
Arizona (M):
Jerome and Bagdad districts (C. M. Conway)
Ray porphyry copper (H. M. Cornwall)
California, Shasta districts (C. M. Conway, M)
Maine-New Hampshire, porphyry with molybdenum (R. G. Schmidt, NC)
Michigan (NC):
Greenland and Rockland quadrangles (J. W. Whitlow)
Michigan copper district (W. S. White)
Virginia, massive sulfides (J. E. Gair, NC)

Crustal studies. *See* Earthquake studies; Geophysics, regional.

Directories:
Department of the Interior information services (E. T. Smith, l, NC)

Drought studies:
Drought in Colorado (T. R. Dosch, w, D)
Floyd River basin (W. L. Steinhilber, w, Iowa City, Iowa)
Seasonal flow characteristics (O. G. Lara, w, Iowa City, Iowa)

Earthquake studies:
Active fault analysis (R. E. Wallace, M)
Comparative elevation studies (R. O. Castle, M)
Computer fault modeling (J. H. Dieterich, M)
Computer operations and maintenance (T. C. Jackson, M)
Crustal inhomogeneity in seismically active areas (S. W. Stewart, M)
Crustal strain (J. C. Savage, M)
Crustal studies (ARPA) (Isidore Zietz, NC)

Earthquake studies—Continued
Dynamic soil behavior (A. T. F. Chen, M)
Earth structure studies (J. H. Healy, M)
Earthquake field studies (W. J. Spence, C. J. Langer, J. N. Jordan, M)
Earthquake-induced ground failures (T. L. Youd, M)
Earthquake-induced landslides (E. L. Harp, M)
Earthquake-induced sedimentary structures (J. D. Sims, M)
Earthquake recurrence and history (R. D. Nason, M)
Eastern United States (R. K. McGuire, D)
Experimental liquefaction potential mapping (T. L. Youd, M)
Fault-zone tectonics (J. C. Savage, M)
Fluid injection, laboratory investigations (J. D. Byerlee, Louis Peselnick, M)
Geologic and geotechnical factors in ground-motion analysis (R. C. Wilson, M)
Geologic parameters of seismic source areas (F. A. McKeown, D)
Ground failure related to the 1811-12 New Madrid earthquakes (S. F. Obermeier, NC)
Ground failures caused by historic earthquakes (D. K. Keefer, D)
Ground-motion modeling and prediction (W. B. Joyner, M)
Ground-motion studies (R. D. Borcherdt, R. P. Maley, M)
Microearthquake data analysis (W. H. K. Lee, M)
National Earthquake Information Service (A. C. Tarr, D)
National Strong-Motion Instrumentation Network (R. B. Matthiesen, M)
New seismic instrumentation for geothermal surveys (P. A. Reasenberg, M)
Nicaragua, Central America, technical assistance in establishing center for earthquake hazard reduction (P. L. Ward, M)
Plate-tectonic studies (E. D. Jackson, M)
Precursory phenomena (P. L. Ward, M)
Prediction, animal behavior studies (P. A. Reasenberg, M)
Prediction monitoring and evaluation (R. N. Hunter, D)
Recurrence intervals along Quaternary faults (K. L. Pierce, D)
Reduction of noise in precursor signals (J. A. Steppe, M)
Relative activity of multiple fault strands (M. G. Bonilla, M)
Reservoir-induced seismicity, statistical approach, (D. E. Stuart-Alexander, M)
Seismic-risk studies (S. T. Algermissen, D)
Seismic-source studies (W. R. Thatcher, M)
Seismic studies for earthquake prediction (C. G. Bufe, M)
Seismicity and Earth structure (J. N. Taggart, D)
Seismological research observatories (J. R. Peterson, Albuquerque, N. Mex.)
Soil engineering research (T. L. Youd, M)
Spectral and time domain analysis of near field recordings of earthquakes (J. B. Fletcher, M)
Stress studies (C. B. Raleigh, M)
Synthetic strong-motion seismograms (W. B. Joyner, M)
Tectonic studies (W. B. Hamilton, D)
Teleseismic search for earthquake precursors (J. W. Dewey, D)
Theoretical seismology (A. F. Espinosa, D)
Worldwide Network of Standard Seismographs (J. R. Peterson, Albuquerque, N. Mex.)
States:
Alaska:
Earthquake hazards:
Anchorage (Ernest Dobrovolny, D)
Coastal communities (R. W. Lemke, D)
Juneau (R. D. Miller, D)
Sitka (L. A. Yehle, D)
Southern part (George Plafker, M)

Earthquake studies—Continued
States—Continued
Alaska—Continued
Microearthquake studies (R. A. Page, M)
Turnagain Arm sediments (A. T. Ovenshine, M)
California (M, except as otherwise noted):
Basement rock studies along San Andreas fault (D. C. Ross)
Continental Shelf fault studies (S. C. Wolf)
Depth of bedrock in the San Francisco Bay region (R. M. Hazlewood)
Earthquake hazards:
San Francisco Bay region (E. E. Brabb)
Southern part (D. M. Morton, Los Angeles)
Foothills fault system (D. E. Stuart-Alexander, M)
Geodetic strain (W. H. Prescott)
Geophysical studies, San Andreas fault (J. H. Healy)
Measurement of seismic velocities for seismic zonation (J. F. Gibbs, R. D. Borcherdt, T. E. Fumal)
Microearthquake studies:
Central part (J. H. Pfluke)
New Melones (J. C. Roller)
Southern part (D. P. Hill)
Recency of faulting:
Coastal California Desert (E. H. Pampeyan)
Eastern Mojave Desert (W. J. Carr)
Tectonics:
Central and northern part (W. P. Irwin)
Central San Andreas fault (D. B. Burke, T. W. Dibblee, Jr.)
Salton Trough tectonics (R. V. Sharp)
Southern part (M. M. Clark)
Theory of wave propagation in anelastic media (R. D. Borcherdt)
Colorado, Rangely (C. B. Raleigh, M)
Idaho, active faults, Snake River Plain (S. S. Oriel, M. H. Hoit, W. E. Scott, D)
Massachusetts, Fault definition, northeastern Massachusetts (A. F. Shride, D)
Missouri, New Madrid fault-zone geophysics (M. F. Kane, D)
Montana, Yellowstone National Park, microearthquake studies (A. M. Pitt, M)
Nevada, tectonics, west-central (E. B. Ekren, D)
New Mexico, seismotectonic analysis, Rio Grande rift (E. H. Baltz, Jr., D)
South Carolina, microearthquake studies (A. C. Tarr, D)
Washington (M):
Earthquake hazards, Puget Sound region (H. D. Gower, P. D. Snavely, Jr.)
Hanford microearthquake studies (J. H. Pfluke)

Ecology:
Estuarine plankton dynamics (J. E. Cloern, w, M)

Engineering geologic studies. *See* Construction and terrain problems; Urban geology.

Environmental assessment:
A. R. Company Coal Creek mine (M. E. MacLachlan, D)
Carter Oil Caballo mine (E. G. A. Weed, l, NC)
Central Utah regional coal (E. S. Davidson, w, M)
Guidelines for administration and management of EIS task forces (K. E. Vanlier, J. W. Allingham, l, NC)
Guidelines for preparation of EIS's (K. E. Vanlier, J. W. Allingham, l, NC)
Kerr-McGee East Gillette mine (L. G. Marcus, l, NC)
Mobil-Consolidation Pronghorn mine (L. G. Marcus, l, NC)
Methodology for monitoring impacts of phosphate development, Idaho (L. G. Marcus, l, NC)
National Petroleum Reserve Alaska environmental analysis (W. J. Schneider, w, M)
Northern Powder River basin, regional coal (Glenn Malmberg, w, D)

Environmental assessment—Continued
Peabody Rochelle mine (L. G. Marcus, l, NC)
Powder River basin uranium (E. S. Santos, D)
Review of environmental impact statements (L. D. Bonham, l, NC)
South Florida environment (B. F. McPherson, w, Miami)
Southern Utah regional coal (E. S. Davidson, w, M)

Environmental geology:
Quaternary dating applications—overview map (K. L. Pierce, D)
States:
Alaska, Peterburg quadrangle (D. A. Brew)
Montana:
Environmental study of the Big Fork-Avon area (I. J. Witkind, D)
Land resources, Helena region (R. G. Schmidt, NC; G. D. Robinson, M)
Utah:
Cedar City 2° quadrangle (K. A. Sargent, D)
Central Utah energy lands (I. J. Witkind, D)
Kaiparowits Plateau coal basin (K. A. Sargent, D)
Wyoming, Hams Fork coal basin (A. B. Gibbons, D)
See also Construction and terrain problems; Land use and environmental impact; Urban geology.

Evapotranspiration:
Evaporation, Colorado lakes (D. B. Adams, w, D)
Evapotranspiration data analyses (T. E. A. van Hylckama, w, Lubbock, Tex.)
Evapotranspiration theory (O. E. Leppanen, w, Bay St. Louis, Miss.)
Mechanics of evaporation (G. E. Koberg, w, D)
Vegetation ecohydrology (R. M. Turner, w, Tucson, Ariz.)

Extraterrestrial studies:
Lunar analog studies:
Explosion craters (D. J. Roddy, Flagstaff, Ariz.)
Lunar data synthesis:
Imbrium and Serenitatis Basins (J. F. McCauley, Flagstaff, Ariz.)
Sample petrology and stratigraphy (H. G. Wilshire, M)
Synoptic lunar geology (D. E. Wilhelms, M)
Lunar microwave (G. R. Olhoeft, Denver)
Lunar sample investigations:
Chemical and X-ray fluorescence analysis (H. J. Rose, Jr., NC)
Lunar igneous-textured rocks (O. B. James, NC)
Major lunar breccia types (E. C. T. Chao, NC)
Mineralogical analyses (R. B. Finkelman, NC)
Oxygen fugacities and crystallization sequence (Motoaki Sato, NC)
Petrologic studies (Edwin Roedder, NC)
Pyroxenes (J. S. Huebner, NC)
Planetary analog studies, mass movements (E. C. Morris, Flagstaff, Ariz.)
Planetary investigations:
Geologic mapping of Mars (D. H. Scott, J. F. McCauley, Flagstaff, Ariz.)
Geologic synthesis of Mars (Harold Masursky, Flagstaff, Ariz.)
Image-processing studies (L. A. Soderblom, Flagstaff, Ariz.)
Mariner Jupiter-Saturn (L. A. Soderblom, Flagstaff, Ariz.)
Mariner Venus-Mercury TV (N. J. Trask, NC)

Extraterrestrial studies—Continued
Planetary investigations—Continued
Mars mineralogy and chemistry, Viking lander (Priestley Toulmin III, H. J. Rose, Jr., NC)
Mars topographic synthesis (S. S. C. Wu, Flagstaff, Ariz.)
Planetary cartography (R. M. Batson, Flagstaff, Ariz.)
Radar applications (G. G. Schaber, Flagstaff, Ariz.)
Viking mission:
Lander (E. C. Morris, Flagstaff, Ariz.)
Orbiter TV (M. H. Carr, M)
Physical properties of Mars (H. J. Moore, M)
Site analysis (Harold Masursky, Flagstaff, Ariz.)

Ferro-alloy metals:
Chromium:
Geochemistry (B. A. Morgan III, NC)
Resource studies (T. P. Thayer, NC)
Molybdenum-rhenium resource studies (R. U. King, D)
States:
North Carolina, tungsten in Hamme district (J. E. Gair, NC)
Oregon, John Day area (T. P. Thayer, NC)
Pennsylvania, State Line district (B. A. Morgan III, NC)

Flood-hazard mapping:
Alabama (C. O. Ming, w, Montgomery)
Arkansas (M. S. Hines, w, Little Rock)
California (J. R. Crippen, w, M)
Colorado (T. R. Dosch, w, D)
Connecticut (M. A. Cervione, Jr., w, Hartford)
Florida (S. D. Leach, w, Tallahassee)
Georgia (McGlone Price, w, Doraville)
Idaho (W. A. Harenberg, w, Boise)
Illinois (B. J. Prugh, w, Champaign)
Indiana (J. B. Swing, w, Indianapolis)
Iowa (O. G. Lara, w, Iowa City)
Kansas (D. B. Richards, w, Lawrence)
Kentucky (C. H. Hannum, w, Louisville)
Louisiana (A. S. Lowe, w, Baton Rouge)
Maine (R. A. Morrill, w, Augusta)
Massachusetts (S. W. Wandle, Jr., w, Boston)
Michigan (R. L. Knutilla, w, Lansing)
Minnesota (G. H. Carlson, w, St. Paul)
Missouri (L. D. Hauth, w, Rolla)
Montana (R. J. Omang, w, Helena)
Nebraska (G. G. Jamison, w, Lincoln)
New Hampshire (S. W. Wandle, Jr., w, Boston, Mass.)
North Carolina (R. W. Coble, w, Raleigh)
North Dakota (O. A. Crosby, w, Bismarck)
Ohio (D. K. Roth, w, Columbus)
Oklahoma (W. B. Mills, w, Oklahoma City)
Oregon (D. D. Harris, w, Portland)
Pennsylvania (L. V. Page, w, Harrisburg)
Puerto Rico (E. D. Cobb, w, San Juan)
South Carolina (W. T. Utter, w, Columbia)
South Dakota (O. J. Larimer, w, Huron)
Texas (J. D. Bohn, w, Austin)
United States (G. W. Edelen, w, NC)
Vermont (S. W. Wandle, Jr., w, Boston, Mass.)
Virginia (P. M. Frye, w, Richmond)
Washington (J. H. Bartells, w, Tacoma)
West Virginia (G. S. Runner, w, Charleston)
Wisconsin (C. L. Lawrence, w, Madison)

Flood-insurance studies:
Alabama (C. O. Ming, w, Montgomery)
Arizona (B. N. Aldridge, w, Tucson)
Arkansas (A. H. Ludwig, w, Little Rock)

Flood-insurance studies—Continued
California (J. R. Crippen, w, M)
Colorado (R. C. Christensen, w, D)
Connecticut (M. A. Cervione, Jr., w, Hartford)
Florida (S. D. Leach, w, Tallahassee)
Georgia (McGlone Price, w, Doraville)
Idaho (W. A. Harenberg, w, Boise)
Illinois (G. W. Curtis, w, Champaign)
Indiana (D. H. Rapp, w, Indianapolis)
Iowa (A. J. Heinitz, w, Iowa City)
Kansas (K. D. Medina, w, Lawrence)
Kentucky (C. H. Hannum, w, Louisville)
Louisiana (D. D. Pyburn, Baton Rouge)
Maine (R. M. Morrill, w, Augusta)
Massachusetts (L. A. Swallow, w, Boston)
Michigan (R. L. Knuttila, w, Lansing)
Minnesota (G. H. Carlson, w, St. Paul)
Missouri (L. D. Hauth, w, Rolla)
Montana (R. J. Omang, w, Helena)
Nebraska (G. G. Jamison, w, Lincoln)
Nevada (C. V. Schroer, w, Carson City)
New Hampshire (L. A. Swallow, w, Boston, Mass.)
New Jersey (R. D. Schopp, w, Trenton)
New Mexico (L. P. Denis, w, Albuquerque)
New York (R. T. Mycyk, w, Albany)
North Carolina (N. N. Jackson, w, Raleigh)
Ohio (D. K. Roth, w, Columbus)
Oklahoma (T. L. Huntzinger, w, Oklahoma City)
Oregon (D. D. Harris, w, Portland)
Pennsylvania (Andrew Voytik, w, Harrisburg)
Puerto Rico (J. R. Harkins, w, San Juan)
Rhode Island (L. A. Swallow, w, Boston, Mass.)
South Carolina (B. H. Whetstone, w, Columbia)
Tennessee (W. J. Randolph, w, Nashville)
Texas (J. D. Bohn, w, Austin)
United States (E. J. Kennedy, w, NC)
Vermont (S. S. Wandle, w, Boston, Mass.)
Virginia (J. R. Mohler, w, Fairfax)
Washington (C. H. Swift, w, Tacoma)
Wisconsin (C. L. Lawrence, w, Madison)

Flood investigations:
Countermeasures, scour and erosion (J. C. Bruce, w, M)
Dating infrequent floods (R. A. Sigafoos, w, NC)
Documentation of extreme floods (H. H. Barnes, Jr., w, NC)
Flow frequency analysis (W. O. Thomas, w, NC)
Model bridge-site report (H. H. Barnes, w, NC)
Nationwide flood-frequency (A. G. Scott, w, NC)
States and territories:
Alabama, floods, bridge-site studies (C. O. Ming, w, Montgomery)
Arkansas (M. S. Hines, w, Little Rock)
Arizona, 1977-78 flood report (B. N. Aldridge, w, Tucson)
California:
Flood hydrology Butte basin (J. C. Blodgett, w, Sacramento)
Floods-small drainage areas (A. O. Waananen, w, M)
Colorado (w, D):
Floods, Elbert County (T. R. Dosch, w, D)
Foothill floods (J. F. McCain, w, D)
Connecticut, Small stream flood characteristics (M. P. Thomas, w, Hartford)
Delaware, Floods small drainage areas (R. H. Simmons, w, Dover)

Flood investigations—Continued
States and territories—Continued
Florida (w, Tampa):
Bridge site studies (W. C. Bridges, w, Tallahassee)
Regional flood-frequency study (M. A. Seijo)
Georgia:
Atlanta flood charactersitics (E. J. Inman, w, Doraville)
Flood and bridge site studies (McGlone Price, w, Doraville)
Urban flood-frequency, Georgia (E. J. Inman, w, Doraville)
Hawaii, Special flood-data collection (R. H. Nakahara, w, Honolulu)
Idaho (W. A. Harenburg, w, Boise)
Illinois, Urban floods in northeastern Illinois (H. E. Allen, Jr., w, Dekalb)
Indiana, flood frequency (R. L. Gold, w, Indianapolis)
Iowa (w, Iowa City):
Flood data for selected bridge sites (O. G. Lara)
Flood profiles, of Iowa streams (O. G. Lara)
Kentucky:
Small-area flood hydrology (J. N. Sullivan, Jr., w, Louisville)
Hydraulics of bridge sites (C. H. Hannum, w, Louisville)
Louisiana, roughness coefficients (G. J. Arcement, w, Baton Rouge)
Maryland, Floods—small drainage areas (D. H. Carpenter, w, Towson)
Massachusetts, Small basin flood flow in Massachusetts (J. S. Wandle, w, Boston)
Minnesota, flood-plain studies (G. H. Carlson, w, St. Paul)
Mississippi, Multiple-bridge hydraulics (B. E. Colson, w, Jackson)
Nevada (w, Carson City):
Environmental study, Nevada (P. A. Glancy)
Flood investigations (Otto Moosburner)
New Jersey, flood peaks and flood plains (R. O. Schopp, w, Trenton)
New Mexico, flood analysis (R. P. Thomas w, Santa Fe)
New York, peak discharge of ungaged streams (Bernard Dunn, w, Albany)
Oklahoma, small watersheds (T. J. Huntzinger, Jr., w, Oklahoma City)
Puerto Rico:
Eloise floods (K. G. Johnson, w, San Juan)
St. Croix flood of October 7-8, 1977 (K. G. Johnson, w, San Juan)
South Carolina, Hydraulic site reports (B. H. Whetstone, w, Columbia)
Tennessee (W. J. Randolph, w, Nashville)
Virginia:
Hydrology, Wytheville fish hatchery (J. R. Hendrick, w, Marion)
Statewide (P. M. Frye, w, Richmond)
Washington, Flood-inundation mapping (J. H. Bartells, w, Tacoma)
Wisconsin (w, Madison):
Bridge flood backwater (D. A. Stedfast, w, Madison)
Flood-control effects on Trout Creek (E. E. Zuehls)
Flood documentation in Wisconsin (P. E. Hughes)
St. Croix scenic river waste study (R. S. Grant)
Wyoming, flood investigations (G. S. Craig, w, Cheyenne)

Fluorspar:
Colorado, Bonanza and Poncha Springs quadrangles (R. E. Van Alstine, NC)
Illinois-Kentucky district, regional structure and ore controls (D. M. Pinckney, D)

Foreign nations, geologic investigations:
- Brazil, mineral, resources and geologic training (S. A. Stanin, Rio de Janeiro)
- Poland
  - Characteristics of coal basins (K. J. Englund, NC)
  - Geochemistry of coal and computerization of coal data (V. E. Swanson, D)
- Saudi Arabia, crystalline shield, geologic and mineral reconnaissance (F. S. Simons, Jiddah)
- Spain, marine mineral resources (P. D. Snavely, Jr., M)
- Thailand, remote-sensing program (J. O. Morgan, Bangkok)

Foreign nations, hydrologic investigations. *See* Water resources, Foreign countries.

Fuels, organic. *See* Coal; Oil shale; Petroleum and natural gas.

Gas, natural. *See* Petroleum and natural gas.

Geochemical distribution of the elements:
- Basin and Range granites (D. E. Lee, D)
- Botanical exploration and research (H. L. Cannon, D)
- Coding and retrieval of geologic data (T. G. Lovering, D)
- Data of geochemistry (Michael Fleischer, NC)
- Data systems (R. V. Mendes, D)
- Element availability:
  - Soils (R. C. Severson, D)
  - Vegetation (L. P. Gough, D)
- Geochemistry of belt rocks (J. J. Connor, D)
- Light stable isotopes (J. R. O'Neil, M)
- Phosphoria Formation, organic carbon and trace element distribution (E. K. Maughan, D)
- Sedimentary rocks, chemical composition (T. P. Hill, D)
- Selenium, tellurium, and thallium, geochemical exploration (H. W. Lakin, D)
- Statistical geochemistry and petrology (A. T. Miesch, D)
- Tippecanoe sequence, Western Craton (L. G. Schultz, D)
- Trace elements in oil shale (W. E. Dean, Jr., D)
- Urban geochemistry (H. A. Tourtelot, D)
- Western coal regions:
  - Geochemical survey of rocks (R. J. Ebens, D)
  - Geochemical survey of soils (R. R. Tidball, D)
  - Geochemical survey of vegetation (J. A. Erdman, D)
  - Geochemical survey of waters (G. L. Feder, D)
- *States:*
- California, Sierra Nevada batholith, geochemical study (F. C. W. Dodge, M)
- Colorado, Mt. Princeton igneous complex (Priestley Toulmin III, NC)
- Pennsylvania, greater Pittsburgh region, environmental geochemistry (R. P. Biggs, Carnegie)

Geochemical prospecting methods:
- Application and evaluation of methods of chemical analysis to diverse geochemical environments (J. G. Viets, D)
- Application of silver-gold geochemistry to exploration (H. W. Laking, D)
- Botanical exploration and research (H. L. Cannon, D)
- Development of effective on-site methods of chemical analysis for geochemical exploration (W. L. Campbell, D)
- Elements in organic-rich material (F. N. Ward, D)
- Gamma-ray spectrometry (J. A. Pitkin, D)
- Geochemical characterization of metallogenic provinces and mineralized areas (G. J. Neuerburg, D)
- Geochemical exploration:
  - Glaciated areas (H. V. Alminas, D)
  - Research in arctic, alpine, and subalpine regions (J. H. McCarthy, D)
  - Techniques:
    - Alpine and subalpine environments (G. C. Curtin, D)

Geochemical prospecting methods—Continued
- Techniques—Continued
  - Arid environments (M. A. Chaffee, D)
- Gold composition analysis in mineral exploration (J. C. Antweiler, D)
- Instrumentation development (R. C. Bigelow, D)
- Jasperoid, relations to ore deposits (T. G. Lovering, D)
- Lateritic areas, southern Appalachian Mountains (W. R. Griffitts, D)
- Mercury, geochemistry (A. P. Pierce, D)
- Mineral exploration methods (G. B. Gott, D)
- Mineralogical techniques in geochemical exploration (Theodore Botinelly, D)
- New mineral storage and identification program (George Van Trump, Jr., D)
- Ore-deposit controls (A. V. Heyl, Jr., D)
- Pattern recognition and clustering methods for the graphical analysis of geochemical data (J. B. Fife, D)
- Research in methods of spectrographic analysis for geochemical exploration (E. L. Mosier, D)
- Sulfides, accessory in igneous rocks (G. J. Neuerberg, D)
- Surface and ground water in geochemical exploration (G. A. Nowlan, D)
- Volatile elements and compounds in geochemical exploration (M. E. Hinkle, D)
- *States:*
- Alaska, geochemical exploration techniques (G. C. Curtin, D)
- New Mexico, Basin and Range part, geochemical reconnaissance (W. R. Griffitts, D)

Geochemistry, experimental:
- Environment of ore deposition (P. B. Barton, Jr., NC)
- Experimental mineralogy (R. O. Fournier, M)
- Fluid inclusions in minerals (Edwin Roedder, NC)
- Fluid zonation in metal deposits (J. T. Nash, M)
- Geologic thermometry (J. S. Huebner, NC)
- Hydrothermal alteration (J. J. Hemley, NC)
- Impact metamorphism (E. C. T. Chao, NC)
- Kinetics of igneous processes (H. R. Shaw, NC)
- Late-stage megmatic processes (G. T. Faust, NC)
- Mineral equilibria, low temperature (E-an Zen, NC)
- Neutron activation (F. E. Senftle, NC)
- Oil shale:
  - Colorado, Utah, and Wyoming (W. E. Dean, Jr., D)
  - Organic geochemistry (R. E. Miller, D)
- Organic geochemistry (J. G. Palacas, D)
- Organometallic complexes, geochemistry (Peter Zubovic, NC)
- Solution-mineral equilibria (C. L. Christ, M)
- Stable isotopes and ore genesis (R. O. Rye, D)
- Statistical geochemistry (A. T. Miesch, D)

Geochemistry, water:
- Chemical constituents of ground water (William Back, w, NC)
- Chemical reactions at mineral surfaces (J. D. Hem, w, M)
- Chemistry of hydrosolic metals (J. D. Hem, w, M)
- Computer modeling of rock-water interactions (J. L. Haas, Jr., NC)
- Elements, distribution in fluvial and brackish environments (V. C. Kennedy, w, M)
- Factors determining solute transfer in the unsaturated zone (Jacob Rubin, W, M)
- Gases, complexes in water (D. W. Fischer, w, NC)
- Geochemistry of geothermal systems (Ivan Barnes, w, M)
- Geochemistry of San Francisco Bay waters and sediments (D. H. Peterson, w, M)
- Geologic perspectives—global carbon dioxide (E. T. Sundquist, w, NC)
- Geothermal trace-element reactions (E. A. Jenne, w, M)
- Interaction of minerals and water in saline environments (B. F. Jones, w, NC)

Geochemistry, water—Continued
Interface hydrochemistry and paleoclimatology (I. J. Winograd, w, NC)
Mineralogic controls of the chemistry of ground water (B. B. Hanshaw, w, NC)
Organic geochemistry (R. L. Malcolm, w, D)
Redox reactions (D. C. Thorstenson, w, NC)
Trace-element partitioning (E. A. Jenne, w, M)
Uranium mill tailings (E. R. Landa, w, NC)
See also Quality of water.

Geochemistry and petrology, field studies:
Basalt, genesis (T. L. Wright, NC)
Basin and Range granites (D. E. Lee, D)
Epithermal deposits (R. G. Worl, D)
Geochemical studies in southeastern States (Henry Bell III, NC)
Geochemistry of diagenesis (K. J. Murata, M)
Geochemistry of marine sediments (W. E. Dean, D)
Geochemistry of Tippecanoe Sequence, Western Craton (L. G. Schultz, D)
Inclusions in basaltic rocks (E. D. Jackson, M)
Layered Dufek intrusion, Antarctica (A. B. Ford, M)
Layered intrusives (N. J. Page, M)
Mercury, geochemistry and occurrence (A. P. Pierce, D)
Nobium and tantalum, distribution in igneous rocks (David Gottfried, NC)
Organic petrology of sedimentary rocks (N. H. Bostick, D)
Rare-earth elements, resources and geochemistry (J. W. Adams, D)
Regional geochemistry (W. E. Dean, Jr., D)
Regional metamorphic studies (H. L. James, M)
Residual minor elements in igneous rocks and veins (George Phair, NC)
Solution transport of heavy metals (G. K. Czamanske, M)
Submarine volcanic rocks, properties (J. G. Moore, M)
Syngenetic ore deposition (C. M. Conway, M)
Thermal waters, origin and characteristics (D. E. White, M)
Trace elements in oil shale (W. E. Dean, Jr., D)
Trondhjemites, major and minor elements, isotopes (Fred Barker, D)
Ultramafic rocks, petrology of alpine types (R. G. Coleman, M)
Uranium, radon and helium—gaseous emanation detection (G. M. Reimer, D)
Western coal regions:
Geochemical survey of rocks (R. J. Ebens, D)
Geochemical survey of soils (R. R. Tidball, D)
Geochemical survey of vegetation (J. A. Erdman, D)
Western energy regions:
Element availability—plants (L. P. Gough, D)
Element availability—rocks (J. M. McNeal, D)
Element availability—soils (R. C. Severson, D)
States:
Alaska (M):
La Perouse layered intrusion (R. A. Loney)
Metasedimentary and metaigneous rocks, southwestern Brooks Range (I. L. Tailleur)
Petersburg quadrangle (D. A. Brew)
Arizona (M):
Ray program:
Mineral Mountain (T. G. Theodore)
Silicate mineralogy, geochemistry (N. G. Banks)
Stocks (S. C. Creasey)
California:
Geochemistry of sediments, San Francisco Bay (D. S. McCulloch, M)
Granitic rocks of Yosemite National Park (D. L. Peck, NC)

Geochemistry and petrology, field studies—Continued
States—Continued
California—Continued
Kings Canyon National Park (J. G. Moore, M)
Long Valley Caldera-Mono Craters volcanic rocks (R. A. Bailey, NC)
Sierra Nevada xenoliths (J. P. Lockwood, M)
Colorado:
Petrology of Mt. Princeton igneous complex (Priestley Toulmin III, NC)
Tertiary-Laramide intrusives (E. J. Young, D)
Hawaii, ankaramites (M. H. Beeson, M)
Idaho, Wood Rive district (W. E. Hall, M)
Idaho-Montana-Wyoming, petrology of the Yellowstone Plateau volcanic field (R. L. Christiansen, M)
Montana:
Diatremes, Missouri River Breaks (B. C. Hearn, Jr., NC)
Geochronology, north-central Montana (B. C. Hearn, Jr., NC; R. F. Marvin, R. E. Zartman, D)
Wolf Creek area, petrology (R. G. Schmidt, NC)
Nevada, igneous rocks and related ore deposits (M. L. Silberman, M)
Pennsylvania, geochemistry of Pittsburgh urban area (H. A. Tourtelot, D)
South Dakota, Keystone pegmatite area (J. J. Norton, Rapid City)

Geochronological investigations:
Carbon-14 method (Meyer Rubin, NC)
Geochronology and rock magnetism (G. B. Dalrymple, M)
Geochronology of uranium ores and their host rocks (K. R. Ludig, D)
Igneous rocks and deformational periods (R. W. Kistler, M)
Lead-uranium, lead-thorium, and lead-alpha methods (T. W. Stern, NC)
Magnetic chronology, Colorado Plateau and environs (D. P. Elston, E. M. Shoemaker, Flagstaff, Ariz.)
Quaternary dating techniques, numerical and relative-age (K. L. Pierce, D)
Radioactive-disequilibrium studies (J. N. Rosholt, D)
San Francisco volcanic field (P. E. Damon, University of Arizona
States:
Alaska, K-Ar dates, southwest Brooks Range (I. L. Tailleur, M; R. B. Forbes, D. L. Turner, Fairbanks)
Colorado, geochronology of Denver area (C. E. Hedge, D)
See also Isotope and nuclear studies.

Geologic mapping:
Map scale smaller than 1:62,500:
Antarctica, Dufek Massif and Forrestal Range, Pensacola Mountains (A. B. Ford, M)
Belt basin study (J. E. Harrison, D)
Columbia River basalt (D. A. Swanson, M)
States:
Alaska (M):
Ambler River and Baird Mountains quadrangles (I. L. Tailleur)
Charley River quadrangle (E. E. Brabb)
Craig quadrangle (G. D. Eberlein, Michael Churkin, Jr.)
Delong Mountains quadrangle (I. L. Tailleur)
Geologic map (H. M. Beikman)
Glacier Bay National Monument (D. A. Brew)
Hughes-Shungnak area (W. W. Patton, Jr.)
Iliamna quadrangle (R. L. Detterman)
Juneau and Taku River quadrangles (D. A. Brew)
Metamorphic facies map (D. A. Brew)
Natural landmarks investigation (R. L. Detterman)
Petersburg quadrangle (D. A. Brew)
St. Lawrence Island (W. W. Patton, Jr.)

Geologic mapping—Continued:
Map scale smaller than 1:62,500—Continued
States—Continued
Arizona (Flagstaff):
North-central part (D. P. Elston)
Phoenix 2-degree quadrangle (T. N. V. Karlstrom)
Shivwits Plateau (Ivo Lucchitta)
Arkansas (B. R. Haley, Little Rock)
California (M):
Environmental maps for land use planning (E. H. Pampeyan)
Tectonic studies, Great Valley area (J. A. Bartow, D. E. Marchand)
Colorado (D):
Colorado Plateau geologic map (D. D. Haynes)
Denver 2-degree quadrangle (B. H. Bryant)
Geologic map (O. L. Tweto)
Greeley 2-degree quadrangle, western half (W. A. Braddock)
Leadville 2-degree quadrangle (O. L. Tweto)
Pueblo 2-degree quadrangle (G. R. Scott)
Sterling 2-degree quadrangle (G. R. Scott)
Idaho (D):
Challis Volcanics (D. H. McIntyre)
Dubois 2-degree quadrangle (M. H. Hait and B. A. Skipp)
Idaho Falls 2-degree quadrangle (M. A. Kuntz)
Preston 2-degree quadrangle (S. S. Oriel)
Snake River Plain, central part, volcanic petrology (H. E. Malde)
Snake River Plain region, eastern part (S. S. Oriel)
Missouri, Rolla 2-degree quadrangle, mineral-resource appraisal (W. P. Pratt, D)
Montana, White Sulphur Springs 2-degree quadrangle (M. W. Reynolds, D)
Nevada:
Elko County:
Central (K. B. Ketner, D)
Countywide (R. A. Hope, M)
Western (R. R. Coats, M)
Geologic map (J. H. Stewart, M)
Lincoln County, Tertiary rocks (G. L. Dixon, D)
New Jersey, Pennsylvania, New York, Newark 2-degree quadrangle (A. A. Drake, Jr., NC)
New Mexico (D):
North Church Rock area (A. R. Kirk)
Sanostee (A. C. Huffman, Jr.)
Santa Fe 2-degree quadrangle, western half (E. H. Baltz, Jr.)
Socorro 2-degree quadrangle, (G. O. Bachman)
North Carolina, Charlotte 2-degree sheet (Richard Goldsmith, NC)
South Carolina, Charlotte 2-degree sheet (Richard Goldsmith, NC)
South Carolina, Georgia, North Carolina, Greenville 2-degree quadrangle (A. E. Nelson, NC)
Utah (M):
Delta 2-degree quadrangle (H. T. Morris)
Richfield 2-degree quadrangle (T. A. Steven, P. D. Rowley)
Tooele 2-degree quadrangle (W. J. Moore)
Wasatch-Uinta Tectonics (Salt Lake City and Ogden 2-degree quadrangles, B. H. Bryant, D)
Washington, Wenatchee 2-degree sheet (R. W. Tabor, R. B. Waitt, Jr., V. A. Frizzell, Jr., M)

Geologic mapping—Continued
Map scale smaller than 1:62,500—Continued
States:
Wyoming:
Geologic map (J. D. Love, Laramie)
Preston 2-degree quadrangle (S. S. Oriel, D)
Wasatch-Uinta Tectonics (Ogden 2-degree quadrangle, B. H. Bryant, D)
Teton Wilderness (J. D. Love, Laramie)
Map scale 1:62,500 and larger:
States and territories:
Alaska:
Anatuvuk Pass (G. B. Shearer, c, Anchorage)
Anchorage area (Ernest Dobrovolny, D)
Bering River coal field (R. B. Sanders, c, Anchorage)
Cape Beaufort-Corwin Bluffs coal field (J. E. Callahan, c, Anchorage)
Geology and mineral resources of the Ketchikan quadrangle (H. C. Berg, M)
Juneau area (R. D. Miller, D)
Kukpowruk River coal field (J. E. Callahan, c, Anchorage)
Nelchina area, Mesozoic investigations (Arthur Grantz, M)
Nenana coal investigations (Clyde Wahrhaftig, M)
Nome area (C. L. Hummel, M)
Utokok River and Kokolik River coal field (J. E. Callahan, c, Anchorage)
West Chichagof-Yakobi Islands (B. R. Johnson, M)
Arizona:
Bowie zeolite area (L. H. Godwin, c, NC)
Cummings Mesas quadrangle (Fred Peterson, c, D)
Hackberry Mountain area (D. P. Elston, Flagstaff)
Mt. Wrightson quadrangle (H. D. Drewes, D)
Ray district, porphyry copper (H. R. Cornwall, M)
Sedona area (D. P. Elston, Flagstaff)
Western Arizona tectonic studies (Ivo Lucchitta, Flagstaff)
California (M, except as otherwise noted):
Coast Range, ultramafic rocks (E. H. Bailey)
Condrey Mountain and Hornbrook quadrangles (P. E. Hotz)
King Range-Chemise area (R. J. McLaughlin)
Long Valley caldera (R. A. Bailey, NC)
Malibu Beach and Topanga quadrangles (R. F. Yerkes)
Merced Peak quadrangle (D. L. Peck, NC)
Northern Coast Ranges (K. F. Fox, Jr.)
Palo Alto, San Mateo, and Montara Mountain quadrangles (E. H. Pampeyan)
Peninsular Ranges (V. R. Todd, La Jolla)
Point Dume and Triunfo Pass quadrangles (R. H. Campbell)
Regional fault studies (E. J. Helley, D. G. Herd, B. F. Atwater)
Ryan quadrangle (J. F. McAllister)
Santa Lucia Range (V. M. Seiders)
Searles Lake area (G. I. Smith)
Sierra Nevada batholith (P. C. Bateman)
The Geysers-Clear Lake area (R. J. McLaughlin)
Western Santa Monica Mountains (R. H. Campbell)
Colorado (D, except as otherwise noted):
Barcus Creek quadrangle (W. J. Hail)
Barcus Creek SE quadrangle (W. J. Hail)
Bonanza quadrangle (R. E. Van Alstine, NC)
Buckhorn Lakes quadrangle (R. G. Dickinson, c, D)
Central City area (R. B. Taylor)
Citadel Plateau (G. A. Izett, c, D)

Geologic mapping—Continued

Map scale 1:62,500 and larger—Continued

States and territories—Continued

Colorado (D, except as otherwise noted)—Continued

Coal mine deformation studies, Somerset mining district (C. R. Dunrud)
Cochetopa area (J. C. Olson)
Courthouse Mountain quadrangle (R. G. Dickinson, c, D)
Denver basin, Tertiary coal zone (P. E. Soister, c, D)
Denver metropolitan area (R. M. Lindvall)
Desert Gulch quadrangle (R. C. Johnson, D)
Disappointment Valley, geology and coal resources (D. E. Ward)
Middle Dry Fork quadrangle (R. C. Johnson, D)
Northern Park Range (G. L. Snyder)
Poncha Springs quadrangle (R. E. Van Alstine, NC)
Rangely NE quadrangle (R. S. Garrigues, c, D)
Rocky Mountain National Park (W. A. Braddock)
Rustic quadrangle (K. L. Shaver)
Savery quadrangle (C. S. V. Barclay, c, D)
Strasburg SW quadrangle (P. E. Soister, c, D)
Thornburgh quadrangle (M. J. Reheis, c, D)
Ward and Gold Hill quadrangles (D. J. Gable)
Washboard Rock quadrangle (R. G. Dickinson, c, D)
Watkins and Watkins SE quadrangles (P. E. Soister, c, D)

Connecticut, Cooperative mapping program (M. H. Pease, Jr., Boston, Mass.)

Georgia, Macon-Gordon district (S. H. Patterson, NC)

Idaho (D, except as otherwise noted):

Bayhorse area (S. W. Hobbs)
Black Pine Mountains (J. F. Smith, Jr.)
Boulder Mountains (C. M. Tschanz)
Goat Mountain quadrangle (M. H. Staatz)
Grouse quadrangle (B. A. Skipp)
Hawley Mountain quadrangle (W. J. Mapel)
Malad SE quadrangle (S. S. Oriel)
Montour quadrangle (H. E. Malde)
Palisades Dam quadrangle (D. A. Jobin, c, D)
Patterson quadrangle (E. T. Ruppel)
Strevell quadrangle (J. F. Smith)
Upper and Lower Red Rock Lake quadrangles (I. J. Witkind)
Wood River district (W. E. Hall, M)
Yellow Pine quadrangle (B. F. Leonard)

Kentucky, cooperative mapping program (E. R. Cressman, Lexington)

Maine:

Blue Hill quadrangle (D. B. Stewart, NC)
Castine quadrangle (D. B. Stewart, NC)
Orland quadrangle (D. R. Wones, NC)
Rumford quadrangle (R. H. Moench, D)
The Forks quadrangle (F. C. Canney, D)

Maryland (NC):

Delmarva Peninsula (J. P. Owens)
Northern Coastal Plain (J. P. Minard)
Western Maryland Piedmont (M. W. Higgins)

Massachusetts:

Boston and vicinity (C. A. Kaye, Boston)
Cooperative mapping program (J. O. Peper, NC)

Michigan, Gogebic Range, western part (R. G. Schmidt, NC)

Geologic mapping—Continued

Map scale 1:62,500 and larger—Continued

States and territories—Continued

Minnesota, Vermilion greenstone belt (P. K. Sims, D)

Montana:

Birney SW quadrangle (S. Volz, c, Casper, Wyo.)
Cooke City quadrangle (J. E. Elliott, D)
Craig quadrangle (R. G. Schmidt, NC)
Crazy Mountains Basin (B. A. Skipp, D)
Decker quadrangle (B. E. Law, c, D)
Elk Park quadrangle (H. W. Smedes, D)
Half Moon Hill quadrangle (V. Neirmeir, c, Casper, Wyo.)
Holmes Ranch quadrangle (N. E. Micklich, c, Casper, Wyo.)
Jordan quadrangle (G. D. Mowat, c, Billings)
Kirby quadrangle (c, Casper, Wyo.)
Lemhi Pass quadrangle (M. H. Staatz, D)
Melrose phosphate field (G. D. Fraser, c, D)
Melrose quadrangle (H. W. Smedes and G. D. Fraser, D)
Northern Pioneer Range, geologic environment (E-an Zen, NC)
Pearl School quadrangle (G. L. Galyardt, c, Casper, Wyo.)
Spring Gulch quadrangle (N. E. Micklich, c, Casper, Wyo.)
Taintor Desert quadrangle (S. Volz, c, Casper, Wyo.)
Tongue River Dam quadrangle (N. E. Micklich c, Casper, Wyo.)
Wolf Creek area, petrology (R. G. Schmidt, NC)

Nebraska, McCook 2-degree quadrangle (G. E. Prichard, D)

Nevada:

Austin quadrangle (E. H. McKee, M)
Bellevue Peak quadrangle (T. B. Nolan, NC)
Carlin region (J. F. Smith, Jr., D)
Jordan Meadow and Disaster Peak quadrangles (R. C. Greene, M)
Kobeh Valley (T. B. Nolan, NC)
Midas-Jarbridge area (R. R. Coats, M)
Round Mountain and Manhattan quadrangles (D. R. Shawe, D)
Spruce Mountain 4 quadrangle (G. D. Fraser, c, D)

New Mexico:

Acoma area (C. H. Maxwell, D)
Alamosa Mesa West quadrangle (D. B. Umshler, c, Roswell)
Alma quadrangle (J. C. Rattë, D)
Bull Basin quadrangle (J. C. Rattë, D)
Church Rock-Smith Lake (C. T. Pierson, D)
Cretaceous stratigraphy, San Juan basin (E. R. Landis, D)
Dillon Mountain quadrangle (J. C. Rattë, D)
Gallup East quadrangle (E. D. Patterson, c, Roswell)
Gallup West quadrangle (J. E. Fassett, c, Farmington)
Glenwood quadrangle (J. C. Rattë, D)
Hillsboro quadrangle (D. C. Hedlund, D)
Holt Mountain quadrangle (J. C. Rattë, D)
Iron Mountain (A. V. Heyl, Jr., D)
Laguna Peak (J. L. Ridgley, D)
Luna quadrangle (J. E. Fassett, c, Farmington)
Manuelito quadrangle (J. E. Fassett, c, Farmington)
Manzano Mountains (D. A. Myers, D)
Mongollon quadrangle (J. C. Rattë, D)
O-Block Canyon quadrangle (J. C. Rattë, D)
Ojo Encino Mesa quadrangle (D. B. Umshler, c, Roswell)

Geologic mapping—Continued

Map scale 1:62,500 and larger—Continued

States and territories—Continued

New Mexico—Continued

Pinos Altos Range (T. L. Finnell, D)
Pueblo Alto Trading Post quadrangle (R. W. Jentgen, c, Farmington)
Raton coal basin, western part (C. L. Pillmore, D)
Reserve quadrangle (J. C. Rattë, D)
Saliz Pass quadrangle (J. C. Rattë, D)
Samson Lake quadrangle (J. E. Fassett, c, Farmington)
Star Lake quadrangle (J. E. Fassett, c, Farmington)
Tanner Lake quadrangle (D. B. Umshler, c, Roswell)
Twin Butte quadrangle (M. L. Millgate, c, Farmington)
Valles Mountains, petrology (R. L. Smith, NC)

New York, Geologic correlations and mineral resources in Precambrian rocks of St. Lawrence lowlands (C. E. Brown, NC)

North Carolina, central Piedmont (A. A. Stromquist, D)

North Dakota:

Clark Butte 15-minute quadrangle (G. D. Mowat, c, Billings, Mont.)
North Almont quadrangle (H. L. Smith, c, D)

Pennsylvania (NC):

Northern anthracite field (M. J. Bergin)
Southern anthracite field (G. H. Wood, Jr.)
Wind Gap and adjacent quadrangles (J. B. Epstein)

Puerto Rico (R. D. Krushensky, NC)

South Dakota:

Black Hills Precambrian (J. A. Redden, Hill City)
Keystone pegmatite area (J. J. Norton, Rapid City)
Medicine Mountain quadrangle (J. C. Rattë, D)

Texas:

Agency Draw NE quadrangle (G. N. Pipiringos, D)
Bates Knolls quadrangle (G. N. Pipiringos, D)
Tilden-Loma Alta area (K. A. Dickinson, D)

Utah (c, D, unless otherwise noted):

Basin Canyon quadrangle (Fred Peterson)
Blackburn Canyon quadrangle (Fred Peterson)
Canaan Peak quadrangle (W. E. Bowers)
Coal mine bumps, Sunnyside mining district (F. W. Osterwald, D)
Confusion Range (R. K. Hose, M)
Crawford Mountains (W. C. Gere, c, M)
East-of-the-Navajo quadrangle (H. D. Zeller)
Fourmile Bench quadrangle (W. E. Bowers)
Horse Flat quadrangle (H. D. Zeller)
Horse Mountain quadrangle (W. E. Bowers)
Jessen Butte quadrangle (E. M. Schell, c, Casper, Wyo.)
Matlin Mountains (V. R. Todd, M)
Needle Eye Point quadrangle (H. D. Zeller)
Oak City area (D. J. Varnes, D)
Ogden 4 NW quadrangle (R. J. Hite)
Pete's Cove quadrangle (H. D. Zeller)
Salt Lake City and vicinity (Richard VanHorn, D)
Sheeprock Mountains, West Tintic district (H. T. Morris, M)
Ship Mountain Point quadrangle (H. D. Zeller)
Sunset Flat quadrangle (Fred Peterson)
Wah Wah Summit quadrangle (L. F. Hintze, Salt Lake City)
Wasatch Front surficial geology (R. D. Miller, D)
Willard Peak area (M. D. Crittenden, Jr., M)

Virginia (NC):

Culpeper basin (K. Y. Lee)

Geologic mapping—Continued

Map scale 1:62,500 and larger—Continued

States and territories—Continued

Virginia—Continued

Delmarva Peninsula (J. P. Owens)
Northern Blue Ridge (G. H. Espenshade)
Rapidan-Rappahannock (Louis Pavlides)

Washington:

Chewelah No. 4 quadrangle (F. K. Miller, M)
Glacier Park area (F. W. Cater, Jr., D)
Northern Okanogan Highlands (C. D. Rinehart, M)
Olympic Peninsula, eastern part (W. M. Cady, D)
Stevens County (R. G. Yates, M)
Togo Mountain quadrangle (R. C. Pearson, D)

Wisconsin, Black River Falls and Hatfield quadrangles (Harry Klemic, NC)

Wyoming (c, D, unless otherwise noted):

Acme quadrangle (B. E. Barnum)
Albany and Keystone quadrangles (M. E. McCallum, D)
Alkali Butte quadrangle (M. W. Reynolds, D)
Appel Butte quadrangle (G. L. Galyardt)
Badwater Creek (R. E. Thaden, D)
Bailey Lake quadrangle (M. L. Schroeder)
Beaver Creek Hills quadrangle (c, Casper)
Betty Reservoir NE quadrangle (N. McKinnie, c, Casper)
Browns Hill quadrangle (C. S. V. Barclay)
Cottonwood Rim quadrangle (C. S. V. Barclay)
Coyote Draw quadrangle (G. L. Galyardt)
Crawford Mountains (W. C. Gere, c, M)
Deer Creek quadrangle (M. L. Schroeder)
Devils Tooth quadrangle (W. G. Pierce, M)
Eagle Peak quadrangle (H. W. Smedes and H. J. Prostka, D)
Eagle Rock quadrangle (S. P. Buck, c, Casper)
Fortin Draw quadrangle (B. E. Law)
Four Bar-J Ranch quadrangle (G. L. Galyardt)
Gillette East quadrangle (B. E. Law)
Grand Teton National Park (J. D. Love, Laramie)
Greenhill quadrangle (S. P. Buck, c, Casper)
Grieve Reservoir quadrangle (C. S. V. Barclay)
Gros Ventre Range (F. S. Simons)
Hilight quadrangle (W. J. Purdon, c, Casper)
Hultz Draw quadrangle (c, Casper)
Ketchum Buttes quadrangle (C. S. V. Barclay)
Little Thunder Reservoir quadrangle (G. C. Martin, c, Casper)
Monarch quadrangle (B. E. Barnum)
Moyer Springs quadrangle (B. E. Law)
Neil Butte quadrangle (S. P. Buck, c, Casper)
North Star School NE quadrangle (S. P. Buck, c, Casper)
North Star School NW quadrangle (S. P. Buck, c, Casper)
North Star School SE quadrangle (L. Jefferies, c, Casper)
Open A Ranch quadrangle (G. C. Martin, c, Casper)
Oriva quadrangle (B. E. Law)
Pickle Pass quadrangle (M. L. Schroeder)
Pine Creek quadrangle (D. A. Jobin)
Pine Mountain-Oil Mountain area (G. J. Kerns, c, Casper)
Piney Canyon NW quadrangle (G. C. Martin, c, Casper)
Piney Canyon SW quadrangle (L. Wackwitz, c, Casper)

Geologic mapping—Continued
Map scale 1:62,500 and larger—Continued
States and territories—Continued
Wyoming—Continued
Reid Canyon quadrangle (G. J. Kerns, c, Casper)
Reno Junction quadrangle (L. Jefferies, c, Casper)
Reno Reservoir quadrangle (G. C. Martin, c, Casper)
Rough Creek quadrangle (S. P. Buck, c, Casper)
Savery quadrangle (C. S. V. Barclay)
Sheridan Pass quadrangle (W. L. Rohrer, c, Casper)
Sheridan quadrangle (E. I. Winger)
Square Top Butte quadrangle (G. J. Kerns, c, Casper)
Teckla quadrangle (J. E. Goolsby, c, Casper)
Teckla SW quadrangle (J. E. Goolsby, c, Casper)
The Gap quadrangle (G. L. Galyardt)
Tullis quadrangle (C. S. V. Barclay)
Turnercrest NE quadrangle (G. C. Martin, c, Casper)
Two Ocean Pass quadrangle (H. W. Smedes, D)
Wapiti quadrangle (W. G. Pierce, M)
Weston SW quadrangle (R. W. Jones, c, Casper)

Geologic-related hazards:
Hazards warning, preparedness, and technical assistance (D. R. Nichols, L, NC)

Geomagnetism:
External geomagnetic-field variations (W. H. Campbell, D)
Geomagnetic-data analysis (C. O. Stearns, D)
Geomagnetic observatories (J. D. Wood, D)
Geomagnetic secular variation (L. R. Alldredge, D)
Magnetic-field analysis and U.S. charts (E. B. Fabiano, D)
World magnetic charts and analysis (E. B. Fabiano, D)

Geomorphology:
Channel adjustment, Cochiti Dam (J. D. Dewey, w, Albuquerque, N. Mex.)
Forest geomorphology, Pacific coast (R. J. Janda, w, M)
Morphology, provenance, and movement of desert sand (E. D. McKee, D)
Quaternary landforms and deposits interpreted from Landsat-1 imagery, Midwest and Great Plains (R. B. Morrison, D)
States:
Arizona, post-1890 A.D. erosion features interpreted from Landsat-1 imagery (R. B. Morrison, D)
Idaho, surficial geology of eastern Snake River Plain (W. E. Scott, M. D. Hait, Jr., D)
Massachusetts, sea-cliff erosion studies (C. A. Kaye, Boston)
New Mexico, Chaco Canyon National Monument (H. E. Malde, D)
Utah, Quaternary geology (W. E. Scott, D)
Wyoming (D):
Wind River Mountains, Quaternary geology (G. M. Richmond)
Yellowstone National Park, glacial and postglacial geology (G. M. Richmond)
See also Sedimentology; Geochronological investigations.

Geophysics, regional:
Airborne and satellite research:
Aeromagnetic studies (M. F. Kane, D)
Electromagnetic research (F. C. Frischknecht, D)
Gamma-ray research (J. S. Duval, D)
Regional Studies (Isidore Zietz, NC)
Antarctica, Pensacola Mountains, geophysical studies (J. C. Behrendt, Woods Hole, Mass.)
Basin and Range geophysical studies (W. E. Davis, M)
Crust and upper mantle:
Aeromagnetic interpretation of metamorphic rocks (Isidore Zietz, NC)

Geophysics, regional—Continued
Crust and upper mantle—Continued
Aeromagnetic studies of the United States (Isidore Zietz, NC)
Analysis of traveltime data (J. C. Roller, M)
Seismicity and Earth structure (J. N. Taggart, D)
Seismologic studies (J. P. Eaton, M)
Engineering geophysics (H. D. Ackermann, D)
Florida Continental Shelf, gravity studies (H. L. Krivoy, NC)
Gravity surveys:
Dona Ana, Otero, Lincoln, Sierra, and Socorro Counties, New Mexico (D. L. Healey, D)
Maryland cooperative (D. L. Daniels, NC)
Ground-water geophysics (W. D. Stanley, D)
Magnetic chronology, Colorado Plateau and environs (D. P. Elston, E. M. Shoemaker, Flagstaff, Ariz.)
Mobile magnetometer profiles, Eastern United States (M. F. Kane, D)
New England, magnetic properties of rocks (Andrew Griscom, M)
Program and systems development (G. I. Evenden, W. L. Anderson, D)
Rainier Mesa (J. R. Ege)
Rocky Mountains, northern (D. L. Peterson, M. D. Kleinkopf, D)
Southeastern States geophysical studies (Peter Popenoe, NC)
Southwestern States geophysical studies (D. L. Peterson, NC)
Thermal modeling investigations (Kenneth Watson, D)
Ultramafic rocks, geophysical studies, intrusions (G. A. Thompson, M)
United States, aeromagnetic surveys (E. R. King, NC)
States and territories:
Alaska, Ambler River and Baird Mountains quadrangles, gravity studies (D. F. Barnes, M)
California, Sierra Nevada, geophysical studies (H. W. Oliver, M)
Idaho, Snake River Plain (D. L. Peterson, D)
Massachusetts, geophysical studies (M. F. Kane, NC)
Minnesota (NC):
Keweenawan rocks, magnetic studies (K. G. Books)
Southern part, aeromagnetic survey (E. R. King)
Nevada, engineering geophysics, Nevada Test Site (R. D. Carroll, D)
New Mexico, Rio Grande graben (L. E. Cordell, D)
Pennsylvania, magnetic properties of rocks (Andrew Griscom, M)
Puerto Rico, seismicity of Puerto Rico (A. C. Tarr, D)

Geophysics, theoretical and experimental:
Borehole electrical techniques in uranium exploration (J. J. Daniels, D)
Borehole geophysical research in uranium exploration (J. H. Scott, D)
Earthquakes, local seismic studies (J. P. Eaton, M)
Elastic and inelastic properties of Earth materials (Louis Peselnick, M)
Electrical properties of rocks (R. D. Carroll, D)
Electrical resistivity studies (A. A. R. Zohdy, D)
ERDA/DOE Geothermal Petrophysics (G. R. Olhoeft, D)
Experimental rock mechanics (C. B. Raleigh, M)
Gamma-ray spectrometry in uranium (J. S. Duval, D)
Gamma-ray spectrometry for uranium exploration in crystalline terranes (J. A. Pitkin, D)
Geomechanical studies, in-situ stress (J. R. Ege, D)
Geophysical data, interpretation using electronic computers (R. G. Henderson, NC)
Geophysical studies relating to uranium deposits in crystalline terranes (D. L. Campbell, D)
Ground-motion studies (J. H. Healy, M)

Geophysics, theoretical and experimental—Continued

Infrared and ultraviolet radiation studies (R. M. Moxham, NC)
Magnetic and luminescent properties (F. E. Senftle, NC)
Magnetic Properties Laboratory (M. E. Beck, Jr., Bellingham, Wash.)
Microwave studies (A. W. England, D)
Mineral Research Petrophysics (G. R. Olhoeft, D)
NASA Electrical properties for the detection and mapping of waters on Mars (G. R. Olhoeft, D)
NASA Laboratory microwave radar and thermal emission studies of basalt soil in vacuum (G.R. Olhoeft, D)
Paleomagnetism, Precambrian and Tertiary chronology (D. P. Elston, Flagstaff, Ariz.)
Petrophysics-Geothermal (G. R. Olhoeft, D)
Remanent magnetization of rocks (C. S. Grommé, M)
Resistivity interpretation (A. A. R. Zohdy, D)
Rock behavior at high temperature and pressure (E. C. Robertson, NC)
Seismicity patterns in time and space (C. G. Bufe, M)
Stress studies (C. B. Raleigh, M)
Theory of gamma rays for geological applications (J. S. Duval, D)
Thermal modeling investigations (Kenneth Watson, D)
Thermodynamic properties of rocks (R. A. Robie, NC)
Ultramafic intrusions, geophysical studies (G. A. Thompson, M)
Uranium geophysics in frontier areas (J. W. Cady, D)
Uranium petrophysics (G. R. Olhoeft, D)
Volcano geophysics (E. T. Endo, M)
States:
California, mass properties of oil-field rocks (L. A. Beyer, M)
Nevada (D):
Nevada Test Site:
Interpretation of geophysical logs (R. D. Carroll)
Seismic velocity measuring techniques (R. D. Carroll)
South Carolina, geoelectrical studies of the Charleston, S.C., earthquake zone (D. L. Campbell, D)
Vermont, in-situ stress in a granite quarry (G. E. Brethauer, D)

Geotechnical investigations:

Electronics instrumentation research for engineering geology (J. B. Bennetti, Jr., D)
Geotechnical measurements and services (H. W. Olsen, D)
In-situ stress, reactor hazards research (T. C. Nichols, Jr., D)
Miscellaneous landslide investigations (R. W. Fleming, D)
Open-pit slope stability (F. T. Lee, D)
Research in rock mechanics (F. T. Lee, D)
Soil engineering research (T. L. Youd, M)
States:
Colorado, coal mine deformation at Somerset (C. R. Dunrud, D)
Utah, coal mine bumps (F. W. Osterwald, D)
Virginia, Reston (S. F. Obermeier, NC)
Western United States, engineering geology investigations in Powder River basin (F. W. Osterwald, D)

Geothermal Investigations:

Broad-band electrical surveys (Mark Landisman, University of Texas)
Colorado Plateau, potential field methods (R. R. Wahl, D)
Convection and thermoelastic effects in narrow vertical fracture spaces:
Analytical techniques (Gunnar Bodvarsson, Oregon State University)
Numerical techniques (R. P. Lowell, Georgia Institute of Technology)
Development of first-motion holography for exploration (Keiiti Aki, Massachusetts Institute of Technology)

Geothermal investigations—Continued

Electrical and electromagnetic methods in geothermal areas (D. B. Jackson, D)
Evaluation of intermediate-period seismic waves as an exploration tool (D. M. Boore, Stanford University)
Evaluation of noble gas studies in exploration (Emanuel Mazor, Weizmann Institute of Science, Rehovot, Israel)
Exploration and characterization from seismic activity (E. A. Page, ENSCO, Inc.)
Geochemical exploration (M. E. Hinkle, D)
Geochemical indicators (A. H. Truesdell, M)
Geochemistry of geopressured systems (Y. K. Kharaka, w. M)
Geophysical characterization of young silicic volcanic centers, eastern Sierran Front (W. F. Isherwood, D)
Geothermal, Coachella Valley (J. H. Robison, w, M)
Geothermal coordination (F. H. Olmsted, w, M)
Geothermal geophysics (D. R. Mabey, D)
Geothermal hydrologic reconnaissance (F. H. Olmsted, w, M)
Geothermal petrophysics (G. R. Olhoeft, D)
Geothermal reservoirs (Manuel Nathenson, M)
Geothermal resource assessment (L. J. P. Muffler, M)
Geothermal studies (A. H. Lachenbruch, M)
Gravity variations as a monitor of water levels (J. M. Goodkind, University of California, San Diego)
Heat flow (J. H. Sass, A. H. Lachenbruch, M)
Isotopic and chemical studies of geothermal gases (Harmon Craig, University of California, San Diego)
Low-frequency electromagnetic prospecting system (J. Clarke and H. F. Morrison, University of California, Berkeley)
Mercury geochemistry as a tool for geothermal exploration (P. R. Buseck, Arizona State University)
Oxygen isotopes (J. R. O'Neil, M)
Physics of geothermal systems (W. H. Diment, M)
Radioactivity series isotopic disequilibrium (J. K. Osmond and J. B. Cowart, Florida State University)
Regional geoelectromagnetic traverse (J. F. Hermance, Brown University)
Regional volcanology (R. L. Smith, NC)
Remote sensing (Kenneth Watson, D)
Rock-water interactions (R. O. Fournier, M)
Seismic exploration (P. L. Ward, M)
Signal processing methods for magnetotellurics (W. C. Hernandez, ENSCO, Inc.)
Statistical characteristics of geothermal resources, Basin and Range province (W. F. Isherwood, D)
Thermal waters (D. E. White, M)
States:
Alaska, geothermal reconnaissance (T. D. Miller, M)
Arizona:
Geothermal water: Salt River Valley (R. P. Ross, w, Flagstaff) Verde Valley (P. P. Ross, w, Flagstaff)
San Francisco volcanic field (E. W. Wolfe, Flagstaff)
California:
Coso area, passive seismology (P. A. Reasenberg, M)
Geology of Long Valley-Mono basin (R. A. Bailey, NC)
Long Valley:
Active seismology (D. P. Hill, M)
Mercury in soils of geothermal areas (R. W. Klusman, Colorado School of Mines)
Microearthquake monitoring:
Imperial Valley (D. P. Hill, M)
The Geysers-Clear Lake (C. G. Bufe, M)
Mt. Lassen thermal areas (L. J. P. Muffler, M)
The Geysers area:
Seismic noise (H. M. Iyer, M)
The Geysers-Clear Lake (B. C. Hearn, Jr., NC)

Geothermal investigations—Continued
States—Continued
California—Continued
The Geysers-Clear Lake area, pre-Tertiary geology (R. J. McLaughlin, M)
Colorado:
Colorado geothermal (R. E. Moran, w, D)
Geochemical and hydrological parameters of geothermal systems (R. H. Pearl, Colorado Geological Survey)
Geothermal resources (G. L. Galyardt, c, D)
Relationship between geothermal resources and ground water (J. C. Romero, Colorado Geological Survey)
Georgia, heat flow and radioactive heat generation studies in Southeastern United States (D. L. Smith, University of Florida)
Hawaii, Kilauea Volcano, potential field methods for subsurface magma mapping (C. J. Zablocki, D)
Idaho:
Raft River surface and subsurface geology (H. R. Covington, D)
Snake River Plain surface and subsurface geology (M. A. Kuntz, D)
Sugar City area (H. J. Prostka, D)
Test drilling, Raft River valley (E. G. Crosthwaite, Boise)
Montana:
Geothermal investigations in Montana (R. B. Leonard, w, Helena)
Geothermal reconnaissance in southwestern Montana (R. A. Chadwick, Montana State University)
Nevada:
Geothermal reconnaissance (R. K. Hose, M)
Black Rock desert geothermal (A. H. Welch, w, Carson City)
New Mexico, evaluation of geothermal potential of the Basin and Range province (G. P. Landis, University of New Mexico)
Oregon:
Geophysical investigation of the Cascade Range (R. W. Couch, Oregon State University)
Geophysical investigations of the Vale-Owyhee geothermal region (R. W. Couch, Oregon State University)
Geothermal reconnaissance (N. S. MacLeod, M)
Hydrologic reconnaissance of geothermal areas (E. A. Sammel, w, M)
Hydrothermal alteration, Cascades (M. H. Beeson, M)
Utah:
Geothermal reconnaissance in Utah (F. E. Rush, w, Salt Lake City)
Geothermal resources (G. L. Galyardt, c, D)
Petrology and geochronology of late Tertiary and Quaternary volcanic rocks (W. P. Nash, University of Utah)
Regional heat flow and geochemical studies (S. H. Ward, University of Utah)
West Virginia, eastern Warm Springs (W. A. Hobba, Jr., w, Morgantown)
Wyoming, Yellowstone thermal areas, geology (M. H. Beeson, M)

Glaciology:
Electromagnetic methods for measuring snow (M. F. Meier, w, Tacoma, Wash.)
Glacier investigations (C. O. Geiger, w, Helena, Mont.)
Ice Age modelling (D. P. Adam, M)
Water, ice, and energy balance of mountain glaciers and ice physics (M. F. Meier, w, Tacoma, Wash.)

Gold:
Composition related to exploration (J. C. Antweiler, D)

Gold—Continued
Great Lakes region (D. A. Seeland, D)
States:
Alaska, Seward Peninsula, nearshore (D. M. Hopkins, M)
California, Klamath Mountains (P. E. Hotz, M)
Montana (D):
Cooke City quadrangle (J. E. Elliott)
Ore deposits, southwestern part (K. L. Wier)
Nevada (M, except as otherwise noted):
Aurora and Bodie districts, Nevada-California (F. J. Kleinhampl)
Carlin mine (A. S. Radtke)
Comstock district (D. H. Whitebread)
Dun Glen quadrangle (D. H. Whitebread)
Goldfield district (R. P. Ashley)
Round Mountain and Manhattan districts (D. R. Shawe, D)
New Mexico, placer deposits (Kenneth Segerstrom, D)
North Carolina, Gold Hill area (A. A. Stromquist, D)
Oregon-Washington, nearshore area (P. D. Snavely, Jr., M)
South Dakota, Keystone area (W. H. Raymond, D)
Wyoming, northwestern part, conglomerates (J. C. Antweiler,
See also Heavy metals.

Ground water-surface water relations:
Bank storage reconnaissance (W. D. Simons, w, M)
States:
Florida (w, Miami, except as otherwise noted):
Hydrologic base, Dade County (L. J. Swayze)
Idaho (w, Boise), hydrology:
Island Park-Henrys Lake (R. L. Whitehead)
Weiser Basin (H. W. Young)
Missouri, hydrology of Ozarks Basin (John Skelton, w, Rolla)
Nebraska, Platte Basin water resources (E. G. Lappala, w, Lincoln)
New Mexico, Pecos River, miscellaneous (G. E. Welder, w, Roswell)
Wisconsin, Hydrology, Cedar Lake (R. S. McLeod, w, Madison)

Heavy metals:
Appalachian region:
Mineral resources, Connecticut-Massachusetts (J. P. D'Agostino, NC)
South-central (A. A. Stromquist, D)
Hydrogeochemistry and biogeochemistry (T. T. Chao, D)
Mineral paragenesis (J. T. Nash, M)
Regional variation in heavy-metals content of Colorado Plateau stratified rocks (R. C. Cadigan, D)
Rocky Mountain region, fossil beach placers (R. S. Houston, Laramie, Wyo.)
Solution transport (G. K. Czamanske, M)
Southeastern States, geochemical studies (Henry Bell III, NC)
States:
Alaska (M):
Gulf of Alaska, nearshore placers (Erk Reimnitz)
Hogatza trend (T. P. Miller)
Southeastern part (D. A. Brew)
Southern Alaska Range (B. L. Reed)
Southwestern part (J. M. Hoare)
Yukon-Tanana Upland (H. L. Foster)
Idaho, Washington Peak quadrangle (D. A. Seeland, D)

Heavy metals—Continued
States—Continued
Nevada:
Aurora and Bodie districts, Nevada-California (F. J. Kleinhampl, M)
Basin and Range (D. R. Shawe, D)

Hydrologic data collection and processing:
Data file for well records (R. S. McLeod, w, Madison, Wis.)
Hydrologic probability models (W. H. Kirby, w, NC)
New Mexico data bank (D. R. Posson, w, Albuquerque)
Store-retrieve hydrologic data (G. W. Hawkins, w, Mineola, N.Y.)
See also Hydrologic instrumentation.

Hydrologic instrumentation:
Chipps Island acoustic flowmeter (S. H. Hoffard, w, M)
Drilling techniques (Eugene Shuter, w, D)
GOES data collection (E. H. Cordes, w, Miami, Fla.)
Hydrologic instrumentation (R. W. Paulson, w, NC)
Instrumentation and environmental studies (G. E. Ghering, w, D)
Instrumentation research, water (F. C. Koopman, w, Bay St. Louis, Miss.)
Interagency sedimentation project (J. V. Skinner, w, Minneapolis, Minn.)
Laser spectroscopy (M. C. Goldberg, w, D)
Optical current meter design (Winchell Smith, w, M)
Satellite data relay project (W. G. Slope, w, NC)
Suspended solids sensors (J. V. Skinner, w, Minneapolis, Minn.)
Susquehanna Landsat-DCS test (J. V. Funt, w, Harrisburg, Pa.)
Techniques of flood-plain mapping (R. H. Brown, w, Bay St. Louis, Miss.)
Telemetry evaluation program (J. F. Turner, w, Tampa, Fla.)
See also Hydrologic data collection and processing.

Hydrology, ground water:
Analysis of ground water systems (S. S. Papadopulos, w, NC)
Appalachian Basin, waste storage (P. M. Brown, w, Raleigh, N. C.)
Aquifer systems:
Field research (B. E. Lofgren, w, Sacramento, Calif.)
Theoretical aspects (D. C. Helm, w, Sacramento, Calif.)
Borehole geophysics (W. S. Keys, w, D)
Climax heater experiment (D. D. Gonzalez, w, D)
Consultation and research (C. V. Theis, w, Albuquerque, N. Mex.)
Digital modeling, ground-water flow (S. P. Larson, w, NC)
Energy transport in ground water (A. F. Moench, w, M)
Fractured hydrogeologic systems (C. R. Faust, w, NC)
Geopressured-geothermal resources (R. H. Wallace, w, Bay St. Louis, Miss.)
Ground-water geophysics research (A. A. R. Zohdy, w, D)
Ground-water staff functions (S. W. Lohman, w, D)
Ground-water tracer studies (R. J. Sun, w, NC)
Hydrologic laboratory (F. S. Riley, w, D)
Hydrology of the Madison aquifer (E. M. Cushing, w, D)
Hydrology of Wilcox Formation with reference to liquid waste emplacement in the Gulf Coastal Plain (R. H. Wallace, Jr., w, Bay St. Louis, Miss.)
Impact of mining on aquifers (N. J. King, w, D)
In-situ stress measurements (J. D. Bredehoeft, w, NC)
Liaison, U.S. Geological Survey-Bureau of Land Management (F. W. Giessner, w, D)
Limestone hydraulic permeability (V. T. Stringfield, w, NC)
Microbes in ground water (G. G. Ehrlich, w, M)
Modeling of geothermal systems (M. L. Sorey, w, M)

Hydrology, ground water—Continued
Northern Great Plains aquifer study (G. A. Dinwiddle, w, D)
Paradox basin hydrology (F. F. Rush, w, D)
Role of confining clays (R. G. Wolff, w, NC)
Southeast limestone aquifer study (R. H. Johnston, w, Atlanta, Ga.)
Transport phenomena in porous media (J. W. Mercer, w, NC)
Tropical carbonate aquifers (William Back, w, NC)
States and territories:
Alabama:
Cretaceous aquifer simulation (R. A. Gardner, w, Montgomery)
Environmental hydrogeology highways (J. C. Scott, w, Montgomery)
Water management, Madison County (J. R. Avrett, w, University)
Alaska (w, Anchorage):
Data summary, Cook Inlet (G. W. Freethey)
Ground-water appraisal, Alaska region (Chester Zenone)
Kenai Borough project (G. S. Anderson)
Arizona:
Ak Chin water supply (R. P. Wilson, w, Tucson)
Ground water to Colorado River (O. J. Loeltz, w, Yuma)
Southern Apache County (T. W. Anderson, w, Flagstaff)
Special site studies (R. D. MacNish, w, Tucson)
Water supply, Lake Mead area (R. L. Laney, w, Phoenix)
Arkansas:
Ground water, lower Mississippi region (J. E. Terry, Jr., w, Little Rock)
Hydrology of Claiborne and Wilcox (M. E. Broom, w, Little Rock)
California:
Central Valley aquifers (G. L. Bertoldi, w, Sacramento)
City of Merced ground water appraisal (R. W. Page, w, Sacramento)
Data Antelope-Valley East Kern (C. E. Lamb, w, Laguna Niguel)
Geohydrology, Mojave River basin (Anthony Buono, w, Laguna Niguel)
Ground water:
Beale Air Force Base (R. W. Page, w, Sacramento)
Hollister area (C. D. Farrar, w, M)
Indian Wells Valley (D. J. Downing, w, Laguna Niguel)
Santa Barbara (J. A. Singer, w, Santa Barbara)
Thousand Oaks (J. J. French, w, Laguna Niguel)
Ground water model—Modesto (C. J. Londquist, w. Sacacramento)
Ground water U.S. Marine Corps Twentynine Palms (W. R. Moyle, w, Laguna Niguel)
Imperial Valley geothermal model (R. E. Miller)
Owens River basin study (W. F. Hardt, w, Laguna Niguel)
Palmdale Bulge earthquake prediction (J. R. Moyle, w, Laguna Niguel)
Redding basin ground water appraisal (M. J. Pierce, w, Sacramenta)
Seawater intrusion, Soquel-Aptos (K. S. Muir, w, M)
Sole-source aquifer studies (G. L. Faulkner, w, M)
Updating ground-water information in the Eureka area (M. J. Johnson, w, M)
Water resources, Vandenberg AFB (C. E. Lamb)
Colorado (w, D):
Arkansas River basin (J. L. Huges, w, Pueblo)
Aquifer testing (F. A. Welder)
Colorado River salinity ground water (J. W. Warner,)
Ground water, Denver basin (D. E. Hillier)
Ground water investigations Rio Blanco County (F. A. Welder, w, Meeker)

Hydrology, ground water—Continued
States and territories—Continued
Colorado—Continued
Ground water studies in coal areas (J. J. D'Lugosz)
High Plains aquifer study (R. G. Borman)
Intensive monitoring northwest Colorado (R. S. Parker)
Roan-Parachute ground-water model (R. H. Dale)
Routt County ground water (T. R. Ford, w, Meeker)
West Slope aquifers (T. F. Giles, w, Grand Junction)
Connecticut (w, Hartford):
Farmington ground-water potential (D. L. Mazzeferro)
Recharge areas for stratified drift (E. H. Handman)
Florida:
Aquifer characteristics in southwest Florida (R. M. Wolansky, w, Tampa)
Biscayne aquifer (Howard Klein, w, Miami)
Dade City ground water (C. H. Tibbals, w, Orlando)
Duval County Floridan aquifer study (B. J. Franks, w, Jacksonville)
Fernandina saltwater intrusion investigation (C. B. Bentley, w, Jacksonville)
Floridan aquifer—Withlacoochee (P. W. Bush, w, Orlando)
Freshwater resources, Big Pine Key (C. E. Hanson, w, Miami)
Geohydrology, citrus irrigation (W. E. Wilson III, w, Tampa)
Ground water—Kissimmee River Basin (R. G. Belles, Jr., w, Orlando)
Hydrology, Cocoa well-field (W. D. Wood, w, Orlando)
Injecting wastes in saline aquifers (F. W. Meyer, w, Miami)
Injecting monitoring, Tampa Bay area (J. J. Hickey, w, Tampa)
New well fields, Dade County (Howard Klein, w, Miami)
Northwest Volusia (A. T. Rutledge, w, Orlando)
Potentiometric maps in Southwest Florida Water Management District (P. D. Ryder, w, Tampa)
Saltwater line, west-central Florida (E. R. Close, w, Tampa)
Sand and gravel aquifer, Escambia (Henry Trapp, w, Tallahasse)
Sarasota disposal well, phase 1 (Horace Sutcliffe, Jr., w, Sarasota)
Shallow aquifer Palm Beach County (A. L. Knight, w, Miami)
St. Johns County Shallow aquifer study (E. C. Hayes, w, Jacksonville)
Storage of storm waters (J. J. Hickey, w, Tampa)
Subsurface disposal—Pinellas (J. J. Hickey, w, Tampa)
Technical assistance, Hillsborough County (J. W. Stewart, w. Tampa)
Technical support,ground water (P. D. Ryder, w. Tampa)
Technical support, Pinellas County (B. F. Joyner, w, Tampa)
Upper East Coast (W. L. Miller, w, Miami)
Water for desalting Florida Keys (F. W. Meyer, w, Miami)
Water resources, Everglades (B. G. Waller, w, Miami)
Water resources, Lake Worth (D. V. Maddy, w, Miami)
Water supply, southwest Brevard County, (Michael Planert, w, Orlando)
Well fields, west central Florida (E. R. Close, w, Tampa)
Winter Haven lakes study (R. C. Reichenbaugh, w, Tampa)
Georgia:
Ground water, Atlanta region (C. W. Cressler, w, Doraville)
Southeast limestone aquifer study (R. E. Krause, w, Doraville)

Hydrology, ground water—Continued
States and territories—Continued
Hawaii (w, Honolulu):
Exploratory drilling (R. L. Soroos)
Honolulu basal aquifer (R. H. Dale)
Kipahulu water resources (R. L. Soroos)
Idaho:
Water resources of the Camas Prairie (H. W. Young, w, Boise)
Water resources, Rockland Valley (H. W. Young, w, Boise)
Illinois, Shallow ground water, McHenry County (J. T. Krohelski, w, DeKalb)
Indiana (w, Indianapolis):
Decatur County (T. K. Greenman, w, Indianapolis)
Elkhart ground water study (T. E. Imbrigiotta, w. Indianapolis)
Ground water availability, Taylorsville (Michael Planert)
Ground water, Upper West Fork of the River basin (W. W. Lapham)
Indiana dunes ground-water study (D. C. Gillies)
Jennings County fracture trace (William Meyer)
Johnson-Morgan ground-water study (D. C. Gillies)
Newton Jasper ground water (R. J. Shedlock)
Regional aquifer study in Indiana (R. J. Shedlock)
Southeast Indiana lineaments (T. K. Greeman, w, Indianapolis)
Vincennes ground-water study (R. J. Shedlock)
Iowa (w, Iowa City):
Cambrian-Ordovician aquifer (W. L. Steinhilber, w, Iowa City)
Hydrology of glaciated carbonate terranes (W. L. Steinhilber)
North-central Iowa (J. W. Cagle)
Pennsylvanian aquifers, coal region (J. C. Cagle, w, Iowa City)
Kansas:
Aquifer test evaluation (J. M. McNellis, w, Lawrence)
Arbuckle Group:
Liquid waste (A. J. Gogel, w, Lawrence)
Geohydrologic maps, southwestern Kansas (E. D. Gutentag, w, Garden City)
Geohydrology for planning in western Kansas (Jack Hume w, Garden City)
Hydrologic data base, Ground Water Management District 3 (H. F. Grubb, w, Garden City)
Sandstone aquifer, southwest Kansas (Jack Hume, w, Garden City)
Kentucky, Mississippi Plateau potentiometric map (T. W. Lambert, w, Louisville)
Louisiana (w, Baton Rouge):
Red River waterway study (J. E. Rogers, w, Alexandria)
Southwestern Louisiana (D. J. Nyman, w, Baton Rouge)
Washington Parish ground water (H. L. Case)
Maine (w, Augusta):
Androscoggin ground water (G. C. Prescott, Jr.)
Ground water in southwestern Maine (G. C. Prescott, Jr.)
Maine sand and gravel aquifers (G. C. Prescott)
Maryland (w, Towson):
Environmental geohydrologic studies (E. G. Otton)
Garrett County well inventory (L. J. Nutter,)
Ground water resources—urbanization Harford County (L. J. Nutter, w, Towson)
Maryland Aquifer Studies III (F. K. Mack)

Hydrology, ground water—Continued
States and territories—Continued
Maryland—Continued
Sole-source aquifer study (C. A. Richardson)
Special studies—ground water (C. A. Richardson)
Western Montgomery County ground water study (E. G. Otten, w, Towson)
Massachusetts (w, Boston):
Cape Cod sole-source aquifer (J. H. Guswa)
Coal hydrology, Massachusetts and Rhode Island (M. H. Frimpter)
Estimating maximum ground water levels (M. H. Frimpton)
Ground water:
Cape Cod (J. H. Guswa)
Martha's Vineyard (D. F. Delaney)
Nantucket (E. H. Walker)
Monitoring Cape Cod's ground water (J. H. Guswa)
Northeastern Massachusetts river basins (R. A. Brackley)
Water resources Blackstone River basin (E. H. Walker)
Michigan:
Ground water of coal deposits, Bay County, Michigan (J. R. Stark, w, Lansing)
Water resources Marquette iron range (N. G. Grannemann, w, Okemos)
Minnesota (w, St. Paul):
Ground-water appraisal, Pelican River sand plain (R. T. Miller)
Ground water:
Big Stone County (W. J. Soukup, St. Paul)
Four-county area (G. F. Lindholm)
Southwestern Minnesota (D. G. Adolphson)
Todd, Cass, Morrison Counties (D. C. Larson)
Lake Williams—water balance (D. I. Siegel)
Pelican River sand plain (D. G. Adolphson)
Reconnaissance of sand-plain aquifers (H. W. Anderson)
Regional aquifer study in Minnesota (H. O. Reeder)
Twin Cities tunnel-system hydrology (E. L. Madsen)
Water resources, Buffalo River (R. J. Wolf)
Mississippi (w, Jackson):
Hydrology-Tennessee-Tombigbee (A. G. Lamonds)
Potentiometric mapping (B. E. Wasson)
Water:
Developing areas (B. E. Wassson)
Southwest-central Mississippi (C. A. Spiers)
Missouri (w, Rolla):
Prosperity ground water (E. J. Harvey)
Regional aquifer system in Missouri (L. F. Emmett)
Water in southeastern Missouri lowlands (R. R. Luckey)
Montana:
Energy Minerals Rehabilitation Inventory and Analysis site studies (N. E. McClymonds, w, Helena)
Geohydrologic maps, Fort Union area (J. D. Stoner, w, Billings)
Geohydrologic maps, Madison aquifer (R. D. Feltis, w, Billings)
Ground water, Swan-Avon Valleys (K. R. Wilke, w, Helena)
Hydrology of paleozic rocks (W. R. Miller, w, Billings)
Mining effects, shallow water (S. E. Slagle, w, Billings)
Northern Great Plains aquifer study (G. M. Pike, w, Helena)
Powder River (W. R. Miller, w, Billings)
Pumpkin Creek (J. D. Stoner, w, Billings)
Water monitoring—coal Montana (K. R. Wilke, w, Helena)

Hydrology, ground water—Continued
States and territories—Continued
Nebraska:
Butler County, Nebraska (M. H. Ginsberg, w, Lincoln)
Hydrology Platte-Loup area NE (E. G. Lappala, w, Lincoln)
Platte-Republican watershed (J. W. Goeke, w, North Platte)
Nevada (w, Carson City):
Beatty disposal site investigation (W. D. Nichols)
Consolidated-rock water supply (T. L. Katzer)
Fernley area water resorces (F. E. Arteaga)
Ground-water levels, Topaz Lake (J. O. Nowlin)
Lemmon Valley geophysics (D. H. Schaefer)
Pumping effects on Devil's Hole (H. L. McQueen)
Storage depletion:
Pahrump Valley (J. R. Harrill)
Water resources, Walker Indian Reservation (D. H. Schaefer)
New Hampshire, ground water in Lamprey River basin (J. E. Cotton, w, Concord)
New Jersey (w, Trenton):
Digital model, Potomac-Raritan-Magothy aquifer system (J. E. Luzier)
Geohydrology, east-central New Jersey (G. M. Farlekas)
Pumpage inventory (William Kam)
New Mexico (w, Albuquerque, except as otherwise noted):
Capulin ground water (D. L. Hart)
Effects of development in northwest New Mexico (F. P. Lyford)
Elephant Butte Irrigation District well-field evaluation (C. A. Wilson, w, Las Cruces)
Geothermal hydrology, Jemez Mountains (F. W. Trainer)
Lower Rio Grande valley (C. A. Wilson)
Navajo Indian Health Service (W. L. Hiss)
Northern High Plains (E. G. Lappala)
Rio Puerco area ground water (P. F. Frenzel)
Roswell Basin, quantitative (G. E. Welder, w, Roswell)
Sandia-Manzano Mountains (D. W. Wlikins)
Water resources:
Acoma Pueblo (F. B. Lyford)
Laguna Reservation (F. P. Lyford)
Mimbres Basin (J. S. McLean)
Santa Fe (W. A. Mourant)
Water supply, Tijeras Canyon (J. D. Hudson)
Zuni (B. R. Ott)
New York:
Buried-channel aquifers, Albany (R. M. Waller, w, Albany)
Geohydrology, North Brookhaven, Long Island (E. J. Koszalka, w, Syosset)
Ground water, Oswego County (D. S. Hammond, w, Albany)
Hydrogeology of Suffolk County, New York (H. M. Jensen, w, Syosset)
Subsurface storage of chilled water (Julian Soren, w, Syosset)
North Carolina, Ground-water network review (M. D. Winner, w, Raleigh)
North Dakota (w, Bismarck, except as otherwise noted):
Ground water:
Bottineau-Rolette, North Dakota (M. R. Burkart)
Logan County (R. L. Klausing)
McHenry and Sheridan Counties (P. G. Randich)
McIntosh County (R. L. Klausing)
McKenzie County (M. G. Croft)
Ground-water availability, Fort Union coal (M. G. Croft)
Hydrology of Madison Group (D. J. Ackerman, w, Grand Forks)
Mining and reclamation, Mercer County (M. E. Crawley)
Northern Great Plains aquifer study (W. R. Scott)

Hydrology, ground water—Continued
States and territories—Continued
Ohio (w, Columbus):
Dayton digital model (S. E. Norris)
Ground water in Geauga County (V. E. Nichols)
Piketon investigation (S. E. Norris)
Salina ground-water hydrology (S. E. Norris)
Subsurface mines as source of water (J. O. Helgesen)
Oklahoma (w, Oklahoma City):
Arbuckle aquifer (R. W. Fairchild)
Ogallala model, Texas County (R. B. Morton)
Oregon (w, Portland):
Bend-Redmond ground water (J. B. Gonthier, w, Portland)
Dalles-Monmouth ground-water study (J. B. Gonthier)
Ground water, Clackamas County (A. R. Leonard)
Ground water, Hood basin (F. J. Frank)
Ground water, Newberg area (F. J. Frank)
John Day fossil beds (F. J. Frank)
Myrtle Creek ground-water study (F. J. Frank)
Reedsport water supply (F. J. Frank)
Special studies (D. D. Harris)
Pennsylvania (w, Harrisburg, except as otherwise noted):
Eisenhower well test (C. R. Wood, w, Harrisburg)
Ground water, Resources of Pike County (L. D. Carswell)
Ground water, central Columbia County (O. B. Lloyd, Jr.)
Hydrogeology:
Erie County (G. R. Schiner, w, Meadville)
Great Valley (A. E. Becher)
Hydrology of Gettysburg Formation (C. R. Wood)
Water levels and quality monitoring (W. C. Roth)
Puerto Rico:
Ground-water appraisal, Caribbean (J. E. Heisel, w, San Juan)
Ground-water reconnaissance, Central Lajas Valley, (H. J. McCoy, w, San Juan)
Water for North Coast rice (J. R. Diaz, w, San Juan)
Water-resources appraisal of St. Croix, Virgin Islands (H. J. McCoy, w, San Juan)
Rhode Island, ground water in Pawcatuck River basin (H. E. Johnston, w, Providence)
South Carolina (w, Conway, except as otherwise noted):
Assessment of ground-water resources (A. L. Zack)
Ground water resources of Sumter and Florence (B. C. Spigner, w, Columbia)
Study of geohydrologic problems (A. L. Zack)
South Dakota:
High Plains aquifer study (H. L. Case, w, Rapid City)
Hydrology of the Madison Group (L. W. Howells, w, Huron)
Northern Great Plains aquifer study (H. L. Case, w, Rapid City)
Water resources, Walworth County (E. P. LeRoux, w, Huron)
Tennessee (w, Nashville):
Ground water in the Nashville Region, Tennessee (D. R. Rima)
Hydrology of hard rock aquifers (E. F. Hollyday)
Memphis aquifer studies (W. S. Parks, w, Memphis)
Texas:
Ground water, Palo Duro Creek Basin (P. L. Rettman, w, San Antonio)
Rusk County ground water (S. J. Halasz, w, Houston)
Salinity control, Brazos and Red Rivers (S. Garza, w, Austin)
Salt dome hydrology (phase I) (J. E. Carr, w, Houston)
Trinity River alluvium (S. Garza, w, Austin)
Utah (w, Salt Lake City):
Coal-related hydrologic data (C. T. Sumsion
Hydrology, Tooele Valley area (A.G. Razem)

Hydrology, ground water—Continued
States and territories—Continued
Utah—Continued
Morgan Valley (J. S. Gates)
Navajo Sandstone, Southwestern Utah (R. M. Cordova)
Reconnaissance, Fish Springs Flat (E. L. Bolke, w, Salt Lake City)
Vermont, ground water in Rutland area (R. E. Willey, w, Montpelier)
Virginia:
Coastal plain studies (H. T. Hopkins, w, Richmond)
Fairfax County urban-area study (R. H. Johnson, w, Fairfax)
Ground water resources, Blue Ridge Parkway (H. T. Hopkins, w, Richmond)
Hydrology of James City County (J. F. Harsh w, Richmond)
Washington (w, Tacoma, except as otherwise noted):
Clallam County water resources (B. W. Drost)
Gig Harbor water resources (B. W. Drost)
Hydrologic basin analysis (K. L. Walters)
Kitsap Peninsula study (A. J. Hansen, Jr.)
Port Gamble water resources (W. E. Lum)
Shoalwater water resources (W. E. Lum)
Spokane ground-water quality (E. L. Bolke)
Swinomish ground water (B. W. Drost)
Water data for coal mining (F. A. Packard)
Water Yakima Reservation (J. A. Skrivan)
West Virginia (w, Charleston):
Ecology and underground coal mining (J. W. Borchers)
Elk River basin study (G. T. Tarver)
Guyandotte River study (J. S. Bader)
Remotely sensed ground water (W. A. Hobba, w, Morgantown)
Water resources of Tug Fork basin (J. S. Bader)
Wisconsin (w, Madison):
Ground water, Dodge County (R. W. Devaul)
Ground-water quality (P. A. Kammerer, Jr.)
Hydrogeologic maps of southeastern Wisconsin (M. G. Sherrill)
Iron River hatchery study (S. M. Hindall)
Washington-Ozaukee Counties (H. L. Young)
Water resources of Forest County (R. P. Novitzki)
Wyoming (w, Cheyenne):
Arikaree Mulestone Flat, Wyoming (D. T. Hoxie)
Bighorn Basin aquifers (M. E. Cooley)
Hanna basin water resources (S. J. Rucker, w, Cheyenne)
High Plains aquifer study (S. W. West)
Model of Bates Hole (K. C. Glover)
Northern Great Plains aquifer study (W. G. Hodson)
Paleozoic hydrology, Power River basin (J. R. Marie)
Tertiary aquifers, Laramie County (M. A. Crist)

Hydrology, surface water:
Channels, sediment loads, and streamflows (G. P. Williams, w, D)
Circulation, San Francisco Bay (T. T. Conomos, w, M)
Evaluation of low-flow runoff (W. D. Simons, w, M)
Hydrology defined by rainfall simulation (G. C. Lusby, w, D)
Isotope fractionation (T. B. Coplen, w, NC)
Numerical simulation (R. A. Baltzer, w, NC)
Runoff simulation (R. W. Lichty, w, NC)
Water-quality-model development and implementation (R. A. Baltzer, w, NC)
States;
Alabama (w, Tuscaloosa):
Environmental study, Birmingham (R. H. Bingham)
Flow charactersitics of streams (C. O. Ming, w, Montgomery)
Mobile River study (J. E. Bowie, w, Montgomery)

Hydrology, surface water—Continued

States—Continued

Alabama—Continued
- Small-stream studies (H. H. Jeffcoat)
- Travel-time studies (H. H. Jeffcoat)

Alaska, water resources of fish sites (G. A. McCoy, Anchorage)

Arizona, Flood hydrology of Arizona (B. N. Aldridge, w, Tucson)

Arkansas (w, Little Rock):
- Arkansas basin flows (G. G. Ducret)
- Characteristics of streams (M. S. Hines)

California (w, Sacramento, except as otherwise noted):
- California lakes and reservoirs (W. L. Bradford, w, M)
- Lake model test (W. L. Bradford, w, M)
- Tidal River discharge computation (R. N. Oltmann)

Colorado (w, D):
- Colorado streamflow statistics (J. F. McCain)
- Instream flow evaluation (D. P. Bauer)
- Inventory of water resources on Ft. Carson (D. A. Wentz)
- Peak discharge small watershed (R. K. Livingston)

Connecticut, Water quality of Lake Waramang (David Grason, w, Hartford)

Delaware, Delaware River master activity (F. T. Schaefer, w, Milford, Pa.)

Florida:
- Freshwater inflow to estuaries (C. L. Goetz, w, Tampa)
- Hillsborough River basin water supply (C. L. Goetz, w, Tampa)
- Hydrograph simulation studies (J. F. Turner, Jr., w, Tampa)
- Hydrology Area B, Sarasota County (H. R. Sutcliffe, w, Sarasota)
- Hydrology of lakes (G. H. Hughes, w, Tallahassee)
- Jumper Creek investigation (Warren Anderson, w, Orlando)
- Low flows in northwestern Florida (R. P. Rumenik, w, Tallahassee)
- Regional flood frequency study (J. F. Turner, w, Tampa)
- Small stream flood frequencies (W. C. Bridges, w, Tallahassee)
- Volusia wetlands delineation (P. W. Bush, w, Orlando)

Georgia (w, Doraville):
- Seasonal low flow (T. R. Dyar)
- Storage requirements for Georgia streams (R. F. Carter)
- Time-of-travel Georgia streams (J. L. Pearman)

Idaho, Bedload in North Fork Teton River (R. P. Williams, w, Boise)

Illinois:
- Dam ratings (L. G. Davis, w, DeKalb)
- Illinois River miles (R. W. Healy, w, Champaign)
- T and K studies on Illinois streams (B. J. Prugh, w, Champaign)

Indiana:
- Coal mine lakes (S. E. Regone, w, Indianapolis)
- Mapping of Big Long Lake (R. R. Contreras, w, Indianapolis)
- River mileage (G. E. Nell, w, Indianapolis)

Kansas (w, Lawrence):
- Channel geometry, coal areas (E. E. Hedman)
- Channel geometry, Kansas River (W. R. Osterkamp)
- Channel geometry regulated streams (E. E. Lawrence)
- Flood investigations (H. R. Hejl, Jr.)
- Sediment-active geometry (W. R. Osterkamp)
- Soldier Creek (W. J. Carswell)

Hydrology, surface water—Continued

States—Continued

Kansas—Continued
- Streamflow characteristics (P. R. Jordan)
- Water yield, Kansas (W. J. Carswell, w, Lawrence)

Kentucky, Green River model study (T. W. Hale, w, Louisville)

Louisiana (w, Baton Rouge):
- Characteristics of streams (M. J. Forbes, Jr.)
- Small-stream flood frequency (A. S. Lowe)

Maine (w, Augusta):
- Drainage areas (D. J. Cowing):
- Hydrology of selected Maine rivers (D. J. Cowing)
- Water resources (G. C. Prescott, w, Augusts)

Maryland, Low-flow studies in Maryland (R. H. Simmons, w, Towson)

Minnesota ,Bridge site, project reports (C. H. Carlson, w, St. Paul)

Mississippi, documentation of bridge backwater (B. E. Colson, w, Jackson)

Montana (w, Helena, unless otherwise noted):
- Bridge-site investigations (R. J. Omang)
- Peak flow, small drainage areas (R. J. Omang)
- Watershed model (L. E. Cary, w, Billings)

Nevada, Lake Mead recreation area flood hazards (Otto Moosburner, w, Carson City)

New Jersey, base flow studies (R. D. Schopp, w, Trenton)

New Mexico, runoff from channel geometry (J. P. Borland, w, Santa Fe)

New York (w, Albany):
- Acid-rain—Adirondacks (D. E. Troutman)
- Low-flow study (B. B. Eissler)
- Reaeration studies (D. E. Troutman)
- Stream gazetteer (L. A. Wagner)
- Time-of-travel studies (D. E. Troutman)

North Carolina (w, Raleigh):
- Channelization effects, Chicod Creek (C. E. Simmons)
- Data site information for 208 study (C. E. Simmons)
- Effect of land use on stream quality (C. E. Simmons)
- Regionalization—minimum streamflows (R. C. Heath)

Ohio (w, Columbus):
- Hydraulics of bridge sites (W. O. Thomas)
- Low flow of Ohio streams (R. I. Mayo)
- Rural hydrology (E. E. Webber, w, Columbus)
- Time-of-travel studies of Ohio streams (A. O. Westfall)

Oklahoma, coal field hydrology (S. J. Playton, w, Oklahoma City)

Oregon, Oregon lakes and reservoirs (D. D. Harris, w, Portland)

Pennsylvania (w, Harrisburg):
- Flow routing, Susquehanna River (D. L. Bingham)
- Low-flow regionalization (H. N. Flippo)
- Mean discharge—Pennsylvania (H. N. Flippo)
- Time of travel, Lehigh River (C. D. Kaufman)

Puerto Rico, Islandwide 208 assistance study (Fernando Gomez-Gomez, w, San Juan)

South Carolina (w, Columbia):
- Data reports, flood forecasting (C. S. Bennett)
- Low-flow characteristics (W. M. Bloxham)

South Dakota (w, Huron):
- Flood-frequency study (L. D. Becker)
- Small-stream flood frequency (L. D. Becker)

Tennessee (w, Nashville, except as otherwise noted):
- Miscellaneous data services (V. J. May)

Hydrology, surface water—Continued

States—Continued

Tennessee—Continued

Tennessee bridge scour (W. J. Randolph)

Texas (w, Austin, except as otherwise noted):

Small watersheds (B. O. Massey)

Trinity River time-of-travel studies (R. H. Ollman, w, Fort Worth)

Utah, mined lands rehabilitation (G. W. Sandberg, w, Cedar City)

Washington (w, Tacoma):

Duwamish toxicant study (E. A. Prych)

Low flow of Washington streams (P. J. Carpenter)

Lower Elwha Project (K. L. Walters)

Makah Project (K. L. Walters)

Newaukum basin study (E. R. Prych)

Tulalip water resources (B. W. Drost)

Unregulated flow at Union Gap (D. E. LaFrance)

Water resources of the Hoh Indian Reservation (W. E. Lum)

West Virginia, small drainage areas (G. S. Runner, w, Charleston)

Wisconsin (w, Madison):

Flood-frequency study (D. H. Conger)

Low-flow stream geometry (L. B. House)

Low-flow study (W. A. Gebert)

Nonpoint source pollution (S. J. Field)

Pheasant Branch study (R. S. Grant)

Streamflow estimates in lake basins (R. P. Novitzki)

Water-quality control (B. K. Holstrom)

See also Evapotranspiration; Flood investigations; Marine hydrology; Plant ecology; Urbanization, hydrologic effects.

Industrial minerals. *See* specific minerals.

Iron:

Resource studies, United States (Harry Klemic, NC)

States:

Michigan, Gogebic County, western part (G. G. Schmidt, NC)

Wisconsin, Black River Falls (Harry Klemic)

Isotope and nuclear studies:

Instrument development (F. J. Jurceka, D)

Isotope fractionation (T. B. Coplen II, w, NC)

Isotope ratios in rocks and minerals (Irving Friedman, D)

Isotopic hydrology (F. J. Pearson, w, NC)

Lead isotopes and ore deposits (R. E. Zartman, D)

Mass spectrometry and isotopic measurements (J. S. Stacey, D)

Nuclear irradiation (G. M. Bunker, D)

Radioisotope dilution (L. P. Greenland, NC)

Reactor facility (G. P. Kraker, Jr., w, D)

Stable isotopes and ore genesis (R. O. Rye, D)

Upper mantle studies (Mitsunobu Tatsumoto, D)

See also Geochronological investigations; Geochemistry, water; Radioactive-waste disposal.

Land resources analysis:

Idaho, eastern Snake River Plain region (S. S. Oriel, D)

Land subsidence:

Geothermal subsidence, Mexicali (B. E. Lofgren, w, Sacramento, Calif.)

Geothermal subsidence research (B. E. Lofgren, w, Sacramento, Calif.)

Land subsidence studies (B. E. Lofgren, w, Sacramento, Calif.)

Land subsidence—Continued

States:

Arizona:

Land subsidence-earth fissures (R. L. Laney, w, Phoenix)

Subsidence fissures, Tucson basin (L. J. Mann, w, Tuscon)

New Jersey, Land subsidence (William Kam, w, Trenton)

New Mexico, land subsidence in the Known Potash Leasing Area (M. L. Millgate, c, Roswell)

Texas, coastal subsidence studies (R. K. Gabrysch, w, Houston)

Land use and environmental impact:

Accuracy assessment of land use and land cover maps produced from Landsat digital data (G. H. Rosenfield, 1, NC)

Barrier island land use and land cover (H. F. Lins, Jr., 1, NC)

Geographic Information Systems software development (W. B. Mitchell, l, NC)

Geographic Information Systems operation and development (W. B. Mitchell, 1, NC)

Hazard prediction and warning, socioeconomic and land use planning implications (R. H. Alexander, l, Boulder, Colo.)

Impact of the oil and gas industry on the Louisiana coast (D. W. Davis, J. L. Place, l, NC)

Land use and land cover:

Land use map accuracy determination (K. A. Fitzpatrick-Lins, l NC)

Land use pattern analysis (C. W. Spurlock, 1, Gainesville, Fla.)

Mapping and data compilation (G. L. Loelkes, l, NC)

Mapping in Alaska based on Landsat digital data (Leonard Gaydos, 1, Moffett Calif.)

Maps and data and other geographic studies (J. R. Anderson, 1, NC)

Land use impact on solar-terrestrial energy systems (R. W. Pease, l, NC)

Mid-Atlantic land information and analysis study (R. H. Alexander, l, NC)

Multidisciplinary studies:

Culpeper Basin earth sciences applications study (A. J. Froelich, NC)

Earth-science information for decisionmakers (R. D. Brown, Jr., M)

Review and analysis of USGS spatial data handling (Olaf Kays, l, NC)

States:

Colorado, environmental and resource demonstration study, Front Range urban corridor (W. R. Hansen, D)

Virginia, Earth-science applications study in Fairfax County (A. J. Froelich, NC)

Washington, Puget Sound region, earth sciences applications study, (B. R. Foxworthy, w, Seattle)

See also Construction and terrain problems; Urban geology; Urban hydrology.

Lead, zinc, and silver:

Lead resources of United States (C. S. Bromfield, D)

Zinc resources of the United States (Helmuth Wedow, Jr., Knoxville, Tenn.)

States:

Alaska, southwest Brooks Range (I. L. Tailleur, M)

Colorado (D):

San Juan Mountains:

Eastern, reconnaissance (W. N. Sharp)

Northwestern (F. S. Fisher)

Lead, zinc, and silver—Continued
States—Continued
Illinois-Kentucky district, regional structure and ore controls (D. M. Pinckney, D)
Nevada (M):
Comstock district (D. H. Whitebread)
Silver Peak Range (R. P. Ashley)
Utah, Park City district (C. S. Bromfield, D)

Limnology:
Interrelations of aquatic ecology and water quality (K. V. Slack, w, M)
Oxygen cycle in streams (R. E. Rathbun, w, Bay St. Louis, Miss.)
Relation of ground water to lakes (T. C. Winter, w, D)
Water quality of impoundments (J. L. Barker, w, Harrisburg, Pa.)
States and territories:
Colorado, lake reconnaissance (D. A. Wentz, w, D)
Maine, Limnological study of lakes (D. J. Cowing, w, Boston, Mass.)
Massachusetts, Hager Pond nutrient study (W. D. Silvey; w, Boston)
Montana, limnology of Valley County lakes (R. F. Ferreira, w, Helena)
Ohio, limnology of selected lakes (C. G. Angelo w, Columbus)
Puerto Rico, Quality of water, Lago Carraizo (Ferdinand Quinones-Marquez,w, San Juan)
Wisconsin, hydrology of lakes (R. W. Devaul, w, Madison)
See also Quality of water.

Lithium:
Cenozic deposit history (J. R. Davis, D)
Exploration for and resource appraisal of nonpegmatite deposits (J. D. Vine, D)
Geochemistry of lithium clays (R. K. Glanzman, D)
Regional distribution (E. F. Brenner-Tourtelot, D)

Lunar geology. *See* Extraterrestrial studies.

Manganese. *See* Ferro-alloy metals.

Marine geology:
Atlantic Continental Shelf:
Environmental impact of petroleum exploration and production (H. J. Knebel, Woods Hole, Mass.)
Geophysics studies (J. C. Behrendt, Woods Hole, Mass.)
Magnetic chronology (E. M. Shoemaker, D. P. Elston, Flagstaff, Ariz.)
New England coastal zone (R. N. Oldale, Woods Hole, Mass.)
Organic geochemistry of Atlantic Continental Shelf and nearshore environments (R. E. Miller, NC)
Site surveys (W. P. Dillon, Woods Hole, Mass.)
Stratigraphy (J. C. Hathaway, Woods Hole, Mass.)
Stratigraphy and structure (J. S. Schlee, Woods Hole Mass.)
Caribbean and Gulf of Mexico:
Coastal environments (H. L. Berryhill, Corpus Christi, Tex.)
Estuaries (C. W. Holmes, Corpus Christi, Tex.)
Mississippi delta studies (L. E. Garrison, Corpus Christi Tex.)
Natural resources and tectonic features (R. G. Martin, Jr., Corpus Christi, Tex.)
Oil migration and diagenesis of sediments (C. W. Holmes, Corpus Christi, Tex.)
Tectonics, Caribbean (J. E. Case, Corpus Christi, Tex.)

Marine geology—Continued
Carribbean and Gulf of Mexico—Continued
Tectonics, Gulf (L. E. Garrison, Corpus Christi, Tex.)
Geotechnical investigations (D. A. Sangrey, D)
Marine mineral resources, worldwide (F. H. Wang, M)
Pacific and Arctic geochemistry of sediments (W. E. Dean, D)
Pacific coast sedimentology (H. E. Clifton, M)
Pacific Ocean, biostratigraphy, deep ocean (J. D. Bukry, La Jolla, Calif.)
Pacific reef studies (J. I. Tracey, Jr., NC)
Small Boat Surveys, Harley J. Knebel (Woods Hole, Mass)
Spanish Continental Margin (Almeria Province) (P. D. Snavely, Jr., H. G. Greene, H. F. Clifton, W. P. Dillon, J. M. Robb, M)
Volcanic geology, Mariana and Caroline Islands (Gilbert Corwin, NC)
World offshore oil and gas (T. H. McCulloh, Seattle, Wash.)
States and territories:
Alaska (M, except as otherwise noted):
Arctic coastal marine processes (Erik Reimnitz)
Beaufort-Chuckchi Sea Continental Shelf (Arthur Grantz)
Beaufort Sea environment studies (P. W. Barnes)
Bering Sea:
General study (D. W. Scholl)
Northern:
Environmental geologic studies (C. H. Nelson)
Sea floor (C. H. Nelson)
Coastal environments (A. T. Ovenshine)
Continental Shelf resources (D. M. Hopkins)
Cook Inlet (L. B. Magoon III)
Gulf of Alaska (B. F. Molnia)
Seward Peninsula, nearshore (D. M. Hopkins)
Tectonic history (R. E. von Huene, NC)
California (M):
Borderlands:
Geologic framework (A. E. Roberts)
Southern part (G. W. Moore)
Continental Margin, central part (E. A. Silver)
La Jolla marine geology laboratory (G. W. Moore)
Monterey Bay (H. G. Greene)
San Francisco Bay:
General study (D. S. McCulloch)
Geochemistry of sediments (D. H. Peterson)
Oregon, land-sea transect, Newport (P. D. Snavely, Jr., M)
Oregon-California, black sands (H. C. Clifton, M)
Oregon-Washington, nearshore (P. D. Snavely, Jr., M)
Puerto Rico, coooperative program (J. V. A. Trumbull, Santurce)
Texas, barrier islands (R. E. Hunter, Corpus Christi)

Marine hydrology:
Hydrologic-oceanographic studies (F. A. Kohout, w, Woods Hole, Mass.)
States and territories:
Maryland, estuarine ecology (R. L. Cory, w, Edgewater)
Puerto Rico, San Juan lagoons (S. R. Ellis, w, San Juan)
See also Hydrology, surface water; Quality of water; Geochemistry, water; Marine geology.

Mercury:
Geochemistry (A. P. Pierce, D)
Mercury deposits and resources (E. H. Bailey, M)
State:
California, Coast Range ultramafic rocks (E. H. Bailey, M)

Meteorites. *See* Extraterrestrial studies.

Mine drainage and hydrology
- Chemical models—coal hydrology (D. C. Thorstenson, w, Dallas, Tex.)
- Water monitoring-coal mining, Northeastern region (F. T. Schaefer, w, NC)
- *States:*
- Georgia, Water monitoring—coal mining (C. L. Sanders, w, D)
- Illinois (w, Champaign):
  - Mine reclamation hydrology (E. A. Magner)
  - Water monitoring-coal mining (L. G. Davis)
- Indiana (w, Indianapolis):
  - Uranium, remote sensing for uranium exploration (G. L. Raines, D)
  - Effects of Strip Mining and Reclamation (D. E. Renn)
- Kentucky (w, Louisville):
  - Coal-mining effects:
    - Grapevine Creek (J. E. Dysart)
  - Downstream effects of coal mining (J. E. Dysart)
  - Water from coal mines (D. S. Mull)
- Maryland, Water monitoring—coal mining (W. W. Staubitz, w, Towson)
- Mississippi, plan for study of lignite hydrology (G. J. Dalsin, w, Jackson)
- Montana, East Trail Creek (W. R. Hotchkiss, w, Helena)
- New Mexico, San Juan coal monitoring (J. D. Dewey, w, Albuquerque)
- Ohio, Mine reclamation, Lake Hope Basin (T. M. Crouch, w, Columbus)
- Pennsylvania (w, Harrisburg):
  - Coal hydrology of Big Sandy Creek (D. L. Bingham)
  - Daylighting—hydrology of Babb Creek (L. A. Reed)
  - Water monitoring—coal mining (J. R. Ritter)
  - Western Middle anthracite hydrology (D. J. Growitz)
- Tennessee, Landsat basin characteristics (E. F. Hollyday, w, Nashville)
- Utah (w, Salt Lake City):
  - Huntington coal hydrology (T. W. Danielson)
  - Ferron sandstone, Castle Valley (G. C. Lines)
  - Water monitoring—coal mining Utah (K. M. Waddell)
- Virginia, Reconnaissance of coal areas (S. M. Rogers, w, Richmond)
- West Virginia (w, Charleston):
  - Deep-mine collapse hydrology (W. H. Hobba)
  - Quantitative mine-water studies (G. G. Wyrick)
  - Water monitoring—coal mining (D. H. Appel)
- Wyoming, water monitoring coal mining (S. A. Druse, w, Cheyenne)

Mineral and fuel resources—compilations and topical studies:
- Application massive sulfides, Virginia deposits (J. E. Gair, NC)
- Arctic mineral-resource investigations (R. M. Chapman, M)
- Basin and Range, geologic studies (F. G. Poole, D)
- Colorado Plateau (R. P. Fischer, D)
- Information bank, computerized (J. A. Calkins, NC)
- Mineral-resource surveys:
  - Mineral resource estimation (W. D. Menzie, M)
  - Mineral resources of Precambrian rocks in St. Lawrence County, New York (C. E. Brown, NC)
  - Minerals for energy production (L. F. Rooney, NC)
  - Primitive and Wilderness Areas:
    - Beaver Creek, Kentucky (K. J. Englund, NC)
    - Big Frog Wilderness Study Area, Tennessee (J. E. Gair, NC)

Mineral and fuel resources—Continued
- Mineral-resource surveys—Continued
  - Primitive and Wilderness Areas—Continued
    - Bob Marshall Wilderness Area, Montana (R. L. Earhart, D)
    - Caney Creek Wilderness, Arkansas (G. E. Erickson, NC)
    - Cohutta Wilderness, Georgia-Tennessee (J. E. Gair, NC)
    - Elkhorn Wilderness Study Area, Montana (W. R. Greenwood, D)
    - Ellicott Rock Wilderness, South Carolina—North Carolina—Georgia (R. W. Luce, NC)
    - Gates of the Mountains Wilderness Area, Montana (M. W. Reynolds, D)
    - Gee Creek Wilderness, Tennessee (J. E. Epstein, NC)
    - Glacier Bay National Monument Wilderness Area, Alaska (D. A. Brew, M)
    - James River Face, Virginia (C. E. Brown, NC)
    - John Muir Wilderness, California (N. K. Huber, M)
    - King Range—Chemise Mountains, California (R. J. McLaughlin, M)
    - Linville Gorge Wilderness, North Carolina (J. P. D'Agostino, NC)
    - Mount Hood and Zigzag Wilderness Areas, Oregon (T. E. C. Keith M)
    - Otter Creek Wilderness, West Virginia (K. J. Englund, NC)
    - Pecos Wilderness, New Mexico (R. H. Moench, D)
    - Rawah Wilderness Area and nearby study areas, Colorado (R. C. Pearson, D)
    - Selway-Bitterroot Wilderness, Idaho and Montana (W. R. Greenwood, D)
    - Shining Rock Wilderness, North Carolina (F. G. Lesure, NC)
    - Sipsey River, Alabama (S. P. Schweinfurth, NC)
    - Snow Mountain Wilderness Area, California (D. Grimes, D)
    - Snowy Range Wilderness Study Area, Wyoming (R. S. Houston, D)
    - Superstition Wilderness, Arizona (D. W. Peterson, D)
    - Washakie Wilderness, Wyoming (J. C. Antwiler, D)
    - West Chichagof-Yakobi Wilderness Study Area, Alaska (B. R. Johnson, M)
- Nonmetallic deposits, mineralogy (B. M. Madsen, M)
- Oil and gas resources:
  - Central and northern California Continental Shelf (C. W. Spencer, D)
  - Outer Continental Shelf (R. B. Powers, E. W. Scott, D)
  - Permian Basin (G. L. Dolton, S. E. Frezon, Keith Robinson, A. B. Coury, K. L. Varnes, D)
  - Petroleum potential of southern California borderland appraised (C. W. Spencer, D)
- Resource analysis, economics of mineral resources (J. H. DeYoung, Jr., NC)
- Wilderness Program:
  - Geochemical services (D. J. Grimes, D)
  - Geophysical services (M. F. Kane, D)
- *States:*
- Alaska (M):
  - AMRAP Program (J. E. Case)
  - Mineral resources (E. H. Cobb)
  - Petersburg quadrangle (D. A. Brew)
  - Southwestern Brooks Range (I. L. Tailleur)
- Colorado, Summitville district, alteration study (R. E. Van Loenen, D)

Mineral and fuel resources—Continued
States—Continued
Missouri, Rolla 2-degree quadrangle, mineral-resource appraisal (W. P. Pratt, D)
Nevada, igneous rocks and related ore deposits (M. L. Silberman, M)
United States:
Central States, mineral-deposit controls (A. V. Heyl, Jr., D)
Iron-resources studies (Harry Klemic, NC)
Lightweight-aggregate resources (A. L. Bush, D)
Metallogenic maps (P. W. Guild, NC)
Northeastern States, peat resources (C. C. Cameron, NC)
Southeastern States, mineral-resource surveys (R. A. Laurence, Knoxville, Tenn.)
Wisconsin, northern, mineral-resource survey (C. E. Dutton, Madison)
See also specific minerals or fuels.

Mineralogy and crystallography, experimental:
Crystal chemistry (Malcolm Ross, NC)
Crystal structure, sulfides (H. T. Evans, Jr., NC)
Electrochemistry of minerals (Motoaki Sato, NC)
Mineralogic services and research (R. C. Erd, M)
Mineralogical crystal chemistry (J. R. Clark, M)
Mineralogy of heavy metals (F. A. Hildebrand, D)
Planetary mineralogical studies (Priestley Toulmin III, NC)
Research on ore minerals (B. F. Leonard, D)
See also Geochemistry, experimental.

Minor elements:
Geochemistry (George Phair, NC)
Niobium:
Colorado, Wet Mountains (R. L. Parker, D)
Niobium and tantalum, distribution in igneous rocks (David Gottfried, NC)
Phosphoria Formation, statigraphy and resources (R. A. Gulbrandsen, M)
Nonpegmatic lithium resources (J. D. Vine, D)
Rare-earth elements, resources and geochemistry (J. W. Adams, D)
Trace-analysis methods, research (F. N. Ward, D)

Model studies, geologic and geophysical:
Computer modeling:
Rock-water interactions (J. L. Haas, Jr., NC)
Tectonic deformation (J. H. Dieterich, M)
Ice Ages (D. P. Adam, M)

Model studies, hydrologic:
Alluvial fan deposition (W. E. Price, w, NC)
Atchafalaya River Basin model (M. E. Jennings, w, Bay St. Louis, Miss.)
Ground-water hydrology, strip-mining areas (J. O. Helgesen, w, Columbus, Ohio)
High Plains Aquifer Study (J. B. Weeks, w, D)
Hydrodynamics of a tidal estuary (R. T. Cheng, w, M)
Miocene aquifer study (E. T. Baker, Jr., w, Austin, Tex.)
Modeling organic solute transport (J. B. Robertson, w, M)
Nevada Test Site hydrologic model (D. I. Leap, w, D)
Numerical simulation (V. C. Lai, w, NC)
Operation models, surface-water systems (M. E. Jennings, w, Bay St. Louis, Miss.)
Physical modeling (V. R. Schneider, w, Bay St. Louis, Miss.)
Rainfall-runoff modeling (G. H. Leavesley, w, D)
Regional Studies Coordination (G. D. Bennett w, NC)
Simulation of hydrogeologic systems (R. L. Cooley, w, D)
Streamflow models (P. R., Jordan, w, Lawrence, Kans.)
Surface-water-quality modeling (S. M. Zand, w, M)
Systems Analysis Laboratory (I. C. James, w, NC)
Transient flow (C. E. Mongan, w, Cambridge, Mass.)
Transport in fluid flow (Akio Ogata, w, M)

Model studies, hydrologic—Continued
Water-quality modeling (D. B. Grove, w, D)
Watershed modeling (J. F. Turner, w, Tampa, Fla.)
States:
Arizona:
Coconino aquifer—Apache County, Arizona (P. P. Ross, w, Phoenix)
Southwest alluvial basins (T. W. Anderson, w, Tucson)
Arkansas (w, Little Rock):
Bartholomew Stream Flow Subsystem (M. E. Broom)
Illinois River model (C. T. Bryant)
California:
Antelope Valley ground water model (J. R. Freckeiton, w, Laguna Niguel)
Digital model of Carmel Valley (M. J. Johnson, w, M)
Ground water Model Fresno County (H. T. Mitten, w, Sacramento)
Impact of Marble Cone Fire (K. W. Lee, w, M)
Sacramento Valley groundwater (P. W. Anttila, w, Sacramento)
Salinas ground-water model (M. J. Johnson, w, M)
Water supply forecast evaluation (K. L. Wahl, w, M)
Colorado:
Geochemical investigation (S. G. Robson, w, D)
Narrows Reservoir model (A. W. Burns, w, D)
Rocky Mountain Arsenal DIMP contamination (S. G. Robson, w, D)
Water management—High Plains (R. G. Borman, w, D)
Delaware:
Aquifer model studies—Delaware (A. L. Hodges, Jr., w, Dover)
Delaware Potomac Aquifer Study (P. P. Leahy, w, Dover)
Florida:
Ground water, Ft. Lauderdale (Ellis Donsky, w, Miami)
Hydrologic effects West-Central Florida (W. E. Wilson, w, Tampa)
Loxahatchee River basin model (D. V. Maddy, w, Miami)
Water resources Ft. Walton Beach area (L. R. Hayes w, Tallahassee)
Watershed modeling (J. F. Turner, w, Tampa)
Georgia (w, Doraville):
Ground water models (H. B. Counts)
Cretaceous-Tertiary Aquifer ( )
Tertiary limestone ( )
Idaho, Rathdrum Prairie aquifer (H. R. Seitz, w, Boise)
Indiana (w, Indianapolis):
Dissolved Oxygen Modeling and Assimilation Studies (S. E. Ragone)
Logansport ground-water study (D. C. Gillies)
Kansas, ground water-surface water, north-central Kansas (L. E. Stullken, w, Garden City)
Maryland (w, Towson):
Aquia-Piney Point-Nanjemoy aquifers (J. F. Williams)
Ground water from Maryland coastal plain (W. B. Fleck)
Small basin modelling (L. J. Nutter)
Massachusetts, De-icing chemicals, ground water (L. R. Frost, w, Boston)
Minnesota, evaluation of quality-of-water, data for management (M. S. McBride, w, St. Paul)
Mississippi:
Documentation of bridge backwater (B. E. Colson, w, Jackson)
Modeling of Tupelo ground-water system (J. M. Kernodle w, Jackson)

Model studies, hydrologic
States—Continued
Mississippi—Continued
Tennessee-Tombigbee Divide digital model (M. S. McBride, w, St. Paul)
Nebraska (w, Lincoln):
High Plains Aquifer Study (M. J. Ellis)
Irrigation districts in southwestern Nebraska (E. G. Lappala)
Willow Creek dam site (E. G. Lappala)
Nevada (w, Carson City):
Eagle Valley ground-water model (F. E. Artega)
Jones-Galena Creek water resources (T. L. Katzer)
Las Vegas Valley Ground-Water Models (J. R. Harrill)
Sediment Transport Model E. FK. Carson R. (T. L. Katzer)
New Jersey (w, Trenton):
Englishtown Formation (W. D. Nichols)
Multilayer Simulation, Central New Jersey (G. M. Farlekas)
Simulation of multilayer aquifer (A. W. Harbaugh)
New York:
Hudson River estuary flow model (W. N. Embree, w, Albany)
Hydrologic modeling, phase 2 (T. E. Reilly, w, Syosset)
Impact and Mitigation of Sewering (G. E. Kimmel, w, Syosset)
Tioughnioga River ground water (O. J. Cosner, w, Albany)
Ohio, Franklin County digital model (E. J. Weiss, w, Columbus)
Oklahoma (w, Oklahoma City):
North Canadian hydrology (R. E. Davis)
Coal Creek Basin, (S. J. Playton)
Great Salt Plains Study (J. E. Reed)
High Plains Aquifer Study (J. E. Reed)
Oregon, Portland Well Field Model (J. E. Luzier, w, Portland)
Pennsylvania (w, Harrisburg):
Delaware River streamflow model (J. O. Shearman)
Flow routing Chemung (J. T. Armbruster)
Flow simulation, Juniata River (J. T. Armbruster)
Laurel Run Dam Failure (J. R. Armbruster)
Schuylkill River Quality of Water (T. H. Yorke)
South Dakota, water resources of Big Sioux Valley (N. C. Koch, w, Huron)
Tennessee, Memphis ground-water model (J. V. Brahana, w, Nashville)
Texas, High Plains Aquifer Study (I. D. Yost, w, Austin)
Utah, Hydrology of Beryl-Enterprise area (R. W. Mower, w, Salt Lake City)
Washington (w, Tacoma):
Columbia River basalt model (D. B. Sapik)
Ground water-surface water model (E. A. Prych)
Spokane drainfield study(J. A. Skrivan)
Wisconsin (w, Madison):
Digital streamflow model, Rock River (W. R. Krug)
Land-Use Changes, Southwest Wisconsin, (W. R. Krug)
Nonpoint pollution in Fox basin (P. E. Hughes)
Wisconsin River model (W. R. Krug)
Wyoming, Digital Model La Grange Area (W. B. Borchert, w, Cheyenne)
Molybdenum. *See* Ferro-alloy metals.
Moon studies. *See* Extraterrestrial studies.
Nickle. *See* Ferro-alloy metals.
Nuclear explosions, geology:
Engineering geophysics, Nevada Test Site (R. D. Carroll, D)
Environmental effects (P. P. Orkild, D)
Geologic investigations:
Computer-stored physical properties data (J. R. Ege, D)
Nevada Test Site:
Nevada Test Site (P. P. Orkild, D)
Northern Yucca Flat and Pahute Mesa (W. D. Quinlivan, D)
Pahute Mesa and central and southern Yucca Flat (G. L. Dixon, D)
Geomechanical investigations, Nevada Test Site (J. R. Ege, D)
Nuclear explosions, hydrology:
Nuclear explosive underground engineering, hydrology (J. E. Weir, w, D)
Yucca flat hydrology (G. C. Doty, w, Mercury, Nev.)
States:
Alaska, hydrology of Amchitka Island Test Site (D. D. Gonzalez, w, D)
Nevada (w, D), Nevada Test Site:
Central, hydrology (G. A. Dinwiddie)
Hydrology (W. W. Dudley, Jr.)
Oil shale:
East-central Uinta Basin (G. N. Pipiringos, D)
Oil shale and associated minerals (J. L. Renner, c, D)
Organic geochemistry (R. E. Miller, D)
Petrology (J. R. Dyni, D)
Regional geochemistry (W. E. Dean, Jr., D)
Stratigraphic studies, eastern Uinta Basin (W. B. Cashion, Jr., D)
Trace elements (W. E. Dean, Jr., D)
States:
Alaska, Anatuvuk Pass (G. B. Shearer, c, Anchorage)
Colorado (D):
Central Roan Cliffs area (W. J. Hall, D)
Lower Yellow Creek area (W. J. Hall)
Piceance Creek basin:
East-central (R. B. O'Sullivan)
Experimental mining (R. P. Snyder)
General (J. R. Donnell)
Northwestern (G. N. Pipiringos)
Stratigraphy of the Green River Formation (R. C. Johnson, D)
Colorado-Utah-Wyoming, geochemistry (W. E. Dean, Jr., D)
Colorado-Wyoming, Eocene rocks (H. W. Roehler, D)
Utah, South 1/2 Nutters Hole quadrangle (W. B. Cashion, Jr., D)
Paleobotany, systematic:
Diatom studies (G. W. Andrews, NC)
Floras:
Cenozoic:
Pacific Northwest (J. A. Wolfe, M)
Western United States and Alaska (J. A. Wolfe, M)
Devonian (J. M. Schopf, Columbus, Ohio)
Paleozoic (S. H. Mamay, NC)
Fossil wood and general paleobotany (R. A. Scott, D)
Modern seeds, California (J. A. Wolfe, D. P. Adam, M)
Plant microfossils:
Mesozoic (R. H. Tschudy, D)
Paleozoic (R. M. Kosanke, D)
Paleoecology:
Faunas, Late Pleistocene, Pacific coast (W. O. Addicott, M)

Paleoecology—Continued
- Fish, Quaternary, California (R. Casteel, D. P. Adam)
- Foraminifera, ecology (M. R. Todd, NC)
- Ostracodes, Recent, North Atlantic (J. E. Hazel, NC)
- Paleoenvironmental studies, Miocene, Atlantic Coastal Plains (T. G. Gibson, NC)
- Pollen, Quaternary, California (D. P. Adam, M)
- *Tempskya*, Southwestern United States (C. B. Read, Albuquerque, N. Mex.)
- Vertebrate faunas, Ryukyu Islands, biogeography (F. C. Whitmore, Jr., NC)

Paleontology, invertebrate, systematic:
- Brachiopods:
  - Carboniferous (Mackenzie Gordon, Jr., NC)
  - Ordovician (R. B. Neuman, NC; R. J. Ross, Jr., D)
  - Upper Paleozoic (J. T. Dutro, Jr., NC)
- Bryozoans, Ordovician (O. L. Karklins, NC)
- Cephalopods:
  - Cretaceous (D. L. Jones, M)
  - Jurassic (R. W. Imlay, NC)
  - Upper Cretaceous (W. A. Cobban, D)
  - Upper Paleozoic (Mackenzie Gordon, Jr., NC)
- Chitinozoans, Lower Paleozoic (J. M. Schopf, Columbus, Ohio)
- Conodonts, Devonian and Mississippian (C. A. Sandberg, D)
- Corals, rugose:
  - Mississippian (W. J. Sando, NC)
  - Silurian-Devonian (W. A. Oliver, Jr., NC)
- Foraminifera:
  - Fusuline and orbitoline (R. C. Douglass, NC)
  - Cenozoic (M. R. Todd, NC)
  - Cenozoic, California and Alaska (P. J. Smith, M)
  - Mississippian (B. A. Skipp, D)
  - Recent, Atlantic shelf (T. G. Gibson, NC)
- Gastropods:
  - Mesozoic (N. F. Sohl, NC)
  - Miocene-Pliocene, Atlantic coast (T. G. Gibson, NC)
  - Paleozoic (E. L. Yochelson, NC)
- Graptolites, Ordovician-Silurian (R. J. Ross, Jr., D)
- Mollusks, Cenozoic, Pacific coast (W. A. Addicott, M)
- Ostracodes:
  - Lower Paleozoic (J. M. Berdan, NC)
  - Upper Cretaceous and Tertiary (J. E. Hazel, NC)
  - Upper Paleozoic (I. G. Sohn, NC)
- Pelecypods:
  - Inoceramids (D. L. Jones, M)
  - Jurassic (R. W. Imlay, NC)
  - Paleozoic (John Pojeta, Jr., NC)
  - Triassic (N. J. Silberling, M)
- Trilobites, Ordovician (R. J. Ross, Jr., D)

Paleontology, stratigraphic:
- Cenozoic:
  - Diatoms, Great Plains, nonmarine (G. W. Andrews, NC)
  - Foraminifera, smaller, Pacific Ocean and islands (M. R. Todd, NC)
  - Mollusks:
    - Atlantic coast, Miocene (T. G. Gibson, NC)
    - Pacific coast, Miocene (W. O. Addicott, M)
  - Pollen and spores, Kentucky (R. H. Tschudy, D)
  - Vertebrates:
    - Atlantic coast (F. C. Whitmore, Jr., NC)
    - Pacific coast (C. A. Repenning, M)
    - Panama Canal Zone (F. C. Whitmore, Jr., NC)
    - Pleistocene (G. E. Lewis, D)

Paleontology, stratigraphic—Continued
- Mesozoic:
  - Pacific coast and Alaska (D. L. Jones, M)
  - Cretaceous:
    - Alaska (D. L. Jones, M)
    - Foraminifera:
      - Alaska (H. R. Bergquist, NC)
      - Atlantic and Gulf Coastal Plains (H. R. Bergquist, NC)
      - Pacific coast (R. L. Pierce, M)
    - Gulf coast and Caribbean (N. F. Sohl, NC)
    - Molluscan faunas, Caribbean (N. F. Sohl, NC)
    - Western Interior United States (W. A. Cobban, D)
  - Jurassic, North America (R. W. Imlay, NC)
  - Triassic, marine faunas and stratigraphy (N. J. Silberling, M)
- Paleozoic:
  - Devonian and Mississippian conodonts, Western United States (C. A. Sandberg, D)
  - Fusuline Foraminifera, Nevada (R. C. Douglass, NC)
  - Mississippian:
    - Stratigraphy and brachiopods, northern Rocky Mountains and Alaska (J. T. Dutro, Jr., NC)
    - Stratigraphy and corals, northern Rocky Mountains (W. J. Sando, NC)
  - Mississippian biostratigraphy, Alaska (A. K. Armstrong, M)
  - Onesquethaw Stage (Devonian), stratigraphy and rugose corals (W. A. Oliver, NC)
  - Ordovician:
    - Bryozoans, Kentucky (O. L. Karklins, NC)
    - Stratigraphy and brachiopods, Eastern United States (R. B. Neuman, NC), Western United States (R. J. Roxx, Jr., D)
  - Paleobotany and coal studies Antarctica (J. M. Schopf, Columbus, Ohio)
  - Palynology of cores from Naval Petroleum Reserve No. 4 (R. A. Scott, D)
  - Pennsylvanian:
    - Fusulinidae:
      - Alaska (R. C. Douglass, NC)
      - North-central Texas (D. A. Myers, D)
    - Spores and pollen, Kentucky (R. M. Kosanke, D)
  - Permian, floras, Southwestern United States (S. H. Mamay, NC)
  - Silurian-Devonian:
    - Corals, northeastern United States (W. A. Oliver, Jr., NC)
    - Upper Silurian-Lower Devonian, Eastern United States (J. M. Berdan, NC)
  - Subsurface rocks, Florida (J. M. Berdan, NC)
  - Upper Paleozoic, Western States (Mackenzie Gordon, Jr., NC)

Paleontology, vertebrate, systematic:
- Artiodactyls, primitive (F. C. Whitmore, Jr., NC)
- Pinnipedia (C. A. Repenning, M)
- Pleistocene fauna, Big Bone Lick, Kentucky (F. C. Whitmore, Jr., NC)
- Tritylodonts, American (G. E. Lewis, D)

Paleotectonic maps. *See* Regional studies and compilations.

Petroleum and natural gas:
- Automatic data-processing system for field and reservoir estimates (K. A. Yenne, c, Los Angeles, Calif.)
- Borehole gravimetry, application to oil exploration (J. W. Schmoker, D)

Petroleum and natural gas—Continued
Catagenesis of organic matter and generation of petroleum (N. H. Bostick, D)
Devonian black shale, Appalachian Basin:
Borehole gravity study (J. W. Schmoker, D)
Clay mineralogy (J. W. Hosterman, NC)
Conodont maturation (A. G. Harris, NC)
Data storage and retrieval system
Geochemical study (G. E. Claypool, D)
Stratigraphy (J. B. Roen, NC)
Structural studies (L. D. Harris, NC)
Uranium and trace-element study (J. S. Leventhal, D)
Gulf of Mexico, oil and gas resources of the Gulf of Mexico (B. M. Miller, D)
Methods of recovery (F. W. Stead, D)
Oil and gas map, North America (W. W. Mallory, D)
Oil and gas resource apprasial methodology and procedures (B. M. Miller, D)
Organic geochemistry (J. G. Palacas, D)
Origin and distribution of natural gases (D. D. Rice, D)
Origin, migration, and accumulation of petroleum (L. C. Price, D)
Petroleum prospecting with helium detector (A. A. Roberts, D)
Rocky Mountain States, seismic detection of stratigraphic traps (R. T. Ryder, D)
Tight gas sands (D. D. Rice, D)
Western Interior Cretaceous studies (C. W. Spencer, D)
Western United States:
Devonian and Mississippian (C. A. Sandberg, D)
Devonian and Mississippian flysch source-rock studies (F. G. Poole, D)
Properties of reservoir rocks (R. F. Mast, D)
Source rocks of Permian age (E. K. Maughan, D)
States:
Alaska (M):
Cook Inlet (L. B. Magoon III)
Northeastern Arctic Slope Federal-State field project (I. F. Palmer, c, Anchorage)
North Slope, petroleum geology (R. D. Carter)
NPRA (National Petroleum Reserve Alaska) Oil and Gas Source Rock Study (L. B. Magoon III, M)
Arkansas, Sandstone reservoirs (B. R. Haley, Little Rock)
California:
Carpenteria and Hondo-Santa Ynez field reserves, OCS (D. G. Griggs, c, Los Angeles)
Eastern Los Angeles basin (T. H. McCulloh, Seattle, Wash.)
Salinas Valley (D. L. Durham, M)
Southern San Joaquin Valley, subsurface geology (J. C. Maher, M)
Colorado (c, D, except as otherwise noted):
Citadel Plateau (G. A. Izett)
Denver Basin, Tertiary coal zone and associated Strata (P. A. Soister)
Grand Junction 2-degree quadrangle (W. B. Cashion, Jr., D)
Piceance Creek basin—low permeability gas sands (R. C. Johnson, D)
Savery quadrangle (C. S. V. Barclay)
New Mexico, San Juan Basin (E. R. Landis, D)
Utah (c, D, except as otherwise noted):
Canaan Peak quadrangle (W. E. Bowers)
Collet Top quadrangle (H. D. Zeller)
Grand Junction 2-degree quadrangle (W. B. Cashion, Jr., D)

Petroleum and natural gas—Continued
Wyoming:
Browns Hill quadrangle (C. S. V. Barclay, c, D)
Lander area phosphate reserve (W. L. Rohrer, c, D)
Pine Mountain-Oil Mountain area (G. J. Kerns, c, Casper)
Reid Canyon quadrangle (G. J. Kerns, c, Casper)
Savery quadrangle (C. S. V. Barclay, c, D)
Square Top Butte quadrangle (W. H. Laraway, c, Casper)
Stratigraphy, lower Upper Cretaceous formations (E. A. Merewether, D)
Wyoming-Montana-North Dakota-South Dakota, Williston Basin (C. A. Sandberg, D)
Petrology. *See* Geochemistry and petrology, field studies.
Phosphate:
Phosphoria Formation, stratigraphy and resources (R. A. Gulbrandsen, M)
States:
Alaska, Anatuvuk Pass (c, Anchorage)
Idaho:
Palisades Dam quadrangle (D. A. Jobin, c, D)
Phosphate resources (Peter Oberlindacher, c, M)
Montana, Melrose phosphate field (G. D. Fraser, c, D)
Nevada, Spruce Mountain 4 quadrangle (G. D. Fraser, c, D)
United States, southeastern phosphate resources (J. B. Cathcart, D)
Utah:
Crawford Mountains (W. C. Gere, c, M)
Ogden 4 NW quadrangle (R. J. Hite, c, D)
Wyoming:
Crawford Mountains phosphate deposits (W. C. Gere, c, M)
Pickle Pass quadrangle (M. L. Schroeder, c, D)
Pine Creek quadrangle (M. L. Schroeder, c, D)
Plant ecology:
Element availability:
Hydrology and Pinyon-Juniper (J. J. Owen, w, D)
Soils (R. C. Severson, D)
Vegetation (L. P. Gough, D)
Periodic plant-growth phenomena and hydrology (R. L. Phipps, w, NC)
Vegetation and hydrology (R. S. Sigafoos, w, NC)
Western coal regions, geochemical survey of vegetation (J. A. Erdman, D)
See also Evapotranspiration; Geochronological investigations; Limnology.
Platinum:
Mineralogy and occurrence (G. A. Desborough, D)
States:
Montana, Stillwater complex (N. J. Page, M)
Wyoming, Medicine Bow Mountains (M. E. McCallum, Fort Collins, Colo.)
Potash:
Arizona, Patagonia area (J. A. Crowley, c, M)
Colorado and Utah, Paradox basin (O. B. Raup, D)
Nevada, alunite (J. A. Crowley, c, M)
New Mexico, Carlsbad, potash and other saline deposits (C. L. Jones, M)
Primitive areas. *See under Mineral and fuel resources*—Compilations and topical studies, mineral-resource surveys.
Public and industrial water supplies. *See* Quality of water; Water resources.
Quality of water:
Atlanta Central Lab atomic absorption (F. E. King, w, Doraville, Ga.)
Atlanta Central Lab automated methods (A. J. Horowitz, w, Doraville, Ga.)

Quality of water—Continued

Atlanta Central Lab—biological analyses (R. G. Lipscomb, w, Doraville, Ga.)
Atlanta Central Lab—manual methods (E. R. Anthony, w, Doraville, Ga.)
Atlanta Central Lab—organic analyses (L. E. Lowe, w, Doraville)
Atlanta Central Lab—special methods (D. K. Leifeste, w, Doraville, Ga.)
Adsorption process models (J. D. Hem, w, M)
Bedload samplers (D. W. Hubbell, w, D)
Benchmark network (R. R. Pickering, w, NC)
Biological information assessment (B. W. Lium, w, Doraville, Ga.)
Central Laboratories (W. A. Beetem, w, NC)
Chemistry of New Zealand waters (I. K. Barnes, w, M)
Data evaluation support (R. E. Gust, w, D)
Denver Central Lab—atomic absorption (D. B. Manigold, w, D)
Denver Central Lab—automated methods (V. C. Marti, w, D)
Denver Central Lab—biological analyses (S. A. Duncan, w, D)
Denver Central Lab—logistical support (R. E. Gust, w, D)
Denver Central Lab—manual methods (S. A. Duncan, w, D)
Denver Central Lab—organic analyses (D. B. Manigold, w, D)
Denver Central Lab—physical properties (R. L. McAvoy, w, D)
Denver Central Lab—radiochemical analyses (S. A. Duncan, w, D)
Denver Central Lab—special methods (R. L. McAvoy, w, D)
Denver Central Laboratory (R. L. McAvoy, w, D)
Development of biological methods (B. W. Lium, w, Atlanta, Ga.)
Development of water methods (B. A. Malo, w, D)
Digital model-waste transport (J. B. Robertson, w, Idaho Falls, Idaho)
Geochemical kinetics studies (H. C. Claassen, w, D)
Geochemical kinetics, volcanic rocks (H. C. Claassen, w, D)
Geochemistry Oil Field Waters, Alaska (Y. K. Kharaka, w, M)
Geochemistry, Western coal region (G. L. Feder, w, D)
Hydraulic Fracturing Waste Disposal (R. J. Sun, w, NC)
Hydrologic interpretations (E. J. Pluhowski, w, NC)
Hydrology of central Nevada (G. A. Dinwiddie, w, D)
Improvement of QW data system (D. A. Goolsby, w, NC)
Instrumentation, petrochemical (W. A. Beetem, w, NC)
Laboratory evaluation (V. J. Janzer, w, D)
Methods coordination (M. W. Skougstad, w, D)
Methods development (W. A. Beetem, w, NC)
Methods development support (D. E. Erdman, w, Doraville, Ga.)
Methods for organics (W. E. Pereira, w, D)
Methods for pesticides (T. R. Steinheimer, w, D)
Methods for trace metals (H. E. Taylor, w, D)
Modeling mineral-water reactions (L. N. Plummer, w, NC)
National river quality (J. F. Ficke, w, NC)
Nevada Test Site geochemistry (A. F. White, w, D)
Nevada Test Site tracer studies (D. I. Leap, w, D)
Nevada Test Site waste management (G. A. Dinwiddie, w, D)
Nevada Test Site waste sites (G. C. Doty, w, Mercury, Nev.)
Nuclear hydrology services (W. W. Dudley, w, D)
Off Nevada Test Site waste sites (J. E. Weir, w, D)

Quality of water—Continued

Organic deep waste storage (R. L. Malcolm, w, D)
Organic polyelectrolytes (R. L. Wershaw, w, D)
Organic substances in streams (R. E. Rathbun, w, Bay St. Louis, Miss.)
Organics in oil-shade residues (J. A. Leenheer, w, D)
Organics in water (D. F. Goerlitz, w, M)
Pesticide monitoring network (R. J. Pickering, w, NC)
Poplar River waste quality (R. C. Averett, w, D)
Potomac Estuary studies (J. P. Bennett, w, NC)
Precipitation quality network (R. J. Pickering, w, NC)
Quality assurance (W. A. Beetem, w, NC)
Quality assurance (L. J. Schroder, w, D)
Quality assurance procedures (L. C. Friedman, w, D)
Radioanalytical methods (L. L. Thatcher, w, D)
Radiochemical Techniques of Water Resources Investigations (V. J. Janzer, w, D)
Radiohydrology of explosion sites (D. D. Gonzalez, w, D)
Radionuclide migration at Nevada Test Site (W. W. Dudley, w, D)
Radionuclides on sediments (D. D. Gonzalez, w, D)
River-water quality and land use (D. J. Lystrom, w, Portland, Ore.)
Standard reference water sample program (M. J. Fishman, w, D)
Temperature modeling in natural streams (A. P. Jackman, w, M)
Thermal modeling (H. E. Jobson, w, Bay St. Louis, Miss.)
Thermal pollution (G. E. Harbeck, Jr., w, D)
Toxic substances in aquatic ecosystems (H. V. Leland, w, M)
Trace-element availability in sediments (S. N. Luoma, w, M)
Transition metal hydrogeochemistry (Edward Callender, w, NC)
Transport in ground water (L. F. Konikow, w, D)
Transuranium research (J. M. Cleveland, w, D)
Turbulent diffusion and thermal loading (Nobuhiro Yotsukura, w, NC)
Water-quality-data evaluation (W. H. Doyle, Jr., w, D)

States and territories:

Alabama:
- Water problems in coal-mine areas (Celso Puente, w, Tuscaloosa)
- Water resources in oil fields (W. J. Powell, w, Tuscaloosa)

Arizona:
- Ground-water, Little Colorado basin (S. G. Brown, w, Tuscon)
- Papago-arsenic in drinking water (L. J. Mann, w, Tuscon)
- Sludge disposal, Flagstaff (T. H. Thompson, w, Flagstaff)

Arkansas (w, Little Rock):
- L'anguille assessment (C. T. Bryant)
- Soil Conservation Service watershed studies (T. E. Lamb)
- Waste-assimilation capacity (C. T. Bryant)

California:
- Colorado River salinity (D. T. Hartley, w, Laguna Niguel)
- Ground-Water Quality Inventory (G. L. Faulkner w, M)
- Ground-water quality, Santa Ana (L. A. Eccles, w, Laguna Niguel)
- Merced River water quality (R. J. Hoffman, w, Sacramento)
- New River water quality (J. G. Setmire, w, Laguna Niguel)
- Quality of water, California streams (W. L. Bradford, w, M)
- San Francisco Bay monitoring (W. L. Bradford, w, M)
- San Francisco Bay urban study (R. D. Brown, M)
- Santa Barbara ground water (C. B. Hutchinson, w, Laguna Niguel)

Quality of water—Continued
States and territories—Continued
California—Continued
Thermograph network evaluation (J. T. Limerinos, w, M)
Water quality studies design-National Park Service (W. L. Bradford, w, M)
Water resources Upper Coachella (Anthony Buono, w, Laguna Niguel)
Colorado (w, D, except as otherwise noted):
Aquatic biology of Piceance Creek (K. J. Covay, w, Meeker)
Effects of feedlots on ground water (S. G. Robson)
Effects of sludge basins on ground water (S. G. Robson)
Hayden powerplant study (G. J. Saulnier, w, Meeker)
In-situ uranium mining (J. W. Warner)
Lowry landfill ground-water quality (N. G. Gaggiani)
Northwestern Colorado water quality (T. R. Ford, w, Meeker)
Quality of water characteristics of Colorado streams (M. W. Gaydos)
Quality of water in underground coal mines (R. E. Moran)
Upper Colorado energy impacts (T. D. Steele)
Water quality, Jefferson County (D. C. Hall)
Yampa Valley ground-water reconnaissance (W. E. Hofstra)
Connecticut, changes in ground-water quality (E. H. Handman, w, Hartford)
Florida:
Dade storm-water quality (H. C. Mattraw, w, Miami)
Drainage wells Orlando area (C. H. Tibbals, w, Orlando)
Environmental studies, statewide (G. A. Irwin, w, Tallahassee)
Ground-water quality, Dade County (Howard Klein, w, Miami)
Lakes Faith, Hope, and Charity (A. G. Lamonds, Jr., w, Orlando)
Radionuclides in ground water (Horace Sutcliffe, Jr., w, Sarasota)
Salt-water intrusion, Cape Coral (D. H. Boggess, w, Fort Myers)
Subsurface waste storage (G. L. Faulkner, w, Tallahassee)
Traffic-related contaminants (H. C. Mattraw, w, Miami)
Water quality:
Broward County (C. B. Sherwood, Jr., w, Miami)
South New River Channel (B. G. Waller, w, Miami)
Georgia (w, Doraville):
Coal region, north Georgia (J. B. McConnell)
Ground water irrigation southwest Georgia (R. G. Grantham)
Quality water of West Point reservoir (J. B. McConnell)
Storm runoff, greater Atlanta area (J. B. McConnell)
Stream quality southwest Georgia, agriculture area (J. B. McConnell)
Hawaii, monitoring of critical ground-water areas (K. J. Takasaki, w, Honolulu)
Idaho (w, Boise):
East Idaho ground-water quality (H. R. Seitz)
Ground-water-quality assessment (H. R. Seitz)
Ground water—quality of water monitoring (R. L. Whitehead)
Illinois (w, Champaign):
Palos Hills waste burial site (L. G. Toler)
Sludge irrigation hydrology (R. F. Fuentes)
Sludge storage in strip-mine land (G. L. Patterson)
Strip mine hydrology (T. P. Brabets)
Indiana (w, Indianapolis):
Ground water, Indiana dunes (W. G. Weist)
Landfill monitoring, Marion County (J. R. Marie)
Surface-water quality study (M. A. Hardy)
Watershed water quality (S. E. Ragone)

Quality of water—Continued
States and territories—Continued
Iowa (w, Iowa City):
Indian-Twin Ponies water quality (L. J. Slack)
Water quality Iowa coal region (W. C. Steinkampf)
Kansas (w, Lawrence):
Contamination of Equus beds (J. M. McNellis)
Enhanced oil recovery, Kansas (D. G. Jorgensen)
Ground-water-quality network evaluations (A. M. Diaz)
Quality of water in mined areas in southeast (A. M. Diaz)
Saline discharge, Smoky Hill River (J. B. Gillespie)
Kansas, Urban storm water quality (A. M. Diaz)
Kentucky (w, Louisville):
Chloroform in alluvial aquifer (R. W. Davis)
Louisville alluvial aquifer test (R. J. Faust)
Louisiana (w, Baton Rouge):
Pollution capacity of streams (R. F. Martien)
Quality of water, Lower Mississippi River (F. C. Wells)
Maine:
Hydrology of Salmon Lake (D. J. Cowing, w, Augusta)
Public inquiries (R. C. Wagner, w, Augusta)
Massachusetts (w, Boston):
Ground-water contamination (D. F. Delaney)
Impact of Otis Air Force Base waste disposal (D. R. LeBlanc)
Lake Cochituate nutrients (F. B. Gay)
Water quality management (M. H. Frimpter)
Minnesota (w, St. Paul):
Coal-tar derivates in ground-water (M. F. Hult)
Ground-water quality network (M. F. Hult)
Karst well hydraulics (M. F. Hult)
Water quality of highway runoff (M. R. Have)
Mississippi, Tennessee-Tombigbee Divide quality-of-water monitoring (C. H. Tate, w, Jackson)
Missouri (w, Rolla):
Prosperity water quality (J. H. Barks)
Urban runoff in Springfield (John Skeleton)
Montana:
Geohydrology of Helena Valley (A. J. Boettcher, w, Helena)
Ground water Poplar basin (R. D. Feltis, w, Billings)
Thermal study—Madison River (A. J. Boettcher, w, Helena)
Nebraska:
Analysis surface-water quality data (R. A. Engberg, w, Lincoln)
Ground-water quality (R. A. Engberg, w, Lincoln)
Nevada (w, Carson City):
Ground-water contamination by explosives wastes (A. S. Van Denburgh)
Ground-water-quality monitoring network (J. O. Nowlin)
Pond seepage, Weed Heights (R. J. LaCamera)
Truckee-Carson assessment (J. O. Nowlin)
New Hampshire:
Effects of waste disposal—Peace Air Force Base (Edward Bradley, w, Augusta)
Eutrophication, Lake Winnisquam (W. D. Silvey, w, Concord)
New Mexico:
Malaga Bend evaluation (J. L. Kunkler, w, Santa Fe)
Quality-of-water monitor in Chaco River basin (Kim Ong, Ong, w, Albuquerque)

Quality of water—Continued
States and territories—Continued
New Mexico—Continued
San Juan River valley (F. P. Lyford, w, Albuquerque)
New York (w, Albany):
Biology of landfill leaching (T. A. Ehlke)
Ground-water pollution, Olean (A. D. Randall)
Organic compounds in ground water (J. T. Turk)
PCB transport in the Upper Hudson (R. J. Archer)
Recharge and nitrates, Cornell Farm (A. D. Randall)
Sediment nutrient dynamics (J. T. Turk)
Westchester County waste management (R. J. Archer)
North Carolina (w, Raleigh):
Chemical quality atmospheric deposition (R. C. Heath)
Effects of channelizing Black River (C. E. Simmons)
Water-quality of major North Carolina rivers (C. C. Daniel)
North Dakota, mining effects, Gascoyne area (M. G. Croft, w, Bismarck)
Ohio (w, Columbus):
Brine investigation (S. E. Norris)
Miscellaneous water resources studies (R. V. Swisshelm,)
Quality of water monitor network (A. A. Gordon)
Rattlesnake Creek water quality (K. F. Evans)
Oklahoma (w, Oklahoma City):
Blue Creek quality (J. K. Kurklin)
Coal hydrology eastern Oklahoma (M. V. Marcher)
Gaines Creek quality, Oklahoma (J. K. Kurklin)
Salt-water infiltration (J. J. D'Lugosz)
Surface water suitability (J. D. Stoner)
Zinc mine water quality (J. D. Stoner)
Oregon (w, Portland):
Portland:
Harbor study (S. W. McKenzie)
Water-quality study (S. W. McKenzie)
Stream quality in Oregon (T. L. Miller)
Water in western Douglas County (D. A. Curtiss)
Willamette River basin low flow (S. W. McKenzie)
Pennsylvania (w, Harrisburg, unless otherwise noted):
Anthracite mine discharge (D. J. Growitz)
Ground-water quality in Pennsylvania (H. E. Koester)
Impoundment, Sleepy Hollow Run (D. R. Williams, w, Pittsburgh)
Little Blue Run Lake—fly ash (D. R. Williams, w, Pittsburgh)
Nonpoint sources Pequea Creek basin (J. R. Ward)
Pennsylvania Gazetteer of streams Part II (L. C. Shaw)
Stream conditions—Chester County (J. J. Murphy w, Philadelphia)
Water quality—Blue Marsh Lake (J. L. Barker)
Water quality in Tioga River basin (J. R. Ward)
Puerto Rico (w, San Juan):
Effects of oil spillage on ground water (Fernando Gomez-Gomez)
Ground water reaction to refinery effluent (J. R. Diaz)
Solid-waste study (Fernando Gomez-Gomez)
Surface impoundents, (J. R. Diaz)
Rhode Island, quality of Rhode Island streams (W. D. Silvey, w, Boston, Mass.)
South Carolina (w, Columbia):
Fluoride in ground water, coastal plain (J. M. Rhett)
Savannah River plant (D. I. Cahal)

Quality of water—Continued
States and territories—Continued
Tennessee, Burial-ground studies at Oak Ridge National Laboratory (D. A. Webster, w, Knoxville)
Texas, Colorado River salinity (Jack Rawson, w, Austin)
Utah (w, Salt Lake City):
Reconnaissance of Utah coal fields (K. M. Waddell)
Surface-water quality:
Dirty Devil River basin (J. C. Mundorff)
Water quality, San Rafael River basin (J. C. Mundorff)
Vermont, ground-water quality (R. E. Willey, w, Montpelier)
Virginia, dredge spoil disposal (J. F. Harsh, w, Richmond)
Washington (w, Tacoma):
Columbia basin demonstration project (P. R. Boucher)
Ground-water-quality network (M. O. Fretwell)
Lake Wilderness nutrients (N. P. Dion)
Salt-water intrusion (N. P. Dion)
Spokane ground water quality (E. L. Bolke)
Sulphur Creek program(P. R. Boucher)
West Virginia, effects of deep mining (J. L. Chisolm, w, Charleston)
Wisconsin (w, Madison):
Ground-water quality, Waukesha County (J. J. Schiller)
Nederlo Creek biota (P. A. Kammerer, Jr.)
Stream reaeration (R. S. Grant)
Wyoming (w, Cheyenne):
Herbicides North Platte (H. R. Schuetz)
In-situ coal, (J. F. Busby)
In-situ oil shale (E. R. Cox)
North Platte reservoirs (S. J. Rucker IV)
Nutrient release, Lake DeSmet (D. J. Wangsness)
See also Geochemistry; Hydrologic instrumentation; Hydrology, surface water; Limnology; Marine hydrology; Sedimentology; Water resources.

Quicksilver. *See* Mercury.

Radioactive materials, transport in water. *See* Geochemistry, water.

Radioactive waste disposal:
Hydrology of nuclear landfill (D. E. Prudic, w, Albany, N.Y.)
Hydrology of salt domes (R. L. Hosman, w, Baton Rouge, La.)
Implications of long-term climate changes (D. P. Adam)
National Overview Atlas (J. P. Ohl, D)
Nevada waste coordination (W. W. Dudley, w, D)
Pierre Shale (G. W. Shurr, D)
Radioactive byproducts in salt (J. W. Mercer, w, Albuquerque, N. Mex.)
Radioactive-waste burial (George Debuchananne, w, NC)
Radioactive-waste-burial study (J. M. Cahill, w, Columbia, S. C.)
Radiohydrology technical coordination (George Debuchananne, w, NC)
Sheffield site investigation (J. B. Foster, w, Champaign, Ill.)
Waste-disposal sites (L. A. Wood, w, NC)
Waste emplacement crystalline rocks inconterminous United States (H. W. Smedes, D)
States:
Idaho, hydrology of subsurface waste disposal (J. T. Barraclough, w, Idaho Falls)
Kentucky, Maxey Flats investigation (H. H. Zehner, w, Louisville)
New Mexico (D):
Eddy and Lea counties, exploratory drilling (C. L. Jones)
Southeastern, waste emplacement (C. L. Jones)
Utah (D):
Paradox Basin (L. M. Gard)

Radioactive-waste disposal—Continued
States—Continued
Utah—Continued
Salt Valley anticline (L. M. Gard)
See also Geochemistry, water.
Rare-earth metals. *See* Minor elements.
Regional studies and compilations, large areas of the United States:
Appalachians-Caledonides synthesis analysis (R. B. Neuman, Washington, D.C.)
Basement rock map (R. W. Bayley, M)
Characterization of crystalline rock terrane (H. W. Smedes and D. J. Gable, D)
Paleotectonic map folios:
Devonian System (E. G. Sable, D)
Mississippian System (L. C. Craig, D)
Pennsylvanian System (E. D. McKee, D)
Physiography of Southeastern United States (J. T. Hack, NC)
Volcanic rocks of the Appalachians (D. W. Rankin, NC)
Remote sensing:
Cartographic applications:
Composite mapping and topographic analysis (D. D. Greenlee, Technicolor Graphics Services, Inc., Sioux Falls, S. Dak.)
Landsat image maps of Cape Cod (R. S. Williams, Jr., l, NC)
Geologic applications:
Airborne and satellite research:
Aeromagnetic studies (M. F. Kane, D)
Development of an automatic analog earthquake processor (J. P. Eaton, M)
Electromagnetic research (F. C. Frischknecht, D)
Fraunhofer line discriminator studies (R. D. Watson, l, Flagstaff, Az.)
Gamma-ray research (J. S. Duyal, D)
Geochemical plant stress (F. C. Canney, D)
Heat Capacity Mapping Mission: Thermal-inertia mapping (Kenneth Watson, D)
Geologic investigations with integrated geophysical and remote sensing data (J. V. Taranik, l, Sioux Falls, S. Dak.)
Geothermal resources (Kenneth Watson, D)
Geologic investigations with integrated data (J. V. Taranik, l, Sioux Falls, S, Dak.)
Infrared surveillance of volcanoes (J. D. Freidman, D)
Interpretation studies (R. H. Henderson, NC)
National aeromagnetic survey (J. R. Henderson, D)
Remote sensing of dynamic geological phenomena and geologic hazards (R. S. Williams, Jr., l, NC)
Remote-sensing geophysics (Kenneth Watson, D)
Satellite magnetometry (R. D. Regan, NC)
Surficial and thematic mapping (T. N. V. Karlstrom, Flagstaff, Ariz.)
Urban geologic studies (T. W. Offield, D)
Volcanic gas monitoring (Motoaki Sato, NC)
Landsat experiments:
Analysis of porphyry copper prospects from Landsat digital data (R. G. Schmidt, NC)
Evaluation of Great Plains area (R. B. Morrison, D)
Iron-absorption band for the discrimination of iron-rich zones (L. C. Rowan, NC)
Linear features of the conterminous United States (W. D. Carter, l, NC)
Morphology, provenance, and movement of desert and seas in Africa, Asia. and Australia (E. D. Mckee, D)
Remote sensing —Continued
Geologic applications—Continued
Landsat experiments—Continued
Optimum Landsat spectral bands (G. L. Raines, D)
Prototype volcano surveillance network (J. P. Eaton, M)
Study of multispectral imagery, northwestern Saudi Arabia (A. J. Bodenlos, NC)
Suspended particulate matter in nearshore surface waters, northeast Pacific Ocean and the Hawaiian Islands (P. R. Carlson, M)
Synthetic stereo in Landsat imagery (Gordon Swann, Flagstaff, Ariz.)
Targeting of mineral exploration effort (J. V. Taranik, l, Sioux Falls, S. Dak.)
Tectonic and mineral-resource investigations, Andes Mountains, South America (W. D. Carter, l, NC)
Thermal surveillance of active volcanoes (J. D. Friedman, NC)
Skylab/EREP studies:
Evaluation of Great Plains area (R. B. Morrison, D)
Marine and coastal processes on the Puerto Rico-Virgin Islands Platform (J. V. A. Trumball, Santurce, P. R.)
Remote-sensing geophysics (Kenneth Watson, D)
Skylab/visual observations:
Desert sand seas (E. D. McKee, D; C. S. Breed, Flagstaff, Ariz.)
Volcanologic features (J. D. Friedman, D)
Time-lapse satellite data for monitoring dynamic hydrologic phenomena (Morris Deutsch, S. Serebreny, l, C)
Uranium, remote sensing for uranium exploration (G. L. Raines, D)
States:
Alaska (M):
Beaufort Sea, inner shelf and coastal sedimentation environment (Erk Reimnitz)
Remote sensing of permafrost and geologic hazards (O. J. Ferrians, Jr.)
Arizona:
Arizona Regional Ecological Test Site:
North-central (D. P. Elston, Flagstaff)
Post-1890 A. D. episode erosion (R. B. Morrison, D)
Basin and Range-Colorado Plateau boundary investigation (D. P. Elston, Ivo Lucchitta, Flagstaff)
Colorado, effects of atmosphere on multispectral mapping rock types by computer, Cripple Creek-Canon City (H. W. Smedes, D)
Colorado-Wyoming, analysis of Cortez-Uinta mineralized areas from Landsat digital data (L. C. Rowan, NC)
New Mexico, analysis of Landsat images of Claunch and vicinity (W. A. Fischer, l, NC)
Texas, monitoring changing geologic features, Texas Gulf Coast (R. B. Hunter, Corpus Christi)
Hydrologic applications:
Aircraft and spacecraft observations of Arctic sea ice (W. J. Campbell, w. Tacoma, Wash.)
Ice Dynamics (W. J. Campbell, w. Tacoma, Wash.)
Hydrologic remote sensing (G. K. Moore, w, Sioux Falls, S. Dak.)
Optical and computer processing and interpretation techniques for Landsat hydrologic and environmental applications (Morris Deutsch, l, NC)
Polar-ice remote sensing (W. J. Campbell, w. Tacoma, Wash.)

Remote sensing—Continued
Hydrologic applications—Continued
Remote sensing, quality of water (M. C. Goldberg, w, D)
Wetlands research (V. P. Carter, w, NC)
Satellite image atlas of glaciers (R. S. Williams, Jr., l, NC)
Sierra Cooperative Pilot Project:
Meterological parameter monitoring with GOES (Donald Rottner, Bureau of Reclamation, Denver, Colo.)
Satellite monitoring of cloud-top temperatures (O. H. Foehner, Bureau of Reclamation, Denver, Colo.)
Targeting, inventorying, and monitoring groundwater resources (J. R. Lucas, Technicolor Graphic Services, Inc., Sioux Falls, S. Dak.)
States:
Alaska, meteor burst telemetry (R. D. Lamke, w, Anchorage)
Arizona (w, Phoenix), snow-cover mapping (H. H. Schumann)
Connecticut, Connecticut River estuary (F. H. Ruggles, Jr., w, Hartford)
Florida, southern, Landsat (A. L. Higer, w, Miami)
Kansas, mined land hydrology, southeast Kansas (A. M. Diaz, w, Lawrence)
Pennsylvania, GOES, Juniata basin (C. D. Kauffman, w, Harrisburg)
Image processing technology, High-resolution film recording system (George Harris, Jr., l, Sioux Falls, S. Dak.)
Land-resource applications:
Colorado River natural resources and land use data inventory (H. D. Newkirk, Bureau of Reclamation, Denver, Colo.)
Development of automatic techniques for land use mapping from remote-sensor data (J. R. Wray, l, NC)
Forest defoliation mapping and drainage assessment (W. G. Rohde, Technicolor Graphic Services, Inc., Sioux Falls S. Dak.)
Impact of strip mining on range resources and wildlife habitat (D. M. Carneggie, l, Sioux Falls, S. Dak.)
Lake Mead National Recreation Area (Nevada and Arizona) (D. Lauer, l, Sioux Falls, S. Dak.)
Land Applications Program (D. R. Hood, Technicolor Graphic Services, Inc., Sioux Falls, S. Dak.)
Land resource analysis using airborne multispectral scanner data (G. R. Johnson, Technicolor Graphic Services, Inc., Sioux Falls, S. Dak.)
Land systems mapping with digital Landsat data (C. J. Robinove, l, NC)
Landsat and aircraft imagery for mine ground stability evaluation (R. K. Rinkenberger, Mine Safety & Health, Admin.., Denver, Colo.)
States:
Arizona, wildland vegetation inventory (W. G. Rohde, Technicolor Graphic Services, Inc., Sioux Falls, S. Dak.)
California, large-scale photographs for range-trend analysis (D. M. Carneggie, l, Sioux Falls, S. Dak.)
Washington, Department of Natural Resources forest classification (G. R. Johnson, Technicolor Graphic Services, Inc., Sioux Falls, S. Dak.)

Reservoirs. *See* Evapotranspiration; Sedimentology.

Resource and land investigations:
Council of State Governments, communication of data needs (J. T. O'Connor, l, NC)
Designation of critical environmental areas (J. T. O'Connor, l, NC)

Resource and land investigations—Continued
Environmental planning and Western coal development (E. T. Smith, l, NC)
Implementing critical resource area programs (E. A. Imhoff, l, NC)
Methodology for siting onshore facilities associated with OCS development in the New England region (W.W. Doyel, l, NC)
Mined-area reclamation and related land use planning (E. A. Imhoff, l, NC)
National Environmental Indicators report (E. T. Smith, l, NC)
State land inventory systems (Olaf Kays, l, NC)
State programs on wild, scenic, and recreational rivers (M. L. Pattison, l, NC)
States:
California, Redwoods National Park (J. T. O'Connor, l, NC)
Washington, Colville Indian Reservation, case study on land use planning (E. T. Smith, l, NC)

Rhenium. *See* Minor elements; Ferro-alloy metals.

Saline minerals:
Mineralogy (B. M. Madsen, M)
States:
Colorado and Utah, Paradox Basin (O. B. Raup, D)
New Mexico, Carlsbad potash and other saline deposits (C. L. Jones, M)
Wyoming, Sweetwater County, Green River Formation (W. C. Culbertson, D)

Saltwater intrusion. *See* Marine hydrology; Quality of water.

Sedimentology:
Arctic fluvial processes, landforms (K. M. Scott, w, Laguna Niguel, Calif.)
Bedload-transport research (W. W. Emmett, w, D)
Channel morphology (L. B. Leopold, w, Berkeley, Calif.)
Coon Creek morphology (S. W. Trimble, w, Los Angeles, Calif.)
Estuarine intertidal environments (J. L. Glenn, w, D)
Measurement of sediment-laden flows (A. G. Scott, w, NC)
Petrology Laboratory (L. G. Schultz, D)
Sediment-hillside morphology (G. P. William, w, D)
Sediment movement in rivers (R. H. Meade, Jr., w, D)
Sediment transport phenomena (D. W. Hubbell, w, D)
Transport processes (C. F. Nordin, w, D)
States:
Alabama, hydrology of Warrior coal field (Celso Puento, w, Tuscaloosa
Alaska:
Coastal environments (A. T. Ovenshine, M)
Hydrology and quality of water of Keta River basin (G. O. Balding, w, Juneau)
Arizona, sediment—Paria River, Lees Ferry (W. B. Garrett, w, Tucson)
California, Los Padres reservoir study (L. F. Trujillo)
Hawaii:
Haiku-Kamooalii-Halawa water quality (S. S. Chinn, w, Honolulu)
Peak flow-sediment discharge relations (B. L. Jones, w, Honolulu)
Idaho, Snake and Clearwater Rivers, sediment (H. R. Spitz, w, Boise)
Illionois, urban construction stream quality (H. E. Allen, w, DeKalb)
Indiana, analysis of sediment data base (L. J. Mansue, w, Indianapolis)
Kansas (w, Lawrence):
Estimation of sediment yield (P. R. Jordan)
Fluvial sediment in northeastern Kansas (C. D. Albert)
Kentucky, sediment characteristics Kentucky streams (R. F. Flint, w, Louisville)
Maryland, trap efficiency—Rock Creek (W. J. Herb, w, Towson)

Sedimentology—Continued
States—Continued
Minnesota, red clay sediment and quality-of-water evaluation (E. G. Giacomini, w, St. Paul)
North Carolina, sediment study (C. E. Simmons, w, Raleigh)
North Dakota (w, Bismarck):
Park River water-quality assessment (D. J. Ackerman)
Water monitoring—coal mining (N. D. Haffield)
Ohio (w, Columbus):
Highway 315 sediment study (D. R. Helsel)
Sediment movement, strip-mined areas (C. G. Angelo)
Sediment yields (P. W. Anttila)
Oregon, water quality, Bull Run watershed (M. V. Shulters, w, Portland)
Pennsylvania (w, Harrisburg):
Highway erosion-control measures (L. A. Reed)
Predicting sediment flow (L. A. Reed)
Study of cobble bed streams (J. R. Ritter)
Tennessee, hydrologic study, coal mining study, New River (W. P. Carey, w, Nashville)
Washington (w, Tacoma):
May Creek sediment study (W. L. Haushild)
Sediment characteristics (L. M. Nelson)
West Viriginia:
Coal River sediment (S. C. Downs, w, Charleston)
Sediment yield of Taylor Run (S. M. Ward, w, Morgantown)
Wisconsin (w, Madison):
Red clay sedimentation (S. M. Hindall)
White River reservoir study (S. M. Hindall)
See also Geochemistry, water; Geochronological investigations; Hydraulics, surface flow; Hydrologic data collection and processing; Stratigraphy and sedimentation; Urbanization, hydrologic effects.

Selenium. *See* Minor elements.

Silver. *See* Heavy metals; Lead, zinc, and silver.

Soil moisture:
Infiltration and drainage (Jacob Rubin, w, M)
Snow hydrology (W. W. Embree, w, Albany, N.Y.)
See also Evapotranspiration.

Spectroscopy:
Mobile spectrographic laboratory (D. J. Grimes, D)
Spectrographic analytical services and research (A. W. Helz, NC; A. T. Meyers, D; Harry Bastron, M)
X-ray spectroscopy (H. J. Rose, Jr., NC; Harry Bastron, M)

Stratigraphy and sedimentation:
Antler flysch, Western United States (F. G. Poole, D)
Middle and late Tertiary history, Northern Rocky Mountains and Great Plains (N. M. Denson, D)
Pennsylvania System stratotype section (G. H. Wood, Jr., NC)
Permian, Western United States (E. K. Maughan, D)
Phosphoria Formation, stratigraphy and resources (R. A. Gulbrandsen, M)
Rocky Mountains and Great Basin, Devonian and Mississippian conodont biostratigraphy (C. A. Sandberg, D)
Sedimentary structures, model studies (E. D. McKee, D)
Tight gas sands (D. D. Rice, D)
States:
Alabama-Florida, stratigraphy (J. A. Miller, w, Tallahassee, Fla.)
Alaska, Cretaceous (D. L. Jones, M)
Arizona:
Hermit and Supai Formations (E. D. McKee, D)

Stratigraphy and sedimentation—Continued
States—Continued
Arizona—Continued
Magnetic chronology, Colorado Plateau and environs (D. P. Elston, E. M. Shoemaker, Flagstaff)
Arizona-New Mexico, paleomagnetic correlation, Colorado Plateau (D. J. Strobell, Flagstaff, Ariz.)
California, southern San Joaquin Valley, subsurface geology (J. C. Maher, M)
Louisiana, Continental Shelf (H. L. Berryhill, Jr., Corpus Christi, Tex.)
Montana, Ruby Range, Paleozoic rocks (E. T. Ruppel, D)
Montana - North Dakota - South Dakota - Wyoming, Williston basin (C. A. Sandberg, D)
Nebraska, central Nebraska basin (G. E. Prichard, D)
Nevada, Indian Trail Formation, abandonment of name (G. L. Dixon, D)
New Mexico, western and adjacent areas, Cretaceous stratigraphy (E. R. Landis, D)
Oregon-California (M), black sands:
Geologic investigations (H. E. Clifton)
Hydrologic investigations (P. D. Snavely, Jr.)
Utah, Promontory Point (R. B. Morrison, D)
Wyoming, Lamont-Baroil area (M. W. Reynolds, D)
See also Paleontology, stratigraphic; *specific areas under* Geologic mapping.

Structural geology and tectonics:
Central Appalachian tectonics (A. A. Drake, Jr., NC)
Contemporary coastal deformation (R. O. Castle, M)
Rock behavior at high temperature and pressure (E. C. Robertson, NC)
Structural studies, Basin and Range (F. G. Poole, D)
States:
Arizona, southeastern tectonics (Harold Drewes, D)
California-Nevada, transcurrent fault analysis, western Great Basin (R. E. Anderson, D)
Nevada, central, east-trending lineaments (G. L. Dixon, D)
See also specific areas under Geologic mapping.

Talc:
New York, Pope Mills and Richville quadrangles (C. E. Brown, NC)

Tantalum. *See* Minor elements.

Thorium:
Analytical support (C. M. Bunker, D)
Investigations of thorium in igneous rocks (M. H. Staatz, D)
States:
Colorado (D):
Cochetopa area (J. C. Olson)
Wet Mountains, thorium resources appraisal (T. J. Armbrustmacher)
Wyoming, Bear Lodge Mountains (M. H. Staatz, D)

Tungsten. *See* Ferro-alloy metals.

Uranium:
Exploration techniques:
Geochemical techniques (R. A. Cadigan, D)
Geochemical techniques of halo uranium (J. K. Otton, D)
Morrison Formation (L. C. Craig, D)
Uranium in streams as an exploration technique (K. J. Wenrich-Verbeek, D)
Genesis of tabular uranium deposits on the Colorado Plateau (R. A. Brooks, D)
Geophysics:
Borehole electrical techniques in uranium exploration (J. J. Daniels, D)

Uranium—Continued
Geophysics—Continued
Borehole geophysical research in uranium exploration (J. H. Scott, D)
Gamma-ray spectrometry in uranium (J. S. Duval, D)
Gamma-ray spectroscopy for uranium exploration in Crystalline terranes (J. A. Pitkin, D)
Geophysical studies relating to uranium deposits in crystalline terranes (D. L. Cambell, D)
Hydrogenochemistry of uranium deposits (C. G. Bowles, D)
Ore-forming processes (H. C. Granger, D)
Paleomagnetism applied to uranium exploration (R. L. Reynolds, D)
Petrophysics (G. R. Olhoeft, D)
Precambrian sedimentary and metasedimentary rocks (F. A. Hills, D)
Radium and other isotopic disintegration products in springs and subsurface water (R. A. Cadigan, J. K. Felmlee, D)
Remote sensing for uranium exploration (G. L. Raines, D)
Resources of radioactive minerals (A. P. Butler, Jr., D)
Resources of United States and world (W. I. Finch, D)
Southern High Plains (W. I. Finch, D)
United States:
Eastern:
Appalachian Basin Paleozoic rocks (A. F. Jacob, D)
Basin analysis as related to uranium potential in Triassic sedimentary rocks (C. E. Turner, D)
Uranium vein deposits (R. I. Grauch, D)
Southwestern, basin analysis related to uranium potential in Permian rocks (J. A. Campbell, D)
Western:
Relation of diagenesis and uranium deposits (M. B. Goldhaber, D)
Vein and disseminated deposits of uranium (J. T. Nash, D)
Uranium daughter products in modern decaying plant remains, in soils, and in stream sediments (K. J. Wenrich-Verbeek, D)
Uranium geophysics in frontier areas (J. W. Cady, D)
Volcanic source rocks (R. A. Zielinski, D)
States:
Arizona-Colorado-New Mexico-Utah, Colorado Plateau (D):
Basin analysis of uranium-bearing Jurassic rocks (Fred Peterson)
Tabular deposits (R. A. Brooks)
Arizona-Nevada-Utah, uranium potential of Basin and Range province (J. E. Peterson, D)
Colorado (D):
Cochetopa Creek uranium-thorium area (J. C. Olson)
Colorado Plateau (Summary) Report (R. P. Fischer)
Marshall Pass uranium (J. C. Olson)
Schwartzwalder mine (E. J. Young)
Uranium-bearing Triassic rocks (R. D. Lupe)
Colorado-New Mexico-Texas-Utah-Wyoming, organic chemistry of uranium (J. S. Leventhal, D)
New Mexico (D):
Acoma area (C. H. Maxwell)
Church Rock-Smith Lake (C. T. Pierson)
Crownpoint uranium studies (J. F. Robertson)
North Church Rock (A. R. Kirk)
San Juan Basin uranium (M. W. Green)
Sanostee (A. C. Huffman, Jr.)
Thoreau uranium studies, New Mexico (J. F. Robertson)
South Dakota-Wyoming, uranium-bearing pipes (C. G. Bowles, D)

Uranium—Continued
States—Continued
Texas:
Coastal Plain, geophysical and geological studies (D. H. Eargle, Austin)
Tilden-Loma Alta area (K. A. Dickinson, D)
Uranium disequilibrium studies (F. E. Senftle, NC)
Texas-Wyoming, roll-type deposits (E. N. Harshman, D)
Utah-Colorado (D):
Moab quadrangle (A. P. Butler, Jr.)
Uinta and Piceance Creek basin (L. C. Craig)
Washington (D), midnite uranium mine (J. T. Nash)
Wyoming (D):
Badwater Creek (R. E. Thaden)
Crooks Peak quadrangle (L. J. Schmitt, Jr.)
Granite as a source rock of uranium (J. S. Stuckless)
Northeastern Great Divide Basin (L. J. Schmitt, Jr.)
Powder River basin (E. S. Santos)
Sagebrush Park quadrangle (L. J. Schmitt, Jr.)
Stratigraphic analysis of Tertiary uranium basins of Wyoming (D. A. Seeland)
Stratigraphic analysis of Western Interior Cretaceous uranium basins (H. W. Dodge, Jr.)

Urban geology:
Alaska (D):
Anchorage area (Ernest Dobrovolny)
Juneau area (R. D. Miller)
Sitka area (L. A. Yehle)
Small coastal communities (R. W. Lemke)
Arizona, Phoenix-Tucson region resources (T. G. Theodore, M)
California (M, except as otherwise noted):
Coastal geologic processes (K. R. Lajoie)
Flatlands materials and their land use significance (E. J. Helley)
Geologic factors in open space (R. M Gulliver)
Hillside materials and their land use significance (C. M. Wentworth, Jr.)
Malibu Beach and Topanga quadrangles (R. F. Yerkes)
Quaternary framework for earthquake studies, Los Angeles Basin (J. C. Tinsley III)
Regional slope stability (T. H. Nilsen)
San Francisco Bay region, environment and resources planning study:
Bedrock geology (M. C. Blake)
Marine geology (D. S. McCulloch)
Open space (C. S. Danielson)
San Andreas fault:
Basement studies (D. C. Ross)
Basin studies (J. A. Bartow)
Regional framework (E. E. Brabb)
Tectonic framework (R. D. Brown)
San Mateo County cooperative (H. D. Gower)
Sargent-Berrocal fault zone (R. J. McLaughlin, D. H. Sorg)
Seismicity and ground motion (W. B. Joyner)
Southern:
Eastern part (D. M. Morton, Riverside)
Western part (R. F. Yerkes)
Colorado (D):
Denver-Front Range urban corridor, remote sensing (T. W. Offield)
Denver metropolitan area (R. M. Lindvall)
Denver mountain soils (P. W. Schmidt)
Denver urban area, regional geochemistry (H. A. Tourtelot)
Denver urban-area study:
Geologic maps:
Boulder-Fort Collins-Greeley area (R. B. Colton)

Urban geology—Continued
Denver urban-area study—Continued
Geologic maps—Continued
Colorado Springs-Castle Rock area (W. R. Hansen)
Greater Denver area (D. E. Trimble)
Land-use classification, Colorado Front Range urban corridor (W. R. Hansen, L. B. Driscoll)
Engineering geology mapping research, Denver region (H. E. Simpson)
Terrain mapping from Skylab data (H. W. Smedes)
Maryland, Baltimore-Washington urban-area study (J. T. Hack, NC)
Massachusetts, Boston and vicinity (C. A. Kaye, Boston)
Montana, geology for planning, Helena region (R. G. Schmidt, NC)
New Mexico, geology of urban development (H. E. Malde, D)
Pennsylvania (NC, except as otherwise noted):
Coal-mining features, Allegheny County (W. E. Davies)
Geochemistry of Pittsburgh urban area (H. A. Tourtelot, D)
Susceptibility to landsliding:
Allegheny County (J. S. Pomeroy)
Beaver, Butler, and Washington Counties (J. S. Pomeroy)
Utah, Salt Lake City and vicinity (Richard VanHorn, D)
Virginia, geohydrologic mapping of Fairfax County (A. J. Froelich, NC)

Urban hydrology:
Analysis of urban flood data in United States (V. B. Sauer, w, Atlanta, Ga.)
Geohydrology, urban planning (H. G. O'Connor, w, Lawrence, Kans.)
Urban-area reconnaissance (W. E. Hale, w, Albuquerque, N. Mex.)
Urban runoff networks (H. H. Barnes, Jr., w, NC)
Urban sedimentology (H. P. Guy, w, NC)
States:
Alaska, Anchorage geohydrology (C. Zenone, w, Anchorage)
California, Perris Valley (M. W. Busby, w, Laguna Niguel)
Colorado:
Climatological atlases, Colorado Front Range urban corridor (W. R. Hansen, D)
Flood frequency, urban areas (R. K. Livingston, w, D)
Front Range urban corridor (D. E. Hillier, w, D)
Storm runoff quality, Denver (S. R. Ellis, w, D)
Florida:
Bay Lake area (E. R. German, w, Orlando)
Leon County (R. P. Rumenik, w, Tallahasse)
Storm water quality south Florida (H. C. Mattraw, w, Miami)
Tampa Bay region (M. A. Lopez, w, Tampa)
Hawaii, hydrology, sediment in Mauna Loa (C. J. Ewart, w, Honolulu)
Indiana, Indianapolis Water Company canal study (William Meyer, w, Indianapolis)
Iowa, flow models, Walnut Creek (O. G. Lara, w, Iowa City)
Kansas, urban runoff, Wichita (D. B. Richards, w, Lawrence)
Kentucky, Northern Kentucky urban hydrology (R. W. Davis, w, Louisville)
Maryland, Rock Creek—Anacostia River (T. W. Yorke, w, Towson)
Mississippi, bridge-site investigations (K. V. Wilson, w, Jackson)
Missouri, stream hydrology, St. Louis (T. W. Alexander, w, Rolla)
New Mexico, urban flood hydrology, Albuquerque (Ralph Clement w, Santa Fe)

Urban hydrology—Continued
States—Continued
New York, solid waste sites, Suffolk (G. E. Kimmel, w, Mineola)
North Carolina, urban hydrology, Charlotte (W. H. Eddins, w, Raleigh)
Ohio (R. P. Hawkinson, w, Columbus)
Oregon (w, Portland):
Bear Creek water-quality study (S. W. McKenzie)
Portland rainfall-runoff study (Antonius Laenen)
Pennsylvania (w, Harrisburg):
Philadelphia (T. G. Ross, w, Philadelphia)
Storm-water measurements (T. G. Ross)
Tennessee:
Effects of urbanization on floods and quality of water (F. N. Lee, w, Nashville)
Memphis Urban Flood Frequency (B. L. Neely, w, Memphis)
Texas (w, Fort Worth, except as otherwise noted):
Austin (M. L. Maderak, w, Austin)
Dallas County urban study (B. B. Hampton)
Dallas urban study (B. B. Hampton)
Fort Worth urban study (R. M. Slade, Jr.)
Houston urban study (Fred Liscum, w, Houston)
San Antonio urban study (Lynn Harmsen, w, San Antonio)
Washington:
Bellevue urban runoff study (W. L. Haushild, w, Tacoma)
Puget Sound urban-area studies (B. L. Foxworthy, w, Tacoma)
Wisconsin, simulation of urban runoff (R. S. Grant, w, Madison)

Vegetation:
Element availability:
Soils (R. C. Severson, D)
Vegetation (L. P. Gough, D)
Elements in organic-rich material (F. N. Ward, D)
Plant geochemistry, urban areas (H. A. Tourtelot, D)
Western coal regions, geochemical survey of vegetation (J. A. Erdman, D)
See also Plant ecology.

Volcanic-terrane hydrology. *See* Artificial recharge.

Volcanology:
Caldron and ash-flow studies (R. L. Smith, NC)
Cascade volcanoes, geodimeter studies (D. A. Swanson, M)
Columbia River basalt (D. A. Swanson, M)
Kimberlites (B. C. Hearn, Jr.)
Regional volcanology (R. L. Smith, NC)
Volcanic-ash chronology (R. E. Wilcox, D)
Volcanic hazards (D. R. Crandell, D)
States:
Arizona, San Francisco volcanic field (J. F. McCauley, M)
Hawaii:
Hawaiian Volcano Observatory (Hawaii National Park)
Seismic studies (P. L. Ward, M)
Submarine volcanic rocks (J. G. Moore, M)
Idaho (D):
Central Snake River Plain, volcanic petrology (H. E. Malde)
Eastern Snake River Plain region (M. A. Kuntz, H. R. Covington)
Montana, Wolf Creek area, petrology (R. G. Schmidt, NC)
New Mexico, Valles Mountains, petrology (R. L. Smith, NC)
Wyoming, deposition of volcanic ash in the Mowry Shale and Frontier Formation (G. P. Eaton, D)

Water budget:
- Hydrologic reconnaissance, West-Central Utah (J. S. Gates, w, Salt Lake City, Utah)
- Water budget Eagle Lake (D. I. Siegel, w, St. Paul, Minn.)

Water resources:
- Central Region field coordination (H. H. Hudson, w, D)
- Chattahoochee intensive river quality (R. N. Cherry, w, Atlanta, Ga.)
- Columbia-North Pacific ground water (B. L. Foxworthy, w, Tacoma, Wash.)
- Comprehensive studies, Pacific Northwest (L. E. Newcomb, w, M)
- Computational hydraulics (V. C. Lai, w, NC)
- Dams, weirs, and flumes (H. J. Tracy, w, Atlanta, Ga.)
- Data coordination, acquisition, and storage:
  - NAWDEX Project (M. D. Edwards, w, NC)
  - Water Data Coordination (R. H. Langford, w, NC)
- East Triassic waste-disposal study (G. L. Bain, w, Raleigh, NC)
- Evaluation of land treatment (R. F. Hadley, w, D)
- Foreign assistance:
  - PL 80-402 (J. R. Jones, w, NC)
  - Section 607 (J. R. Jones, w, NC)
- Foreign countries, Saudi Arabia, Saudi Arabian advisory services (G. C. Tibbits, Jr. w, NC)
- General hydrologic research (R. L. Nace, w, Raleigh, NC)
- Ground water, Missouri Basin (O. J. Taylor, w, D)
- Ground-water appraisal, New England region (Allen Sinnott, w, Trenton, NJ)
- Hydrology of land use change (D. J. Lystrom, w, NC)
- Intensive river-quality assessment (D. A. Rickert, w, Portland, Oreg.)
- Intermediate-depth drilling (L. C. Dutcher, w, M)
- International activities (J. R. Jones, w, NC)
- Monitoring design, coal regions (H. H. Hudson, w, D)
- Modeling principles (J. P. Bennett, w, NC)
- National assessment (D. W. Moody, w, NC)
- Network design (M. E. Moss, w, NC)
- Northeastern Region field coordination (J. W. Geurin, w, NC)
- Northwest water-resources data center (N. A. Kallio, w, Portland, Oreg.)
- Off-road vehicle use (C. T. Snyder, w, M)
- Polaris operations (T. T. Conomos, w, M)
- Powell arid lands centennial (R. F. Hadley, w, D)
- Quality-of-water accounting network (R. J. Pickering, w, NC)
- Rehabilitation potential, energy lands (L. M. Shown, w, D)
- Reservoir bank storage study (T. H. Thompson, w, M)
- Southeastern Region field coordination (C. L. Holt, w, Atlanta, Ga.)
- State aid, miscellaneous (J. R. Jones, w, NC)
- Water for coal conversion, Upper Missouri River basin (O. O. Taylor, w, D)
- Water-resource activities (J. R. Carter, w, D)
- Waterway treaty engineering studies (J. A. Bettendorf, w, NC)
- Western Region field coordination (L. E. Newcomb, w, M)
- *States and territories:*
- Alabama:
  - Drainage areas (J. C. Scott, w, Montgomery)
  - Low flows of Alabama streams (R. H. Bingham, w, Tuscaloosa)
  - Plans, reports, and information (W. J. Powell, w, Tuscaloosa)

Water resources—Continued
- *States and territories—Continued*
- Alaska (w, Anchorage, except as otherwise noted):
  - Arctic resources (J. M. Childers)
  - Coal resources study (D. R. Scully)
  - Collection of basic records analysis (D. R. Lamke, w, Anchorage)
  - Geohydrology Delta-Clearwater area (R. F. Brown)
  - Municipal water supply (G. S. Anderson)
  - North Slope study (G. L. Nelson, w, Fairbanks)
  - North Star project (G. L. Nelson, w, Fairbanks)
  - Water resources of national petroleum reserves (C. E. Sloan, w, Anchorage)
- Arizona:
  - Black Mesa hydrologic study (C. K. Bell, w, Tucson)
  - Black Mesa monitoring program (C. K. Bell, w, Flagstaff)
  - Coconino Sandstone water budget, Navajo County (L. J. Mann, w, Flagstaff)
  - Sedona ground-water availability (G. W. Levings, w, Flagstaff)
  - Verde Valley water resources (S. J. Owen, w, Tucson)
  - Water resources of the Papago Reservation (L. J. Mann, w, Tucson)
- Arkansas (w, Little Rock):
  - Cache River aquifer-stream system (M. E. Broom)
  - Characteristics of streams (M. S. Hines)
  - Investigations and hydrologic information (R. T. Sniegocki)
  - Lignite hydrology (J. E. Terry, w, Little Rock)
  - Time-of-travel study (T. E. Lamb)
- California:
  - Delta isotope study (W. L. Bradford, w, M)
  - Ground water:
    - Death Valley (D. J. Downing, w, Laguna Niguel)
    - Joshua Tree (D. J. Downing, w, Laguna Niguel)
    - Madera area, ground-water model (C. J. Landquist w, Sacramento)
    - Santa Cruz (K. S. Muir, w, M)
  - Indian reservations (C. E. Lamb, w, M)
  - Power plant siting—Desert basins (J. H. Koehler, w, Laguna Niguel)
  - San Antonio Creek ground water appraisal (C. B. Hutchinson, w, Laguna Niguel)
    - Water, Redwood National Park (S. H. Hofford, w, M)
  - Water resources California desert (J. H. Koehler, w, Laguna Niguel)
- Colorado (w, D, except as otherwise noted):
  - Areawide water-quality inventory (L. J. Britton)
  - Coal rehabilitation (G. H. Leavesley)
  - Ground water:
    - Potentiometric surface mapping (F. A. Welder)
    - Southwestern Colorado (R. E. Brogden)
    - U.S. Bureau of Mines prototype mine (J. B. Weeks)
  - Hydrology:
    - El Paso County (R. E. Fidler, w, Pueblo)
    - Naval Oil Shale Reserve No. 1 (G. H. Leavesley)
    - Parachute-Roan Creek Basin (O. B. Adams, w, Grand Junction)
    - San Luis Valley (R. K. Livingston, w, Pueblo)
    - South Platte River basin, Henderson to State line (R. T. Hurr)
  - Intensive monitoring, Raton, Colorado (D. P. Bauer)
  - Quality of water:
    - Boulder County (D. C. Hall)
    - Geochemical investigations (S. G. Robson)
  - Regional monitoring (Gerhard Kuhn)

Water resources—Continued
States and territories—Continued
Colorado—Continued
Regional monitoring, Raton Mesa (A. P. Hall, w, Pueblo)
Sediment yield, Piceance Basin (V. C. Norman)
Spring hydraulics (G. J. Saulnier)
Water monitoring—coal mining Colorado (J. R. Little, w, D)
Water resources, Park-Teller County (K. E. Goddard, w, D)
Yampa River basin assessment (T. D. Steele)
Connecticut (w, Hartford):
Ground water, Southbury-Woodbury (D. L. Mazzaferro)
Hydrogeology, south-central Connecticut (F. P. Haeni)
Integrated hydrologic network (R. L. Melvin)
Part 7, Upper Connecticut River basin (R. B. Ryder)
Part 9, Farmington River basin (F. P. Haeni)
Part 10, Lower Connecticut River basin (L. A. Weiss)
Short-term studies (C. E. Thomas, Jr.)
Florida:
Annual hydrologic report, southwestern Florida (K. W. Causseaux, w, Tampa)
Broward County (C. B. Sherwood, Jr., w, Miami)
Caloosahatchee River study (T. H. O'Donnell, w, Ft. Myers)
East Boundary area investigation (B. G. Waller, w, Miami)
Ground water:
Aquifer mapping, south Florida (Howard Klein, w, Miami)
Hallandale area (W. A. Pitt, w, Miami)
Hollywood area (W. A. Pitt, w, Miami)
Hydrogeology, middle Peace basin (W. E. Wilson III, w, Tampa)
Hydrology,Manatee County (D. P. Brown, w, Sarasota)
Ochlockonee River basin investigation (C. A. Pascale, w, Tallahassee)
Potentiometric surface, St. Petersburg-Tampa (C. B. Hutchinson, w, Tampa)
Sand-gravel aquifer, Pensacola (Henry Trapp, w, Tallahassee)
Santa Fe River basin (J. D. Hunn, w, Tallahassee)
Sewage effluent disposal, irrigation (M. C. Yurewics, Tallahassee)
Shallow aquifer, Brevard County (J. M. Frazee, Jr., w, Winter Park)
Technical assistance, south Florida (Howard Klein, w, Miami)
Urban hydrology, Englewood area (Horace Sutcliffe, Jr., w, Sarasota)
Verna well field (Horace Sutcliffe, Jr., w, Sarasota)
Water resources:
Duval and Nassau counties (G. W. Leve, w, Jacksonville)
Martin County (R. A. Miller, w, Miami)
Tequesta (A. L. Knight, w, Miami)
Hydrogeologic maps, Seminole County (W. D. Wood, w, Winter Park)
Hydrogeology, Osceola Forest (P. R. Seaber, w, Tallahassee)
Lee County (D. H. Boggess, w, Ft. Myers)
Palm Beach County (J. N. Fischer, w, Miami)
Quality of water:
Estuarine hydrology, Tampa Bay (C. R. Goodwin, w, Tampa)
Solid waste, Hillsborough County (Mario Fernandez, Jr., w, Tampa)

Water resources—Continued
States and territories—Continued
Florida—Continued
Quality of Water:
Technical assistance, Department of Environmental Regulation (G. A. Irwin, w, Tallahassee)
Special studies, technical assistance (C. S. Conover, w, Tallahassee)
Surface water:
Lakes in southwest Florida (R. C. Reichenbaugh, w, Tampa)
Manasota technical assistance (Horace Sutcliffe, Jr., w, Sarasota)
Technical assistance:
Northwest Florida Water Management District (W. B. Mann, w, Tallahassee)
Suwanee River Water Management District (J. C. Rosenau, w, Tallahassee)
Water Atlas (S. D. Leach, w, Tallahassee)
Water resources, Hendry County (T. H. O'Donnell, w, Miami)
Water resources of Manasota basin (K. W. Causseaus, w, Tampa)
Water resources, Orange County (C. H. Tibbals, w, Winter Park)
Western Collier County (W. J. Haire, w, Miami)
Georgia (w, Doraville):
Cretaceous (L. D. Pollard)
Hydrology of the Albany area (R. E. Krause)
Information system (J. R. George)
Hawaii (w, Honolulu):
Biology-morphology Wailuku River (J. J. S. Yee, w, Honolulu)
Data management, Guam (C. J. Huxel, Jr.)
Topical studies (F. T. Hidaka)
Idaho (w, Boise):
Flow in Silver Creek, Idaho (J. A. Moreland)
Ground-water-quality assessment (H. R. Seitz)
Kootenai Board—WWT (E. F. Hubbard)
Special studies (C. A. Thomas)
Streamflow evaluation, Upper Snake River (C. A. Thomas)
Indiana (w, Indianapolis):
Ground water near Fort Wayne (Michael Planert)
Plate map books for board of Health (B. P. Robinson)
Iowa (w, Iowa City):
Bedrock mapping (R. E. Hansen)
Low flow, Iowa streams (O. G. Lara)
Kansas (w, Lawrence, except as otherwise noted):
Geohydrology Arkansas River valley southwest Kansas (R. A. Barker, w, Garden City)
Glacial deposits (J. E. Denne, w, Lawrence)
Special hydrologic investigations (H. G. O'Conner)
Saline water Wellington Formation (A. J. Gogel, w, Lawrence)
Water supply in droughts (H. G. O'Conner)
Kentucky (w, Louisville):
Covington-Lexington-Louisville triangle (D. S. Mull)
Ground water, Ohio River valley (J. M. Kernodle)
Somerset hydrology (R. W. Davis)
Louisiana (w, Baton Rouge):
Baton Rouge area (C. D. Whiteman, Jr.)
Lignite hydrology (J. L. Snider, w, Alexandria)
Ground water:
Grammercy area (G. T. Cardwell)
Kisatchie Forest area (J. E. Rogers, w, Alexanderia)
Terrace aquifer, central Louisiana (J. L. Snider)

Water resources—Continued
States and territories—Continued
Louisiana—Continued
New Orleans area (D. C. Dial)
Reports on special topics (M. J. Forbes)
Site studies (J. E. Rogers)
Surface water:
Flood hydraulics and hydrology (B. L. Neely, Jr.)
Velocity of Louisiana Streams (A. J. Calandro)
Maine, public inquiries (E. S. Denison w, Boston, Mass.)
Massachusetts (w, Boston):
Coastal southeastern Massachusetts, Wareham to Seekonk (G. D. Tasker)
Connecticut River lowlands (E. H. Walker)
Deicing chemicals, ground water (L. R. Frost)
Nashua River basin (R. A. Brackley)
Northeast, Coastal basins (F. B. Gay)
Public inquiries (E. S. Denison)
Michigan (w, Lansing, except as otherwise noted):
Erosion in St. Joseph Basin (T. R. Cummings)
Geohydrology, environmental planning (F. R. Twenter)
Ground water:
Models, Muskegon County (W. B. Fleck)
West Uppir Peninsula (C. J. Doonan)
Minnesota (w, St. Paul):
Impact of copper-nickel mining (P. G. Olcott)
Twin Cities ground-water study (J. H. Guswa)
Mississippi (w, Jackson):
Aquifer maps for Mississippi (E. H. Boswell)
Salt Dome hydrology in Mississippi (C. A. Spiers, w, Jackson)
Water assimilation (G. A. Bednar)
Missouri, irrigation water, Audrian County (L. F. Emmett)
Montana (w, Helena, except as otherwise noted):
Ground water:
Fort Belknap (R. D. Feltis, w, Billings)
Fort Union Formation (S. E. Slagle, w, Billings)
Hydrology, lower Flathead (A. J. Boettche)
"Saline seeps" (B. D. Lewis, w, Billings)
Special investigations (J. A. Moreland)
Water supplies for national parks, monuments, and recreation areas (J. A. Moreland)
Nebraska (w, Lincoln):
Hydrogeology of southwest Nebraska (E. G. Lappala)
Movement of nitrogen into aquifers (L. R. Petri)
Time-of-travel data (L. R. Petri)
Nevada (w, Carson City):
Aquifers in the Fallon area (P. A. Glancy)
Topical studies (P. A. Glancy)
Water supply:
Cold Spring Valley (A. S. Van Denburgh)
Mining districts (H. A. Shamberger)
New Hampshire (w, Concord):
Ground-water reconnaissance, river basins (J. E. Cotton)
Public inquiries (J. V. Skinner)
New Jersey (w, Trenton):
Problem river studies (J. C. Schornick, Jr.)
Quantification nonpoint pollution (J. C. Schornick, Jr.)
Short-term studies (William Kam)
Geophysical logging (R. L. Walker)
Water resources, Wharton Tract (A. S. Poggiol)
New Mexico (w, Albuquerque):
Bureau of Indian Affairs water-supply investigations (F. P. Lyford)
Coal-lease areas, northwest New Mexico (J. R. Hejl)

Water resources—Continued
States and territories—Continued
New Mexico—Continued
Ground water:
Capitan Limestone (W. L. Hiss)
Harding County (F. D. Trauger)
Miscellaneous activities, State Engineering (W. A. Mourant)
White Sands Missile Range, water levels and pumpage (H. D. Hudson)
Pojoaque River analyses (G. A. Hearne)
Water resources, Acoma and Laguna Reservations (F. P. Lyford)
Water resources, Mimbres Basin (J. S. McLean)
New York (w, Syosset, except as otherwise noted):
Basin recharge with sewage effluent (R. C. Prill)
Hydrogeology of southeast Nassau County (H. F. H. Ku)
Long Island water quality (B. G. Katz)
Nassau County, ground-water (Chabot Kilburn)
Short-term studies (L. A. Martens, w, Albany)
Suffolk County, water-quality observation well program (Julian Soren)
Water resources, South Fork, Long Island (Bronius Nemickas)
North Carolina (w, Raleigh):
Hydrology of Albermarle-Pamlico area (C. C. Daniel)
Public water supplies (T. M. Robison)
Surface water:
Hydrology of estuaries (G. L. Geisse)
Requests for data (H. N Jackson)
North Dakota (w, Bismarck, except as otherwise noted):
Ground water:
Billings-Golden Valley Slope (L. O. Anna)
Dickey-Lamoure (J. S. Downey)
Hydrologic changes due to mining (W. F. Horak)
Morton County (D. J. Ackerman)
Ramsey County (R. D. Hutchinson)
Ransom-Sargent (C. A. Armstrong)
Special investigations (O. A. Crosby)
Rattlesnake Butte area hydrology (W. F. Horak)
Wibaux-Beach deposit hydrology (W. F. Horak, Jr.)
Northern Mariana Islands, Water resources information—Northern Marianas (D. A. Davis, w, Honolulu, Haw.)
Oklahoma (w, Oklahoma City):
Ground water, Antlers Sand (D. L. Hart, Jr.)
Monitor Oklahoma coal field (J. S. Havens, w, Oklahoma City)
Requests, special investigations (J. H. Irwin)
Pennsylvania (w, Harrisburg, except as otherwise noted):
Allegheny River basin Level-B study (D. B. Richards, w, Meadville)
Ground-water resources of Monroe County (L. D. Carswell, w, Philadelphia)
Ground water:
Chester County (L. J. McGreevy, w, West Chester)
Cumberland Valley (A. E. Beecher)
Ground-water resources of the Williamsport area (O. B. Lloyd)
Quality of water, highway construction effects on streams (J. F. Truhlar, Jr.)
Western Pennsylvania (G. R. Schiner)
Puerto Rico (w, San Juan):
Contingent requests (E. D. Cobb)
Geohydrology of landfills, (Fernando Gomez-Gomez, w, San Juan)

Water resources—Continued
States and territories—Continued
Puerto Rico—Continued
Hydrologic systems modeling (M. A. Lopez)
St. Thomas water-resources appraisal (H. J. McCoy)
Rhode Island, public inquiries (H. E. Johnston, w, Providence)
South Carolina (w, Columbia):
Cooper River rediversion (P. W. Johnson)
Reconnaissance of estuaries (F. A. Johnson)
South Dakota (w, Huron, except as otherwise noted):
Cheyenne and Standing Rock Indian Reservations (L. W. Howells)
Clark County (L. J. Hamilton)
Deuel and Hamlin Counties (Jack Kume, w, Vermillion)
Water resources:
Aurora and Jerauld Counties (L. J. Hamilton)
Davison-Hanson Counties (J. E. Powell, w, E. F. Le Roux)
Miner County (Jack Kume, w, Vermillion)
Yankton County (J. E. Powell, w, Huron)
Tennessee , Terrace- deposits study (W. S. Parks, w, Memphis)
Texas:
Edwards aquifer, Austin area (M. L. Maderak, w, Austin)
Ground water:
El Paso (D. E. White, w, El Paso)
Houston (R. K. Gabrysch, w, Houston)
Model study, Chicot and Evangeline aquifers (W. R. Meyer, w, Houston)
Orange County (G. W. Bonnet, w, Houston)
Rio Grande environmental study (J. S. Gates, w, El Paso)
Salt encroachment at Houston (D. G. Jorgensen, w, Houston)
San Antonio (R. D. Reeves, w, San Antonio)
Quality of water, bays and estuaries (D. C. Hahl, w, Houston)
Trust territory, water-resource information (D. A. Davis, w, Honolulu, Hawaii)
Utah (w, Salt Lake City, except as otherwise noted):
Central Wasatch Plateau (C. T. Sumsion)
Environmental impacts (Donald Price)
Ground water:
Oil-shale hydrology (K. L. Lindskov)
Statewide ground-water conditions (J. C. Stephens)
Navajo Sandstone, east-central Utah (J. W. Hood)
Navajo Sandstone, southeastern Utah (J. W. Hood)
Program enhancement (Theodore Arnow)
Quality of water, Flamingo Gorge Reservoir (E. L. Bolke)
Surface water:
Canal-loss studies (R. W. Cruff)
Inflow to Great Salt Lake (J. C. Mundorff)
Vermont:
Ground water, Upper Winooski Basin (A. L. Hodges, Jr., w, Montpelier)
Public inquiries (R. E. Willey, w, Montpelier)
Water quality, Black River (W. D. Silvey, w, Boston, Mass.)
Virginia (w, Richmond):
Ground water:
Geohydrologic data (R. L. Wait)
Hydrology of Prince William Forest Park (H. T. Hopkins)
Hydrology of the Great Dismal Swamp (J. F. Harsh)
South of James River (O. J. Cosner)
Surface water, project planning and public inquiries (P. M. Frye)

Water resources—Continued
States and territories—Continued
Washington (w, Tacoma):
Ground water:
Special hydrologic problems (R. J. Carpenter)
Test drillings (K. L. Walters)
Inquiries (J. R. Williams)
Model simulation for water management (J. A. Skrivan)
Quileute project (L. M. Nelson)
Real-time data collection (R. R. Adsit)
Tulalip water resources (B. W. Drost)
West Virginia (w, Charleston):
Saline ground water (J. B. Foster)
Studies for unforeseen needs (G. G. Wyrick, w, Morgantown)
Wisconsin (w, Madison):
Ground water, Columbia County (C. A Harr)
Low flow of small streams (S. J. Field)
Nederlo Creek hydrololgy (P. A. Kammerer, w, Madison)
Quality of water:
Ground-water-quality monitoring (C. A. Harr)
Menomonee River sediment study (E. R. Zuehls)
Washington county sediment study (S. M. Hindall)
Surface water, drainage areas (E. W. Henrich)
Wyoming (w, Cheyenne):
Arikaree Formation, Lusk (M. A. Crist)
Effluent monitor, national parks (E. R. Cox)
Green River basin water supply (H. W. Lowham)
Water resources, Powder River basin (M. E. Lowry)

Water use:
National water use data program (J. R. Ruggles, w, NC)
States and territories:
Alaska, water use (L. D. Patrick, w, Anchorage)
California, water use (J. R. Crippen, w, M)
Colorado, water use (R. R. Hurr, w, D)
Connecticut, water use (F. P. Haeni, w, Hartford)
Florida:
Ground-water use, Peace basin (A. D. Duerr, w, Tampa)
Water use, (S. D. Leach, w, Tallahassee)
Georgia, water use (R. F. Carter, w, Doraville)
Hawaii, water-use data (R. H. Nakahara, w, Honolulu)
Illinois, water use (D. E. Winget, w, Champaign)
Kansas:
Estimating ground-water withdrawals (C. H. Baker, Jr., w, Lawrence)
Water use (C. H. Baker, Jr., w, Lawrence)
Louisiana, water use, 1975 (G. C. Cardwell, w, Baton Rouge)
Maryland, water use (F. K. Mack, w, Towson)
Massachusetts, water use (J. A. Baker, w, Boston)
Michigan, water use (F. R. Twenter, w, Lansing)
Minnesota, water use (E. L. Madsen, w, St. Paul)
Mississippi, water use (J. A. Callahan, w, Jackson)
North Carolina, water use (R. W. Coble, w, Raleigh)
Nebraska, availability and use of water, Nebraska (E. K. Steele, w, Lincoln)
New Mexico, water use (W. K. Dein, w, Santa Fe)
Nevada, water use (C. V. Schroer, w, Carson City)
North Dakota, water use (Dale Frink, w, Bismarck)
Ohio, water use (R. M. Hathaway, w, Columbus)
Oregon, water use (L. E. Hubbard, w, Portland)
Pennsylvania, water use (A. E. Becher, w, Harrisburg)
Puerto Rico, water use (Fernando Gomez-Gomez, w, San Juan)
Tennessee, water use (R. L. Gold, w, Nashville)
Texas, water use (E. T. Baker, w, Austin)

Water use—Continued

States and territories—Continued

Utah, water use (R. W. Cruff, w, Salt Lake City)

Virginia, water use (H. T. Hopkins, w, Richmond)

Washington, water use (E. H. Gavock, w, Tacoma)

West Virginia, water use (G. G. Wyrick, w, Charleston)

Wisconsin, water use (R. S. McLeod, w, Madison)

Waterpower classification:

California (c, Sacramento):

Kings River basin, examination of pumped storage sites (W. T. Smith)

Mokelumne River Basin, examination of pumped storage sites (D. E. Wilson)

Review of withdrawals, Owens River basin Westside tributaries (R. D. Morgan)

Upper San Joaquin River basin, examination of pumped storage sites (W. T. Smith)

Waterpower—Continued

California—Continued

Westside tributaries (R. D. Morgan)

Idaho, Pahsimeroi River, reservoir and dam site (K. J. St. Mary c, Portland, Oreg.)

Oregon (c, Portland), Review of withdrawals:

Clackamas River basin (L. O. Moe)

Coquille River basin (S. R. Osborne)

Nestucca River basin (K. J. St. Mary)

South Umpqua River (L. O. Moe)

Wilderness Program. *See* Primitive and Wilderness Areas *under* Mineral and fuel resources—compilations and topical studies, mineral-resources surveys.

Zeolites:

California (southeastern), Oregon, and Arizona (R. A. Sheppard, D)

Zinc. *See* Lead, zinc, and silver.

SUBJECT INDEX

A

absolute age *see also* geochronology; isotopes
absolute age—dates
basalt: Age and composition of Jingu Seamount 181
— Age and strontium isotopic composition of the Honolulu Volcanics 180
— Age of Emperor Seamounts confirms hot-spot hypothesis 180
— Minimum age of Mieji Seamount 180-181
— Rubidium-strontium systematics of Hawaiian-Emperor Seamount chain basalts 181
— Volcanic recurrence intervals and volcanic hazards in the eastern Snake River Plain in Idaho 71-72
basanite: Age of Black Point dike, Oahu and Yarmouth interglaciation 180
gneiss: Age of Archean events in the Big Horn Mountains of Wyoming 184
— Geochronology 333
granite: New age of metaplutonic rocks in the Survey Pass quadrangle, Brooks Range 95
— Two-mica granite and the Mesoappalachian-Avaltonian boundary in New Hampshire 37
granodiorite: Age of Davidson Granodiorite and mineralization in Comstock Lode mining district of western Nevada 79-80
migmatite: More Archean rocks in Utah 70
minerals: Potassium-argon ages of Mesozoic mafic rocks of the Pensacola Mountains 191-192
— Potassium-argon geochronology of Mesozoic mafic rocks of the Pensacola Mountains 336
obsidian: Pliocene rhyolite in the Sevier Plateau, Utah 73
peat: Age of Everglades peat 21
plagioclase: Mesozoic radiometric ages in Precambrian rocks 95
plutonic rocks: Geochronology of intrusion and prophyry copper ores, Globe-Miami, Arizona 5
sediments: Quaternary deposits and soils, Sierra Nevada foothills 85-86
shells: Corrections for marine shell radiocarbon dates 192
— Holocene submergence of the southern New England inner Continental Shelf 141
volcanic rocks: Potassium-argon ages of volcanic rocks in the Murrieta area of California 86-87
zircon: Constraints on the genesis of uranium ores in the Midnite Mine, Washington, from geochronologic and lead-isotope investigations 46
— Lower Archean gneiss from Wyoming 190
— New data on the age of the Independence dike swarm in eastern California 184
— Preliminary Proterozoic lead ages on zircon from augen gneiss, Big Delta quadrangle 96
absolute age—interpretation
K/Ar: Cenozoic events in west-central Arizona 82-83
overprinting: Regional geochronology of the Willow Creek area 96
seamounts: Hawaiian Island-Emperor Seamount studies 180-181
aeromagnetic surveys *see* magnetic surveys *under* geophysical surveys *under* Alaska; Oklahoma; Saudi Arabia
Afars and Issas Territory *see* Djibouti
Afghanistan—economic geology
metals: Afghanistan-Iran-Turkey 321
Africa *see also* Djibouti; Egypt; Kenya; Liberia; South Africa
Africa—economic geology
fluorspar: Fluorspar resources of Africa 1
Alabama—hydrogeology
hydrology: Alabama 112
— Regionalization of low flow in Alabama streams 112
Alabama—stratigraphy
Cretaceous: Cyclicity of Upper Cretaceous sedimentary rocks 64
Alaska—areal geology
Arctic region: Geology of Alaska bordering Arctic Ocean 94
regional: Alaska 91-100
— East-central 95-96
— Northern 94-95
— Southeastern 97-100
— Southern 96-97
— Southwestern 97
— Statewide 91-94
Alaska—economic geology
metals: Copper and molybdenum in Nabesna, Alaska 296
— Geochemical anomalies in the Mystery Mountains, Medfra quadrangle, Alaska 4
mineral resources: Alaska Mineral Resource Assessment Program 91-93
— Geophysical ore guides in south-central Alaska 97
— Mineral resources and aeromagnetic studies of Glacier Bay National Monument 97-99
— Mineral resources in Kuiu-Etolin Islands Tertiary volcanic and intrusive belt 99
— Resources data summarized 93
molybdenum: Quartz Hill molybdenum deposit, Ketchikan quadrangle, Alaska 3-4
petroleum: Alaska 23-25
— Discovery of potential source rocks for petroleum, eastern Gulf of Alaska 150
— Geochemical exploration for petroleum in a permafrost environment, North Slope 24
— New information on age and petroleum potential of Lisburne Group (Carboniferous and Permian), North Slope 23
— Origin of North Slope oil and gas 23
— Petroleum geology of Cook Inlet Basin 24-25
— Petroleum potential of Lower Cretaceous deltaic sandstones, North Slope 23-24

uranium: Epigenetic uranium mineralization, Alaska 44
— Uranium studies in interior Alaska 39
Alaska—engineering geology
geologic hazards: Research in geologic hazards 251
permafrost: Geochemical exploration for petroleum in a permafrost environment, North Slope 24
— Model for predicting offshore permafrost in the Beaufort Sea 94-95
Alaska—environmental geology
land use: Landsat used to map vegetation in Alaska 307
maps: Landsat used to map vegetation in Alaska 307
Alaska—geochronology
Devonian: New age of metaplutonic rocks in the Survey Pass quadrangle, Brooks Range 95
Mesozoic: Mesozoic radiometric ages in Precambrian rocks 95
Paleocene: Regional geochronology of the Willow Creek area 96
Proterozoic: Preliminary Proterozoic lead ages on zircon from augen gneiss, Big Delta quadrangle 96
Alaska—geomorphology
glacial geology: Columbia Glacier, Alaska 204-205
— Glacier ice and water balance 203
— Glacier inventories 203-204
Alaska—geophysical surveys
gravity surveys: Gravity surveys 240
magnetic surveys: Mineral resources and aeromagnetic studies of Glacier Bay National Monument 97-99
remote sensing: Copper and molybdenum in Nabesna, Alaska 296
— Landsat used to map vegetation in Alaska 307
seismic surveys: Gas-charged sediment areas in the northern Gulf of Alaska 152-153
— Seafloor thermogenic gas seep, Norton Sound 154-155
surveys: Airborne pulse sounding of Alaskan glaciers 174
Alaska—hydrogeology
ground water: Geohydrology of the Fairbanks North Star Borough 129
hydrology: Alaska 129-130
— Hydrology and water quality of the Keta River basin 129-130
springs: Geohydrology of the Delta-Clearwater area 129
— Hot spring area, Circle quadrangle 96
Alaska—oceanography
continental shelf: Crustal structure, abyssal basins and Continental Shelf beneath the Bering Sea 154
marine geology: Alaskan continental margin 150-155
sedimentation: Bottom boundary layers and sediment transport, Norton Sound in Alaska 154
— Comparison of sedimentation in Yakutat and Icy Bays, Alaska 151
— Holocene sediment volume on the northeast Gulf of Alaska Continental Shelf and the sediment contribution of present-day rivers 151-152
— Movement of bedforms in the lower Cook Inlet, Alaska 152
— Neoglacial sedimentation in Glacier Bay, Alaska 150-151
— Sedimentation in coastal embayments of the northern Gulf of Alaska 151
— Volcanic ash in surficial sediments of the Kodiak Shelf, western Gulf of Alaska 152
Alaska—petrology
igneous rocks: Cumulate gabbro and pillow basalt associated with the Mount Sorenson ultramafic complex 96
— Intrusive belts of southeastern Alaska 99-100
— Trondhjemite in the Talkeetna Mountains, south-central Alaska 97
Alaska—stratigraphy
Carboniferous: Paleotectonic setting of the Carboniferous of Alaska 93-94
Cretaceous: Dinoflagellates helpful in North Slope biostratigraphy 217
Jurassic: Upper Jurassic shallow-water sandstones of the Bering Sea continental margin 153
Paleozoic: Late Paleozoic fossils in ophiolite, northeastern Alaska 95
— New analysis of paleomagnetic data from Alexander terrane 99
— Paleozoic and Triassic paleomagnetism of the Alexander terrane, southeastern Alaska 168
— Reconstruction of Paleozoic continental margin in Alaska and accreted terranes 93
Pennsylvanian: New information on age and petroleum potential of Lisburne Group (Carboniferous and Permian), North Slope 23
Precambrian: Exotic Precambrian rocks in southwestern Alaska 97
— Review of Precambrian rocks of Alaska 93
Alaska—tectonophysics
crust: Gravity surveys 240
plate tectonics: Microplate tectonics 94
— Paleotectonic setting of the Carboniferous of Alaska 93-94
— Reconstruction of Paleozoic continental margin in Alaska and accreted terranes 93
algae—biostratigraphy
Ordovician: Ordovician Vinini Formation of northern Nevada 80-81
algae—Coccolithophoraceae
Miocene: Planktonic microfossils and the lower-middle Miocene boundary in the California borderland 157
algae—diatoms
Quaternary: Quaternary paleolimnology of Lake Valencia, Venezuela 214
algae—stromatolites
Holocene: Algal stromatolites (oncolites), Onondaga Lake, New York 228
aluminum—resources
evaluation: Copper-aluminum substitution model 14-15
global: World aluminum (bauxite) resources 1
americium—isotopes
Am-241: Errors in gross radioactivity measurements 234
angiosperms—floral studies
Paleogene: Early Tertiary flora found in New Mexico 217
Antarctica—general
current research: Antarctic programs 336-338
Antarctica—geochemistry
weathering: Mineralogy of surface encrustations in the Orville Coast area 337
Antarctica—geochronology
Cenozoic: Magnetic correlation of upper Cenozoic Dry Valley Drilling Project cores 336-337
Mesozoic: Potassium-argon ages of Mesozoic mafic rocks of the Pensacola Mountains 191-192
— Potassium-argon geochronology of Mesozoic mafic rocks of the Pensacola Mountains 336
Antarctica—geomorphology
glacial geology: Former more extensive glacial ice in the Orville Coast area 337-338
Antarctica—petrology
igneous rocks: Application to volcanic rocks in Antarctica 187
intrusions: Geologic field study of the Dufek intrusion 336
Antarctica—structural geology
tectonics: Structural geology and paleomagnetism of the Orville Coast area 337
Appalachians—areal geology
regional: Appalachian Highlands and the Coastal Plains 60-65
Appalachians—economic geology
coal: Dissolved sulfate loads, an index of mining activity 261
natural gas: Appalachian Basin 31-33
— Fracture reservoirs in Devonian black shale 32-33
— Gas generation in Devonian black shale 31
— Late Devonian black shale sedimentation and possible gas exploration areas 32
— New method for computing organic-carbon content of Devonian shale 33
Appalachians—engineering geology
slope stability: Landslide investigations in the Appalachian Plateau 254-255
Appalachians—environmental geology
pollution: Subsurface waste nuclide migration at Maxey Flats storage site near Morehead, Kentucky 264
— Tritium tracer tests successful at Oak Ridge National Laboratory in Tennessee 264

Appalachians—geochemistry
organic materials: Sources of organic matter in Devonian black shales 33

Appalachians—stratigraphy
Ordovician: Lower-Middle Ordovician boundary in the north-central Appalachian Basin 219

Appalachians—structural geology
maps: Synthesis and analysis of Appalachian orogen 100
tectonics: Synthesis and analysis of Appalachian orogen 100
— Thrust plates in the Blue Ridge 63
— Two-mica granite and the Mesoappalachian-Avaltonian boundary in New Hampshire 37

aquifers *see under* ground water

Arabian Peninsula *see also* Oman; Saudi Arabia

Arabian Peninsula—seismology
crust: Seismic profile 332-333

Arabian Peninsula—tectonophysics
mantle: Regional gravity studies 333

Archean *see also under* geochronology *under* Utah; Wyoming

archeology *see* archaeology *under* stratigraphy *under* Middle East

Arctic Ocean—stratigraphy
changes of level: Model for predicting offshore permafrost in the Beaufort Sea 94-95

Arizona—economic geology
copper: Geochronology of intrusion and prophyry copper ores, Globe-Miami, Arizona 5
— Porphyry copper in Arizona 295-296
— Volatile gases useful in geochemical exploration 12
geothermal energy: Intermediate-temperature geothermal waters found in the Verde Valley, Arizona 194
uranium: Geological setting for uranium deposits in the Data Creek basin, west-central Arizona 43
— Uranium potential of Cenozoic rocks of the Basin and Range province, Arizona 43

Arizona—engineering geology
land subsidence: Arizona 130
— Earth fissures form in alluvial deposits that overlie buried bedrock irregularities 276
— Geophysical studies over subsidence fissures 175
— Mechanisms of ground failure associated with ground-water withdrawal 277

Arizona—environmental geology
geologic hazards: Analysis of flood-data network for regional information 270
— Potential flood and debris hazards at Willow Beach 130

Arizona—geochronology
Cenozoic: Cenozoic events in west-central Arizona 82-83

Arizona—geomorphology
impact features: Basin and crater studies 285-286

Arizona—geophysical surveys
remote sensing: Porphyry copper in Arizona 295-296
— Radar investigations 284-285

Arizona—hydrogeology
springs: Intermediate-temperature geothermal waters found in the Verde Valley, Arizona 194

Arizona—paleobotany
Plantae: Plant societies along a bajada in southern Arizona 220

Arizona—stratigraphy
Mississippian: Chesterian channels discovered in western Grand Canyon, Arizona 29
Ordovician: Ordovician Montoya Group extended westward in southeastern Arizona 83

Arkansas—stratigraphy
Paleocene: Post-Midwayan (Paleocene) uplift at margin of Mississippi embayment in northeastern Arkansas 66

arsenic—abundance
ground water: High arsenic concentrations in ground-water samples from northern Malheur County 132

asbestos—production
human ecology: The asbestos minerals and cancer incidence 177-178

Asia *see also* Afghanistan; Arabian Peninsula; China; India; Indonesia; Iran; Japan; Pakistan

Asia—economic geology
mineral resources: Assistance to intergovernmental organizations 312-313

associations—general
IGCP: International Geological Correlation Program 317-318

Atlantic Coastal Plain—areal geology
regional: Appalachian Highlands and the Coastal Plains 60-65

Atlantic Coastal Plain—economic geology
phosphate: Extension of phosphorite-bearing strata underneath Atlantic Continental Shelf of United States 3
water resources: Ancestral Potomac River deposits in Fairfax County, Virginia 303
— Southeastern region 112-118

Atlantic Coastal Plain—engineering geology
earthquakes: Eastern United States 247-248

Atlantic Coastal Plain—environmental geology
ecology: Central Atlantic Regional Ecological Test Site 306-307
— Studies of benthic fauna in the Potomac River Estuary 159
land use: Development of Atlantic-Gulf barrier islands 309
— Land use map accuracy determination 307
maps: Land use map accuracy determination 307
pollution: Tritium migration at Barnwell, South Carolina 264

Atlantic Coastal Plain—geophysical surveys
maps: Temporal mapping with Landsat data 344
— Upper Chesapeake Bay 344-345
remote sensing: Temporal mapping with Landsat data 344
— Upper Chesapeake Bay 344-345
— Wetland studies 301

Atlantic Coastal Plain—hydrogeology
ground water: Potentiometric surface of Cretaceous aquifer, Atlantic Coastal Plain 111
hydrology: Atlantic Coast 159
— Factors influencing seasonal distributions of biochemically reactive substances in the Potomac River 159

Atlantic Coastal Plain—oceanography
continental shelf: Reefs and hardgrounds of the Georgia Bight 142-143
— Stratigraphic test wells on the outer Continental Shelf 144
— Stratigraphy and structure of the Atlantic Continental Margin 143
marine geology: Atlantic Continental Margin 141-145

Atlantic Coastal Plain—stratigraphy
changes of level: Shoreline datum planes in the southeastern United States 214-215
Neogene: Sedimentary environments in the Neogene of the central Atlantic Coastal Plain 216

Atlantic Ocean—economic geology
petroleum: OCS lease sales for oil and gas 165-166
— Organic geochemistry of a stratigraphic test well, Southeast Georgia Embayment 144-145
— Stratigraphic test wells on the outer Continental Shelf 144
phosphate: Extension of phosphorite-bearing strata underneath Atlantic Continental Shelf of United States 3

Atlantic Ocean—environmental geology
pollution: Trace metals and an area of possible sediment accumulation on the North Atlantic Continental Shelf 141-142

Atlantic Ocean—oceanography
continental slope: Observations from a submersible of slumps on the upper Continental Slope south of Georges Bank 142

Atlantic Ocean—tectonophysics
crust: Origin of the East Coast Magnetic Anomaly 143-144
— Stratigraphy and structure of the Atlantic Continental Margin 143

Australasia *see also* New Zealand

Australia *see also* Northern Territory

automatic data processing—economic geology
cartography: An experimental technique for delineating areas best suited for mining of coal 71
data analysis: Petroleum resource analysis 15
— Prospector computer consultant 13-14

— Resource analysis 13-15
data bases: Computerized Resources Information Bank 13
— Geothermal resources file 13
data handling: National Coal Resources Data System, Phase II 13
data systems: Computerization of the Nation's coal resources 19
information systems: Resource information systems 13
— Resource information systems and analysis 13-15
models: Computer modeling of ore-forming processes 47
— Copper-aluminum substitution model 14-15
— Mineral resource assessment 14
— Uranium resource appraisal and decision modeling 14

automatic data processing—engineering geology
models: Evaluation of dam-break flood-wave models 270

automatic data processing—environmental geology
computer programs: Statistical design of sampling techniques 307
information systems: Geographic information systems software development 309

automatic data processing—general
cartography: Point-transfer eye test 341
— Space oblique mercator projection 345
data storage: Photogrammetric archival storage system 342
digital techniques: Building DLG-2 digital files directly from stereomodels 340-341
— Coordinate transformation system 343-344
— Digital cartography 342-344
— Digital data editing system 343
— Digital profile recording and output system 343
— Digital readout and reference system for cartographic camera 343
timesharing: Remote-access, error-free computer timesharing 15

automatic data processing—geochemistry
computer programs: Computer programs simulate distribution of aqueous uranium species 268
models: Computer modeling 335
neutron activation analysis: Neutron activation of geologic materials 232
simulation: Feedback effects analyzed in salt dissolution 268

automatic data processing—geophysical surveys
computer programs: Surface self-potential distributions as indicators of subsurface geothermal activity 198-199
data analysis: Data analysis laboratory 290
data handling: Tests of hydrologic-data relay systems 300
well-logging: Computer model of gamma spectra in boreholes 267
— Computer programs to relate acoustic waveforms and fracture permeability in boreholes 268

automatic data processing—hydrogeology
data acquisition: Data coordination, acquisition, and storage 134-136
— Office of Water-Data Coordination 134-135
data bases: Index to ground-water monitor wells in Louisiana 122-123
— National Water Data Exchange 135-136
— Prototype water-use data systems in Connecticut, Kansas, and Virginia 137-138
— Urban water program 136-137
data handling: Data-management system 136
data storage: Water-data storage system 135
— Water use 137
maps: Computer-composite hydrogeologic maps for Fairfax County, Virginia 303
models: Conversion of a three-dimensional analog model to a three-dimensional digital model 210
— Flood frequency 136-137
— Model development 211-212
— Modeling of urban storm-water processes 136

automatic data processing—methods
applications: Computer managed meetings 346
data processing: Batch computing 346
— Time sharing 346
technology: Computer technology 346

automatic data processing—seismology
data bases: Seismic data bases 238

B

Basin and Range Province—areal geology
regional: Basin and Range region 78-83

Basin and Range Province—economic geology
gold: Age of Davidson Granodiorite and mineralization in Comstock Lode mining district of western Nevada 79-80
lithium: Origin and distribution of lithium-rich clay deposits 16
metals: Metals in Devonian marine strata in central Nevada 80
mineral resources: Mineral-resource studies 78-80
uranium: Alteration aureoles in McDermitt caldera in Nevada and Oregon 79
— Uranium potential of Cenozoic rocks of the Basin and Range province, Arizona 43

Basin and Range Province—stratigraphy
research: Stratigraphic and structural studies 80-83

Basin and Range Province—structural geology
neotectonics: Possible paleoseismic belt in Nevada Test Site region 82
tectonics: Cenozoic events in west-central Arizona 82-83
— Southward-directed thrusting of Mesozoic age in northeastern Nevada 81

batholiths *see under* intrusions

bauxite—resources
global: World aluminum (bauxite) resources 1

Bering Sea—geophysical surveys
seismic surveys: Seafloor thermogenic gas seep, Norton Sound 154-155

Bering Sea—oceanography
sedimentation: Bottom boundary layers and sediment transport, Norton Sound in Alaska 154
— Sources of surficial sediment, southern Bering Sea 153-154
— Wave-generated sand and gravel ribbons in the Bering Sea 155
sediments: Manganese-rich sediment from the Aleutian Basin, southern Bering Sea 154

Bering Sea—seismology
crust: Crustal structure, abyssal basins and Continental Shelf beneath the Bering Sea 154

Bering Sea—tectonophysics
plate tectonics: Upper Jurassic shallow-water sandstones of the Bering Sea continental margin 153

Black Sea—stratigraphy
Quaternary: Computer modeling 335

Bolivia—economic geology
brines: Bolivian Altiplano salars 186
lithium: Bolivia 321

Brazil—hydrogeology
hydrology: Brazil 321-322

brines *see also under* economic geology *under* Bolivia; Saudi Arabia

brines—evaluation
general: Evaluation of brines 185-187

brines—properties
viscosity: Method for extrapolating the viscosity of geothermal brines derived 193
— Viscosity of ionic substances 198

C

calcium—abundance
orthoquartzite: Calcium-poor quartzites in eastern Nevada 81

California—areal geology
regional: California 83

California—economic geology
copper: Volcanogenic massive sulfide deposits in the northern Klamath Mountains, California and Oregon 4
geothermal energy: Apparent stress changes at The Geysers 197
— Conductive heat flow in the Randsburg area in California 193
— Electromagnetic soundings at Randsberg Known Geothermal Resource Area (KGRA) 173-174
— Geothermal resource evaluation, Minarets Wilderness, California 55
— Limits of hot-water geothermal system in The Geysers-Clear Lake geothermal area 197

— Low-velocity body lies under Coso Hot Springs 197
— Magma body postulated under Clear Lake Volcanics from teleseismic P-wave delays 197
— Two-dimensional-inversion of seismic attenuation observations at Coso Hot Springs Known Geothermal Resource Area 200
— Variometer array used to detect electrical conductors and telluric currents in the crust 192
— Volatile gases useful in geochemical exploration 12
metals: Metallogeny in California 4
petroleum: California 30
— Maturation of organic matter and generation of petroleum in Tertiary oil basins 30
— Petroleum potential of central and northern California Outer Continental Shelf 148-149
— Petroleum potential of plate boundary 30
phosphate: Known extent of California phosphate deposit enlarged 17
thorium: New thorium resource numbers calculated for vein-type occurrences 52

California—engineering geology
earthquakes: Northern California 243-244
— Southern California 244-246
geologic hazards: Foothill fault system in Sierra Nevada, California 259
— Geologic hazards of the northern California-Oregon Outer Continental Shelf and slope 149
— Lineament studies in the San Joaquin Valley, California 259-260
land subsidence: Mechanisms of ground failure associated with ground-water withdrawal 277
— Subsidence of peatland varies with depositional environment 277
slope stability: Landslide activity in the Pacific Palisades area of Los Angeles, California, in 1978 254

California—environmental geology
ecology: Distributions of carbon and stable-carbon isotopes in waters and sediments of San Francisco Bay 162
— History, landforms, and vegetation of San Francisco Bay tidal marshes 159-160
— Natural and anthropogenic influences on benthic-community structure in San Francisco Bay 160
— Plankton dynamics in San Francisco Bay 161
— Population biology and production of Gemma gemma in San Francisco Bay 161
— Sources and sinks of oxygen, carbon, nitrogen, and silica in San Francisco Bay 161-162
— Temporal dynamics of copper, zinc, and silver related to freshwater discharge in southern San Francisco Bay 160-161
geologic hazards: Environmental geology of the southern California borderland 147
— History of flooding in Butte Basin between 1878 and 1978 131
— San Joaquin Valley windstorm, December 20, 1977 206
land use: Environmental impacts of off-road vehicles 87
— Regional agencies use of earth-science products from the San Francisco Bay Regional Study 303-304
pollution: Biotic and abiotic uptake of added nitrate and phosphate in a northern California stream 227-228
— Trace-metal form and bioavailability in estuarine sediments 223
reclamation: Sierra Cooperative Pilot Project 292

California—geochronology
Mesozoic: New data on the age of the Independence dike swarm in eastern California 184
Neogene: Potassium-argon ages of volcanic rocks in the Murrieta area of California 86-87
Pleistocene: Absolute age of main marine terrace in Pacific Palisades 86
Quaternary: Paleomagnetism of the Clear Lake Volcanics, California 167-168
— Quaternary deposits and soils, Sierra Nevada foothills 85-86

California—geophysical surveys
electromagnetic surveys: Electromagnetic soundings at Randsberg Known Geothermal Resource Area (KGRA) 173-174
gravity surveys: Gravity map of California 175
— Gravity surveys 240
— Southern California high-precision gravity networks 175-176
heat flow: Conductive heat flow in the Randsburg area in California 193
— New heat flow results from southern California 241
maps: Gravity map of California 175
remote sensing: Radar investigations 284-285
— Sierra Cooperative Pilot Project 292
surveys: Lineament studies in the San Joaquin Valley, California 259-260

California—hydrogeology
ground water: Indian Wells Valley water-level predictions 130
hydrology: Availability of water for irrigational use, Santa Rosa Indian Reservation 130
— California 130-131
— Computation of tidal river discharge 130-131
thermal waters: Limits of hot-water geothermal system in The Geysers-Clear Lake geothermal area 197

California—oceanography
marine geology: San Francisco Bay 148
ocean circulation: Movement and equilibrium of bedforms in central San Francisco Bay, California 159
sedimentation: Sediment transport on the San Pedro Shelf, California 147
— Sediment transport processes on the Monterey Deep-Sea Fan 150

California—petrology
igneous rocks: Upper Cenozoic rhyolites of the southern Sierra Nevada, California 181-182
intrusions: Jurassic granitic rocks in the western Sierra Nevada 84
metamorphic rocks: Paleozoic metasedimentary rocks in eastern Mojave Desert 84
metaplutonic rocks: Character of Peninsular Ranges batholith 84-85

California—seismology
crust: Low-velocity body lies under Coso Hot Springs 197
— Magma body postulated under Clear Lake Volcanics from teleseismic P-wave delays 197
— Root of the Sierra Nevada 83-84
— Two-dimensional-inversion of seismic attenuation observations at Coso Hot Springs Known Geothermal Resource Area 200
earthquakes: Apparent stress changes at The Geysers 197
— Earthquake swarms 242-243
— Foreshock studies 239
— Magnetic studies 242
— Strength of the San Andreas 241

California—stratigraphy
Cenozoic: Vanished alluvial-fan complex in the Riverside Area 87
Holocene: Sierra Nevada Holocene lake records 205-206
Miocene: Late Miocene paleogeography of the Santa Cruz Region in California 147-148
— Light-stable isotopes applied to paleoclimatology 205
— Planktonic microfossils and the lower-middle Miocene boundary in the California borderland 157
Quaternary: Central Valley Quaternary studies 206-207
— Chrysomonad cysts as a paleoecological tool 206
— Ice-Age pollen record from coastal California 206
— Quaternary studies in the Los Angeles area 86

California—structural geology
neotectonics: Historic deformation in the Garlock fault-Slate Range area 85
— Silvers record past Garlock fault movements 85
— Southern California high-precision gravity networks 175-176
tectonics: Melones fault north of Downieville 83

California—tectonophysics
crust: Crustal deformation 240-241
— Gravity surveys 240
— Variometer array used to detect electrical conductors and telluric currents in the crust 192

plate tectonics: Geologic framework of the southern California borderland 146-147
— Magma sources and tectonic setting of Clear Lake Volcanics, California 181
— Plate tectonics of the western United States 83

Cambrian *see also under* stratigraphy *under* Montana

Cambrian—paleontology
Mollusca: Cambrian primitive mollusks 219

Canada *see also* Appalachians; Atlantic Coastal Plain; Great Lakes; Great Lakes region; Great Plains; Manitoba; Northwest Territories; Rocky Mountains

carbon—isotopes
analysis: Carbon isotopes as a correlation tool 33
C-13/C-12: Carbon-13/carbon-12 isotope fractionation of organic matter associated with uranium ores induced by alpha irradiation 47-48
— Distributions of carbon and stable-carbon isotopes in waters and sediments of San Francisco Bay 162
C-14: Compilation of carbon-14 data 224

carbonate rocks *see under* sedimentary rocks

Carboniferous *see also under* stratigraphy *under* Alaska; Colorado; Europe; Wyoming

catalogs—seismology
earthquakes: Seismic data bases 238

Cenozoic *see also under* geochronology *under* Antarctica; Arizona; Idaho; *see also under* stratigraphy *under* California; Eastern U.S.

Cenozoic—paleontology
research: Mesozoic and Cenozoic studies 214-218

Central America *see also* Guatemala; Nicaragua

cesium—abundance
analcime: Analcime a notable concentrator of cesium in Yellowstone geyser basins 196

changes of level *see also under* stratigraphy *under* Arctic Ocean; Atlantic Coastal Plain; Micronesia; New England; Washington

chemical analysis—methods
chromatography: Anionic constituents 233
— Organic constituents 233-234
neutron activation analysis: Neutron activation 232
— Neutron activation of geologic materials 232
research: Analytical chemistry 231
— Analytical methods 231-232

chemical analysis—techniques
applications: Analysis of water 232-234
— The measurement of uranium content in metallic ores, sediments, and water 231
sample preparation: Analytical methodology useful in geochemical exploration 12
— Errors in gross radioactivity measurements 234
— Spectrophotometric determination of tungsten in rocks 231

China—general
current research: People's Republic of China 329-330

chromatography *see under* methods *under* chemical analysis

chromite *see also under* economic geology *under* Oregon

chromite—affinities
ophiolite: Stratigraphic position of chromite deposits in selected ophiolite complexes 9

chromite—resources
global: Chromite resources 1

clastic rocks *see under* sedimentary rocks

clastic sediments *see under* sediments

clay mineralogy—areal studies
Basin and Range Province: Origin and distribution of lithium-rich clay deposits 16
Western Interior: Partings in western coals 22

clay mineralogy—experimental studies
organic materials: Clay-humic complexes 186

coal *see also under* economic geology *under* Appalachians; Colorado; Eastern U.S.; Great Plains; Illinois; Montana; New Mexico; Pennsylvania; Rocky Mountains; United States; Utah; Virginia; West Virginia; Western Interior; Wyoming

coal—deposits
experimental studies: Dating, geochemistry, and petrology of peat, lignite, and coal 21-23

coal—genesis
deltas: Coal beds in deltaic paleoenvironments 20

coal—resources
data handling: National Coal Resources Data System, Phase II 13

Coelenterata—Rugosa
Devonian: Devonian coral biostratigraphy 218-219

Colorado—economic geology
coal: Douglas Creek arch area, Colorado 21
— Rank and methane content of western coals 20
metals: Sulfur isotope studies at Creede, Colorado 191
natural gas: Depositional environments of gas-bearing Upper Cretaceous rocks in northwestern Colorado 27
— Sedimentation and petroleum potential of fluvial part of Mesaverde Group, Piceance Creek basin, Colorado 27
oil shale: Quantitative mineralogy of Colorado oil shale 35
petroleum: Oil-bearing eolian sandstones, Colorado 27
— Petroleum in northwestern Colorado 295
thorium: New thorium resource numbers calculated for vein-type occurrences 52
— Thorium resources in the Wet Mountains of Colorado 51-52
uranium: Genesis of the Schwartzwalder uranium deposit, Colorado 39-40
— Geochemical expression of uranium in carbonate rocks, Pitch Mine, Colorado 38
— Pre-Belden unconformity in the Marshall Pass district, Colorado 38-39
— Regional geologic setting of the Cochetopa uranium district, Colorado 39
— Uranium and thorium in Precambrian crystalline rocks of the Medicine Bow Mountains, North Central Colorado 39
— Uranium in central Colorado soil profiles 44

Colorado—engineering geology
land subsidence: Lands above underground coal mines should be developed with caution 276-277
slope stability: Large-scale gravitational slope movement in Colorado 255
waste disposal: Methane gas from landfill deposits in Denver area of Colorado 303

Colorado—environmental geology
geologic hazards: Flood hydrology of foothill streams in Colorado 270
— Methane gas from landfill deposits in Denver area of Colorado 303
land use: Mountain soils mapping in Front Range Urban Corridor, Colorado 303
— Resource inventory of Grand Valley, Colorado 292
maps: Mountain soils mapping in Front Range Urban Corridor, Colorado 303
pollution: Colorado 273
waste disposal: Hydrology of coal-spoil piles near Hayden 121

Colorado—geochemistry
isotopes: Strontium isotopes and minor-element geochemistry of alkaline rocks, Wet Mountains, Colorado 190

Colorado—geophysical surveys
remote sensing: Petroleum in northwestern Colorado 295
— Resource inventory of Grand Valley, Colorado 292

Colorado—hydrogeology
ground water: Dawson-aquifer model converted 121
— Effects of a cattle feedlot on ground-water quality 120
— Ground-water resources of Crowley County 121
hydrology: Colorado 120-121
— Historical perspective of the South Platte River 120

Colorado—mineralogy
orthosilicates: Sapphirine in host rocks of Precambrian sulfide deposits, Wet Mountains, Colorado 7

Colorado—stratigraphy
Carboniferous: Pre-Belden unconformity in the Marshall Pass district, Colorado 38-39

Colorado—structural geology
tectonics: Major tectonic zone across southern Colorado 73-74

Colorado—tectonophysics
heat flow: Heat production in the southern Rocky Mountains, Colorado 198
Colorado Plateau—tectonophysics
heat flow: Heat production in the southern Rocky Mountains, Colorado 198
Columbia Plateau—petrology
lava: Source areas and distribution of Columbia River Basalt Group in Washington 183
congresses *see* symposia
Connecticut—economic geology
water resources: Prototype water-use data systems in Connecticut, Kansas, and Virginia 137-138
Connecticut—environmental geology
pollution: Sources of nutrients in Lake Waramaug, Connecticut 229
Connecticut—geomorphology
glacial geology: Deglaciation of central Connecticut 59
Connecticut—structural geology
tectonics: A new look at the Chester syncline, eastern Connecticut 58-59
conodonts—biostratigraphy
Devonian: Eight lateral biofacies within a single Upper Devonian conodont zone 218
Ordovician: Lower-Middle Ordovician boundary in the north-central Appalachian Basin 219
— Ordovician Montoya Group extended westward in southeastern Arizona 83
Paleozoic: Melones fault north of Downieville 83
— Stratigraphy first, structure second 80
Permian: Late Paleozoic fossils in ophiolite, northeastern Alaska 95
conservation *see also under* environmental geology *under* United States
conservation—environment
desertification: Monitoring desertification 294
conservation—natural resources
forests: Forest defoliation 294
programs: Cooperative projects with the U. S. Fish and Wildlife Service 291
continental shelf *see also under* oceanography *under* Alaska; Atlantic Coastal Plain; New Jersey; Oregon; Texas
continental slope *see also under* oceanography *under* Atlantic Ocean; Washington
copper *see also under* economic geology *under* Arizona; California; Idaho; Montana; Nevada; Oman; Virginia
copper—resources
evaluation: Copper-aluminum substitution model 14-15
Cretaceous *see also under* geochronology *under* Nevada; *see also under* stratigraphy *under* Alabama; Alaska; Georgia; Gulf Coastal Plain; New Mexico; North America; Northwest Territories; Utah; Western Interior
crust *see also under* seismology *under* Arabian Peninsula; Bering Sea; California; Great Basin; Hawaii; Nevada; Red Sea region; Wyoming; *see also under* tectonophysics *under* Alaska; Atlantic Ocean; California
crystal chemistry *see also* minerals
crystal growth *see also* minerals
crystal structure *see also* minerals
crystal structure—sulfides
bartonite: Bartonite, $K_6Fe_{20}S_{27}$ 177
djurleite: Djurleite and chalcocite, Cu_xS 177
erdite: Crystal structures of alkali-iron copper sulfide minerals; erdite, $NaFeS_2 \cdot 2H_2O$ 176-177
rasvumite: Rasvumite, KFe_2S_3 177
crystallography *see also* mineralogy

D

deformation *see also* geophysics; structural analysis
deformation—experimental studies
compression: Mode of deformation of Rosebud coal; Colstrip, Montana 310
creep: Rheology of rocks and rock-forming minerals 171
deformation—field studies
creep: Crustal deformation 240-241
mylonitization: Mylonitization of the Salem Gabbro-Diorite intrusive complex 57
petrofabrics: Simultaneous crystallization and deformation in ophiolite complexes 8-9
recrystallization: Character of Peninsular Ranges batholith 84-85
stress: Clastic dikes; a key to Tertiary regional stress fields in the Northwest Olympic Peninsula 88
— Strength of the San Andreas 241
Delaware—hydrogeology
ground water: Multiaquifer model, Kent County, Delaware 208-209
deltas *see under* environment *under* sedimentation
Devonian *see also under* geochronology *under* Alaska; *see also under* stratigraphy *under* Nevada; North America
Devonian—stratigraphy
biostratigraphy: Devonian coral biostratigraphy 218-219
— Eight lateral biofacies within a single Upper Devonian conodont zone 218
diagenesis *see also* sedimentation
diagenesis—effects
reservoir properties: Early fresh-water diagenesis produces limestone with favorable oil reservoir properties 34
— Influence of diagenesis on reservoir properties of some Upper Cretaceous sandstones, Uinta Basin, Utah 27-28
diagenesis—indicators
geologic thermometry: Diagenetic laumontite–a low-temperature paleothermometer 157
magnetic anomalies: Aeromagnetic detection of diagenetic magnetite over oil fields 33-34
diagenesis—materials
sandstone: Determination of pre-cementation porosity and permeability in sandstones 45
diastrophism *see* orogeny
diatoms *see under* algae
dikes *see under* intrusions
Dinoflagellata *see under* palynomorphs
Djibouti—economic geology
water resources: Djibouti 322
domes *see under* style *under* folds

E

Earth—magnetic field
Fourier analysis: Representation of geomagnetic field by local functions 169
observations: Geomagnetism 168-169
— Magnetic stations for the International Magnetospheric Study (IMS) 169
secular variations: Electromagnetic refraction in the mantle and secular change 169
— Geomagnetic secular change 168-169
— Improved selection of geomagnetically quiet-day levels 169
— Magnetic variations from external sources 169
earthquakes *see also* engineering geology; seismology; *see also under* engineering geology *under* Atlantic Coastal Plain; California; Japan; Mississippi Valley; New Jersey; New Mexico; Utah; Washington; *see also under* seismology *under* California; catalogs; Greece; Guatemala; Hawaii; Nicaragua; Oregon; Peru; symposia; United States; Wyoming
earthquakes—effects
ground motion: Correlation between ground failure and seismic intensity 257
— Ground motion 249-250
— Ground shaking hazard and risk 250
landslides: Earthquake-induced landslides 255-257
— Landslides caused by historic earthquakes 256
— Landslides caused by recent earthquakes 256-257
liquefaction: Research in soils engineering 252-253
earthquakes—genesis
subduction zones: Numerical modeling 241
earthquakes—mechanism
faults: Fault stability 241-242
research: Earthquake mechanics and prediction studies 238-243
seismic sources: Earthquake source mechanisms 248-249
earthquakes—prediction
precursors: Earthquake precursors 242
— Radon and water level 242
— Tilt 242
Eastern Hemisphere *see also* Africa; Antarctica; Arctic Ocean; Asia; Atlantic Ocean; Europe
Eastern U.S.—economic geology
coal: Hazardous elements in eastern coal resources 22
water resources: Northeastern region 102-112

— Regional studies 103
— Southeastern region 112-118
Eastern U.S.—engineering geology
geologic hazards: Eastern United States 247-248
Eastern U.S.—geochemistry
organic materials: Origin of methane in peat, coal, and eastern Devonian shale 22-23
Eastern U.S.—stratigraphy
Cenozoic: Shoreline datum planes in the southeastern United States 214-215
ecology *see also under* environmental geology *under* Atlantic Coastal Plain; California; North Carolina; Pacific Coast; Virginia
ecology—Invertebrata
streams: Invertebrate drift in a meadow and a canyon reach of a mountain stream 227
— Water-quality effects of underground coal mining 227
ecology—Pisces
streams: Relation between pH and fish kills in Oyster Creek, New Jersey 221
ecology—Plantae
bajadas: Plant societies along a bajada in southern Arizona 220
drought: Severity of droughts estimated from tree rings 220
floods: Flood related movement of scree 220
research: Plant ecology 220
economic geology—practice
programs: Resource Attache Program 318-319
Egypt—economic geology
mineral resources: Egypt 322-323
elastic waves *see under* seismology
electrical logging *see* well-logging
electrical surveys *see under* geophysical surveys *under* Florida; Hawaii; Idaho
electromagnetic surveys *see under* geophysical surveys *under* California
energy sources *see also under* economic geology *under* Indonesia; Pacific region; Pakistan; Peru; Turkey; United States
energy sources—production
effects: Hydrologic aspects of energy 260-261
energy sources—resources
global: Resource Attache Program 318-319
international cooperation: Assistance in studying energy resources 311-312
nuclear energy: Nuclear-fuel resources 36-53
engineering geology *see also* deformation; environmental geology; geodesy; geophysical methods; ground water; land subsidence; mining geology; nuclear facilities; rock mechanics; soil mechanics
engineering geology—general
research: Engineering geology 251-253
engineering geology—methods
photogrammetry: Image control targets 342
— Photogrammetric archival storage system 342
— Photogrammetry 340-342
environmental geology *see also* engineering geology
environmental geology—general
research: Climate 205-207
— Environmental geochemistry 275
Eocene *see also under* geochronology *under* Washington; *see also under* stratigraphy *under* Wyoming
epeirogeny *see also* orogeny
Eurasia *see also* Black Sea
Europe *see also* the individual nations
Europe—stratigraphy
Carboniferous: The Late Devonian and Early Mississippian ostracode genus Pseudoleperditia 218
evaporites *see also under* chemically precipitated rocks *under* sedimentary rocks
explosions—nuclear explosions
military geology: Geology and hydrology related to national security 261-263

F

faults—displacements
active faults: Active faults in Houston, Texas 259
— Basin structure in Culpeper, Virginia 258-259
— Fault stability 241-242
— Foothill fault system in Sierra Nevada, California 259
— Historic deformation in the Garlock fault-Slate Range area 85
— Potassium-argon ages of volcanic rocks in the Murrieta area of California 86-87
— Silvers record past Garlock fault movements 85
decollement: Large-scale detachment faulting of Eocene volcanic rocks, southeastern Absaroka Range, Wyoming 74-75
overthrust faults: Large scale nappes in Southwest Oregon 87-88
strike-slip faults: Bald Butte fault in the Helena area of Montana 77
thrust faults: Cenozoic events in west-central Arizona 82-83
— Late Alleghenian thrusting in New Jersey 60-61
— Muldoon Canyon thrust in south-central Idaho 76-77
— Revised interpretation of thrust faults in the southern Flint Creek Range, western Montana 77-78
— Southward-directed thrusting of Mesozoic age in northeastern Nevada 81
— Structure of southwestern Virgin Mountains, southeastern Nevada 82
— Tectonic style and history, north end of the Pioneer Mountains in Montana 75-76
— Thrust faulting indicated by relationship of Catskill and Pocono Formations in northeastern Pennsylvania 62
— Thrust faults in the ultramafic belt, northern Vermont 57
— Thrust plates in the Blue Ridge 63
— Thrusting and lateral faulting, Northwest Washington 88-89
— Younger-over-older thrust plates in southeastern Idaho 76
faults—distribution
cumulates: Faulting in the Duluth Complex 66
fault zones: A structural analysis of the Norumbega fault zone 56
gneiss: Ancient fault sets in northern Michigan 67
growth faults: Faulting in banded upper zone of the Stillwater Complex 6
high-angle faults: A new look at the Chester syncline, eastern Connecticut 58-59
faults—effects
mylonite: Mylonitization of the Salem Gabbro-Diorite intrusive complex 57
faults—systems
lineaments: Structure of the Choteau 2-degree quadrangle, Montana 78
orientation: Fault systems in the Boston Basin of Massachusetts 57
rift zones: Rio Grande rift, New Mexico 78
fission-track dating *see under* geochronology
Florida—economic geology
peat: Age of Everglades peat 21
petroleum: Gulf of Mexico and Florida 30-31
— Reservoir porosity in Sunniland Limestone (Lower Cretaceous), southern Florida 31
— Source rock potential, South Florida Basin, Florida 31
phosphate: Florida phosphate resources enlarged by drilling 17-18
water resources: Suwannee River Water Management District, Florida 293
Florida—engineering geology
waterways: Water loss in the flood diversion link between the Hillsborough River and the Tampa Bypass Canal 116
Florida—environmental geology
geologic hazards: Flood frequency 136-137
— Flood-stage frequency relations of lakes in Florida 270-271
land use: Interrelation of census and USGS land use data 309
pollution: Caloosahatchee River assessment 274
— Chemistry and hydrology of Winter Haven chain of lakes 228-229
— Subsurface storage of liquid industrial waste 273
— Subsurface storage of liquid wastes in Florida 274
— Water quality of the Hillsborough River 113-114
waste disposal: Biochemical activity following subsurface waste injection 222-223
— Geohydrological assessment of a landfill in Pinellas County 114
— Sewage-effluent disposal by spray irrigation 115

Florida—geophysical surveys
electrical surveys: Resistivity soundings in Florida 175
— Surface resistivity used to locate the saltwater-freshwater interface 113
remote sensing: Suwannee River Water Management District, Florida 293
Florida—hydrogeology
ground water: Application of a numerical model in simulating water-level changes in the Floridan aquifer 209
— Deep cavernous zone in the Floridan Aquifer 114
— Leaky confined conditions at Pensacola well 114
— Potential of contamination increased by ground-water pumpage in Lee County 113
— Saltwater intrusion in the city of Cape Coral 114-115
— Shallow aquifers replacing deep artesian aquifers as Hendry County water supply 116
— Test well probes hydrogeology beneath Tampa Bay 113
— The Biscayne Aquifer 115
— Water availability in St. Johns County 113
— Water quality of the Floridan Aquifer, Manatee County 114
hydrology: Data-management system 136
— Hydrologic resources of the Ochlockonee River basin area 112-113
— Modeling of urban storm-water processes 136
— Natural sulfate contamination of the Santa Fe River 115
— Water quality in Everglades National Park 115
— Water use in southwestern Florida in 1977 138
surveys: Florida 112-116
Florida—oceanography
ocean circulation: Tidal circulation in Tampa Bay, Florida 158
reefs: Coral reefs and man's influence on them 158
fluid inclusions—interpretation
hydrothermal solutions: Light-stable isotope and fluid-inclusion studies of the East Tintic district in Utah 190-191
folds—orientation
recumbent folds: Early recumbent folding in Silurian turbidite section, Maine 56-57
superposed folds: Relationship between superimposed folding and geologic history in the Georgia Piedmont 63-64
folds—style
anticlines: Metamorphism and structural relationships in the Kings Mountain area of the Carolinas 63
domes: Differential deformation of the Grenville Complex and its basement in St. Lawrence County, New York 59
— The Oliverian domes, re-evaluated 60
synclines: A new look at the Chester syncline, eastern Connecticut 58-59
folds—systems
anticlinoria: Flat Swamp Member of the Cid Formation extended 62-63
foliation *see also* structural analysis
forests *see under* natural resources *under* conservation
fossils *see* appropriate fossil group
fossils, problematic *see* problematic fossils
foundations *see also* rock mechanics; soil mechanics
framework silicates *see under* minerals

G

genesis of ore deposits *see* mineral deposits, genesis
geochemistry—applications
environmental geology: Environmental geochemistry 275
geochemistry—general
research: Experimental and theoretical geochemistry 176
— Geochemistry, mineralogy, petrology 176-188
— Geochemistry of water 185-187
— Isotope and nuclear geochemistry 188-192
— Water-rock interactions 185
geochemistry—methods
factor analysis: Extended Q-mode factor analysis 187-188
research: Analytical methods 231-232
statistical methods: Statistical geochemistry and petrology 187-188
— Universal data transformation 187
geochemistry—processes
precipitation: Porous media model studies of sandstone-type uranium deposits 50-51
reduction: Relationship of modern groundwater chemistry to the origin and rereduction of south Texas roll-front uranium deposit 50
geochemistry—surveys
California: Sources and sinks of oxygen, carbon, nitrogen, and silica in San Francisco Bay 161-162
— Temporal dynamics of copper, zinc, and silver related to freshwater discharge in southern San Francisco Bay 160-161
North Dakota: Geochemical processes in mining areas in North Dakota 221-222
— Lignite decomposition 186
Western U.S.: Geochemical survey of the western energy regions 275
geochronology *see also* absolute age
geochronology—fission-track dating
apatite: Dating of the Climax Stock; Nevada Test Site 191
zircon: Age of Davidson Granodiorite and mineralization in Comstock Lode mining district of western Nevada 79-80
geochronology—methods
research: Advances in geochronometry 191-192
geochronology—paleomagnetism
lava: Paleomagnetism of the Clear Lake Volcanics, California 167-168
magnetostratigraphy: Magnetic correlation of upper Cenozoic Dry Valley Drilling Project cores 336-337
secular variations: Geomagnetic secular variation during Holocene time 168
geochronology—racemization
shells: Absolute age of main marine terrace in Pacific Palisades 86
— Amino acid dating of shell deposits at Willapa Bay 89
geochronology—tephrochronology
correlation: Tephrochronology 71
geochronology—thermoluminescence
soils: Thermoluminescence properties of soil carbonate 192
geochronology—tree rings
drought: Severity of droughts estimated from tree rings 220
geodesy—methods
topography: Topographic surveys and mapping 339-345
geodesy—surveys
California: Historic deformation in the Garlock fault-Slate Range area 85
United States: Gravity surveys 240
geologic hazards *see also* land subsidence; *see also under* engineering geology *under* Alaska; California; Eastern U.S.; Greece; Louisiana; Mississippi; Montana; Nevada; Oregon; Pacific Coast; South Carolina; Texas; United States; Virginia; Washington; Western U.S.; *see also under* environmental geology *under* Arizona; California; Colorado; Florida; Georgia; Idaho; Illinois; Iowa; Louisiana; Massachusetts; Missouri; Nevada; New York; Oregon; Pacific Coast; Utah; Washington; Wisconsin
geologic hazards—earthquakes
data bases: Seismic data bases 238
ground motion: Correlation between ground failure and seismic intensity 257
— Ground motion 249-250
— Ground shaking hazard and risk 250
landslides: Earthquake-induced landslides 255-257
— Landslides caused by historic earthquakes 256
— Landslides caused by recent earthquakes 256-257
liquefaction: Research in soils engineering 252-253
mechanism: Earthquake source mechanisms 248-249
research: Active faults, seismotectonic framework and earthquake potential 243
— Earthquake hazards studies 243-251
— Earthquake studies 235-253
geologic hazards—floods
erosion: Countermeasures for hydraulic problems at bridges 269-270
hydrology: Hydrologic studies 213-214
maps: Flood mapping 271-272

models: Evaluation of dam-break flood-wave models 270
research: Flood-frequency studies 270-271
— Floods 269-272
— Outstanding floods 269-270

geologic hazards—land subsidence
karst: Land subsidence and collapse over soluble rocks 277
research: Land subsidence 275-277

geologic hazards—landslides
case studies: Areal and regional studies 253-255
research: Landslide hazards 253-257
— Topical studies of landslides 255

geologic hazards—observations
remote sensing: Cooperative projects with the Mine Safety and Health Administration 292

geologic hazards—prediction
research: Geology and hydrology applied to hazard assessment and environment 235-278
— Hazards information and warnings 277-278
response: Research on public response to geologic hazards 309

geologic hazards—site exploration
nuclear facilities: Reactor hazards 257-260

geology—general
publications: Book reports 349
— Book reports 350
— Books and maps 347
— By mail 350
— How to obtain publications 349-350
— Maps and charts 349-350
— Maps and charts 350
— National Technical Information Service 350
— Open-file reports 348
— Over the counter 349-350
— Publications issued 348-349
— Publications program 347-348
— U. S. geological survey publications 347-350

geology—practice
international cooperation: Assistance to intergovernmental organizations 312-313
— International cooperation in the Earth Science 311-341
— International Geological Correlation Program 317-318
— Participant training and technology transfer 313
— Scientific and technical assistance 311-319
— Scientific cooperation and research 313, 317

geology—research
general: Geologic and hydrologic principles, processes, and techniques 167-234
international cooperation: International commission representation 319-320
— Summary by country 321
military geology: Geology and hydrology related to national security 261-263

geomorphology *see also* glacial geology

geomorphology—fluvial features
channel geometry: Channel changes 201-202
channels: Channel characteristics identify losing stream reaches 118

geomorphology—lacustrine features
extinct lakes: Early Holocene history of Lake Bonneville 205
salars: Bolivian Altiplano salars 186

geomorphology—landform evolution
alluvial fans: Vanished alluvial-fan complex in the Riverside Area 87
basins: Quaternary studies in the Los Angeles area 86
drainage patterns: Late Miocene drainage patterns in Southeast Washington 90-91
— Summary of late Cenozoic history of the Wind River basin and adjacent uplands in Wyoming 75
rivers: An ancestral Hudson River valley of the Continental Shelf off New Jersey 142
uplifts: Geomorphology of New England 59-60

geomorphology—maps
remote sensing: Wenatchee, Washington 345
terrain classification: Integrated terrain mapping 295

geomorphology—methods
statistical methods: Curve-fitting techniques 202-203

geomorphology—processes
cratering: Basin and crater studies 285-286
wind erosion: Eolian processes 202
— Wind as a geologic agent in desert climates 207

geomorphology—shore features
deltas: Historical changes of shoreline and wetland in Puget Sound region 89-90
marshes: History, landforms, and vegetation of San Francisco Bay tidal marshes 159-160
terraces: Pleistocene terraces at Willapa Bay, Washington 149-150

geomorphology—solution features
karst: Dissolution history, southeastern New Mexico 70
— Land subsidence and collapse over soluble rocks 277

geomorphology—volcanic features
calderas: Withington Creek caldera 73
lava fields: Field mapping of the Craters of the Moon lava field, Idaho 72
— Structurally complex roots of a caldera near Questa, New Mexico 72
quantitative geomorphology: Quantitative morphology of volcanoes 285

geophysical methods—electrical methods
applications: Electrical techniques for geothermal exploration 193
resistivity: Calculation of resistivities of two-dimensional structures 173
— Field procedure and data reduction (with HP 97-67) for total field resistivity surveys 192-193
— Nonlinear complex resistivity 169-170
self-potential methods: Calculation of self-potential anomalies 173
— Surface self-potential distributions as indicators of subsurface geothermal activity 198-199

geophysical methods—electromagnetic methods
interpretation: Electromagnetic response of inhomogeneous overburden 173
— Electromagnetic soundings at Randsberg Known Geothermal Resource Area (KGRA) 173-174
radar methods: Impulse radar for geologic mapping 170
— Radar investigations 284-285

geophysical methods—magnetic methods
applications: Variometer array used to detect electrical conductors and telluric currents in the crust 192
interpretation: Magnetization directions from magnetic anomalies 172
— Model for magnetic-anomaly inversion 172-173
— Vector aeromagnetic data 173

geophysical methods—magnetotelluric methods
applications: Magnetotelluric method for geothermal prospecting 199
techniques: Field tests of real-time magnetotelluric systems 173

geophysical methods—methods
applications: Gravity variation at microgal level 199
techniques: Applied geophysical techniques 172-176

geophysical methods—radioactivity methods
instruments: Scintillator used as fast neutron detector 48

geophysical surveys *see* electrical surveys *under* geophysical surveys *under* Florida; Hawaii; Idaho; *see* electromagnetic surveys *under* geophysical surveys *under* California; *see* gravity surveys *under* geophysical surveys *under* Alaska; California; Oregon; Saudi Arabia; *see* magnetic surveys *under* geophysical surveys *under* Alaska; Oklahoma; Saudi Arabia; *see* radioactivity surveys *under* geophysical surveys *under* Montana; *see* seismic surveys *under* geophysical surveys *under* Alaska; Bering Sea; Great Lakes; Hawaii; Idaho; Saudi Arabia; Wyoming; *see* surveys *under* geophysical surveys *under* Alaska; California; Mexico; Montana; *see also* geophysical methods

geophysics *see also* deformation; engineering geology

geophysics—experimental studies
pyroxene: Electrical conductivity of pyroxenes 170-171
— Rheology of rocks and rock-forming minerals 171

geophysics—general
research: Geophysics 167-176

Georgia—environmental geology
geologic hazards: Flood in northeastern Georgia resulting from failure of dam on Toccoa Creek 269
land use: Land use map accuracy determination 307
— Statistical comparisons of land use mapping at 1:24,000 and 1:100,000 scales 307-308
maps: Land use map accuracy determination 307
— Statistical comparisons of land use mapping at 1:24,000 and 1:100,000 scales 307-308
pollution: Effect of nitrification on the oxygen balance of the upper Chattahoochee River in Georgia 223

Georgia—hydrogeology
ground water: Saltwater encroachment in a carbonate-aquifer system at Brunswick 116
— Water-bearing openings in crystalline rocks found to be horizontal fractures 116
hydrology: Georgia 116

Georgia—oceanography
reefs: Reefs and hardgrounds of the Georgia Bight 142-143

Georgia—stratigraphy
Cretaceous: Cyclicity of Upper Cretaceous sedimentary rocks 64

Georgia—structural geology
tectonics: Relationship between superimposed folding and geologic history in the Georgia Piedmont 63-64
— Warwoman lineament extention 65

geosynclines *see also* orogeny

geotechnics *see* engineering geology

geothermal energy *see also under* economic geology *under* Arizona; California; Gulf Coastal Plain; Hawaii; Idaho; Louisiana; Montana; South Dakota; Texas; United States; Utah; Western U.S.; Wyoming

geothermal energy—exploration
electrical methods: Electrical techniques for geothermal exploration 193
— Surface self-potential distributions as indicators of subsurface geothermal activity 198-199
gravity methods: Gravity variation at microgal level 199
indicators: High helium isotope ratios associated with geothermal fluids 199
— Relationship between the silica geothermometer and known regional heat flow 200
magnetotelluric methods: Magnetotelluric method for geothermal prospecting 199
remote sensing: Evaluation of geothermal heat flux models 299
well-logging: Transient temperature inversions in geothermal boreholes 199

geothermal energy—production
global: World geothermal energy producers canvassed 54

geothermal energy—properties
brines: Method for extrapolating the viscosity of geothermal brines derived 193
— Viscosity of ionic substances 198
geologic thermometry: Magnesium correction determined for sodium-potassium-calcium geothermometer 193
geothermal systems: Geothermal systems 192-200
reservoir properties: Electrical properties of geothermal materials 170
— Transient pressure analysis in vapor-dominated geothermal systems 192

geothermal energy—resources
data bases: Geothermal resources file 13

glacial geology *see also* geomorphology

glacial geology—general
research: Glaciology 203-205

glacial geology—glacial features
glacial lakes: Glacial Lake Taunton Deposits 58
— Middle-Wisconsinan glacial lake in Scobey, Montana, area 69-70
moraines: Geology and limnology of the Alpine Wilderness Area 90
— Readvance produces Ellisville moraine 58

glacial geology—glaciation
deglaciation: Deglaciation of central Connecticut 59
— Retreat of ice left eastern upland of Massachusetts subject to deep freeze 58
deposition: Comparison of sedimentation in Yakutat and Icy Bays, Alaska 151
— Further studies of two classic geologic sites of Massachusetts 141
— Neoglacial sedimentation in Glacier Bay, Alaska 150-151
— Sedimentation in coastal embayments of the northern Gulf of Alaska 151
extent: Former more extensive glacial ice in the Orville Coast area 337-338
ice movement: Summary of late Cenozoic history of the Wind River basin and adjacent uplands in Wyoming 75

glacial geology—glaciers
atlas: Satellite image atlas of glaciers 295
inventory: Glacier inventories 203-204
observations: Airborne pulse sounding of Alaskan glaciers 174
— Columbia Glacier, Alaska 204-205
water balance: Glacier ice and water balance 203

glaciation *see under* glacial geology

glaciers *see under* glacial geology

gold *see also under* economic geology *under* Basin and Range Province; Wyoming

granite *see also under* granite-granodiorite family *under* igneous rocks

Graptolithina—biostratigraphy
Ordovician: Ordovician rocks in Monitor Hills, south-central Nevada 82

gravity surveys *see under* geophysical surveys *under* Alaska; California; Oregon; Saudi Arabia

Great Basin—economic geology
petroleum: Continuous lacustrine sedimentation of Paleogene source beds in the Great Basin 29
— Great Basin and southwestern United States 28-30
— Petroleum source beds in Permian Phosphoria Formation, northeastern Great Basin 29

Great Basin—geochemistry
organic materials: Sources of organic matter in Devonian black shales 33

Great Basin—seismology
crust: Crustal thinning in northwest Nevada 199-200

Great Lakes—geophysical surveys
seismic surveys: Geology of central Lake Michigan 65
— Lake Michigan 65

Great Lakes region—areal geology
regional: Central region 65-67

Great Lakes region—environmental geology
pollution: Contamination potential of the Silurian dolomite aquifer in eastern Wisconsin 111
— Waste tritium migration in ground water, Cook County, Illinois 264

Great Plains—areal geology
regional: Rocky Mountains and Great Plains 67-78

Great Plains—economic geology
coal: Geochemical survey of the western energy regions 275
natural gas: Facies relations of low-permeability Cretaceous reservoirs in the Northern Great Plains 25
— Rocky Mountains and Great Plains 25-28
phosphate: Phosphate investigation, Rocky Mountains and Great Plains 17-18

Great Plains—environmental geology
pollution: Highly fractured lignite at the Gascoyne mine in Bowman County, North Dakota 260-261

Great Plains—hydrogeology
hydrology: Relation of ground-water pumping for irrigation to energy use 138

Great Plains—petrology
igneous rocks: Igneous studies 71-73

Great Plains—stratigraphy
research: Stratigraphic studies 67-71

Great Plains—structural geology
tectonics: Tectonic and geophysical studies 73-78

Greece—engineering geology
geologic hazards: Earthquake investigations 251
— The Thessaloniki earthquake 243

Greece—seismology
earthquakes: Earthquake investigations 251
— The Thessaloniki earthquake 243

ground water *see also* hydrogeology; hydrology

ground water—aquifers
models: Aquifer-model studies 208-209
— Evaluation of aquifer parameters 208
— Model of a two-aquifer system 208
pyroclastics: Hydrochemistry of volcanic aquifers 185
— Kinetic model 185
ground water—contamination
organic materials: Organic compounds in ground water 272-273
simulation: Computer programs simulate distribution of aqueous uranium species 268
water quality: Leaching profiles in volcanic glasses 185
ground water—geochemistry
sulfur: Stability of polysulfides 186-187
ground water—movement
cycles: Ground-water flow near lakes 224-225
ground water—recharge
research: Recharge studies 209-210
ground water—surveys
Alaska: Geohydrology of the Delta-Clearwater area 129
— Geohydrology of the Fairbanks North Star Borough 129
— Hydrology and water quality of the Keta River basin 129-130
Arizona: Arizona 130
Biscayne Aquifer: The Biscayne Aquifer 115
Buffalo Aquifer: Two-dimensional model of the Buffalo aquifer 108
California: Availability of water for irrigational use, Santa Rosa Indian Reservation 130
— Indian Wells Valley water-level predictions 130
Chicot Aquifer: Model study of the Chicot and Evangeline aquifers, Texas Gulf Coast 209
Colorado: Colorado 273
— Effects of a cattle feedlot on ground-water quality 120
— Ground-water resources of Crowley County 121
Dawson Aquifer: Dawson-aquifer model converted 121
Delaware: Multiaquifer model, Kent County, Delaware 208-209
Djibouti: Djibouti 322
Eastern U.S.: Regional studies 103
Edwards Aquifer: Lithology of the Edwards aquifer 211
Florida: Leaky confined conditions at Pensacola well 114
— Potential of contamination increased by ground-water pumpage in Lee County 113
— Resistivity soundings in Florida 175
— Saltwater intrusion in the city of Cape Coral 114-115
— Shallow aquifers replacing deep artesian aquifers as Hendry County water supply 116
— Subsurface storage of liquid industrial waste 273
— Subsurface storage of liquid wastes in Florida 274
— Surface resistivity used to locate the saltwater-freshwater interface 113
— Test well probes hydrogeology beneath Tampa Bay 113
— Water availability in St. Johns County 113
— Water use in southwestern Florida in 1977 138
Floridan Aquifer: Application of a numerical model in simulating water-level changes in the Floridan aquifer 209
— Biochemical activity following subsurface waste injection 222-223
— Deep cavernous zone in the Floridan Aquifer 114
— Geohydrological assessment of a landfill in Pinellas County 114
— Hydrologic resources of the Ochlockonee River basin area 112-113
— Natural sulfate contamination of the Santa Fe River 115
— Sewage-effluent disposal by spray irrigation 115
— Water loss in the flood diversion link between the Hillsborough River and the Tampa Bypass Canal 116
— Water quality of the Floridan Aquifer, Manatee County 114
Georgia: Saltwater encroachment in a carbonate-aquifer system at Brunswick 116
— Water-bearing openings in crystalline rocks found to be horizontal fractures 116
Great Plains: Relation of ground-water pumping for irrigation to energy use 138
Gulf Coastal Plain: Geopressured zones 186
Idaho: Ground-water-quality assessment, northern Idaho 131
— Hydrologic conditions in Rockland Valley 131-132
Illinois: Waste tritium migration in ground water, Cook County, Illinois 264
Indiana: Availability of ground water in the upper White River basin 104
— Effects of seepage from fly-ash settling ponds and construction dewatering on ground-water levels at the Indiana Dunes National Lakeshore 103-104
— Evaluation of ground water in Elkhart County 104
— Flow model of the unconsolidated aquifers near Logansport 105
— Irrigation and ground water in Newton and Jasper Counties 104
— Saline ground water near Vincennes well field 104
Iowa: Study to determine hydrology of sandstone aquifers in the coal-bearing Pennsylvanian strata 121
— Test drilling of aquifers in northwestern Iowa 122
Jasper Aquifer: Ground water in Jasper aquifer 127
Kansas: Changes in historic patterns of a stream-aquifer system 21
— Chemical quality of ground water in Kansas 122
— Hydrologic conditions in the Equusbeds region 122
— Methods of estimating ground-water withdrawals for irrigation 138
— Potentiometric surface–Arbuckle Group 210
— Simulation of multiaquifer system along Arkansas River valley, southwestern Kansas 208
— Stream-aquifer model of north-central Kansas 225
Kentucky: Subsurface waste nuclide migration at Maxey Flats storage site near Morehead, Kentucky 264
Kenya: Kenya 326
Louisiana: Index to ground-water monitor wells in Louisiana 122-123
— Saltwater encroachment at Baton Rouge 123
Maryland: Drilling phase of modeling project completed 105
Massachusetts: Ground-water contamination by secondary treated wastewater 274
— Nutrient content of ground water 274
Michigan: Ground water in Marquette County 105
— Model study of Michigan coal deposit 106
— Water resources of the Marquette Iron Range area 105-106
Midwest: Targeting, inventorying, and monitoring ground-water resources 294
Minnesota: Appraisal of ground-water in central Minnesota 106-107
— Design for a ground-water-quality monitoring network 106
— Effect of copper and nickel mining on surface and ground water in northeastern Minnesota 106
— Ground-water appraisal of sand-plain areas 107
— Lake budget in Minnesota 225
— Minnesota 272
— Minnesota and Wisconsin 108
— Shallow aquifers in southwestern Minnesota 106
— Spread of contaminants through multiaquifer wells in southeastern Minnesota 107
— Use of surficial aquifers increasing in Minnesota 107
Mississippi: Geohydrology of three Mississippi salt domes 265
— Significance of saturated soils in coastal plains 301
Missouri: Deep wells in Audrain County 123
— Extreme fractionation of $^{234}U/^{238}U$ isotopes within a Missouri aquifer 188
— Hydrology of Ozark basins in Missouri 225
Montana: Coal hydrology and geochemical studies in the Powder River basin, Montana and Wyoming 260

— Geohydrology of the Helena Valley 124
— Ground-water resources of part of the Flathead Indian Reservation 124
— Hydrogeology of the Fort Union coal region 124
— Hydrology of Prairie Dog Creek 124
— Regional-scale aquifers investigated in Montana 124
— Saline-seep development in Hailstone basin 123-124
— Seepage runs in Federal coal-lease areas 124
— Third test well completed in the Madison Aquifer 120
Nebraska: Tracer studies at sites in Nebraska and Texas 209-210
Nevada: Development of a relation for steady-state dumping rate in Eagle Valley 132
New Hampshire: Ground-water resources of the Lamprey River basin 108-109
New Mexico: Aquifer near Capulin 124-125
— Ground-water conditions in the vicinity of Elephant Butte Irrigation District well field 125-126
— Ground-water resources of the lower Rio Grande Valley area of New Mexico 126
— Projected ground-water pumpage from uranium mines in northwestern New Mexico 125
New York: Aquifer storage of chilled water for air conditioning at Kennedy Airport, New York 210
— Conversion of a three-dimensional analog model to a three-dimensional digital model 210
— Hydrogeology of artificial-recharge site 109
— New York 272-273
— Streamflow augmentation 225
— The role of the unsaturated zone in artificial recharge 109
New Zealand: New Zealand 328
North Carolina: Freshwater availability on offshore barrier islands 117
— Water-level measurements in observation wells 117-118
North Dakota: Glaciofluvial aquifers in McIntosh County 127
— Ground-water availability and quality in Billings, Golden Valley, and Slope Counties 126
— Hydrology of Wibaux-Beach deposit 126
— Major aquifers in buried valleys 127
— Outwash plain in Logan County 126
— Results of test drilling in Bottineau and Rolette Counties 126
Ohio: Subsurface mines as a water source 110
Oregon: High arsenic concentrations in ground-water samples from northern Malheur County 132
— Hydrological system of the Bend-Redmond area 133
— Iron distribution and geochemistry in a coastal dunes aquifer at Coos Bay 132
Pennsylvania: Vertical ground-water movement in abandoned mine shafts in Pennsylvania 261
— Water-supply capability of shale in south-central Pennsylvania 110
Rathdrum Prairie Aquifer: Hydrology of Rathdrum Prairie aquifer 131
Saudi Arabia: Water-personnel development 334
— Water-resources advisory services 332
South Carolina: Tritium migration at Barnwell, South Carolina 264
South Dakota: Large, low-temperature geothermal resource in Paleozoic rocks of South Dakota 54-55
— Pumping test of a Niobrara Marl aquifer in northeastern Aurora County 127
— Saline ground water in Clark County 127
Tennessee: Channel characteristics identify losing stream reaches 118
— Locating successful well sites in Jefferson County 118
— Tritium tracer tests successful at Oak Ridge National Laboratory in Tennessee 264
Texas: Geohydrology of salt domes in northeastern Texas 264-265
— Relationship of modern groundwater chemistry to the origin and rereduction of south Texas roll-front uranium deposit 50
Turkey: Turkey 334-336
United States: Summary appraisals of the Nation's ground-water resources 210-211
— The regional aquifer-system analysis program 139-140
Utah: Chemical mass-transfer model of spring water 221
— Digital model of ground-water flow in Tooele Valley 128
— Navajo Sandstone a source of ground water for future energy-related development 128
— Navajo Sandstone an important aquifer in southwestern Utah 127-128
— Potential effects of stripping coal from the Ferron Sandstone aquifer, Utah 261
Vermont: Ground-water quality 110
Virginia: Ancestral Potomac River deposits in Fairfax County, Virginia 303
— Chemical quality of ground water in Fairfax County 110-111
— Computer-composite hydrogeologic maps for Fairfax County, Virginia 303
— Ground-water reconnaissance of the Blue Ridge Parkway 110
— Ground-water resources, James City County 111
— Potentiometric surface of Cretaceous aquifer, Atlantic Coastal Plain 111
— Relation of highway construction to water quality 111
Washington: Seawater intrusion along the Washington coast 133
— Water-resource investigations on Indian reservations in Washington 133-134
Wisconsin: Contamination potential of the Silurian dolomite aquifer in eastern Wisconsin 111
— Maintaining lake levels by using ground water 225

Guatemala—geochemistry
trace elements: Water-extractable trace metals in volcanic eruption clouds 183-184

Guatemala—seismology
earthquakes: Guatemala 323

Gulf Coastal Plain—areal geology
regional: Appalachian Highlands and the Coastal Plains 60-65

Gulf Coastal Plain—economic geology
geothermal energy: Use of hydrogeologic mapping techniques in identifying potential geopressured-geothermal reservoirs 54
lignite: Gulf Coast lignite 21
maps: Use of hydrogeologic mapping techniques in identifying potential geopressured-geothermal reservoirs 54
oil and gas fields: Geopressured zones 186
petroleum: Gulf of Mexico and Florida 30-31
— New appraisal of oil and gas resources, western Gulf of Mexico 30
thorium: Uranium and thorium content in weathering profiles of the Catahoula Tuff, South Texas coastal plain 44

Gulf Coastal Plain—engineering geology
waste disposal: Geohydrology of salt domes in northeastern Texas 264-265
— Geohydrology of three Mississippi salt domes 265
— Subsurface storage of liquid industrial waste 273
— Subsurface storage of liquid wastes in Florida 274

Gulf Coastal Plain—environmental geology
land use: Development of Atlantic-Gulf barrier islands 309
pollution: Biochemical activity following subsurface waste injection 222-223
waste disposal: Geochemistry of geopressured geothermal waters in coastal Louisiana and Texas 260

Gulf Coastal Plain—oceanography
ocean circulation: Gulf Coast 158

Gulf Coastal Plain—stratigraphy
Cretaceous: Cyclicity of Upper Cretaceous sedimentary rocks 64

Gulf of Mexico—economic geology
natural gas: Gulf of Mexico and Florida 30-31
— New appraisal of oil and gas resources, western Gulf of Mexico 30
— Origin of Cenozoic natural gas accumulations, western Gulf of Mexico 30
petroleum: OCS lease sales for oil and gas 165-166

Gulf of Mexico—oceanography
marine geology: Gulf of Mexico 145-146
ocean waves: Effects of cyclic loading on underconsolidated sediments 146

Gulf of Mexico—structural geology
salt tectonics: Late Tertiary tectonics event in the southwestern Gulf of Mexico 145
— Origin of Cenozoic natural gas accumulations, western Gulf of Mexico 30

H

Hawaii—economic geology
geothermal energy: A proposed source mechanism for Kilauean self-potential anomalies 196

Hawaii—geochronology
Quaternary: Age and strontium isotopic composition of the Honolulu Volcanics 180
— Age of Black Point dike, Oahu and Yarmouth interglaciation 180

Hawaii—geophysical surveys
electrical surveys: A proposed source mechanism for Kilauean self-potential anomalies 196
seismic surveys: Crustal structure beneath Kilauea Volcano 195-196

Hawaii—petrology
lava: Molokai petrologic studies 179-180
volcanology: Hawaiian volcano studies 178-180
— Radio-telemetered volcanic gas monitoring in Hawaii 176

Hawaii—seismology
crust: Crustal structure beneath Kilauea Volcano 195-196
earthquakes: Global correlation of magma ascent and earthquake energy 179

Hawaii—tectonophysics
mantle: Mantle structure of Hawaiian volcanoes investigated 179
plate tectonics: Hawaiian Island-Emperor Seamount studies 180-181
— Rubidium-strontium systematics of Hawaiian-Emperor Seamount chain basalts 181

Hawaii—volcanology
Kilauea: Kilauea Volcano quiescent during FY 1978 178-179
— Papa'u Seamount, a submarine landslide deposit off the Island of Hawaii 158
Mauna Loa: Mauna Loa continues slow inflation 179

heat flow *see also under* geophysical surveys *under* California; *see also under* tectonophysics *under* Colorado; Colorado Plateau; Idaho; Nevada; Rocky Mountains

heat flow—measurement
remote sensing: Evaluation of geothermal heat flux models 299

heat flow—regional patterns
applications: Relationship between the silica geothermometer and known regional heat flow 200

heat flow—temperature
transient phenomena: Transient temperature inversions in geothermal boreholes 199

heat flow—thermal conductivity
mechanism: Thermal-conduction mechanisms in rocks and minerals 198

heavy minerals *see also* placers

helium—isotopes
ratios: High helium isotope ratios associated with geothermal fluids 199

Holocene *see also under* geochronology *under* Massachusetts; Pacific Coast; Virginia; Western U.S.; *see also under* stratigraphy *under* California; Utah

Hungary—general
current research: Hungary 323

hydrocarbons *see under* organic materials

hydrogeology *see also* ground water; hydrology

hydrogeology—general
military geology: Geology and hydrology related to national security 261-263
publications: Surface-water, quality-of-water, and ground-water-level records 347
research: Geochemistry of water 185-187
— Miscellaneous studies 211

hydrogeology—methods
automatic data processing: Data coordination, acquisition, and storage 134-136
— National Water Data Exchange 135-136
— Office of Water-Data Coordination 134-135
— Water-data storage system 135
remote sensing: Ground-water information on Landsat imagery 301

hydrology *see also* ground water; hydrogeology

hydrology—atmospheric precipitation
rainfall: Isotopes indicate rain-soil interaction 185

hydrology—cycles
evaporation: Evaporation and transpiration 226
— Relationship of evaporation to wind-speed for an open channel 226
evapotranspiration: Selecting an equation for computing potential evapotranspiration in an arid area 226
research: Relation between surface water and ground water 224-225

hydrology—general
military geology: Geology and hydrology related to national security 261-263
programs: International Hydrological Program 313
publications: State hydrologic unit maps 347-348
— State list of publications on hydrology and geology 347
— State water-resources investigations folders 348
— Surface-water, quality-of-water, and ground-water-level records 347
research: Geologic and hydrologic principles, processes, and techniques 167-234
— Ground-water hydrology 207-211

hydrology—limnology
closed systems: Closed-basin lake systems 185-186
lakes: Ground-water flow near lakes 224-225
research: Limnology and potamology 227-229
sedimentation: Sedimentation in lakes and streams 202

hydrology—methods
automatic data processing: Data coordination, acquisition, and storage 134-136
— Flood frequency 136-137
— Modeling of urban storm-water processes 136
— National Water Data Exchange 135-136
— Office of Water-Data Coordination 134-135
— Water-data storage system 135
mathematical methods: Model development 211-212
remote sensing: Applications to hydrologic studies 300-301
— Enhancement of surface-water features by principal components transform of Landsat data 301
— Tests of hydrologic-data relay systems 300

hydrology—rivers and streams
channel geometry: Channel changes 201-202
erosion: Countermeasures for hydraulic problems at bridges 269-270
hydraulics: Open-channel hydraulics 212-213
research: Surface-water hydrology 211-214
sedimentation: Sediment transport 201
streamflow: Hydrologic studies 213-214

hydrology—snow
meltwater: Snowmelt-runoff prediction models 203

hydrology—surveys
Alabama: Alabama 112
— Regionalization of low flow in Alabama streams 112
Alaska: Alaska 129-130
Arkansas River: Changes in historic patterns of a stream-aquifer system 21
Arkansas River valley: Simulation of multiaquifer system along Arkansas River valley, southwestern Kansas 208
Atlantic Coastal Plain: Atlantic Coast 159
Blackfoot River basin: Idaho 273
California: Availability of water for irrigational use, Santa Rosa Indian Reservation 130
— Biotic and abiotic uptake of added nitrate and phosphate in a northern California stream 227-228
— California 130-131

Caloosahatchee River: Caloosahatchee River assessment 274
Chattahoochee River: Effect of nitrification on the oxygen balance of the upper Chattahoochee River in Georgia 223
Colorado: Colorado 120-121
— Flood hydrology of foothill streams in Colorado 270
— Hydrology of coal-spoil piles near Hayden 121
Connecticut: Prototype water-use data systems in Connecticut, Kansas, and Virginia 137-138
— Sources of nutrients in Lake Waramaug, Connecticut 229
Dead Sea: Jordan 326
Eastern U.S.: Northeastern region 102-112
— Southeastern region 112-118
Florida: Chemistry and hydrology of Winter Haven chain of lakes 228-229
— Data-management system 136
— Flood-stage frequency relations of lakes in Florida 270-271
— Florida 112-116
— Natural sulfate contamination of the Santa Fe River 115
— Water quality in Everglades National Park 115
— Water use in southwestern Florida in 1977 138
Georgia: Georgia 116
Great Plains: Relation of ground-water pumping for irrigation to energy use 138
Hillsborough River: Water loss in the flood diversion link between the Hillsborough River and the Tampa Bypass Canal 116
— Water quality of the Hillsborough River 113-114
Hudson River: PCB transport in the upper Hudson River 272
— Transport of PCB's in the Hudson River 109
Idaho: Hydrologic conditions in Rockland Valley 131-132
— Hydrology of Rathdrum Prairie aquifer 131
— Idaho 131-132
— Invertebrate drift in a meadow and a canyon reach of a mountain stream 227
Illinois: Illinois 103
— Illinois 273
— Sludge-irrigation hydrology 103
Illinois River: Time-of-travel measured in Peoria Pool of the Illinois River 103
Indiana: Availability of ground water in the upper White River basin 104
— Effects of seepage from fly-ash settling ponds and construction dewatering on ground-water levels at the Indiana Dunes National Lakeshore 103-104
— Indiana 103-105
Indonesia: Indonesia 324
Iowa: Effects of urbanization on flood-flow characteristics of Walnut Creek basin 121-122
— Iowa 121-122
— Water quality of Iowa's coal region 122
Kansas: Kansas 122
— Kansas 273
— Methods of estimating ground-water withdrawals for irrigation 138
— Stream-aquifer model of north-central Kansas 225
Keta River: Hydrology and water quality of the Keta River basin 129-130
Kickapoo River basin: Flood of July 1978 in Kickapoo River basin, Wisconsin 269
Lake Koshkonong: Digital model predicts effects of powerplant water use on lake levels and river flow in Wisconsin 138
Lake Valencia: Quaternary paleolimnology of Lake Valencia, Venezuela 214
Louisiana: Insecticides in Louisiana oxbow lake beds 274
— Louisiana 122-123
— Magnitude and frequency of peak discharges on small streams in Louisiana 271
Maryland: Maryland 105
Massachusetts: Flood magnitude and frequency in three regions of Massachusetts 271
— Massachusetts 105
— Nutrient content of ground water 274
— Water quality in the Blackstone River basin 105
Michigan: Michigan 105
— Water resources of the Marquette Iron Range area 105-106
Minnesota: Effect of copper and nickel mining on surface and ground water in northeastern Minnesota 106
— Lake budget in Minnesota 225
— Minnesota 106-108
— Minnesota and Wisconsin 108
— Water quality established before highway construction 107
— Water-quality monitoring in Voyageurs National Park 107
Mississippi: Significance of saturated soils in coastal plains 301
Mississippi River: Volatile and semivolatile organics in the lower Mississippi River in Louisiana 223-224
Missouri: Hydrology of Ozark basins in Missouri 225
— Missouri 123
— Technique for estimating the magnitude and frequency of floods in St. Louis County 123
Montana: Flood-prone areas in Helena, Montana 271-272
— Hydrology of Prairie Dog Creek 124
— Limnological characteristics of small Montana reservoirs 228
— Montana 123-124
— Seepage runs in Federal coal-lease areas 124
Nevada: Development of a relation for steady-state dumping rate in Eagle Valley 132
— Flood-frequency relations for small streams in Nevada 271
— Nevada 132
New Hampshire: New Hampshire 108-109
New Jersey: Impact of land-use changes on water resources 109
— New Jersey 109
— Relation between pH and fish kills in Oyster Creek, New Jersey 221
New Mexico: Ground-water conditions in the vicinity of Elephant Butte Irrigation District well field 125-126
— Ground-water resources of the lower Rio Grande Valley area of New Mexico 126
— Hydrology of coal areas in northwestern New Mexico 125
— New Mexico 124-126
New York: Magnitude and frequency of floods on unregulated rural streams in New York 271
— New York 109
— Streamflow augmentation 225
North Carolina: Chemical characteristics of unpolluted streams 116-117
— Hydrologic effects of land clearing and drainage, Albemarle-Pamlico Peninsula 117
— Hydrology of Chicod Creek basin 117
— North Carolina 116-118
— Water-quality trend analysis 220-221
North Dakota: Highly fractured lignite at the Gascoyne mine in Bowman County, North Dakota 260-261
— Major factors controlling sediment runoff in Park River watershed 126
— North Dakota 126-127
Ochlockonee River basin: Hydrologic resources of the Ochlockonee River basin area 112-113
Ohio: A reconnaissance of biological and chemical characteristics of selected Ohio lakes 228
— Ohio 110
Onondaga Lake: Algal stromatolites (oncolites), Onondaga Lake, New York 228
Oregon: Hydrological system of the Bend-Redmond area 133
— Irrigation-return flow from pastures and orchards in Bear Creek basin, Jackson County 132
— Oregon 132-133
— Wide range of conditions represented in western Oregon flood-frequency analysis 133
Pennsylvania: Low-flow frequency of ungaged streams 110
— Pennsylvania 110
— Water quality of Tulpehocken Creek, Pennsylvania, prior to impoundment of Blue Marsh Lake 229
Potomac River: Ancestral Potomac River deposits in Fairfax County, Virginia 303
— Factors influencing seasonal distributions of biochemically reactive substances in the Potomac River 159

— Studies of benthic fauna in the Potomac River Estuary 159
Powder River basin: Coal hydrology and geochemical studies in the Powder River basin, Montana and Wyoming 260
Rio Negro: Brazil 321-322
Sacramento River: Computation of tidal river discharge 130-131
— History of flooding in Butte Basin between 1878 and 1978 131
Saint Joseph River basin: Land conservation related to water quality 222
Saudi Arabia: Water-personnel development 334
Skunk River: Flood profiles of Skunk River and tributaries in Iowa 271
Sooes River: Flood elevations for the Sooes River 134
South Dakota: South Dakota 127
South Platte River valley: Effects of a cattle feedlot on ground-water quality 120
— Historical perspective of the South Platte River 120
South Santiam River: A preliminary evaluation of dissolved-oxygen depletion in the South Santiam River 133
Tennessee: Channel characteristics identify losing stream reaches 118
— Tennessee 118
Texas: Texas 127
— Urban water quality 137
— Water quality of selected reservoirs in Texas 229
Turkey: Turkey 334-336
United States: National stream quality accounting network completed 138-139
— River quality assessment program 139
Utah: Utah 127-128
Venezuela: Venezuela 336
Vermont: Vermont 110
Virginia: Dissolved sulfate loads, an index of mining activity 261
— Virginia 110
Washington: Geology and limnology for resource planning and management, Alpine Lakes Wilderness Area, Washington 302-303
— Geology and limnology of the Alpine Wilderness Area 90
— Washington 133-134
— Water-quality effects of underground coal mining 227
— Water-resource investigations on Indian reservations in Washington 133-134
Western Interior: Central region 118-128
— Multistate studies 120
Western U.S.: Western region 128-134
Williams Lake: Water balance of Williams Lake, north-central Minnesota 107
Wisconsin: Hydrology of the Mole Lake Indian Reservation area in Forest County 111
— Maintaining lake levels by using ground water 225
— Wisconsin 111-112
— Wisconsin wetlands affect streamflow and sediment yields 111-112

hydrology—techniques
chemical analysis: Analysis of water 232-234
— Errors in gross radioactivity measurements 234
— Metallic constituents 232-233
research: New hydrologic instruments and techniques 229-230

hydrothermal alteration *see under* processes *under* metasomatism

I

Idaho—economic geology
copper: Proterozoic Z stratabound copper occurrences 5-6
geothermal energy: Correlation of cyclic sediments between Raft River geothermal wells 195
— Drill holes give a deeper view into eastern Snake River plain, Idaho 195
— Evaluation of the geothermal potential of the Inel area in Idaho, with deep Schlumberger soundings 194
— Seismic refraction at Idaho National Engineering Laboratory, Eastern Snake River plain 194
petroleum: Mississippian source rocks in Utah and Idaho 28-29
phosphate: Phosphate resources in Permian Phosphoria Formation of east-central Idaho 78-79
thorium: New thorium resource numbers calculated for vein-type occurrences 52

Idaho—engineering geology
waste disposal: Volcanic recurrence intervals and volcanic hazards in the eastern Snake River Plain in Idaho 71-72

Idaho—environmental geology
geologic hazards: Volcanic recurrence intervals and volcanic hazards in the eastern Snake River Plain in Idaho 71-72
pollution: Idaho 273

Idaho—geochemistry
strontium: Initial strontium values of rocks from the Pioneer Mountains 72-73
trace elements: Idaho 273

Idaho—geochronology
Cenozoic: Tephrochronology 71

Idaho—geomorphology
fluvial features: Channel changes 201-202
volcanic features: Withington Creek caldera 73

Idaho—geophysical surveys
electrical surveys: Evaluation of the geothermal potential of the Inel area in Idaho, with deep Schlumberger soundings 194
seismic surveys: Seismic refraction at Idaho National Engineering Laboratory, Eastern Snake River plain 194

Idaho—hydrogeology
ground water: Ground-water-quality assessment, northern Idaho 131
hydrology: Hydrologic conditions in Rockland Valley 131-132
— Hydrology of Rathdrum Prairie aquifer 131
— Idaho 131-132
— Invertebrate drift in a meadow and a canyon reach of a mountain stream 227

Idaho—petrology
igneous rocks: Origin of voids in volcanic bedrock at Teton damsite, Idaho 182
intrusions: Tertiary intrusions in the Cretaceous Idaho Batholith 73
maps: Field mapping of the Craters of the Moon lava field, Idaho 72

Idaho—stratigraphy
Proterozoic: A new Proterozoic Y stratigraphic unit, east-central Idaho 67

Idaho—structural geology
tectonics: Muldoon Canyon thrust in south-central Idaho 76-77
— Subsurface model for an area of the eastern Snake River plain 78
— Younger-over-older thrust plates in southeastern Idaho 76

Idaho—tectonophysics
heat flow: Heat-flow map for State of Idaho 200
maps: Heat-flow map for State of Idaho 200

igneous rocks *see also* magmas; metamorphic rocks; metasomatism; phase equilibria

igneous rocks—alkalic composition
isotopes: Strontium isotopes and minor-element geochemistry of alkaline rocks, Wet Mountains, Colorado 190

igneous rocks—andesite-rhyolite family
rhyolite: Chemical and petrographic subdivision of Precambrian rhyolites in Missouri 183
— Pliocene rhyolite in the Sevier Plateau, Utah 73
— Upper Cenozoic rhyolites of the southern Sierra Nevada, California 181-182

igneous rocks—basalt family
geochemistry: Emission spectrographic analysis for trace elements in basalts from core holes near Charleston, South Carolina 231-232

igneous rocks—diorite family
trondhjemite: Trondhjemite in the Talkeetna Mountains, south-central Alaska 97

igneous rocks—granite-granodiorite family
granite: Two-mica granite and the Mesoappalachian-Avaltonian boundary in New Hampshire 37
petrology: Jurassic granitic rocks in the western Sierra Nevada 84

igneous rocks—hypabyssal rocks
magnetic susceptibility: Tertiary intrusions in the Cretaceous Idaho Batholith 73

igneous rocks—mafic composition
age: Potassium-argon ages of Mesozoic mafic rocks of the Pensacola Mountains 191-192

igneous rocks—petrology
research: Igneous studies 71-73

igneous rocks—plutonic rocks
distribution: Intrusive belts of southeastern Alaska 99-100
factor analysis: Application of granitic rocks of the Granite Mountains, Wyoming 188
genesis: Plutonic rocks and magmatic processes 184
geochemistry: Initial strontium values of rocks from the Pioneer Mountains 72-73
petrology: Study of silicic plutonic rocks 332

igneous rocks—pyroclastics and glasses
tuff: Origin of voids in volcanic bedrock at Teton damsite, Idaho 182

igneous rocks—ultramafic family
kimberlite: Neodymium isotopic composition of kimberlites 189
ophiolite: Cumulate gabbro and pillow basalt associated with the Mount Sorenson ultramafic complex 96
— Oman 327-328
— Thrusting and lateral faulting, Northwest Washington 88-89

igneous rocks—volcanic rocks
factor analysis: Application to volcanic rocks in Antarctica 187
geochemistry: Strontium and lead isotopic composition in volcanic rocks from Peru and New Hebrides; genesis of calc-alkaline lava 188-189
petrology: The Oliverian domes, re-evaluated 60
— Volcanic rocks and processes 178-184

Illinois—economic geology
coal: Detailed lithology near coal seams indicated by borehole and hole-to-hole logging 171

Illinois—environmental geology
geologic hazards: Flood frequency 136-137
pollution: Illinois 273
— Sludge-irrigation hydrology 103
waste disposal: Tunnel aids investigation near Sheffield, Illinois 264
— Waste tritium migration in ground water, Cook County, Illinois 264

Illinois—hydrogeology
hydrology: Illinois 103
— Time-of-travel measured in Peoria Pool of the Illinois River 103

impact statements *see also under* environmental geology *under* Montana

impact statements—land use
research: Environmental impact studies 310

incertae sedis *see* problematic fossils

inclusions *see also* fluid inclusions

India—geophysical surveys
remote sensing: India 323-324

Indiana—hydrogeology
ground water: Evaluation of ground water in Elkhart County 104
— Flow model of the unconsolidated aquifers near Logansport 105
— Irrigation and ground water in Newton and Jasper Counties 104
— Saline ground water near Vincennes well field 104
hydrology: Availability of ground water in the upper White River basin 104
— Effects of seepage from fly-ash settling ponds and construction dewatering on ground-water levels at the Indiana Dunes National Lakeshore 103-104
— Indiana 103-105

Indonesia—economic geology
energy sources: Energy resources 324-325

Indonesia—engineering geology
waterways: Indonesia 324

Indonesia—tectonophysics
maps: Tectonics of the Indonesian region 324-325
plate tectonics: Tectonics of the Indonesian region 324-325

industrial minerals *see also under* economic geology *under* Nevada

intrusions—age
absolute age: Potassium-argon ages of Mesozoic mafic rocks of the Pensacola Mountains 191-192

intrusions—batholiths
petrology: A more complex Sebago batholith 57
— Character of Peninsular Ranges batholith 84-85
strontium: Initial strontium values of rocks from the Pioneer Mountains 72-73

intrusions—dikes
age: Age of Black Point dike, Oahu and Yarmouth interglaciation 180
dike swarms: New data on the age of the Independence dike swarm in eastern California 184

intrusions—layered intrusions
gabbro: Geologic field study of the Dufek intrusion 336
structure: Faulting in banded upper zone of the Stillwater Complex 6

intrusions—plutons
age: New age of metaplutonic rocks in the Survey Pass quadrangle, Brooks Range 95
distribution: Jurassic granitic rocks in the western Sierra Nevada 84

intrusions—stocks
age: Dating of the Climax Stock; Nevada Test Site 191
— Geochronology of intrusion and prophyry copper ores, Globe-Miami, Arizona 5
mineralization: Zoned mineralization around a hidden stock in west-central Utah 5

intrusions—structure
field studies: Tertiary intrusions in the Cretaceous Idaho Batholith 73

Invertebrata *see also* Coelenterata; Graptolithina; Mollusca; Ostracoda; problematic fossils; Radiolaria; Trilobita

Invertebrata—ecology
streams: Invertebrate drift in a meadow and a canyon reach of a mountain stream 227
— Water-quality effects of underground coal mining 227

Iowa—environmental geology
geologic hazards: Flood profiles of Skunk River and tributaries in Iowa 271
land use: Effects of urbanization on flood-flow characteristics of Walnut Creek basin 121-122
— Study to determine hydrology of sandstone aquifers in the coal-bearing Pennsylvanian strata 121

Iowa—hydrogeology
ground water: Test drilling of aquifers in northwestern Iowa 122
hydrology: Iowa 121-122
— Water quality of Iowa's coal region 122

Iowa—stratigraphy
Mississippian: The Late Devonian and Early Mississippian ostracode genus Pseudoleperditia 218

Iran—economic geology
metals: Afghanistan-Iran-Turkey 321
mining geology: CENTO training program 313

Iran—geophysical surveys
remote sensing: Iran 325

iron *see also under* economic geology *under* Pacific Coast; Virginia; West Virginia

iron—abundance
ground water: Iron distribution and geochemistry in a coastal dunes aquifer at Coos Bay 132

isostasy *see also under* structural geology *under* Washington

isotope dating *see* absolute age

isotopes *see also* absolute age; geochronology

isotopes—abundance
radioactive isotopes: Identification of possible uranium province in central Wyoming through radio-element distribution in crystalline basement rocks 47
surface water: Isotopes indicate rain-soil interaction 185

isotopes—americium
Am-241: Errors in gross radioactivity measurements 234

isotopes—analysis
stable isotopes: Light-stable isotope and fluid-inclusion studies of the East Tintic district in Utah 190-191
— Stable isotopes 190-191

isotopes—carbon
analysis: Carbon isotopes as a correlation tool 33
C-13/C-12: Carbon-13/carbon-12 isotope fractionation of organic matter associated with uranium ores induced by alpha irradiation 47-48
— Distributions of carbon and stable-carbon isotopes in waters and sediments of San Francisco Bay 162
C-14: Compilation of carbon-14 data 224

isotopes—helium
ratios: High helium isotope ratios associated with geothermal fluids 199
isotopes—igneous rocks
volcanic rocks: Strontium and lead isotopic composition in volcanic rocks from Peru and New Hebrides; genesis of calc-alkaline lava 188-189
isotopes—lead
Pb-206/Pb-204: Lead isotopes applied to mineral exploration 12
isotopes—neodymium
Nd-144/Nd-143: Neodymium isotopic composition of kimberlites 189
isotopes—radon
Rn-222: Value of radon measurements for uranium prospecting 49
isotopes—strontium
Sr-87/Sr-86: Age and strontium isotopic composition of the Honolulu Volcanics 180
— Strontium isotopes and minor-element geochemistry of alkaline rocks, Wet Mountains, Colorado 190
isotopes—sulfur
S-34/S-32: Sulfur isotope studies at Creede, Colorado 191
isotopes—tracers
research: Isotope tracer studies 188-190
isotopes—uranium
U-238/U-234: Extreme fractionation of $^{234}U/^{238}U$ isotopes within a Missouri aquifer 188
Israel—general
current research: Israel 325

J

Japan—engineering geology
earthquakes: Japan 325-326
Jordan—economic geology
water resources: Jordan 326
Jupiter—areal geology
maps: Planetary cartography and photogrammetry 283-284
Jupiter—exploration
Galileo Mission: The Galileo Mission 280
Voyager: The Voyager Mission 280
Jurassic *see also under* stratigraphy *under* Alaska

K

Kansas—economic geology
water resources: Prototype water-use data systems in Connecticut, Kansas, and Virginia 137-138
Kansas—environmental geology
pollution: Kansas 273
waste disposal: Potentiometric surface–Arbuckle Group 210
Kansas—hydrogeology
ground water: Chemical quality of ground water in Kansas 122
— Hydrologic conditions in the Equusbeds region 122
hydrology: Changes in historic patterns of a stream-aquifer system 21
— Kansas 122
— Methods of estimating ground-water withdrawals for irrigation 138
— Simulation of multiaquifer system along Arkansas River valley, southwestern Kansas 208
— Stream-aquifer model of north-central Kansas 225
karst *see under* solution features *under* geomorphology
Kentucky—environmental geology
waste disposal: Subsurface waste nuclide migration at Maxey Flats storage site near Morehead, Kentucky 264
Kenya—environmental geology
land use: Kenya 326

L

lakes *see under* environment *under* sedimentation; *see under* limnology *under* hydrology
land subsidence—geologic bazards
research: Land subsidence 275-277
land subsidence—solution features
karst: Land subsidence and collapse over soluble rocks 277
land use *see also under* environmental geology *under* Alaska; Atlantic Coastal Plain; California; Colorado; Florida; Georgia; Gulf Coastal Plain; Iowa; Kenya; New Jersey; New Mexico; North Carolina; Pacific Coast; United States; Virginia; Washington; Western U.S.; Wisconsin
land use—classification
coal: Coal resource occurrence/coal development potential (CRO/CDP) reports 164
— Known recoverable coal resource areas 164
geothermal energy: Known geothermal resource areas 164
mineral resources: Classification and evaluation of mineral lands 163-164
— Classified land 163
— Known leasing areas for potassium, phosphate, and sodium 164
oil and gas fields: Known geologic structures of producing oil and gas fields 163-164
— Onshore oil and gas lease sales 164
water resources: Waterpower classification–preservation of reservoir sites 164-165
land use—controls
mineral resources: Supervision of mineral leasing 165
land use—general
research: Land use and environmental impact 302-310
land use—management
petroleum: Management of oil and gas resources on the Outer Continental Shelf 165-166
— OCS lease sales for oil and gas 165-166
land use—maps
cartography: Cooperative land use mapping and data projects 306
— Geographic information systems software development 309
— Land use and land cover and associated maps 304-306
— Land use and land cover change mapping of urban areas 306
— Land use and land cover maps and data and other geographic studies 304-309
— Land use change detection and map update 308-309
— Statistical design of sampling techniques 307
land use—natural resources
management: Management of natural resources on Federal and Indian lands 163-166
land use—planning
research: Multidisciplinary studies in support of land-use planning and decision-making 302-304
land use—remote sensing
maps: Integrated terrain mapping 295
mines: Impact of surface mining 292-293
programs: Cooperative projects with states 293
— Cooperative projects with the Bureau of Land Management 290-291
— Cooperative projects with the National Park Service 291
landslides *see under* earthquakes *under* geologic hazards; *see under* slope stability
lava *see also* igneous rocks; magmas
lava—age
absolute age: Volcanic recurrence intervals and volcanic hazards in the eastern Snake River Plain in Idaho 71-72
lava—distribution
lava flows: Source areas and distribution of Columbia River Basalt Group in Washington 183
lava—geochemistry
trace elements: Magma sources and tectonic setting of Clear Lake Volcanics, California 181
— Molokai petrologic studies 179-180
— Strontium and lead isotopic composition in volcanic rocks from Peru and New Hebrides; genesis of calc-alkaline lava 188-189
lava—observations
lava fields: Field mapping of the Craters of the Moon lava field, Idaho 72
— Structurally complex roots of a caldera near Questa, New Mexico 72
lava—petrology
rhyolite: Pliocene rhyolite in the Sevier Plateau, Utah 73
lead *see also under* economic geology *under* Virginia
lead—isotopes
Pb-206/Pb-204: Lead isotopes applied to mineral exploration 12
ratios: Strontium and lead isotopic composition in volcanic rocks from Peru and New Hebrides; genesis of calc-alkaline lava 188-189

lead-zinc deposits—resources
global: Lead and zinc resources of the United States and of the World 2-3
Liberia—areal geology
maps: Liberia 326
lignite *see also under* economic geology *under* Gulf Coastal Plain; North Dakota
lignite—deposits
experimental studies: Dating, geochemistry, and petrology of peat, lignite, and coal 21-23
limestone *see also under* carbonate rocks *under* sedimentary rocks
limnology *see under* hydrology
lineation *see also* structural analysis
lithium *see also under* economic geology *under* Basin and Range Province; Bolivia; Nevada
lithium—affinities
uranium: Association of lithium with uranium 16
lithium—analysis
autoradiography: Autoradiographic method of lithium determination 16-17
lithium—resources
sedimentary rocks: Lithium investigations in sedimentary and volcanic rocks 15-17
Louisiana—economic geology
geothermal energy: Geochemistry of geopressured geothermal waters in coastal Louisiana and Texas 260
Louisiana—engineering geology
geologic hazards: Effects of cyclic loading on underconsolidated sediments 146
— Inundation maps of urban areas 272
maps: Inundation maps of urban areas 272
Louisiana—environmental geology
geologic hazards: Magnitude and frequency of peak discharges on small streams in Louisiana 271
pollution: Insecticides in Louisiana oxbow lake beds 274
— Volatile and semivolatile organics in the lower Mississippi River in Louisiana 223-224
Louisiana—hydrogeology
ground water: Index to ground-water monitor wells in Louisiana 122-123
— Saltwater encroachment at Baton Rouge 123
hydrology: Louisiana 122-123
lunar studies *see* Moon

M

magmas *see also* igneous rocks; intrusions; lava
magmas—genesis
hot spots: Magma sources and tectonic setting of Clear Lake Volcanics, California 181
processes: Plutonic rocks and magmatic processes 184
magnesium—geochemistry
thermal waters: Magnesium correction determined for sodium-potassium-calcium geothermometer 193
magnetic field *see under* Earth
magnetic surveys *see under* geophysical surveys *under* Alaska; Oklahoma; Saudi Arabia
Maine—economic geology
peat: Peat resources in Minnesota and Maine 3
Maine—petrology
intrusions: A more complex Sebago batholith 57
Maine—structural geology
folds: Early recumbent folding in Silurian turbidite section, Maine 56-57
structural analysis: A structural analysis of the Norumbega fault zone 56
Mammalia—biostratigraphy
Cenozoic: Late Cenozoic vertebrate biochronology 215
Mammalia—faunal studies
Cenozoic: Vertebrate faunas of Gay Head, Martha's Vineyard, Massachusetts 216
manganese—abundance
sediments: Manganese-rich sediment from the Aleutian Basin, southern Bering Sea 154
Manitoba—engineering geology
waste disposal: Borehole geophysical logs of granitic rocks in Manitoba, Canada 268
mantle *see also under* seismology *under* Nevada; *see also under* tectonophysics *under* Arabian Peninsula; Hawaii; Moon
mantle—properties
conductivity: Electromagnetic refraction in the mantle and secular change 169
maps *see also under* areal geology *under* Jupiter; Liberia; Mars; Mercury Planet; New Mexico; *see also under* economic geology *under* Gulf Coastal Plain; Texas; Wyoming; *see also under* engineering geology *under* Louisiana; Mississippi; Montana; United States; *see also under* environmental geology *under* Alaska; Atlantic Coastal Plain; Colorado; Georgia; *see also under* geomorphology *under* Washington; *see also under* geophysical surveys *under* Atlantic Coastal Plain; California; Moon; Saudi Arabia; *see also under* hydrogeology *under* automatic data processing; United States; Virginia; *see also under* structural geology *under* Appalachians; *see also under* tectonophysics *under* Idaho; Indonesia
maps—cartography
automatic data processing: Building DLG-2 digital files directly from stereomodels 340-341
— Coordinate transformation system 343-344
— Digital cartography 342-344
— Digital data editing system 343
— Digital profile recording and output system 343
— Digital readout and reference system for cartographic camera 343
— Photogrammetric archival storage system 342
— Point-transfer eye test 341
field studies: Field surveying 339-342
— Inertial surveying with span mark 339-340
— Surveying from the air using inertial technology 339
instruments: Cartographic equipment 345
— Microdotter 345
land use: Cooperative land use mapping and data projects 306
— Geographic information systems software development 309
— Land use and land cover and associated maps 304-306
— Land use and land cover change mapping of urban areas 306
— Land use and land cover maps and data and other geographic studies 304-309
— Land use change detection and map update 308-309
— Statistical design of sampling techniques 307
photogrammetry: Numerical orientation of Kelsh K-100 plotter 341
— Photogrammetry 340-342
photography: Arbitrary photocoordinate pass points 340
— Image control targets 342
— Mapping from high-resolution and high-altitude panchromatic photographs 340
— "Natural" color image maps from color infrared film 342
— Planimetric compilation from orthophotographs 341
programs: Topographic surveys and mapping 339-345
projections: Space oblique mercator projection 345
remote sensing: Landsat-3 return beam vidicon images 344
— Satellite image maps 344-345
— Satellite technology 344-345
maps—general
publications: Maps and charts 349-350
— Maps and charts 350
marine geology *see also* oceanography; *see also under* oceanography *under* Alaska; Atlantic Coastal Plain; California; Gulf of Mexico; Pacific Coast; United States
marine geology—observations
deep-sea environment: Deep-sea relief, sediments, and mineral deposits 156-157
processes: Marine geologic processes 157-158
Mars—areal geology
maps: Planetary cartography and photogrammetry 283-284
Mars—exploration
Viking: The Viking Mars Mission 279
Mars—geochronology
cratering: Image chronology on Mars 283
Mars—geomorphology
channels: Fluvial history of Mars 281
eolian features: Eolian features on Mars 282-283
permafrost: Geophysics applied to permafrost on Mars 174-175

processes: Mass wasting and periglacial processes on Mars 281-282
volcanic features: Volcanic deposits on Mars 282

Maryland—hydrogeology
ground water: Drilling phase of modeling project completed 105
hydrology: Maryland 105

Massachusetts—engineering geology
shorelines: Cape Cod, Massachusetts 294

Massachusetts—environmental geology
geologic hazards: Flood magnitude and frequency in three regions of Massachusetts 271
pollution: Ground-water contamination by secondary treated wastewater 274
— Nutrient content of ground water 274
— Trace metals of Boston Harbor sediments 141

Massachusetts—geochronology
Holocene: Holocene submergence of the southern New England inner Continental Shelf 141

Massachusetts—geomorphology
glacial geology: Further studies of two classic geologic sites of Massachusetts 141
— Glacial Lake Taunton Deposits 58
— Readvance produces Ellisville moraine 58

Massachusetts—hydrogeology
hydrology: Massachusetts 105
— Water quality in the Blackstone River basin 105

Massachusetts—paleontology
Vertebrata: Vertebrate faunas of Gay Head, Martha's Vineyard, Massachusetts 216

Massachusetts—stratigraphy
Miocene: Miocene sporomorphs from Massachusetts 215-216
Pennsylvanian: Narragansett Basin extends to Massachusetts coast 57
Quaternary: Retreat of ice left eastern upland of Massachusetts subject to deep freeze 58

Massachusetts—structural geology
faults: Fault systems in the Boston Basin of Massachusetts 57
— Mylonitization of the Salem Gabbro-Diorite intrusive complex 57

mathematical geology *see also* automatic data processing

meetings *see* symposia

Melanesia *see also* New Hebrides

melange *see under* interpretation *under* structural analysis

mercury *see also under* economic geology *under* Oregon

Mercury Planet—areal geology
maps: Geologic mapping of Mercury 283
— Planetary cartography and photogrammetry 283-284

Mesozoic *see also under* geochronology *under* Alaska; Antarctica; California; *see also under* stratigraphy *under* New Mexico

Mesozoic—paleontology
research: Mesozoic and Cenozoic studies 214-218

metals *see also* aluminum; arsenic; bauxite; magnesium; manganese; tungsten; *see also under* economic geology *under* Afghanistan; Alaska; Basin and Range Province; California; Colorado; Iran; Michigan; Missouri; Montana; Saudi Arabia; South Carolina; Turkey; United States; Utah; Western Interior

metals—abundance
sediments: Trace metals and an area of possible sediment accumulation on the North Atlantic Continental Shelf 141-142
— Trace metals of Boston Harbor sediments 141

metals—analysis
chemical analysis: Metallic constituents 232-233

metals—exploration
biogeochemical methods: Biogeochemical investigations 12

metals—geochemistry
trace elements: Trace-metal form and bioavailability in estuarine sediments 223

metals—resources
data bases: Computerized Resources Information Bank 13

metamorphic rocks *see also* igneous rocks; metamorphism; metasomatism

metamorphic rocks—distribution
metamorphic belts: Exotic Precambrian rocks in southwestern Alaska 97

metamorphic rocks—facies
greenschist facies: Paleozoic cataclastic deformation and low-grade metamorphism of Proterozoic rocks in the northern Virginia Blue Ridge 62

metamorphic rocks—gneisses
geochemistry: Initial strontium values of rocks from the Pioneer Mountains 72-73
petrology: The Oliverian domes, re-evaluated 60

metamorphic rocks—lithostratigraphy
Proterozoic: Archean and Proterozoic structural and stratigraphic details of the Hartville uplift in Wyoming 69

metamorphic rocks—metaplutonic rocks
petrology: Character of Peninsular Ranges batholith 84-85

metamorphic rocks—metasedimentary rocks
metaconglomerate: Archean-Proterozoic boundary in Laramie Mountains in Wyoming may contain radioactive conglomerates 36-37
petrology: Paleozoic metasedimentary rocks in eastern Mojave Desert 84

metamorphic rocks—mylonites
distribution: Mylonitization of the Salem Gabbro-Diorite intrusive complex 57

metamorphic rocks—petrology
general: Metamorphic rocks and processes 184-185

metamorphic rocks—schists
greenstone: Greenstone in Devonian Slaven Chert in north-central Nevada 81
mineral assemblages: Mineral equilibria of slightly calcic pelitic schists in Barrovian regional metamorphism 184-185

metamorphism—grade
low-grade metamorphism: Paleozoic cataclastic deformation and low-grade metamorphism of Proterozoic rocks in the northern Virginia Blue Ridge 62

metamorphism—regional metamorphism
grade: Metamorphism and structural relationships in the Kings Mountain area of the Carolinas 63
mineral assemblages: Mineral equilibria of slightly calcic pelitic schists in Barrovian regional metamorphism 184-185

metasomatism—processes
hydrothermal alteration: Alteration associated with a fault zone in the Carolina slate belt, South Carolina 8

meteor craters *see also* meteorites

meteorites—geochemistry
Moama: Origin and history of the adcumulate eucrite, Moama 189

Mexico *see also* Gulf Coastal Plain

Mexico—economic geology
mineral resources: Mexico 326-327

Mexico—geophysical surveys
surveys: Deep-tow studies of the East Pacific Rise off Mexico 157

Michigan—economic geology
metals: Chemical data from the Hemlock Formation, Ned Lake quadrangle, Michigan 8
thorium: Thorium and uranium resources in Goodrich Quartzite upgraded 37
uranium: Paleocurrent studies contribute to uranium resource evaluation in Upper Peninsula of Michigan 38
— Paleogeography of the Jacobsville Sandstone, Michigan 38
water resources: Water resources of the Marquette Iron Range area 105-106

Michigan—environmental geology
pollution: Land conservation related to water quality 222

Michigan—hydrogeology
ground water: Ground water in Marquette County 105
— Model study of Michigan coal deposit 106
hydrology: Michigan 105

Michigan—stratigraphy
Proterozoic: Michigan 65-66
— Revision in Proterozoic X stratigraphy in Marenisco-Watersmeet area, northern Michigan 65-66

Michigan—structural geology
tectonics: Ancient fault sets in northern Michigan 67

Micronesia—stratigraphy
changes of level: Reef limestones of the Palau Islands, trust territory of the Pacific Islands 156

Middle East *see also* Israel; Jordan; Turkey

Middle East—economic geology
tin: Afghanistan-Iran-Turkey 321

Middle East—stratigraphy
archaeology: Jordan 326

Midwest—economic geology
water resources: Targeting, inventorying, and monitoring ground-water resources 294

Midwest—engineering geology
waste disposal: Hydraulic properties of Cretaceous shale 210

Midwest—geophysical surveys
remote sensing: Targeting, inventorying, and monitoring ground-water resources 294

mineral deposits, genesis—controls
depth: Depth limitation to uranium deposition, Powder River basin, Wyoming and Montana 42
— Uranium ore deposit controls in the Powder River basin 42
geochemical controls: Organic acids on the move 45
— Organo-clay complexes in uranium deposits 44
— Porous media model studies of sandstone-type uranium deposits 50-51
— Relationship of modern groundwater chemistry to the origin and rereduction of south Texas roll-front uranium deposit 50
paleogeographic controls: Paleogeography of the Jacobsville Sandstone, Michigan 38
structural controls: Pre-Belden unconformity in the Marshall Pass district, Colorado 38-39

mineral deposits, genesis—lead
mineralization: Factors affecting the origin of stratabound massive sulfide deposits of the Great Gossan Lead (GGL), southwestern Virginia 8

mineral deposits, genesis—lithium
brines: Origin of commercial lithium brines 15-16
environment: Origin and distribution of lithium-rich clay deposits 16

mineral deposits, genesis—metals
age: Age of Davidson Granodiorite and mineralization in Comstock Lode mining district of western Nevada 79-80

mineral deposits, genesis—processes
epigene processes: Epigenetic uranium mineralization, Alaska 44
hydrothermal processes: Alteration associated with a fault zone in the Carolina slate belt, South Carolina 8
— Genesis of the Schwartzwalder uranium deposit, Colorado 39-40
— Gold-mineralized areas in Manhattan quadrangle have potential for molybdenum-porphyry deposits 5
supergene processes: Constraints on the genesis of uranium ores in the Midnite Mine, Washington, from geochronologic and lead-isotope investigations 46
volcanism: Big Mike sulfide deposit in northwestern Nevada 79
— Volcanogenic massive sulfide deposits in the northern Klamath Mountains, California and Oregon 4
weathering: Uranium and thorium content in weathering profiles of the Catahoula Tuff, South Texas coastal plain 44

mineral deposits, genesis—uranium
experimental studies: Obsidian, perlite, and felsite as sources of uranium: an experimental study 46
mineralization: The Ruby Well No. 1 uranium mine, McKinley County, New Mexico 41
roll-type deposits: Computer modeling of ore-forming processes 47

mineral exploration—biogeochemical methods
experimental studies: Biogeochemical investigations 12

mineral exploration—geobotanical methods
copper: Botanical investigations 12
ore guides: Molybdenum in catclaw mimosa as a possible indicator of uranium 51

mineral exploration—geochemical methods
anomalies: Geochemical anomalies in the Mystery Mountains, Medfra quadrangle, Alaska 4
aureoles: Alteration aureoles in McDermitt caldera in Nevada and Oregon 79
isotopes: Lead isotopes applied to mineral exploration 12
metals: Chemical data from the Hemlock Formation, Ned Lake quadrangle, Michigan 8
— Geochemical-reconnaissance results 10-11
soil sampling: Volatile gases useful in geochemical exploration 12
stream sediments: Relative uranium scavenging affects of organic matter, clays, and iron and manganese oxides 49-50
trace elements: Analytical methodology useful in geochemical exploration 12
— Palladium, platinum, and rhodium 335
— Pyritic alteration in northern Keg Mountains, Utah 71
uranium: Association of lithium with uranium 16
— The measurement of uranium content in metallic ores, sediments, and water 231

mineral exploration—geological methods
metals: Mineral belt studies 332

mineral exploration—geophysical methods
electromagnetic methods: Mining geophysics 332
magnetic methods: Mineral resources and aeromagnetic studies of Glacier Bay National Monument 97-99
ore guides: Geophysical ore guides in south-central Alaska 97
radioactivity methods: Scintillator used as fast neutron detector 48
uranium: Geophysical studies of a uranium deposit in southern Utah 174
— Geophysical study of gneiss domes and two-mica granites 51

mineral exploration—hydrological methods
uranium: Radium and uranium in mineral springs 48-49
— Source for the anomalous uranium in surface waters of the Ojo Caliente area in New Mexico 49
— Uranium source potential estimated from radium and radon concentrations in flowing water 48

mineral exploration—methods
applications: Geochemical and geophysical techniques in resource assessments 10-12

mineral exploration—ore guides
drainage patterns: Present-day stream valleys as guides to uranium deposits in Wyoming 42-43
helium: Helium detection for uranium exploration 49
isotopes: Identification of possible uranium province in central Wyoming through radio-element distribution in crystalline basement rocks 47
radon: Value of radon measurements for uranium prospecting 49
thermoluminescence: Some applications of thermoluminescence to uranium prospecting 45
uranium: Borehole magnetic susceptibility probe detects low-level anomalies 171
— Physical-property changes associated with roll-front uranium deposits 171

mineral exploration—programs
lead-zinc deposits: Poland 331-332
lithium: Bolivia 321
metals: Afghanistan-Iran-Turkey 321
mineral resources: Mexico 326-327

mineral exploration—remote sensing
copper: Copper and molybdenum in Nabesna, Alaska 296
— Porphyry copper in Arizona 295-296
lead-zinc deposits: Regional structures interpreted from Landsat data 298
multispectral analysis: Visible and near-infrared multispectral aircraft images used to distinguish altered rocks 299
programs: Targeting mineral exploration 295-296
spectral analysis: Altered-rock spectra in the visible and near infrared 172
— Near-infrared spectra of alteration minerals and the potential for use in remote-sensing applications 172
— Visible and near-infrared spectra of rocks from a chromite-rich area in Oregon 171-172
uranium: Mineral exploration at Claunch, New Mexico 295

mineral exploration—techniques
data analysis: Prospector computer consultant 13-14

mineral prospecting *see* mineral exploration

mineral resources *see also under* economic geology *under* Alaska; Asia; Basin and Range Province; Egypt; Mexico; North America; United States

mineral resources—exploration
geochemical methods: Geochemical and geophysical techniques in resource assessments 10-12

mineral resources—resources
chemical resources: Chemical resources 15-18
data analysis: Resource analysis 13-15
data bases: Computerized Resources Information Bank 13
evaluation: Mineral resource assessment 14
— Prospector computer consultant 13-14
global: Resource Attache Program 318-319
— United States and world mineral resource assessments 1-3
information systems: Resource information systems 13
— Resource information systems and analysis 13-15

mineralogy—general
research: Geochemistry, mineralogy, petrology 176-188
— Mineralogic studies and crystal chemistry 176-178

minerals *see also* crystal structure

minerals—chain silicates, pyroxene group
pyroxene: Electrical conductivity of pyroxenes 170-171

minerals—framework silicates
analcime: Analcime a notable concentrator of cesium in Yellowstone geyser basins 196

minerals—framework silicates, zeolite group
laumontite: Diagenetic laumontite–a low-temperature paleothermometer 157

minerals—occurrence
weathering crust: Mineralogy of surface encrustations in the Orville Coast area 337

minerals—orthosilicates
sapphirine: Sapphirine in host rocks of Precambrian sulfide deposits, Wet Mountains, Colorado 7
stillwellite: Rare earth borosilicate in magnetite ore 8

minerals—oxides
iron oxides: Relative uranium scavenging affects of organic matter, clays, and iron and manganese oxides 49-50

minerals—sulfides
bartonite: Bartonite, $K_6Fe_{20}S_{27}$ 177
djurleite: Djurleite and chalcocite, Cu_xS 177
erdite: Crystal structures of alkali-iron copper sulfide minerals; erdite, $NaFeS_2 \cdot 2H_2O$ 176-177
rasvumite: Rasvumite, KFe_2S_3 177
sphalerite: Sphalerite in Interior Basin coals 22

mining geology—evaluation
coal: An experimental technique for delineating areas best suited for mining of coal 71

mining geology—methods
remote sensing: Cooperative projects with the Mine Safety and Health Administration 292
— Impact of surface mining 292-293

mining geology—objectives
human ecology: The asbestos minerals and cancer incidence 177-178

mining geology—practice
international cooperation: CENTO training program 313

Minnesota—economic geology
peat: Peat resources in Minnesota and Maine 3
water resources: Targeting, inventorying, and monitoring ground-water resources 294

Minnesota—environmental geology
pollution: Minnesota 272

Minnesota—geophysical surveys
remote sensing: Targeting, inventorying, and monitoring ground-water resources 294

Minnesota—hydrogeology
ground water: Appraisal of ground-water in central Minnesota 106-107
— Design for a ground-water-quality monitoring network 106
— Ground-water appraisal of sand-plain areas 107
— Shallow aquifers in southwestern Minnesota 106
— Spread of contaminants through multiaquifer wells in southeastern Minnesota 107
— Two-dimensional model of the Buffalo aquifer 108
— Use of surficial aquifers increasing in Minnesota 107
hydrology: Effect of copper and nickel mining on surface and ground water in northeastern Minnesota 106
— Lake budget in Minnesota 225
— Minnesota 106-108
— Minnesota and Wisconsin 108
— Water balance of Williams Lake, north-central Minnesota 107
— Water quality established before highway construction 107
— Water-quality monitoring in Voyageurs National Park 107

Minnesota—structural geology
faults: Faulting in the Duluth Complex 66
— Minnesota 66

Miocene *see also under* geochronology *under* Nevada; *see also under* stratigraphy *under* California; Massachusetts; Washington

Mississippi—engineering geology
geologic hazards: Inundation maps of urban areas 272
maps: Inundation maps of urban areas 272
waste disposal: Geohydrology of three Mississippi salt domes 265

Mississippi—geophysical surveys
remote sensing: Significance of saturated soils in coastal plains 301

Mississippi Valley—areal geology
Mississippi Embayment: Central region 65-67
— Mississippi embayment 66-67

Mississippi Valley—engineering geology
earthquakes: Eastern United States 247-248

Mississippi Valley—geophysical surveys
remote sensing: Regional structures interpreted from Landsat data 298

Mississippi Valley—stratigraphy
Pliocene: Age and mode of deposition of so-called "Lafayette formation" in northern Mississippi embayment 66

Mississippi Valley—structural geology
tectonics: Post-Midwayan (Paleocene) uplift at margin of Mississippi embayment in northeastern Arkansas 66
— Regional structures interpreted from Landsat data 298

Mississippian *see also under* stratigraphy *under* Arizona; Iowa; Nevada

Missouri—economic geology
lead-zinc deposits: Regional structures interpreted from Landsat data 298
metals: Copper, cobalt, and nickel in Viburnum Trend 7

Missouri—environmental geology
geologic hazards: Technique for estimating the magnitude and frequency of floods in St. Louis County 123

Missouri—hydrogeology
ground water: Deep wells in Audrain County 123
— Extreme fractionation of $^{234}U/^{238}U$ isotopes within a Missouri aquifer 188
hydrology: Hydrology of Ozark basins in Missouri 225
— Missouri 123

Missouri—petrology
igneous rocks: Chemical and petrographic subdivision of Precambrian rhyolites in Missouri 183

Mollusca—biostratigraphy
Cretaceous: Biostratigraphy of Cretaceous nonmarine mollusks from the Western Interior of North America 217-218

Mollusca—Bivalvia
ecology: Population biology and production of Gemma gemma in San Francisco Bay 161
— Temporal dynamics of copper, zinc, and silver related to freshwater discharge in southern San Francisco Bay 160-161
Eocene: Reproduction of glochidium larva in an Eocene nonmarine bivalve 217

Mollusca—occurrence
Cambrian: Cambrian primitive mollusks 219

molybdenum *see also under* economic geology *under* Alaska; Nevada

Montana—economic geology
coal: Coal hydrology and geochemical studies in the Powder River basin, Montana and Wyoming 260

copper: Botanical investigations 12
— Proterozoic Z stratabound copper occurrences 5-6
geothermal energy: A hydrothermal system near Ennis, Montana 193-194
metals: Significant mineral potential in Elkhorn Wilderness Study Area, Montana 9
platinum: Faulting in banded upper zone of the Stillwater Complex 6
thorium: New thorium resource numbers calculated for vein-type occurrences 52
uranium: Depth limitation to uranium deposition, Powder River basin, Wyoming and Montana 42
— Uranium ore deposit controls in the Powder River basin 42

Montana—engineering geology
geologic hazards: Flood-prone areas in Helena, Montana 271-272
land subsidence: Subsidence of reclaimed coal mine spoils, Colstrip, Montana 310
maps: Flood-prone areas in Helena, Montana 271-272

Montana—environmental geology
impact statements: Mode of deformation of Rosebud coal; Colstrip, Montana 310
— Subsidence of reclaimed coal mine spoils, Colstrip, Montana 310

Montana—geochemistry
strontium: Initial strontium values of rocks from the Pioneer Mountains 72-73

Montana—geomorphology
glacial geology: Middle-Wisconsinan glacial lake in Scobey, Montana, area 69-70

Montana—geophysical surveys
radioactivity surveys: Interpretation of aerial gamma-ray data from the northern part of the Boulder batholith 300
surveys: Electrical and magnetic studies of Belt green beds 174

Montana—hydrogeology
ground water: Geohydrology of the Helena Valley 124
— Ground-water resources of part of the Flathead Indian Reservation 124
— Hydrogeology of the Fort Union coal region 124
— Hydrology of Prairie Dog Creek 124
— Regional-scale aquifers investigated in Montana 124
— Saline-seep development in Hailstone basin 123-124
— Third test well completed in the Madison Aquifer 120
hydrology: Limnological characteristics of small Montana reservoirs 228
— Montana 123-124
— Seepage runs in Federal coal-lease areas 124
springs: A hydrothermal system near Ennis, Montana 193-194

Montana—stratigraphy
Cambrian: Trilobite from the Silver Hill Formation 67-68
Paleogene: Magnetostratigraphy of lower Tertiary rocks in the Powder River basin 167
Proterozoic: Eastern extent of the Proterozoic Y Belt basin, Montana 68

Montana—structural geology
tectonics: Bald Butte fault in the Helena area of Montana 77
— Revised interpretation of thrust faults in the southern Flint Creek Range, western Montana 77-78
— Structure of the Choteau 2-degree quadrangle, Montana 78
— Tectonic style and history, north end of the Pioneer Mountains in Montana 75-76

Moon—general
research: Lunar and Planetary Geoscience Consortium 286-287
— Lunar investigations 285-289

Moon—geochemistry
isotopes: Implications from Luna 24 to U-Pb evolution in the lunar mantle 189-190

Moon—geomorphology
cratering: Basin and crater studies 285-286
rilles: Volcanism and tectonism studies 286

Moon—geophysical surveys
maps: Lunar and planetary mapping 344
remote sensing: Lunar and planetary mapping 344

Moon—petrology
breccia: Consortium of Apollo 17 breccias 287-288

Moon—tectonophysics
mantle: Electrical conductivity of pyroxenes 170-171

mud volcanoes *see also* volcanology

N

natural gas *see also under* economic geology *under* Appalachians; Colorado; Great Plains; Gulf of Mexico; New Mexico; Utah; Western Interior

natural gas—exploration
techniques: New exploration and production techniques 33-35

natural resources *see under* conservation

Nebraska—hydrogeology
ground water: Tracer studies at sites in Nebraska and Texas 209-210
hydrology: Historical perspective of the South Platte River 120

neodymium—isotopes
Nd-144/Nd-143: Neodymium isotopic composition of kimberlites 189

Neogene *see also under* geochronology *under* California; *see also under* stratigraphy *under* Atlantic Coastal Plain

neotectonics *see also under* structural geology *under* Basin and Range Province; California; Wyoming

Nevada—economic geology
copper: Big Mike sulfide deposit in northwestern Nevada 79
industrial minerals: Novaculite in Nevada 18
lithium: Origin of commercial lithium brines 15-16
molybdenum: Gold-mineralized areas in Manhattan quadrangle have potential for molybdenum-porphyry deposits 5
oil shale: Geology and oil-shale resources of the Elko West and Elko East 7 1/2′ quadrangles, Elko County, Nevada 35
— Metals in Devonian marine strata in central Nevada 80
selenium: Selenium in Paleozoic eugeosynclinal rocks in central Nevada 5
silver: Age of Davidson Granodiorite and mineralization in Comstock Lode mining district of western Nevada 79-80
thorium: Alteration aureoles in McDermitt caldera in Nevada and Oregon 79

Nevada—engineering geology
geologic hazards: Possible paleoseismic belt in Nevada Test Site region 82
waste disposal: Complexity of structure and hydrology of Eleana Formation confirmed at Syncline Ridge, Nevada Test Site 265-266

Nevada—environmental geology
geologic hazards: Flood-frequency relations for small streams in Nevada 271

Nevada—geochronology
Cretaceous: Dating of the Climax Stock; Nevada Test Site 191
Miocene: Age of Davidson Granodiorite and mineralization in Comstock Lode mining district of western Nevada 79-80

Nevada—hydrogeology
hydrology: Development of a relation for steady-state dumping rate in Eagle Valley 132
— Nevada 132

Nevada—sedimentary petrology
sedimentary rocks: Formation of conglomerates from submarine slides 34
sedimentation: Calcium-poor quartzites in eastern Nevada 81

Nevada—seismology
crust: Crustal thinning in northwest Nevada 199-200
mantle: Teleseismic P-wave study at the Battle Mountain heat-flow high, Nevada, shows a deep, high-velocity intrusion present 193

Nevada—stratigraphy
Devonian: Greenstone in Devonian Slaven Chert in north-central Nevada 81
Mississippian: Age of type Pablo Formation in central Nevada 82
Ordovician: Ordovician rocks in Monitor Hills, south-central Nevada 82
— Ordovician Vinini Formation of northern Nevada 80-81
Paleozoic: Paleozoic rocks in southern East Range, northwestern Nevada 81

— Stratigraphy first, structure second 80
Permian: Southward-directed thrusting of Mesozoic age in northeastern Nevada 81
Triassic: Triassic continental and marine rocks correlated by sedimentary features 81

Nevada—structural geology
tectonics: Structure of southwestern Virgin Mountains, southeastern Nevada 82

Nevada—tectonophysics
heat flow: Teleseismic P-wave study at the Battle Mountain heat-flow high, Nevada, shows a deep, high-velocity intrusion present 193

New England—areal geology
regional: New England and the Adirondacks 56-60

New England—geochronology
Paleozoic: Two-mica granite and the Mesoappalachian-Avaltonian boundary in New Hampshire 37

New England—geomorphology
landform evolution: Geomorphology of New England 59-60

New England—geophysical surveys
remote sensing: Cape Cod, Massachusetts 294

New England—stratigraphy
changes of level: Holocene submergence of the southern New England inner Continental Shelf 141

New England—structural geology
folds: The Oliverian domes, re-evaluated 60

New Hampshire—economic geology
uranium: Two-mica granite and the Mesoappalachian-Avaltonian boundary in New Hampshire 37

New Hampshire—hydrogeology
ground water: Ground-water resources of the Lamprey River basin 108-109
hydrology: New Hampshire 108-109

New Hebrides—geochemistry
isotopes: Strontium and lead isotopic composition in volcanic rocks from Peru and New Hebrides; genesis of calc-alkaline lava 188-189

New Jersey—economic geology
uranium: Organo-clay complexes in uranium deposits 44

New Jersey—engineering geology
earthquakes: Eastern United States 247-248

New Jersey—environmental geology
land use: Impact of land-use changes on water resources 109
pollution: Relation between pH and fish kills in Oyster Creek, New Jersey 221

New Jersey—hydrogeology
hydrology: New Jersey 109

New Jersey—oceanography
continental shelf: An ancestral Hudson River valley of the Continental Shelf off New Jersey 142

New Jersey—structural geology
tectonics: Late Alleghenian thrusting in New Jersey 60-61

New Mexico—areal geology
maps: Geologic map of the Arroyo del Agua quadrangle, Rio Arriba County, New Mexico 41-42

New Mexico—economic geology
coal: Rank and methane content of western coals 20
— San Juan Basin, New Mexico 20
natural gas: Oil and gas resources of Permian Basin, West Texas and southeastern New Mexico 29-30
uranium: Carbon-13/carbon-12 isotope fractionation of organic matter associated with uranium ores induced by alpha irradiation 47-48
— Disconformities in the Grants, New Mexico, mineral belt and their relationship to uranium occurrence 40-41
— Mineral exploration at Claunch, New Mexico 295
— Relative uranium scavenging affects of organic matter, clays, and iron and manganese oxides 49-50
— Source for the anomalous uranium in surface waters of the Ojo Caliente area in New Mexico 49
— The Ruby Well No. 1 uranium mine, McKinley County, New Mexico 41
— Uranium potential in Rio Grande rift basins 52
water resources: Ground-water resources of the lower Rio Grande Valley area of New Mexico 126

New Mexico—engineering geology
earthquakes: Western United States excluding California 246-247
waste disposal: Dissolution history of evaporite beds defined 267
— Hydrologic testing of strata associated with Permian bedded salt 267
— Waste isolation pilot plant site, southeastern New Mexico 267

New Mexico—environmental geology
land use: Projected ground-water pumpage from uranium mines in northwestern New Mexico 125

New Mexico—geomorphology
solution features: Dissolution history, southeastern New Mexico 70

New Mexico—geophysical surveys
remote sensing: Mineral exploration at Claunch, New Mexico 295

New Mexico—hydrogeology
ground water: Aquifer near Capulin 124-125
hydrology: Ground-water conditions in the vicinity of Elephant Butte Irrigation District well field 125-126
— Hydrology of coal areas in northwestern New Mexico 125
— New Mexico 124-126

New Mexico—paleobotany
Plantae: Early Tertiary flora found in New Mexico 217

New Mexico—stratigraphy
Cretaceous: Cretaceous stratigraphic studies 41
— High energy beds in the Dilco 42
Mesozoic: Disconformities in the Grants, New Mexico, mineral belt and their relationship to uranium occurrence 40-41
Ordovician: Ordovician Montoya Group extended westward in southeastern Arizona 83

New Mexico—structural geology
tectonics: Rio Grande rift, New Mexico 78
— Structurally complex roots of a caldera near Questa, New Mexico 72

New York—areal geology
Adirondack Mountains: New England and the Adirondacks 56-60

New York—economic geology
rare earths: Rare earth borosilicate in magnetite ore 8

New York—engineering geology
reservoirs: Aquifer storage of chilled water for air conditioning at Kennedy Airport, New York 210

New York—environmental geology
geologic hazards: Magnitude and frequency of floods on unregulated rural streams in New York 271
pollution: Column studies of waste-water infiltration 222
— New York 272-273
— PCB transport in the upper Hudson River 272
— Transport of PCB's in the Hudson River 109

New York—hydrogeology
ground water: Conversion of a three-dimensional analog model to a three-dimensional digital model 210
— Hydrogeology of artificial-recharge site 109
— The role of the unsaturated zone in artificial recharge 109
hydrology: Algal stromatolites (oncolites), Onondaga Lake, New York 228
— New York 109
— Streamflow augmentation 225

New York—structural geology
tectonics: Differential deformation of the Grenville Complex and its basement in St. Lawrence County, New York 59
— Lineaments related to subsurface geology in Salina Salt Basin, New York and Pennsylvania 265

New Zealand—hydrogeology
ground water: New Zealand 328

Nicaragua—seismology
earthquakes: Nicaragua 239

noble gases *see also* helium; radon

nodules—manganese
distribution: Small scale distribution patterns of manganese nodules 3
observations: Manganese nodules from three equatorial North Pacific test sites 156

nonmetals *see also* sulfur

North America *see also* Appalachians; Atlantic Coastal Plain; Great Lakes; Great Lakes region; Great Plains; Gulf Coastal Plain; Mexico; Rocky Mountains; United States

North America—economic geology
mineral resources: Circum-Pacific Energy and Mineral Resources Program 318

North America—paleontology
Mammalia: Late Cenozoic vertebrate biochronology 215

North America—stratigraphy
Cretaceous: Biostratigraphy of Cretaceous nonmarine mollusks from the Western Interior of North America 217-218
Devonian: The Late Devonian and Early Mississippian ostracode genus Pseudoleperditia 218
Triassic: Paleozoic and Triassic paleomagnetism of the Alexander terrane, southeastern Alaska 168

North America—tectonophysics
plate tectonics: Petroleum potential of plate boundary 30

North Carolina—economic geology
uranium: Uranium resources in the Grandfather Mountain Window in North Carolina 52-53

North Carolina—environmental geology
ecology: Wetland studies 301
land use: Hydrologic effects of land clearing and drainage, Albemarle-Pamlico Peninsula 117
pollution: Water-quality trend analysis 220-221

North Carolina—hydrogeology
ground water: Freshwater availability on offshore barrier islands 117
— Water-level measurements in observation wells 117-118
hydrology: Chemical characteristics of unpolluted streams 116-117
— Hydrology of Chicod Creek basin 117
— North Carolina 116-118

North Carolina—stratigraphy
Paleozoic: Flat Swamp Member of the Cid Formation extended 62-63

North Carolina—structural geology
tectonics: Metamorphism and structural relationships in the Kings Mountain area of the Carolinas 63

North Dakota—economic geology
lignite: Geochemical processes in mining areas in North Dakota 221-222
— Highly fractured lignite at the Gascoyne mine in Bowman County, North Dakota 260-261

North Dakota—engineering geology
slope stability: Soil slides in southwestern North Dakota 253-254

North Dakota—environmental geology
pollution: Geochemical processes in mining areas in North Dakota 221-222
— Lignite decomposition 186

North Dakota—geochemistry
weathering: Highly fractured lignite at the Gascoyne mine in Bowman County, North Dakota 260-261

North Dakota—hydrogeology
ground water: Glaciofluvial aquifers in McIntosh County 127
— Ground-water availability and quality in Billings, Golden Valley, and Slope Counties 126
— Hydrology of Wibaux-Beach deposit 126
— Major aquifers in buried valleys 127
— Outwash plain in Logan County 126
— Results of test drilling in Bottineau and Rolette Counties 126
hydrology: Major factors controlling sediment runoff in Park River watershed 126
— North Dakota 126-127

Northern Hemisphere *see also* Africa; Arctic Ocean; Asia; Atlantic Ocean; Europe; North America; Pacific Ocean

Northern Territory—geomorphology
impact features: Basin and crater studies 285-286

Northwest Territories—stratigraphy
Cretaceous: Paleoenvironment of Cretaceous silicoflagellates north of Baffin Island 156-157

nuclear explosions *see under* explosions

nuclear facilities—geologic hazards
research: Reactor hazards 257-260

O

ocean circulation *see also under* oceanography *under* California; Florida; Gulf Coastal Plain; Texas; United States

ocean floors *see also under* oceanography *under* Pacific Ocean

ocean waves *see also under* oceanography *under* Gulf of Mexico

oceanography—sea ice
research: Sea-ice studies 230-231

Ohio—engineering geology
waste disposal: Thickness of bedded salt in northeastern Ohio 265

Ohio—environmental geology
pollution: A reconnaissance of biological and chemical characteristics of selected Ohio lakes 228

Ohio—hydrogeology
ground water: Subsurface mines as a water source 110
hydrology: Ohio 110

oil and gas fields *see also under* economic geology *under* Gulf Coastal Plain; United States

oil shale *see also under* economic geology *under* Colorado; Nevada; Utah; Western Interior

oil shale—production
pollution: Comparison of spent shale and soil as sorbents for retort waste water 35

Oklahoma—geophysical surveys
magnetic surveys: Aeromagnetic detection of diagenetic magnetite over oil fields 33-34

Oman—economic geology
copper: Oman 327-328

ophiolite *see under* ultramafic family *under* igneous rocks

Ordovician *see also under* stratigraphy *under* Appalachians; Arizona; Nevada; New Mexico; Pennsylvania

ore guides *see under* mineral exploration

Oregon—economic geology
chromite: Visible and near-infrared spectra of rocks from a chromite-rich area in Oregon 171-172
mercury: Alteration aureoles in McDermitt caldera in Nevada and Oregon 79
zinc: Volcanogenic massive sulfide deposits in the northern Klamath Mountains, California and Oregon 4

Oregon—engineering geology
geologic hazards: Geologic hazards of the northern California-Oregon Outer Continental Shelf and slope 149

Oregon—environmental geology
geologic hazards: Wide range of conditions represented in western Oregon flood-frequency analysis 133

Oregon—geophysical surveys
gravity surveys: Geophysical exploration 11-12

Oregon—hydrogeology
ground water: High arsenic concentrations in ground-water samples from northern Malheur County 132
— Iron distribution and geochemistry in a coastal dunes aquifer at Coos Bay 132
hydrology: A preliminary evaluation of dissolved-oxygen depletion in the South Santiam River 133
— Hydrological system of the Bend-Redmond area 133
— Irrigation-return flow from pastures and orchards in Bear Creek basin, Jackson County 132
— Oregon 132-133

Oregon—oceanography
continental shelf: Stratigraphic and tectonic framework, Oregon-Washington Continental Margin 149

Oregon—seismology
earthquakes: Seismicity studies of the Mount Hood, Oregon, area 195

Oregon—structural geology
tectonics: Large scale nappes in Southwest Oregon 87-88
— Oregon 87-81

Oregon—volcanology
Newberry Volcano: Latest eruptions at Newberry Volcano in Oregon 182-183

organic materials—abundance
black shale: New method for computing organic-carbon content of Devonian shale 33
— Sources of organic matter in Devonian black shales 33
ground water: Minnesota 272
— New York 272-273
— Organic compounds in ground water 272-273

organic materials—alteration
thermal alteration: Maturation of organic matter and generation of petroleum in Tertiary oil basins 30
— Mississippian source rocks in Utah and Idaho 28-29

organic materials—analysis
chemical analysis: Organic constituents 233-234

organic materials—detection
surface water: Volatile and semivolatile organics in the lower Mississippi River in Louisiana 223-224

organic materials—experimental studies
biodegradation: Adsorption of ketones in water 224
— Bacterial growth kinetics with acetone as a substrate 224

organic materials—geochemistry
clay: Organo-clay complexes in uranium deposits 44
clay minerals: Clay-humic complexes 186
isotopes: Carbon-13/carbon-12 isotope fractionation of organic matter associated with uranium ores induced by alpha irradiation 47-48
oxides: Relative uranium scavenging affects of organic matter, clays, and iron and manganese oxides 49-50
source rocks: Organic geochemistry of a stratigraphic test well, Southeast Georgia Embayment 144-145

organic materials—humates
analysis: Organic acids on the move 45

organic materials—hydrocarbons
aromatic hydrocarbons: Composition and source of petroleum 157
methane: Origin of methane in peat, coal, and eastern Devonian shale 22-23

organic materials—kerogen
abundance: Metals in Devonian marine strata in central Nevada 80

organic materials—properties
thermochemical properties: Thermochemistry of maturation of fossil fuels 176

orogeny—extent
Allegheny Orogeny: Late Alleghenian thrusting in New Jersey 60-61

orthosilicates *see under* minerals

Ostracoda—biostratigraphy
Mississippian: The Late Devonian and Early Mississippian ostracode genus Pseudoleperditia 218

oxides *see under* minerals

P

Pacific Coast—economic geology
iron: Volcanogenic massive sulfide deposits in the northern Klamath Mountains, California and Oregon 4
springs: Limits of hot-water geothermal system in The Geysers-Clear Lake geothermal area 197

Pacific Coast—engineering geology
geologic hazards: Northern California 243-244
— Southern California 244-246

Pacific Coast—environmental geology
ecology: Historical changes of shoreline and wetland in Puget Sound region 89-90
geologic hazards: Quaternary studies in the Los Angeles area 86
land use: Pacific Northwest Regional Commission 293

Pacific Coast—geochronology
Holocene: Corrections for marine shell radiocarbon dates 192

Pacific Coast—geomorphology
glacial geology: Glacier ice and water balance 203

Pacific Coast—geophysical surveys
remote sensing: Pacific Northwest Regional Commission 293
— Washington Department of Natural Resources 293

Pacific Coast—hydrogeology
springs: Geothermometry applied to hot springs in western United States 194-195

Pacific Coast—oceanography
marine geology: California to Washington 146-150
— Pacific coast 159-162
— Pacific continental margin 146-150

Pacific Coast—tectonophysics
plate tectonics: Melones fault north of Downieville 83
— Origin of melanges of the Olympic Peninsula 88
— Petroleum potential of plate boundary 30
— Plate tectonics of the western United States 83

Pacific Ocean *see also* Bering Sea; Micronesia

Pacific Ocean—oceanography
nodules: Manganese nodules from three equatorial North Pacific test sites 156
ocean floors: Deep-tow studies of the East Pacific Rise off Mexico 157
reefs: Reef limestones of the Palau Islands, trust territory of the Pacific Islands 156
sediments: Mixing of equatorial Pacific siliceous clays 156

Pacific Ocean—tectonophysics
plate tectonics: Age and composition of Jingu Seamount 181
— Age of Emperor Seamounts confirms hot-spot hypothesis 180
— Hawaiian Island-Emperor Seamount studies 180-181
— Minimum age of Mieji Seamount 180-181
— Rubidium-strontium systematics of Hawaiian-Emperor Seamount chain basalts 181

Pacific region—economic geology
energy sources: Circum-Pacific Energy and Mineral Resources Program 318
phosphate: Phosphate resources of the Circumpacific region 1-2

Pakistan—economic geology
energy sources: Pakistan 328-329
mining geology: CENTO training program 313

Paleocene *see also under* geochronology *under* Alaska; *see also under* stratigraphy *under* Arkansas; Rocky Mountains

paleoclimatology—Cenozoic
Mississippi Valley: Age and mode of deposition of so-called "Lafayette formation" in northern Mississippi embayment 66

paleoclimatology—Holocene
California: Sierra Nevada Holocene lake records 205-206
Utah: Early Holocene history of Lake Bonneville 205

paleoclimatology—Miocene
California: Light-stable isotopes applied to paleoclimatology 205

paleoclimatology—Quaternary
California: Central Valley Quaternary studies 206-207
— Ice-Age pollen record from coastal California 206
Massachusetts: Retreat of ice left eastern upland of Massachusetts subject to deep freeze 58

paleoecology—Neogene
Atlantic Coastal Plain: Sedimentary environments in the Neogene of the central Atlantic Coastal Plain 216

paleoecology—palynomorphs
Quaternary: Ice-Age pollen record from coastal California 206

paleoecology—Protista
Cretaceous: Paleoenvironment of Cretaceous silicoflagellates north of Baffin Island 156-157
Quaternary: Chrysomonad cysts as a paleoecological tool 206

Paleogene *see also under* stratigraphy *under* Montana; Wyoming

paleogeography—Cenozoic
California: Vanished alluvial-fan complex in the Riverside Area 87

paleogeography—Miocene
California: Late Miocene paleogeography of the Santa Cruz Region in California 147-148

paleogeography—Pennsylvanian
Massachusetts: Narragansett Basin extends to Massachusetts coast 57

paleogeography—Proterozoic
Michigan: Paleogeography of the Jacobsville Sandstone, Michigan 38

paleogeography—Quaternary
California: Quaternary studies in the Los Angeles area 86

paleomagnetism—Cenozoic
Antarctica: Magnetic correlation of upper Cenozoic Dry Valley Drilling Project cores 336-337

paleomagnetism—Cretaceous
Antarctica: Structural geology and paleomagnetism of the Orville Coast area 337

paleomagnetism—Holocene
Western U.S.: Geomagnetic secular variation during Holocene time 168
paleomagnetism—interpretation
clinker: Paleomagnetic method for determining burning rates of ancient coal seam fires 167
rocks: Rock magnetism 167-168
paleomagnetism—Paleogene
Western Interior: Magnetostratigraphy of lower Tertiary rocks in the Powder River basin 167
paleomagnetism—Paleozoic
Alaska: New analysis of paleomagnetic data from Alexander terrane 99
paleomagnetism—Phanerozoic
Alaska: Paleozoic and Triassic paleomagnetism of the Alexander terrane, southeastern Alaska 168
paleomagnetism—Proterozoic
Saudi Arabia: Geophysical laboratory 333
Western Interior: Paleomagnetic poles and polarity zonation in the Proterozoic Belt Supergroup 167
paleomagnetism—Quaternary
California: Paleomagnetism of the Clear Lake Volcanics, California 167-168
paleontology—general
research: Paleontology 214-220
Paleozoic *see also under* geochronology *under* New England; *see also under* stratigraphy *under* Alaska; Nevada; North Carolina; Pennsylvania
Paleozoic—paleontology
research: Paleozoic studies 218-219
palynomorphs—biostratigraphy
Devonian: Late Paleozoic fossils in ophiolite, northeastern Alaska 95
palynomorphs—Dinoflagellata
Cretaceous: Dinoflagellates helpful in North Slope biostratigraphy 217
palynomorphs—miospores
Miocene: Miocene sporomorphs from Massachusetts 215-216
Quaternary: Ice-Age pollen record from coastal California 206
paragenesis—metals
South Carolina: Alteration associated with a fault zone in the Carolina slate belt, South Carolina 8
peat *see also under* economic geology *under* Florida; Maine; Minnesota
peat—deposits
age: Dating, geochemistry, and petrology of peat, lignite, and coal 21-23
Pelecypoda *see* Bivalvia *under* Mollusca
Pennsylvania—economic geology
coal: Contaminants in coal 21
— Petrology of the Upper Freeport coal bed, Indiana County, Pennsylvania 21-22
uranium: Organo-clay complexes in uranium deposits 44
Pennsylvania—engineering geology
waste disposal: Lineaments related to subsurface geology in Salina Salt Basin, New York and Pennsylvania 265
Pennsylvania—environmental geology
pollution: Vertical ground-water movement in abandoned mine shafts in Pennsylvania 261
— Water quality of Tulpehocken Creek, Pennsylvania, prior to impoundment of Blue Marsh Lake 229
Pennsylvania—geomorphology
weathering: Quaternary deposits and soils of the Central Susquehanna Valley in Pennsylvania 64-65
Pennsylvania—hydrogeology
ground water: Water-supply capability of shale in south-central Pennsylvania 110
hydrology: Low-flow frequency of ungaged streams 110
— Pennsylvania 110
Pennsylvania—stratigraphy
Ordovician: Lower-Middle Ordovician boundary in the north-central Appalachian Basin 219
Paleozoic: Thrust faulting indicated by relationship of Catskill and Pocono Formations in northeastern Pennsylvania 62
Quaternary: Quaternary deposits and soils of the Central Susquehanna Valley in Pennsylvania 64-65
Pennsylvania—structural geology
tectonics: Tectonic history of Shochary Ridge in Pennsylvania 61-62
Pennsylvanian *see also under* stratigraphy *under* Alaska; Massachusetts
permafrost *see also under* engineering geology *under* Alaska
permafrost—engineering properties
research: Research in permafrost engineering 253
Permian *see also under* stratigraphy *under* Nevada
Peru—economic geology
energy sources: Peru 330-331
Peru—geochemistry
isotopes: Strontium and lead isotopic composition in volcanic rocks from Peru and New Hebrides; genesis of calc-alkaline lava 188-189
Peru—seismology
earthquakes: Peru 239-240
petroleum *see also under* economic geology *under* Alaska; Atlantic Ocean; California; Colorado; Florida; Great Basin; Gulf Coastal Plain; Gulf of Mexico; Idaho; Rocky Mountains; Southwestern U.S.; Texas; United States; Utah; Wyoming
petroleum—exploration
techniques: New exploration and production techniques 33-35
petroleum—genesis
migration: Primary migration of crude oil 33
reservoir rocks: Early fresh-water diagenesis produces limestone with favorable oil reservoir properties 34
— Formation of conglomerates from submarine slides 34
petroleum—geochemistry
aromatic hydrocarbons: Composition and source of petroleum 157
maturation: Thermochemistry of maturation of fossil fuels 176
petroleum—production
reservoir rocks: Prediction of oil and gas production from chalk reservoirs 34-35
petroleum—resources
data analysis: Petroleum resource analysis 15
petrology—general
research: Geochemistry, mineralogy, petrology 176-188
petrology—methods
factor analysis: Extended Q-mode factor analysis 187-188
statistical methods: Statistical geochemistry and petrology 187-188
phase equilibria—mineral assemblages
interpretation: Mineral equilibria of slightly calcic pelitic schists in Barrovian regional metamorphism 184-185
phase equilibria—theoretical studies
phase diagrams: Unary and binary multisystem net for $n+k$ ($k \leq 6$) phases 176
phosphate *see also under* economic geology *under* Atlantic Coastal Plain; Atlantic Ocean; California; Florida; Great Plains; Idaho; Pacific region; Rocky Mountains
Pisces—faunal studies
Cenozoic: Vertebrate faunas of Gay Head, Martha's Vineyard, Massachusetts 216
placers—gold
Wyoming: Origin and value of Dickie Springs gold placer deposit, central Wyoming 6-7
placers—heavy minerals
Utah: Uranium and thorium in placer deposits 43-44
planetology *see also* Jupiter; Mars; Mercury Planet; Moon; Venus
planetology—general
research: Astrogeology 279-289
— Planetary investigations 279-285
planetology—theoretical studies
geochemistry: Extraterrestrial oxygen fugacities 288-289
Plantae *see also* algae; angiosperms; palynomorphs; problematic fossils; Protista
Plantae—ecology
bajadas: Plant societies along a bajada in southern Arizona 220
drought: Severity of droughts estimated from tree rings 220
floods: Flood related movement of scree 220
Plantae—floral studies
Paleogene: Early Tertiary flora found in New Mexico 217
plate tectonics *see also under* tectonophysics *under* Alaska; Bering Sea; California; Hawaii; Indonesia; North America; Pacific Coast; Pacific Ocean

plate tectonics—subduction
subduction zones: Numerical modeling 241
platinum *see also under* economic geology *under* Montana; Turkey; Wyoming
Pleistocene *see also under* geochronology *under* California; *see also under* stratigraphy *under* Washington
Pliocene *see also under* geochronology *under* Utah; *see also under* stratigraphy *under* Mississippi Valley
plutons *see under* intrusions
Poland—economic geology
lead-zinc deposits: Poland 331-332
pollution *see also under* environmental geology *under* Appalachians; Atlantic Coastal Plain; Atlantic Ocean; California; Colorado; Connecticut; Florida; Georgia; Great Lakes region; Great Plains; Gulf Coastal Plain; Idaho; Illinois; Kansas; Louisiana; Massachusetts; Michigan; Minnesota; New Jersey; New York; North Carolina; North Dakota; Ohio; Pennsylvania; Red Sea region; Texas; Utah; Virginia; Washington; Western U.S.; Wyoming
pollution—experimental studies
oil shale: Comparison of spent shale and soil as sorbents for retort waste water 35
pollution—human ecology
medical geology: Minerals and environmental health 177-178
— The asbestos minerals and cancer incidence 177-178
pollution—pollutants
coal: Contaminants in coal 21
— Hazardous elements in eastern coal resources 22
organic materials: Adsorption of ketones in water 224
— Bacterial growth kinetics with acetone as a substrate 224
pollution—waste disposal
radioactive waste: Radioactive wastes and the geologic and hydrologic environments 263-269
pollution—water
ground water: Organic compounds in ground water 272-273
research: Effects of pollutants on water quality 272-274
— Hydrologic aspects of energy 260-261
water quality: Chemical, physical, and biological characteristics of water 220-224
— Effects of mining on water quality 273
Precambrian *see also under* stratigraphy *under* Alaska; Saudi Arabia; Wyoming
Precambrian—paleontology
research: Precambrian studies 219-220
problematic fossils—biostratigraphy
Ordovician: Ordovician Vinini Formation of northern Nevada 80-81
problematic fossils—occurrence
Proterozoic: Ediacarian (?) age fossils from Saudi Arabia 219-220
Proterozoic *see also under* geochronology *under* Alaska; Saudi Arabia; *see also under* stratigraphy *under* Idaho; Michigan; Montana; Washington; Western Interior; Wyoming
Protista—Silicoflagellata
Cretaceous: Paleoenvironment of Cretaceous silicoflagellates north of Baffin Island 156-157
Protozoa *see* Protista
Puerto Rico—economic geology
sand: Potential sand resources of the northeast Puerto Rico shelf 155
Puerto Rico—environmental geology
waste disposal: Treated sewage effluent used for sugarcane irrigation 210
Puerto Rico—oceanography
sedimentation: Sedimentation patterns on the Puerto Rico insular shelf 155

Q

Quaternary *see also under* geochronology *under* California; Hawaii; Washington; *see also under* stratigraphy *under* Black Sea; California; Massachusetts; Pennsylvania; Venezuela

R

radioactive dating *see* absolute age
radioactivity surveys *see under* geophysical surveys *under* Montana
Radiolaria—biostratigraphy
Devonian: Greenstone in Devonian Slaven Chert in north-central Nevada 81
Mississippian: Age of type Pablo Formation in central Nevada 82
— Late Paleozoic fossils in ophiolite, northeastern Alaska 95
radium—abundance
water: Radium and uranium in mineral springs 48-49
— Uranium source potential estimated from radium and radon concentrations in flowing water 48
radon—abundance
water: Uranium source potential estimated from radium and radon concentrations in flowing water 48
radon—isotopes
Rn-222: Value of radon measurements for uranium prospecting 49
rare earths *see also* neodymium; *see also under* economic geology *under* New York; Western U.S.
rare earths—abundance
meteorites: Origin and history of the adcumulate eucrite, Moama 189
reclamation *see also under* environmental geology *under* California; United States
reclamation—natural resources
programs: Cooperative projects with the Bureau of Reclamation 292
Red Sea—remote sensing
geophysical surveys: Red Sea Commission 312
Red Sea region—environmental geology
pollution: Red Sea Commission 312
Red Sea region—seismology
crust: Seismic profile 332-333
reefs *see also under* oceanography *under* Florida; Georgia; Pacific Ocean
regional geology *see* areal geology under the appropriate area term
remote sensing *see also* geophysical methods; *see also under* geophysical surveys *under* Alaska; Arizona; Atlantic Coastal Plain; California; Colorado; Florida; India; Iran; Midwest; Minnesota; Mississippi; Mississippi Valley; Moon; New England; New Mexico; Pacific Coast; Saudi Arabia
remote sensing—applications
cartography: Landsat-3 return beam vidicon images 344
— Satellite image maps 344-345
— Satellite technology 344-345
— Surveying from the air using inertial technology 339
defoliation: Forest defoliation 294
environment: Studying the global environment 294-295
general: Applications to geologic studies 297-300
ground water: Ground-water information on Landsat imagery 301
heat flux: Evaluation of geothermal heat flux models 299
hydrology: Applications to hydrologic studies 300-301
land use: Impact of surface mining 292-293
mineral exploration: Targeting mineral exploration 295-296
monitoring: Monitoring the environment 290-294
slope stability: High-resolution sensing techniques for slope-stability studies 255
terrain classification: Integrated terrain mapping 295
waste disposal: Lineament studies help characterize waste disposal study areas 297-298
remote sensing—automatic data processing
cartography: Space oblique mercator projection 345
data analysis: Data analysis laboratory 290
data handling: Tests of hydrologic-data relay systems 300
remote sensing—general
programs: Cooperative projects with states 293
— Cooperative projects with the Bureau of Land Management 290-291
— Cooperative projects with the Bureau of Reclamation 292
— Cooperative projects with the Mine Safety and Health Administration 292
— Cooperative projects with the National Park Service 291
— Cooperative projects with the U. S. Fish and Wildlife Service 291

research: Remote sensing and advanced techniques 290-302

remote sensing—imagery
color imagery: "Natural" color image maps from color infrared film 342
glaciers: Satellite image atlas of glaciers 295
interpretation: Correction of Landsat images 290
— Image control targets 342
— Water depth from Landsat images 290
multispectral analysis: Visible and near-infrared multispectral aircraft images used to distinguish altered rocks 299
side-scanning methods: Geometric correction of flight-path curvature in SLAR imagery 301

remote sensing—instruments
airborne methods: Data from airborne instruments 296-297

remote sensing—interpretation
data analysis: Integration of remotely sensed data with other data 290
principal components analysis: Enhancement of surface-water features by principal components transform of Landsat data 301
spectral analysis: Altered-rock spectra in the visible and near infrared 172
— Near-infrared spectra of alteration minerals and the potential for use in remote-sensing applications 172
— Visible and near-infrared spectra of rocks from a chromite-rich area in Oregon 171-172

remote sensing—methods
luminescence: Fraunhofer line discriminator experiments 296-297
photogeologic methods: Mapping from high-resolution and high-altitude panchromatic photographs 340
— Planimetric compilation from orthophotographs 341
photogrammetry: Photogrammetry 340-342
radar methods: Experimental data to help design the space shuttle radar system 299
satellite methods: Earth Resources Observation Systems program 290
thermal inertia: Further refinement in thermal-inertia mapping 298-299

reservoirs *see also under* engineering geology *under* New York

rhyolite *see under* andesite-rhyolite family *under* igneous rocks

rift zones *see under* systems *under* faults

rock mechanics *see also* soil mechanics

rock mechanics—deformation
creep: Rheology of rocks and rock-forming minerals 171
research: Research in rock mechanics 251-252

rock mechanics—failure
coal: Mode of deformation of Rosebud coal; Colstrip, Montana 310

rock mechanics—materials, properties
electrical properties: Electrical properties of geothermal materials 170
— Geophysical laboratory 333
research: Petrophysics 169-172
saprolite: Properties of saprolite as related to slope stability 255
shale: Hydraulic properties of Cretaceous shale 210
thermal properties: Thermal-conduction mechanisms in rocks and minerals 198

Rocky Mountains—areal geology
regional: Rocky Mountains and Great Plains 67-78

Rocky Mountains—economic geology
coal: Geochemical survey of the western energy regions 275
— Lands above underground coal mines should be developed with caution 276-277
petroleum: Rocky Mountains and Great Plains 25-28
phosphate: Phosphate investigation, Rocky Mountains and Great Plains 17-18
thorium: Uranium and thorium in Precambrian crystalline rocks of the Medicine Bow Mountains, North Central Colorado 39
uranium: Uranium potential of Sierra Madre and Medicine Bow Mountains, Wyoming 46

Rocky Mountains—petrology
igneous rocks: Igneous studies 71-73

Rocky Mountains—stratigraphy
Paleocene: Cretaceous-Tertiary boundary in gas-bearing beds of southeastern Uinta Basin, Utah 28
research: Stratigraphic studies 67-71

Rocky Mountains—structural geology
tectonics: Tectonic and geophysical studies 73-78

Rocky Mountains—tectonophysics
heat flow: Heat production in the southern Rocky Mountains, Colorado 198

S

salt tectonics *see also under* structural geology *under* Gulf of Mexico

sand *see also under* economic geology *under* Puerto Rico; West Indies

sandstone *see also under* clastic rocks *under* sedimentary rocks

Saudi Arabia—economic geology
brines: Evaporite studies 333
metals: Mineral belt studies 332
— Mining geophysics 332
water resources: Water-personnel development 334
— Water-resources advisory services 332

Saudi Arabia—general
current research: Saudi Arabia 332-334

Saudi Arabia—geochronology
Proterozoic: Geochronology 333

Saudi Arabia—geophysical surveys
gravity surveys: Regional gravity studies 333
magnetic surveys: Regional magnetic studies 333
maps: Regional magnetic studies 333
remote sensing: Remote sensing 336-337
seismic surveys: Seismic profile 332-333

Saudi Arabia—paleontology
problematic fossils: Ediacarian (?) age fossils from Saudi Arabia 219-220

Saudi Arabia—petrology
igneous rocks: Study of silicic plutonic rocks 332

Saudi Arabia—stratigraphy
Precambrian: Study of Precambrian formations 332

Saudi Arabia—tectonophysics
paleomagnetism: Geophysical laboratory 333

sea water—geochemistry
estuaries: Factors influencing seasonal distributions of biochemically reactive substances in the Potomac River 159
evolution: Computer modeling 335

sedimentary petrology—general
research: Sedimentology 200-203

sedimentary rocks *see also* sedimentary structures; sedimentation; sediments

sedimentary rocks—carbonate rocks
chalk: Prediction of oil and gas production from chalk reservoirs 34-35
geochemistry: Carbon isotopes as a correlation tool 33
limestone: Early fresh-water diagenesis produces limestone with favorable oil reservoir properties 34
— Reservoir porosity in Sunniland Limestone (Lower Cretaceous), southern Florida 31
— Source rock potential, South Florida Basin, Florida 31

sedimentary rocks—chemically precipitated rocks
evaporites: Thickness of bedded salt in northeastern Ohio 265

sedimentary rocks—clastic rocks
black shale: Fracture reservoirs in Devonian black shale 32-33
— Gas generation in Devonian black shale 31
— Late Devonian black shale sedimentation and possible gas exploration areas 32
— New method for computing organic-carbon content of Devonian shale 33
— Sources of organic matter in Devonian black shales 33
conglomerate: Formation of conglomerates from submarine slides 34
eolianite: Oil-bearing eolian sandstones, Colorado 27
lithofacies: Sedimentation and petroleum potential of fluvial part of Mesaverde Group, Piceance Creek basin, Colorado 27
novaculite: Novaculite in Nevada 18

orthoquartzite: Calcium-poor quartzites in eastern Nevada 81
pyroclastics: Correlation of Eocene volcaniclastic rocks, southeastern Absaroka Range in northwestern Wyoming 68-69
sandstone: Determination of pre-cementation porosity and permeability in sandstones 45
— Influence of diagenesis on reservoir properties of some Upper Cretaceous sandstones, Uinta Basin, Utah 27-28
saprolite: Properties of saprolite as related to slope stability 255
shale: Hydraulic properties of Cretaceous shale 210

sedimentary rocks—environmental analysis
shelf environment: Cyclicity of Upper Cretaceous sedimentary rocks 64

sedimentary rocks—lithostratigraphy
correlation: Triassic continental and marine rocks correlated by sedimentary features 81

sedimentary rocks—properties
reservoir properties: Facies relations of low-permeability Cretaceous reservoirs in the Northern Great Plains 25

sedimentary structures *see also* sedimentary rocks; sediments

sedimentary structures—soft sediment deformation
clastic dikes: Clastic dikes; a key to Tertiary regional stress fields in the Northwest Olympic Peninsula 88

sedimentation—controls
structural controls: Fracture reservoirs in Devonian black shale 32-33

sedimentation—cyclic processes
transgression: Cyclicity of Upper Cretaceous sedimentary rocks 64

sedimentation—deposition
alluvial fans: Age and mode of deposition of so-called "Lafayette formation" in northern Mississippi embayment 66
basins: Quaternary studies in the Los Angeles area 86

sedimentation—environment
brackish-water environment: Computer modeling 335
coastal environment: Comparison of sedimentation in Yakutat and Icy Bays, Alaska 151
— Neoglacial sedimentation in Glacier Bay, Alaska 150-151
— Sedimentary environments in the Neogene of the central Atlantic Coastal Plain 216
— Sedimentation in coastal embayments of the northern Gulf of Alaska 151
deltas: Coal beds in deltaic paleoenvironments 20
— Depositional environments of gas-bearing Upper Cretaceous rocks in northwestern Colorado 27
— Emery and Wasatch Plateau basins, Utah 20
— Glacial Lake Taunton Deposits 58
— Hams Fork Basin, Wyoming 20
— San Juan Basin, New Mexico 20
high-energy environment: High energy beds in the Dilco 42
lakes: Continuous lacustrine sedimentation of Paleogene source beds in the Great Basin 29
— Sierra Nevada Holocene lake records 205-206
rivers: Sedimentation and petroleum potential of fluvial part of Mesaverde Group, Piceance Creek basin, Colorado 27

sedimentation—processes
mass movements: Papa'u Seamount, a submarine landslide deposit off the Island of Hawaii 158
slumping: Formation of conglomerates from submarine slides 34
— Observations from a submersible of slumps on the upper Continental Slope south of Georges Bank 142

sedimentation—provenance
detritus: Possible source of sand-size detritus, Tertiary Marfa Basin, Texas 40
factor analysis: Sources of surficial sediment, southern Bering Sea 153-154
orthoquartzite: Calcium-poor quartzites in eastern Nevada 81
paleocurrents: Late Devonian black shale sedimentation and possible gas exploration areas 32
— Paleocurrent studies contribute to uranium resource evaluation in Upper Peninsula of Michigan 38
rivers: Holocene sediment volume on the northeast Gulf of Alaska Continental Shelf and the sediment contribution of present-day rivers 151-152

sedimentation—transport
marine transport: Bottom boundary layers and sediment transport, Norton Sound in Alaska 154
— Movement and equilibrium of bedforms in central San Francisco Bay, California 159
— Movement of bedforms in the lower Cook Inlet, Alaska 152
— Sedimentation patterns on the Puerto Rico insular shelf 155
— Trace metals and an area of possible sediment accumulation on the North Atlantic Continental Shelf 141-142
— Wave-generated sand and gravel ribbons in the Bering Sea 155
marine transports: Volcanic ash in surficial sediments of the Kodiak Shelf, western Gulf of Alaska 152
stream transport: Major factors controlling sediment runoff in Park River watershed 126
— Sediment transport 201
— Sediment transport on the San Pedro Shelf, California 147
— Sedimentation in lakes and streams 202
turbidity currents: Sediment transport processes on the Monterey Deep-Sea Fan 150
wind transport: Eolian processes 202
— Wind as a geologic agent in desert climates 207

sediments *see also* sedimentary rocks; sedimentary structures; sedimentation

sediments—chemically precipitated sediments
weathering crust: Mineralogy of surface encrustations in the Orville Coast area 337

sediments—clastic sediments
colluvium: Quaternary deposits and soils, Sierra Nevada foothills 85-86
till: Readvance produces Ellisville moraine 58
volcanic ash: Volcanic ash in surficial sediments of the Kodiak Shelf, western Gulf of Alaska 152

sediments—composition
siliceous composition: Mixing of equatorial Pacific siliceous clays 156

sediments—distribution
thickness: Holocene sediment volume on the northeast Gulf of Alaska Continental Shelf and the sediment contribution of present-day rivers 151-152

sediments—geochemistry
manganese: Manganese-rich sediment from the Aleutian Basin, southern Bering Sea 154
trace metals: Trace-metal form and bioavailability in estuarine sediments 223

sediments—pore water
geochemistry: Anionic constituents 233

sediments—properties
acoustical properties: Gas-charged sediment areas in the northern Gulf of Alaska 152-153
— Seafloor thermogenic gas seep, Norton Sound 154-155

seismic surveys *see under* geophysical surveys *under* Alaska; Bering Sea; Great Lakes; Hawaii; Idaho; Saudi Arabia; Wyoming

seismology *see also* engineering geology

seismology—crust
elastic waves: Intermediate-period seismic studies in Yellowstone Caldera 200
low-velocity zones: Low-velocity body lies under Coso Hot Springs 197
— Magma body postulated under Clear Lake Volcanics from teleseismic P-wave delays 197
P-waves: Crustal structure beneath Kilauea Volcano 195-196
— Root of the Sierra Nevada 83-84
velocity structure: Crustal thinning in northwest Nevada 199-200

seismology—earthquakes
data bases: Seismic data bases 238
foreshocks: Foreshock studies 239
ground motion: Earthquake investigations 251
— Ground motion 249-250
— Ground shaking hazard and risk 250
mechanism: Apparent stress changes at The Geysers 197
— Earthquake mechanics and prediction studies 238-243

— Fault stability 241-242
occurrence: The Thessaloniki earthquake 243
precursors: Earthquake precursors 242
— Magnetic studies 242
— Radon and water level 242
— Tilt 242
prediction: Crustal deformation 240-241
— Gravity surveys 240
— Strength of the San Andreas 241
publications: Earthquake Information Bulletin 350
— Earthquake publications 348
research: Earthquake studies 235-253
— Operations and special investigations 235-236
seismic sources: Earthquake source mechanisms 248-249
swarms: Earthquake swarms 242-243
symposia: Guatemala 323

seismology—elastic waves
attenuation: Two-dimensional-inversion of seismic attenuation observations at Coso Hot Springs Known Geothermal Resource Area 200

seismology—interior
profiles: Seismic profile 332-333

seismology—mantle
high-velocity zones: Teleseismic P-wave study at the Battle Mountain heat-flow high, Nevada, shows a deep, high-velocity intrusion present 193

seismology—microseisms
geothermal energy: Yellowstone seismometer net detects geothermal seismic noise 196

seismology—observatories
international cooperation: Assistance to intergovernmental organizations 312-313
networks: Seismic network studies 236-238

seismology—seismicity
changes: Changes in Yellowstone seismicity patterns observed 196
geologic hazards: Possible paleoseismic belt in Nevada Test Site region 82
research: Seismicity 235-238
— Seismicity 238-239
seismic gaps: Nicaragua 239
— Peru 239-240
— Seismic gaps 239-240
seismotectonics: Active faults, seismotectonic framework and earthquake potential 243
— Numerical modeling 241

seismology—volcanology
earthquakes: Global correlation of magma ascent and earthquake energy 179
seismicity: Seismicity studies of the Mount Hood, Oregon, area 195

shale *see under* clastic rocks *under* sedimentary rocks

shore features *see under* geomorphology

shorelines *see also under* engineering geology *under* Massachusetts

silver *see also under* economic geology *under* Nevada

slope stability *see also* engineering geology; geomorphology; *see also under* engineering geology *under* Appalachians; California; Colorado; North Dakota; Utah; Virginia; Wyoming

slope stability—landslides
case studies: Areal and regional studies 253-255
earthquakes: Earthquake-induced landslides 255-257
— Landslides caused by historic earthquakes 256
— Landslides caused by recent earthquakes 256-257
failure: Correlation between ground failure and seismic intensity 257
research: Landslide hazards 253-257
— Topical studies of landslides 255

slope stability—site exploration
techniques: High-resolution sensing techniques for slope-stability studies 255

soil mechanics *see also* rock mechanics

soil mechanics—case studies
earthquakes: Research in soils engineering 252-253

soils—chemistry
isotopes: Isotopes indicate rain-soil interaction 185

soils—surveys
California: Quaternary deposits and soils, Sierra Nevada foothills 85-86
— San Joaquin Valley windstorm, December 20, 1977 206
Colorado: Mountain soils mapping in Front Range Urban Corridor, Colorado 303
Mississippi: Significance of saturated soils in coastal plains 301
Pennsylvania: Quaternary deposits and soils of the Central Susquehanna Valley in Pennsylvania 64-65
Puerto Rico: Treated sewage effluent used for sugarcane irrigation 210

South Africa—geomorphology
impact features: Basin and crater studies 285-286

South America *see also* Bolivia; Brazil; Peru; Venezuela

South Carolina—economic geology
metals: Alteration associated with a fault zone in the Carolina slate belt, South Carolina 8

South Carolina—engineering geology
geologic hazards: Charleston, South Carolina 257-258

South Carolina—environmental geology
waste disposal: Tritium migration at Barnwell, South Carolina 264

South Carolina—geochemistry
trace elements: Emission spectrographic analysis for trace elements in basalts from core holes near Charleston, South Carolina 231-232

South Carolina—structural geology
tectonics: Metamorphism and structural relationships in the Kings Mountain area of the Carolinas 63
— Warwoman lineament extention 65

South Dakota—economic geology
geothermal energy: Large, low-temperature geothermal resource in Paleozoic rocks of South Dakota 54-55
uranium: Helium detection for uranium exploration 49

South Dakota—engineering geology
waste disposal: Potential for radioactive-waste disposal in Pierre Shale 127

South Dakota—hydrogeology
ground water: Pumping test of a Niobrara Marl aquifer in northeastern Aurora County 127
— Saline ground water in Clark County 127
hydrology: South Dakota 127
thermal waters: Large, low-temperature geothermal resource in Paleozoic rocks of South Dakota 54-55

Southern Hemisphere *see also* Africa; Antarctica; Atlantic Ocean; Pacific Ocean

Southwestern U.S.—economic geology
petroleum: Great Basin and southwestern United States 28-30

spectrometry *see* spectroscopy

spectroscopy—methods
emission spectroscopy: Emission spectrographic analysis for trace elements in basalts from core holes near Charleston, South Carolina 231-232
— Emission spectroscopy 231-232
— Induction coupled plasma spectroscopy 231

spectroscopy—techniques
applications: The measurement of uranium content in metallic ores, sediments, and water 231
sample preparation: Spectrophotometric determination of tungsten in rocks 231

springs *see also* ground water; *see also under* hydrogeology *under* Alaska; Arizona; Montana; Pacific Coast; Tennessee; Utah; Virginia

standard materials—analysis
accuracy: Analytical precision for inorganic determinations 234
calibration: Errors in gross radioactivity measurements 234

stromatolites *see under* algae

strontium—isotopes
Sr-87/Sr-86: Age and strontium isotopic composition of the Honolulu Volcanics 180
— Strontium and lead isotopic composition in volcanic rocks from Peru and New Hebrides; genesis of calc-alkaline lava 188-189
— Strontium isotopes and minor-element geochemistry of alkaline rocks, Wet Mountains, Colorado 190

structural analysis *see also* folds

structural analysis—faults
fault zones: A structural analysis of the Norumbega fault zone 56

structural analysis—folds
fold axes: Southward-directed thrusting of Mesozoic age in northeastern Nevada 81

interference patterns: Relationship between superimposed folding and geologic history in the Georgia Piedmont 63-64

structural analysis—interpretation
flow structures: Origin of voids in volcanic bedrock at Teton damsite, Idaho 182
interference patterns: Metamorphism and structural relationships in the Kings Mountain area of the Carolinas 63
— Tectonic history of Shochary Ridge in Pennsylvania 61-62
melange: Large scale nappes in Southwest Oregon 87-88
— Origin of melanges of the Olympic Peninsula 88
ophiolite: Simultaneous crystallization and deformation in ophiolite complexes 8-9

structural petrology *see* structural analysis

sulfides *see under* minerals

sulfur—geochemistry
aqueous solutions: Stability of polysulfides 186-187

sulfur—isotopes
S-34/S-32: Sulfur isotope studies at Creede, Colorado 191

sulphur *see* Sulfur

surveys—current research
U. S. Geological Survey: USGS quadrangle evolution for Department of Energy 52

surveys—research
U. S. Geological Survey: How to obtain publications 349-350
— Publications issued 348-349
— Publications program 347-348
— U. S. geological survey publications 347-350

symposia—general
research: International commission representation 319-320

symposia—hydrogeology
hydrology: Venezuela 336

symposia—seismology
earthquakes: Guatemala 323

T

tectonics *see also* faults; folds; orogeny; structural analysis; *see also under* structural geology *under* Antarctica; Appalachians; Basin and Range Province; California; Colorado; Connecticut; Georgia; Great Plains; Idaho; Michigan; Mississippi Valley; Montana; Nevada; New Jersey; New Mexico; New York; North Carolina; Oregon; Pennsylvania; Rocky Mountains; South Carolina; Washington

tektites *see also* meteorites

Tennessee—environmental geology
waste disposal: Tritium tracer tests successful at Oak Ridge National Laboratory in Tennessee 264

Tennessee—hydrogeology
hydrology: Channel characteristics identify losing stream reaches 118
— Tennessee 118
springs: Locating successful well sites in Jefferson County 118

tephrochronology *see under* geochronology

Tertiary *see also under* geochronology *under* Utah

Texas—economic geology
geothermal energy: Use of hydrogeologic mapping techniques in identifying potential geopressured-geothermal reservoirs 54
maps: Use of hydrogeologic mapping techniques in identifying potential geopressured-geothermal reservoirs 54
petroleum: Oil and gas resources of Permian Basin, West Texas and southeastern New Mexico 29-30
uranium: Mineralogic residence of uranium in roll-type deposits 46-47
— Molybdenum in catclaw mimosa as a possible indicator of uranium 51
— Possible source of sand-size detritus, Tertiary Marfa Basin, Texas 40
— Relationship of modern groundwater chemistry to the origin and rereduction of south Texas roll-front uranium deposit 50
— Uranium and thorium content in weathering profiles of the Catahoula Tuff, South Texas coastal plain 44

Texas—engineering geology
geologic hazards: Active faults in Houston, Texas 259
land subsidence: Pattern of land-surface subsidence changing in the Houston-Galveston area, Texas 275-276
waste disposal: Geohydrology of salt domes in northeastern Texas 264-265

Texas—environmental geology
pollution: Urban water quality 137
— Water quality of selected reservoirs in Texas 229

Texas—hydrogeology
ground water: Ground water in Jasper aquifer 127
— Lithology of the Edwards aquifer 211
— Model study of the Chicot and Evangeline aquifers, Texas Gulf Coast 209
— Tracer studies at sites in Nebraska and Texas 209-210
hydrology: Modeling of urban storm-water processes 136
— Texas 127
thermal waters: Geochemistry of geopressured geothermal waters in coastal Louisiana and Texas 260

Texas—oceanography
continental shelf: Cooperative study of the Texas inner Continental Shelf 145
ocean circulation: Seasonal drift patterns off the Texas coast 146
— Turbidity structures in Corpus Christi Bay, Texas 145

thermal conductivity *see under* heat flow

thermal waters *see also under* hydrogeology *under* California; South Dakota; Texas; Western U.S.; Wyoming

thermal waters—temperature
geologic thermometry: Magnesium correction determined for sodium-potassium-calcium geothermometer 193

thermoluminescence *see under* geochronology

thorium *see also under* economic geology *under* California; Colorado; Gulf Coastal Plain; Idaho; Michigan; Montana; Nevada; Rocky Mountains; Utah; Wyoming

thrust faults *see under* displacements *under* faults

tin *see also under* economic geology *under* Middle East

trace elements *see under* geochemical methods *under* mineral exploration; *see under* geochemistry *under* Guatemala; Idaho; lava; metals; South Carolina

Triassic *see also under* stratigraphy *under* Nevada; North America; Utah

Trilobita—biostratigraphy
Cambrian: Trilobite from the Silver Hill Formation 67-68

tungsten—analysis
spectroscopy: Spectrophotometric determination of tungsten in rocks 231

Turkey—economic geology
energy sources: Turkey 334-336
metals: Afghanistan-Iran-Turkey 321
mining geology: CENTO training program 313
platinum: Palladium, platinum, and rhodium 335

Turkey—general
research: Results of previous programs 336

U

underground water *see* ground water

United States *see also* the individual states and regions

United States—areal geology
regional: Regional geologic investigations 56-100
— Regional studies and compilations of large areas 100

United States—economic geology
coal: Coal analysis 19-23
— Coal resource occurrence/coal development potential (CRO/CDP) reports 164
— Computerization of the Nation's coal resources 19
— Estimates of coal resources 20-21
— Field studies 19-23
— Known recoverable coal resource areas 164
— Participation in the interagency EMRIA program 19
energy sources: Mineral-fuel investigations 19-55
geothermal energy: Geothermal resources 53-55
— Known geothermal resource areas 164
— U. S. geothermal resource assessment updated 53-54
lead-zinc deposits: Lead and zinc resources of the United States and of the World 2-3

metals: Geochemical-reconnaissance results 10-11
mineral resources: Geologic studies of mining districts and mineral-bearing regions 3-9
— Mineral-resource investigations 1-18
— Mineral resource investigations of wilderness areas 9-10
— United States and world mineral resource assessments 1-3
oil and gas fields: Known geologic structures of producing oil and gas fields 163-164
— Onshore oil and gas lease sales 164
petroleum: Management of oil and gas resources on the Outer Continental Shelf 165-166
— Oil and gas resources 23-35
uranium: USGS quadrangle evolution for Department of Energy 52
water resources: National stream quality accounting network completed 138-139
— National water quality programs 138-139
— River quality assessment program 139
— Special water-resource programs 134-140
— State water-resources investigations folders 348
— Summary appraisals of the Nation's ground-water resources 210-211
— The regional aquifer-system analysis program 139-140
— Urban water program 136-137
— Water-resource investigations 101-140
— Water use 137

United States—engineering geology
geologic hazards: Maps of flood-prone areas 272
maps: Engineering geologic map of the United States 251
— Maps of flood-prone areas 272

United States—environmental geology
conservation: Management of natural resources on Federal and Indian lands 163-166
— Waterpower classification–preservation of reservoir sites 164-165
land use: Urban water program 136-137
reclamation: Participation in the interagency EMRIA program 19

United States—hydrogeology
maps: State hydrologic unit maps 347-348

United States—oceanography
marine geology: Coastal and marine geology 141-158
— Island possessions and territories 155-156
— Marine geology and coastal hydrology 141-162
ocean circulation: Estuarine and coastal hydrology 158-162

United States—seismology
earthquakes: Operations and special investigations 235-236
— Seismic network studies 236-238

uranium *see also under* economic geology *under* Alaska; Arizona; Basin and Range Province; Colorado; Michigan; Montana; New Hampshire; New Jersey; New Mexico; North Carolina; Pennsylvania; Rocky Mountains; South Dakota; Texas; United States; Utah; Washington; Western Interior; Wyoming

uranium—affinities
lithium: Association of lithium with uranium 16

uranium—analysis
chemical analysis: The measurement of uranium content in metallic ores, sediments, and water 231

uranium—exploration
hydrological methods: Uranium source potential estimated from radium and radon concentrations in flowing water 48
ore guides: Physical-property changes associated with roll-front uranium deposits 171
— Some applications of thermoluminescence to uranium prospecting 45
— Value of radon measurements for uranium prospecting 49

uranium—genesis
experimental studies: Obsidian, perlite, and felsite as sources of uranium: an experimental study 46
geochemical controls: Porous media model studies of sandstone-type uranium deposits 50-51
host rocks: Determination of pre-cementation porosity and permeability in sandstones 45
roll-type deposits: Computer modeling of ore-forming processes 47

uranium—isotopes
U-238/U-234: Extreme fractionation of $^{234}U/^{238}U$ isotopes within a Missouri aquifer 188

uranium—ore deposits
ore guides: Borehole magnetic susceptibility probe detects low-level anomalies 171

uranium—resources
evaluation: Uranium resource appraisal and decsison modeling 14

Utah—economic geology
coal: Emery and Wasatch Plateau basins, Utah 20
— Potential effects of stripping coal from the Ferron Sandstone aquifer, Utah 261
geothermal energy: Geothermal well logged at Roosevelt Hot Springs in Utah 197-198
metals: Light-stable isotope and fluid-inclusion studies of the East Tintic district in Utah 190-191
— Pyritic alteration in northern Keg Mountains, Utah 71
— Zoned mineralization around a hidden stock in west-central Utah 5
natural gas: Cretaceous-Tertiary boundary in gas-bearing beds of southeastern Uinta Basin, Utah 28
oil shale: Detailed geologic investigation of the Agency Draw Northeast Quadrangle, East-central Uinta Basin, Utah 35-36
petroleum: Mississippian source rocks in Utah and Idaho 28-29
thorium: Uranium and thorium in placer deposits 43-44
uranium: Coffinite ores of the Tony M mine in Utah 47
— Geophysical studies of a uranium deposit in southern Utah 174
— Uranium in the Cutler Formation, Lisbon Valley, Utah 40
— Uranium source potential estimated from radium and radon concentrations in flowing water 48

Utah—engineering geology
earthquakes: Western United States excluding California 246-247
slope stability: Lateral-spreading landslide near Ogden, Utah 255
— Visible and concealed geologic hazards in central Utah 70-71
waste disposal: Paradox Basin, Utah, explored for high-level waste repository location 266-267

Utah—environmental geology
geologic hazards: Visible and concealed geologic hazards in central Utah 70-71
pollution: Potential effects of stripping coal from the Ferron Sandstone aquifer, Utah 261

Utah—geochronology
Archean: More Archean rocks in Utah 70
Pliocene: Pliocene rhyolite in the Sevier Plateau, Utah 73
Tertiary: Marysvale volcanic chronology 191

Utah—hydrogeology
ground water: Digital model of ground-water flow in Tooele Valley 128
— Navajo Sandstone a source of ground water for future energy-related development 128
— Navajo Sandstone an important aquifer in southwestern Utah 127-128
hydrology: Utah 127-128
springs: Chemical mass-transfer model of spring water 221
— Sources of water discharged from Fish Springs 128
— Springs in the northern Wasatch Plateau 128
— Uranium source potential estimated from radium and radon concentrations in flowing water 48

Utah—sedimentary petrology
diagenesis: Influence of diagenesis on reservoir properties of some Upper Cretaceous sandstones, Uinta Basin, Utah 27-28

Utah—stratigraphy
Cretaceous: Cretaceous-Tertiary boundary in gas-bearing beds of southeastern Uinta Basin, Utah 28
Holocene: Early Holocene history of Lake Bonneville 205

Triassic: Triassic continental and marine rocks correlated by sedimentary features 81

V

varves *see* lacustrine features *under* geomorphology

Venezuela—economic geology
water resources: Venezuela 336

Venezuela—stratigraphy
Quaternary: Quaternary paleolimnology of Lake Valencia, Venezuela 214

Venus—exploration
Pioneer: The Pioneer Venus Mission 279-280
planning: Radar investigations 284-285

Vermont—hydrogeology
ground water: Ground-water quality 110
hydrology: Vermont 110

Vermont—structural geology
faults: Thrust faults in the ultramafic belt, northern Vermont 57

Vertebrata *see also* Mammalia; Pisces; problematic fossils

Vertebrata—faunal studies
Cenozoic: Vertebrate faunas of Gay Head, Martha's Vineyard, Massachusetts 216

Virginia—areal geology
Roseland District: Geology of the Roseland district, Virginia Blue Ridge 8

Virginia—economic geology
coal: Southwestern Virginia 20-21
copper: Possible stratiform-copper occurrence in Devonian rocks in Virginia 10
iron: Large submarginal iron resources in Virginia and West Virginia Wilderness Study Areas 10
lead: Factors affecting the origin of strata-bound massive sulfide deposits of the Great Gossan Lead (GGL), southwestern Virginia 8
water resources: Prototype water-use data systems in Connecticut, Kansas, and Virginia 137-138

Virginia—engineering geology
geologic hazards: Basin structure in Culpeper, Virginia 258-259
— Piedmont tectonic features in Virginia 258
— Structure of the Coastal Plain, Virginia 259
slope stability: Flood related movement of scree 220
— Properties of saprolite as related to slope stability 255

Virginia—environmental geology
ecology: Wetland studies 301
land use: Ancestral Potomac River deposits in Fairfax County, Virginia 303
pollution: Dissolved sulfate loads, an index of mining activity 261

Virginia—geochronology
Holocene: Severity of droughts estimated from tree rings 220

Virginia—hydrogeology
ground water: Chemical quality of ground water in Fairfax County 110-111
— Ground-water reconnaissance of the Blue Ridge Parkway 110
— Ground-water resources, James City County 111
— Potentiometric surface of Cretaceous aquifer, Atlantic Coastal Plain 111
hydrology: Virginia 110
maps: Computer-composite hydrogeologic maps for Fairfax County, Virginia 303
springs: Relation of highway construction to water quality 111

Virginia—petrology
metamorphism: Paleozoic cataclastic deformation and low-grade metamorphism of Proterozoic rocks in the northern Virginia Blue Ridge 62

volcanic features *see under* geomorphology

volcanism *see under* volcanology

volcanoes *see under* volcanology

volcanology—volcanism
age: Marysvale volcanic chronology 191
— Potassium-argon ages of volcanic rocks in the Murrieta area of California 86-87
calderas: Structurally complex roots of a caldera near Questa, New Mexico 72
— Withington Creek caldera 73
eruptions: Studies of volcanic ejecta and gasses 183-184
geologic hazards: Volcanic recurrence intervals and volcanic hazards in the eastern Snake River Plain in Idaho 71-72
petrology: Cenozoic volcanism in western United States 181-183
processes: Volcanic rocks and processes 178-184

volcanology—volcanoes
Guatemala: Water-extractable trace metals in volcanic eruption clouds 183-184
Hawaii: Hawaiian volcano studies 178-180
— Mantle structure of Hawaiian volcanoes investigated 179
— Radio-telemetered volcanic gas monitoring in Hawaii 176
Kilauea: A proposed source mechanism for Kilauean self-potential anomalies 196
— Crustal structure beneath Kilauea Volcano 195-196
— Kilauea Volcano quiescent during FY 1978 178-179
— Papa'u Seamount, a submarine landslide deposit off the Island of Hawaii 158
Mauna Loa: Mauna Loa continues slow inflation 179
Mount Hood: Seismicity studies of the Mount Hood, Oregon, area 195
Newberry Volcano: Latest eruptions at Newberry Volcano in Oregon 182-183

W

Washington—areal geology
regional: Washington 88-91

Washington—economic geology
uranium: Constraints on the genesis of uranium ores in the Midnite Mine, Washington, from geochronologic and lead-isotope investigations 46
— Geophysical study of gneiss domes and two-mica granites 51
— Uranium and thorium in granitic rocks of northeastern Washington 36
water resources: Water-resource investigations on Indian reservations in Washington 133-134

Washington—engineering geology
earthquakes: Western United States excluding California 246-247
geologic hazards: Flood elevations for the Sooes River 134

Washington—environmental geology
geologic hazards: Changes in valley environment caused by floods of December 1977, Mount Rainier, Washington 269
land use: Geology and limnology for resource planning and management, Alpine Lakes Wilderness Area, Washington 302-303
— Historical changes of shoreline and wetland in Puget Sound region 89-90
— Historical changes of shorelines and wetland at river deltas, Puget Sound region, Washington 302
— Washington Department of Natural Resources 293
pollution: Water-quality effects of underground coal mining 227

Washington—geochronology
Eocene: Constraints on the genesis of uranium ores in the Midnite Mine, Washington, from geochronologic and lead-isotope investigations 46
Quaternary: Amino acid dating of shell deposits at Willapa Bay 89

Washington—geomorphology
maps: Wenatchee, Washington 345
weathering: Geology and limnology of the Alpine Wilderness Area 90

Washington—hydrogeology
ground water: Seawater intrusion along the Washington coast 133
hydrology: Washington 133-134

Washington—oceanography
continental slope: Stratigraphic and tectonic framework, Oregon-Washington Continental Margin 149

Washington—petrology
lava: Source areas and distribution of Columbia River Basalt Group in Washington 183

Washington—stratigraphy
changes of level: Historical changes of shoreline and wetland in Puget Sound region 89-90
Miocene: Late Miocene drainage patterns in Southeast Washington 90-91

Pleistocene: Pleistocene terraces at Willapa Bay, Washington 149-150
Proterozoic: Stratigraphy of the Windermere Group 91

Washington—structural geology
isostasy: Postglacial isostatic uplift of the Puget Lowland 89
tectonics: Clastic dikes; a key to Tertiary regional stress fields in the Northwest Olympic Peninsula 88
— Origin of melanges of the Olympic Peninsula 88
— Tertiary history of the Straight Creek Fault and the Olympic-Wallowa Lineament 90
— Thrusting and lateral faulting, Northwest Washington 88-89

waste disposal *see also under* engineering geology *under* Colorado; Gulf Coastal Plain; Idaho; Manitoba; Midwest; Mississippi; Nevada; New Mexico; Ohio; Pennsylvania; South Dakota; Texas; Utah; *see also under* environmental geology *under* Colorado; Florida; Gulf Coastal Plain; Illinois; Kansas; Kentucky; Puerto Rico; South Carolina; Tennessee

waste disposal—liquid waste
storage: Disposal and storage studies 210
waste water: Comparison of spent shale and soil as sorbents for retort waste water 35

waste disposal—radioactive waste
case studies: Regional studies 264-267
effects: Computer programs simulate distribution of aqueous uranium species 268
— Effects of heat-induced fluid flow near a buried canister of high-level radioactive waste 267
— Feedback effects analyzed in salt dissolution 268
experimental studies: Tritium removed from tritiated water by bacteria 268-269
research: Geochemistry 268-269
— Geophysics 267-268
— Radioactive wastes and the geologic and hydrologic environments 263-269
— Studies of low-level radioactive-waste disposal sites 264
site exploration: Computer programs to relate acoustic waveforms and fracture permeability in boreholes 268

waste disposal—site exploration
remote sensing: Lineament studies help characterize waste disposal study areas 297-298

water resources *see also under* economic geology *under* Atlantic Coastal Plain; Connecticut; Djibouti; Eastern U.S.; Florida; Jordan; Kansas; Michigan; Midwest; Minnesota; New Mexico; Saudi Arabia; United States; Venezuela; Virginia; Washington; Western Interior; Western U.S.

waterways *see also under* engineering geology *under* Florida; Indonesia

waterways—canals
evaporation: Relationship of evaporation to windspeed for an open channel 226

waterways—channels
hydraulics: Open-channel hydraulics 212-213

waterways—erosion
bridges: Countermeasures for hydraulic problems at bridges 269-270

weathering *see also under* geochemistry *under* Antarctica; North Dakota; *see also under* geomorphology *under* Pennsylvania; Washington

weathering—igneous rocks
volcanic glass: Leaching profiles in volcanic glasses 185

well-logging—applications
geothermal energy: Correlation of cyclic sediments between Raft River geothermal wells 195
— Drill holes give a deeper view into eastern Snake River plain, Idaho 195
— Geothermal well logged at Roosevelt Hot Springs in Utah 197-198

well-logging—automatic data processing
boreholes: Computer programs to relate acoustic waveforms and fracture permeability in boreholes 268

well-logging—interpretation
fractures: Borehole geophysical logs of granitic rocks in Manitoba, Canada 268
gravity anomalies: Effects of terrain on borehole gravity data 34
lithology: Detailed lithology near coal seams indicated by borehole and hole-to-hole logging 171
structure: Subsurface model for an area of the eastern Snake River plain 78
temperature: Transient temperature inversions in geothermal boreholes 199

well-logging—radioactivity
automatic data processing: Computer model of gamma spectra in boreholes 267
gamma-ray methods: Borehole capture gamma-ray analysis 23
techniques: Development of a borehole neutron generator 267

well-logging—techniques
boreholes: Development of hole-to-hole and deep-penetrating electrical and acoustic borehole-geophysical systems 171

West Indies *see also* Puerto Rico

West Indies—economic geology
sand: Sand deposits of the Virgin Island platform 155-156

West Virginia—economic geology
coal: Coal resources of Cranberry Wilderness Study Area, West Virginia 9-10
iron: Large submarginal iron resources in Virginia and West Virginia Wilderness Study Areas 10

Western Hemisphere *see also* Atlantic Ocean; North America; Pacific Ocean

Western Interior—economic geology
coal: Partings in western coals 22
— Rank and methane content of western coals 20
— Sphalerite in Interior Basin coals 22
metals: Lead isotopes applied to mineral exploration 12
natural gas: Prediction of oil and gas production from chalk reservoirs 34-35
oil shale: Oil shale resources 35-36
uranium: Radium and uranium in mineral springs 48-49
water resources: Central region 118-128

Western Interior—hydrogeology
hydrology: Multistate studies 120

Western Interior—stratigraphy
Cretaceous: Biostratigraphy of Cretaceous nonmarine mollusks from the Western Interior of North America 217-218
Proterozoic: Paleomagnetic poles and polarity zonation in the Proterozoic Belt Supergroup 167

Western U.S.—economic geology
geothermal energy: Geothermometry applied to hot springs in western United States 194-195
rare earths: Thorium and rare earth resources occur in disseminated deposits in the Bear Lodge Mountains in Wyoming 51
water resources: Western region 128-134

Western U.S.—engineering geology
geologic hazards: Western United States excluding California 246-247

Western U.S.—environmental geology
land use: Geochemical survey of the western energy regions 275
pollution: Compilation of carbon-14 data 224

Western U.S.—geochronology
Holocene: Geomagnetic secular variation during Holocene time 168

Western U.S.—hydrogeology
thermal waters: A hydrothermal system near Ennis, Montana 193-194
— Geothermometry applied to hot springs in western United States 194-195
— Intermediate-temperature geothermal waters found in the Verde Valley, Arizona 194

Western U.S.—petrology
volcanology: Cenozoic volcanism in western United States 181-183

Wisconsin—environmental geology
geologic hazards: Flood of July 1978 in Kickapoo River basin, Wisconsin 269
land use: Digital model predicts effects of powerplant water use on lake levels and river flow in Wisconsin 138

Wisconsin—geomorphology
fluvial features: Channel changes 201-202

Wisconsin—hydrogeology
ground water: Contamination potential of the Silurian dolomite aquifer in eastern Wisconsin 111
hydrology: Hydrology of the Mole Lake Indian Reservation area in Forest County 111
— Maintaining lake levels by using ground water 225
— Minnesota and Wisconsin 108
— Wisconsin 111-112
— Wisconsin wetlands affect streamflow and sediment yields 111-112

Wyoming—areal geology
Seminoe Mountains: New data on geology of Seminoe Mountains 69
Wyoming—economic geology
coal: An experimental technique for delineating areas best suited for mining of coal 71
— Coal maps, 1:100,000-scale 19-20
— Hams Fork Basin, Wyoming 20
— Weston SW quadrangle, Wyoming 21
geothermal energy: Intermediate-period seismic studies in Yellowstone Caldera 200
— Yellowstone seismometer net detects geothermal seismic noise 196
gold: Origin and value of Dickie Springs gold placer deposit, central Wyoming 6-7
maps: An experimental technique for delineating areas best suited for mining of coal 71
— Coal maps, 1:100,000-scale 19-20
petroleum: Geometry and history of petroleum-bearing sandstone units of early Late Cretaceous age in eastern Wyoming 25-26
— Stratigraphic relations of Mississippian and Pennsylvanian rocks and possible oil entrapment in western Wyoming 26-27
platinum: Platinum-group minerals in the New Rambler copper-nickel deposit, southeastern Wyoming 6
thorium: New thorium resource numbers calculated for vein-type occurrences 52
— Thorium and rare earth resources occur in disseminated deposits in the Bear Lodge Mountains in Wyoming 51
uranium: Archean-Proterozoic boundary in Laramie Mountains in Wyoming may contain radioactive conglomerates 36-37
— Depth limitation to uranium deposition, Powder River basin, Wyoming and Montana 42
— Identification of possible uranium province in central Wyoming through radioelement distribution in crystalline basement rocks 47
— Mineralogic residence of uranium in roll-type deposits 46-47
— Present-day stream valleys as guides to uranium deposits in Wyoming 42-43
— Uranium ore deposit controls in the Powder River basin 42
— Uranium potential of Sierra Madre and Medicine Bow Mountains, Wyoming 46
Wyoming—engineering geology
land subsidence: Lands above underground coal mines should be developed with caution 276-277
slope stability: Landslides near Kemmerer, Wyoming 255-256
Wyoming—environmental geology
pollution: Coal hydrology and geochemical studies in the Powder River basin, Montana and Wyoming 260
Wyoming—geochronology
Archean: Age of Archean events in the Big Horn Mountains of Wyoming 184
— Lower Archean gneiss from Wyoming 190
Wyoming—geophysical surveys
seismic surveys: Geophysical exploration 11-12
Wyoming—hydrogeology
thermal waters: Analcime a notable concentrator of cesium in Yellowstone geyser basins 196
Wyoming—paleontology
Mollusca: Reproduction of glochidium larva in an Eocene nonmarine bivalve 217
Wyoming—petrology
igneous rocks: Application of granitic rocks of the Granite Mountains, Wyoming 188
Wyoming—seismology
crust: Intermediate-period seismic studies in Yellowstone Caldera 200
earthquakes: Changes in Yellowstone seismicity patterns observed 196
Wyoming—stratigraphy
Carboniferous: Stratigraphic relations of Mississippian and Pennsylvanian rocks and possible oil entrapment in western Wyoming 26-27
Eocene: Correlation of Eocene volcaniclastic rocks, southeastern Absaroka Range in northwestern Wyoming 68-69
Paleogene: Magnetostratigraphy of lower Tertiary rocks in the Powder River basin 167
Precambrian: Archean-Proterozoic boundary in Laramie Mountains in Wyoming may contain radioactive conglomerates 36-37
Proterozoic: Archean and Proterozoic structural and stratigraphic details of the Hartville uplift in Wyoming 69
Wyoming—structural geology
neotectonics: Large-scale detachment faulting of Eocene volcanic rocks, southeastern Absaroka Range, Wyoming 74-75
— Summary of late Cenozoic history of the Wind River basin and adjacent uplands in Wyoming 75

X

X-ray analysis—X-ray fluorescence
techniques: Loss-On-Fusion method for determining volatiles in geochemical samples 232
— X-ray fluorescence 232
X-ray fluorescence *see under* X-ray analysis

Z

zinc *see also under* economic geology *under* Oregon

INVESTIGATOR INDEX

A

Aaron, J. M. 142
Ackerman, D. J. 126
Ackerman, H. D. 257, 266
Ackermann, H. D. 194
Adam, D. P. 205, 206
Adolphson, D. G. 106
Ager, T. A. 214
Aggarwal, H. R. 285
Ahmad, Z. 313
Albers, J. P. 4
Albert, C. D. 122, 273
Aleinikoff, J. A. 37
Alexander, R. H. 309
Alexander, T. W. 123
Algermissen, S. T. 250
Alldredge, L. R. 169
Allen, H. E. 136
Allen, R. W. 29
Alley, W. M. 136
Alminas, H. V. 10
Altschuler, Z. S. 21, 325
Anderson, H. W., Jr. 107
Anderson, P. 295
Anderson, R. C. 11
Anderson, R. E. 246
Anderson, W. H. 291, 325
Anderson, W. L. 173
Andreasen, G. E. 333
Andrews, D. J. 248
Angelo, C. G. 228
Anna, L. O. 126
Annell, C. S. 231
Antweiler, J. C. 6, 10
Aquino, R. 206
Arcement, G. J. 272
Archer, R. J. 109
Arihood, L. D. 104
Armbruster, J. T. 110
Armbrustmacher, T. J. 51, 52, 190
Armstrong, C. A. 126
Arnold, J. R. 286
Aronson, D. A. 109
Arteaga, F. E. 132
Arth, J. G. 72, 184
Arthur, D. W. G. 282
Aruscavage, P. J. 231
Ashley, R. P. 79, 172
Attanasi, E. D. 15
Atwater, B. 159
Atwater, B. F. 206
Avanzino, R. J. 227
Awramik, S. M. 219

B

Babcock, H. M. 328
Bachman, G. O. 70, 267
Bacon, C. R. 181
Baedecker, P. A. 232
Bailey, E. H. 313
Bailey, R. A. 55
Baird, A. K. 279
Baker, C. H. 138
Baker, C. H., Jr. 137
Baker, E. T., Jr. 127
Baker, J. L. 229
Bakun, W. H. 239
Balding, G. O. 129
Ball, M. M. 142
Balsley, J. R. 326
Baltz, E. H., Jr. 246
Barker, F. 184
Barker, J. A. 87
Barker, R. A. 21, 208
Barnes, D. F. 240
Barnes, J. W. 313
Barnes, P. W. 94
Barnes, W. 230
Barnum, B. E. 21
Barr, D. 209
Barron, J. A. 317
Bartells, J. N. 134
Barthmaier, E. W. 293
Bartlow, J. A. 259
Barton, P. B. 191
Bassari, M. 333
Bassett, R. L. 209
Basu, A. R. 189
Batchelder, J. N. 73, 76, 190
Bateman, P. C. 317
Bath, G. D. 261
Batson, R. M. 283
Bauer, W. L. 290
Baysinger, J. P. 31
Bazzari, M. 333
Becher, A. E. 110
Beck, R. E. 325
Beeson, M. H. 179
Beetem, W. A. 224
Behrendt, J. C. 143, 247, 336
Bell, H., III 8, 65
Bennett, J. P. 201
Berg, H. C. 91, 99
Bergeron, M. P. 104
Bergin, M. J. 62
Bethke, P. M. 191
Beverage, J. P. 229
Bhattacharyya, B. K. 172, 173
Bielefeld, M. J. 286
Billingsly, G. 29
Bingham, D. L. 121
Bingham, R. H. 112
Bird, K. J. 23
Bischoff, J. L. 156
Bisdorf, R. 116
Bisdorf, R. J. 175
Blackwelder, B. W. 66, 214
Blackwell, D. D. 200
Blakely, R. J. 11, 172
Blank, H. R., Jr. 332
Blodget, W. H. 336
Blodgett, J. C. 131, 269
Blunt, D. J. 89
Boettcher, A. J. 124
Boggess, D. H. 114
Bohor, B. F. 22
Bonelli, J. E. 232
Bonham, S. M. 261
Bonner, K. G. 290
Boone, D. M. 200
Borman, R. G. 120
Bortleson, G. C. 89, 302
Bostick, N. H. 30
Botbol, J. M. 13, 14, 15
Bothner, M. H. 141, 142
Boudette, E. L. 37
Bouma, A. H. 152
Bowan, R. W. 14
Bowin, C. O. 143
Bowles, C. G. 49
Bown, T. M. 74
Boyce, J. M. 280
Boyer, S. J. 336
Brabb, E. E. 243, 318
Brabets, T. P. 273
Bradbury, J. P. 214
Breed, C. S. 202, 207, 282
Brenner-Tourtelot, E. F. 16
Bressler, S. L. 167
Brethauer, G. E. 261
Brew, D. A. 97, 99
Brice, J. C. 269
Briqueu, L. 188
Briskey, J. A., Jr. 2
Brock, M. R. 37
Brook, C. A. 53
Brookins, D. 95
Brown, C. E. 59
Brown, D. E. 213
Brown, D. P. 114
Brown, G. E. 177
Brown, G. F. 319, 336
Brown, P. M. 111, 260
Brown, T. M. 68
Brown, W. E., Jr. 284
Brune, J. N. 83
Bryant, B. H. 70
Bucknam, R. C. 246
Bufe, C. G. 197, 239, 251
Bukry, J. D. 150, 156, 157
Buono, A. 130
Burford, R. O. 240
Burke, D. B. 244
Burkham, D. E. 202
Butler, H. M. 235
Butman, B. 141
Byerly, M. I. 231
Byerly, P. 83
Byers, F. M., Jr. 261
Byrne, R. 206

C

Cacchione, D. A. 147, 154
Cadigan, R. A. 48

Cady, J. W. 51
Cagle, J. W. 121
Cahill, J. M. 264
Cain, D. J. 160
Cain, D. L. 121
Cain, J. C. 169
Calk, L. C. 84, 158
Calkins, J. A. 13
Cameron, C. C. 3
Campbell, D. L. 257
Campbell, E. Y. 231
Campbell, J. A. 40, 44
Campbell, R. H. 277
Campbell, W. H. 169
Campbell, W. J. 230
Cannon, W. F. 3, 67
Carey, W. P. 201
Cargill, S. M. 317
Carlson, K. H. 30
Carlson, M. A. 235
Carlson, P. R. 150, 151, 152
Carlson, R. R. 6
Carmony, N. B. 213
Carneggie, D. M. 292
Carothers, W. W. 260
Carr, J. E. 209, 264
Carr, M. H. 279, 280, 281
Carr, W. J. 82
Carrara, P. E. 337
Carroll, R. D. 261
Carter, C. 93
Carter, V. 301
Carter, W. D. 317, 319
Case, J. E. 97
Cashion, W. B. 28
Cassidy, R. J. 30
Cathcart, J. B. 17
Cathrall, J. D. 99
Causaras, C. 116
Cavanaugh, E. T. 25
Cecil, C. B. 21
Cecil, F. E. 48
Chambers, M. J. 307
Champion, D. C. 72
Champion, D. E. 168
Chao, E. C. T. 21, 330
Chao, T. T. 12
Chapman, R. H. 175
Chen, J. 184
Chidester, A. H. 317, 326
Childs, J. R. 154
Chintu Lai 211
Christensen, R. C. 270
Christian, R. P. 279
Chrzastowski, M. J. 89, 302
Church, J. P. 85
Churkin, M., Jr. 93, 168
Claassen, H. C. 185
Clague, D. A. 179, 180, 181
Clark, A. L. 317
Clark, B. C. 279
Clark, J. R. 176, 177
Clark, M. M. 244
Clark, P. E. 286
Clarke, S. H., Jr. 147, 149
Claypool, G. E. 23, 24, 29, 31, 144, 150
Clifton, H. E. 89
Clisham, T. J. 28
Cloern, J. E. 148, 161
Cloud, P. E., Jr. 219
Clynne, M. A. 193
Coats, R. R. 81
Cobb, E. H. 93
Cobb, J. C. 22
Cobban, W. A. 25
Coleman, R. G. 317, 327
Collins, C. A. 132
Colson, B. E. 272
Colton, R. B. 69
Condit, C. D. 283
Connor, C. L. 4, 95
Conomos, T. J. 159
Contont, C. C. 319
Conway, C. M. 332
Cook, H. E. 34
Cooley, R. L. 208
Coonrad, W. L. 97
Cooper, A. K. 153, 154
Cooper, R. W. 66
Coplen, T. B., Jr. 311
Cordell, L. E. 78, 298
Cordes, E. H. 300
Cordova, R. M. 127
Corwin, G. 156, 317
Cory, R. L. 159
Costa, J. E. 213
Cotton, J. E. 108
Coury, A. B. 29
Covington, H. R. 195
Cragwall, J. S., Jr. 313
Craig, H. 199
Crandall, D. R. 277
Crawley, M. E. 221, 260
Creasey, S. C. 5
Crenshaw, G. L. 12
Cressler, C. W. 116
Crim, W. D. 10
Croft, M. G. 260
Cronin, T. M. 214
Crouch, J. K. 157
Crouch, T. M. 110
Csejtey, B., Jr. 96, 97
Cummings, T. R. 222
Cunningham, C. G. 191
Cunninham, C. G. 5
Cushing, E. M. 103, 120
Czamanske, G. K. 176, 177, 317

D

Dalrymple, G. B. 71, 180, 181
Dana, P. 130
Daniel, C. C., III 117, 220
Daniels, J. J. 171
Danielson, T. W. 128
Danilchik, W. 20
Davidson, D. F. 319
Davies, M. 283
Davies, W. E. 254
Davis, G. H. 311, 319
Davis, J. R. 15, 321
Dawdy, D. R. 136
Dean, V. C. 24
Dean, W. E. 228
Dean, W. E., Jr. 153, 154
Dearborn, L. L. 129
DeBuchananne, G. D. 311
DeBuchannane, G. D. 313
Dempsey, W. J. 261
Denny, C. S. 59
Desborough, G. A. 5, 80
Dethier, D. P. 90, 302
Dewey, J. W. 236, 239
Diaz, A. M. 273
Diaz, J. R. 210
Dibble, W. E., Jr. 15
Dickinson, K. A. 44
Dieterich, J. H. 241
Dillon, W. P. 144
Dilonardo, A. L. 336
Dion, N. P. 133
Dixon, H. R. 69
Dodge, F. C. W. 84
Dodge, H. W., Jr. 42
Doe, B. R. 12
Doherty, D. J. 195
Dolton, G. L. 29
Domenico, J. A. 321
Donaldson, F. G. 328
Donnelly, J. M. 167, 181, 197
Donovan, T. J. 33
Donzeau, M. 333
Dooley, J. R., Jr. 16
Dorsey, M. E. 137
Doty, G. C. 261
Doukas, M. P. 243
Downey, H. D. 15
Doyle, W. H., Jr. 136
Draeger, W. C. 326
Drake, A. A., Jr. 60, 61
Drake, D. E. 147, 154
Dresler, P. V. 159
Drew, L. J. 15
Drewes, H. B. 83
Drost, B. W. 133
Duba, A. G. 170
Duerr, A. D. 138
Duffield, W. A. 181
Dunn, B. 271
Dunn, M. L. 10
Dunrud, C. R. 276
Durbin, T. J. 132
Dutro, J. T., Jr. 67, 93, 94
Duty, D. W. 57
Dyni, J. R. 35

E

Eberlein, G. D. 93, 168
Ebling, J. L. 270
Edelen, G. W., Jr. 272
Ege, J. R. 277
Ehlke, T. A. 223
Ehrlich, G. G. 222, 274
Elliott, J. E. 332
Elliott, R. L. 3
Ellsworth, W. L. 179, 238
Elston, D. P. 167, 336
Embree, G. F. 182, 195
Emerson, R. L. 224
Emmett, L. F. 123
Emmett, W. W. 201
Emmons, P. J. 121
Engel, M. E. 290
England, A. W. 336
Englund, K. J. 20
Erd, R. C. 176, 177

Erdman, J. A. 51
Ericksen, G. E. 319, 321
Erickson, D. W. 106
Erickson, J. R. 264
Erickson, R. L. 10
Eskanasy, D. 141
Espenshade, G. H. 62
Espinosa, A. F. 249, 319, 323
Ethridge, F. G. 50
Euster, H. P. 185
Evans, H. T., Jr. 177
Evert, W. A. 261

F

Fabiano, E. B. 168
Faizi, S. 261
Farmer, A. 291
Farrar, C. D. 194
Faust, C. R. 267
Feltis, R. D. 124
Fernald, A. T. 261
Fernandez, M., Jr. 114
Ferrebee, W. M. 141
Ferreira, R. F. 228
Ferrigno, J. G. 295
Ficklin, W. H. 10
Field, M. E. 147, 149
Field, S. J. 202
Finkelman, R. B. 21
Fischer, W. A. 295, 319
Fish, J. E. 116
Fisher, D. W. 186, 260
Fishman, M. J. 232, 233
Fitch, F. H. 332
Fitterman, D. V. 173
Fitzpatrick, D. J. 114
Flanigan, V. J. 174
Fleck, R. J. 333
Fleming, R. W. 253
Fletcher, J. P. B. 248
Flippo, H. N., Jr. 110
Flores, J. M. 20
Flores, R. M. 20
Foehner, O. H. 292
Foose, M. P. 8, 14, 66
Force, E. R. 8
Ford, A. B. 191, 336
Forgey, R. L. 33
Fornari, D. J. 158
Foster, H. L. 96
Foster, J. B. 264
Fouch, T. D. 28, 29
Fouda, A. A. 322
Fournier, R. O. 193, 330
Fox, K. F., Jr. 88
Frederiksen, N. O. 215
Freeman, V. L. 20
Frenzel, P. F. 125
Fretwell, J. D. 113
Fretwell, M. O. 227
Frezon, S. E. 29
Friedman, I. 205
Friedman, J. D. 266, 297
Friedman, L. C. 234
Frischknecht, F. C. 173, 326
Frisken, J. G. 326
Frizzell, V. A., Jr. 90
Froelich, A. J. 303
Fryberger, S. G. 27
Fuentes, R. F. 103
Fuis, G. S. 239, 242
Fumal, T. E. 249
Fusillo, T. V. 109, 221
Fuste, L. A. 227
Futa, K. 181

G

Gabrysch, R. K. 275
Gair, J. E. 8, 317
Galanis, S. P., Jr. 241
Gallagher, D. B. 308
Gammon, P. 301
Garbarino, J. R. 232
Garber, M. S. 222
Garcia, M. 181
Garrison, L. E. 146
Garrison, R. E. 317
Gates, J. S. 128
Gatson, K. W. 311
Gawarecki, S. J. 312, 313
Gay, F. B. 274
Gehring, D. G. 291
George, R. P., Jr. 4
Gettings, M. E. 333
Gettings, M. G. 333
Giacomini, E. G. 108
Gibbons, A. B. 255
Gibbs, J. F. 249
Gibson, T. G. 216
Gill, H. E. 116
Gillies, D. C. 104, 105
Glanzman, R. K. 16
Glick, E. E. 66
Gloersen, P. 230
Goddard, G. L. 201
Goddard, P. L. 118
Godsy, E. M. 222, 274
Goetz, C. L. 113
Goff, F. E. 181, 197
Gogel, A. J. 210
Gohn, G. S. 257
Goldberg, M. C. 233
Goldhaber, M. G. 50
Goldich, S. S. 187
Gonthier, J. B. 132, 133
Gonzales, D. D. 261
Goodkind, J. M. 199
Goodwin, C. R. 158
Gottfried, D. 231
Gower, H. D. 246
Graczyk, D. J. 202
Graff, P. J. 46
Granger, H. C. 45, 47
Grannemann, N. G. 105
Grant, R. S. 201, 202
Grauch, R. I. 47
Green, M. W. 40
Green, S. M. 193, 195
Greene, H. G. 147
Greenlee, D. D. 290, 295
Greenwood, W. R. 9
Griffitts, W. R. 10
Grimes, D. J. 12
Griscom, A. 97, 243, 259
Grogan, D. R. 28
Grolier, M. J. 202, 207, 282
Gromme, C. S. 97, 99, 167, 168
Gross, T. N. 122
Grosz, O. M. 226
Grove, D. B. 273
Grow, J. A. 143
Growitz, D. J. 261
Grybeck, D. 97
Guffanti, M. 53
Guild, P. W. 319
Gutentag, E. D. 138

H

Hackett, O. M. 313
Hadley, D. G. 219
Haeberli, W. 204
Haeni, F. P. 137
Hahn, S. S. 227
Halasz, S. J. 264
Hall, W. E. 73
Hallet, B. 206
Halley, R. B. 31, 34
Hamet, J. 189
Hamilton, L. J. 127
Hamilton, M. S. 14
Hamilton, W. B. 83, 324
Hammett, K. M. 211
Hampton, M. A. 152
Hanley, J. H. 217
Hanley, J. T. 14
Hanna, W. F. 9, 243
Hansen, B. P. 274
Hansen, W. R. 303
Haranczyk, C. 331
Harbaugh, A. W. 210
Harden, J. W. 85, 206
Harlow, D. H. 239
Harned, D. A. 220
Harp, E. L. 256, 325
Harris, A. G. 219
Harris, D. D. 133
Harris, L. D. 32, 219
Harrison, J. E. 5
Harsh, J. F. 111
Hart, D. L., Jr. 124
Hartz, R. W. 94
Harvey, E. J. 225
Harwood, D. S. 243
Hatch, N. L., Jr. 57
Hayes, E. C. 113
Hayes, L. R. 209
Hays, W. W. 249
Healey, D. L. 261
Hearn, B. C., Jr. 167, 181
Hedge, C. E. 70, 181, 190
Hedges, L. S. 127
Hein, J. R. 153, 317
Heindl, L. A. 313, 319, 322
Heinitz, A. J. 271
Hejl, H. R. 125
Helgerson, A. K. 89, 302
Helgesen, J. O. 110
Helley, E. J. 243
Hem, J. D. 186
Hemley, J. J. 326
Henderson, S. E. 116
Hendrick, W. E., Jr. 111
Hennessy, J. L. 144
Henry, V. J. 142

Herb, W. J. 202, 213
Herd, D. G. 243
Herkelrath, W. N. 192
Hertz, E. 290
Herz, N. 8
Hess, A. E. 268
Hess, G. R. 150, 157
Heyl, A. V. 7
Hietanen-Makela, A. M. 83
Higgins, B. B. 257
Higgins, M. W. 63
Hildenbrand, T. G. 247, 298
Hill, D. P. 179, 195, 238
Hill, G. W. 146
Hill, H. R. 230
Hillhouse, J. W. 168
Hills, F. A. 36
Hinkle, M. E. 12
Hitchcock, T. 197
Hite, R. J. 266
Hoare, J. M. 97
Hobbs, R. G. 330
Hobbs, S. W. 67
Hodges, C. A. 282
Hodson, J. N. 265
Hoffard, S. H. 229
Holdsworth, B. 81, 95
Hollyday, E. F. 118
Holmes, C. W. 145, 155
Holmes, M. L. 157
Holt, H. E. 283
Holt, M. F. 106
Holzer, T. L. 277
Hood, D. R. 293
Hood, J. W. 128
Hoover, D. B. 193, 265
Hoover, L. 317
Hopkins, D. M. 94
Hopkins, H. T. 110, 111, 137
Horak, W. F. 126
Horton, J. W., Jr. 63
Hose, R. K. 80, 82
Hotchkiss, W. R. 124, 260
Houston, R. S. 46
Hovland, R. D. 78
Howard, K. A. 15, 84
Howell, D. G. 30, 146
Howells, L. W. 54
Hubbard, L. E. 133
Hubbard, L. L. 133
Hubbell, D. W. 229
Hubert, A. E. 12, 321
Hudson, J. H. 34, 158
Hudson, T. 3
Huebner, J. S. 170
Huff, L. C. 313
Huffman, A. C., Jr. 23
Hughes, B. A. 233
Hughes, P. E. 269
Huie, C. 99, 336
Hull, J. E. 115
Hull, R. W. 273
Hult, M. F. 107, 272
Hunn, J. D. 115
Hunt, G. R. 171, 172
Hunt, S. J. 99
Hunter, R. E. 148, 155
Hupp, C. R. 220
Husid, R. 323
Hyde, J. H. 277

I

Imbrigiotta, T. E. 104
Irwin, W. P. 243
Iyer, H. M. 193, 195, 196, 197
Izett, G. A. 70, 71, 246, 267

J

Jachens, R. C. 175, 240
Jackson, R. O. 319
Jahns, R. H. 253
Jaksha, L. H. 236
James, O. B. 287
Janzer, V. J. 234
Jarrett, R. D. 213
Jenkins, E. C. 261
Jennings, M. E. 136, 211
Jobson, H. E. 211, 226
Johnson, B. R. 97
Johnson, C. E. 242
Johnson, D. A. 283
Johnson, G. R. 170, 284, 293, 294
Johnson, G. W. 232
Johnson, M. G. 13
Johnson, R. B. 255
Johnson, R. C. 27
Johnson, R. G. 141
Johnson, T. V. 286
Johnston, J. E. 21
Johnston, M. J. 242
Johnston, R. H. 303
Jones, B. F. 185, 186, 325
Jones, D. L. 81, 82, 93, 94, 95
Jones, J. R. 326
Jones, M. 99, 168
Jones, M. L. 201
Jordan, J. N. 235
Jordan, P. R. 202
Junkins, J. 345

K

Kachadoorian, R. 251, 253, 277
Kaczanowski, G. 194
Kalliokoski, J. O. K. 38
Kane, M. F. 323, 326
Kaplan, I. R. 157
Karlstrom, K. E. 46
Karma, A. S. 45
Katock, R. 21
Katzer, T. L. 201
Kauahikaua, J. P. 173
Kauffman, E. G. 217
Kaufman, A. A. 199
Kaye, C. A. 57, 215, 216
Keefer, D. K. 252, 256, 325
Keighin, C. W. 27
Keil, K. 279
Keith, T. E. C. 96, 196
Keller, G. V. 199
Kellogg, K. 333
Kellogg, K. S. 337
Kennedy, G. L. 86
Kennedy, V. C. 185, 227
Kent, B. H. 19
Kestin, J. P. 198
Ketner, K. B. 18, 80
Keys, W. S. 127, 197, 267, 268
Khan, A. S. 29, 30
Kharaka, Y. K. 186, 260
Kieffer, H. 280
Kimball, B. A. 221
King, B. S. 232
King, C. Y. 242
King, H. D. 10
King, N. E. 240
King, S. C. 10
Kinney, D. M. 319
Kirby, S. H. 171
Kirk, A. R. 41
Kistler, R. W. 191, 336
Kiteley, L. W. 27
Klasner, J. S. 67
Klausing, R. L. 126, 127
Klein, H. 115
Klein, J. M. 121
Kleinkopf, M. D. 326
Klemic, H. 8
Klitgord, K. D. 143
Knapton, J. R. 260
Knebel, H. J. 142
Knepper, D. H., Jr. 298
Knott, J. M. 324
Knudson, C. F. 319
Kockelman, W. J. 303, 318
Kohout, F. A. 334
Konikow, L. F. 273
Konnert, J. A. 176
Kork, J. O. 71
Kosanke, R. B. 29
Koski, R. A. 4
Kraemer, T. F. 53
Krimmel, R. M. 203
Krivoy, H. L. 144
Krohn, M. D. 265, 297
Kromhardt, A. P. 129
Kruer, S. A. 128
Krug, W. R. 138
Kuberry, R. W. 169
Kulp, K. P. 229
Kuntz, M. A. 71, 72
Kurtz, H. F. 1
Kvenvolden, K. A. 89, 152, 154

L

Lachenbruch, A. H. 53, 241
Lahr, J. C. 236
Lai, C. 130
Lancelot, J. R. 188
Land, L. F. 270
Landing, E. 219
Landwehr, J. M. 336
Laney, R. L. 130, 276
Lang, S. M. 323
Langer, C. J. 235, 236
Langer, W. H. 59, 303
Lanphere, M. A. 93, 97, 180, 181
Lantz, R. J. 157
Lapham, W. W. 104
Lappala, E. G. 209
Lara, O. G. 121
Larsen, F. D. 58
Larson, G. J. 58

Larson, J. D. 110
Larson, S. P. 121, 328
Lauer, D. T. 291
Laurin, G. S. 311
Lawson, A. C. 83
Leahy, P. P. 208
Leavesley, G. H. 211
LeBlanc, D. R. 274
Lee, D. E. 81
Lee, R. W. 260
Lee, W. H. K. 238, 244
Leenheer, J. A. 35, 321
Lefebvre, R. H. 72
Leiggi, P. A. 7
Lemon, E. M., Jr. 257
Leo, G. W. 60
Leonard, R. B. 193
Leone, H. L., Jr. 274
Lesure, F. G. 10
Leve, G. W. 114
Leventhal, J. S. 33, 47
Levings, G. W. 124
Levy, W. P. 151
Lewis, B. D. 123, 124, 260
Lichtenstein, B. R. 286
Lichty, R. W. 211
Liddicoat, J. 257
Lidwin, R. A. 111
Lidz, B. 158
Lidz, B. H. 34
Lindh, A. G. 238, 239
Lindholm, G. F. 107
Lindsey, D. A. 68
Lindvall, R. M. 303
Lines, G. C. 261
Ling, C. H. 301
Ling, H. S. 307
Lipin, B. R. 1, 9
Lipman, P. W. 72
Lisowski, M. 240
Livingston, R. K. 121
Lockner, D. A. 238
Lodde, P. F. 249
Loesch, T. L. 326
Loferski, P. J. 8
Lofgren, B. E. 326
London, E. B. H. 59
Lopez, D. 73
Lopez, M. A. 136, 270
Loskot, C. 209
Loucks, R. R. 6
Love, J. D. 6, 75
Lovell, M. D. 195
Lowe, A. S. 271
Lowell, R. P. 199
Lubeck, C. M. 31
Lucas, J. R. 293, 294, 301, 326
Lucchitta, B. K. 281, 286
Lucchitta, I. 82
Luce, R. W. 8, 65
Ludington, S. D. 9
Ludwig, K. R. 46
Luepke, G. 149
Luoma, S. N. 160, 223
Lupe, R. D. 81
Luther, E. 206
Luzier, J. E. 132
Lyford, F. P. 125
Lyons, P. C. 57
Lystrom, D. J. 136
Lyttle, P. T. 61

M

Mabey, D. R. 53, 78
MacKenzie, G., Jr. 29
MacKinnon, D. A. 207
MacKinnon, D. T. 219
MacLeod, N. S. 182
Maderak, M. L. 137, 211
Magoon, L. B., III 23, 24
Maher, J. C. 322
Mahood, A. 206
Majchszak, F. L. 32
Maley, R. P. 251, 312
Mallory, M. J. 130, 208
Mamay, S. H. 95
Mandle, R. J. 105
Manheim, F. T. 3
Mankinen, E. A. 167
Mantis, C. E. 239
March, R. 204
Marchand, D. E. 64, 85, 206
Mariner, R. H. 53
Markewich, H. W. 75
Marks, S. M. 197
Marlow, M. S. 153
Marshall, S. L. 122
Martin, A., Jr. 104
Martin, C. M. 273
Martin, E. A. 145
Martin, R. G. 145
Martinez, M. 235
Massey, B. C. 136
Masursky, H. 279, 280, 281, 283, 319
Matson, D. L. 286
Matthiesen, R. B. 329
Matti, J. C. 87
Mattick, R. E. 143, 144, 330
Mattraw, H. C. 136
Maughan, E. K. 26, 29
Maurer, D. K. 230
May, F. E. 217
May, R. J. 192
Mayo, L. R. 203, 204
McBroome, L. A. 303
McCallum, M. E. 6, 39
McCammon, R. B. 14
McCarthy, J. H., Jr. 10
McCauley, J. F. 202, 207, 280, 282
McClymonds, N. E. 124, 326
McCulloch, D. S. 148, 159
McCulloh, T. H. 157
McDonald, M. G. 106
McEvilly, T. V. 239
McGee, K. A. 176
McGill, J. T. 86, 254
McGuire, R. K. 249
McKee, E. D. 29
McKelvey, V. E. 319
McKenzie, S. W. 132
McLean, H. 30, 153
McLeod, R. S. 225
McNally, K. C. 242
McNeal, J. M. 51
McNellis, J. M. 122, 202
McPherson, B. F. 274
Mehnert, H. H. 73, 191, 246
Meier, M. F. 203, 204
Meissner, C. R. 9, 20
Menard, H. W. 330
Mendieta, H. B. 229
Menzie, W. D., II 14
Mercer, J. W. 267
Merewether, E. A. 25
Merriam, D. 317
Metzger, A. E. 286
Meyer, W. 103
Meyer, W. R. 209
M'Gonigle, J. W. 20
Miesch, A. T. 187, 188
Milazzo, V. A. 308
Millard, H. T., Jr. 188, 232
Miller, B. M. 30, 330
Miller, C. D. 277
Miller, C. H. 252
Miller, F. K. 91
Miller, J. A. 111
Miller, J. E. 211
Miller, R. A. 115, 136
Miller, R. D. 255
Miller, R. E. 144
Miller, R. L. 330
Miller, R. W. 273
Miller, S. H. 298
Miller, T. P. 39
Miller, W. A. 290
Miller, W. R. 9
Milton, D. J. 62, 285
Ming, C. O. 272
Minkin, J. A. 21
Missimer, T. M. 114
Mitchell, G. D. 116
Mitsunobu, T. 188
Moench, A. F. 192
Molnia, B. F. 150, 151, 152
Momenzadeh, M. 313
Moore, D. O. 334
Moore, G. K. 301, 319, 323, 325
Moore, H. J., Jr. 282
Moore, J. G. 158
Moosburner, O. 130, 271
Morgan, J. O. 319
Morgan, J. W. 232
Morrell, R. P. 99
Morris, H. T. 2, 71, 190
Morrison, H. F. 198
Morrison, K. 219
Morrissey, D. J. 261
Mortensen, C. E. 242
Morton, D. M. 86, 87, 277
Morton, J. L. 86, 95
Mory, P. C. 9
Mosier, E. L. 6, 10, 231
Moss, M. E. 336
Moss, M. R. 270
Mossotti, V. G. 232
Motooka, J. M. 10, 231
Moyle, W. R., Jr. 130
Mudge, M. R. 78
Muffler, L. J. P. 53, 196
Muller, D. C. 261
Mullineaux, D. R. 277
Munson, B. E. 19
Murata, K. J. 205
Myette, C. F. 106, 225
Mytton, J. W. 20

N

Nackowski, M. P. 313
Naeser, C. W. 71, 191, 246
Nakamura, N. 189
Nakata, J. K. 87, 206
Nash, J. T. 36, 38, 43, 52
Nason, R. D. 249
Natland, J. H. 180
Nehring, N. L. 194, 197
Nelson, A. E. 63
Nelson, C. A. 290
Nelson, C. H. 154
Nelson, W. H. 97
Neuman, R. B. 100, 317
Newell, M. F. 184
Newell, W. L. 258, 259
Nichols, D. J. 28
Nichols, F. H. 148, 160
Nichols, T. C., Jr. 251
Nilsen, T. H. 318
Noble, E. A. 319, 330
Normark, W. R. 150, 157
Norris, S. E. 265
Novitzki, R. P. 111
Nowlan, G. A. 10

O

Oaksford, E. T. 109
Oberbeck, V. R. 285
Oberhansley, G. G. 182
Oberlindacher, P. 78
Obermeier, S. F. 252, 255
O'Donnell, T. H. 114, 116
O'Hara, C. J. 141
Ojakangas, R. W. 38
Oldale, R. N. 141
Olhoeft, G. R. 169, 170, 174, 284
Olimpio, J. C. 264
Olive, W. W. 66, 322, 330
Oliver, H. W. 175
Oliver, W. A., Jr. 218
Olson, A. C. 13, 19
Olson, J. C. 38, 39, 52
Olson, W. A., Jr. 311
Oltmann, R. N. 130
Omang, R. J. 271
O'Neil, J. R. 79, 190
Oppenheimer, D. H. 196, 197
Oriel, S. S. 76, 195
Orkild, P. P. 261
Orr, D. G. 295, 325
Osberg, P. H. 56, 100
Osterkamp, W. R. 202
Osterwald, F. W. 276
Otton, J. K. 16, 43
Overstreet, W. C. 321

P

Packard, F. A. 227
Page, L. R. 322
Paillet, F. L. 268
Pakiser, L. C., Jr. 83
Palacas, J. G. 31
Pankratz, L. W. 276
Papadopulos, S. S. 332, 334
Parker, A. 154
Parkhurst, D. L. 268
Parliman, D. J. 131
Parrett, C. 271
Pascale, C. A. 112, 273, 274
Patterson, G. L. 103
Patterson, S. H. 1, 319
Pavlides, L. 258
Pawlowska, J. 331
Payne, G. A. 107, 108
Pearl, J. E. 88
Pearson, F. J. 311
Pedder, A. E. H. 218
Pelselnick, L. 240
Peper, J. D. 58
Pereira, W. E. 233
Perkins, D. M. 250
Person, W. J. 235
Peters, N. E. 224, 272
Peterson, D. H. 159, 161
Peterson, F. 45
Pettinger, L. R. 291, 292, 326
Phair, G. 198
Phillips, J. D. 257, 297
Phillips, J. S. 265
Phillips, R. L. 147
Pierce, H. W. 43
Pierce, K. L. 303
Pierson, C. T. 40, 45, 51
Pike, R. J. 286
Pike, R. J., Jr. 285
Pike, R. S. 30
Pilkey, O. J. 142
Pinckney, D. J. 186
Pinder, G. F. 121
Piotrowski, R. G. 32
Piper, D. Z. 156
Pipiringos, G. N. 35
Pitman, J. K. 27
Pitt, A. M. 196
Plafker, G. 150
Platt, L. B. 76
Plummer, L. N. 268
Podwysocki, M. H. 265, 297
Pohn, H. A. 265, 297
Pojeta, J., Jr. 219
Polcyn, F. 290
Pollard, D. D. 241
Pollock, D. W. 264
Pomeroy, P. W. 235
Poole, F. G. 5, 80, 82
Popenoe, P. 142
Post, A. 203, 204
Potori, J. E. 109
Potter, R. W., II 193
Powers, R. B. 29, 30
Pratt, W. P. 183
Prescott, W. H. 240
Price, L. C. 33
Priestly, K. F. 199
Prill, R. C. 109
Prinz, W. C. 65
Proctor, P. D. 10
Puckett, L. J. 220
Purdy, R. W. 216
Pyen, G. S. 232, 233

R

Rachlin, J. 261
Radbruch-Hall, D. 251, 255
Radtke, A. S. 80
Raines, G. L. 326
Ramseier, R. O. 230
Randich, P. G. 127
Rasmussen, L. A. 230
Ratcliffe, N. M. 247
Rathbun, R. E. 212
Ray, C. E. 216
Raymond, R. H. 130
Raymond, W. H. 7
Razem, A. C. 128
Reasenberg, P. A. 197
Reed, R. C. 37
Reed, W. E. 157
Reilly, T. E. 210
Reimer, G. M. 49
Reimnitz, E. 94, 230
Reinemund, J. A. 317, 336
Reinhardt, J. 64, 219
Remmenga, E. E. 30
Repenning, C. A. 215
Repetski, J. E. 83, 219
Rettig, S. L. 15, 186, 321
Reussow, J. P. 104
Reynolds, M. W. 5, 68
Reynolds, R. L. 46, 50, 336
Rice, D. D. 25, 30
Richards, P. W. 319
Ridgley, J. L. 41
Rinella, F. 133
Rinkenberger, R. K. 292
Risacher, F. 186
Robbin, D. M. 34
Roberts, A. A. 24, 33
Roberts, A. E. 17
Roberts, E. D. 194
Roberts, R. J. 79
Robertson, E. C. 198
Robertson, J. F. 41
Robin, R. L. 228
Robinove, C. J. 294, 295
Robinson, K. 29
Robinson, P. 60
Robinson, S. W. 192
Roddy, D. J. 285
Roedder, E. W. 331
Roen, J. B. 32
Rogers, A. M. 236, 249
Rogers, S. M. 261
Rohde, W. G. 290
Rooney, L. F. 333
Root, D. H. 15
Rose, H. J., Jr. 279
Roseboom, E. H., Jr. 176
Ross, D. C. 85
Ross, M. 177
Ross, P. P. 194
Ross, R. J., Jr. 80, 329
Roth, E. F. 249
Roure, F. 87
Rowan, L. C. 297, 299, 326
Rowe, J. J. 232
Rowley, P. D. 73
Roybal, R. G. 125, 126
Rozelle, J. W. 326

Rubin, D. M. 148, 159
Rumen, L. L. 33
Rundle, J. B. 241
Ruppel, B. D. 157
Rush, F. E. 266
Russ, D. P. 247
Russell, L. S. 217
Ruthven, R. W. 311
Ryan, B. J. 121
Ryder, R. T. 11
Rye, R. O. 50, 191
Ryer, T. A. 20
Rytuba, J. J. 79

S

Saindon, L. G. 211
Sakamoto, C. M. 206
Samuel, E. A. 53
Sanchez, J. 20
Sandberg, C. A. 28, 218
Sandeen, W. M. 209
Sanders, C. L. 269
Santos, E. S. 42
Sanzolone, R. F. 12
Sarna-Wojcicki, A. M. 244, 277
Sass, J. H. 53, 193, 241
Sato, M. 176, 288
Sauer, C. G. 208
Sauer, S. P. 325, 326
Sauer, V. B. 269
Savage, J. C. 240, 319
Savage, W. Z. 251
Sawyer, M. B. 45
Schaake, J. C., Jr. 136
Schaber, G. G. 282, 284, 299
Schaefer, B. E. 284
Schafer, J. P. 59
Schamberger, M. 291
Scheetz, N. D. 311
Schemel, L. E. 162
Schimschal, U. 267
Schlee, J. S. 143
Schmidt, P. W. 303
Schmidt, R. G. 77
Schmoker, J. W. 33, 34
Schoenberg, M. E. 272
Schoff, S. L. 330
Scholl, D. W. 153
Scholle, P. A. 33, 34, 144
Schornick, J. C. 221
Schroder, L. J. 224
Schroeder, R. A. 272
Schruben, P. G. 1, 13
Schultz, D. J. 211
Schultz, D. M. 144
Schuster, R. L. 253
Schweitering, J. F. 32
Scott, D. H. 281, 282, 286
Scott, E. W. 29, 30
Scott, J. H. 171
Scott, R. A. 95
Scott, W. E. 205
Sebetich, M. J. 227
Seeland, D. A. 42
Segall, P. 241
Segerstrom, K. 6
Seidel, D. C. 16
Seitz, H. R. 131, 201
Senftle, F. E. 311
Shaffer, G. L. 13
Shampine, W. J. 334
Sharp, R. V. 244
Shaw, H. R. 53, 179, 268
Shawe, D. R. 5
Shedlock, R. J. 104
Sheehan, C. A. 291
Sheldon, R. P. 1, 317
Sheridan, D. M. 7
Sherrill, M. G. 111, 264
Sherrod, D. R. 182
Shideler, G. L. 145
Shinn, E. A. 34, 158
Shoemaker, E. M. 280
Shope, W. G., Jr. 300
Showen, C. R. 313, 326
Shride, A. F. 57
Shultz, D. J. 224
Shurr, G. W. 25
Siegel, D. I. 106, 107
Sigafoos, R. S. 269
Sikonia, W. G. 203, 204
Silberling, N. J. 81, 94
Silberman, M. L. 4, 79, 95, 96
Simmons, C. E. 116, 117
Simpson, R. W., Jr. 172
Simpson, S. L. 266, 297
Sims, J. D. 205
Sims, P. K. 65
Sinclair, W. C. 113, 228
Sinding-Larsen, R. 14
Singer, D. A. 13, 14
Sinnott, A. 103
Sisler, F. A. 268
Skinner, J. V. 229
Skipp, B. A. 76
Skipp, B. L. 29
Skogerboe, R. K. 232
Slack, J. F. 8
Slack, K. V. 227
Slack, L. J. 115, 122
Slade, R. M. 137, 211
Slater, L. 240
Slater, R. A. 142
Slater, W. H. 277
Smith, B. D. 174
Smith, C. 124
Smith, D. B. 183
Smith, G. I. 85, 205
Smith, J. G. 3
Smith, K. A. 321
Smith, M. A. 144
Smith, R. L. 15, 53, 321
Smith, W. 229
Snavely, P. D., Jr. 88, 149, 319
Snyder, G. L. 69
Snyder, J. P. 345
Soderblom, L. A. 279, 280, 283, 286
Sohm, J. E. 112
Sohn, I. G. 218
Solomon, B. J. 35
Sonnevil, R. A. 99
Soren, J. 210
Sorensen, M. L. 81
Sousa, T. M. 319
Spence, W. J. 235, 236, 239, 323
Spencer, D. W. 123
Spiers, C. A. 265
Spiker, E. 162
Spiker, E. C. 141
Spirakis, C. S. 45
Staatz, M. H. 51, 52
Stacey, J. S. 190
Stanley, R. S. 57
Stanley, W. D. 173
Stark, J. R. 106
Stearns, C. O. 169
Stearns, H. 180
Steinbrugge, K. V. 250
Stephens, C. D. 236
Stephens, D. W. 224, 233
Steppe, J. A. 242
Stern, T. W. 84, 96, 184
Stetz, D. J. 294
Steven, T. A. 73
Stevens, H. H., Jr. 229
Stevens, T. A. 5, 191
Stewart, R. M. 238, 239
Stickney, M. C. 197
Stoeser, D. B. 332
Stokoe, K. H. 249
Stone, B. D. 57, 58
Stone, J. R. 59
Stone, P. 84
Stoner, J. D. 124
Stover, C. W. 235
Strange, W. E. 175, 240
Stuart-Alexander, D. E. 259
Stuart, W. D. 241
Stuber, H. A. 35
Stuckless, J. S. 187, 188
Stullken, L. E. 225
Suczek, C. A. 81
Sugiura, M. 169
Sulam, D. 225
Sumioka, S. S. 133
Sunada, K. K. 50
Suneson, N. H. 82
Susuki, T. 86
Sutley, S. J. 231
Sutphin, L. M. 313
Swain, F. M. 111
Swanberg, C. A. 200
Swanson, D. A. 90, 183
Swanson, J. A. 13
Swanson, J. R. 53
Szabo, B. J. 188

T

Tabor, R. W. 90
Tai, D. Y. 233
Tangborn, W. V. 203, 211
Tanner, A. B. 49
Taranik, J. V. 295, 296
Tarr, A. C. 238
Tasker, G. D. 270
Tatsumoto, M. 189
Taylor, F. A. 253
Taylor, H. E. 232
Taylor, M. E. 67
Taylor, R. E. 53, 54
Taylor, T. A. 268
Teleki, P. G. 323
Thaden, R. E. 42
Thatcher, L. L. 273
Thatcher, W. R. 240, 241

Thayer, T. P. 1, 8, 9
Theisen, A. F. 296
Theobald, P. K., Jr. 326
Thomas, C. A. 212
Thompson, C. L. 21
Thompson, J. K. 161
Thompson, W. B. 56
Thor, D. R. 154
Thorson, R. M. 89
Thorstenson, D. C. 186, 221, 260, 268
Threlkeld, C. N. 31
Thurmond, C. J. 116
Tibbitts, G. C., Jr. 334
Tilley, L. J. 227
Tinsley, J. C., III 86
Tippens, C. L. 173
Todd, V. R. 84
Todd, W. J. 291
Toimil, L. J. 230
Tolbert, G. E. 319
Toulmin, P., III 279
Towie, J. N. 192
Trabant, D. C. 203, 204
Trapp, H., Jr. 114
Trautwein, C. M. 290, 291, 295, 296
Trescott, P. C. 121, 328
Trimble, D. E. 253
Tripp, R. B. 321
Troutman, B. M. 211
Troutman, D. E. 212, 224
Truesdell, A. H. 311
Trumbull, J. V. A. 155
Tschudy, R. H. 45
Tucci, P. 103
Tugal, T. 313
Turk, J. T. 109
Turner, D. L. 97
Turner, J. F. 211, 300
Turner-Peterson, C. 44
Turner, R. L. 326
Turner, R. M. 213, 220, 226
Tweto, O. L. 73

U

Ucok, H. 170
Unruh, D. M. 189
Uthman, M. 333

V

Van Alstine, R. E. 1
Van der Voo, R. 99, 168
Van Driel, J. N. 303
van Hylckama, T. E. A. 220, 226
Van Loenen, S. D. 45
Varnes, D. J. 255
Varnes, K. L. 29
Vecchioli, J. 274
Vedder, J. G. 30, 146
Vennum, W. R. 337
Verbeck, E. R. 259
Viets, J. G. 10, 231
Vietti, B. T. 30
Vine, J. D. 15
Volckmann, R. P. 258

W

Waddell, K. M. 136
Wagner, J. R. 112
Wahl, K. D. 122
Wahlberg, J. S. 5
Wait, R. L. 334
Wallace, A. R. 43
Wallace, C. A. 77
Wallace, R. E. 329
Wallace, R. H., Jr. 53, 54
Waller, B. G. 115
Walters, K. L. 133
Walthall, K. L. 311
Waltz, F. A. 290
Wandle, S. W., Jr. 271
Wanek, A. R. 15
Wang, F. H. 312
Ward, A. W., Jr. 207
Ward, F. N. 231
Ward, L. W. 66
Ward, R. W. 200
Wardlaw, B. R. 80
Warren, C. G. 47
Washington, C. L. 261
Watkins, F. A. 113
Watkins, J. A. 286
Watson, B. A. 76
Watson, D. E. 167
Watson, J. 317
Watson, K. 298, 299, 326
Watson, R. D. 296
Watterson, J. R. 12
Watts, K. C., Jr. 10
Watts, R. D. 174, 266
Weaver, C. S. 195
Webster, D. A. 264
Wedow, H., Jr. 331
Weed, E. G. A. 57
Weems, R. E. 257
Wehmiller, J. F. 86
Weiblen, P. W. 187
Weiner, E. R. 233
Weiner, M. S. 220
Wells, F. C. 223
Wenrich-Verbeek, K. J. 9, 49
Wentworth, C. M., Jr. 247, 325
Wershaw, R. W. 186
Wesselman, J. B. 53, 54
Wesson, R. L. 319
Westphal, B. 188
Whetten, J. T. 88
White, A. F. 185, 261
White, D. E. 54
White, R. R. 125, 126
Whitehead, D. H. 81
Whiteman, C. D., Jr. 123
Whitmore, F. C., Jr. 215, 216
Wieczorek, G. F. 256
Wier, J. E., Jr. 265
Wiggins, L. B. 170
Wiitala, S. W. 271
de Wijs, H. J. 187
Wilcox, D. E. 129
Wilder, H. B. 220
Wilhelms, D. E. 285, 286
Wilke, K. R. 124
Willey, R. E. 110
Williams, B. B. 10
Williams, G. P. 120
Williams, R. P. 201
Williams, R. S., Jr. 121, 294, 295
Wilshire, H. G. 87, 206
Wilson, C. A. 125, 126
Wilson, L. A. 67
Wilson, L. D. 136
Wilson, M. E. 244
Wilson, R. C. 257
Windolph, J. F., Jr. 9
Winikka, C. C. 130
Winner, M. D., Jr. 117
Winter, T. C. 107, 224
Wintsch, R. P. 58
Witkind, I. J. 70
Wold, R. J. 65
Wolf, R. J. 108
Wolfe, J. A. 217
Wolff, R. G. 210
Wollitz, L. E. 261
Wones, D. R. 56
Woo, C. C. 3
Wood, S. H. 244
Woodham, W. M. 300
Wright, D. L. 174
Wright, T. L. 90, 183
Wrucke, C. T., Jr. 81
Wu, S. S. C. 283
Wyerman, T. A. 185
Wynn, J. C. 171, 332

Y

Yenne, K. A. 330
Yerkes, R. F. 244, 251
Yotsukura, N. 212
Youd, T. L. 252
Young, E. J. 39
Young, H. W. 131
Younger, J. 228
Yukutake, T. 169
Yurewicz, M. C. 115

Z

Zablocki, C. J. 196
Zambresky, L. F. 249
Zand, S. M. 227
Zartman, R. E. 190, 331
Zech, R. S. 43
Zehner, H. H. 264
Zeliber, J. L., Jr. 268
Zellweger, G. M. 227
Zembrzuski, T. J., Jr. 271
Zen, E-an 67, 72, 75, 176, 184
Zenone, C. 276
Ziegler, W. 218
Zielinski, R. A. 46, 183
Zoback, M. D. 241
Zohdy, A. A. R. 173, 175, 192, 194, 322
Zubovic, P. 22
Zucca, J. J. 195
Zwally, H. J. 230

☆ U.S. GOVERNMENT PRINTING OFFICE: 1980 O— 311-344/90